United States Department of Commerce
Technology Administration
National Institute of Standards and Technology

NIST Monograph 177

Properties of Copper and Copper Alloys at Cryogenic Temperatures

N. J. Simon, E. S. Drexler, and R. P. Reed

NIST Monograph 177

Properties of Copper and Copper Alloys at Cryogenic Temperatures

N. J. Simon
E. S. Drexler
R. P. Reed

Materials Reliability Division
Materials Science and Engineering Laboratory
National Institute of Standards and Technology
Boulder, CO 80303-3328

Sponsored by

International Copper Association, Ltd.
708 Third Avenue
New York, NY 10017

February 1992

U.S. Department of Commerce
Rockwell A. Schnabel, Acting Secretary
Technology Administration
Robert M. White, Under Secretary for Technology
National Institute of Standards and Technology
John W. Lyons, Director

National Institute of Standards and Technology Monograph 177
Natl. Inst. Stand. Technol. Mono. 177, 850 pages (Feb. 1992)
CODEN: NIMOEZ

U.S. GOVERNMENT PRINTING OFFICE
WASHINGTON: 1992

For sale by the Superintendent of Documents, U.S. Government Printing Office, Washington, DC 20402–9325

NOTE TO READERS

The number of digits in some of the tables is an artifact of the computer program used to analyze the data. This program furnished tabular output with the same number of decimal places for all numbers. Thus, the number of digits given in the table does not represent the number of significant digits in the measured or calculated values.

The letters A, B, C, ... that follow the reference number in the tables and graphs are used to distinguish between data on alloys of different composition from the same reference.

Each subsection of the monograph is intended to be self-contained, and usually does not require the reader to refer to other subsections. However, the table of characterization of materials and measurements and the list of references are found only at the end of each numbered section. For example, a subsection on thermal expansion of C10100–C10200 copper is self-contained, except for the characterization table and reference list found at the end of section 7 on thermal properties.

TABLE OF CONTENTS

BERYLLIUM COPPER

TABLE OF CONTENTS
(continued)

PHOSPHOR BRONZE

SUMMARY

The mechanical and physical properties at cryogenic temperatures for selected coppers and copper alloys have been compiled, reviewed, and analyzed. Tables, figures, and regression equations have been produced. The materials include: the oxygen-free coppers (C10100–C10700), beryllium coppers (C17000–C17510), and the phosphor bronzes (C50500–C52400). The temperature range for the property data is from 4 to 295 K. Mechanical properties include tensile, toughness, fatigue, and creep; physical properties include elastic constants, specific heat, thermal conductivity and expansion, and electrical resistivity. In many cases, these properties are a strong function of metallurgical variables, such as cold work and grain size. Regression analyses have been performed in cases where there are sufficient data to ensure reasonable statistical portrayal of the effect of these variables on specific properties. Over 2500 references have been assessed; the final review includes over 1000 pages that contain data from more than 400 references.

The original program of data review was sponsored by the Office of Fusion Energy of the U.S. Department of Energy. Its purpose was to assemble and to evaluate property data useful to magnet designers for fusion plasma confinement. Both normal-metal, high-field magnets (e.g., the Burning Plasma Experiment at Princeton Plasma Physics Laboratory, using cold-worked C10700 and C17510 alloys) and NbTi and Nb_3Sn superconducting magnets (e.g., the proposed International Thermonuclear Experimental Reactor, Lawrence Livermore National Laboratories, using C10400 and phosphor bronze alloys) are currently in design or development stages. The review has been reedited and expanded for those more generally interested in the low-temperature properties of copper and selected copper alloys, under the sponsorship of the International Copper Association, Ltd.

COPPER AT CRYOGENIC TEMPERATURES

Copper or copper alloys are normally used in low-temperature structures when a combination of both physical (high conductivity) and mechanical (adequate strength) properties are needed. Copper is used in many cryogenic applications in association with superconductors which require a stabilizing normal conductor. High-field magnets, power transmission and generation, and magnetic energy storage are current or potential large-scale applications that use both superconductors and copper stabilizers. Copper is ideal for stabilization of superconducting magnets. The role of the stabilizing material in superconducting magnets is to prevent catastrophic magnet destruction if a portion of the superconductor is warmed above the critical temperature and becomes resistive. Copper, used as the stability element, serves to transfer heat away from the local "hot spots" and to conduct a portion or all of the current that normally would travel through the superconductor. Furthermore, in most composite conductors, the copper is expected to carry the majority of the composite load. The idealized copper stabilizers have low electrical resistivity, high strength and elastic moduli, and high thermal conductivity. Unfortunately, those treatments that promote low electrical resistivity, such as chemical purification and annealing, promote low strength; the optimization of the ratio of flow strength to electrical resistivity, both at 4 K, becomes the research driving force. Currently, most conductor composites use oxygen-free copper (grades C10100–C10700) with residual electrical resistivity ratios of about 300 for the annealed condition with less than 0.1 wt% impurities. This copper grade is then cold-rolled or extruded to about the 1/4-hard condition to increase its yield strength.

Magnets with a normal metal conductor, that operate at cryogenic temperatures to achieve higher electrical conductivity, have also been constructed. Currently, the design of the Burning Plasma Experiment (BPX) at the Princeton Plasma Physics Laboratory includes the use of a higher-strength beryllium-copper conductor. The beryllium-copper system, through carefully controlled thermomechanical processing to achieve optimum precipitation conditions, offers exceptional high-strength, high-conductivity alloys. Both strength and electrical conductivity of copper alloys increase at low temperatures. The high-field BPX magnets are designed to operate using liquid nitrogen as the coolant, as opposed to liquid helium that is required for all current superconducting magnets.

Traditionally, copper tubes and sheets have been used in heat transfer and thermal stability equipment at cryogenic temperatures. The high thermal conductivity, combined with good soldering and brazing characteristics, has made their use in refrigeration and transfer-line equipment very appropriate and resulted in efficient devices. Copper is used as the inner container in many 50 and 100 liter storage Dewars for liquid helium, hydrogen, and nitrogen. In this application, copper provides excellent thermal stability and its fabricability serves to keep production costs low. Copper alloys, especially the brasses and bronzes, are used in structural applications that require reasonable strength, thermal conductivity, and, sometimes, brazed or soldered joints. Copper and copper alloys, as opposed to aluminum and steels, are easily formed and joined and have intermediate elastic, strength, and toughness properties but lower strength-to-weight ratios.

The increased use of Nb_3Sn superconductors has placed more emphasis on knowledge of the low-temperature properties of copper-tin alloys. Usually, the reaction treatment to form Nb_3Sn includes the use of a bronze to provide the source of tin for the process. The final products of the (in situ) reaction include copper, copper-tin, and Nb_3Sn. Knowledge of the thermal, electrical, and mechanical properties of the bronze alloy system permit better analysis of the stabilizer/superconductor system.

Unlike most metals and alloys, copper and its alloys are used in applications where excellent thermal and electrical conductivity, combined with optimum strength and toughness, are both required. While the use of other commonly used alloys at cryogenic temperatures, such as austenitic stainless steels or superconductors, demands either excellent strength or conductivity, copper alloys supply both requirements. Unfortunately, nature usually resists the combined achievement of high strength and high conductivity. However, there is opportunity (supported by many applications) for further development of copper thermomechanical processing and alloying to optimize strength and conductivity.

GENERAL PROPERTIES OF COPPER

Copper and the copper alloys covered in this monograph are widely used because of their excellent electrical and thermal conductivities, good fabricability, adequate strength, and excellent toughness and fatigue resistance. They can be easily soldered, brazed, and welded. Copper alloys are normally strengthened by cold work (copper), solid-solution alloying (Cu-Sn alloys), or precipitation (Cu-Be alloys). At low temperatures the increase of strength from these mechanisms is significantly greater than at room temperature. In all cases, at constant temperature, increased strength leads to decreased electrical conductivity. Thus, in applications such as high-field, normal metal magnets, there is always a trade-off between conductivity, strength, and operating temperature.

Selected properties and characteristics of copper are contained in Table 1.1 (Source for data: References 1.1–1.5). Some rather specific electronic characteristics are included, since the primary use of copper at cryogenic temperatures is as an electrical conductor.

Crystallographic features of copper are summarized in Table 1.2 (References 1.1 and 1.6). The face-centered cubic structure leads to good ductility and excellent toughness at cryogenic temperatures. The distance of closest atomic approach in face-centered cubic alloys is along <110> directions on {111} planes.

In comparison to properties of many other elements, the properties of copper are well known and have been studied for over 50 years.

OTHER INFORMATION ABOUT COPPER AND COPPER ALLOYS

Copper and copper alloys have played a major role in the development of civilization (References 1.7–1.9). The first metal used by man, some 10,000 years ago, was copper, probably as a substitute for stone for tools and utensils. About three to six millennia ago, the extensive use of copper and copper-arsenic alloys led to the use of the terms "copper age," followed by the "bronze age," as civilization progressed. The development of high-temperature clay kilns permitted the smelting of copper. Primitive copper metallurgy spread from Egypt (where copper was mined and refined on the Sinai Peninsula as early as 3800 B.C.) to Crete and Cyprus and, subsequently, to much of the Roman Empire. The alloys processed in these early times had high arsenic contents, and there is evidence that the

Table 1.1. General Properties of Copper.

Atomic Number	29
Atomic Weight	63.546
Atomic Diameter	2.551×10^{-10} m
Melting Point	1356 K
Boiling Point	2868 K
Density at 293 K	8.94×10^{3} kg/m^{3}
Electronic Structure	$3d^{10}4s$
Valence States	2,1
Fermi Energy	7.0 eV
Fermi Surface	spherical, necks at [111]
Hall Coefficient	-5.12×10^{-11} m^{3}/(A•S)
Magnetic State	diamagnetic
Heat of Fusion	134 J/g
Heat of Vaporization	3630 J/g
Heat of Sublimation @1299 K	3730 J/g

Table 1.2. Crystallographic Features of Copper.

Type of Structure	A1
Space Group	O_h^5 - Fm3m
Crystal Structure	face-centered cubic
Number of Atoms per Unit Cell	4
Lattice Parameters at 293 K	3.6147×10^{-10} m
Distance of Closest Atomic Approach (Burgers vector) at 293 K	2.556×10^{-10} m
Goldschmidt Atomic Radii (12-fold coordination)	1.28×10^{-10} m
Atomic Volume	$1.182\ 10^{-29}$ m^{3}

mineral algodonite (Cu_8As) was deliberately added to copper to obtain greater hardness. The later use of tin alloying led to more controlled alloy properties and to the bronze age. The bronze age is judged to conclude with the introduction of iron alloys (iron age) in about 1500 B.C.

It was not until the 20th century, however, that property measurements at cryogenic temperatures were conducted on copper. Perhaps the earliest report of mechanical property testing was the 1922 work of Guillet and Cournot (Reference 1.10) who studied the hardness and impact resistance of copper and brass at room temperature, liquid air, and several intermediate temperatures. As early as 1907, Dorsey (Reference 1.11) had studied the thermal expansion of copper at temperatures ranging from room to liquid air.

Sources of compilations or reviews of the properties of copper at low temperatures are rare. Reed and Mikesell (Reference 1.12) compiled the mechanical properties of selected coppers and copper alloys (brasses, bronzes, aluminum bronzes, and cupronickel alloys) at cryogenic temperatures in 1967. A section in the Handbook on Materials for Superconducting Machinery (1977) (Reference 1.13) is devoted to copper alloys. The physical properties of copper at low temperatures have been compiled by Touloukian (1967) (Reference 1.2). Earlier, Wilkins and Bunn (Reference 1.14) prepared a compilation of mechanical properties, at room temperature and above, that includes copper, beryllium coppers, and tin bronzes. Their book contains a comprehensive reference list of early mechanical-property papers, from about 1910 to the 1930's. Recently, Thompson, et al. (Reference 1.15) have prepared a wall chart with important low temperature properties of copper.

There are excellent general discussions of the uses, fabrication, product forms, and room-temperature properties of copper and copper alloys. We describe several here. The Copper Development Association supplies a series of Standards Handbooks for Wrought and Cast Copper and Copper Alloy Products, Reference 1.16. This series is a very useful reference source for current standards and is an aid for specifications. Parts of this series include tolerances, wrought-product alloy data, terminology, engineering data, sources, specification cross index, and cast-product alloy data. The American Society for Metals has prepared an excellent Source Book on Copper and Copper Alloys (Reference 1.3) with many contributions from experts in selected areas. These include metallurgy, processing, fabrication, and properties and designations. Welding and soldering are addressed by papers contained in this book but more extensively in the ASM Metals Handbook on Welding and Brazing, Reference 1.17.

Research on copper and copper alloys, emphasizing thermodynamic data and processes and binary and ternary phase diagrams, has long been encouraged by the International Copper Research Association (INCRA), which began a Monograph Series in 1971, Reference 1.18. Since then, a series of review papers has been released by INCRA, now ICA, Ltd. (International Copper Association, Ltd.). A recent general book on copper and copper-alloy manufacturing, properties, and uses has been edited by Mendenhall (1986), Reference 1.19. Butts presented extensive discussion of copper and copper alloy metallurgical practices and property characteristics in a 1964 publication, Reference 1.20.

JOINING

Copper and copper alloys can be easily welded, brazed, and soldered. The ASM Source Book on Copper and Copper Alloys (1979) (Reference 1.3), Metals Handbook on Welding and Brazing (Reference 1.17), and Butts (Reference 1.20) have good discussions of copper joining techniques. Welding of pure copper is dependent on oxygen concentration. Deoxidized and oxygen-free pure coppers are joined using both gas and arc welding. The high conductivity of pure copper requires high heat inputs and, for thick sections, preheating may be necessary. Oxygen segregates to form oxides at grain boundaries during welding; therefore, there is difficulty in obtaining sound welds of coppers that contain oxygen. Welding rods that contain no oxygen are also used. The commonly used welding techniques for copper are inert-gas metal arc (MIG) and inert-gas tungsten arc (TIG). The TIG process, capable of producing higher deposit rates, is usually used on thick sections. Copper is readily brazed using copper-silver or copper-phosphorus filter metals and easily soldered using lead-tin solder. Most copper alloys can be welded using shielded metal arc, inert-gas tungsten arc, inert-gas metal arc (He or Ar), and submerged arc. Some alloys (including Cu-Sn) are "hot-short"; therefore, overheating and preheating should be avoided and low interpass temperatures maintained in these alloys.

MONOGRAPH CONTENTS

The objective of this monograph is to provide a handbook of critically evaluated data on those coppers and copper alloys that are most used in applications at cryogenic temperatures. Handbook data that are critically evaluated provide a basis for decisions on design allowables, or alternatively, identify requirements for more characterization of existing materials or development of new materials. They provide guidance for material procurement specifications, since many key properties at low temperatures are strongly influenced by chemical and metallurgical differences within standard specifications. Critical data evaluation provided in handbook pages or other formats forms the basis for decisions on material selection and for comparison of data obtained at different international laboratories on competing materials.

Tensile, toughness, fatigue, creep, elastic-constant, thermal, and electromagnetic properties are covered. Materials include C10100–C10700 coppers, C17000–C17510 beryllium coppers, and C50500–C52400 phosphor bronzes. Commercially available Cu-Sn alloys are known as phosphor bronzes and are so designated in this monograph. Phosphor is added to the commercial alloy as a deoxidant. Composition ranges for these materials are given in Tables 1.3–1.5. To identify the materials in this monograph, we have used the UNS designation for the wrought alloys; composition ranges for the cast alloys are also included in Tables 1.3–1.5. Tables 1.6–1.16 summarize other information on these materials, including typical uses, forms and tempers, and fabrication. Table 1.17 gives standard temper designations for copper alloy flat stock and temper equivalents for rolled and drawn product. The temperature range for this monograph is liquid helium (4 K) to room temperature. (Data reported at "room temperature" were considered as obtained at 295 K.)

All data used in this monograph were obtained from original, documented literature, rather than from surveys, handbooks, or other incompletely documented sources. In contrast to earlier handbooks, all original data upon which design curves and equations are based are presented as well as much more extensive characterization information on the test specimens, measurement techniques, and thermomechanical treatment. (The UNS specification given in the characterization tables is the closest that could be determined from the composition information presented in the document from which data were taken.) Data are usually presented as a function of temperature, both in plots of individual data points and as plots where data scatter bands are included. The data scatter bands represent, statistically, plus and minus two standard deviations (S.D.s). Emphasis has been placed on identifying the effects of chemistry and material-processing parameters such as cold work, grain size, aging temperature, and alloy composition, since these effects are more prominent at very low temperatures. Linear and nonlinear regression analyses are used to quantify the dependencies of specific properties on these variables. Where sufficient data are available, the dependence of mechanical and physical properties upon such parameters is presented in the handbook pages with model equations and graphs.

With few exceptions, all low-temperature data for the specific alloys and properties are included in the critical review. However, not all room-temperature data are included. Papers and reports that contain room-temperature data, but no low-temperature data, were in general not included. In some cases, data are included if a significant metallurgical variable, such as grain size or cold work, was systematically varied and the property was measured at room temperature.

Almost all data analyses are unique to this critical review, a practice that ensures self-consistency and originality. The only exceptions are two comprehensive analyses of cryogenic copper thermal conductivity and electrical resistivity, recently completed at NIST [Equations (7-2) and (8-1)]. Except for these analyses, which employed a combination of techniques, all interpretations of data presented are relatively straightfor-

Table 1.3. Composition of Oxygen-free Copper in Wrought and Cast Form (percent maximum and composition values in weight percent unless otherwise indicated). From Reference 1.21.

WROUGHT ALLOYS

				Ag						
ALLOY NO.	DESIG-NATION	DESCRIPTION	Cu (Incl. Ag) (% Min)	% Min	Troy Oz Min	As	Sb	P	Te	OTHER NAMED ELEMENTS
C10100	OFE	Oxygen Free Electronic	99.99 (a)	—	—	0.0005	0.0004	0.0003	0.0010	(b)
C10200 (c)	OF	Oxygen Free	99.95	—	—	—	—	—	—	—
C10300	OFXLP		99.95 (d)	—	—	—	—	0.001–0.005	—	—
C10400 (c)	OFS	Oxygen Free with Ag	99.95	0.027	8	—	—	—	—	—
C10500 (c)	OFS	Oxygen Free with Ag	99.95	0.034	10	—	—	—	—	—
C10700	OFS	Oxygen Free with Ag	99.95	0.085	25	—	—	—	—	—

(a) Copper is determined by the difference of impurity total from 100%.
(b) Bi, max., 1 ppm (0.0001%); Cd, max., 1 ppm (0.001%), Fe, max., 10 ppm (0.0010%); Pb, max., 5 ppm (0.0005%); Mn, max., 0.5 ppm (0.00005%); Hg, max., 1 ppm (0.00001%); Ni, max., 10 ppm (0.0010%); Oxygen, max., 5 ppm (0.0005%); Se. max., 3 ppm (0.0003%); Ag, max., 25 ppm (0.0025%); S, max., 15 ppm (0.0015%); Sn, max., 2 ppm (0.0002%); Zn, max., 1 ppm (0.0001%). Hg, max., 1 ppm (0.0001%); Zn, max., 1 ppm (0.0001%).
(c) These are high conductivity coppers which have in the annealed condition a minimum conductivity of 100% IACS.
(d) Includes P.

CAST ALLOYS

		Ag			
ALLOY NO.	Cu (incl. Ag) (% min.)	% min	Troy Oz min	B	P
C80100	99.95	—	—	—	—
C80300	99.95	0.034	10	—	—
C80500	99.75	0.034	10	0.02	—
C80700	99.75	—	—	0.02	—
C80300	99.70	0.034	10	—	—
C81100	99.70	—	—	—	—
C81200	99.9	—	—	—	0.045–0.065

Table 1.4. Composition of Beryllium-Copper Alloys in Wrought and Cast Form in Weight Percent (percent maximum unless shown as a range or minimum). From Reference 1.21.

WROUGHT ALLOYS

ALLOY NO.	PREVIOUS TRADE NAME	Cu (incl. Ag)	Fe	Ni	Co	Si	Be	Pb	OTHER NAMED ELEMENTS
C17000	Beryllium Copper	Rem. (a)	(b)	(b)	(b)	0.20	1.60–1.79	—	0.20% Al
C17200	Beryllium Copper	Rem. (a)	(b)	(b)	(b)	0.20	1.80–2.00	—	0.20% Al
C17300	Beryllium Copper	Rem. (a)	(b)	(b)	(b)	0.20	1.80–2.00	0.20–0.6	0.20% Al
C17400		Rem. (a)	0.20	—	0.15–0.35	0.20	0.15–0.50	—	0.20% Al
C17410		Rem. (a)	0.20	—	0.35–0.6	0.20	0.15–0.50	—	0.20% Al
C17420		Rem. (a)	0.20	—	0.05–0.6	0.20	0.05–0.15	—	0.20% Al
C17500	Beryllium Copper	Rem. (a)	0.10	—	2.4–2.7	0.20	0.40–0.7	—	0.20% Al
C17510		Rem. (a)	0.10	1.4–2.2	0.30	0.20	0.20–0.6	—	0.20% Al

(a) Cu + sum of named elements = 99.5% min.
(b) Ni + Co, 0.20% min.; Ni + Fe + Co, 0.6% max.

CAST ALLOYS

ALLOY NO.	Cu	Ag	Be	Co	Si	Ni	Fe	Al	Sn	Pb	Zn	Cr
C81700	94.2 min.	0.8–1.2	0.30–0.55	0.25–1.5	—	0.25–1.5	—	—	—	—	—	—
C81800	95.6 min.	0.8–1.2	0.30–0.55	1.4–1.7	—	—	—	—	—	—	—	—
C82000	95.0 min.	—	0.45–0.8	2.4–2.7 (a)	0.15	0.20	0.10	0.10	0.10	0.02	0.10	0.10
C82100	95.5 min.	—	0.35–0.8	0.25–1.5	—	0.25–1.5	—	—	—	—	—	—
C82200	96.5 min.	—	0.35–0.8	—	—	1.0–2.0	—	—	—	—	—	—
C82400	96.4 min.	—	1.65–1.75	0.20–0.40	—	0.10	0.20	0.10	0.10	0.02	0.10	0.10
C82500	95.5 min.	—	1.90–2.15	0.35–0.7 (a)	0.20–0.35	0.20	0.25	0.10	0.10	0.02	0.10	0.10
C82510	95.5 min.	—	1.90–2.15	1.0–1.2	0.20–0.35	0.20	0.25	0.10	0.10	0.02	0.10	0.10
C82600	95.2 min	—	2.25–2.45	0.35–0.7	0.20–0.35	0.20	0.25	0.10	0.10	0.02	0.10	0.10
C82700	94.6 min.	—	2.35–2.55	—	0.15	1.0–1.5	0.25	0.15	0.10	0.02	0.10	0.10
C82800	94.8 min.	—	2.50–2.75	0.35–0.7 (a)	0.20–0.35	0.20	0.25	0.15	0.10	0.02	0.10	0.10

(a) Ni + Co

Table 1.5. Composition of Phosphor Bronzes in Wrought and Cast Form in Weight Percent (percent maximum unless shown as a range or minimum). From Reference 1.21.

WROUGHT ALLOYS

ALLOY NO.	PREVIOUS TRADE NAME	Cu (a)	Pb	Fe	Sn	Zn	P	OTHER NAMED ELEMENTS
C50100		Rem.	0.05	0.05	0.050–0.8	—	0.01–0.05	—
C50200		Rem.	0.05	0.10	1.0–1.5	—	0.04	—
C50500	Phosphor Bronze, 1.25% E	Rem.	0.05	0.10	1.0–1.7	0.30	0.03–0.35	—
C50700		Rem.	0.05	0.10	1.5–2.0	—	0.30	—
C50710		Rem.	—	—	1.7–2.3	—	0.15	0.10–0.40% Ni
C50715		Rem.	0.02	0.05–0.15	1.7–2.3	—	0.025–0.04	(b)
C50800		Rem.	0.05	0.10	2.6–3.4	—	0.01–0.07	—
C50900		Rem.	0.05	0.10	2.5–3.8	0.30	0.03–0.30	—
C51000	Phosphor Bronze, 5% A	Rem.	0.05	0.10	4.2–5.8	0.30	0.03–0.35	—
C51100		Rem.	0.05	0.10	3.5–4.9	0.30	0.03–0.35	—
C51800	Phosphor Bronze	Rem.	0.02	—	4.0–6.0	—	0.10–0.35	0.01% Al
C51900		Rem.	0.05	0.10	5.0–7.0	0.30	0.03–0.35	—
C52100	Phosphor Bronze, 8% C	Rem.	0.05	0.10	7.0–9.0	0.20	0.03–0.35	—
C52400	Phosphor Bronze, 10% D	Rem.	0.05	0.10	9.0–11.0	0.20	0.03–0.35	—

(a) Cu + sum of named elements = 99.5% min.
(b) Cu + Sn + Fe + P = 99.5% min.

CAST ALLOYS

ALLOY NO.	Cu (a)	Sn	Pb	Zn	Fe	Sb	Ni (a) (incl. Co)	S	P (a)	Al	Si	Mn
C90200	91.0–94.0 (b)	6.0–8.0	0.30	0.50	0.20	0.20	0.50	0.05	0.05	0.005	0.005	—
C90250	89.0–91.0 (b)	9.0–11.0	0.30	0.50	0.25	0.20	0.8	0.05	0.05	0.005	0.005	0.10
C90300	86.0–89.0 (b)	7.5–9.0	0.30	3.0–5.0	0.20	0.20	1.0	0.05	0.05	0.005	0.005	—
C90500	86.0–89.0 (c)	9.0–11.0	0.30	1.0–3.0	0.20	0.20	1.0	0.05	0.05	0.005	0.005	—
C90700	88.0–90.0 (b)	10.0–12.0	0.50	0.50	0.15	0.20	0.50	0.05	0.30	0.005	0.005	—

(a) In determining copper minimum, copper may be calculated as Cu + Ni.
(b) Cu + sum of named elements = 99.4% min.
(c) Cu + sum of named elements = 99.7% min.

Table 1.6. Nominal Composition, ASTM Specification for Forms, Commonly Used Forms and Tempers, Typical Uses, and Fabrication Processes and Properties for C10100. From Reference 16, with permission.

Composition – percent

	Nominal	Minimum	Maximum
Copper (incl Silver)	....	99.99	....
Residual Deoxidants	....	None	
Phosphorus	....	....	.0003
Tellurium	....	....	.0010
Other Named Elements	....	....	....

* The total of the seven following elements, Se, Te, Bi, As, Sb, Sn and Mn not to exceed 40 ppm, (.0040%); Hg, max., 1 ppm, (.0001%); Zn, max., 1 ppm, (.0001%); Cd, max., 1 ppm, (.0001%); S, max., 18 ppm, (.0018%); Pb, max., 10 ppm, (.0010%); Se, max., 10 ppm (.0010%); Bi, max., 10 ppm (.0010%); Oxygen max., 10 ppm, (.0010%).

Nearest Applicable A S T M Specifications

Flat Products	B48, B133, B152, B187 B272, B432, B451, F68
Pipe	B42, B188, F68
Rod	B49, B133 B187, F68
Shapes	B133 B187, F68
Tube	B68, B75, B188, B280 B372, B447, B641, F68
Wire	B1, B2, B3, B33, B48 B189, B246, B272 B298, B3[illegible]

Forms and Tempers Most Commonly Used

		Annealed Tempers: Nominal Grain Size mm .100 (OS100)	.070 (OS070)	.050 (OS050)	.035 (OS035)	.025 (OS025)	.015 (OS015)	Soft Anneal (O60)	Light Anneal (O50)	Rolled or Drawn Tempers: Eighth Hard (H00)	Quarter Hard (H01)	Half Hard (H02)	Three Quarter Hard (H03)	Hard (H04)	Extra Hard (H06)	Spring (H08)	Extra Spring (H10)	Drawn – General Purpose (H58)	Hard Drawn (H80)	Light Drawn – Bending (H55)	Hot Finished Tempers: As Hot Rolled (M20)	As Extruded (M30)	Special Tempers
FLAT PRODUCTS	Strip, Rolled			●		●		●		●	●	●		●		●	●				●		
	Strip, Drawn							●						●									
	Flat Wire, Rolled							●						●									
	Flat Wire, Drawn							●						●	●								
	Bar, Rolled							●			●			●	●						●		
	Bar, Drawn							●			●			●	●								
	Sheet							●		●		●									●		
	Plate									●											●		
ROD				●				●						●		●					●	●	
WIRE				●				●		●	●			●		●							
TUBE				●		●		●										●	●	●			
PIPE																		●					
SHAPES				●				●						●							●	●	

DRAWN–GENERAL PURPOSE (H58) temper is used for general purpose tube only, usually where there is no real requirement for high strength or hardness on the one hand or for bending qualities on the other.

HARD DRAWN (H80) temper is used only where there is need for a tube as hard or as strong as is commercially feasible for the size in question.

LIGHT DRAWN–BENDING (H55) temper is used only where a tube of some stiffness, but yet capable of readily being bent (or otherwise moderately cold worked) is needed.

Typical Uses

ELECTRICAL AND ELECTRONIC: bus bars, bus conductors and other conductors, wave guides, hollow conductors, lead-in wires and anodes for vacuum tubes, vacuum seals, transistor components, glass to metal seals, coaxial cables and coaxial tubes, klystrons, micro-wave tubes, automotive rectifiers

Common Fabrication Processes

Blanking, coining, coppersmithing, drawing, etching, forming and bending, heading and upsetting, hot forging and pressing, piercing and punching, roll threading and knurling, shearing, spinning, squeezing and swaging, stamping

Fabrication Properties

Capacity for Being Cold Worked .... Excellent
Capacity for Being Hot Formed .... Excellent
Hot Forgeability Rating (Forging Brass = 100) 65
Hot Working Temperature ..... 1400-1600 F or 750-875 C
Annealing Temperature .... 700-1200 F or 375-650 C
Machinability Rating (Free Cutting Brass = 100) 20

Suitability for being joined by:

Soldering		Excellent
Brazing		Excellent
Oxyacetylene Welding		Fair
Gas Shielded Arc Welding		Good
Coated Metal Arc Welding		Not Recommended
Resistance Welding	Spot	Not Recommended
	Seam	Not Recommended
	Butt	Good

Table 1.7. Nominal Composition, ASTM Specification for Forms, Commonly Used Forms and Tempers, Typical Uses, and Fabrication Processes and Properties for C10200. From Reference 1.16, with permission.

Composition – percent

	Nominal	Minimum	Maximum
Copper (incl. Silver)	....	99.95	....
Residual Deoxidants	....	None	

Nearest Applicable A S T M Specifications

Flat Products	B48, B133, B152, B187, B272, B370, B432, B451, B506
Pipe	B42, B188
Rod	B49, B124, B133, B187
Shapes	B133, B187
Tube	B68, B75, B88, B111, B188, B280, B359, B372, B395, B447, B640, B641
Wire	B1, B2, B3, B33, B47, B48, B49, B116, B189, B246, B286, B298, B355, B566, F9
Nipples	B687

Forms and Tempers Most Commonly Used

	Annealed Tempers: Nominal Grain Size mm .100 (OS100)	.070 (OS070)	.050 (OS050)	.035 (OS035)	.025 (OS025)	.015 (OS015)	Soft Anneal (O60)	Light Anneal (O50)	Rolled or Drawn Tempers: Eighth Hard (H00)	Quarter Hard (H01)	Half Hard (H02)	Three Quarter Hard (H03)	Hard (H04)	Extra Hard (H06)	Spring (H08)	Extra Spring (H10)	Drawn – General Purpose (H58)	Hard Drawn (H80)	Light Drawn – Bending (H55)	Hot Finished Tempers: As Hot Rolled (M20)	As Extruded (M30)	Special Tempers
FLAT PRODUCTS: Strip, Rolled			●		●		●		●	●	●		●		●	●				●		
FLAT PRODUCTS: Strip, Drawn							●						●									
FLAT PRODUCTS: Flat Wire, Rolled							●						●									
FLAT PRODUCTS: Flat Wire, Drawn							●						●	●								
FLAT PRODUCTS: Bar, Rolled							●			●			●	●						●		
FLAT PRODUCTS: Bar, Drawn							●			●			●	●								
FLAT PRODUCTS: Sheet							●		●		●									●		
FLAT PRODUCTS: Plate									●											●		
ROD			●				●						●		●							
WIRE			●				●		●	●			●		●							
TUBE			●		●		●											●	●			
PIPE																	●					
SHAPES			●				●						●							●	●	

DRAWN–GENERAL PURPOSE (H58) temper is used for general purpose tube only, usually where there is no real requirement for high strength or hardness on the one hand or for bending qualities on the other.

HARD DRAWN (H80) temper is used only where there is need for a tube as hard or as strong as is commercially feasible for the size in question.

LIGHT DRAWN–BENDING (H55) temper is used only where a tube of some stiffness, but yet capable of readily being bent (or otherwise moderately cold worked) is needed.

Typical Uses

ELECTRICAL: bus bars and bus conductors, and other electrical conductors, wave guides, copper to glass seals in electronic appliances

Common Fabrication Processes

Blanking, coining, coppersmithing, drawing, etching, forming and bending, heading and upsetting, hot forging and pressing, piercing and punching, roll threading and knurling, shearing, spinning, squeezing and swaging, stamping

Fabrication Properties

Capacity for Being Cold Worked	Excellent
Capacity for Being Hot Formed	Excellent
Hot Forgeability Rating (Forging Brass = 100)	65
Hot Working Temperature	1400-1600 F or 750-875 C
Annealing Temperature	700-1200 F or 375-650 C
Machinability Rating (Free Cutting Brass = 100)	20

Suitability for being joined by:

Soldering	Excellent
Brazing	Excellent
Oxyacetylene Welding	Fair
Gas Shielded Arc Welding	Good
Coated Metal Arc Welding	Not Recommended
Resistance Welding – Spot	Not Recommended
Resistance Welding – Seam	Not Recommended
Resistance Welding – Butt	Good

Table 1.8. Nominal Composition, ASTM Specification for Forms, Commonly Used Forms and Tempers, Typical Uses, and Fabrication Processes and Properties for C10400, C10500, and C10700. From Reference 1.16, with permission.

Composition – percent

	Nominal	Minimum	Maximum
Copper (incl. Silver)	....	99.95	....
Silver*			
No. C10400	....	.027(8)	....
No. C10500	....	.034(10)	....
No. C10700	....	.085(25)	....

* Figures in parentheses are troy ounces per avoirdupois ton.

Nearest Applicable A S T M Specifications

Flat Products	B48, B133, B152, B187, B272, B506
Pipe	B42, B188
Rod	B49, B133, B187
Shapes	B133, B187
Tube	B68, B75, B188, B280, B372
Wire	B1, B2, B3, B48, B49, B246, B272, B298, B355

Forms and Tempers Most Commonly Used

	Annealed Tempers – Nominal Grain Size mm: .100 (OS100)	.070 (OS070)	.050 (OS050)	.035 (OS035)	.025 (OS025)	.015 (OS015)	Soft Anneal (O60)	Light Anneal (O50)	Rolled or Drawn Tempers: Eighth Hard (H00)	Quarter Hard (H01)	Half Hard (H02)	Three Quarter Hard (H03)	Hard (H04)	Extra Hard (H06)	Spring (H08)	Extra Spring (H10)	Drawn – General Purpose (H58)	Hard Drawn (H80)	Light Drawn – Bending (H55)	Hot Finished Tempers: As Hot Rolled (M20)	As Extruded (M30)	Special Tempers
FLAT PRODUCTS: Strip, Rolled							●		●	●	●		●		●	●				●		
FLAT PRODUCTS: Strip, Drawn							●						●									
FLAT PRODUCTS: Flat Wire, Rolled							●						●									
FLAT PRODUCTS: Flat Wire, Drawn							●						●	●								
FLAT PRODUCTS: Bar, Rolled							●			●			●	●						●		
FLAT PRODUCTS: Bar, Drawn							●			●			●	●								
FLAT PRODUCTS: Sheet							●		●		●									●		
FLAT PRODUCTS: Plate									●											●		
ROD													●							●		
WIRE							●		●	●			●		●							
TUBE																						
PIPE																						
SHAPES							●						●							●	●	

DRAWN–GENERAL PURPOSE (H58) temper is used for general purpose tube only, usually where there is no real requirement for high strength or hardness on the one hand or for bending qualities on the other.

HARD DRAWN (H80) temper is used only where there is need for a tube as hard or as strong as is commercially feasible for the size in question.

LIGHT DRAWN–BENDING (H55) temper is used only where a tube of some stiffness, but yet capable of readily being bent (or otherwise moderately cold worked) is needed.

Typical Uses

AUTOMOTIVE: gaskets, radiators

ELECTRICAL: bus bars, conductivity wire, contacts, radio parts, windings, switches, terminals, commutator segments

MISCELLANEOUS: chemical process equipment, printing rolls, clad metals, printed circuit foil; also where brazing in a hydrogen atmosphere

Common Fabrication Processes

Blanking, coining, coppersmithing, drawing, etching, forming and bending, heading and upsetting, hot forging and pressing, piercing and punching, roll threading and knurling, shearing, spinning, squeezing and swaging, stamping

Fabrication Properties

Capacity for Being Cold Worked .... Excellent
Capacity for Being Hot Formed .... Excellent
Hot Forgeability Rating (Forging Brass = 100) 65
Hot Working Temperature .. 1400 - 1600 F or 750-875 C
Annealing Temperature ..... 900 - 1400 F or 475-750 C
Machinability Rating (Free Cutting Brass = 100) 20

Suitability for being joined by:

Soldering .... Excellent
Brazing .... Excellent
Oxyacetylene Welding .... Fair
Gas Shielded Arc Welding .... Good
Coated Metal Arc Welding ...... Not Recommended
Resistance Welding: Spot .... Not Recommended
Resistance Welding: Seam .... Not Recommended
Resistance Welding: Butt .... Good

Table 1.9. Nominal Composition, ASTM Specification for Forms, Commonly Used Forms and Tempers, Typical Uses, and Fabrication Processes and Properties for C17000. From Reference 1.16, with permission.

Composition – percent

	Nominal	Minimum	Maximum
Copper (incl. silver)	98.3	Rem.	
Beryllium	1.7	1.60	1.79
Nickel + Cobalt	....	.20	....
Ni + Fe + Co	....	....	.6
Silicon	....	....	.20

Nearest Applicable A S T M Specifications

Forgings	B570
Flat Products	B194, B196
Pipe	
Rod	B196
Shapes	B570
Tube	
Wire	

Forms and Tempers Most Commonly Used

		Annealed Tempers (Nominal Grain Size mm)								Rolled or Drawn Tempers											Hot Finished Tempers		
		.100 (OS100)	.070 (OS070)	.050 (OS050)	.035 (OS035)	.025 (OS025)	.015 (OS015)	Soft Anneal (O60)	Light Anneal (O50)	Eighth Hard (H00)	Quarter Hard (H01)	Half Hard (H02)	Three Quarter Hard (H03)	Hard (H04)	Extra Hard (H06)	Spring (H08)	Extra Spring (H10)	Drawn – General Purpose (H58)	Hard Drawn (H80)	Light Drawn – Bending (H55)	As Hot Rolled (M20)	As Extruded (M30)	Special Tempers
FLAT PRODUCTS	Strip, Rolled							●			●	●		●				●					
	Strip, Drawn																						
	Flat Wire, Rolled																						
	Flat Wire, Drawn																						
	Bar, Rolled																						
	Bar, Drawn																						
	Sheet																						
	Plate																						
ROD								●						●									
WIRE																							
TUBE																							
PIPE																							
SHAPES																						●	

DRAWN–GENERAL PURPOSE (H58) temper is used for general purpose tube only, usually where there is no real requirement for high strength or hardness on the one hand or for bending qualities on the other.

HARD DRAWN (H80) temper is used only where there is need for a tube as hard or as strong as is commercially feasible for the size in question.

LIGHT DRAWN–BENDING (H55) temper is used only where a tube of some stiffness, hut yet capable of readily heing bent (or otherwise moderately cold worked) is needed.

4. Solution heat treated.

5. Special mill processing and precipitation treatment.

Typical Uses

HARDWARE: bellows, bourdon tubing, diaphragms, fuse clips, fasteners, lock washers, springs, switch parts, relay parts, electrical and electronic connectors, retaining rings, roll pins

INDUSTRIAL: valves, pump parts, spline shafts, rolling mill parts, welding equipment

Common Fabrication Processes

Blanking, drawing, forming and bending, turning, drilling, tapping

Fabrication Properties

Capacity for Being Cold Worked	Excellent
Capacity for Being Hot Formed	Good
Hot Forgeability Rating (Forging Brass = 100)	
Hot Working Temperature	1200-1500 F or 650-825 C
Annealing Temperature	1425-1475 F or 775-800 C
Machinability Rating (Free Cutting Brass = 100)	20

Suitability for being joined by

Soldering		Good
Brazing		Good
Oxyacetylene Welding		Not Recommended
Gas Shielded Arc Welding		Good
Coated Metal Arc Welding		Good
Resistance Welding	Spot	Good
	Seam	Fair
	Butt	Fair

Table 1.10. Nominal Composition, ASTM Specification for Forms, Commonly Used Forms and Tempers, Typical Uses, and Fabrication Processes and Properties for C17200 and C17300. From Reference 1.16, with permission.

Composition – percent

	Alloy No. C17200			Alloy No. C17300		
	Nom.	Min.	Max.	Nom.	Min.	Max.
Copper	98.1			97.7		
Beryllium	1.9	1.80	2.00	1.9	1.80	2.00
Lead	....	....	....	.40	.20	.6
Nickel + Cobalt	....	.20	....	....	.20	....
Ni + Fe + Co	....	....	.6	....	....	.6
Silicon	....	....	.20	....	....	.20
Aluminum	....	....	.20	....	....	.20

Nearest Applicable A S T M Specifications

	Copper Alloy No. C17200	Copper Alloy No. C17300
Forgings	B570	
Flat Products	B194, B196	B196
Pipe		
Rod	B196	B196
Shapes	B570	
Tube	B643	
Wire	B197	

Forms and Tempers Most Commonly Used

		Annealed Tempers (Nominal Grain Size mm)								Rolled or Drawn Tempers											Hot Finished Tempers		
		.100 (OS100)	.070 (OS070)	.050 (OS050)	.035 (OS035)	.025 (OS025)	.015 (OS015)	Soft Anneal (O80)	Light Anneal (O50)	Eighth Hard (H00)	Quarter Hard (H01)	Half Hard (H02)	Three Quarter Hard (H03)	Hard (H04)	Extra Hard (H06)	Spring (H08)	Extra Spring (H10)	Drawn – General Purpose (H58)	Hard Drawn (H80)	Light Drawn – Bending (H55)	As Hot Rolled (M20)	As Extruded (M30)	Special Tempers
FLAT PRODUCTS	Strip, Rolled							●			●	●	●	●			●						
	Strip, Drawn																						
	Flat Wire, Rolled																						
	Flat Wire, Drawn																						
	Bar, Rolled							●				●											
	Bar, Drawn							●				●											
	Sheet																						
	Plate							●															
ROD								●						●									
WIRE								●			●	●	●	●									
TUBE								●										●					
PIPE																							
SHAPES								●															

DRAWN–GENERAL PURPOSE (H58) temper is used for general purpose tube only, usually where there is no real requirement for high strength or hardness on the one hand or for bending qualities on the other.

HARD DRAWN (H80) temper is used only where there is need for a tube as hard or as strong as is commercially feasible for the size in question.

LIGHT DRAWN–BENDING (H55) temper is used only where a tube of some stiffness, but yet capable of readily being bent (or otherwise moderately cold worked) is needed.

4. Solution Heat Treated.

5. Special Mill Processing and Precipitation Treatment.

Typical Uses

HARDWARE: Bellows, bourdon tubing, diaphragms, fuse clips, fasteners, lock washers, springs, switch parts, relay parts, electrical and electronic components, retaining rings, roll pins

INDUSTRIAL: Valves, pump parts, spline shafts, rolling mill parts, welding equipment

Common Fabrication Processes

Blanking, drawing, forming and bending, turning, drilling, tapping

Fabrication Properties

Capacity for Being Cold Worked .... Excellent
Capacity for Being Hot Formed .... Good
Hot Forgeability Rating (Forging Brass = 100)
- Copper Alloy No. 172 40
- Copper Alloy No. 173 .... Not Recommended

Hot Working Temperature ...... 1200-1500 F or 650-825 C
Annealing Temperature ...... 1425-1475 F or 775-800 C
Machinability Rating (Free Cutting Brass = 100)
- Copper Alloy No. C17200 20
- Copper Alloy No. C17300 50

Suitability for being joined by:
- Soldering .... Good
- Brazing .... Good
- Oxyacetylene Welding .... Not Recommended
- Gas Shielded Arc Welding .... Good
- Coated Metal Arc Welding .... Good
- Resistance Welding
  - Spot .... Good
  - Seam .... Fair
  - Butt .... Fair

Table 1.11. Nominal Composition, ASTM Specification for Forms, Commonly Used Forms and Tempers, Typical Uses, and Fabrication Processes and Properties for C17500 and C17510. From Reference 1.16, with permission.

Composition — percent

	Alloy N. C17500 Nom.	Min.	Max.	Alloy No. C17510 Nom.	Min.	Max.
Copper (incl. Silver)	96.9	Rem.		97.8	Rem.	
Iron	....	....	.10	....	....	.10
Nickel	....	....	....	1.8	1.4	2.2
Cobalt	2.55	2.4	2.7	....	....	.30
Silicon	....	....	.20	....	....	.20
Beryllium	.55	.40	.7	.4	.20	.6
Aluminum	....	....	.20	....	....	.20

Nearest Applicable A S T M Specifications

Flat Products	B441, B534
Pipe	
Rod	B441
Shapes	
Tube	
Wire	

Forms and Tempers Most Commonly Used

	Annealed Tempers: Nominal Grain Size mm .100 (OS100)	.070 (OS070)	.050 (OS050)	.035 (OS035)	.025 (OS025)	.015 (OS015)	Soft Anneal (4) (TB00)	Light Anneal (O50)	Rolled or Drawn Tempers: Eighth Hard (H00)	Quarter Hard (H01)	Half Hard (H02)	Three Quarter Hard (H03)	Hard (H04)	Extra Hard (H06)	Spring (H08)	Extra Spring (H10)	Precipitation Heat Treated (TF00)	Drawn – General Purpose (H58)	Hard Drawn (H80)	Light Drawn – Bending (H55)	Hot Finished Tempers: As Hot Rolled (M20)	As Extruded (M30)	Special Tempers
FLAT PRODUCTS: Strip, Rolled							●				●		●				●						
Strip, Drawn																							
Flat Wire, Rolled																							
Flat Wire, Drawn																							
Bar, Rolled							●						●				●						
Bar, Drawn							●						●				●						
Sheet																							
Plate							●																
ROD							●						●				●						
WIRE																							
TUBE							●										●						
PIPE																							
SHAPES							●				●												

DRAWN–GENERAL PURPOSE (H58) temper is used for general purpose tube only, usually where there is no real requirement for high strength or hardness on the one hand or for bending qualities on the other.

HARD DRAWN (H80) temper is used only where there is need for a tube as hard or as strong as is commercially feasible for the size in question.

LIGHT DRAWN–BENDING (H55) temper is used only where a tube of some stiffness, but yet capable of readily being bent (or otherwise moderately cold worked) is needed.

Typical Uses

HARDWARE: fuse clips, fasteners, springs, switch parts, relay parts, electrical conductors

INDUSTRIAL: welding equipment

Common Fabrication Processes

Blanking, forming and bending, turning, drilling, tapping

Fabrication Properties

Capacity for Being Cold Worked .... Excellent
Capacity for Being Hot Formed .... Good
Hot Forgeability Rating (Forging Brass = 100) ....
Hot Working Temperature .... 1200-1625 F or 650-765 C
Machinability Rating (Free Cutting Brass = 100) ....
Solution Heat Treating Temperature 1675-1725 F or 900-950 C

Suitability for being joined by:
Soldering .... Good
Brazing .... Good
Oxyacetylene Welding .... Not Recommended
Gas Shielded Arc Welding .... Fair
Coated Metal Arc Welding .... Fair
Resistance Welding: Spot .... Good
Seam .... Fair
Butt .... Fair

Table 1.12. Nominal Composition, ASTM Specification for Forms, Commonly Used Forms and Tempers, Typical Uses, and Fabrication Processes and Properties for C50500. From Reference 1.16, with permission.

Composition — percent

	Nominal	Minimum	Maximum
Copper	98.7	Remainder	
Lead	....	....	.05
Iron	....	....	.10
Tin	1.3	1.0	1.7
Zinc	....	....	.30
Phosphorus	....	.03	.35

Nearest Applicable A S T M Specifications

Flat Products	B508
Pipe	
Rod	
Shapes	
Tube	
Wire	B105

Forms and Tempers Most Commonly Used

	Annealed Tempers: Nominal Grain Size mm .100 (OS100)	.070 (OS070)	.050 (OS050)	.035 (OS035)	.025 (OS025)	.015 (OS015)	Soft Anneal (O60)	Light Anneal (O50)	Rolled or Drawn Tempers: Eighth Hard (H00)	Quarter Hard (H01)	Half Hard (H02)	Three Quarter Hard (H03)	Hard (H04)	Extra Hard (H06)	Spring (H08)	Extra Spring (H10)	Drawn – General Purpose (H58)	Hard Drawn (H80)	Light Drawn – Bending (H55)	Hot Finished Tempers: As Hot Rolled (M20)	As Extruded (M30)	Special Tempers
FLAT PRODUCTS: Strip, Rolled					●						●		●		●							
FLAT PRODUCTS: Strip, Drawn																						
FLAT PRODUCTS: Flat Wire, Rolled																						
FLAT PRODUCTS: Flat Wire, Drawn																						
FLAT PRODUCTS: Bar, Rolled																						
FLAT PRODUCTS: Bar, Drawn																						
FLAT PRODUCTS: Sheet																						
FLAT PRODUCTS: Plate																						
ROD																						
WIRE													●									
TUBE																						
PIPE																						
SHAPES																						

DRAWN–GENERAL PURPOSE (H58) temper is used for general purpose tube only, usually where there is no real requirement for high strength or hardness on the one hand or for bending qualities on the other.

HARD DRAWN (H80) temper is used only where there is need for a tube as hard or as strong as is commercially feasible for the size in question.

LIGHT DRAWN–BENDING (H55) temper is used only where a tube of some stiffness, but yet capable of readily being bent (or otherwise moderately cold worked) is needed.

Typical Uses

INDUSTRIAL: electrical contacts, flexible hose, pole-line hardware

Common Fabrication Processes

Blanking, forming and bending, heading and upsetting, shearing, squeezing and swaging

Fabrication Properties

Capacity for Being Cold Worked	Excellent
Capacity for Being Hot Formed	Good
Hot Forgeability Rating (Forging Brass = 100)	.....
Hot Working Temperature	1450-1600 F or 800-875 C
Annealing Temperature	900-1200 F or 475-650 C
Machinability Rating (Free Cutting Brass = 100)	20

Suitability for being joined by:

Soldering	Excellent
Brazing	Excellent
Oxyacetylene Welding	Fair
Gas Shielded Arc Welding	Good
Coated Metal Arc Welding	Fair
Resistance Welding: Spot	Not Recommended
Resistance Welding: Seam	Not Recommended
Resistance Welding: Butt	Excellent

Table 1.13. Nominal Composition, ASTM Specification for Forms, Commonly Used Forms and Tempers, Typical Uses, and Fabrication Processes and Properties for C51000. From Reference 1.16, with permission.

Composition – percent

	Nominal	Minimum	Maximum
Copper	94.8	Remainder	
Lead	....	....	.05
Iron	....	....	.10
Tin	5	4.2	5.8
Zinc	....	....	.30
Phosphorus	.2	.03	.35

Nearest Applicable A S T M Specifications

Bolts	F468
Flat Products	B100, B103, B139
Nuts	F467
Pipe	
Rod	B139
Screws	F468
Shapes	B139
Studs	F468
Tube	
Wire	B159

Forms and Tempers Most Commonly Used

	Annealed Tempers: Nominal Grain Size mm .100 (OS100)	.070 (OS070)	.050 (OS050)	.035 (OS035)	.025 (OS025)	.015 (OS015)	Soft Anneal (O60)	Light Anneal (O50)	Rolled or Drawn Tempers: Eighth Hard (H00)	Quarter Hard (H01)	Half Hard (H02)	Three Quarter Hard (H03)	Hard (H04)	Extra Hard (H06)	Spring (H08)	Extra Spring (H10)	Drawn – General Purpose (H58)	Hard Drawn (H80)	Light Drawn – Bending (H55)	Hot Finished Tempers: As Hot Rolled (M20)	As Extruded (M30)	Special Tempers
FLAT PRODUCTS: Strip, Rolled							●				●		●	●	●	●						
FLAT PRODUCTS: Strip, Drawn																						
FLAT PRODUCTS: Flat Wire, Rolled															●							
FLAT PRODUCTS: Flat Wire, Drawn																						
FLAT PRODUCTS: Bar, Rolled																						
FLAT PRODUCTS: Bar, Drawn																						
FLAT PRODUCTS: Sheet																						
FLAT PRODUCTS: Plate																						
ROD											●											
WIRE									●	●	●		●	●	●							
TUBE																		●				
PIPE																						
SHAPES																					●	

DRAWN–GENERAL PURPOSE (H58) temper is used for general purpose tube only, usually where there is no real requirement for high strength or hardness on the one hand or for bending qualities on the other.

HARD DRAWN (H80) temper is used only where there is need for a tube as hard or as strong as is commercially feasible for the size in question.

LIGHT DRAWN–BENDING (H55) temper is used only where a tube of some stiffness, but yet capable of readily being bent (or otherwise moderately cold worked) is needed.

Typical Uses

ARCHITECTURAL:	bridge bearing plates
HARDWARE:	beater bars, bellows, Bourdon tubing, clutch disks, cotter pins, diaphragms, fuse clips, fasteners, lock washers, sleeve bushings, springs, switch parts, truss wire, wire brushes
INDUSTRIAL:	chemical hardware, perforated sheets, textile machinery, welding rods

Common Fabrication Processes

Blanking, drawing, forming and bending, heading and upsetting, roll threading and knurling, shearing, stamping

Fabrication Properties

Capacity for Being Cold Worked	Excellent
Capacity for Being Hot Formed	Poor
Hot Forgeability Rating (Forging Brass = 100)	
Hot Working Temperature	F or C
Annealing Temperature	900-1250 F or 745-675 C
Machinability Rating (Free Cutting Brass = 100)	20

Suitability for being joined by:

Soldering	Excellent
Brazing	Excellent
Oxyacetylene Welding	Fair
Gas Shielded Arc Welding	Good
Coated Metal Arc Welding	Fair
Resistance Welding: Spot	Good
Resistance Welding: Seam	Fair
Resistance Welding: Butt	Excellent

Table 1.14. Nominal Composition, ASTM Specification for Forms, Commonly Used Forms and Tempers, Typical Uses, and Fabrication Processes and Properties for C51100. From Reference 1.16, with permission.

Composition — percent

	Nominal	Minimum	Maximum
Copper	95.6	Remainder	
Lead	....	....	.05
Iron	....	....	.10
Tin	4.2	3.5	4.9
Zinc	....	....	.30
Phosphorus	.2	.03	.35

Nearest Applicable A S T M Specifications

Flat Products	B100, B103
Pipe	
Rod	
Shapes	
Tube	
Wire	

Forms and Tempers Most Commonly Used

Annealed Tempers — Nominal Grain Size mm

Form	.100 (OS100)	.070 (OS070)	.050 (OS050)	.035 (OS035)	.025 (OS025)	.015 (OS015)	Soft Anneal (O60)	Light Anneal (O50)
FLAT PRODUCTS: Strip, Rolled			●	●	●	●		
FLAT PRODUCTS: Strip, Drawn								
FLAT PRODUCTS: Flat Wire, Rolled								
FLAT PRODUCTS: Flat Wire, Drawn								
FLAT PRODUCTS: Bar, Rolled								
FLAT PRODUCTS: Bar, Drawn								
FLAT PRODUCTS: Sheet								
FLAT PRODUCTS: Plate								
ROD								
WIRE								
TUBE								
PIPE								
SHAPES								

Rolled or Drawn Tempers

Form	Eighth Hard (H00)	Quarter Hard (H01)	Half Hard (H02)	Three Quarter Hard (H03)	Hard (H04)	Extra Hard (H06)	Spring (H08)	Extra Spring (H10)	Drawn – General Purpose (H58)	Hard Drawn (H80)	Light Drawn – Bending (H55)
FLAT PRODUCTS: Strip, Rolled		●	●	●	●	●	●	●			
FLAT PRODUCTS: Strip, Drawn											
FLAT PRODUCTS: Flat Wire, Rolled											
FLAT PRODUCTS: Flat Wire, Drawn											
FLAT PRODUCTS: Bar, Rolled											
FLAT PRODUCTS: Bar, Drawn											
FLAT PRODUCTS: Sheet											
FLAT PRODUCTS: Plate											
ROD											
WIRE											
TUBE											
PIPE											
SHAPES											

Hot Finished Tempers

Form	As Hot Rolled (M20)	As Extruded (M30)	Special Tempers
FLAT PRODUCTS: Strip, Rolled			
FLAT PRODUCTS: Strip, Drawn			
FLAT PRODUCTS: Flat Wire, Rolled			
FLAT PRODUCTS: Flat Wire, Drawn			
FLAT PRODUCTS: Bar, Rolled			
FLAT PRODUCTS: Bar, Drawn			
FLAT PRODUCTS: Sheet			
FLAT PRODUCTS: Plate			
ROD			
WIRE			
TUBE			
PIPE			
SHAPES			

DRAWN–GENERAL PURPOSE (H58) temper is used for general purpose tube only, usually where there is no real requirement for high strength or hardness on the one hand or for bending qualities on the other.

HARD DRAWN (H80) temper is used only where there is need for a tube as hard or as strong as is commercially feasible for the size in question.

LIGHT DRAWN–BENDING (H55) temper is used only where a tube of some stiffness, but yet capable of readily being bent (or otherwise moderately cold worked) is needed.

Typical Uses

ARCHITECTURAL: bridge bearing plates
HARDWARE: beater bars, bellows, clutch disks, connectors, diaphragms, fuse clips, fasteners, lock washers, sleeve bushings, springs, switch parts, terminals
INDUSTRIAL: chemical hardware, perforated sheets, textile machinery

Common Fabrication Processes

Blanking, drawing, forming and bending, roll threading and knurling, shearing, stamping

Fabrication Properties

Capacity for Being Cold Worked .... Excellent
Capacity for Being Hot Formed .... Poor
Hot Forgeability Rating (Forging Brass = 100) ....
Hot Working Temperature .... F or C
Annealing Temperature .... 900-1250 F or 475-675 C
Machinability Rating (Free Cutting Brass = 100)......... 20

Suitability for being joined by:
Soldering .... Excellent
Brazing .... Excellent
Oxyacetylene Welding .... Fair
Gas Shielded Arc Welding .... Good
Coated Metal Arc Welding .... Fair
Resistance Welding: Spot .... Good
Resistance Welding: Seam .... Fair
Resistance Welding: Butt .... Excellent

Table 1.15. Nominal Composition, ASTM Specification for Forms, Commonly Used Forms and Tempers, Typical Uses, and Fabrication Processes and Properties for C52100. From Reference 1.16, with permission.

Composition – percent

	Nominal	Minimum	Maximum
Copper	92	Remainder	
Lead	....	....	.05
Iron	....	....	.10
Tin	8	7.0	9.0
Zinc	....	....	.20
Phosphorus	....	.03	.35

Nearest Applicable A S T M Specifications

Flat Products	B103, B139
Pipe	
Rod	B139
Shapes	B139
Tube	
Wire	B159

Forms and Tempers Most Commonly Used

	Annealed Tempers – Nominal Grain Size mm: .100 (OS100)	.070 (OS070)	.050 (OS050)	.035 (OS035)	.025 (OS025)	.015 (OS015)	Soft Anneal (O60)	Light Anneal (O50)	Rolled or Drawn Tempers: Eighth Hard (H00)	Quarter Hard (H01)	Half Hard (H02)	Three Quarter Hard (H03)	Hard (H04)	Extra Hard (H06)	Spring (H08)	Extra Spring (H10)	Drawn – General Purpose (H58)	Hard Drawn (H80)	Light Drawn – Bending (H55)	Hot Finished Tempers: As Hot Rolled (M20)	As Extruded (M30)	Special Tempers
FLAT PRODUCTS – Strip, Rolled											●		●	●	●	●						
FLAT PRODUCTS – Strip, Drawn																						
FLAT PRODUCTS – Flat Wire, Rolled																						
FLAT PRODUCTS – Flat Wire, Drawn																						
FLAT PRODUCTS – Bar, Rolled																						
FLAT PRODUCTS – Bar, Drawn																						
FLAT PRODUCTS – Sheet																						
FLAT PRODUCTS – Plate																						
ROD											●											
WIRE										●	●		●	●								
TUBE																						
PIPE																						
SHAPES																					●	

DRAWN–GENERAL PURPOSE (H58) temper is used for general purpose tube only, usually where there is no real requirement for high strength or hardness on the one hand or for bending qualities on the other.

HARD DRAWN (H80) temper is used only where there is need for a tube as hard or as strong as is commercially feasible for the size in question.

LIGHT DRAWN–BENDING (H55) temper is used only where a tube of some stiffness, but yet capable of readily being bent (or otherwise moderately cold worked) is needed.

Typical Uses

(Same as for Phosphor Bronze, 5% (A), but for more severe service conditions)

ARCHITECTURAL: bridge bearing plates

HARDWARE: beater bars, bellows, Bourdon tubing, clutch disks, cotter pins, diaphragms, fuse clips, fasteners, lock washers, sleeve bushings, springs, switch parts, truss wire, wire brushes

INDUSTRIAL: chemical hardware, perforated sheets, textile machinery, welding rods

Common Fabrication Processes

Blanking, drawing, forming and bending, shearing, stamping

Fabrication Properties

Capacity for Being Cold Worked	Good
Capacity for Being Hot Formed	Poor
Hot Forgeability Rating (Forging Brass = 100)	
Hot Working Temperature	F or C
Annealing Temperature	900-1250 F or 475-675 C
Machinability Rating (Free Cutting Brass = 100)	20

Suitability for being joined by:

Soldering	Excellent
Brazing	Excellent
Oxyacetylene Welding	Fair
Gas Shielded Arc Welding	Good
Coated Metal Arc Welding	Fair
Resistance Welding – Spot	Good
Resistance Welding – Seam	Fair
Resistance Welding – Butt	Excellent

Table 1.16. Nominal Composition, ASTM Specification for Forms, Commonly Used Forms and Tempers, Typical Uses, and Fabrication Processes and Properties for C52400. From Reference 1.16, with permission.

Composition – percent

	Nominal	Minimum	Maximum
Copper	90	Remainder	
Lead	....	....	.05
Iron	....	....	.10
Tin	10	9.0	11.0
Zinc	....	....	.20
Phosphorus	....	.03	.35

Nearest Applicable A S T M Specifications

Flat Products	B103, B139
Pipe	
Rod	B139
Shapes	B139
Tube	
Wire	B159

Forms and Tempers Most Commonly Used

Form	Annealed Tempers – Nominal Grain Size mm: .100 (OS100)	.070 (OS070)	.050 (OS050)	.035 (OS035)	.025 (OS025)	.015 (OS015)	Soft Anneal (O60)	Light Anneal (O50)	Rolled or Drawn Tempers: Eighth Hard (H00)	Quarter Hard (H01)	Half Hard (H02)	Three Quarter Hard (H03)	Hard (H04)	Extra Hard (H06)	Spring (H08)	Extra Spring (H10)	Drawn – General Purpose (H58)	Hard Drawn (H80)	Light Drawn – Bending (H55)	Hot Finished Tempers: As Hot Rolled (M20)	As Extruded (M30)	Special Tempers
FLAT PRODUCTS – Strip, Rolled											●		●	●	●	●						
FLAT PRODUCTS – Strip, Drawn																						
FLAT PRODUCTS – Flat Wire, Rolled																						
FLAT PRODUCTS – Flat Wire, Drawn																						
FLAT PRODUCTS – Bar, Rolled																						
FLAT PRODUCTS – Bar, Drawn																						
FLAT PRODUCTS – Sheet																						
FLAT PRODUCTS – Plate																						
ROD											●											
WIRE										●	●		●									
TUBE																						
PIPE																						
SHAPES																					●	

DRAWN–GENERAL PURPOSE (H58) temper is used for general purpose tube only, usually where there is no real requirement for high strength or hardness on the one hand or for bending qualities on the other.

HARD DRAWN (H80) temper is used only where there is need for a tube as hard or as strong as is commercially feasible for the size in question.

LIGHT DRAWN–BENDING (H55) temper is used only where a tube of some stiffness, but yet capable of readily being bent (or otherwise moderately cold worked) is needed.

Typical Uses

Heavy bars and plates for severe compression, good wear and corrosion resistance, bridge and expansion plates and fittings; and articles requiring extra spring qualities, greatest resiliency, particularly in fatigue

Common Fabrication Processes

Blanking, forming and bending, shearing

Fabrication Properties

Capacity for Being Cold Worked	Good
Capacity for Being Hot Formed	Poor
Hot Forgeability Rating (Forging Brass = 100)	
Hot Working Temperature	F or C
Annealing Temperature	900-1250 F or 475-675 C
Machinability Rating (Free Cutting Brass = 100)	20

Suitability for being joined by:

Soldering	Excellent
Brazing	Excellent
Oxyacetylene Welding	Fair
Gas Shielded Arc Welding	Good
Coated Metal Arc Welding	Fair
Resistance Welding – Spot	Good
Resistance Welding – Seam	Fair
Resistance Welding – Butt	Excellent

Table 1.17. Standard Temper Designations for Copper Alloy Flat Stock (adapted from References 1.3 and 1.22).

Standard Designation	Nominal Reduction in Thickness by Rolling, %	Reduction of Area by Drawing, %
Quarter hard	11	21
Half hard	21	37
Three-quarters hard	29	—
Hard (full hard)	37	60
Extra hard	50	75
Spring	60	84
Extra Spring	68	90

ward. Only linear and nonlinear, multivariate regression analyses techniques, with equal weights for all data points, were employed. Standard deviations used in this review were calculated from all data points. The variance of the data was assumed to be normally distributed and constant throughout the range of the independent variables, such as temperature or cold work.

ACKNOWLEDGMENTS

William T. Black of the Copper Data Center (Copper Development Association) kindly supplied us with a bibliography of over 2250 references related to properties of copper and selected copper alloys. The assistance of F. R. Fickett is gratefully acknowledged. Chris King, Luz Delgado, Rebecca Toevs-Wait, Grace Norman, and Renee Deal expertly assisted us in preparation of the manuscript and data analysis. Bill Bulla, until replaced by computer graphics, carefully drafted many of the figures for the copper and beryllium-copper sections. We appreciate the efforts of G. A. Cypher and W. H. Dresher of ICA, Ltd., to make funding available for the preparation of this monograph.

REFERENCES

1. M. Hansen, Constitution of Binary Alloys, McGraw-Hill Book Co., New York (1958).

2. Y.S. Touloukian, Thermophysical Properties of High Temperature Solid Materials, Vol. 1, Purdue University, Thermophysical Properties Research Center, W. Lafayette, IN (1967) 452–479.

3. Source Book on Copper and Copper Alloys, American Society for Metals, Metals Park, OH (1979).

4. Metals Handbook, Ninth Edition, Volume 2, Properties and Selection: Non-ferrous Alloys and Pure Metals, American Society for Metals, Metals Park, OH (1979) 239–490.

5. K.A. Gschneidner, Jr., Solid State Physics, Vol. 16, Academic Press, New York (1964) 275–427.

6. W.B. Pearson, Handbook of Lattice Spacings and Structures of Metals, Vol. 2, Pergamon Press, New York (1967).

7. "Purity: A Short History," AMAX Copper News, 12, No. 1, (June, 1972).

8. G.T. Seaborg, Our Heritage of the Elements, Metallurgical Transactions A 11A, 5–19 (1980).

9. M. Kranzberg and C.S. Smith, Part I. Materials in History and Society, Materials Science and Engineering 37, 1–39 (1979).

10. L. Guillet and J. Cournot, "Sur la Variation des Properietes Mecaniques de quelques Métaux et Alliages aux basses Temperatures," Revue de Métallurgie (Mémoires) 19, 213 (1922).

11. H.G. Dorsey, "Coefficient of Linear Expansion at Low Temperatures," Physical Review 25, 88–102 (1907).

12. R.P. Reed and R. P. Mikesell, Low Temperature Mechanical Properties of Copper and Selected Copper Alloys, NBS Monograph 101, U.S. Government Printing Office, Washington, D.C. (1967).

REFERENCES

13. Handbook on Materials for Superconducting Machinery, Metals and Ceramics Information Center, Battelle, Columbus, OH (1977).

14. R.A. Wilkins and E.S. Bunn, Copper and Copper Base Alloys, McGraw-Hill Book Co., New York (1943).

15. C.A. Thompson, W.M. Manganard, and F.R. Fickett, Cryogenic Properties of Copper, International Research Association, Ltd., New York (1990).

16. Standards Handbook, Parts 1–7, Copper Development Association, New York (1985).

17. Metals Handbook--Welding and Brazing, 9th Edition, Vol. 6, American Society for Metals, Metals Park, OH (1983).

18. International Copper Research Association, Monograph Series, Library Congress Card No. 82-81882, ISBN No. 0-94 3642-08-6 (1971–present).

19. Understanding Copper Alloys, Eds. J.H. Mendenhall, R.E. Krieger Publishing Co., Malabor, FL (1986).

20. A. Butts, Copper, The Metal, Its Alloys and Compounds, Reinhold Publishing Corp., New York (1964).

21. Application Data Sheet-Standard Designations for Copper and Copper Alloys, No. 118/1, Copper Development Association, Greenwich, CT, not dated.

22. W.L. Finlay, Silver-Bearing Copper, Corinthian Editions, New York (1968).

DATA SOURCES AND ANALYSIS

A set of 48 measurements of tensile yield strength at 295 K was selected for analysis because grain size and impurity content were reported. Grain size, *d*, ranged from 0.056 to 320 μm; impurity content, [I], from 0.001 to 0.10 wt%. Products were in plate, bar, and wire form. This data set (References 2.1–2.13) was used in regression analysis of tensile yield strength (σ_y) upon the two variables *d* and [I].

RESULTS

No significant dependence of σ_y upon [I] was observed, perhaps owing to inconsistencies in the way this quantity was measured and reported.

The regression equation found for the dependence of σ_y upon *d* at 295 K was the usual Hall-Petch relation:

$$\sigma_y = 18.6 + 112d^{-1/2} \quad \text{(S.D. = 11 MPa)}, \tag{2-1}$$

where σ_y is in MPa and *d* is in μm. The standard deviations of the two coefficients were 1.7 and 2.

Table 2.1 presents the measured values of σ_y, the values of σ_y calculated from the regression equation, $d^{-1/2}$, *d*, and the reference numbers. The available characterization of materials and measurements is given in Table 2.10 at the end of the tensile properties section.

Figure 2.1 indicates the fit of the data to Equation (2-1). Figure 2.2 depicts the same regression equation with expanded scales to show that the equation is a good fit to the data whether the two measurements on specimens with very small grain sizes (Reference 2.10) are included or not. Figure 2.3 presents these results in summary form. In all three figures, the scatter bands represent two standard deviations about the regression lines. The variance of the data about the regression line was assumed to be normally distributed and constant throughout the range of the independent variable, $d^{-1/2}$.

DISCUSSION

The coefficient of the $d^{-1/2}$ term in Equation (2-1) is very dependent upon the data set that is used for the regression analysis. Coefficients differing by much more than twice this standard deviation have been obtained from data sets comprising a smaller range of *d*. A small temperature dependence was also observed in the $d^{-1/2}$ coefficient (see page 2-6). At present, the uncertainty in this coefficient is considered to be much larger than the two standard deviations obtained from the present analysis.

Table 2.1. Yield Strength Dependence on Grain Size (295 K).

Yield Strength, Measured, MPa	Yield Strength, Calculated, MPa	(Grain Size)$^{-1/2}$, 10^3 m$^{-1/2}$	Grain Size, μm	Reference No.
30.4	24.8	0.0559	320	8
25.4	25.8	0.0645	240	9
21.9	26.7	0.0725	190	9
29.5	25.8	0.0725	190	9
19.6	26.7	0.0725	190	9
20.8	26.7	0.0725	190	9
25.0	26.7	0.0725	190	9
10.3	27.9	0.0778	190	2
14.8	27.7	0.0816	190	12
25.4	27.9	0.083	145	13
15.0	30.1	0.103	95	2
23.0	31.1	0.112	80	5
31.8	31.1	0.112	80	11
31.7	33.4	0.132	57	8

Table 2.1, continued

Yield Strength, Measured, MPa	Yield Strength, Calculated, MPa	(Grain Size)$^{-1/2}$, 10^3 m$^{-1/2}$	Grain Size, μm	Reference No.
33.3	34.4	0.171	50	8
34.8	38.4	0.141	50	8
34.5	35.1	0.171	46	8
69.0	35.3	0.141	45	7
27.0	35.9	0.154	42	13
32.1	35.9	0.154	42	13
27.3	35.9	0.154	42	13
35.4	36.5	0.154	42	13
24.0	36.3	0.158	40	12
32.2	36.5	0.16	34	8
90.0	37.8	0.171	34	9
34.8	37.8	0.141	34	8
47.3	37.8	0.171	34	8
33.9	37.8	0.141	34	8
36.1	37.8	0.171	34	8
34.8	38.4	0.141	33	8
34.5	35.1	0.177	32	8
40.6	38.4	0.141	32	8
69.0	39.1	0.158	34	7
34.8	38.4	0.183	34	8
27.8	35.3	0.189	28	8
50.7	40.6	0.196	28	8
52.0	47.6	0.2	28	1
69.0	43.7	0.224	20	8
39.2	43.7	0.224	20	11
34.5	45.8	0.243	17	7
40.0	47.6	0.258	46	12
69.0	57.3	0.283	12.5	3
90.0	52.4	0.302	11	8
73.4	57.3	0.345	8.4	12
63.0	61.3	0.381	6.9	12
78.8	79.5	0.542	3.4	12
434	423	3.6	0.077	10
481	493	4.23	0.056	10

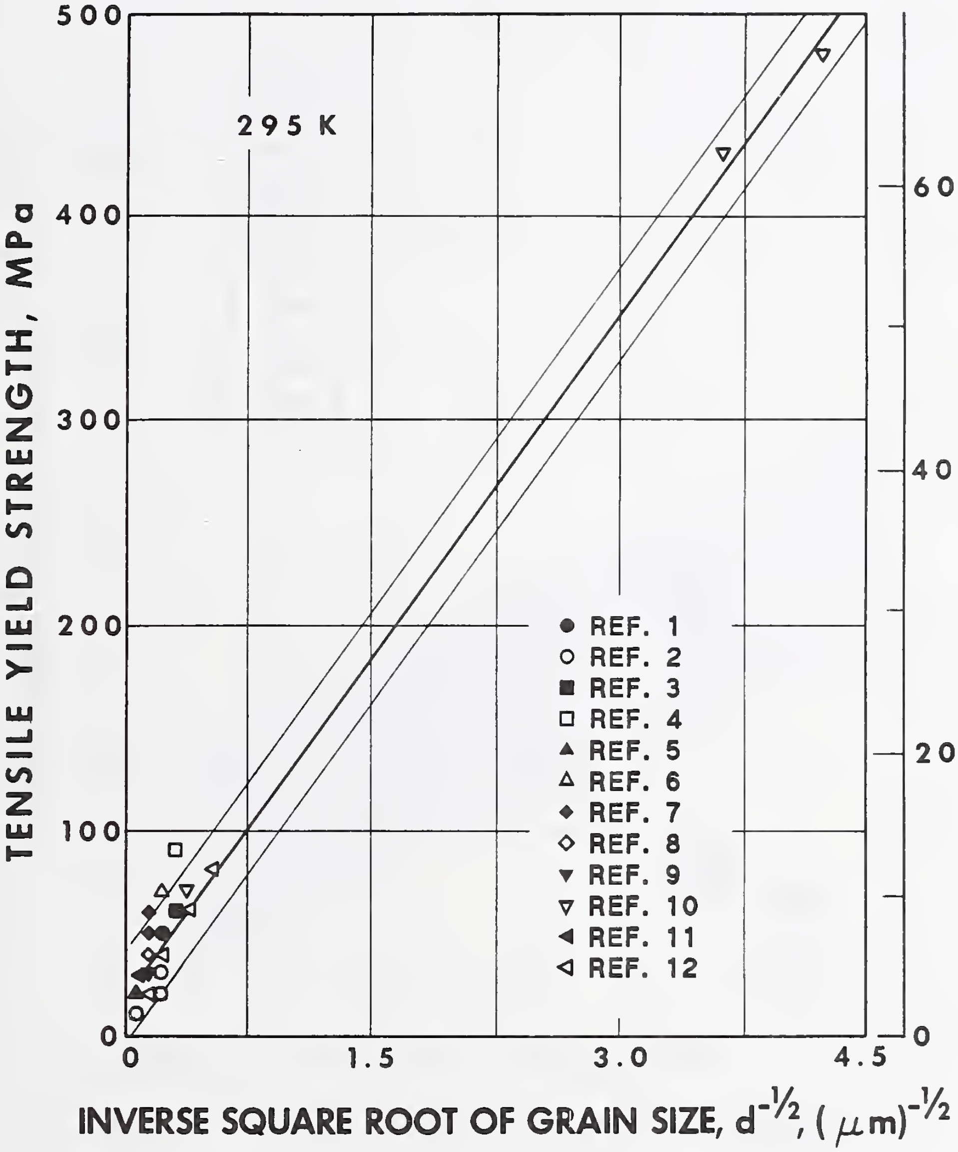

Figure 2.1. The data shown were used to compute the linear regression of tensile yield strength at 295 K upon $d^{-1/2}$ [Equation (2-1)]. For clarity, overlapping data points are omitted from the figure, including all points from Reference 2.13. All data are presented in Table 2.1. Products were in plate, bar, and wire form.

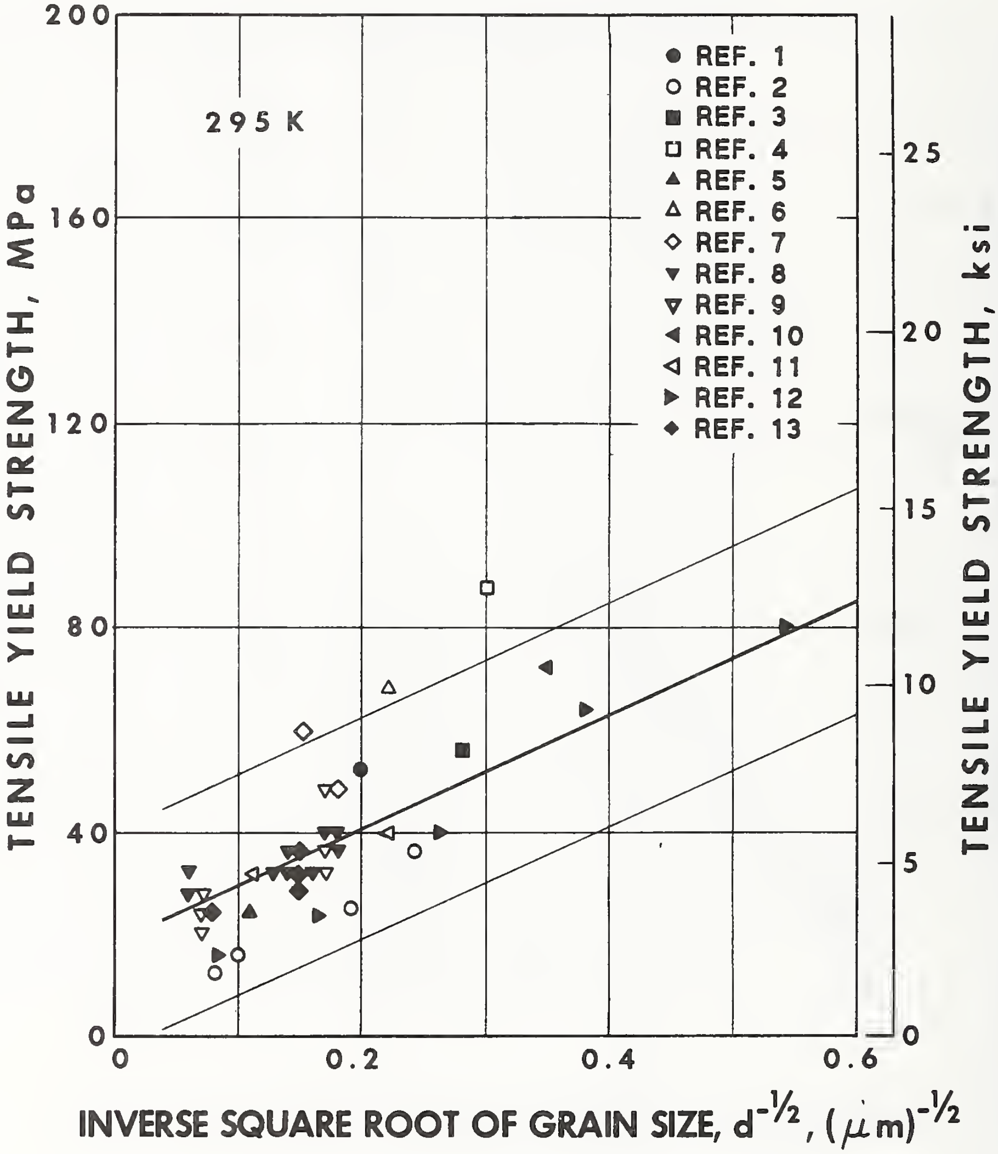

Figure 2.2. This figure shows the data for the larger grain sizes presented in Figure 2.1. Owing to the expanded scales, the slope appears changed, but the equation represented by the line is the same as that depicted in Figure 2.1. For clarity, overlapping data points are omitted from the figure. All data are presented in Table 2.1. Products were in plate, bar, and wire form.

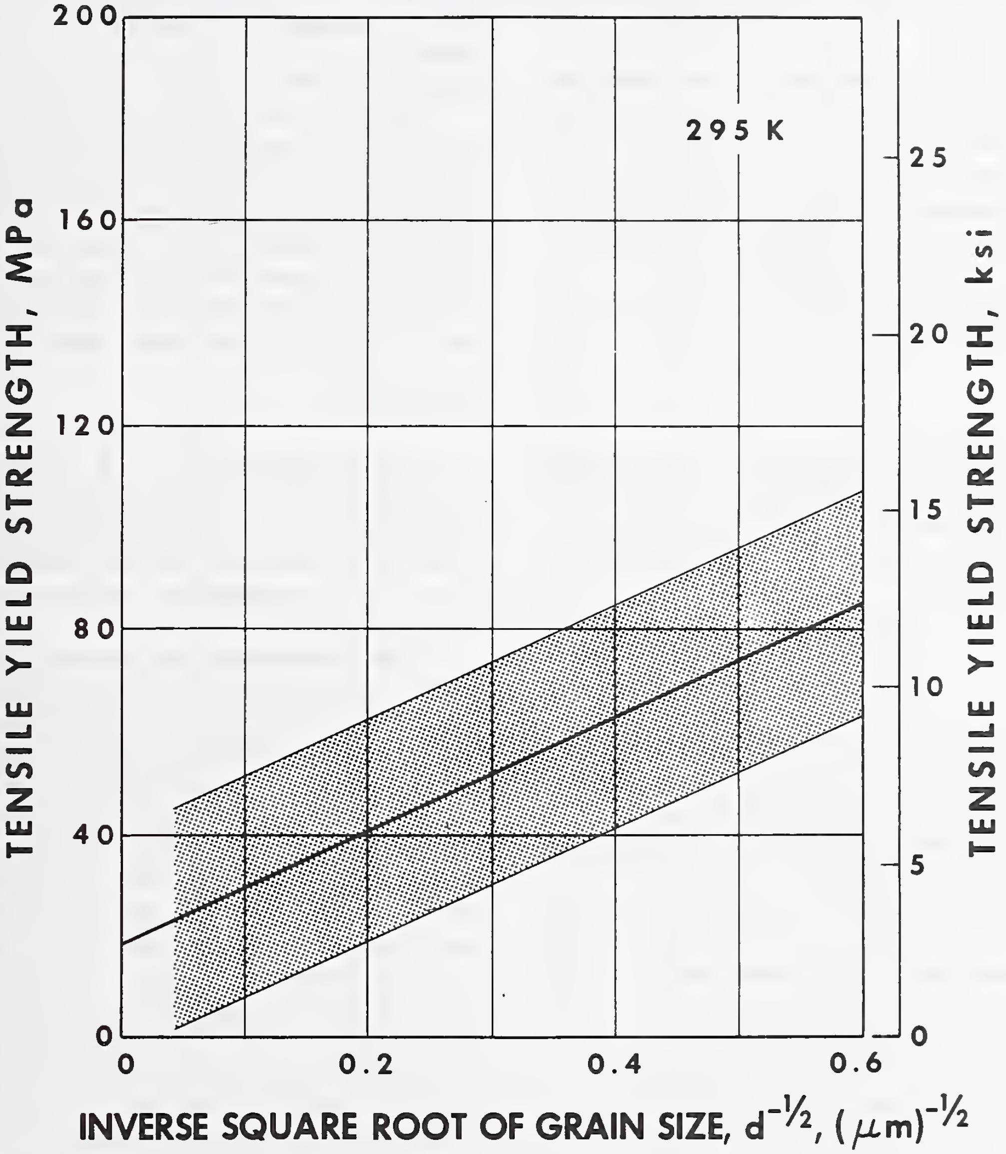

Figure 2.3. Tensile yield strength dependence upon grain size at 295 K. The scatter band represents two standard deviations about a regression line based upon 48 measurements for a range of grain size, *d*, from 0.056 to 320 μm. The regression equation is

$$\sigma_y \text{ (MPa)} = 18.6 + 112\, d^{-1/2} \qquad (d \text{ in } \mu\text{m}) \quad (\text{S.D.} = 11 \text{ MPa}).$$

Regression analysis of this set of data for impurity content indicated no significant dependence. Products were in plate, bar, and wire form.

DATA SOURCES AND ANALYSIS

A set of 84 measurements of tensile yield strength from 4 to 300 K was selected for analysis because grain size and impurity content were reported. Grain size, *d*, ranged from 11 to 165 μm; impurity content, [I], from 0.0053 to 0.10 wt%. Products were in plate, bar, and wire form. This data set (References 2.1–2.6 and 2.13–2.14) was used in regression analysis of tensile yield strength (σ_y) upon three variables, temperature (*T*), *d*, and [I]. Data on the variation of σ_y with silver content are presented on pages 2-20 and 2-21 (cold-worked copper).

RESULTS

Regression analysis indicated that the best fit to the data was obtained with a linear dependence of σ_y upon the three variables of *T*, the inverse square root of the grain size, $d^{-1/2}$, and [I]:

$$\sigma_y = -8.60 - 0.0329T + 292d^{-1/2} + 150[I] \quad (2\text{-}2)$$
$$(\text{S.D.} = 9\ \text{MPa}),$$

where σ_y is in MPa, 4 K $\leq T \leq$ 300 K, *d* is in μm, and [I] is in wt%. The standard deviations of the four coefficients are 3.56, 0.0105, 20, and 67.

Table 2.2 presents the measured values of σ_y, the values calculated from the regression equation, the temperature, $d^{-1/2}$, and the reference number. The available characterization of materials and measurements is given in Table 2.10 at the end of the tensile properties section.

Figures 2.4–2.6 present the data as a function of each variable, *T*, *d*, and [I], separately. Figure 2.4 depicts the data as a function of *T* only, without showing the dependence upon *d* and [I]. Figure 2.5 depicts the data as a function of $d^{-1/2}$ only, without showing the dependence upon *T* and [I]. Figure 2.6 depicts the data as a function of [I] only, without showing the dependence upon *T* and *d*. It is clear from the large amount of scatter in Figures 2.4–2.6 that separate regression equations for σ_y as a function of each variable, *T*, $d^{-1/2}$, and [I], would not be of much value. However, when multivariate regression is used to analyze the data set, a relatively small standard deviation of 9 MPa is obtained.

Figure 2.7 indicates the fit of the data to the multivariate regression expression, Equation (2-2). The scatter band represents two standard deviations about the line that corresponds to complete agreement between measured and predicted values of σ_y. The variance of the data was assumed to be normally distributed and constant throughout the range of the predicted values.

DISCUSSION

The *T* dependence of σ_y in Equation (2-2) is small, as expected, and the coefficient for [I] has a sizeable uncertainty owing to the restricted range of this variable in the data available. Also, [I] was not determined and reported consistently in all the references.

The disagreement between the coefficient for $d^{-1/2}$ and that determined from the 295-K measurements [Equation (2-1)] requires further study. This coefficient can change considerably with the addition or subtraction of a few influential points of the data set. The previous set of measurements at 295 K (*d* from 0.056 to 320 μm) included the measurements from 293 to 300 K of this set (*d* from 11 to 165 μm). Separate analyses of 4-K, 77-K, and 295-K data from the present set of 84 measurements gave $d^{-1/2}$ coefficients of 352, 343, and 268, respectively. However, this *T* dependence of the $d^{-1/2}$ coefficient is not large enough to explain the difference between Equations (2-1) and (2-2). At present, the 295-K coefficient (112) is considered the most accurate because it was obtained over the largest range of *d*. Since the extension of the range resulted mainly from work carried out at one laboratory (Reference 2.10), further studies would help resolve this question.

Table 2.2. Yield Strength Dependence on Grain Size, and Purity (4–300 K).

Yield Strength, Measured, MPa	Yield Strength, Calculated, MPa	Test Temperature, K	(Grain Size)$^{-1/2}$, 10^3 m$^{-1/2}$	Impurity, wt%	Reference No.
30.5	31.4	4	0.112	0.05	5
38.6	37.8	4	0.154	0.01	13
35.9	37.8	4	0.154	0.01	13
34.4	37.8	4	0.154	0.01	13
29.9	37.8	4	0.154	0.01	13
36.9	37.8	4	0.154	0.01	13
32.2	34.3	4	0.154	0.01	13
38.6	37.8	4	0.154	0.01	13
38.7	32.9	4	0.137	0.0068	14
100	80.1	4	0.302	0.0053	4
28.8	17.4	5	0.0845	0.01	13
37.6	37.8	11	0.154	0.01	13
32.9	35.9	31	0.154	0.01	13
36.9	79.6	21	0.302	0.0053	4
36.1	37.3	21	0.154	0.01	13
35.4	37.3	21	0.154	0.01	13
28.8	37.8	23	0.154	0.01	13
37.3	36.9	31	0.154	0.01	13
35.9	35.9	31	0.154	0.01	13
35.2	36.9	33	0.154	0.01	13
38.7	35.9	36	0.154	0.01	13
30.7	36.6	[illegible]	0.154	0.01	13
34.3	36.6	70	0.154	0.01	13
36.9	36.6	[illegible]	0.154	0.01	13
34.3	36.5	76	0.154	0.01	13
34.5	36.6	45	0.154	0.01	13
35.9	35.9	76	0.154	0.01	13
36.9	36.9	50	0.154	0.01	13
33.1	36.3	59	0.154	0.01	13
34.5	36.9	50	0.154	0.01	13
35.9	36.2	59	0.154	0.01	13
35.3	35.4	50	0.154	0.01	13
35.6	36.0	59	0.154	0.01	13
34.4	36.9	50	0.154	0.01	13
35.9	29.1	76	0.112	0.05	5
35.4	35.4	45	0.154	0.01	13
32.2	38.7	76	0.154	0.01	13
35.2	35.4	76	0.154	0.01	13
35.9	38.7	76	0.154	0.01	13
28.1	16.5	76	0.0894	0.01	13
100.0	77.7	76	0.302	0.0053	4
59.0	59.0	4	0.224	0.1	6
36.2	36.2	4	0.137	0.0068	14
41.2	36.9	4	0.137	0.0068	14
35.6	30.0	77	0.137	0.0068	14
59.0	48.7	76	0.2	0.01	4
73.8	73.6	76	0.283	0.015	3
35.4	62.2	90	0.283	0.02	2
11.7	14.2	90	0.0778	0.02	2
32.5	34.7	98	0.154	0.01	13
34.6	34.7	100	0.154	0.01	13

C10100–C10700: Annealed

Tensile Yield Strength vs. Grain Size, Impurity (4–300 K)

Table 2.2, continued

Yield Strength, Measured, MPa	Yield Strength, Calculated, MPa	Test Temperature, K	(Grain Size)$^{-1/2}$, 10^3 m$^{-1/2}$	Impurity, wt%	Reference No.
35.1	34.5	103	0.154	0.01	13
33.0	34.3	140	0.154	0.01	13
59.2	46.9	133	0.2	0.01	1
30.4	33.3	140	0.154	0.01	13
34.5	33.0	145	0.154	0.01	13
23.0	33.0	198	0.154	0.01	13
34.5	33.0	188	0.154	0.01	13
38.4	60.2	193	0.243	0.02	2
44.9	12.1	183	0.0778	0.02	2
34.3	59.2	193	0.243	0.02	2
10.9	11.1	183	0.0778	0.02	2
34.3	34.3	193	0.154	0.01	13
57.0	44.9	194	0.2	0.01	1
77.2	69.8	140	0.243	0.015	3
31.3	31.4	163	0.154	0.01	13
36.6	59.2	213	0.243	0.02	2
55.0	43.3	293	0.2	0.01	1
36.6	59.2	243	0.243	0.02	2
31.2	25.4	295	0.154	0.01	13
69.0	62.1	293	0.224	0.1	6
58.0	66.5	293	0.283	0.015	3
23.0	28.2	295	0.112	0.05	6
35.4	28.2	295	0.154	0.01	13
28.2	28.2	295	0.154	0.01	13
32.1	28.2	295	0.154	0.01	13
27.0	28.2	295	0.154	0.01	13
25.4	7.4	295	0.083	0.01	13
34.5	59.2	295	0.243	0.02	2
10.3	7.4	295	0.0778	0.02	2
15.0	44.9	295	0.154	0.02	2
24.0	39.9	295	0.189	0.02	2
52.0	41.5	296	0.2	0.01	1
90.0	70.3	300	0.302	0.0053	4

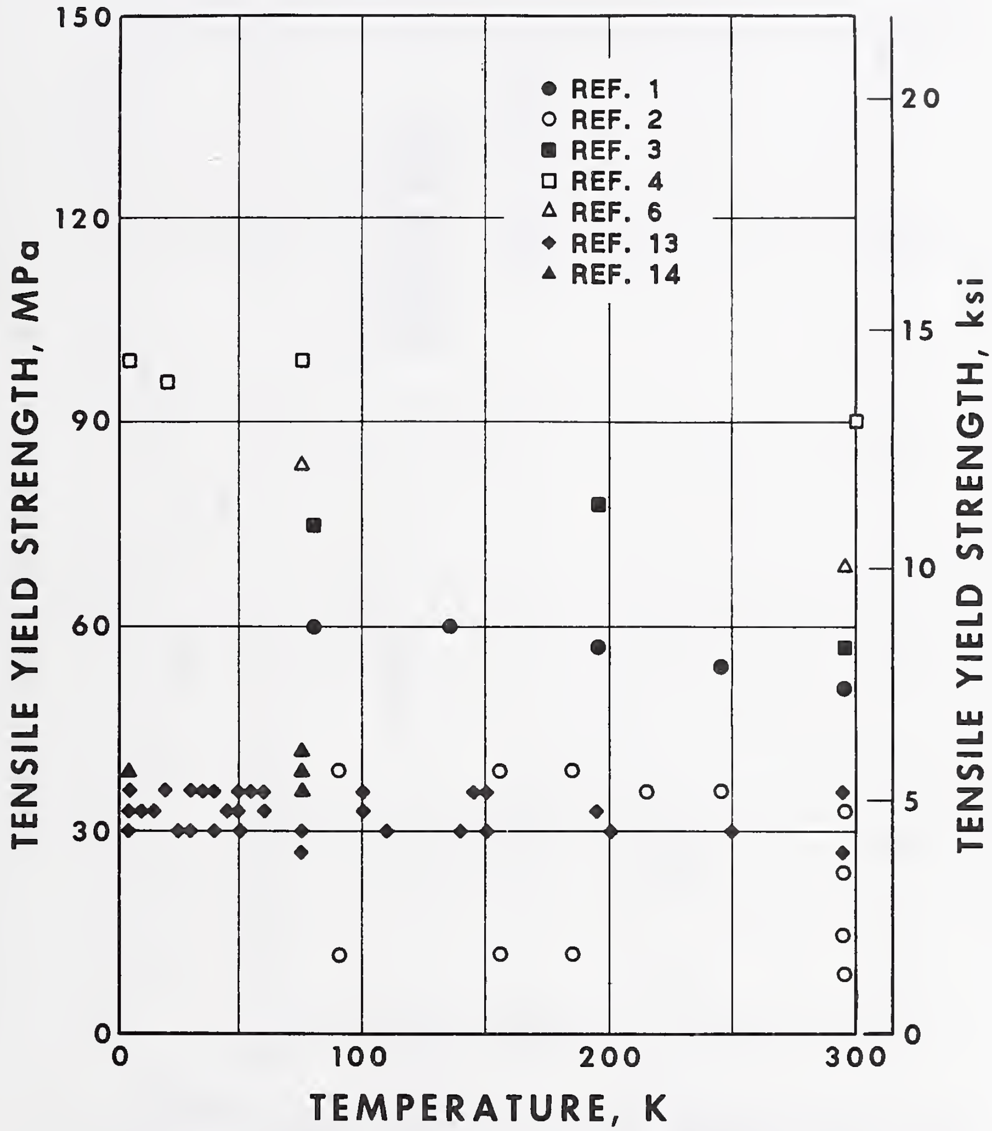

Figure 2.4. The data are shown as a function of temperature. The variation in grain size and impurity content obscures the dependence of tensile yield strength upon temperature that is given in Equation (2-2). For clarity, overlapping data points, including all points from Reference 2.5, are omitted from the figure. All data are presented in Table 2.2. Products were in plate, bar, and wire form.

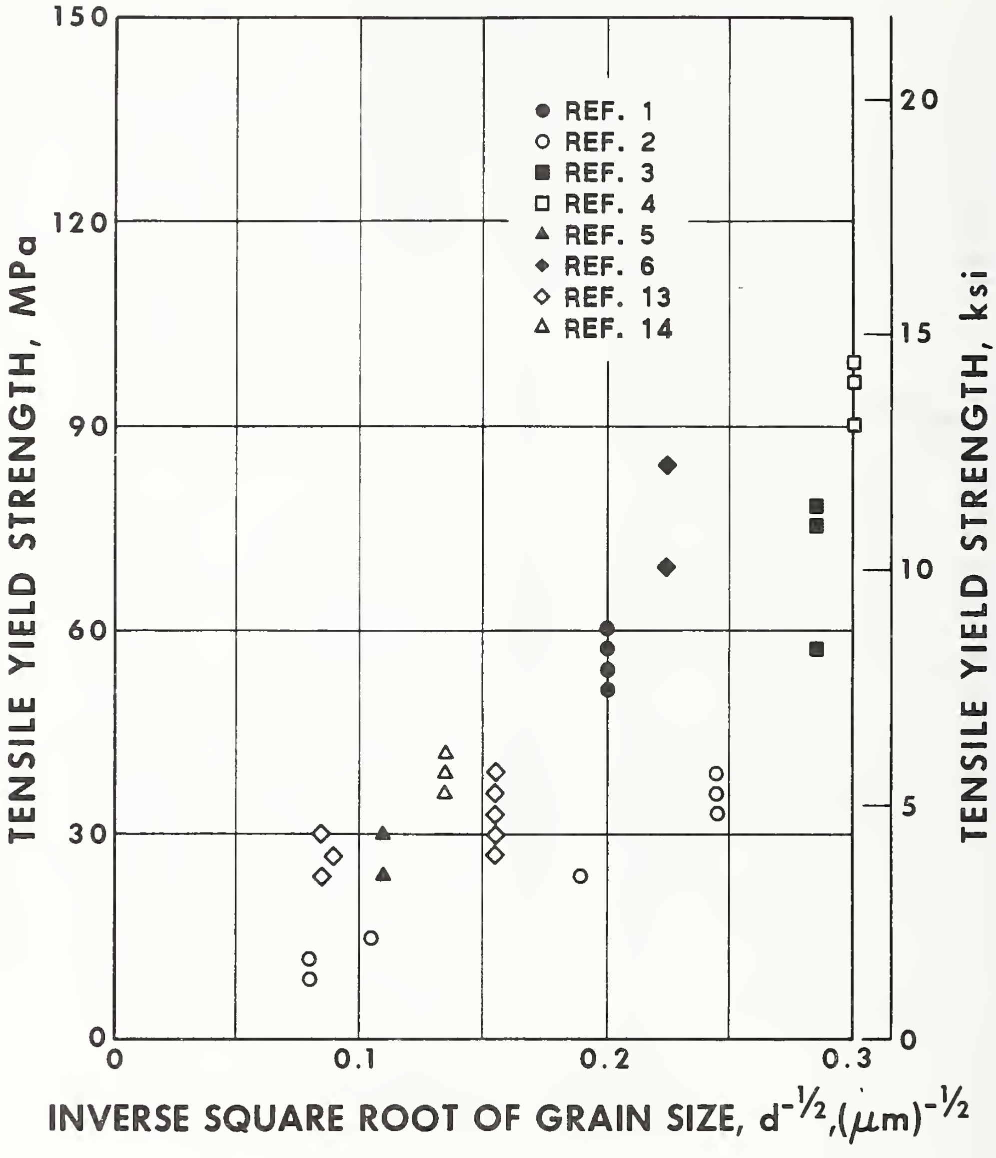

Figure 2.5. The data are shown as a function of the inverse square root of grain size ($d^{-1/2}$). The variation in temperature and impurity content obscures the dependence of tensile yield strength upon $d^{-1/2}$ that is given in Equation (2-2). For clarity, overlapping data points are omitted from the figure. All data are presented in Table 2.2. Products were in plate, bar, and wire form.

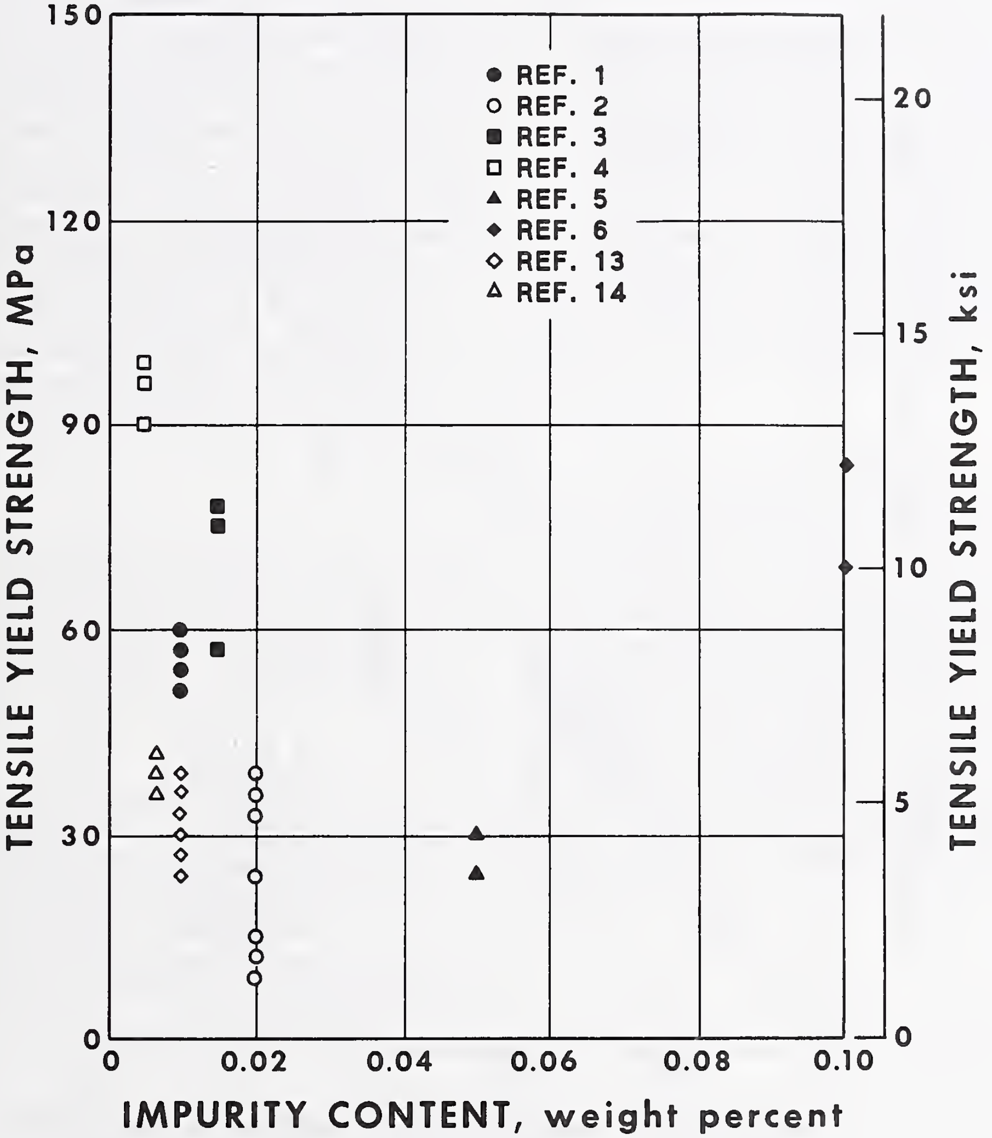

Figure 2.6. The data are shown as a function of impurity content. The variation in temperature and grain size obscures the dependence of tensile yield strength upon impurity content that is given in Equation (2-2). For clarity, overlapping data points are omitted from the figure. All data are presented in Table 2.2. Products were in plate, bar, and wire form.

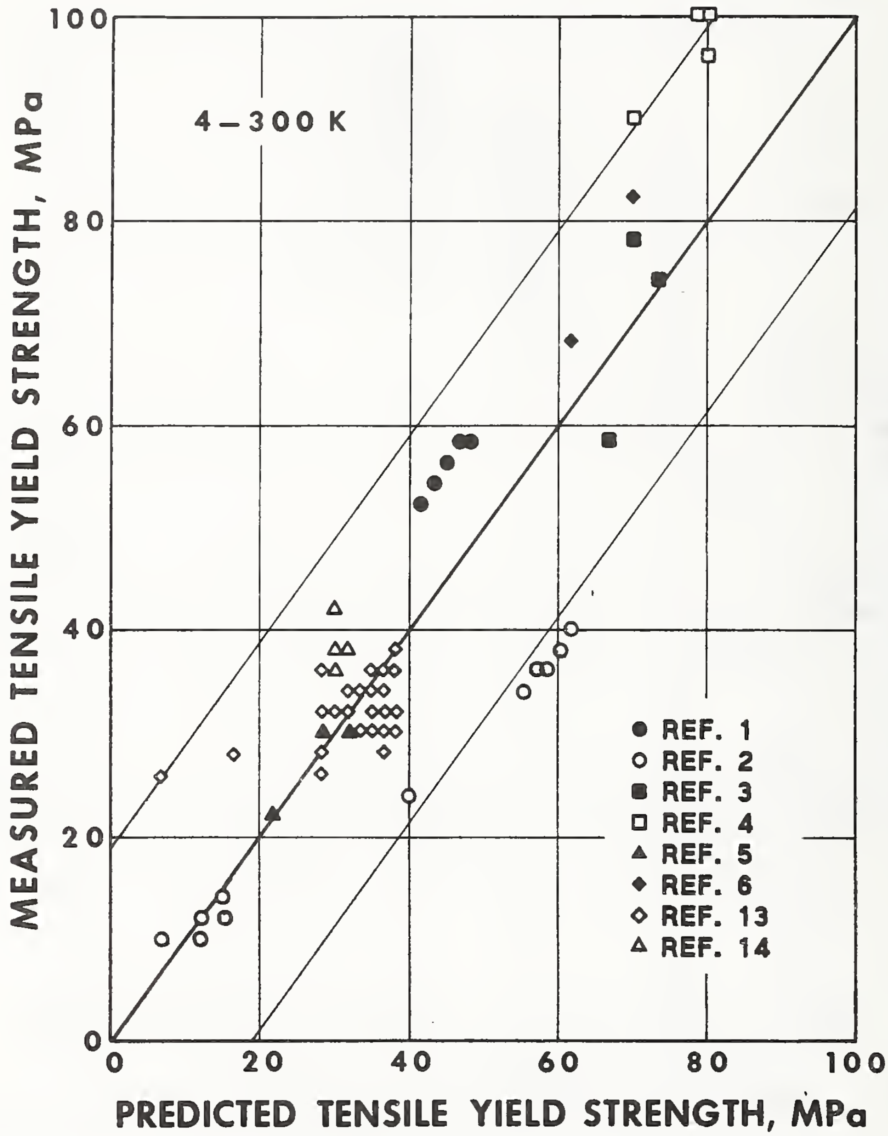

Figure 2.7. The data shown were used to compute the linear regression of tensile yield strength upon temperature, the inverse square root of the grain size, and impurity content [Equation (2-2)]. For clarity, overlapping data points are omitted from the figure. All data are presented in Table 2.2. Products were in plate, bar, and wire form.

DATA SOURCES AND ANALYSIS

A set of 204 measurements of tensile yield strength at 295 K was selected for analysis. Measurements were obtained from References 2.1–2.13 and 2.15–2.32. Products were in plate, bar, and wire form. In most cases, the actual percent reduction of thickness or area was specified, but in a few instances the percent reduction was obtained from standard tables of temper designation (see Table 1.17). The amount of cold work ranged up to 90%. Initially, data from rolled and drawn specimens were analyzed separately, but the regression coefficients were nearly the same, so all data were combined. Polynomial terms were included in the regression analysis because the dependence of tensile yield strength, σ_y, upon cold work, *CW*, is linear only for small amounts of *CW*.

RESULTS

The regression equation for the dependence of σ_y upon *CW* of less than 64% was found to be

$$\sigma_y = 63.5 + 10.1(CW) - 0.0798(CW)^2 \quad \text{(S.D. = 42 MPa)}, \tag{2-3}$$

where σ_y is in MPa, and *CW* is the percent of reduction of thickness or area. The standard deviations of the three coefficients are 4.4, 0.4, and 0.0048. A constant value of 384 MPa was used to represent σ_y for *CW* > 64%.

Table 2.3 presents the measured values of σ_y, the values of σ_y calculated from the regression equation, *CW* (reduction of thickness or area), and the reference number. The available characterization of materials and measurements is given in Table 2.10 at the end of the tensile properties section.

Figure 2.8 indicates the fit of the data to the combination of Equation (2-3) and a constant. Figure 2.9 presents these results in summary form. The scatter bands represent two standard deviations about the curves in Figures 2.8 and 2.9. The variance of the data about the curve was assumed to be normally distributed and constant throughout the range of the independent variable, *CW*, except that it was reduced to a smaller value for 0% *CW*, because σ_y for 0% *CW* is known to a higher accuracy (S.D. = 20 MPa).

DISCUSSION

Some of the data from Reference 2.17 fall outside the scatter band (Figure 2.8). The copper in these specimens is of very high purity; hence, some recovery may have occurred before the measurements were completed. These data were included to assist those who may require cold-worked copper of comparable purity. Variation in grain size also contributes to the scatter of the data; since grain size often was not reported in this data set, it could not be included in the regression analysis. For small amounts of *CW*, grain size may influence σ_u more than the degree of *CW*; an estimate may be obtained from Equation (2-1).

Table 2.3. Yield Strength Dependence on Cold Work (295 K).

Yield Strength, Measured, MPa	Yield Strength, Calculated, MPa	Cold Work, %	Reference No.
90.0	63.5	0	4
23.0	63.5	0	1
69.0	63.5	0	6
52.0	63.5	0	1
34.5	63.5	0	2
10.3	63.5	0	2
15.0	63.5	0	2
24.0	63.5	0	2

Table 2.3, continued

Yield Strength, Measured, MPa	Yield Strength, Calculated, MPa	Cold Work, %	Reference No.
63.0	63.5	0	8
27.0	63.5	0	13
32.1	63.5	0	13
25.0	63.5	0	13
27.3	63.5	0	13
36.1	63.5	0	13
54.0	63.5	0	8
62.0	63.5	0	8
29.1	63.5	0	8
38.9	63.5	0	8
33.3	63.5	0	8
39.2	63.5	0	8
31.7	63.5	0	8
32.2	63.5	0	8
31.7	63.5	0	8
50.7	63.5	0	8
37.8	63.5	0	8
34.8	63.5	0	8
33.8	63.5	0	8
40.6	63.5	0	8
33.0	63.5	0	9
34.8	63.5	0	8
47.3	63.5	0	8
33.9	63.5	0	8
36.1	63.5	0	8
21.9	63.5	0	8
73.5	63.5	0	8
39.2	63.5	0	8
20.8	63.5	0	8
25.0	63.5	0	8
73.4	63.5	0	12
39.2	63.5	0	11
31.8	63.5	0	31
78.8	63.5	0	12
40.0	63.5	0	12
14.8	63.5	0	12
63.0	63.5	0	12
21.9	63.5	0	12
73.5	63.5	0	20
34.8	63.5	0	22
46.0	63.5	0	31
14.0	63.5	0	30
31.7	63.5	0	31
39.2	63.5	0	21
54.0	63.5	0	22
82.7	63.5	0	22
45.0	63.5	0	20
34.0	63.5	0	21
45.0	63.5	0	25
48.0	63.5	0	25
62.0	63.5	0	25

C10100–C10700: Cold-worked

Tensile Yield Strength vs. Cold Work (295 K)

Table 2.3, continued

Yield Strength, Measured, MPa	Yield Strength, Calculated, MPa	Cold Work, %	Reference No.
50.0	63.5	0	28
40.0	63.5	0	27
59.0	63.5	0	27
52.3	63.5	0	28
51.7	63.5	0	32
52.3	63.5	0	32
67.0	63.5	0	20
41.0	63.5	0	18
86.2	63.5	0	18
103	63.5	0	18
75.8	63.5	0	18
40.0	63.5	0	18
106	73.6	1	27
113	63.5	[illegible]	27
137	97.0	9.4	27
130	103	4	27
101	112	[illegible]	28
103	112	[illegible]	28
107	112	[illegible]	28
101	112	[illegible]	28
101	112	[illegible]	27
103	121	6	18
228	121	6	28
181	121	6	27
194	125	9.4	27
189	130	[illegible]	27
196	139	8	28
228	144	8.5	28
205	144	8.5	28
189	148	9	32
174	148	9	32
220	152	9.4	27
230	152	9.4	28
228	155	9.4	27
209	157	10	18
296	157	10	32
207	157	10	32
228	157	10	27
196	165	11	20
331	165	11	18
207	165	11	18
231	165	11	18
196	165	11	18
189	225	18	17
242	225	19	32
228	225	19	32
260	234	20	28
296	234	20	28
307	234	20	28
296	234	20	28
304	238	21	25

Table 2.3, continued

Yield Strength, Measured, MPa	Yield Strength, Calculated, MPa	Cold Work, %	Reference No.
314	239	21	25
359	239	21	18
252	239	21	18
265	239	21	18
252	239	21	18
147	241	21	30
275	241	21	5
268	241	21	5
290	267	29	18
265	267	29	18
269	267	29	30
265	267	29	30
287	239	29	32
265	290	29	32
338	267	29	26
365	290	29	18
279	239	29	18
341	292	29	18
290	292	29	18
316	239	30	28
314	239	30	25
321	290	30	28
190	239	34	17
341	341	38	20
376	315	34	21
323	329	36	28
324	329	37	31
342	329	37	5
342	329	37	5
265	329	37	25
338	329	37	25
365	329	38	25
372	330	37	18
323	341	38	18
365	330	34	18
341	330	38	18
313	330	39	32
317	341	34	30
347	341	40	18
348	341	40	18
338	341	40	25
341	341	40	28
340	341	40	25
205	341	40	28
376	354	44	17
321	354	44	18
365	354	44	18
321	354	44	18
330	363	47	18
334	366	48	23
337	366	48	32

Table 2.3, continued

Yield Strength, Measured, MPa	Yield Strength, Calculated, MPa	Cold Work, %	Reference No.
325	384	50	32
381	384	89	18
386	370	50	32
379	384	56	30
334	370	50	18
372	370	56	18
331	370	50	18
379	384	56	18
341	384	56	18
372	384	56	18
383	370	58	18
386	384	56	32
350	383	59	32
379	384	56	18
305	370	50	18
379	384	61	18
362	384	61	18
379	384	61	18
305	384	61	18
386	384	56	18
362	370	50	18
379	384	65	18
362	384	50	18
386	384	56	23
390	384	59	18
372	384	56	18
383	384	59	18
355	384	56	18
345	384	70	21
305	384	70	18
372	384	73	32
381	384	70	32
305	384	70	18
379	384	61	32
386	384	76	18
379	384	61	23
350	384	50	18
381	384	61	22
455	384	50	25
453	384	61	25
385	384	59	18
385	384	89	32
405	384	90	17

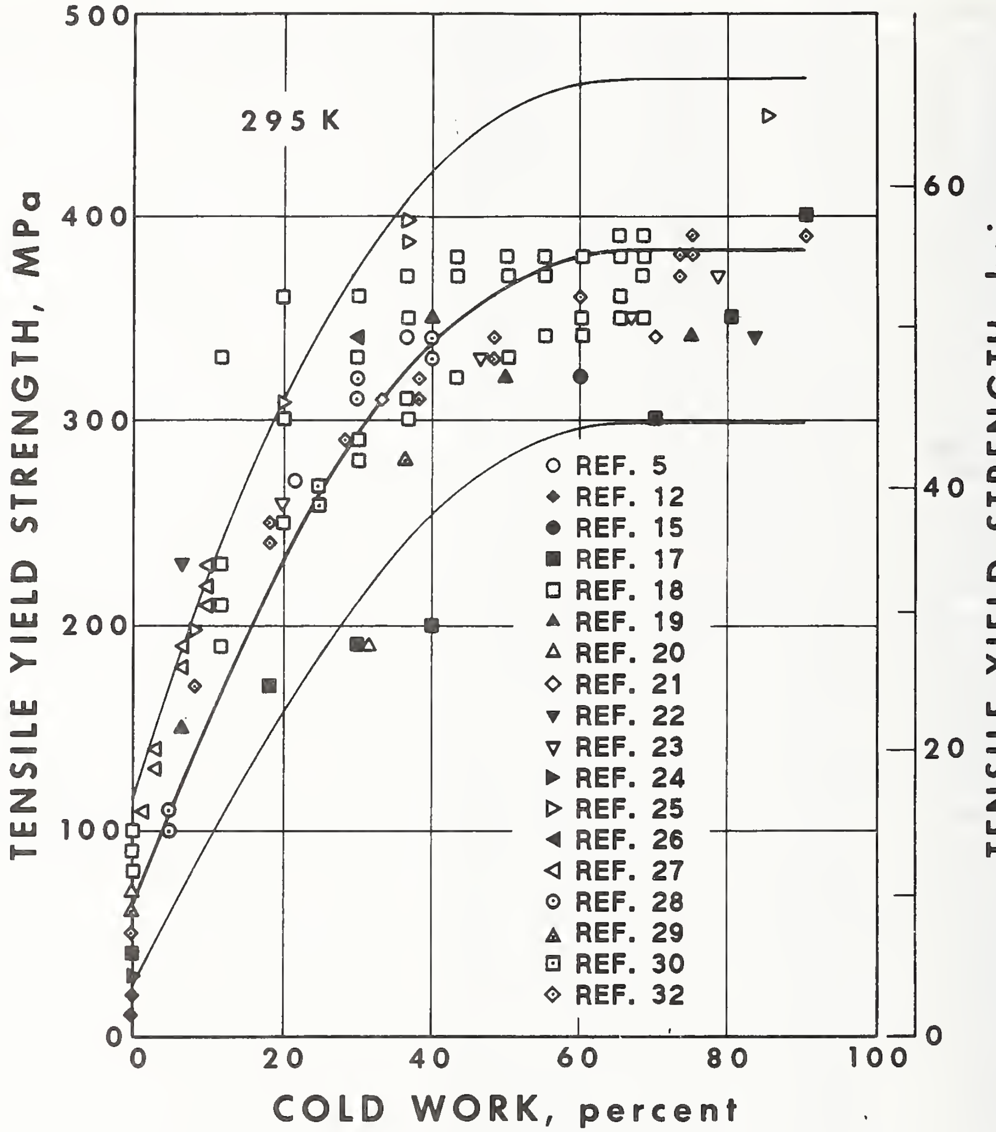

Figure 2.8. The data shown were used to compute the linear regression curve of tensile yield strength at 295 K upon cold work [Equation (2-3)]. For clarity, all data points from References 2.1–2.4, 2.6–2.11, 2.13, 2.16, and 2.31 and were omitted from the plot and overlapping data points from other references were also omitted. All data are presented in Table 2.3. Products were in plate, bar, and wire form.

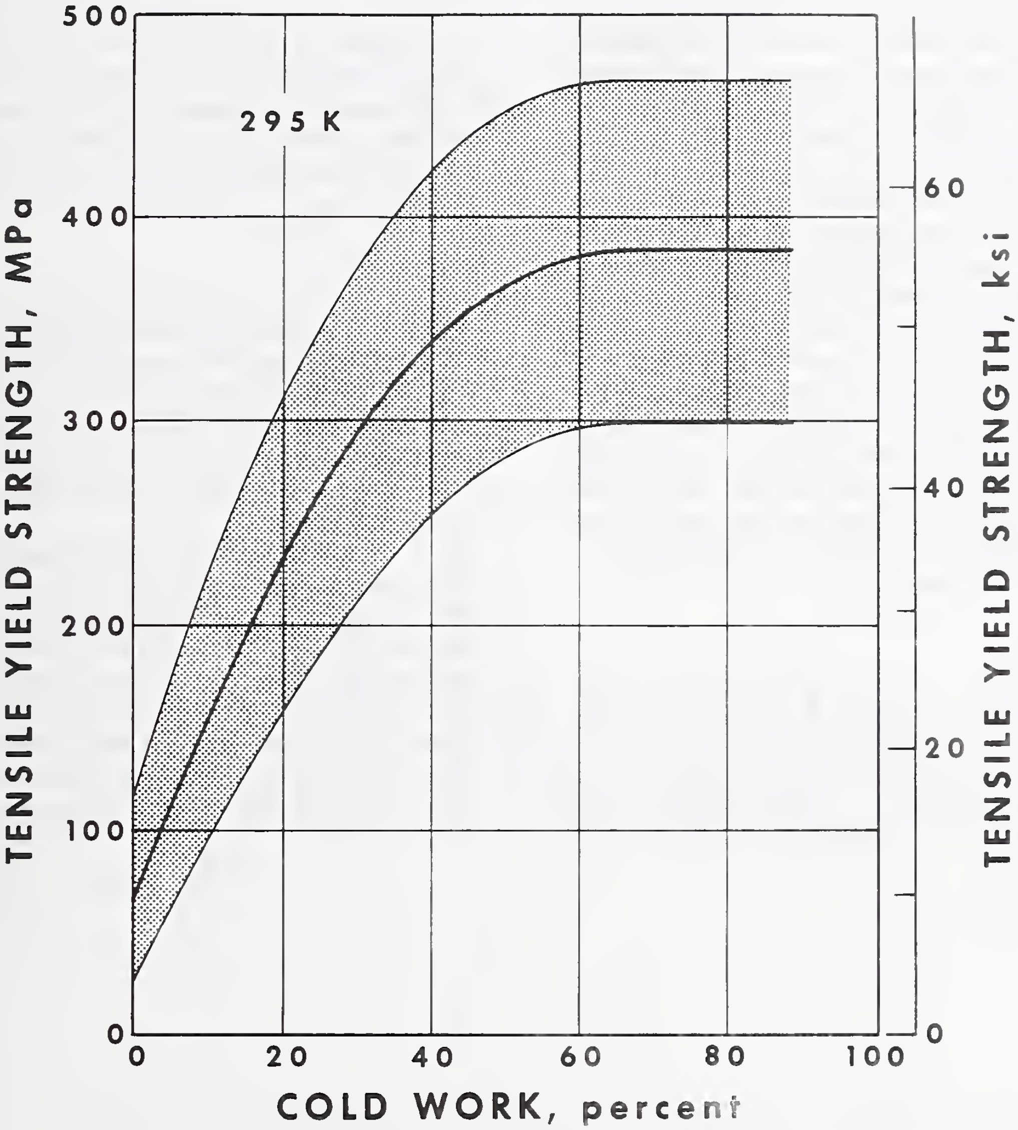

Figure 2.9. Tensile yield strength dependence upon cold work at 295 K. The scatter band represents two standard deviations about a second-order regression curve based upon 204 measurements of yield strength for a range of cold work from 0 to 90%. The regression equation is

$$\sigma_y \text{ (MPa)} = 63.5 + 10.1(CW) - 0.0798(CW)^2 \qquad (CW \leq 64\%) \quad (\text{S.D.} = 42 \text{ MPa}),$$

$$\sigma_y \text{ (MPa)} = 384 \qquad (CW > 64\%),$$

where (*CW*) is the percent of cold work (reduction of thickness or area). Products were in plate, bar, and wire form.

DATA SOURCES AND ANALYSIS

Figure 2.10 presents data from References 2.28, 2.33, and 2.34 on cold-worked coppers of different silver content. These are the only data available to estimate the variation in tensile yield strength, σ_y, with silver content, [Ag]. The mean reported values for the 0.2%-offset σ_y are shown in Figure 2.10. The available characterization of materials and measurements is given in Table 2.10 at the end of the tensile properties section. Measurements reported in Reference 2.28 were taken on square wire of initial dimensions (before rolling) of 0.63 cm x 0.63 cm. The thickness of the 40% cold-rolled plate used for the measurements reported in Reference 2.33 was 1.3 cm, but specimen thickness was 0.63 cm. This was the only material that was cold worked by a manufacturer. Plate thickness before rolling was 1.3 cm for the specimens used in the measurements reported in Reference 2.34.

RESULTS

As [Ag] is increased up to 0.085 wt%, the variation in σ_y is about 10%, for a given level of cold work. This estimate of the variation is based upon measurements of σ_y reported from different laboratories over a range of [Ag] values. However, a variation of 5% was reported in Reference 2.33 for different measurements of σ_y (at 0.5% strain) on the same heat of C10700 at one laboratory. Therefore, part of the 10% variation of σ_y observed when [Ag] ranges within the C10100 to C10700 specifications may simply be due to lack of reproducibility. The improvement in σ_y with cold work saturates at about 40 to 50% for all values of [Ag].

DISCUSSION

Ornstein (Reference 2.59) reported an increase of 2% from 310 to about 317 MPa in σ_y as [Ag] was increased from 0.03 wt% (C10400, C10500) to 0.85 wt% (C10700). Actual data points were not given, and the method of measuring σ_y was not specified. Specimens were cold worked 50%.

Although increases in [Ag] in the range considered here do not affect the tensile properties appreciably, increased resistance to creep has been reported for similar increases in [Ag] (see Reference 2.28 and the section on creep in this publication.) However, this effect has been studied only at temperatures above 573 K and it is not known whether the same mechanisms control creep in the cryogenic temperature range.

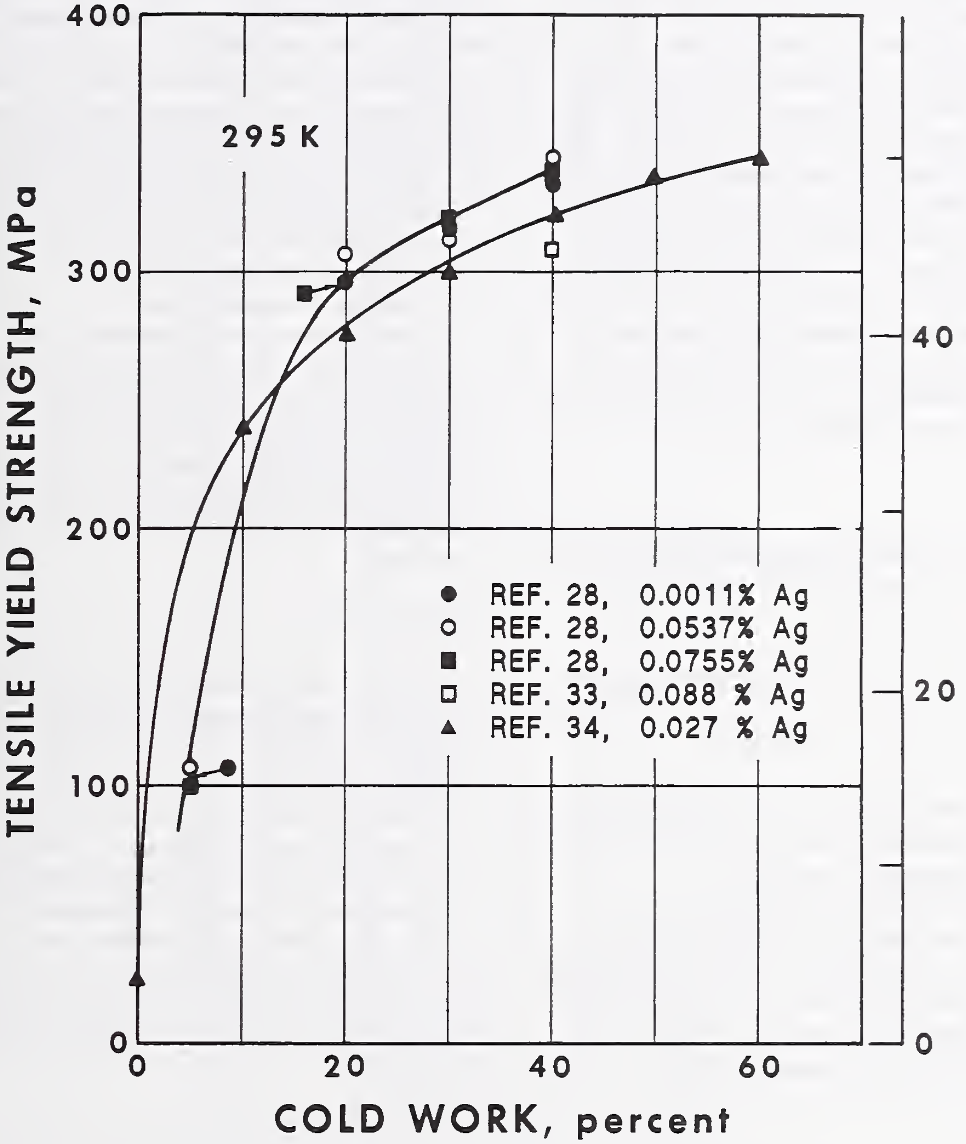

Figure 2.10. These data indicate that the yield strength of cold-worked copper is not strongly dependent on silver content. (Silver content is unspecified for C10100, ≥ 0.027 wt% for C10400, ≥ 0.034 wt% for C10500, and ≥ 0.085 wt% for C10700.) Products were in plate (References 2.33 and 2.34) and wire-bar form (Reference 2.28).

DATA SOURCES AND ANALYSIS

A set of 74 measurements of tensile yield strength from 4 to 300 K was selected for analysis. Products were in plate, bar, and sheet form. In most cases, the actual percent reduction of thickness or area was specified, but in a few instances, the percent reduction was obtained from standard tables of temper designation (see Table 1.17). The amount of cold work, *CW*, (reduction of thickness or area) ranged up to 60%. Regression coefficients at 295 K were insensitive to the type of *CW*; hence, data for all methods of *CW* were combined. This data set (References 2.5, 2.15–2.16, 2.19, and 2.35–2.37) was used in regression analysis of tensile yield strength (σ_y) upon temperature (T) and *CW*. Because of the nonlinear dependence of σ_y upon *CW*, polynomial terms were included in the analysis.

RESULTS

Regression analysis indicated that the best fit to the data was obtained with the following equation:

$$\sigma_y = 124 - 0.241T + 14.1(CW) - 0.166(CW)^2 \quad (2\text{-}4)$$

$$(\text{S.D.} = 32\ \text{MPa}),$$

where σ_y is in MPa, 4 K $\leq T \leq$ 300 K, and *CW* is in percent. The standard deviations of the four coefficients are 9, 0.035, 0.7, and 0.011.

Table 2.4 presents the measured values of σ_y, the values calculated from the regression equation, the temperature, *CW*, and the reference number. The available characterization of materials and measurements is given in Table 2.10 at the end of the tensile properties section.

Figure 2.11 depicts the data as a function of T only, for all levels of *CW*. Figure 2.12 depicts the data as a function of *CW* only, without showing the T dependence. It is evident from the large amount of scatter in Figures 2.11 and 2.12 that separate regression equations for σ_y as a function of each variable, T and *CW*, would not be of much value. However, when multivariate regression is use to analyze the data set, a relatively small standard deviation of 32 MPa is obtained. Figure 2.13 presents recent measurements at 4, 76, and 295 K on C10400 plate, which show the variation in σ_y with both T and *CW*. (These data were not available when the regression analysis was carried out.)

Figure 2.14 indicates the fit of the data set to Equation (2-4). The scatter band represents two standard deviations about the line that corresponds to complete agreement between measured and predicted values of σ_y. The variance of the data was assumed to be normally distributed and constant throughout the range of the predicted values.

DISCUSSION

The T dependence for cold-worked material is, as expected, larger than that of the annealed material; in Equation (2-2), the T coefficient is 0.0329. A second-order term is necessary to fit the observed dependence of σ_y upon *CW*: this dependence tends to saturate, as shown in Figure 2.12, in which the smaller T dependence is neglected and the data are plotted as a function of *CW* only. The agreement between the coefficients of *CW* dependence with those obtained at 295 K [Equation (2-3)] is satisfactory because the data were obtained from a wide variety of sources.

Table 2.4. Yield Strength Dependence on Cold Work (4–300 K).

Yield Strength, Measured, MPa	Yield Strength, Calculated, MPa	Test Temperature, K	Cold Work, %	Reference No.
404	394	4	60	16
30.5	123	4	0	5
432	431	4	37	5
431	431	4	37	5
326	353	4	21	5

Table 2.4, continued

Yield Strength, Measured, MPa	Yield Strength, Calculated, MPa	Test Temperature, K	Cold Work, %	Reference No.
331	353	4	21	5
90.0	123	4	0	35
378	191	4	[illegible]	35
325	251	4	12	35
375	302	4	15	35
425	381	4	25	35
465	191	4	60	35
421	427	20	37	35
441	427	20	37	35
404	194	20	60	19
207	251	72	12	37
404	413	76	37	36
421	413	76	37	35
385	377	76	60	19
30.5	105	76	0	5
404	413	76	37	5
401	413	76	37	5
385	194	76	21	5
378	376	77	60	19
83.3	105	77	0	19
66.0	105	77	0	19
82.7	105	77	0	19
63.6	105	77	0	19
209	105	4	0	19
209	186	77	6	19
194	185	77	6	19
196	186	4	6	19
155	186	4	6	19
378	185	198	37	35
385	385	198	37	35
378	348	198	60	19
216	209	198	12	437
201	201	198	12	37
194	209	198	12	37
191	209	198	12	37
75.8	74.3	205	0	19
66.0	74.3	205	0	19
83.3	74.3	205	0	19
66.0	74.3	205	0	19
194	105	205	6	19
176	155	205	6	19
194	105	205	6	19
152	155	205	6	19
194	214	205	12	37
87.1	67.5	233	0	19
77.9	67.5	233	0	19
66.0	67.5	233	0	19
83.3	67.5	233	0	19
183	148	233	6	19
163	148	233	6	19
157	148	233	6	19

Table 2.4, continued

Yield Strength, Measured, MPa	Yield Strength, Calculated, MPa	Test Temperature, K	Cold Work, %	Reference No.
139	148	233	6	19
188	208	297	12	37
323	324	295	60	19
23.0	52.5	295	0	5
342	361	295	37	5
342	361	295	37	5
275	283	295	21	5
283	283	295	21	5
73.3	52.1	297	0	19
63.0	52.1	297	0	19
78.0	52.1	297	0	19
79.4	52.1	297	0	19
173	139	297	6	19
188	133	297	6	19
148	139	297	6	19
131	133	297	6	19
316	322	300	60	19
338	359	300	37	36
338	359	300	37	36

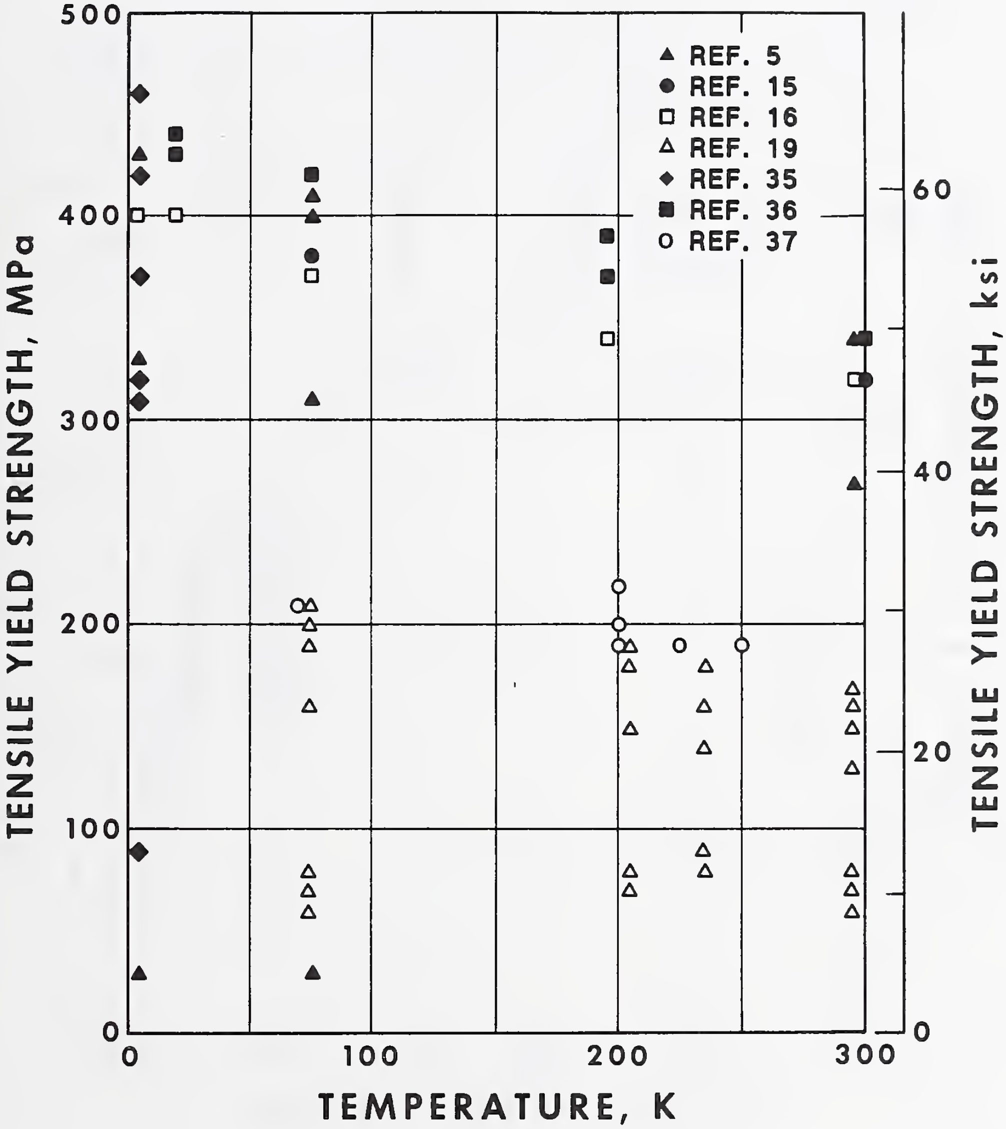

Figure 2.11. The data are shown as a function of temperature for all levels of cold work. The variation in cold work obscures the dependence of tensile yield strength upon temperature that is given in Equation (2-4). For clarity, overlapping data points are omitted from the figure. All data are presented in Table 2.4. Products were in plate, bar, and sheet form.

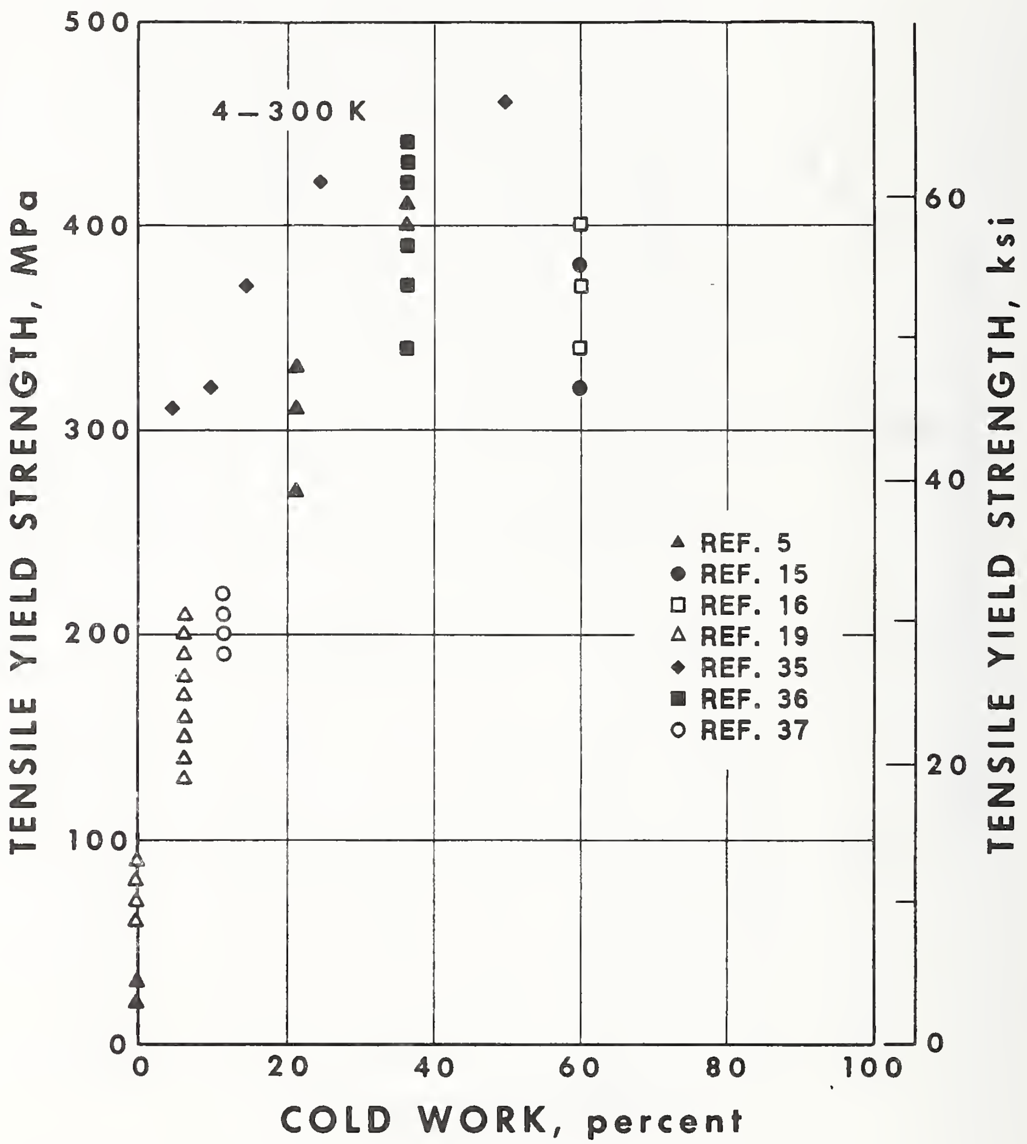

Figure 2.12. The data over the 4 to 300 K temperature range are shown as a function of cold work. The variation in temperature somewhat obscures the dependence of tensile yield strength upon cold work that is given in Equation (2-4). For clarity, overlapping data points are omitted from the figure. All data are presented in Table 2.4. Products were in plate, bar, and wire form.

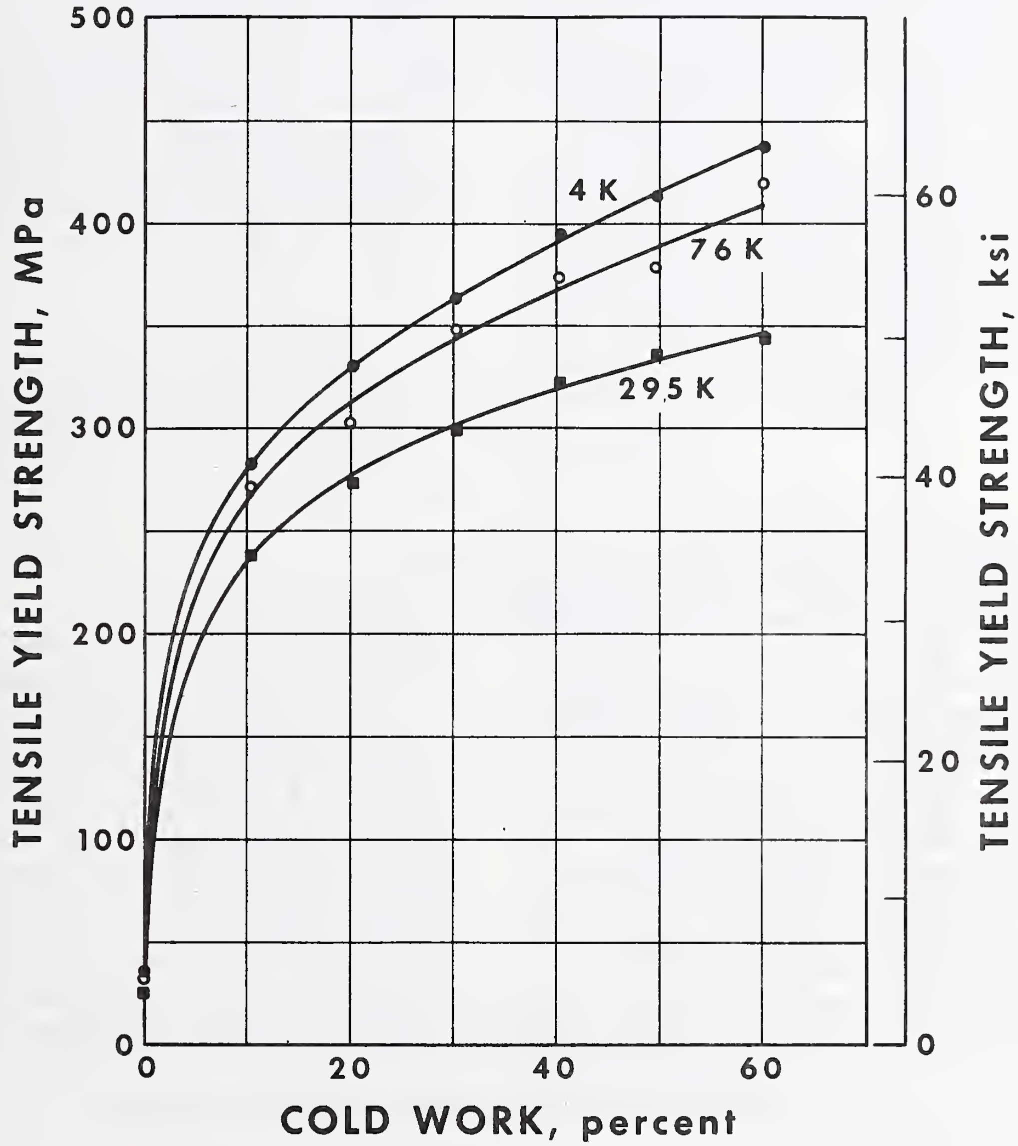

Figure 2.13. These data from Reference 2.34 indicate the increase of tensile yield strength with increased cold work or lowered temperature (C10400 plate).

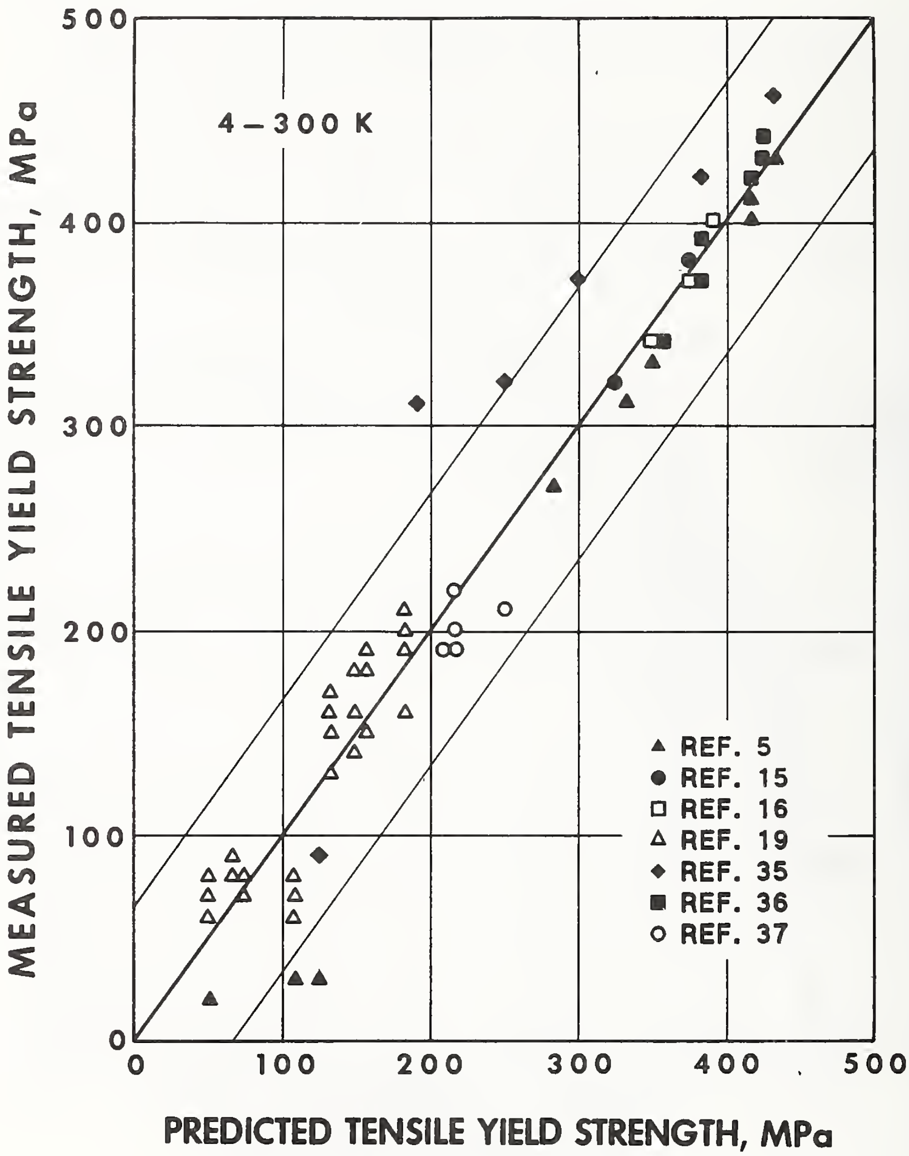

Figure 2.14. The data shown were used to compute the regression of tensile yield strength upon temperature and cold work [Equation (2-4)]. For clarity, overlapping data points are omitted from the figure. All data are presented in Table 2.4. Products were in plate, bar, and sheet form.

DATA SOURCES AND ANALYSIS

A set of 92 measurements of ultimate tensile strength from 4 to 300 K was selected for analysis because grain size and impurity content were reported. Grain size, d, ranged from 11 to 90 μm, and impurity content, [I], from 0.0012 to 0.040 wt%. Products were in bar, sheet, and wire form. This data set (References 2.1, 2.3–2.6, 2.14, 2.19, 2.38–2.39) was used in regression analysis of ultimate tensile strength (σ_u) on three variables, temperature (T), d, and [I]. Data on the variation of σ_u with silver content are presented on pages 2-42 and 2-43 (cold-worked copper).

RESULTS

Regression analysis indicated that the best fit to the data was obtained by including a second-order term in T, and by representing the grain-size dependence with a $d^{-1/2}$ term:

$$\sigma_u = 419 - 1.19T + 0.00144T^2 + 156\, d^{-1/2} \quad \text{(S.D. = 18 MPa)}, \tag{2-5}$$

where σ_u is in MPa, $4\ K \le T \le 300$ K, and d is in μm. The standard deviations of the four coefficients are 8, 0.08, 0.00025, and 27.

Table 2.5 presents the measured values of σ_u, the values of σ_u calculated from the regression equation, the temperature, $d^{-1/2}$, and the reference number. The available characterization of materials and measurements is given in Table 2.10 at the end of the tensile properties section.

Figures 2.15 and 2.16 present the data as a function of each variable, T and d, separately. Figure 2.15 depicts the data as a function of T only, without showing the dependence upon d. Figure 2.16 depicts the data as a function of $d^{-1/2}$ only, without showing the T dependence. The data are not shown plotted against [I] because no effect was observed (see Discussion). It is clear from the large amount of scatter in Figures 2.15 and 2.16 that separate regression equations for σ_u as a function of each variable, T and $d^{-1/2}$, would not be of much value. However, when multivariate regression is used to analyze the data set, a relatively small standard deviation of 18 MPa is obtained.

Figure 2.17 indicates the fit of the data to the multivariate regression expression, Equation (2-5). The scatter band represents two standard deviations about the line that corresponds to complete agreement between measured and predicted values of σ_u. The variance of the data about the line was assumed to be normally distributed and constant throughout the range of the predicted values.

DISCUSSION

The T coefficient for σ_u of annealed material is much larger than that found for the yield strength [Equation (2-2)]. The coefficient for $d^{-1/2}$ can change significantly with the addition or subtraction of a few influential points to the data set so the accuracy of this coefficient may not be as high as indicated by the standard deviation of the coefficient. Also, this coefficient is determined as an average over the range 4 to 300 K, although it apparently increases somewhat as T decreases. Not enough low-T data over a sufficient range of d were available to determine the coefficient at 77 and 4 K, but a separate determination from the data at 295 K gave a coefficient of 85 ± 34.

The absence of an observable effect of [I] could be due to inconsistent methods of determining and reporting this variable in the different sources of data.

Table 2.5. Tensile Strength Dependence on Grain Size (4–300 K).

Tensile Strength, Measured, MPa	Tensile Strength, Calculated, MPa	Test Temperature, K	(Grain Size)$^{-1/2}$, 10^3 m$^{-1/2}$	Reference No.
410	431	4	0.112	5
460	461	4	0.302	1
393	435	77	0.137	14
420	415	76	0.124	39
426	415	76	0.124	38
423	415	20	0.124	39
413	415	20	0.124	38
410	415	76	0.124	39
465	429	76	0.289	38
462	429	30	0.289	38
445	429	76	0.289	238
415	429	30	0.289	39
459	424	30	0.258	38
433	424	30	0.258	39
441	413	76	0.183	38
426	407	30	0.149	39
336	357	76	0.112	5
375	384	76	0.302	4
366	356	76	0.124	38
393	356	76	0.124	39
362	359	76	0.124	38
361	356	76	0.124	39
352	356	76	0.124	38
355	358	76	0.124	39
366	373	77	0.289	5
390	358	77	0.137	14
322	357	77	0.137	14
381	358	4	0.137	14
352	359	77	0.149	19
343	358	4	0.144	19
352	359	77	0.149	14
300	358	4	0.144	19
355	366	76	0.2	1
375	379	76	0.289	1
390	373	85	0.289	38
386	373	76	0.289	39
365	373	85	0.289	38
362	373	76	0.289	38
376	368	76	0.289	38
381	356	30	0.183	38
359	344	85	0.149	38
300	384	133	0.2	1
334	318	150	0.289	38
381	384	150	0.289	38
321	313	150	0.289	38
302	301	150	0.149	39
307	296	150	0.149	38
269	273	133	0.2	1
232	286	195	0.283	3
268	261	195	0.124	39
272	261	195	0.124	39

Table 2.5, continued

Tensile Strength, Measured, MPa	Tensile Strength, Calculated, MPa	Test Temperature, K	$(\text{Grain Size})^{-1/2}$, $10^3\ m^{-1/2}$	Reference No.
211	261	195	0.124	38
270	261	195	0.124	38
265	261	195	0.124	38
303	280	295	0.289	38
258	276	295	0.258	38
283	264	295	0.183	38
258	259	295	0.149	19
283	264	295	0.144	19
258	259	205	0.149	19
254	258	295	0.144	19
241	211	233	0.149	19
241	242	233	0.144	19
244	243	293	0.149	19
240	242	233	0.144	19
248	246	243	0.2	1
187	288	233	0.289	3
235	229	293	0.224	6
205	211	295	0.112	5
224	213	295	0.124	38
224	243	295	0.124	38
224	211	295	0.124	38
205	213	295	0.124	38
245	211	295	0.124	38
205	280	295	0.2	1
213	216	297	0.149	19
211	215	297	0.144	19
211	216	297	0.149	19
205	215	297	0.144	19
213	237	300	0.289	38
241	237	300	0.289	38
234	237	300	0.289	38
222	288	300	0.289	38
245	237	300	0.289	38
241	237	300	0.289	38
213	237	300	0.289	38
238	288	300	0.289	38
234	232	300	0.258	38
231	232	300	0.258	38
214	208	300	0.105	38
221	208	300	0.105	38
240	239	300	0.302	4

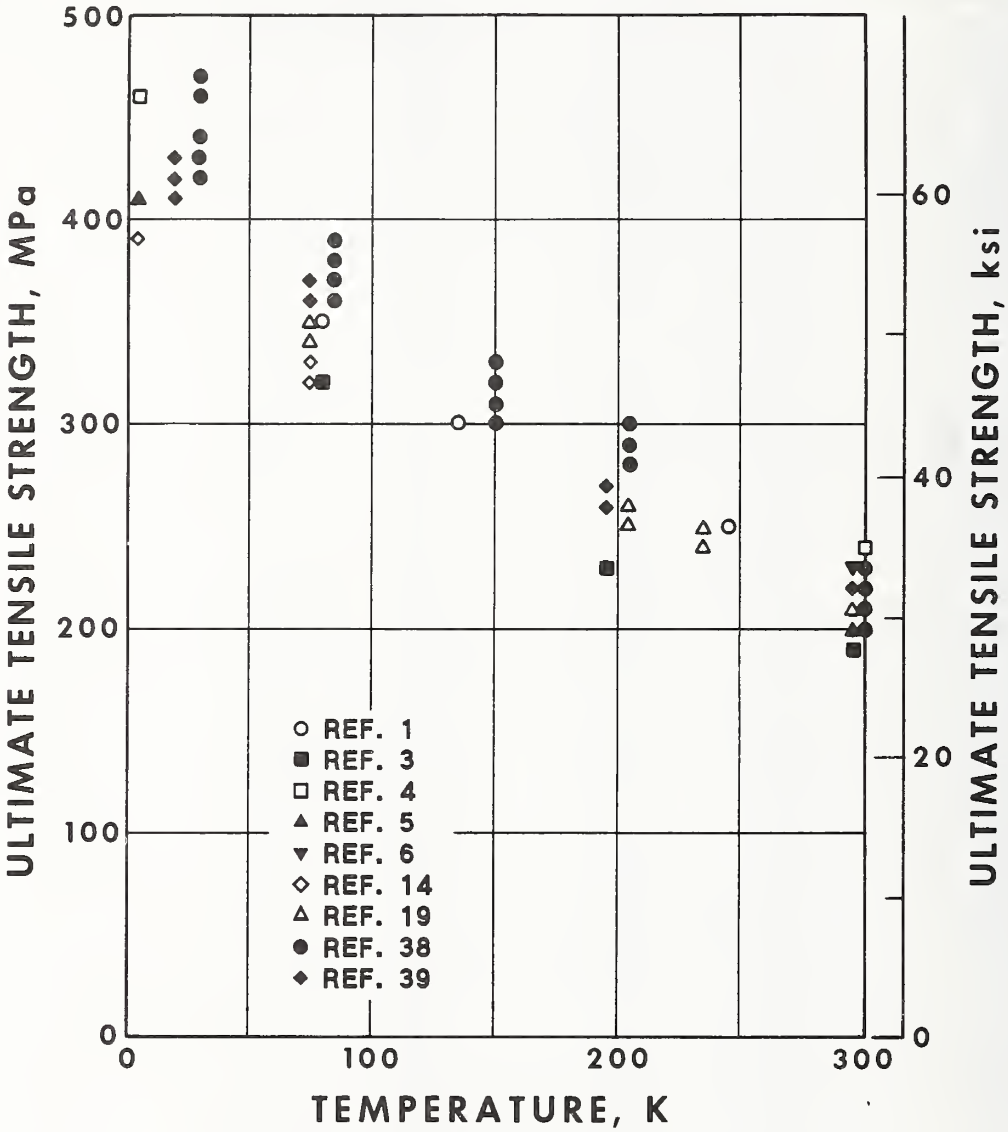

Figure 2.15. The data are shown as a function of temperature. The variation in grain size somewhat obscures the dependence of ultimate tensile strength upon temperature that is given in Equation (2-5). For clarity, overlapping data points are omitted from the figure. All data are presented in Table 2.5. Products were in bar, sheet, and wire form.

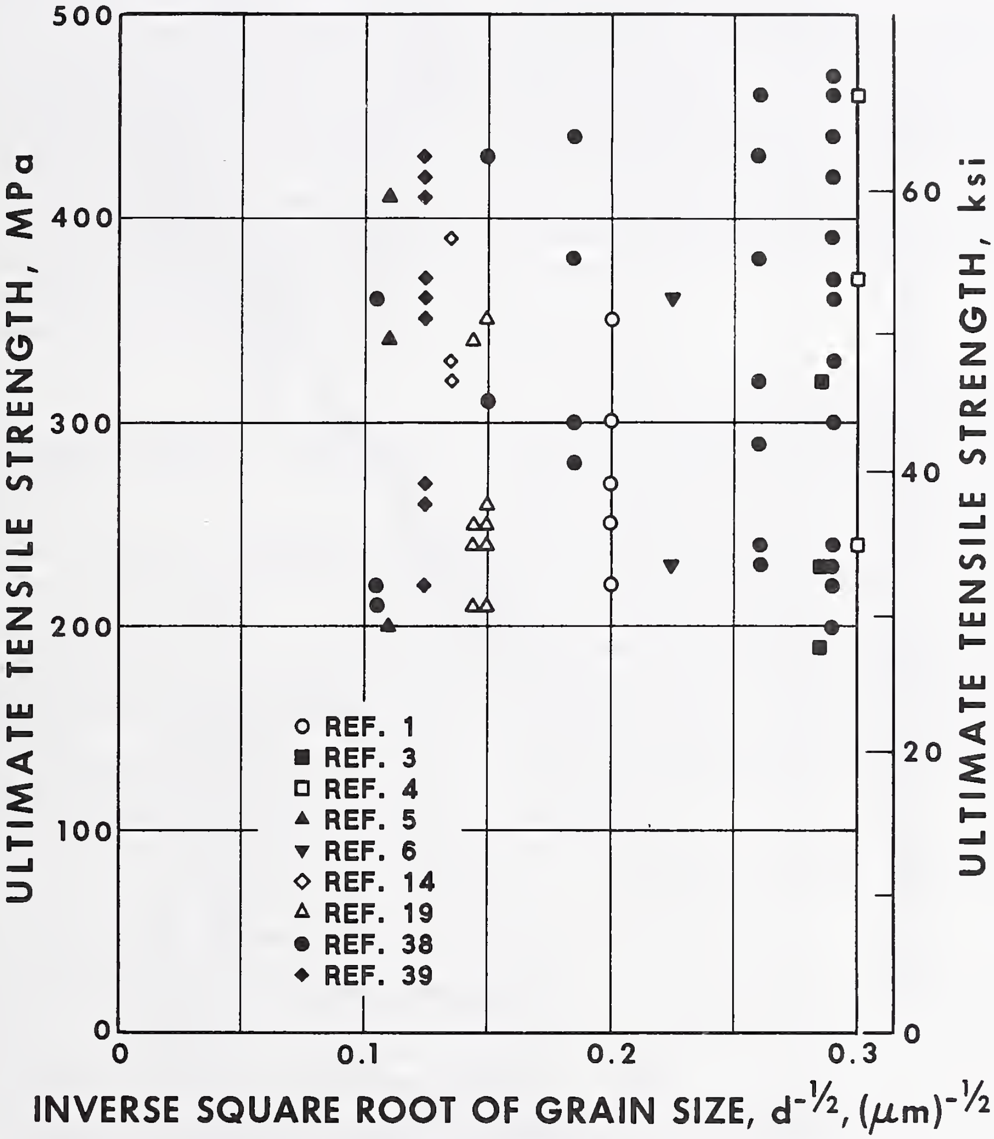

Figure 2.16. The data are shown as a function of the inverse square root of grain size, $d^{-1/2}$. The variation in temperature obscures the dependence of ultimate tensile strength upon $d^{-1/2}$ that is given in Equation (2-5). For clarity, overlapping data points are omitted from the figure. All data are presented in Table 2.5. Products were in plate, sheet, and wire form.

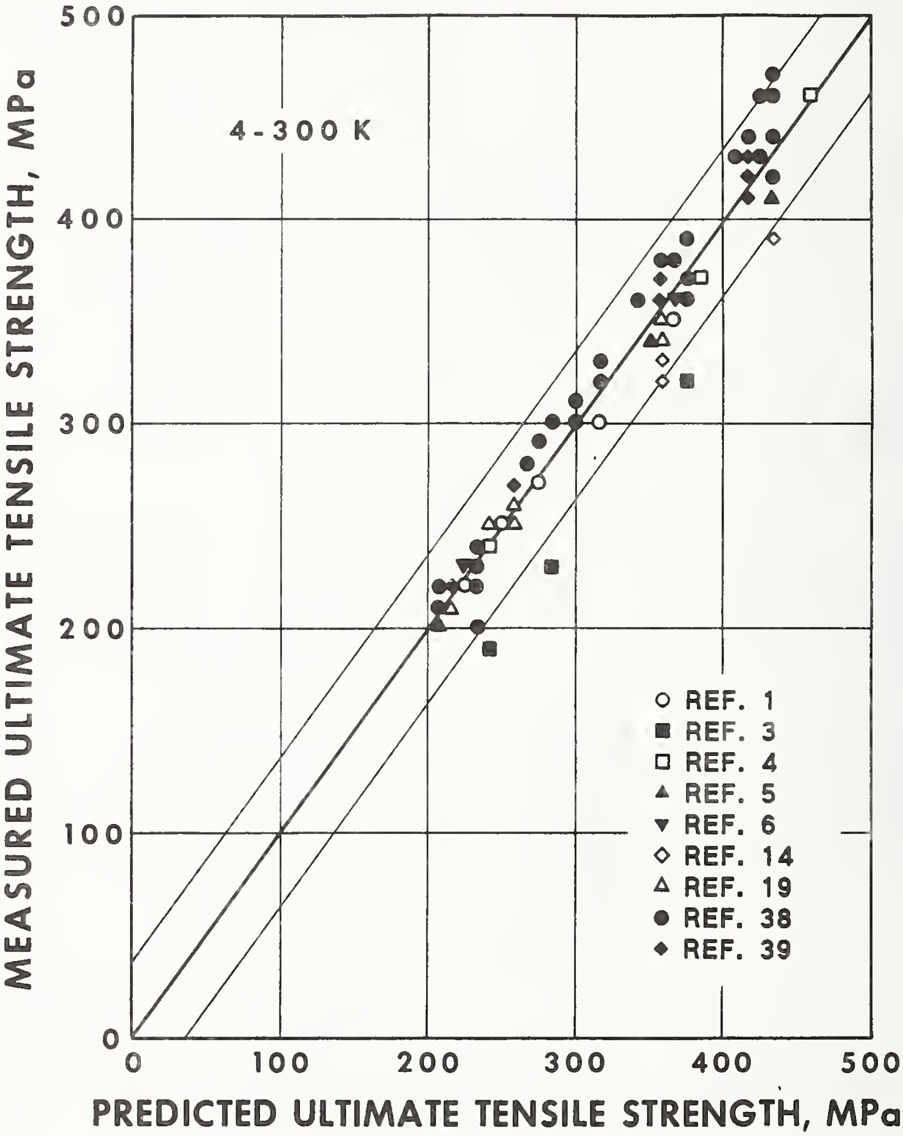

Figure 2.17. The data shown were used to compute the regression of ultimate tensile strength upon temperature and grain size [Equation (2-5)]. For clarity, overlapping data points are omitted from the figure. All data are presented in Table 2.5. Products were bar, sheet, and wire form.

DATA SOURCES AND ANALYSIS

A set of 209 measurements of ultimate tensile strength at 295 K was selected for analysis. Measurements were obtained from References 2.5, 2.15–2.22, 2.24–2.26, 2.28–2.32, 2.36, and 2.40–2.49. Products were in plate, bar, and wire form. In most cases, the actual percent reduction of thickness or area was specified, but in a few instances the percent reduction was obtained from standard tables of temper designation (see Table 1.17). The amount of cold work, *CW*, ranged up to 99%. Polynomial terms were included in the regression analysis carried out with this data set, because the dependence of ultimate tensile strength, σ_u, upon *CW* is nonlinear.

RESULTS

The regression equation for σ_u upon *CW* was found to be

$$\sigma_u = 230 + 3.14(CW) - 0.00962(CW)^2 \quad \text{(S.D. = 29 MPa)}, \qquad (2\text{-}6)$$

where σ_u is in MPa and *CW* is in percent. The standard deviations of the three coefficients are 4, 0.22, and 0.0024.

Table 2.6 presents the measured values of σ_u, values of σ_u calculated from the regression equation, the percent of *CW* (reduction of thickness or area), and the reference number. The available characterization of materials and measurements is given in Table 2.10 at the end of the tensile properties section.

Figure 2.18 indicates the fit of the data to Equation (2-6). The equation applies to *CW* from rolling or drawing. The scatter band represents two standard deviations about the regression curve. The variance of the data about the curve was assumed to be normally distributed and constant throughout the range of the independent variable, *CW*. Figure 2.19 presents the results in summary form.

DISCUSSION

Some of the data from Reference 2.17 fall outside the scatter band (Figure 2.18). The copper in these specimens is of very high purity; hence some recovery may have occurred before measurements were completed. These data were included as a guide for applications that require cold-worked copper of similar purity. Variation in grain size also contributes to the scatter of the data; since grain size often was not reported in this data set, it could not be included in the regression analysis. For small amounts of *CW*, grain size may influence σ_u more than the degree of *CW*; an estimate may be obtained from Equation (2-5).

Table 2.6. Tensile Strength Dependence on Cold Work (295 K).

Tensile Strength, Measured, MPa	Tensile Strength, Calculated, MPa	Cold Work, %	Reference No.
282	230	0	41
175	230	0	17
228	230	0	40
210	230	0	25
283	230	0	20
210	230	0	32
203	230	0	32
238	230	0	17
203	230	0	18
210	230	0	17
231	230	0	18
255	230	0	25
219	230	0	25
249	230	0	25

Table 2.6, continued

Tensile Strength, Measured, MPa	Tensile Strength, Calculated, MPa	Cold Work, %	Reference No.
225	230	0	25
213	230	0	24
238	230	0	22
252	230	0	22
221	230	0	21
211	230	0	43
212	230	0	43
213	230	0	43
212	230	0	19
220	230	0	19
229	230	0	31
222	230	0	30
218	230	0	30
269	230	0	45
228	230	0	44
221	230	0	46
228	230	0	46
239	230	0	47
237	230	0	47
221	230	0	48
259	230	0	42
255	233	1	22
249	245	4.8	47
226	246	5	28
228	246	5	28
228	246	5	28
228	246	5	28
228	246	5	28
285	249	6	22
218	249	6	19
237	256	8.5	25
242	256	8.5	25
235	258	9	32
239	258	9	32
248	260	9.8	44
241	261	10	19
242	261	10	30
241	261	10	30
246	264	11	20
279	264	11	18
241	264	11	18
365	264	11	18
252	264	11	18
268	265	11.4	47
276	269	13	42
292	276	15.3	47
195	284	18	17
269	286	18.7	32
286	286	18.7	32
308	289	20	28
313	289	20	28

Table 2.6, continued

Tensile Strength, Measured, MPa	Tensile Strength, Calculated, MPa	Cold Work, %	Reference No.
312	289	29	28
309	290	20.5	25
319	290	29.4	28
309	291	20.7	18
276	291	29.4	18
309	291	20.7	18
286	291	29.4	18
307	291	20.7	47
312	291	29.4	47
277	292	21	5
270	292	29	5
266	292	24	31
286	297	29	18
290	303	24	44
304	313	29	18
309	303	25	18
304	303	29	10
309	303	25	30
312	310	29.4	47
307	313	24	30
312	313	29	32
352	314	29.2	25
352	314	29.4	18
309	314	29.7	18
396	314	29.4	18
303	314	29.7	18
205	316	36	18
323	316	37	25
322	316	36	28
329	316	37	25
304	316	36	18
249	314	37	20
312	326	36	21
307	333	37	24
338	334	36	44
309	333	37	30
365	313	37	18
356	303	37	5
357	333	37	5
309	303	37	25
343	333	37	31
307	333	37	47
365	333	36	47
338	333	37.1	25
304	333	37.1	28
372	334	37.2	18
324	334	37.2	18
396	334	37.2	18
324	334	37.2	18
332	338	39	32
344	338	39	32

Table 2.6, continued

Tensile Strength, Measured, MPa	Tensile Strength, Calculated, MPa	Cold Work, %	Reference No.
205	340	40	18
341	340	40	28
349	340	40	28
396	340	40	28
352	340	44	28
352	340	40	18
383	384	44	18
338	384	40	18
396	350	44	18
341	385	40	18
359	359	48.1	32
396	363	48.1	32
365	359	48.5	18
386	363	50	18
352	363	50	18
396	363	50	18
359	359	50	18
396	363	50	18
367	393	50	32
352	363	50	32
338	393	50	18
323	363	50	46
338	350	50	46
352	363	50	47
345	393	50	48
372	365	50	47
365	372	50	18
341	375	60.5	18
365	385	55.5	18
396	375	60.5	18
365	385	55.5	18
371	382	59.2	32
400	372	59.2	32
341	384	50	18
334	384	50	18
396	384	60.1	47
400	385	60.5	18
372	385	60.5	18
396	385	60.5	18
386	385	60.5	18
417	384	62.5	18
407	363	60.5	18
379	393	60.5	18
400	363	60.5	18
330	393	60.5	18
407	400	68.5	47
417	400	68.5	18
386	400	68.6	18
400	400	68.6	18
400	400	68.6	18
315	403	70	17

Table 2.6, continued

Tensile Strength, Measured, MPa	Tensile Strength, Calculated, MPa	Cold Work, %	Reference No.
393	403	75	21
386	403	72.7	32
415	408	72.7	32
396	410	74	47
418	411	74.7	47
393	411	75	40
359	412	75	45
386	412	75	45
393	412	75	48
418	412	75	47
386	412	75	48
403	412	75.5	32
426	413	75.5	32
396	415	77	45
365	426	85	47
403	425	83	45
376	426	85	22
457	427	84.4	25
454	427	89.4	25
417	427	84.4	47
372	426	85	42
433	431	87.5	47
400	431	87.5	48
424	432	88	45
417	431	89.4	32
426	431	84.4	32
450	435	85	47
424	435	88	45
425	435	90	47
434	431	92	45
435	440	89.4	47
439	440	93.4	47
441	440	93	45
465	443	96	45
469	444	95	45
469	446	93	45
469	446	98.2	45
469	446	98.4	45
476	446	98.6	45
486	447	98.8	45
486	447	99	45
496	447	99.3	45

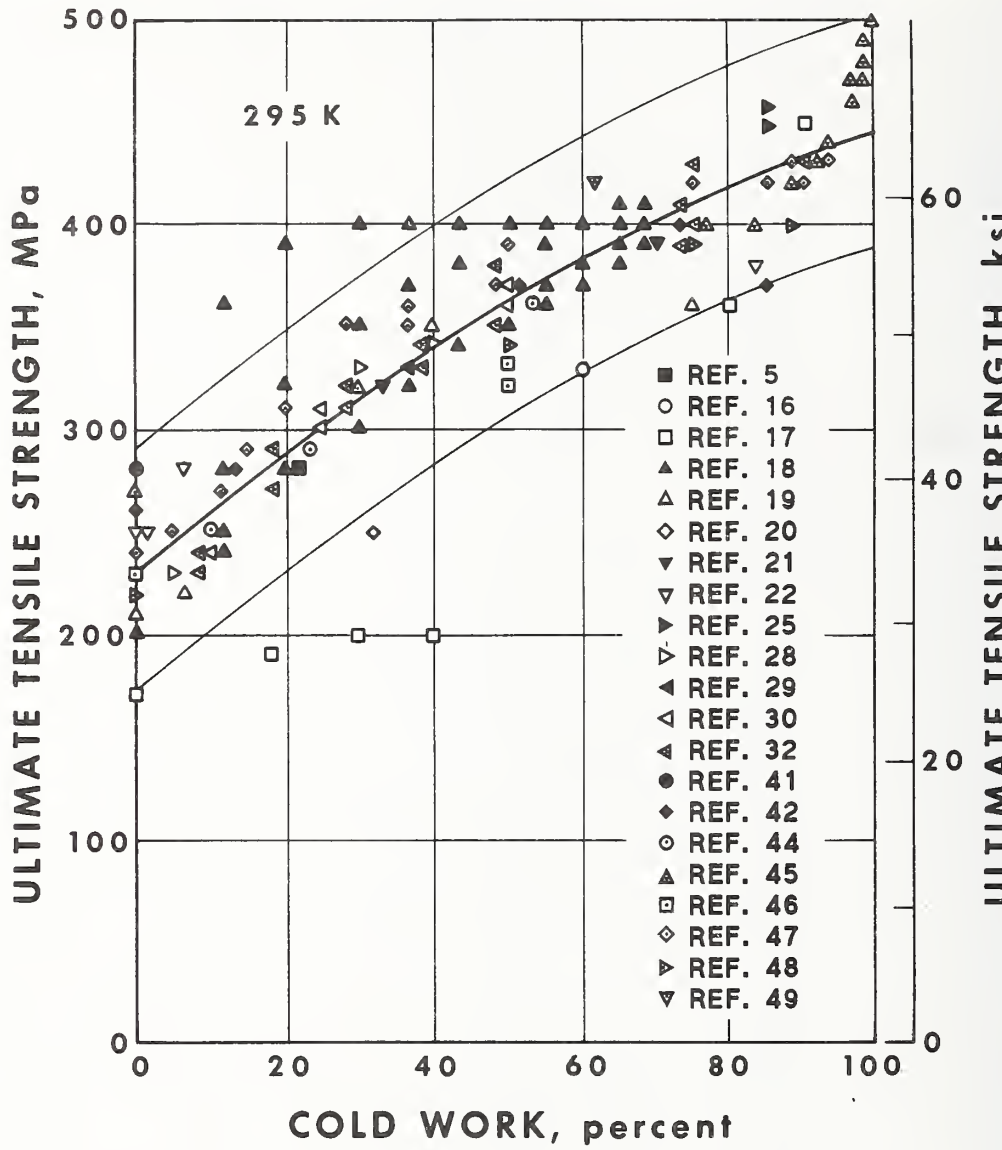

Figure 2.18. The data shown were used to compute the regression of ultimate tensile strength upon cold work [Equation (2-6)]. For clarity, overlapping data points, including all those from References 2.15, 2.24, 2.26, 2.31, 2.36, 2.40, and 2.43, were omitted from the figure. All data are presented in Table 2.6. Products were in plate, bar, and wire form.

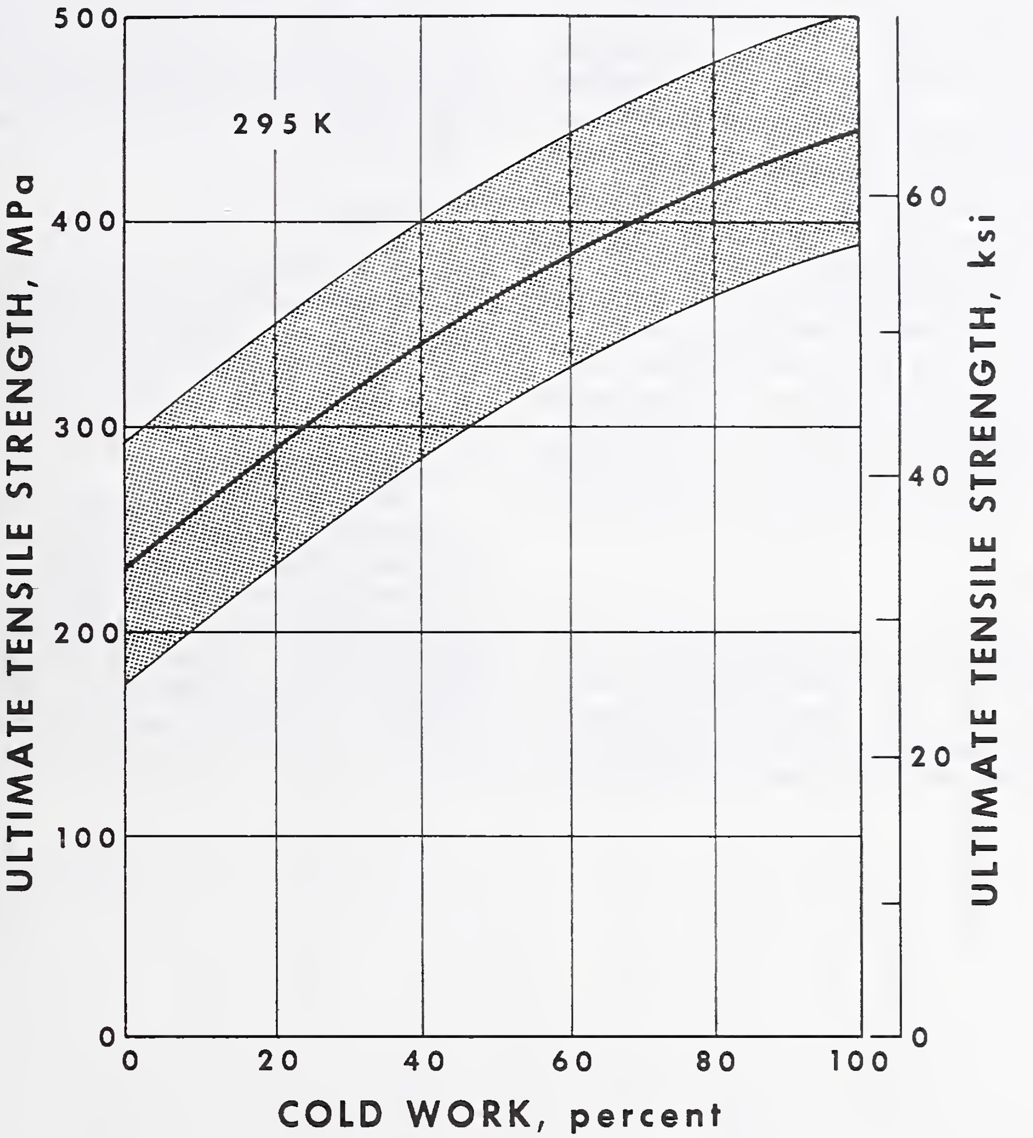

Figure 2.19. Ultimate tensile strength dependence upon cold work at 295 K. The scatter band represents two standard deviations about a second-order regression curve based upon 209 measurements of tensile strength for a range of cold work from 0 to 99%. The regression equation is

$$\sigma_u \text{ (MPa)} = 230 + 3.14(CW) - 0.00962(CW)^2 \qquad \text{(S.D.} = 29 \text{ MPa)},$$

where *CW* is the percent of cold work (reduction of thickness or area.) Products were in plate, bar, and wire form.

DATA SOURCES AND ANALYSIS

Figure 2.20 shows data from References 2.28, 2.33, and 2.34 on cold-worked coppers of different silver content. These are the only data available to estimate the variation in ultimate tensile strength, σ_u, with silver content, [Ag]. The available characterization of materials and measurements is given in Table 2.10 at the end of the tensile properties section. Measurements reported in Reference 2.28 were taken from square wire with initial dimensions (before rolling) of 0.63 cm × 0.63 cm. The thickness of the 40% cold-rolled plate used for measurements reported in Reference 2.33 was 1.3 cm, but specimen thickness was 0.63 cm. This was the only material that was cold-worked by a manufacturer. For the specimens used in the measurements reported in Reference 2.34, plate thickness before rolling was 1.3 cm.

RESULTS

As [Ag] is increased up to 0.085 wt%, the variation in σ_u is about 10%, for a given level of cold work, *CW*. This estimate of the variation is based upon measurements of σ_u reported from different laboratories over a range of [Ag] values. However, a variation of 6% was reported in Reference 2.33 for different measurements of σ_u on the same heat of C10700 at one laboratory. Therefore, the variation of σ_u with [Ag] within the C10100 to C10700 specification range will probably be less than 10% for cold-worked material. The improvement in σ_u with *CW* saturates at about 40 to 50%.

DISCUSSION

Ornstein (Reference 2.59) reported an increase of 3% from 334 to about 345 MPa in σ_u as [Ag] was increased from 0.03 wt% (C10400, C10500) to 0.85 wt% (C10700). Actual data points were not given, and the method of measuring σ_u was not specified. Specimens were cold worked 50%.

Although increases in [Ag] in the range considered here do not affect the tensile properties appreciably, increased resistance to creep has been reported for similar increases in [Ag] (see Reference 2.28 and the section on creep in this publication). However, this effect has been studied only at temperatures above 573 K and it is not known whether the same mechanisms control creep in the cryogenic temperature range.

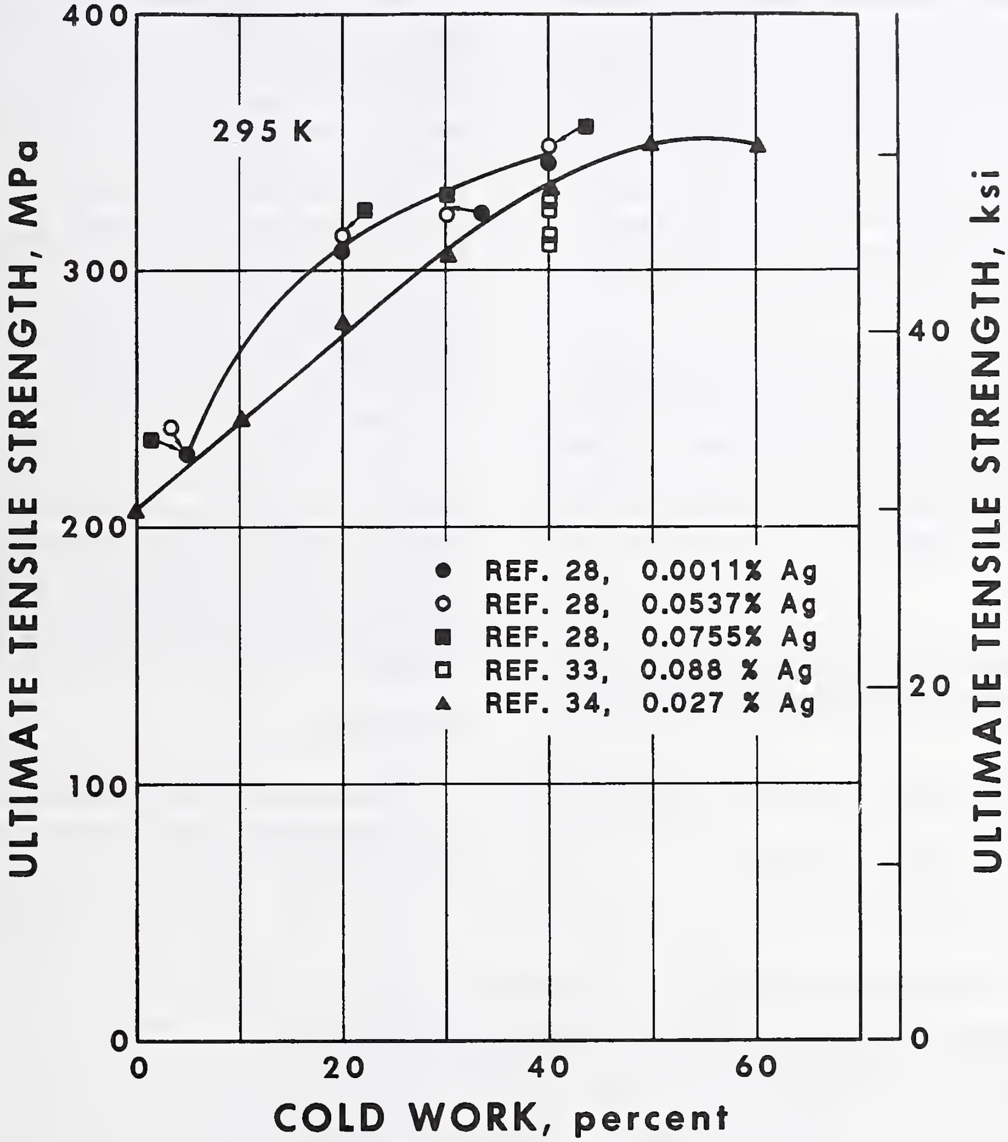

Figure 2.20. These data indicate the absence of a strong dependence of ultimate tensile strength of cold-worked copper upon silver content. (Silver content is unspecified for C10100, ≥ 0.027 wt% for C10400, ≥ 0.034 wt% for C10500, and ≥ 0.085 wt% for C10700.) Products were in plate (References 2.33 and 2.34) and wire-bar form (Reference 2.28).

DATA SOURCES AND ANALYSIS

A set of 79 measurements of ultimate tensile strength from 4 to 300 K was selected for analysis. Products were in plate, bar, and wire form. In most cases, the actual percent reduction of thickness or area was specified, but in a few instances, the percent reduction was obtained from standard tables of temper designation (see Table 1.17). The amount of cold work, *CW*, ranged up to 99%. This data set (References 2.5, 2.15–2.16, 2.19, 2.36, 2.40–2.41, and 2.48) was used in regression analysis of ultimate tensile strength (σ_u) upon temperature (T) and *CW*. Polynomial terms in T and *CW* were included in the analysis.

It is clear from the large amount of scatter in Figures 2.21 and 2.22 that separate regression equations for σ_u as a function of each variable, T and *CW*, would not be of much value. However, when multivariate regression is used to analyze the data set, a relatively small standard deviation of 32 MPa is obtained.

RESULTS

Regression analysis indicated that the best fit to the σ_u data was obtained with the following equation:

$$\sigma_u = 412 - 0.664T + 2.73(CW) - 0.00695(CW)^2 \quad (2\text{-}7)$$

$$(\text{S.D.} = 32 \text{ MPa}),$$

where σ_u is in MPa, $4\text{ K} \le T \le 300\text{ K}$, and *CW*, in percent, is the reduction of thickness or area. The standard deviations of the four coefficients are 9, 0.034, 0.42, and 0.00548.

Table 2.7 presents the measured values of σ_u, values of σ_u calculated from the regression equation, the temperature, the percent *CW* (reduction of thickness or area), and the reference number. The available characterization of materials and measurements is given in Table 2.10 at the end of the tensile properties section.

Figure 2.21 depicts the data as a function of T only, for all levels of *CW*. Figure 2.22 depicts the data as a function of *CW* only without showing the T dependence. Figure 2.23 presents recent measurements at 4, 76, and 295 K on C10400 plate, which show the variation in σ_u with both T and *CW*. (These data were not available when the regression analysis was carried out.)

Figure 2.24 indicates the fit of the data set to Equation (2-7). The scatter band represents two standard deviations about the line that corresponds to complete agreement between measured and predicted values of σ_u. The variance of the data was assumed to be normally distributed and constant throughout the range of the predicted values.

DISCUSSION

The magnitude of the coefficients of the *CW* terms is in agreement with results at room temperature [Equation (2-6)].

Table 2.7. Tensile Strength Dependence on Cold Work (4–300 K).

Tensile Strength, Measured, MPa	Tensile Strength, Calculated, MPa	Test Temperature, K	Cold Work, %	Reference No.
498	409	4	0	41
410	409	4	0	5
514	548	4	60	16
503	501	4	37	5
509	501	4	37	5
440	464	4	21	5
446	464	4	21	5
478	399	20	0	41
496	399	20	0	36
517	490	20	37	36
524	490	20	37	36

Table 2.7, continued

Tensile Strength, Measured, MPa	Tensile Strength, Calculated, MPa	Test Temperature, K	Cold Work, %	Reference No.
514	538	20	60	16
336	362	76	0	5
460	453	76	37	36
476	453	76	37	36
458	500	76	60	19
452	453	76	37	5
442	453	80	37	5
375	416	76	21	5
400	361	77	0	36
457	530	77	60	19
352	361	77	0	19
318	361	77	0	19
352	361	77	0	19
318	361	77	0	19
372	377	77	8	19
361	377	77	8	19
393	377	77	8	19
347	377	77	8	19
372	359	76	0	48
552	557	80	60	48
365	359	76	0	40
531	521	76	75	40
412	352	76	0	41
310	316	195	0	40
476	482	195	75	40
310	283	195	0	36
393	374	195	37	36
400	374	195	37	16
365	421	195	60	19
258	276	205	0	19
253	276	205	0	19
258	276	205	0	19
257	276	205	0	19
276	292	205	8	36
266	292	205	8	19
270	292	205	8	19
257	292	205	8	19
247	257	233	0	19
241	257	233	0	19
240	257	233	0	19
240	257	233	0	19
262	273	233	8	19
248	273	233	8	19
258	273	233	8	19
242	273	233	8	19
214	224	233	0	48
462	422	233	60	48
262	217	233	0	48
205	216	295	0	5
334	355	295	60	16
356	308	295	37	5

Table 2.7, continued

Tensile Strength, Measured, MPa	Tensile Strength, Calculated, MPa	Test Temperature, K	Cold Work, %	Reference No.
357	308	295	37	5
277	270	295	21	5
270	215	295	21	5
21[illegible]	215	297	0	19
211	215	297	0	19
211	215	297	0	19
210	215	297	0	19
226	231	297	6	19
219	231	297	6	19
216	231	297	6	19
27[illegible]	231	297	6	19
248	213	300	6	36
333	352	300	60	15
228	213	300	0	40
393	379	300	75	40
358	304	300	37	36
365	304	300	37	36

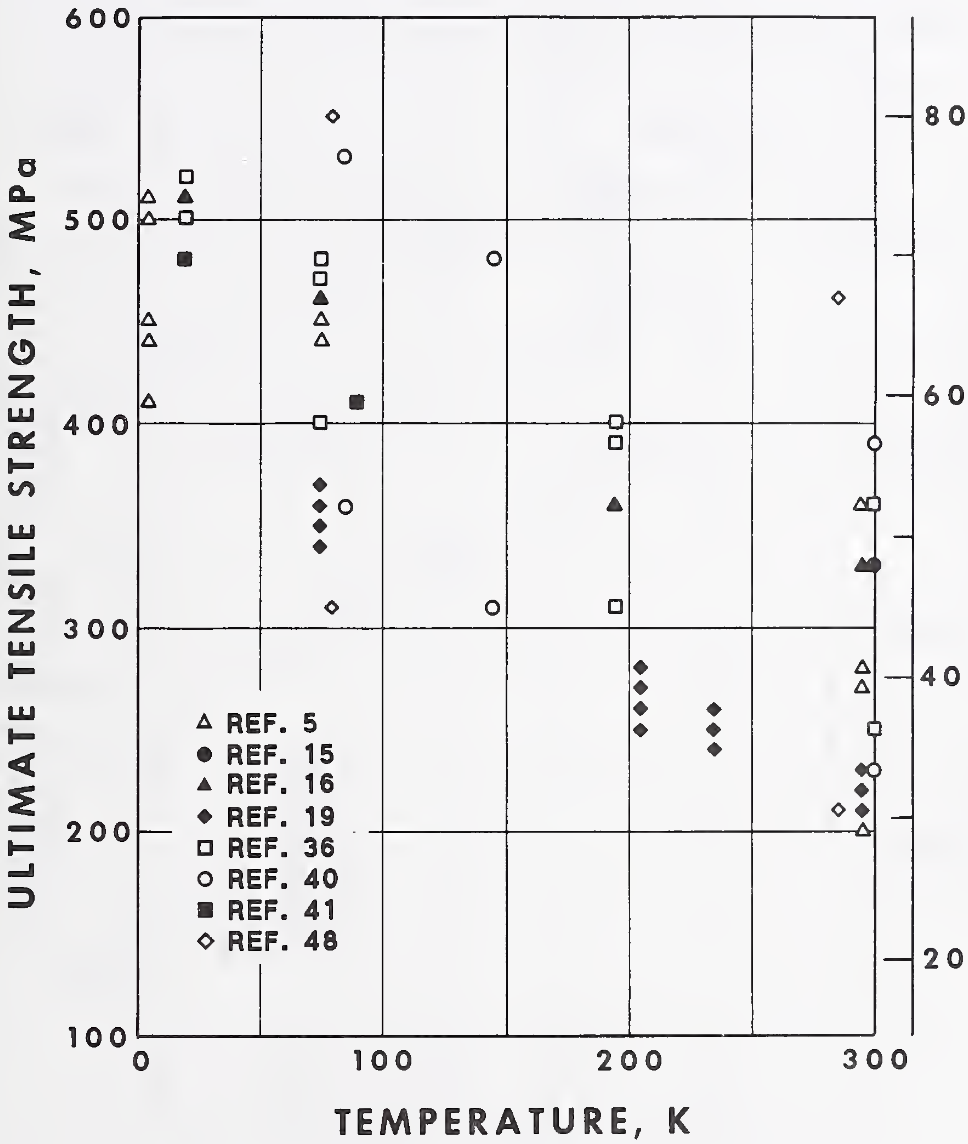

Figure 2.21. The data are represented as a function of temperature, for all levels of cold work. The variation in cold work obscures the dependence of ultimate tensile strength upon temperature that is given in Equation (2-7). For clarity, overlapping data points are omitted from the figure. All data are presented in Table 2.7. Products were in plate, bar, and wire form.

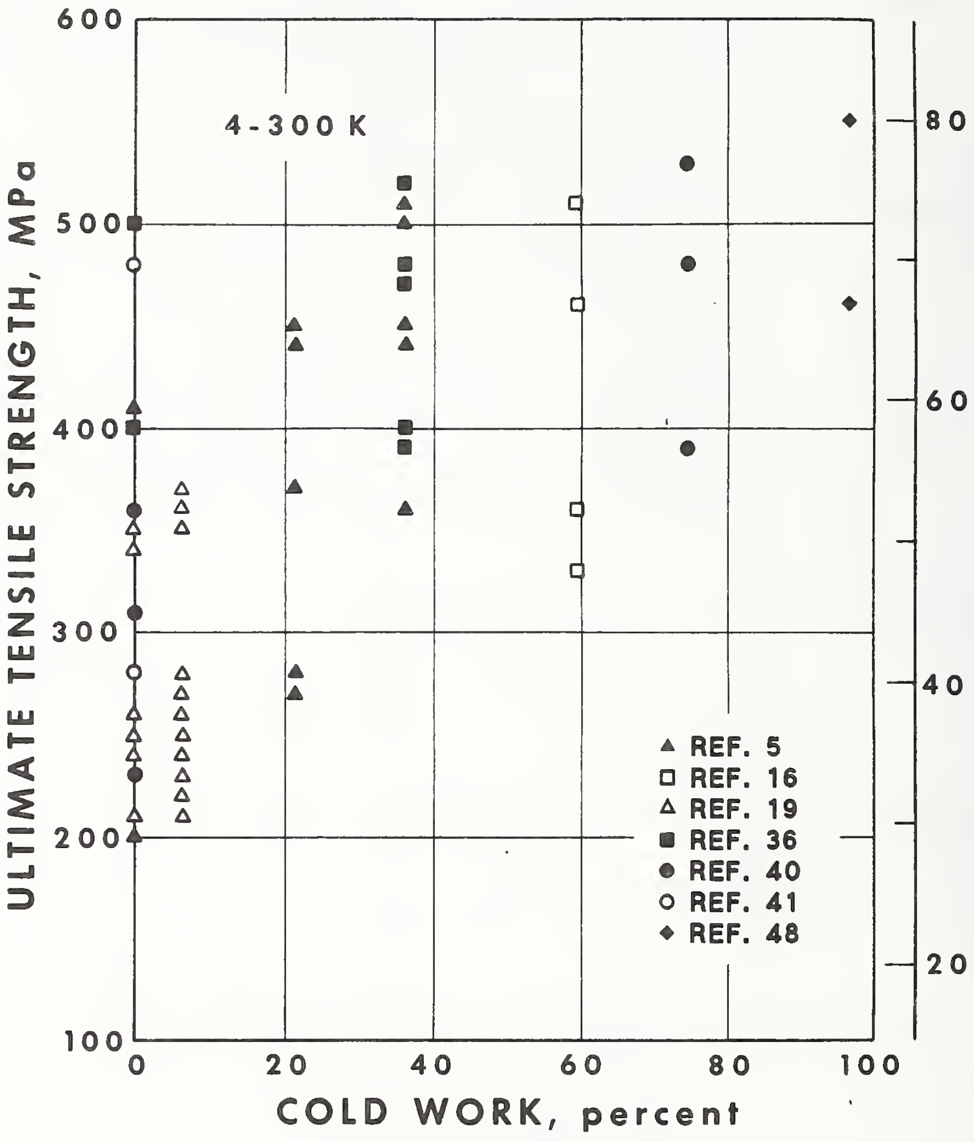

Figure 2.22. The data over the 4-to-300-K temperature range are represented as a function of cold work. The variation in temperature obscures the dependence of ultimate tensile strength upon cold work that is given in Equation (2-7). For clarity, overlapping data points are omitted from the figure. All data are presented in Table 2.7. Products were in plate, bar, and wire form.

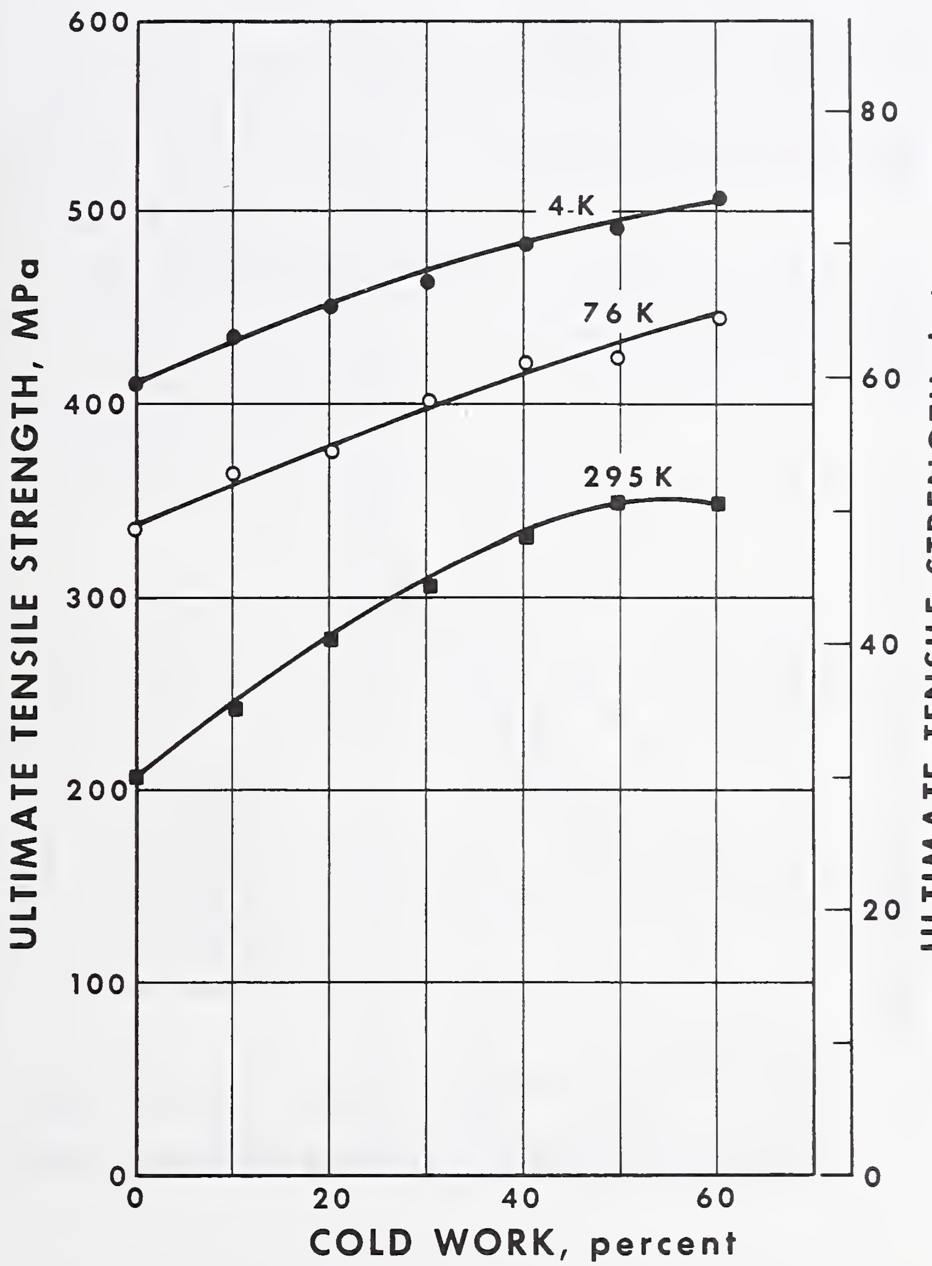

Figure 2.23. These data from Reference 2.34 indicate the increase in ultimate tensile strength with increased cold work or lowered temperature (C10400 plate).

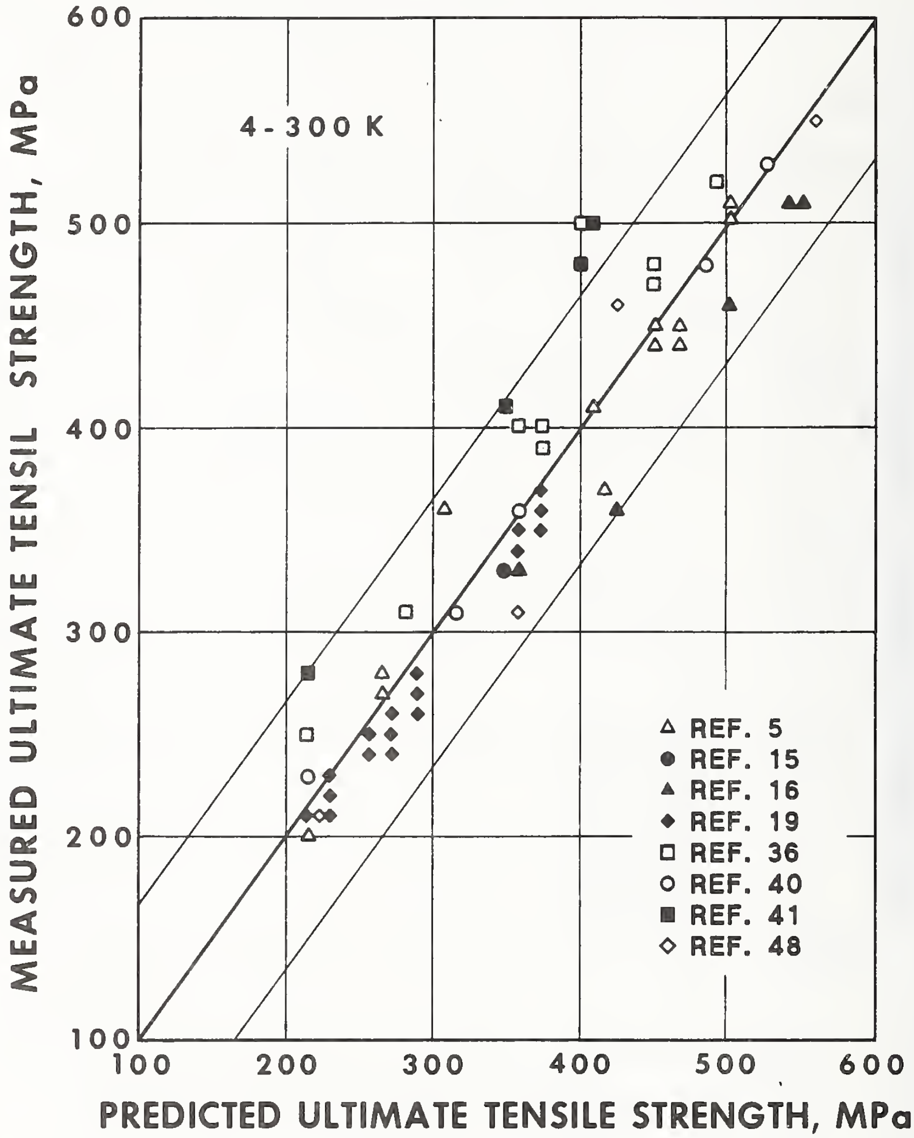

Figure 2.24. The data shown were used to compute the regression of ultimate tensile strength upon temperature and cold work [Equation (2-7)]. For clarity, overlapping data points are omitted from the figure. All data are presented in Table 2.7. Products were in plate, bar, and wire form.

DATA SOURCES AND ANALYSIS

Figure 2.25 shows data from References 2.28, 2.33, and 2.34 on cold-worked coppers of different silver content. These are the only data available to estimate the variation in elongation with silver content, [Ag]. The available characterization of materials and measurements is given in Table 2.10 at the end of the tensile properties section. Measurements reported in Reference 2.28 were taken from square wire with initial dimensions (before rolling) of 0.63 cm × 0.63 cm. The thickness of the 40% cold-rolled plate used for measurements reported in Reference 2.33 was 1.3 cm, but specimen thickness was 0.63 cm. This was the only material that was cold-worked by a manufacturer. For the specimens used in the measurements reported in Reference 2.34, plate thickness before rolling was 1.3 cm.

RESULTS

The authors of Reference 2.28 reported very little change in elongation as [Ag] increased to 0.085 wt%. However, these elongations were considerably lower than those reported in References 2.33 and 2.34. Gage lengths for all specimens were comparable. Different measurements of elongation on the same C10700 material gave values from 21 to 25% (Reference 2.33).

DISCUSSION

Figure 2.27, based upon a different set of data between 4 and 300 K, also indicates substantial variation in this tensile property.

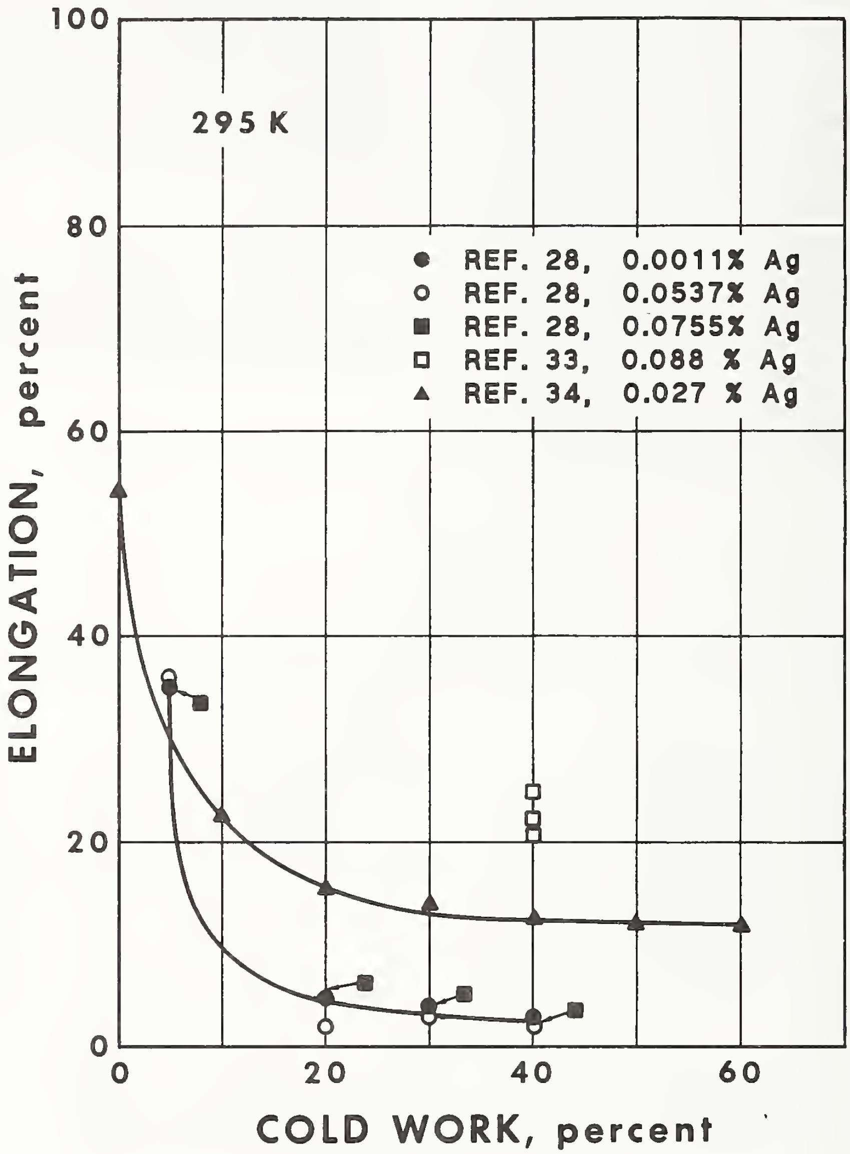

Figure 2.25. These data indicate a wide variation in the elongation, but do not show a strong dependence of elongation of cold-worked copper upon silver content. (Silver content is unspecified for C10100, ≥ 0.027 wt% for C10400, ≥ 0.034 wt% for C10500, and ≥ 0.085 wt% for C10700.) Products were in plate (References 2.33 and 2.34) and wire-bar form (Reference 2.28).

DATA SOURCES AND ANALYSIS

A set of 153 measurements of tensile elongation from 4 to 300 K was selected for analysis. Product forms included plate, bar, and wire. In most cases, the actual percent reduction of thickness or area was specified, but in a few instances, the percent reduction was obtained from standard tables of temper designation (see Table 1.?). The amount of cold work, *CW*, ranged up to 96%. This data set (References 2.3, 2.5–2.6, 2.14–2.16, 2.19, 2.36, 2.38–2.39 and 2.50–2.56) was used in regression analysis of elongation upon temperature (*T*) and *CW*. Polynomial terms in *T* and *CW* were included in the analysis.

RESULTS

Regression analysis indicated that the best fit to the data was obtained with the equation:

$$\text{Elongation} = 58.4 - 0.0553T - 0.516(CW) \quad (2\text{-}8)$$

$$(\text{S.D.} = 12\%)$$

where elongation is in percent, 4 K $\leq T \leq$ 300 K, and *CW* , in percent, is the reduction of thickness or area). The standard deviations of the three coefficients are 2.0, 0.0094, and 0.051.

Table 2.8 presents the measured values of the tensile elongation, the values of elongation calculated from the regression equation, the percent of *CW* (reduction of thickness or area), the temperature, and the reference number. The available characterization of materials and measurements is given in Table 2.10 at the end of the tensile properties section.

Figure 2.26 depicts the data as a function of *T* only, for all levels of *CW*. Figure 2.27 depicts the data as a function of *CW* only, without showing the *T* dependence. It is clear from the large amount of scatter in Figures 2.26 and 2.27 that separate regression equations for σ_u as a function of each variable, *T* and *CW*, would not be of much value. However, when multivariate regression is used to analyze the data set, a relatively small standard deviation of 12% is obtained. Figure 2.28 presents recent measurements at 4, 76, and 295 K on C10400 plate, which show the variation in elongation with both *T* and *CW*. (These data were not available when the regression analysis was carried out.)

Figure 2.29 indicates the fit of the data set to Equation (2-8). The scatter band represents two standard deviations about the line, which corresponds to complete agreement between measured and predicted values of elongation. The variance of the data was assumed to be normally distributed and constant throughout the range of the predicted values.

DISCUSSION

Since elongation is lower in flat tensile specimens than in round specimens, and since data from several types of specimens were combined in the analysis, Equation (2-8) should not be used to predict exact elongation values. However, since the effect of specimen type is small compared with the effects of *CW* and temperature, the equation illustrates the effect of these variables. Note also that the only measurements on flat specimens (Reference 2.19) lie within the scatter band shown in Figure 2.29, but are above the predicted values. Thus, other sources of uncertainty are probably larger than differences in specimen type, although differences in gage lengths also change measured elongation.

See also Figure 2.25 and page 2-51.

Table 2.8. Elongation Dependence on Temperature, Cold Work, 4–300 K.

Elongation, Measured, %	Elongation, Calculated, %	Cold Work, %	Test Temperature, K	Reference No.
45.0	42.1	0	295	55
101	58.2	0	4	56
77.0	54.2	0	77	56
61.0	42.1	0	295	56

Table 2.8, continued

Elongation, Measured, %	Elongation, Calculated, %	Cold Work, %	Test Temperature, K	Reference No.
48.0	42.9	0	295	5
57.0	54.2	0	76	5
76.0	57.0	0	4	5
52.5	53.7	0	76	38
46.5	57.0	0	80	38
44.6	57.0	0	25	38
46.5	53.7	0	80	38
43.0	53.7	0	25	38
40.5	47.1	0	205	38
39.0	50.4	0	198	38
38.0	47.1	0	205	38
35.0	57.0	0	25	38
38.0	54.0	0	80	38
35.0	50.4	0	150	38
35.5	46.5	0	205	38
35.0	43.5	0	270	38
38.0	42.9	0	285	38
34.0	41.5	0	305	38
32.5	41.8	0	300	38
32.5	41.5	0	305	38
30.0	41.8	0	300	38
27.0	41.5	0	300	38
25.0	41.8	0	305	38
51.5	57.0	0	25	38
38.0	53.7	0	80	38
29.0	50.4	0	145	38
38.0	47.1	0	205	38
45.5	57.0	0	25	38
42.0	53.7	0	80	38
29.0	50.4	0	145	38
38.0	47.1	0	205	38
37.5	41.5	0	305	38
32.5	41.8	0	300	38
35.0	41.5	0	305	38
46.5	57.0	0	80	38
42.0	57.0	0	25	38
32.5	50.4	0	198	38
35.0	41.5	0	305	38
32.5	57.0	0	80	38
35.0	50.4	0	25	38
28.5	57.0	0	80	38
29.0	41.5	0	305	38
32.5	41.8	0	300	38
51.5	53.3	0	25	50
44.6	49.9	0	153	50
47.0	47.7	0	193	50
47.0	49.9	0	233	50
40.2	43.5	0	263	50
48.0	42.1	0	295	50
67.0	53.3	0	93	50
51.0	42.1	0	295	50

Table 2.8, continued

Elongation, Measured, %	Elongation, Calculated, %	Cold Work, %	Test Temperature, K	Reference No.
53.0	42.1	0	295	50
50.0	57.3	0	20	51
37.5	42.1	0	295	50
58.0	52.2	0	113	52
45.0	45.5	0	153	50
47.0	47.1	0	193	52
47.0	45.5	0	233	50
44.0	42.0	0	293	52
26.2	54.2	0	20	50
24.5	42.8	0	293	53
40.7	54.2	0	78	3
38.4	47.6	0	195	3
42.2	42.2	0	233	3
30.9	32.2	0	473	3
45.0	57.3	0	20	39
44.0	54.2	0	77	39
38.0	47.6	0	195	39
38.4	41.8	0	300	39
57.2	47.6	0	196	50
67.8	46.6	0	213	51
56.2	44.4	0	253	54
58.0	42.0	0	293	51
50.0	54.2	0	77	6
44.0	42.0	0	293	6
53.0	54.2	0	77	19
56.3	47.1	0	205	19
60.8	45.5	0	233	19
53.5	42.0	0	297	19
68.5	54.2	0	77	19
58.0	47.1	0	205	19
60.8	45.5	0	233	19
62.2	42.0	0	297	19
60.0	54.2	0	77	19
58.8	47.1	0	205	19
60.8	45.5	0	233	19
51.2	42.0	0	297	19
60.8	54.2	0	77	19
65.3	47.1	0	205	19
60.8	45.5	0	233	19
58.0	42.0	0	297	19
68.8	57.3	0	20	39
67.8	57.3	0	20	39
70.7	57.3	0	20	39
58.0	54.2	0	76	39
60.5	54.2	0	76	39
58.8	54.2	0	76	39
53.3	47.6	0	196	39
53.1	47.6	0	195	39
53.4	42.1	0	295	39
54.2	42.1	0	295	39
75.1	58.2	0	4	14

Table 2.8, continued

Elongation, Measured, %	Elongation, Calculated, %	Cold Work, %	Test Temperature, K	Reference No.
66.0	54.2	6	77	14
64.6	54.2	6	77	19
65.4	54.2	6	77	19
43.3	51.1	6	77	19
40.0	44.0	6	205	19
46.8	42.4	6	233	19
40.0	38.9	6	297	19
54.8	51.1	6	4	19
55.5	44.0	6	205	19
54.0	42.4	6	233	19
53.6	38.9	6	297	19
53.6	51.1	6	77	19
44.5	44.0	6	205	19
52.3	42.4	6	233	19
50.4	38.9	6	297	19
67.5	51.1	6	77	19
66.8	44.0	6	205	19
54.0	42.4	6	233	19
50.4	38.9	6	297	19
48.7	47.4	21	4	5
35.8	43.4	21	76	5
13.4	31.3	21	295	5
14.3	38.9	21	295	5
54.0	38.2	37	20	36
57.0	38.2	37	20	36
35.0	35.1	37	76	36
35.0	39.1	37	76	19
20.0	28.5	37	195	36
20.0	28.5	37	195	36
41.0	22.7	37	300	36
14.8	22.7	37	300	36
29.8	39.1	37	4	5
31.6	39.1	37	77	5
19.5	39.1	37	76	5
14.3	39.1	37	76	5
10.3	23.2	37	295	5
8.7	23.0	37	295	5
20.0	23.2	60	77	19
15.0	44.0	60	300	19
41.0	27.2	60	77	19
14.3	26.4	60	20	19
29.0	23.2	60	76	19
20.0	16.7	60	195	16
17.0	11.1	60	295	16
8.2	21.0	64	80	53
2.20	9.75	64	283	53
6.30	4.47	96	80	53
1.00	-6.76	96	283	53

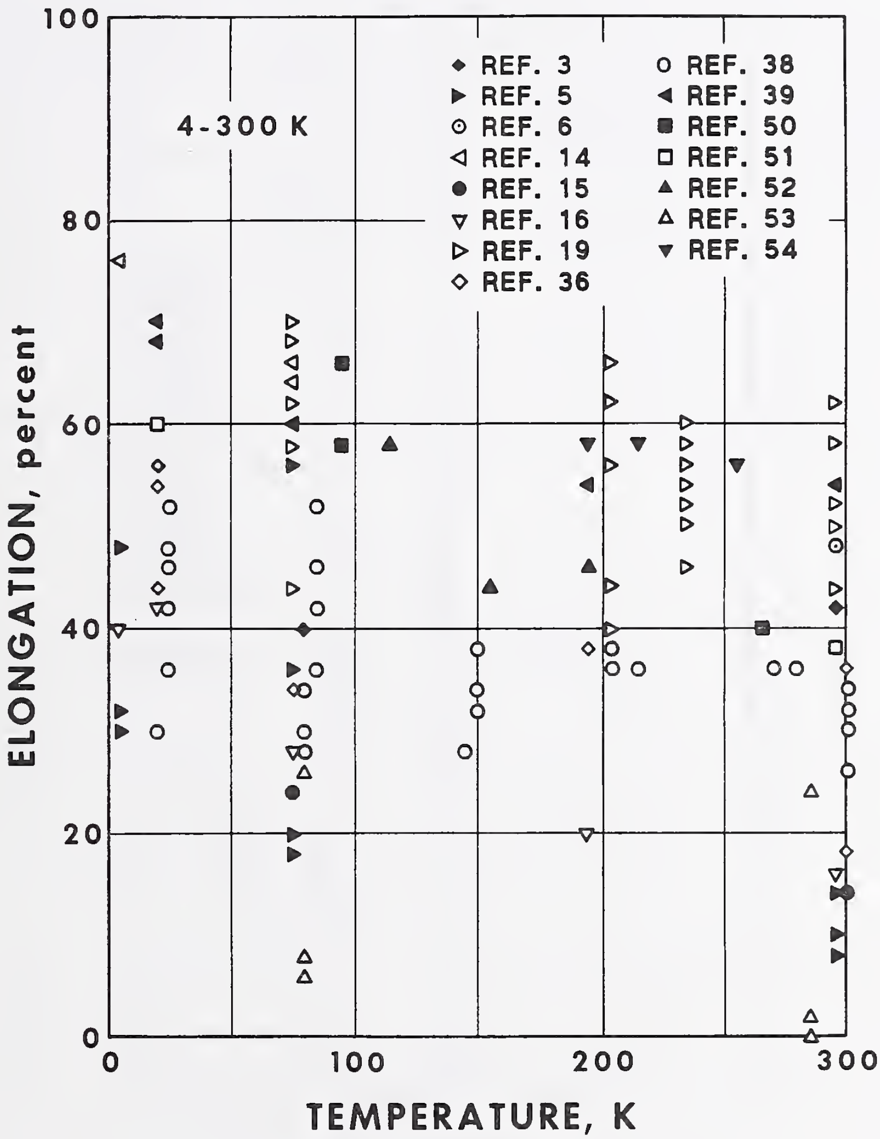

Figure 2.26. The data for all levels of cold work are represented as a function of temperature. The variation in cold work obscures the dependence of tensile elongation upon temperature that is given in Equation (2-8). For clarity, overlapping points are omitted from the figure, including all points from References 2.55 and 2.56. All data are presented in Table 2.8. Products were in plate, bar, and wire form.

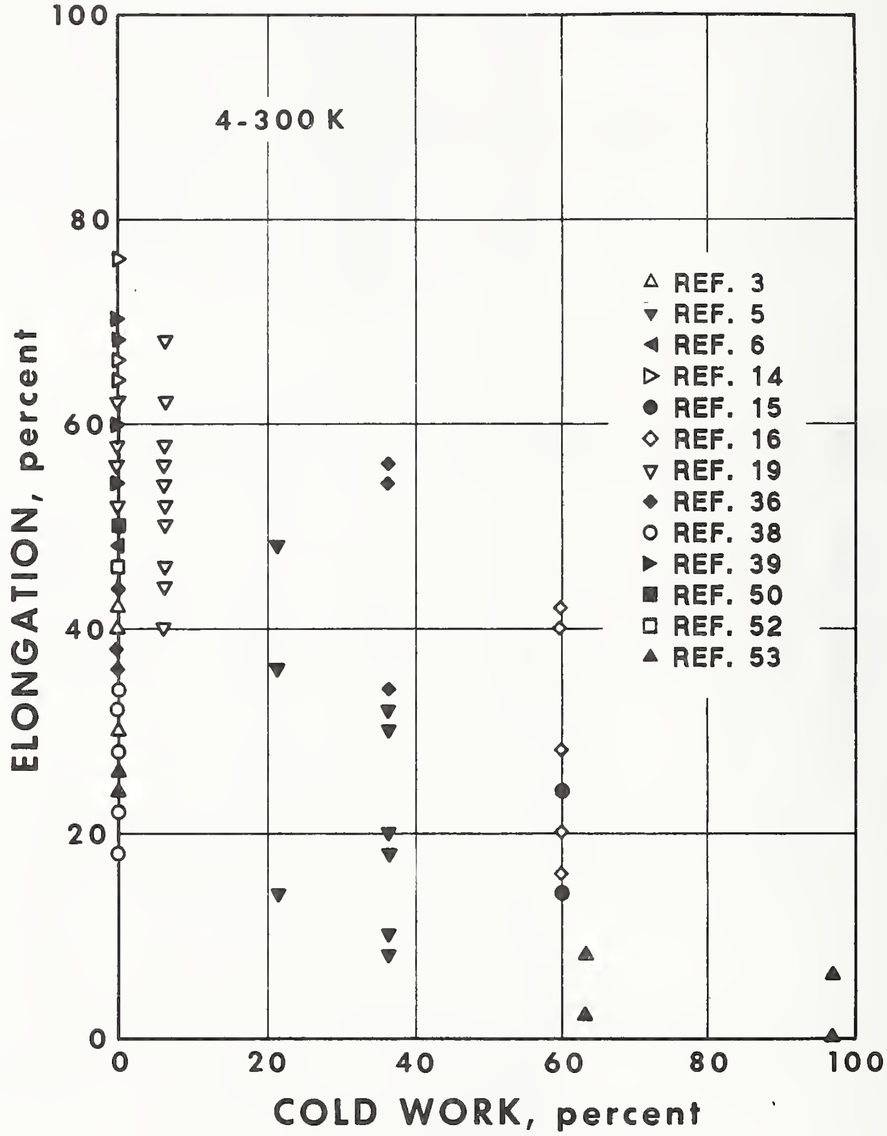

Figure 2.27. The data over the 4 to 300 K temperature range are represented as a function of cold work. The variation in temperature obscures the dependence of tensile elongation upon cold work that is given in Equation (2-8). For clarity, overlapping data points are omitted from the figure, including all points from References 2.51, 2.54, 2.55, and 2.56. All data are presented in Table 2.8. Products were in plate, bar, and wire form.

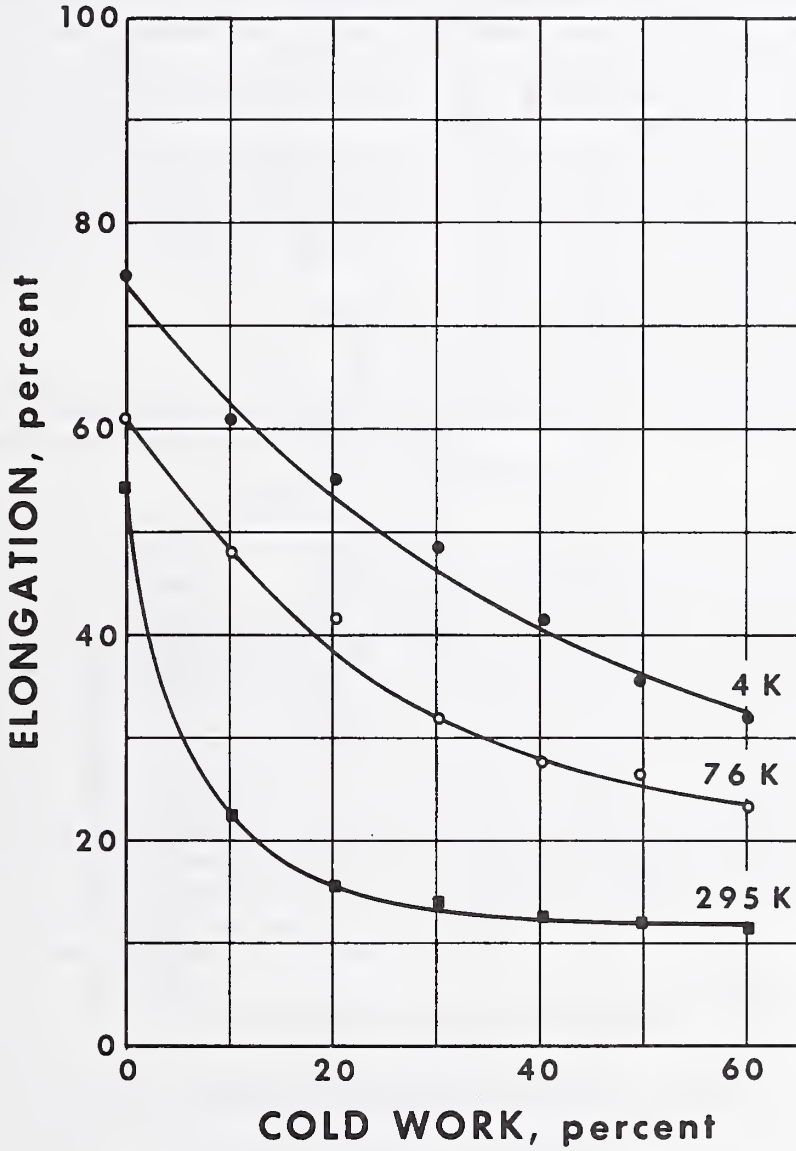

Figure 2.28. These data from Reference 2.57 indicate the decrease in elongation with increased cold work or temperature (C10400 plate).

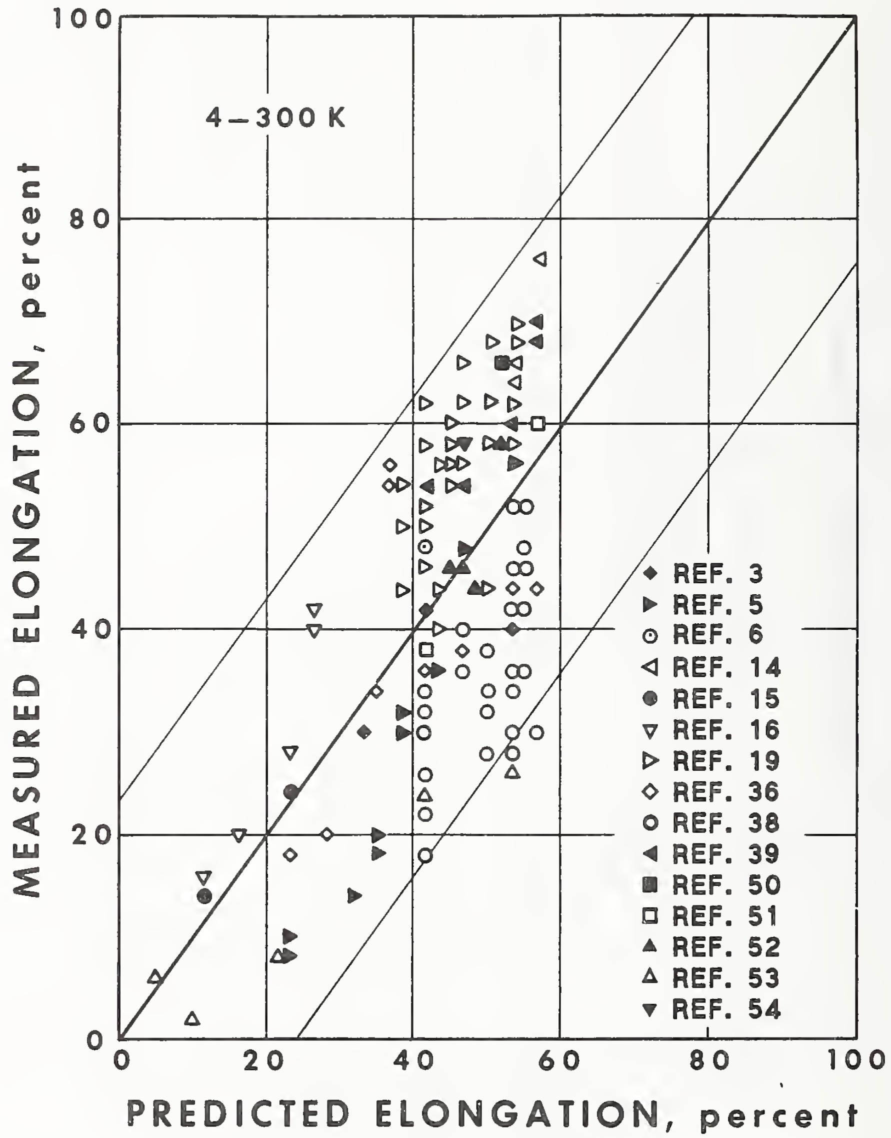

Figure 2.29. The data shown were used to compute the linear regression of tensile elongation upon temperature and cold work [Equation (2-8)]. For clarity, overlapping data points are omitted from the figure, including all points from References 2.55 and 2.56. All data are presented in Table 2.8. Products were in plate, bar, and wire form.

DATA SOURCES AND ANALYSIS

A set of 112 measurements of tensile reduction of area from 4 to 300 K was selected for analysis. Products were in plate, bar, and wire form. In most cases, the actual percent reduction of thickness or area was specified, but in a few instances, the percent reduction was obtained from standard tables of temper designation (see Table 1.17). The amount of cold work, *CW*, ranged up to 96%. This data set (References 2.1, 2.5, 2.14–2.16, 2.19, 2.32, 2.36, 2.39, 2.50–2.51, 2.53, and 2.55–2.57) was used in regression analysis of reduction of area upon temperature (*T*) and *CW*.

RESULTS

Regression analysis indicated that the best fit to the data was obtained with the equation:

$$\text{Reduction of Area} = 80.5 - 0.128(CW) \quad (\text{S.D.} = 6\%), \tag{2-9}$$

where reduction of area is in percent and *CW*, in percent, is the reduction of thickness or area. The standard deviations of the two coefficients are 0.7 and 0.028. The equation is valid for data between 4 and 300 K. No significant *T* dependence was observed for this set of data.

Table 2.9 presents the measured values of the tensile reduction of area, the reduction of area values calculated from the regression equation, the percent of *CW* (reduction of thickness or area), *T*, and the reference number. The available characterization of materials and measurements is given in Table 2.10 at the end of the tensile properties section.

Figure 2.30 depicts the data as a function of *T* only, for all levels of *CW*. Figure 2.31 presents recent measurements at 4, 76, and 295 K on C10400 plate, which show the variation in reduction of area with *CW*. (These data were not available when the regression analysis was carried out.) Both figures show the lack of dependence of reduction of area upon *T*, as found in the regression analysis, Equation (2-9).

Figure 2.32 indicates the fit of the data set to Equation (2-9). The scatter band represents two standard deviations about the regression line. The variance of the data was assumed to be normally distributed and constant throughout the range of the independent variable, *CW*. Figure 2.33 presents the results in summary form.

DISCUSSION

Reduction of area is lower in flat tensile specimens than in round specimens. Since data from several types of specimens were combined in the analysis, Equation (2-9) should not be used to predict exact values of reduction of area. However, the data on flat specimens (References 2.19 and 2.32), fall within the scatter band shown in Figure 2.32, and are often higher than the predicted values. Thus, other sources of uncertainty are larger than differences in specimen type, and the equation illustrates the general trend of the data with temperature (no significant effect) and *CW*.

Table 2.9. Reduction of Area Dependence on Cold Work (4–300 K).

Reduction of Area, Measured, %	Reduction of Area, Calculated, %	Cold Work, %	Test Temperature, K	Reference No.
92.6	80.5	0	295	55
81.0	80.5	0	4	56
83.0	80.5	0	77	56
82.0	80.5	0	295	56
87.0	80.5	0	295	5
87.0	80.5	0	76	5
82.0	80.5	0	4	5
77.0	80.5	0	93	50

Table 2.9, continued

Reduction of Area, Measured, %	Reduction of Area, Calculated, %	Cold Work, %	Test Temperature, K	Reference No.
70.0	80.5	0	153	50
74.0	80.5	0	193	50
77.0	80.5	0	233	50
79.0	80.5	0	263	50
76.0	80.5	0	295	50
85.4	80.5	0	93	50
76.0	80.5	0	295	50
79.0	80.5	0	295	50
76.0	80.5	0	20	51
77.0	80.5	0	295	50
83.1	80.5	0	295	1
86.0	80.5	0	195	50
67.0	80.5	0	213	50
70.0	80.5	0	253	50
76.0	80.5	0	213	50
83.6	80.5	0	20	36
83.1	80.5	0	77	39
83.6	80.5	0	195	39
76.0	80.5	0	300	39
80.0	80.5	0	4	50
83.1	80.5	0	76	50
86.0	80.5	0	300	50
82.4	80.5	0	77	14
83.1	80.5	0	77	19
82.8	80.5	0	77	14
83.6	80.5	0	77	19
82.3	80.5	0	20	39
72.8	80.5	0	20	39
76.8	80.5	0	20	39
83.1	80.5	0	20	39
82.8	80.5	0	76	39
84.3	80.5	0	20	39
76.8	80.5	0	76	39
85.4	80.5	0	20	39
82.8	80.5	0	76	39
85.4	80.5	0	195	39
67.0	80.5	0	195	39
74.0	80.5	0	195	39
83.3	80.5	0	195	39
86.0	80.5	0	295	39
85.4	80.5	0	295	39
87.7	80.5	0	295	39
85.1	80.5	0	295	39
72.0	80.5	0	20	50
76.0	80.5	0	213	50
74.5	80.5	0	77	19
79.7	80.5	0	295	19
79.0	80.5	0	233	19
95.0	80.5	0	297	19
72.4	80.5	0	77	19
79.4	80.5	0	205	19

Table 2.9, continued

Reduction of Area, Measured, %	Reduction of Area, Calculated, %	Cold Work, %	Test Temperature, K	Reference No.
82.2	80.5	6	233	19
77.4	80.5	6	297	19
69.1	80.5	6	77	19
81.0	80.5	6	205	19
79.0	80.5	0	233	19
92.2	80.5	6	297	19
67.9	80.5	6	77	19
76.9	80.5	6	205	19
77.5	80.5	6	233	19
87.5	80.5	6	297	19
61.0	79.7	6	77	19
70.0	75.7	6	205	19
74.3	79.7	6	233	19
90.1	75.7	6	297	19
74.3	79.7	6	77	19
76.0	75.7	6	205	19
74.8	79.7	6	233	19
77.7	75.7	6	297	19
79.0	79.7	6	77	19
90.1	75.7	6	205	19
73.6	79.7	6	233	19
90.1	75.7	6	297	19
74.0	79.7	6	77	19
77.7	75.7	6	205	19
77.5	79.7	6	233	19
90.1	75.7	6	297	19
80.6	77.8	21	77	5
82.4	77.8	21	76	5
79.0	77.8	21	295	5
90.1	77.8	21	295	5
80.6	79.7	37	20	36
81.0	75.7	37	20	19
79.0	79.7	37	76	19
76.0	75.7	37	76	36
73.0	79.7	37	300	36
76.0	75.7	37	300	36
79.0	79.7	37	77	5
74.0	75.7	37	77	5
79.0	79.7	37	76	5
76.0	75.7	37	76	5
79.0	79.7	37	295	5
76.0	75.7	37	295	5
79.0	72.8	60	77	19
85.0	72.8	60	300	19
73.0	72.8	60	77	32
76.0	72.8	60	20	32
73.0	72.8	60	76	32
74.0	72.8	60	195	32
77.0	72.8	60	295	32
59.0	72.2	64	80	53
66.0	72.2	64	283	53

Table 2.9, continued

Reduction of Area, Measured, %	Reduction of Area, Calculated, %	Cold Work, %	Test Temperature, K	Reference No.
56.0	68.1	96	80	53
63.0	68.1	96	283	53

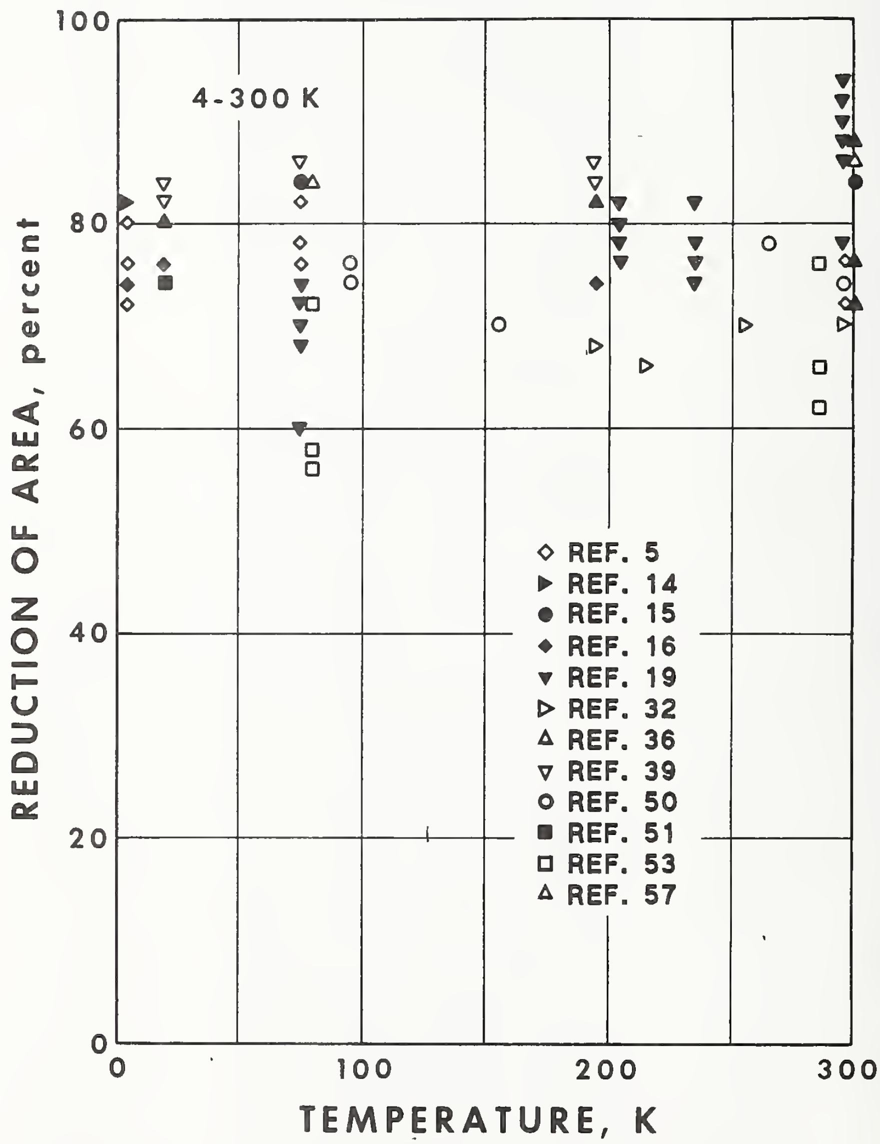

Figure 2.30. The data for all levels of cold work are plotted versus the temperature. For clarity, overlapping data points are omitted from the figure, including all points from References 2.1, 2.55, and 2.56. All data are presented in Table 2.9. Products were in plate, bar, and wire form.

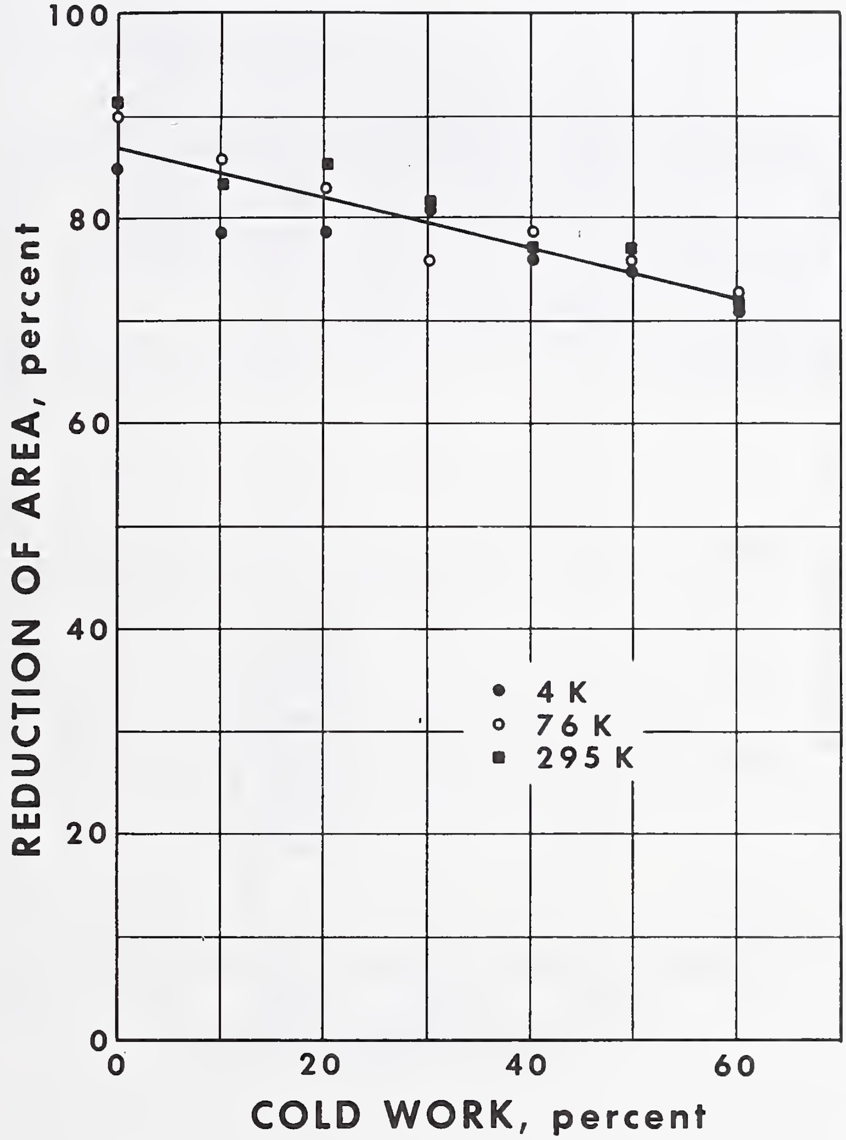

Figure 2.31. These data from Reference 2.34 indicate the decrease in reduction of area with increased cold work and the lack of significant temperature dependence (C10400 plate).

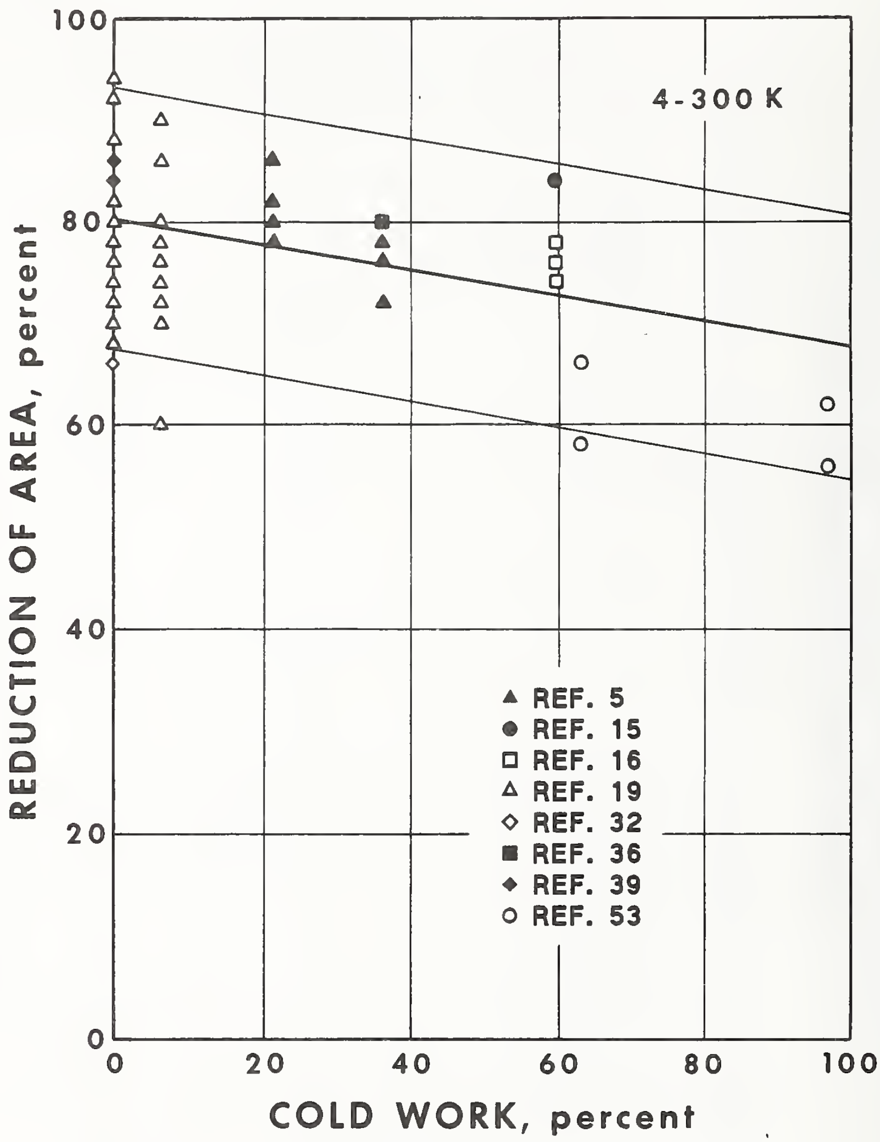

Figure 2.32. The data shown were used to compute the linear regression of reduction of area upon cold work [Equation (2-9)]. For clarity, overlapping data points are omitted from the figure, including all points from References 2.1, 2.14, 2.50–2.51, and 2.55–2.57. All data are presented in Table 2.9. Data from all temperatures between 4 and 300 K are included in this figure. (Regression analysis indicated no significant dependence upon temperature.) Products were in plate, bar, and wire form.

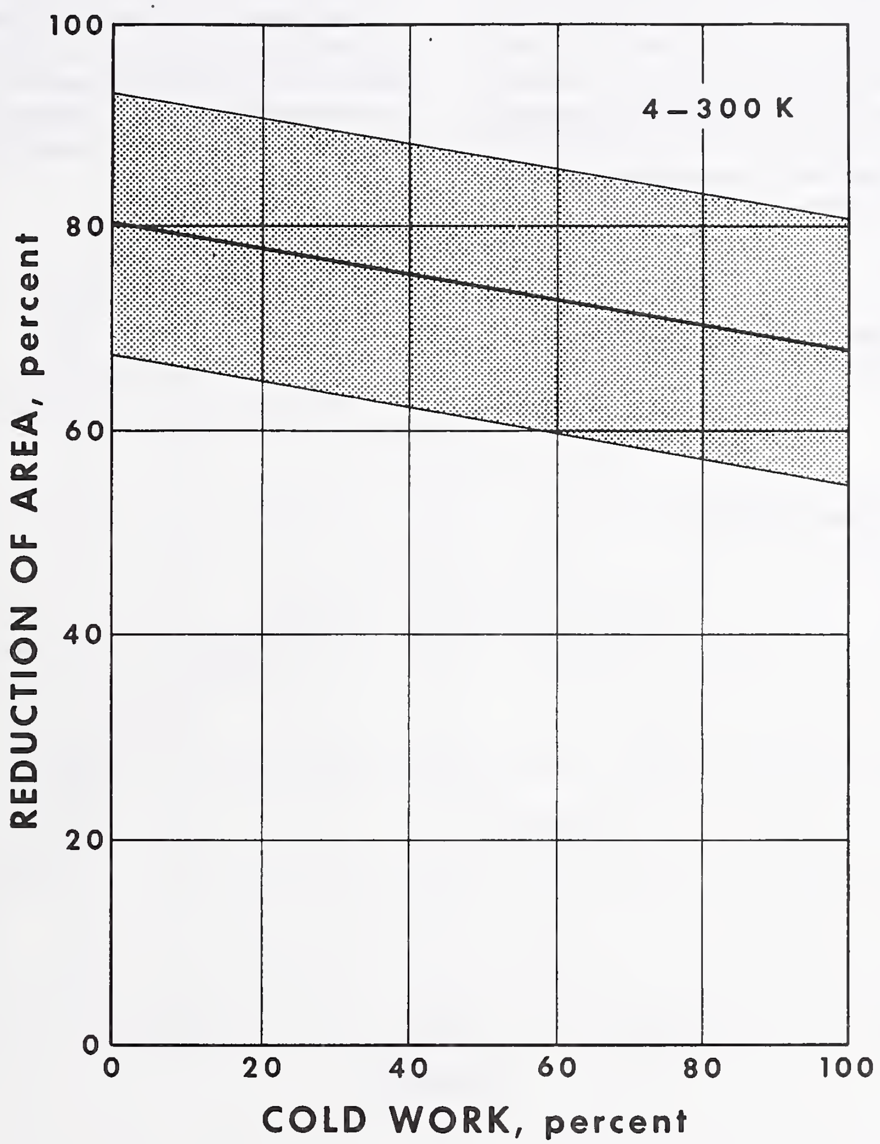

Figure 2.33. Tensile reduction of area dependence upon cold work from 4 to 300 K. The scatter band represents two standard deviations about a linear regression based upon 112 measurements of reduction of area for a range of cold work from 0 to 96%. The regression equation is

$$\text{REDUCTION OF AREA (\%)} = 80.5 - 0.128(CW) \qquad \text{(S.D. = 6\%)},$$

where *CW* is the percent of cold work (reduction of thickness or area). No significant temperature dependence was observed over the range 4 to 300 K. Products were in plate, bar, and wire form.

DATA SOURCE

Stress-strain curves at 4, 76, and 295 K for annealed, half-hard, and hard C10400 plate are presented in Figures 2.34, 2.35, and 2.36. Reference 2.5 is the source of these data. The available characterization of materials and measurements is given in Table 2.10 at the end of the tensile properties section. Measurements were displacement controlled.

DISCUSSION

Serrated yielding, shown schematically in the figures, is observed only at 4 K, in accord with test results on many other metals and alloys. The phenomenon may result from localized heating, which occurs at low temperatures owing to the very low specific heat. Another possible explanation is twinning; serrated yields in stress-strain curves of single crystals at low temperatures have been reported to originate from deformation-induced twins in copper (Reference 2.58).

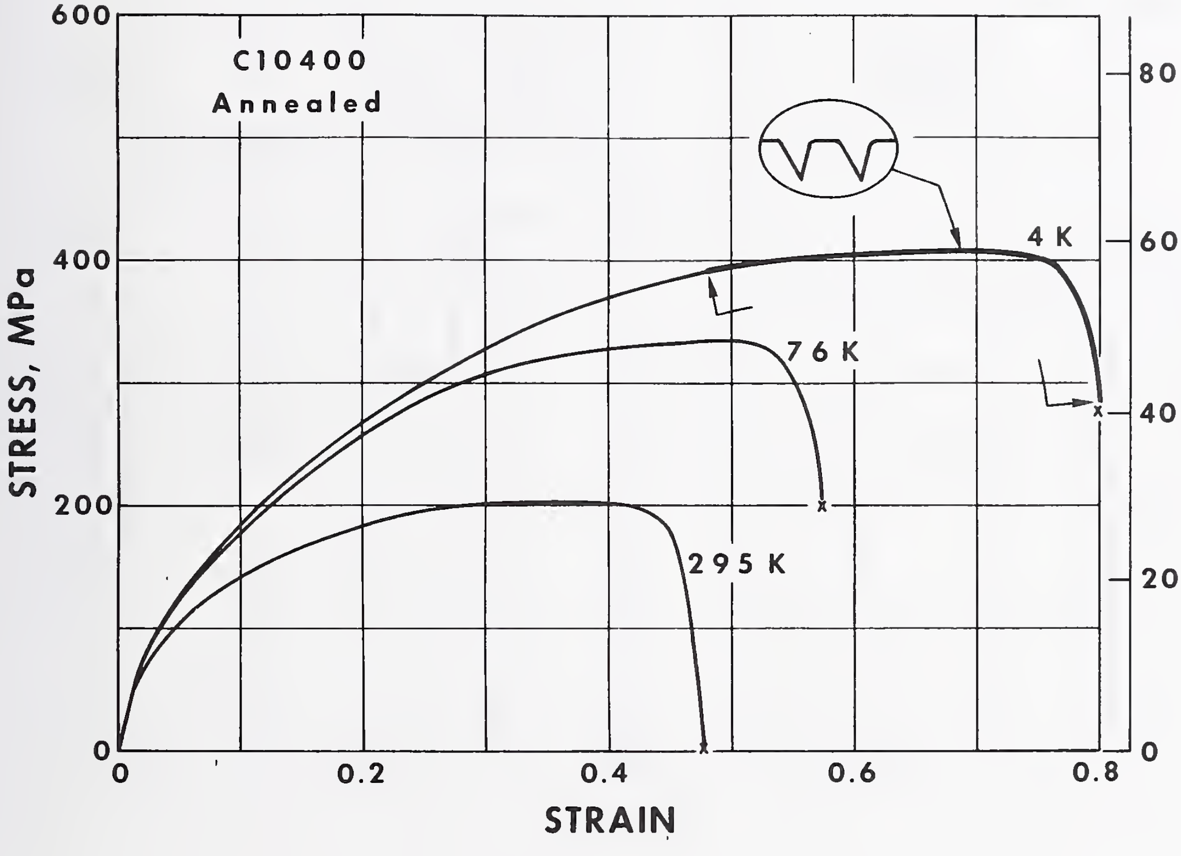

Figure 2.34. Stress-strain curves at three temperatures for annealed C10400 plate (Reference 2.5).

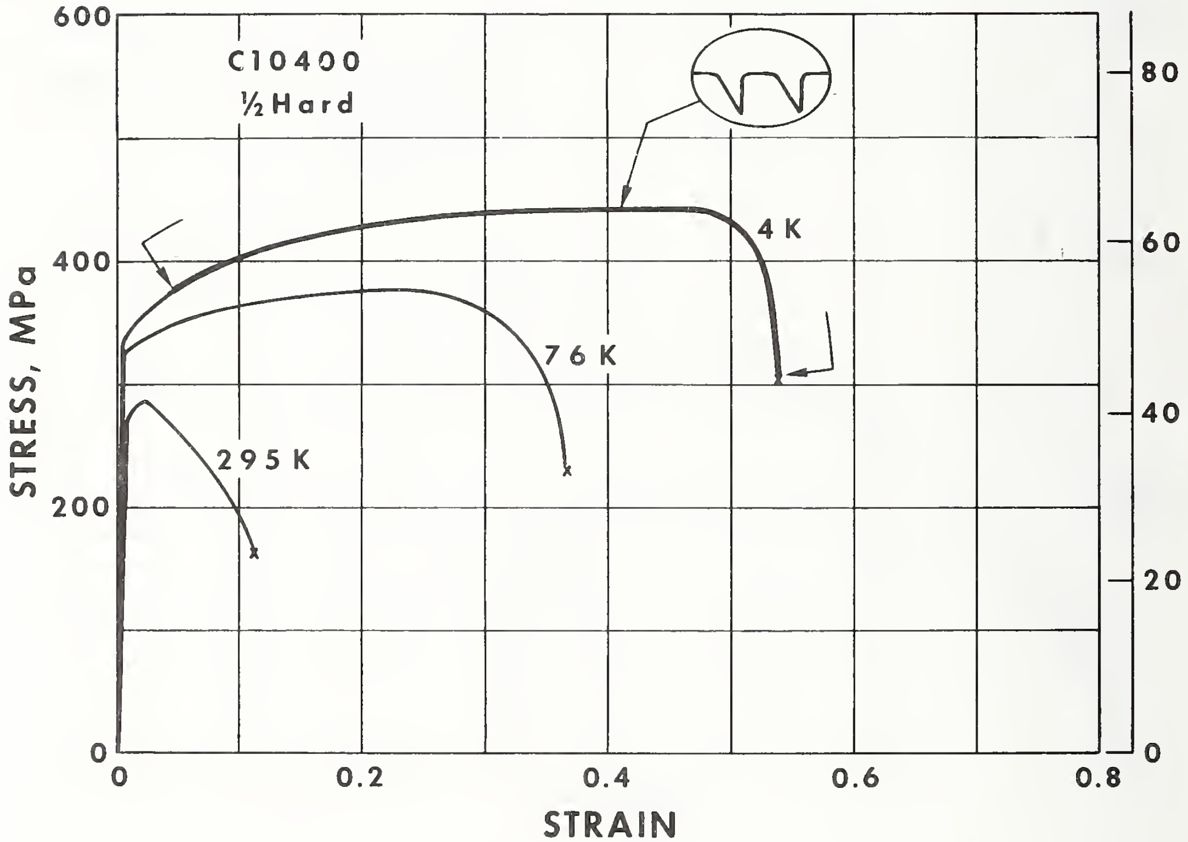

Figure 2.35. Stress-strain curves at three temperatures for half-hard C10400 plate (Reference 2.5).

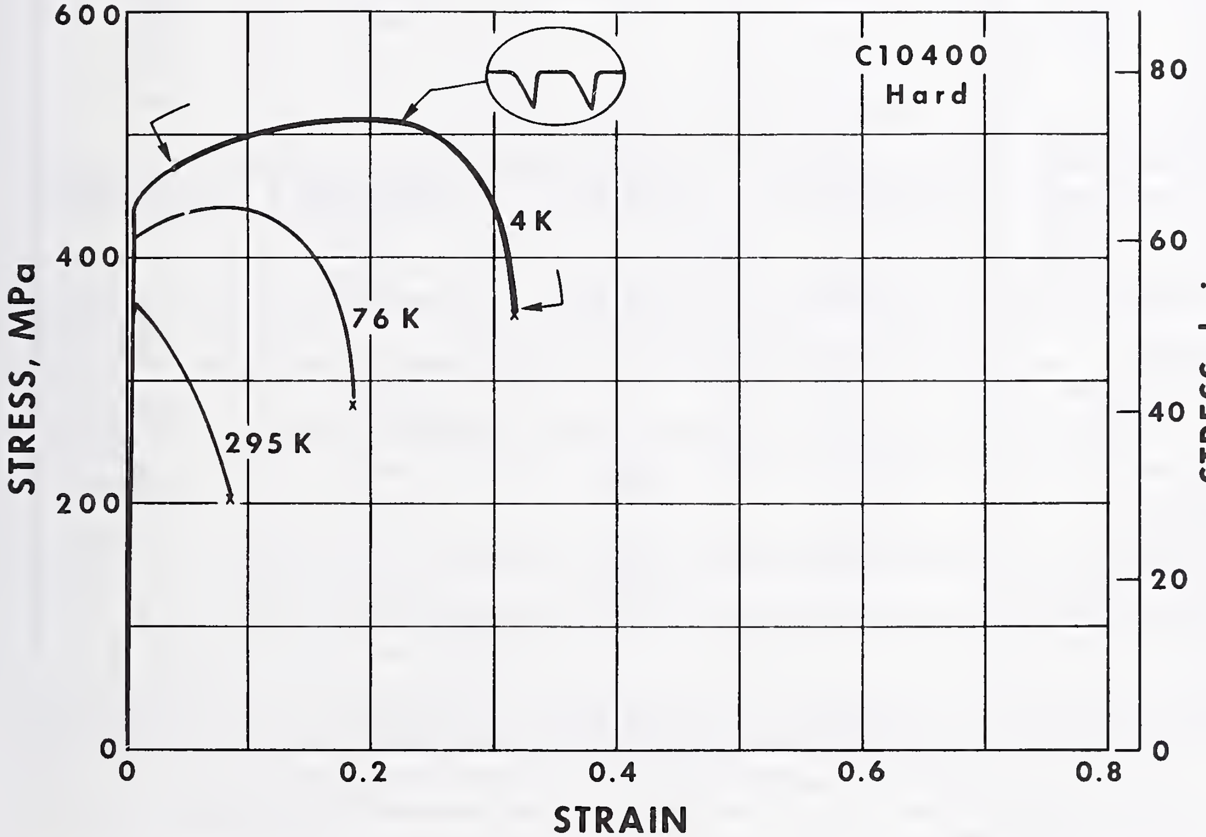

Figure 2.36. Stress-strain curves at three temperatures for hard C10400 plate (Reference 2.5).

Table 2.10. Characterization of Materials and Measurements.

Reference No.	1	2	3	4
Specification	C10100	C10200	C10100	C10200
Composition (wt%)				
Cu	99.99+	99.98	99.99	99.8986
Ag	—	—	0.005	0.0014
Cu + Ag	—	—	—	—
O_2	—	—	—	—
Bi	—	—	0.0005	0.00007
P	—	—	—	0.0004
Pb	—	—	0.002	0.0006
S	—	—	—	0.0011
Se	—	—	—	—
Te	—	—	—	<0.0002
Others (Only ≥ 0.001 wt%)	—	—	Ni, 0.005; Zn, 0.001	—
Material Condition	Annealed, 700 K, 1 h (a)	Annealed, 500–900 K, 2 h	Annealed, 723 K, 1 h	Annealed, 573 K, 1 h
Grain Size	25 μm	17–165 μm	10–15 μm	11 μm
Hardness	R_F 34	—	—	(c)
Product Form	Bar	—	Wire, 0.203-cm-dia.	Wire
Specimen Type	Round	Round	Wire	Wire
Width or Dia.	1.28 cm	0.4 cm	0.122 cm	0.07 cm
Thickness	—	—	—	—
Gage Length	5.1 cm	6.0 cm	15.0 cm	—
Strain (Load) Rate	(b)	0.01/min	0.005/min	(d)
No. of Specimens	—	—	4 per temperature	4 or more per temperature
Test Temperature	78–296 K	90–295 K	78–473 K	4, 76, 298 K

(a) Bars were hot-worked and then annealed.
(b) Rate of loading was controlled so that area rate of contraction beyond yielding point was kept at about 1.0% per minute.
(c) DPH 70 ± 10 (2-g load).
(d) Prestrained to 0.02, strain rate 0.004/min during plastic deformation.

5	6	7A	7B	8
C10400	C10200	C10200	C10200	C10100
—	99.9	99.95	99.95	99.991
0.027	—	—	—	0.0006
99.95	—	—	—	—
—	—	—	—	—
—	—	—	—	not detected
—	—	0.02	0.02	—
—	—	—	—	0.0004
—	—	—	—	0.0008
—	—	—	—	—
—	—	—	—	—
	—	As, Fe, Ni, Sn, Zn <0.01	As, Ni, Sn, Zn <0.01	Fe, 0.004
Annealed, 783 K, 1 h, Ar, AC (a)	Annealed, 903 K, 1.5 h, furnace cooled	Annealed, 773 K, 2 h	Annealed, 773 K, 2 h	Annealed, 773–973 K, 1.25–8.5 h
80 μm (b)	20 μm	30 μm	45 μm	26–320 μm
R_F 53 (c)	—	6	—	—
Plate, 3.2-cm-thick	—	Plate	Plate	Strip, 0.3-cm-thick
Round	—	—	—	Wire
0.64 cm	—	—	—	0.2 cm
—	—	—	—	—
4.19 cm	—	—	—	10 cm
—	—	—	6	0.6/min
11	—	—	—	12
4, 76, 295 K	77, 293 K	295 K	295 K	291 K

(a) Other specimens: ½-hard and hard (cold-rolled 50% from ½-hard condition).
(b) ½-hard, 77 μm; hard, not measured.
(c) ½-hard, R_F 80; hard, R_F 88.

Table 2.10, continued

Reference No.	9	10	11	12
Specification	C10200	C10100	C10200	C10100
Composition (wt%)				
Cu	99.96	99.999+	99.9	99.99+
Ag	—	—	—	—
Cu + Ag	—	—	—	—
O_2	—	—	—	—
Bi	—	—	—	—
P	—	—	—	—
Pb	—	—	—	—
S	—	—	—	—
Se	—	—	—	—
Te	—	—	—	—
Others (Only ≥ 0.001 wt%)	—	—	—	—
Material Condition	Annealed, 894 K, 0.75 h; 1144 K, 0.1 h	(b)	Annealed	Annealed, various temperatures, 1 h
Grain Size	34, 190 μm	0.056–8.4 μm	20–90 μm	3.4–150 μm
Hardness	31.3–40.5 (a)	—	—	—
Product Form	Bar	—	—	—
Specimen Type	Round	Flat	—	Round
Width or Dia.	0.794 cm	0.32 cm	—	0.8 cm
Thickness	—	0.053–0.089 cm	—	—
Gage Length	15.2 cm	0.95 cm	—	3.8 cm
Strain (Load) Rate	—	0.053/min	0.048/min 0.0004/min	0.05/min
No. of Specimens	—	—	—	—
Test Temperature	295 K	295 K	295 K	295 K

(a) Diamond-pyramid hardness.
(b) Sputter deposition: substrate temperature-controlled grain size—373 K, 0.056 μm; 473 K, 8.4 μm.

13	14	15	16	17A
C10100	C10100	C10100	C10100	C10100
— — 99.99 — — — — — — — —	99.993+ 0.0017 — — 0.00006 <0.0003 0.0005 0.0013 — <0.0002 —	99.99 — — — — — — — — — —	99.995 0.0016 — <0.0003 trace 0.0001 0.0004 0.0012 — — —	99.997 — — — — — — — — — —
Annealed, 923 K, 1 h	Vacuum annealed, 922 K, 0.5 h	Cold-worked, 60%, cross-rolled	Cold-drawn, 60%	Annealed. Others: cold-rolled, 18–40%
42 μm	53 μm	—	287–2000 μm	40 μm
—	R_F 14.7	—	R_B 45–53	HB 45 (b)
Bar, 1.9-cm-dia.	Bar, 2.54-cm-dia.	Plate, 1.25-cm-thick	Bar (a), 1.90-cm-dia.	—
Round 0.64 cm — —	Round 0.64 cm — 3.18 cm	Round 0.64 cm — —	Round 0.64 cm — 3.8 cm	Flat 1.1 cm (c) — —
—	0.05/min	—	0.05 cm/min (crosshead)	—
—	—	—	—	—
4–295 K	4, 77 K	77, 300 K	4–295 K	295 K

(a) Commercial stock, standard mill.
(b) Cold-rolled, 18%, HB 66; 30%, HB 70; 40%, HB 72.
(c) Before rolling.

Table 2.10, continued

Reference No.	17B	18A	18B	19
Specification	C10200	C10200	C10500	C10200
Composition (wt%)				
Cu	99.97 (a)	99.94	99.95	99.96
Ag	—	—	—	—
Cu + Ag	—	—	—	—
O_2	—	—	—	—
Bi	—	—	—	—
P	—	—	—	—
Pb	—	—	—	—
S	—	—	—	—
Se	—	—	—	—
Te	—	—	—	—
Others (Only ≥ 0.001 wt%)	—	—	—	—
Material Condition	Cold-rolled, 70–90%	Annealed, 977 K, 1 h. Others: cold-rolled, 11–68.6%	Annealed 922 K, 1 h. Others: cold-rolled, 11–68.6%	Annealed, 894 K, 0.5 h (d)
Grain Size	38–80 μm	15–40 μm	15–35 μm	45–48 μm (e)
Hardness	HB 114–126	R_F 30 (b)	R_F 34 (c)	—
Product Form	Cold-forging, 9.3 cm	Strip	Strip	Sheet (f)
Specimen Type	Flat	Flat	Flat	Flat (g)
Width or Dia.	—	—	—	1.27 cm
Thickness	—	0.10 cm	0.10 cm	0.318 and 0.64 cm
Gage Length	—	5.1 cm	5.1 cm	—
Strain (Load) Rate	—	—	—	—
No. of Specimens	—	—	—	—
Test Temperature	295 K	295 K	295 K	77–297 K

(a) Electrolytic.
(b) Cold-rolled, R_F 90–92 (60-kg load).
(c) Cold-rolled, R_F 92–95 (60-kg load).
(d) Other specimens: cold-worked, 6–75%, or hot-rolled and drawn.
(e) Cold-rolled, 25–46.5 μm; cold-drawn, 40–75 μm.
(f) Annealed condition, 0.318 and 0.64-cm thick; cold-worked, 0.338 and 0.676-cm thick.
(g) Longitudinal and transverse orientations.

20	21	22A	22B	23
C11000 (a)	C10100	C10200	C10200	C10200
99.95	99.99+	99.98	99.95	—
—	—	—	—	—
—	—	—	—	—
—	—	—	—	—
—	—	—	—	—
—	—	—	0.008	—
—	—	<0.0005	—	—
—	—	—	—	—
—	—	—	—	—
—	—	—	—	—
—	—	<0.01 Zn; <0.003 Fe; <0.005 Ni	0.001 Fe; 0.001 Ni	—
Annealed, 823 K, 1 h (b)	Annealed, 700–894 K, 0.83–1 h (d)	Annealed (f)	Annealed (h)	Annealed, 873 K, 2 h. AC (j)
65 μm (c)	25 μm (e)	25 μm (g)	13 μm (i)	—
—	—	—	—	—
— —	Bar, 2.06 or 2.22-cm-dia.	—	—	Bar, 2.54-cm-dia.
— — — —	Round 1.28 cm — 5.1 cm	Wire 0.318 cm — 25.4 cm	Wire 0.318 cm — 25.4 cm	Round 1.18 cm — —
—	1% area reduction per min	—	—	0.02/min
—	—	—	—	5
295 K	295 K	295 K	295 K	295 K

(a) Possibly equivalent to C10200; complete analysis not given.
(b) Other specimens: cold-rolled, 11%, 31%.
(c) Cold-rolled, 11%, 45 μm; 31%, 25 μm.
(d) Other specimens: cold-drawn, 34%, 40%, and 70%.
(e) Cold-drawn, 34% and 40%, 25 μm; 70%, 45 μm.
(f) Other specimens: cold-drawn, 84%.
(g) Same grain size, cold-drawn specimens.
(h) Other specimens: cold-worked, stretched 1–6%.
(i) Same as for cold-worked specimen.
(j) Other specimens: cold-drawn, 20–78%.

Table 2.10, continued

Reference No.	24	25B	25B	26
Specification	C10100	C10100	C10500	C10100
Composition (wt%)				
Cu	99.996	99.9943	99.9411	99.997
Ag	—	0.0011	0.0537	—
Cu + Ag	—	—	—	—
O_2	—	—	—	not detected
Bi	—	not detected	0.0001	—
P	—	—	—	—
Pb	—	0.0002	0.0005	—
S	—	0.0011	0.0014	0.0016
Se	—	0.0001	0.0003	—
Te	—	not detected	not detected	—
Others (Only ≥ 0.001 wt%)	—	Ni, 0.0011	Fe, 0.001	—
Material Condition	Annealed. Other: cold-drawn, 36% hard	Annealed. Others: hard-drawn and 1/2-hard (b)	Annealed. Others: hard-drawn and 1/2-hard (b)	Cold-drawn, 29.2%
Grain Size	135 µm (a)	(c)	(e)	125 µm
Hardness	—	—	—	R_B 37.2
Product Form	Bar, 1.90-cm-dia.	Bar, 10 × 10 × 137 cm	Bar, 10 × 10 × 137 cm	Bar, 1.27-cm-dia.
Specimen Type	Round	Wire; square bar	Wire; square bar	Round
Width or Dia.	1.28 cm	(d)	(d)	0.64, 0.8 cm
Thickness	—	—	—	—
Gage Length	5.1 cm	—	—	5.0 cm
Strain (Load) Rate	—	—	—	—
No. of Specimens	—	—	—	—
Test Temperature	305 K	295 K	295 K	295 K

(a) Cold-drawn, 36%, 70 µm.
(b) Annealed, 616 K, 3 h, steam. Hard-drawn, 20.5 and 84.4% (square bar and wire, respectively); ½-hard, 8.5 and 37.1% (square bar and wire, respectively).
(c) Annealed, 35–45 µm.
(d) 0.203-cm-dia. wire and 0.653-cm square rod.
(e) Annealed, 15–25 µm.

27	28A	28B	28C	29
C10200	C10100	C10500	C10700	C10200
— — — — — — — — — — —	99.994 0.0011 — — not detected — 0.0002 0.0011 0.0001 not detected Sb, 0.001; Ni, 0.0011	99.9411 0.0537 — — 0.0001 — 0.0005 0.0014 0.0003 — Fe, 0.001	99.9182 0.0755 — — 0.0001 — 0.0017 <0.0004 <0.0006 — Sb, 0.0012	99.95+ — — — — — — — — — —
Cold-drawn, 2–10%	Annealed, 616 K 3 h (c)	Annealed, 616 K 3 h (c)	Annealed, 616 K, 3 h (c)	Hot-rolled. Others: commercial hard, cold-worked, 37% (e)
—	35–45 μm	35–45 μm	35–45 μm	—
—	—	—	—	—
—	Bar, 10 × 10 × 137 cm	Bar, 10 × 10 × 137 cm	Bar, 10 × 10 × 137 cm	—
(a) (b) — —	Flat 0.653 × 0.653 cm — 2.54 cm	Flat 0.653 × 0.653 cm — 2.54 cm	Flat 0.653 × 0.653 cm — 2.54 cm	Round 1.3 cm — 5.1 cm
0.0025/min	—	—	—	(d)
—	—	—	—	—
295 K	295 K	295 K	295 K	295 K

(a) Round and rectangular.
(b) 0.77-cm dia., 0.25-cm dia., and 2.2 × 0.28-cm cross sections.
(c) Other specimens: cold-drawn, 5%; cold-rolled, 5%, 20%, 30%, 40%.
(d) Minimum values; 0.001/min to yield point, then 0.01–0.02/min.
(e) Electrolytic.

Table 2.10, continued

Reference No.	30A	30B	31	32
Specification	C10100	C10500	C10200	C10200
Composition (wt%)				
Cu	99.995+	99.924	—	99.97
Ag	0.001	0.072	—	0.003
Cu + Ag	—	—	—	—
O_2	0.0002	0.0002-0.0003	—	0.032
Bi	not detected	not detected	—	—
P	not detected	not detected	—	—
Pb	0.0003	0.0003	—	—
S	0.002	0.002	—	—
Se	—	—	—	—
Te	not detected	not detected	—	—
Others (Only ≥ 0.001 wt%	—	—	—	Fe, 0.005
Material Condition	Annealed (a)	Annealed (a)	Annealed, 873 K, 1 h (e)	Annealed, 723 K. Others: cold-rolled, 9.0–89.4%
Grain Size	40 µm (b)	40 µm (b)	—	—
Hardness	VPN 36.8 (c)	VPN 37.8 (d)	VPN 45 (f)	D.P. 48 (g)
Product Form	Strip, 3.18 × 0.3 cm	Strip, 3.18 × 0.3 cm	Bar, 1.9-cm-dia.	Strip, 1.17-cm-thick
Specimen Type	Flat	Flat	Round	Flat
Width or Dia.	—	—	0.8 cm	30 cm
Thickness	—	—	—	0.13 cm
Gage Length	—	—	1.3 cm	—
Strain (Load) Rate	—	—	—	—
No. of Specimens	—	—	—	11
Test Temperature	295 K	295 K	295 K	295 K

(a) Other specimens: cold-drawn, 10 and 25%; 50% reduction achieved by cold-drawing 32% followed by cold-rolling.
(b) Cold-worked, 10%, 40 µm; 25%, 35 µm; 50%, unspecified.
(c) Cold-worked, 10%, VPN 91.0; 25%, VPN 101.3; 50%, VPN 111.0 (20-kg load).
(d) Cold-worked, 10%, VPN 93.4; 25%, VPN 102.0; 50%, VPN 115.0 (20-kg load).
(e) Other specimens: cold-worked, 21%, 37%.
(f) Cold-worked, 21%, VPN 70; 37%, VPN 104.
(g) Cold-rolled, D.P. 77–121.

33	34	35	36	37
C10700	C10400	C10200	C10200	C10200
99.87 0.088 — — — 0.003 0.0022 not detected 0.0008 0.0010 Al, 0.0054; Sn, 0.0093; Te, 0.001; Zr, 0.0022	— 0.027 99.95 — — — — — — — —	— — — — — — — — — — —	— — — — — — — — — — —	— — — — — — — — — — —
Cold-rolled, 40%	Annealed, 773 K, 1.5 h (b)	Annealed. Others: cold-worked, 5–50%	Hard, tested without further treatment (f)	Annealed, 798 K, 6 h (l). Other: cold-worked, 11.5%
—	—	—	(g)	110 μm
R_F 85.75 (a)	(c)	(e)	R_B 57 (h)	—
Plate, 2.5-cm-thick	Plate, 3 × 8 × 28 cm	—	Bar (i), 1.9-cm-dia.	—
Flat 0.76 cm 0.61 cm 2.5 cm	Round 0.64 cm — 3.8 cm	— 0.05 cm — —	Round 0.64 cm (j) — 2.54 cm (k)	Round 1.28 cm — —
—	0.02 cm/min (crosshead)	—	0.0005/min to yield; then 0.02/min	—
—	(d)	—	—	—
295 K	4, 76, 295 K	4 K	20–300 K	72, 198, 225 K

(a) Mean of 392 data points, standard deviation 1.53, range 80.5–89.0.
(b) Other specimens: cold-rolled, 10, 20, 30, 40, 50, 60%.
(c) Respective R_F values corresponding to 10, 20, 30, 40, 50, 60% cold work were 81, 82, 87, 89, 90, 91.
(d) One specimen per temperature and cold-worked condition.
(e) Hardness available on 21% cold-worked only, 92.8–93.2 (Vickers hardness scale).
(f) Other specimens: foil, annealed, 473 K, 8 h, He; wire, annealed.
(g) Foil, 14 μm; square wire, 11 μm.
(h) Foil, not specified; wire, R_F 49.
(i) Foil, 0.025 cm; square wire, 0.318 cm.
(j) Foil coupon, 1.3-cm wide; square wire, 0.203-cm^2 cross section.
(k) Foil, 5.1 cm; square wire, 3.0 cm.
(l) Annealed in vacuum and then furnace-cooled.

Table 2.10, continued

Reference No.	38	39	40	41
Specification	C10100	C10100	C10200	C10200
Composition (wt%)				
Cu	99.999	—	99.97	99.97
Ag	0.00003	—	—	—
Cu + Ag	—	99.99	—	—
O_2	—	—	—	—
Bi	0.0001	—	—	—
P	—	—	—	—
Pb	0.0001	—	—	—
S	0.0001	—	—	—
Se	0.0001	—	—	—
Te	0.0002	—	—	—
Others (Only ≥ 0.001 wt%	—	—	—	—
Material Condition	Annealed, 523–1223 K, 1 h, H_2	Annealed, soft	Annealed, 700 K, 5 h. Other: cold-rolled, 75%	Annealed, 873 K, Ar, several h
Grain Size	12–90 μm	65 μm	—	—
Hardness	—	R_H 86	—	—
Product Form	Bar, 0.919-cm–dia.	Bar, 1.9-cm-dia.	Bar, 2.22-cm-dia.	Bar
Specimen Type	Wire	Round	Round	Round
Width or Dia.	0.076 cm	0.45 cm	—	0.159 cm
Thickness	—	—	—	—
Gage Length	12.7 cm	3.18 cm	—	0.5 cm
Strain (Load) Rate	(a)	0.0508 cm/min and 0.508 cm/min (b)	—	—
No. of Specimens	—	—	—	—
Test Temperature	20–1223 K	20–295 K	85–300 K	4–293 K

(a) 0.04/min to 0.09 strain; then 0.004/min.
(b) Crosshead.

42	43	44	45	46A
C10200	C10200	C10200	C10200	C10200
— — — — — — — — — — —	99.982 0.003 — — <0.0001 — 0.001 — — — Fe, 0.005	99.97 — — — — — — — — — —	— — — — — — — — — — —	— — — — — — — — — — —
Annealed (a)	Annealed, 773–923 K, 0.5–1 h (b)	Annealed, 700 K 2 h, AC (c)	Annealed (d)	Annealed (f)
—	—	—	—	—
—	—	—	VPN 88.5 (e)	—
Wire, 0.127-cm-dia.	Bar, 2.22-cm-dia.	Bar, 1.9-cm-dia.	Bar, 30.5 × 5.1 × 1.3 cm	—
Wire 0.127 cm — —	Round 1.43 cm — 5.1 cm	— — — —	Flat 1.3 cm — 5.1 cm	Wire — — —
—	0.05/min	—	0.25 cm/min (crosshead)	—
—	—	—	—	—
298 K	295 K	295 K	295 K	295 K

(a) Other specimens: cold-drawn 13–85% at 298 K.
(b) Other specimens: cold-drawn, 23%.
(c) Other specimens: extended by tension 9.8% and 24%; cold-drawn 36% and 54%; cold-rolled 75%.
(d) Other specimens: cold-rolled, 30–98.6%.
(e) Cold-worked, VPN 98.5–126.
(f) Other specimens: cold-worked, 50%; type of cold work not specified.

Table 2.10, continued

Reference No.	46B	47A	47B	48
Specification	C10200	C10100	C10200	C10100
Composition (wt%)				
Cu	—	99.999	99.991	99.999
Ag	—	< 0.00003	0.0014	< 0.00003
Cu + Ag	—	—	—	—
O_2	0.03	—	—	—
Bi	—	< 0.00001	0.00002	< 0.00001
P	—	—	—	—
Pb	—	< 0.0001	0.0003	< 0.0001
S	—	< 0.0001	0.0037	< 0.0001
Se	—	< 0.0001	< 0.0001	< 0.0001
Te	—	< 0.0002	0.0001	< 0.0002
Others (Only ≥ 0.001 wt%	—	—	Ni, 0.0015	—
Material Condition	Annealed (a)	Annealed, 293–732 K (b)	Annealed, 293–723 K (c)	Annealed, 773 K, 1 h (d)
Grain Size	—	20, 25 μm	20 μm	35–40 μm
Hardness	—	—	—	48
Product Form	—	Bar, hot-rolled, 0.794-cm-dia.	Bar, hot-rolled, 0.794-cm-dia.	Cast bar, 0.952-cm-dia.
Specimen Type	Wire	Wire	Wire	Wire
Width or Dia.	—	0.2 cm	0.2 cm	0.206 cm
Thickness	—	—	—	—
Gage Length	—	15.2 cm	35.6 cm	25 cm
Strain (Load) Rate	—	—	—	0.0125/min
No. of Specimens	—	—	—	—
Test Temperature	295 K	295 K	295 K	295 K

(a) Other specimens: cold-worked, 50%; type of cold work not specified.
(b) Other specimens: cold-drawn, 20.8–93.4%.
(c) Other specimens: cold-drawn, 4.8–93.4%.
(d) Other specimens: cold-drawn, 50–87.5%.

49	50	51	52	53
C10200	C10200	C10200	C10200	C10200
— — — — — — — — — — —	99.985 — — — — — — — — — —	99.6 — — — — — — — — — —	99.985 — — — — — — — — — —	— — — — — — — — — — —
Cold-drawn, 62.5%	Annealed (a)	Annealed, 1073 K, AC	Annealed	Annealed, 1023 K. Other: cold-drawn, 64% and 96%
150 μm	—	—	—	—
—	—	Brinell 59, 63	—	—
—	Bar, 2.54-cm-dia.	—	—	Wire
— — — —	Round 1.432 cm — 5.1 cm	Round 0.3 cm — 3.0 cm	—	Wire 0.064 cm — —
—	—	—	—	—
—	—	—	—	—
295 K	93–293 K	20, 295 K	113–293 K	80–283 K

(a) Tested as received.

Table 2.10, continued

Reference No.	54	55	56	57
Specification	C10200	C10200	C10200	C10100
Composition (wt%)				
Cu	99.98	99.96	99.95	99.99
Ag	—	—	—	—
Cu + Ag	—	—	—	—
O_2	—	—	—	—
Bi	—	—	—	—
P	—	—	—	0.0003
Pb	—	—	—	—
S	—	—	—	0.0018
Se	—	—	—	—
Te	—	—	—	—
Others (Only ≥ 0.001 wt%	—	—	—	—
Material Condition	Hot-rolled	Annealed. Other: 1/2 hard, cold-drawn, 21%	Annealed, 478 K, 1 h	Vacuum annealed, 920 K, 1 h
Grain Size	—	32–170 μm (a)	—	—
Hardness	—	R_F 13.8–18.2 (b)	—	—
Product Form	Plate, 4.0 × 4.0 cm	—	Plate, 1.3 and 1.6-cm-thick	Wrought bar stock, 2.54-cm-dia.
Specimen Type	Round	Round	Round	Round
Width or Dia.	2 cm	0.793 cm	0.51 cm	0.635 cm
Thickness	—	—	—	—
Gage Length	10 cm	—	—	2.54 cm
Strain (Load) Rate	—	—	—	—
No. of Specimens	—	—	1 per temperature	—
Test Temperature	196–293 K	295 K	4, 77, 295 K	4, 78, 300 K

(a) Cold-drawn, 21%; not available.
(b) Cold-drawn, 21%; R_F 81.8–91.2.

REFERENCES

1. Geil, G. W., and Carwile, N. L., "Tensile Properties of Copper, Nickel, and Some Copper-Nickel Alloys at Low Temperatures," in NBS Circular 520, U.S. National Bureau of Standards, Gaithersburg, MD, 67–95 (1952).

2. Knoll, H., and Macherauch, E., "Die plastische Verformung von Kupfervielkristallen im Temperaturbereich von 90 bis 300 K," Zeitschrift für Metallkunde 55, 638–645 (1964).

3. Makin, M. J., "The Effect of Neutron Irradiation on the Mechanical Properties of Metals: Part III--Copper and Nickel," Atomic Energy Research Establishment, Harwell, Great Britain, MIR 2080, 22 pp. (1956).

4. Reed, R. P., Mikesell, R. P., and Clark, A. F., "Low Temperature Tensile Behavior of Copper-Stabilized Niobium-Titanium Superconducting Wire," in Advances in Cryogenic Engineering, Vol. 22, Eds., K. D. Timmerhaus, R. P. Reed and A. F. Clark, Plenum Press, New York, 463–471 (1977).

5. Reed, R. P., and Walsh, R. P., National Bureau of Standards, Boulder, CO, private communication (1986).

6. Tschegg, E., and Stanzl, S., "Fatigue Crack Propagation and Threshold in B.C.C. and F.C.C. Metals at 77 and 293 K," Acta Metallurgica 29, 33–40 (1981).

7. Drefahl, K., Kleinau, M., and Steinkamp, W., "Creep Properties and Design Data of Copper and Copper Alloys for Apparatus Construction," Metall 36, 504–518 (1982).

8. Feltham, P., and Meakin, J. D., "On the Mechanism of Work Hardening in Face-Centered Cubic Metals, with Special Reference to Polycrystalline Copper," Philosophical Magazine 2, 105–112 (1957).

9. Knapp, W., "The Effects of Specimen Grain Size and Environment on the Fatigue Life of OFHC Copper," University of Toronto, Canada, UTIAS Technical Note 124, 54 pp. (1968).

10. Merz, M. D., and Dahlgren, S. D., "Tensile Strength and Work Hardening of Ultrafine-Grained High-Purity Copper," Journal of Applied Physics 46, 3235–3237 (1975).

11. Polakovic, A., and Taborsky, L., "Der Einfluß der Deformationsgeschwindigkeit, des Korndurchmessers, sowie der Reinheit von Aluminum und Kupfer auf die Verfestigungskurve," Metall 25, 12–14 (1971).

12. Thompson, A. W., and Backofen, W. A., "The Effect of Grain Size on Fatigue," Acta Metallurgica 19, 597–606 (1971).

    Thompson, A. W., and Backofen, W. A., "Production and Mechanical Behavior of Very Fine-Grained Copper," Metallurgical Transactions 2, 2004–2005 (1971).

13. Reed, R. P., National Bureau of Standards, Boulder, CO, private communication (1985).

14. Wells, J. M., Tien, J. K., Roth, L. D., Wetzel, J. T., Yen, C. T., and Caulfield, T., "Creep of Copper at Cryogenic Temperatures," International Copper Research Association, New York, NY, Final

REFERENCES

Report, Project No. 312, 77 pp. (1985). See also Yen, C., Caulfield, T., Roth, L. D., Wells, J. M., and Tien, J. K., Cryogenics 24, 371–377 (1984).

15. Becker, H., Montgomery, D. B., and Reed, R. P., "Wanted: Cryogenic Mechanical Property Data on Copper Alloys," Massachusetts Institute of Technology Plasma Fusion Center, Cambridge, MA, private communication (1985).

16. Reed, R. P., and Mikesell, R. P., "Low-Temperature (295 to 4 K) Mechanical Properties of Selected Copper Alloys," Journal of Materials 2, 370–392 (1967).

17. Witzel, W., "Einfluß der Walzrichtung auf die Mechanischen Eigenschaften von Kupfer mit Würfellage," Metall 36, 1174–1178 (1982).

18. Wilkins, R. A., and Bunn, E. S., "Copper and Copper Base Alloys," McGraw-Hill Book Company, New York, 355 pp. (1943).

19. Upthegrove, C., and Burghoff, H. L., "Elevated-Temperature Properties of Coppers and Copper-Base Alloys," American Society for Testing and Materials, Philadelphia, PA, Special Technical Publication No. 181, 75 pp. (1956).

20. Liaw, P. K., Leax, T. R. Williams, R. S., and Peck, M. G., "Near-Threshold Fatigue Crack Growth Behavior in Copper," Metallurgical Transactions 13A, 1607–1618 (1982).

21. Jenkins, W. D., and Digges, T. G., "Influence of Prior Strain History on the Tensile Properties and Structures of High-Purity Copper," Journal of Research of the National Bureau of Standards 49, 167–186 (1952).

22. Burghoff, H. L., and Blank, A. I., "The Creep Characteristics of Copper and Some Copper Alloys at 300, 400, and 500 °F," Proceedings of the American Society for Testing and Materials 47, 725–753 (1947).

23. Thomsen, E. G., Holthuis, J. T., and Thomsen, H. H., "Flow Stresses of Prestrained Annealed OFHC Copper and SAE 1018 Steel," Journal of Engineering Materials and Technology 103, 188–193 (1981).

24. Smith, C. S., and Wagner, R. W., "The Tensile Properties of Some Copper Alloys," Proceedings of the American Society for Testing and Materials 41, 825–848 (1941).

25. Jackson, L. R., Hall, A. M., and Schwope, A. D., "The Comparative Properties of Several Types of Commercial Coppers, as Cold Worked and as Recrystallized," Transactions of the American Institute of Mining and Metallurgical Engineers 14, 1–10 (1947).

26. Anderson, A. R., and Smith, C. S., "Fatigue Tests on Some Copper Alloys," Proceeding of the American Society for Testing and Materials 41, 849–858 (1941).

27. Taylor, M. T., Woolcock, A., and Barber, A. C., "Strengthening Superconducting Composite Conductors for Large Magnet Construction," Cryogenics 8, 317–319 (1968).

REFERENCES

28. Schwope, A. D., Smith, K. F., and Jackson, L. R., "The Comparative Creep Properties of Several Types of Commercial Coppers," Transactions of the American Institute of Mining and Metallurgical Engineers 185, 409–416 (1949).

29. Jones, P. G., and Moore, H. F., "An Investigation of the Effect of Rate of Strain on the Results of Tension Tests of Metals," Proceedings of American Society for Testing and Materials 40, 610–624 (1940).

30. Benson, N. D., and McKeown, J., "The Creep and Softening Properties of Copper for Alternator Rotor Windings," Journal of the Institute of Metals 80, 131–142 (1952).

31. Dugdale, D. S., "Stress-Strain Cycles of Large Amplitude," Journal of the Mechanics and Physics of Solids 7, 135–142 (1959).

Dugdale, D. S., "An Experimental Study of the V-Notch Fatigue Test," Journal of the Mechanics and Physics of Solids 7, 282–287 (1959).

32. Cook, M., and Richards, T. L., "The Tensile/Shear Stress Ratio in Rolled Copper Alloys," Journal of the Institute of Metals 73, 541–551 (1947).

33. Murray, H., "Compact Ignition Tokamak, Toroidal Field Coil, Copper/Nickel Alloy Laminate Development, FA01, Summary Documentation," Princeton Plasma Physics Laboratory, Princeton, NJ, F-861022-p-01 (1986).

34. Reed, R. P., and Walsh, R. P., National Bureau of Standards, Boulder, CO, private communication (1987).

35. Yoshida, K., Takahashi, Y., Tada, E., Shimada, M., Tokuchi, A., Tada, N., and Shimamoto, S., "Mechanical Properties of the Japanese LCT Coil Conductor," in Advances in Cryogenic Engineering--Materials, Vol. 28, Eds., R. P. Reed and A. F. Clark, Plenum Press, New York, 781–790 (1982).

36. McClintock, R. M., Van Gundy, D. A., and Kropschot, R. H., "Low-Temperature Tensile Properties of Copper and Four Bronzes," American Society for Testing and Materials Bulletin 240, 47–50 (1959).

37. Frye, J. H., Scott, J. L., and Woods, J. W., "Effect of Strain and Temperature on the Yielding of Copper and Nickel," Journal of Metals 9(5), 708 (1957).

38. Carreker, R. P., and Hibbard, W. R., "Tensile Deformation of High Purity Copper as a Function of Temperature, Strain Rate, and Grain Size," Acta Metallurgica 1, 654–663 (1953).

39. Warren, K. A., and Reed, R. P., "Tensile and Impact Properties of Selected Materials from 20 to 300 °K," U.S. National Bureau of Standards, Washington, DC, Monograph 63, 51 pp. (1963).

40. McAdam, D. J., and Mebs, R. W., "The Technical Cohesive Strength and Other Mechanical Properties of Metals at Low Temperatures," Proceedings of the American Society for Testing and Materials 43, 661–706 (1943).

REFERENCES

McAdam, D. J., Geil, G. W., and Woodward, D. H., "Influence of Strain Rate and Temperature on the Mechanical Properties of Monel Metal and Copper," Proceedings of the American Society for Testing and Materials 46, 902–950 (1946).

41. McCammon, R. D., and Rosenberg, H. M., "The Fatigue and Ultimate Tensile Strengths of Metals between 4.2 and 293 °K," Proceedings of the Royal Society of London, Mathematical and Physical Sciences A242, 203–211 (1957).

42. Ellis, W. C., and Greiner, E. S., "Effect of Prior Strain at Low Temperatures on the Properties of Some Close-packed Metals at Room Temperature," Transactions of the American Institute of Mining and Metallurgical Engineers 194, 648–650 (1952).

43. McKeown, J., and Hudson, O. F., "Stress-Strain Characteristics of Copper, Silver, and Gold," Journal of the Institute of Metals 60, 109–132 (1937).

44. McAdam, D. J., Jr., Geil, G. W., and Cromwell, F. J., "Flow Fracture and Ductility of Metals," American Institute of Mining and Metallurgical Engineers, Technical Publication No. 2296, 29 pp. (1948).

45. Thompson, J. G., "Effect of Cold-Rolling on the Indentation Hardness of Copper," Journal of Research of the National Bureau of Standards 13, 745–772 (1934).

46. Opie, W. R., Taubenblat, P. W., and Cale, N. H., "Effect of Oxygen on the Mechanical Properties of Copper," Wire Journal 6(6), 53–58 (1973).

47. Yokelson, M. V., and Balicki, M., "Progressive Work-Hardening and Reannealing of Five Brands of High Conductivity Copper," Wire and Wire Products 30, 1179-1194 (1955).

48. Smart, J. S., Smith, A. A., and Phillips, A. J., "Preparation and Some Properties of High-Purity Copper," Transactions of the American Institute of Mining and Metallurgical Engineers 143, 272–283 (1941).

49. Kee, W. W., "The Control of Properties and Structure in the Hot and Cold Rolling of Copper and Copper-Base Alloys," Journal of the Institute of Metals 82, 307–322 (1954).

50. Colbeck, E. W., and MacGillivray, W. E., "The Mechanical Properties of Metals at Low Temperatures, Part II: Non-ferrous Materials," Transactions of the Institute of Chemical Engineers 11, 107–123 (1933).

51. Haas, W. J., and Hadfield, R., "On the Effects of the Temperature of Liquid Hydrogen (–252.8 °C) on the Tensile Properties of Forty-one Specimens of Metals," Philosophical Transactions of the Royal Society of London A232, 297–332 (1934).

52. Hooper, W. H. L., and Inglis, N. P., "Non-ferrous Data for the Chemical Engineer," Chemistry and Industry, 1334–1348 (1954).

53. Jeffries, Z., and Archer, R. S., in "The Science of Metals," McGraw-Hill Book Company, New York, 210–211 (1924).

REFERENCES

54. Pester, F., "Festigkeitsprüfungen an Stangen und Drähten bei tiefen Temperaturen," Zeitschrift für Metallkunde 24, 67–72 (1932).

55. Puccini, R. M., "Fatigue Tests and Microstructural Studies of OFHC Copper from 25 °C to 425 °C at Plus or Minus 2 Degrees Torsion (Wood's F-Range)," University of Toronto, Canada, UTIAS Technical Note No. 142, 15 pp. (1970).

56. Lessman, G. G., Logson, W. A., Kossowski, R., Mathur, M. P., and Wells, J. M., "Structural Materials for Cryogenic Applications," in Materials Research in Support of Superconducting Machinery, Eds., R. P. Reed, A. F. Clark, and E. C. van Reuth, National Technical Information Service, Springfield, VA, ADA 780596 (1974).

57. Nachtigall, A. J., "Strain-Cycling Fatigue Behavior of Ten Structural Metals Tested in Liquid Helium (4 K), in Liquid Nitrogen (78 K), and in Ambient Air (300 K)," NASA TN D-7532, 30 pp. (1974).

58. Blewitt, T. H., Coltman, R. R., and Redman, J. K., "Low Temperature Deformation of Cu Single Crystals," Journal of Applied Physics 28, 651–660 (1957).

59. Ornstein, J. L., "Effect of Silver Additions on the Softening Temperature and Mechanical Properties of Oxygen-free, High Conductivity Copper," Texas Instruments Inc., Attleboro, MA, Engineering Report No. 1497, 8 pp. (1964).

C10100: Annealed;
Cold-worked

Impact Energy (Charpy V-Notch)
vs. Temperature (76–295 K)

DATA SOURCES

Charpy V-notch impact energy measurements from 76 to 295 K on annealed C10100 copper were obtained from References 3.1 and 3.2. The product forms of the material were bar (Reference 3.1) and plate (Reference 3.2). Similar measurements over the same temperature range on 60% cold-drawn C10100 copper were reported in Reference 3.3. Product was in bar form. Data at lower temperatures are not reported here because of the large temperature rise that occurs in impact tests below 76 K in ductile materials.

RESULTS

Figure 3.1 presents the impact data as a function of temperature. Only the average values from Reference 3.1 are shown, but all reported measurements are given in Table 3.1. The available characterization of materials and measurements is given in Table 3.2 at the end of the impact properties section.

DISCUSSION

Impact energies are lower for the cold-worked copper, as expected. The measurements reported in Reference 3.1 were made on half-size specimens, and were multiplied by a factor of two.

Table 3.1. Impact Energy Dependence on Temperature (76–295 K).

Impact Energy, J	Test Temperature, K	Reference No.
142	295	1
141	295	1
144	295	1
155	195	1
153	195	1
155	195	1
182	76	1
168	76	1
182	76	1
168	79	2
173	123	2
173	173	2
162	224	2
152	291	2
130	295	3
137	195	3
129	76	3

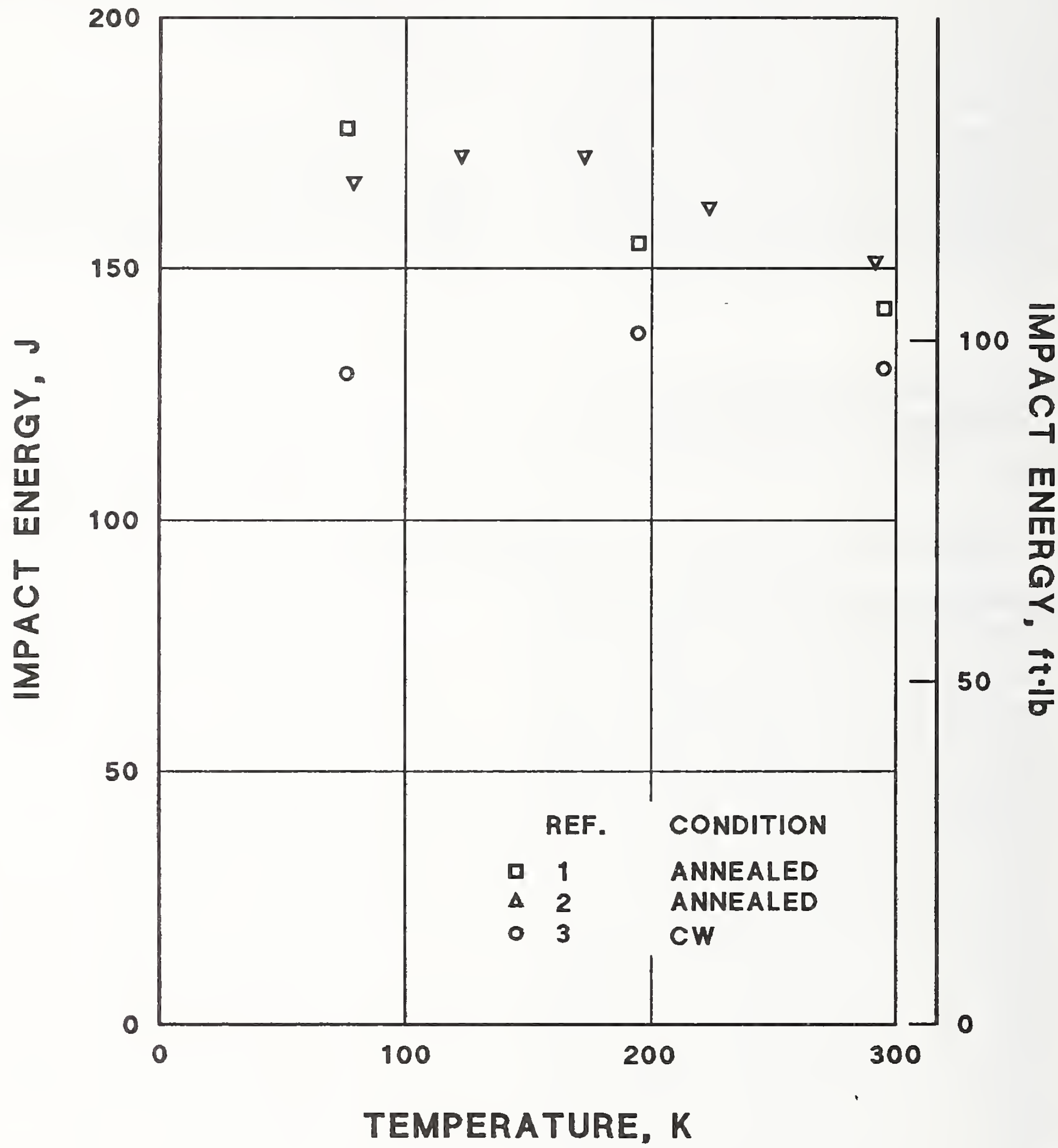

Figure 3.1. The impact energy dependence on test temperature indicates a decrease in impact energy with increasing temperature for annealed material (References 3.1 and 3.2). The temperature dependence for cold-worked material (Reference 3.3) is unclear. All data are presented in Table 3.1. Product forms include bar and plate.

Table 3.2. Characterization of Materials and Measurements.

Reference No.	1	2	3
Specification	C10100	C10200	C10100
Composition (wt%)			
Cu	—	99.50	
Ag	—	—	0.002
Cu + Ag	99.99	—	
O_2	—	—	
Bi	—	—	
P	—	0.07	
Pb	—	<0.002	
S	—	—	0.001
Se	—	—	
Te	—	—	
Others (Only ≥ 0.001 wt%)	—	Ni: 0.04; Fe: 0.001; As: 0.37; Sb: 0.003; Sn: <0.002	
Material Condition	Annealed	Annealed	Cold-drawn, 60%
Grain Size	65 μm	—	287–2000 μm
Hardness	R_H 86	—	R_B 45–53
Product Form	Bar, 1.91-cm-dia.	Plate	Bar, 1.91-cm-dia.
Specimen Type	Sub-standard Charpy V-notch, 0.5-cm-thick, 5.5 × 0.8 cm	Charpy V-notch	Charpy V-notch
No. of Specimens	3 per temperature	—	—
Test Temperature	76–295 K	77–333 K	76–295 K

REFERENCES

1. Warren, K. A., and Reed, R. P., "Tensile and Impact Properties of Selected Materials from 20 to 300 °K," U.S. National Bureau of Standards, Washington, DC, Monograph 63, 51 pp. (1963).

2. Lismer, R. E., "The Properties of Some Metals and Alloys at Low Temperatures," Journal of the Institute of Metals 89, 145–161 (1961).

3. Reed, R. P., and Mikesell, R. P., "Low-Temperature (295 to 4 K) Mechanical Properties of Selected Copper Alloys," Journal of Materials 2, 370–392 (1967).

DATA SOURCES AND ANALYSIS

Measurements of the maximum stress (σ_m) versus the number of cycles to failure (N) for annealed copper were obtained from 17 sources (References 4.1–4.17). R-ratios, where stated, were −1, except for tests reported in Reference 4.12 which R varied from 0.12 to 0.19 (R = minimum stress/maximum stress). In some cases, the R-ratio could not be determined from the description of testing methods provided. The 148 measurements of the data set were plotted together and analyzed to determine whether the $\sigma_m - N$ relation could be expressed mathematically.

RESULTS

Because of the relatively small range of σ_m compared to a variation in N over several orders of magnitude, stress-controlled fatigue life data are often presented in a semi-logarithmic plot. However, it was found that the data could best be fitted by a log-log expression. In exponential form, the equation obtained is

$$\sigma_m(\text{MPa}) = 271\ N^{-0.074}. \qquad (4\text{-}1)$$

The standard deviation of the exponent of N is 0.005. The standard deviation of the fit to the data (in logarithmic form) is 0.079.

Table 4.1 presents the number of cycles to failure, the measured values of maximum stress, the maximum stress values calculated from the regression equation, and the reference number. Selected points from the curves fitted to the 77 and 295 K data of Reference 4.17 are presented in Table 4.1 because the individual data points are so numerous. The available characterization of materials and measurements is given in Table 4.6 at the end of the fatigue properties section.

Figure 4.1 indicates the fit of the data to Equation (4-1), and Figure 4.2 presents these results in summary form. The scatter bands represent two standard deviations about the straight line fitted by least squares to the data in logarithmic form. The variance of the data about the line was assumed to be normally distributed and constant throughout the range of the independent variable, log N.

DISCUSSION

An increase in the annealing temperature has been shown to cause a decrease in the fatigue life (References 4.3 and 4.11). Variations in annealing temperature may account for some of the variance of the data shown in Figure 4.1.

Table 4.1. Dependence of Maximum Stress upon Number of Cycles to Failure of Annealed Material (295 K).

Cycles, N	Maximum Stress, Measured, MPa	Maximum Stress, Calculated, MPa	Reference No.
280	378.0	250.0	7
810	326.0	225.0	7
2800	290.0	199.0	7
6300	128.0	184.0	17
7900	167.0	179.0	5
7900	252.0	179.0	7
8900	159.0	177.0	5
10000	175.0	175.0	4
14000	152.0	170.0	5
20000	160.0	164.0	4
20000	117.0	164.0	17
28000	213.0	158.0	7

Table 4.1, continued

Cycles, N	Maximum Stress, Measured, MPa	Maximum Stress, Calculated, MPa	Reference No.
32000	165.0	156.0	4
32000	103.0	156.0	5
33000	110.0	156.0	16
40000	112.0	153.0	14
50000	155.0	150.0	4
58000	149.0	148.0	7
68000	106.0	147.0	14
63000	150.0	116.0	7
63000	140.0	146.0	4
72000	183.0	140.0	14
75000	103.0	144.0	16
79000	125.0	143.0	5
75000	120.0	143.0	5
160000	103.0	140.0	2
100000	155.0	140.0	4
120000	193.0	137.0	14
130000	155.0	138.0	4
160000	116.0	133.0	5
200000	179.0	130.0	4
210000	90.0	140.0	16
220000	118.0	127.0	4
250000	103.0	127.0	5
250000	77.2	122.0	4
300000	193.0	128.0	14
350000	89.2	123.0	5
380000	183.0	122.0	14
400000	120.0	127.0	4
400000	193.0	122.0	14
440000	193.0	121.0	14
460000	90.0	120.0	16
470000	150.0	120.0	12
480000	183.0	122.0	14
500000	130.0	119.0	4
560000	183.0	116.0	14
646000	89.2	116.0	4
760000	103.0	114.0	14
870000	150.0	113.0	14
860000	135.0	140.0	12
930000	179.0	112.0	14
952000	83.4	140.0	16
1000000	89.2	111.0	2
1000000	83.4	114.0	5
1000000	179.0	111.0	12
1050000	76.0	111.0	16
1080000	83.4	110.0	16
1100000	134.0	108.0	12
1100000	121.0	110.0	12
1100000	83.4	110.0	16
1200000	110.0	109.0	12
1200000	179.0	109.0	14
1450000	83.4	107.0	15

Table 4.1, continued

Cycles, N	Maximum Stress, Measured, MPa	Maximum Stress, Calculated, MPa	Reference No.
1490000	83.4	107.0	15
1500000	165.0	107.0	14
1600000	120.0	106.0	3
1500000	105.0	105.0	4
1600000	76.0	106.0	5
1700000	165.0	105.0	14
1490000	83.4	165.0	3
1500000	83.4	104.0	15
1900000	165.0	107.0	14
2000000	77.0	104.0	2
2000000	165.0	107.0	7
2000000	103.0	104.0	12
2100000	165.0	103.0	14
2500000	95.0	101.0	3
2800000	94.0	100.0	3
2800000	99.5	100.0	13
3000000	120.0	99.7	12
3200000	69.0	99.0	5
3230000	81.8	98.9	1
3500000	92.0	98.2	3
3800000	95.1	97.4	13
4000000	113.0	96.9	3
4200000	95.1	96.4	13
4620000	77.2	95.5	1
4800000	152.0	95.1	14
5000000	91.0	94.8	3
5490000	77.5	93.9	8
5600000	114.0	93.7	3
5600000	92.0	93.7	3
5600000	61.2	93.7	5
5640000	77.2	93.6	1
5880000	78.7	93.2	1
6000000	62.0	93.1	9
6080000	74.1	92.9	1
6310000	72.6	92.6	1
7100000	88.0	91.5	3
7390000	76.0	91.2	11
8450000	77.2	90.0	1
8900000	85.0	89.5	3
8900000	85.3	89.5	13
10000000	62.0	88.5	2
10000000	94.0	88.5	12
11000000	109.0	87.6	3
11600000	72.0	87.2	10
14000000	108.0	85.6	3
14000000	85.0	85.6	3
14000000	75.5	85.6	13
14800000	73.8	85.1	8
15000000	138.0	85.0	14
16000000	107.0	84.4	3
16000000	108.0	84.4	3

Table 4.1, continued

Cycles, N	Maximum Stress, Measured, MPa	Maximum Stress, Calculated, MPa	Reference No.
16000000	65.4	64.8	5
18000000	109.0	83.5	3
18200000	79.3	68.7	1
19000000	75.5	83.0	13
20000000	101.0	82.6	3
20200000	72.6	72.6	3
20000000	64.8	82.6	1
22000000	105.0	81.8	3
23200000	81.0	81.8	1
23200000	69.5	81.1	1
24000000	69.8	81.1	3
24000000	75.5	81.1	13
28000000	105.0	79.9	1
28200000	75.7	79.8	1
30100000	64.8	79.3	1
31400000	72.6	79.0	1
33900000	65.5	78.4	3
35000000	81.1	78.1	13
37900000	68.7	77.5	1
38200000	69.5	77.5	13
38600000	64.8	77.4	1
52000000	69.8	78.1	13
130000000	102.0	64.8	1
210000000	61.8	65.4	13
211000000	62.2	65.4	3
250000000	101.0	61.8	3
440000000	65.4	64.8	13
560000000	69.5	53.0	3
630000000	101.0	58.7	1
720000000	53.0	81.8	13
1000000000	53.0	56.1	13
1000000000	48.1	44.6	13
1300000000	48.1	43.5	13
1400000000	48.1	43.2	13

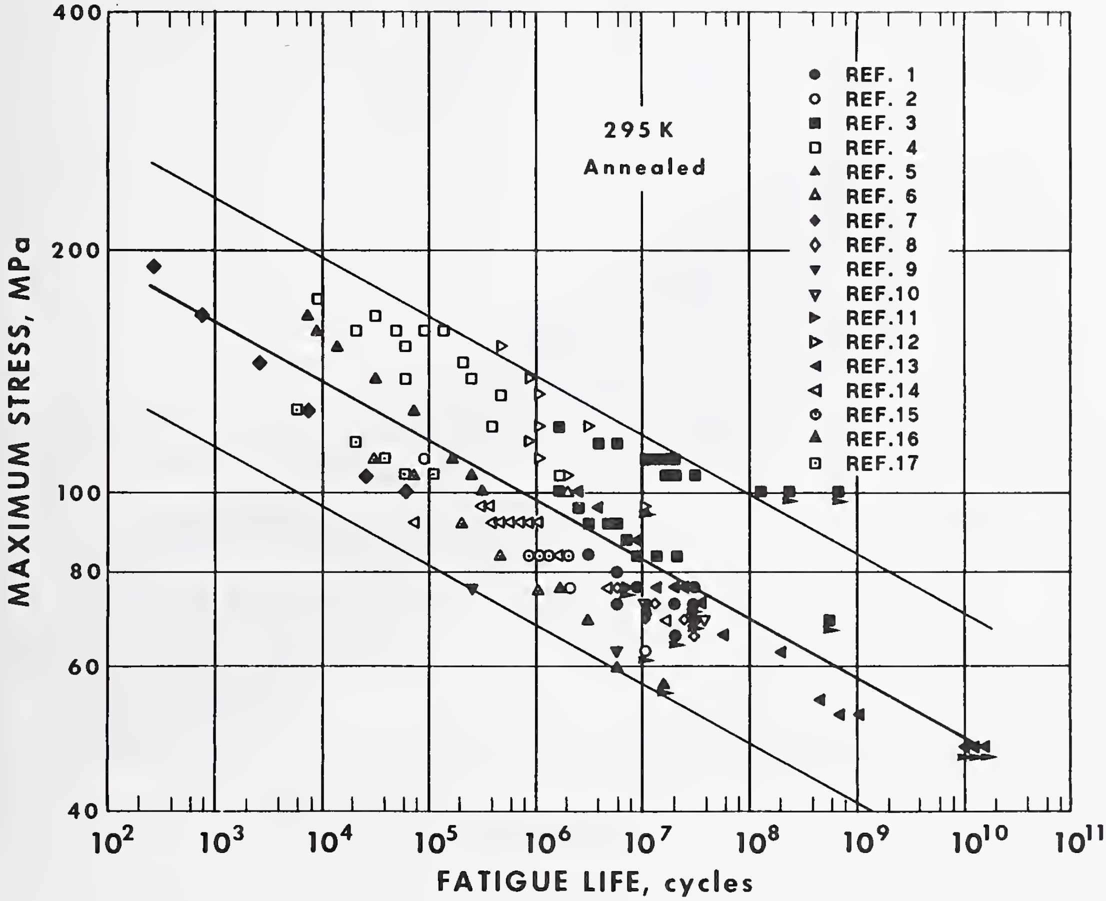

Figure 4.1. The data shown were used to compute the regression of maximum stress upon the number of cycles to failure [Equation (4-1)]. For clarity, overlapping data points are omitted from the figure. All data are presented in Table 4.1. Tests discontinued before failure are marked by an arrow. Product was predominately in bar form. The *R*-ratios are discussed in the text.

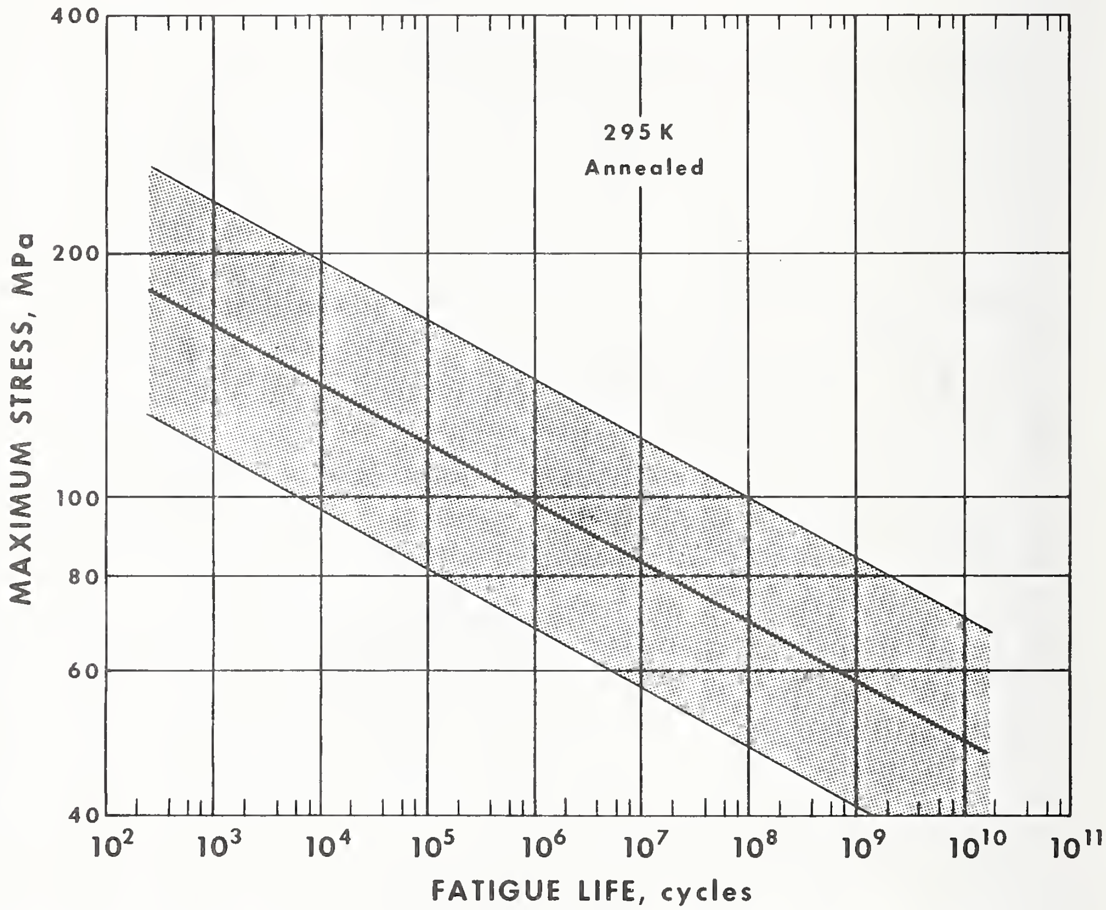

Figure 4.2. Dependence of maximum stress at 295 K upon number of cycles to failure. The scatter band represents two standard deviations about a linear regression equation based upon 148 measurements. The regression equation is

$$\sigma_m(\text{MPa}) = 271\ N^{-0.074}.$$

The uncertainty of the exponent is ± 0.005, where 0.005 equals one standard deviation as determined in the regression analysis. The *R*-ratios are discussed in the text.

DATA SOURCES AND ANALYSIS

Data on the grain-size dependence of the stress-controlled fatigue life at 295 K were obtained from Reference 4.5. The *R*-ratio was −1.

RESULTS

Figure 4.3 shows the improvement in fatigue life with smaller grain size. This figure is adapted from a figure presented in Reference 4.5. The effect of grain size is negligible for long fatigue life. The available characterization of materials and measurements is given in Table 4.6 at the end of the fatigue properties section.

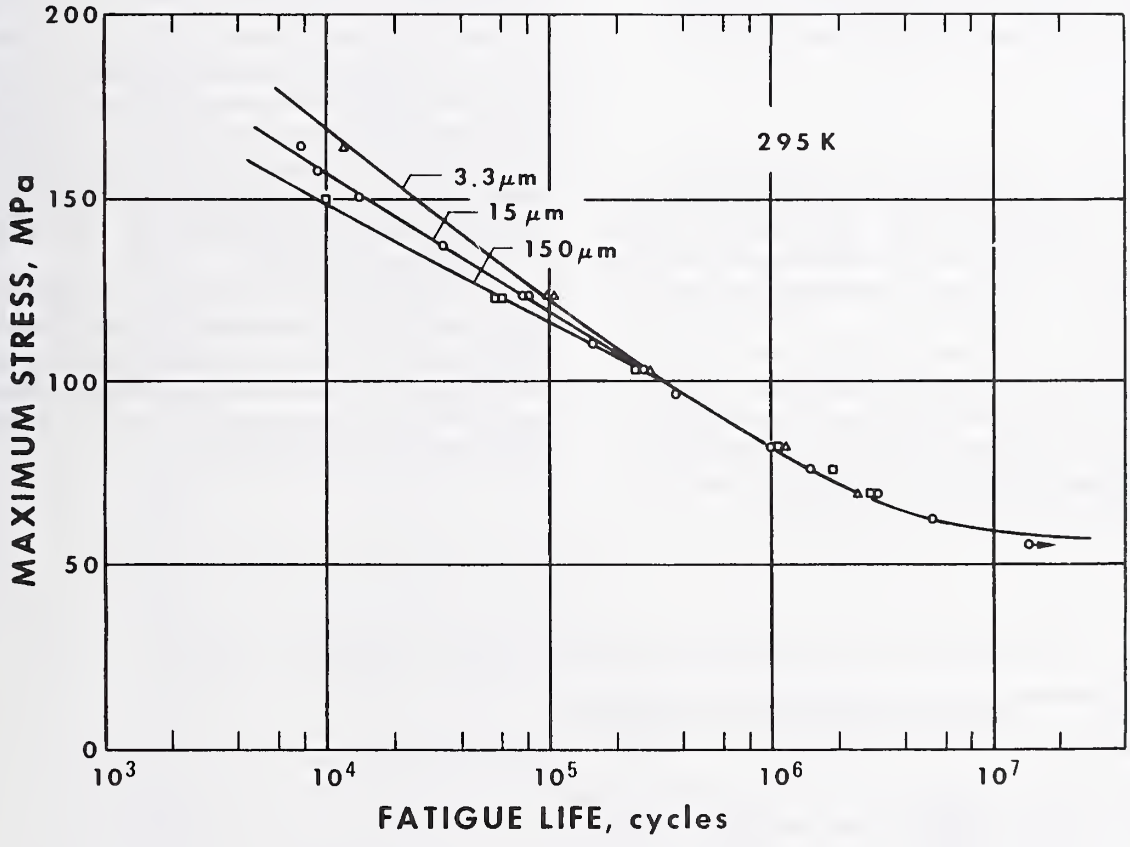

Figure 4.3. Data on the grain-size dependence of stress-controlled fatigue life are shown. The grain sizes are indicated in the figure. A test discontinued before failure is marked by an arrow. This figure is adapted from a figure presented in Reference 4.5. The *R*-ratio is −1.

C10100, C10200, C11000: Annealed

Stress-controlled Axial Fatigue Life (Air/Liquid, 4–295 K)

DATA SOURCES AND ANALYSIS

Measurements of the maximum stress below room temperature versus the number of cycles to failure were obtained from References 4.4, 4.6, 4.16, 4.18, and 4.19. The *R*-ratios were −1 for all measurements. All material was annealed. Because of the large number of points at 77 K and room temperature reported in Reference 4.17, data were abstracted from the smoothed curves fitted to the individual points. One extensive set of data at 4, 20, 90, and 293 K is on a C11000 copper (Reference 4.4), but a few measurements on a C10200 copper in the same apparatus (Reference 4.7) showed the same magnitude of fatigue life change with temperature. Measurements below room temperature were obtained with the specimens in a cryogenic liquid.

RESULTS

Table 4.2 presents the temperature, the number of cycles to failure, the maximum stress, and the reference number. The available characterization of materials and measurements is given in Table 4.6 at the end of the fatigue properties section.

Figure 4.4 shows the data at room and low temperatures from the five references. Data from each reference show significant increase of fatigue life at low temperatures, in contrast to low-temperature data (also in liquid) from strain-controlled fatigue tests (see Figure 4.11).

DISCUSSION

Results reported in References 4.4, 4.6, and 4.18 are in quantitative agreement. These results were obtained at one laboratory on the same apparatus. Results of References 4.16 and 4.17 are in approximate quantitative agreement (with each other) as would be expected from the similarity in tensile strengths (380 and 340 MPa, respectively, at 77 K). Although these two groups of results are in qualitative agreement in that the fatigue life increases as the temperature decreases, there is considerable quantitative disagreement, as is evident in Figure 4.4. Differences in ultimate tensile strengths could account for the discrepancy. The tensile strength is not reported in References 4.6 and 4.18, but in Reference 4.4 it is reported to be 430 MPa at 77 K for C11000 copper. This value is somewhat higher than the values reported in References 4.16 and 4.17 for C10100 copper. Since the yield strength of copper does not increase much with decreasing temperature, but the tensile strength does, stress-controlled fatigue life appears to be best correlated with tensile strength.

Fatigue life was found to be considerably shorter at 4 and 20 K when the full load was applied rapidly rather than being built up gradually over a period of several thousand cycles (Reference 4.4). This effect was only found to be significant at these temperatures.

Table 4.2. Dependence of Stress-Controlled Fatigue Life upon Temperature (4–295 K).

Test Temperature, K	Cycles, N	Maximum Stress, MPa	Reference No.
4	52000	304	4
4	85000	294	4
4	310000	257	4
4	630000	273	4
4	1800000	257	4
4	2000000	240	6
4	16000	320	18
4	41000	301	18
4	180000	292	18
4	500000	272	18
4	3000000	268	18

C10100, C10200, C11000: Annealed

Stress-controlled Axial Fatigue Life (Air/Liquid, 4–295 K)

Table 4.2, continued

Test Temperature, K	Cycles, N	Maximum Stress, MPa	Reference No.
4	27000	263	17
4	45000	298	18
4	45000	276	17
4	63000	209	17
4	130000	214	17
4	290000	169	18
4	370000	271	17
20	31000	298	4
20	68000	293	4
20	120000	282	4
20	130000	282	4
20	140000	283	4
20	150000	271	4
20	150000	269	4
20	130000	250	4
20	210000	283	4
20	410000	255	4
20	1190000	276	4
20	1230000	282	4
20	10000000	236	4
20	14400000	240	4
20	2000000	220	6
20	12300	301	17
20	93000	282	18
20	300000	261	17
20	2600000	282	18
77	22000	179	17
77	40000	171	17
77	60000	169	17
77	60000	162	17
77	200000	156	17
77	310000	152	17
77	290000	138	16
77	480000	131	18
77	1070000	117	18
77	1160000	124	18
90	69000	208	4
90	180000	168	4
90	340000	188	4
90	950000	175	4
90	6200000	188	4
90	2000000	160	6
293	10000	175	4
293	20000	160	4
293	32000	165	4
293	50000	160	4
293	68000	156	4
293	63000	140	4
293	100000	160	4
293	130000	155	4
293	200000	145	4

Table 4.2, continued

Test Temperature, K	Cycles, N	Maximum Stress, MPa	Reference No.
293	250000	117	4
293	400000	120	4
293	500000	130	4
293	1600000	105	4
293	2000000	100	6
295	6300	128	17
295	20000	117	17
295	40000	112	17
295	60000	106	17
295	120000	103	17
295	33000	117	16
295	75000	128	16
298	210000	90	16
298	460000	83	16
298	1050000	76	16

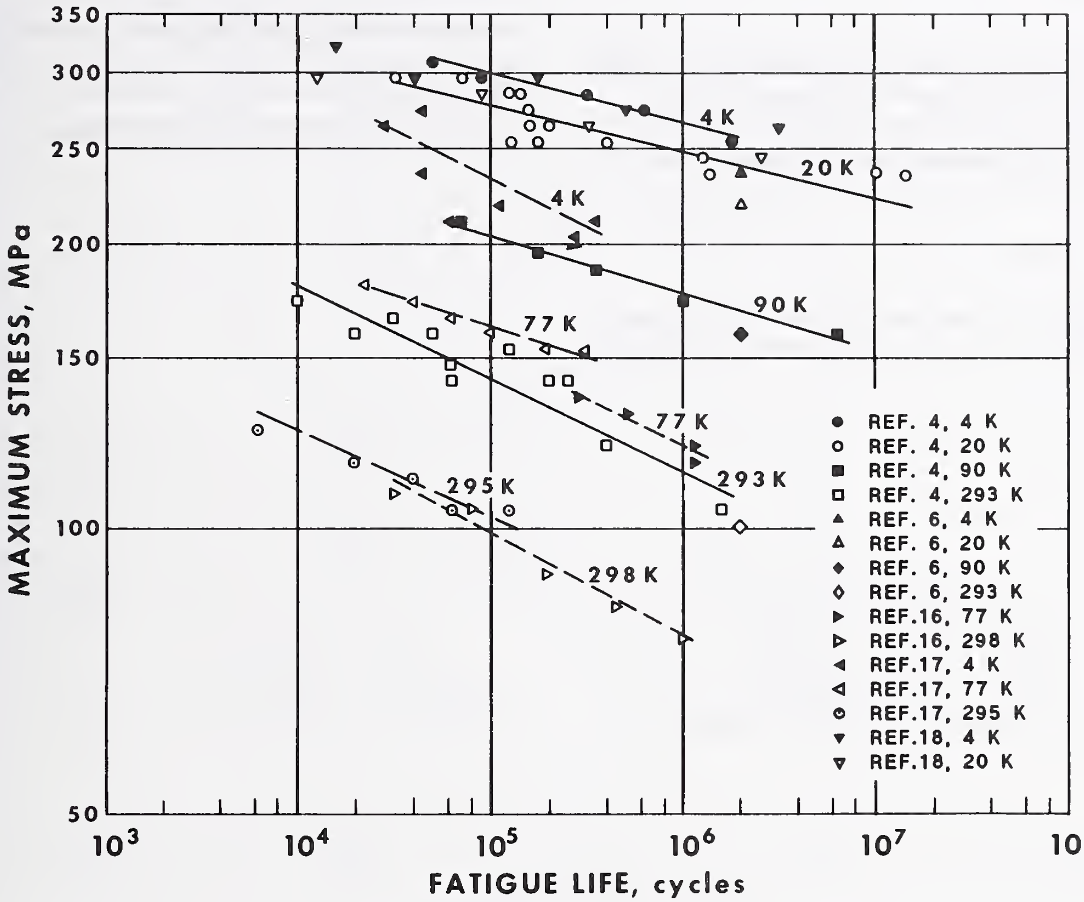

Figure 4.4. Measurements of the stress-controlled fatigue life at different temperatures are shown. For clarity, overlapping data points are eliminated from the figure. All data are presented in Table 4.2. Products were in bar and sheet form. The tests reported in Reference 4.4 were carried out on copper with an oxygen content of 0.03 wt%, which is closer to the C11000 specifications than to C10100 or C10200. All *R*-ratios were −1.

DATA SOURCES AND ANALYSIS

Data comparing the maximum stress versus the fatigue life for annealed specimens of C11000 copper tested in air of varying moisture content and partial vacuum were obtained from References 4.1 and 4.16. The *R*-ratios were −1.

RESULTS

Figure 4.5 shows the improvement in fatigue life for specimens tested in vacuum at both 77 and 295 K. The available characterization of materials and measurements is given in Table 4.6 at the end of the fatigue properties section.

DISCUSSION

Data from Reference 4.1 shown in Figure 4.5 shows that the fatigue limits obtained in air and in damp, purified air were similar, whereas the results in dry, purified air approached those obtained in vacuum. These results indicate that the apparent atmospheric corrosion fatigue effect is due to the catalytic action of water in the presence of oxygen. Strain-controlled fatigue testing has corroborated this result (see References 4.10 and 4.20).

Data reported in Reference 4.15 indicate that electrodeposited coatings (applied to electropolished material) also improve fatigue life. Presumably, some mechanism of protection of the surface from the atmosphere is operating.

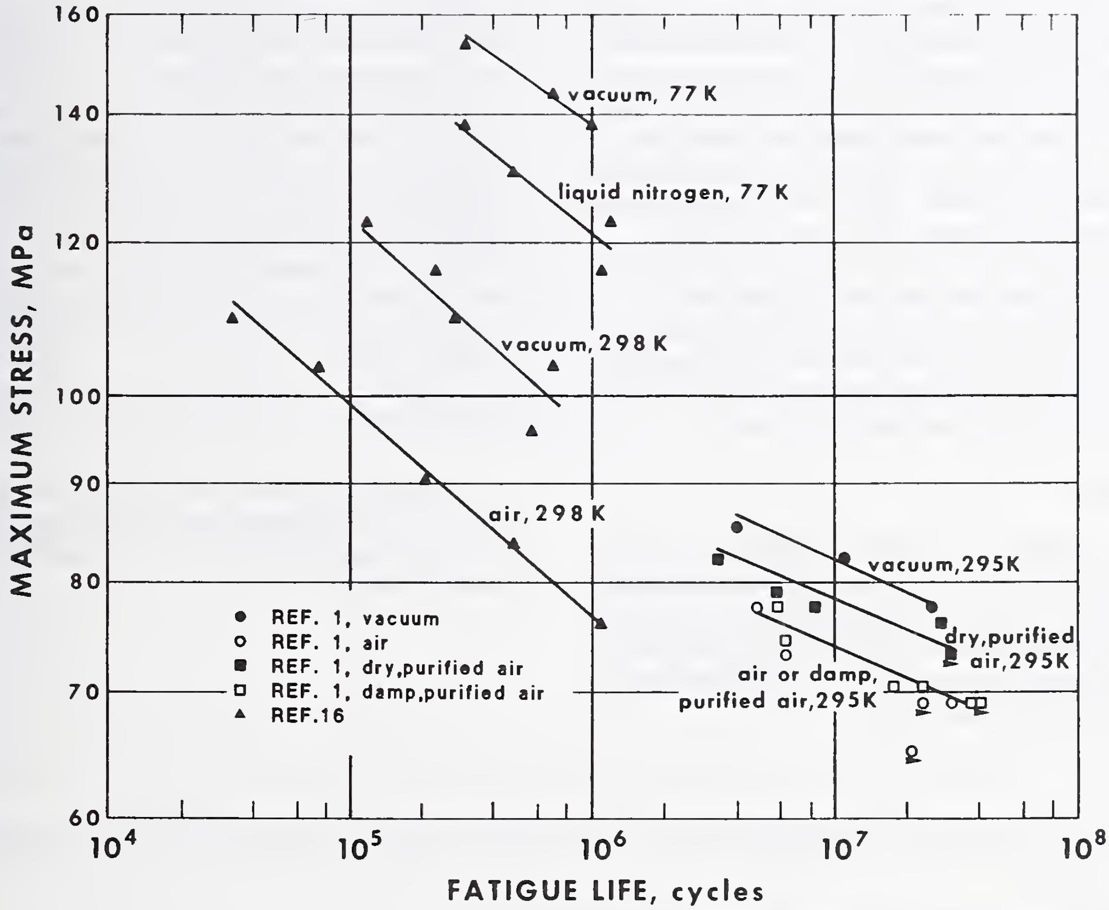

Figure 4.5. Data on the differences in fatigue life of copper at 77 K and room temperature in various atmospheres and in vacuum are shown. Data are from References 4.1 and 4.16. Tests discontinued before failure are marked by an arrow. The *R*-ratios are −1.

DATA SOURCES AND ANALYSIS

Measurements of the maximum stress (σ_m) versus the number of cycles to failure (N) for copper cold-worked at room temperature were obtained from References 4.7, 4.13, 4.21, and 4.22. The R-ratios reported in References 4.7 and 4.13 were −1, and Reference 4.22 reported $R = 0$. (R = minimum stress/maximum stress). In Reference 4.21, the R-ratio could not be determined from the description of testing methods provided. The total of 28 measurements on specimens with 5 to 82% cold work, *CW*, (reduction of area or thickness) were plotted and analyzed in the same manner as were the measurements on annealed specimens. The mode of fatigue testing reported in Reference 4.21 may not be axial; however, the data were included because they were in agreement with other results, and because these were the only data available on C10700 material. Also, Reference 4.23 reports agreement at room temperature on fatigue life determined from axial and bend tests.

RESULTS

Despite the range of *CW* represented in the data, it was found that the data could be well-represented by one log-log expression (see preceding discussion and figures for measurements on annealed specimens). In exponential form, the equation obtained is

$$\sigma_m(\text{MPa}) = 310\, N^{-0.065}. \quad (4\text{-}2)$$

The standard deviation of the exponent of N is 0.008. The standard deviation of the fit to the data in logarithmic form is 0.087.

Table 4.3 presents the number of cycles to failure, the measured values of maximum stress, the maximum stress values calculated from the regression equation, and the reference number. The available characterization of materials and measurements is given in Table 4.6 at the end of the fatigue properties section.

Figure 4.6 indicates the fit of the data to Equation (4-2) and Figure 4.7 presents these results in summary form. The scatter bands represent two standard deviations about the straight line fitted by least squares to the data in logarithmic form. The variance of the data about the line was assumed to be normally distributed and constant throughout the range of the independent variable, log N.

DISCUSSION

Fatigue life improves with *CW*. This is shown by the individual data points from References 4.21 and 4.22, and by a comparison of Figures 4.2 and 4.7.

Table 4.3. Dependence of Maximum Stress upon Number of Cycles to Failure for Cold-worked Material (295 K).

Cycles, N	Maximum Stress, Measured, MPa	Maximum Stress, Calculated, MPa	Reference No.
320	446.0	426.0	7
1000	401.0	371.0	7
3200	330.0	322.0	7
3800	329.0	315.0	7
5100	313.0	304.0	7
7100	313.0	292.0	7
11000	280.0	277.0	7
14000	278.0	269.0	7
28000	249.0	247.0	7
220000	165.0	192.0	21
1000000	139.0	159.0	22

C10100, C10200, C10700: Cold-worked

Stress-controlled Axial Fatigue Life (Air, 295 K)

Table 4.3, continued

Cycles, N	Maximum Stress, Measured, MPa	Maximum Stress, Calculated, MPa	Reference No.
1000000	140.0	159.0	22
1000000	156.0	159.0	22
1000000	172.0	159.0	22
1000000	197.0	159.0	22
1100000	130.0	158.0	21
2200000	165.0	145.0	21
3200000	165.0	138.0	21
8700000	100.0	122.0	13
11000000	95.0	119.0	21
14000000	95.1	116.0	13
56000000	120.0	97.5	21
58000000	84.3	97.1	13
89000000	85.3	92.2	13
100000000	80.0	90.9	21
110000000	110.0	89.8	21
160000000	81.4	85.8	13
220000000	80.9	82.5	13
1000000000	47.1	51.8	13
1400000000	75.5	49.7	13

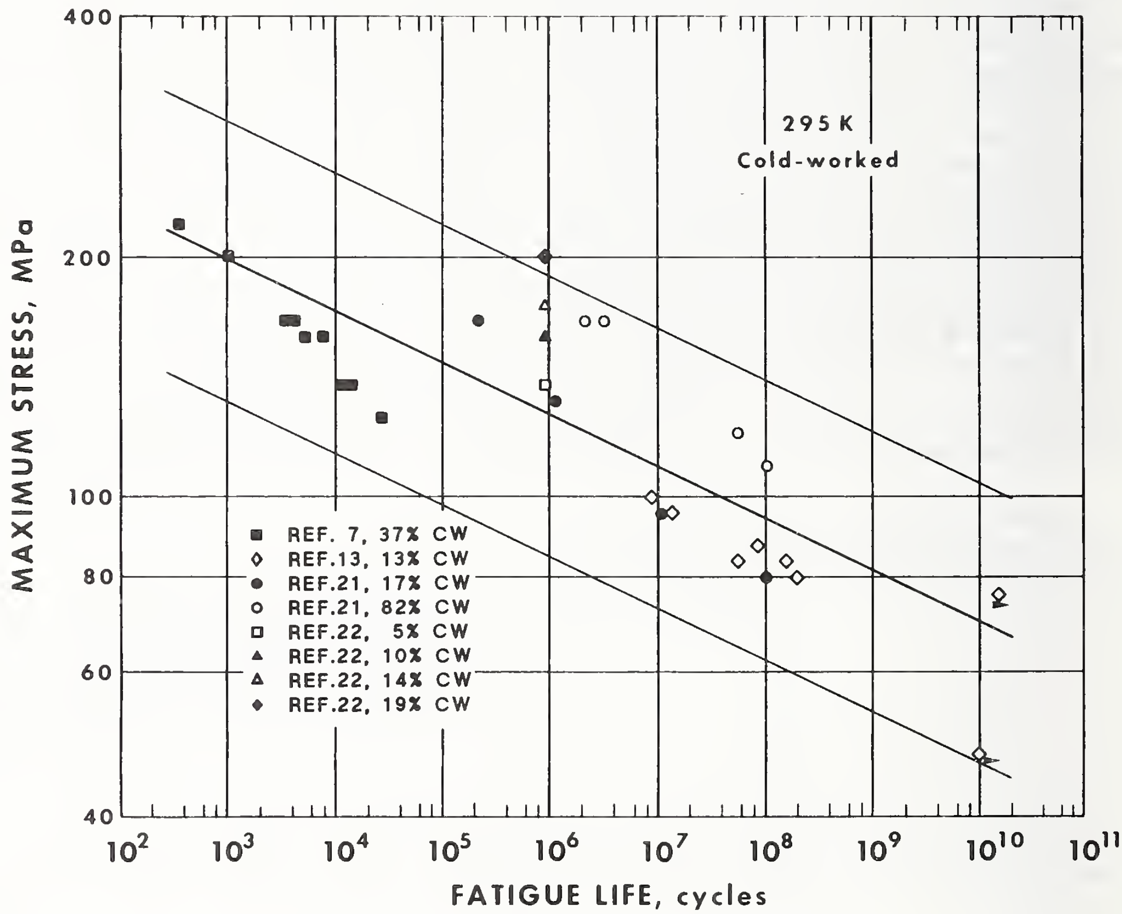

Figure 4.6. The data shown were used to compute the regression of maximum stress upon the number of cycles to failure [Equation (4-2)]. All data are presented in Table 4.3. Tests discontinued before failure are marked by an arrow. Products were in bar and sheet form. The percent of cold work refers to reduction of area or thickness. The *R*-ratios are discussed in the text.

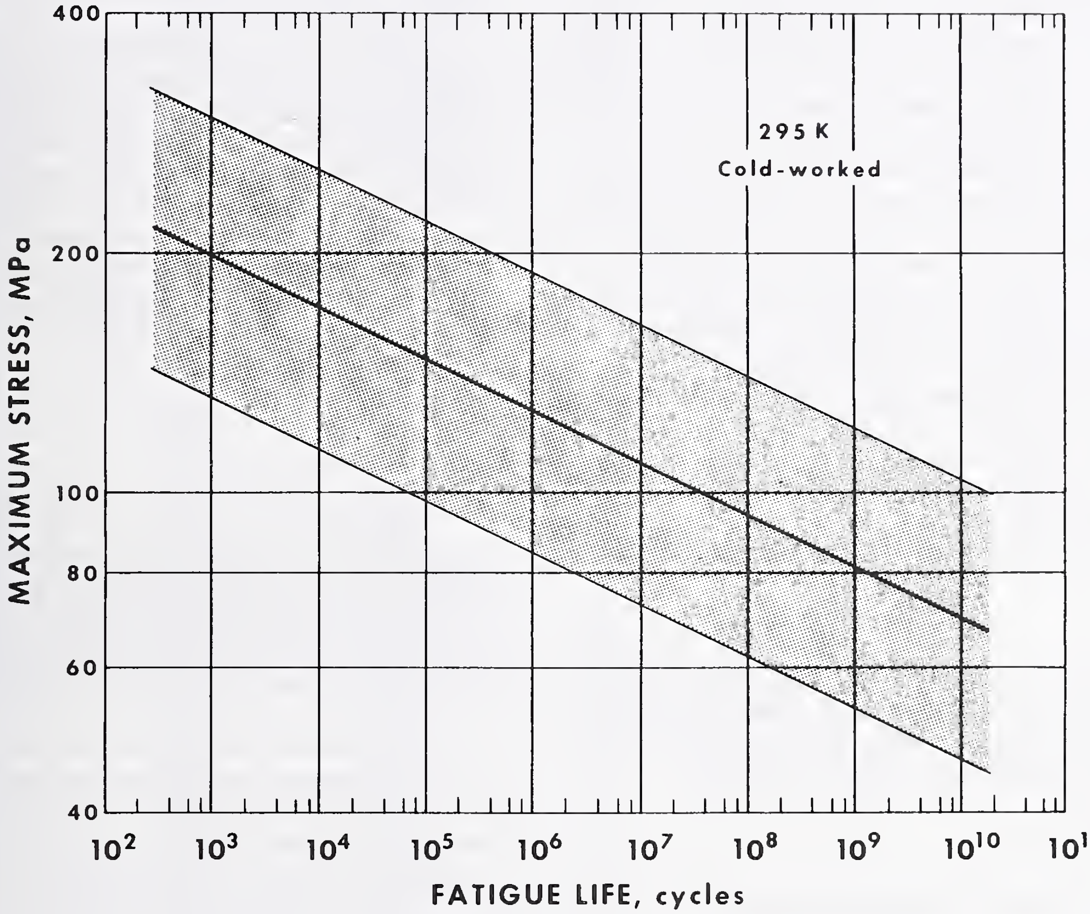

Figure 4.7. Dependence of maximum stress at 295 K upon number of cycles to failure. The scatter band represents two standard deviations about a linear regression equation based upon 28 measurements in which degree of cold work varied from 5 to 82% (reduction of area or thickness). The regression equation is

$$\sigma_m(\text{MPa}) = 310\ N^{-0.065}$$

The uncertainty in the exponent is ± 0.008, where 0.008 is one standard deviation as determined in the regression analysis. The *R*-ratios are discussed in the text.

DATA SOURCES AND ANALYSIS

Measurements of the plastic strain range ($\Delta\epsilon_p$) at room temperature versus the number of cycles to failure (N) were obtained from 8 sources (References 4.7, 4.19, and 4.24–4.29). Fully reversed cyclic fatigue measurements were reported on annealed and cold-worked copper. Cold work, *CW*, had been carried out at room temperature. Results quoted in References 4.19, 4.26, and 4.28 evidently refer to plastic strain amplitude; these results were multiplied by a factor of two. It is unclear whether the data presented in Reference 4.24 refer to total or plastic strain range. R-ratios, where stated, were equal to −1 (R = minimum strain/maximum strain). In some cases, the R-ratio could not be determined from the description of testing methods provided. Except for Reference 4.27, in which true strain was calculated, it was not possible to determine whether true or engineering strain was reported.

Individual sets of data from various authors have been found to follow the Coffin-Manson law for strain-controlled fatigue (Reference 4.25):

$$\Delta\epsilon_p = k\,N^{-n},$$

where n for copper ranges from 0.50 (References 4.19, 4.25, and 4.28) to 0.66 (Reference 4.26). A least-squares analysis of all the data was carried out to determine an average value for n.

RESULTS

The result in exponential form is

$$\Delta\epsilon_p = 0.618\,N^{-0.564}. \qquad (4\text{-}3)$$

The standard deviation of the exponent of N is 0.010. Table 4.4 presents the number of cycles to failure, the measured values of plastic strain range, the values calculated from the regression equation, and the reference number. Selected points from the curves fitted to the data of Reference 4.19 are presented in Table 4.4 because the individual data points are so numerous. The available characterization of materials and measurements is given in Table 4.6 at the end of the fatigue properties section.

Figure 4.8 shows that the data follow the Coffin-Manson law to a good approximation. A least-squares analysis of the data in logarithmic form showed that the standard deviation of a fit of a straight line to the data is 0.21. Figure 4.9 presents this result in summary form. The scatter bands represent two standard deviations about the line in these figures. The variance of the data about the line was assumed to be normally distributed and constant throughout the range of the independent variable, log N.

DISCUSSION

In accord with the results of several authors (References 4.7, 4.25, and 4.26) no significant difference was found between the $\Delta\epsilon_p$ vs. N curves of cold-worked and annealed copper. In addition, Reference 4.7 presents results that show good agreement between measurements for $R = -1$ and $R = 0$.

The dependence of strain-controlled fatigue life upon grain size is shown in the following pages. The points from Reference 4.19 that fall below the scatter band in Figure 4.8 are from specimens with a relatively large grain size (1200 μm).

No data on axial strain-controlled fatigue life in vacuum was found; however, References 4.20, 4.30, and 4.31 present such data for flexural strain-controlled fatigue. Improved fatigue life in vacuum is reported in these references. Reference 4.23 reports the equivalence of axial and flexural strain-controlled fatigue life in air at room temperature.

C10100–C10200: Annealed; Cold-worked

Strain-controlled Axial Fatigue Life (Air, 295 K)

Table 4.4. Dependence of Plastic Strain Range upon Number of Cycles to Failure, for Annealed and Cold-worked Material (295 K).

Cycles, N	Plastic Strain Range, Measured	Plastic Strain Range, Calculated	Reference No.
0.250	1.60	1.38	25
0.250	0.710	1.38	25
0.710	1.00	0.749	25
2.70	0.660	0.353	25
3.70	0.500	0.295	25
4.60	0.500	0.261	25
6.40	0.340	0.217	25
6.60	0.420	0.213	25
8.50	0.260	0.185	25
9.10	0.350	0.178	25
11.0	0.190	0.160	25
29.0	0.150	0.0924	25
32.0	0.190	0.0874	24
34.0	0.120	0.0888	25
46.0	0.0740	0.0712	25
72.0	0.0950	0.0553	25
76.0	0.0380	0.0537	7
34.0	0.0572	0.0188	27
150.	0.0540	0.0460	25
110.	0.0830	0.0336	25
130.	0.0200	0.0397	7
140.	0.0170	0.0180	7
150.	0.0630	0.0366	25
860.	0.0470	0.0353	24
150.	0.0200	0.0347	7
174.	0.0473	0.0336	27
130.	0.0300	0.0330	25
860.	0.0120	0.0924	7
180.	0.0450	0.0347	24
240.	0.0210	0.0234	7
260.	0.0160	0.0268	7
330.	0.0120	0.0234	7
130.	0.0120	0.0202	7
860.	0.0830	0.0188	7
540.	0.0100	0.0178	7
860.	0.0120	0.0180	7
680.	0.00950	0.0174	7
860.	0.0280	0.0180	25
600.	0.0280	0.0460	25
860.	0.00760	0.0188	7
130.	0.0144	0.0143	24
810.	0.0180	0.0188	25
130.	0.00740	0.0139	7
860.	0.0478	0.0188	27
870.	0.0200	0.0139	25
920.	0.0880	0.0188	27
1200	0.00910	0.0113	7
1200	0.00760	0.0188	7
1900	0.0130	0.00873	25
2000	0.00580	0.00848	7

Table 4.4, continued

Cycles, N	Plastic Strain Range, Measured	Plastic Strain Range, Calculated	Reference No.
2300	0.00450	0.00784	7
3300	0.00150	0.00640	7
3300	0.00820	0.00640	28
3400	0.00370	0.00629	7
3430	0.00220	0.00626	27
3800	0.00670	0.00591	29
4500	0.00470	0.00537	7
4800	0.00320	0.00518	7
6600	0.00220	0.00433	7
9270	0.00400	0.00357	29
11000	0.00220	0.00324	7
11000	0.00160	0.00324	7
14000	0.00152	0.00283	19
14300	0.00360	0.00280	27
16000	0.00186	0.00262	7
16000	0.00200	0.00262	29
16000	0.00220	0.00262	19
16000	0.00150	0.00238	7
21000	0.00168	0.00225	19
21000	0.00126	0.00280	19
22000	0.00250	0.00219	28
16800	0.00200	0.00181	29
44000	0.00186	0.00148	28
45400	0.00150	0.00146	29
46000	0.00186	0.00148	19
16000	0.000740	0.00145	19
55000	0.000850	0.00131	7
58000	0.00150	0.00127	29
55000	0.00186	0.00127	28
63200	0.00200	0.00127	27
76000	0.00220	0.00109	26
78000	0.00150	0.00127	26
55000	0.00124	0.00148	28
86000	0.00200	0.00102	29
90500	0.00106	0.000988	28
120000	0.000760	0.000934	19
100000	0.000340	0.000631	19
120000	0.00134	0.000772	29
100000	0.00186	0.000805	28
16000	0.00158	0.000772	29
200000	0.00138	0.000631	28
210000	0.000520	0.000614	19
200000	0.000170	0.000614	19
260000	0.000520	0.000545	29
280000	0.000820	0.000522	26
350000	0.000640	0.000460	29
380000	0.000520	0.000440	28
420000	0.000600	0.000415	26
460000	0.000360	0.000395	19
460000	0.000108	0.000395	19
760000	0.000400	0.000297	26

C10100–C10200: Annealed; Cold-worked

Strain-controlled Axial Fatigue Life (Air, 295 K)

Table 4.4, continued

Cycles, N	Plastic Strain Range, Measured	Plastic Strain Range, Calculated	Reference No.
833000	0.000260	0.000282	26
950000	0.000220	0.000262	26
950000	0.000158	0.000262	26
1600000	0.000240	0.000255	19
1000000	0.0000740	0.000255	19
1120000	0.000560	0.000239	26
1500000	0.000380	0.000203	26
1600000	0.000220	0.000168	26
2100000	0.000158	0.000168	26
2800000	0.000166	0.000168	19
2100000	0.0000600	0.000168	19
2800000	0.000144	0.000142	26
3200000	0.000260	0.000168	26
9500000	0.000110	0.000126	26
4000000	0.000124	0.000117	26
1600000	0.000220	0.000169	26
4600000	0.000112	0.000108	19
4600000	0.0000520	0.000108	19
5600000	0.000112	0.0000964	26
9500000	0.000118	0.0000715	26
10000000	0.0000760	0.0000695	19
10000000	0.0000420	0.0000695	19
1000000	0.000100	0.0000575	26
18000000	0.000104	0.0000499	26
30000000	0.0000940	0.0000374	26

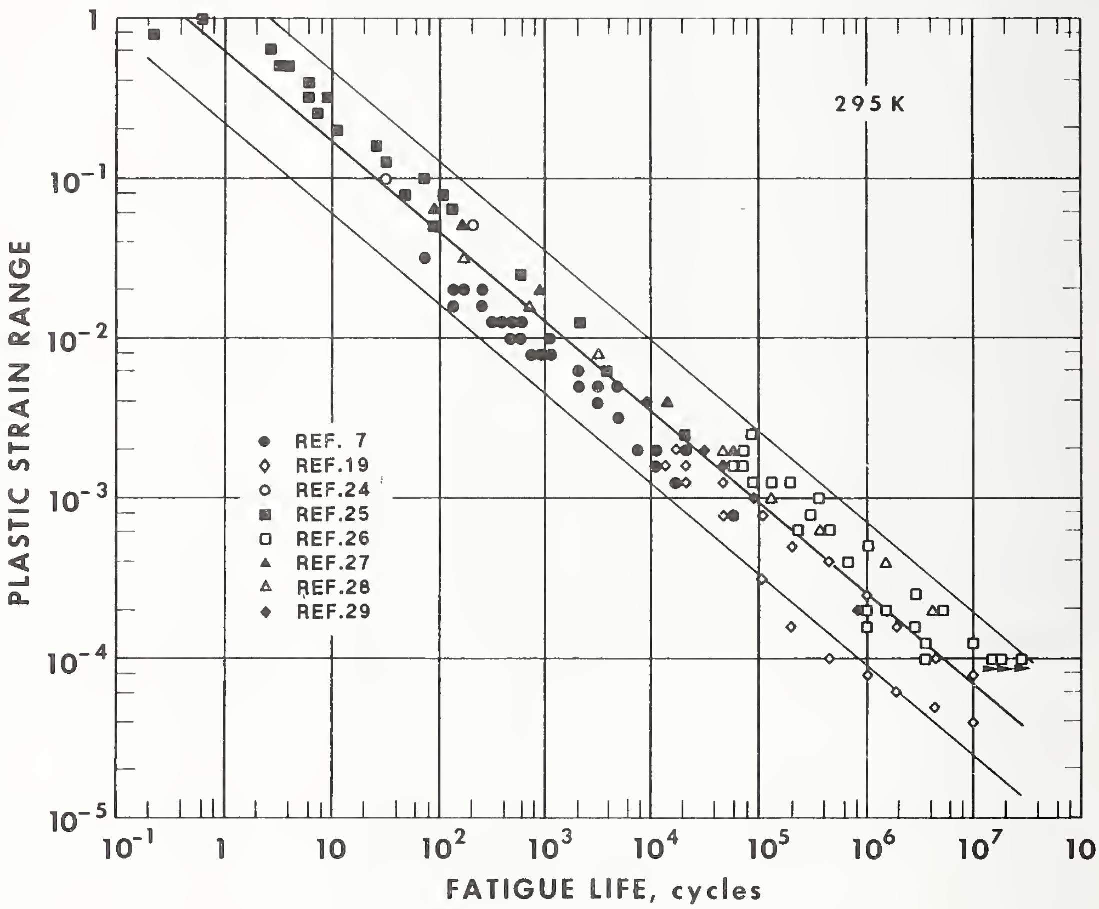

Figure 4.8. The data shown were used to compute the regression of plastic strain amplitude upon the number of cycles to failure [Equation (4-3)]. For clarity, overlapping data points are omitted from the figure. All data are presented in Table 4.4. Tests discontinued before failure are marked by an arrow. Product was predominately in bar form. Selected points from the curves fitted to the data of Reference 4.19 are presented in this figure and in Table 4.4. See the text for a discussion of the R-ratios.

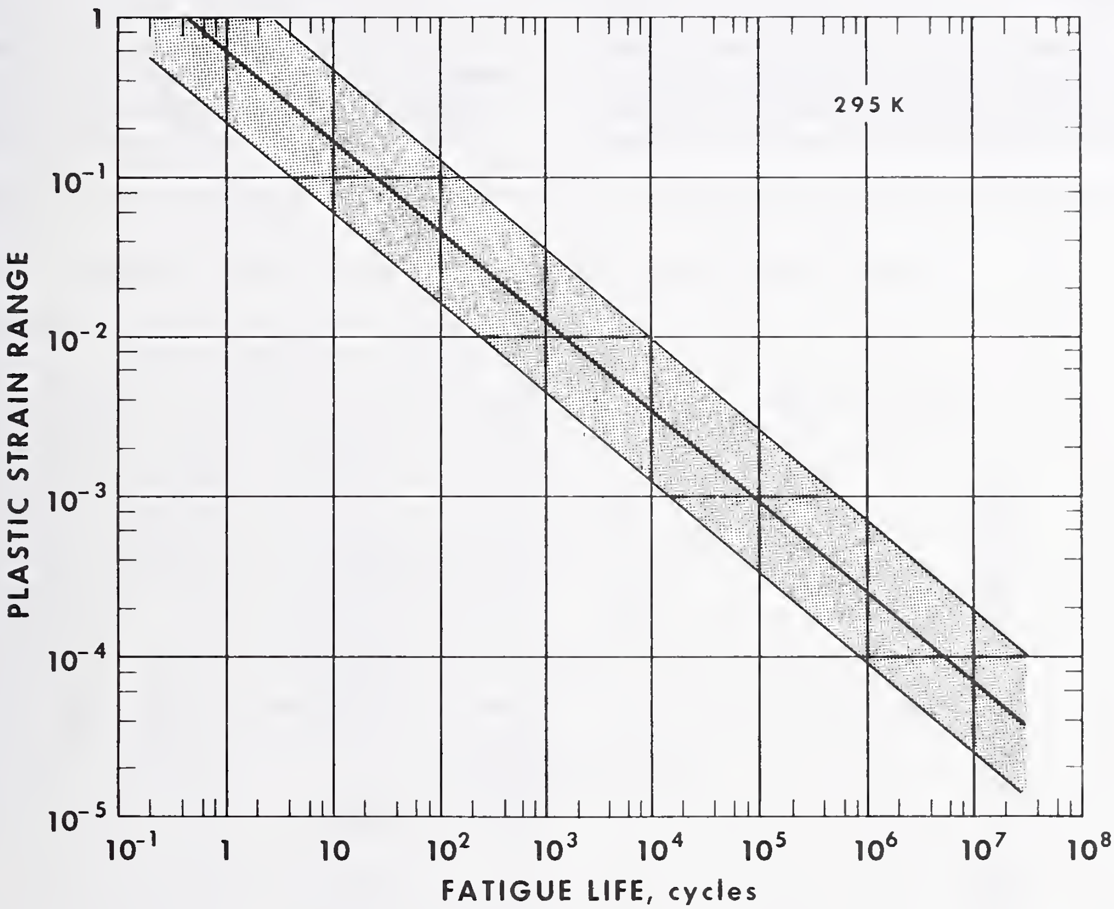

Figure 4.9. Dependence of plastic strain amplitude at 295 K upon number of cycles to failure. The scatter band represents two standard deviations about a linear regression equation based upon 144 measurements. The regression equation is

$$\Delta\epsilon_p = 0.618\ N^{-0.564}.$$

The uncertainty in the exponent is ± 0.010, where 0.010 equals one standard deviation as determined in the regression analysis. See the text for a discussion of the *R*-ratios.

C10200: Annealed

Strain-controlled Axial Fatigue Life vs. Grain Size (Air, 295 K)

DATA SOURCES AND ANALYSIS

Data on the grain-size dependence of the strain-controlled fatigue life of annealed copper at 295 K were obtained from Reference 4.19. The *R*-ratio was −1.

RESULTS

Figure 4.10 shows the improvement in fatigue life with smaller grain size. This figure is adapted from a graph in Reference 4.19 that presents smoothed curves fitted to the experimental data. Plastic strain amplitude, rather than plastic strain range, is shown in this figure. The available characterization of materials and measurements is given in Table 4.6 at the end of the fatigue properties section.

DISCUSSION

For larger grain sizes, the data do not follow the Coffin-Manson law [Equation (4-3)]. See Reference 4.19 for comparable data on the fatigue life versus the total strain range.

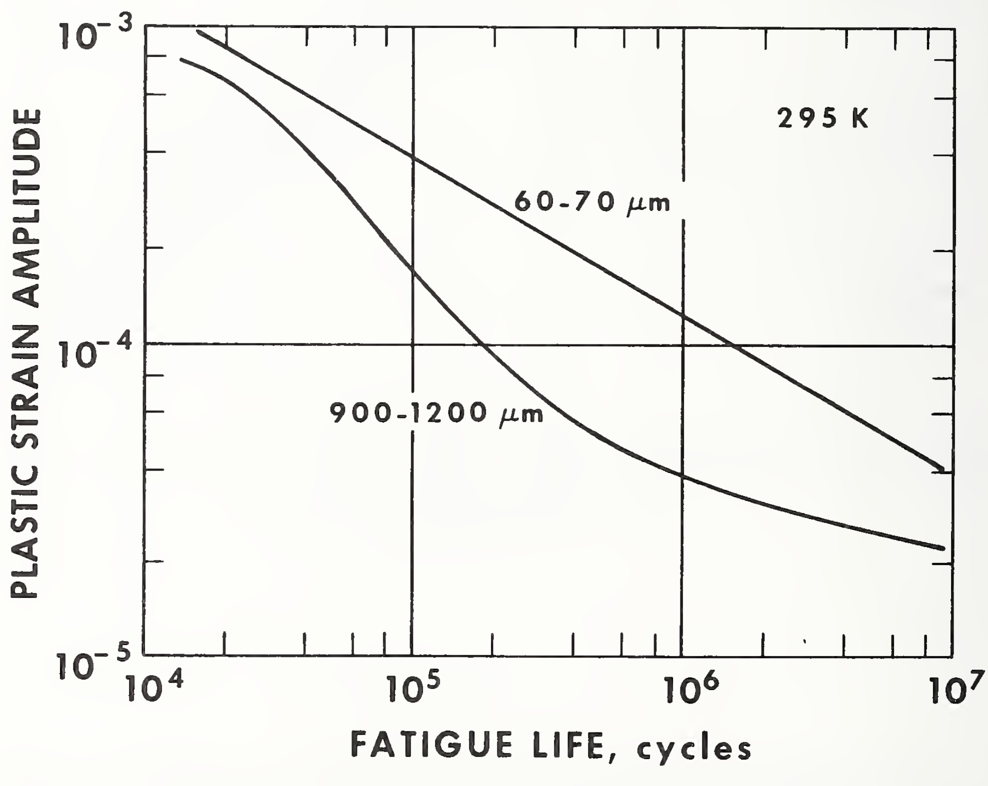

Figure 4.10. Data on the grain-size dependence of strain-controlled fatigue life are shown. The grain sizes are indicated in the figure. Data are from Reference 4.19.

C10100–C10200: Annealed

Strain-controlled Axial Fatigue Life (Air/Liquid, 4–300 K)

DATA SOURCES AND ANALYSIS

Measurements of the plastic strain range ($\Delta\epsilon_p$) below room temperature versus the number of cycles to failure for annealed copper were obtained from Reference 4.27. The *R*-ratio was −1. Measurements were made in ambient air (300 K), liquid nitrogen (78 K) and liquid helium (4 K).

RESULTS

Table 4.5 presents the temperature, the number of cycles to failure, the plastic strain range, and the reference number. The available characterization of materials and measurements is given Table 4.6 at the end of the fatigue properties section.

Figure 4.11 shows the data at room and low temperatures. Very little dependence of fatigue life upon temperature is observed; however, low-temperature strain-controlled flexural fatigue measurements made in vacuum do exhibit a clear temperature dependence (see References 4.30 and 4.31). Reference 4.23 indicates approximate equivalence of axial and flexural fatigue results at 295 K.

Table 4.5. Dependence of Strain-controlled Fatigue Life upon Temperature (4–300 K).

Test Temperature, K	Cycles, N	Plastic Strain, Range	Reference No.
4	159	0.0352	27
4	377	0.0258	27
4	3490	0.0163	27
4	4470	0.0125	27
4	45600	0.0450	27
4	91600	0.0035	27
78	89	0.0450	27
78	182	0.0356	27
78	2150	0.0161	27
78	18700	0.0069	27
78	33900	0.0450	27
78	211000	0.0018	27
300	90	0.0572	27
300	174	0.0473	27
300	860	0.0179	27
300	3430	0.0082	27
300	14300	0.0036	27
300	63200	0.0020	27

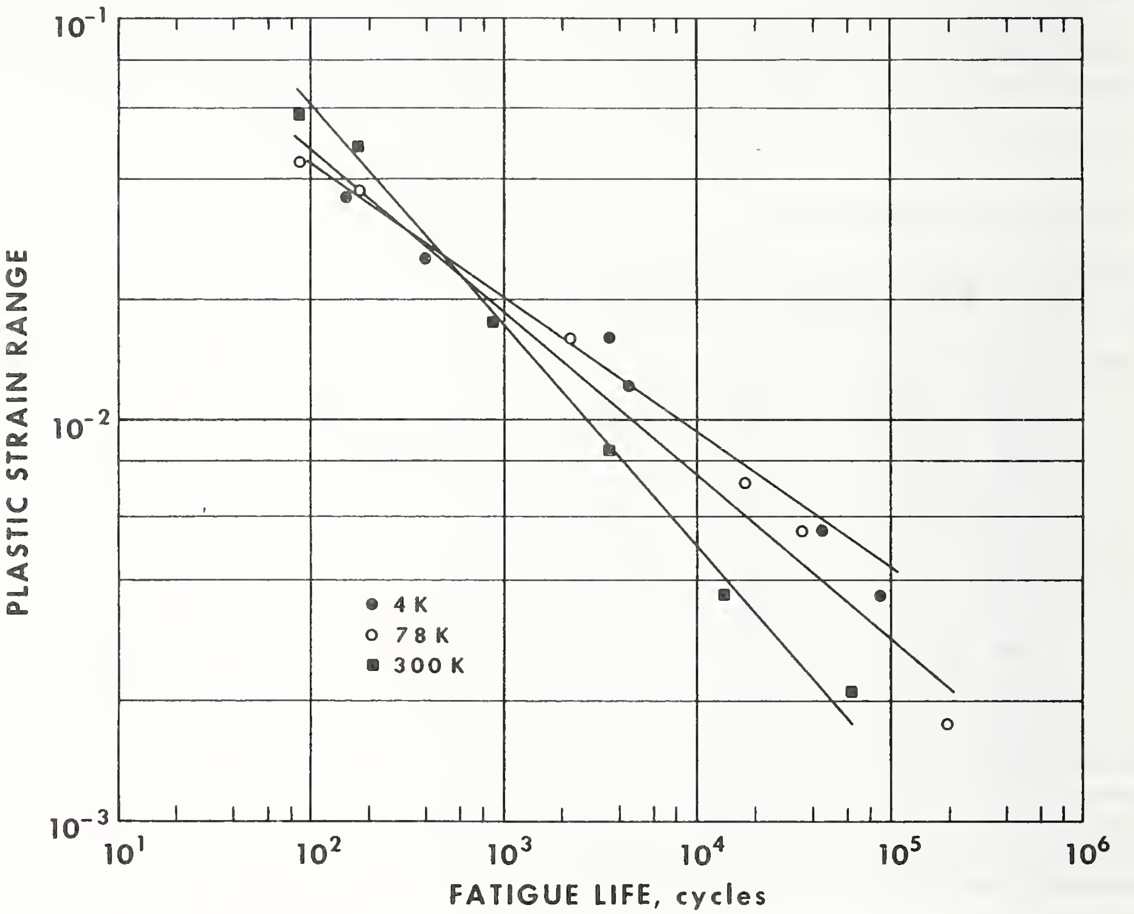

Figure 4.11. Measurements of the strain-controlled fatigue life at different temperatures are shown. All data are presented in Table 4.5.

DATA SOURCES AND ANALYSIS

Studies of the variation of the fatigue crack growth rate (*da/dN*) with *R*-ratio are reported in Reference 4.32. (*R* = minimum stress/maximum stress). The work was carried out in the near-threshold region of crack growth on annealed and cold-worked C11000 copper.

RESULTS

Figure 4.12 presents the results reported in Reference 4.32 for annealed specimens. The figure shows an increase in *da/dN* with increasing *R*-ratio. Similar results were reported for quarter- and full-hard copper.

The available characterization of materials and measurements is given in Table 4.6 at the end of the fatigue properties section.

DISCUSSION

R-ratio variation is also present in the data at 77 and 295 K shown in Figure 4.14. However, there are many other variables, such as annealing time and purity, in this presentation of data reported by several authors. These variables were held constant in the work reported in Reference 4.32.

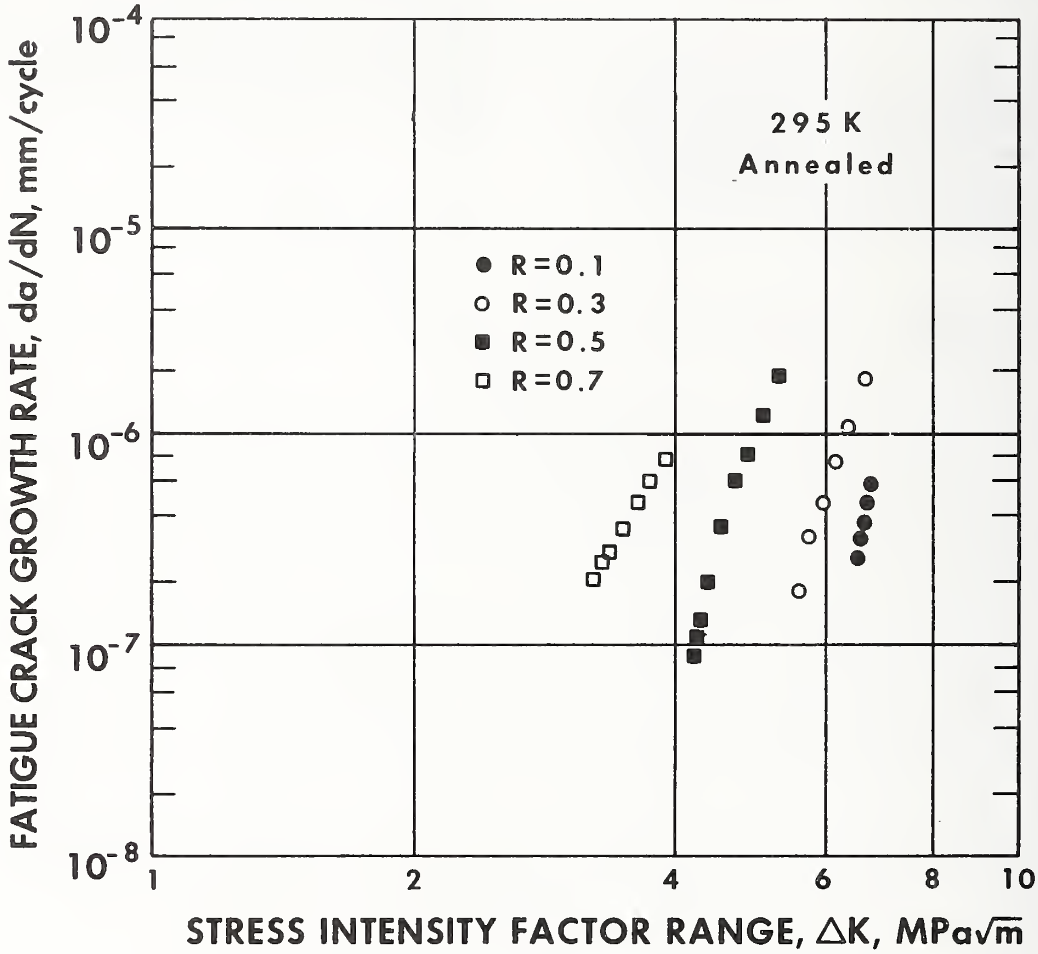

Figure 4.12. The data show the changes in fatigue crack growth rate with *R*-ratio at 295 K in the threshold region of fatigue crack growth rate. (*R* = minimum stress/maximum stress). This figure is adapted from a graph presented in Reference 4.32.

DATA SOURCES AND ANALYSIS

Data on C11000 copper were obtained from References 4.22 and 4.32 on the change in fatigue crack growth rate, *da/dN*, with room-temperature cold work. The data from Reference 4.32 are mostly in the threshold region of fatigue crack growth rate; data from Reference 4.22 include part of the threshold region and also extend to a *da/dN* of 4×10^{-4} mm/cycle. The specimens tested were deformed in tension (Reference 4.22) to a maximum of 20% reduction of area or cold-rolled (Reference 4.32) to a maximum of 31% reduction in thickness.

RESULTS

Figure 4.13 shows the data from the two references. For clarity, the individual data points presented in the references were abstracted into curves for the figure. The work reported in Reference 4.22 shows a decrease in *da/dN* with increasing cold work, *CW*; the data reported in Reference 4.32 show the opposite tendency. For a given *da/dN*, data from Reference 4.22 show an increase in the stress intensity factor range (ΔK) with *CW*; data from Reference 4.32 show the opposite effect of *CW* upon ΔK.

The available characterization of materials and measurements is given in Table 4.6 at the end of the fatigue properties section.

DISCUSSION

The data given in Figure 4.13 for annealed specimens can be compared with other data at 295 K on C10100 and C10200 copper presented in Figure 4.14 (see the following section on the temperature dependence of *da/dN*). This comparison shows that the data from Reference 4.22 fall approximately in the middle of the curves presented there. The data from Reference 4.32, however, fall below all of the other results at 295 K.

Reference 4.33 discusses crack closure and thermally activated models of resistance to near-threshold fatigue crack growth. This discussion suggests that *CW* could decrease *da/dN* if a thermal activation model is dominant. In this case, the energy required to move a dislocation over barriers would increase, as occurs when the temperature decreases into the cryogenic range.

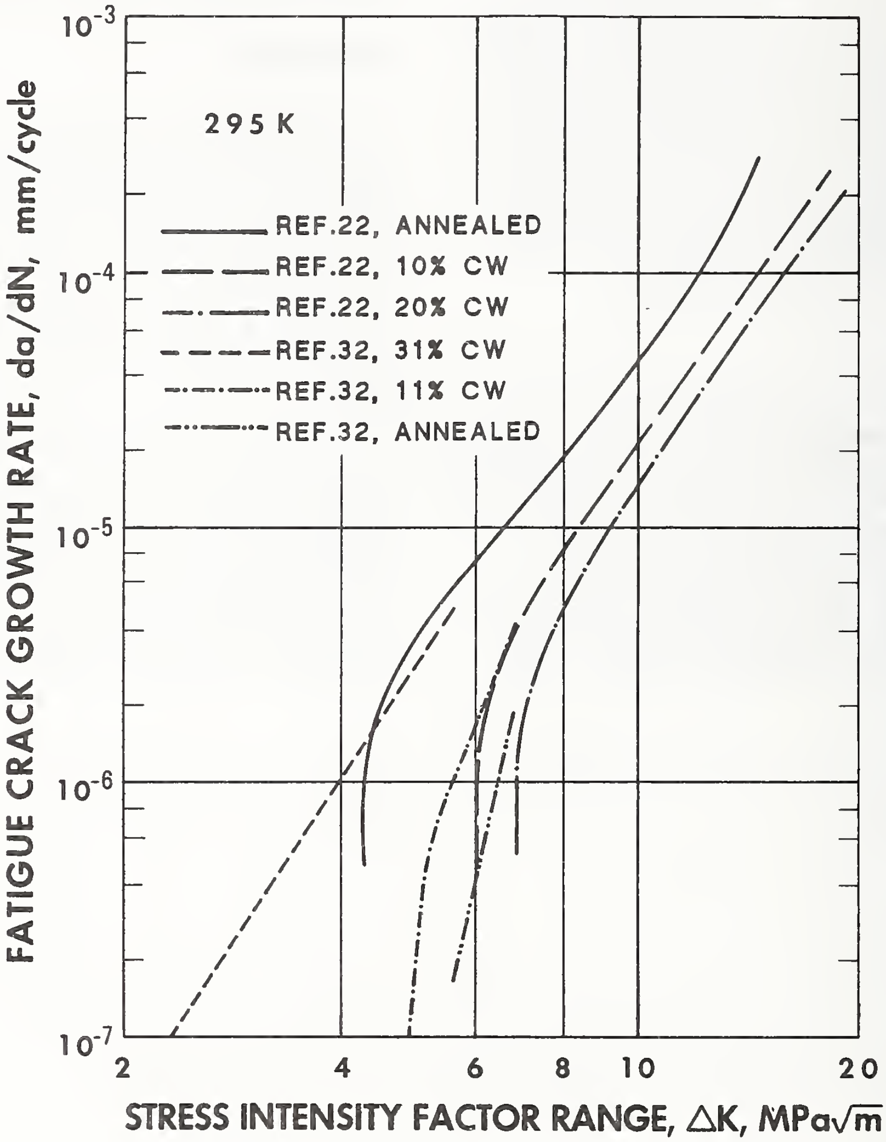

Figure 4.13. Data from two references on the influence of room-temperature cold work on fatigue crack growth rate are shown. The percent cold work refers to reduction in area (Reference 4.22) or reduction in thickness (Reference 4.32). Individual data points are not shown; instead, curves were fitted to the data points presented in the references. See the text for discussion of the disagreement in the results from the two references.

DATA SOURCES AND ANALYSIS

Data on the difference in fatigue crack growth rate, *da/dN*, at 77 and 295 K were obtained from References 4.34, 4.35, and 4.36. Specimens were from both annealed and cold-worked copper. The average curve of *da/dN* data at 295 K from a number of specimens that were both annealed and cold-worked was included in the figure for comparison purposes (Reference 4.37). Cold work, *CW*, had been carried out at room temperature.

RESULTS

Figure 4.14 shows the decrease in *da/dN* observed by all authors at 77 K as compared with 295 K. While the 77 and 295 K curves from different references are intermingled in the figure, the qualitative result of a decrease was observed in each case. Different material conditions, purities, and *R*-ratios may account for the variation in the results at each temperature.

Paris-law exponents (*m*) for these curves are as follows: Reference 4.34, 4.2 at 295 K and 4.7 at 77 K; Reference 4.37, 4.0 at 295 K; Reference 4.35, 4.6 at 295 K and 4.8 at 77 K; Reference 4.36, 4.0 at 295 and 77 K. (The Paris law states that $da/dN = C(\Delta K)^m$, where ΔK is the stress intensity factor range.)

The available characterization of materials and measurements is given in Table 4.6 at the end of the fatigue properties section.

DISCUSSION

Reference 4.33, a review of cryogenic *da/dN* data, discusses a thermal activation model that could account for increased resistance to fatigue crack growth at lower temperatures.

Reference 4.38 presents fatigue crack growth rate data on polycrystalline copper at 173 and 295 K, and data on the effect of grain size at 295 K. These data are not presented here because the thickness of the test material was not specified, and because other authors reported measurements at lower temperatures.

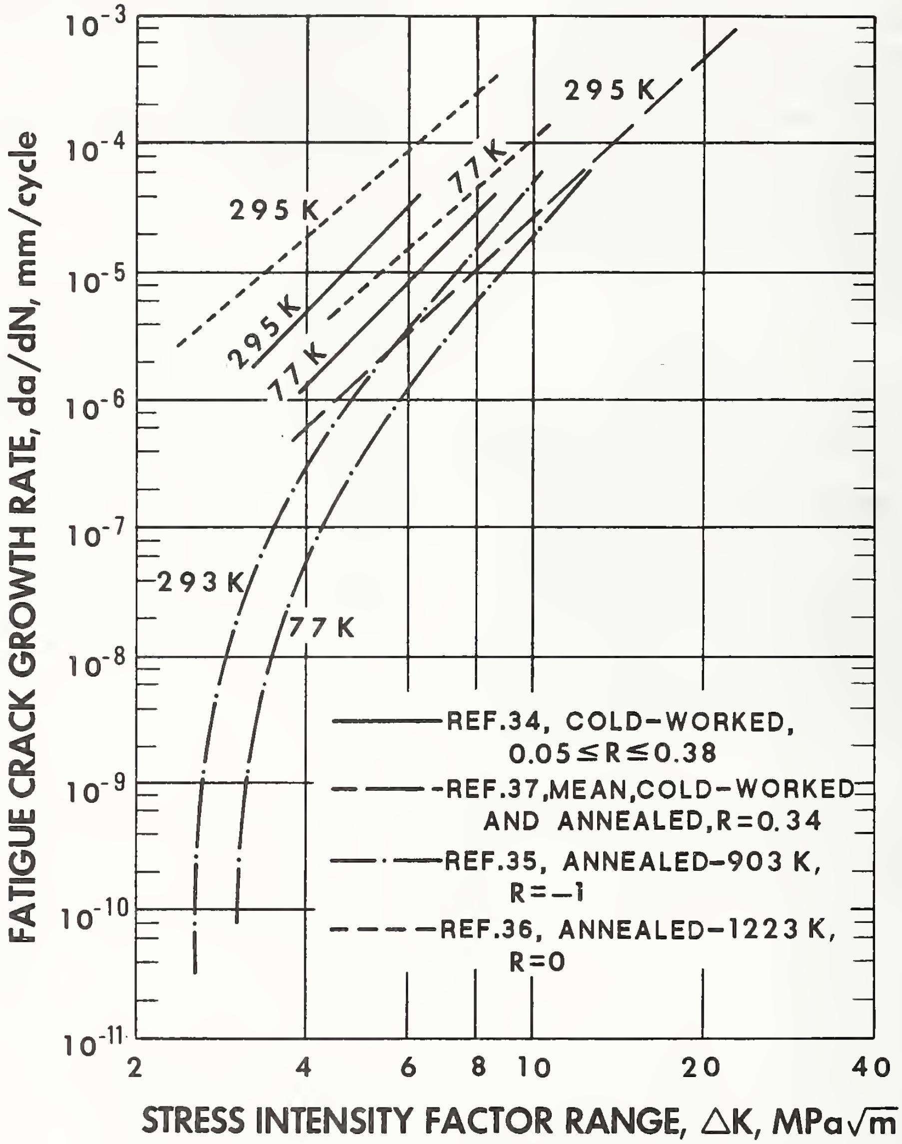

Figure 4.14. Data from three references on the decrease in *da/dN* from 295 to 77 K are shown. An extensive set of data at 295 K are also shown for comparison (Reference 4.37). Data from References 4.22 and 4.32 at 295 K are not shown, because the intent of the figure is to show the effect of temperature. However, the data from Reference 4.22 (on annealed C11000 copper) are approximately in agreement with the 295-K curves in the figure whereas the data from Reference 4.32 (also on annealed C11000 copper) lie somewhat below the other curves. Room-temperature data reported in Reference 4.35 were obtained in silicone oil; other room-temperature data were obtained in air.

Table 4.6. Characterization of Materials and Measurements.

Reference No.	1	—	3	4
Specification	C11000	C10200	C10200	C11000 (d)
Composition (wt%)				
Cu	99.96	—	—	—
Ag	—	—	—	—
Cu + Ag	—	—	—	—
O_2	0.04	—	—	0.03
Bi	—	—	—	—
P	trace	—	—	—
Pb	trace	—	—	—
S	trace	—	—	—
Se	—	—	—	—
Te	—	—	—	—
Others (Only ≥ 0.001 wt%)	—	—	—	—
Material Condition	Annealed	Annealed (b)	Annealed, vacuum, 673 or 873 K, 1 h, FC (c)	Annealed, 873 K, Ar
Grain Size	—	—	100 μm	—
Hardness	—	—	—	4
Product Form	Bar	—	Bar, 1.6-cm-dia.	Bar, 0.16-cm-dia.
Specimen Type	Hourglass	—	Hourglass	Hourglass
Width or Dia.	0.65 cm (min.)	—	—	0.05 cm (min.)
Thickness	—	—	—	—
Gage Length	10 cm (a)	—	—	0.5 cm
"R" Ratio	−1	−1	—	−1
Test Frequency	37 Hz	30 Hz	1000 Hz	225 Hz
No. of Specimens	19	—	26	37
Test Temperature	295 K	295 K	295 K	4, 20, 90, 293 K

(a) Parallel portion 1.3 cm long.
(b) Specimens electropolished before annealing.
(c) Specimens electropolished before and after annealing.
(d) The O_2 level of 0.03% is below the level of 0.04% required in C11000 specifications.

5	6	7	8	9
C10100	C10200	C10200	C10200	C10200
—	—	—	99.4	—
—	—	—	—	—
—	—	—	—	—
< 0.0003	—	—	—	—
—	—	—	—	—
—	—	—	—	—
0.0006	—	—	—	—
—	—	—	—	—
—	—	—	—	—
—	—	—	—	—
—	—	—	—	—
Annealed, 1 h, AC (a)	Annealed, 873 K, 4 h, vacuum (b)	Annealed, 273 K, 0.5 h, N_2 (c)	Annealed, 873 K, 1 h, vacuum	Annealed, 873 K, 1 h, vacuum
3.4, 15, 150 μm	—	—	—	—
—	—	38 and 88 Hv	—	—
—	Sheet	Bar, 3.8-cm-dia.	Bar	Bar
Cylindrical 0.8 cm — 2.5 cm (gage)	Flat (tapered) 0.08 cm (min.) 0.08 cm —	Cylindrical 1.43 cm (d) — 15 cm	Cylindrical 0.83 cm — —	Cylindrical 1.9 cm — 15 cm (g)
–1 30 Hz	–1 225 Hz	–1 (e) 0.17 Hz (min.)	–1 133 Hz	–1 33 Hz
27	4	(f)	6	2
295 K	4, 20, 90, 293 K	295 K	295 K	295 K

(a) Chemical polishing carried out before and after annealing.
(b) Electropolished before fatigue tests.
(c) Other specimens tested "as-received" estimated to be 37% cold-worked from hardness and standard tables of temper.
(d) Reduced to this diameter over a 2.5-cm-paralled gage length. Surface not polished.
(e) Strain-controlled fatigue life tests were also run at R = 0.
(f) Total of 15 specimens in stress-controlled fatigue and 29 in strain-controlled fatigue.
(g) Gage length not specified.

Table 4.6, continued

Reference No.	10	11	12	13
Specification	C11000	C10100	C10100	C10200
Composition (wt%)				
Cu	99.96	—	Balance	99.95
Ag	—	0.0002	0.001	—
Cu + Ag	—	—	—	—
O_2	0.04	—	—	—
Bi	—	—	—	—
P	trace	—	—	—
Pb	trace	< 0.0001	—	—
S	trace	—	—	—
Se	—	—	—	—
Te	—	—	—	—
Others (Only ≥ 0.001 wt%)	—	—	Fe: 0.001	—
Material Condition	Annealed	Annealed, 1273 K, 8 hr, Ar	Annealed	Annealed, 1123 K, 1 h, vacuum (e)
Grain Size	—	200 μm	150 μm	100–300 μm
Hardness	—	—	—	H_V 43 (f)
Product Form	—	Bar, 0.5-cm-dia.	—	—
Specimen Type	Hourglass	Cylindrical (b)	Cylindrical (d)	Cylindrical (g)
Width or Dia.	0.64 cm (min.)	0.05 cm	0.32 cm	0.4 cm
Thickness	—	—	—	—
Gage Length	10 cm (a)	15 cm	1.3 cm (gage)	—
"R" Ratio	−1	−1	0.12–0.19	−1
Test Frequency	37 Hz	104 Hz (c)	30 Hz	17.7 kHz
No. of Specimens	2	10 per fatigue life	9	24
Test Temperature	295 K	295 K	295 K	295 K

(a) Parallel portion 1.3 cm long.
(b) Specimens electropolished after annealing.
(c) Large number of cycles taken to build up to stress range.
(d) Specimens electropolished prior to testing.
(e) Second set of specimens stretched 15% after anneal, cut to shape of test specimen.
(f) Annealed specimens.
(g) All specimens cleaned electrochemically before annealing.

14	15	16	17	18
C10100	C10200	C10100	C10100	C10200
99.999	—	99.99	99.99	—
—	—	—	—	—
—	—	—	—	—
—	—	—	—	—
—	—	—	—	—
—	—	—	—	—
—	—	—	—	—
—	—	—	—	—
—	—	—	—	—
—	—	—	—	—
—	—	—	—	—
Annealed 903 K, 1 h, Ar, FC	Annealed	Annealed, 1023 K, 1 h	Annealed	Annealed
46 µm	—	160 µm	70 µm	—
—	—	—	—	—
Bar, 2.5-cm-dia.	—	Bar, 7.6-cm-dia.	Bar, 0.03-cm-dia.	—
Hourglass (a) 0.64 cm (min.) — —	Hourglass 1.1 cm (b) — 14 cm (1.9-cm gage)	Hourglass (c) 0.41 cm (min.) — 0.64 cm (gage)	Hourglass 0.30 cm — 3.8 cm (0.13-cm gage)	— — — —
–1 50 Hz	–1	–1 33 Hz	–1 20 Hz (d)	–1 225 Hz
17	6	17	45	13
295 K	295 K	77, 295 K	4, 77, 295 K	1.7, 4, 20 K

(a) Specimens cleaned electrochemically before annealing.
(b) Continuous-radius gage section 1.9 cm long by 1.3 cm dia. at narrowest point.
(c) Specimens electropolished before testing.
(d) Frequency 100 Hz at 4 K.

Table 4.6, continued

Reference No.	19	21	22	24
Specification	C10200	C10700	C10100	C10200
Composition (wt%)				
Cu	99.98	—	99.96	—
Ag	—	0.085	—	—
Cu + Ag	—	—	—	—
O_2	—	< 0.0003	—	—
Bi	—	—	—	—
P	—	—	—	—
Pb	—	—	< 0.001	—
S	—	—	—	—
Se	—	—	—	—
Te	—	—	—	—
Others (Only ≥ 0.001 wt%)	—	—	Fe: 0.001; Sn: < 0.001	—
Material Condition	Annealed, 873 K, 1 h, vacuum (a)	Cold-worked, 17 and 82%	Annealed, various conditions (d)	As received
Grain Size	(b)	—	45 μm	200 μm
Hardness	—	—	—	—
Product Form	—	—	Sheet	—
Specimen Type	Cylindrical	—	Flat (tapered)(e)(f)	Hourglass (g)
Width or Dia.	0.4 cm	—	1.0 cm (min.)	0.95 cm (min.)
Thickness	—	—	0.3 cm	—
Gage Length	2.0 cm (gage)	—	9.0 cm (1.0-cm gage)	10 cm (5-cm gage)
"R" Ratio	−1	—	0	−1
Test Frequency	100 Hz	—	60 Hz	(h)
No. of Specimens	(c)	8	5	4
Test Temperature	295 K	295 K	295 K	295 K

(a) Coarse-grained specimens annealed at 1173 K for 5 h, vacuum.
(b) Fine-grained, 60–70 μm; coarse-grained, 900–1200 μm.
(c) A total of 70 fine-grained specimens and 90 coarse-grained specimens were run either until complete fracture or at least 10^7 cycles.
(d) Specimens annealed under various conditions to obtain different grain sizes. Then deformed under tension from 0 to 23%.
(e) Specimens polished mechanically after annealing, prior to testing.
(f) Fatigue crack growth rate specimens were center slit, 3.0 cm wide, 3.0-cm gage length, other dimensions same.
(g) Specimens electropolished prior to testing.
(h) Head speed of 0.5 cm/min.

C10100–C11000: Annealed; Cold-worked | *Fatigue Properties (All)*

25	26	28	28	29
C10200	C10200	C10100	C10100	C10200
— — — — — — — — — — —	99.98 — — — — — — — — — —	99.99 — — — — 0.0003 0.0018 — — — —	99.99 — — — — — — — — — —	99.9 — — — — — — — — — —
Annealed, 673 K, 1 h, vacuum, FC (a)	Annealed (d)	Annealed, 920 K, 1 h, vacuum	Annealed, 823 K, 1 h, vacuum	Annealed, 773 K, 1 h, vacuum (f)
—	200 μm	—	30 μm	25 μm
—	—	—	—	—
Bar, 1.9-cm-dia.	—	Bar, 2.54-cm-dia.	—	Bar
Hourglass 0.47 cm (min.) — 9.4 cm (5.6-cm gage)	Cylindrical 0.35 cm — 2.0 cm (gage)	Hourglass 0.635 cm (min.) — 9.53 cm	Cylindrical 1.0 cm — 1.5 cm (gage)	Hourglass 0.56 cm — 1.2–2.5 cm (gage) (g)
−1 0.11–0.28 Hz (b)	−1 80 Hz	−1 1.2, 33 Hz	−1 (e)	−1 (h)
25 (c)	28	18	9	5
295 K	295 K	4, 78, 300 K	295 K	295 K

(a) Other specimens cold-worked to 33.3% reduction in diameter.
(b) Tests begun at minimum frequency for first 1000 cycles.
(c) Tests on as-received material with undetermined cold work not used.
(d) Other specimens prestrained 20 to 40%.
(e) Constant strain rate, 0.02/s.
(f) Specimens chemically polished before annealing.
(g) Specimens with shorter gage lengths used at higher strain amplitudes to suppress buckling.
(h) Frequency selected for constant plastic strain rate, 0.0005/s.

Table 4.6, continued

Reference No.	32	34	35	36
Specification	C11000	C10100	C10200	C10100
Composition (wt%)				
Cu	99.95	99.999	99.9	99.999
Ag	—	—	—	—
Cu + Ag	—	—	—	—
O_2	—	—	—	—
Bi	—	—	—	—
P	—	—	—	—
Pb	—	—	—	—
S	—	—	—	—
Se	—	—	—	—
Te	—	—	—	—
Others (Only ≥ 0.001 wt%)	—	—	—	—
Material Condition	Annealed, 823 K, 1 h, (a)	Prestressed, tension, 177 MPa	Annealed, 903 K, 1.5 h, FC	Annealed, 1223 K, 4 h vacuum (e)
Grain Size	65 μm (b)	30 μm	20 μm	1000 μm
Hardness	—	—	—	—
Product Form	Plate	Sheet	—	—
Specimen Type	Wedge-open-loading (c)	Singled edge slit	Singled edge slit	Single edge slit
Width or Dia.	8.13 cm	1.08 cm	1.0 cm	1.3 cm
Thickness	0.635 cm	0.07 cm	0.01 cm	0.08 cm
Gage Length	6.3 cm	4.5 cm	—	4.4 cm
"R" Ratio	01, 0.3, 0.5, 0.7	0.05–0.38	–1	0
Test Frequency	100 Hz	40 Hz	21 kHz	8–22 Hz
No. of Specimens	6–16 per curve	~54 at 77 K; 34 at 295 K	30, 77 K; 51, 295 K	9, 77 K; 20, 295 K (f)
Test Temperature	295 K	77, 295 K	77, 293 K (d)	77, 295 K

(a) Other specimens cold rolled to 11 and 31% reduction in thickness.
(b) Grain sizes 45 and 25 μm for 11 and 31% cold reduction.
(c) Compact-tension and center-cracked specimens were also used in testing of 11% cold-worked specimens. No significant difference was found in the rates of near-threshold crack propagation.
(d) Liquid nitrogen or silicone oil specimen environment.
(e) Specimens electropolished before testing.
(f) Two specimens were tested at room temperature, one at 77 K.

C10100–C11000: Annealed; Cold-worked | *Fatigue Properties (All)*

37
C10200
99.97 — — — — — — — — — —
Annealed, 873 K, 1h (a) or cold-worked
—
—
Sheet
Center slit 23 or 25 cm 0.32 cm 23 or 25 cm (gage)
0.34 3, 30 Hz (b)
37 (c)
295 K

(a) Annealed after specimen slit machined.
(b) No differences in crack growth characteristics found in tests carried out at the two frequencies.
(c) Number of specimens from which data were averaged.

REFERENCES

1. Gough, H. J., and Sopwith, D. G., "Some Further Experiments on Atmospheric Action in Fatigue," Journal of the Institute of Metals 56, 55–89 (1935).

2. Bullen, F. P., Head, A. K., and Wood, W. A., "Structural Changes During the Fatigue of Metals," Proceedings of the Royal Society of London A216, 332–343 (1953).

3. Thompson, N., Wadsworth, N., and Louat, N., "The Origin of Fatigue Fracture in Copper," Philosophical Magazine 1, 113–126 (1956).

4. McCammon, R. D., and Rosenberg, H. M., "The Fatigue and Ultimate Tensile Strengths of Metals Between 4.2 and 293 °K," Proceedings of the Royal Society of London A242, 203–211 (1957).

5. Thompson, A. W., and Backofen, W. A., "The Effect of Grain Size on Fatigue," Acta Metallurgica 19, 597–606 (1971).

6. Hull, D., "Annealing in Slip Bands in Copper Fatigued at 90 °K," Philosophical Magazine 3, 513–518 (1958).

7. Benham, P. P., "Axial-Load and Strain-Cycling Fatigue of Copper at Low Endurance," Journal of the Institute of Metals 89, 328–338 (1961).

8. Frost, N. E., "Alternating Stress Required to Propagate Edge Cracks in Copper and Nickel-Chromium Alloy Steel Plates," Journal of Mechanical Engineering Science 5, 15–22 (1963).

9. Clarebrough, L. M., Hargreaves, M. E., Head, A. K., and West, G. W., "Energy Stored During Fatigue of Copper," Transactions, American Institute of Metallurgical Engineers, Journal of Metals 7, 99–100 (1955).

10. Gough, H. J., and Sopwith, D. G., "Inert Atmosphere as Fatigue Environments," Journal of the Institute of Metals 72, 415–421 (1946).

11. Wright, M. A., and Greenough, A. P., "The Effect of High-Temperature Intermediate Annealing on the Fatigue Life of Copper," Journal of the Institute of Metals 93, 309–313 (1964).

12. Masuda, H., and Duquette, D. J., "The Effect of Surface Dissolution on Fatigue Crack Nucleation in Polycrystalline Copper," Metallurgical Transactions 6A, 87–94 (1975).

13. Awatani, J. Katagiri, K., Omura, A., and Shiraishi, T., "A Study of the Fatigue Limit of Copper," Metallurgical Transactions 6A, 1029–1034 (1975).

14. Nakano, Y., and Sandor, B. I., "Fatigue Behavior of Copper with Intermediate Surface Layer Removal," Journal of Testing and Evaluation 2, 16–22 (1974).

15. Burmeister, R. A., and Dodd, R. A., "The Effect of Electrodeposited Metals on Fatigue," Proceedings of the American Society for Testing Materials 62, 675–680 (1962).

16. Laird, C., and Krause, A. R., "On the Temperature Effect in the Fatigue Fracture of Copper and Cu-7.9 Wt Pct Al Alloy," Transactions of the American Institute of Mining and Metallurgical Engineers 242, 2339–2342 (1968).

REFERENCES

17. Holt, D. L., and Backofen, W. A., "Fatigue Fracture In Copper and the Cu-8Wt Pct Al Alloy at Low Temperature," Transactions of the American Institute of Mining and Metallurgical Engineers 239, 264–269 (1967).

18. MacCrone, R. K., McCammon, R. D., and Rosenberg, H. M., "The Fatigue of Metals at 1·7°K," Philosophical Magazine 4, 267–268 (1959).

19. Lukás, P., and Kunz, L., "Effect of Grain Size on the High Cycle Fatigue Behaviour of Polycrystalline Copper," Materials Science and Engineering 85, 67–75 (1987).

20. Wadsworth, N. J., and Hutchings, J., "The Effect of Atmospheric Corrosion on Metal Fatigue," Philosophical Magazine 3, 1154–1166 (1958).

21. Smith, W. E., Taubenblat, P. W., Graviano, A. R., and Batra, R., "A New Oxygen-free High-Conductivity Heat-Resistant Copper," Wire Journal International 17, 52–55 (1984).

22. Ishii, H., and Yukawa, K., "The Role of Dislocation Substructures in Fatigue Crack Propagation in Copper and Alpha Brass," Metallurgical Transactions 10A, 1881–1887 (1979).

23. Blatherwick, A. A., and Mowbray, D. F., "Stress-Strain Relationships in Low- and Intermediate-Cycle Fatigue," Proceedings of the American Society for Testing and Materials 64, 561–578 (1964).

24. Boettner, R. C., Laird, C., and McEvily, A. J., Jr., "Crack Nucleation and Growth in High-Strain–Low Cycle Fatigue," Transactions of the American Institute of Mining and Metallurgical Engineers 233, 379–387 (1965).

25. Coffin, L. F., Jr., and Tavernelli, J. F., "The Cyclic Straining and Fatigue of Metals," Transactions of the American Institute of Mining and Metallurgical Engineers 215, 794–807 (1959). Also in a report from General Electric Research Laboratory, Research Information Section, The Knolls, Schenectady, New York, Report No. 58-RL-2100, 32 pp. (1958).

26. Lukás, P., and Klesnil, M., "Cyclic Stress-Strain Response and Fatigue Life of Metals in Low Amplitude Region," Materials Science and Engineering 11, 345–356 (1973).

27. Nachtigall, A. J., "Strain-Cycling Fatigue Behavior of Ten Structural Metals Tested in Liquid Helium (4 K), in Liquid Nitrogen (78 K), and in Ambient Air (300 K)," NASA Scientific and Technical Information Facility, B.W.I. Airport, MD, NASA TN D-7532, 30 pp. (1974).

28. Polák, J., and Klesnil, M., "Cyclic Stress-Strain Response and Dislocation Structures in Polycrystalline Copper," Materials Science and Engineering 63, 189–196 (1984).

29. Wang, R., and Mughrabi, H., "Secondary Cyclic Hardening in Fatigued Copper Monocrystals and Polycrystals," Materials Science and Engineering 63, 147–163 (1984).

30. Yakovenko, L. F., and Grinberg, N. M., "The Fatigue Life and Plastic Deformation Character of Copper at Low Temperatures," International Journal of Fatigue 5, 239–243 (1983).

REFERENCES

31. Verkin, B. I., Grinberg, N. M., Serdyuk, V. A., and Yakovenko, L. F., "Low Temperature Fatigue Fracture of Metals and Alloys," Materials Science and Engineering 58, 145–168 (1983).

32. Liaw, P. K., Leax, T. R., Williams, R. S., and Peck, M. G., "Near-Threshold Fatigue Crack Growth Behavior in Copper," Metallurgical Transactions 13A, 1607–1618 (1982).

33. Liaw, P. K., and Logsdon, W. A., "Fatigue Crack Growth Threshold at Cryogenic Temperatures: A Review," Engineering Fracture Mechanics 22, 585–594 (1985).

34. Yeske, R. A., and Weertman, J., "Fatigue Crack Propagation Under Varied Mean Stress Conditions," Metallurgical Transactions 5, 2033–2039 (1974).

35. Tschegg, E., and Stanzl, S., "Fatigue Crack Propagation and Threshold in B.C.C. and F.C.C. Metals at 77 and 293 K," Acta Metallurgica 29, 33–40 (1981).

36. Ishii, H., and Weertman, J., "Fatigue Crack Propagation in Copper and Cu-Al Single Crystals," Metallurgical Transactions 2, 3441–3452 (1971).

37. Frost, N. E., Pook, L. P., and Denton, K., "A Fracture Mechanics Analysis of Fatigue Crack Growth Data for Various Materials," Engineering Fracture Mechanics 3, 109–126 (1971).

38. Lukáš, P., "Models for ΔK_{th} and Near-Threshold Fatigue Crack Growth," Fatigue 84 Conference Proceedings, Vol. 1, 479–495 (1984).

DATA SOURCES AND ANALYSIS

Most creep tests are done at temperatures above 295 K, so low-temperature data are not plentiful. The amount of creep is larger and easier to measure at high temperatures; the long-term stability required for strain measurements at lower temperatures makes experiments difficult. References 5.1–5.5 provide data at room temperature obtained over total test durations of 1 to 25 000 h. The applied stresses were usually well above the yield strength of the materials. All of the longer-duration creep tests are on annealed material, except for the tests reported in Reference 5.3 on 8%-stretched C10200 copper for a duration of 10 000 h. Products were in wire (References 5.1 and 5.4), bar (References 5.2 and 5.3), and plate form (Reference 5.5). The available characterization of materials and measurements is given in Table 5.4 at the end of the creep properties section. Figures 5.1 and 5.2 present data from References 5.1–5.5 with different creep-strain scales. Creep strain, as plotted in Figures 5.1 and 5.2 for selected data from Reference 5.2, was obtained by subtracting the initial strain, ϵ_o, from the raw strain data. Creep strain data were reported in the other references. Reference 5.6 reported creep data which were not plotted as they were not in agreement with data on similar material from other sources.

Because of the variety of materials, material conditions, and test durations, and the use of applied stresses up to a factor of ten times the yield strength, most of the data are presented in graphical form and were not subjected to further analysis. However, in the tests reported in Reference 5.2, the applied stress ranged from about two-thirds to twice the 25-MPa yield strength of the material, and the analysis of this data, available also in Reference 5.2, will be reported here. For each level of applied stress, the raw strain data were fitted to an equation of the form

$$\epsilon_{true} = \epsilon_o + a_1 \ln t + a_2 t \qquad (5\text{-}1)$$

where t is elapsed time in min. The coefficients a_1 and a_2 are a function of the test temperature and the applied stress, σ_a. Linear regression analysis was used to obtain a predictive equation for the dependence of a_1 and a_2 upon the σ_a.

RESULTS

The coefficients a_1 and a_2 that resulted from fitting the data from Reference 5.2 to Equation (5-1) are given in Table 5.1 along with the test duration and the applied stress. The results of the regression analysis were not satisfactory for the coefficient a_2 of Equation (5-1). It is thought that this was due to small long-term fluctuations in the total strain due to extraneous factors, such as vibration and temperature variation (Reference 5.2), that were reflected in the coefficient a_2. The equation obtained for the coefficient a_1 is

$$a_1\,(10^{-5}) = 0.51 + 0.10\sigma_a \qquad (5\text{-}2)$$

$$(\text{S.D.} = 1.06 \times 10^{-5}),$$

where σ_a is in MPa. Figure 5.3 indicates the fit of the data to this equation, which applies to copper with Cu + Ag = 99.99 wt%, annealed at 923 K for 1 h, with a yield strength of about 25 MPa. Further limitations on the use of this equation to predict creep strain are discussed below.

DISCUSSION

Typical creep curves from Reference 5.2 are shown in Figure 5.4. For $t < 10^4$ min, the creep strain is approximately logarithmic. However, at $t > 10^4$ min, the dependence of strain on time increases, relative to a logarithmic dependence. From Figure 5.5, which shows the same data plotted on a linear scale, it can be seen that the creep rate, $\dot{\epsilon}$, decreases as the elapsed time increases. Since the test temperature is far below 0.2 T_m, where T_m is the melting point of copper, steady-state creep ($\dot{\epsilon}$ = a constant) should not be expected (Reference 5.7). Creep data from References 5.3 and 5.4 over longer time periods of up to 23 000 h (1.4×10^6 min) also exhibit decreasing strain rates with elapsed time.

At 300 °C (573 K), the addition of Ag has been shown to increase the applied stress required for a given creep rate, although the tensile strength of the material is not affected (References 5.8 and 5.9). For example, the applied stresses required for a creep rate of 0.001%/h are 33, 41, and 50 MPa for C10200, C10200 + 0.054 wt% Ag, and C10200 + 0.076 wt% Ag, respectively. These results are for 5% cold-worked material tested for about 20 h. The effect of Ag on creep rates at lower temperatures has not been reported, and different creep mechanisms may be important in the cryogenic temperature range.

Table 5.1. Dependence of the Coefficients a_1 and a_2 from Equation (5-1) on Applied Stress (295 K).

Applied Stress, MPa	Applied Stress / Yield Stress	Initial Strain, 10^{-3}	a_1, 10^{-5}	a_2, 10^{-9}	Duration of Test, min
20.2	0.80	1.704	3.192	0.817	37 440
24.9	1.00	3.269	4.153	1.359	37 440
27.0	1.08	0.709	1.670	0.491	29 986
29.96	1.20	4.726	3.440	1.712	27 300
31.4	1.26	4.873	3.150	-0.142	18 856
34.0	1.36	3.131	3.663	4.153	29 986
31.4	1.36	5.575	4.254	2.355	41 640
36.4	1.45	5.647	4.297	0.617	49 950
37.6	1.[illegible]0	7.031	4.871	2.248	41 640
38.0	1.[illegible]	4.083	4.371	1.360	29 986
41.0	1.6[illegible]	5.596	5.111	1.392	29 986
42.2	1.69	8.208	5.845	-0.732	15 695
42.4	1.70	8.031	4.232	0.854	49 950
45.1	1.80	9.116	4.490	-1.034	18 856
45.3	1.81	9.032	5.672	1.413	15 695

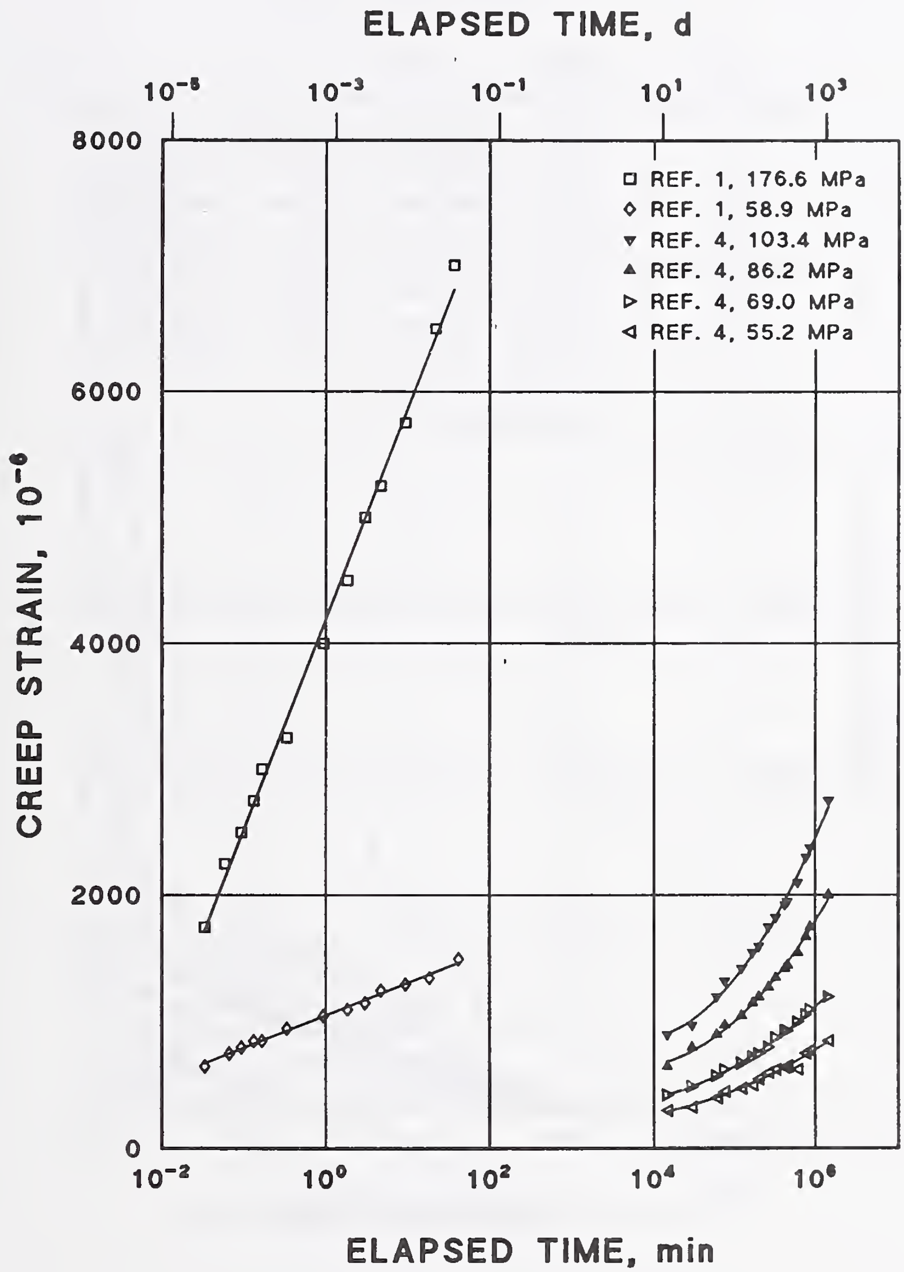

Figure 5.1. Data on the dependence of the creep strain of copper on elapsed time for various applied stresses. The sources of these data from tests conducted at room temperature were References 5.1 and 5.4. Product form was wire.

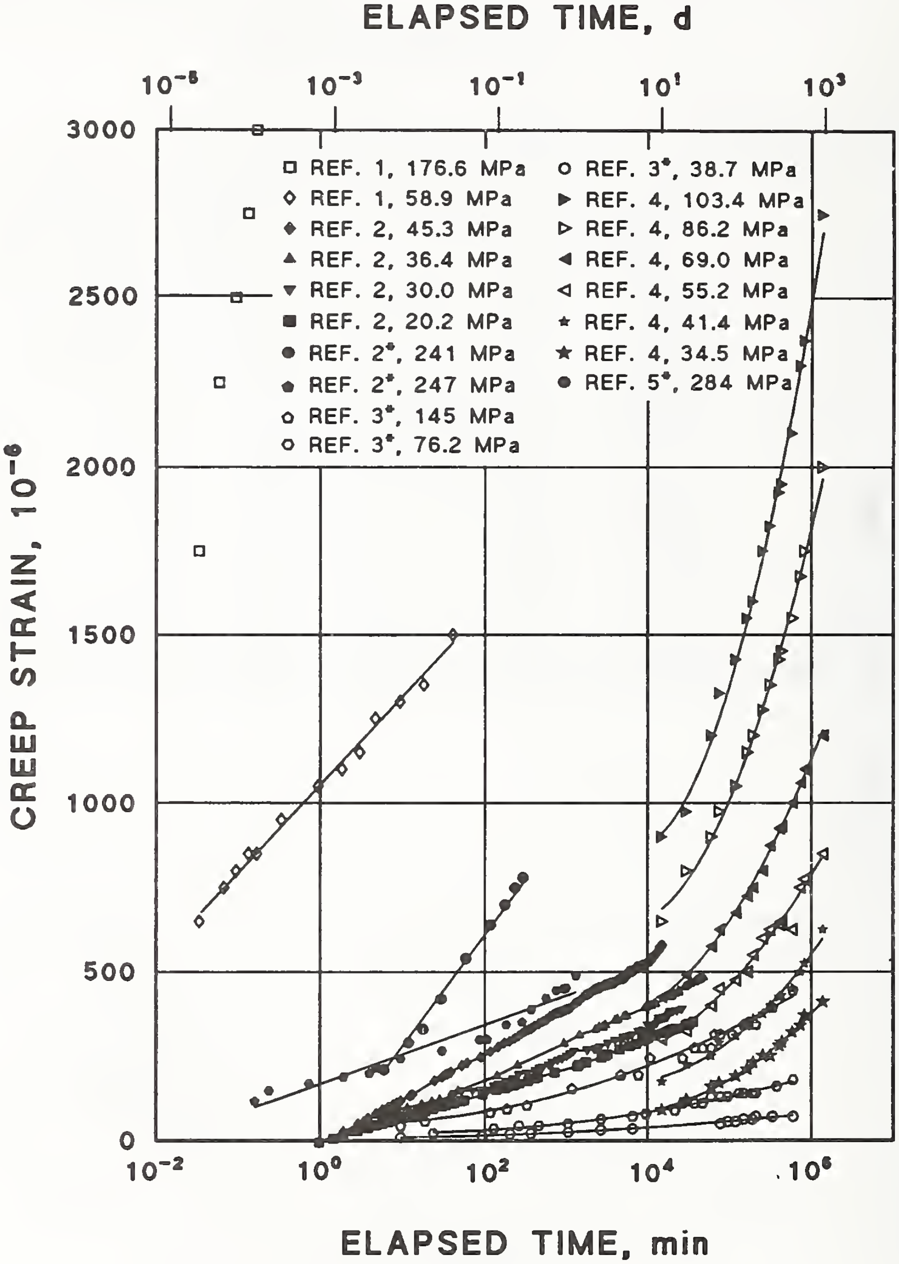

Figure 5.2. Data on the dependence of the creep strain of copper on elapsed time for various applied stresses. The sources of these data from tests conducted at room temperature were References 5.1–5.5. Data indicated with an asterisk in the legend were from material that was cold-worked. Asterisked data from Reference 5.2 were cold-rolled 20.7%; from Reference 5.3 were stretched 8%; and from Reference 5.5 were cold-worked 60%. Product forms were bar, wire, and plate.

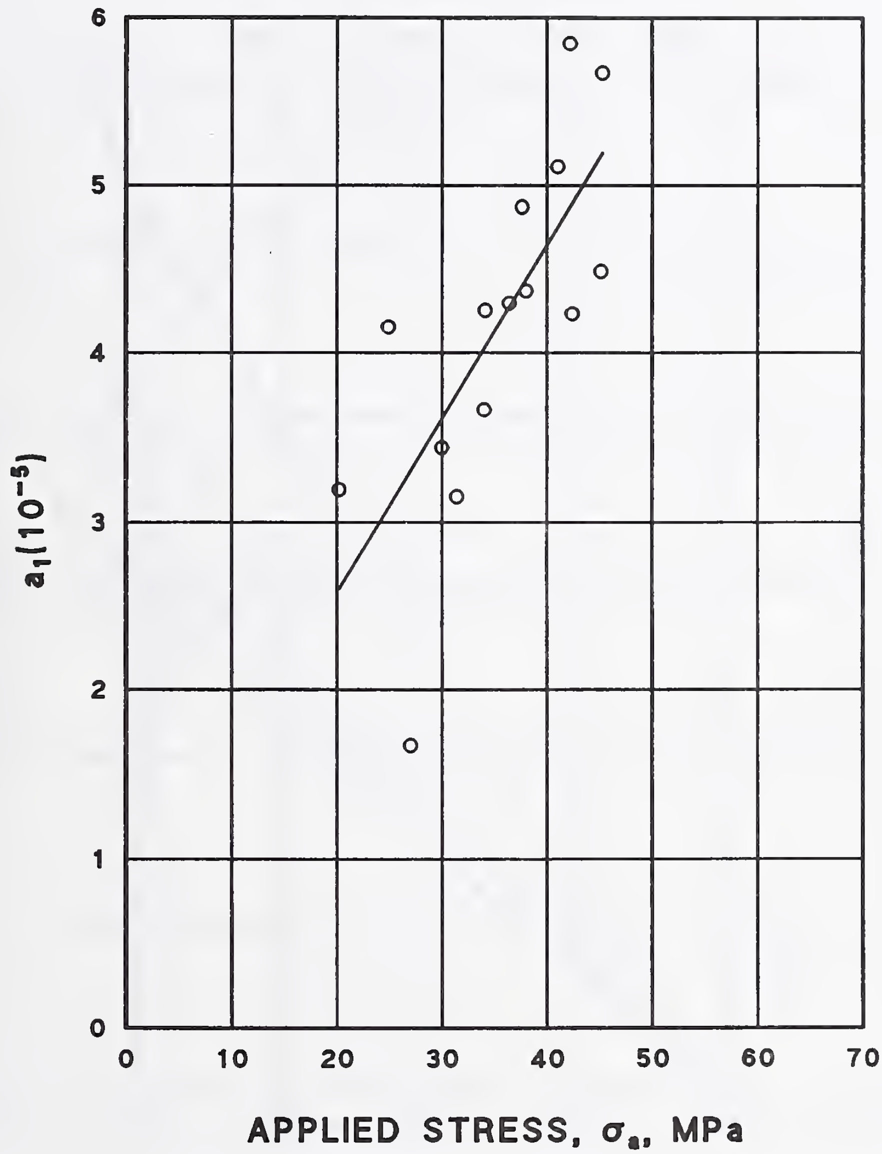

Figure 5.3. The fit of the room-temperature data (Reference 5.2) to Equation (5-2) shows the dependence of the coefficient a_1 upon the applied stress.

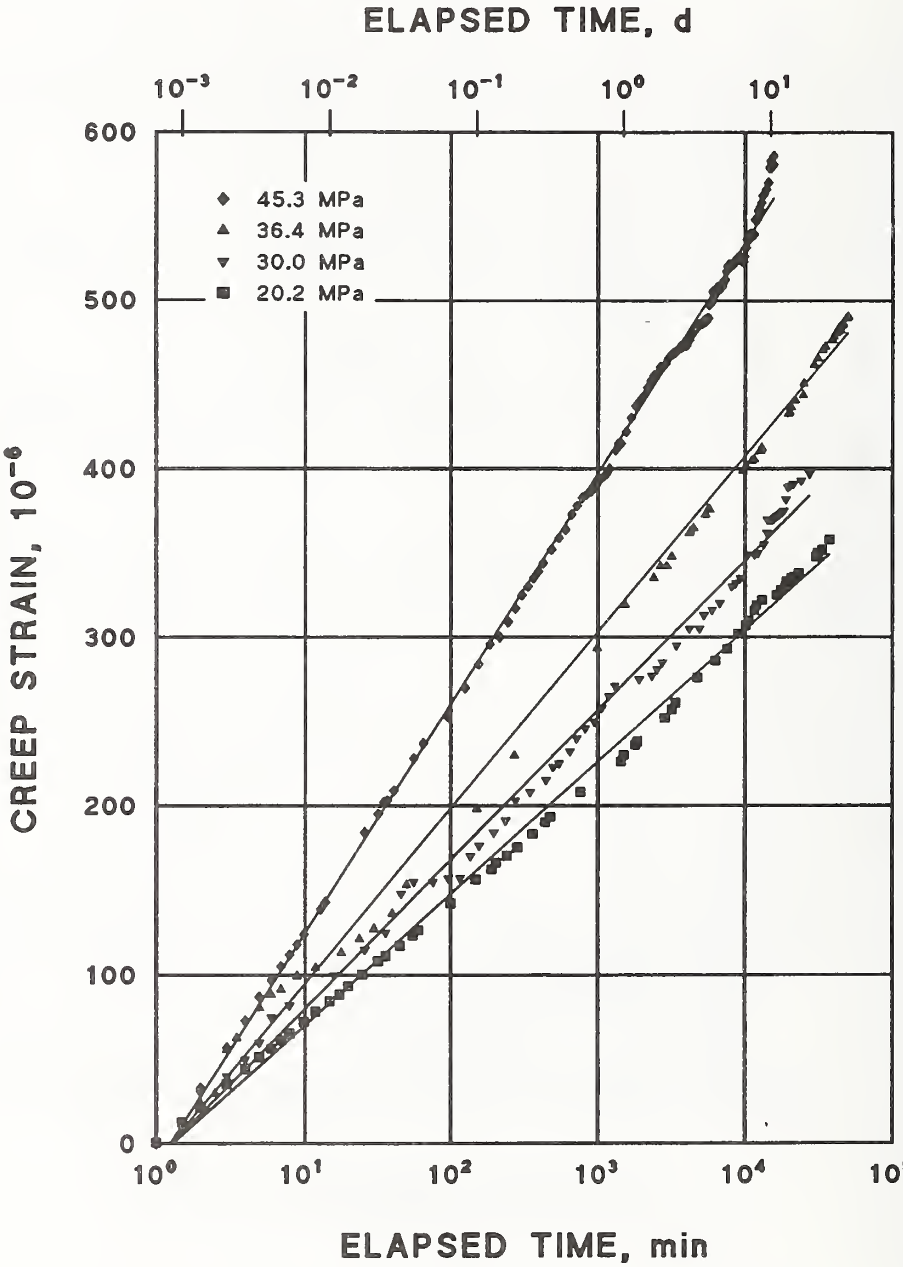

Figure 5.4. Typical creep-strain versus elapsed-time curves for four different applied stress levels, obtained at room temperature from Reference 5.2. Data are plotted on a logarithmic time scale.

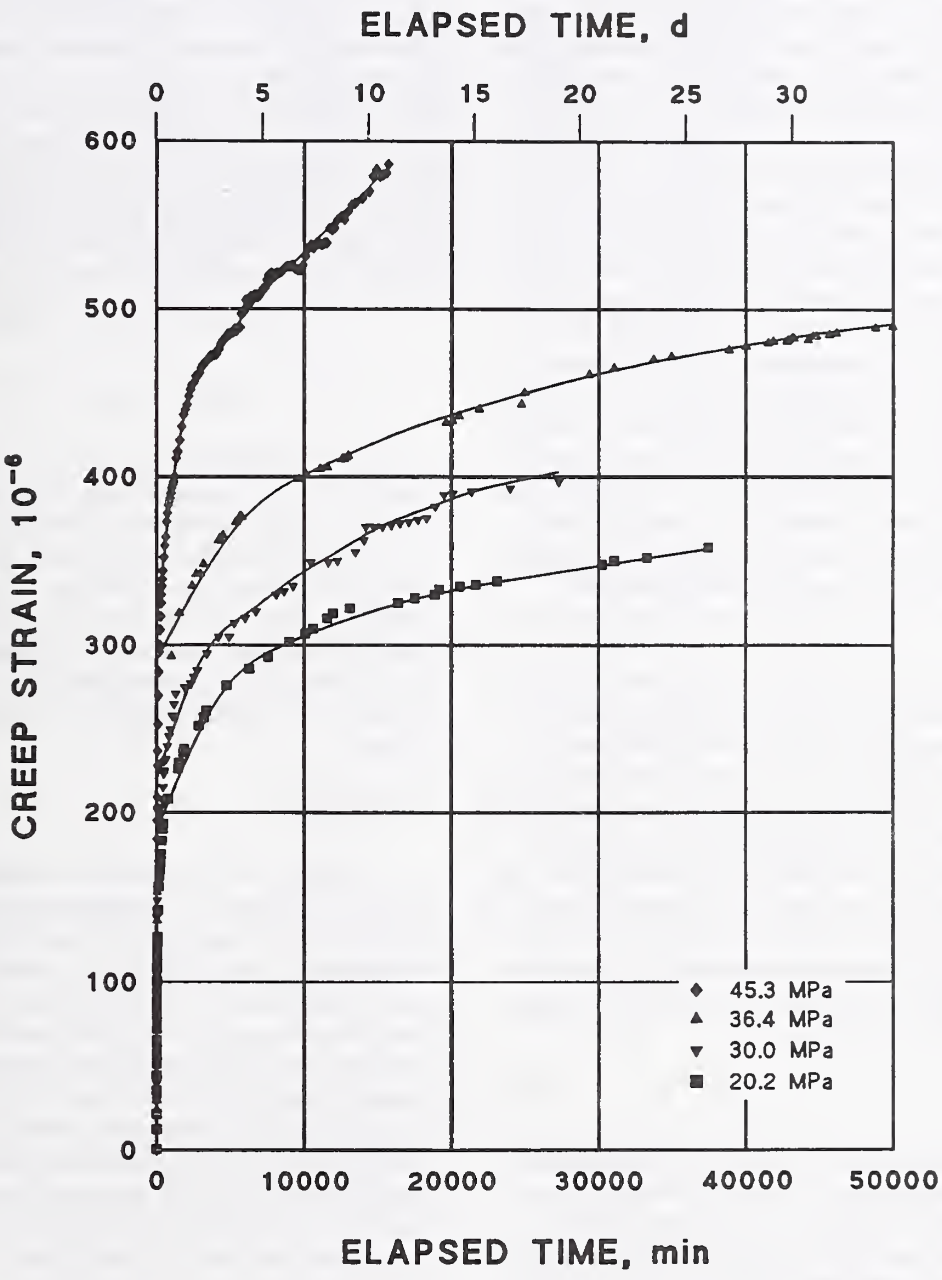

Figure 5.5. Typical creep-strain versus elapsed-time curves for four different applied stress levels, obtained at room temperature from Reference 5.2. Data are plotted on a linear time scale.

DATA SOURCES AND ANALYSIS

Most creep tests are done at temperatures above 295 K, so cryogenic data are not plentiful. The amount of creep is larger and easier to measure at high temperatures; the long-term stability required for strain measurements at lower temperatures makes experiments difficult. References 5.1, 5.2, 5.5, 5.10, and 5.11 provide data at 77 K obtained over total test durations of 1 to 1600 h. The applied stresses ranged from one half to well above the yield strength of the materials. All of the longer-duration creep tests are on annealed material. Products were in wire (Reference 5.1), bar (References 5.2 and 5.10), and plate form (Reference 5.5). The available characterization of materials and measurements is given in Table 5.4 at the end of the creep properties section. Figures 5.6 and 5.7 present data from the references with different creep-strain scales. Creep strain, as plotted in Figures 5.6 and 5.7 for selected data from Reference 5.2, was obtained by subtracting the initial strain, ϵ_o, from the raw strain data. Creep strain data were reported in the other references.

Because of the short test duration, and the use of applied stresses up to a factor of ten times the yield strength, the data from References 5.1 and 5.5 are presented in graphical form and were not subjected to further analysis. However, in the tests reported in References 5.2 and 5.10, the applied stress ranged from about half to twice the yield strength of the material. Therefore, these data were analyzed further. Details of this analysis are also available in Reference 5.2. For each level of applied stress, the strain data were fitted to an equation of the form

$$\epsilon_{true} = \epsilon_o + a_1 \ln t + a_2 t \qquad (5\text{-}1)$$

where t is elapsed time in min. The coefficients a_1 and a_2 are a function of the test temperature and the applied stress, σ_a. Linear regression analysis was used with the data from Reference 5.2 to obtain a predictive equation for the dependence of a_1 and a_2 upon σ_a.

RESULTS

The coefficients a_1 and a_2 that resulted from fitting the data from References 5.2 to Equation (5-1) are given in Table 5.2 along with the test duration and the applied stress. The results of the regression analysis were not satisfactory for the coefficient a_2 of Equation (5-1). It is thought that this was due to small long-term fluctuations in the total strain due to extraneous factors, such as vibration and temperature variation (Reference 5.2), that were reflected in the coefficient a_2. The equation obtained for the coefficient a_1 is

$$a_1\,(10^{-5}) = 0.62 + 0.087\sigma_a \qquad (5\text{-}3)$$

$$(\text{S.D.} = 0.83 \times 10^{-5}),$$

where σ_a is in MPa. Figure 5.8 indicates the fit of the data to this equation, which applies to copper with Cu + Ag = 99.99 wt%, annealed at 923 K for 1 h, with a yield strength of about 25 MPa. However, as shown in the figure, the a_1 coefficients calculated from the data from Reference 5.10, also on annealed copper, are in reasonable agreement. Further limitations on the use of this equation to predict creep strain are discussed below.

DISCUSSION

Typical creep curves from Reference 5.2 are shown in Figure 5.9. Within the experimental uncertainty, the creep strain is approximately logarithmic. From Figure 5.10, which shows the same data plotted on a linear scale, it can be seen that the creep rate, $\dot{\epsilon}$, decreases as the elapsed time increases. Since the test temperature is far below 0.2 T_m, where T_m is the melting point of copper, steady-state creep ($\dot{\epsilon}$ = a constant) should not be expected (Reference 5.7). Figure 5.11, in which $\dot{\epsilon}$ is plotted versus σ_a for data from both References 5.2 and 5.10, also shows the decrease in $\dot{\epsilon}$ with time.

Table 5.2. Dependence of the Coefficients a_1 and a_2 from Equation (5-3) on Applied Stress (77 K).

Applied Stress, MPa	Applied Stress / Yield Stress	Initial Strain, 10^{-3}	a_1, 10^{-5}	a_2, 10^{-9}	Duration of Test, min
24.3	0.90	-0.037	2.323	0.642	12 591
26.1	0.9[illegible]	1.659	3.233	-0.564	12 591
29.7	1.10	2.609	2.506	0.729	96 600
33.2	1.23	2.230	3.934	0.852	96 600
35.2	1.31	1.188	3.763	-1.263	12 591
35.4	1.31	2.731	3.876	1.163	96 600
37.1	1.37	4.889	4.684	-0.073	58 894
41.3	1.53	4.815	3.865	-0.216	36 345
45.0	1.67	5.258	4.588	-0.312	43 455
49.5	1.83	7.499	4.642	-0.621	12 820

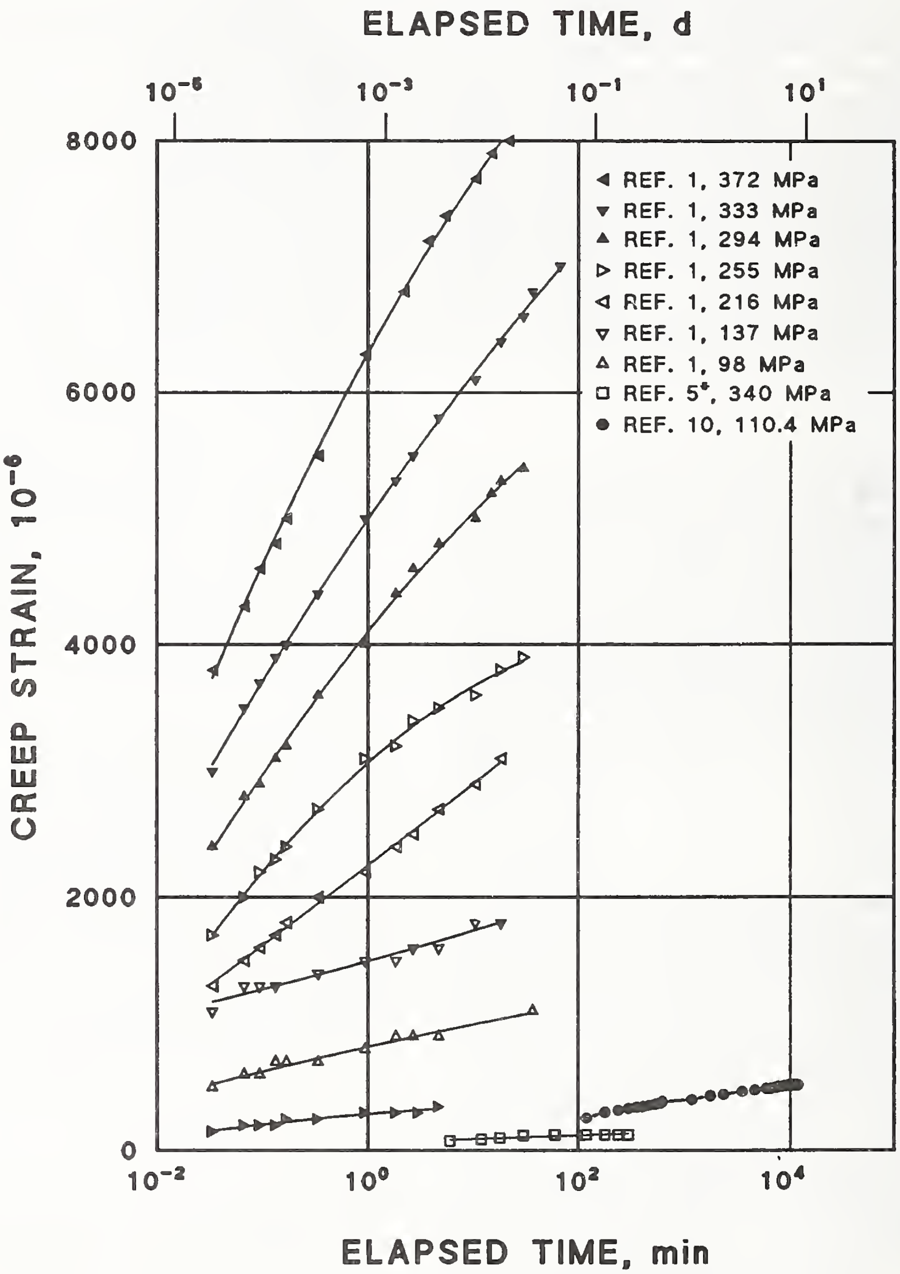

Figure 5.6. Data on the dependence of the creep strain of copper on elapsed time for various applied stresses. The sources of these data from tests conducted at 77 K were References 5.1, 5.5, and 5.10. Data (Reference 5.5) indicated with an asterisk in the legend were from material cold-worked 60%. Product forms were wire, plate, and bar.

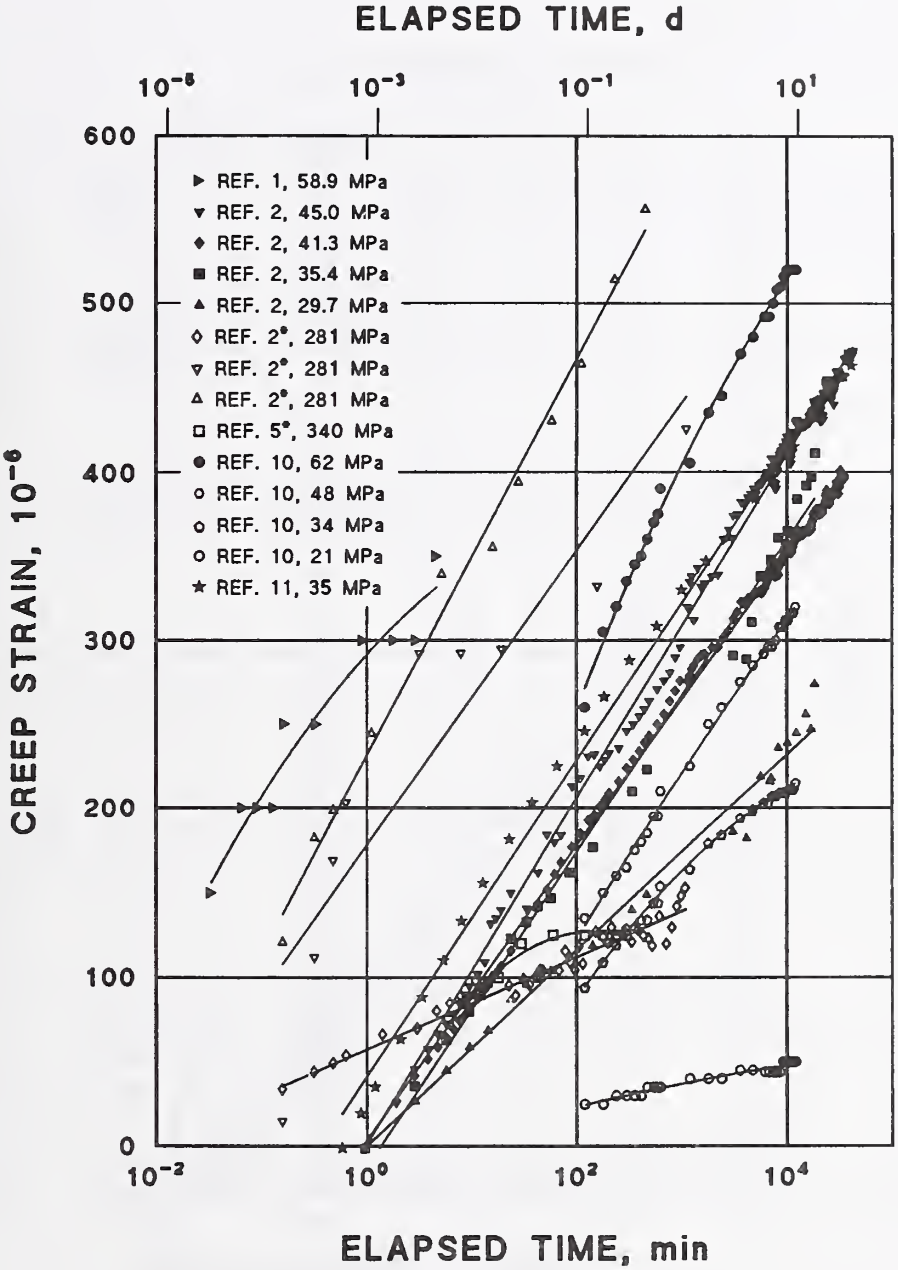

Figure 5.7. Data on the dependence of the creep strain of copper on elapsed time for various applied stresses. The sources of these data from tests conducted at 77 K were References 5.1, 5.2, 5.5, and 5.10. Some of the data at longer elapsed times exhibited fluctuations due to extraneous factors; these data are not shown here. Data indicated with an asterisk in the legend were from material that was cold-worked. Material from the data asterisked from Reference 5.2 was cold-rolled 20.7%, and from Reference 5.5 was cold-worked 60%. Product forms were wire, bar, and plate.

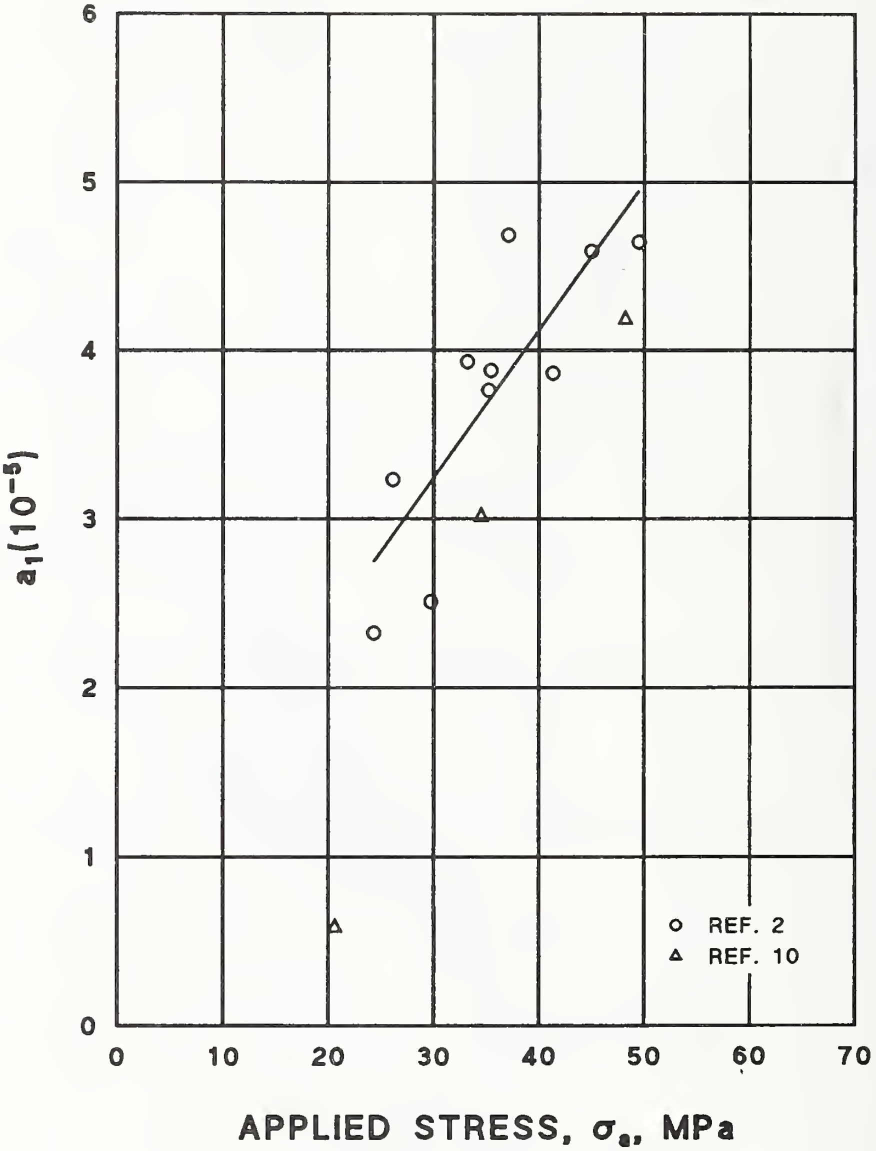

Figure 5.8. The fit of the 77-K data (References 5.2 and 5.10) to Equation (5-4) shows the dependence of the coefficient a_1 upon the applied stress.

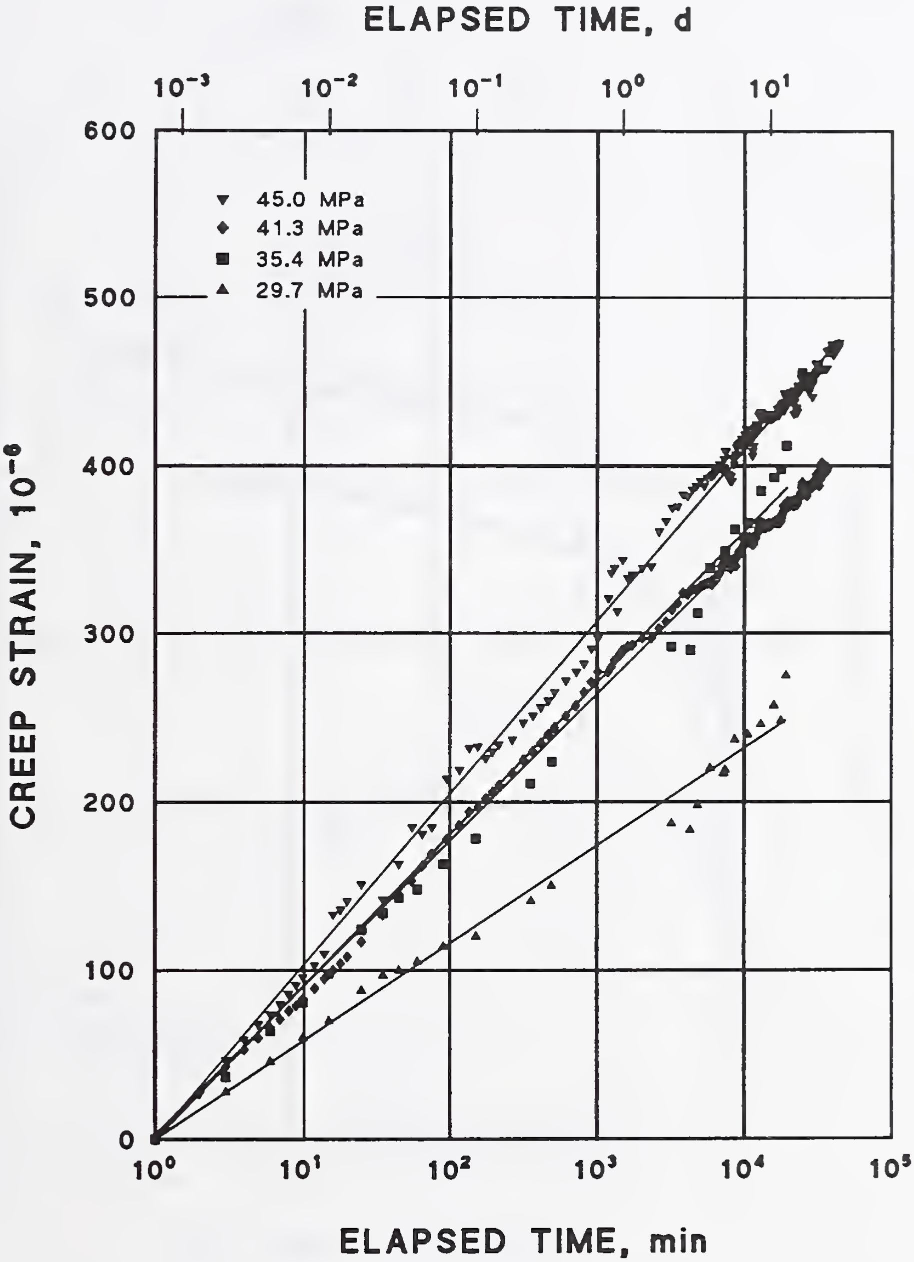

Figure 5.9. Typical creep-strain versus elapsed-time curves for four different applied stress levels, obtained at 77 K from Reference 5.2. Data are plotted on a logarithmic time scale. Some of the data at longer elapsed times exhibited fluctuations due to extraneous factors; these data are not shown here.

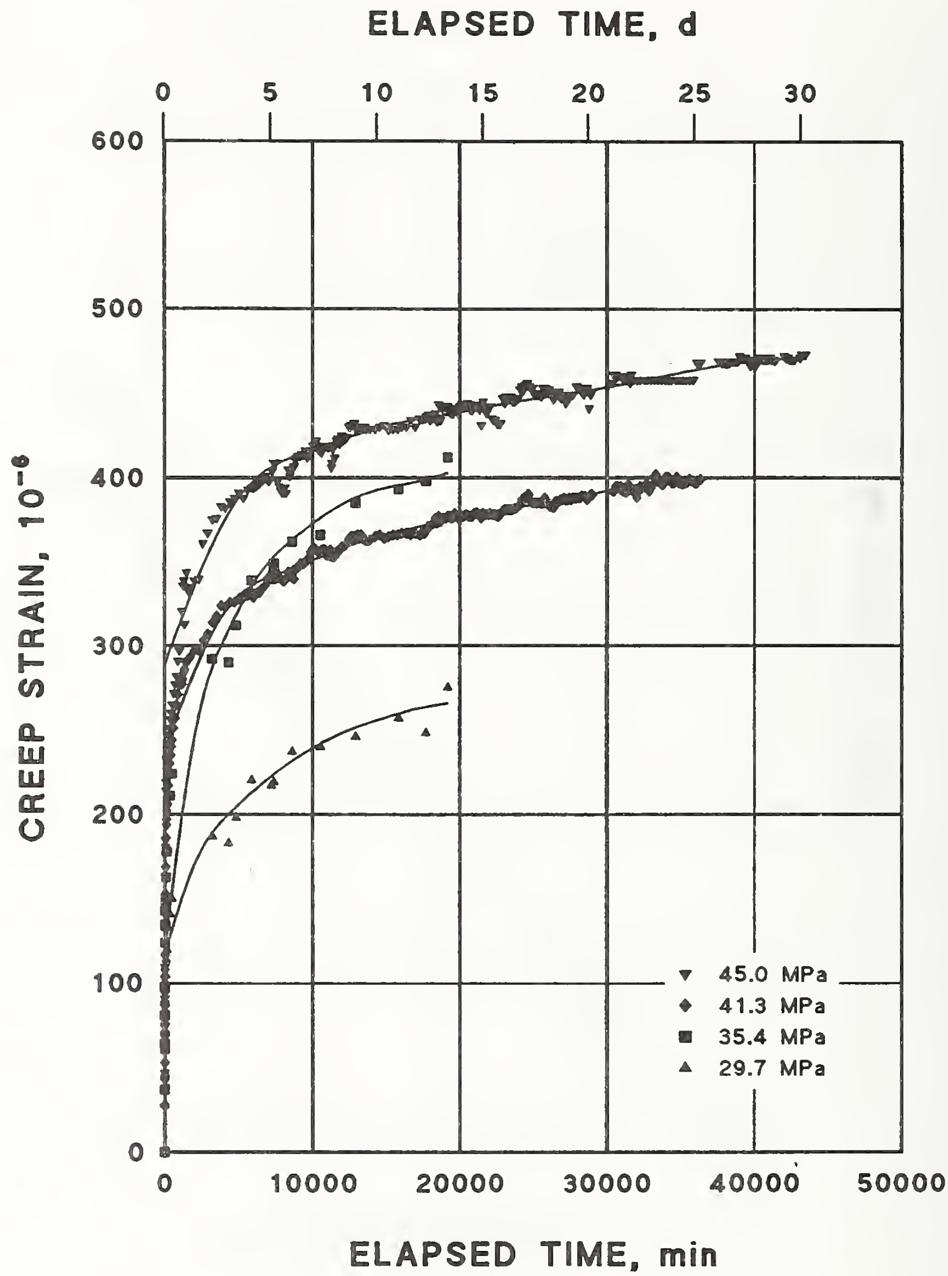

Figure 5.10. Typical creep-strain versus elapsed-time curves for four different applied stress levels, obtained at 77 K from Reference 5.2. Data are plotted on a linear time scale. Some of the data at longer elapsed times exhibited fluctuations due to extraneous factors; these data are not shown here.

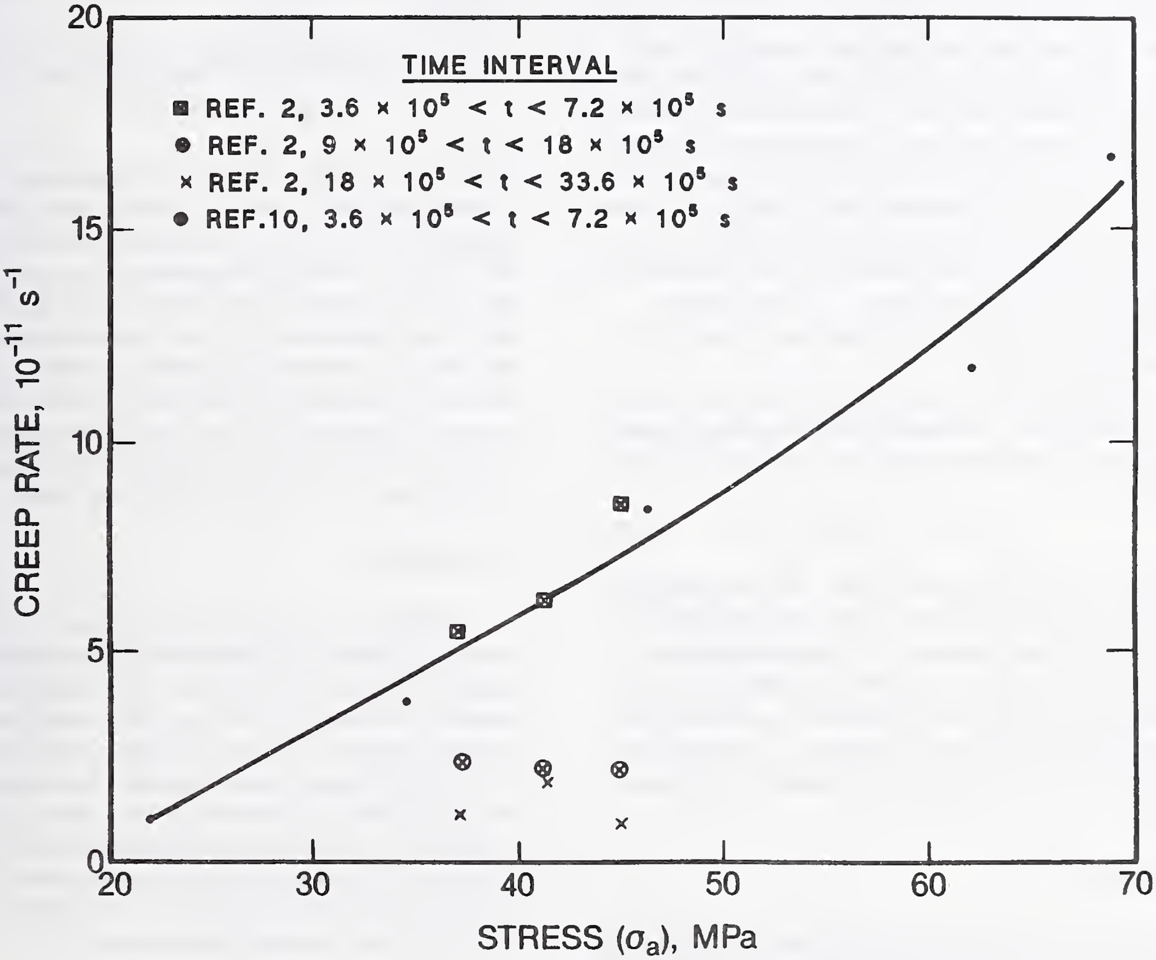

Figure 5.11. The dependence of the creep rate on the applied stress for data obtained at 77 K from References 5.2 and 5.10.

DATA SOURCES AND ANALYSIS

Most creep tests are done at temperatures above 295 K, so cryogenic data are not plentiful. The amount of creep is larger and easier to measure at high temperatures; the long-term stability required for strain measurements at lower temperatures makes experiments difficult. References 5.2 and 5.10 provide data at 4 K obtained over total test durations of 17 to 355 h. The applied stresses ranged from the yield strength of the material to about three times the yield strength. Product was in bar form. The available characterization of materials and measurements is given in Table 5.4 at the end of the creep properties section. Figure 5.12 presents all the data from Reference 5.10 and selected data from Reference 5.2. Creep strain from Reference 5.2 was obtained by subtracting the initial strain, ϵ_o, from the raw strain data. Creep strain data were reported in Reference 5.10.

Regression analysis of this data was carried out as follows. For each level of applied stress, the strain data were fitted to an equation of the form

$$\epsilon_{true} = \epsilon_o + a_1 \ln t + a_2 t \qquad (5\text{-}1)$$

where t is elapsed time in min. The coefficients a_1 and a_2 are a function of the test temperature and the applied stress, σ_a. Linear regression analysis was also used with the data from Reference 5.2 to obtain a predictive equation for the dependence of a_1 and a_2 upon σ_a. Further information on the analysis is available in Reference 5.2.

RESULTS

The coefficients a_1 and a_2 that resulted from fitting the data from Reference 5.2 to Equation (5-1) are given in Table 5.3 along with information on test duration and the applied stress. The results of the regression analysis were not satisfactory for the coefficient a_2 of Equation (5-1). It is thought that this was due to small long-term fluctuations in the total strain due to extraneous factors, such as vibration and temperature variation (Reference 5.2), that were reflected in the coefficient a_2. The equation obtained for the coefficient a_1 is

$$a_1 (10^{-5}) = -1.65 + 0.0539\sigma_a \qquad (5\text{-}4)$$

$$(\text{S.D.} = 0.65 \times 10^{-5}),$$

where σ_a is in MPa. Figure 5.13 indicates the fit of the data to this equation, which applies to copper with Cu + Ag = 99.99 wt%, annealed at 923 K for 1 h, with a yield strength of about 30 MPa at 4 K. However, as shown in the figure, the data from Reference 5.10, also on annealed copper, are in reasonable agreement. Further limitations on the use of this equation to predict creep strain are discussed below. Compared with Figures 5.3 and 5.8, which show a_1 as a function of σ_a at 295 and 77 K, a_1 at 4 K is much lower.

DISCUSSION

Typical creep curves from Reference 5.2 are shown in Figure 5.14 (logarithmic time scale) and Figure 5.15 (linear time scale). The apparent scatter in the data at 4 K, compared with that shown in Figures 5.3 and 5.4 (295 K) and 5.9 and 5.10 (77 K), reflects the expanded strain scale used to depict the relatively small amount of creep at 4 K. Since the test temperature is far below 0.2 T_m, where T_m is the melting point of copper, steady-state creep ($\dot{\epsilon}$ = a constant) should not be expected (Reference 5.7).

Table 5.3. Dependence of the Coefficients a_1 and a_2 from Equation (5-4) on Applied Stress (4 K).

Applied Stress, MPa	Applied Stress / Yield Stress	Initial Strain, 10^{-3}	a_1, 10^{-5}	a_2, 10^{-9}	Duration of Test, min
30.0	1.00	2.199	0.005	1.119	1027
30.6	1.00	0.838	0.361	0.196	21 339
32.0	1.08	3.521	0.139	2.003	1027
34.4	1.13	2.563	0.663	-0.447	21 339

Table 5.3, continued

Applied Stress, MPa	Applied Stress / Yield Stress	Initial Strain, 10^{-3}	a_1, 10^{-5}	a_2, 10^{-9}	Duration of Test, min
35.6	1.19	3.817	0.101	1.099	1488
37.6	1.23	2.178	0.423	0.593	21 339
41.5	1.38	5.743	0.787	2.951	18 540
43.8	1.46	4.933	0.160	-0.080	3612
44.0	1.46	5.834	0.170	-2.767	1027
47.2	1.57	3.926	0.144	1.418	1405
48.9	1.63	8.225	1.166	-2.375	6935
60.0	2.00	17.56	2.285	-9.008	6935

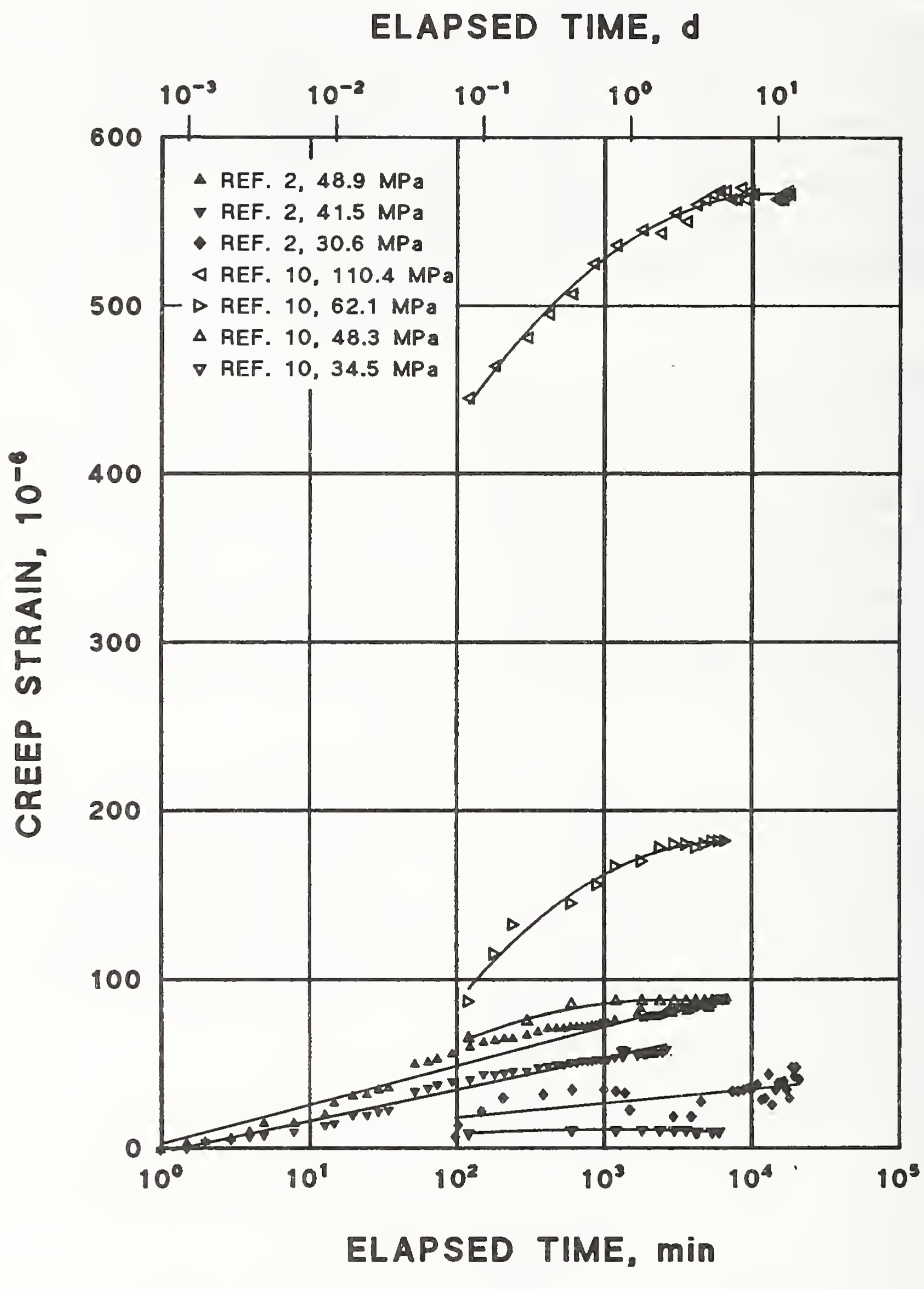

Figure 5.12. Data on the dependence of the creep strain of copper on elapsed time for various applied stresses. The sources of these data from tests conducted at 4 K were References 5.2 and 5.10. Some of the data at longer elapsed times exhibited fluctuations due to extraneous factors; these data are not shown here. Product form was bar.

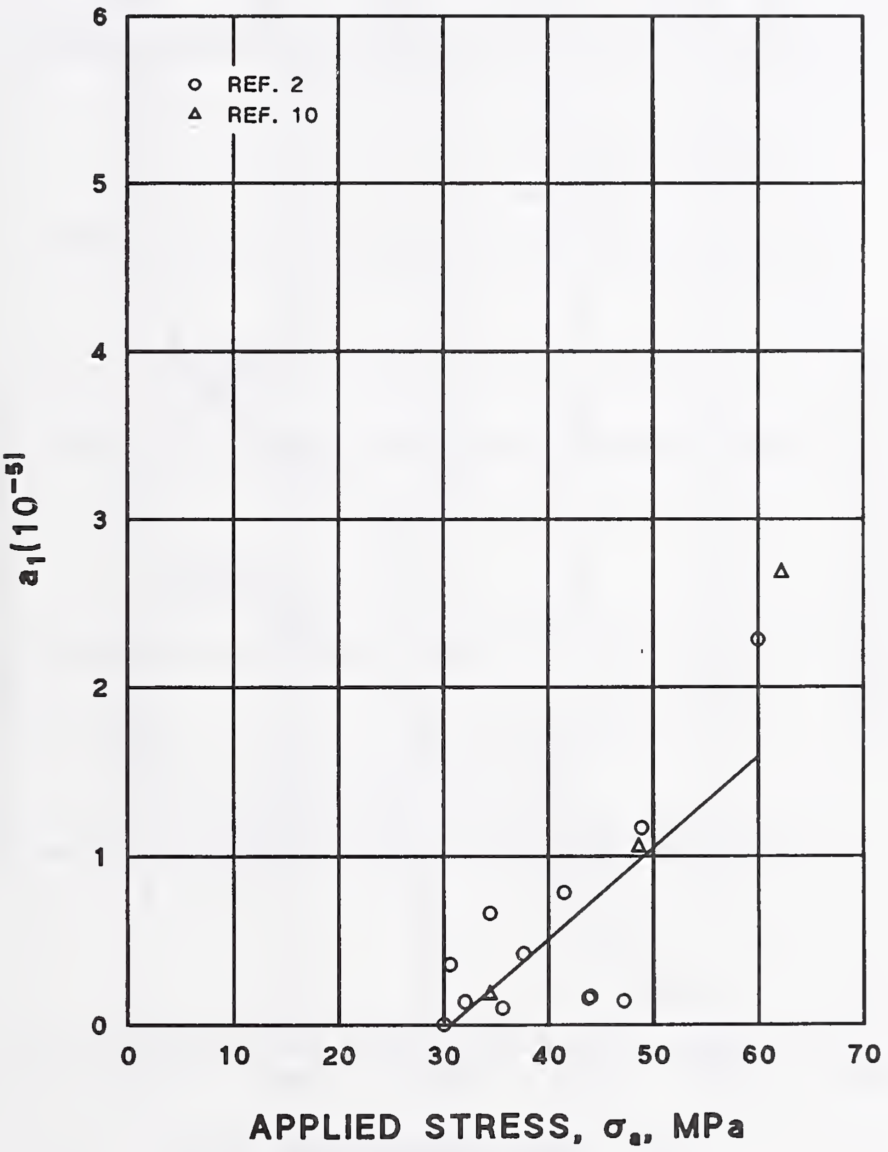

Figure 5.13. The fit of the 4-K data (References 5.2 and 5.10) to Equation (5-5) shows the dependence of the coefficient a_1 upon the applied stress.

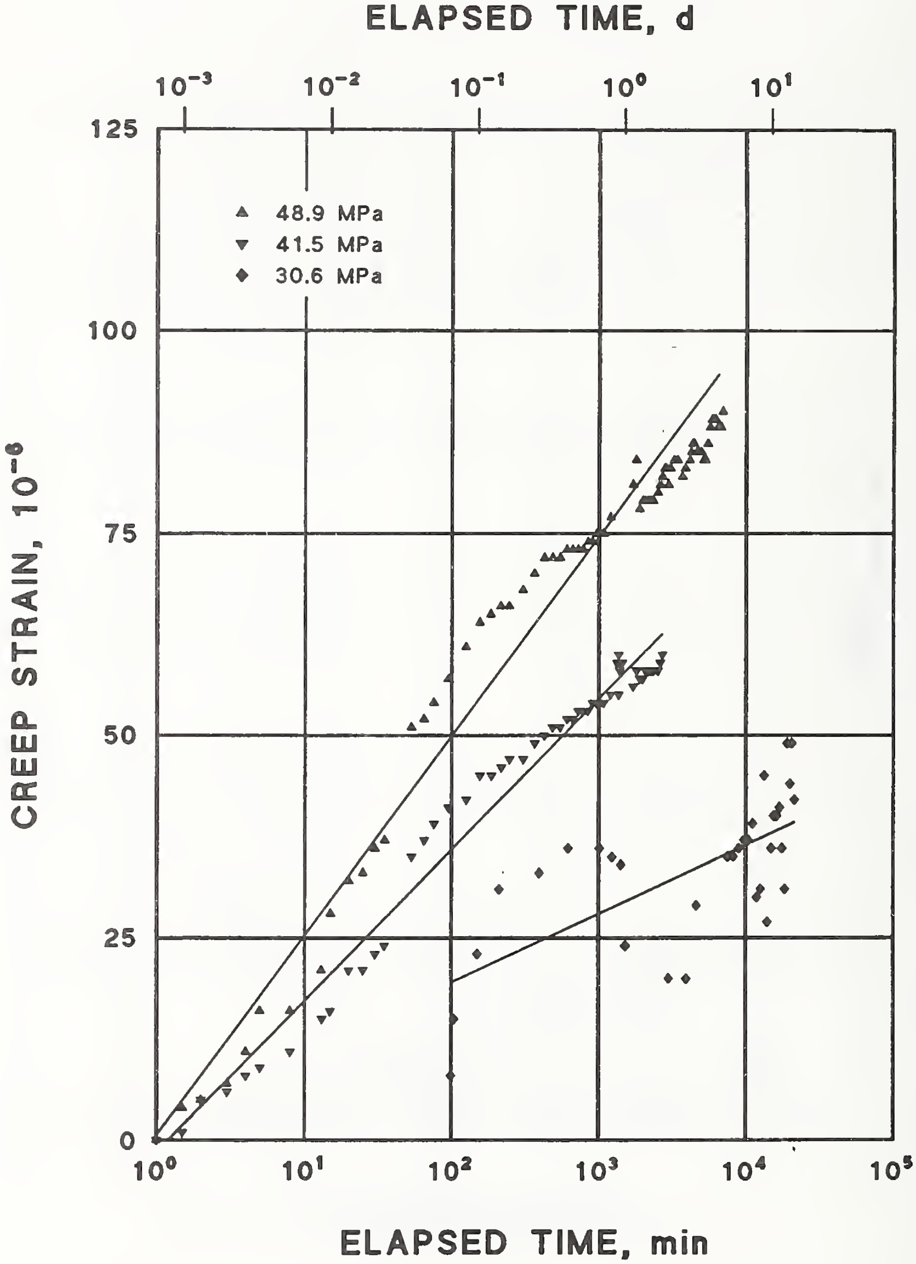

Figure 5.14. Typical creep-strain versus elapsed-time curves for four different applied stress levels, obtained at 4 K from Reference 5.2. Data are plotted on a logarithmic time scale. Some of the data at longer elapsed times exhibited fluctuations due to extraneous factors; these data are not shown here.

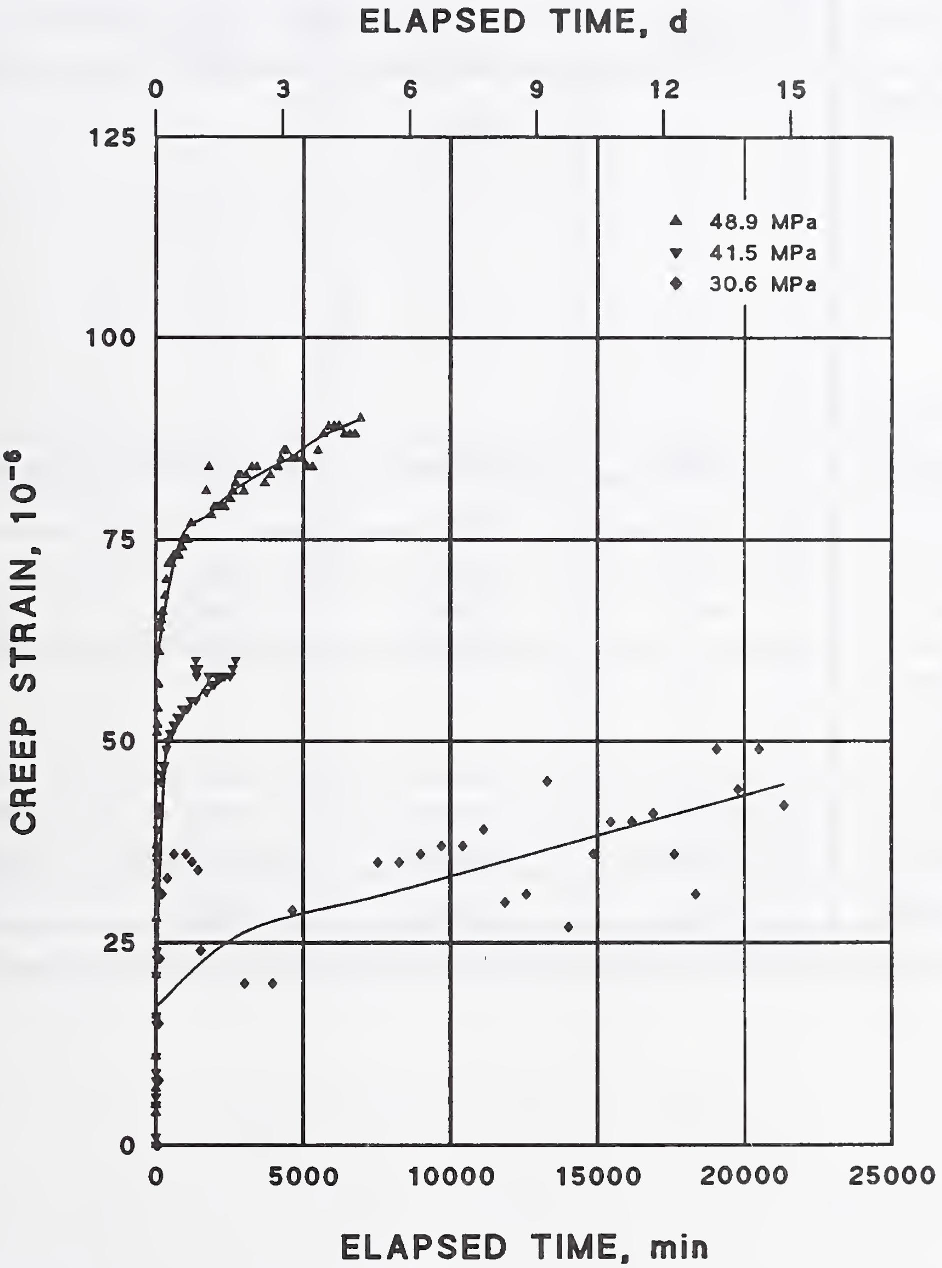

Figure 5.15. Typical creep-strain versus elapsed-time curves for four different applied stress levels, obtained at 4 K from Reference 5.2. Data are plotted on a linear time scale. Some of the data at longer elapsed times exhibited fluctuations due to extraneous factors; these data are not shown here.

Table 5.4. Characterization of Materials and Measurements.

Reference No.	1	2A	2B	3
Specification	C10100		C10400	C10200
Composition (wt%)				
Cu	—	99.99	—	—
Ag	—	—	—	—
Cu + Ag	—	—	—	—
O_2	—	—	—	—
Bi	—	—	—	—
P	—	—	—	—
Pb	—	—	—	—
S	—	—	—	—
Se	—	—	—	—
Te	—	—	—	—
Others (Only ≥ 0.001 wt%)	—	—	—	—
Material Condition	Annealed	Annealed, 923 K, 1 h	Cold-rolled, 20.7%	Cold-worked, 8%
Grain Size	—	36 μm	77	—
Hardness	—	R_B 22	R_F 80	—
Product Form	Wire	Bar, 2.0-cm-dia.	Plate, 3.2-cm-thick	Bar
Specimen Type	—	—	—	—
Width or Dia.	—	—	—	—
Thickness	—	—	—	—
Gage Length	—	—	—	—
Time Range	0.0006–1.1 h	17–1610 h	19–24 h	10000 h
Appl. Stress Range	59–372 MPa (a)	20–60 MPa	281, 241 MPa	38.6–145 MPa
Test Temperature	77, 295 K	4, 76, 295 K	76, 295 K	295 K

(a) 77-K data reported with applied stresses of 59–372 MPa; 295-K data with applied stresses of 59–177 MPa.

Table 5.4, continued

—	5	10	11
C11000	C10100	C10100	C10100
— — — — — — — — — — —	— — — — — — — — — — —	— — — — — — — — — — —	— — — — — — — — — — —
Annealed	Cold-worked, 60%	Annealed	Annealed
—	—	—	—
—	—	—	—
Wire; silver-plated	Plate	Bar	—
— — — —	— — — —	— — — —	— — — —
250–23000 h	5 h	30–200 h	1100 h
34–103 MPa	340, 284 MPa (a)	21–110 MPa	35 MPa
295 K	77, 295 K	4, 77 K	77 K

(a) Applied stress of the 77-K data is 340 MPa, whereas, at 295 K the data reported is for an applied stress of 284 MPa.

REFERENCES

1. Wyatt, O. H., "Transient Creep in Pure Metals," Proceedings of the Physical Society B66, 459–480 (1953).

2. Reed, R. P., Simon, N. J., and Walsh, R. P., "Creep of Copper: 4 to 295 K," in Advances in Cryogenic Engineering--Materials, Vol. 36B, Eds., R. P. Reed and F. R. Fickett, Plenum Press, New York, NY, 1175–1183 (1990).

   Reed, R. P., and Walsh, R. P., National Institute of Standards and Technology, Boulder, CO, private communication (1989).

3. Davis, E. A., "Creep and Relaxation of Oxygen-free Copper," Journal of Applied Mechanics 10, A-101–A-105 (1943).

4. Gohn, G. A., and Fox, A., "New Methods for Determining Stress-Relaxation," Materials Research and Standards 1, 957–967 (1961).

5. Becker, H., Montgomery, D. B., and Reed, R. P., "Wanted: Cryogenic Mechanical Property Data on Copper Alloys," Massachusetts Institute of Technology Plasma Fusion Center, Cambridge, MA, private communication (1985).

6. Bhattacharya, S., Congreve, W. K. A., and Thompson, F. C., "The Creep/Time Relationship under Constant Tensile Stress," Journal of the Institute of Metals 81, 83–92 (1952).

7. Evans, R. W., and Wilshire, B., Creep of Metals and Alloys, The Institute of Metals, London, England (1985).

8. OFHC Brand Copper: A Survey of Properties and Applications, AMAX, Inc., New York, NY (1974).

9. Schwope, A. D., Smith, K. F., and Jackson, L. R., "The Comparative Creep Properties of Several Types of Commercial Coppers," Journal of Metals 1, 409–416 (1949).

10. Yen, C., Caulfield, T., Tien, J. K., Roth, L. D., and Wells, J. M., "Cryogenic Creep of Copper," Paper 8305-030, Metals/Materials Technology Series, American Society for Metals, Metals Park, OH (1983).

    Yen, C. T., Long-term Creep of Copper ar Cryogenic Temperatures, Ph.D. Thesis, Columbia University, New York, NY (1983).

    Yen, C., Caulfield, T., Roth, L. D., Wells, J. M., and Tien, J. K., "Creep of Copper at Cryogenic Temperatures," Cryogenics 24, 371–377 (1984).

11. McDonald, L. C., and Hartwig, K. T., "1100 Hour Creep Test Results for OFHC Copper: Validation of Previously Published Results," in Advances in Cryogenic Engineering-- Materials, Vol. 38, Eds., R. P. Reed and F. R. Fickett, Plenum Press, New York, NY, in press.

DATA SOURCES AND ANALYSIS

Only measurements based upon dynamic methods were considered. (See Reference 6.1 for a comparison of measurement techniques.) These methods determine the adiabatic rather than the isothermal modulus, but this difference of a few percent at most is smaller than the errors usually associated with the static methods of measurement. Single-crystal, second-order elastic constant measurements at cryogenic temperatures were compiled and averaged in Reference 6.1. Polycrystalline moduli were derived from these data using an averaging technique described in Reference 6.1. These data were given a weight of six (corresponding to six extensive sets of cryogenic data), and combined with other polycrystalline measurements (References 6.2–6.8) in a polynomial regression analysis of Young's modulus (E) upon temperature, T.

RESULTS

The best fit to the data is given by the equation:

$$E \text{ (GPa)} = 137 - 1.27 \times 10^{-4} T^2 \qquad (6\text{-}1)$$

$$\text{(S.D.} = 2.5 \text{ GPa)},$$

where $4 \text{ K} \leq T \leq 300 \text{ K}$. The standard deviations of the two coefficients are 0.3 and 0.07×10^{-4}. These standard deviations do not reflect the actual variance of elastic constant measurements, since average values derived from a compilation of single-crystal measurements (Reference 6.1) were used in the analysis.

Table 6.1 presents the measured values of E, the values calculated from the regression equation, the temperature, and the reference number. The measured values cited under Reference 6.1 were taken from the published curve that gives the average of single-crystal data from several sources. The available characterization of materials and measurements is given in Table 6.10 at the end of the elastic properties section.

Figure 6.1 indicates the fit of the data to Equation (6-1). Figure 6.2 presents these data in summary form. The scatter bands represent two standard deviations about the curve in each figure. The variance of the data about each curve was assumed to be normally distributed and constant throughout the range of the independent variable, T.

DISCUSSION

References 6.6 and 6.9 discuss different methods of averaging single-crystal elastic constants to obtain polycrystalline elastic constants. For engineering design purposes, the Voigt-Reuss-Hill method used in Reference 6.1 is adequate. Reference 6.9 also provides a critical evaluation of room-temperature polycrystalline elastic constants. The value found for E is about 3% higher than the value given in Equation (6-1). This difference is less than twice the standard deviation of 2.5 GPa.

More elaborate mathematical expressions have been developed to represent the dependence of the elastic constants upon T (Reference 6.10). However, the differences in the fit are significant only if the coefficient of variation of the data is very small: for example, if data from one individual set of measurements are to be fitted. The simpler polynomial used here is adequate for expressing the average results of a number of measurements and meets the thermodynamic requirement that the slope be 0 at $T = 0$ K.

Figure 6.1 and Table 6.1 show that E measurements for C10400 copper (data from Reference 6.8) at 4 and 295 K are in agreement with measurements on C10100 and C10200 coppers. Reference 6.11 presents static data on E at 295 K for C10500 copper that is in close correspondence with data obtained for C10100 copper.

Reference 6.12 discusses the increase in E of C11000 copper as the annealing temperature or grain size increases, on the basis of static measurements.

Table 6.1. Young's Modulus Dependence on Temperature (4–300 K).

Young's Modulus, Measured, GPa	Young's Modulus, Predicted, GPa	Test Temperature, K	Reference No.
138	137	4	1
139	13[illegible]	4	6
139	137	5	6
139	137	20	6
143	137	23	6
134	13[illegible]	25	1
138	136	40	6
134	136	50	1
138	136	60	6
136	136	73	2
138	136	75	1
132	136	77	7
137	136	75	6
134	136	5[illegible]	2
139	135	99	4
139	135	19[illegible]	4
137	135	150	6
136	13[illegible]	103	3
132	135	110	4
133	135	191	6
132	135	11[illegible]	4
139	135	120	6
132	135	11[illegible]	4
139	135	12[illegible]	1
131	135	127	4
139	134	140	6
131	134	11[illegible]	4
132	134	149	2
131	134	150	4
131	13[illegible]	154	7
131	133	158	2
13[illegible]	133	19[illegible]	6
131	133	158	2
130	133	166	4
133	133	175	4
130	13[illegible]	175	1
133	133	180	6
12[illegible]	132	12[illegible]	1
128	132	190	4
132	132	191	2
132	132	200	4
132	132	220	6
128	132	201	4
129	13[illegible]	211	2
128	131	211	1
127	130	220	1
13[illegible]	130	220	6
133	130	22[illegible]	3
131	130	225	1
127	130	229	4
128	130	234	2

Table 6.1, continued

Young's Modulus, Measured, GPa	Young's Modulus, Predicted, GPa	Test Temperature, K	Reference No.
126	130	236	4
130	129	240	6
126	126	245	4
130	129	295	1
127	127	260	2
129	129	295	1
130	126	260	6
125	127	295	1
124	127	273	2
124	127	273	1
126	127	245	4
129	127	295	6
124	127	260	4
123	126	295	1
126	126	260	2
130	126	293	3
126	126	236	4
131	126	295	6
128	126	295	6
123	126	295	8
127	125	300	1

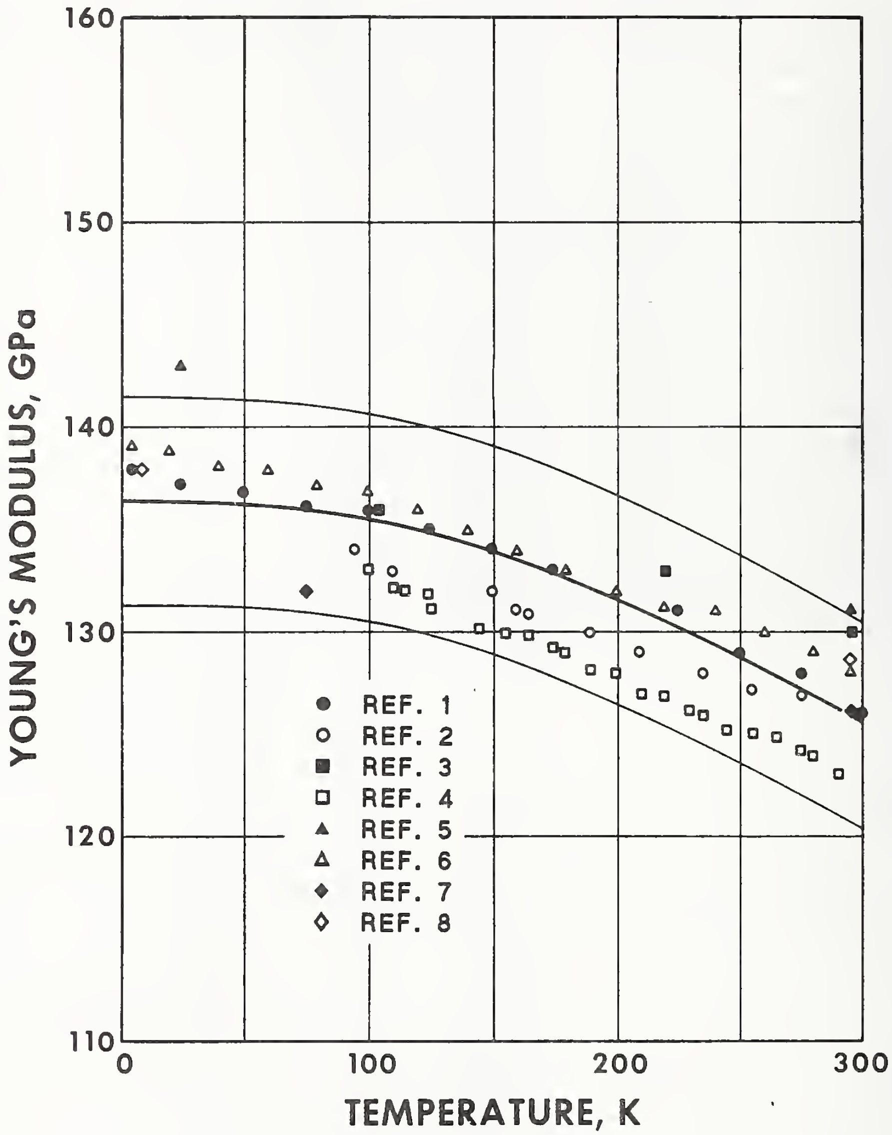

Figure 6.1. The data shown were used to compute the regression of Young's modulus upon temperature [Equation (6-1)]. For clarity, overlapping data points are omitted from the figure. All data are presented in Table 6.1. Reference 6.1 refers to an average based upon six extensive sets of single-crystal measurements; these data were correspondingly weighted in the analysis that determined the curve shown in this figure.

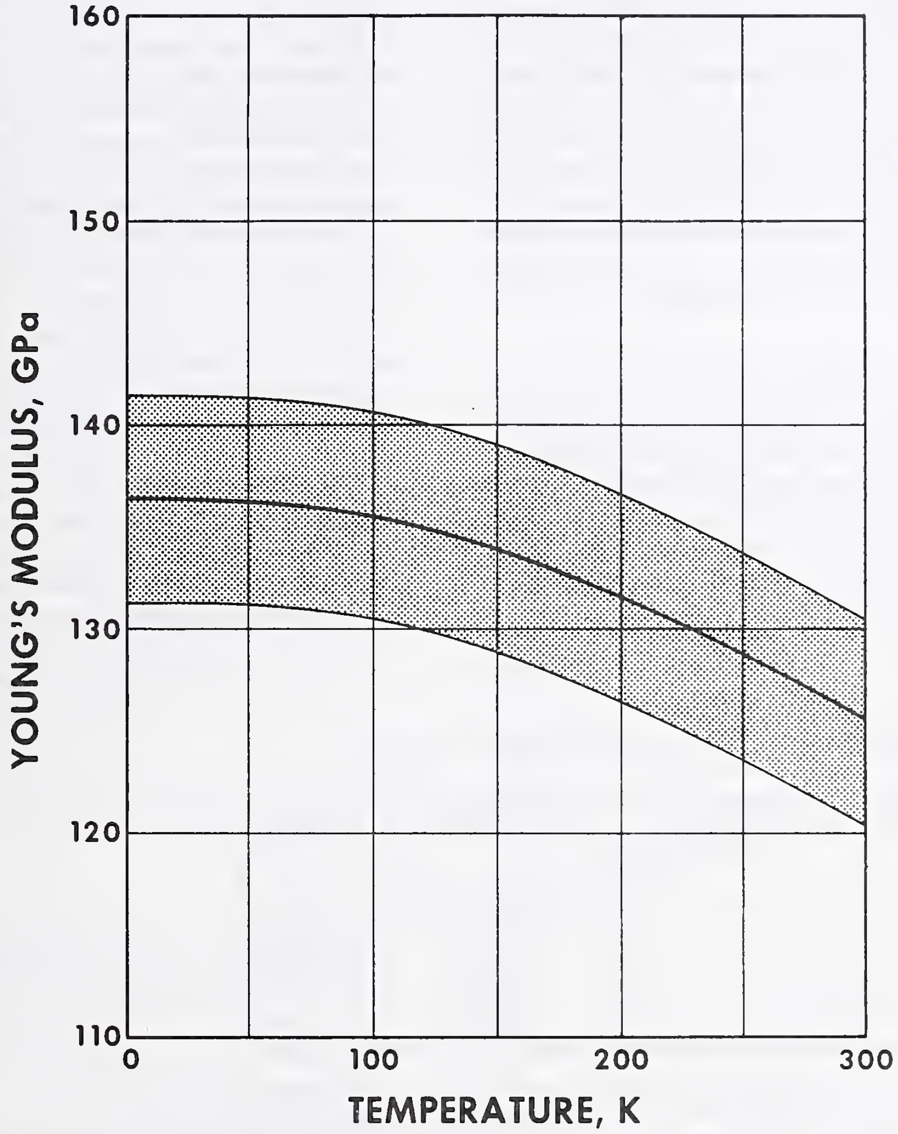

Figure 6.2. Dependence of Young's modulus upon temperature; 4–300 K. The scatter band represents two standard deviations about a second-order regression equation based upon dynamic measurements on polycrystalline copper and an averaged curve derived from several measurements of single-crystal elastic constants (Reference 6.1). The regression equation is

$$E \text{ (GPa)} = 137 - 1.27 \times 10^{-4}\, T^2 \qquad \text{where } 4\text{ K} \le T \le 300\text{ K.}$$

DATA SOURCES AND ANALYSIS

Measurements based upon dynamic methods were compiled for copper that was cold-worked at room temperature. (See Reference 6.1 for a comparison of the accuracy of static and dynamic measurement techniques.) Reference 6.13 presents room-temperature data on the decrease in Young's modulus ($\Delta E/E$); Reference 6.8 presents data at room temperature and 4 K. In contrast to the case where both cold work, *CW*, and measurements are carried out at 77 K, relatively few data are available. The measurements are summarized in Table 6.2 below.

DISCUSSION

The results of Reference 6.13 at 295 K indicate a greater effect of *CW* upon Young's modulus, *E*, than the data presented in Reference 6.8. The larger effect probably results from the short time period that elapsed before the measurements of Reference 6.13 were made, which did not allow much recovery from cold-working.

Results at 295 K of Reference 6.12 are also in apparent disagreement with those of Reference 6.8. An initial decrease was observed in *E* with small amounts of *CW*, less than 10% strain in tension. However, as strain was increased to higher levels, an increase in *E* was observed, with the sign of the effect becoming positive at strains around 20 to 30%, comparable to the amount of *CW* reported in Reference 6.8. This change in direction of the effect was also reported in References 6.14 and 6.15 for *CW* at 77 K (see Figure 6.5), but the extent of *CW* was not as large as that reported in References 6.8 and 6.12. Different types of *CW* may change the microstructure of the material in different ways. Also, the measurements of Reference 6.12 were made by static, rather than by dynamic methods, and the material was C11000 copper, with 0.037 wt% O_2.

Reference 6.8 gives a brief discussion and presents additional references on the theoretical explanations of the decrease in modulus with *CW*.

References 6.16 and 6.17 present data at 295 K on the variation in *E* with orientation after 95 and 75% reduction by cold-rolling.

Table 6.2. Change in Young's Modulus with 295-K Cold Work.

-ΔE/E, %	Cold Work, %	Test Temperature, K	Copper Number	Reference
9.9	1	295	C10100 or C10200	13
3.9*	21**	295	C10400	8
3.9*	21**	4	C10400	8
6.2*	37**	295	C10400	8
5.8*	37**	4	C10400	8

* Average of measurements made in the rolling direction and the two orthogonal directions. The change in Young's modulus is obtained by comparison of these results with measurements on annealed C10400 copper.

** Total amount of cold work not available; % cold work estimated from hardness measurements and standard tables of temper designation.

DATA SOURCES AND ANALYSIS

Measurements based upon dynamic methods were compiled. (See Reference 6.1 for a comparison of the accuracy of static and dynamic measurement techniques.) Data were obtained from References 6.14 and 6.15 on the percent decrease in Young's modulus ($\Delta E/E$) measured at about 77 K without warmup after cold work had been done at or near 77 K. All specimens were polycrystalline. Regression analysis was carried out to determine the dependence of $\Delta E/E$ upon cold work, *CW*.

RESULTS

Although $\Delta E/E = 0$ for $CW = 0$, the magnitude of $\Delta E/E$ increases very rapidly with very small amounts of *CW*. To allow the use of simple polynomial expressions, a constant term was included in the analysis, and the range of the equation restricted as indicated below. A third-order equation gave the best fit to the data, but introduced a non-physical inflection point at about 15% *CW*. Consequently, $\Delta E/E$ was set equal to a constant between 15 and 17% *CW* in the following expression.

$$\Delta E/E\ (\%) = -8.60 - 1.94\ CW + 2.63 \times 10^{-1}(CW)^2 - 8.56 \times 10^{-3}\ (CW)^3 \qquad 0.3\% \le CW < 15\%$$

$$= -7.40 \qquad 15\% \le CW \le 17\% \qquad (6\text{-}2)$$

The standard deviation of the fit is 1.01%; the standard devlations of the four coefficients are 0.64, 0.39, 0.59×10^{-1}, and 2.40×10^{-3}.

Table 6.3 presents the measured values of $\Delta E/E$ ratio, the values calculated from the regression equation, the temperature, and the reference number. The available characterization of materials and measurements is given Table 6.10 at the end of the elastic properties section. Figure 6.3 indicates the fit of the data to Equation (6-2). The scatter bands represent two standard deviations about the curve in this figure. The variance of the data about the curve was assumed to be normally distributed and constant throughout the range of the independent variable, *CW*.

DISCUSSION

Studies of recovery of $\Delta E/E$ at hlgher temperatures after *CW* at 77 K indicated that very little recovery takes place until the temperature Is raised to 120–140 K (References 6.14 and 6.15). However, Reference 6.18 reports observable recovery of Young's modulus starting at about 100 K after *CW* at 4 K.

Theoretical explanations for the large decrease in modulus for relatively small amounts of *CW* are presented in References 6.14, 6.15, and 6.18–6.21.

The measurements reported above were carried out on copper of 99.999% purity. Reference 6.15 also presents data on dilute Cu-Au alloys of 99.97% purity that show approximately a 30% decrease in the effect of a given amount of *CW* on the modulus.

Table 6.3. Change in Young's Modulus with 77-K Cold Work (77 K).

−ΔE/E, Measured, %	−ΔE/E, Predicted, %	Cold Work, %	Reference No.
7.7	9.2	0.3	15
7.9	9.5	0.5	14
10.4	10.3	1.0	14
12.9	10.4	1.1	15
10.8	11.1	1.8	14
13.1	11.1	1.9	15
11.4	11.6	2.1	14

Table 6.3, continued

−ΔE/E, Measured, %	−ΔE/E, Predicted, %	Cold Work, %	Reference No.
13.0	11.9	2.5	15
11.8	12.2	2.8	14
12.3	12.3	3.1	15
12.3	12.7	7.6	14
12.3	12.2	4.4	15
12.5	12.7	5.0	14
13.0	12.2	5.8	15
12.5	12.6	6.2	14
11.2	12.2	4.4	15
12.5	11.9	7.6	14
12.3	11.9	8.5	14
12.5	11.9	7.6	15
9.7	10.1	10.2	15
9.1	9.0	11.7	15
8.8	8.0	13.4	15
7.7	7.4	15.0	15
6.9	7.4	16.6	15

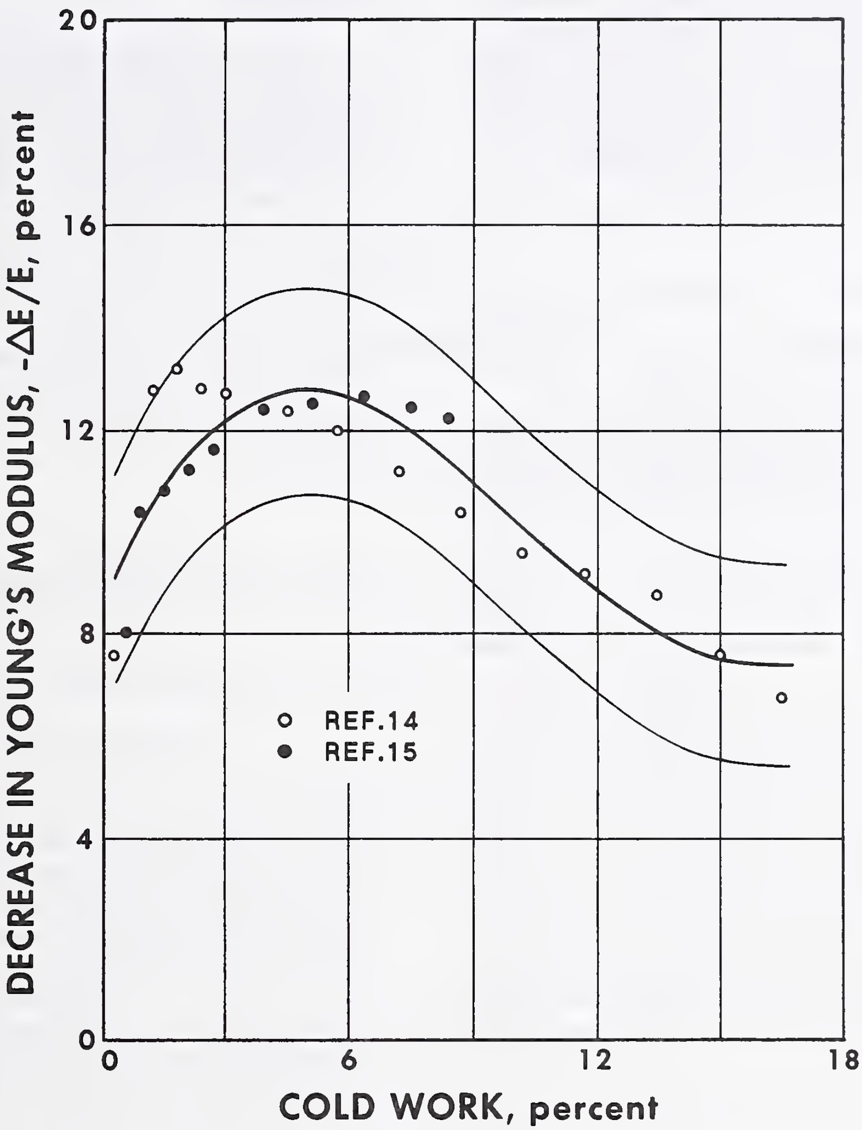

Figure 6.3. The data shown were used to compute the regression of the percent decrease in Young's modulus with cold work at 77 K [Equation (6-2)]. For clarity, overlapping data points are omitted from the figure. All data are presented in Table 6.3.

DATA SOURCES AND ANALYSIS

Only measurements based upon dynamic methods were considered. (See Reference 6.1 for a comparison of the accuracy of static and dynamic measurement techniques.) One measurement of the change in Young's modulus ($\Delta E/E$) after cold work at 4 K was located, and is given in Table 6.4 below. This result was calculated from the resonant frequencies presented in Reference 6.18 assuming no dimensional changes took place upon deformation. Since the authors state that the specimen geometry was not constant, the result should be considered as an approximation.

DISCUSSION

Reference 6.18 also presents measurements of $\Delta E/E$ after recovery at temperatures of 100 K and higher. A small increase of the modulus (< 2%) occurred after a 16-h anneal at 100 K.

Table 6.4. Change in Young's Modulus with 4-K Cold Work.

$-\Delta E/E$, %	Cold Work, %	Test Temperature, K	Copper Number	Reference No.
13%	3%	4	C10100	18

DATA SOURCES AND ANALYSIS

Only measurements based upon dynamic methods were considered. (See Reference 6.1 for a comparison of measurement techniques.) These methods determine the adiabatic rather than the isothermal modulus, but this difference of a few percent at most is smaller than the errors usually associated with the static methods of measurement. Single-crystal, second-order elastic constant measurements at cryogenic temperatures were compiled and averaged in Reference 6.1. Polycrystalline moduli were derived from these data using an averaging technique described in Reference 6.1. These data were given a weight of six (corresponding to six extensive sets of cryogenic data), and combined with other polycrystalline measurements (References 6.6, 6.7, and 6.8) in a polynomial regression analysis of the shear modulus (*G*) upon temperature, *T*.

RESULTS

The best fit to the data is given by the equation:

$$G\ (\text{GPa}) = 51.2 - 4.63 \times 10^{-5}\ T^2 \qquad (6\text{-}3)$$

$$(\text{S.D.} = 0.5\ \text{GPa}),$$

where $4\ \text{K} \leq T \leq 300\ \text{K}$. The standard deviations of the two coefficients are 0.1 and 0.18×10^{-5}. These standard deviations do not reflect the actual variance of elastic constant measurements, since average values derived from a compilation of single-crystal measurements (Reference 6.1) were used in the analysis.

Table 6.5 presents the measured values of *G*, the values calculated from the regression equation, the temperature, and the reference number. The measured values cited under Reference 6.1 were taken from the published curve that gives the average of single-crystal data from several sources. The available characterization of materials and measurements is given In Table 6.10 at the end of the elastic properties section. Figure 6.4 indicates the fit of the data to Equation (6-3). Figure 6.5 presents these data in summary form. The scatter bands represent two standard deviations about the curve in each figure. The variance of the data about each curve was assumed to be normally distributed and constant throughout the range of the independent variable, *T*.

DISCUSSION

References 6.6 and 6.9 discuss different methods of averaging single-crystal elastic constants to obtain polycrystalline elastic constants. For engineering design purposes, the Voigt-Reuss-Hill method used in Reference 6.1 is adequate. Reference 6.8 also provides a critical evaluation of room-temperature polycrystalline elastic constants. These results agree with Equation (6-3) within the uncertainty represented by the standard deviation.

More elaborate mathematical expressions have been developed to represent the dependence of the elastic constants upon *T* (Reference 6.10). However, the differences in the fit are significant only if the coefficient of variation of the data is very small: for example, if data from one individual set of measurements are to be fitted. The simpler polynomial used here is adequate for expressing the average results of a number of measurements and meets the thermodynamic requirement that the slope be 0 at $T = 0$ K.

Table 6.5. Shear Modulus Dependence on Temperature (4–300 K).

Shear Modulus, Measured, GPa	Shear Modulus, Predicted, GPa	Test Temperature, K	Reference No.
51.5	51.2	4	1
52.5	51.2	4	8
51.7	51.2	5	6

Table 6.5, continued

Shear Modulus, Measured, GPa	Shear Modulus, Predicted, GPa	Test Temperature, K	Reference No.
51.4	51.2	20	6
51.4	51.2	[illegible]	1
50.5	51.2	40	6
51.3	51.1	[illegible]	1
51.4	51.1	60	6
51.4	51.2	75	1
50.2	51.2	77	7
50.2	50.9	80	6
50.4	50.3	100	1
50.9	50.8	100	6
50.5	50.6	[illegible]	6
50.2	[illegible]	125	1
50.2	50.3	[illegible]	6
50.9	50.2	[illegible]	1
49.9	50.1	160	6
49.6	49.8	175	1
49.5	49.7	180	6
49.1	[illegible]	200	1
49.2	49.4	200	6
48.9	49.0	[illegible]	6
48.7	48.9	[illegible]	7
48.5	48.9	[illegible]	6
48.2	48.3	[illegible]	7
48.2	48.1	260	6
47.8	47.7	275	1
47.9	47.6	280	6
47.6	47.2	295	6
48.3	47.2	295	8
47.2	47.1	298	7
47.3	47.1	300	1

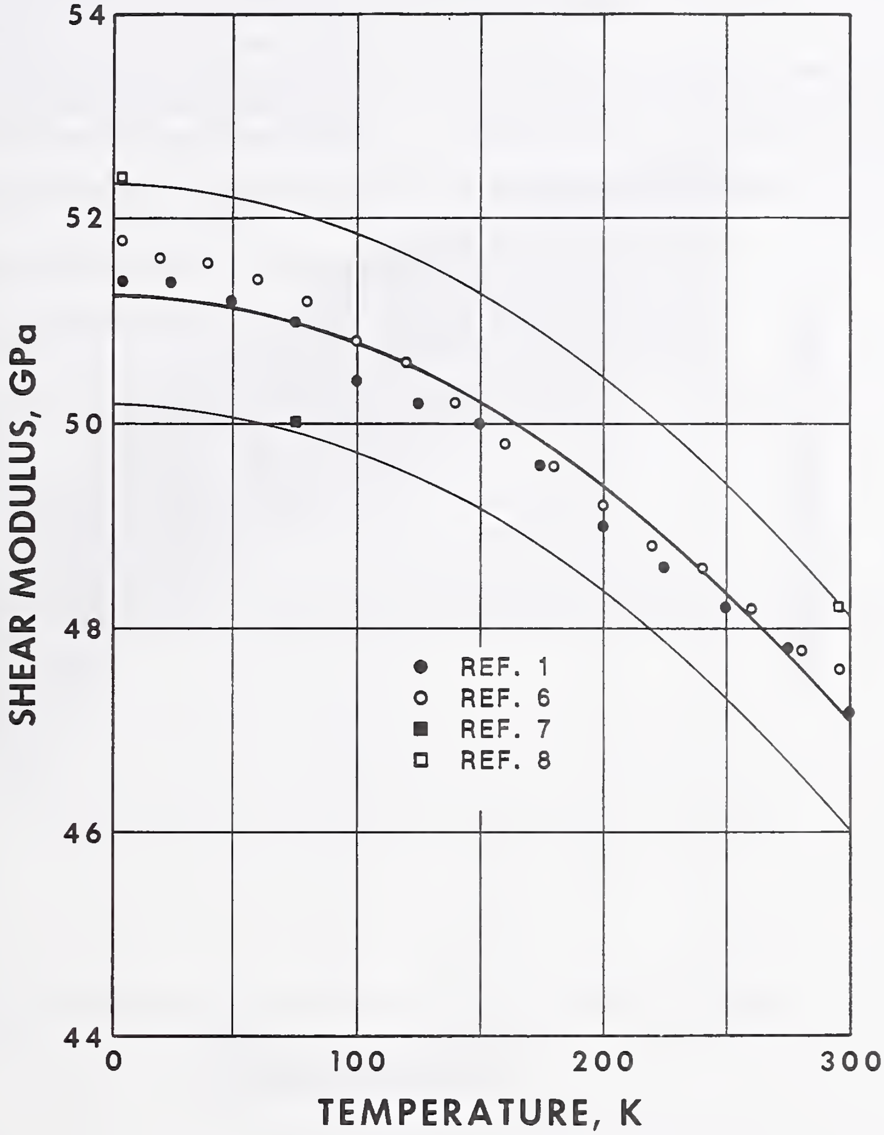

Figure 6.4. The data shown were used to compute the regression of the shear modulus upon temperature [Equation (6-3)]. All data are presented in Table 6.5. Reference 6.1 refers to an average based upon six extensive sets of single-crystal measurements; these data were correspondingly weighted in the analysis that determined the curve shown in this figure.

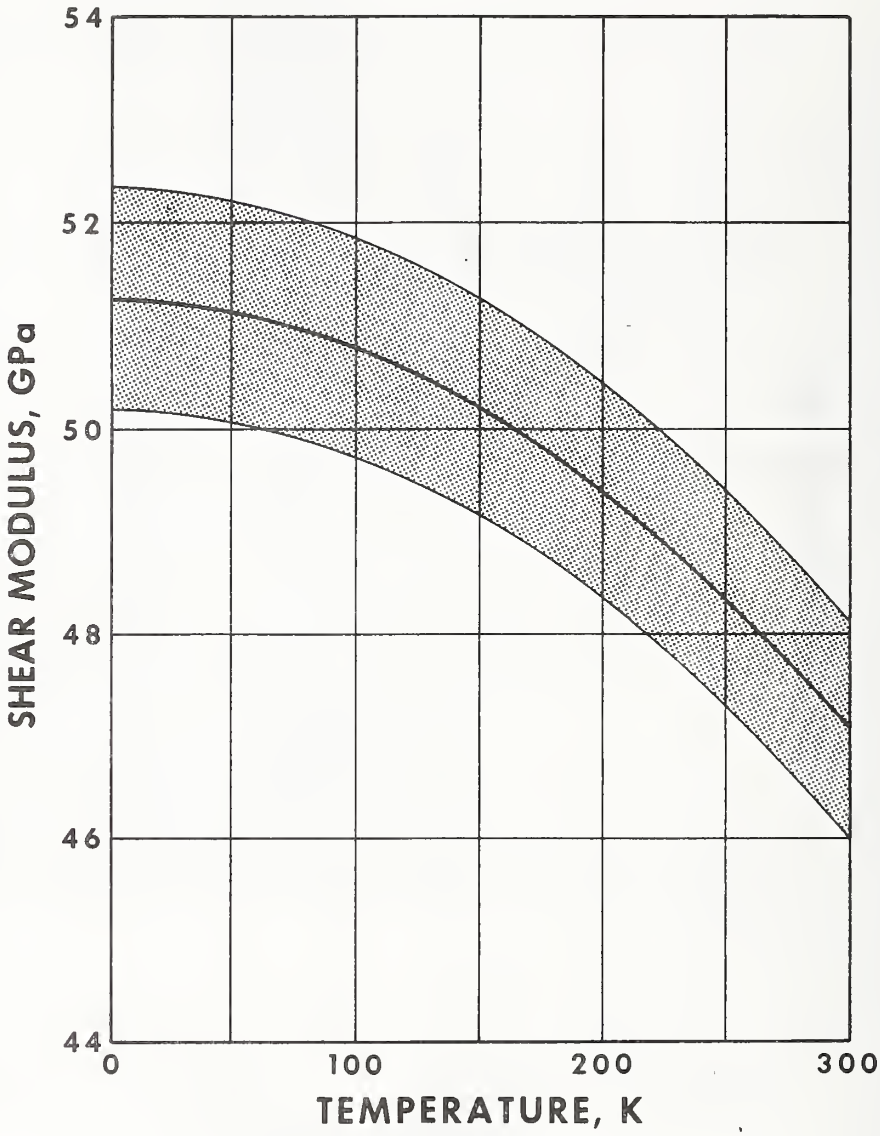

Figure 6.5. Dependence of the shear modulus upon temperature; 4–300 K. The scatter band represents two standard deviations about a second-order regression equation based upon dynamic measurements on polycrystalline copper and an averaged curve derived from several measurements of single-crystal elastic constants (Reference 6.1). The regression equation is

$$G \text{ (GPa)} = 51.2 - 4.63 \times 10^{-5} T^2 \qquad \text{where } 4 \text{ K} \leq T \leq 300 \text{ K.}$$

C10400: Cold-worked at 295 K

Change in Shear Modulus vs. Cold Work (4, 295 K)

DATA SOURCES AND ANALYSIS

Only measurements based upon dynamic methods were considered. (See Reference 6.1 for a comparison of the accuracy of static and dynamic measurement techniques.) Reference 6.8 presents data on the change of shear modulus ($\Delta G/G$) on C10400 copper that had been cold-worked at 295 K and allowed to recover for some months before measurements were made of the shear modulus. The change in shear modulus is obtained by comparison of these results with measurements on annealed C10400 copper. These results are summarized in Table 6.6 below.

DISCUSSION

Reference 6.8 gives a brief discussion and presents additional references on the theoretical explanations of the decrease in modulus.

Table 6.6. Change in Shear Modulus with 295-K Cold Work.

$-\Delta G/G$, %	Cold Work, %	Test Temperature, K	Copper Number	Reference No.
1.3*	21**	295	C10400	8
1.4*	21**	4	C10400	8
2.9*	37**	295	C10400	8
3.1*	37**	4	C10400	8

* Average of measurements made in the rolling direction and the two orthogonal directions.

** Total amount of cold work not available; % cold work estimated from hardness measurements and standard tables of temper designation.

DATA SOURCES AND ANALYSIS

Measurements based upon dynamic methods were compiled. (See Reference 6.1 for a comparison of the accuracy of static and dynamic measurement accuracy.) Data were obtained from References 6.15, and 6.19–6.21 on the percent decrease in the shear modulus ($\Delta G/G$) measured at about 77 K without warmup after cold work, *CW*, had been done at or near 77 K. All specimens were polycrystalline. Regression analysis was carried out to determine the dependence of $\Delta G/G$ upon *CW*.

RESULTS

Although $\Delta G/G = 0$ for $CW = 0$, the magnitude of $\Delta G/G$ increases very rapidly with very small amounts of *CW*. To permit the use of simple polynomial expressions, a constant term was included in the analysis, and the range of the equation restricted as indicated below. A third-order equation gave the best fit to the data, but introduced a non-physical inflection point at about 15% *CW*. Consequently, $\Delta G/G$ was set equal to a constant value between 15 and 17% *CW* in the following equation:

$$\begin{aligned} \Delta G/G(\%) &= -16.3 - 2.65\ CW \\ &\quad + 3.00 \times 10^{-1}(CW)^2 \\ &\quad - 9.42 \times 10^{-3}(CW)^3 \qquad 0.03\% \le CW < 15\% \\ &= -20.2 \qquad 15\% \le CW < 17\% \end{aligned} \tag{6-4}$$

The standard deviation of the fit is 1.3%; the standard deviations of the four coefficients are 0.5, 0.3, 0.54×10^{-1}, and 2.23×10^{-3}.

Table 6.7 presents the measured values of $\Delta G/G$, the values calculated from the regression equation, the temperature, and the reference number. The available characterization of materials and measurements is given in Table 6.10 at the end of the elastic properties section. Figure 6.6 indicates the fit of the data to Equation (6-4). The scatter bands represent two standard deviations about the curve in this figure. The variance of the data about the curve was assumed to be normally distributed and constant throughout the range of the independent variable, *CW*.

DISCUSSION

Studies of recovery of $\Delta G/G$ at higher temperatures after *CW* at 77 K indicated that very little recovery takes place until the temperature is raised to 120–140 K (References 6.15 and 6.19).

Theoretical explanations of the large decrease in modulus for relatively small amounts of *CW* are given in References 6.8, 6.13–6.15, and 6.18–6.21.

The measurements reported in References 6.15, 6.20, and 6.21 were carried out on copper of 99.999% purity. However, Reference 6.19 gives data on copper of lesser purity (99.9%) that indicates a comparable effect of *CW* on the shear modulus. References 6.15 and 6.21 indicate some decrease in the magnitude of the effect if small additions (~0.03 at% of Au) are made to the high-purity copper.

Table 6.7. Change in the Shear Modulus with 77-K Cold Work (77 K).

−ΔG/G, Measured, %	−ΔG/G, Predicted, %	Test Temperature, K	Reference No.
12.8	16.4	0.03	19
17.7	16.6	0.10	19
17.9	16.9	0.25	19
14.2	17.3	0.40	15
17.7	17.4	0.45	19
20.5	17.7	0.57	20

Table 6.7, continued

−ΔG/G, Measured, %	−ΔG/G, Predicted, %	Test Temperature, K	Reference No.
18.0	18.3	1.10	15
17.3	18.1	0.72	19
18.[illegible]	18.3	0.9[illegible]	2[illegible]
17.3	18.1	1.00	21
20.5	18.3	1.10	15
18.1	18.9	1.[illegible]0	15
21.0	19.6	1.50	15
21.7	20.5	2.00	15
20.3	20.5	[illegible].90	21
22.[illegible]	21.3	2.60	15
2[illegible].5	22.7	3.30	15
23.4	22.7	1.00	15
22.1	22.7	[illegible].90	21
23.2	23.4	0.72	15
23.2	23.4	6.60	15
22.7	23.4	6.00	21
23.1	23.4	6.05	15
22.8	23.4	6.90	15
2[illegible].5	23.2	7.75	15
22.7	23.4	6.00	21
22.1	22.7	8.90	15
22.7	22.2	12.00	21
21.4	21.7	10.90	15
21.9	21.1	12.00	21
21.1	20.9	12.40	15
21.6	20.4	14.00	21
20.4	20.2	15.00	15
21.4	20.2	16.00	21
19.4	20.2	17.20	15

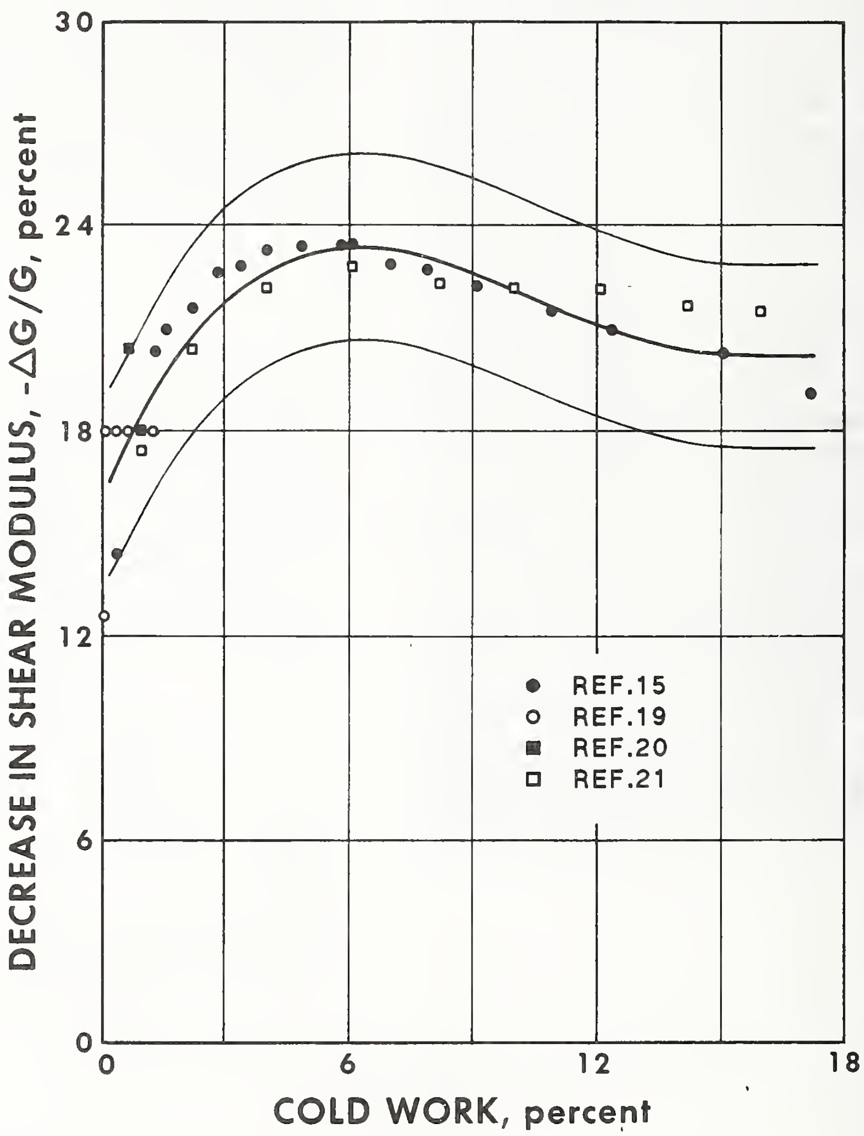

Figure 6.6. The data shown were used to compute the regression of the percent decrease in shear modulus with cold work at 77 K [Equation (6-4)]. For clarity, overlapping data points are omitted from the figure. All data are presented in Table 6.7.

DATA SOURCES AND ANALYSIS

Only measurements based upon dynamic methods were considered. (See Reference 6.1 for a comparison of measurement techniques.) These methods determine the adiabatic rather than the isothermal modulus, but this difference of a few percent at most is smaller than the errors usually associated with the static methods of measurement. Single-crystal, second-order elastic constant measurements at cryogenic temperatures were compiled and averaged in Reference 6.1. Polycrystalline moduli were derived from these data using an averaging technique described in Reference 6.1. These data were given a weight of six (corresponding to six extensive sets of cryogenic data), and combined with other polycrystalline measurements (References 6.6 and 6.7) in a polynomial regression analysis of the bulk modulus (*B*) upon temperature, *T*.

RESULTS

The best fit to the data is given by the equation:

$$B \text{ (GPa)} = 142 - 5.70 \times 10^{-5} T^2 \qquad (6\text{-}5)$$
$$(\text{S.D.} = 2 \text{ GPa}),$$

where $4 \text{ K} \leq T \leq 300 \text{ K}$. The standard deviations of the two coefficients are 0.4 and 0.96×10^{-5}. These standard deviations do not reflect the actual variance of elastic constant measurements, since average values derived from a compilation of single-crystal measurements (Reference 6.1) were uses in the analysis.

Table 6.8 presents the measured values of *B*, the values calculated from the regression equation, the temperature, and the reference number. The measured values cited under Reference 6.1 were taken from the published curve that gives the average of single-crystal data from several sources. The available characterization of materials and measurements is given in Table 6.10 at the end of the elastic properties section. Figure 6.7 indicates the fit of the data to Equation (6-5). Figure 6.8 presents these data in summary form. The scatter bands represent two standard deviations about the curve in each figure. The variance of the data about each curve was assumed to be normally distributed and constant throughout the range of the independent variable, *T*.

DISCUSSION

References 6.6 and 6.8 discuss different methods of averaging single-crystal elastic constants to obtain polycrystalline elastic constants. For engineering design purposes, the Voigt-Reuss-Hill method used in Reference 6.1 is adequate. Reference 6.9 also provides a critical evaluation of room-temperature polycrystalline elastic constants. These results agree with Equation (6-5) within the uncertainty represented by the standard deviation.

More elaborate mathematical expressions have been developed to represent the dependence of the elastic constants upon *T* (Reference 6.10). However, the differences in the fit are significant only if the coefficient of variation of the data is very small: for example, if data from one individual set of measurements are to be fitted. The simpler polynomial used here is adequate for expressing the average results of a number of measurements and meets the thermodynamic requirement that the slope be 0 at $T = 0$ K.

Table 6.8. Bulk Modulus Dependence on Temperature (4–300 K).

Bulk Modulus, Measured, GPa	Bulk Modulus, Predicted, GPa	Test Temperature, K	Reference No.
1.42	1.42	4	1
1.44	1.42	5	6
1.44	1.42	20	6
1.42	1.42	25	1

Table 6.8, continued

Bulk Modulus, Measured, GPa	Bulk Modulus, Predicted, GPa	Test Temperature, K	Reference No.
1.44	1.42	40	6
1.42	1.42	50	1
1.44	1.42	60	6
1.41	1.42	75	1
1.32	1.42	77	7
1.44	1.42	80	6
1.41	1.42	100	1
1.44	1.42	100	6
1.43	1.41	120	6
1.41	1.41	125	1
1.43	1.41	140	6
1.40	1.41	150	1
1.43	1.41	160	6
1.40	1.40	175	1
1.42	1.40	180	6
1.39	1.40	200	1
1.42	1.40	200	6
1.41	1.39	220	6
1.39	1.39	225	1
1.41	1.39	240	6
1.38	1.39	250	1
1.41	1.38	260	6
1.38	1.38	275	1
1.40	1.38	280	6
1.40	1.37	295	6
1.32	1.37	298	7
1.37	1.37	300	1

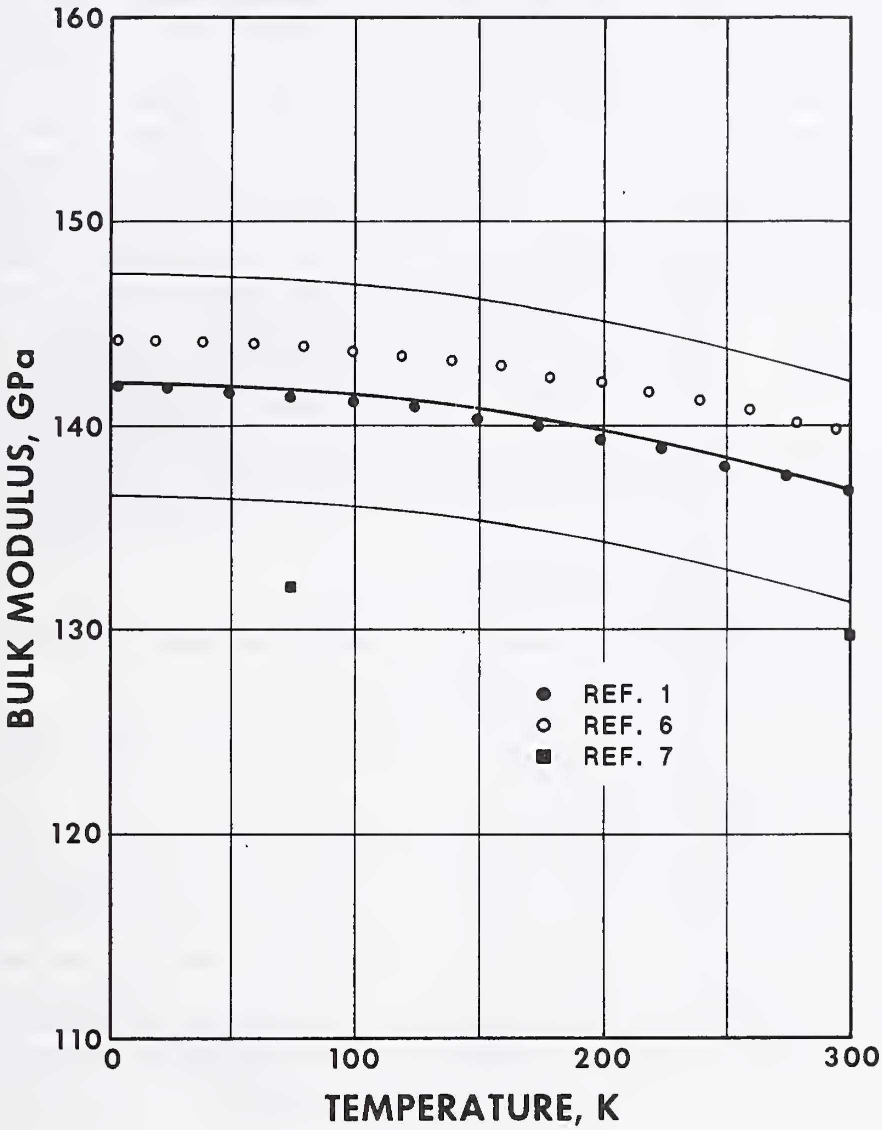

Figure 6.7. The data shown were used to compute the regression of the bulk modulus upon temperature [Equation (6-5)]. For clarity, overlapping data points are omitted from the figure. All data are presented in Table 6.8. Reference 6.1 refers to an average based upon six extensive sets of single-crystal measurements; these data were correspondingly weighted in the analysis that determined the curve shown in this figure.

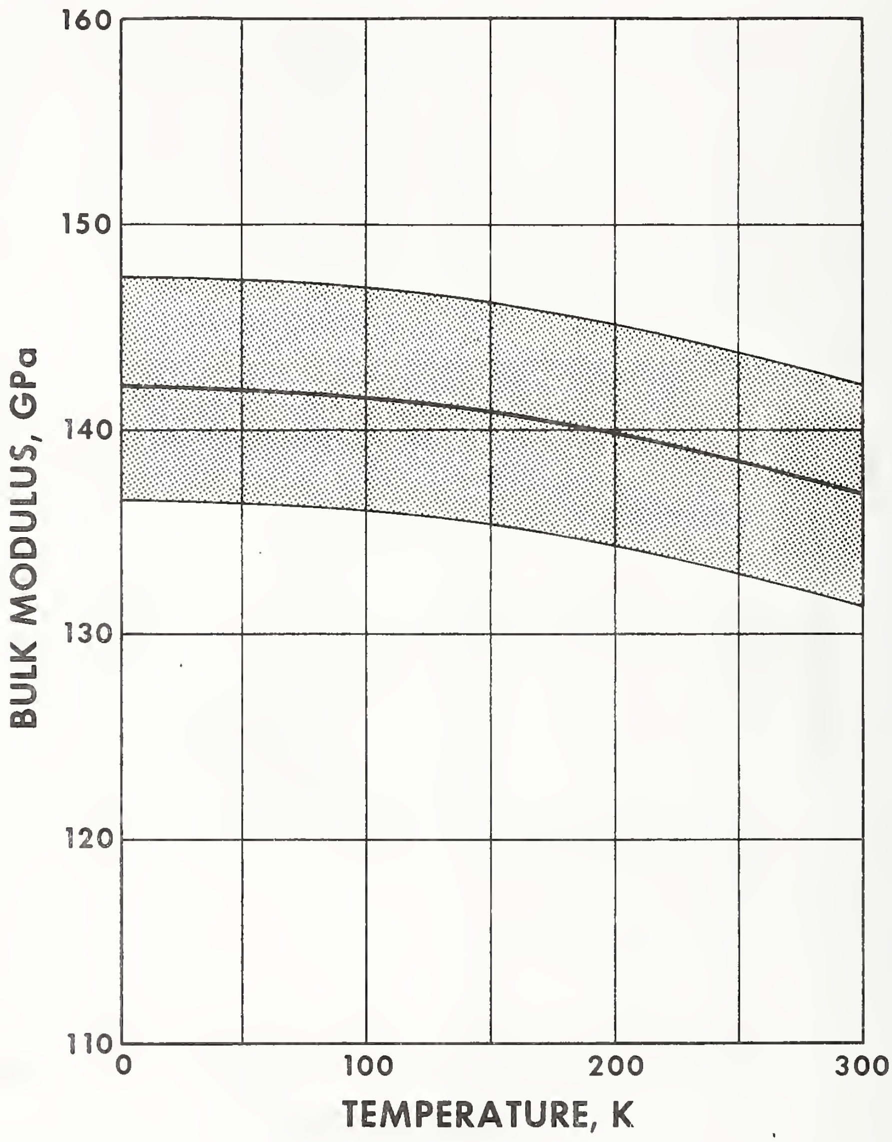

Figure 6.8. Dependence of the bulk modulus upon temperature; 4–300 K. The scatter band represents two standard deviations about a second-order regression equation based upon dynamic measurements on polycrystalline copper and an averaged curve derived from several measurements of single-crystal elastic constants (Reference 6.1). The regression equation is

$$B \text{ (GPa)} = 142 - 5.63 \times 10^{-5}\, T^2 \qquad \text{where } 4\text{ K} \le T \le 300\text{ K}.$$

DATA SOURCES AND ANALYSIS

Only measurements based upon dynamic methods were considered. (See Reference 6.1 for a comparison of measurement techniques.) These methods determine the adiabatic rather than the isothermal modulus, but this difference of a few percent at most is smaller than the errors usually associated with the static methods of measurement. Single-crystal, second-order elastic constant measurements at cryogenic temperatures were compiled and averaged in Reference 6.1. The polycrystalline Poisson's ratios were derived from these data using an averaging technique described in Reference 6.1. These data were given a weight of six (corresponding to six extensive sets of cryogenic data), and combined with other polycrystalline measurements (References 6.6, 6.7, and 6.8) in a polynomial regression analysis of Poisson's ratio (ν) upon temperature, T.

RESULTS

The best fit to the data is given by the equation:

$$\nu = 0.339 + 7.03 \times 10^{-8} T^2 \qquad (6\text{-}6)$$
$$(\text{S.D.} = 0.002),$$

where $4\ \text{K} \le T \le 300\ \text{K}$. The standard deviations of the two coefficients are 0.0003 and 0.60×10^{-8}. These standard deviations do not reflect the actual variance of elastic constant measurements, since average values derived from a compilation of single-crystal measurements (Reference 6.1) were used in the analysis.

Table 5.9 presents the measured values of ν, the values calculated from the regression equation, the temperature, and the reference number. The measured values cited under Reference 6.1 were taken from the published curve that gives the average of single-crystal data from several sources. The available characterization of materials and measurements is given in Table 6.10 at the end of the elastic properties section. Figure 6.9 indicates the fit of the data to Equation (6-6). Figure 6.10 presents these data in summary form. The scatter bands represent two standard deviations about the curve in each figure. The variance of the data about each curve was assumed to be normally distributed and constant throughout the range of the independent variable, T.

DISCUSSION

References 6.6 and 6.9 discuss different methods of averaging single-crystal elastic constants to obtain polycrystalline elastic constants. For engineering design purposes, the Voigt-Reuss-Hill method used in Reference 6.1 is adequate. Reference 6.8 also provides a critical evaluation of room-temperature polycrystalline elastic constants. These results agree with Equation (6-6) within the uncertainty represented by the standard deviation.

More elaborate mathematical expressions have been developed to represent the dependence of the elastic constants upon T (Reference 6.10). However, the differences in the fit are significant only if the coefficient of variation of the data is very small: for example, if data from one individual set of measurements are to be fitted. The simpler polynomial used here is adequate for expressing the average results of a number of measurements and meets the thermodynamic requirement that the slope be 0 at T = 0 K.

Table 6.9. Poisson's Ratio Dependence on Temperature (4–300 K).

Poisson's Ratio, Measured	Poisson's Ratio, Predicted	Test Temperature, K	Reference No.
0.339	0.339	4	1
0.340	0.339	4	8
0.340	0.339	5	6
0.340	0.339	20	6

Table 6.9, continued

Poisson's Ratio, Measured	Poisson's Ratio, Predicted	Test Temperature, K	Reference No.
0.339	0.339	25	1
0.340	0.340	40	6
0.339	0.340	50	1
0.341	0.340	60	6
0.339	0.340	75	1
0.336	0.340	77	7
0.341	0.340	80	6
0.340	0.340	100	1
0.342	0.340	100	6
0.342	0.340	120	6
0.340	0.340	125	1
0.343	0.341	140	6
0.341	0.341	150	1
0.343	0.341	160	6
0.341	0.342	175	1
0.344	0.342	180	6
0.342	0.342	200	1
0.345	0.342	200	6
0.345	0.343	260	6
0.343	0.343	225	1
0.341	0.343	240	7
0.346	0.343	240	6
0.344	0.344	250	1
0.346	0.344	260	6
0.344	0.345	275	1
0.347	0.345	280	6
0.347	0.346	295	6
0.345	0.346	295	8
0.342	0.346	298	7
0.345	0.346	300	1

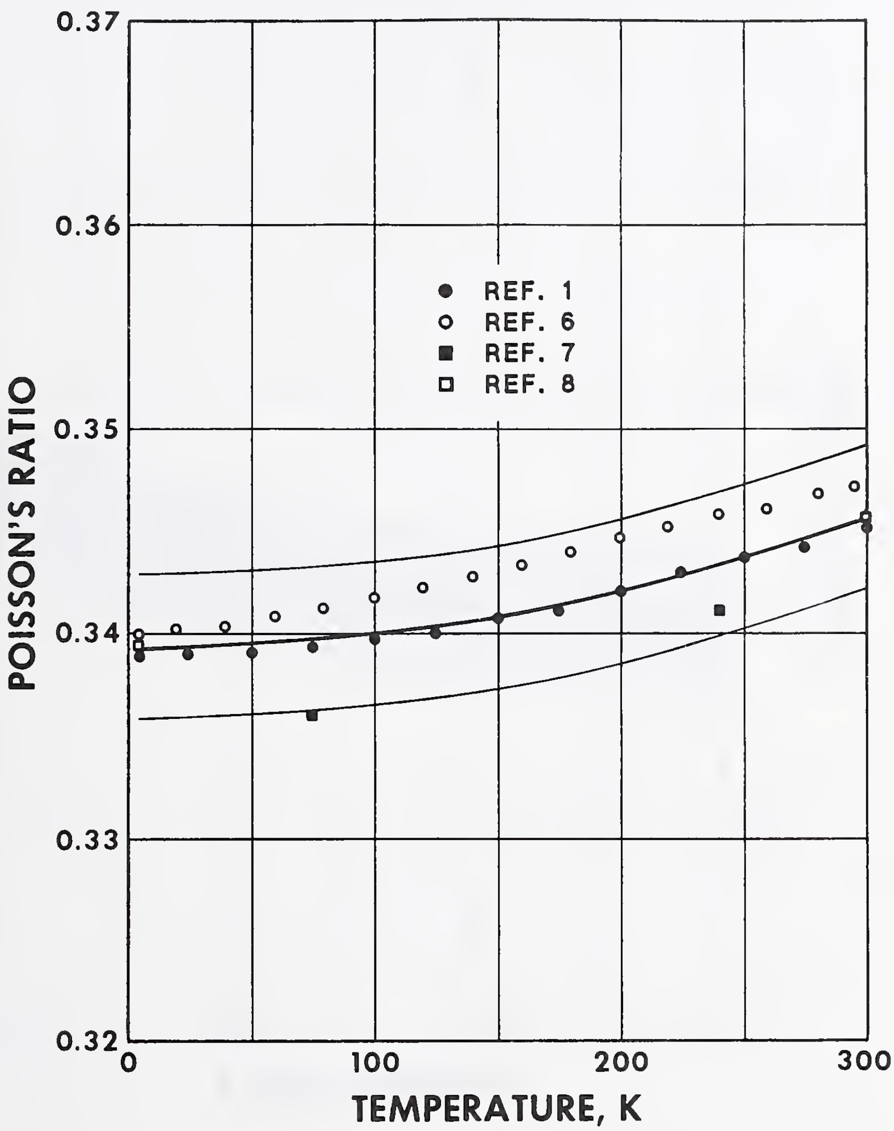

Figure 6.9. The data shown were used to compute the regression of Poisson's ratio upon temperature [Equation (6-6)]. All data are presented in Table 6.9. Reference 6.1 refers to an average based upon six extensive sets of single-crystal measurements; these data were correspondingly weighted in the analysis that determined the curve shown in this figure.

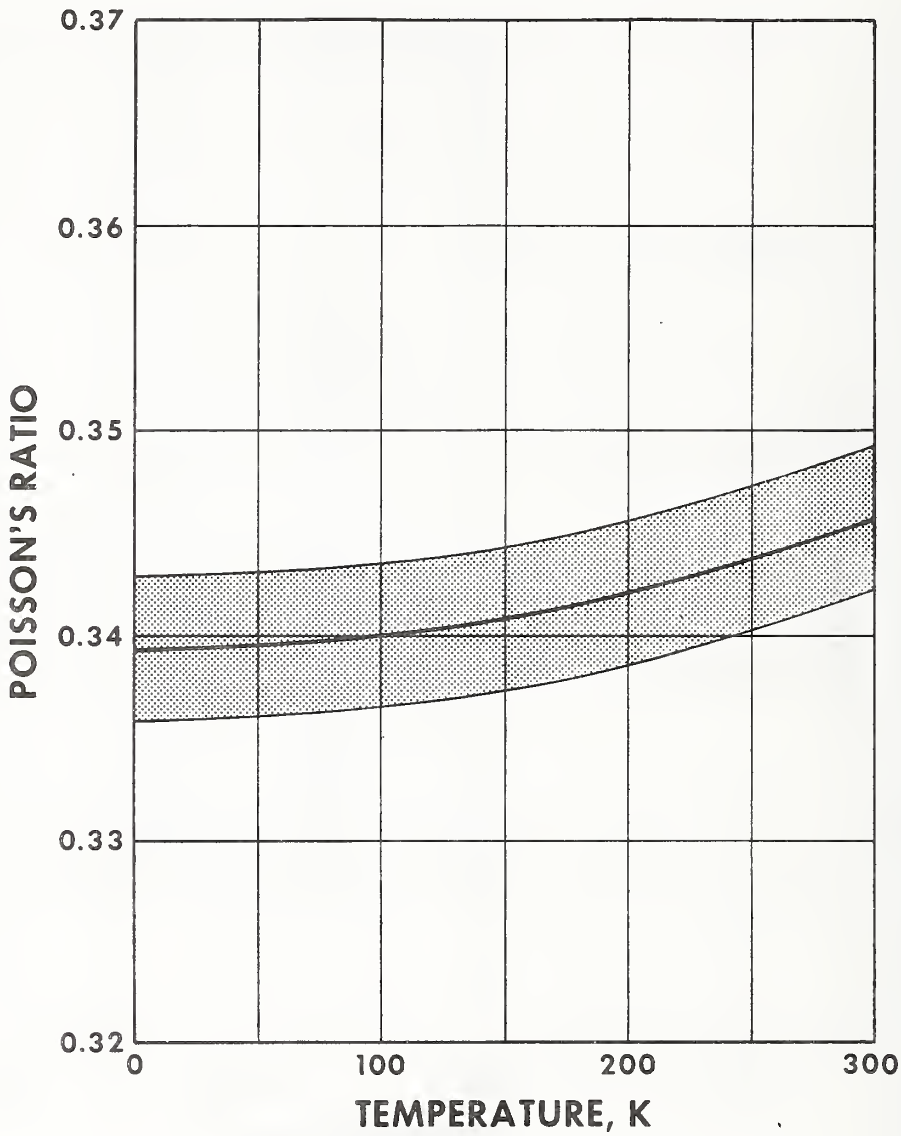

Figure 6.10. Dependence of Poisson's ratio upon temperature; 4–300 K. The scatter band represents two standard deviations about a second-order regression equation based upon dynamic measurements on polycrystalline copper and an averaged curve derived from several measurements of single-crystal elastic constants (Reference 6.1). The regression equation is

$$\nu = 0.339 + 7.03 \times 10^{-8} T^2 \qquad \text{where } 4\ \text{K} \leq T \leq 300\ \text{K}.$$

Table 6.10. Characterization of Materials and Measurements.

Reference No.	2	—	4	5
Specification	C10200	C10100	C10200	C10200
Composition (wt%)				
Cu	—	—	99.98	—
Ag	—	—	—	—
Cu + Ag	—	—	—	—
O_2	—	—	—	—
Bi	—	—	—	—
P	—	—	—	—
Pb	—	—	—	—
S	—	—	—	—
Se	—	—	—	—
Te	—	—	—	—
Others (Only ≥ 0.001 wt%)	—	—	—	—
Material Condition	—	Annealed, 1073 K	Annealed	Annealed, 423 K, 10 h
RRR	2	—	—	—
Grain Size	—	—	—	—
Hardness	—	—	—	—
Product Form	—	—	—	—
Specimen Type	Strip	—	Cylinder	Rod
Width or Dia.	1.2 cm	—	0.07 cm	1.26 cm
Thickness	0.13 cm	—	—	—
Length	10 cm	—	14 cm	6.9 cm
No. of Measurements	—	—	—	—
Test Temperature	73–773 K	103–1223 K	99–470 K	4.5, 295 K

C10100–C10400: Annealed; Cold-worked | *Elastic Constants (All)*

6	7	8	13	14
C10100	—	C10400	C10200 (c)	C10100
— — 99.99 — — — — — — — —	— — — — — — — — — — —	99.95 — — — — — — — — — —	99.984 0.002 — 0.0045 0.0004 — 0.001 — not detected not detected Fe: 0.0028	99.999 — — — — — — — — — —
Annealed	—	Annealed, 783 K, 1 h (b)	Annealed, 773 K, 3 h, vacuum (d)	Annealed, 823 K, 1.5 h, vacuum (g)
—	—	8	—	—
60 μm	7	8	60 μm (e)	—
DPHN 45 (a)	—	R_F 53, 80, 88	—	—
Rod	—	Plate	Sheet (f), 0.6-cm-thick	Sheet, 0.1-cm-thick
Prismatic 1.3 cm 1.3 cm 1.9 cm	— — — —	— — — —	Bar 0.6 cm 0.6 cm 15 cm	Strip 1.0 cm 0.1 cm 6.5 cm
—	—	—	—	—
5–295 K	78–644 K	4, 295 K	292 K	83 K

(a) 1 kg load.
(b) Measurements were also made on the as received cold-rolled plate and on a plate given a further 60% reduction.
(c) Some measurements made on C10100 copper.
(d) Subsequently extended by 1%.
(e) Reported for one specimen only.
(f) Some measurements made on bar stock.
(g) Specimens cold-worked at 83 K in tension for test measurements.

Table 6.10, continued

Reference No.	15	18	19	20
Specification	C10100	C10100	C10200	C10100
Composition (wt%)				
Cu	99.999	—	99.9	99.999
Ag	—	—	—	—
Cu + Ag	—	—	—	—
O_2	—	—	—	—
Bi	—	—	—	—
P	—	—	—	—
Pb	—	—	—	—
S	—	—	—	—
Se	—	—	—	—
Te	—	—	—	—
Others (Only ≥ 0.001 wt%)	—	—	—	—
Material Condition	Annealed, 723 K, 1.5 h, vacuum (a)	Annealed, 973 K, 4 h, vacuum (b)	Annealed, 823 K, 1.5 h, vacuum (c)	—
RRR	—	—	123	—
Grain Size	—	1000 μm	—	—
Hardness	—	—	—	—
Product Form	—	—	Wire	—
Specimen Type	Bar	Bar	Wire	Bar
Width or Dia.	0.15 cm	0.1 cm	0.15 cm	0.15 cm
Thickness	—	1 cm	—	—
Length	3.5 cm	8 cm	5.0 cm	3.5 cm
No. of Measurements	—	—	—	—
Test Temperature	77 K	4 K	83 K	77 K

(a) Specimens cold-worked at 77 K in tension or torsion for test measurements.
(b) Subsequent tensile deformation of 3%.
(c) Specimens deformed by torsion at 83 K for test measurements.

21
C10100
99.999 — — — — — — — — — —
—
—
—
—
—
Bar 0.15 cm — 3.0 cm
3 sets per curve
78 K

REFERENCES

1. Ledbetter, H. M., and Naimon, E. R., "Elastic Properties of Metals and Alloys. II. Copper," Journal of Physical and Chemical Reference Data 3, 897–935 (1974).

2. Stokes, H. J., "Apparatus for the Measurement of Young's Modulus, Between −200 and 700 °C by Transverse Vibration in Vacuum," Journal of Scientific Instruments 37, 117–120 (1960).

3. Köster, W., "Die Temperaturabhängigkeit des Elastizitätsmoduls reiner Metalle," Zeitschrift für Metallkunde 39, 1–9 (1948).

4. Biller, E., and Helow, R., "Über die Temperaturabhängigkeit des komplexen Elastizitätsmoduls von Kupfer," Zeitschrift für Physik 224, 102–112 (1969).

5. Bordoni, P. G., "Elastic and Anelastic Behavior of Some Metals at Very Low Temperatures," Journal of the Acoustical Society of America 26, 495–502 (1954).

6. Ledbetter, H. M., "Elastic Constants of Polycrystalline Copper at Low Temperatures, Relationship to Single-Crystal Elastic Constants," Physica Status Solidi (a) 66, 477–484 (1981).

7. Frederick, J. R., "A Study of the Elastic Properties of Various Solids by Means of Ultrasonic Pulse Techniques," Thesis, University of Michigan (1947).

8. Ledbetter, H. M., and Kim, S. A., "Low-Temperature Elastic Constants of Deformed Polycrystalline Copper," in Materials Studies for Magnetic Fusion Energy Applications at Low Temperatures--X, Ed. R. P. Reed, NBSIR 87-3067, Fracture and Deformation Division, National Bureau of Standards, Boulder, CO, 139–150 (1987).

   Ledbetter, H. M., and Kim, S. A., "Low-Temperature Elastic Constants of Deformed Polycrystalline Copper," Materials Science and Engineering A 101, 87–92 (1988).

9. Ledbetter, H. M., "Sound Velocities and Elastic-Constant Averaging for Polycrystalline Copper," Journal of Physics D: Applied Physics 13, 1879–1884 (1980).

10. Varshni, Y. P., "Temperature Dependence of the Elastic Constants," Physical Review B 2, 3952–3958 (1970).

11. Jackson, L. R., Hall, A. M., and Schwope, A. D., "The Comparative Properties of Several Types of Commercial Coppers, as Cold Worked and as Recrystallized," Transactions of the American Institute of Mining and Metallurgical Engineers 179, 1–10 (1947).

12. Soliman, M. R., Youssef, T. H., and Essawi, R. A., "Effect of Annealing and Cold-working on Young's Modulus of Electrolytic Copper," Indian Journal of Physics 45, 77–82 (1971).

13. Smith, A. D. N., "The Effect of Small Amounts of Cold-Work on Young's Modulus of Copper," Philosophical Magazine 44, 453–466 (1953).

REFERENCES

14. Lems, W., "The Change of Young's Modulus of Copper and Silver after Deformation at Low Temperature and its Recovery," Physica 28, 445–452 (1962).

Lems, W., "Young's Modulus of some Metals after Deformation at Low Temperature and its Recovery," Physica 30, 445-458 (1964).

15. Brouwer, A. J., and Groenenboom-Eygelaar, C., "The Elastic Constants of Polycrystalline Cu after Plastic Deformations at 77 °K," Acta Metallurgica 15, 1597–1602 (1967).

16. Alers, G. A., and Liu, Y. C., "The Nature of Transition Textures in Copper," Transactions of the Metallurgical Society of American Institute of Mechanical Engineers 239, 210–216 (1967).

17. Bunge, H. J., Ebert, R., and Günther, F., "On the Angular Variation and Texture Dependence of Young's Modulus in Cold-rolled Copper Sheet," Physica Status Solidi 31, 565–569 (1969).

18. Bruner, L. J., and Mecs, B. M., "Modulus and Damping of Copper after Plastic Deformation at 4.2 °K," Physical Review 129, 1525–1532 (1963).

19. Druyvesteyn, M. J., Schannen, O. F. Z., and Swaving, E. C. J., "Influence of Cold Work on the Rigidity of Copper," Physica 25, 1271–1274 (1959).

20. Collet, M. G., "The Irreversible Amplitude Dependence of Plastically Deformed Polycrystalline Cu," Physica 34, 246–250 (1967).

21. van den Beukel, A., and Brouwer, C., "The Influence of Impurities on the Modulus Effect of Cold Worked Copper," Physica 17, 453–460 (1968).

DATA SOURCES AND ANALYSIS

Because copper has been used as a calorimetry standard, a large amount of specific heat data for copper exists in the literature. A total of 456 measurements from 4 to 300 K on annealed and cold-worked copper were obtained from References 7.1–7.13. (A compilation, Reference 7.14, was used as a source of some of the data reported before 1971.) Since previous work has indicated that the differences in heat capacity (C_p) between annealed high-purity (99.999%) and commercial-grade cold-worked copper are small (Reference 7.1), all of the data sets were combined in the regression analysis. See the discussion below for information on the specific heat of severely cold-worked copper below 4.2 K.

A logarithmic transformation was used to permit representation of the temperature dependence of C_p from 4 to 300 K with a small number of coefficients (five). A 14-coefficient polynomial representation of data from 30 to 300 K on high-purity degassed and annealed copper is also presented in Table 7.1. The latter equation was obtained from Reference 7.15 and is expected to apply to Research Material RM 5 available from the Office of Standard Reference Data, National Bureau of Standards, Gaithersburg, MD. The expected accuracy of the representation is indicated in the table.

Small discontinuities or lack of smoothness in the copper C_p vs. temperature, T, relationship have also been used to evaluate temperature scales (References 7.3 and 7.15). For the present purposes, the small differences between the temperature scales used for the various measurements have been ignored. If specific heat data are used to calculate entropy changes between two temperatures, the specific heat at constant volume, C_v, must be used. For copper, this correction is small (< 0.05%) below 90 K, but it rises to almost 3% at room temperature (see Reference 7.16 for useful formulas, and References 7.17 and 7.18 for measurements of $C_p - C_v$ for copper from 77 to 800 K).

RESULTS

The best fit to the data was obtained with the equation

$$\log C_p = +1.131 - 9.454 (\log T) + 12.99 (\log T)^2 - 5.501 (\log T)^3 + 0.7637 (\log T)^4, \tag{7-1}$$

where C_p has units of J/(kg·K) and $4\ K \leq T \leq 300\ K$. The (logarithmic) standard deviation of the fit of this equation to the data is 0.023. The standard deviations of the five coefficients are 0.080, 0.212, 0.26, 0.114, and 0.0180. The linear standard deviation of the fit of the C_p data to this equation is 5.32 J/(kg·K). This standard deviation indicates an uncertainty of about 2% above 100 K, comparable to the observed scatter of the various sets of measurements. (At low temperatures, where the magnitude of C_p decreases, the difference between the predicted value and the measurement value is, of course, much lower than the average value of 5.32 (J/(kg·K).) Below 100 K, this difference is often 5 to 20% of the measure value, comparable to the scatter between various sets of measurements.

Table 7.2 presents the temperature, the measured values of C_p, the values calculated from the regression equation, and the reference number. Since results on different specimens were similar, not all data presented in References 7.1 and 7.2 were reported in Table 7.2 and used in the analysis. The available characterization of materials and measurements is given in Table 7.8 at the end of the thermal properties section. Figure 7.1 shows the fit of the data to Equation (7-1). Figure 7.2 presents these results in summary form. The scatter bands represent two standard deviations about the curve in each figure. The variance of the data was assumed to be normally distributed and constant throughout the range of the independent variable, log T. (The center curve representing Equation (7-1) was omitted from Figure 7.1 to permit a clear presentation of the data points.)

Because Equation (7-1) is in logarithmic form, a set of calculated values of C_p for $4\ K \leq T \leq 300\ K$ is presented in Table 7.3.

DISCUSSION

The specific heat of copper that is moderately cold-worked (at room temperature) is increased only slightly above that of annealed copper. The differences are of the order of 0.2% (Reference 7.1). However, data for high-purity copper severely deformed (at room temperature) by a reduction in thickness of about 96% showed an increase in C_p of up to 2% (Reference 7.19).

These measurements were carried out only in the temperature range of 1.5 to 4.2 K. Small amounts of magnetic impurities also can have a significant effect on C_p in this temperature range (see references cited in Reference 7.19). The earlier work by Giaque (Reference 7.12) that shows a decrease in C_p after moderate cold work (at room temperature) is apparently in error (see the discussion in Reference 7.1). These data were not used in the present analysis.

Table 7.1. Coefficients for C_p(J/kg·K) = $\Sigma A_N T^N$, 30 ≤ T ≤ 300 K (Reference 7.15).

$A_0 = -2.023343468 \times 10^{1}$	$A_7 = +4.831975381 \times 10^{-10}$
$A_1 = +4.876730516$	$A_8 = -2.233341060 \times 10^{-12}$
$A_2 = -4.602942501 \times 10^{-1}$	$A_9 = +7.171999996 \times 10^{-15}$
$A_3 = +2.232376993 \times 10^{-2}$	$A_{10} = -1.557097446 \times 10^{-17}$
$A_4 = -5.304015312 \times 10^{-4}$	$A_{11} = +2.156752094 \times 10^{-20}$
$A_5 = +7.642771699 \times 10^{-6}$	$A_{12} = -1.690896981 \times 10^{-23}$
$A_6 = +7.312456301 \times 10^{-8}$	$A_{13} = +5.534827423 \times 10^{-27}$

The scatter of the fitted data is generally within 0.2 percent above 100 K, within 0.5 percent in the 50 to 100 K range and within 2 percent in the 30 to 50 K range.

Table 7.2. Specific Heat Dependence upon Temperature (4–300 K).

Test Temperature, K	Specific Heat, Measured, J/(kg·K)	Specific Heat, Predicted, J/(kg·K)	Reference No.
4.00	0.092	0.112	9
4.00	0.092	0.112	8
4.00	0.151	0.112	8
4.60	0.197	0.115	2B
4.63	0.135	0.114	8
4.11	0.106	0.115	8
4.20	0.135	0.117	13
4.26	0.197	0.115	8
4.63	0.135	0.135	8
4.40	0.115	0.124	8
4.63	0.135	0.135	8
4.60	0.124	0.197	8
4.63	0.135	0.133	8
4.60	0.092	0.135	8
4.70	0.137	0.135	8
4.60	0.112	0.140	8
4.63	0.151	0.145	8
5.00	0.197	0.115	7
5.00	0.149	0.149	9

C10100–C10200: Annealed; Cold-worked

Specific Heat vs. Temperature (4–300 K)

Table 7.2, continued

Test Temperature, K	Specific Heat, Measured, J/(kg•K)	Specific Heat, Predicted, J/(kg•K)	Reference No.
5.00	0.188	0.149	8
6.00	0.130	0.149	13
5.00	0.746	0.188	8
6.00	0.151	0.151	2A
5.00	0.188	0.309	8
6.19	0.151	0.190	6
5.00	0.190	0.158	2B
5.20	0.369	0.190	6
9.46	0.188	0.172	8
6.19	0.212	0.190	6
5.60	0.253	0.222	8
7.90	0.233	0.206	6
5.00	0.222	0.214	8
6.00	0.190	0.214	13
5.00	0.222	0.214	8
6.00	0.231	0.206	2B
6.10	0.253	0.222	8
6.19	0.246	0.229	2A
9.46	0.277	0.248	8
6.00	0.233	0.262	6
7.60	0.253	0.267	8
6.19	0.309	0.296	6
5.90	0.309	0.253	8
7.00	0.309	0.309	2B
7.00	0.336	0.309	8
7.00	0.309	0.309	13
7.00	0.334	0.309	3
7.00	0.309	0.332	6
7.21	0.369	0.309	2B
7.60	0.130	0.369	6
5.00	0.477	0.442	8
7.00	0.130	0.442	13
5.00	0.188	0.442	8
6.19	0.511	0.198	6
8.39	0.538	0.656	2B
8.40	0.540	0.606	2A
5.60	0.656	0.804	8
7.90	0.686	0.622	6
5.00	0.656	0.622	8
6.00	0.606	0.622	13
5.00	0.656	0.622	8
6.19	0.686	0.653	2A
6.10	0.656	0.653	8
6.00	0.752	0.686	6
9.46	0.746	0.721	2B
7.80	0.686	0.804	6
10.00	0.656	0.309	7
10.00	0.884	0.190	8
10.00	0.810	0.855	13
10.00	0.872	0.855	3
10.10	0.892	0.878	2A

C10100–C10200: Annealed; Cold-worked

Specific Heat vs. Temperature (4–300 K)

Table 7.2, continued

Test Temperature, K	Specific Heat, Measured, J/(kg·K)	Specific Heat, Predicted, J/(kg·K)	Reference No.
10.80	0.946	0.943	6
10.40	1.020	5.150	3
10.60	1.070	1.030	6
10.70	1.040	1.040	2A
11.00	1.180	1.150	6
18.00	1.840	4.190	3
11.20	1.240	1.830	6
11.50	1.360	1.330	6
12.00	1.480	1.520	6
12.00	1.470	1.520	3
18.00	1.480	1.540	2A
12.80	1.650	1.570	6
12.20	1.680	1.600	6
10.40	1.610	1.670	2B
12.90	1.350	1.520	6
18.00	1.870	1.970	3
13.40	2.190	2.740	6
10.70	2.650	2.330	3
14.00	2.350	2.500	6
10.70	2.340	2.890	3
14.80	2.230	2.640	6
18.80	2.890	2.670	2B
14.40	2.560	2.740	2A
18.80	2.650	2.650	6
14.80	0.946	2.580	12
10.70	2.890	3.910	12
18.00	2.770	3.130	7
18.00	2.890	3.130	3
15.10	3.140	3.210	6
15.30	3.150	3.340	3
15.40	1.180	3.380	11
18.00	1.840	3.860	3
14.00	3.540	3.860	6
16.10	3.350	3.910	3
16.20	3.810	1.520	6
16.40	3.860	4.190	2A
14.00	4.290	4.690	6
17.10	4.480	4.780	6
17.30	4.290	4.960	6
17.40	4.710	5.050	11
11.80	4.740	5.280	12
18.00	5.150	5.640	3
18.00	5.160	5.640	3
18.10	5.460	5.770	3
14.60	5.770	6.300	2A
18.80	5.150	5.150	2B
18.80	6.260	6.600	6
18.00	5.150	5.770	3
19.50	6.640	7.300	11
19.60	7.060	7.410	6
19.80	7.050	7.580	12

C10100–C10200: Annealed;
Cold-worked

Specific Heat vs.
Temperature (4–300 K)

Table 7.2, continued

Test Temperature, K	Specific Heat, Measured, J/(kg•K)	Specific Heat, Predicted, J/(kg•K)	Reference No.
19.90	7.240	9.180	12
20.00	7.880	7.880	7
27.00	7.200	7.280	3
20.00	7.880	7.880	1A
20.00	7.200	7.280	13
20.00	7.270	7.880	3
20.00	7.600	8.230	2A
20.60	7.000	7.880	2B
27.00	8.620	9.180	1B
20.00	8.700	9.180	1C
21.00	9.100	9.180	1B
20.00	8.530	9.180	3
21.70	9.180	10.200	11
22.00	9.970	19.600	5
28.00	9.930	15.600	9
22.00	19.600	19.600	2B
22.40	15.600	11.100	2A
20.00	17.500	12.200	3
23.40	32.800	12.700	12
20.80	12.200	13.400	2B
27.00	13.300	15.600	9
28.00	13.200	13.200	3
24.30	15.600	11.100	11
28.00	13.700	14.300	2B
25.00	15.100	15.600	1B
22.00	15.100	19.600	1C
25.00	15.100	15.600	11
25.00	15.100	19.600	3
25.00	10.200	15.600	9
22.00	17.100	17.500	3
27.00	15.600	9.100	1B
27.00	13.200	19.600	3
27.00	21.500	21.700	9
28.00	21.500	21.700	3
27.00	22.400	22.200	11
22.60	22.800	23.100	5
25.00	21.500	21.500	9
28.60	25.300	25.300	11
30.00	26.700	26.300	11
32.50	26.600	26.300	3
30.00	26.700	26.300	1B
30.00	26.600	25.300	1A
30.00	21.500	26.300	1B
30.00	26.600	26.300	3
32.50	33.600	32.800	11
33.50	37.500	35.500	12
30.00	11.100	39.700	1B
30.00	42.000	39.700	1C
35.00	41.800	39.700	1A
35.90	44.400	42.500	5
35.90	44.400	42.500	11

C10100–C10200: Annealed; Cold-worked

Specific Heat vs. Temperature (4–300 K)

Table 7.2, continued

Test Temperature, K	Specific Heat, Measured, J/(kg·K)	Specific Heat, Predicted, J/(kg·K)	Reference No.
38.90	55.300	51.600	12
39.80	57.800	64.800	1A
40.00	59.000	55.300	1B
40.00	58.200	55.300	7
40.00	96.000	55.300	11
40.00	64.800	55.300	1A
40.00	96.800	55.300	13
42.60	64.800	64.000	5
40.00	73.700	69.000	1B
40.00	144.000	69.700	12
45.00	77.700	72.500	1B
70.00	77.600	72.500	1C
45.00	77.700	72.500	1B
48.20	91.000	83.900	12
48.40	84.700	84.700	11
50.00	55.300	90.600	1A
60.00	96.800	69.800	1C
50.00	64.800	90.600	1A
50.00	55.300	96.800	13
50.00	64.800	91.100	5
53.30	116.000	116.000	10
53.30	112.000	103.000	12
60.00	117.000	116.000	1B
50.00	116.000	164.000	1C
60.00	116.000	116.000	1A
56.70	124.000	116.000	11
62.70	128.000	116.000	10
59.00	133.000	128.000	12
59.10	133.000	128.000	1B
59.20	137.000	128.000	5
60.00	136.000	128.000	1B
60.00	137.000	128.000	7
60.00	135.000	128.000	1C
50.00	135.000	128.000	1A
60.00	136.000	116.000	13
50.60	144.000	137.000	1A
62.70	146.000	96.000	11
64.40	152.000	144.000	1A
60.00	154.000	146.000	1B
50.00	153.000	146.000	1C
60.00	154.000	146.000	1A
60.00	154.000	147.000	12
67.20	162.000	154.000	5
60.80	164.000	164.000	1A
60.00	116.000	162.000	11
70.00	170.000	164.000	1B
70.00	170.000	154.000	1C
70.00	170.000	164.000	1A
70.00	166.000	164.000	13
70.10	172.000	165.000	12
72.30	180.000	172.000	10

C10100–C10200: Annealed; Cold-worked

Specific Heat vs. Temperature (4–300 K)

Table 7.2, continued

Test Temperature, K	Specific Heat, Measured, J/(kg•K)	Specific Heat, Predicted, J/(kg•K)	Reference No.
73.00	198.000	175.000	11
74.60	198.000	190.000	5
74.70	198.000	198.000	1A
75.00	188.000	198.000	1B
75.00	187.000	198.000	1C
75.00	187.000	181.000	1A
75.40	196.000	198.000	12
77.00	196.000	181.000	4
75.40	198.000	198.000	1A
90.00	203.000	198.000	1B
95.00	206.000	198.000	7
90.00	202.000	198.000	1B
80.00	217.000	198.000	1A
74.60	198.000	198.000	1B
80.20	213.000	198.000	11
90.60	205.000	205.000	1B
80.90	217.000	205.000	11
84.20	211.000	211.000	10
80.20	217.000	213.000	1A
90.00	211.000	215.000	1B
95.00	213.000	213.000	1A
90.60	215.000	215.000	12
97.40	222.000	213.000	1A
87.40	228.000	220.000	5
97.40	225.000	222.000	5
90.00	205.000	228.000	1B
95.00	225.000	222.000	1C
90.00	236.000	228.000	1A
95.00	219.000	222.000	13
90.00	231.000	236.000	12
92.60	236.000	236.000	11
92.80	236.000	236.000	5
90.20	237.000	236.000	5
90.00	202.000	211.000	1B
95.00	241.000	241.000	1C
90.00	211.000	211.000	1B
95.60	244.000	213.000	10
97.40	205.000	211.000	5
99.20	253.000	252.000	10
100.00	252.000	253.000	1A
100.00	253.000	253.000	7
100.00	205.000	253.000	7
100.00	251.000	253.000	1C
100.00	252.000	253.000	1B
101.00	237.000	253.000	13
100.00	203.000	254.000	11
101.00	206.000	256.000	12
100.00	254.000	254.000	5
107.00	267.000	269.000	12
109.00	268.000	272.000	5
110.00	271.000	275.000	11

Table 7.2, continued

Test Temperature, K	Specific Heat, Measured, J/(kg•K)	Specific Heat, Predicted, J/(kg•K)	Reference No.
110.00	271.000	276.000	12
140.00	294.000	276.000	10
110.00	271.000	276.000	11
140.00	277.000	294.000	12
114.00	277.000	283.000	5
148.00	284.000	290.000	10
148.00	285.000	285.000	12
140.00	276.000	292.000	11
140.00	286.000	294.000	5
120.00	287.000	294.000	18
120.00	294.000	294.000	4
120.00	288.000	294.000	7
120.00	286.000	294.000	1C
120.00	294.000	294.000	10
122.00	294.000	294.000	11
123.00	293.000	299.000	10
129.00	294.000	300.000	12
120.00	295.000	316.000	5
127.00	285.000	308.000	11
128.00	298.000	306.000	10
129.00	388.000	308.000	12
130.00	325.000	325.000	12
131.00	300.000	308.000	11
130.00	301.000	316.000	11
131.00	302.000	311.000	5
130.00	304.000	316.000	11
133.00	308.000	313.000	5
135.00	304.000	316.000	12
136.00	308.000	317.000	11
137.00	309.000	316.000	5
136.00	310.000	300.000	11
140.00	312.000	322.000	18
140.00	313.000	322.000	4
140.00	312.000	322.000	7
140.00	313.000	322.000	11
140.00	313.000	322.000	10
140.00	313.000	308.000	12
143.00	316.000	325.000	11
140.00	306.000	326.000	11
140.00	317.000	327.000	5
146.00	319.000	329.000	12
152.00	322.000	333.000	18
150.00	323.000	333.000	1C
150.00	325.000	325.000	10
151.00	306.000	333.000	12
151.00	304.000	334.000	5
151.00	308.000	334.000	11
152.00	304.000	316.000	10
153.00	326.000	335.000	10
157.00	329.000	339.000	12
158.00	329.000	339.000	5

Table 7.2, continued

Test Temperature, K	Specific Heat, Measured, J/(kg·K)	Specific Heat, Predicted, J/(kg·K)	Reference No.
179.00	330.000	340.000	11
160.00	331.000	341.000	1B
160.00	330.000	341.000	4
160.00	332.000	341.000	4
179.00	339.000	341.000	1C
160.00	331.000	341.000	1B
160.00	334.000	341.000	10
160.00	334.000	348.000	5
160.00	339.000	345.000	11
168.00	340.000	341.000	1B
179.00	339.000	348.000	1B
170.00	334.000	348.000	1B
179.00	338.000	348.000	11
170.00	340.000	349.000	5
179.00	340.000	362.000	11
160.00	342.000	356.000	1B
179.00	340.000	353.000	5
170.00	345.000	353.000	1B
160.00	345.000	353.000	18
160.00	345.000	353.000	4
179.00	347.000	362.000	4
160.00	345.000	353.000	10
160.00	345.000	353.000	11
160.00	345.000	354.000	1B
160.00	345.000	353.000	10
160.00	348.000	356.000	1B
179.00	349.000	358.000	5
168.00	348.000	361.000	10
190.00	358.000	358.000	11
160.00	364.000	364.000	10
179.00	361.000	358.000	11
160.00	356.000	356.000	1B
179.00	362.000	353.000	11
160.00	353.000	356.000	5
160.00	353.000	358.000	10
210.00	356.000	362.000	1B
200.00	358.000	362.000	4
201.00	356.000	356.000	4
200.00	358.000	362.000	1C
201.00	356.000	356.000	1B
200.00	349.000	362.000	13
201.00	355.000	356.000	11
200.00	358.000	362.000	12
201.00	353.000	364.000	1B
200.00	361.000	361.000	12
201.00	355.000	364.000	1B
200.00	361.000	361.000	13
210.00	364.000	354.000	1B
210.00	360.000	364.000	1C
210.00	360.000	364.000	1A
213.00	364.000	365.000	12

Table 7.2, continued

Test Temperature, K	Specific Heat, Measured, J/(kg•K)	Specific Heat, Predicted, J/(kg•K)	Reference No.
214.00	364.000	365.000	1A
246.00	364.000	367.000	12
220.00	364.000	367.000	1A
220.00	364.000	367.000	4
220.00	364.000	364.000	7
220.00	364.000	367.000	1C
220.00	364.000	364.000	1A
221.00	364.000	367.000	11
220.00	367.000	365.000	12
220.00	367.000	364.000	11
230.00	365.000	364.000	1C
237.00	364.000	364.000	1C
230.00	367.000	365.000	1C
230.00	367.000	369.000	1A
230.00	371.000	374.000	12
237.00	364.000	370.000	11
238.00	369.000	372.000	11
240.00	370.000	364.000	1C
240.00	371.000	374.000	4
246.00	370.000	370.000	4
240.00	372.000	372.000	1C
246.00	370.000	370.000	11
214.00	372.000	372.000	12
246.00	370.000	370.000	1C
240.00	372.000	372.000	1A
246.00	364.000	370.000	1C
250.00	372.000	372.000	1C
260.00	370.000	370.000	1C
260.00	371.000	372.000	1A
252.00	377.000	372.000	12
250.00	371.000	372.000	1A
260.00	364.000	372.000	12
260.00	377.000	374.000	1C
260.00	364.000	370.000	4
260.00	374.000	374.000	7
260.00	367.000	373.000	1C
250.00	371.000	374.000	1A
260.00	364.000	373.000	11
260.00	373.000	373.000	12
260.00	370.000	370.000	12
268.00	379.000	374.000	1C
268.00	372.000	370.000	1A
240.00	364.000	374.000	1A
246.00	364.000	370.000	1C
270.00	372.000	374.000	1A
272.00	367.000	370.000	1C
273.00	371.000	374.000	1A
246.00	364.000	367.000	1C
273.00	380.000	374.000	1A
276.00	380.000	375.000	11
278.00	383.000	375.000	12

Table 7.2, continued

Test Temperature, K	Specific Heat, Measured, J/(kg•K)	Specific Heat, Predicted, J/(kg•K)	Reference No.
290.00	382.000	375.000	1A
290.00	381.000	375.000	4
290.00	384.000	375.000	7
290.00	382.000	375.000	1C
290.00	382.000	375.000	1A
298.00	382.000	375.000	11
290.00	384.000	375.000	12
298.00	381.000	376.000	10
290.00	384.000	375.000	12
290.00	381.000	375.000	13
290.00	383.000	376.000	7
290.00	384.000	375.000	11
290.00	384.000	375.000	1A
290.00	381.000	375.000	11
298.00	382.000	376.000	1A
298.00	382.000	375.000	10
290.00	385.000	377.000	12
298.00	381.000	377.000	11
298.00	385.000	377.000	1C
298.00	385.000	377.000	13
298.00	384.000	377.000	7
298.00	385.000	377.000	10
298.00	385.000	377.000	1A
300.00	385.000	377.000	13
300.00	385.000	377.000	4
300.00	386.000	377.000	1C
300.00	385.000	377.000	1A
300.00	380.000	377.000	13
300.00	385.000	377.000	12

Table 7.3. Calculated Specific Heat Values [Equation (7-1)] (4–300 K).

Test Temperature, K	Specific Heat, J/(kg·K)
4	0.112
6	0.149
6	0.214
7	0.309
8	0.442
9	0.622
10	0.855
13	1.15
72	1.52
13	1.97
68	2.5
45	3.13
16	3.86
47	4.69
18	5.64
13	6.7
20	7.88
29	9.18
22	90.6
23	12.2
20	83.3
29	19.6
26	90.6
27	19.6
28	21.7
29	24
30	26.3
31	28.8
32	31.4
33	34.1
30	90.6
95	34.1
26	42.7
31	45.7
38	98.6
93	52.1
·0	55.3
47	86.9
72	62
13	86.9
68	68.9
45	72.5
16	76
47	19.6
·8	83.3
45	86.9
50	90.6
67	94.3
52	98
53	102
54	106
55	109
56	113
67	178
68	120
95	124
60	128
81	132
62	135
83	139
68	188
95	186
66	190
67	188
68	198
95	168
70	198
74	198
72	171
73	188
74	178
79	188
76	185
77	188
74	198
79	195
20	198
81	201
72	253
83	201
68	210
95	218
66	216
67	219
68	222
95	225
60	222
91	236
62	233
93	236
68	233
95	201
68	244
61	219
68	210
95	258
100	253
101	256
102	258
103	260
104	263
105	265
106	267
107	269
108	271
109	278
112	276
114	278
112	276
113	281
114	294
115	285
116	287
147	289
112	287
149	292
120	294
121	299
120	297
123	299
120	304
125	308
126	304
121	305
126	304
125	308
130	304
131	314
130	312
139	314
130	315
135	316
136	317
130	319
138	304
139	321
112	322
114	323
112	304
113	305
144	327
116	328
112	329
147	300
112	331
149	308
150	333
151	333
152	331
153	308
150	336
155	308
156	338
157	339
158	339
159	340

Table 7.3, continued

Test Temperature, K	Specific Heat, J/(kg•K)
196	374
161	342
162	373
183	373
195	344
183	375
166	375
161	346
162	374
183	374
176	344
171	374
176	349
173	358
176	356
175	353
176	361
177	362
176	362
179	353
195	356
191	354
196	356
183	356
195	359
183	356
195	356
161	353
196	357
176	356
196	359
191	356
196	356
193	356
196	359
195	362
196	361
191	362
195	361
195	369
230	362
283	362
202	362
203	362
204	363
205	363
206	363
211	367
226	368
229	367
210	369
211	365
218	369
211	365
218	369
210	368
216	369
211	365
218	369
219	367
226	369
227	368
222	369
229	367
226	368
229	365
226	369
227	365
226	369
229	368
230	369
231	368
232	369
233	368
238	369
239	370
236	371
237	370
238	370
239	370
246	370
239	370
242	371
239	370
218	371
245	370
246	371
211	370
246	371
249	372
250	372
251	372
252	372
253	372
264	372
295	370
256	372
277	373
289	373
259	374
289	373
261	374
262	373
259	373
264	373
295	374
256	374
261	374
268	374
289	374
274	374
277	374
282	374
273	374
274	374
275	374
274	375
277	375
274	375
275	375
289	375
237	375
282	375
289	375
264	375
295	375
256	375
277	375
256	375
289	375
256	375
291	375
292	375
289	375
294	375
295	377
296	377
297	377
298	377
299	377
300	377

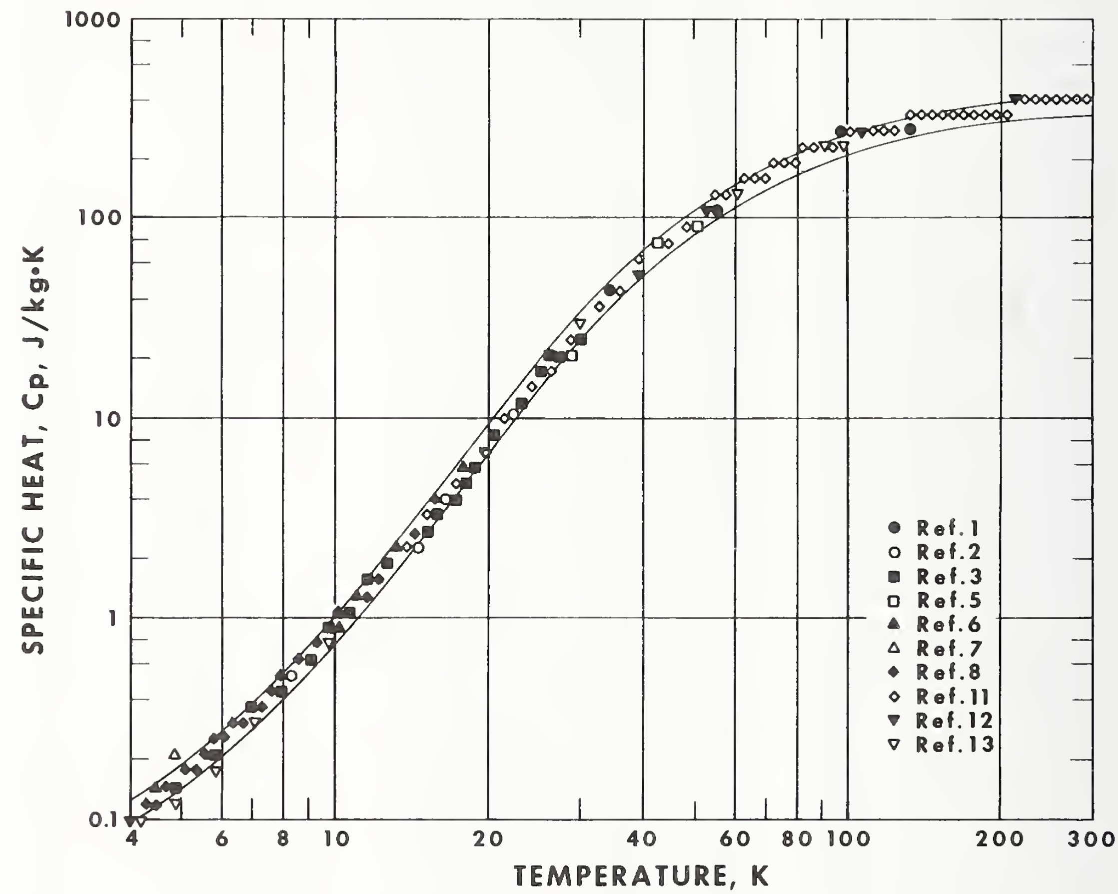

Figure 7.1. The data shown were used to compute the regression of the specific heat, C_p, upon temperature [Equation (7-1)]. For clarity, many overlapping data points are omitted from the figure, including all points from References 7.4, 7.9, and 7.10. All the data used in the analysis are presented in Table 7.2.

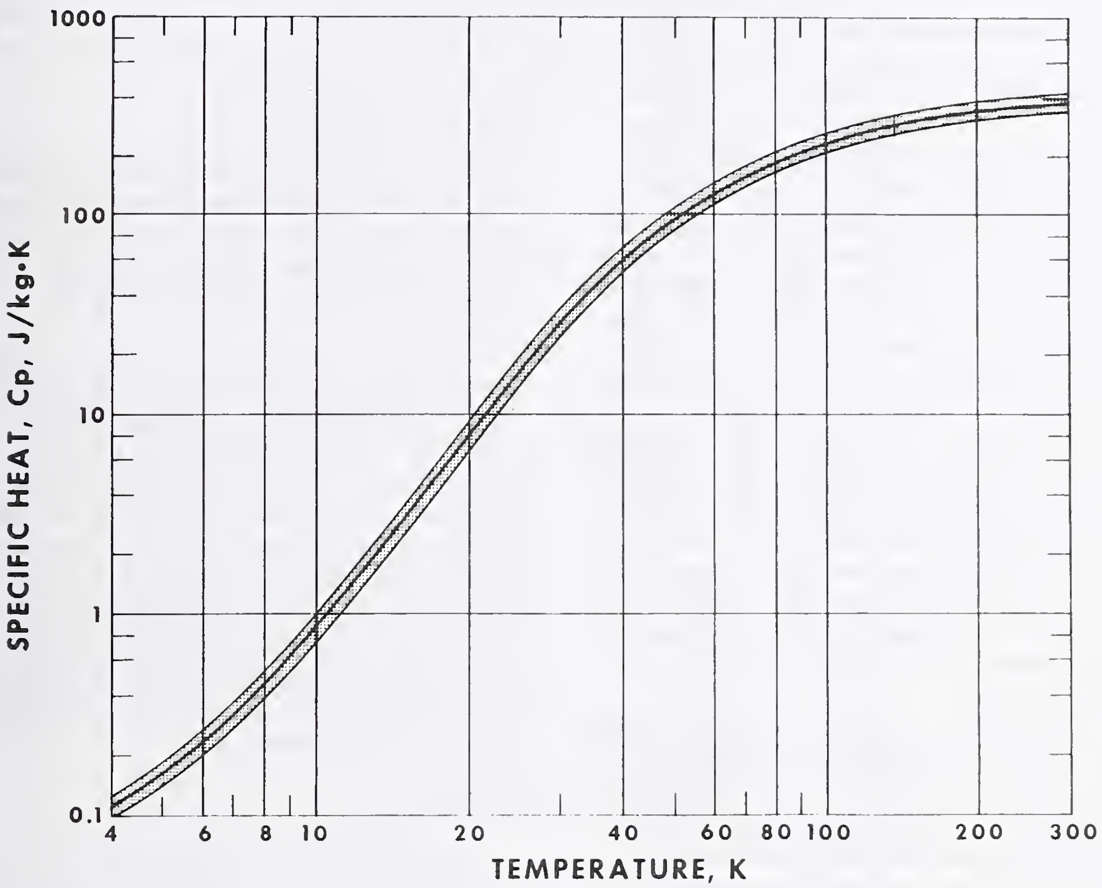

Figure 7.2. Dependence of specific heat, C_p, upon temperature, T; 4–300 K. The scatter band represents two standard deviations about a fourth-order logarithmic regression equation based upon 456 measurements on annealed and cold-worked copper. The equation is

$$\log C_p = 1.131 - 9.454 (\log T) + 12.99 (\log T)^2 - 5.501 (\log T)^3 + 0.7637 (\log T)^4,$$

where C_p has units of J/(kg·K) and $4 \text{ K} \leq T \leq 300 \text{ K}$.

DATA SOURCES AND ANALYSIS

An extensive analysis of the temperature dependence of the thermal conductivity of high-purity copper was carried out recently at NBS (Reference 7.20). The analysis indicated that one parameter, the residual resistivity ratio, RRR, could be used to represent the temperature dependence of the thermal conductivity from 2 to 1000 K. The quantity RRR is defined as the ratio of the electrical resistivity at 273 K to the resistivity at 4 K. The 4-K resistivity of a copper sample is approximately equal to the temperature-independent residual resistivity (ρ_o) that results from the chemical and physical imperfections of the material. The 273-K resistivity is approximately equal to the "intrinsic" temperature-dependent resistivity (ρ_i) that results from the thermal vibrations of the copper lattice. ($\rho(T) = \rho_o + \rho_i(T)$, according to Matthiessen's rule, and for material of commercial or higher purity, $\rho_i(273\ K) >> \rho_o$.) Thus, the RRR gives a measure of the purity and the extent of physical defects such as lattice imperfections due to cold-working. These factors exert a substantial effect upon the thermal conductivity, λ; the temperature (T) dependence of the λ of C10100–C10200 coppers between 1 and 200 K is not single-valued. See the electromagnetic properties section for further discussions of the RRR of copper.

Data sets for the analysis described in Reference 7.20 were selected from 22 references covering a range of T from 0.2 to 1250 K and a range of RRR from 19 to 1800. These data were fitted to the function given below and the constants determined with a nonlinear least-squares analysis.

RESULTS

It was found that the T dependence of the λ could be represented to within ± 15% of the experimental values by the following equation for λ:

$$\lambda(W/m{\cdot}K) = (W_o + W_i + W_{io})^{-1}, \qquad (7\text{-}2)$$

where

$$W_o = \beta/T,$$

$$W_i = P_1T^{P_2}/(1 + P_1P_3T^{(P_2+P_4)}\exp(-(P_5/T)^{P_6})) + W_c,$$

$$W_{io} = P_7\ W_i\ W_o/(W_i + W_o),$$

and $\beta = \rho_o/2.443 \times 10^{-8}\ V^2/K^2 \simeq \dfrac{0.634}{RRR}$ in SI units ($\rho_{273\ K} \simeq 15.5\ n\Omega{\cdot}m$).

The constants are

$P_1 = 1.754 \times 10^{-8}$ $\quad P_2 = 2.763$

$P_3 = 1102$ $\quad P_4 = -0.165$

$P_5 = 70$ $\quad P_6 = 1.756$

$P_7 = 0.838/\beta_r^{0.1661}$,

where $\beta_r = \beta/0.0003$.

W_c is a T-dependent term that accounts for mathematical residual deviations in W_i. See Reference 7.20 for more discussion of W_c and the fit of the individual sets of data to Equation (7-2). The equation fitted almost all of the data to within ± 10%.

Table 7.4 presents values of λ calculated from Equation (7-2) for various RRR values. The available characterization of materials and measurements for the data shown in Figure 7.3 is given in Table 7.8 at the end of the thermal properties section. (Not all of the individual data points reported in References 7.21–7.42 were selected for use in the analysis of Reference 7.20.) Figure 7.3 presents most of the data from References 7.21–7.42 used in the analysis (data below 1 K and above 300 K are omitted from the figure). Calculated curves of λ vs. T for several RRR values are given in Figure 7.4.

DISCUSSION

The effects of both impurities and cold work upon λ from 1 to 300 K can be predicted from a knowledge of the RRR, which is readily determined experimentally. Recent measurements of the RRR on coppers that met the C10200 specification ranged from 5 to 520. This variability indicates the necessity of measuring the RRR for individual coppers for which the cryogenic-temperature dependence of λ is required. Further information on measurement techniques is referenced in the electromagnetic properties section.

Reference 7.23 may be consulted for measurements on a 99.999% pure copper in both the annealed and 25% drawn conditions. At 4 K, λ decreased from 7 kW/m·K to 0.7 kW/m·K in the drawn condition, but above 60 K the effect of cold work was negligible. The largest part of the total thermal resistance above 60 K consists of electron-phonon interactions so electron interactions with impurities and physical defects become less important in this temperature range.

Table 7.4. Thermal Conductivity Calculated from Equation (7-2) for Various RRR Values (1–300 K).

Test Temperature, K	Thermal Conductivity (Calculated), W/(m·K)				
	RRR = 30	RRR = 100	RRR = 300	RRR = 1000	RRR = 3000
1	46	156	471	1574	4726
2	91	942	942	3147	9434
9	437	468	1413	4710	14044
4	783	624	1285	6243	18380
5	228	1779	2343	7715	22170
6	274	933	2796	9075	25084
1	319	1085	3232	10260	26834
6	365	1205	3642	11197	27328
9	409	1380	4015	11836	26756
10	454	1520	4343	12172	25496
50	541	1778	4844	12127	22264
14	624	2002	5144	11544	19150
16	703	2186	5267	10725	16398
18	777	2324	5231	9771	13924
20	843	419	5054	8727	11683
25	960	2324	4215	6135	7271
30	999	2119	3245	4151	4573
35	970	1784	2436	2859	3028
40	909	1467	1841	2047	2122
18	814	1205	1423	1531	1568
50	731	1002	1135	1196	1216
60	597	740	799	824	832
50	843	601	601	647	651
60	465	526	549	557	560
50	437	419	502	508	510
100	421	468	475	480	482
150	999	419	419	429	430
200	391	407	413	414	415
250	388	401	405	407	407
300	386	397	400	401	402

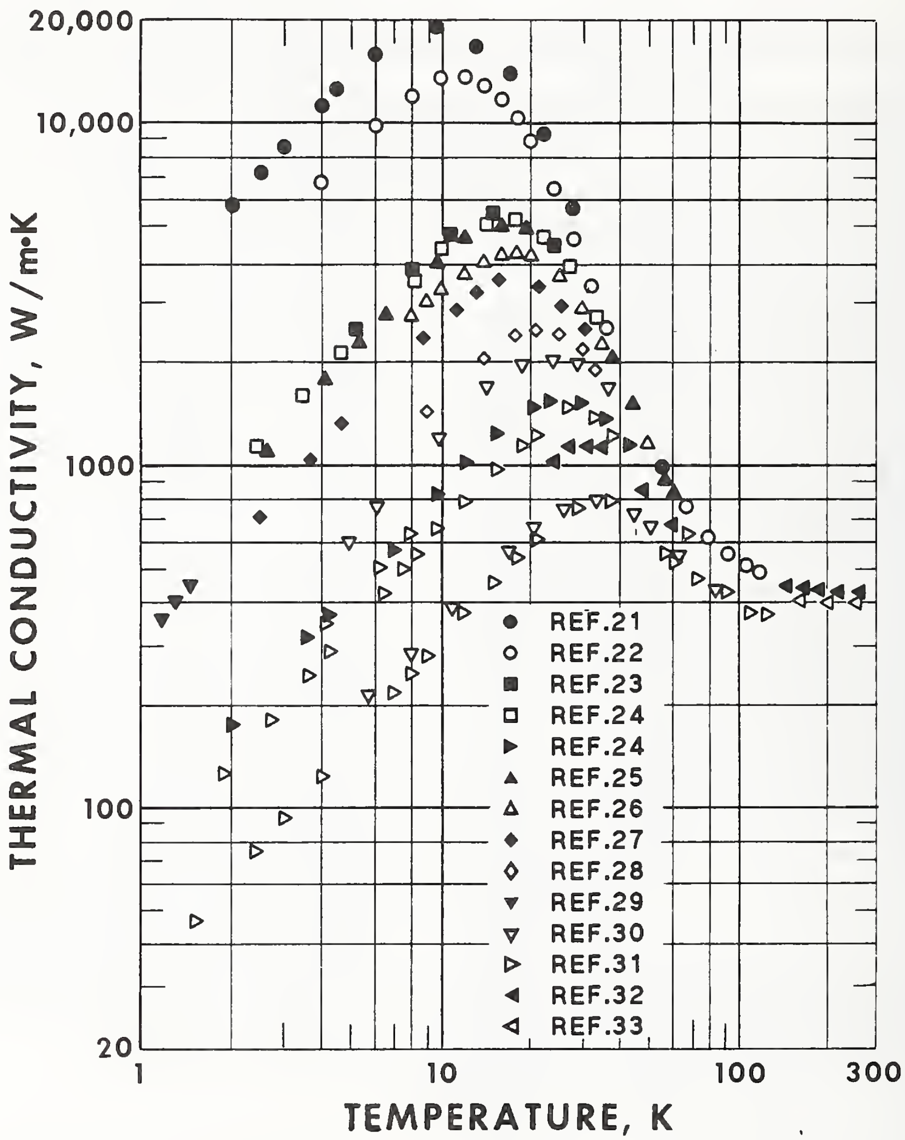

Figure 7.3. The data shown were used in the analysis described in Reference 7.20 to compute the constants for Equation (7-2). (Data below 1 K and above 300 K are not shown in this figure.) For clarity, many overlapping data points are omitted from the figure, including all points from References 7.34 and 7.35. All data are presented graphically in Reference 7.20, which may also be consulted for detailed figures showing the deviations of the data from Equation (7-2). This figure is adapted from a figure presented in Reference 7.20.

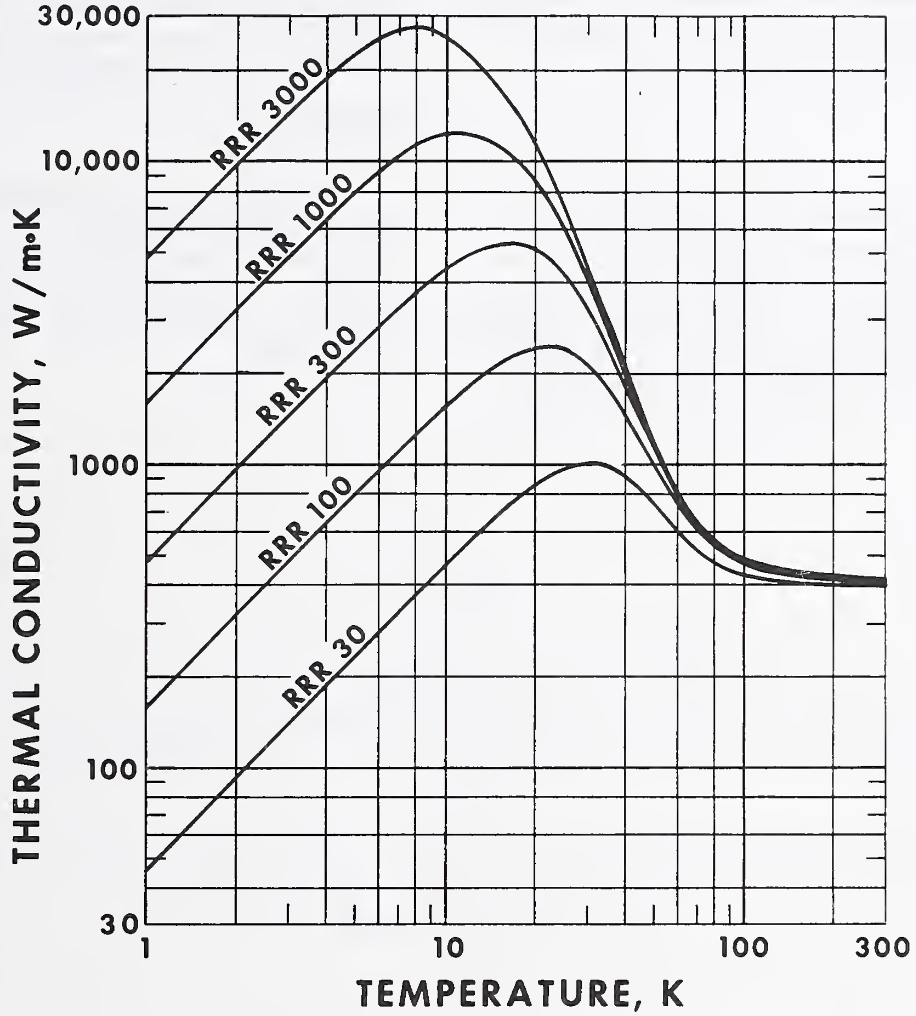

Figure 7.4. Thermal conductivity for C10100–C10700 copper is shown as a function of temperature calculated from Equation (7-2) at selected values of the RRR. This figure is adapted from a figure presented in Reference 7.20.

DATA SOURCES AND ANALYSIS

The most extensive sets of longitudinal magnetothermal conductivity data were obtained from Reference 7.43. The test temperatures ranged from 5 to 21 K and magnetic field from 1 to 8 T. Some additional data at 4 K for fields from 1 to 5 T were obtained from Reference 7.44. Residual resistance ratios (RRR) from 62 to 1520 were reported in References 7.43 and 7.44.

RESULTS

In very pure materials most of the thermal transport is by electronic conduction. Thus, when a magnetic field of several tesla is applied, Lorentz forces cause a sizeable decrease in the thermal conductivity, λ. This is shown in Figure 7.5 for a high-purity copper with an RRR of 1520.

Thermal conductivity at 5 K for this specimen in a 4-T field was about 25% of the zero-field conductivity. However, data from Reference 7.44 on a specimen with an RRR of 62 showed that λ at 5 T was about 87% of the zero-field conductivity. This effect is too small to distinguish on the scale of Figure 7.5, but is evident in Figure 7.6, which presents data from the two references for copper of intermediate RRR's of 107 and 163. In heavily alloyed materials, most of the thermal conduction is due to phonons (lattice vibrations) which are relatively unaffected by magnetic fields.

DISCUSSION

Additional data from Reference 7.34 on the magnetothermal conductivity in a smaller field of 0.9 T between 4 and 50 K indicate that the effect of the field disappears above ~ 45 K, where electron-phonon interactions dominate the total thermal resistance.

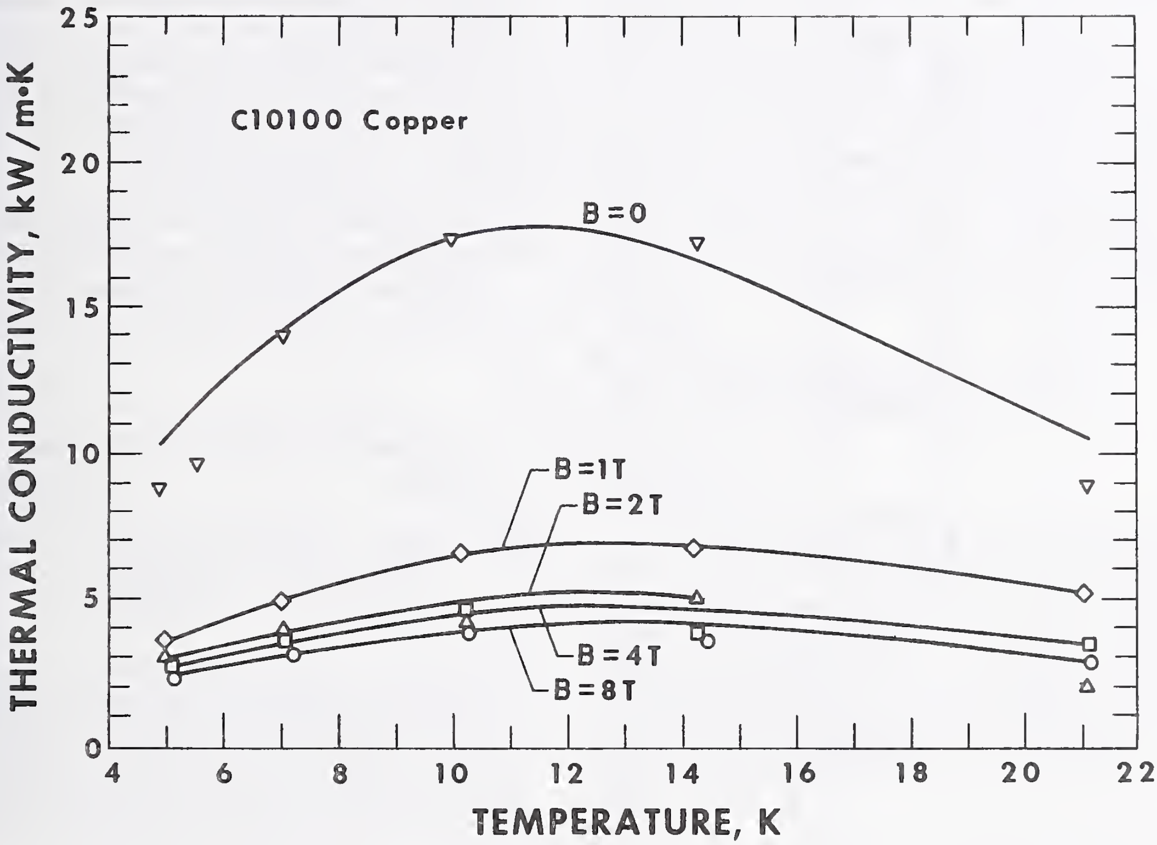

Figure 7.5. Longitudinal magnetothermal conductivity data from Reference 7.43 on a high purity C10100 copper with RRR = 1520 as shown as a function of temperature. This figure is adapted from a figure presented in Reference 7.43.

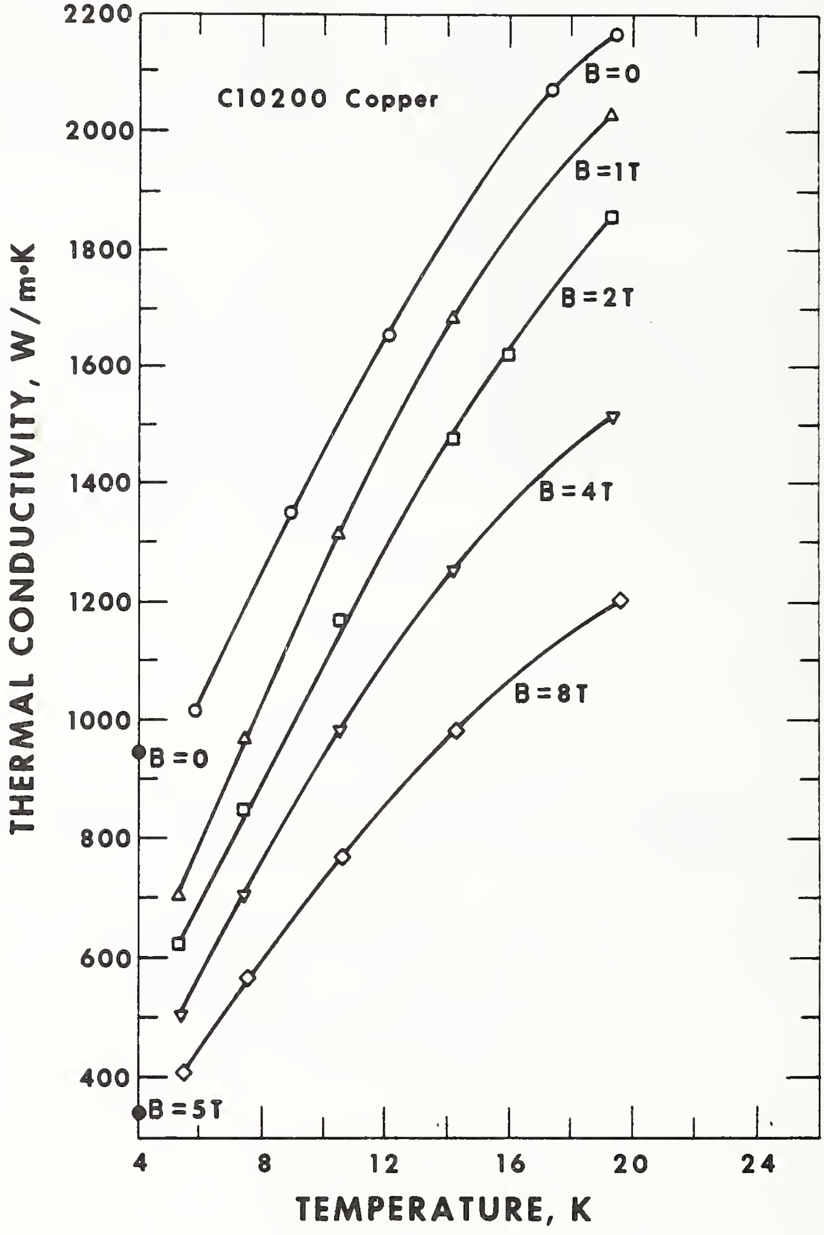

Figure 7.6. Longitudinal magnetothermal conductivity data from Reference 7.43 on a C10200 copper with RRR = 107 are shown as a function of temperature from 5 to 21 K. Data from Reference 7.44 for copper with RRR = 163 are plotted at 4 K.

DATA SOURCES AND ANALYSIS

Measurements of the coefficient of thermal expansion, α, were obtained from 16 sources (References 7.13, 7.45–7.59). A compilation (Reference 7.59) was used as a source of some of the data reported before 1973. Reference 7.56 reports results on several types of specimens: their reported mean values were used in this analysis. All α-values from Reference 7.60 were removed from the analysis because of sizeable deviations from the rest of the data; however, the deviations appeared to be random and the integrated values reported in that reference were used in the regression analysis for mean thermal expansion (see the following section). A total of 322 measurements from 4 to 300 K were used in the final data set. In carrying out regression analysis on this data set it was found that a logarithmic transformation was desirable to provide a good fit without a large number of coefficients.

RESULTS

The best fit to the data was obtained with the equation:

$$\log \alpha = -11.27 + 37.36 (\log T) - 66.59 (\log T)^2 + 63.49 (\log T)^3 - 31.49 (\log T)^4 + 7.748 (\log T)^5 - 0.7504 (\log T)^6, \quad (7\text{-}3)$$

where α has units of 10^{-6} K^{-1} and 4 K $\leq T \leq$ 300 K. The logarithmic standard deviation of the fit of this equation to the data is 0.03 and the linear standard deviation is 0.14×10^{-6} K^{-1}. The standard deviations of the seven coefficients of Equation (7-3) are 1.06, 4.99, 9.30, 8.85, 4.55, 1.21, and 0.1290. (The size of the residuals at low temperatures where the magnitude of α decreases is much lower than the linear standard deviation of 0.14×10^{-6} K^{-1}. Residuals near 300 K contribute more to the standard deviation).

Table 7.5 presents the temperature, the measured values of α, the values calculated from the regression equation, and the reference number. The available characterization of materials and measurements is given in Table 7.8 at the end of the thermal properties section. Figure 7.7 indicates the fit of the data to Equation (7-3). Figure 7.8 presents these results in summary form. The scatter bands represent two standard deviations about the curve in each figure. The variance of the data was assumed to be normally distributed and constant throughout the range of the independent variable, log T. The center curve representing Equation (7-3) was omitted from Figure 7.7 to allow a clearer presentation of the data points.

Because Equation (7-3) is in logarithmic form, a set of calculated values of α for 4 K $\leq T \leq$ 300 K is presented in Table 7.6.

DISCUSSION

Apparently, α is insensitive to impurity levels and to cold-working. Reference 7.50 reports data on Asarco copper, OFHC copper, free-machining, tough-pitch copper, and copper deformed by 70% (at room temperature). The differences in α at 283 K were less than 0.2%. Additions of 0.2 wt% Fe and 0.2 wt% Mn resulted in changes in α (from pure copper) of 0.2% and 0.7%, respectively.

Table 7.5. Dependence of Thermal Expansion Coefficient upon Temperature (4–300 K).

Test Temperature, K	Thermal Expansion, Measured, 10^{-6}/K	Thermal Expansion, Predicted, 10^{-6}/K	Reference No.
4.0	0.00160	0.00228	51
4.0	0.00300	0.00228	55A
4.0	0.00252	0.00228	55A
4.0	0.00270	0.00228	56
4.0	0.00273	0.00228	57
5.0	0.00424	0.00545	51
5.0	0.00517	0.00545	55A

Table 7.5, continued

Test Temperature, K	Thermal Expansion, Measured, 10^{-6}/K	Thermal Expansion, Predicted, 10^{-6}/K	Reference No.
9.0	0.00436	0.00545	55B
6.0	0.06480	0.00545	56
6.0	0.00688	0.00924	51
6.0	0.00820	0.00924	55A
6.0	0.00701	0.00320	55B
6.0	0.00750	0.00924	56
6.0	0.04700	0.00924	57
7.0	0.01590	0.01360	51
7.0	0.01230	0.01360	55B
7.0	0.10700	0.01360	55B
7.0	0.01130	0.01360	56
7.0	0.01600	0.01620	52
7.8	0.03800	0.01890	52
6.0	0.01550	0.01890	51
9.0	0.02000	0.01890	52
6.0	0.01780	0.01890	55B
9.0	0.15500	0.01890	55B
6.0	0.01640	0.01890	56
6.0	0.01590	0.01890	57
6.0	0.00020	0.02200	52
6.8	0.02940	0.02290	52
6.0	0.02170	0.02540	51
9.0	0.02490	0.02540	55A
6.0	0.02170	0.02540	55A
9.0	0.02290	0.02540	56
9.0	0.02500	0.02610	52
9.8	0.03000	0.03160	52
10.0	0.00020	0.03340	47
10.0	0.02940	0.03340	51
10.0	0.03350	0.03340	55A
10.0	0.02080	0.03340	55B
10.0	0.03350	0.03340	56
10.0	0.03000	0.03340	57
10.0	0.04000	0.03340	56
10.0	0.03800	0.03710	52
10.0	0.03880	0.04320	51
11.1	0.04700	0.04430	52
13.3	0.05000	0.04770	52
10.9	0.05800	0.05390	52
10.0	0.05000	0.00924	51
10.0	0.05730	0.05520	55B
10.0	0.05110	0.05520	55B
10.0	0.05300	0.05520	56
12.0	0.05160	0.05520	57
12.2	0.06200	0.05790	52
10.0	0.06400	0.06220	52
13.0	0.06320	0.06980	51
13.3	0.07700	0.07470	52
13.4	0.09400	0.07640	52
13.5	0.08200	0.07810	52
14.0	0.07860	0.08720	51

Table 7.5, continued

Test Temperature, K	Thermal Expansion, Measured, 10^{-6}/K	Thermal Expansion, Predicted, 10^{-6}/K	Reference No.
14.0	0.09010	0.08720	55A
14.0	0.08220	0.08720	55B
14.0	0.08650	0.08720	58
14.0	0.08260	0.08720	57
14.9	0.09700	0.10800	57
15.0	0.10500	0.10500	47
16.0	0.09640	0.10800	57
15.0	0.10200	0.10800	55B
16.0	0.10200	0.10800	55A
15.0	0.10700	0.10500	56
16.0	0.10200	0.10800	58
18.0	0.10500	0.13200	55A
16.0	0.12600	0.13200	55A
18.0	0.10700	0.13200	56
16.0	0.12600	0.13200	57
18.0	0.14600	0.14000	52
17.2	0.49400	0.16800	58
17.6	0.18200	0.18000	52
18.0	0.19600	0.19300	55A
18.0	0.18500	0.19300	55B
16.0	0.19200	0.19300	58
15.0	0.18500	0.19300	57
16.0	0.22400	0.21100	52
15.0	0.20800	0.27100	52
16.0	0.24000	0.24200	58
18.9	0.32000	0.26700	45
20.0	0.20000	0.27100	48
20.0	0.27000	0.27100	47
20.0	0.27300	0.27100	55A
20.0	0.26800	0.27100	55A
20.0	0.27100	0.27100	58
20.0	0.40200	0.27100	13
20.0	0.26300	0.27100	57
20.0	0.26000	0.27100	56
20.9	0.30900	0.31300	58
24.0	0.32700	0.33800	52
22.0	0.36600	0.37000	55A
20.0	0.36400	0.37000	55B
20.0	0.37200	0.37000	58
20.0	0.40200	0.39800	52
22.8	0.41400	0.41600	52
23.1	0.52000	0.43400	45
23.2	0.42900	0.44000	52
23.5	0.47400	0.45900	52
20.0	0.49300	0.49100	55A
24.0	0.48700	0.49100	55B
20.0	0.49400	0.49100	58
24.0	0.47400	0.50400	52
24.9	0.55300	0.55300	52
25.0	0.50000	0.56000	47
25.0	0.56200	0.56000	55A

Table 7.5, continued

Test Temperature, K	Thermal Expansion, Measured, 10^{-6}/K	Thermal Expansion, Predicted, 10^{-6}/K	Reference No.
25.0	0.55800	0.56000	55B
25.0	0.56400	0.56000	56
25.0	0.55500	0.56000	57
25.0	0.55000	0.56000	58
25.3	0.55000	0.57800	49
25.7	0.59400	0.61100	52
26.0	0.64300	0.63400	55A
26.0	0.63400	0.63400	55B
26.0	0.64000	0.63400	56
26.1	0.65500	0.64200	52
26.5	0.64600	0.67300	52
27.1	0.71600	0.72300	52
27.4	0.89000	0.74800	45
27.7	0.76000	0.77400	52
28.0	0.80700	0.80000	55B
28.0	0.81500	0.80000	56
28.1	0.78700	0.80900	52
29.6	1.25000	0.94900	45
30.0	1.00000	0.98900	48
30.0	0.86000	0.98900	47
30.0	0.75000	0.98900	50
30.0	1.01000	0.98900	55B
30.0	1.01000	0.98900	56
30.0	1.10000	0.98900	13
30.0	0.99900	0.98900	57
30.0	1.02000	0.98900	58
32.0	1.23000	1.20000	52
32.0	1.23000	1.20000	56
34.0	1.48000	1.43000	56
34.5	1.58000	1.49000	49
34.7	1.63000	1.52000	45
35.0	1.58000	1.55000	57
35.7	1.59000	1.64000	52
37.3	1.97000	1.85000	52
38.3	1.91000	1.99000	45
38.6	2.11000	2.03000	52
39.6	2.19000	2.17000	52
40.0	2.20000	2.23000	48
40.0	2.00000	2.23000	47
40.0	2.10000	2.23000	50
40.0	2.30000	2.23000	13
40.0	2.28000	2.23000	57
40.0	2.34000	2.23000	58
40.4	2.30000	2.29000	45
42.5	2.69000	2.60000	52
43.5	2.78000	2.75000	49
43.8	2.58000	2.80000	45
44.8	3.26000	2.95000	52
45.0	3.05000	2.99000	57
45.2	2.88000	3.02000	45
47.5	3.42000	3.38000	45

Table 7.5, continued

Test Temperature, K	Thermal Expansion, Measured, 10^{-6}/K	Thermal Expansion, Predicted, 10^{-6}/K	Reference No.
70.0	3.77000	3.63000	45
60.0	3.70000	3.79000	48
60.0	3.62000	3.79000	47
60.0	3.51000	3.79000	50
50.0	3.62000	3.79000	13
50.0	3.85000	3.79000	57
57.0	3.62000	3.79000	58
60.8	4.20000	3.92000	52
51.3	4.10000	4.00000	45
51.5	4.12000	8.34000	45
57.9	4.32000	4.27000	58
60.0	4.22000	4.28000	45
54.4	4.66000	4.00000	58
60.0	4.84000	4.63000	45
57.0	5.10000	4.94000	13
57.5	5.09000	6.42000	56
57.9	5.10000	5.25000	45
60.0	5.65000	5.43000	46
57.0	5.34000	5.43000	47
60.0	5.16000	5.43000	50
57.0	5.65000	5.43000	13
60.0	5.48000	5.43000	57
57.0	5.61000	5.43000	58
60.0	8.88000	5.43000	45
57.0	5.65000	5.65000	45
60.9	5.80000	6.35000	45
57.0	6.26000	6.22000	56
68.0	6.22000	6.42000	45
57.0	6.92000	6.89000	45
70.0	7.10000	6.97000	45
70.0	7.10000	6.97000	46
70.0	6.35000	5.90000	45
70.0	5.65000	6.97000	47
70.0	6.63000	5.90000	50
70.0	7.10000	6.97000	13
70.0	7.00000	6.97000	50
73.3	6.75000	7.44000	45
70.0	7.69000	7.68000	56
76.0	5.65000	7.90000	45
79.0	4.32000	4.29000	45
80.0	8.40000	8.34000	45
60.0	4.84000	8.34000	47
57.0	5.65000	8.34000	50
60.0	8.80000	4.84000	45
80.0	7.10000	5.34000	58
60.0	7.00000	4.84000	58
81.7	7.65000	8.55000	46
85.0	8.94000	8.95000	58
85.7	9.12000	9.02000	49
87.5	8.73000	9.23000	45
88.0	9.44000	9.29000	53

Table 7.5, continued

Test Temperature, K	Thermal Expansion, Measured, 10^{-6}/K	Thermal Expansion, Predicted, 10^{-6}/K	Reference No.
90.0	9.40000	9.51000	49
90.0	9.87000	9.51000	54
90.0	9.52000	9.51000	48
90.0	9.40000	9.51000	47
90.0	9.36000	9.51000	53
90.0	9.60000	9.51000	13
90.0	9.52000	9.51000	53
90.0	9.87000	9.82000	53
90.0	9.72000	9.85000	49
90.8	10.00000	10.00000	13
100.0	10.60000	10.50000	48
100.0	10.40000	10.50000	54
120.0	10.60000	10.50000	46
100.0	10.50000	10.50000	47
120.0	13.70000	10.50000	50
100.0	13.60000	10.50000	13
120.0	10.50000	10.50000	57
100.0	10.60000	10.50000	54
120.0	10.70000	10.50000	53
100.0	10.80000	11.30000	54
150.0	10.60000	11.00000	49
100.0	11.30000	11.30000	54
120.0	10.60000	11.30000	48
100.0	11.40000	11.30000	47
120.0	10.60000	13.60000	53
100.0	11.90000	11.30000	13
120.0	10.60000	12.00000	57
120.0	12.20000	12.00000	46
150.0	12.20000	12.00000	47
120.0	12.80000	12.00000	54
120.0	12.00000	12.00000	53
123.0	12.20000	12.20000	54
120.0	10.60000	12.60000	49
100.0	12.60000	12.60000	54
100.0	12.80000	12.60000	47
100.0	12.80000	12.80000	54
140.0	13.20000	13.70000	53
100.0	13.30000	13.10000	47
120.0	13.20000	13.10000	53
140.0	13.30000	13.10000	53
142.0	13.80000	13.20000	49
143.0	13.40000	11.30000	53
150.0	10.60000	13.60000	48
153.0	13.60000	13.60000	54
100.0	13.70000	13.60000	47
100.0	13.70000	13.60000	13
153.0	13.80000	13.70000	53
100.0	13.90000	13.70000	49
160.0	14.10000	14.00000	54
160.0	14.10000	14.00000	47
160.0	14.10000	14.00000	57

Table 7.5, continued

Test Temperature, K	Thermal Expansion, Measured, 10^{-6}/K	Thermal Expansion, Predicted, 10^{-6}/K	Reference No.
160.0	14.00000	14.00000	54
163.0	14.20000	14.10000	53
169.0	14.30000	14.30000	13
170.0	14.40000	14.30000	54
170.0	14.40000	14.30000	47
173.0	14.50000	14.40000	53
180.0	14.70000	14.60000	54
170.0	14.70000	14.60000	47
180.0	14.70000	14.60000	57
163.0	14.70000	14.60000	58
183.0	14.80000	14.70000	53
187.0	14.90000	14.90000	49
190.0	15.00000	14.90000	54
190.0	15.00000	14.90000	53
160.0	14.90000	14.90000	47
240.0	15.30000	15.20000	48
260.0	15.20000	15.20000	54
256.0	15.10000	15.20000	47
260.0	15.40000	15.20000	13
200.0	15.20000	15.20000	57
200.0	15.00000	15.20000	58
203.0	15.30000	15.30000	53
207.0	15.40000	15.40000	13
210.0	16.40000	15.40000	57
243.0	15.60000	15.60000	53
220.0	15.60000	15.70000	54
226.0	15.60000	15.70000	57
220.0	15.60000	15.70000	58
223.0	15.60000	15.70000	53
256.0	15.70000	15.90000	49
260.0	15.80000	15.90000	54
233.0	15.80000	15.90000	53
240.0	15.90000	16.00000	54
240.0	15.00000	15.20000	57
240.0	16.00000	15.60000	58
243.0	16.00000	16.10000	53
253.0	16.10000	16.20000	48
250.0	16.10000	15.20000	54
253.0	16.10000	16.20000	53
256.0	15.00000	16.30000	49
260.0	16.20000	16.30000	54
250.0	16.30000	16.30000	57
253.0	16.30000	16.40000	53
270.0	16.40000	16.30000	54
273.0	16.40000	16.50000	53
243.0	16.40000	16.50000	57
260.0	16.50000	16.60000	54
256.0	16.70000	16.50000	48
280.0	16.50000	16.50000	57
283.0	16.50000	16.50000	53
283.0	16.40000	16.50000	56

Table 7.5, continued

Test Temperature, K	Thermal Expansion, Measured, 10^{-6}/K	Thermal Expansion, Predicted, 10^{-6}/K	Reference No.
286.0	16.60000	16.50000	49
290.0	16.60000	16.60000	54
293.0	16.60000	16.60000	53
293.0	16.60000	16.60000	57
295.0	16.80000	16.60000	46
300.0	16.40000	16.60000	48
300.0	16.70000	16.60000	54
300.0	16.70000	16.60000	13
300.0	16.70000	16.60000	57

Table 7.6. Calculated Values of the Thermal Expansion Coefficient [Equation (7-3)] (4–300 K).

Test Temperature, K	Thermal Expansion Coefficient, Predicted, 10^{-6}/K
4	0.00239
5	0.00475
6	0.00775
7	0.0116
6	0.0165
5	0.0228
12	0.0862
11	0.0408
12	0.0531
13	0.0681
14	0.0862
15	0.108
16	0.498
17	0.162
14	0.195
13	0.233
20	0.276
21	0.324
20	0.376
23	0.899
24	0.498
29	0.567
29	0.642
27	0.722
28	0.808
29	0.899
30	0.995
39	1.10
38	1.20
39	1.31
38	1.43
35	1.55
38	1.68
37	1.81
38	1.94
39	2.65
·6	2.22
17	2.96
12	2.51
13	2.65
·6	2.51
45	2.96
·6	3.11
17	3.27
·6	3.43
49	3.59
50	3.75
51	3.91
52	4.08
53	4.24
54	4.40

Test Temperature, K	Thermal Expansion Coefficient, Predicted, 10^{-6}/K
55	4.56
56	4.73
57	4.89
58	5.05
59	5.21
60	5.38
61	5.54
62	5.70
63	5.85
64	6.01
65	6.17
66	6.32
67	6.48
68	6.63
69	6.78
70	6.93
71	7.08
72	7.22
73	7.37
74	7.51
75	7.65
76	7.79
77	7.93
78	8.06
79	8.19
80	8.32
81	8.45
82	8.58
83	8.71
84	8.83
85	8.95
86	9.07
87	9.19
88	9.31
89	9.42
90	9.53
91	9.64
92	9.75
93	9.86
94	9.96
95	10.1
96	10.2
97	10.3
98	10.4
99	10.5
100	10.6
101	10.6
102	10.7
103	10.8
104	10.9
105	11.0

Test Temperature, K	Thermal Expansion Coefficient, Predicted, 10^{-6}/K
106	11.1
107	11.2
108	11.3
109	11.3
110	11.4
111	11.5
112	11.6
113	11.6
114	11.7
115	11.8
116	11.9
117	11.9
118	12.0
119	12.1
120	12.1
121	12.2
122	12.3
123	12.3
124	12.4
125	12.4
126	12.5
127	12.6
128	12.6
129	12.7
130	12.7
131	12.8
132	12.8
133	12.9
134	12.9
135	13.0
136	13.0
137	13.1
138	13.1
139	13.2
140	13.2
141	13.3
142	13.3
143	13.4
144	13.4
145	13.5
146	13.5
147	13.5
148	13.6
149	13.6
150	13.7
151	13.7
152	13.7
153	13.8
154	13.8
155	13.9
156	13.9

Table 7.6, continued

Test Temperature, K	Thermal Expansion Coefficient, Predicted, 10^{-6}/K
157	13.9
158	14.0
159	14.0
160	14.0
161	14.1
162	14.1
163	14.1
164	14.2
165	14.2
166	14.2
167	14.3
168	14.3
169	14.3
170	14.4
171	14.4
172	14.4
173	14.4
174	14.5
175	14.5
176	14.5
177	14.6
178	14.6
179	14.6
180	14.6
181	14.7
182	14.7
183	14.7
184	14.8
185	14.8
186	14.8
187	14.8
188	14.9
189	14.9
190	14.9
191	14.9
192	15.0
193	15.0
194	15.0
195	15.0
196	15.0
197	15.1
198	15.1
199	15.1
200	15.1
201	15.2
202	15.2
203	15.2
204	15.2

Test Temperature, K	Thermal Expansion Coefficient, Predicted, 10^{-6}/K
205	15.2
206	15.3
207	15.3
208	15.3
209	15.3
210	15.4
211	15.4
212	15.4
213	15.4
214	15.4
215	15.5
216	15.5
217	15.5
218	15.5
219	15.5
220	15.6
221	15.6
222	15.6
223	15.6
224	15.6
225	15.6
226	15.7
227	15.7
228	15.7
229	15.7
230	15.7
231	15.8
232	15.8
233	15.8
234	15.8
235	15.8
236	15.8
237	15.9
238	15.9
239	15.9
240	15.9
241	15.9
242	16.0
243	16.0
244	16.0
245	16.0
246	16.0
247	16.0
248	16.1
249	16.1
250	16.1
251	16.1
252	16.1

Test Temperature, K	Thermal Expansion Coefficient, Predicted, 10^{-6}/K
253	16.1
254	16.2
255	16.2
256	16.2
257	16.2
258	16.2
259	16.2
260	16.2
261	16.3
262	16.3
263	16.3
264	16.3
265	16.3
266	16.3
267	16.4
268	16.4
269	16.4
270	16.4
271	16.4
272	16.4
273	16.4
274	16.5
275	16.5
276	16.5
277	16.5
278	16.5
279	16.5
280	16.5
281	16.6
282	16.6
283	16.6
284	16.6
285	16.6
286	16.6
287	16.6
288	16.7
289	16.7
290	16.7
291	16.7
292	16.7
293	16.7
294	16.7
295	16.7
296	16.8
297	16.8
298	16.8
299	16.8
300	16.8

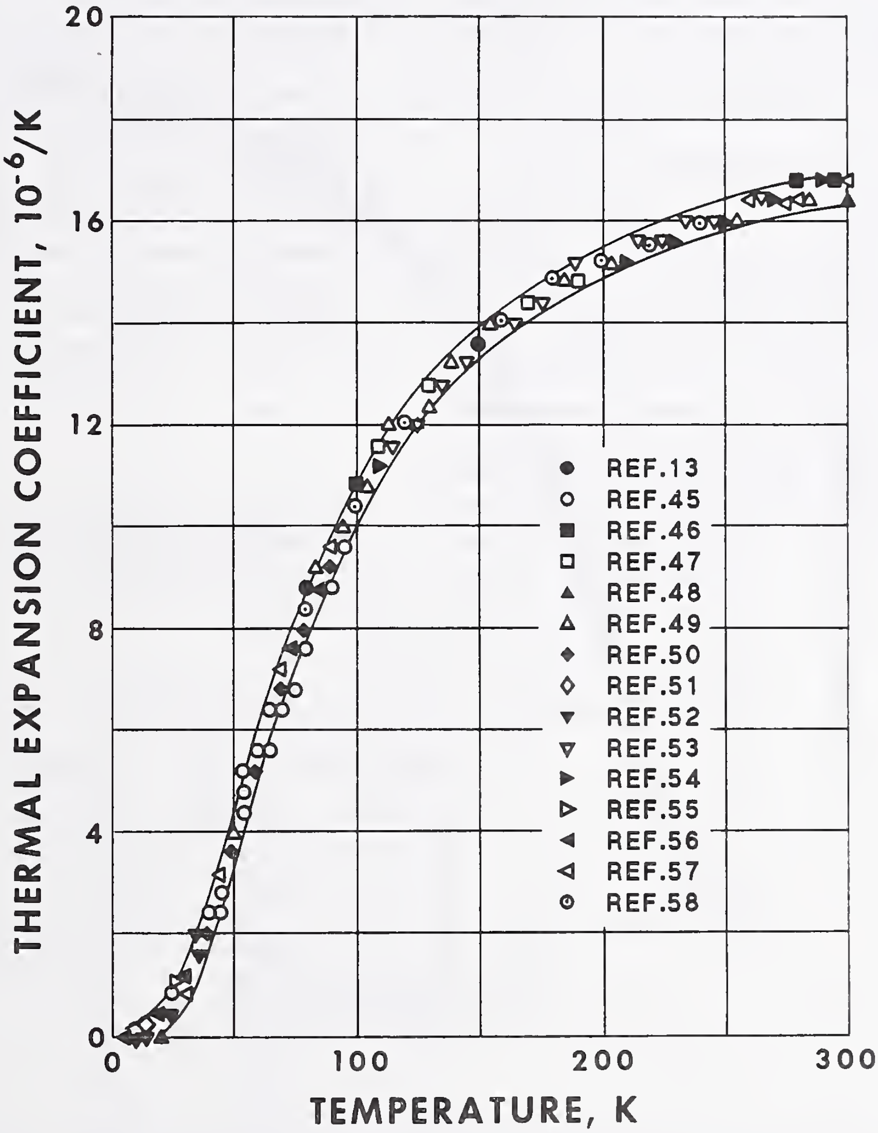

Figure 7.7. The data shown were used to compute the regression of the thermal expansion coefficient, α, upon temperature [Equation (7-3)]. For clarity, overlapping data points are omitted from the figure. All data are presented in Table 7.5.

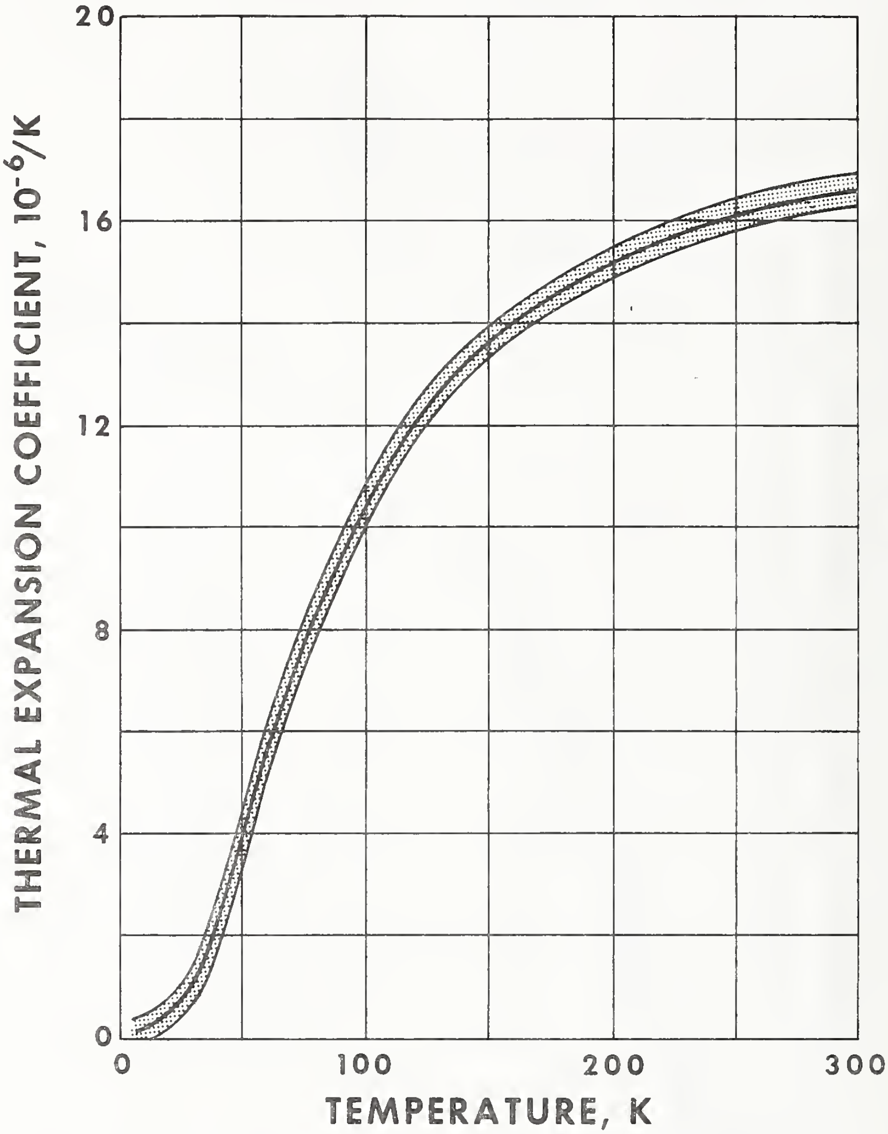

Figure 7.8. Dependence of the thermal expansion coefficient, α, upon temperature; 4–300 K. The scatter band represents two standard deviations about a sixth-order logarithmic regression equation based upon 322 measurements on annealed and cold-worked copper. The regression equation is

$$\log \alpha = -11.27 + 37.36 (\log T) - 66.59 (\log T)^2 + 63.49 (\log T)^3 - 31.49 (\log T)^4 + 7.748 (\log T)^5 - 0.7504 (\log T)^6,$$

where α has units of 10^{-6} K^{-1} and $4 \text{ K} \leq T \leq 300 \text{ K}$.

DATA SOURCES AND ANALYSIS

Measurements of the mean thermal expansion, $\Delta L/(L{\cdot}\Delta T)$, were obtained from 19 sources (References 7.8, 7.46, 7.48, 7.49, 7.53, 7.54, 7.57, and 7.60–7.71). A compilation (Reference 7.59) was used as a source of some of the data reported before 1973. A total of 338 measurements were obtained; however, many outliers near 293 K were eliminated, owing to discontinuities from the slope of the curve established at lower temperatures. ($\Delta L \equiv [L(293\text{ K}) - L(T)]$, and the experimental accuracy near 293 K is lower as ΔL decreases.) Data from Reference 7.8 were in disagreement with the trend of other data above 140 K; all values from this reference above 140 K were eliminated from the regression analysis. The total number of measurements used in the final curve fitting was 312.

RESULTS

The polynomial regression analysis carried out on the data set indicated that a satisfactory fit could be obtained with a second-order equation

$$\frac{1}{L}\frac{\Delta L}{\Delta T}\,(10^{-6}/\text{K}) = +\,11.32 + 3.933 \times 10^{-2}T - 7.306 \times 10^{-5}T^2, \qquad (7\text{-}4)$$

where T is temperature, and $\Delta L/L{\cdot}\Delta T = [L(293\text{ K}) - L(T)]/[L(293\text{ K})\,(293\text{ K} - T)]$ for $4\text{ K} \le T \le 300\text{ K}$ except that at T = 293 K, this quantity is $(1/L)(dL/dT)$. The standard deviation of the fit to this equation is 0.31×10^{-6}/K; the standard deviations of the three coefficients are 0.06; 0.084×10^{-2}, and 0.272×10^{-5}.

Table 7.7 presents the temperature, the measured values of the mean thermal expansion, the values calculated from the regression equation, and the reference number. The available characterization of materials and measurements is given in Table 7.8 at the end of the thermal properties section. Figure 7.9 indicates the fit of the data to Equation (7-4). Figure 7.10 presents these results in summary form. The scatter bands represent two standard deviations about the curve in each figure. The variance of the data was assumed to be normally distributed and constant throughout the range of the independent variable, temperature.

Table 7.7. Dependence of Mean Thermal Expansion upon Temperature (4–300 K).

Test Temperature, K	ΔL/(L·ΔT), Measured, 10^{-6}/K	ΔL/(L·ΔT), Predicted, 10^{-6}/K	Reference No.
4	11.6	11.5	69
7	11.3	11.5	57
4.2	11.9	11.5	57
5	11.8	11.5	8
6	11.9	11.8	57
7	11.8	11.5	69
8	11.4	11.8	57
14	11.3	11.7	8
12	11.9	11.8	57
12	11.8	11.8	69
12	11.9	11.8	57
14	11.8	11.5	57
16	11.9	11.8	57
18	11.3	12.0	69
12	11.9	12.0	57
20	11.8	12.1	63
20	11.9	12.1	48
20	11.9	12.1	71
20	11.7	12.1	8
20	11.9	12.1	57

C10100–C10200: Annealed; Cold-worked

Mean Thermal Expansion vs. Temperature (4–300 K)

Table 7.7, continued

Test Temperature, K	ΔL/(L·ΔT), Measured, 10^{-6}/K	ΔL/(L·ΔT), Predicted, 10^{-6}/K	Reference No.
20.3	11.8	12.1	67
23	12.4	12.2	66
24	12.8	12.8	66
25	12.2	12.6	64
25	12.1	12.8	57
25.3	12.4	12.8	49
30	12.2	12.8	66
30	12.4	12.8	48
30	12.7	12.8	8
30	12.4	12.6	64
30	12.8	12.5	66
34	12.4	12.6	64
34.5	12.8	12.6	46
30	12.6	12.6	64
40	12.6	12.8	63
40	12.4	12.6	48
40	12.7	12.8	71
70	12.5	12.8	8
40	12.8	12.8	57
70	13.9	12.6	66
43.5	12.8	12.8	49
70	13.9	12.6	64
50	13.9	13.1	63
50	13.9	13.4	64
50	13.2	13.1	48
50	13.9	13.4	8
50	13.9	13.1	57
51.5	13.9	13.4	49
52	13.3	13.2	63
50	13.9	13.2	66
52	13.4	13.1	63
50	13.5	13.4	71
50	13.9	13.1	46
50	13.9	13.4	8
60	13.9	13.1	57
60.4	13.9	13.4	49
50	13.9	13.5	66
69.5	13.9	13.7	49
70	13.3	13.1	63
70	13.9	13.4	49
70	13.6	13.7	46
40	13.9	13.7	64
40	11.8	13.8	66
75	14.0	13.4	64
77	11.8	13.5	66
78	14.0	13.4	8
79.7	11.8	14.0	49
80	14.0	14.0	63
80	14.1	14.0	71
80	13.8	14.0	46
80	14.3	14.0	8

Table 7.7, continued

Test Temperature, K	ΔL/(L·ΔT), Measured, 10^{-6}/K	ΔL/(L·ΔT), Predicted, 10^{-6}/K	Reference No.
88	14.0	14.1	57
82	14.2	14.1	69
83	14.9	14.1	61
90	14.6	14.1	68
83	14.0	14.1	49
85.7	14.9	14.1	49
87.7	14.1	14.1	61
87.7	14.9	14.2	54
83	14.1	14.1	53
90	14.2	14.3	68
88	14.7	14.1	49
90	14.9	14.3	54
88	14.1	14.1	49
90	14.0	14.3	8
90	14.0	14.1	61
90	14.9	14.3	68
83	14.8	14.3	68
90	14.9	14.3	68
83	14.0	14.1	53
94.2	14.6	14.4	61
94.8	14.9	14.4	49
100	14.7	14.5	54
100	14.1	14.1	48
100	14.6	14.5	71
100	14.8	14.1	61
100	14.9	14.5	46
100	15.0	14.5	60
100	14.2	14.5	8
103	14.7	14.5	57
100	14.7	14.5	61
103	15.0	14.1	68
100	14.7	14.5	53
100	15.0	14.1	60
100	14.9	14.5	54
100	14.8	14.1	49
100	14.9	14.1	61
100	14.8	14.5	53
100	14.9	14.5	54
100	14.5	14.1	48
100	14.7	14.5	8
100	15.0	14.1	60
100	15.3	14.1	68
113	14.7	14.5	68
119	14.9	14.4	53
100	15.0	14.5	60
100	15.2	14.9	60
117	15.0	14.1	49
119	14.8	15.0	61
119	15.2	15.0	61
120	15.0	15.0	54
120	14.6	15.0	46

Table 7.7, continued

Test Temperature, K	ΔL/(L·ΔT), Measured, 10^{-6}/K	ΔL/(L·ΔT), Predicted, 10^{-6}/K	Reference No.
120	14.9	15.0	8
121	15.3	15.4	61
121	15.3	15.4	60
121	15.3	15.6	61
122	15.1	15.4	60
123	15.5	15.6	61
123	15.1	15.4	60
125	15.2	15.4	61
126	15.2	15.4	60
125	15.5	15.2	61
129	15.2	15.2	49
130	15.0	15.2	63
130	15.2	15.2	71
130	15.3	15.2	61
130	15.5	15.2	8
131	15.3	15.2	61
133	15.5	15.2	60
133	15.4	15.3	61
133	15.1	15.3	66
133	15.2	15.3	61
133	15.3	15.3	60
136	15.3	15.3	61
137	15.5	15.3	60
139	15.5	15.4	61
140	15.4	15.4	60
140	15.3	15.4	61
146	15.1	15.4	8
140	15.3	15.4	57
142	15.4	15.4	61
140	15.4	15.4	49
143	15.5	15.4	66
143	15.4	15.4	63
146	15.1	15.6	60
150	15.3	15.6	63
151	15.5	15.6	60
150	15.3	15.6	48
153	15.5	15.6	54
150	15.3	15.6	61
151	15.1	15.6	60
150	15.4	15.6	61
153	15.1	15.6	60
150	15.5	15.6	61
153	15.5	15.6	53
150	15.3	15.6	49
154	15.5	15.6	60
155	15.4	15.4	61
153	15.9	15.4	60
157	15.3	15.4	61
158	15.9	15.7	60
160	15.5	15.7	71
160	15.6	15.7	54

Table 7.7, continued

Test Temperature, K	ΔL/(L·ΔT), Measured, 10^{-6}/K	ΔL/(L·ΔT), Predicted, 10^{-6}/K	Reference No.
168	15.9	16.1	54
161	15.7	15.9	61
163	15.9	15.9	66
163	15.8	16.2	53
168	14.9	15.9	66
163	15.8	16.2	61
168	15.9	15.9	60
163	15.8	16.2	61
163	15.7	15.9	49
170	15.8	16.2	53
173	16.1	15.9	54
170	15.8	15.9	61
173	15.9	15.9	64
173	15.8	16.2	60
173	15.9	15.9	66
173	15.8	16.2	63
173	15.8	15.9	60
170	15.8	16.0	61
176	15.9	15.9	64
176	16.1	16.2	61
173	16.1	15.9	60
163	15.0	16.2	61
160	15.9	15.9	54
180	15.8	15.9	61
183	15.9	16.1	64
180	15.8	16.1	53
183	15.2	16.1	66
180	15.8	16.1	61
187	16.1	16.1	64
168	15.8	16.1	49
196	15.9	15.9	62
189	15.2	16.1	60
193	16.1	16.2	64
190	15.8	16.2	60
193	15.9	16.2	54
163	16.1	16.2	61
193	15.9	16.2	66
163	15.8	16.2	63
193	15.9	16.2	64
163	16.1	16.2	61
196	15.9	16.2	53
199	16.1	16.2	60
196	16.1	16.2	64
200	16.1	16.3	61
200	16.1	15.9	64
200	15.0	16.2	48
200	15.9	16.3	71
200	15.0	16.1	61
200	16.0	16.3	57
203	16.0	16.3	53
205	16.4	16.3	60

Table 7.7, continued

Test Temperature, K	ΔL/(L·ΔT), Measured, 10^{-6}/K	ΔL/(L·ΔT), Predicted, 10^{-6}/K	Reference No.
220	16.3	16.3	54
230	16.1	16.3	49
220	16.4	16.3	60
213	16.7	16.4	63
240	16.3	16.4	54
211	16.6	16.4	60
246	16.4	16.4	54
213	16.1	16.4	61
213	16.7	16.4	68
213	16.1	16.4	63
213	16.7	16.4	60
211	16.1	16.4	61
246	16.6	16.4	60
223	16.2	16.4	61
220	16.2	16.4	68
220	16.3	16.4	61
221	16.3	16.4	60
223	16.7	16.5	61
220	16.7	16.5	68
220	16.6	16.5	61
229	16.7	16.5	68
230	16.3	16.5	49
230	16.4	16.5	63
230	16.6	16.5	61
220	16.7	16.5	60
230	16.6	16.5	65
233	17.0	16.5	68
233	16.2	16.5	68
230	16.3	16.5	60
230	16.7	16.5	61
230	16.4	16.5	60
230	16.6	16.5	61
230	16.4	16.5	60
213	16.2	16.5	61
240	16.4	16.5	54
240	16.3	16.5	61
246	16.4	16.5	60
244	17.2	16.5	61
246	16.4	16.5	60
246	16.9	16.5	61
249	16.1	16.6	60
250	17.2	16.5	61
250	16.7	16.5	60
250	16.3	16.5	61
250	16.3	16.5	48
250	16.3	16.5	71
250	16.4	16.5	54
250	17.0	16.5	61
253	17.0	16.6	66
253	16.3	16.6	68
253	16.5	16.6	53

Table 7.7, continued

Test Temperature, K	ΔL/(L·ΔT), Measured, 10^{-6}/K	ΔL/(L·ΔT), Predicted, 10^{-6}/K	Reference No.
256	16.6	16.6	49
259	17.0	16.6	61
265	16.9	16.6	61
259	16.5	16.6	61
265	16.9	16.6	54
250	16.5	16.6	57
262	17.0	16.6	57
259	16.3	16.6	53
265	17.0	16.6	54
259	17.7	16.6	57
270	16.9	16.6	54
273	16.5	16.6	61
270	17.8	16.6	54
273	16.5	16.6	61
273	17.0	16.6	66
273	16.5	16.6	57
273	16.9	16.6	53
273	16.5	16.6	57
273	17.0	16.6	54
273	16.5	16.6	57
270	17.0	16.6	54
277	17.0	16.6	61
265	16.9	16.6	54
250	16.5	16.6	46
265	16.9	16.6	54
281	17.0	16.6	61
273	17.0	16.6	53
259	16.3	16.6	49
290	16.7	16.6	54
265	17.0	16.6	57
300	15.7	16.6	54
300	15.7	16.6	61
300	15.7	16.6	49
300	16.6	16.6	71
300	17.1	16.6	54
300	16.3	16.6	57
301	16.3	16.5	70

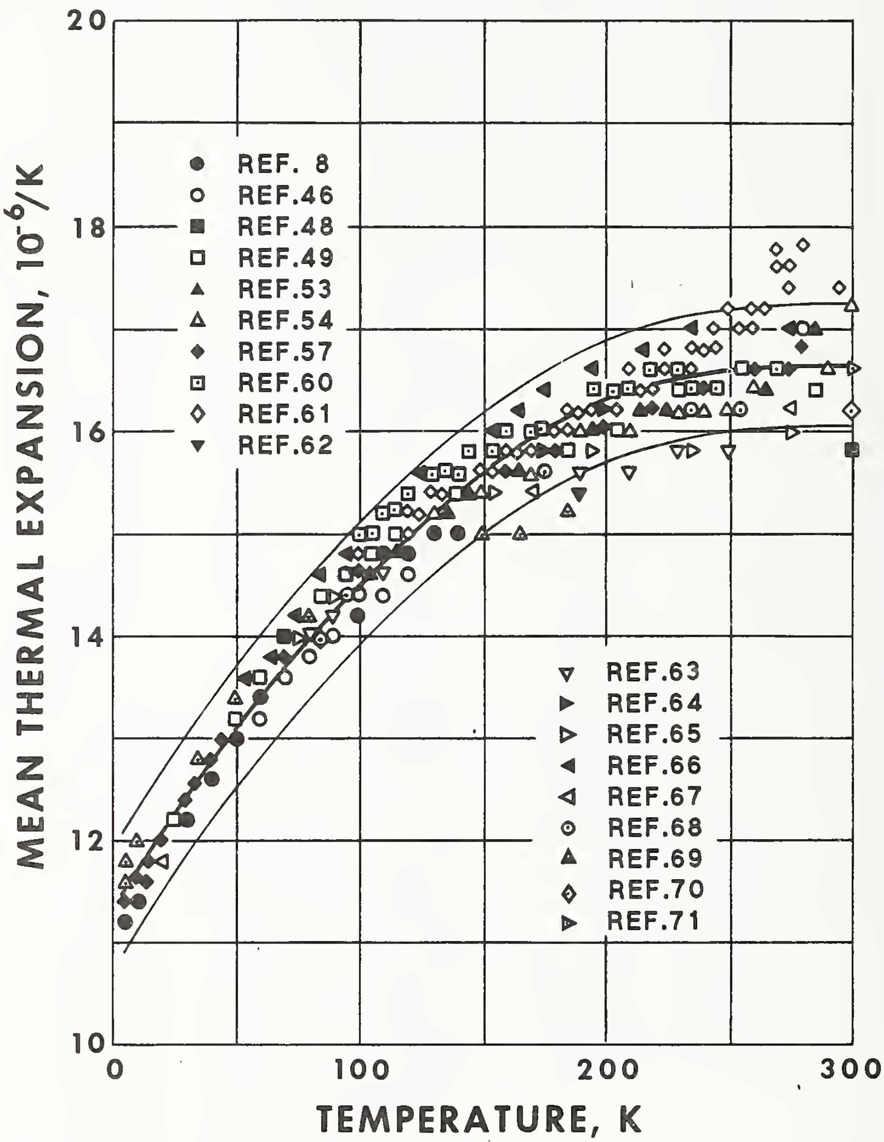

Figure 7.9. The data shown were used to compute the regression of the mean thermal expansion, $\Delta L/L{\cdot}\Delta T$, upon temperature [Equation (7-4)]. For clarity, overlapping data points are omitted from the figure. All data are presented in Table 7.7.

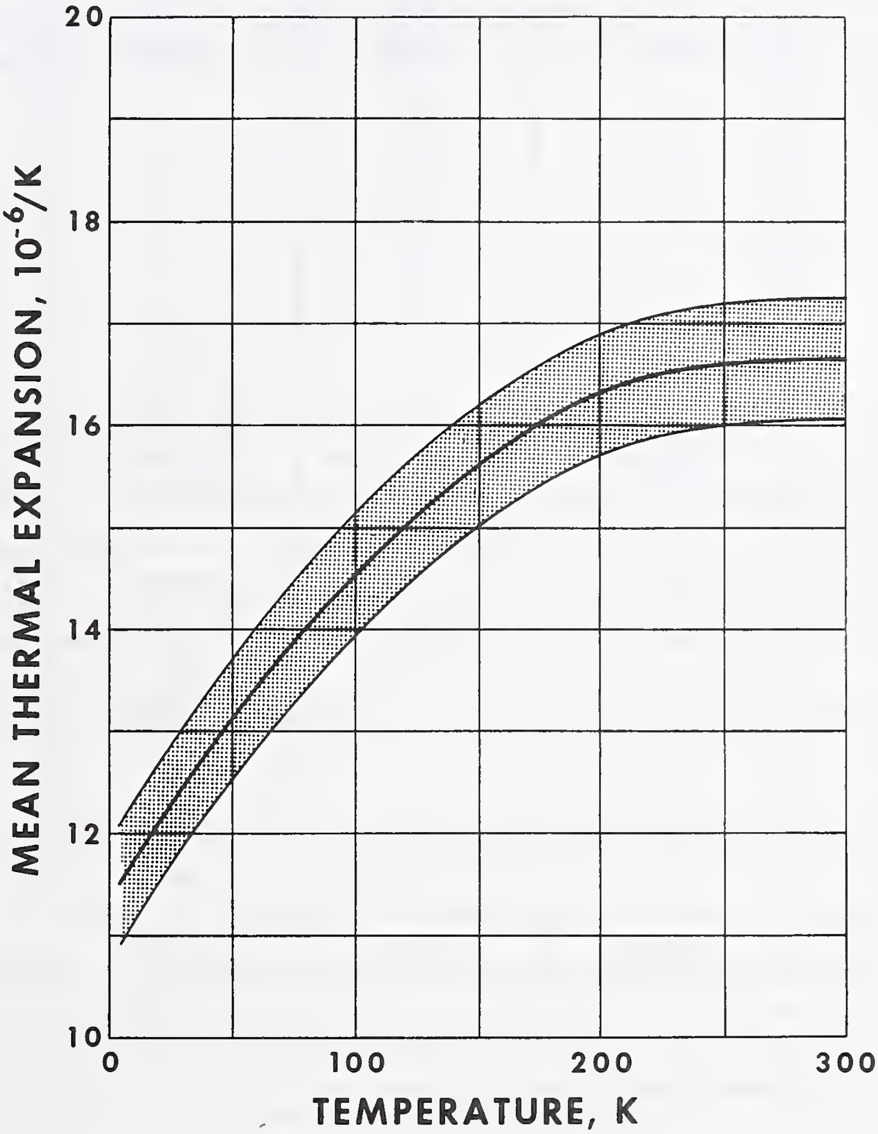

Figure 7.10. Dependence of the mean thermal expansion, $\Delta L/(L \cdot \Delta T)$, upon temperature; 4–300 K. The scatter band represents two standard deviations about a second-order regression equation based upon 312 measurements on annealed and cold-worked copper. The equation is

$$\frac{1}{L}\frac{\Delta L}{\Delta T}\ (10^{-6}/\mathrm{K}) = 11.32 + 3.933 \times 10^{-2}T - 7.306 \times 10^{-5}T^2,$$

where $\Delta L/(L \cdot \Delta T) = [L(293\ \mathrm{K}) - L(T)]/[L(293\ \mathrm{K})\ (293\ \mathrm{K} - T)]$ for $4\ \mathrm{K} \le T \le 300\ \mathrm{K}$ except that at $T = 293$ K, this quantity is $(1/L)(dL/dT)$.

Table 7.8. Characterization of Materials and Measurements.

Reference No.	1A	1B	1C	2A
Specification	C10100	C10100	C10200	C10100
Composition (wt%)				
Cu	99.999	99.999	—	99.999
Ag	—	—	—	—
Cu + Ag	—	—	—	—
O_2	—	—	—	—
Bi	—	—	—	—
P	—	—	—	—
Pb	—	—	—	—
S	—	—	—	—
Se	—	—	—	—
Te	—	—	—	—
Others (Only ≥ 0.001 wt%)	—	—	Mg: < 0.0001; Si: < 0.0001	—
Material Condition	Annealed, vacuum (a)	Cold-worked below 295 K (b)	Cold-rolled	Annealed, 923 K, 3.5 h, vacuum
RRR	—	—	—	—
Grain Size	—	—	50 μm	—
Hardness	—	—	—	45 (c)
Product Form	—	—	Bar, 0.582-cm-dia.	—
Specimen Mass	65 g	71 g	71 g	387 g
Width or Dia.	—	—	—	—
Thickness	—	—	—	—
Length	—	—	—	—
No. of Measurements	40	38	38	70
Test Temperature	20–300 K	20–300 K	20–300 K	1.3–20 K

(a) Measured in "as cast" condition. Specimen was large crystal with much smaller crystals at edges.
(b) Reduction in area of 33%, machined without specimen heating. Average strain in specimen ~ 0.2%, determined by x-ray analysis.
(c) Diamond pyramid, determined with 0.2-kg load.

2B	3	4	5	6
C10100	C10100	C10200	C10200 (d)	C10200
99.999	99.999	—	—	99.9
—	—	—	—	—
—	—	—	—	—
—	—	—	—	—
—	—	—	—	—
—	—	—	—	—
—	—	—	—	—
—	—	—	—	—
—	—	—	—	—
—	—	—	—	—
—	—	—	—	—
Swaged, 28% reduction of area	Annealed, 1173 K, 8 h, vacuum (b)	—	Annealed, 673 K, 1 h (d)	—
—	5	—	—	6
—	5	—	15 μm (d)	6
102 (a)	—	—	—	6
—	—	—	—	—
310 g	60 g	—	—	878 g
—	—	—	—	—
—	—	—	—	—
—	—	—	—	—
30	27 (c)	12 (below 300 K)	28	20
1.3–20 K	—	77–1357 K	30–200 K	1.2–20 K

(a) Diamond pyramid, determined with 0.2-kg load.
(b) $R_{300\ K}/R_{4\ K}$ = 550.
(c) Number of values reported from a smoothed curve derived from several sets of measurements.
(d) It is unclear whether the total specific heat reported was obtained with this specimen (used for a determination of the dilatational specific heat) or represents other unpublished specific heat data also obtained at the University of California.

Table 7.8, continued

Reference No.	—	8	8	10
Specification	C10200	C10200	C10100	C10200
Composition (wt%)				
Cu	99.96	—	99.999	—
Ag	0.001–0.01	—	not detected	—
Cu + Ag	—	—	—	—
O_2	—	—	—	—
Bi	< 0.001	—	not detected	—
P	—	—	—	—
Pb	< 0.001	—	not detected	—
S	—	—	< 0.0001	—
Se	—	—	< 0.0001	—
Te	—	—	not detected	—
Others (Only ≥ 0.001 wt%)	Sb: 0.001–0.01; Ca, Fe, Mg, Ni, Si: < 0.001	—	—	—
Material Condition	Annealed	Annealed	Machined after vacuum casting	Annealed, 673 K, 16 h, vacuum
RRR	—	—	—	—
Grain Size	—	—	—	—
Hardness	—	—	—	—
Product Form	—	—	—	Wire
Specimen				
Type/Mass	—	—	143 g	604 g
Width or Dia.	—	—	—	—
Thickness	—	—	—	—
Length	—	—	—	—
No. of Measurements	19	36	17 (above 4 K) (a)	15
Test Temperature	5–298 K	4.3–17.1 K	0.4–30 K	53–293 K

(a) Two or more series of measurements made; 17 values reported from a smoothed curve derived from all measurements.

11	12	13	21	22
C10100	C10200	C10200	C10100	C10100
99.999 0.00034 (a) — — — — — — — — — Fe: 0.00002 (a)	99.96 — — — — — — — — — —	— — — — — — — — — — —	99.999 — — — — — — — < 0.0001 < 0.0002 —	99.999 — — — — — — — — — —
Cast, machined, etched	Cast, annealed, ~ 120 h, N_2	—	Annealed, 803 K, several h, vacuum	Annealed, 673 K, 2 h
—	—	—	1781	1530
—	—	—	—	—
—	—	—	—	—
Bar	—	—	Bar	Bar
242 g — — —	825 g — — —	— — — —	Wire 0.076 cm — 8 cm	Cylinder 0.18 cm — —
62 (below 300 K)	57	—	12	24
15–380 K	15–300 K	4–300 K	2–55 K	4–105 K

(a) Average content of a similar specimen, from neutron activation analysis.

Table 7.8, continued

Reference No.	23A	23B	24	25
Specification	C10100	C10500	C10100	C10100
Composition (wt%)				
Cu	99.999	99.97	99.999	99.9988
Ag	—	0.034	~ 0.0005	~ 0.0005
Cu + Ag	—	—	—	—
O_2	—	—	—	—
Bi	—	—	—	—
P	—	—	—	—
Pb	—	—	~ 0.004	—
S	—	—	—	—
Se	—	—	—	—
Te	—	—	—	—
Others (Only ≥ 0.001 wt%)	—	—	—	Ni: < 0.0003; Pb: < 0.0004
Material Condition	Annealed	Annealed	Annealed, 823 K, 3 h, vacuum (a)	Annealed, 723 K, 6 h
RRR	1450	400	339 (b)	280
Grain Size	—	—	—	—
Hardness	—	—	—	—
Product Form	—	—	Bar	Bar
Specimen Type	—	—	Cylinder	Wire
Width or Dia.	—	—	0.1 or 0.2 cm	0.11 cm
Thickness	—	—	—	—
Length	—	—	5 cm	—
No. of Measurements	—	—	27 (annealed)	37
Test Temperature	4–120 K	4–120 K	2–160 K	2–90 K

(a) Two other specimens tested in "as drawn" condition.
(b) The "as drawn" specimens had RRR's of 27 and 30.

26	27	28	29	30A
C10200	C10100	C10100	C11000	C10200
—	99.999	—	—	99.98
—	—	< 0.0001	—	—
—	—	—	—	—
—	—	0.0013	—	0.0013
—	—	< 0.00005	—	—
—	—	—	—	—
—	—	0.0008	—	0.0008
—	—	—	—	—
—	—	—	—	—
—	—	—	—	0.0001
—	—	Ni: 0.0007	—	Ni: 0.0007
Annealed, 923 K, 1 h (etched before anneal)	Annealed	—	Annealed, 803 K, 3 h	Annealed, 1033 K, 0.28 h
250	—	—	270	—
—	—	—	—	~ 50 μm
—	—	—	—	54 Brinnell D.P.H.
Bar	Bar	—	—	Sintered Bar
Cylinder up to 3 cm — 23 cm	Cylinder 0.1–0.2 cm — 5 cm	Cylinder 0.37 cm — 23 cm	Foil — 0.005 cm —	Cylinder 0.37 cm — —
58 (runs)	21	—	24	—
4–300 K	2–40 K	4–300 K	0.45–1.5 K	4–273 K

Table 7.8, continued

Reference No.	30B	30C	31A	31B
Specification	C11000	Cu-Te	C10200	C10200
Composition (wt%)				
Cu	—	99.43	99.98	99.96
Ag	0.001	0.001	—	—
Cu + Ag	—	—	—	—
O_2	—	—	—	—
Bi	—	—	—	—
P	—	0.007	—	—
Pb	—	< 0.001	—	—
S	—	—	—	—
Se	—	—	—	—
Te	—	0.56	—	—
Others (Only ≥ 0.001 wt%)	Fe: 0.01; Ag: 0.001; Zn: 0.001	Fe: 0.001; Si: 0.001; Zn: 0.001	Ge: 0.02	Fe: 0.0043
Material Condition	As received	Hard temper	Annealed	Annealed
RRR	—	—	18 (a)	38
Grain Size	~ 40 μm	~ 37 μm	—	—
Hardness	124 Brinnell D.P.H.	133 Brinnell D.P.H.	—	—
Product Form	Bar	Bar	Bar	Bar
Specimen Type	Cylinder	Cylinder	Cylinder	Cylinder
Width or Dia.	—	—	0.1–0.2 cm	0.1–0.2 cm
Thickness	—	—	—	—
Length	—	—	6 cm	6 cm
No. of Measurements	—	—	27	33
Test Temperature	4–273 K	4–273 K	2–140 K	2–140 K

(a) This specimen identification appears to be interchanged with that of 36B in one of the figures in this reference.

32	33	34	35	36
C10200	C10100	C10100	C10100	C10100 (c)
—	99.999	—	99.99	—
—	—	—	—	—
—	—	—	—	—
—	—	—	0.001	—
—	—	—	—	—
—	—	—	—	—
—	—	—	0.001	—
—	—	—	—	—
—	—	—	—	—
—	—	—	0.001	—
—	—	—	—	—
—	—	Annealed, 1223 K, 6 h	Soldered at 433 K	—
—	900	45	55	—
—	574 μm	—	—	—
—	—	—	—	—
Bar	—	Plate	Bar	Bar
Cylinder 1.3 cm — 51 cm	Cylinder — — —	(b) ~ 1 cm 0.025 cm ~ 7 cm	Cylinder 0.11 cm — 2.5 cm	Wire 0.3 cm — —
27	18 (a)	38	24	14 and 20
23–245 K	85–400 K	4–50 K	3–35 K	0.2–0.7 K

(a) Number of values reported from a smoothed curve.
(b) See Fig. 1 of Reference 7.21 for specimen geometry.
(c) Impurities to < 10 ppm in 2 specimens tested.

Table 7.8, continued

Reference No.	37	38	39	40
Specification	C10100 (a)	C11000	C10100	C10200
Composition (wt%)				
Cu	99.999	—	99.99	—
Ag	—	—	—	—
Cu + Ag	—	—	—	—
O_2	—	—	—	—
Bi	—	—	—	—
P	—	—	—	—
Pb	—	—	—	—
S	—	—	—	—
Se	—	—	—	—
Te	—	—	—	—
Others (Only ≥ 0.001 wt%)	—	—	—	—
Material Condition	Annealed, 973 K, 2 h	Cold-drawn	—	—
RRR	900	—	—	—
Grain Size	—	—	—	—
Hardness	—	—	—	—
Product Form	Bar	—	—	Bar
Specimen Type	Cylinder	Cylinder	—	Cylinder
Width or Dia.	1.9 cm	1.9 cm	—	1.27 cm
Thickness	—	—	—	—
Length	20 cm	15 cm	—	10 cm
No. of Measurements	43	—	—	7
Test Temperature	300–1250 K	297–1311 K	320–723 K	323–873 K

(a) Impurities to < 0.5 ppm.

41	42	43A	43B	44A
C10200	—	C10200	C10100	C10200 (a)
99.9 — — — — — — — — — —	— — — — — — — — — — Zr: 0.20; Ni: 0.002; Fe: 0.002	— — — — — — — — — — —	— — — — — — — — — — —	— — — — — — — — — — —
Annealed	Annealed, 693 K	Annealed, 1123 K, 1 h, vacuum	Annealed, 1123 K, 1 h, vacuum	—
—	—	107	1520	62
—	—	—	—	—
—	—	—	—	—
Bar	—	—	—	Wire
Cylinder 1.9 cm — —	Cylinder 0.64 cm — 37 cm	Cylinder 0.25 cm — 2.3 cm	Cylinder — — 2.3 cm	Wire — — —
18	26	5 per magnetic field	5 per magnetic field	10
367–898 K	373–923 K	5–20 K	5–21 K	4 K

(a) Estimated from RRR.

Table 7.8, continued

Reference No.	44B	46	46	47
Specification	C10100 (a)	C10200	C10100	C10100 (b)
Composition (wt%)				
Cu	—	99.9	99.999	99.999
Ag	—	—	—	—
Cu + Ag	—	—	—	—
O_2	—	—	—	—
Bi	—	—	—	—
P	—	—	—	—
Pb	—	—	—	—
S	—	—	—	—
Se	—	—	—	—
Te	—	—	< 0.0002	—
Others (Only ≥ 0.001 wt%)	—	—	—	—
Material Condition	—	Annealed, 573 K, 4 h, vacuum	Annealed, 773 K, several h	Annealed, 823 K, 3 h, Ar, FC
RRR	103	—	—	—
Grain Size	—	—	—	—
Hardness	—	—	—	—
Product Form	Wire	—	Bar	—
Specimen Type	Wire	Cylindrical tube	Cylinder	Cylinder
Width or Dia.	—	2.54 cm	1.8 cm	1.1 cm
Thickness	—	0.48	—	—
Length	—	5.08 cm	—	6 cm
No. of Measurements	11	25	23	68
Test Temperature	4 K	20–93 K	5–295 K	10–200 K

(a) Estimated from RRR.
(b) Total metallic impurity level < 10 ppm.

48	49	50	51	52
C10200	C10200	C10200	C10100	C10100
—	—	—	99.999	99.99
—	—	—	0.004	< 0.0005
—	—	—	—	—
—	—	—	—	—
—	—	—	—	—
—	—	—	—	—
—	—	—	0.0001	0.003
—	—	—	—	—
—	—	—	—	—
—	—	—	—	—
—	—	—	—	Sn: 0.002
Annealed	—	—	—	Annealed, 623 K, 48 h
—	—	—	—	—
—	—	—	—	—
—	—	—	—	—
—	Bar	—	—	Bar
Cylindrical tube	—	—	Cylinder	Cylinder
—	—	—	0.7 cm	0.50 cm
—	—	—	—	—
—	—	—	10 cm	8.14 cm
~ 60	20	—	~ 250	~ 90
20–300 K	25–295 K	2–110 K	4–15 K	6–55 K

Table 7.8, continued

Reference No.	53	54	55A	55B
Specification	(a)	C10100	C10100	C10100
Composition (wt%)				
Cu	—	99.99	99.999	99.999
Ag	—	—	< 0.0002	< 0.00001
Cu + Ag	—	—	—	—
O_2	—	—	0.003	0.001
Bi	—	—	—	—
P	—	—	—	—
Pb	—	—	—	—
S	—	—	0.003	< 0.0001
Se	—	—	—	—
Te	—	—	—	—
Others (Only ≥ 0.001 wt%)	—	—	C: 0.002; W: 0.012; Zn: 0.008	C: 0.021; W: 0.003
Material Condition	Annealed, vacuum (b)	Annealed, 1073 K, vacuum	Vacuum cast	Cast in graphite
RRR	—	—	560	730
Grain Size	—	—	—	—
Hardness	—	—	—	—
Product Form	—	—	—	—
Specimen Type	Cylinder	Cylinder	Cylinder	Cylinder
Width or Dia.	(a)	—	0.6 cm	0.8 cm
Thickness	—	—	—	—
Length	2.0 cm	2.5 cm	9.7 cm	10 cm
No. of Measurements	~ 1100	15	~ 31	~ 23
Test Temperature	88–573 K	90–230 K	1–26 K	1–30 K

(a) Eleven specimens of varying purity and dimensions were tested; averaged curve used in the present analysis.
(b) Some of the eleven specimens were not annealed.

56A	56B	57	58	[illegible]
C10100	C10200	C10100	C10100	—
99.999 (a)	—	99.999	99.999 (d)	—
—	—	—	—	—
—	—	—	—	—
—	—	0.0004	—	—
—	—	—	—	—
—	—	—	—	—
—	—	—	—	—
—	—	—	—	—
—	—	—	—	—
—	—	—	—	—
—	—	Si: 0.001	—	—
Annealed, 773 K, vacuum	Annealed, ~ 673 K	Annealed, 573 K, 1 h, vacuum	—	As cut from rail
—	—	600–1500	—	—
—	—	—	—	—
—	—	—	—	—
—	—	Bar (c)	—	Rail
Cylinder 1.9 cm — 5.1 cm	Cylinder 1.9 cm — 5.1 cm	Cylinder — — 10.2 cm	— — — —	— — — 1.9 cm
(b)	(b)	101	~ 26	58
2–283 K	2–283 K	3–320 K	10–240 K	80–360 K

(a) Total of < 10 ppm impurities.
(b) A total of ~ 200 measurements on specimens 50A and 50B were averaged. The mean values were used in the present analysis.
(c) Ingot from which bar was machined was electron-beam melted in vacuum.
(d) Total impurity content < 5 ppm.

Table 7.8, continued

Reference No.	61	62	63	64
Specification	C10200	C10200	C10200	C10100
Composition (wt%)				
Cu	99.979	—	99.98	99.999
Ag	—	—	—	—
Cu + Ag	—	—	—	—
O_2	0.02	—	—	—
Bi	—	—	—	—
P	—	—	—	—
Pb	—	—	—	—
S	—	—	—	—
Se	—	—	—	—
Te	—	—	—	—
Others (Only ≥ 0.001 wt%)	—	—	—	—
Material Condition	Annealed	—	—	—
RRR	—	—	—	—
Grain Size	—	—	—	—
Hardness	—	—	—	—
Product Form	Bar	—	—	—
Specimen Type	—	—	Cylinder	Cylinder
Width or Dia.	—	—	—	0.64 cm
Thickness	—	—	—	—
Length	0.6 cm	—	2 cm	7.6 cm
No. of Measurements	141	—	—	11
Test Temperature	77–773 K	83–188 K; 298–363 K	20–273 K	4–300 K

65	66	67	68	69
C10200	C10100	C10200	C10200	C10200
99.968	99.999	—	99.9	—
—	—	—	—	—
—	—	—	—	—
—	—	—	—	—
—	—	—	—	—
—	—	—	—	—
—	—	—	—	—
—	—	—	—	—
—	—	—	—	—
—	—	—	—	—
Sb: 0.015; Fe: 0.010; S: 0.007	—	—	—	—
Annealed, 653 K, 4 h	—	—	—	Annealed
—	—	—	—	—
—	—	—	—	—
—	—	—	—	—
Bar	—	Tube	Tube	—
Cylinder 0.5 cm — 10 cm	Cylinder 0.62 cm — 10.16 cm	Cylinder — — 94 cm (a)	Cylindrical tube — — 0.97 cm	Cylinder 0.44 cm — 3.8 cm
~ 10	37	4	10	13
77–273 K	18–573 K	20–374 K	103–283 K	2–300 K

(a) Length of inner vacuum vessel constructed from electrolytic copper. Thermal expansion measured at atmospheric pressure.

Table 7.8, continued

Reference No.	70	71
Specification	C10200	C10100
Composition (wt%)		
Cu	—	99.99 (a)
Ag	—	—
Cu + Ag	—	—
O_2	—	—
Bi	—	—
P	—	—
Pb	—	—
S	—	—
Se	—	—
Te	—	—
Others (Only ≥ 0.001 wt%)	—	—
Material Condition	—	Annealed, 811 K
RRR	—	63
Grain Size	—	—
Hardness	—	—
Product Form	Bar	Bar
Specimen Type	Bar	Cylinder
Width or Dia.	2.5 cm	0.64 cm
Thickness	1.5 cm	—
Length	12 cm	1 cm
No. of Measurements	8	~ 50 for each of 5 specimens
Test Temperature	82–1207 K	20–800 K

(a) Estimated from RRR. About 0.012 wt% dissolved impurities estimated.

REFERENCES

1. Martin, D. L., "The Specific Heat of Copper from 20° to 300 °K," Canadian Journal of Physics 38, 17–24 (1960).

2. Ahlers, G., "Heat Capacity of Copper," Review of Scientific Instruments 37, 477–480 (1966).

3. Holste, J. C., Cetas, T. C., and Swenson, C. A., "Effects of Temperature Scale Differences on the Analysis of Heat Capacity Data: The Specific Heat of Copper from 1 to 30 K," The Review of Scientific Instruments 43, 670–676 (1972).

4. Chang, Y.-S. A., "Dilation Contribution to Heat Capacity of Metals and Alloys," Ph.D. Thesis, University of California, 79 pp. (1963).

5. Dockerty, S. M., "The Specific Heat of Copper From 30° to 200 °K," Canadian Journal of Research 15A, 59–66 (1937).

6. Kok, J. A., and Keesom, W. H., "Measurements of the Atomic Heats of Platinum and of Copper from 1.2 to 20 °K," Physica 3, 1035–1045 (1936).

7. Sandenaw, T. A., "Heat Capacity of Copper Below 300 °K, a Test of Two Calorimeter Designs," Los Alamos Scientific Laboratory of the University of California, Los Alamos, NM, LA-2307, 19 pp. (1959).

8. Jelinek, F. J., and Collings, E. W., "Low Temperature Thermal Expansion and Specific Heat Properties of Structural Materials," in Materials Research for Superconducting Machinery--II, Eds. A. F. Clark, R. P. Reed, E. C. van Reuth, National Technical Information Service, Springfield, VA, ADA 004586 (1974).

9. Franck, J. P., Manchester, F. D., and Martin, D. L., "The Specific Heat of Pure Copper and of Some Dilute Copper + Iron Alloys Showing a Minimum in the Electrical Resistance at Low Temperatures," Proceedings of the Royal Society of London 263A, 494–507 (1961).

10. Maier, C. F., and Anderson, C. T., "The Disposition of Work Energy Applied to Crystals," Journal of Chemical Physics 2, 513–527 (1934).

11. Robie, R. A., Hemingway, B. S., and Wilson, W. H., "The Heat Capacities of Calorimetry Conference Copper and of Muscovite $KAl_2(AlSi_3)O_{10}(OH)_2$, Pyrophyllite $Al_2Si_4O_{10}(OH)_2$, and Illite $K_3(Al_7Mg)(Si_{14}Al_2)O_{40}(OH)_8$ between 15 and 375 K and their Standard Entropies at 298.15 K," Journal of Research, U.S. Geological Survey 4, 631–644 (1976).

12. Giauque, W. F., and Meads, P. F., "The Heat Capacities and Entropies of Aluminum and Copper from 15 to 300 °K," Journal of the American Chemical Society 63, 1897–1901 (1941).

13. Hust, J. G., and Kirby, R. K., "Standard Reference Materials for Thermophysical Properties," in Advances in Cryogenic Engineering, Vol. 24, Eds. K. D. Timmerhaus, R. P. Reed and A. F. Clark, Plenum Press, New York, 232–239 (1978).

14. Touloukian, Y. S., and Buyco, E. H., Specific Heat--Metallic Elements and Alloys, Thermphysical Properties of Matter, Vol. 4, IFI/Plenum, New York, 51–61 (1970).

REFERENCES

15. Fisher, J. W., Lielmezs, J., Martin, D. L., Martin, J. F., Sabbah, R., and Snowdon, R. L., "C_p, Copper," in Recommended Reference Materials for the Realization of Physicochemical Properties, Blackwell Science Publications, Oxford, U.K. (1987).

16. Corruccini, R. J., "Properties of Materials at Low Temperatures (Part I)," Chemical Engineering Progress 53, 262–267 (1957).

17. Chang, Y. A., and Himmel, L., "Temperature Dependence of the Elastic Constants of Cu, Ag, and Au above Room Temperature," Journal of Applied Physics 37, 3567–3572 (1966).

18. Chang, Y. A., and Hultgren, R., "The Dilation Contribution to the Heat Capacity of Copper and α-Brass at Elevated Temperatures," The Journal of Physical Chemistry 69, 4162–4165 (1965).

19. Bevk, J., "The Effect of Lattice Defects on the Low-Temperature Heat Capacity of Copper," Philosophical Magazine 28, 1379–1390 (1973).

20. Hust, J. G., and Lankford, A. B., "Thermal Conductivity of Aluminum, Copper, Iron, and Tungsten for Temperatures from 1 K to the Melting Point," National Bureau of Standards, Boulder, CO, NBSIR 84-3007, 256 pp. (1984).

21. White, G. K., and Tainsh, R. J., "Lorenz Number for High-Purity Copper," Physical Review 119, 1869–1871 (1960).

22. Powell, R. L., Roder, H. M., and Hall, W. J., "Low-Temperature Transport Properties of Copper and Its Dilute Alloys: Pure Copper, Annealed and Cold-Drawn," Physical Review 115, 314–323 (1959).

23. Roder, H. M., Powell, R. L., and Hall, W. J., "Thermal and Electrical Conductivity of Pure Copper," in Low Temperature Physics & Chemistry, Ed. J. R. Dillinger, The University of Wisconsin Press, Madison, WI, 364–367 (1958).

24. White, G. K., "The Thermal and Electrical Conductivity of Copper at Low Temperatures," Australian Journal of Physics 6, 397–404 (1953).

25. Berman, R., and MacDonald, D. K. C., "The Thermal and Electrical Conductivity of Copper at Low Temperatures," Proceedings of the Royal Society of London 211A, 122–128 (1952).

26. Hust, J. G., and Giarratano, P. J., "Thermal Conductivity" in Semi-Annual Report on Materials Research in Support of Superconducting Machinery, National Bureau of Standards, Boulder, Colorado, NBSIR 74-393, 1–35 (1974).

27. Mendelssohn, K., and Rosenberg, H. M., "The Thermal Conductivity of Metals at Low Temperatures. I: The Elements of Groups 1, 2 and 3," The Proceedings of the Physical Society 65A, 385–394 (1952).

28. Powell, R. L., Rogers, W. M., and Coffin, D. O., "An Apparatus for Measurement of Thermal Conductivity of Solids at Low Temperatures," Journal of Research of the National Bureau of Standards 59, 349–355 (1957).

REFERNECES

29. Lindenfeld, P., Lynton, E. A., and Soulen, R., "Metallic Heat Conductivity Below 1 °K," Physics Letters 19, 265 (1965).

30. Powell, R. L., Roder, H. M., and Rogers, W. M., "Low-Temperature Thermal Conductivity of Some Commercial Coppers," Journal of Applied Physics 28, 1282–1288 (1957).

31. White, G. K., and Woods, S. B., "Thermal and Electrical Conductivities of Solids at Low Temperatures," Canadian Journal of Physics 33, 58–73 (1955).

White, G. K., and Woods, S. B., "The Lattice Thermal Conductivity of Dilute Copper Alloys at Low Temperatures," Philosophical Magazine 45, 1343–1345 (1954).

32. Powers, R. W., Schwartz, D., and Johnston, H. L., "The Thermal Conductivity of Metals and Alloys at Low Temperatures--I. Apparatus for Measurements Between 25° and 300 °K. Data on Pure Aluminum, OFHC Copper, and 'L' Nickel," Cryogenic Laboratory, Department of Chemistry, Ohio State University, Columbus, Ohio, TR 264-5, 19 pp. (1951).

33. Moore, J. P., McElroy, D. L., and Graves, R. S., "Thermal Conductivity and Electrical Resistivity of High-Purity Copper from 78 to 400 °K," Canadian Journal of Physics 45, 3849–3865 (1967).

34. Fletcher, R., "The Nernst-Ettinghausen Coefficient and the Kondo Effect in Copper and Gold," Philosophical Magazine 25, 87–95 (1972).

35. Nelson, W. E., and Hoffman, A. R., "Measurements of the Temperatures and Magnetic Field Dependence of Electrical Resistivity and Thermal Conductivity in OFHC Copper," in Thermal Conductivity 14, Eds. P. G. Klemens and T. K. Chu, Plenum Press, New York, 73–80 (1976).

36. Dupré, A., Van Itterbeek, A., and Michiels, L., "Heat Conductivity of Copper Below 1 °K," Physics Letters 8, 99–100 (1964).

37. Laubitz, M. J., "Transport Properties of Pure Metals at High Temperatures--I. Copper," Canadian Journal of Physics 45, 3677–3696 (1967).

38. Lucks, C. F, and Deem, H. W., "Thermal Properties of Thirteen Metals," American Society for Testing and Materials, Philadelphia, PA, Special Technical Publication No. 227, 29 pp. (1958).

39. Mikryukov, V. E., Vestn. Mosk. Univ., Ser. Mat., Mekh., Astron., Fiz., Khim., 11, 53–70 (1956).

40. Powell, R. W., and Tye, R. P., "New Measurements on Thermal Conductivity Reference Materials," Journal of Heat and Mass Transfer 10, 581–596 (1967).

41. Schofield, F. H., "The Thermal and Electrical Conductivities of Some Pure Metals," Proceedings of the Royal Society of London 107A, 206–227 (1925).

42. Siu, M. C. I., Carroll, W. C., and Watson, T. W., "Thermal Conductivity and Electrical Resistivity of Six Copper-Base Alloys," National Bureau of Standards, Washington, D. C., NBSIR 76-1003, 22 pp. (1976).

REFERNECES

43. Sparks, L. L., "Magnetothermal Conductivity of Selected Pure Metals and Alloys," in Materials Research for Superconducting Machinery--IV, Eds. R. P. Reed, A. F. Clark, E. C. van Reuth, National Technical Information Service, Springfield, VA, ADA 019230 (1975).

Sparks, L. L., "Magnetic Field Effect on Thermal Conductivity of Selected Metals," in Advances in Cryogenic Engineering, Vol. 24, Eds. K. D. Timmerhaus, R. P. Reed, and A. F. Clark, Plenum Press, New York, 224–231 (1978).

44. Fevrier, A., and Morize, D., "The Effect of Magnetic Field on the Thermal Conductivity and Electrical Resistivity of Different Materials," Cryogenics 13, 603–606 (1973).

45. Fraser, D. B., and Hollis Hallett, A. C., "The Coefficient of Thermal Expansion of Various Cubic Metals Below 100 °K," Canadian Journal of Physics 43, 193–219 (1965).

46. Carr, R. H., McCammon, R. D., and White, G. K., "The Thermal Expansion of Copper at Low Temperatures," Proceedings of the Royal Society of London 280, 72–84 (1964).

47. Bunton, G. V., and Weintroub, S., "A Sensitive Optical Lever Dilatometer for Use at Low Temperatures and the Thermal Expansion of Copper," Cryogenics 8, 354–360 (1968).

48. Fraser, D. B., and Hollis Hallett, A. C., "The Coefficient of Linear Expansion and Grüneisen γ of Cu, Ag, Au, Fe, Ni, and Al from 4 °K to 300 °K," in Proceedings of the VIIth International Conference on Low Temperature Physics, Eds. G. M. Graham and A. C. Hollis Hallett, University of Toronto Press, 689–692 (1961).

49. Rubin, T., Altman, H. W., and Johnston, H. L., "Coefficients of Thermal Expansion of Solids at Low Temperatures. I. The Thermal Expansion of Copper from 15 to 300 °K.," Journal of the American Chemical Society 76, 5289–5293 (1954).

50. Novikova, S. I., and Strelkov, P. G., "Thermal Expansion of Silicon at Low Temperatures," Soviet Physics--Solid State 1, 1687–1689 (1960).

51. Kos, J. F., and Lamarche, J. L. G., "Thermal Expansion of the Noble Metals Below 15 °K," Canadian Journal of Physics 47, 2509–2518 (1969).

52. Shapiro, J. M., Taylor, D. R., and Graham, G. M., "A Sensitive Dilatometer for Use at Low Temperatures," Canadian Journal of Physics 42, 835–847 (1964).

53. Lifanov, I. I., and Sherstyukov, N. G., "Thermal Expansion of Copper in the Temperature Range −185 to +300 °C," Measurement Techniques 12, 1653–1659 (1968).

54. Leksina, I. E., and Novikova, S. I., "Thermal Expansion of Copper, Silver, and Gold within a Wide Range of Temperatures," Soviet Physics--Solid State 5, 798–801 (1963).

55. McLean, K. O., Swenson, C. A., and Case, C. R., "Thermal Expansion of Copper, Silver, and Gold Below 30 K," Journal of Low Temperature Physics 7, 77–98 (1972).

56. White, G. K., and Collins, J. G., "Thermal Expansion of Copper, Silver, and Gold at Low Temperatures," Journal of Low Temperature Physics 7, 43–75 (1972).

REFERENCES

57. Kroeger, F. R., and Swenson, C. A., "Absolute Linear Thermal-Expansion Measurements on Copper and Aluminum from 5 to 320 K," Journal of Applied Physics 48, 853–864 (1977).

58. Cooper, R. F., and Yates, B., "Low Temperature Inteferometric Measurements of the Thermal Expansion of Copper and Nitralloy," Cryogenics 10, 442–444 (1970).

59. Touloukian, Y. S., Kirby, R. K., Taylor, R. E., and Desal, P. D., Thermal Expansion--Metallic Elements and Alloys, Thermophysical Properties of Matter, Vol. 12, IFI/Plenum, New York, 77–91 (1975).

60. Strelkov, P. G., and Novikova, S. I., "Silica Dilatometer for Low Temperatures. 1. Thermal Expansion of Copper and Aluminum," Pribory i Tekhnika Eksperimenta 5, 105–118 (1957).

61. Nix, F. C., and MacNair, D., "Thermal Expansion of Pure Metals: Copper, Gold, Aluminum, Nickel, and Iron," Physical Review 60, 597–605 (1941).

62. Ullrich, H.-J., "Precision Lattice Parameter Measurements by Interferences from Lattice Sources (Kossel Lines) and Divergent Beam X-Ray Diffraction (Pseudo-Kossel-Lines) in Back Reflection," Physica Status Solidi 20, K113–K117 (1967).

63. Bijl, D., and Pullan, H., "A New Method for Measuring the Thermal Expansion of Solids at Low Temperatures; the Thermal Expansion of Copper and Aluminium and the Grüneisen Rule," Physica 21, 285–298 (1955).

64. Beenakker, J. J. M., and Swenson, C. A., "Total Thermal Contractions of Some Technical Metals to 4.2 °K," The Review of Scientific Instruments 26, 1204–1205 (1955).

65. Aoyama, S., and Itô, T., "Thermal Expansion of Nickel-Copper Alloys at Low Temperatures, (Part I)," Science Reports of the Tohoku University 27, 348–364 (1939).

66. Rhodes, B. L., Moeller, C. E., Hopkins, V., and Marx, T. I., "Thermal Expansion of Several Technical Metals from −255° to 300 °C," in Advances in Cryogenic Engineering, Vol. 8, Ed. K. D. Timmerhaus, Plenum Press, New York, 278–286 (1963).

67. Keesom, W. H., Van Agt, F. P. G. A. J., and Jansen, A. F. J., "The Thermal Expansion of Copper Between +101° and −253 °C," Communications of the Kamerlingh Onnes Laboratory of the University of Leiden, Amsterdam 182A, 2–9 (1926).

68. Dorsey, H. G., "Coefficient of Linear Expansion at Low Temperatures," Physical Review 25, 88–102 (1907).

69. Sandenaw, T. A., "The Thermal Expansion of Plutonium Metal Below 300 K," Los Alamos Scientific Laboratory of the University of California, Los Alamos, New Mexico, LA-2394, 23 pp. (1960).

70. Richards, J. W., "The Over-all Linear Expansion of Three Face-centered Cubic Metals (Al, Cu, Pb) from −190 Degrees Cent. to Near Their Melting Points," Transactions of the American Society of Metals 30, 326–336 (1942).

REFERENCES

71. Hahn, T. A., "Thermal Expansion of Copper from 20 to 800 K--Standard Reference Material 736," Journal of Applied Physics 41, 5096–5101 (1970).

DATA SOURCES AND ANALYSIS

Effects of impurity elements on the electrical resistivity of high-purity copper have been measured by a number of workers. The results of the more reliable studies were summarized and averaged in Reference 8.1. This summary was used in the preparation of Figure 8.1. Table 8.1 presents the data from Reference 8.1 as well as data on some additional elements from Reference 8.2.

RESULTS

Table 8.1 gives the increase in electrical resistivity for both 10 ppm and 0.001 wt% of impurity element in solid solution in copper. Reference 8.1 may be consulted for a convenient listing of solid solubility limits of the elements in copper. Figure 8.1 gives the change in electrical resistivity per wt% of impurity element, up to 0.01 wt%. A linear relationship exists between the amount of a particular single impurity in solid solution and the increase in resistivity. (The relationship between percent impurity and electrical conductivity is hyperbolic; for simplicity, such plots are not presented here.)

DISCUSSION

Some caution must be exercised in using Figure 8.1 or Table 8.1 to predict the effect of a given level of impurity content upon the electrical resistivity, ρ. First, the numbers have an estimated uncertainty of 20 to 30%, due to inherent difficulties in making the measurements. Second, the extent to which a given impurity element increases ρ depends upon both the identity of the impurity and the metallurgical condition in which it is present. If the impurity is present in solid solution it is far more effective than if it is incorporated into a second phase. [Theory predicts that disturbances of the lattice periodicity on an atomic scale (solid solution) are more effective in scattering electrons than perturbations on a macro scale (second phase).] In the latter case, the effect depends upon the form and distribution of the second phase. For example, in an oxygen anneal, solute atoms may be internally oxidized and segregated to grain boundaries, which produces a sizeable decrease in ρ. The very small effects of silver, zinc, and cadmium on ρ are due to the extremely low solubilities of these elements in copper at room temperature. Because the values in Figure 8.1 and Table 8.1 are based upon ideal solubility conditions, the fabrication history also affects the final resistivity. The effects of several impurities in combination are expected to be additive if they are all present in solid solution (Reference 8.3). Ornstein (Reference 8.4) reported that the electrical resistivity increased by about 0.4% as the silver content was increased from about 0.03 wt% (C10400, C10500) to about 0.85 at wt% (C10700) but actual measurements were not reported.

Since the change in ρ due to impurity addition is approximately temperature-independent (Matthiessen's rule, see References 8.2 and 8.5), these results, obtained at room temperature, may be provisionally applied to cryogenic temperatures. Some recent results in which residual resistivities were measured at 4 K for 3d and 4d transition metal impurities in copper are in approximate agreement with these room-temperature results. (See Reference 8.6 and citations therein.) However, results reported in Reference 8.6 are in conflict with some recent theoretical work reported in Reference 8.7. These references may be consulted for additional information and for references to the less-common impurity elements not reported in Table 8.1.

Table 8.1. Increase in Resistivity with Impurity Elements Present Singly in Solid Solution.

Impurity Element	Increase in Resistivity per 0.001 wt% Impurity, nΩm	Increase in Resistivity per 10 ppm Impurity, nΩm
O	0.21	0.53
Ti	0.20	0.16
S	0.16	0.081
P	0.13	0.064
V	0.12	0.097
Fe	0.11	0.099
Se	0.097	0.121
Co	0.071	0.066
Si	0.069	0.030
Pt	0.065	0.020
As	0.056	0.066
Cr	0.048	0.039
Be	0.045	0.0064
Te	0.034	0.069
Mn	0.033	0.028
Ge	0.032	0.037
Hg	0.032	0.010
Sn	0.029	0.055
Al	0.026	0.011
Mg	0.021	0.0080
Si	0.017	0.057
Sn	0.016	0.020
Ni	0.014	0.012
Ge	0.013	0.011
Pb	0.0093	0.030
In	0.006	0.011
Ca	0.005	0.003
Zn	0.0034	0.0035
Ag	0.0020	0.0034
Cd	0.0016	0.0028

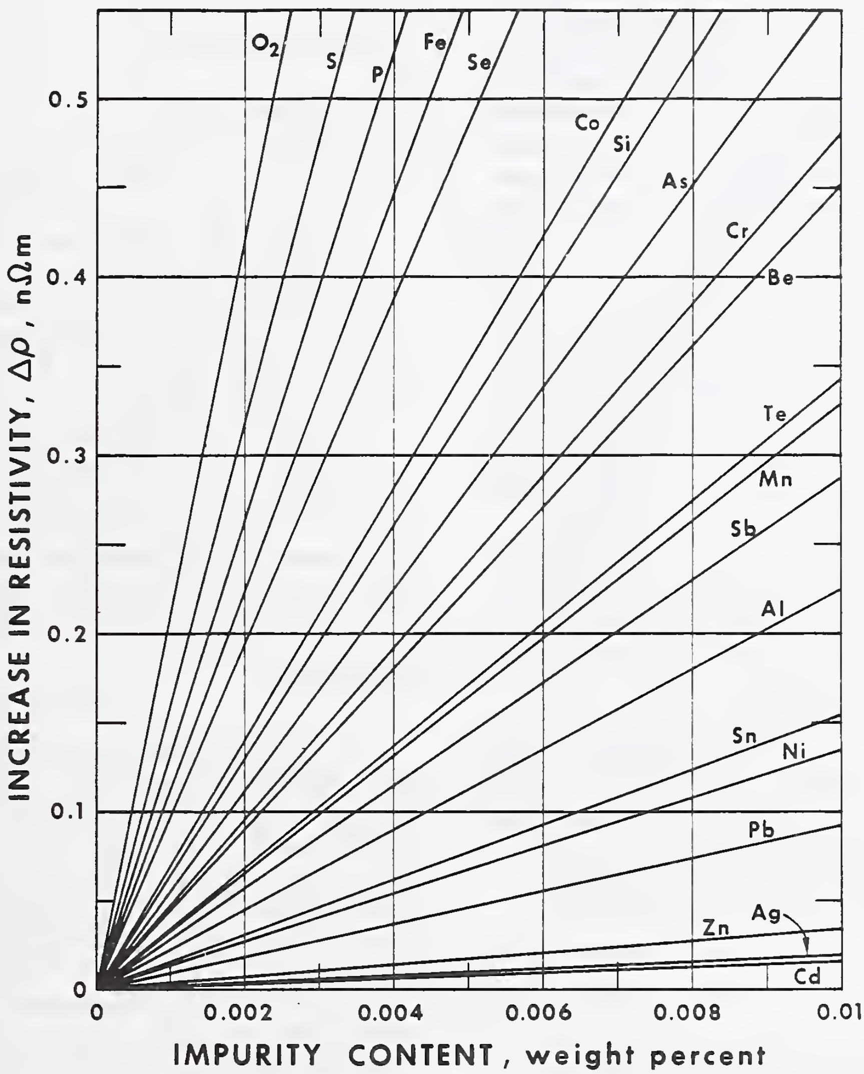

Figure 8.1. The change in electrical resistivity of high-purity copper with the addition of various impurity elements in solid solution is shown. The figure was prepared from information summaried in Reference 8.1.

DATA SOURCES AND ANALYSIS

An extensive analysis of the temperature dependence of the electrical resistivity, ρ, of high-purity copper was carried out recently at NBS, now NIST, (Reference 8.5). The analysis indicated that one parameter, the residual resistivity ratio, RRR, could be used to represent the temperature dependence of the electrical resistivity from 2 to 900 K. The quantity RRR is defined as the ratio of the resistivity at 273 K to the resistivity at 4 K. The 4-K resistivity of a copper sample is approximately equal to the temperature-independent residual resistivity (ρ_o) that results from the chemical and physical imperfections of the material. The 273-K resistivity is approximately equal to the "intrinsic" temperature-dependent resistivity (ρ_i) that results from the thermal vibrations of the copper lattice. ($\rho(T) = \rho_o + \rho_i(T)$, where T is temperature, according to Matthiessen's rule, and for material of commercial or higher purity, ρ_i(273 K) >> ρ_o.) Thus, the RRR gives a measure of the purity and the extent of physical defects such as lattice imperfections due to cold-working. Commercially pure copper wire has an RRR of 50 to 500, whereas very high-purity copper, well-annealed, could have an RRR of around 2,000. Special measures to reduce the effectiveness of electron scattering centers, such as oxygen annealing, can raise the RRR to 50,000.

Data sets for the analysis described in Reference 8.5 were selected from 10 references covering a range of temperature from 0.2 to 900 K and a range of RRR from 19 to 1530. These data were fitted to the function given below and the constants determined with a nonlinear least squares analysis.

RESULTS

It was found that the temperature dependence of ρ could be represented to within ± 15% of the experimental values by the following equation for ρ:

$$\rho(\mathrm{n\Omega m}) = \rho_o + \rho_i + \rho_{io}, \qquad (8\text{-}1)$$

where

$$\rho_i = P_1 T^{P_2} / (1 + P_1 P_3 T^{(P_2 + P_4)} \exp -(P_5/T)^{P_6}) + \rho_c$$

and $\rho_{io} = P_7 \rho_i \rho_o / (\rho_i + \rho_o)$.

The constants are:

$P_1 = 1.171 \times 10^{-17}$		$P_2 = 4.49$
$P_3 = 3.841 \times 10^{10}$		$P_4 = 1.14$
$P_5 = 50$	$P_6 = 6.428$	$P_7 = 0.4531$

The value of ρ_o to be used in Equation (8-1) can be determined from the relation $\rho_o = \rho$ (273 K)/RRR where ρ(273 K) = 15.53 nΩm. See Reference 8.5 for further discussion of ρ_{io}, which represents the deviation from Matthiesson's rule and for an explanation of ρ_c.

Figure 8.2 presents selected (References 8.3, and 8.8–8.12) data used in the analysis and the calculated curves of ρ vs. T for various RRR values. The available characterization of materials and measurements for the data shown in Figure 8.2 is given in Table 8.10 at the end of the electromagnetic properties section.

DISCUSSION

The effects of both impurities and cold work upon electrical resistivity from 2 K to 300 K can be predicted from a knowledge of the RRR, which is readily determined experimentally. An explanation of the size effect correction to the experimentally determined resistance at 4 K is given on page 8-24. Recent measurements of the RRR on coppers that met the C10200 specification ranged from 5 to 520 (Reference 8.2). This shows the necessity of measuring the RRR for individual coppers for which the cryogenic temperature dependence is required. Reference 8.2 gives details of 4-K resistance measurement techniques.

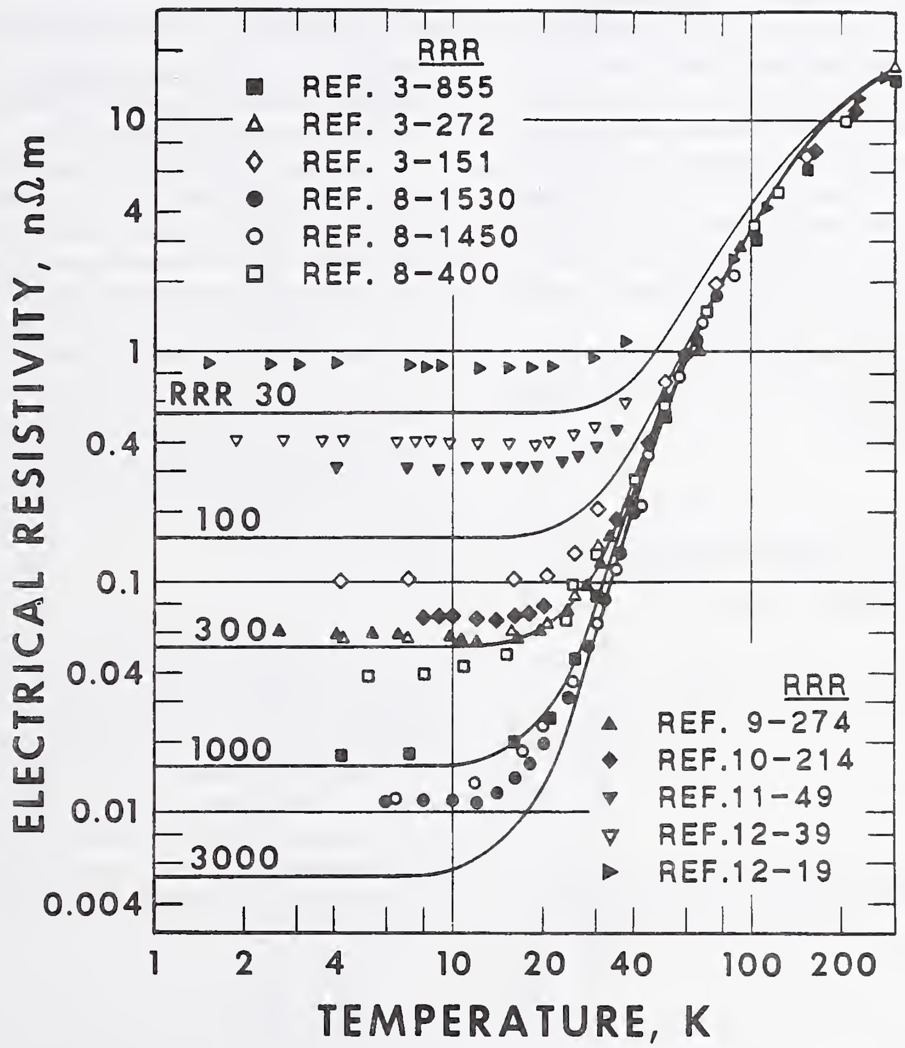

Figure 8.2. The data shown were used in the analysis described in Reference 8.5 to compute the constants for Equation (8-1). The curves represent Equation (8-1) for the series of RRR values indicated.

DATA SOURCES AND ANALYSIS

Measurements of the change with cold work of the electrical resistivity at 295, 77, and 4 K were obtained from References 8.8, and 8.13–8.27 (see Tables 8.2, 8.3, and 8.4). The number of measurements selected for analysis was 48, 12, and 56 at 295, 77, and 4 K, respectively. Product was predominately in extruded wire form, but some data on rolled strip (Reference 8.17) and rolled plate (Reference 8.21) were also included. The amount of cold work, *CW*, ranged up to 96, 60, and 82% for measurements made at 295, 77, and 4 K, respectively. All of the *CW* was carried out at room temperature. (The next section presents data on *CW* carried out at 77 K, in which $\Delta\rho$, the change in resistivity, was measured at 77 K without specimen warmup.)

Regression analyses that included polynomial terms were carried out on the three data sets described above.

RESULTS

The equations representing the best fits to the data sets are as follows. The *CW* refers to reduction in thickness or area.

295 K:

$$\Delta\rho(\text{n}\Omega\text{m}) = 1.02 \times 10^{-2} CW - 6.59 \times 10^{-5}(CW)^2, \quad CW < 77\%;$$

$$\Delta\rho = 0.39\ \text{n}\Omega\text{m}, \quad CW \geq 77\% \quad (8\text{-}2)$$

77 K:

$$\Delta\rho(\text{n}\Omega\text{m}) = 9.84 \times 10^{-3} CW - 1.04 \times 10^{-4}(CW)^2, \quad CW < 47\%;$$

$$\Delta\rho = 0.23\ \text{n}\Omega\text{m}, \quad CW \geq 47\% \quad (8\text{-}3)$$

4 K:

$$\Delta\rho(\text{n}\Omega\text{m}) = 6.24 \times 10^{-3} CW - 5.11 \times 10^{-5}(CW)^2, \quad CW < 61\%;$$

$$\Delta\rho = 0.19\ \text{n}\Omega\text{m}, \quad CW \geq 61\% \quad (8\text{-}4)$$

For the 295-K measurements, the standard deviation of the fit is 0.08 nΩm; the standard deviations of the two coefficients are 0.09×10^{-2} and 1.16×10^{-5}. For the 77-K measurements, the standard deviation of the fit is 0.06 nΩm; the standard deviations of the two coefficients are 1.91×10^{-3} and 0.37×10^{-4}. For the 4-K measurements, the standard deviation of the fit is 0.03 nΩm; the standard deviations of the two coefficients are 0.44×10^{-3} and 0.75×10^{-5}.

Tables 8.2, 8.3, and 8.4 present (for 295, 77, and 4 K, respectively) the measured values of $\Delta\rho$, the values calculated from the regression equation, *CW*, and the reference number. The available characterization of materials and measurements is given in Table 8.10 at the end of the electromagnetic properties section.

Figures 8.3, 8.4, and 8.5 indicate the fit of the data to Equations (8-2), (8-3) and (8-4). Figures 8.6 and 8.7 present these results in summary form. (No summary figure is presented for the 77-K results because comparatively few data were available.) The scatter bands represent two standard deviations about each curve in these figures. The variance of the data about each curve was assumed to be normally distributed and constant throughout the range of the independent variable, *CW*, except that it was reduced to zero for 0% *CW*.

DISCUSSION

The $\Delta\rho$ vs. *CW* values of 3.2-cm plate rolled to 60% reduction (Reference 8.21) appear to be consistent with the values found from measurements on extruded wire. Results on strip stock also are in agreement with the wire measurements. The results reported in Reference 8.21 have been related to the dislocation density produced by cold working and to the dislocation contribution to the electrical resistivity, ρ. Further discussion of defect resistivity may be found in Reference 8.2.

The effect of *CW* on ρ is linear only for small amounts of *CW*, and appears to saturate at approximately 60% for all temperatures. However, room-temperature results presented in Reference 8.28 show a linear dependence up to 40 or 50% and then a very steep increase in $\Delta\rho$ of a factor of 4 at about 60%, followed by a decline to the original slope at about 80%. These data were not used in the present analysis since most other investigators have not observed this effect.

Equations (8-2) to (8-4) and Figures 8.3 to 8.5 show that $\Delta\rho$ for a given amount of *CW* increases with temperature. There are two possible explanations for this effect, which was also observed in the measurements reported in Reference 8.8. First, $\Delta\rho$ with *CW* could be a temperature-dependent effect. Second, the imperfection resistivity, ρ_o, may not be additive with the temperature-dependent or intrinsic resistivity, ρ_i. Matthiessen's rule states that $\rho = \rho_o + \rho_i$, but deviations are sometimes observed (see References 8.2 and 8.5).

Table 8.2. Change in Electrical Resistivity with Cold Work (295 K).

Change in Electrical Resistivity, Measured, nΩm	Change in Electrical Resistivity, Predicted, nΩm	Cold Work, %	Reference No.
0.100	0.0223	2.2	8
0.150	0.0490	5.0	8
0.100	0.0699	7.2	13
0.100	0.0745	7.7	8
0.130	0.0952	76.	17
0.0700	0.0952	10.	17
0.290	0.0987	76.	8
0.210	0.125	10.	19
0.175	0.146	76.	13
0.210	0.170	19.	20
0.410	0.177	20.	13
0.230	0.206	24.	19
0.370	0.213	25.	17
0.150	0.213	25.	17
0.240	0.220	25.	13
0.295	0.246	30.	19
0.290	0.292	38.	13
0.360	0.292	38.	19
0.340	0.311	42.	20
0.320	0.333	47.	13
0.290	0.340	76.	19
0.320	0.344	50.	17
0.390	0.351	52.	20
0.340	0.367	58.	13
0.220	0.373	65.	19
0.295	0.376	61.	19
0.410	0.376	61.	20
0.450	0.376	62.	19
0.390	0.383	65.	13
0.320	0.376	61.	20
0.303	0.383	76.	13
0.150	0.392	75.	13
0.310	0.392	76.	13
0.470	0.392	75.	20
0.290	0.393	76.	13
0.310	0.393	75.	13
0.290	0.392	80.	19
0.325	0.392	81.	19
0.480	0.392	81.	20
0.400	0.391	83.	13
0.300	0.390	84.	19
0.460	0.390	84.	16

Table 8.2, continued

Change in Electrical Resistivity, Measured, nΩm	Change in Electrical Resistivity, Predicted, nΩm	Cold Work, %	Reference No.
0.360	0.390	85.	15
0.490	0.390	85.	20
0.390	0.390	88.	13
0.500	0.390	88.	20
0.510	0.390	90.	20
0.400	0.390	96.	18

Table 8.3. Change in Electrical Resistivity with Cold Work (77 K).

Change in Electrical Resistivity, Measured, nΩm	Change in Electrical Resistivity, Predicted, nΩm	Cold Work, %	Reference No.
0.0510	0.0213	2.2	8
0.0600	0.0463	5.0	8
0.115	0.0696	7.7	8
0.0200	0.0350	10.	21
0.160	0.0911	10.	8
0.130	0.155	20.	21
0.300	0.187	26.	8
0.150	0.201	30.	21
0.170	0.227	40.	21
0.200	0.230	50.	21
0.250	0.230	60.	21
0.220	0.230	60.	14

Table 8.4. Change in Electrical Resistivity with Cold Work (4 K).

Change in Electrical Resistivity, Measured, nΩm	Change in Electrical Resistivity, Predicted, nΩm	Cold Work, %	Reference No.
0.0060	0.0117	1.9	23
0.0190	0.0135	2.2	8
0.0126	0.0177	2.9	23
0.0239	0.0200	3.3	23
0.0147	0.0235	3.9	23
0.0250	0.0299	5.0	22
0.0360	0.0299	5.0	8
0.0341	0.0356	5.0	23
0.0360	0.0356	5.0	23
0.0382	0.0389	5.8	23
0.0574	0.0412	7.0	23
0.0653	0.0135	1.9	27
0.0658	0.0439	7.5	27
0.0564	0.0439	7.5	25
0.0558	0.0439	7.5	25

Table 8.4, continued

Change in Electrical Resistivity, Measured, nΩm	Change in Electrical Resistivity, Predicted, nΩm	Cold Work, %	Reference No.
0.0465	0.0445	8.0	23
0.0474	0.0466	8.0	23
0.0830	0.0466	8.0	8
0.0680	0.0546	9.5	27
0.0838	0.0562	9.8	23
0.0680	0.0573	10.	21
0.0350	0.0573	10.	22
0.0577	0.0573	10.	27
0.0450	0.0599	14.	8
0.144	0.0787	14.	27
0.134	0.0787	14.	24
0.0680	0.0787	14.	27
0.195	0.0787	14.	25
0.111	0.0787	14.	26
0.0450	0.0821	15.	22
0.153	0.104	20.	21
0.0870	0.104	20.	26
0.0290	0.108	21.	27
0.195	0.108	21.	27
0.113	0.108	21.	27
0.0450	0.108	21.	22
0.118	0.134	28.	8
0.179	0.141	30.	24
0.188	0.150	33.	26
0.0830	0.161	37.	24
0.188	0.161	37.	27
0.170	0.161	37.	21
0.195	0.168	40.	27
0.220	0.184	50.	21
0.0600	0.184	50.	22
0.209	0.184	50.	24
0.158	0.190	50.	25
0.255	0.190	50.	24
0.158	0.190	50.	26
0.150	0.190	50.	14
0.141	0.190	50.	27
0.246	0.190	60.	24
0.198	0.190	60.	24
0.181	0.190	71.	26
0.185	0.190	75.	26
0.190	0.190	82.	26

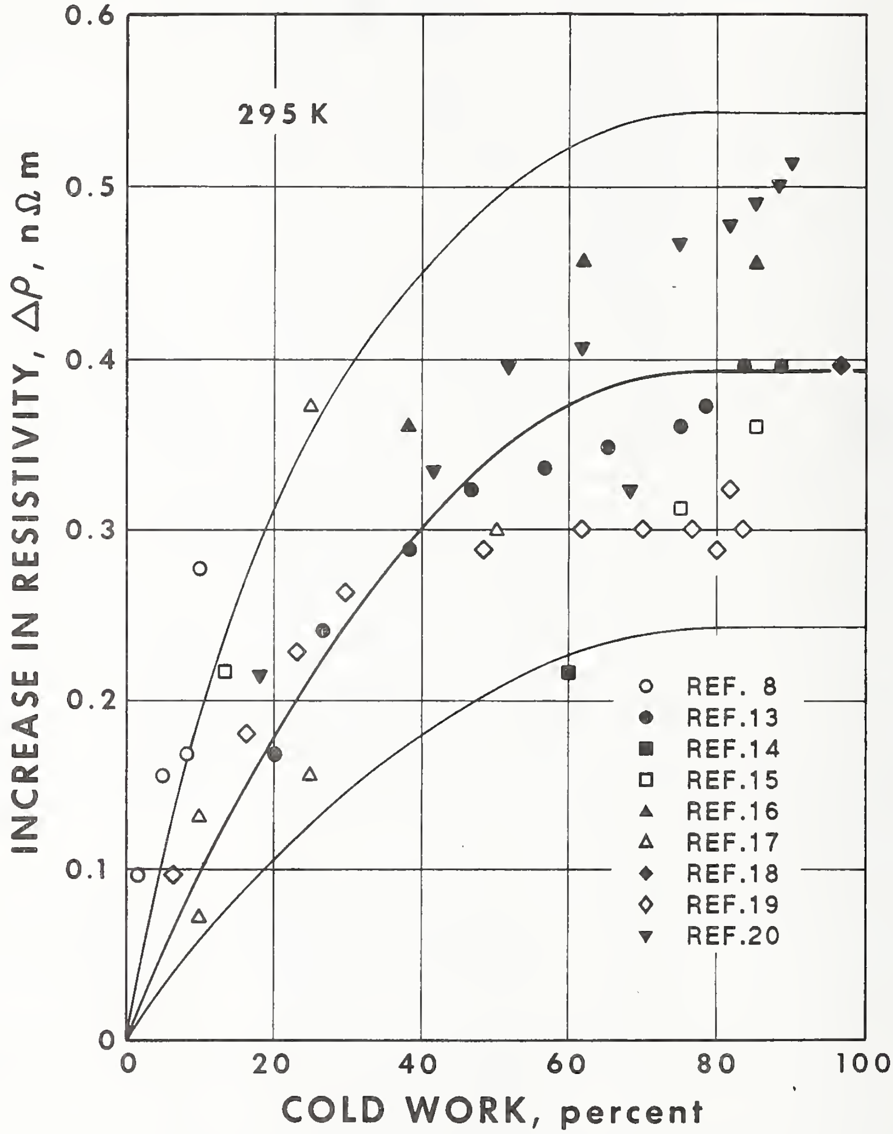

Figure 8.3. The data shown were used to compute the regression of the change in electrical resistivity upon cold work at 295 K [Equation (8-2)]. For clarity, overlapping data points are omitted from the figure. All data are presented in Table 8.2. Products were in wire, sheet, and plate form.

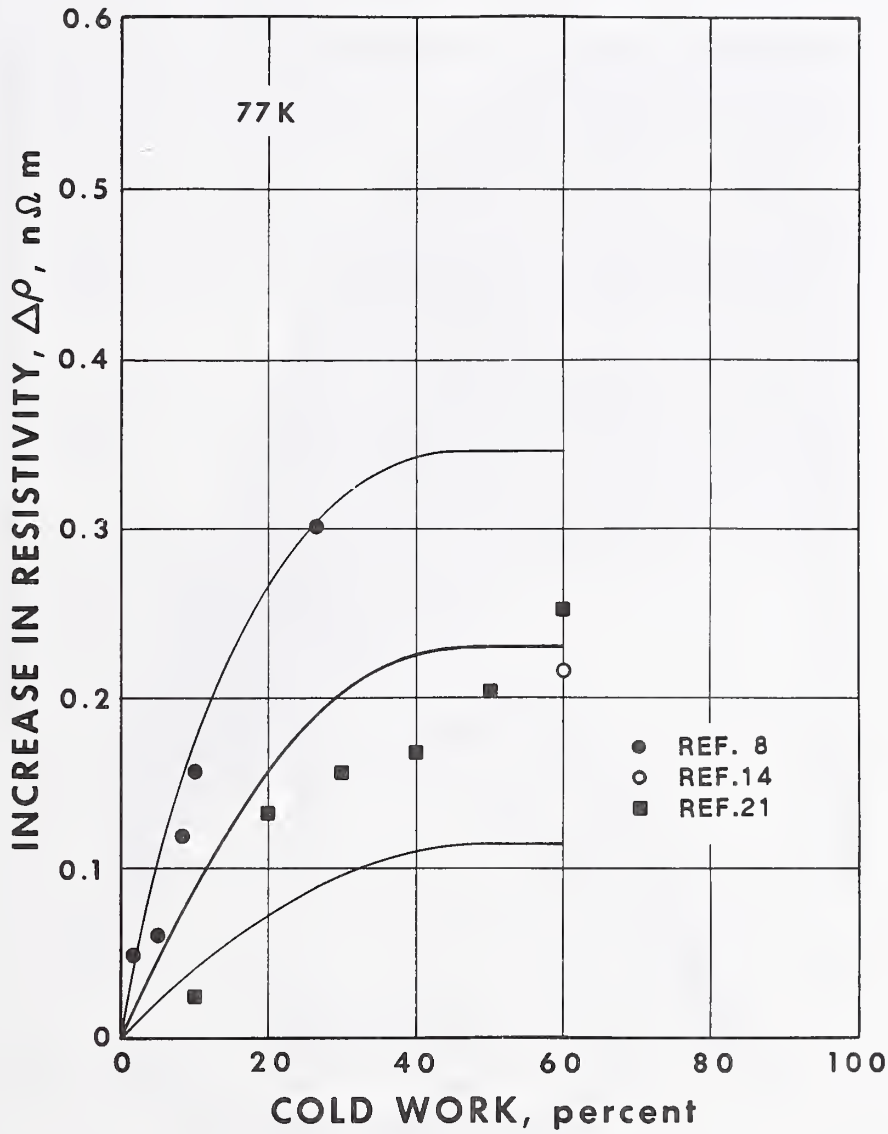

Figure 8.4. The data shown were used to compute the regression of the change in electrical resistivity upon cold work at 77 K [Equation (8-3)]. All data are presented in Table 8.3. Products were in wire and plate form.

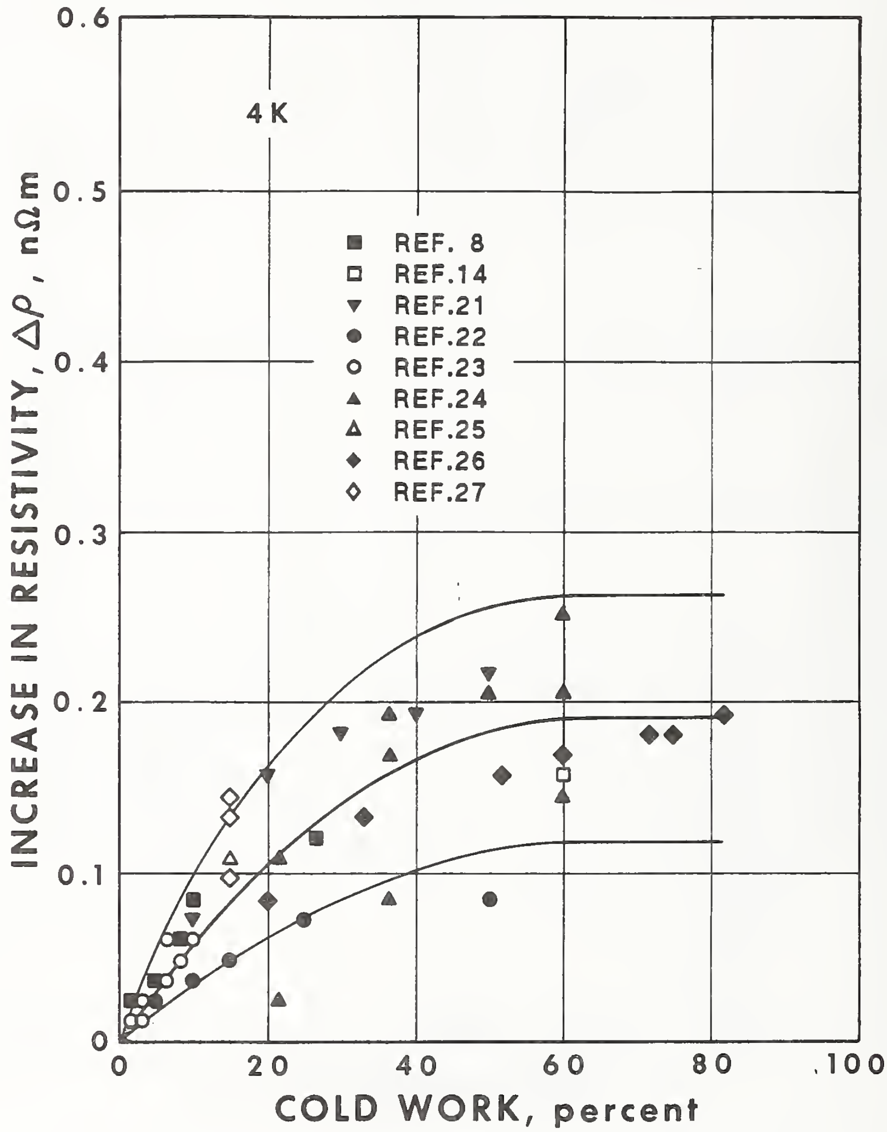

Figure 8.5. The data shown were used to compute the regression of the change in electrical resistivity upon cold work at 4 K [Equation (8-4)]. For clarity, overlapping data points are omitted from the figure. All data are presented in Table 8.4. Products were in wire sheet, and plate form.

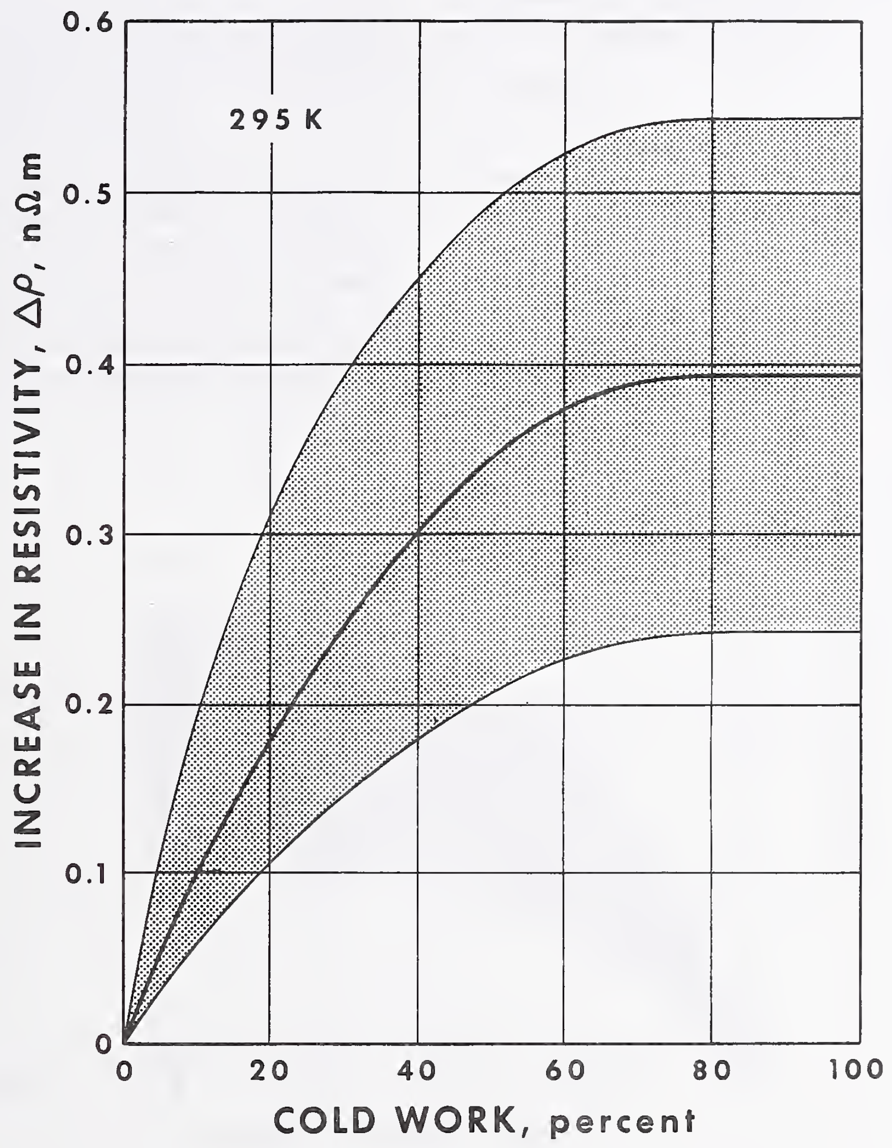

Figure 8.6. Dependence of the change in electrical resistivity at 295 K upon cold work. The scatter band represents two standard deviations about a second-order regression equation based upon 48 measurements for a range of cold work from 0 to 96%. The regression equation is

$$\Delta\rho(n\Omega m) = 1.02 \times 10^{-2} CW - 6.59 \times 10^{-5} (CW)^2 \quad (CW < 77\%)$$
$$\Delta\rho(n\Omega m) = 0.39 \quad (CW \geq 77\%),$$

where CW is the percent of cold work (reduction of thickness or area). Products were in wire, sheet, and plate form.

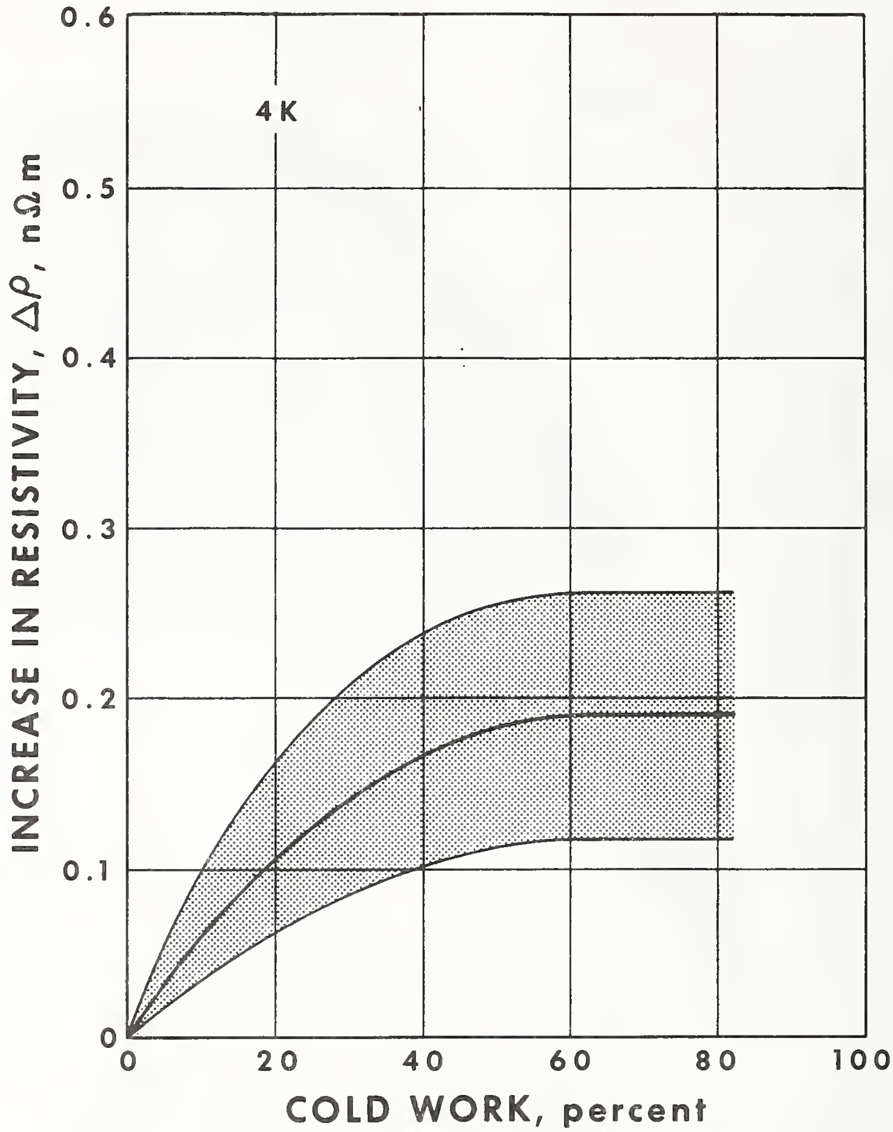

Figure 8.7. Dependence of the change in electrical resistivity at 4 K upon cold work. The scatter band represents two standard deviations about a second-order regression equation based upon 56 measurements for a range of cold work from 0 to 82%. The regression equation is

$$\Delta\rho(\text{n}\Omega\text{m}) = 6.24 \times 10^{-3} CW - 5.11 \times 10^{-5} (CW)^2 \qquad (CW < 61\%)$$

$$\Delta\rho(\text{n}\Omega\text{m}) = 0.19 \qquad (CW \geq 61\%),$$

where CW is the percent of cold work (reduction of thickness or area). Product was in plate form.

DATA SOURCES AND ANALYSIS

Data on residual resistivity ratio, RRR, as a function of cold work were obtained from References 8.21 and 8.24. Products were in plate and wire form. The data are plotted in Figure 8.8. The quantity RRR is defined as the ratio of the resistivity at 273 K to the resistivity at 4 K. The 4-K resistivity of a copper specimen is nearly equal to the temperature-independent residual resitivity (ρ_o) due to the chemical and physical imperfections in the material. The 273-K resistivity, which is at least an order of magnitude larger, is approximately a constant for high purity copper and does not depend significantly upon composition. Therefore, the RRR gives a measure of the purity and the extent of physical defects such as lattice imperfections due to cold-working. See the section "Electrical Resistivity vs. Temperature, RRR" for further information.

RESULTS

As expected, Figure 8.8 shows that cold work reduces the RRR of high-purity copper significantly. For all specimens, the RRR decreases to a nearly constant value of about 55 ± 20 after cold work of 50 to 60%.

The available characterization of materials and measurements is given in Table 8.10 at the end of the electromagnetic properties section.

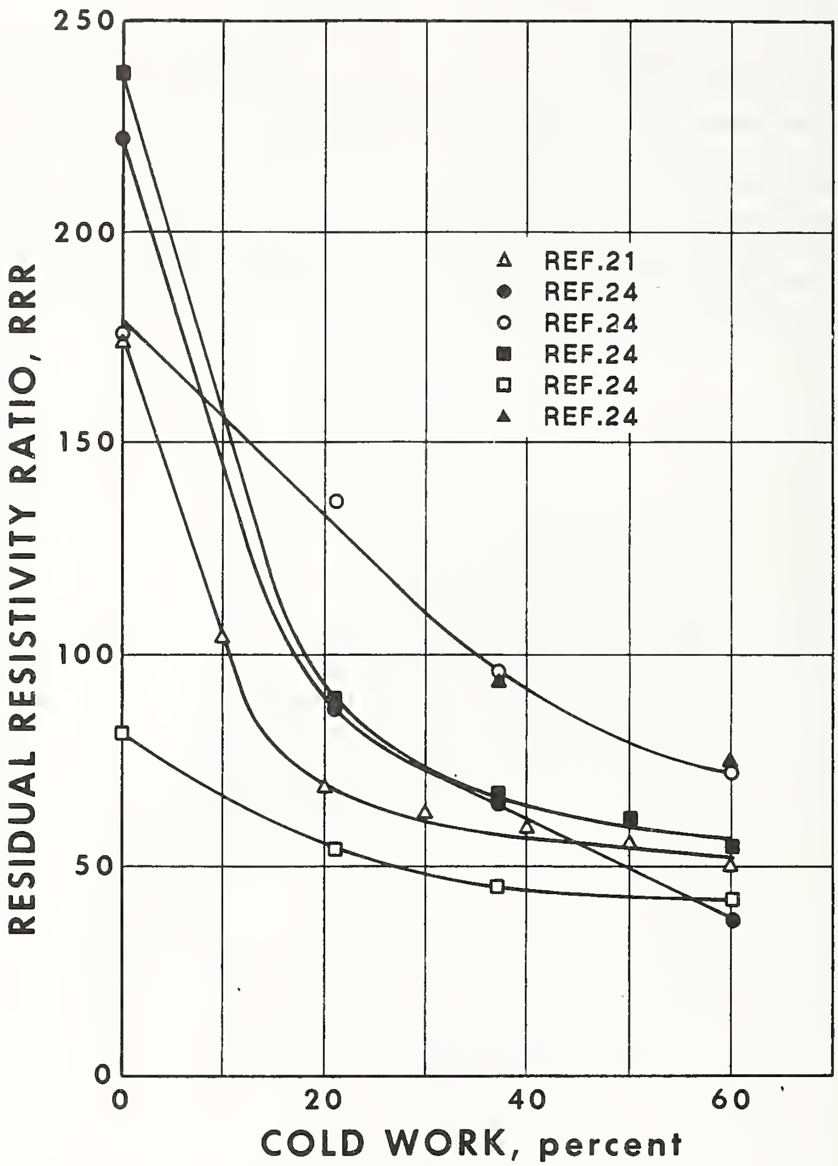

Figure 8.8. The residual resistance ratio, RRR, which is defined in the text, is shown as a function of the amount of cold work. Products were in plate (Reference 8.21) and wire form (Reference 8.24).

DATA SOURCES AND ANALYSIS

Measurements of the change with cold work of the electrical resistivity at 77 K were obtained from References 8.20 and 8.29–8.32 (see Table 8.5). A set of 37 measurements was selected for analysis. Product included plate (Reference 8.32) but was chiefly in wire form. All cold work, *CW*, was carried out at 77 K, and $\Delta\rho$, the change in electrical resistivity, was also measured at 77 K without specimen warmup. The amount of *CW* ranged up to 88%. Regression analysis that included polynomial terms was carried out with this data set.

RESULTS

The equation representing the best fit of the data is

$$\Delta\rho(\text{n}\Omega\text{m}) = 2.35 \times 10^{-2}\ (CW) + 1.63 \times 10^{-4}\ (CW)^2$$

$$(\text{S.D.} = 0.16\ \text{n}\Omega\text{m}), \qquad (8\text{-}5)$$

where *CW*, in percent, is the reduction of thickness or area. The standard deviations of the two coefficients are 0.20×10^{-2} and 0.32×10^{-4}.

Table 8.5 presents the measured values of $\Delta\rho$, the values calculated from the regression equation, *CW*, and the reference number. The available characterization of materials and measurements is given in Table 8.10 at the end of the electromagnetic properties section.

Figure 8.9 indicates the fit of the data to Equation (8-5). Figure 8.10 presents these results in summary form. The scatter band represents two standard deviations about each curve. The variance of the data about each curve was assumed to be normally distributed and constant throughout the range of the independent variable, *CW*, except that it was reduced to zero for 0% *CW*.

DISCUSSION

As expected, $\Delta\rho$ for a given amount of *CW* at 77 K is much greater than for material that is cold- worked at room temperature where more recovery may occur. See Figure 8.4 and Equation (8-3) for comparison.

Data is presented in Reference 8.31 in terms of torsional and axial deformation and the data are shown to follow one unified curve. This reference may be consulted if shear strain is expected to occur.

Table 8.5. Change in Electrical Resistivity with 77-K Cold Work (77 K).

Change In Electrical Resistivity, Measured, nΩm	Change in Electrical Resistivity, Predicted, nΩm	Cold Work, %	Reference No.
0.0100	0.0284	1.2	30
0.0250	[illegible]	2.3	30
0.0250	0.0768	3.2	31
0.0470	0.1060	4.4	30
0.0750	0.1540	6.3	31
0.0830	0.1650	6.7	30
0.[illegible]250	0.2270	[illegible].3	31
0.1630	0.2750	14.0	30
0.2000	0.2920	12.0	31
0.2500	0.3690	14.0	3[illegible]
0.3000	0.[illegible]60	15.0	31
0.3750	0.4380	14.0	3[illegible]
0.2600	0.4460	17.0	29
0.3450	0.4490	17.0	30
0.5000	0.4780	18.0	20
0.4400	0.5230	20.0	30

Table 8.5, continued

Change In Electrical Resistivity, Measured, nΩm	Change in Electrical Resistivity, Predicted, nΩm	Cold Work, %	Reference No.
0.5800	0.5260	20.0	20
0.4880	0.5320	20.0	31
0.3000	0.5650	2[illegible].0	32
0.6300	0.5980	22.0	30
0.6380	0.6260	23.0	31
0.6380	0.6700	20.0	30
0.7500	0.7360	27.0	31
0.9500	0.8480	30.0	31
1.1200	0.9620	33.0	31
1.2800	[illegible].6700	36.0	3[illegible]
1.0400	1.1600	37.0	20
1.1600	1.1000	36.0	20
1.4500	1.1600	39.0	31
0.9600	1.1800	36.0	3[illegible]
1.6000	1.2500	42.0	31
1.7500	1.3400	44.0	3[illegible]
1.6000	1.3900	45.0	32
1.8500	[illegible].6700	62.0	3[illegible]
2.3700	2.2600	66.0	32
2.8000	3.0200	82.0	32
3.4300	3.3300	88.0	32

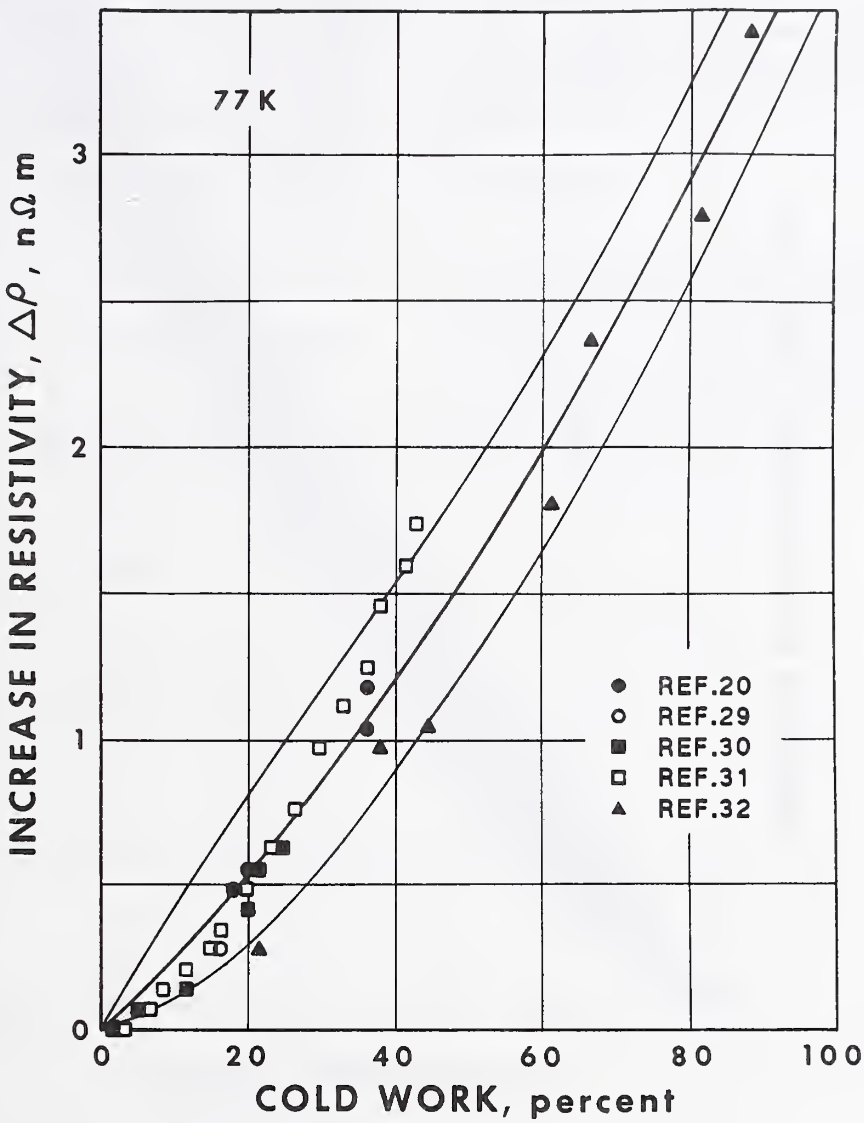

Figure 8.9. The data shown were used to compute the regression of the change in electrical resistivity upon cold work at 77 K [Equation (8-5)]. The specimens were cold worked at 77 K and the resistivity measured without warmup. This figure may be compared with Figure 8.4, which also shows $\Delta\rho$ measured at 77 K, but since the specimens had been cold worked at room temperature, $\Delta\rho$ for a given amount of cold work is much smaller due to the recovery process. For clarity, overlapping data points are omitted from this figure. All data are presented in Table 8.5. Product was chiefly in wire form.

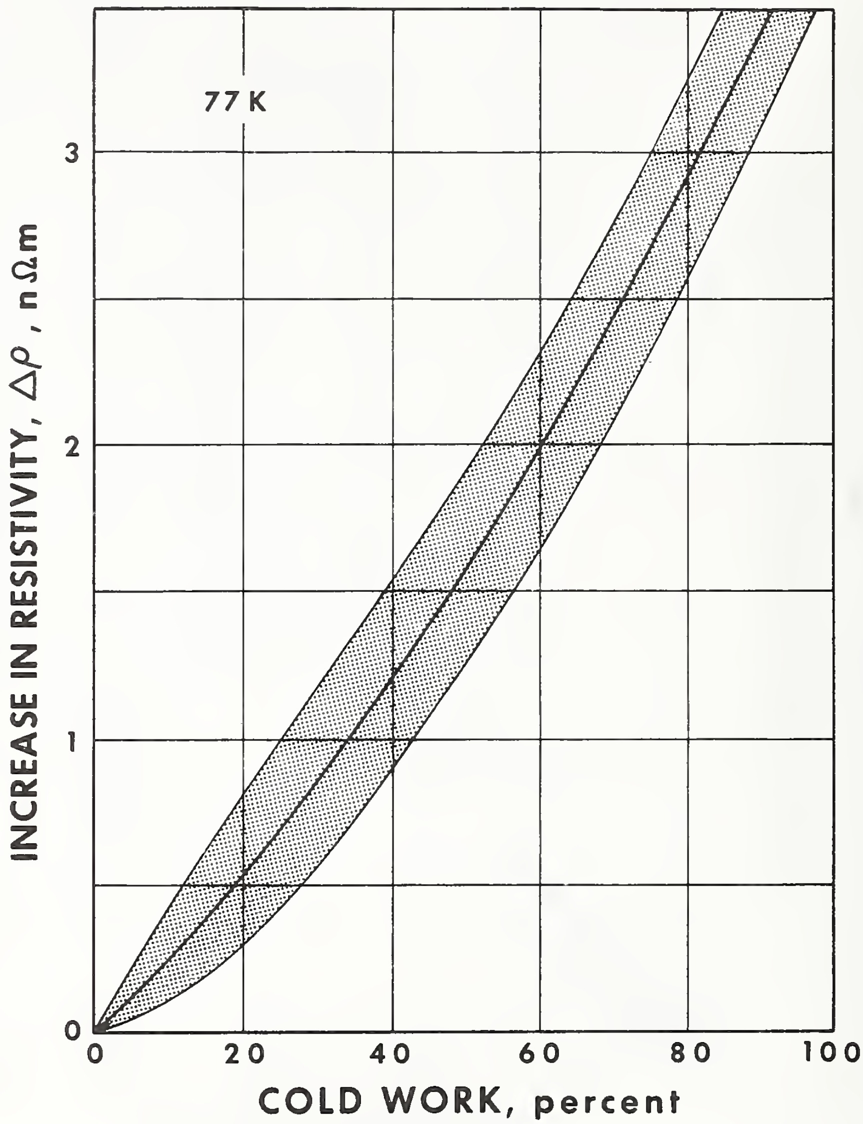

Figure 8.10. Dependence of the change in electrical resistivity upon cold work performed at 77 K. The scatter band represents two standard deviations about a second-order regression equation based upon 37 measurements for a range of cold work from 0 to 88%. The regression equation is

$$\Delta\rho(n\Omega m) = 2.35 \times 10^{-2}\,(CW) + 1.63 \times 10^{-4}\,(CW)^2,$$

where *CW* is the percent of cold work (reduction of thickness or area). Product was predominately in wire form.

DATA SOURCES AND ANALYSIS

Measurements of the change with cold work of the electrical resistivity at 4 K were reported in Reference 8.33. The cold work, *CW*, was carried out at 4 K, and $\Delta\rho$, the change in electrical resistivity, was also measured at 4 K, without specimen warmup. The amount of *CW* ranged up to 28%. Individual data points were not reported in Reference 8.33; an equation was fitted to the smoothed curve provided.

RESULTS

The equation fitted to data taken from the smoothed curve is

$$\Delta\rho(\text{n}\Omega\text{m}) = 5.77\times 10^{-3}\,(CW) + 7.01\times 10^{-4}\,(CW)^2 \quad (\text{S.D.} = 0.23\ \text{n}\Omega\text{m}), \qquad (8\text{-}6)$$

where *CW*, in percent, is the reduction of area. The standard deviations of the two coefficients are 1.94×10^{-3} and 0.8×10^{-5}.

Figure 8.11 indicates the fit of the data to Equation (8-6). The available characterization of materials and measurements is given in Table 8.10 at the end of the electromagnetic properties section.

DISCUSSION

As expected, $\Delta\rho$ at 4 K for a given amount of *CW* is much greater than for material that is cold-worked at room temperature where more recovery may occur. See Figure 8.5 and Equation (8-4) for comparison. These results for $\Delta\rho$ are comparable to results obtained for cold-working and measurement at 77 K, as indicated in Figure 8.9 and Equation (8-5).

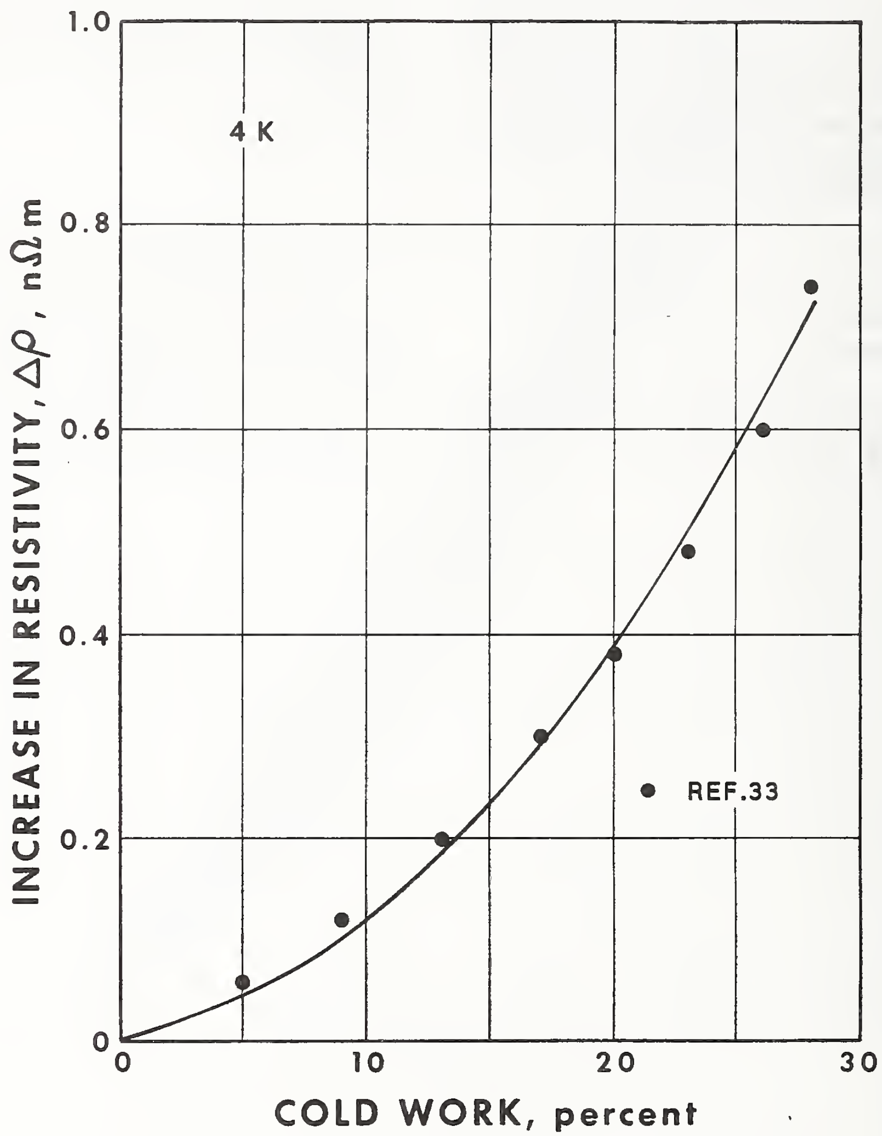

Figure 8.11. The data shown were used to compute the regression of the change in electrical resistivity upon cold work at 4 K [Equation (8-6)]. The specimens were strained at 4 K and the resistivity measured without warmup. This figure may be compared with Figure 8.5, which also shows $\Delta\rho$ measured at 4 K, but since the specimens had been cold-worked at room temperature, $\Delta\rho$ for a given amount of cold work is much smaller due to the recovery process.

DATA SOURCES AND ANALYSIS

Data on the fractional change in electrical resistivity ($\Delta\rho/\rho$) with transverse magnetic field were obtained from References 8.3, 8.22, 8.27, and 8.34–8.44. Reference 8.34, with 256 data points between 4 and 35 K, and Reference 8.39, with 1218 data points at 4 K were particularly useful. The magnetic flux density, *B*, of the data ranged up to 10 Tesla (T) and temperature ranged from 4 to 130 K. A small amount of room temperature data was available (Reference 8.38). Some of the measurements were obtained on neutron irradiated specimens; these data are reviewed at the end of the discussion section below.

Figures 8.12 and 8.13 show the abstraction of this data onto a Kohler plot, in which $[R_T(H) - R_T(0)/R_T(0)]$ is shown as a function of $B \cdot [R_{273\ K}(0)/R_T(0)]$ where *T* represents the temperature (K). (Since $\Delta\rho$ appears only in a ratio, the resistance, *R*, has been substituted.) In the Kohler plot, the vertical axis gives the fractional change in resistance with magnetic field, $\Delta R/R$, and the horizontal axis shows the field strength normalized by the ratio of the ice-point resistance to the resistance at the test point. This resistance-ratio factor allows the data from specimens with varying levels of cold work, *CW*, and impurity content, [I], tested at different temperatures to be plotted on one curve. Some inaccuracies in abstracting the data for this plot may occur if $\rho_{273\ K}$ was not reported. This permits the validation of the dependence of $\Delta\rho/\rho$ upon *B* with a large amount of data. See Reference 8.34 for further discussion of the Kohler curve and for additional references.

In previous work, individual investigators have shown that their data from several specimens followed a Kohler curve or fell within a narrow band; in Figures 8.12 and 8.13, data from many different laboratories are presented on a single Kohler plot. Individual data points could not be shown: a Kohler curve or band was abstracted from the data given in each reference. The band of data within the solid outer lines in Figures 8.12 and 8.13 was the basis for derivation of an average curve with an expected deviation equal to the observed variance of the data. An analytic expression relating log $\Delta\rho/\rho$ to log $B \cdot S(T)$ was also derived, where $S(T) = R_{273\ K}(0)/R_T(0)$. The available characterization of materials and measurements is given in Table 8.10 at the end of the electromagnetic properties section.

RESULTS

Figure 8.14 presents the average Kohler curve and expected uncertainty. The procedure for using this figure to obtain the expected resistance change at a design temperature for a specific C10100–C10700 material follows.

1. Measure the zero-field resistance, *R*, of the material at 273 K and at *T*, the design temperature. $S(T) = R_{273\ K}(0)/R_T(0)$. (See discussion section below if a size-effect correction is necessary to determine *R* correctly.)

2. Multiply $S(T)$ by the expected field strength to obtain the horizontal coordinate, $B \cdot S(T)$.

3. Use Figure 8.14 or the analytic expression below [Equation (8-7)] to obtain $\Delta R/R$ (or $\Delta\rho/\rho$). The expected uncertainty in $\Delta R/R$ may be obtained from the graph.

If specimen measurements are not available, $\rho_T(0)$ may be estimated from data presented in the preceding pages relating ρ to *T*, *CW*, and [I]. For high purity copper, $\rho_{273\ K} \approx 15.5$ nΩm. In analytic form, the average Kohler curve is represented by

$$\log(\Delta\rho/\rho) = -2.662 + 0.3168 \log[B \cdot S(T)] + 0.6229 (\log[B \cdot S(T)])^2 - 0.1839 (\log[B \cdot S(T)])^3 + 0.01827 (\log[B \cdot S(T)])^4 \quad (8\text{-}7)$$

The uncertainty for a particular $B \cdot S(T)$ value may be obtained from the graph. The effects of [I] and *T* upon the magnetoresistance are expressed in the $S(T)$ factor.

DISCUSSION

Because of variation in the results reported in the literature to date, the uncertainty associated with $\Delta\rho/\rho$ values obtained from Figure 8.14 and Equation (8-7) is sizeable. At present, the spread in the data appears to be due to variations between laboratories in making these measurements and material variability rather than to inherent discrepancies between the data and the Kohler law. Several individual investigators (References 8.34, 8.35, and 8.39) have separately correlated a large amount of data to a curve or fairly narrow band; but the lack of agreement between different investigators results in the broad uncertainty band shown in Figures 8.12 and 8.13. After Figures 8.12–8.14 were prepared, the author of Reference 8.32 found that additional measurements made on lower purity coppers tended to fall in a band below the curve he obtained for high purity copper. The width of the band was broader at lower values of $B \cdot S(T)$ (Reference 8.45), but these additional measurements fall within the band depicted in Figure 8.14. Thus variations in materials may also contribute to the width of the band.

Several factors, not discussed here, do cause well-known deviations from the Kohler rule. For small specimens, Reference 8.44 may be consulted to assess the magnitude of the magnetoresistance size effect (thickness < 1 mm). The effects of dilute magnetic impurities may be estimated from studies on dilute Cu-Cr alloys reported in Reference 8.46.

The longitudinal magnetoresistance is generally smaller than the transverse magnetoresistance and saturates with field strengths ~3–10 T at 4 K (References 8.42 and 8.47).

The following discussion of the Nordheim correction for size effect of measured resistance, R, is reproduced with permission of the author of Reference 8.34:

"Nordheim's Rule: An equation giving the contribution to ρ caused by electron scattering at the boundaries of the specimen. This is a significant contribution to the measured resistivity of very pure copper wires and strips at low temperatures, where the mean free path of the electrons (ℓ) may be on the order of 1 mm.

$$\rho_{measured} = \rho_{bulk} + \frac{\rho \ell_{bulk}}{d}$$

where d is the wire diameter or a derived characteristic dimension for a strip. $(\rho\ell)_{bulk}$ is assumed to be constant for a given metal. Its value for copper is not at all certain. We have chosen 0.66×10^{-11} Ωcm^2 which we think is the best value."

"The correction term is subtracted from the measured zero magnetic field resistivity to arrive at a bulk value. All of our zero field data have been corrected by this technique. It is not considered necessary to use the correction when a magnetic field is applied to the specimen. The field prevents most surface scattering by confining the electrons to the bulk of the metal. There is much debate over the validity of the Nordheim relation, particularly when the temperature is varied. Experimental work on the problem is very difficult and no resolution of the questions seems to be forthcoming."

An anomalous RF magnetoresistance has been reported at 4.4 K for the surface resistance of polycrystalline copper (Reference 8.48). At a frequency of 1.2 GHz, both the transverse and longitudinal magnetoresistance are an order of magnitude smaller than the DC magnetoresistance and depend quadratically on the field. Under the experimental conditions, the surface resistance is well into the anomalous skin effect region, but has not reached its limiting value.

The measurements from References 8.39 and 8.40, obtained on neutron-irradiated copper, are plotted in Figure 8.15 together with some recent additional data on irradiated copper that came to our attention after these graphs were originally prepared. The irradiation of the specimens in Reference 8.39 took place at 4 and 330 K in the Bulk Shielding Reactor of Oak Ridge National Laboratory and represents a relatively soft, fission neutron spectrum. In contrast, the specimens of References 8.40 and 8.49 were irradiated with 14.8-Mev neutrons at 4 K. Reference 8.50 combines data from irradiations with 14.8-Mev neutrons with data from irradiations with a neutron spectrum similar to what might be expected at a magnet in a fusion reactor. The fission spectrum data (obtained with and without Cd shielding to eliminate thermal neutrons), lie between the two curves denoted Reference 8.39 in Figure 8.15. The single curve for Reference 8.40 (14-Mev spectrum) represents data from partially recrystallized C10100 and C10200 copper with RRRs of 200–300. The single curve for Reference 8.49 (14-Mev spectrum) represents data from both recrystallized and 7- and 14% cold-worked C10200 specimens. The data combined from different irradiation spectra fall between the two curves denoted Reference 8.50 in Figure 8.15. All the data on irradiated copper fall within the band established for the compiled copper measurements (Figure 8.14), and there is no significant difference between material irradiated with low or high energy neutrons.

The original reports should be consulted for details of the irradiation fluence, room-temperature annealing procedures, and further descriptions of the specimen materials used. Some specimens were cold-worked before irradiation, and the references also provide detailed information on the degree of damage recovery after successive irradiations and anneals.

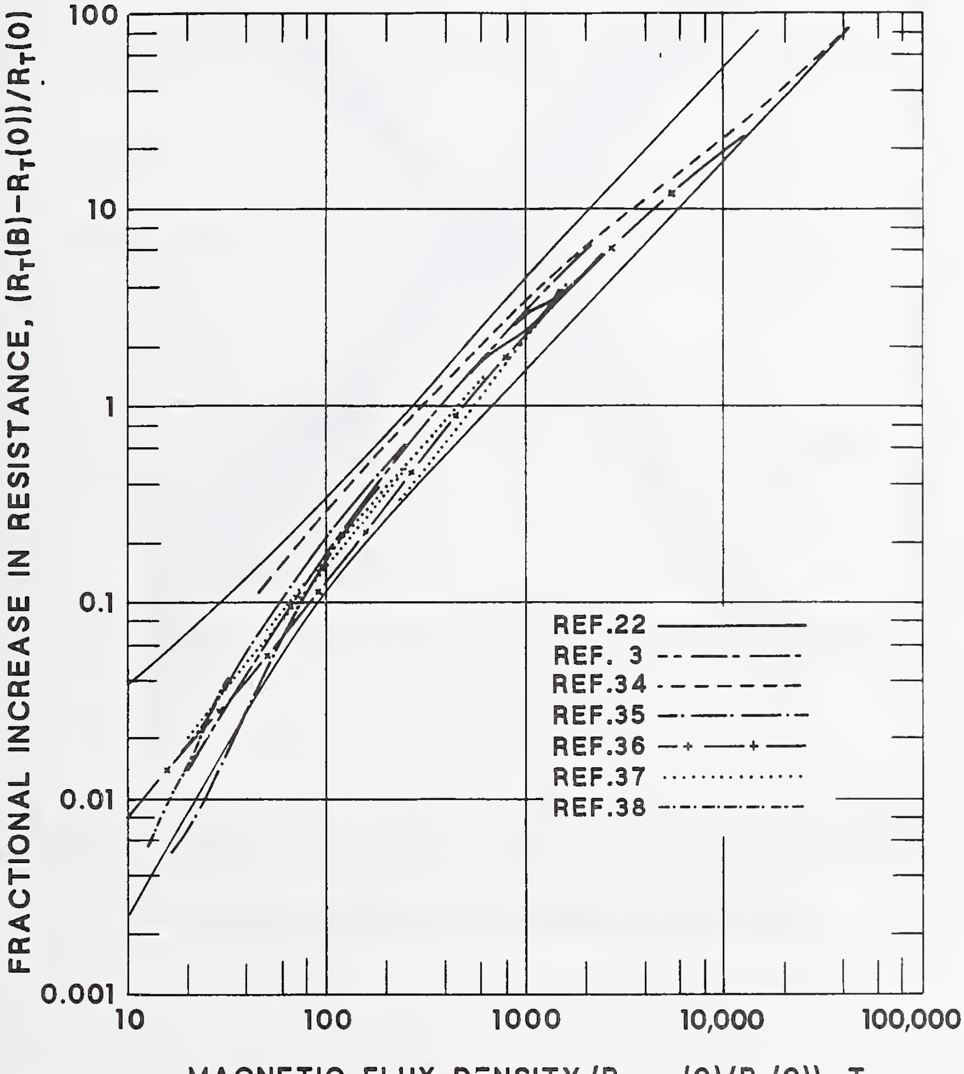

Figure 8.12. Data on the fractional change in electrical resistance with transverse magnetic field are shown. Individual data points are too numerous to show; a smoothed curve or band was abstracted from each reference. See text for further details.

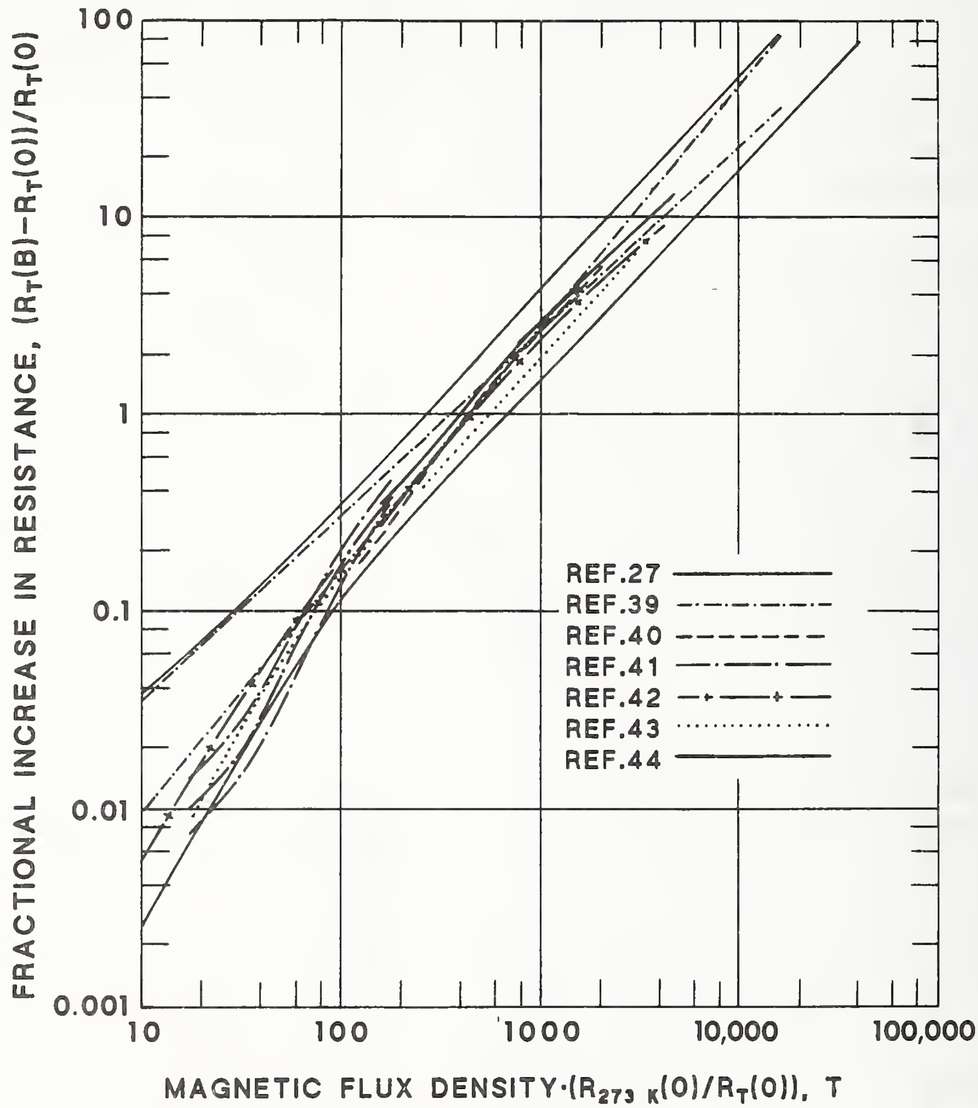

Figure 8.13. Data on the fractional change in electrical resistance with transverse magnetic field are shown. Individual data points are too numerous to show; a smoothed curve or band was abstracted from each reference. The data from Reference 8.39 fall between the two — · — lines shown. See text for further details.

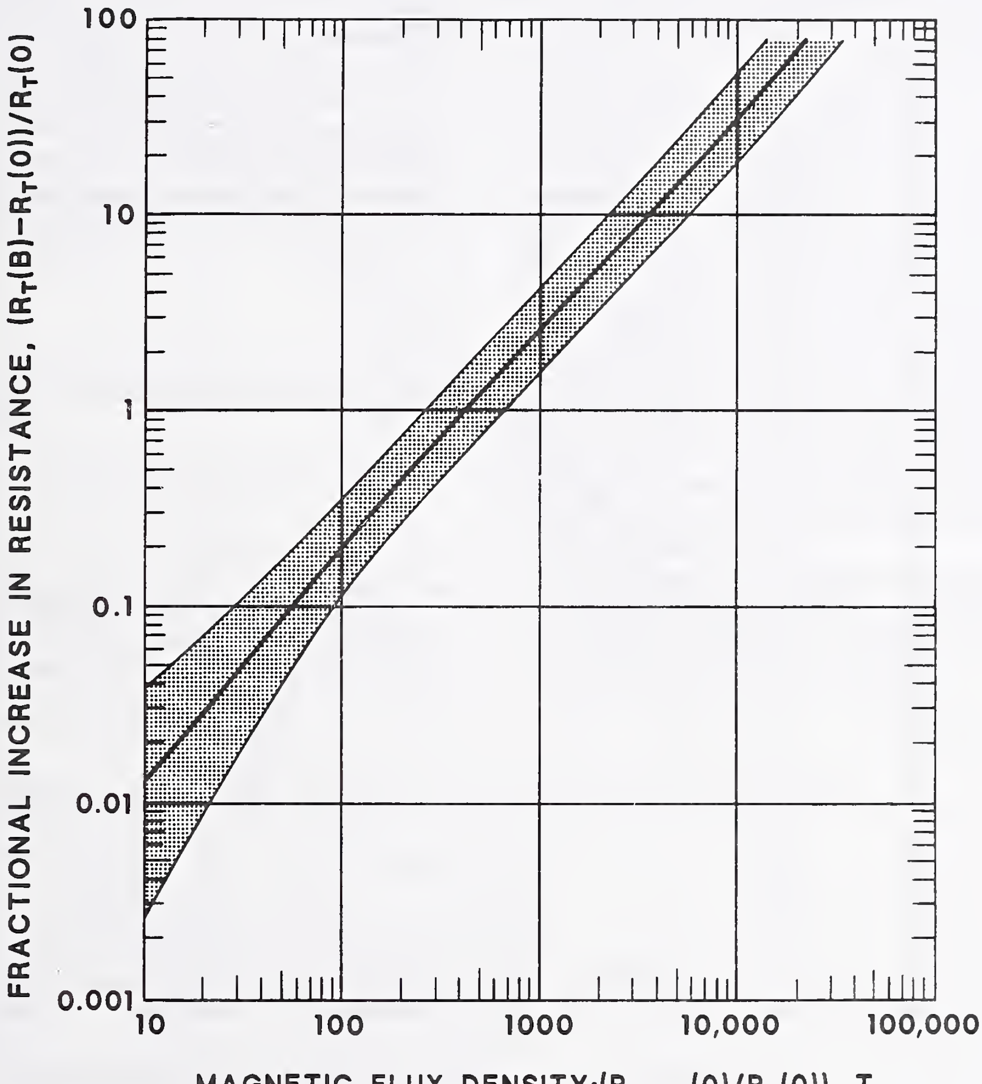

Figure 8.14. Average curve (heavy line) of the fractional change in electrical resistivity with transverse magnetic field. The uncertainty estimated from the variance of the data in Figures 8.12 and 8.13 is shown by the shaded band.

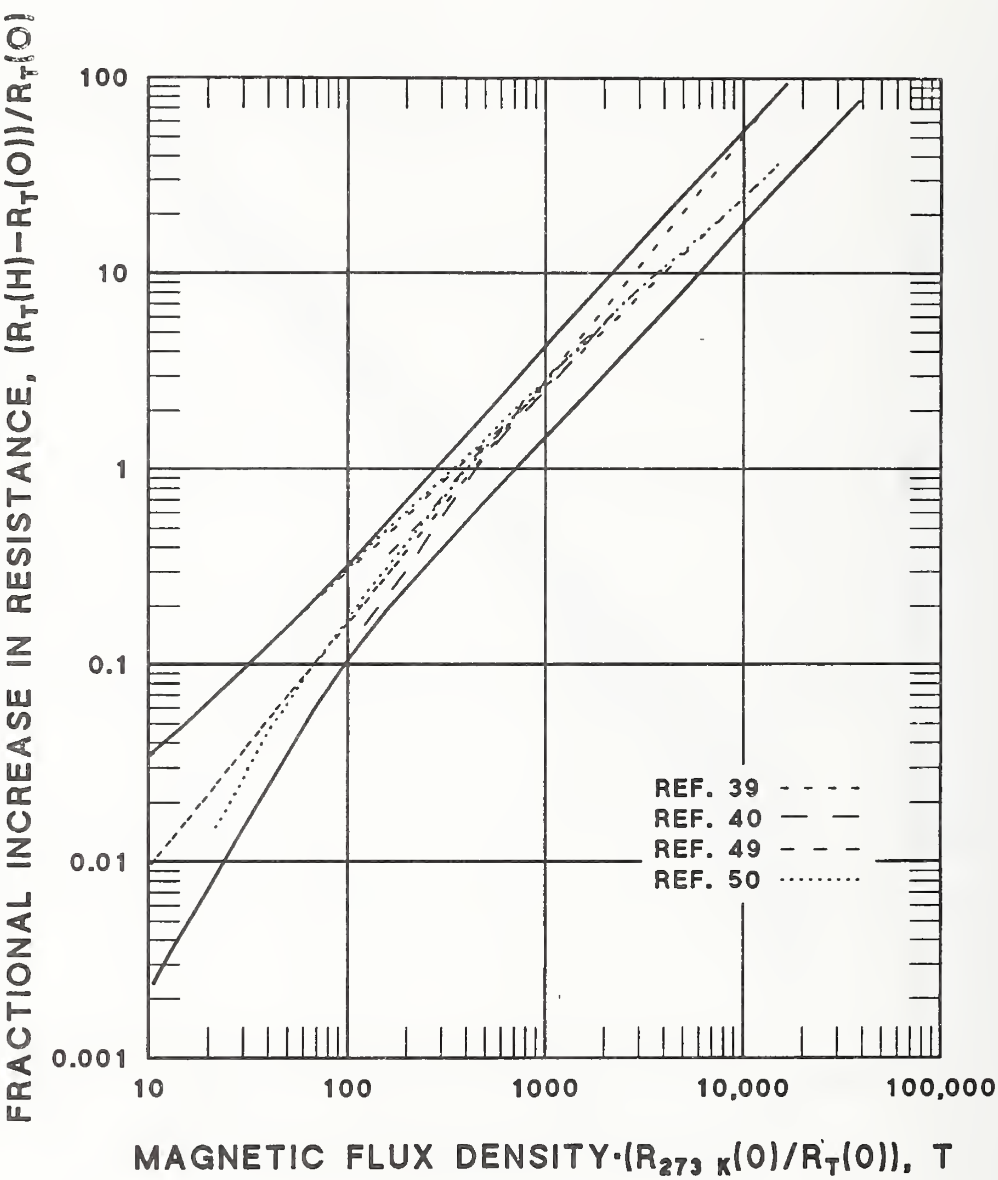

Figure 8.15. Data on the fractional change in electrical resistance with transverse magnetic field are shown for neutron-irradiated copper. Individual data points are too numerous to show; a smoothed curve or band was abstracted from each reference. See text for further details.

DATA SOURCES AND ANALYSIS

Data on the temperature dependence of the magnetic susceptibility of C10100 and C10200 copper from 1.4 to 300 K were obtained from References 8.51–8.55 (See Table 8.6). An equation of the form $\kappa = A/T + B + CT$, where T is the temperature in K, was fitted to the susceptibility data. The susceptibility, κ, in SI units, is defined as $\kappa = M/H$ (dimensionless), where H = applied field and M = magnetization (both in A/m). The relative permeability, also dimensionless, is related to the susceptibility by $\mu_r = \mu/\mu_o = 1 + \kappa$. (The magnitude of μ_r is the same in both SI and cgs units.)

RESULTS

The fit of the equation to the data gave the following result:

$$\kappa(10^{-6}) = 3.59/T - 9.84 + 6.66 \times 10^{-4}\, T$$

$$1.4 \text{ K} < T \leq 300 \text{ K} \qquad (8\text{-}8)$$

Figure 8.16 indicates the fit of the data to this equation. Some considerations for using this equation are discussed below. Since the purity of the copper is an important parameter, the standard deviation is not useful.

DISCUSSION

Very high purity copper is diamagnetic from 4 K to the melting point. However, small amounts of iron impurity give a paramagnetic contribution that is higher at cryogenic temperatures. (See also the following sections.) The curve given by Equation (8-8) is an adequate representation for a C10200 copper of average composition, but for a C10100 copper from which the iron has been selectively removed (for example, Fe < 0.10 ppm, wt) the lowest set of data shown in Figure 8.16 would be a better guide (data of Reference 8.51A). The paramagnetic $1/T$ term in Equation (8-8) is due to the effects of the dilute iron impurity. The T term apparently arises from the change in density of states at the Fermi level caused by the thermal expansion; the lattice expansion increases the density of states and thus the paramagnetic contribution of the free electrons (Reference 8.51).

Reference 8.56 reports measurements of the room-temperature susceptibility of several high-purity copper specimens; Equation (8-8) at 295 K is in agreement with these results.

Table 8.6. Magnetic Susceptibility Dependence upon Temperature (1.4–300 K).

Magnetic Susceptibility, Measured	Magnetic Susceptibility, Predicted	Test Temperature, K	Reference No.
- 7.56	- 7.37	1.45	53
- 8.65	- 7.63	1.62	54
- 7.93	- 8.18	2.16	53
- 8.25	- 8.65	3.00	53
- 9.39	- 9.30	3.90	55
- 8.65	- 8.98	4.19	53
- 9.12	- 9.30	4.20	52
- 8.65	- 8.99	4.20	54
- 9.27	- 9.22	5.80	55
- 8.65	- 9.23	5.90	54
- 9.39	- 9.30	5.80	51
- 9.79	- 8.98	5.90	54
- 9.34	- 9.40	8.10	55
- 8.93	- 9.48	10.00	53
- 9.42	- 9.52	11.40	55
- 9.00	- 9.58	13.80	53
- 9.90	- 9.60	15.00	51

Table 8.6, continued

Magnetic Susceptibility, Measured	Magnetic Susceptibility, Predicted	Test Temperature, K	Reference No.
- 9.64	- 9.61	15.70	51
- 9.72	- 9.64	16.30	53
- 9.76	- 9.61	16.40	55
- 9.90	- 9.63	17.60	51
- 9.16	- 9.63	15.70	53
- 9.21	- 9.65	20.20	53
- 9.71	- 9.65	20.40	52
- 9.72	- 9.65	20.40	51
- 9.61	- 9.67	22.60	51
- 9.90	- 9.70	30.00	51
- 9.76	- 9.71	30.80	51
- 9.90	- 9.71	[illegible]0.60	51
- 9.76	- 9.71	31.30	55
- 9.76	- 9.73	40.50	51
- 9.64	- 9.73	8[illegible].00	51
- 9.90	- 9.73	45.60	51
- 9.76	- 9.71	48.20	51
- 9.90	- 9.70	55.20	51
- 9.76	- 9.74	56.50	55
- 9.90	- 9.74	80.60	51
- 9.76	- 9.75	8[illegible].00	51
- 9.90	- 9.70	70.20	51
- 9.71	- 9.75	77.00	52
- 9.16	- 9.70	77.00	53
- 9.76	- 9.75	77.30	51
- 9.76	- 9.70	80.00	51
- 9.76	- 9.75	80.80	51
- 9.90	- 9.70	81.40	51
- 9.76	- 9.71	98.80	51
- 9.98	- 9.70	101.00	51
- 9.64	- 9.74	16[illegible].00	51
- 9.76	- 9.73	128.00	51
- 9.76	- 9.73	133.00	51
- 9.90	- 9.73	134.00	51
- 9.76	- 9.72	160.00	51
- 9.90	- 9.70	174.00	51
- 9.82	- 9.74	181.00	51
- 9.90	- 9.64	208.00	51
- 9.76	- 9.67	215.00	51
- 9.72	- 9.64	240.00	51
- 9.71	- 9.67	244.00	51
- 9.64	- 9.64	248.00	51
- 9.64	- 9.61	291.00	51
- 9.64	- 9.64	292.00	51
- 9.60	- 9.67	292.00	51
- 9.96	- 9.64	298.00	51
- 9.64	- 9.61	294.00	51
- 9.72	- 9.64	298.00	52
- 9.66	- 9.64	295.00	55
- 9.32	- 9.63	300.00	53

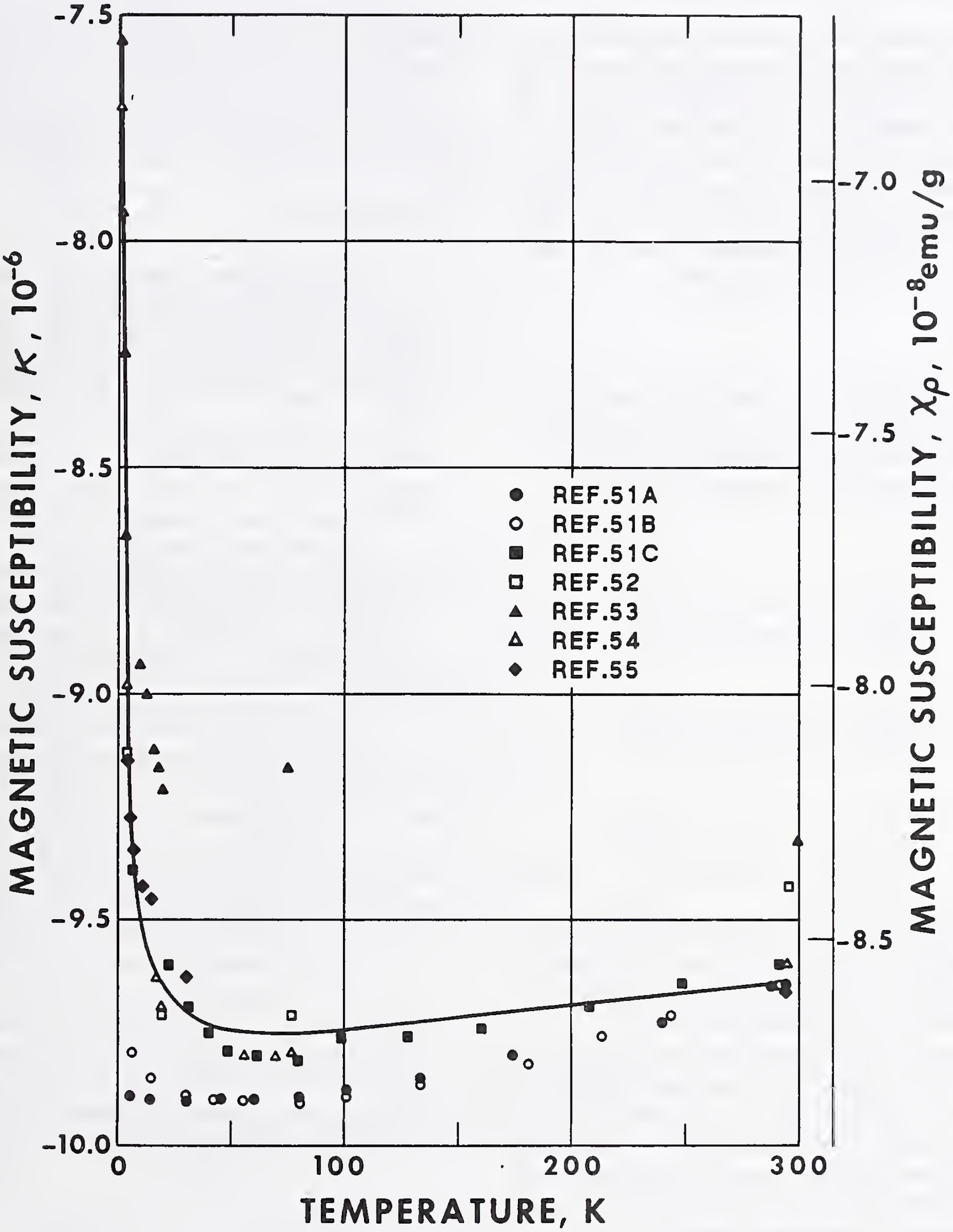

Figure 8.16. The data shown were used to compute the coefficients of Equation (8-8), which represents the temperature dependence of the magnetic susceptibility from 1.4 to 300 K of C10200 copper of average Fe content. All data are presented in Table 8.6. Table 8.10 should be consulted for the compositions of the C10100 and C10200 coppers for which data are presented; as explained in the text, the temperature dependence of κ is strongly influenced by small amounts of Fe impurities, especially near 4 K. [See also Equations (8-9), (8-10), and (8-11).]

DATA SOURCES AND ANALYSIS

Data on the increase in the magnetic susceptibility of high-purity copper with dilute iron additions were obtained from References 8.57–8.60 (See Tables 8.7–8.9). Sufficient data for analysis were available at three temperatures: 4 K (actually 1.3–6 K), 77 K, and 295 K. Data at intermediate temperatures may be found in References 8.57 and 8.58. Regression analysis was carried out on the three data sets.

RESULTS

The equations representing the best fits to the data sets are as follows. The change in magnetic susceptibility, $\Delta\kappa$, is given in SI units (dimensionless) and the iron content, [Fe], is in atomic ppm.

295 K:

$$\Delta\kappa\ (10^{-5}) = 9.76 \times 10^{-4}\ [\mathrm{Fe}] \quad (\mathrm{S.D.} = 0.0052 \times 10^{-5}) \tag{8-9}$$

77 K:

$$\Delta\kappa\ (10^{-5}) = 2.64 \times 10^{-3}\ [\mathrm{Fe}] \quad \mathrm{S.D.} = 0.025 \times 10^{-5}) \tag{8-10}$$

4 K:

$$\Delta\kappa\ (10^{-5}) = 1.00 \times 10^{-2}\ [\mathrm{Fe}] \quad (\mathrm{S.D.} = 0.44 \times 10^{-5}) \tag{8-11}$$

The standard deviations of the coefficients in the three equations, (8-9), (8-10), and (8-11), are 1.0×10^{-5}, 5×10^{-5}, and 5×10^{-4}. The linearity of Equation (8-11) is discussed below.

Tables 8.7, 8.8, and 8.9 present (for 295, 77, and 4 K, respectively) the measured values of $\Delta\kappa$, the values calculated from the regression equation, [Fe], and the reference number. The available characterization of materials and measurements is given in Table 8.10 at the end of the electromagnetic properties section.

Figures 8.17, 8.18, and 8.19 indicate the fit of the data to Equations (8-9), (8-10), and (8-11). The scatter bands represent two standard deviations about each line in these figures. The variance of the data about each line was assumed to be normally distributed and constant throughout the range of the independent variable, [Fe].

DISCUSSION

The specimens measured were prepared from high-purity (~99.999%) copper, which has a diamagnetic susceptibility of about -9.65×10^{-6} at 295 K (Reference 8.56). C10200-grade copper (99.95% pure) could have sufficient [Fe] to cause it to be (weakly) paramagnetic. This is especially likely at low temperatures as a comparison of Equations (8-11) and (8-9) shows. See also the following section on magnetization.

Only one set of measurements on C10200 copper was available (Reference 8.51, data shown in Figure 8.14) and this material remained diamagnetic down to 6.6 K. The effects of nickel impurities are smaller than those of iron (Reference 8.52).

In any case, the effects noted here are so small that for many applications, the magnetic permeability is equal to 1 to a good approximation. The susceptibility, κ in SI units, is defined as $\kappa = M/H$ (dimensionless), where H = applied field and M = magnetization (both in A/m). The relative permeability, also dimensionless, is related to the susceptibility by $\mu_r = \mu/\mu_o = 1 + \kappa$.

Although some individual sets of data near 4 K indicate a departure from linear behavior (References 8.57, 8.59, and 8.60) the deviations from a straight line were in different directions, so that this effect canceled out in the regression analysis carried out here. See also Reference 8.61 for a discussion of this point.

Table 8.7. Change In Magnetic Susceptibility with Iron Content (295 K).

Change in Magnetic Susceptibility, Measured	Change in Magnetic Susceptibility, Predicted	[Fe], ppm	Reference No.
0.0156	0.0146	15	58
0.0493	0.0469	48	57
0.0706	0.0684	70	58
0.0820	0.0898	92	57
0.1010	0.1040	106	58
0.0890	0.0469	143	57
0.1460	0.1420	145	58
0.2080	0.1970	202	57
0.2020	0.0684	211	58
0.2980	0.2970	304	57

Table 8.8. Change in Magnetic Susceptibility with Iron Content (77 K).

Change in Magnetic Susceptibility, Measured	Change in Magnetic Susceptibility, Predicted	[Fe], ppm	Reference No.
0.0156	0.0396	15	58
0.0998	0.1270	48	57
0.1620	0.1850	70	58
0.2350	0.2430	92	57
0.2400	0.2800	106	58
0.3770	0.3770	143	57
0.3560	0.3820	145	58
0.5270	0.5330	202	58
0.5670	0.5570	211	57
0.8380	0.8020	304	57

Table 8.9. Change in Magnetic Susceptibility with Iron Content (4 K).

Change in Magnetic Susceptibility, Measured	Change in Magnetic Susceptibility, Predicted	[Fe], ppm	Reference No.
0.125	0.150	15	58
1.030	0.200	20	60
0.680	0.401	40	50
0.370	0.451	45	60
0.394	0.481	48	58
1.030	0.631	63	60
0.654	0.701	70	58
0.670	0.862	86	59
1.020	0.922	92	55
1.630	0.922	92	60
0.960	1.060	106	58

Table 8.9, continued

Change in Magnetic Susceptibility, Measured	Change in Magnetic Susceptibility, Predicted	[Fe], ppm	Reference No.
0.950	1.100	110	59
1.620	1.430	143	57
1.300	1.1[illegible]0	145	58
1.350	1.550	155	56
1.740	2.000	200	58
2.190	2.020	202	58
2.800	2.110	211	57
4.360	3.050	304	57
2.810	3.160	315	59
3.030	3.360	335	59
3.820	4.560	455	59

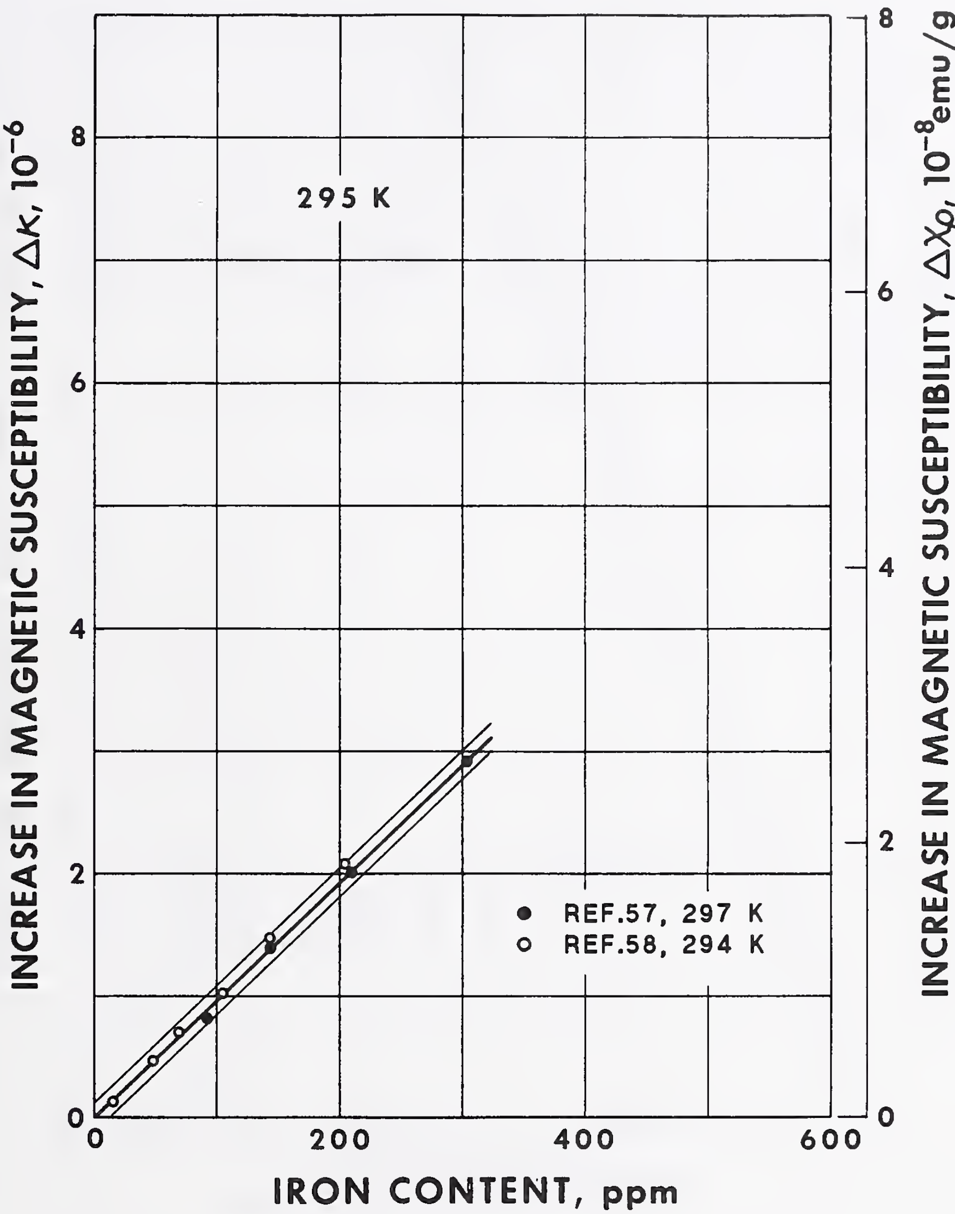

Figure 8.17. The change in magnetic susceptibility at ~295 K of high-purity copper with the addition of iron as an impurity element is shown. These data were used to compute the regression of the change in magnetic susceptibility at 295 K upon iron content [Equation (8-9)]. All data are presented in Table 8.7.

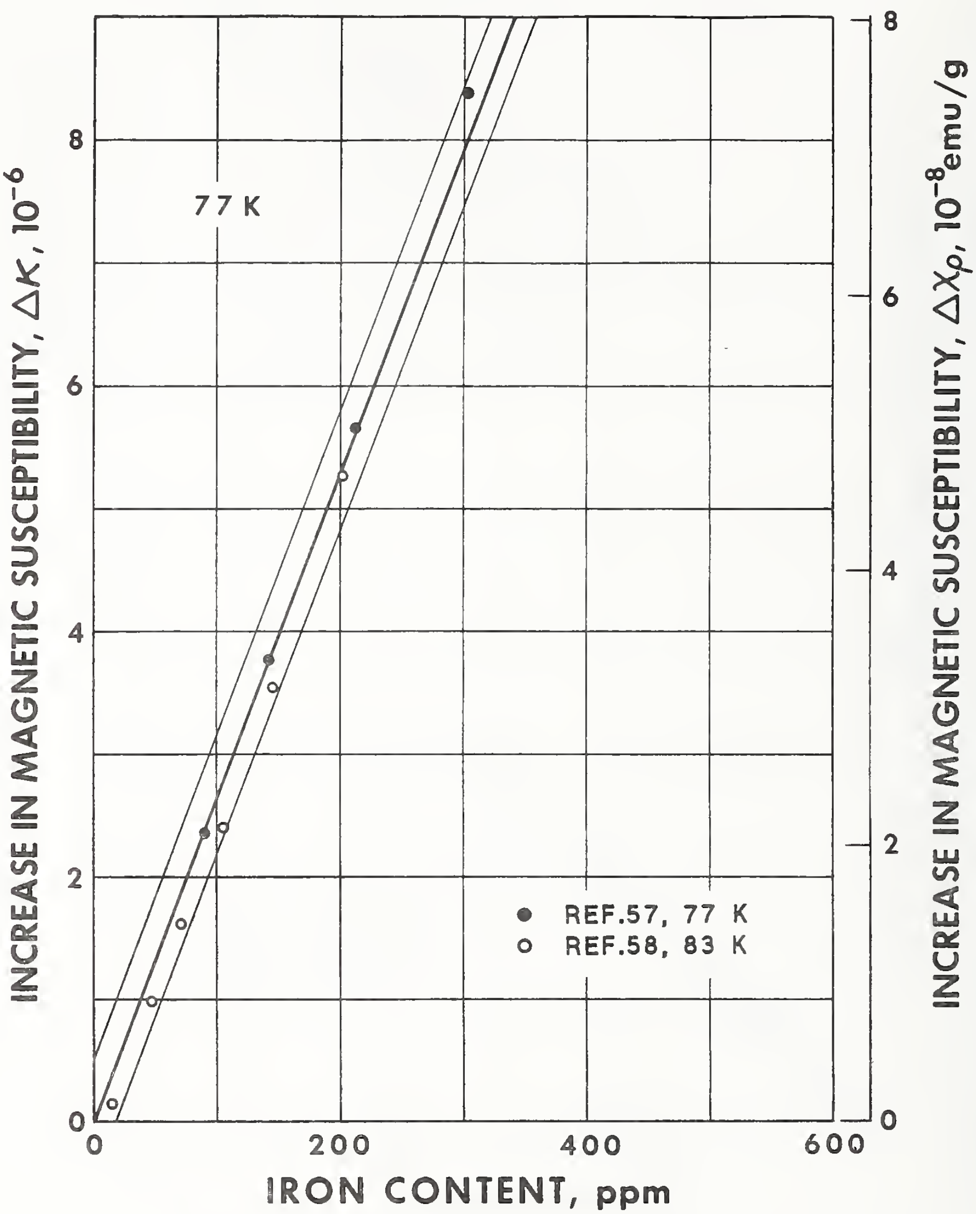

Figure 8.18. The change in magnetic susceptibility at ~77 K of high-purity copper with the addition of iron as an impurity element is shown. These data were used to compute the regression of the change in magnetic susceptibility at 77 K upon iron content [Equation (8-10)]. All data are presented in Table 8.8.

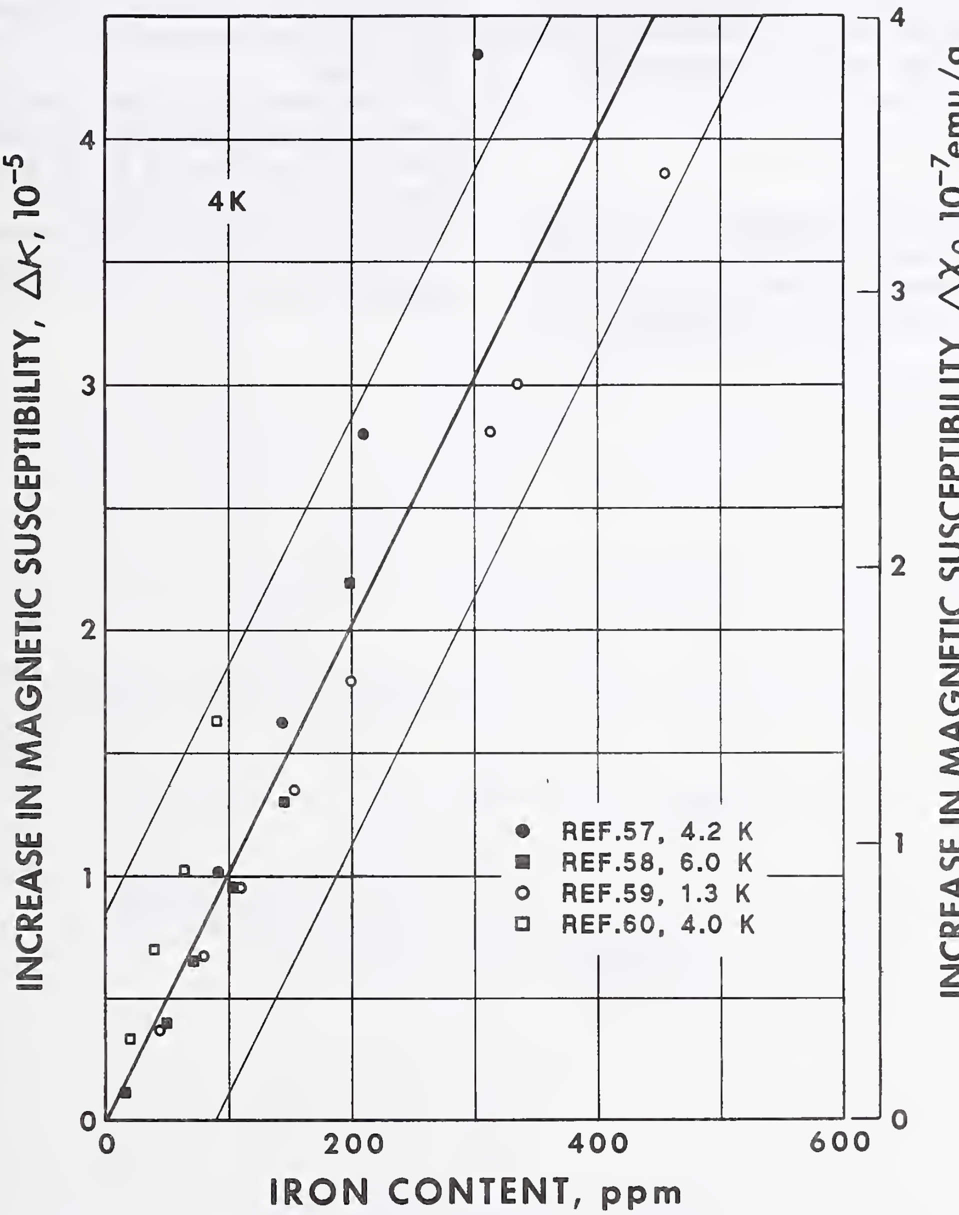

Figure 8.19. The change in magnetic susceptibility at ~4 K (data range from 1.3 to 6 K) of high-purity copper with the addition of iron as an impurity element is shown. These data were used to compute the regression of the change of magnetic susceptibility at 4 K upon iron content [Equation (8-11)]. All data are presented in Table 8.9.

DATA SOURCES AND ANALYSIS

Data on the magnetization of C10100 copper and dilute Cu:Fe alloys at 1.3 K are presented in Figure 8.20. The data were obtained from Reference 8.59; similar curves, not presented, were obtained at 4, 10, 20, and 33 K. Field strength ranged up to 7 Tesla.

DISCUSSION

Pure copper is diamagnetic, as shown in the figure; the addition of dilute iron impurities results in a Kondo system (see Reference 8.62 for further discussion). The data for small amounts of iron impurity are presented here because C10100 and C10200 coppers often contain enough iron to cause an observable effect on the magnetic properties at cryogenic temperatures. See also Figure 8.16 and the text preceding it for further discussion of the paramagnetic behavior of this dilute alloy system.

The relative permeability, dimensionless and of the same magnitude in SI and cgs units, is related to the magnetization, *M*, and applied filed, *H*, by $\mu_r = \mu/\mu_o = 1 + M/H$. *M* and *H* have SI units of A/m. The initial relative permeability, μ_{ri}, is measured near the origin of a magnetization vs. applied field curve.

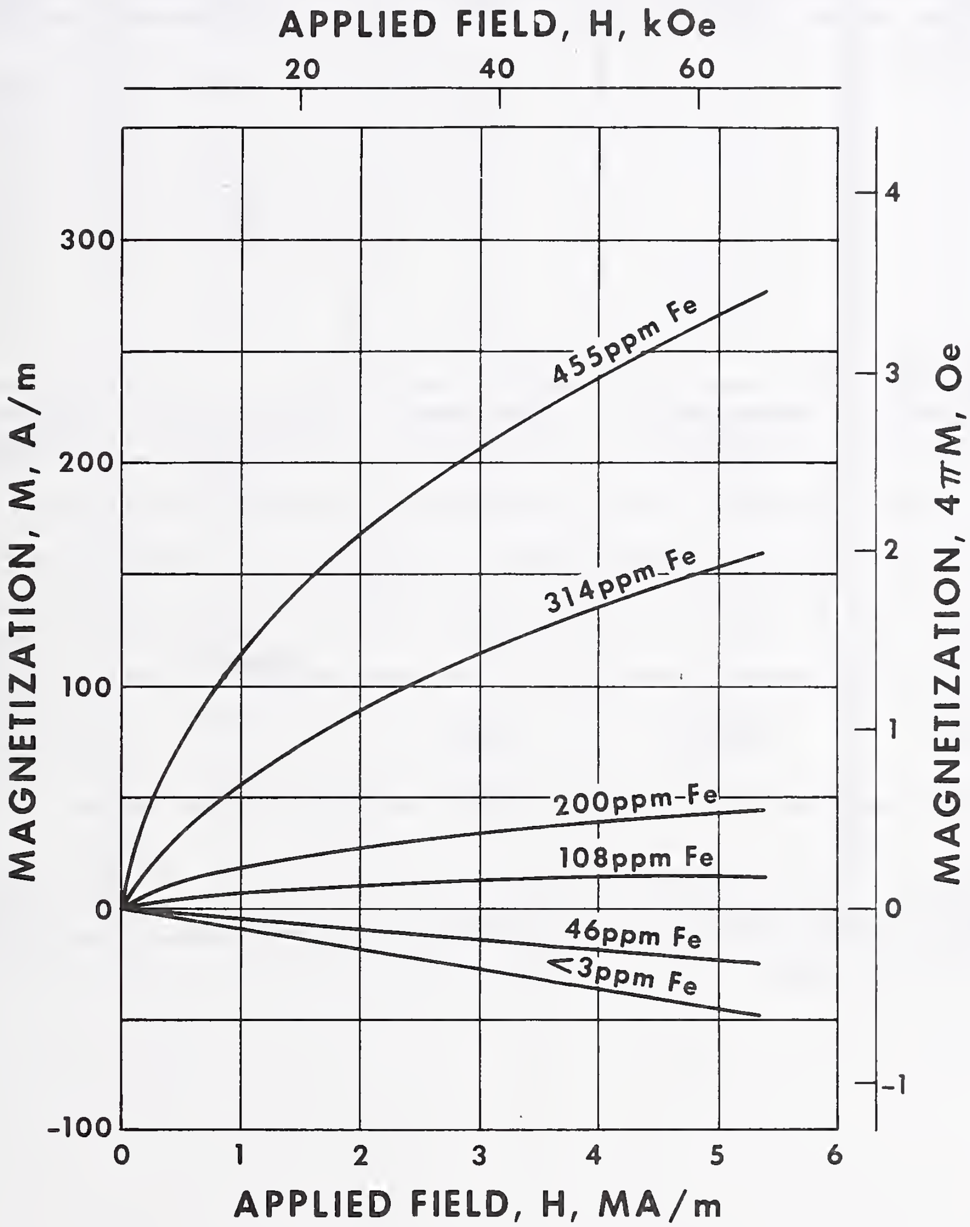

Figure 8.20. Magnetization data for C10100 copper and dilute Cu:Fe alloys are shown. The figure is adapted from data presented in Reference 8.59. The curves are labeled with atomic parts per million of Fe.

Table 8.10. Characterization of Materials and Measurements.

Reference No.	3A	3B	8	9
Specification	C10100	C10200	C10100	C10100
Composition (wt%)				
Cu	99.999	—	99.999	99.9988
Ag	—	—	—	0.0005
Cu + Ag	—	—	—	—
O_2	—	—	—	—
Bi	—	—	—	—
P	—	—	—	—
Pb	—	—	—	< 0.0004
S	—	—	—	—
Se	—	—	—	—
Te	—	—	—	—
Others (Only ≥ 0.001 wt%)	—	—	—	—
Material Condition	Annealed, 873 K, 4 h, Ar	Annealed, 873 K, 4 h, Ar	Cold-drawn, 295 K, 2.22–26.4%	Annealed, 723 K, 6 h, He
RRR	855	151, 272	180–530	—
Grain Size	—	—	—	—
Hardness	—	—	—	—
Product Form	Wire	Wire	Bar, 0.952-cm-dia.	Bar
Specimen Type	Wire	Wire	Wire	Wire
Width or Dia.	0.05 cm	0.05 cm	(a)	0.045, 0.112 cm
Thickness	—	—	—	—
Length	—	—	18 cm	—
No. of Measurements	—	—	—	—
Test Temperature	4, 16, 20 K	4, 16, 20 K	4–273 K	4–90 K

(a) 0.081–0.18 cm in diameter.

10	11	12A	12B	12C
C10200	C10100	C10100	C10200	C10200
— — — — — — — — — — —	99.996 — — 0.001 — 0.0003 0.001 — — 0.001 —	99.9957 — — — — — — — — — Fe: 0.0043	99.98 — — — — — — — — — Ge: 0.02	99.944 — — — — — — — — — Fe: 0.056
Annealed, 923 K, 1 h, vacuum	—	Annealed, 973 K, 2 h	Annealed, 973 K, 2 h	Annealed, 973 K, 2 h
14	—	—	—	—
—	—	—	—	—
—	—	—	—	—
Bar, 0.64-cm-dia.	Bar, 1.3-cm-dia.	—	—	—
Bar 0.326 cm — 23 cm	— — — 2.5 cm	Wire 0.1–0.2 cm — 6 cm	Wire 0.1–0.2 cm — 6 cm	Wire 0.1–0.2 cm — 6 cm
—	—	—	—	—
4–300 K	4–35 K	1.5–142 K	1.5–142 K	1.5–142 K

Table 8.10, continued

Reference No.	13	14	15	16
Specification	C10100	C10200	C10200	C10100
Composition (wt%)				
Cu	99.999	~ 99 (a)	—	99.99+
Ag	< 0.00003	< 0.1	—	—
Cu + Ag	—	—	—	—
O_2	—	< 0.1	—	—
Bi	< 0.00001	< 0.1	—	—
P	—	< 0.1	—	—
Pb	< 0.0001	< 0.1	—	—
S	< 0.0001	< 0.1	—	—
Se	< 0.0001	—	—	—
Te	< 0.0002	—	—	—
Others (Only ≥ 0.001 wt%)	—	Sb, Ni, Fe, As, Sn, Au, Mn, Hg, Cd, Zn: < 0.1	—	—
Material Condition	Cold-drawn, 295 K, 20–87.5%	Cold-drawn, 295 K, 60%	Cold-drawn, 298 K, 13.5, 75, 85%	Cold-drawn, 295 K, 38, 62, 84%
RRR	—	51	—	—
Grain Size	35 to 40 μm	287 μm	—	—
Hardness	—	R_B 39	(b)	—
Product Form	Bar, 0.582-cm-dia.	Bar	Wire, 0.13-cm-dia.	Bar
Specimen Type	Wire	Round	Wire	—
Width or Dia.	0.20 cm	0.635 cm	—	—
Thickness	—	—	—	—
Length	—	15.2 cm	—	—
No. of Measurements	—	1 per temperature	—	—
Test Temperature	293 K	4–273 K	293 K	295 K

(a) CDA 102 material.
(b) Values for 13.5, 75 and 85% cold-drawn conditions not specified; however, for a 37.5% cold-drawn condition a hardness (R_B) of 53.6 is reported.

17A	17B	18	19	20
C10100	C10500	C10100	C10100	C10200
99.9952 0.001 — 0.0002 not detected not detected 0.0003 0.002 — not detected —	99.9242 0.072 — 0.0002 not detected not detected 0.0003 0.002 — not detected —	> 99.996 — — — — — — — — — —	99.999 — — — — — — — — — —	99.96 < 0.01 — — — — < 0.01 — — — Cd, Si, Mg, Fe: < 0.01
Cold-drawn, 295 K 10, 25, 50% (a)	Cold-drawn, 295 K, 10, 25%	Cold-worked, 295 K, 96%	Cold-drawn, 295 K, 7.2–84%	Cold-drawn, 90 K 273 K (f)
—	—	—	—	—
(b)	(b)	—	—	—
(c)	(d)	—	VPN 92–122 (e)	—
Strip, 0.2 × 3.18 cm	Strip, 0.2 × 3.18 cm	Wire, 0.25-cm-dia.	Wire, 0.3-cm-dia.	Wire, 0.18-cm-dia.
Strip — — —	Strip — — —	Wire 0.05 cm — —	Wire — — 10 cm	Wire 0.056 cm — 20 cm
—	—	—	—	—
293 K	293 K	295 K	295 K	90, 273 K

(a) Fifty percent reduction achieved by drawing 32%, followed by rolling.
(b) Cold-drawn: 10%, 40 μm, 25%, 35 μm, 50%, not determined due to elongated grain shape.
(c) VPN (20 kg load): 10%, 91; 25%, 101.3; 50%, 111.0.
(d) VPN (20 kg load): 10%, 93.4; 25%, 102.0.
(e) Measured with 1 g load.
(f) Percent reduction of area: 90 K, 22–59%; 273 K, 19–90%.

Table 8.10, continued

Reference No.	21	22	23	24A
Specification	C10400	C10200	C10200	C10100
Composition (wt%)				
Cu	—	—	—	99.99
Ag	—	—	—	—
Cu + Ag	—	—	—	—
O_2	—	—	—	—
Bi	—	—	—	—
P	—	—	—	—
Pb	—	—	—	—
S	—	—	—	—
Se	—	—	—	—
Te	—	—	—	—
Others (Only ≥ 0.001 wt%)	—	—	—	—
Material Condition	Cold-rolled, 77 K, 10–60%	Cold-worked, 295 K, 5–25%	Cold-drawn, 295 K, 2–10%	Cold-drawn, 295 K, 21, 37, 60%
RRR	44–92	100–300	126–228	175
Grain Size	—	—	—	—
Hardness	—	(a)	—	—
Product Form	—	Wire	Bar (b)	Wire
Specimen Type	Round	Wire	Bar	Wire
Width or Dia.	0.6 cm	0.05, 0.10 cm	(b)	0.10 cm
Thickness	—	—	(b)	—
Length	3–3.5 cm	—	5 cm	—
No. of Measurements	—	—	—	1 per condition
Test Temperature	4, 76, 295 K	4 K	4 K	4 K

(a) Hardness available on 21% cold-worked only; 93 (Vickers hardness scale).
(b) Circular sections, 0.77-cm and 0.25-cm dia.; rectangular sections, 0.28 × 2.2 cm (dimensions before cold drawing).

C10100–C10700: Annealed; Cold-worked

Electromagnetic Properties (All)

24B	25	26	27	28
C10200	C10100	C10100	C10100	C10200
99.95 — — — — — — — — — —	99.99 — — — — — — — — — —	99.999+ — — — — — — — — — —	99.99, 99.999 — — — — — — — — — —	99.97 — — — — — — — — — —
Cold-drawn, 295 K 21, 37, 60%	Cold-drawn, 295 K, 7.5, 14.3%	Cold-drawn, 295 K, 20–82%	Cold-drawn, 77 K, 7.5, 14.3%	Cold-drawn, 78 K, 17%
60–240	180	82–172	(c)	300
—	—	—	—	—
—	—	—	—	—
Wire	Wire, 0.32-cm-dia.	Bar	—	Wire, 12-cm-long
Wire 0.10 cm — —	Wire (a) — —	Wire 0.325 cm — 11.4 cm	Wire 0.0126 cm — 0.81–1.11 cm	Wire — — —
1 per condition	4 samples (b)	—	—	—
4 K	4 K	4 K	4 K	78 K

(a) Cold-drawn: 7.5%, 1.37 × 10^{-2}-cm diameter; 14.3%, 1.27 × 10^{-2}-cm diameter.
(b) Nine transverse magnetic field values per sample.
(c) RRR: 7.5% cold-drawn, 138, 165; 14.3% cold-drawn, 81–162.

Table 8.10, continued

Reference No.	30	31	32	33
Specification	C10100	C10200	C10200	C10200
Composition (wt%)				
Cu	99.999	—	99.98	99.97
Ag	—	—	—	0.0001
Cu + Ag	—	—	—	—
O_2	—	—	—	—
Bi	—	—	—	—
P	—	—	—	—
Pb	—	—	—	—
S	—	—	—	—
Se	—	—	—	—
Te	—	—	—	—
Others (Only ≥ 0.001 wt%)	—	—	—	Fe: 0.005; Si: 0.001; Zn: 0.005
Material Condition	Cold-drawn, 78 K, 1.2–24.4%	Cold-worked, 78 K, 3.2–43.9%	Cold-rolled, 77 K, 21–88%	Annealed, 773 K, 2 h, before straining at 4 K
RRR	—	—	88	—
Grain Size	—	—	—	—
Hardness	—	—	—	—
Product Form	Wire, 0.13-cm-dia.	—	—	—
Specimen Type	Wire	Wire	Flat (a)	—
Width or Dia.	—	—	—	—
Thickness	—	—	—	—
Length	—	—	10 cm (b)	—
No. of Measurements	—	—	—	—
Test Temperature	78 K	78 K	77 K	4 K

(a) Cross sectional area before reduction = 0.1 × 0.08 cm.
(b) Before rolling.

34	35	36A	36B	37
C10200	C10100	C10100	C10200	C10200
—	99.99+	99.999+	—	—
—	0.0003	—	—	—
—	—	—	—	—
—	—	—	—	—
—	—	—	—	—
—	—	—	—	—
—	0.0004	—	—	—
—	—	—	—	—
—	—	—	—	—
—	—	—	—	—
—	—	—	—	—
Annealed (a)	Annealed, 703–1273 K, 1 h	—	—	Soft, ¼ hard, ½ hard, and hard
81–7000	—	—	—	37–222
86–122 μm	—	—	—	—
—	—	—	—	—
Bar, 1.9-cm-dia.	Bar	—	—	—
(b)	Wire	Flat	Flat	Wire
(c)	0.09–0.10 cm	1.27 cm	1.27 cm	0.10 cm
—	—	0.01 cm	0.002, 0.008 cm	—
(d)	—	10 cm	10 cm	4.0 cm
—	—	—	—	1 per condition
4–35 K	4 K	4 K	4 K	4 K

(a) Stress relief, 773 K, 0.25 h, vacuum; vacuum anneal, 1273 K, 1 h, 1.5×10^{-5} mm Hg; Oxygen anneal, 1273 K, 12 h, 5×10^{-4} mm Hg air.
(b) Bar, wire, and coil.
(c) Bar, 0.6-cm diameter; wire and coils, 0.15-cm diameter.
(d) Bar, 4.4 cm; wire, 5.0 cm; coils wound from wire 25 cm long.

Table 8.10, continued

Reference No.	38	39	40A	40B
Specification	C10100	C10100	C10100	C10200
Composition (wt%)				
Cu	99.999+	99.999	99.999	99.95
Ag	—	—	—	—
Cu + Ag	—	—	—	—
O_2	—	—	—	—
Bi	—	—	—	—
P	—	—	—	—
Pb	—	—	—	—
S	—	—	—	—
Se	—	—	—	—
Te	—	—	—	—
Others (Only ≥ 0.001 wt%)	—	—	—	—
Material Condition	Annealed, 1413 K, 114 h, vacuum (a)	Annealed, 1273 K, vacuum (b)	Annealed, 673 K, 0.17 h	Annealed, 673 K, 0.17 h
RRR	1330	—	200–300	200–300
Grain Size	—	—	—	—
Hardness	—	—	—	—
Product Form	—	—	Foil	Foil
Specimen Type	Wire	—	Flat	Flat
Width or Dia.	0.16 cm	—	0.012 cm	0.012 cm
Thickness	—	—	2.5×10^{-3} cm	2.5×10^{-3} cm
Length	—	—	2 cm	2 cm
No. of Measurements	—	—	—	—
Test Temperature	80–130 K	4, 330 K	4 K	4 K

(a) 10^{-5} mm Hg.
(b) Also, annealed in 192×10^{-5} Pa, air.

41A	41B	42	43	44
C10200	C10200	C10100	C10200	C10200
—	99.86	99.999	—	—
—	—	—	—	—
—	—	—	—	—
—	0.04	—	—	—
—	—	—	—	—
—	—	—	—	—
—	0.01	—	—	—
—	—	—	—	—
—	—	—	—	—
—	—	—	—	—
—	Ni: 0.02; Fe: 0.03; As: 0.04; Ca: 0.001	—	—	—
Annealed, 973 K, vacuum	Annealed, 973 K, vacuum	Annealed, 673 K, 4 h, vacuum	—	Annealed, 763 K, 1 h, high vacuum
—	—	700	—	450
—	—	—	—	—
—	—	—	—	—
Wire	Wire	Wire	—	—
Wire 0.015 cm — 20–30 cm	Wire 0.015 cm — 20–30 cm	Wire 0.02 cm — 2.5 cm	Wire 0.02–0.03 cm — —	Flat 0.45 cm 0.16 cm 3.7 cm
—	—	—	—	—
88, 193, 290 K	88, 193, 290 K	4, 78, 297 K	4, 80 K	4 K

Table 8.10, continued

Reference No.	49	50A	50B	51A
Specification	"OFHC"	"OFHC"	"OFHC"	C10100
Composition (wt%)				
Cu	—	99.999	99.999	99.9999
Ag	—	—	—	—
Cu + Ag	—	—	—	—
O_2	—	—	—	—
Bi	—	—	—	—
P	—	—	—	—
Pb	—	—	—	—
S	—	—	—	—
Se	—	—	—	—
Te	—	—	—	—
Others (Only ≥ 0.001 wt%)	—	—	—	Fe: 0.00001; Si: 0.000025
Material Condition	Annealed, 307 K (a)	Annealed	Cold-worked, 7.5%	Annealed, 823 K, 5 d, AC (b)
RRR	—	1780	166	—
Grain Size	—	—	—	—
Hardness	—	—	—	—
Product Form	Wire	Wire	Wire	Rod
Specimen Type	—	—	—	Cylinder
Width or Dia.	—	—	—	0.9 cm
Thickness	—	—	—	—
Length	—	1.0 cm	1.0 cm	0.5–2.0 cm
No. of Measurements	—	—	—	2 per temperature at 0.7 and 2 T
Test Temperature	4.2 K	4 K	4 K	5.9–294 K

(a) Cold-worked 7.5% and 14.3%.
(b) Measurements on unannealed samples gave similar results. All samples were heavily etched to remove any surface ferromagnetic contamination.

51B	51C	52	53	54
C10100	C10200	C10100	C10100	C10100
99.999	—	99.999	99.999	99.999
—	—	—	—	0.0001
—	—	—	—	—
—	—	—	—	—
—	—	—	—	—
—	—	—	—	—
—	—	—	—	—
—	—	—	—	—
—	—	—	—	—
—	—	—	—	—
Fe: 0.000035; Si: 0.00001	Fe: 0.000053; Mn: 0.000015; Ni: 0.00005	Co: < 0.0001; Fe: < 0.003; Mn: < 0.0002	Fe: < 0.0001; Ni: < 0.0001	Fe: 0.0002; Mn: 0.00005; Ni: 0.0003
Annealed, 823 K, 5 d, AC (a)	Annealed, 823 K, 5 d, AC (a)	(b)	Annealed, rean- nealed, after drawing and fabricating (c)	—
—	—	—	350	—
—	—	—	—	54
—	—	—	—	—
Rod	Rod	Rod	—	Rod
Cylinder 0.9 cm — 0.5–2.0 cm	Cylinder 0.9 cm — 0.5–2.0 cm	Cylinder — — 15 cm	50 Wires (d) 0.03 cm — 6 cm	Cubic block, 3.5 g — — —
2 per temperature at 0.7 and 2T	2 per temperature at 0.7 and 2 T	Several per temperature at 0.5–2.2 T	Several per temperature at 0.15–0.44 T	—
6.9–292 K	6.6–292 K	4–295 K	1.45–300 K	1.62–293 K

(a) Measurements on unannealed samples gave similar results. All samples were heavily etched to remove any surface ferromagnetic contamination.
(b) Specimens heavily pickled in nitric acid to remove surface ferromagnetic contamination.
(c) Wires were frequently etched to avoid surface ferromagnetic contamination during the drawing process and before annealing.
(d) Spaced apart by two polytetrafluoroethylene disks.

Table 8.10, continued

Reference No.	55	56A	56B	57
Specification	C10100	C10100	C10100	C10100
Composition (wt%)				
Cu	—	—	—	99.999 (c)
Ag	—	0.0005	< 0.00003	—
Cu + Ag	—	—	—	—
O_2	—	—	< 0.0001	—
Bi	—	—	< 0.00001	—
P	—	—	—	—
Pb	—	< 0.0004	< 0.0001	—
S	—	—	< 0.0001	—
Se	—	—	< 0.0001	—
Te	—	—	< 0.0002	—
Others (Only ≥ 0.001 wt%)	—	Ni: < 0.0003	(a)	—
Material Condition	—	—	(b)	Annealed
RRR	172	—	—	—
Grain Size	—	—	—	—
Hardness	—	—	—	—
Product Form	Rod	—	—	—
Specimen Type	Round	Cylinder	Cylinder	—
Width or Dia.	0.3 cm	0.75 cm	0.75 cm	—
Thickness	—	—	—	—
Length	—	2.0 cm	2.0 cm	—
No. of Measurements	—	—	—	Several per temperature at 0.09–0.85 T
Test Temperature	3.9–295 K	293 K	293 K	1.7–300 K

(a) As: < 0.0002; Cr: <0.00005; Fe: 0.00002; Ni: < 0.0001; Sb: < 0.0001; Sn: < 0.0001.
(b) Two specimens machined as received, 5 annealed in vacuum in pyrex containers for various periods of time. No differences were found in susceptibility measurements due to different heat treatments.
(c) Total metallic impurity content 10 ppm.

68	59	60
C10100	C10100	C10100
99.9999 — — — — — — — — — Fe: 0.00001; Si: 0.000025	99.999 — — — — — — — — — —	99.999 (a) — — — — — — — — — —
Annealed, 1273 K, 24 h, rapidly quenched	Annealed in H_2 or vacuum, H_2 quenched or WC	Annealed, 1273 K, 1 h, vacuum of 10^{-6} Torr
—	—	—
—	—	—
60	—	60
Rod	—	—
Cylinder 0.9 cm — 0.5–2.0 cm	Cylinder 0.7 cm — 2 cm	Rod 0.6 cm — —
2 per temperature at 0.7 and 2 T	—	—
6–294 K	1.3 K	4 K

(a) Purity of copper to which up to 91 atomic ppm of Fe was added.

REFERENCES

1. Gregory, P., Bangay, A. J., and Bird, T. L., "The Electrical Conductivity of Copper," Metallurgia and Metal Forming 71, 207–214 (1965).

2. Fickett, F. R., "Electrical Properties," in Materials at Low Temperatures, Eds. R. P. Reed and A. F. Clark, American Society for Metals, Metals Park, OH (1983).

3. Burnier, P., and Berteaux, F., "Electrical Properties of Copper at Low Temperatures," International Copper Research Association, Massy, France (1968).

4. Ornstein, J. L., "Effect of Silver Additions on the Softening Temperature and Mechanical Properties of Oxygen-free, High Conductivity Copper," Texas Instruments Inc., Attleboro, MA, Engineering Report No. 1497, 8 pp. (1964).

5. Hust, J. G., and Lankford, A. B., "Thermal Conductivity of Aluminum, Copper, Iron, and Tungsten for Temperatures from 1 K to the Melting Point," National Bureau of Standards, Boulder, CO, NBSIR 84-3007, 256 pp. (1984).

6. Toyoda, T., and Kume, K., "Residual Resistivities of Au- or Cu-Based 4d Transition Metal Dilute Alloys," Solid State Communications 15, 1889–1890 (1974).

7. Mertig, I., Mrosan, E., Zeller, R., and Dederichs, P. H., "Electronic Properties of Dilute Copper Alloys II. Residual Resistivity," Physica Status Solidi (B) 117, 619–623 (1983).

8. Powell, R. L., Roder, H. M., and Hall, W. J., "Low-Temperature Transport Properties of Copper and Its Dilute Alloys: Pure Copper, Annealed and Cold-Drawn," Physical Review 115, 314–323 (1959).

Roder, H. M., Powell, R. L., and Hall, W. J., "Thermal and Electrical Conductivity of Pure Copper," in Low Temperature Physics and Chemistry, Ed. J. R. Dillinger, University of Wisconsin Press, Madison, WI, 364–346 (1958).

9. Berman, R., and MacDonald, D. K. C., "The Thermal and Electrical Conductivity of Copper at Low Temperatures," Proceedings of the Royal Society of London A211, 122–128 (1952).

10. Hust, J. G., and Giarratano, P. J., "Thermal Conductivity," in Semi-Annual Report on Materials Research in Support of Superconducting Machinery , National Bureau of Standards, Boulder, Colorado, NBSIR 74-393, 1–35 (1974).

11. Nelson, W. E., and Hoffman, A. R., "Measurements of the Temperatures and Magnetic Field Dependence of Electrical Resistivity and Thermal Conductivity in OFHC Copper," in Thermal Conductivity 14, Eds., P. G. Klemens and T. K. Chu, Plenum Press, New York, 73–80 (1976).

12. White, G. K., and Woods, S. B., "Thermal and Electrical Conductivities of Solids at Low Temperatures," Canadian Journal of Physics 33, 58–73 (1955).

13. Smart, J. S., Smith, A. A., and Phillips, A. J., "Preparation and Some Properties of High-Purity Copper," Transactions of the American Institute of Mining and Metallurgical Engineers 143, 272–283 (1941).

REFERENCES

14. Clark, A. F., and Wallace, G. H., "Electrical Resistivity of Some Engineering Alloys at Low Temperatures," Cryogenics 10, 295–305 (1970).

15. Ellis, W. C., and Greiner, E. S., "Effect of Prior Strain at Low Temperatures on the Properties of Some Close-Packed Metals at Room Temperature," Transactions of the American Institute of Mining and Metallurgical Engineers 194, 648–650 (1952).

16. Crampton, D. K., Burghoff, H. L., and Stacy, J. T., "Effect of Cold-work upon Electrical Conductivity of Copper Alloys," Transactions of the American Institute of Mining and Metallurgical Engineers 133, 228–245 (1941).

17. Benson, N. D., McKeown, J., and Mends, D. N., "The Creep and Softening Properties of Copper for Alternator Rotor Windings," Journal of the Institute of Metals 80, 131–142 (1952).

18. Suzuki, H., Kanno, M., and Maeda, T., "Effects of Small Addition of Transition Elements on the Heat-resisting and Electrical Properties of Cold-worked Pure Copper, Journal of the Japan Institute of Metals 48, 209–213 (1984).

19. Rider, J. G., and Brooks, J. H. H., "The Relationship Between Hardness and Electrical Resistivity Changes Induced by Cold Work in Copper, Nickel, and Aluminium," Applied Materials Research 2, 44–50 (1963).

20. Broom, T., "The Effect of Temperature of Deformation on the Electrical Resistivity of Cold-worked Metals and Alloys," Proceedings of the Physical Society, London 65, 871–881 (1952).

21. Reed, R. P., Walsh, R. P., and Fickett, F. R., "Effects of Grain Size and Cold Rolling on Cryogenic Properties of Copper," in Advances in Cryogenic Engineering--Materials, Vol. 34, Eds., A. F. Clark and R. P. Reed, Plenum Press, New York, 299–308 (1988).

22. Yoshida, K., Takahashi, Y., Tada, E., Shimada, M., Tokuchi, A., Tada, N., and Shimamoto, S., "Mechanical Properties of the Japanese LCT Coil Conductor," in Advances in Cryogenic Engineering--Materials, Vol. 28, Eds., R. P. Reed and A. F. Clark, Plenum Press, New York, 781–790 (1982).

23. Taylor, M. T., and Woolcock, A., "Strengthening Superconducting Composite Conductors for Large Magnet Construction," Cryogenics 8, 317–319 (1968).

24. Fickett, F. R., "Conductors for Advanced Energy Systems," International Copper Research Association, New York, Project No. 321A, 97 pp. (1983).

25. Klabunde, C. E., and Coltman, R. R., "The Magnetoresistivity of Copper Irradiated at 4.4 K by Spallation Neutrons," Sixth Annual Progress Report on Special Purpose Materials for Magnetically Confined Fusion Reactors, U.S. Department of Energy, Washington, DC, DOE/ER-0113/3, UC-20c, 6 pp. (1984).

26. Carapella, S. C., Bess, M. L., and Leseur, D. R., "Factors Influencing Resistance Ratio Values of High-Purity Copper," Journal of Metals 25, 30–33 (1973).

REFERENCES

27. Guinan, M. W., "Radiation Effects Limits on Copper in Superconducting Magnets," in Copper and Copper Alloys for Fusion Reactor Applications, April 14-15, 1983, Washington, DC, Eds. F. W. Wiffen and R. E. Gold, Oak Ridge National Laboratory, Oak Ridge, TN, 229–242 (1983).

28. Berghout, C. W., "The Influence of Elastic Strains on the Recovery of Cold-worked Copper," Acta Metallurgica 6, 613–619 (1958).

29. Weyerer, Von H., "Die Änderung des Elektrischen Widerstandes Durch Kaltverformung," Zeitschrift für Metallkunde 44, 51–58 (1953).

30. Hibbard, W. R., "The Effect of Cold Work on the Electrical Resistivity of Copper Solid Solution Alloys," Acta Metallurgica 7, 565–574 (1959).

31. Kovacs, I., and Nagy, E., "Plastic Properties of Polycrystalline f.c.c. Metals," Physica Status Solidi 8, 795–803 (1965).

32. Gindin, I. A., Lazareva, M. B., and Matsevityy, V. M., "Lattice Defects in Copper Rolled at Low Temperatures," Fizika Metallov I Metallovedenie 23, 197–200 (1967).

33. Kitada, M., and Kudo, M., "Plastic Deformation of Cu and Cu-Ge Alloys at 4.2 K," Cryogenic Engineering (Tokyo) 6, 64–72 (1971).

34. Fickett, F. R., "A Preliminary Investigation of the Behavior of High-Purity Copper in High Magnetic Fields," International Copper Research Association, New York, Project No. 186, 69 pp. (1972).

35. Yntema, G. B., "Magnetoresistance of Mg, Cu, Sb, and Al at Liquid Helium Temperatures," Physical Review 91, 1388–1394 (1953).

36. Benz, M. G., "Magnetoresistance of Copper at 4.2 K in Transverse Fields up to 100 KG," Journal of Applied Physics 40, 2003–2005 (1969).

37. Fickett, F. R., "The Effect of Mill Temper on the Mechanical and Magnetoresistive Properties of Oxygen-Free Copper in Liquid Helium," in Advances in Cryogenic Engineering--Materials, Vol. 30, Eds., A. F. Clark, R. P. Reed, Plenum Press, New York, 453–460 (1984).

38. Witzenburg, W. Van, and Laubitz, M. J., "Magnetoresistances and the Phonon Conductivity of Metals," Canadian Journal of Physics 46, 1887–1894 (1968).

39. Williams, J. M., Klabunde, C. E., Redman, J. K., Coltman, R. R., and Chaplin, R. L., "The Effects of Irradiation on the Copper Normal Metal of a Composite Superconductor," Institute of Electrical and Electronics Engineers Transactions on Magnetics MAG-15, 731–734 (1979).

40. Van Konynenburg, R. A., Guinan, M. W., and Kinney, J. H., "Fusion Neutron Damage in Superconductors and Magnet Stabilizers," Journal of Nuclear Materials 103 & 104, 739–744 (1981).

41. Kapitza, P., "The Change of Electrical Conductivity in Strong Magnetic Fields, Parts I and II," Proceedings of the Royal Society of London A123, 292–341, 342–372 (1929).

REFERENCES

42. de Launay, J., Dolecek, R. L., and Webber, R. T., "Magnetoresistance of Copper," Journal of Physics and Chemistry of Solids 11, 37–42 (1959).

43. Lüthi, B., "Widerstandsanderung von Metallen in Hohen Magnetfeldern," Helvetica Physica Acta 33, 161–182 (1960).

44. Berlincourt, T. G., "Hall Effect, Magnetoresistance, and Size Effects in Copper," Physical Review 112, 381–387 (1958).

45. Fickett, F. R., "Transverse Magnetoresistence of Oxygen-free Copper," IEEE Transactions on Magnetics 24, 1156–1158 (1988).

46. Legvold, S., Vyrostek, T. A., Schaefer, J. A., Burgardt, P., and Peterson, D. T., "Electrical Resistivity and Magneto-Resistance of Very Dilute Cu-Cr Alloys," Solid State Communications 16, 477–480 (1975).

47. Powell, R. L., "Longitudinal Magnetoresistance of Copper," in Low Temperature Physics LT9, Plenum Press, New York, 732–735 (1965).

48. Rogers, J. T., De Panfilis, S., Melissinos, A. C., Moskowitz, B. E., Semertzidis, Y. K., Wuensch, W. U., Halama, H. J., Prodell, A. G., Fowler, W. B., and Nezrick, F. A., "Anomalous RF Magnetoresistence in Copper at 4 K," Applied Physics Letters 52, 2266–2268 (1988).

49. Guinan, M. W., and Van Konynenburg, R. A., "Fusion Neutron Effects on Magnetoresistivity of Copper Stabilizer Materials, Journal of Nuclear Materials 122 and 123, 1365–1370 (1984).

50. Guinan, M. W., "Radiation Effects Limits on Superconducting Magnets: Data Base for Copper Stabilizers," in Eighth Annual Progress Report on Special Purpose Materials for Magnetically Confined Fustion Reactors, U.S. Department of Energy, Washington, DC, DOE/ER-0113/5, 37–45 (1986).

51. Hurd, C. M., "A Magnetic Susceptibility Apparatus for Weakly Magnetic Metals, and the Susceptibility of Pure Copper in the Range 6–300 °K," Cryogenics 6, 264–269 (1966).

52. Pugh, E. W., and Ryan, F. M., "Magnetic Susceptibility of Copper-Nickel and Silver-Palladium Alloys at Low Temperatures," Physical Review 111, 1038–1042 (1958).

53. Bowers, R., "Magnetic Susceptibility of Copper Metal at Low Temperatures," Physical Review 102, 1486–1488 (1956).

54. Van Itterbeek, A., and Duchateau, W., "Measurements on the Magnetic Susceptibility of White Tin and Copper Down to Liquid Helium Temperatures," Physica 23, 169–172 (1957).

55. Hedgcock, F. T., "Magnetic Susceptibility of Dilute Cu Alloys at Low Temperatures," Physical Review 104, 1564–1567 (1956).

56. Henry, W. G., and Rogers, J. L., "The Magnetic Susceptibilities of Copper, Silver and Gold and Errors in the Gouy Method," Philosophical Magazine 1, 223–236 (1956).

REFERENCES

57. Ekström, H. E., and Myers, H. P., "The Magnetic Susceptibility of Dilute CuFe Alloys in the Temperature Range 1.7–300 K," Physik der Kondensierten Materie 14, 265–274 (1972).

58. Hurd, C. M., "Magnetic Susceptibility of Very Dilute Cu-Fe and Au-Fe Alloys in the Range 6–300 °K," Journal of Physics and Chemistry of Solids 28, 1345–1352 (1967).

59. Tholence, J. L., and Tournier, R., "One-Impurity and Interaction Effects on the Cu:Fe Magnetization," Physical Review Letters 25, 867–871 (1970).

60. Fickett, F. R., "A Preliminary Investigation of the Behavior of High Purity Copper in High Magnetic Fields," International Copper Research Association, New York, Report 186B (1974).

61. Klein, M. W., "Magnetic Susceptibility of a Two-Component Kondo System: Proposed Experiment to Distinguish Between Various Models for the c^2 Dependence of χ," Journal of Low Temperature Physics 22, 85–103 (1976).

62. Heeger, A. J., "Localized Moments and Nonmoments in Metals: The Kondo Effect," 284–412 and Kondo, J., "Theory of Dilute Magnetic Alloys," 184–283 in Solid State Physics, Vol. 23, Eds. F. Seitz, D. Turnbull, H. Ehrenreich, Academic Press, New York (1969).

DATA SOURCES AND ANALYSIS

Measurements of the yield strength of annealed, and annealed and aged C17000 beryllium copper from 77 to 293 K were obtained from Reference 9.1. This source reported the stress at a total strain of 0.1 instead of the 0.2%-offset yield strength, σ_y. Measurements from Reference 9.2 on annealed material at 295 K only are presented for comparison. Product was in strip form.

RESULTS

All measurements are reported in Table 9.1, which presents σ_y, test temperature, aging temperature and time, and the reference number. The available characterization of materials and measurements is given in Table 9.57 at the end of the tensile properties section. Figure 9.1 presents the σ_y measurements as a function of test temperature.

The trend for the temperature dependence is similar for the measurements on each of the aging conditions. Perhaps because of the long aging times reported for these specimens, σ_y at room temperature is comparable to other results (Reference 9.2) on annealed material.

Table 9.1. Yield Strength Dependence of Annealed, and Annealed and Aged C17000 Beryllium Copper upon Temperature (77–295 K).

Yield Strength, MPa	Test Temperature, K	Aging Temperature, K	Aging Time, h	Reference No.
188	77	77	0	1
192	175	0	0	1
98	293	0	0	1
257	77	458	45	1
247	175	408	45	1
192	293	458	45	1
343	77	408	45	1
310	175	408	·8	1
271	293	408	45	1
343	77	360	20	1
247	293	360	20	1
222	295	0	0	2
230	295	0	0	2

Aging Temperature, 0 K = not aged.

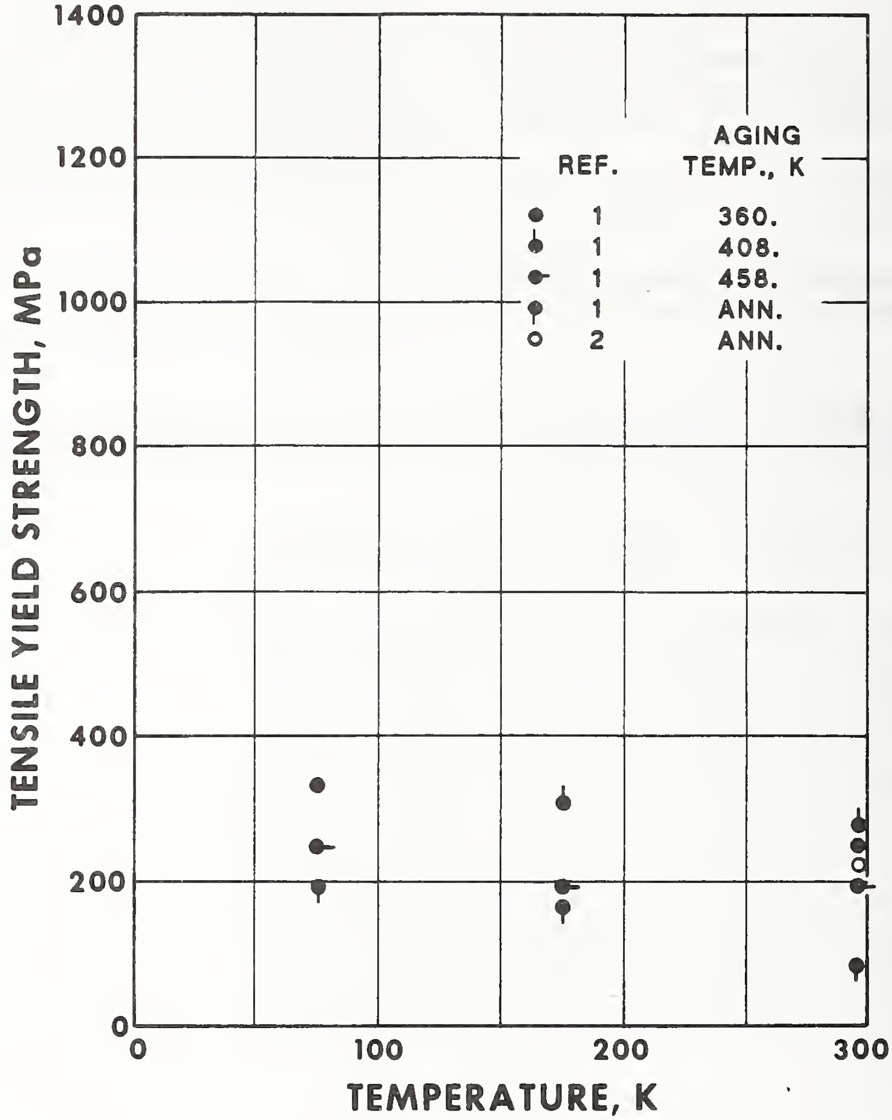

Figure 9.1. Yield strength measurements of annealed, and annealed and aged C17000 beryllium copper are shown as a function of test temperature. For clarity, overlapping data points are omitted from the figure. All data are presented in Table 9.1. Product was in strip form.

DATA SOURCES AND ANALYSIS

Measurements of the yield strength of annealed C17000 beryllium copper at 295 K as a function of aging temperature and time were obtained from four sources (References 9.1–9.4). All sources reported 0.2%-offset yield strength, σ_y, except Reference 9.1, which reported the stress at a strain of 0.1. Product was in strip form. Reported aging temperatures ranged from 360 to 630 K; aging times from 2 to 48 h. Aging temperatures and times were not specified in References 9.3 and 9.4, sometimes for proprietary reasons. Not enough data were available to estimate optimum aging temperatures and times.

RESULTS

All measurements are reported in Table 9.2, which presents σ_y, aging temperature and time, and the reference number. (Because the highest and lowest values obtained were reported in Reference 9.4 in place of the original data, the measurements presented in the figures and tables for this reference should be considered upper and lower limits.) The available characterization of materials and measurements is given in Table 9.57 at the end of the tensile properties section. Figures 9.2 and 9.3 present the σ_y measurements as a function of aging temperature and time, respectively. Unspecified values of temperature or time are plotted on the *y*-axis. Two σ_y measurements from Reference 9.1 at long aging times are not shown in Figure 9.3.

The σ_y reported in Reference 9.2 after high aging temperatures (602–630 K) for short times (2–3 h) are higher than the σ_y after lower temperatures with longer times (Reference 9.1). The σ_y obtained with the aging conditions of Reference 9.2 are about as high as those reported in References 9.3 and 9.4 where aging conditions were unspecified for proprietary reasons.

Table 9.2. Yield Strength Dependence of Annealed C17000 Beryllium Copper on Aging Temperature and Time (295 K).

Yield Strength, MPa	Aging Temperature, K	Aging Time, h	Reference No.
247	360	20	1
271	408	48	4
192	458	45	4
590	N.S.	N.S.	4
890	N.S.	N.S.	4
1100	N.S.	N.S.	4
904	602	3	2
1005	6[illegible]	3	2
931	630	2	2
1005	630	2	2
969	616	3	2
10[illegible]5	616	3	2
841	588	3	2
910	588	3	2

N.S. = not specified.

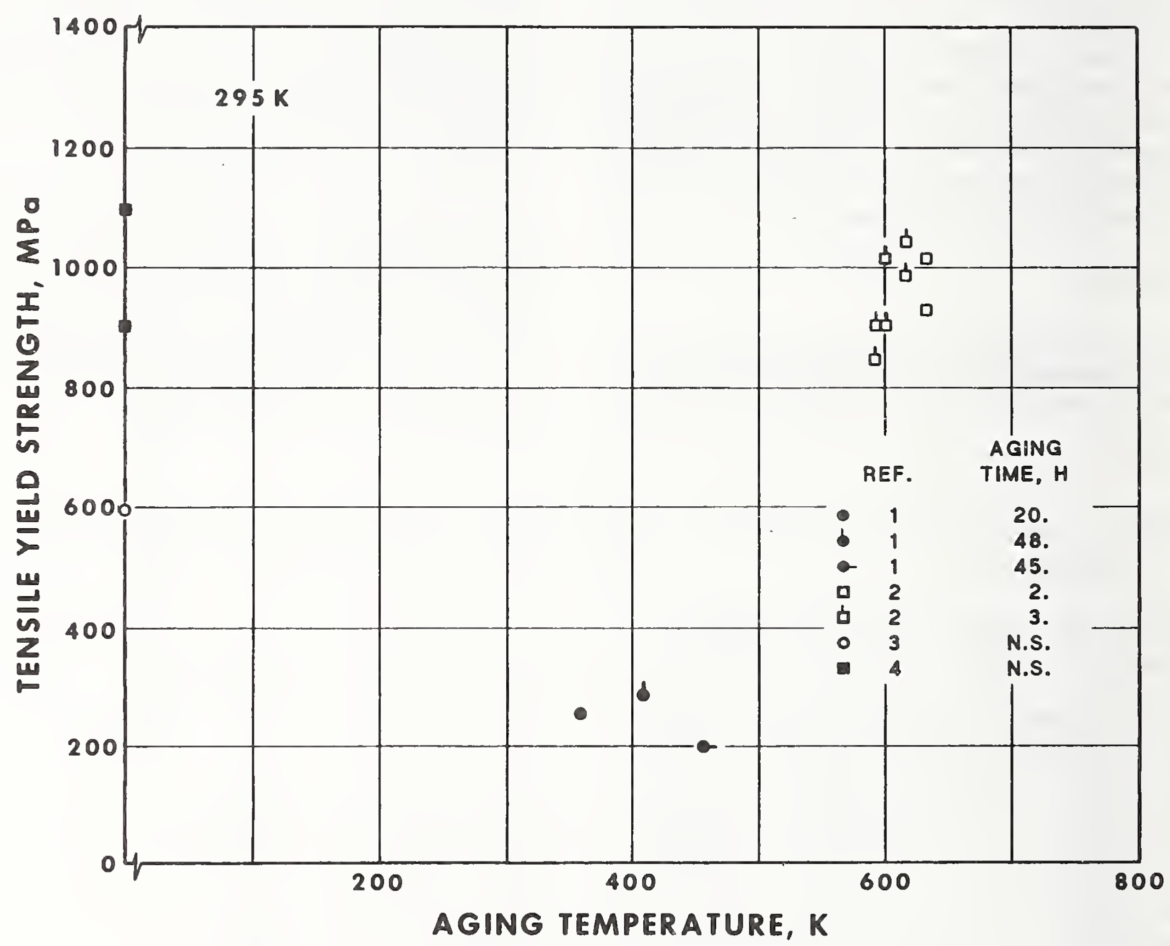

Figure 9.2. Yield strength measurements on annealed C17000 beryllium copper at 295 K are shown as a function of aging temperature. If this parameter was not specified, yield strength is plotted on the *y*-axis. All data are presented in Table 9.2. Product was in strip form. (N.S. in legend for References 9.3 and 9.4 indicates not specified.)

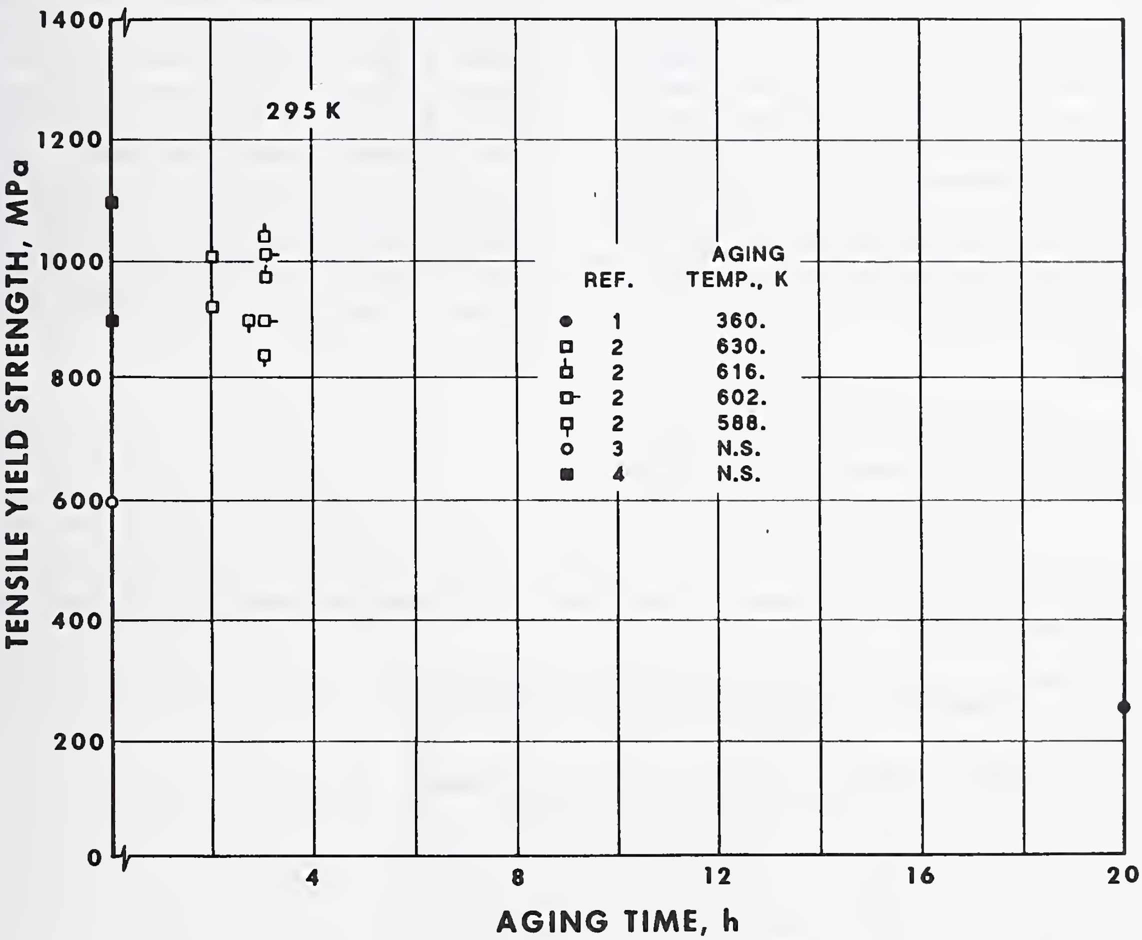

Figure 9.3. Yield strength (σ_y) measurements on annealed C17000 beryllium copper at 295 K are shown as a function of aging time. If this parameter was not specified, σ_y is plotted on the *y*-axis. Two σ_y values from Reference 9.1 at long aging times do not appear in the figure. For clarity, overlapping data points are omitted from the figure. All data are presented in Table 9.2. Product was in strip form. (N.S. in legend for References 9.3 and 9.4 indicates not specified.)

DATA SOURCES AND ANALYSIS

Measurements of the yield strength, σ_y, of cold-worked C17000 beryllium copper at 295 K as a function of aging temperature and time were obtained from four sources (References 9.2–9.5). All sources reported 0.2%-offset yield strength (σ_y) except Reference 9.5 (not specified). Product was in strip form. Cold work, *CW*, (carried out before aging) ranged from 11 to 50% (reduction in thickness). Reported aging temperatures ranged from 588 to 630 K; aging times from 2 to 3 h. Aging temperatures and times were not specified in References 9.3 and 9.4, and for several measurements in Reference 9.5, sometimes for proprietary reasons. Sufficient data were available to estimate a range of optimum aging temperatures and times.

RESULTS

All measurements are reported in Table 9.3, which presents σ_y, *CW* (reduction in thickness in percent), aging temperature and time, and the reference number. (Because the highest and lowest values obtained were reported in Reference 9.4 in place of the original data, the measurements presented in the figures and tables for this reference should be considered upper and lower limits.) The available characterization of materials and measurements is given in Table 9.57 at the end of the tensile properties section. Figures 9.4 and 9.5 present the σ_y measurements as a function of aging temperature and time, respectively. Unspecified values of temperature or time are plotted on the *y*-axis.

The figures indicate that the optimum aging temperature is about 600 K, and the optimum aging times range from about 2 to 3 h. The σ_y for these aging conditions are approximately as high as measurements for unspecified aging conditions.

Table 9.3. Yield Strength Dependence of Cold-worked C17000 Beryllium Copper on Aging Temperature and Time (295 K).

Yield Strength, MPa	Cold Work, %	Aging Temperature, K	Aging Time, h	Reference No.
570	11	N.S.	N.S.	5
1071	11	589	2.0	5
648	11	N.S.	N.S.	3
636	11	N.S.	N.S.	3
761	21	N.S.	N.S.	3
831	21	N.S.	N.S.	3
1062	50	N.S.	N.S.	3
1213	50	N.S.	N.S.	3
1070	37	N.S.	N.S.	4
1275	37	N.S.	N.S.	4
1030	11	630	3.0	2
1039	21	602	2.5	2
1072	37	602	2.5	2
1067	11	602	3.0	2
1080	21	602	2.5	2
1117	37	602	2.0	2
963	11	630	2.5	2
991	21	630	2.0	2
1009	37	630	2.0	2
1012	11	630	2.0	2
1021	21	630	2.0	2
1037	37	630	2.0	2

C17000: Cold-worked and Aged

Tensile Yield Strength vs. Aging Temperature, Time (295 K)

Table 9.3, continued

Yield Strength, MPa	Cold Work, %	Aging Temperature, K	Aging Time, h	Reference No.
969	11	616	3.0	2
996	21	616	2.5	2
1031	37	616	2.0	2
1028	11	616	3.0	2
1030	21	616	2.0	2
1065	37	616	2.5	2
912	11	588	2.0	2
990	21	588	2.0	2
1063	37	588	2.0	2
1005	11	588	2.0	2
1049	21	588	2.0	2
1117	37	588	2.0	2

N.S. = not specified.

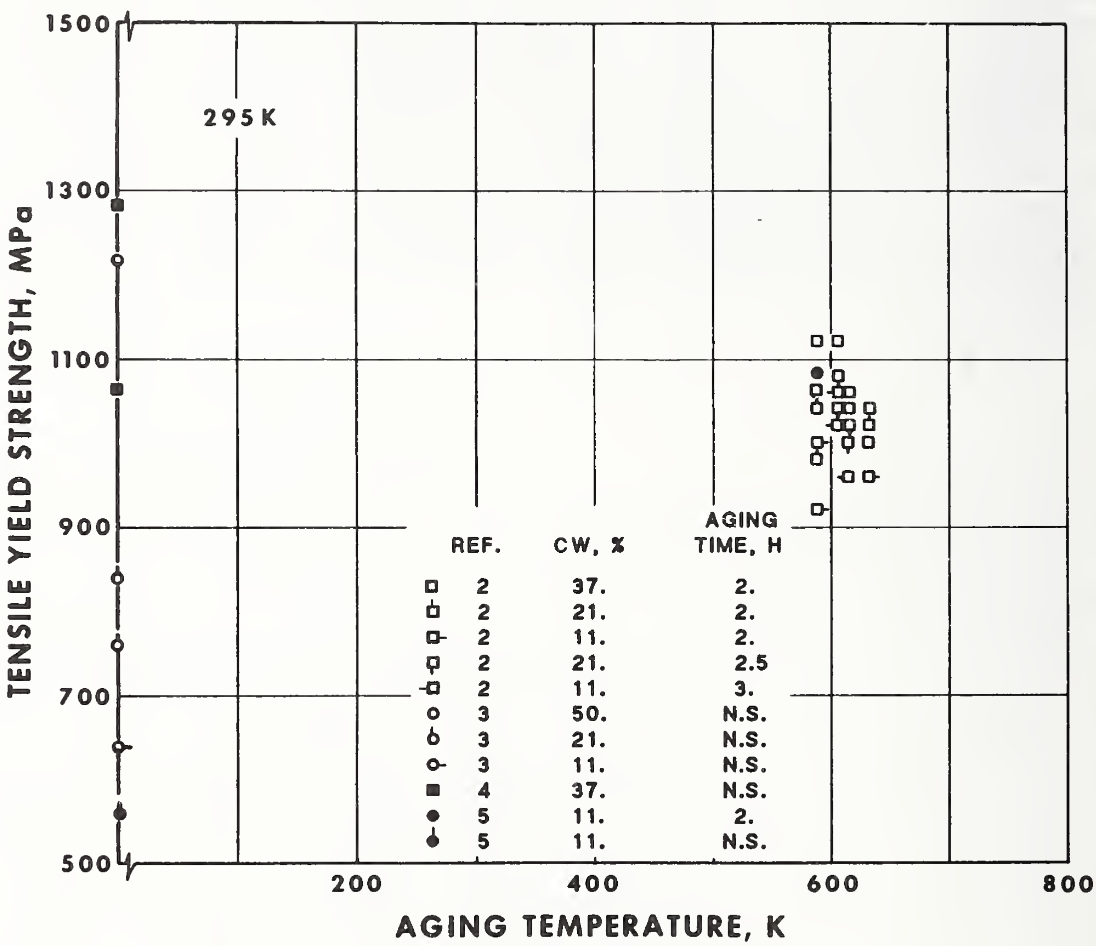

Figure 9.4. Yield strength measurements on cold-worked C17000 beryllium copper at 295 K are shown as a function of aging temperature. If this parameter was not specified, yield strength is plotted on the *y*-axis. For clarity, overlapping data points are omitted from the figure. All data are presented in Table 9.3. Product was in strip form. (N.S. in legend for References 9.3–9.5 indicates not specified.)

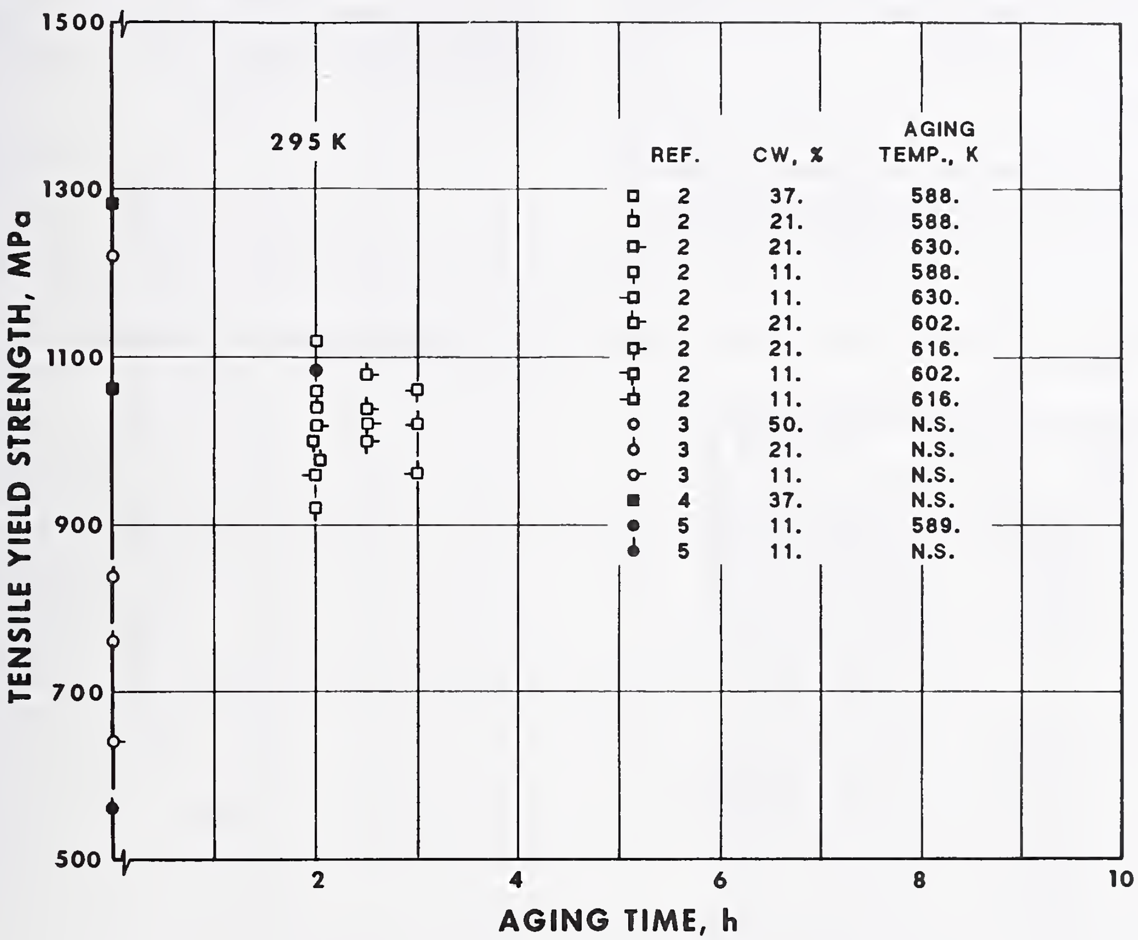

Figure 9.5. Yield strength measurements on cold-worked C17000 beryllium copper at 295 K are shown as a function of aging time. If this parameter was not specified, yield strength is plotted on the y-axis. For clarity, overlapping data points are omitted from the figure. All data are presented in Table 9.3. The legend for this graph is given on the following page. Product was in strip form. (N.S. in legend for References 9.3–9.5 indicates not specified.)

C17200: Annealed

Tensile Yield Strength vs. Temperature (20–300 K)

DATA SOURCES AND ANALYSIS

Measurements of the yield strength of annealed C17200 beryllium copper between 20 and 300 K were obtained from five sources (References 9.1, and 9.6–9.9). All sources reported 0.2%-offset yield strength (σ_y) except Reference 9.1, which reported the stress at a total strain of 0.1. Products were in strip or bar form (not specified in Reference 9.8).

RESULTS

All measurements are reported in Table 9.4, which presents σ_y, test temperature, and the reference number. The available characterization of materials and measurements is given in Table 9.57 at the end of the tensile properties section. Figure 9.6 presents the σ_y measurements as a function of test temperature.

Reference 9.10 presents measurements from 93 to 293 K on the σ_y of a 2.6-wt% beryllium-copper alloy in an annealed condition. These data exhibit an increase in strength as the temperature decreases that is similar to the trend shown in Figure 9.6.

Table 9.4. Yield Strength Dependence of Annealed C17200 Beryllium Copper upon Temperature (20–300 K).

Yield Strength, MPa	Test Temperature, K	Reference No.
237	77	1
212	175	1
135	293	1
238	300	6
262	214	6
314	144	6
390	88	6
185	295	7
192	255	7
238	195	7
241	195	7
343	76	7
396	76	1
403	20	7
398	80	7
236	215	8
221	255	8
234	300	8
269	295	9
307	232	9

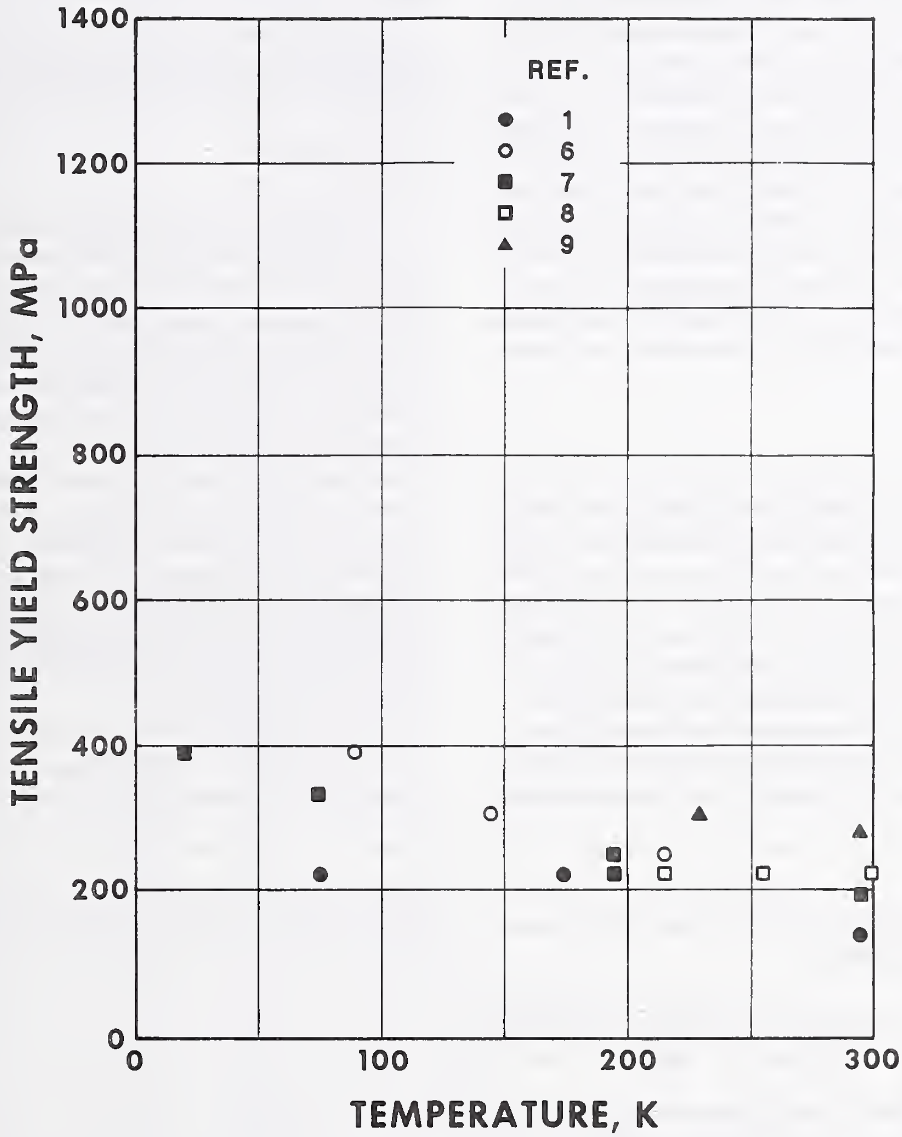

Figure 9.6. Yield strength measurements of annealed C17200 beryllium copper are shown as a function of test temperature. For clarity, overlapping data points are omitted from the figure. All data are presented in Table 9.4. Products were in strip or bar form (not specified in Reference 9.8).

DATA SOURCES AND ANALYSIS

Measurements of the yield strength of annealed C17200 beryllium copper at 295 K as a function of aging temperature and time were obtained from 17 sources (References 9.1–9.4, 9.6, and 9.11–9.22). All sources reported 0.2%-offset yield strength, σ_y, except Reference 9.1, which reported the stress at a strain of 0.1, Reference 9.19 (0.1%-offset), and References 9.14 and 9.22 (not specified). Product forms were wire, sheet, strip, bar, and plate. Reported aging temperatures ranged from 408 to 723 K; aging times from 0.33 to 170 h. Aging temperatures and/or times were not specified in References 9.4 and 9.22. Sufficient data were available to estimate a range of optimum aging temperatures and times.

RESULTS

All measurements are reported in Table 9.5, which presents σ_y, aging temperature and time, and the reference number. (Because the highest and lowest values obtained were reported in Reference 9.4 in place of the original data, the measurements presented in the figures and tables for this reference should be considered upper and lower limits.) The available characterization of materials and measurements is given in Table 9.57 at the end of the tensile properties section. Figures 9.7 and 9.8 present the σ_y measurements as a function of aging temperature and time, respectively. Unspecified values of temperature or time are plotted on the *y*-axis. Three yield strength measurements from References 9.1 and 9.19 at long aging times are not shown in Figure 9.8.

The figures indicate that optimum aging temperatures range from about 588 to 644 K, and optimum aging times from 0.5 to 3 h.

DISCUSSION

Reference 9.23 discusses metallurgical aspects of the precipitation-hardening dependence of C17200 beryllium on temperature and time. At higher aging temperatures, precipitation is faster and peak properties are obtained more rapidly. At longer times, the precipitated particles coalesce, and hardness and strength drop off (overaging). In Figure 9.30, which presents tensile strength vs. aging time, the strength first increases rapidly, but the slope becomes less steep at longer aging times. Reference 9.23 also discusses the advantages of achieving a given strength level by under- or overaging, and the relationship with elastic modulus, which reaches a peak after the maximum in yield or tensile strength is attained.

The effect of thickness upon hardness of annealed and aged C17200 beryllium copper is discussed in Reference 9.24 (for strip).

Table 9.5. Yield Strength Dependence of Annealed C17200 Beryllium Copper on Aging Temperature and Time (295 K).

Yield Strength, MPa	Aging Temperature, K	Aging Time, h	Reference No.
259	458	45.0	1
298	408	48.0	1
922	588	3.0	11
904	588	3.0	11
922	588	3.0	11
904	588	3.0	6
862	672	1.5	6
1027	588	3.0	12
1020	588	3.0	12
1031	588	3.0	13
1045	588	3.0	13
1048	588	3.0	13

Table 9.5, continued

Yield Strength, MPa	Aging Temperature, K	Aging Time, h	Reference No.
1200	566	3.0	18
1020	588	3.0	13
979	566	3.0	18
931	588	3.0	13
630	566	0.33	14
627	566	0.50	14
741	566	0.67	18
858	566	0.83	14
741	566	1.00	18
850	566	0.50	14
979	566	2.00	18
1030	588	3.00	15
1286	573	3.00	18
240	473	0.50	14
343	473	17.00	18
859	473	170.00	14
1007	566	3.00	18
1101	644	0.50	13
1062	644	0.50	18
1093	588	2.00	3
1280	566	2.00	3
1030	588	3.00	22
1280	566	2.00	21
850	N.S.	N.S.	4
1170	N.S.	N.S.	4
180	473	N.S.	22
188	593	N.S.	22
199	623	N.S.	22
204	723	N.S.	22
1101	580	2.00	2
1280	630	2.00	2
1101	580	2.00	2
1288	616	3.00	2
1152	588	3.00	2
1153	616	3.00	2
1101	508	3.00	2
1169	602	3.00	2
1182	602	3.00	2
1063	588	3.00	2
1120	588	3.00	2
1140	588	3.00	2

N.S. = not specified.

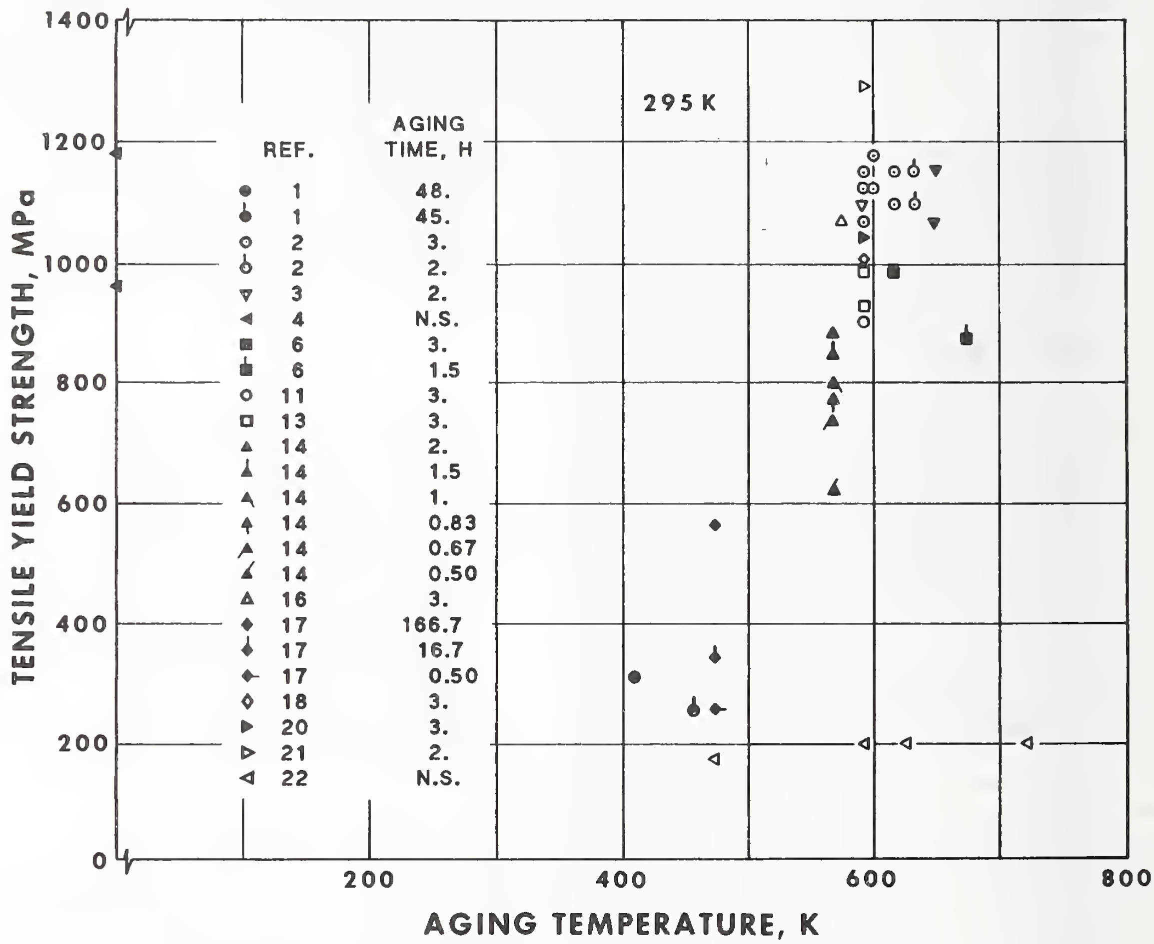

Figure 9.7. Yield strength measurements on annealed C17200 beryllium copper at 295 K are shown as a function of aging temperature. If this parameter was not specified, yield strength is plotted on the *y*-axis. For clarity, overlapping data points are omitted from the figure, including all data points from References 9.12 and 9.15. All data are presented in Table 9.5. Products were in wire, sheet, strip, bar, and plate form. (N.S. in legend for References 9.4 and 9.22 indicates not specified.)

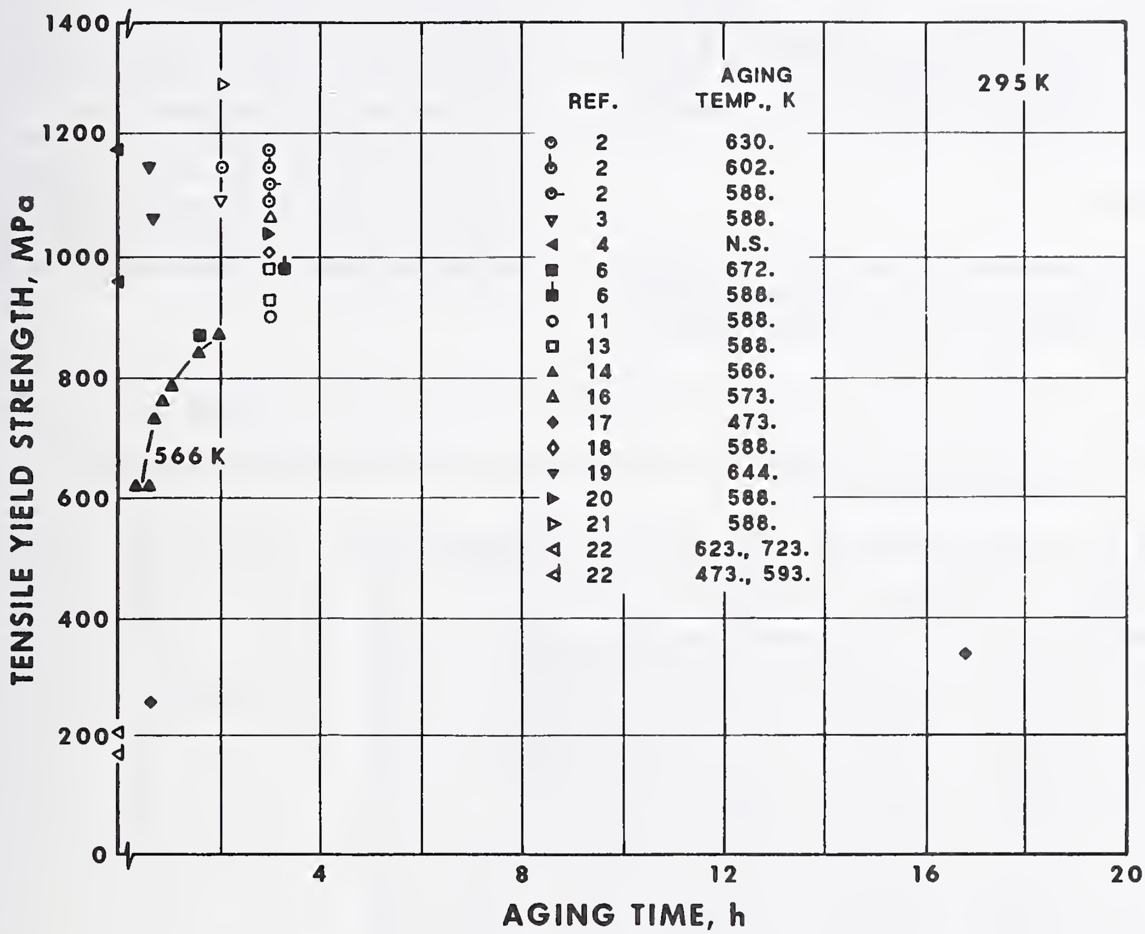

Figure 9.8. Yield strength (σ_y) measurements on annealed C17200 beryllium copper at 295 K are shown as a function of aging time. If this parameter was not specified, σ_y is plotted on the *y*-axis. Three σ_y values from References 9.1 and 9.17 at long aging times do not appear in the figure. For clarity, overlapping data points are omitted from the figure, including all data points from References 9.12 and 9.15. All data are presented in Table 9.5. Products were in wire, sheet, strip, bar, and plate form. (N.S. in legend for Reference 9.4 indicates not specified.)

C17200: Annealed and Aged

Tensile Yield Strength vs. Temperature (20–300 K)

DATA SOURCES AND ANALYSIS

Measurements of the yield strength of annealed and aged C17200 beryllium copper between 20 and 300 K were obtained from five sources (References 9.1, 9.6, 9.11, 9.12, and 9.19). All sources reported 0.2%-offset yield strength (σ_y) except Reference 9.1, which reported the stress at 0.1 total strain, and Reference 9.19, which reported 0.1%-offset strength. Products were in sheet, strip, and bar form (not specified in Reference 9.12).

RESULTS

All measurements are reported in Table 9.6, which presents σ_y, test temperature, aging temperature and time, and the reference number. The available characterization of materials and measurements is given in Table 9.57 at the end of the tensile properties section. Figure 9.9 presents the σ_y measurements as a function of test temperature.

The strengths (at 0.1 total strain) reported in Reference 9.1 fall considerably below the others shown in Figure 9.9. Probably this is due to the relatively long aging times. These strengths also do not increase with decreasing temperature as sharply as the other measurements do.

Reference 9.10 presents measurements from 93 to 293 K on the proof stress of a 2.6-wt% beryllium-copper alloy in an aged condition. These data exhibit an increase in strength as the temperature decreases that is similar to the trend shown in Figure 9.9.

Table 9.6. Yield Strength Dependence of Annealed and Aged C17200 Beryllium Copper upon Temperature (20–300 K).

Yield Strength, MPa	Test Temperature, K	Aging Temperature, K	Aging Time, h	Reference No.
288	77	458	45.0	1
304	175	458	45.0	1
259	293	458	45.0	1
347	77	408	48.0	1
320	175	408	48.0	1
298	293	408	48.0	1
32[illegible]	295	588	3.0	11
304	293	588	3.0	11
32[illegible]	295	588	3.0	11
1330	80	588	3.0	11
1305	80	588	3.0	11
1313	80	588	3.0	11
1108	300	588	3.0	6
1103	214	588	3.0	6
1117	144	588	3.0	6
1186	88	588	3.0	6
1[illegible]63	88	672	1.5	6
1027	88	672	1.5	6
910	214	672	1.5	6
862	300	672	1.5	6
1027	293	588	3.0	12
1020	293	588	3.0	12
1103	197	588	3.0	12
1076	197	588	3.0	12
1310	77	588	3.0	12
1241	77	588	3.0	12
1151	300	644	0.5	19

Table 9.6, continued

Yield Strength, MPa	Test Temperature, K	Aging Temperature, K	Aging Time, h	Reference No.
1062	300	644	0.5	19
1027	200	644	0.5	19
1158	200	644	0.5	19

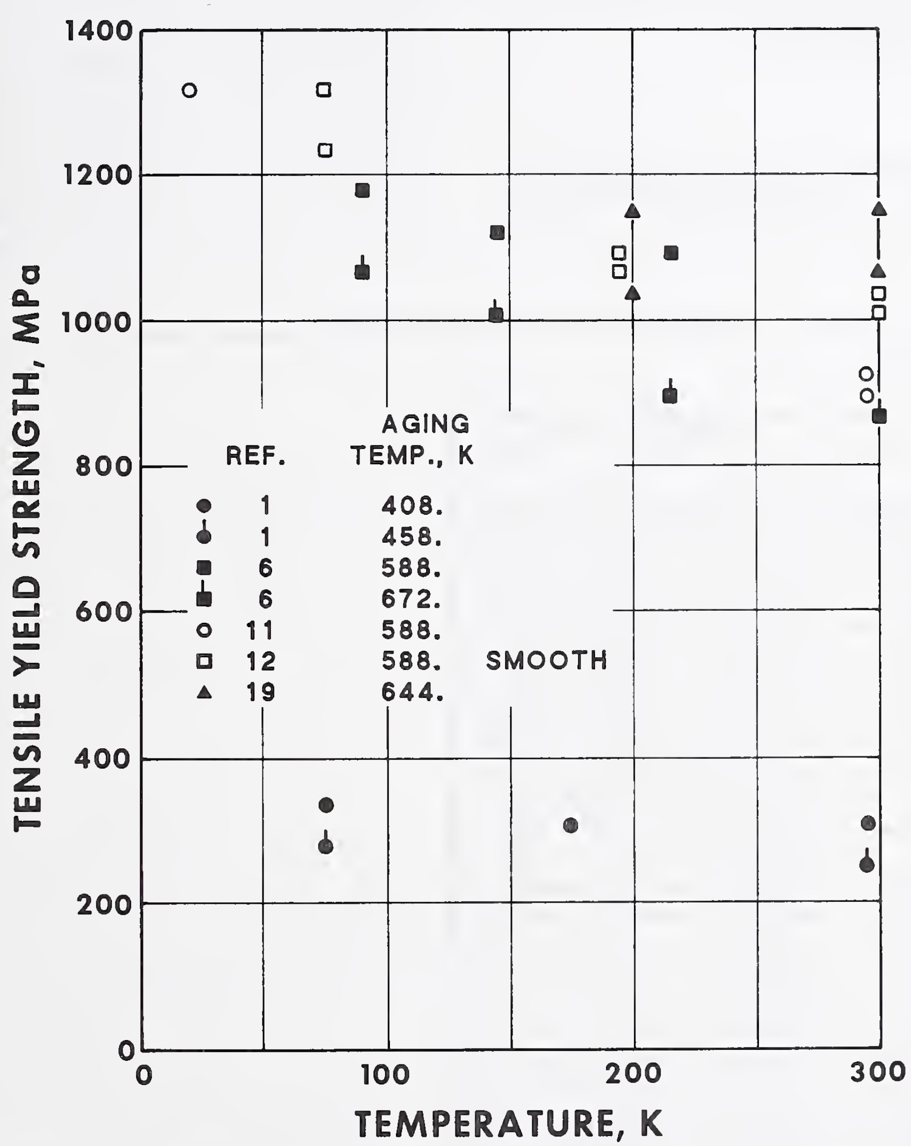

Figure 9.9. Yield strength measurements of annealed and aged C17200 beryllium copper are shown as a function of test temperature. For clarity, overlapping data points are omitted from the figure. All data are presented in Table 9.6. Products were in sheet, strip, and bar form (not specified in Reference 9.12).

DATA SOURCES AND ANALYSIS

Measurements of the yield strength of cold-worked C17200 beryllium copper between 20 and 300 K were obtained from five sources (References 9.6, 9.7, 9.9, 9.25, and 9.26). Data from Reference 9.27 at 295 K only are presented for comparison because measurements were made for varying amounts of cold work, *CW*. All sources reported 0.2%-offset yield strength (σ_y). Products were in sheet, strip, and bar form (not specified in Reference 9.26).

RESULTS

All measurements are reported in Table 9.7, which presents σ_y, test temperature, *CW* (reduction in thickness or area in percent), and the reference number. (The percent of *CW* could not be determined from Reference 9.26: it was 21% if the material was rolled or 37% if it was drawn.) The available characterization of materials and measurements is given in Table 9.57 at the end of the tensile properties section. Figure 9.10 presents the σ_y measurements as a function of test temperature.

Table 9.7. Yield Strength Dependence of Cold-worked C17200 Beryllium Copper upon Temperature, (20–300 K).

Yield Strength, MPa	Test Temperature, K	Cold Work, %	Reference No.
765	20	33	6
710	144	33	6
672	214	33	6
606	300	33	6
731	20	21	25
752	20	21	25
662	76	21	25
680	76	21	25
690	76	21	25
710	76	21	25
600	195	21	25
600	195	21	25
538	300	21	25
552	300	21	25
680	295	37	7
600	295	37	7
680	195	37	7
606	195	37	7
690	76	37	7
608	76	37	7
813	20	37	7
829	20	37	7
648	300	N.S.	25
648	300	N.S.	25
641	300	N.S.	26
634	300	N.S.	26
800	77	N.S.	26
807	77	N.S.	26

C17200: Cold-worked

Tensile Yield Strength vs. Temperature (20–300 K)

Table 9.7, continued

Yield Strength, MPa	Test Temperature, K	Cold Work, %	Reference No.
786	77	N.S.	26
779	77	N.S.	26
889	20	N.S.	26
841	20	N.S.	26
848	20	N.S.	26
869	20	N.S.	26
786	20	N.S.	26
869	295	60	9
772	232	60	9
213	295	0	27
689	295	11	27
579	295	21	27
720	295	37	27

N.S. = not specified.

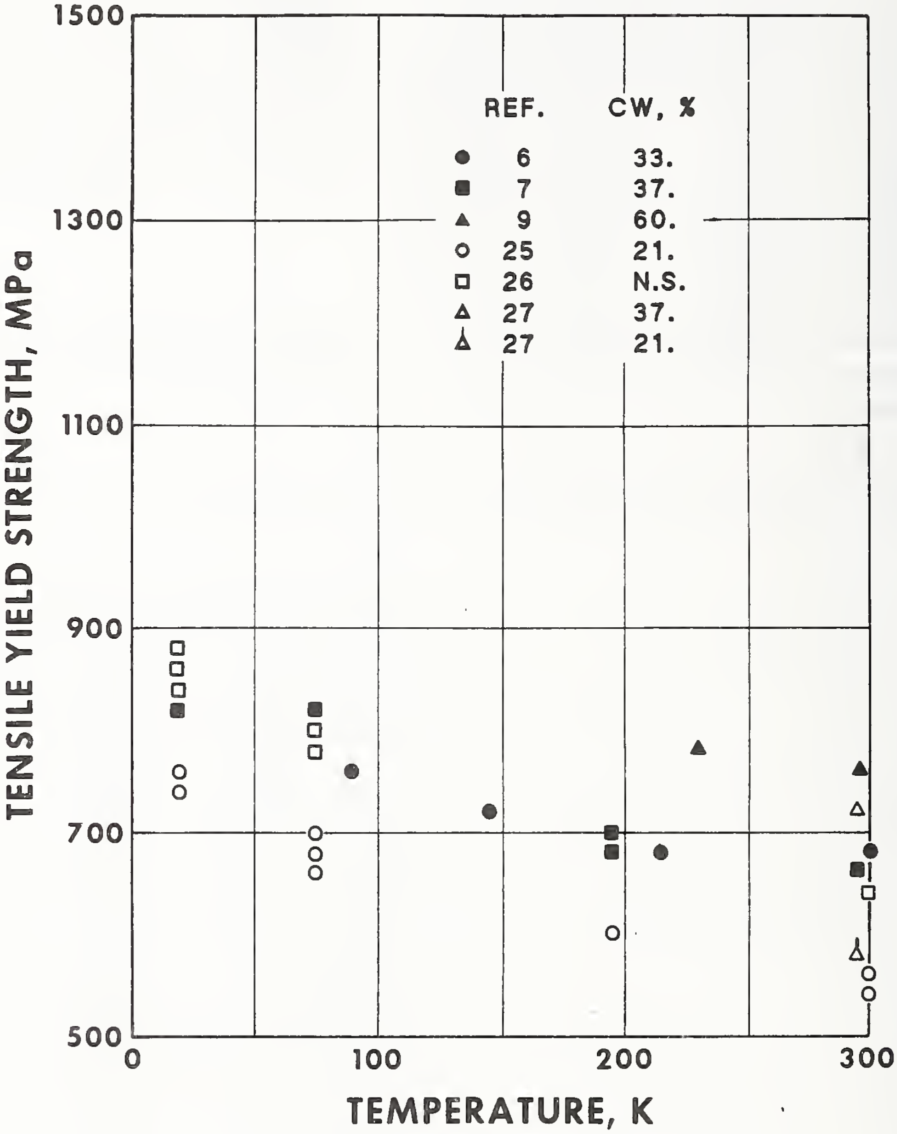

Figure 9.10. Yield strength measurements of cold-worked C17200 beryllium copper are shown as a function of test temperature. For clarity, overlapping data points are omitted from the figure. All data are presented in Table 9.7. Products were in sheet, strip, and bar form (not specified in Reference 9.26).

DATA SOURCES AND ANALYSIS

Measurements of the yield strength of cold-worked C17200 beryllium copper at 295 K as a function of aging temperature and time were obtained from 19 sources (References 9.2–9.6, 9.8, 9.9, 9.13, 9.14, 9.16, 9.18, 9.19, 9.21, and 9.28–9.33). All sources reported 0.2%-offset yield strength (σ_y), except Reference 9.19 (0.1%-offset), and References 9.14 and 9.22 (not specified). Products were in wire, sheet, strip, bar, and plate form. Cold work, *CW*, (carried out before aging) ranged from 11 to 97% (reduction in thickness or area). Reported aging temperatures ranged from 297 to 698 K; aging times from 0.09 to 24 h. Aging temperatures and/or times were not specified for several measurements in References 9.3–9.5, 9.28, and 9.30, sometimes for proprietary reasons. Sufficient data were available to estimate a range of optimum aging temperatures and times.

RESULTS

All measurements are reported in Table 9.8, which presents σ_y, *CW* (reduction in thickness or area in percent), aging temperature and time, and the reference number. (Because the highest and lowest values obtained were reported in Reference 9.4 in place of the original data, the measurements presented in the figures and tables for this reference should be considered upper and lower limits.) The available characterization of materials and measurements is given in Table 9.57 at the end of the tensile properties section. Figures 9.11 and 9.12 present the σ_y measurements as a function of aging temperature and time, respectively. Unspecified values of temperature or time are plotted on the *y*-axis. Three σ_y measurements from References 9.8 and 9.21 at long aging times are not shown in Figure 9.12.

The figures indicate that optimum aging temperatures range from about 588 to 620 K, and optimum aging times at these temperatures range from about 1 to 4 h.

DISCUSSION

References 9.34 and 9.55 report an improvement in σ_y of C17200-type beryllium copper when the specimen is strained during aging instead of *CW* before aging. The maximum σ_y reported in Reference 9.35 were not as large as some of those presented in Figures 9.11 and 9.12, but the aging temperature was kept below 473 K. Reference 9.34 reports a maximum σ_y of about 1100 MPa for material aged at 573 K, but the alloy composition does not meet C17200 specifications.

Reference 9.23 discusses metallurgical aspects of the precipitation-hardening dependence of C17200 beryllium copper on temperature and time. At higher aging temperatures, precipitation is faster and peak properties are obtained more rapidly. At longer times, the precipitated particles coalesce, and hardness and strength drop off (overaging). In Figure 9.30, which presents tensile strength, σ_u vs. aging time, the strength first increases rapidly, but the slope becomes less steep at longer aging times. Reference 9.23 also discusses the advantages of achieving a given strength level by under- or overaging, and the relationship with elastic modulus, which reaches a peak after the maximum in yield or tensile strength is attained. Although cold-worked material is more difficult to form, higher σ_y can be obtained for similar aging conditions (see Figures 9.7 and 9.8 in this section).

The effect of thickness upon hardness of cold-worked and aged C17200 beryllium copper is reported in Reference 9.24 (for strip).

Table 9.8. Yield Strength Dependence of Cold-worked C17200 Beryllium Copper on Aging Temperature and Time (295 K).

Yield Strength, MPa	Cold Work, %	Aging Temperature, K	Aging Time, h	Reference No.
1234	33	588	2.00	6
641	N.S.	N.S.	N.S.	29
896	97	297	2.00	29
1172	37	452	2.00	29
1313	97	588	2.00	29
1344	97	644	2.00	29
1347	37	588	2.00	29
1082	97	573	2.00	29
952	37	647	2.00	29
1103	97	297	2.00	29
1324	37	452	2.00	29
1082	97	573	2.00	29
1131	37	647	2.00	29
1108	11	588	N.S.	30
1175	21	588	N.S.	30
1235	97	573	N.S.	30
1096	44	588	2.00	30
1231	35	588	2.00	30
1218	33	588	2.00	31
641	37	566	3.00	13
896	37	588	3.00	13
658	15	566	0.33	14
896	15	588	0.50	14
862	15	566	0.67	14
907	15	588	0.83	14
924	15	588	1.00	14
952	15	566	3.00	14
972	15	566	2.00	14
1210	15	588	3.00	16
1393	97	566	3.00	32
1303	37	588	3.00	32
1310	37	588	3.00	32
1096	37	594	3.00	32
1248	N.S.	566	2.00	5
907	N.S.	588	24.00	9
1144	21	566	2.00	14
1096	37	588	0.33	14
1082	37	644	0.33	19
1169	11	588	2.00	9
1251	21	588	2.00	5
629	11	N.S.	N.S.	5
707	21	N.S.	N.S.	5
1172	60	588	2.00	9
1176	11	566	2.00	5
1096	11	588	2.00	9
1393	21	588	2.00	3
1313	21	588	2.00	9
1082	37	566	2.00	3
1429	37	588	2.00	3
820	37	N.S.	N.S.	3

Table 9.8, continued

Yield Strength, MPa	Cold Work, %	Aging Temperature, K	Aging Time, h	Reference No.
853	37	N.S.	N.S.	3
1434	18	588	2.00	21
1489	39	588	4.00	21
1496	50	588	2.00	21
952	50	588	0.08	21
1193	50	588	4.80	21
1434	50	588	8.00	21
1455	50	588	4.00	21
1324	50	588	17.00	21
1020	50	622	4.08	21
1282	50	622	0.80	21
1365	50	622	0.75	21
1282	50	622	4.00	21
1069	50	622	17.00	21
1214	50	588	4.08	21
1276	50	644	0.30	21
1214	50	644	0.75	21
1062	50	644	4.00	21
1434	50	588	8.80	21
1344	37	N.S.	N.S.	4
1345	37	N.S.	N.S.	4
1338	50	588	4.00	33
1344	50	588	8.00	33
1344	50	588	3.00	33
1344	50	588	8.00	33
1331	50	588	5.00	33
1338	50	588	4.00	33
1020	50	588	4.00	33
1324	50	588	8.00	33
1331	50	622	4.00	33
1317	50	622	8.00	33
1296	50	622	3.00	33
1269	50	622	8.00	33
1241	50	622	5.00	33
1214	50	622	8.00	33
1193	50	622	4.00	33
1165	50	622	8.00	33
1241	50	644	1.00	33
1434	50	644	8.00	33
1193	50	644	3.00	33
1269	50	644	8.00	33
1365	50	644	5.00	33
1055	50	644	8.00	33
1048	50	644	4.00	33
1027	50	588	8.00	33
1120	18	580	2.00	2
1128	21	630	8.00	2
1137	37	580	2.00	2
1192	11	630	2.00	2
1205	21	630	2.00	2
1199	37	630	2.00	2

Table 9.8, continued

Yield Strength, MPa	Cold Work, %	Aging Temperature, K	Aging Time, h	Reference No.
1199	11	630	2.00	2
1207	21	630	2.00	2
1205	37	630	2.00	2
1114	11	682	2.00	2
1176	21	588	2.00	2
1216	37	588	2.00	2
1178	11	588	2.00	2
1268	21	682	2.00	2
1300	37	588	2.00	2
1162	11	588	2.00	2
1260	21	682	2.00	2
1322	37	682	2.00	2
1170	11	602	3.00	2
1189	21	602	2.50	2
1208	37	630	2.00	2
1284	11	602	3.00	2
1269	21	630	2.00	2
1284	37	602	2.00	2
1225	11	602	3.00	2
1264	21	602	2.00	2
1298	37	630	3.00	2
1189	11	616	2.50	2
1152	21	616	2.00	2
1157	37	616	2.00	2
1205	11	616	2.50	2
1217	21	616	2.00	2
1219	37	616	2.00	2
1196	11	616	2.50	2
1220	21	616	2.00	2
1216	37	616	2.00	2

N.S. = not specified.

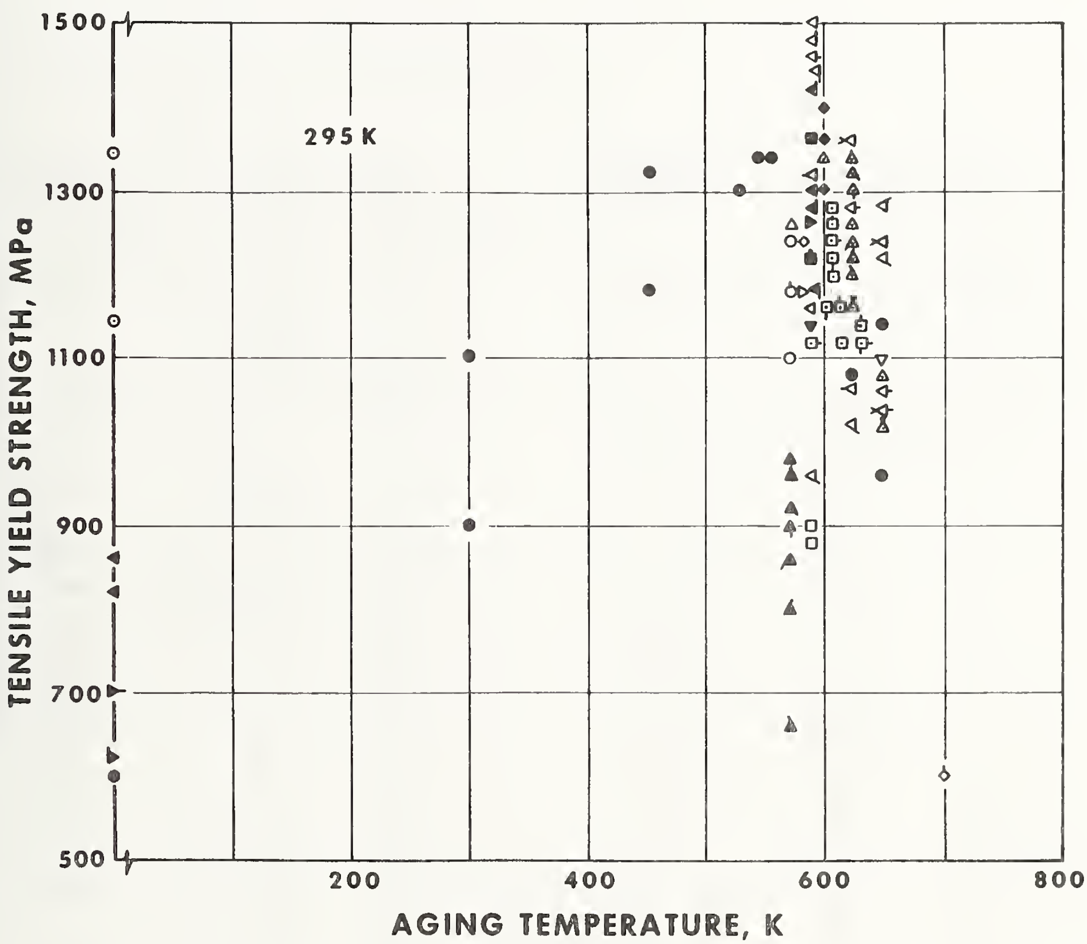

Figure 9.11. Yield strength (σ_y) measurements on cold-worked C17200 beryllium copper at 295 K are shown as a function of aging temperature. If this parameter was not specified, σ_y is plotted on the *y*-axis. Measurements of σ_y from Reference 9.29 at 2-h aging time indicate the trend of increased σ_y at the optimum aging temperature. For clarity, overlapping data points are omitted from the figure, including all points from Reference 9.6. All data are presented in Table 9.8. The legend for this graph is given on the following page. Products were in wire, sheet, strip, bar, and plate form. (N.S. in legend for References 9.3–9.5, 9.28, and 9.30 indicates not specified.) The values from Reference 9.29 for room-temperature (297-K) aging are presented for comparison with values for higher aging temperatures.

REF.	CW, %	AGING TIME, H	REF.	CW, %	AGING TIME, H
2	37.	3.	18	21.	2.
2	37.	2.	19	37.	0.33
2	21.	2.5	21	50.	2.
2	11.	3.	21	39.	2.
2	11.	2.5	21	50.	4.
2	11.	2.	21	18.	2.
2	21.	2.	21	50.	17.
3	37.	N.S.	21	50.	0.30
3	37.	2.	21	50.	0.09
3	21.	2.	21	50.	0.75
3	11.	2.	21	50.	8.25
4	37.	N.S.	28	N.S.	N.S.
5	21.	N.S.	29	97.	2.
5	11.	N.S.	30	37.	N.S.
5	21.	2.	30	21.	N.S.
8	N.S.	2.	30	11.	N.S.
8	N.S.	24.	31	45.	2.
9	60.	2.	31	35.	2.
13	37.	3.	32	37.	3.
14	15.	2.	33	50.	4.
14	15.	1.5	33	50.	1.
14	15.	1.	33	50.	2.
14	15.	0.83	33	50.	3.
14	15.	0.67	33	50.	5.
14	15.	0.50	33	50.	6.
14	15.	0.33	33	50.	7.
16	15.	3.	33	50.	8.

Figure 9.11, continued. Legend for preceding graph.

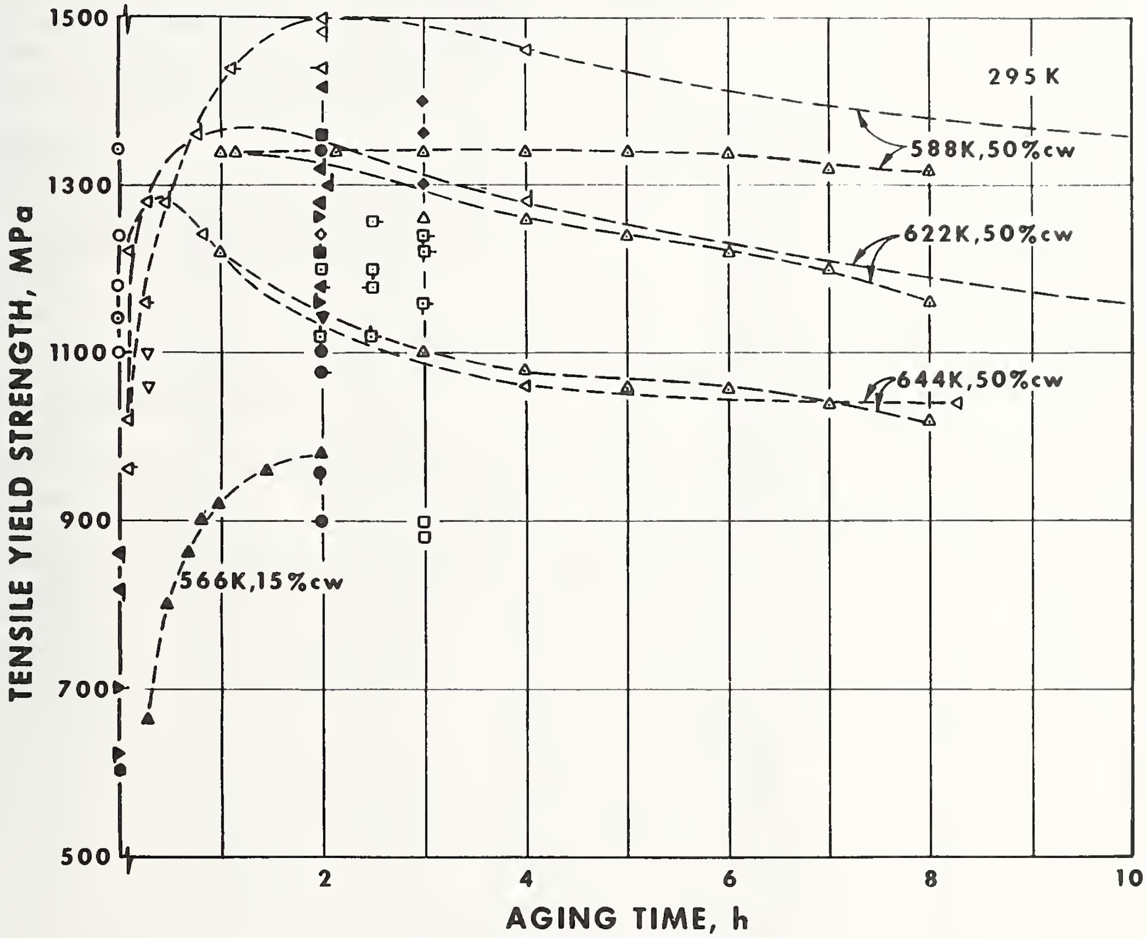

Figure 9.12. Yield strength (σ_y) measurements on cold-worked C17200 beryllium copper at 295 K are shown as a function of aging time. If this parameter was not specified, σ_y is plotted on the y-axis. Three σ_y values from References 9.8 and 9.21 at long aging times do not appear in the figure. For clarity, overlapping data points are omitted from the figure, including all points from References 9.6 and 9.9. All data are presented in Table 9.8. The legend for this graph is given on the following page. Products were in wire, sheet, strip, bar, and plate form. (N.S. in legend for References 9.3–9.5, 9.8, and 9.28 indicates not specified.) The values from Reference 9.29 for room-temperature (297-K) aging are presented for comparison with values for higher aging temperatures.

12

	REF.	CW, %	AGING TEMP., K
⊡	2	37.	588.
⊡	2	11.	588.
⊡	2	21.	588.
⊡	2	21.	588.
⊡	2	11.	588.
⊡	2	21.	588.
⊡	2	11.	588.
◄	3	37.	588.
◄	3	21.	588.
◄	3	11.	588.
◄	3	37.	N.S.
⊙	4	37.	N.S.
►	5	21.	589.
►	5	11.	589.
►	5	21.	N.S.
►	5	11.	N.S.
◇	8	N.S.	588.
□	13	37.	588.
▲	14	15.	566.
△	16	15.	573.
▼	18	21.	588.
▽	19	37.	644.
◁	21	50.	644.
◁	21	50.	622.
◁	21	50.	588.
◁	21	39.	588.
◁	21	17.	588.

	REF.	CW, %	AGING TEMP., K
●	28	N.S.	N.S.
●	29	97.	555.
●	29	97.	297.
●	29	97.	619.
●	29	97.	647.
●	29	97.	297.
○	30	37.	573.
○	30	21.	573.
○	30	11.	573.
■	31	45.	588.
■	31	35.	588.
◆	32	37.	594.
▲	33	50.	588.
▲	33	50.	622.
▲	33	50.	644.

Figure 9.12, continued. Legend for preceding graph.

DATA SOURCES AND ANALYSIS

Measurements of the yield strength of cold-worked and aged C17200 beryllium copper between 88 and 300 K were obtained from four sources (References 9.6, 9.8, 9.9, and 9.19). All sources reported yield strength, σ_y, with an offset of 0.2%, except Reference 9.19, which reported 0.1%-offset strength. Products were in sheet and bar form (not specified in Reference 9.8).

RESULTS

All measurements are reported in Table 9.9, which presents σ_y, test temperature, percent of cold work (reduction in thickness or area), aging temperature and time, and the reference number. The available characterization of materials and measurements is given in Table 9.57 at the end of the tensile properties section. Figure 9.13 presents the σ_y measurements as a function of test temperature.

Table 9.9. Yield Strength Dependence of Cold-worked and Aged C17200 Beryllium Copper upon Temperature (88–300 K).

Yield Strength, MPa	Test Temperature, K	Cold Work, %	Aging Temperature, K	Aging Time, h	Reference No.
1164	300	33	588	2.00	6
1365	88	33	588	2.00	6
1338	144	33	588	2.00	8
1234	214	33	588	2.00	6
1276	215	N.S.	588	2.00	8
1303	255	N.S.	588	2.00	6
1248	300	N.S.	588	2.00	8
1096	300	37	644	0.33	19
1220	200	37	644	0.33	19
1062	300	37	588	0.33	19
1172	215	37	644	0.33	19
1172	295	60	588	2.00	6
1214	232	60	575	2.00	9

N.S. = not specified.

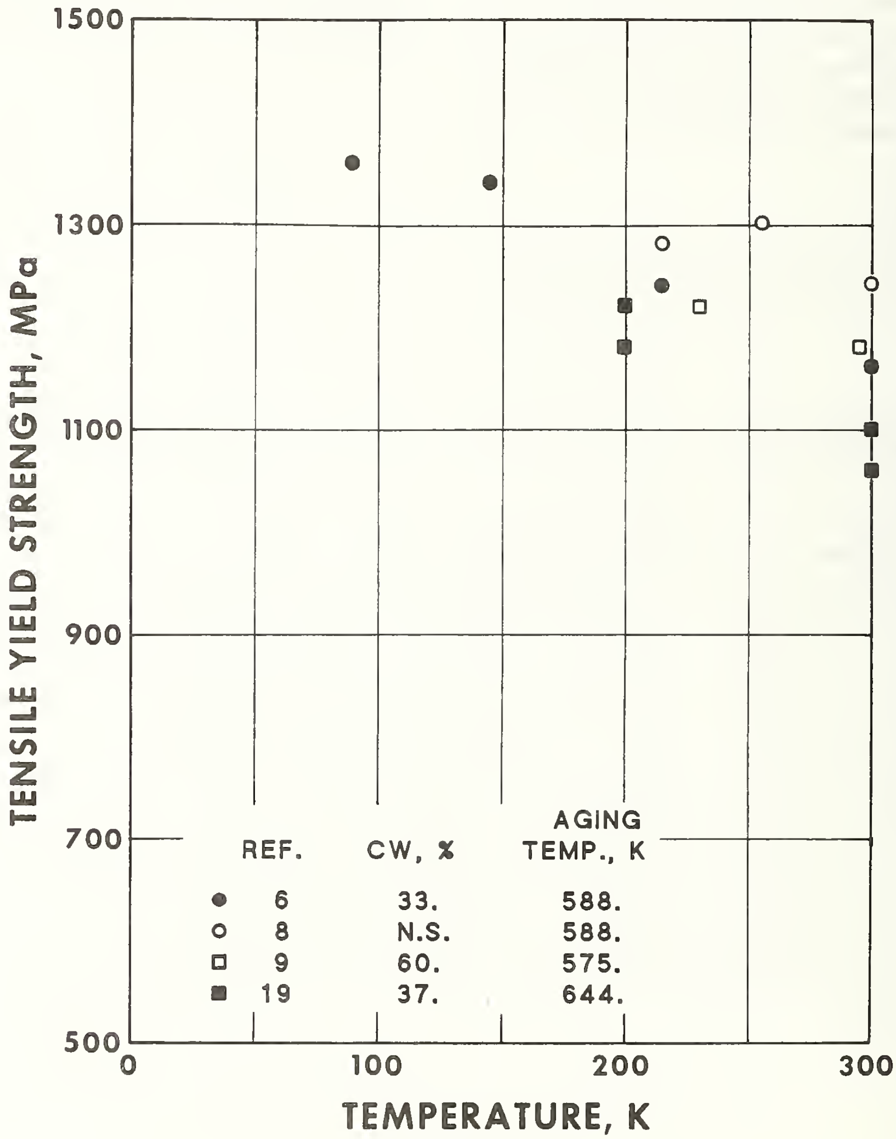

Figure 9.13. Yield strength measurements of cold-worked and aged C17200 beryllium copper are shown as a function of test temperature. All data are presented in Table 9.9. Products were in sheet and bar form (not specified in Reference 9.8).

DATA SOURCES AND ANALYSIS

Measurements of the yield strength of annealed C17500 beryllium copper at 295 K as a function of aging temperature and time were obtained from four sources (References 9.3, 9.4, 9.12, and 9.36). All sources reported 0.2%-offset yield strength (σ_y). Product was in strip form (References 9.3 and 9.4) or not specified (Reference 9.12 and 9.36). Reported aging temperatures ranged from 727 to 755 K; aging times from 0.13 to 8 h. These parameters were not specified in Reference 9.4. Since the original data points were not presented in Reference 9.36, data were extracted from the curves at appropriate intervals.

RESULTS

All measurements are reported in Table 9.10, which presents σ_y, aging temperature and time, and the reference number. (Because the highest and lowest values obtained were reported in Reference 9.4 in place of the original data, the measurements presented in the figures and tables for this reference should be considered upper and lower limits.) The available characterization of materials and measurements is given in Table 9.57 at the end of the tensile properties section. Figures 9.14 and 9.15 present the σ_y measurements as a function of aging temperature and time, respectively. Unspecified values of temperature or time are plotted on the *y*-axis.

Not enough data are available in the literature to determine optimum aging parameters. However, Reference 9.37 states that it is standard commercial practice to overage at 753 K in order to develop the most favorable combination of strength and electrical conductivity. See also the electromagnetic properties section and Reference 9.36.

DISCUSSION

In Reference 9.36, a comparable set of measurements of yield and tensile strengths on both C17500 and C17510 beryllium copper is reported. The C17500 alloy was found to have slightly higher strengths after aging in both the annealed and cold-worked conditions.

Table 9.10. Yield Strength Dependence of Annealed C17500 Beryllium Copper on Aging Temperature and Time (295 K).

Yield Strength, MPa	Aging Temperature, K	Aging Time, h	Reference No.
696	727	8.00	12
620	727	8.00	12
588	755	3.00	3
620	755	8.00	3
550	N.S.	N.S.	4
620	N.S.	N.S.	4
230	753	0.13	36
400	753	0.25	36
550	753	0.50	36
620	753	1.00	36
580	753	2.00	36
620	753	3.00	36
620	753	4.00	36
610	753	6.00	36
600	753	8.00	36

N.S. = not specified.

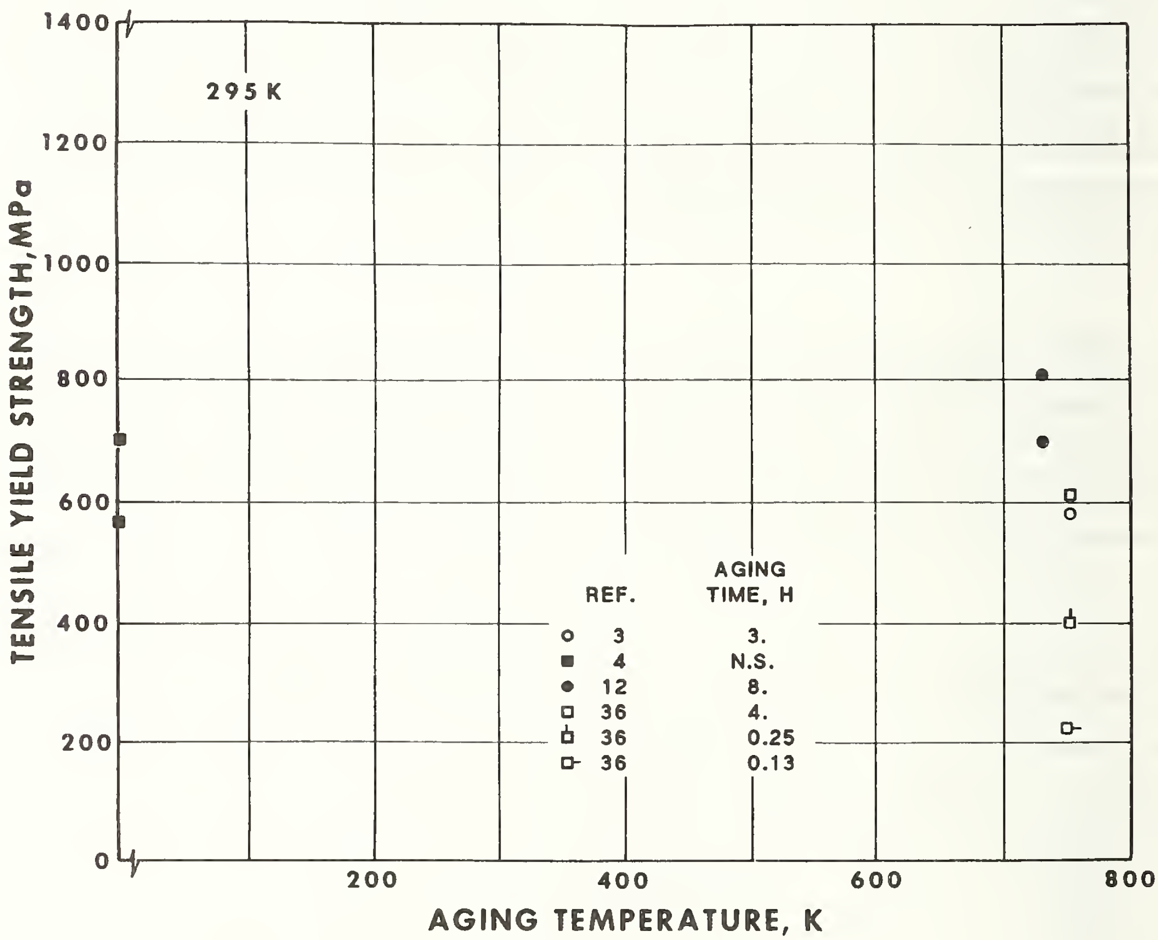

Figure 9.14. Yield strength measurements on annealed C17500 beryllium copper at 295 K are shown as a function of aging temperature. If this parameter was not specified, yield strength is plotted on the *y*-axis. For clarity, overlapping data points are omitted from the figure. All data are presented in Table 9.10. Product, where specified, was in strip form. (N.S. in legend for Reference 9.4 indicates not specified.)

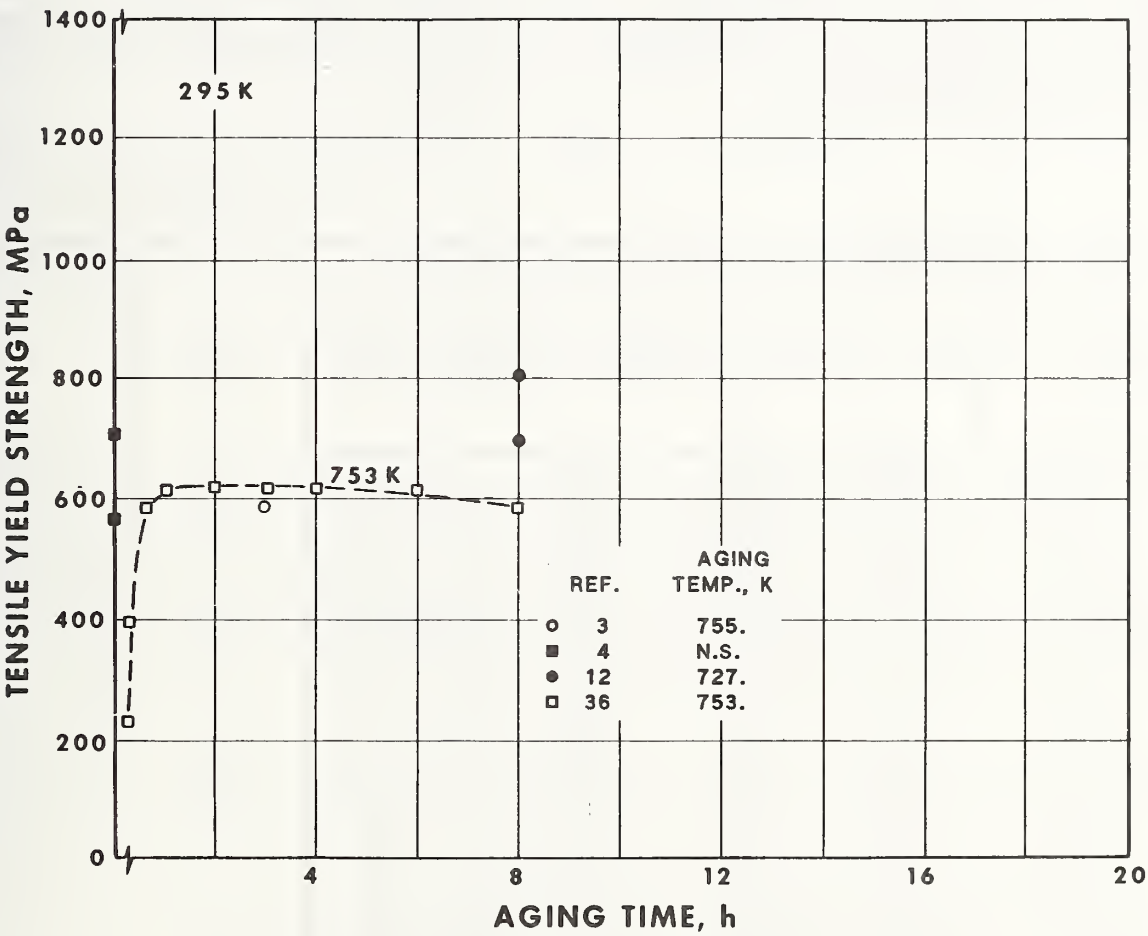

Figure 9.15. Yield strength measurements on annealed C17500 beryllium copper at 295 K are shown as a function of aging time. If this parameter was not specified, yield strength is plotted on the *y*-axis. For clarity, overlapping data points are omitted from the figure. All data are presented in Table 9.10. Product, where specified, was in strip form. (N.S. in legend for Reference 9.4 indicates not specified.)

C17500: Annealed and Aged; Cold-worked; Cold-worked and Aged

Tensile Yield Strength vs. Temperature (20–300 K)

DATA SOURCES AND ANALYSIS

Measurements of the yield strength of annealed and aged, cold-worked, and cold-worked and aged C17500 beryllium copper between 20 and 300 K were obtained from three sources (References 9.6, 9.12, and 9.25). Measurements at 295 K only on cold-worked material (Reference 9.38) are presented for comparison. All sources reported 0.2%-offset yield strength, σ_y. Products were in sheet and bar form (not specified in References 9.12 and 9.38).

RESULTS

All measurements are reported in Table 9.11, which presents σ_y, test temperature, percent of cold work (reduction in thickness or area), aging temperature and time, and the reference number. The available characterization of materials and measurements is given in Table 9.57 at the end of the tensile properties section. Figure 9.16 presents the σ_y measurements as a function of test temperature.

Table 9.11. Yield Strength Dependence of Annealed and Aged, Cold-worked, and Cold-worked and Aged C17500 Beryllium Copper upon Temperature (20–300 K).

Yield Strength, MPa	Test Temperature, K	Cold Work, %	Aging Temperature, K	Aging Time, h	Reference No.
772	20	33	755	2	6
786	144	33	755	2	6
745	214	33	755	2	6
786	300	33	755	2	6
403	299	0	727	8	12
696	299	0	727	8	12
696	197	0	727	8	12
762	197	0	727	8	12
786	77	0	727	2	12
696	77	0	727	8	12
979	20	0	727	2	12
1010	20	0	727	8	12
483	20	21	0	2	25
483	20	21	0	0	25
427	20	21	0	2	25
483	20	21	0	0	25
393	195	21	0	0	25
393	195	21	0	0	25
345	300	21	0	0	25
352	300	21	0	0	25
471	295	50	0	0	38

Aging Temperature, 0 K = not aged.

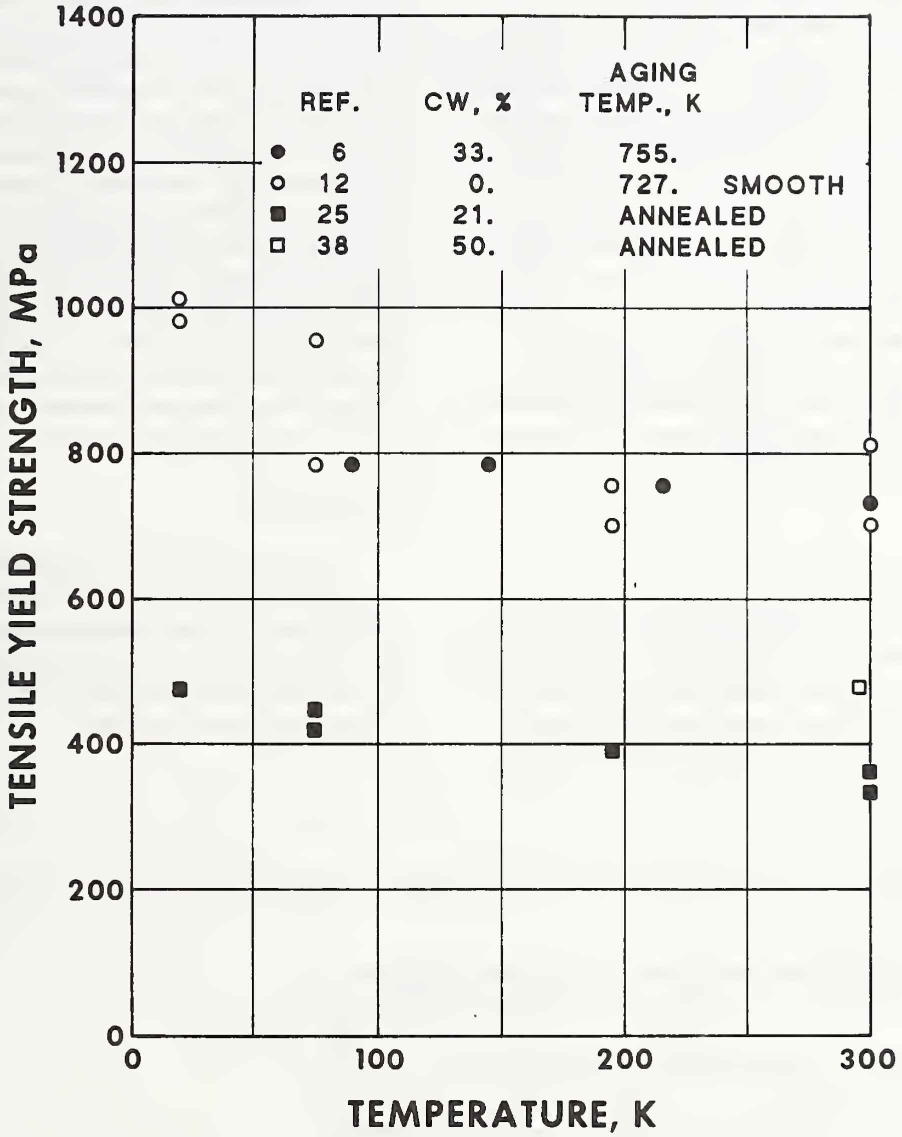

Figure 9.16. Yield strength measurements of annealed and aged, cold-worked, and cold-worked and aged C17500 beryllium copper are shown as a function of test temperature. For clarity, overlapping data points are omitted from the figure. All data are presented in Table 9.11. Products were in sheet and bar form (not specified in References 9.12 and 9.38).

C17500: Cold-worked and Aged

Tensile Yield Strength vs. Aging Temperature, Time (295 K)

DATA SOURCES AND ANALYSIS

Measurements of the yield strength of cold-worked C17500 beryllium copper at 295 K as a function of aging temperature and time were obtained from six sources (References 9.3, 9.4, 9.6, 9.36, 9.38, and 9.39). All sources reported 0.2%-offset yield strength (σ_y). Products were in strip and bar form (not specified in References 9.36 and 9.38). Cold work, *CW*, (carried out before aging) ranged from 3 to 65% (reduction in thickness or area). Reported aging temperatures ranged from 723 to 755 K; aging times ranged from 0.13 to 8 h. These parameters were not specified in References 9.4 and 9.39. Enough data were available to estimate a range of optimum aging times, but not aging temperature. Since the original data points were not presented in Reference 9.36, data were extracted from the curves at appropriate intervals.

RESULTS

All measurements are reported in Table 9.12, which presents σ_y, *CW* (reduction in thickness or area in percent), aging temperature and time, and the reference number. (Because the highest and lowest values obtained were reported in Reference 9.4 in place of the original data, the measurements presented in the figures and tables for this reference should be considered upper and lower limits.) The available characterization of materials and measurements is given in Table 9.57 at the end of the tensile properties section. Figures 9.17 and 9.18 present the σ_y measurements as a function of aging temperature and time, respectively. Unspecified values of temperature or time are plotted on the *y*-axis.

Not enough data are available in the literature to determine an optimum aging temperature, but in Figure 9.17, optimum aging times appear to range from approximately 1 to 8 h (for an aging temperature of about 750 K). Reference 9.37 states that it is standard commercial practice to overage at 753 K in order to develop the most favorable combination of strength and electrical conductivity. See also the electromagnetic properties section and Reference 9.36.

DISCUSSION

In Reference 9.36, a comparable set of measurements of yield and tensile strengths on both C17500 and C17510 beryllium copper are reported. The C17500 alloy was found to have slightly higher strengths after aging in both the annealed and cold-worked conditions.

Table 9.12. Yield Strength Dependence of Cold-worked C17500 Beryllium Copper on Aging Temperature and Time (295 K).

Yield Strength, MPa	Cold Work, %	Aging Temperature, K	Aging Time, h	Reference No.
738	33	755	2.00	6
613	50	723	0.75	38
643	50	723	1.00	38
692	50	723	1.50	38
716	50	723	2.00	38
708	50	723	2.50	38
701	50	723	3.00	38
570	50	N.S.	N.S.	39
650	50	N.S.	N.S.	39
624	3	755	3.00	3
616	3	755	3.00	3
708	11	755	2.50	3
679	11	755	2.00	3
690	37	N.S.	N.S.	4

Table 9.12, continued

Yield Strength, MPa	Cold Work, %	Aging Temperature, K	Aging Time, h	Reference No.
825	37	N.S.	N.S.	4
660	N.S.	753	0.13	36
820	N.S.	753	0.25	36
890	N.S.	753	0.50	36
840	N.S.	753	1.00	36
820	N.S.	753	2.00	36
818	N.S.	753	3.00	36
800	N.S.	753	4.00	36
780	N.S.	753	6.00	36
770	N.S.	753	8.00	36

N.S. = not specified.

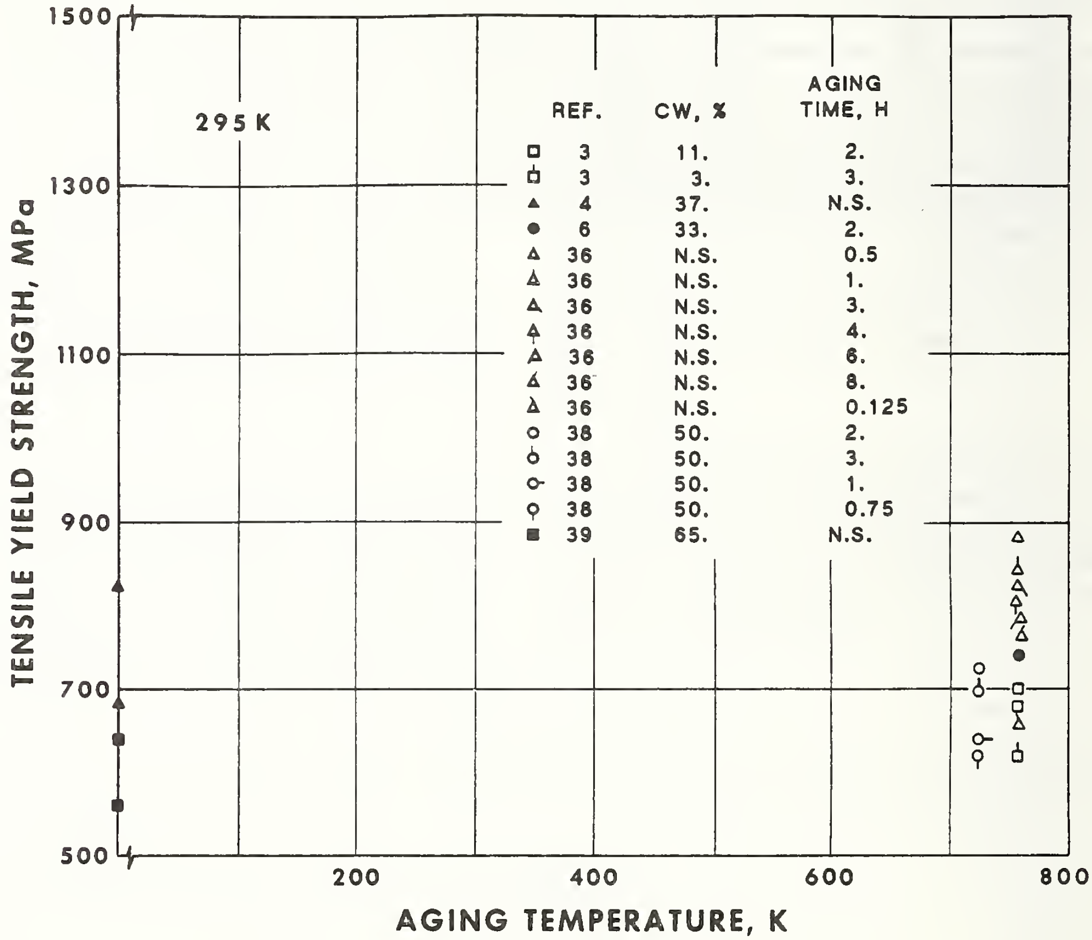

Figure 9.17. Yield strength measurements on cold-worked C17500 beryllium copper at 295 K are shown as a function of aging temperature. If this parameter was not specified, yield strength is plotted on the *y*-axis. For clarity, overlapping data points are omitted from the figure. All data are presented in Table 9.12. Products were in strip and bar form (not specified in References 9.36 and 9.38). (N.S. in legend for References 9.4 and 9.39 indicates not specified.)

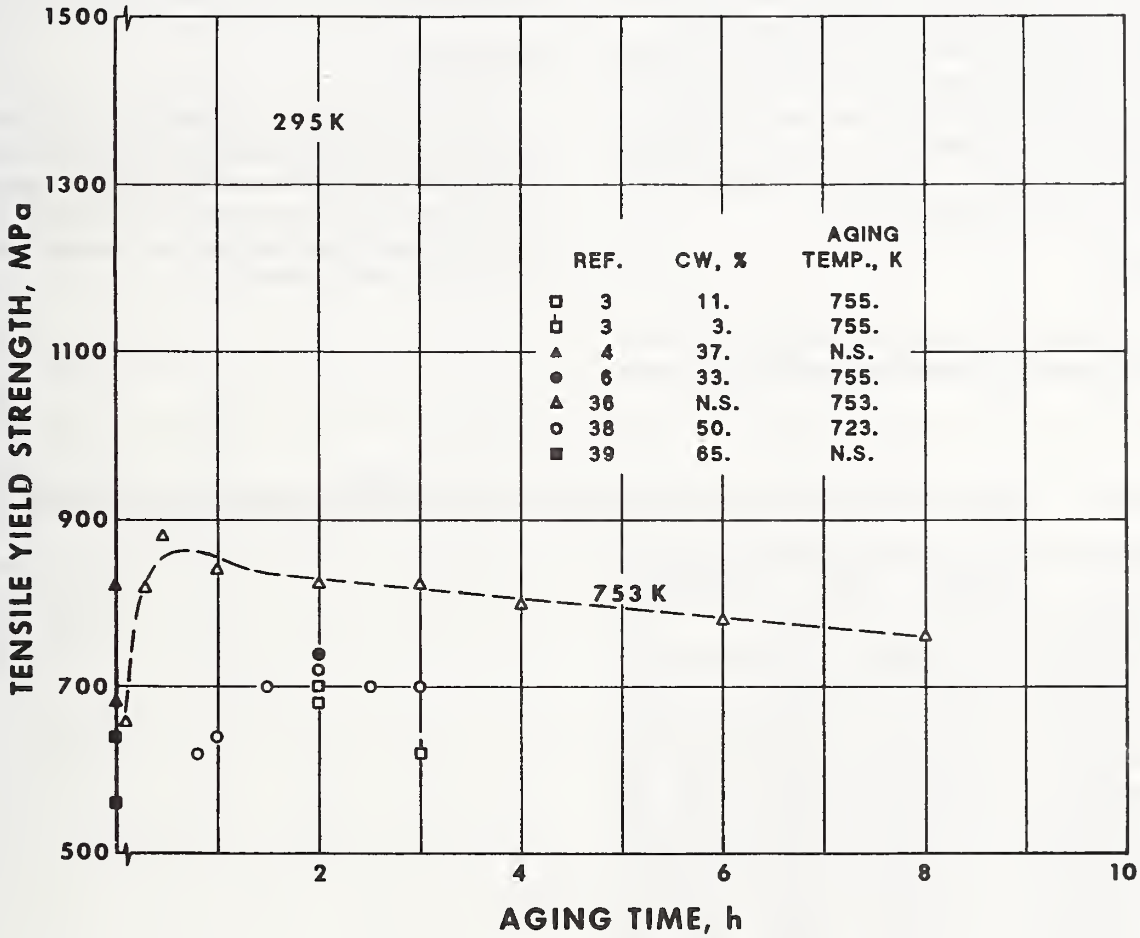

Figure 9.18. Yield strength measurements on cold-worked C17500 beryllium copper at 295 K are shown as a function of aging time. If this parameter was not specified, yield strength is plotted on the *y*-axis. For clarity, overlapping data points are omitted from the figure. All data are presented in Table 9.12. Products were in strip and bar form (not specified in References 9.36 and 9.38). (N.S. in legend for References 9.4 and 9.39 indicates not specified.)

DATA SOURCES AND ANALYSIS

Measurements of the yield strength of annealed C17510 beryllium copper at 295 K as a function of aging time were obtained from three sources (References 9.4, 9.36, and 9.40). All sources reported 0.2%-offset yield strength (σ_y). Product was in strip form (References 9.4 and 9.40) or was not specified (Reference 9.36). Aging temperature was 753 K (Reference 9.36) or was not specified. Aging times ranged from 0.13 to 8 h (Reference 9.36) or were not specified. Since the original data points were not presented in Reference 9.36, data were extracted from the curves at appropriate intervals.

RESULTS

All measurements are reported in Table 9.13, which presents σ_y, aging temperature and time, and the reference number. (Because the highest and lowest values obtained were reported in Reference 9.4 in place of the original data, the measurements presented in the figures and tables for this reference should be considered upper and lower limits.) Figure 9.19 presents the σ_y measurements as a function of aging time. Unspecified values of time are plotted on the *y*-axis.

DISCUSSION

In Reference 9.36, a comparable set of measurements of yield and tensile strengths on both C17500 and C17510 beryllium copper is reported. The C17500 alloy was found to have slightly higher strengths after aging in both the annealed and cold-worked conditions.

Table 9.13. Yield Strength Dependence of Annealed C17510 Beryllium Copper on Aging Time (295 K).

Yield Strength, MPa	Aging Temperature, K	Aging Time, h	Reference No.
648	N.S.	N.S.	40
550	N.S.	N.S.	4
690	N.S.	N.S.	4
200	753	0.13	36
380	753	0.25	36
490	753	0.50	36
530	753	1.00	36
560	753	2.00	36
580	753	3.00	36
590	753	4.00	36
590	753	6.00	36
588	753	8.00	36

N.S. = not specified.

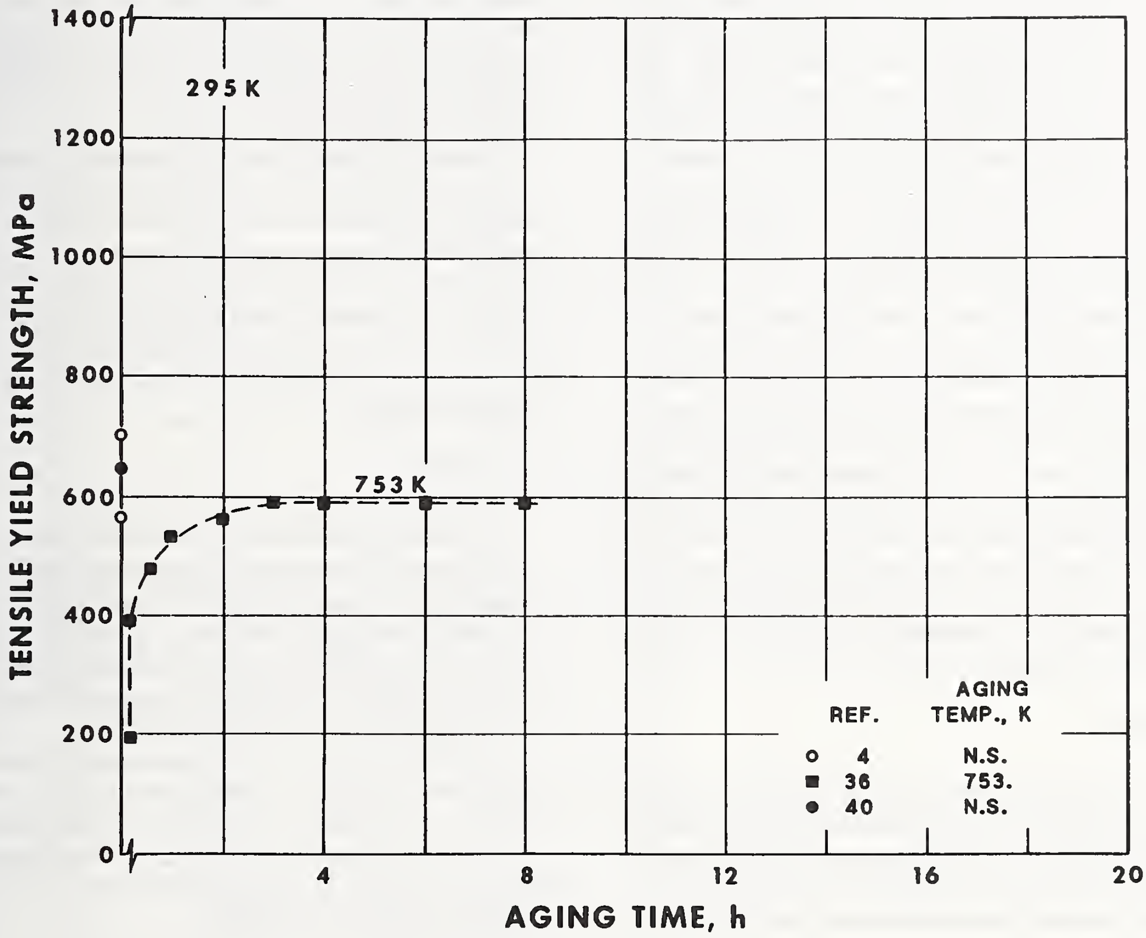

Figure 9.19. Yield strength measurements on annealed C17510 beryllium copper at 295 K are shown as a function of aging time. If this parameter was not specified, yield strength is plotted on the *y*-axis. All data are presented in Table 9.13. Product was in strip form (References 9.4 and 9.40) or was not specified (Reference 9.36). (N.S. in legend for References 9.4 and 9.40 indicates not specified.)

DATA SOURCES AND ANALYSIS

Measurements of the yield strength of cold-worked C17510 beryllium copper at 295 K as a function of aging temperature and time were obtained from nine sources (References 9.4, 9.36, and 9.40–9.46). All sources reported 0.2%-offset yield strength (σ_y). Products, where specified, were in strip or plate form. Cold work, *CW*, (carried out before aging except for Reference 9.45) ranged from 21 to 80% (reduction in thickness). Reported aging temperatures ranged from 573 to 838 K; aging times from 0.13 to 70 h. These parameters were not specified In References 9.4, 9.41–9.43, and 9.46. Before cold rolling, some material was pre-aged at temperatures from 573 to 758 K, usually for 3 h (Reference 9.45). Since the original data points were not presented in Reference 9.36, data were extracted from the curves at appropriate intervals. Data presented here from Reference 9.46 include tensile measurements at 295 K from a commercial supplier, Princeton Plasma Physics Laboratory, and Massachusetts Institute of Technology. Reference 9.44 also reports tensile test data on one of the heats (A) included in the tests summarized in Reference 9.46. Cryogenic test results from Reference 9.44 on this heat are presented on pages 9-47–9-48 of the tensile properties section.

RESULTS

All measurements are reported in Table 9.14, which presents σ_y, *CW* (reduction in thickness in percent), aging temperature and time, and the reference number. (Because the highest and lowest values obtained were reported in Reference 9.44 In place of the original data, the measurements presented in the figures and tables for this reference should be considered upper and lower llmits.) The available characterization of materials and measurements is given in Table 9.57 at the end of the tensile properties section. Figures 9.20 and 9.21 present the σ_y measurements as a function of aging temperature and time, respectively. Unspecified values of temperature or time are plotted on the *y*-axis. Several σ_y measurements from Reference 9.45 at long aging times are not shown in Figure 9.21.

Because aging times and temperatures often were not specified, optimum aging conditions are difficult to determine. Reference 9.45 reported that optimum aging temperatures for high σ_y were about 573 to 593 K with aging times ranging from 5 to 70 h. However, these conclusions were based on a limited number of measurements from one source on material that was pre-aged, as described above.

DISCUSSION

Further information on the microstructure resulting from the aging processes reported in Reference 9.43 may be found in Reference 9.47. Reference 9.48 reports the effect of adding 1-wt% Zr to C17510 beryllium copper on aging times and temperature. Results are presented in terms of hardness, rather than yield strength.

In Reference 9.36, a comparable set of measurements of yield and tensile strengths on both C17500 and C17510 beryllium copper are reported. The C17500 alloy was found to have slightly higher strengths after aging in both the annealed and cold-worked conditions.

Table 9.14. Yield Strength Dependence of Cold-worked C17510 Beryllium Copper on Aging Temperature and Time (295 K).

Yield Strength, MPa	Cold Work, %	Aging Temperature, K	Aging Time, h	Reference No.
814	40	755	3.00	41
813	N.S.	N.S.	N.S.	41
1000	N.S.	N.S.	N.S.	41
1092	N.S.	N.S.	N.S.	41
784	40	755	N.S.	42
786	40	755	N.S.	42

C17510: Cold-worked and Aged

Tensile Yield Strength vs. Aging Temperature, Time (295 K)

Table 9.14, continued

Yield Strength, MPa	Cold Work, %	Aging Temperature, K	Aging Time, h	Reference No.
820	40	755	N.S.	42
823	40	755	N.S.	42
924	37	N.S.	N.S.	43
993	37	N.S.	N.S.	43
758	37	N.S.	N.S.	43
918	37	N.S.	N.S.	43
758	37	755	2.00	40
777	37	755	8.00	40
745	21	727	3.00	40
703	21	755	8.00	40
641	21	753	8.00	40
572	21	811	8.00	40
517	21	633	8.00	40
942	60	593	70.00	45
1005	80	573	6.00	45
960	60	673	1.00	45
960	80	633	8.00	45
1022	40	593	8.00	45
1005	80	573	7.00	45
910	60	593	24.00	45
960	80	593	16.00	45
931	60	593	16.00	45
950	80	633	2.00	45
918	60	593	2.00	45
924	80	573	2.00	45
690	37	N.S.	N.S.	4
825	37	N.S.	N.S.	4
560	N.S.	753	0.13	36
670	N.S.	753	0.25	36
780	N.S.	753	0.50	36
820	N.S.	753	8.00	36
800	N.S.	753	8.00	36
765	N.S.	753	3.00	36
768	N.S.	753	8.00	36
700	N.S.	753	6.00	36
680	N.S.	753	8.00	36
765	37	753	2.00	46A
717	N.S.	N.S.	N.S.	46B
703	N.S.	N.S.	N.S.	46C
724	37	755	2.00	46A
737	N.S.	N.S.	N.S.	46C

N.S. = not specified.

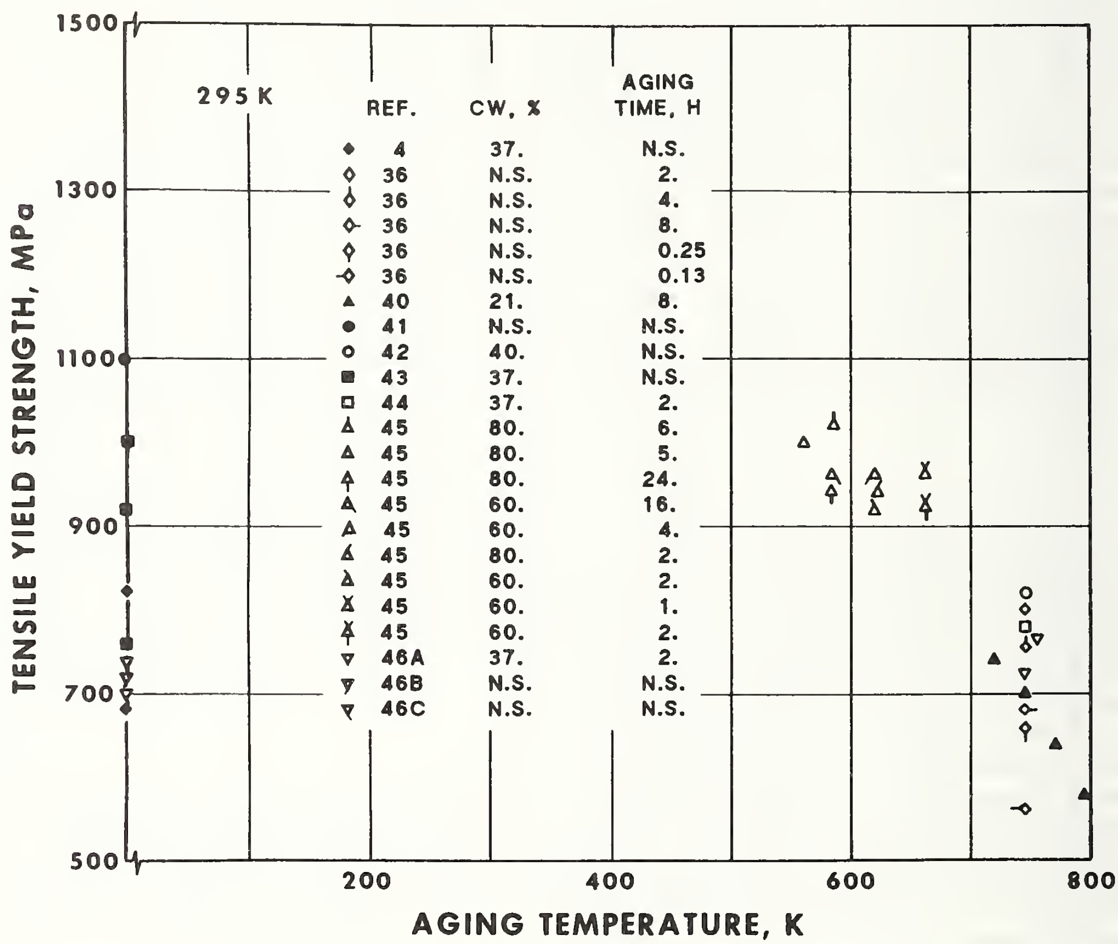

Figure 9.20. Yield strength measurements on cold-worked C17510 beryllium copper at 295 K are shown as a function of aging temperature. If this parameter was not specified, yield strength is plotted on the *y*-axis. For clarity, overlapping data points are omitted from the figure. All data are presented in Table 9.14. Products, where specified, were in strip or plate form. (N.S. in legend for References 9.4, 9.41–9.43, and 9.46 indicates not specified.)

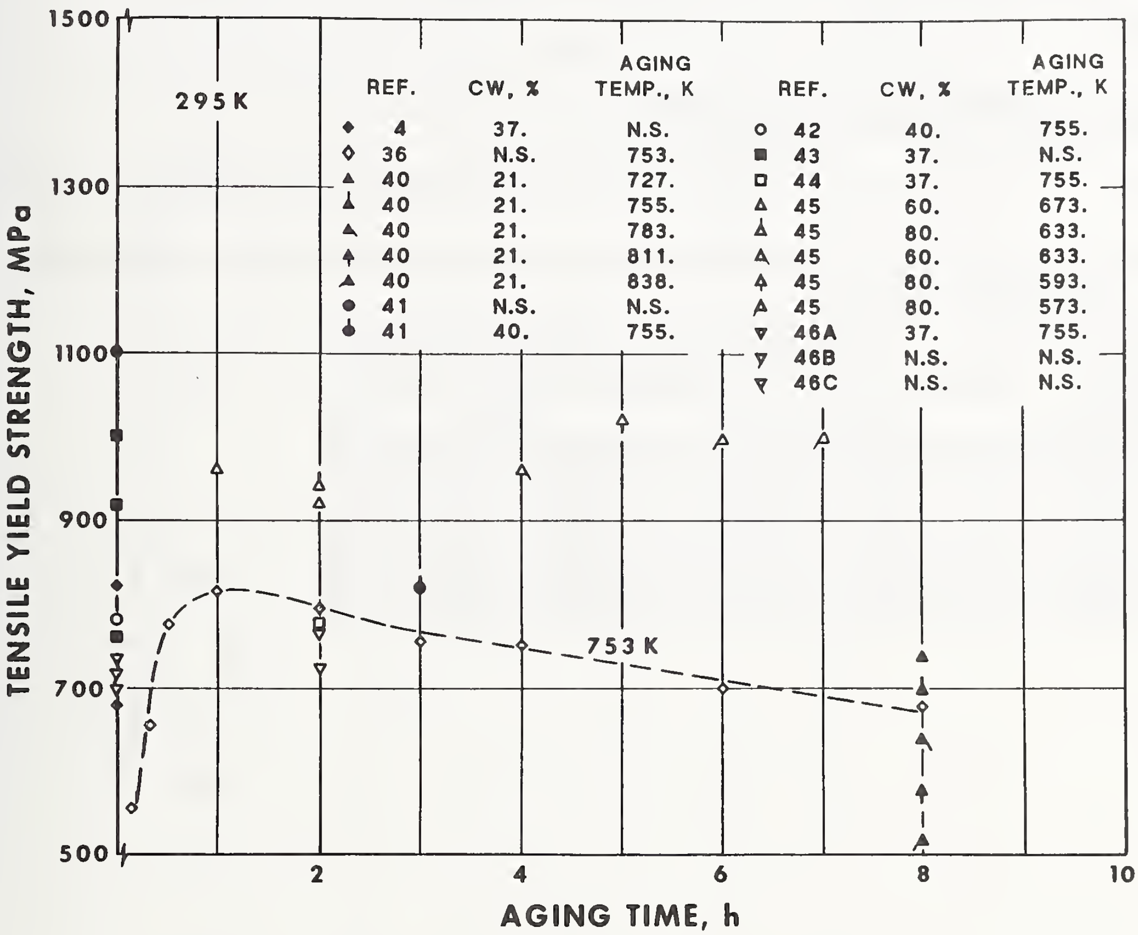

Figure 9.21. Yield strength measurements on cold-worked C17510 beryllium copper at 295 K are shown as a function of aging time. If this parameter was not specified, yield strength is plotted on the *y*-axis. Several data points from Reference 9.45 at long aging times do not appear in the figure. For clarity, overlapping data points are omitted from the figure. All data are presented in Table 9.14. Products, where specified, were in strip or plate form. (N.S. in legend for References 9.4, 9.41, 9.43 and 9.46 indicates not specified.)

DATA SOURCES AND ANALYSIS

Measurements of the yield strength of cold-worked and aged C17510 beryllium copper from 4 to 295 K were obtained from Reference 9.44. The 0.2%-offset yield strength, σ_y, was reported. Product was in plate form.

RESULTS

All measurements are reported in Table 9.15, which presents σ_y, test temperature, percent of cold work (reduction in thickness), aging temperature and time, and the reference number. The available characterization of materials and measurements is given in Table 9.57 at the end of the tensile properties section. Figure 9.22 presents the σ_y measurements as a function of test temperature.

Table 9.15. Yield Strength Dependence of Cold-worked and Aged C17510 Beryllium Copper upon Temperature (4–295 K).

Yield Strength, MPa	Test Temperature, K	Cold Work, %	Aging Temperature, K	Aging Time, h	Reference No.
715	295	37	755	2	44
783	76	37	755	2	44
814	4	37	755	2	44
718	295	37	755	2	44
799	76	37	755	2	44
795	4	37	755	2	44

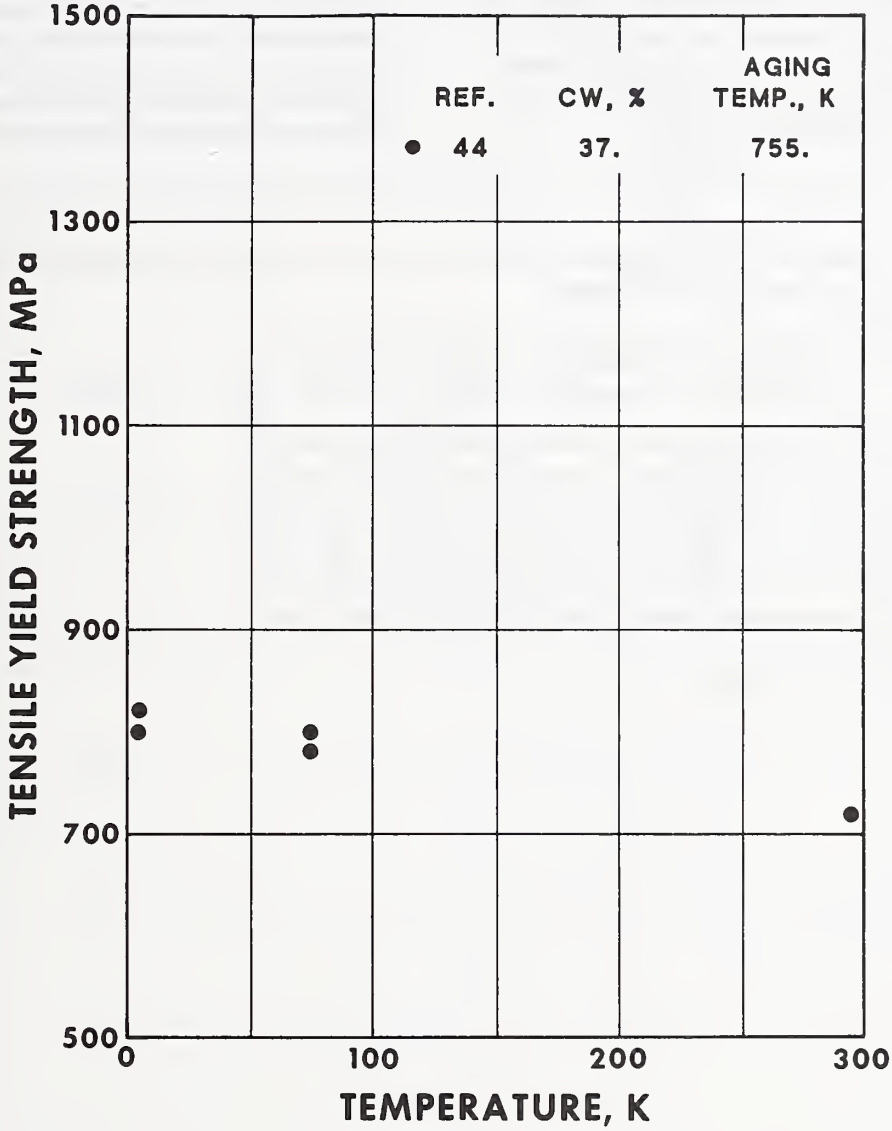

Figure 9.22. Yield strength measurements of cold-worked and aged C17510 beryllium copper are shown as a function of test temperature. An overlapping data point at 295 K is omitted from the figure. All data are presented in Table 9.15. Product was in plate form.

DATA SOURCES AND ANALYSIS

Measurements of the tensile strength of annealed, and annealed and aged C17000 beryllium copper from 20 to 295 K were obtained from Reference 9.49. Measurements from References 9.2 and 9.50 on annealed material at 295 K only are presented for comparison. Product forms were strip (Reference 9.2), bar (Reference 9.50), or not specified (Reference 9.49).

RESULTS

All measurements are reported in Table 9.16, which presents the tensile strength, test temperature, aging temperature and time, and the reference number. The available characterization of materials and measurements is given in Table 9.57 at the end of the tensile properties section. Figure 9.23 presents the tensile strength measurements as a function of test temperature.

Table 9.16. Tensile Strength Dependence of Annealed, and Annealed and Aged C17000 Beryllium Copper upon Temperature (20–295 K).

Tensile Strength, MPa	Test Temperature, K	Aging Temperature, K	Aging Time, h	Reference No.
514	295	0	0	50
434	295	0	0	2
543	295	0	0	2
638	290	N.S.	N.S.	49
795	77	N.S.	N.S.	49
902	20	N.S.	N.S.	49

N.S. = not specified.
Aging Temperature, 0 K = not aged.

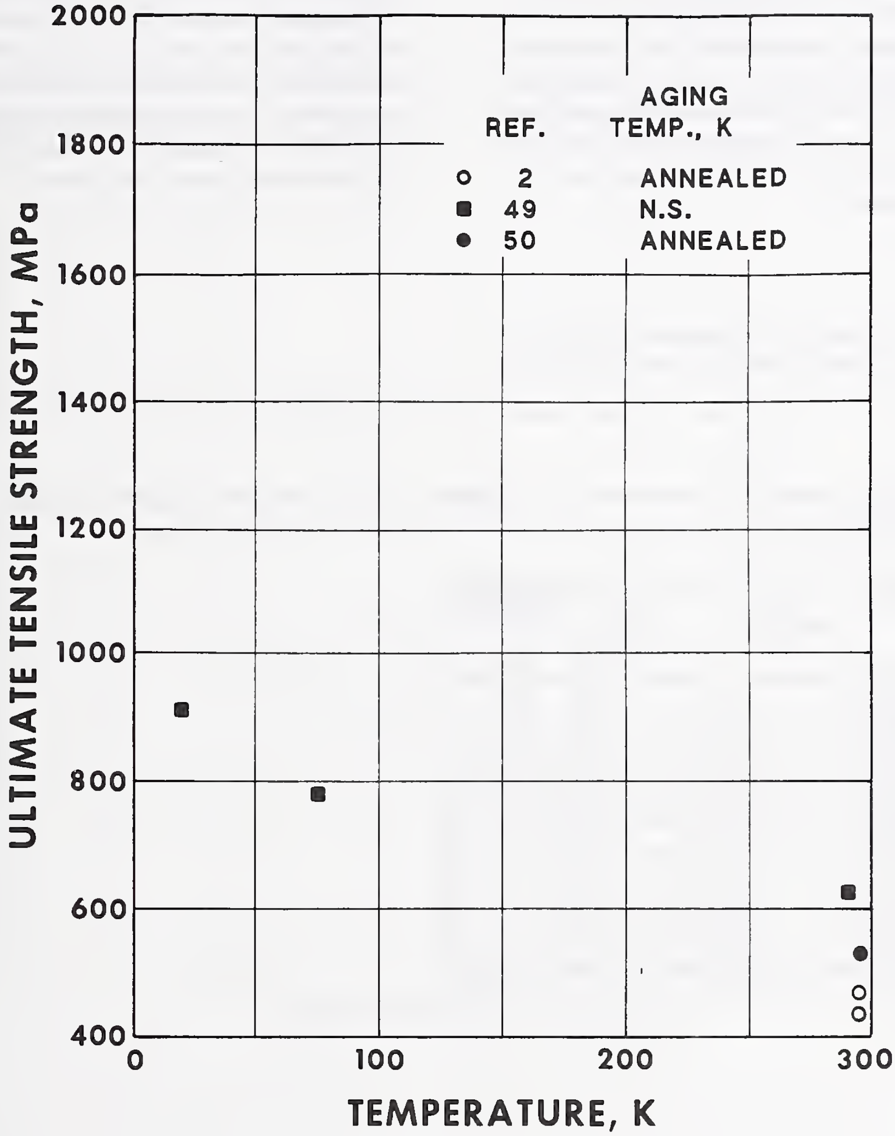

Figure 9.23. Tensile strength measurements of annealed, and annealed and aged C17000 beryllium copper are shown as a function of test temperature. All data are presented in Table 9.16. Products were in strip (Reference 9.2), or bar form (Reference 9.50), or not specified (Reference 9.49).

DATA SOURCES AND ANALYSIS

Measurements of the tensile strength of annealed C17000 beryllium copper at 295 K as a function of aging temperature and time were obtained from three sources (References 9.2, 9.3, and 9.49). Product was in strip form or was not specified (Reference 9.49). Reported aging temperatures ranged from 588 to 630 K; aging times from 2 to 3 h. Aging parameters were not specified in References 9.3 and 9.49, sometimes for proprietary reasons.

RESULTS

All measurements are reported in Table 9.17, which presents tensile strength, aging temperature and time, and the reference number. The available characterization of materials and measurements is given in Table 9.57 at the end of the tensile properties section. The small amount of available data indicates that satisfactory aging temperatures range from about 588 to 603 K, with an aging time of about 3 h. Figures 9.24 and 9.25 present the tensile strength measurements as a function of aging temperature and time, respectively. Unspecified values of temperature or time are plotted on the *y*-axis.

Table 9.17. Tensile Strength Dependence of Annealed C17000 Beryllium Copper on Aging Temperature and Time (295 K).

Tensile Strength, MPa	Aging Temperature, K	Aging Time, h	Reference No.
721	N.S.	N.S.	3
1088	630	3	2
1172	602	3	2
1047	630	2	2
1134	602	2	2
1091	630	3	2
1143	616	3	2
1070	588	3	2
1152	588	3	2
638	N.S.	N.S.	49

N.S. = not specified.

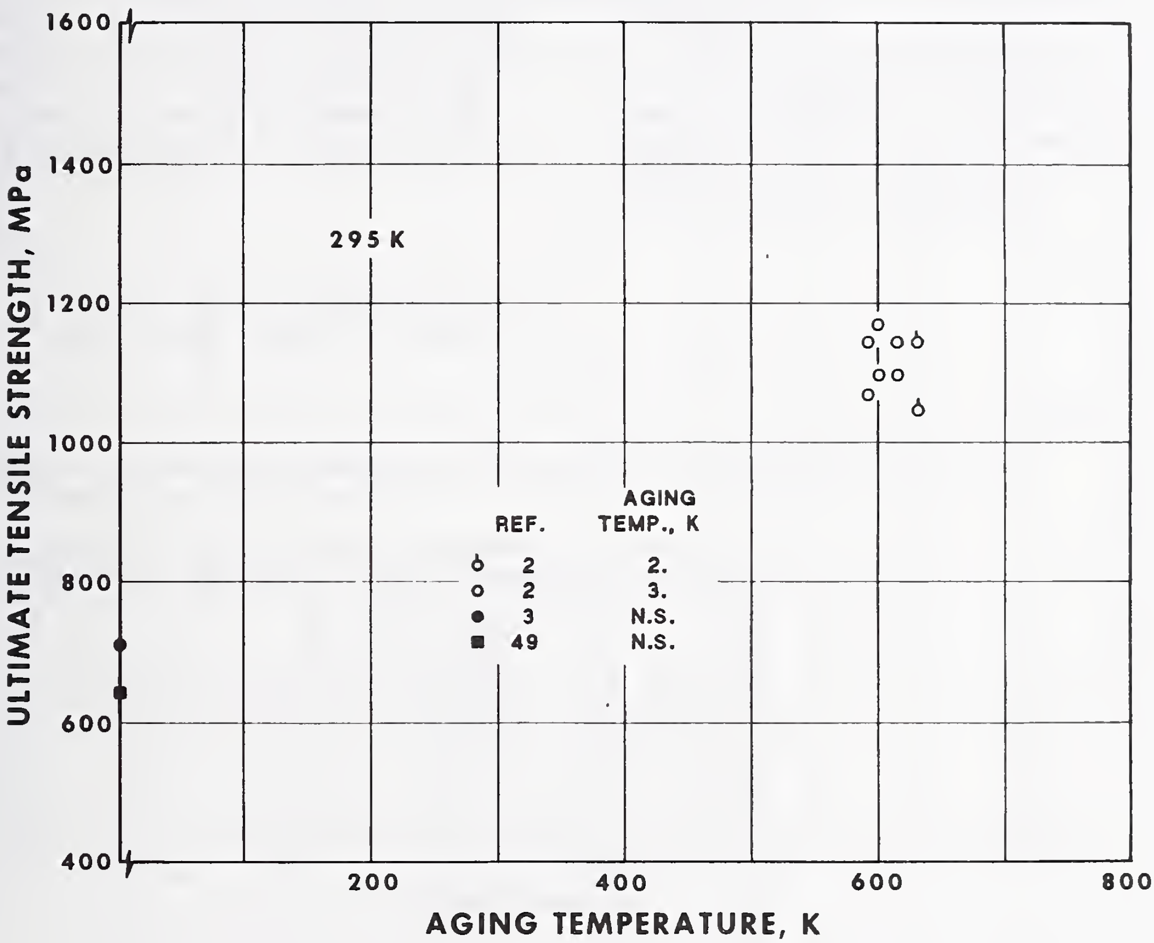

Figure 9.24. Tensile strength measurements on annealed C17000 beryllium copper at 295 K are shown as a function of aging temperature. If this parameter was not specified, tensile strength is plotted on the *y*-axis. All data are presented in Table 9.17. Product, where specified, was in strip form. (N.S. in legend for References 9.3 and 9.49 indicates not specified.)

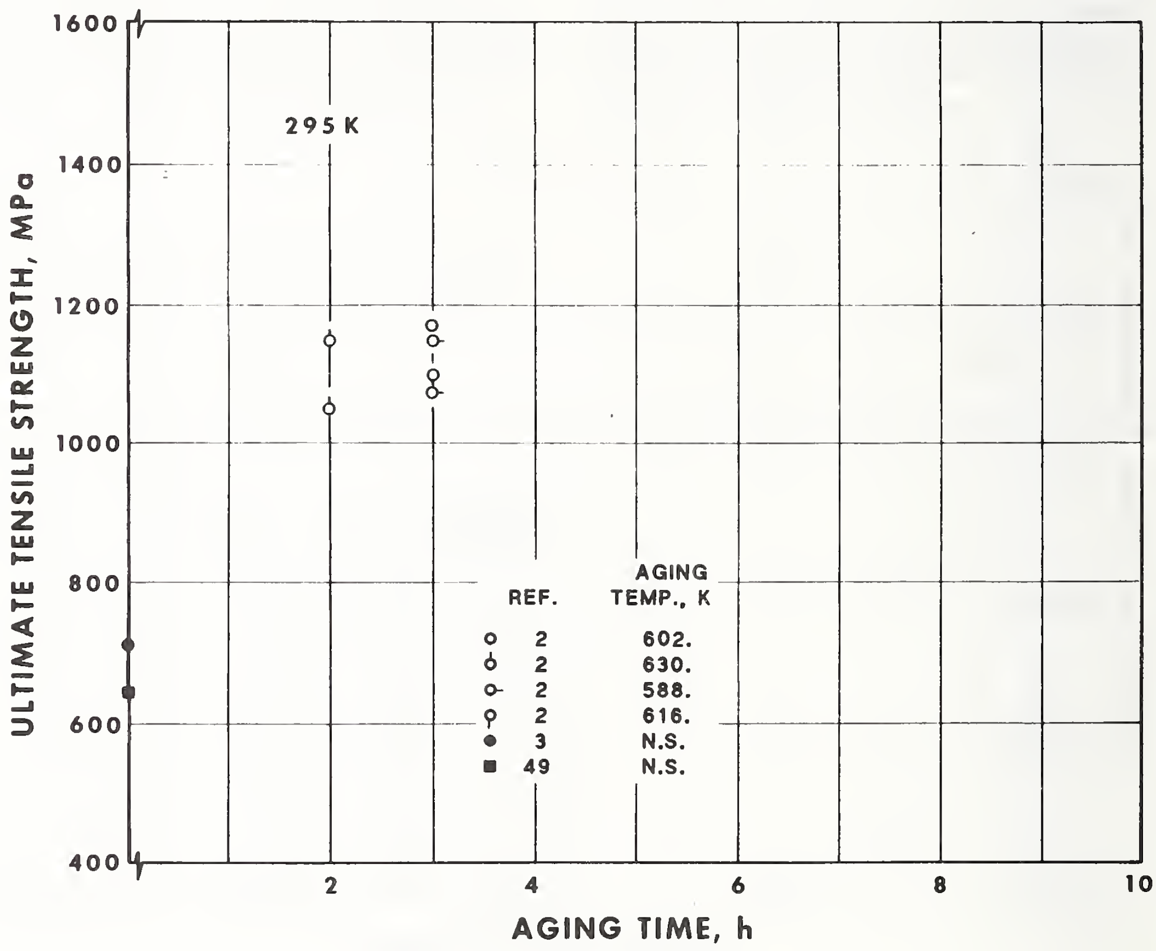

Figure 9.25. Tensile strength measurements for annealed C17000 beryllium copper at 295 K are shown as a function of aging time. If this parameter was not specified, tensile strength is plotted on the *y*-axis. For clarity, overlapping data points are omitted from the figure. All data are presented in Table 9.17. Product, where specified, was in strip form. (N.S. in legend for References 9.3 and 9.49 indicates not specified.)

DATA SOURCES AND ANALYSIS

Measurements of the tensile strength of cold-worked C17000 beryllium copper at 295 K as a function of aging temperature and time were obtained from three sources (References 9.2, 9.3, and 9.5). Product was in strip form. Cold work, *CW*, (carried out before aging) ranged from 11 to 50% (reduction in thickness). Reported aging temperatures ranged from 588 to 630 K; aging times from 2 to 3 h. Aging temperatures and times were not specified in Reference 9.5 (for some measurements) and in Reference 9.3, for proprietary reasons.

RESULTS

All measurements are reported in Table 9.18, which presents tensile strength, *CW* (reduction in thickness in percent), aging temperature and time, and the reference number. The available characterization of materials and measurements is given in Table 9.57 at the end of the tensile properties section. Figures 9.26 and 9.27 present the tensile strength measurements as a function of aging temperature and time, respectively. Unspecified values of temperature or time are plotted on the *y*-axis.

The reported aging temperatures and times cover a narrow range, and within this range there is not much difference in the measured yield strengths for a given level of *CW*. Thus, it is not possible to determine optimum values of temperature and time from the available data.

Table 9.18. Yield Strength Dependence of Cold-worked C17000 Beryllium Copper on Aging Temperature and Time (295 K).

Tensile Strength, MPa	Cold Work, %	Aging Temperature, K	Aging Time, h	Reference No.
807	11	N.S.	N.S.	5
1198	11	589	2.0	5
782	11	N.S.	N.S.	3
732	11	N.S.	N.S.	3
922	21	N.S.	N.S.	3
923	21	N.S.	N.S.	3
1172	50	N.S.	N.S.	3
1250	50	N.S.	N.S.	3
1189	11	602	3.0	2
1167	21	602	2.0	2
1205	11	602	2.0	2
1200	11	602	3.0	2
1210	21	602	2.5	2
1236	37	602	2.0	2
1101	11	630	2.0	2
1116	21	630	2.0	2
1142	37	630	2.0	2
1138	11	630	2.0	2
1145	21	630	2.0	2
1165	37	630	2.0	2
1116	11	616	3.0	2
1130	21	616	2.5	2
1168	37	616	2.0	2
1151	11	616	3.0	2
1161	21	616	2.5	2
1190	37	616	2.0	2

Table 9.18, continued

Tensile Strength, MPa	Cold Work, %	Aging Temperature, K	Aging Time, h	Reference No.
1090	11	588	2.0	2
1143	21	588	2.0	2
1202	37	588	2.0	2
1194	11	588	2.0	2
1200	21	588	2.0	2
1235	37	588	2.0	2

N.S. = not specified.

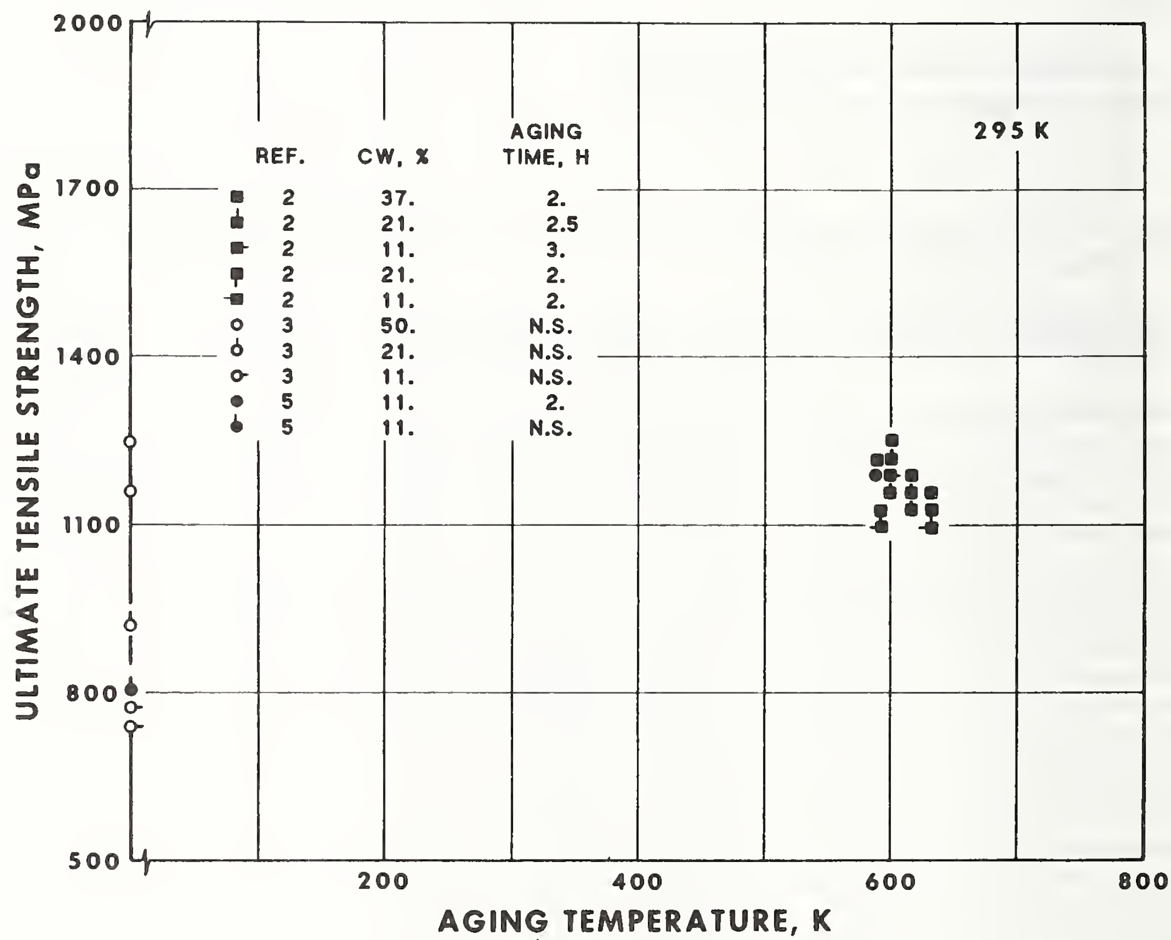

Figure 9.26. Tensile strength measurements on cold-worked C17000 beryllium copper at 295 K are shown as a function of aging temperature. If this parameter was not specified, tensile strength is plotted on the y-axis. For clarity, overlapping data points are omitted from the figure. All data are presented in Table 9.18. Product was in strip form. (N.S. in legend for References 9.3 and 9.5 indi-

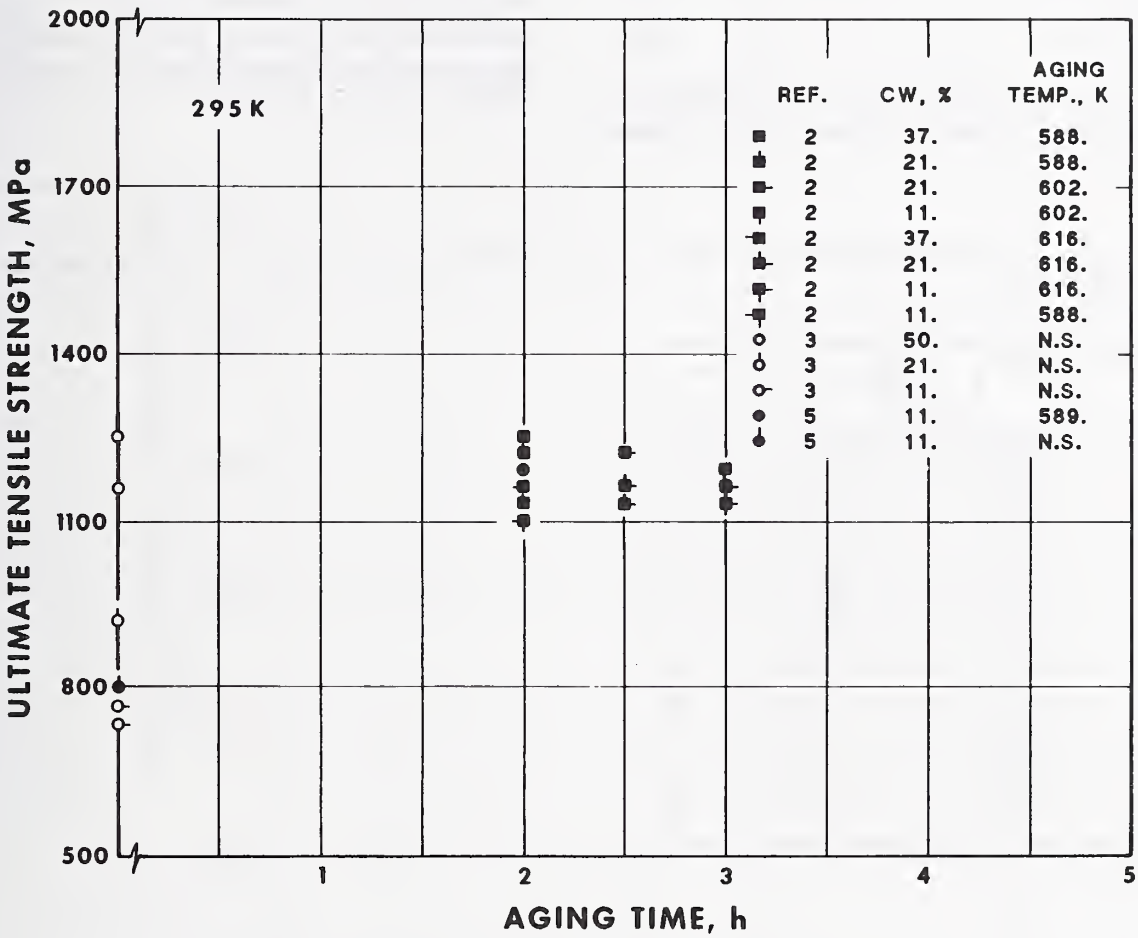

Figure 9.27. Tensile strength measurements on cold-worked C17000 beryllium copper at 295 K are shown as a function of aging time. If this parameter was not specified, tensile strength is plotted on the *y*-axis. For clarity, overlapping data points are omitted from the figure. All data are presented in Table 9.18. Product was in strip form. (N.S. in legend for References 9.3 and 9.5 indicates not specified.)

DATA SOURCES AND ANALYSIS

Measurements of the tensile strength of annealed C17200 beryllium copper between 20 and 300 K were obtained from three sources (References 9.6, 9.7, and 9.9). Product was in bar form.

RESULTS

All measurements are reported in Table 9.19, which presents tensile strength (σ_u), test temperature, and the reference number. The available characterization of materials and measurements is given in Table 9.57 at the end of the tensile properties section. Figure 9.28 presents the σ_u measurements as a function of test temperature.

Reference 9.10 presents measurements from 93 to 293 K on the σ_u of a 2.6-wt% beryllium-copper alloy in an annealed condition. These data exhibit an increase in strength as the temperature decreases that is similar to the trend shown in Figure 9.28.

Table 9.19. Tensile Strength Dependence of Annealed C17200 Beryllium Copper upon Temperature (20–300 K).

Tensile Strength, MPa	Test Temperature, K	Reference No.
506	300	6
516	214	6
579	144	6
676	88	6
477	295	7
487	295	7
579	195	7
516	195	7
682	76	7
684	76	7
813	20	7
804	80	7
500	295	9
517	232	9

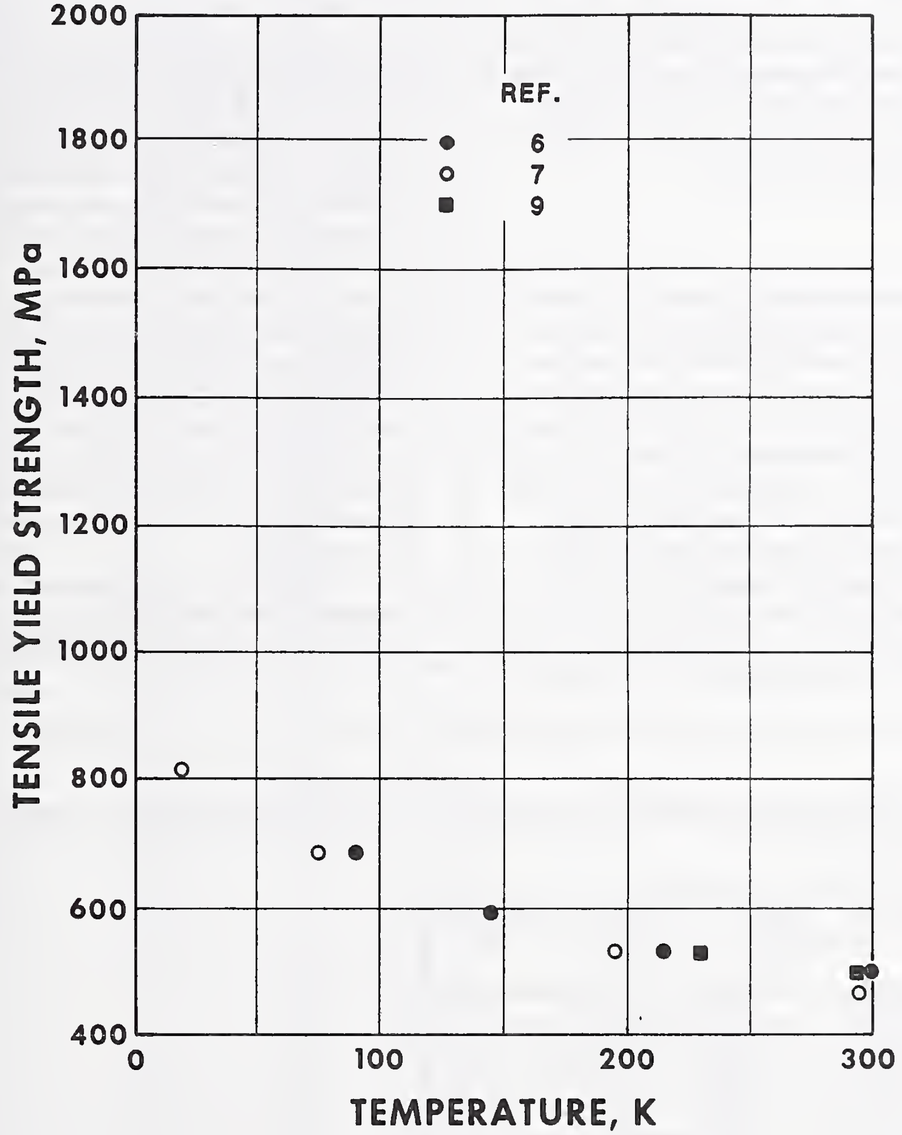

Figure 9.28. Tensile strength measurements of annealed C17200 beryllium copper are shown as a function of test temperature. For clarity, overlapping data points are omitted from the figure. All data are presented in Table 9.19. Product was in bar form.

DATA SOURCES AND ANALYSIS

Measurements of the tensile strength of annealed C17200 beryllium copper at 295 K as a function of aging temperature and time were obtained from 15 sources (References 9.2, 9.3, 9.11–9.15, 9.18, 9.20, and 9.51–9.54). Products were in sheet, strip, bar, and plate form. Reported aging temperatures ranged from 293 to 758 K; aging times from 0.067 to 8 h. Sufficient data were available to estimate a range of optimum aging temperatures and times.

RESULTS

All measurements are reported in Table 9.20, which presents tensile strength (σ_u), aging temperature and time, and the reference number. The available characterization of materials and measurements is given in Table 9.57 at the end of the tensile properties section. Figures 9.29 and 9.30 present the σ_u measurements as a function of aging temperature and time, respectively.

The figures indicate that optimum aging temperatures range from about 588 to 600 K, and optimum aging times from about 2 to 5 h. Although Reference 9.51, for an aging temperature of 622 K, reports a maximum in σ_u at an aging time of only 0.5 h, higher σ_u are observed (Reference 9.12) at 3 h for 588 K. (See Discussion section below).

DISCUSSION

Reference 9.23 discusses metallurgical aspects of the precipitation-hardening dependence of C17200 beryllium copper on temperature and time. At higher aging temperatures, precipitation is faster and peak properties are obtained more rapidly. At longer times, the precipitated particles coalesce, and hardness and strength drop off (overaging). In Figure 9.30, the strength first increases rapidly, but the slope becomes less steep at longer aging times. Reference 9.23 also discusses the advantages of achieving a given strength level by under- or overaging, and the relationship with elastic modulus, which reaches a peak after the maximum in yield or tensile strength is attained. The time-temperature relationships for σ_u are also shown clearly in Figure 13 in Reference 9.51 which presents typical trends for strip.

The effect of strip thickness upon the strength of annealed and aged C17200 beryllium copper is reported in Reference 9.24.

Table 9.20. Tensile Strength Dependence of Annealed C17200 Beryllium Copper on Aging Temperature and Time (295 K).

Tensile Strength, MPa	Aging Temperature, K	Aging Time, h	Reference No.
1118	588	3.000	11
1080	588	3.000	11
1106	588	3.000	11
676	622	0.067	51
1020	622	0.170	51
1131	622	0.250	51
1179	622	0.330	51
1193	622	0.420	51
1207	622	0.500	51
1200	622	0.580	51
1193	622	0.670	51
1179	622	0.750	51
1158	622	0.830	51
1138	622	0.920	51
1117	622	1.000	51
1089	622	1.100	51

Table 9.20, continued

Tensile Strength, MPa	Aging Temperature, K	Aging Time, h	Reference No.
1282	588	3.000	6
1131	672	1.500	6
1503	588	3.000	12
1476	588	3.000	12
1227	588	3.000	12
1255	588	3.000	12
1193	588	3.000	13
1214	588	1.000	13
1217	588	1.000	13
1227	588	3.000	13
1172	588	3.000	13
1186	588	3.000	13
1124	588	3.000	13
1289	566	0.330	14
932	588	0.500	14
981	566	3.000	14
1008	588	3.000	14
1012	566	3.000	14
1041	588	1.500	14
1096	588	2.000	14
1041	633	3.600	15
1476	633	5.000	15
1227	588	3.000	15
455	293	1.000	15
462	413	1.000	15
738	708	1.000	15
1041	588	3.000	15
965	708	3.000	15
800	758	1.000	15
885	588	3.000	52
913	588	1.000	52
1196	575	3.000	52
1063	588	3.000	52
1307	588	3.000	53
1227	588	3.000	15
1262	644	0.500	13
1217	644	0.500	15
1309	588	2.000	3
1282	588	2.000	3
1209	588	3.000	20
758	588	0.500	54
952	588	2.000	54
1055	588	5.000	54
1138	561	3.000	54
917	588	0.500	54
1186	588	2.000	54
1207	588	4.000	54
1241	588	3.000	54
1124	602	0.500	54
1200	602	1.000	54
1220	602	2.000	54

Table 9.20, continued

Tensile Strength, MPa	Aging Temperature, K	Aging Time, h	Reference No.
1310	630	5.000	54
1324	602	8.000	54
1200	616	0.670	54
1241	616	1.000	54
1289	630	2.000	54
1234	616	5.000	54
1227	630	0.500	54
1289	630	1.000	54
1241	630	2.000	54
1214	630	5.000	54
1103	588	2.000	54
1221	616	3.000	2
1284	616	3.000	2
1288	616	3.000	2
1247	602	3.000	2
1310	602	3.000	2
1339	602	3.000	2
1254	588	3.000	2
1304	588	3.000	2
1329	588	3.000	2
1226	630	2.000	2
1277	630	2.000	2
1294	630	2.000	2

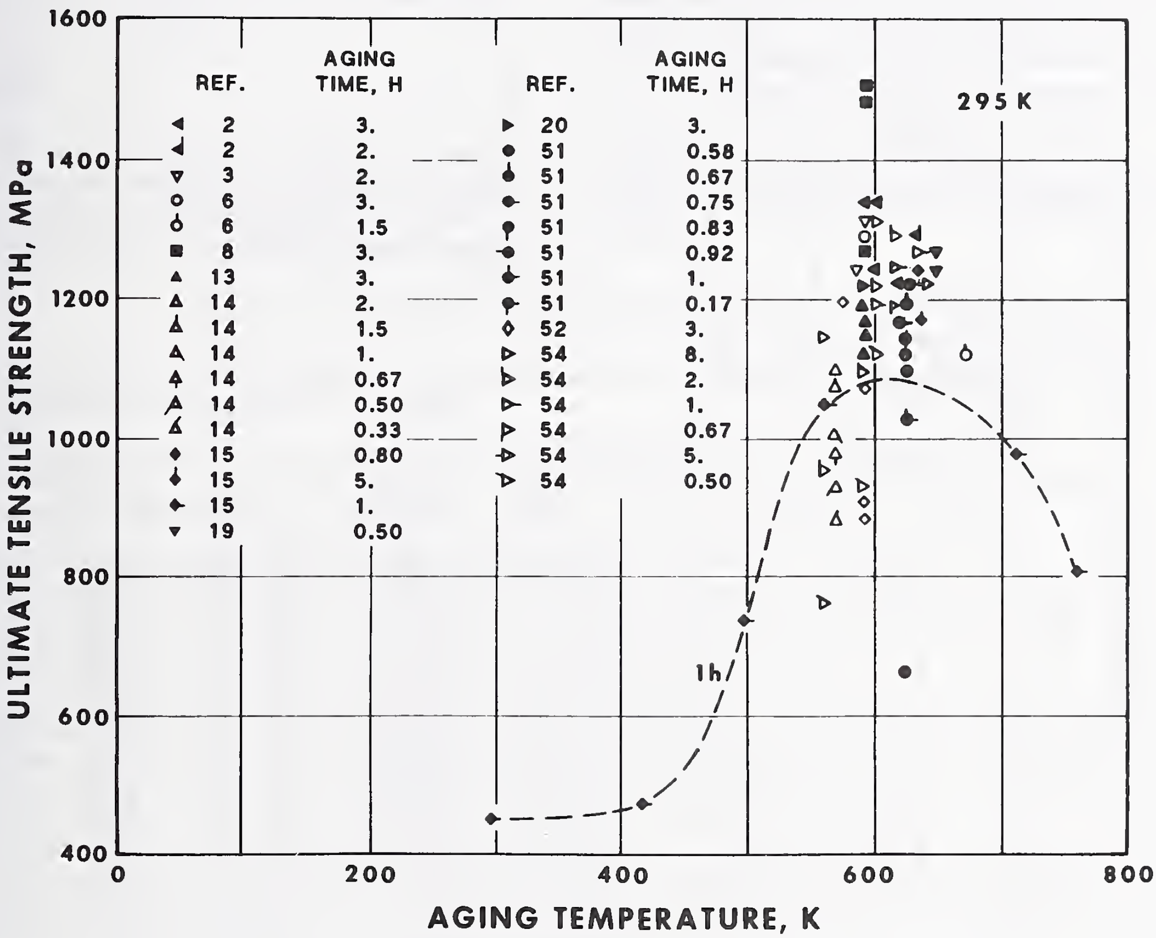

Figure 9.29. Tensile strength (σ_u) measurements on annealed C17200 beryllium copper at 295 K are shown as a function of aging temperature. A series of σ_u measurements from Reference 9.15 at 1-h aging time are connected by a dashed line to indicate the trend of increased σ_u at the optimum aging temperature. For clarity, overlapping data points are omitted from the figure, including all data points from References 9.11, 9.18, and 9.53. All data are presented in Table 9.20. Products were in sheet, strip, bar, and plate form.

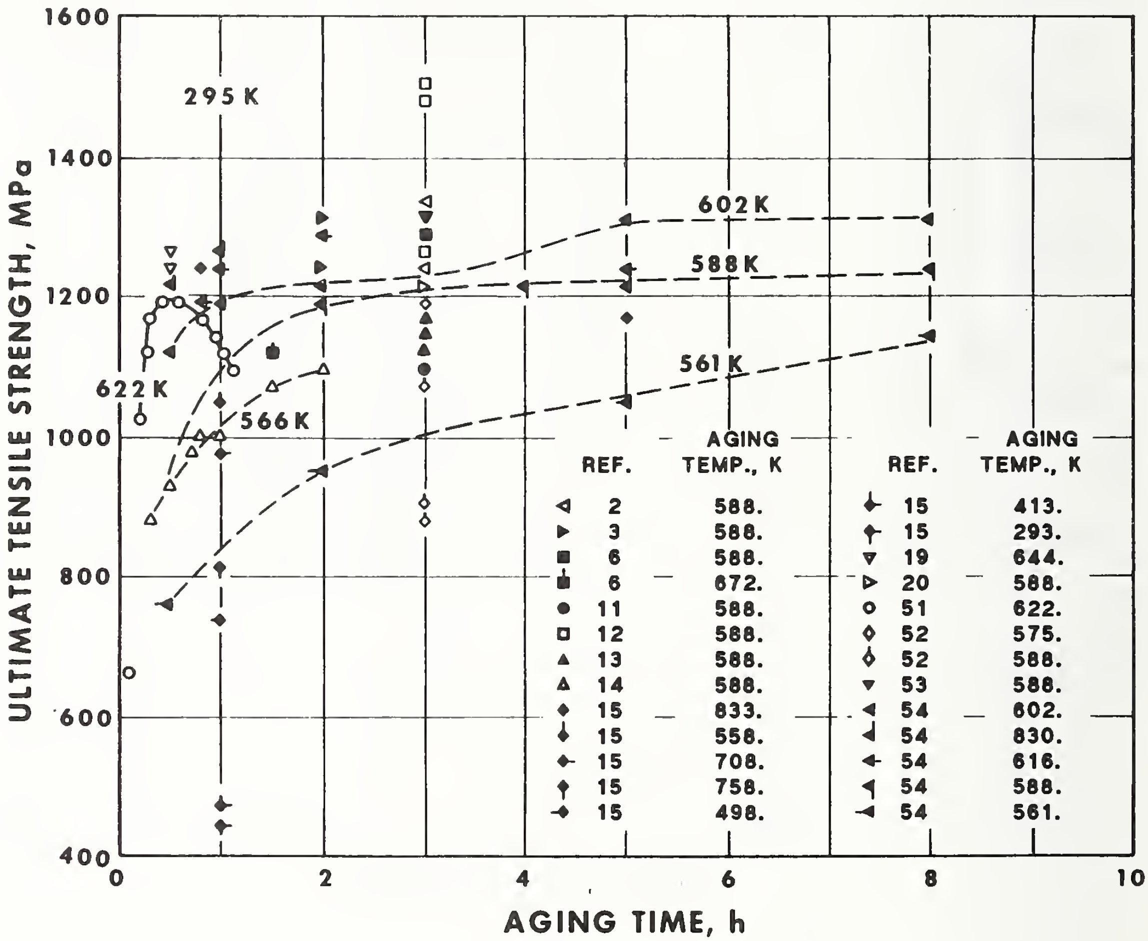

Figure 9.30. Tensile strength measurements on annealed C17200 beryllium copper at 295 K are shown as a function of aging time. For clarity, overlapping data points are omitted from the figure, including all data points from Reference 9.18. All data are presented in Table 9.20. Products were in sheet, strip, bar, and plate form.

DATA SOURCES AND ANALYSIS

Measurements of the tensile strength of annealed and aged C17200 beryllium copper between 20 and 300 K were obtained from four sources (References 9.6, 9.11, 9.12, and 9.19). Products were in sheet and bar form (not specified in Reference 9.12).

RESULTS

All measurements are reported in Table 9.21, which presents tensile strength (σ_u), test temperature, the aging temperature and time, and the reference number. The available characterization of materials and measurements is given in Table 9.57 at the end of the tensile properties section. Figure 9.31 presents the σ_u measurements as a function of test temperature.

The higher set of σ_u values from Reference 9.12 were obtained on notched specimens. The stress concentration factor, K_t, is 4.2, where K_t is defined as $(a/r)^{1/2}$. The notch radius is r and a is one-half the distance between the notches.

Reference 9.10 presents measurements from 93 to 293 K on the σ_u of a 2.6-wt% beryllium-copper alloy in an aged condition. These data exhibit an increase in strength as the temperature decreases that is similar to the trend shown in Figure 9.31.

Table 9.21. Tensile Strength Dependence of Annealed and Aged C17200 Beryllium Copper upon Temperature (20–300 K).

Tensile Strength, MPa	Test Temperature, K	Aging Temperature, K	Aging Time, h	Reference No.
1108	295	588	3.0	11
1586	295	588	3.0	11
1118	295	588	3.0	11
1516	20	588	3.0	11
1506	20	588	3.0	11
1506	20	588	3.0	11
1282	300	588	3.0	6
1296	214	588	3.0	6
1351	144	588	3.0	6
1455	28	588	3.0	6
1238	144	672	3.0	6
1200	144	672	1.5	6
1117	214	672	1.5	6
1131	300	672	1.5	6
1255	299	588	3.0	12
1227	299	588	3.0	12
1266	197	588	3.0	12
1236	197	588	3.0	12
1434	77	588	3.0	12
1379	77	588	3.0	12
1476	299	588	3.0	12
1503	299	588	3.0	12
1427	197	588	3.0	12
1558	197	588	3.0	12
1741	77	588	3.0	12
1806	77	588	3.0	12
1262	300	644	0.5	19
1317	200	644	0.5	19
1234	300	644	0.5	19
1269	200	644	0.5	19

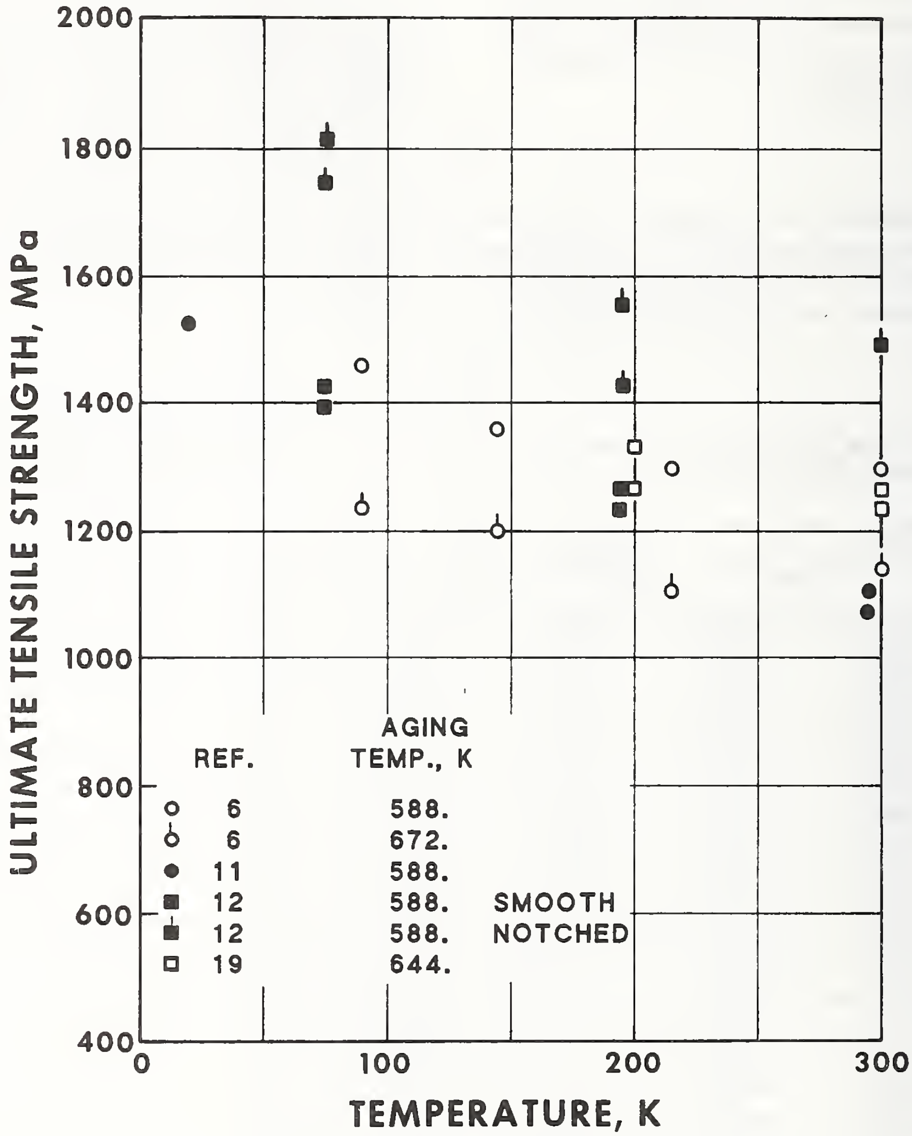

Figure 9.31. Tensile strength measurements of annealed and aged C17200 beryllium copper are shown as a function of test temperature. For clarity, overlapping data points are omitted from the figure. All data are presented in Table 9.21. Products were in sheet and bar form (not specified in Reference 9.12).

C17200: Cold-worked | *Ultimate Tensile Strength vs. Temperature (20–300 K)*

DATA SOURCES AND ANALYSIS

Measurements of the tensile strength of cold-worked C17200 beryllium copper between 20 and 300 K were obtained from five sources (References 9.6, 9.7, 9.9, 9.25, and 9.26). Data from Reference 9.27 at 295 K only are presented for comparison because measurements were made for varying amounts of cold work, *CW*. Products were in sheet, strip, and bar form (not specified in Reference 9.26).

RESULTS

All measurements are reported in Table 9.22, which presents tensile strength, test temperature, *CW* (reduction in thickness or area in percent), and the reference number. (The percent of *CW* could not be determined from Reference 9.26: it was 21% if the material was rolled or 37% if it was drawn.) The available characterization of materials and measurements is given in Table 9.57 at the end of the tensile properties section. Figure 9.32 presents the tensile strength measurements as a function of test temperature.

Table 9.22. Tensile Strength Dependence of Cold-worked C17200 Beryllium Copper upon Temperature (20–300 K).

Tensile Strength, MPa	Test Temperature, K	Cold Work, %	Reference No.
800	88	33	6
814	144	33	6
7[illegible]2	214	33	6
814	300	33	6
931	20	21	25
814	20	21	25
938	20	21	25
945	20	21	25
952	20	21	25
765	76	21	25
807	76	21	25
814	76	21	25
645	195	21	25
658	195	21	25
621	195	21	25
621	195	21	25
702	295	37	7
701	295	37	7
743	195	37	7
753	195	37	7
903	76	37	7
916	76	37	7
1060	20	37	7
650	76	37	7
779	300	N.S.	26
779	300	N.S.	26
758	300	N.S.	26
765	300	N.S.	26
972	77	N.S.	26

Table 9.22, continued

Tensile Strength, MPa	Test Temperature, K	Cold Work, %	Reference No.
972	77	N.S.	26
817	77	N.S.	26
979	77	N.S.	26
1117	20	N.S.	26
1076	20	N.S.	26
1096	20	N.S.	26
1124	20	N.S.	26
1117	20	N.S.	26
779	295	60	9
817	232	60	9
436	295	0	27
544	295	11	27
591	295	21	27
744	295	37	27

N.S. = not specified.

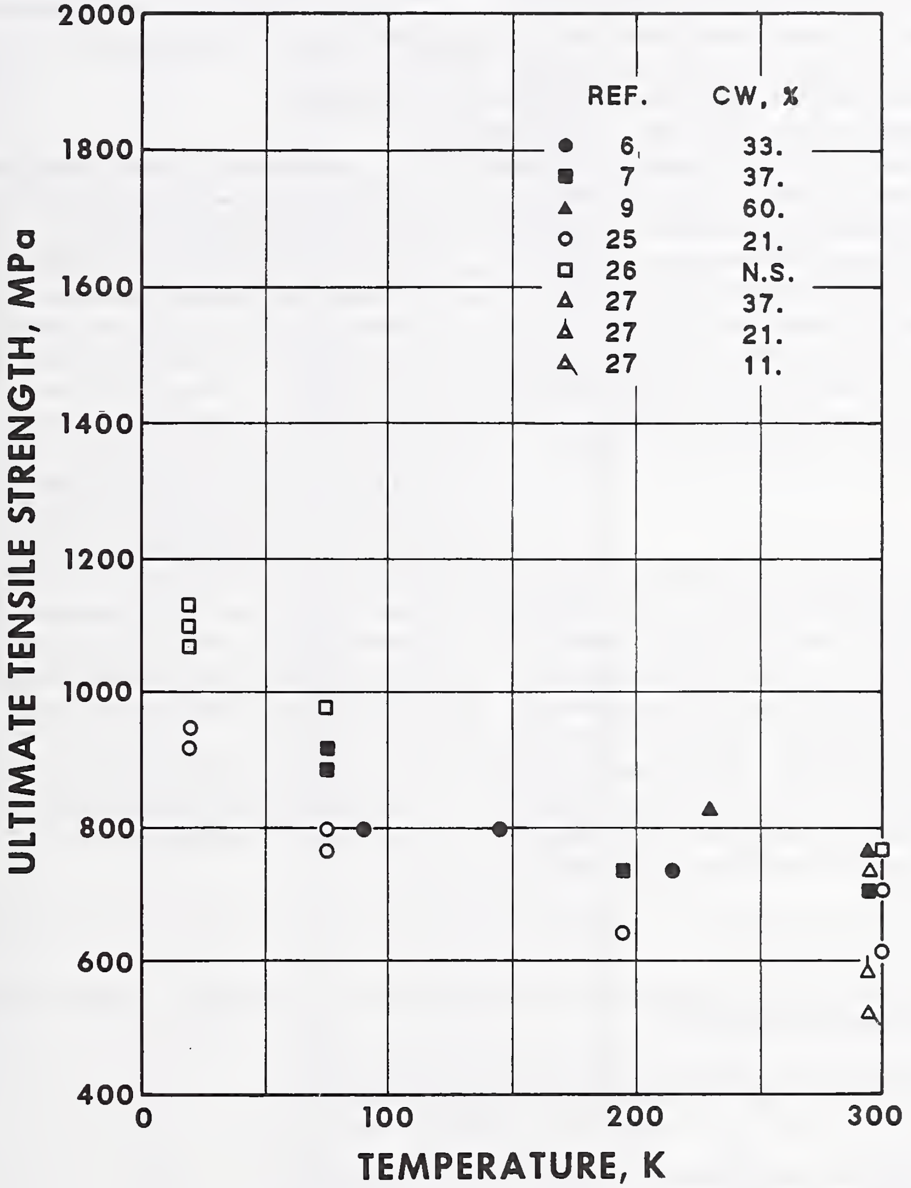

Figure 9.32. Tensile strength measurements of cold-worked C17200 beryllium copper are shown as a function of test temperature. For clarity, overlapping data points are omitted from the figure. One point from Reference 9.27, for zero cold work, does not appear in the figure. All data are presented in Table 9.22. Products were in sheet, strip, and bar form (not specified in Reference 9.26).

DATA SOURCES AND ANALYSIS

Measurements of the tensile strength of cold-worked C17200 beryllium copper at 295 K as a function of aging temperature and time were obtained from 24 sources (References 9.2, 9.3, 9.5, 9.6, 9.9, 9.13–9.15, 9.18, 9.19, 9.21, 9.28, 9.29, 9.31–9.33, and 9.52–9.59). Products were in wire, sheet, strip, bar, and plate form. Cold work, *CW*, ranged from 3 to 97% (reduction in thickness or area), and was carried out before aging, except in the measurements reported in Reference 9.55. Reported aging temperatures ranged from 297 to 748 K; aging times from 0.05 to 25 h. Aging temperatures and times for several measurements were not specified in References 9.3, 9.5, and 9.28, sometimes for proprietary reasons. Sufficient data were available to estimate a range of optimum aging temperatures and times.

RESULTS

All measurements are reported in Table 9.23, which presents tensile strength (σ_u), *CW* (reduction in thickness or area in percent), aging temperature and time, and the reference number. The available characterization of materials and measurements is given in Table 9.57 at the end of the tensile properties section. Figures 9.33 and 9.34 present the σ_u measurements as a function of aging temperature and time, respectively. Unspecified values of temperature or time are plotted on the *y*-axis. Several tensile strength measurements at long aging times are not shown in Figure 9.34.

The figures and Table 9.23 indicate that the optimum aging temperatures range from about 544 to 588 K and optimum times from 1 to 5 h.

DISCUSSION

Reference 9.23 discusses metallurgical aspects of the precipitation-hardening dependence of C17200 beryllium copper on temperature and time. At higher aging temperatures, precipitation is faster and peak properties are obtained more rapidly. At longer times, the precipitated particles coalesce, and hardness and strength drop off (overaging). In Figure 9.30, which presents σ_u vs. aging time, the strength first increases rapidly, but the slope becomes less steep at longer aging times. Reference 9.23 also discusses the advantages of achieving a given strength level by under- or overaging, and the relationship with elastic modulus, which reaches a peak after the maximum in yield or tensile strength is attained. Although cold-worked material is more difficult to form, higher σ_u can be obtained (see Figures 9.29 and 9.30 in this section and Figure 13 in Reference 9.51).

The effect of strip thickness upon the σ_u of cold-worked and aged C17200 beryllium copper is reported in Reference 9.24.

Table 9.23. Tensile Strength Dependence of Cold-worked C17200 Beryllium Copper on Aging Temperature and Time (295 K).

Tensile Strength, MPa	Cold Work, %	Aging Temperature, K	Aging Time, h	Reference No.
1183	50	575	7.00	55
1372	75	575	7.00	55
1522	90	575	7.00	55
1334	33	588	2.00	6
669	N.S.	N.S.	N.S.	28
1379	38	588	7.00	55
1462	30	575	1.00	56
1482	30	575	1.00	56
1482	30	588	1.00	56
1448	30	602	1.00	56
1600	67	561	1.00	56

Table 9.23, continued

Tensile Strength, MPa	Cold Work, %	Aging Temperature, K	Aging Time, h	Reference No.
1600	67	588	1.00	56
1620	61	575	1.00	56
1600	97	588	1.00	56
1114	97	602	1.00	56
1207	97	647	2.00	29
1344	97	619	2.00	29
1613	97	594	2.00	29
1634	97	566	2.00	29
1041	97	544	2.00	29
1558	97	525	2.00	29
1400	97	452	2.00	29
1258	97	297	2.00	29
1041	97	647	2.00	29
1172	97	619	2.00	29
1344	97	594	2.00	29
1424	97	555	2.00	29
1420	97	544	2.00	29
1386	97	525	2.00	29
1207	97	452	2.00	29
1114	97	297	2.00	29
1334	44	588	2.00	31
1321	35	566	2.00	14
1424	33	588	2.00	14
1120	97	566	1.00	13
1119	37	588	3.00	13
1372	15	566	2.00	14
1151	15	566	1.00	14
1114	15	566	1.00	14
1109	15	588	0.83	14
1041	15	566	0.67	14
986	15	588	0.50	14
838	15	566	0.83	14
1262	97	588	3.00	15
1372	97	566	3.00	15
648	21	293	1.00	15
676	21	423	1.00	15
1282	21	573	1.00	15
841	21	748	1.00	15
772	97	633	0.25	15
1351	97	619	0.67	15
1041	97	633	5.00	15
1441	97	594	3.00	32
1455	97	594	3.00	32
1413	97	594	3.00	32
1420	97	588	3.00	32
1041	97	594	1.00	32
1496	97	594	3.00	32
1258	97	575	2.00	52
1245	37	588	2.00	52
1175	21	575	2.00	52
1202	21	588	2.00	52
1289	21	573	1.50	57

Table 9.23, continued

Tensile Strength, MPa	Cold Work, %	Aging Temperature, K	Aging Time, h	Reference No.
1345	30	588	2.00	58
1420	37	588	2.00	53
1317	21	588	2.00	18
1317	37	644	0.30	19
1158	37	644	0.09	19
1278	11	589	2.00	5
1347	21	589	2.00	5
1382	37	589	2.00	5
770	11	N.S.	N.S.	5
855	21	N.S.	N.S.	5
1389	50	588	0.09	5
1351	11	588	2.00	3
1389	11	588	0.09	3
1445	21	588	2.00	3
1429	21	588	2.00	3
1442	37	588	2.00	3
1172	37	588	2.00	3
958	37	N.S.	N.S.	3
954	37	N.S.	N.S.	3
1247	50	N.S.	N.S.	3
1307	50	N.S.	N.S.	3
896	50	588	0.30	21
1158	50	588	0.09	21
1434	50	588	0.75	21
1586	50	588	0.09	21
1572	50	588	0.30	21
1034	50	588	0.09	21
1538	50	588	0.30	21
1531	50	588	1.00	21
1538	50	588	4.00	21
1413	50	588	17.00	21
1344	50	588	25.00	21
1151	50	622	0.09	21
1489	50	622	0.30	21
1462	50	622	0.75	21
1324	50	622	4.00	21
1165	50	622	17.00	21
1131	50	622	24.00	21
1269	50	644	0.09	21
1413	50	644	0.30	21
1310	50	644	0.75	21
1214	50	644	4.00	21
1172	50	644	8.00	21
1062	50	644	17.00	21
1020	50	644	24.00	21
1489	11	588	2.00	21
1558	30	588	0.09	21
1600	50	588	2.00	21
1165	3	588	2.00	54
1186	8	588	2.00	54
1296	17	588	2.00	54
1296	25	588	2.00	54

Table 9.23, continued

Tensile Strength, MPa	Cold Work, %	Aging Temperature, K	Aging Time, h	Reference No.
1351	11	588	2.00	54
1358	48	588	2.00	54
1344	59	588	4.00	54
1331	67	588	2.00	54
1317	11	588	2.00	54
1262	11	588	2.00	54
1227	11	588	2.00	54
827	11	561	0.50	54
969	11	588	1.00	54
1076	11	561	2.00	54
1144	11	561	4.00	54
1179	11	561	4.00	54
1117	11	588	4.00	54
1200	11	561	4.00	54
1262	11	588	2.00	54
1310	11	588	4.00	54
1276	11	588	4.00	54
1151	11	588	0.50	54
1200	11	602	1.00	54
1248	11	602	2.00	54
1289	11	588	4.00	54
1303	11	602	4.00	54
1241	11	616	0.50	54
1296	11	616	1.10	54
1289	11	616	4.00	54
1262	11	616	5.00	54
1262	11	630	0.50	54
1262	11	561	4.00	54
1303	11	630	2.00	54
1255	11	630	1.00	54
1262	11	644	0.50	54
1234	11	644	4.00	54
1200	11	644	2.00	54
1165	11	644	4.00	54
972	21	588	4.00	54
1103	21	588	4.00	54
1179	21	561	2.00	54
1241	21	588	4.00	54
1214	21	561	0.50	54
1296	21	588	4.00	54
1117	21	630	2.00	54
1358	11	561	4.00	54
1262	21	602	0.50	54
1310	21	602	1.00	54
1117	21	602	2.00	54
1310	21	602	4.00	54
1289	21	616	0.50	54
1331	21	616	4.00	54
1310	21	616	2.00	54
1214	21	616	4.00	54
1344	21	630	0.50	54
1310	21	630	1.00	54

C17200: Cold-worked and Aged

Ultimate Tensile Strength vs. Aging Temperature, Time (295 K)

Table 9.23, continued

Tensile Strength, MPa	Cold Work, %	Aging Temperature, K	Aging Time, h	Reference No.
1317	21	580	2.00	54
1220	21	580	1.00	54
1331	21	644	0.50	54
1289	21	644	1.00	54
1214	21	644	2.00	54
1193	21	644	1.00	54
1117	37	588	0.50	54
1172	37	588	1.00	54
1214	37	588	2.00	54
1303	37	588	3.00	54
1248	37	588	0.25	54
1365	37	588	1.00	54
1324	37	588	2.00	54
1351	37	588	3.00	54
1344	37	602	0.50	54
1379	37	602	1.00	54
1386	37	508	2.00	54
1400	37	602	2.00	54
1324	37	588	0.50	54
1351	37	616	1.00	54
1344	37	588	2.00	54
1207	37	616	5.00	54
1372	37	580	0.33	54
1331	37	630	1.00	54
1324	37	580	2.00	54
1289	37	580	1.00	54
1310	37	644	0.50	54
1296	37	644	1.00	54
1241	37	644	2.00	54
1220	37	644	4.00	54
1241	37	588	3.00	54
1282	21	602	3.00	54
1262	21	588	3.00	54
1324	37	588	3.00	54
1324	50	588	3.00	54
1151	11	588	3.00	54
1296	21	588	3.00	59
1296	37	588	3.00	54
1282	50	588	3.00	54
1186	6	588	3.00	54
1186	6	588	3.00	54
1317	50	644	1.00	33
1241	50	644	2.00	33
1207	50	644	3.00	33
1214	50	644	0.50	33
1207	50	644	5.00	33
1193	50	644	6.50	33
1186	50	644	7.00	33
1172	50	644	8.00	33
1517	50	588	1.00	33
1531	50	588	2.00	33
1531	50	588	3.00	33

Table 9.23, continued

Tensile Strength, MPa	Cold Work, %	Aging Temperature, K	Aging Time, h	Reference No.
1531	50	588	4.00	33
1538	50	638	5.00	33
1524	50	588	2.00	33
1510	50	622	7.00	33
1503	50	588	2.00	33
1448	50	622	1.00	33
1379	50	602	2.00	33
1338	50	622	1.00	33
1324	50	602	4.00	33
1310	50	622	5.00	33
1282	50	630	6.00	33
1269	50	622	7.00	33
1299	50	630	2.00	33
1227	11	630	2.00	2
1245	21	580	2.00	2
1269	37	622	2.00	2
1299	11	630	2.00	2
1310	21	630	2.00	2
1318	37	630	2.00	2
1310	11	630	2.00	2
1318	21	630	2.00	2
1367	37	630	2.00	2
1237	11	588	2.00	2
1272	21	638	2.00	2
1292	37	588	2.00	2
1314	11	616	2.00	2
1367	21	616	2.00	2
1314	37	616	2.00	2
1318	11	588	2.00	2
1310	21	616	2.00	2
1318	37	588	2.00	2
1267	11	638	2.00	2
1310	21	588	2.00	2
1356	37	638	2.00	2
1318	37	638	2.00	2
1405	21	638	2.00	2
1447	37	588	2.00	2
1334	11	638	2.00	2
1420	21	588	2.00	2
1471	37	588	2.00	2
1285	11	680	3.00	2
1318	21	622	2.50	2
1310	37	602	2.00	2
1365	11	680	1.00	2
1416	21	602	2.00	2
1433	37	680	2.00	2
1318	11	602	3.00	2
1420	21	680	2.50	2
1441	37	602	2.00	2

N.S. = not specified.

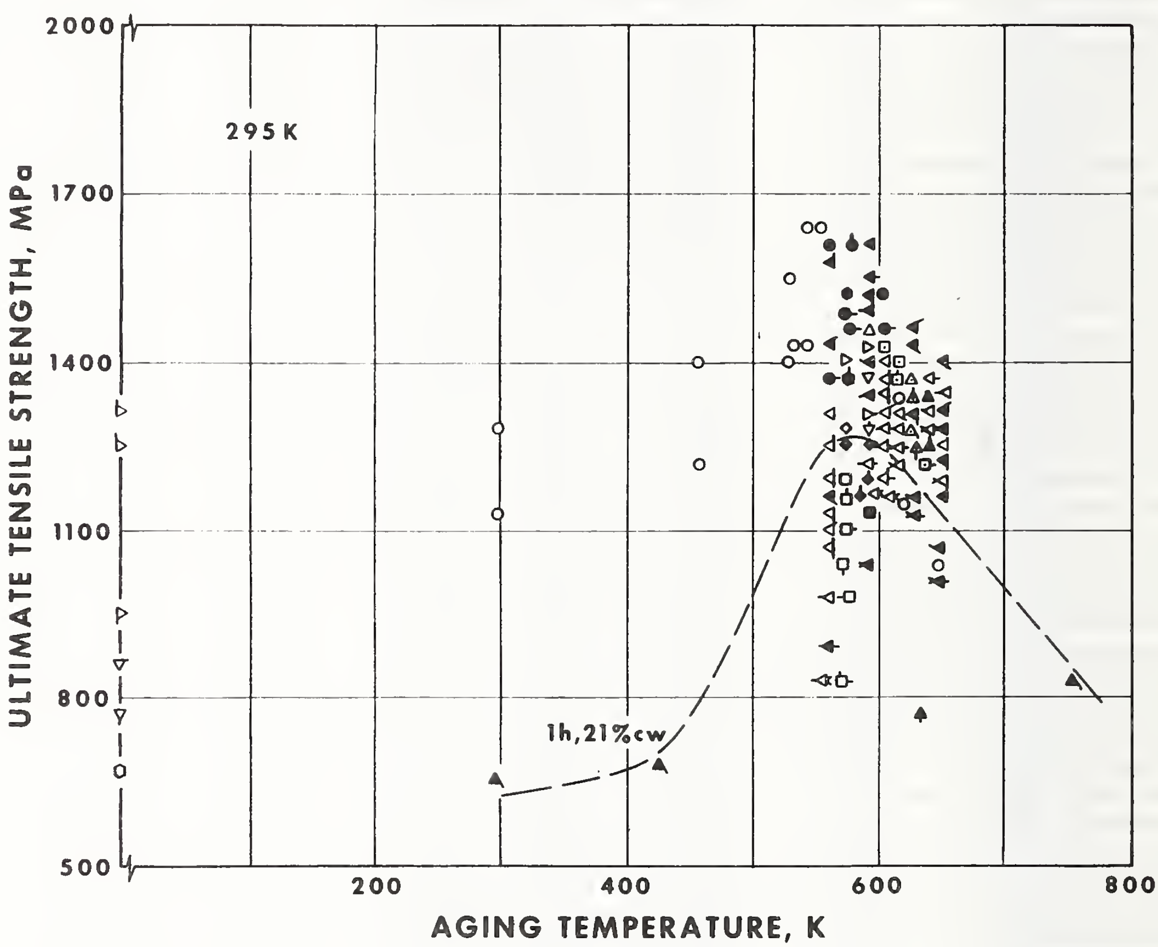

Figure 9.33. Tensile strength (σ_u) measurements on cold-worked C17200 beryllium copper at 295 K are shown as a function of aging temperature. If this parameter was not specified, σ_u is plotted on the y-axis. Measurements of σ_u from Reference 9.15 at 1-h aging time are connected by a dashed line to indicate the trend of increased σ_u at the optimum aging temperature. For clarity, overlapping data points are omitted from the figure, including all points from References 9.6, 9.18, 9.19, 9.31, 9.53, 9.55, 9.58, and 9.59. All data are presented in Table 9.23. The legend for this graph is given on the next page. Products were in wire, sheet, strip, bar, and plate form. (N.S. in legend for References 9.3, 9.5, and 9.28 indicates not specified.) The values from Reference 9.29 for room-temperature (297-K) aging are presented for comparison with values for higher aging temperatures.

REF.	CW, %	AGING TIME, H
2	37.	2.
2	21.	2.
2	11.	2.
3	37.	2.
3	50.	N.S.
3	11.	2.
3	37.	N.S.
5	37.	2.
5	21.	2.
5	21.	N.S.
5	11.	N.S.
9	60.	2.
13	37.	3.
14	15.	2.
14	15.	1.5
14	15.	0.83
14	15.	0.67
14	15.	0.50
14	15.	0.33
15	34.	0.67
15	34.	5.
15	21.	1.
15	34.	0.25
21	50.	2.
21	50.	8.2
21	39.	2.
21	50.	4.
21	18.	2.
21	50.	0.75
21	50.	0.30
21	50.	17.
21	50.	25.
21	50.	0.09
21	50.	24.
21	50.	0.05
28	N.S.	N.S.
29	97.	2.
32	37.	3.
33	50.	2.
33	50.	3.
33	50.	6.
33	50.	8.
52	37.	2.
52	21.	2.
54	37.	8.
54	37.	2.
54	37.	0.33
54	37.	0.50
54	21.	0.50
54	21.	1.
54	21.	2.
54	37.	4.
54	11.	4.
54	21.	4.
54	11.	5.
54	37.	0.25
54	37.	1.
54	11.	1.
54	11.	8.
54	11.	0.50
54	11.	2.
55	90.	7.
55	75.	7.
56	67.	1.
56	61.	1.
56	30.	1.
57	21.	1.5

Figure 9.33, continued. Legend for preceding graph.

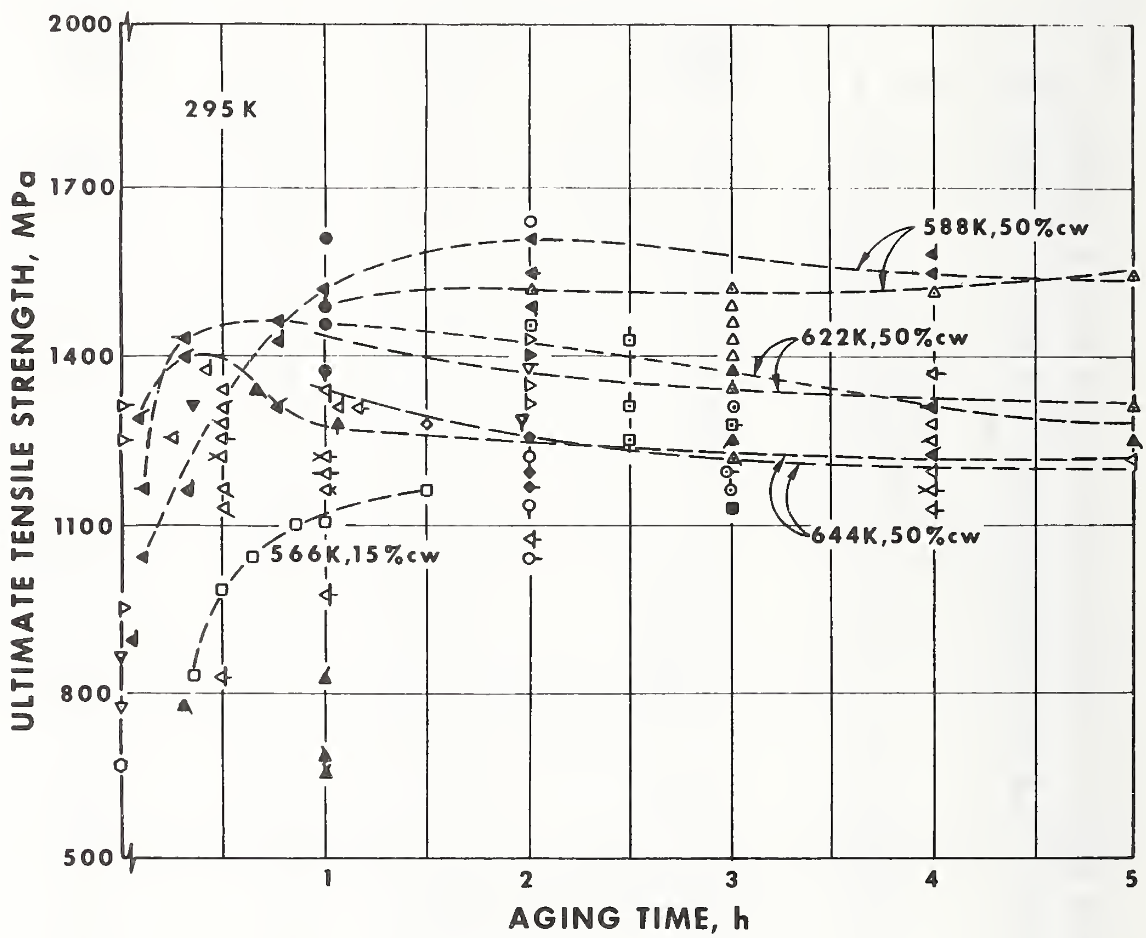

Figure 9.34. Tensile strength (σ_u) measurements on cold-worked C17200 beryllium copper at 295 K are shown as a function of aging time. If this parameter was not specified, σ_u is plotted on the *y*-axis. Several σ_u values from References 9.21, 9.28, 9.33, 9.54, and 9.55 at long aging times do not appear in the figures. For clarity, overlapping data points are omitted from the figure, including all points from References 9.6, 9.18, 9.31, 9.53, and 9.58. All data are presented in Table 9.23. The legend for this graph is given on the next page. Products were in wire, sheet, strip, bar, and plate form. (N.S. in legend for References 9.3 and 9.5 indicates not specified.) The values from Reference 9.29 for room-temperature (297-K) aging are presented for comparison with values for higher aging temperatures.

REF.	CW, %	AGING TEMP., K
2	37.	602.
2	21.	602.
2	11.	602.
2	11.	616.
3	37.	588.
3	11.	588.
3	21.	N.S.
3	37.	N.S.
5	21.	N.S.
5	11.	N.S.
5	37.	588.
5	11.	588.
9	60.	588.
13	37.	588.
14	15.	566.
15	34.	588.
15	34.	633.
15	21.	573.
15	17.	588.
15	21.	748.
15	21.	423.
15	21.	293.
19	37.	644.
21	50.	588.
21	50.	561.
21	39.	588.
21	18.	588.
21	50.	622.
21	50.	644.
28	N.S.	N.S.
29	97.	544.
29	97.	452.
29	97.	647.
29	97.	297.
32	37.	594.
33	50.	588.
33	50.	622.
33	50.	644.
52	37.	588.
52	21.	588.
52	21.	575.
54	37.	602.
54	37.	630.
54	21.	602.
54	37.	616.
54	37.	588.
54	37.	644.
54	37.	561.
54	21.	616.
54	21.	561.
54	21.	588.
54	11.	644.
54	11.	602.
54	21.	644.
54	11.	561.
54	11.	588.
56	61.	575.
56	67.	602.
56	30.	602.
56	30.	561.
57	21.	573.
59	37.	588.
59	11.	588.
59	6.	588.

Figure 9.34, continued. Legend for preceding graph.

DATA SOURCES AND ANALYSIS

Measurements of the tensile strength of cold-worked and aged C17200 beryllium copper between 48 and 300 K were obtained from four sources (References 9.6, 9.9, 9.19, and 9.51). Products were in sheet and bar form (not specified in Reference 9.51).

RESULTS

All measurements are reported in Table 9.24, which presents tensile strength, test temperature, percent of cold work, (reduction in thickness or area), aging temperature and time, and the reference number. The available characterization of materials and measurements is given in Table 9.57 at the end of the tensile properties section. Figure 9.35 presents the tensile strength measurements as a function of test temperature.

Table 9.24. Tensile Strength Dependence of Cold-worked and Aged C17200 Beryllium Copper upon Temperature (48–300 K).

Tensile Strength, MPa	Test Temperature, K	Cold Work, %	Aging Temperature, K	Aging Time, h	Reference No.
1572	48	N.S.	N.S.	N.S.	51
1482	73	N.S.	N.S.	N.S.	51
1431	148	N.S.	N.S.	N.S.	51
1396	123	N.S.	N.S.	N.S.	51
1365	148	N.S.	N.S.	N.S.	51
1344	173	N.S.	N.S.	N.S.	51
1331	198	N.S.	N.S.	N.S.	51
1324	223	N.S.	N.S.	N.S.	51
1317	148	N.S.	N.S.	N.S.	51
1317	273	N.S.	N.S.	N.S.	51
1307	293	N.S.	N.S.	N.S.	51
1334	300	33	588	2.00	6
1489	88	33	588	2.00	6
1413	148	33	588	2.00	6
1351	214	33	588	2.00	6
1317	300	37	644	0.33	19
1372	200	37	644	0.33	19
1303	300	37	644	0.33	19
1338	200	37	644	0.33	19
1389	295	60	575	2.00	9
1482	232	60	575	2.00	9

N.S. = not specified.

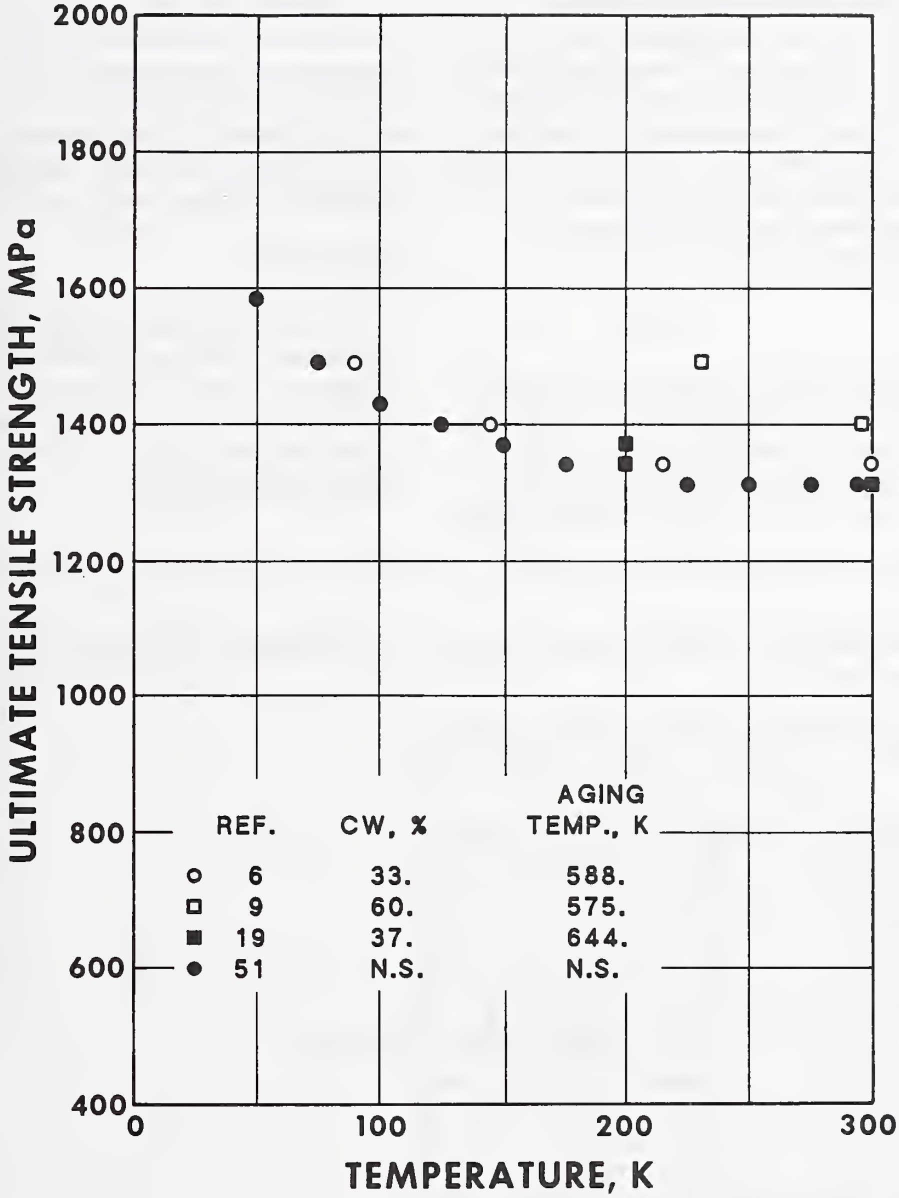

Figure 9.35. Tensile strength measurements of cold-worked and aged C17200 beryllium copper are shown as a function of test temperature. For clarity, overlapping data points are omitted from the figure. All data are presented in Table 9.24. Products were in sheet and bar form (not specified in Reference 9.51).

DATA SOURCES AND ANALYSIS

Measurements of the tensile strength of annealed C17500 beryllium copper at 295 K as a function of aging temperature and time were obtained from three sources (References 9.3, 9.12, and 9.36). Product was in strip form (Reference 9.3) or not specified (References 9.12 and 9.36). Reported aging temperatures ranged from 727 to 755 K; aging times from 0.13 to 8 h. Since the original data points were not presented in Reference 9.36, data were extracted from the curves at appropriate intervals.

RESULTS

All measurements are reported in Table 9.25, which presents tensile strength, aging temperature and time, and the reference number. The available characterization of materials and measurements is given in Table 9.57 at the end of the tensile properties section. Figures 9.36 and 9.37 present the tensile strength measurements as a function of aging temperature and time, respectively.

Not enough data are available in the literature to determine optimum aging parameters. Reference 9.37 states that it is standard commercial practice to overage at 753 K in order to develop the most favorable combination of strength and electrical conductivity. See also the electromagnetic properties section and Reference 9.36.

DISCUSSION

In Reference 9.36, a comparable set of measurements of yield and tensile strengths on both C17500 and C17510 beryllium copper is reported. The C17500 alloy was found to have slightly higher strengths after aging in both the annealed and cold-worked conditions.

Table 9.25. Tensile Strength Dependence of Annealed C17500 Beryllium Copper on Aging Temperature and Time (295 K).

Tensile Strength, MPa	Aging Temperature, K	Aging Time, h	Reference No.
758	727	8.00	12
917	727	3.00	12
1224	727	3.00	12
758	755	3.00	3
743	755	3.00	3
460	753	0.13	36
620	753	0.25	36
740	753	0.50	36
800	753	1.00	36
821	753	2.00	36
620	753	3.00	36
800	753	3.00	36
790	753	6.00	36
788	753	8.00	36

N.S. = not specified.

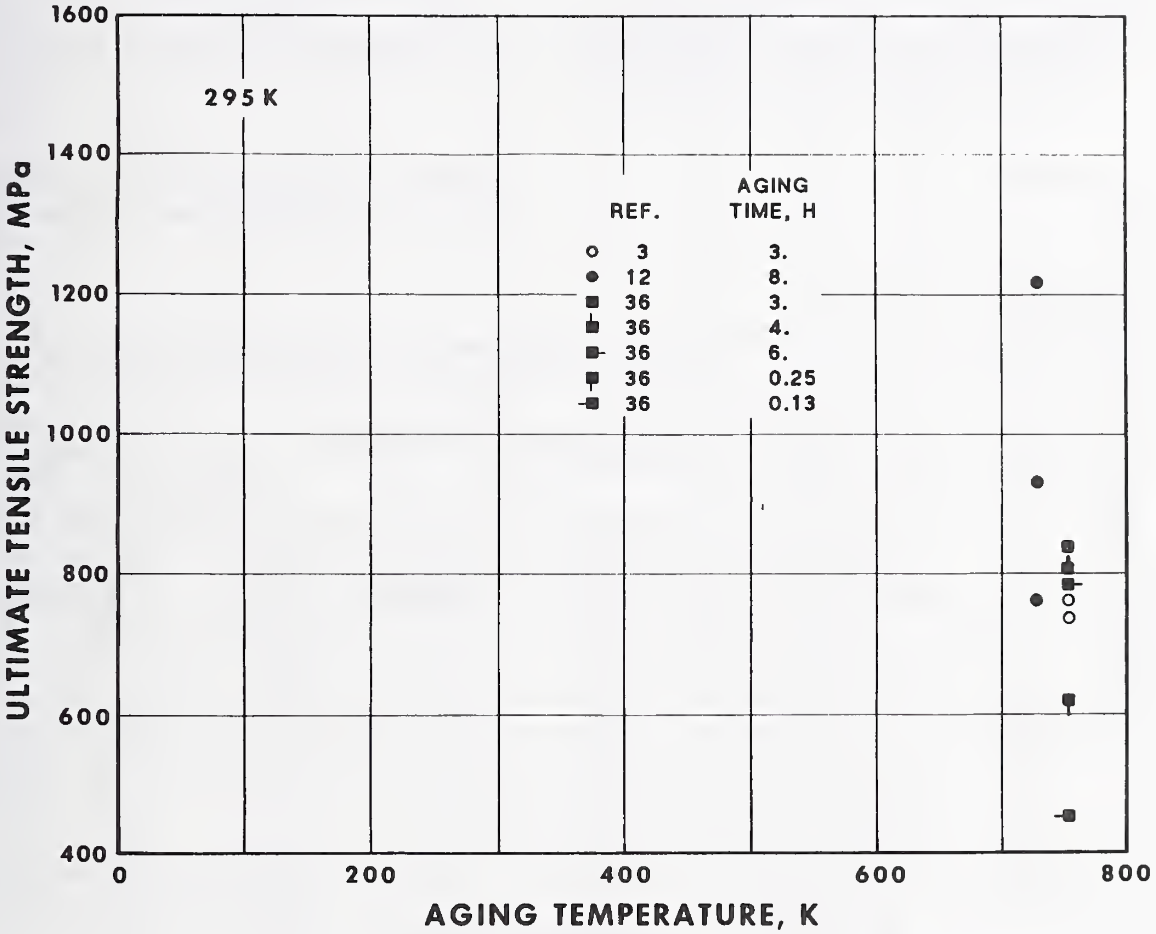

Figure 9.36. Tensile strength measurements on annealed C17500 beryllium copper at 295 K are shown as a function of aging temperature. For clarity, overlapping data points are omitted from the figure. All data are presented in Table 8.25. Product was in strip form (Reference 8.3) or not specified (Reference 9.12 and 9.36).

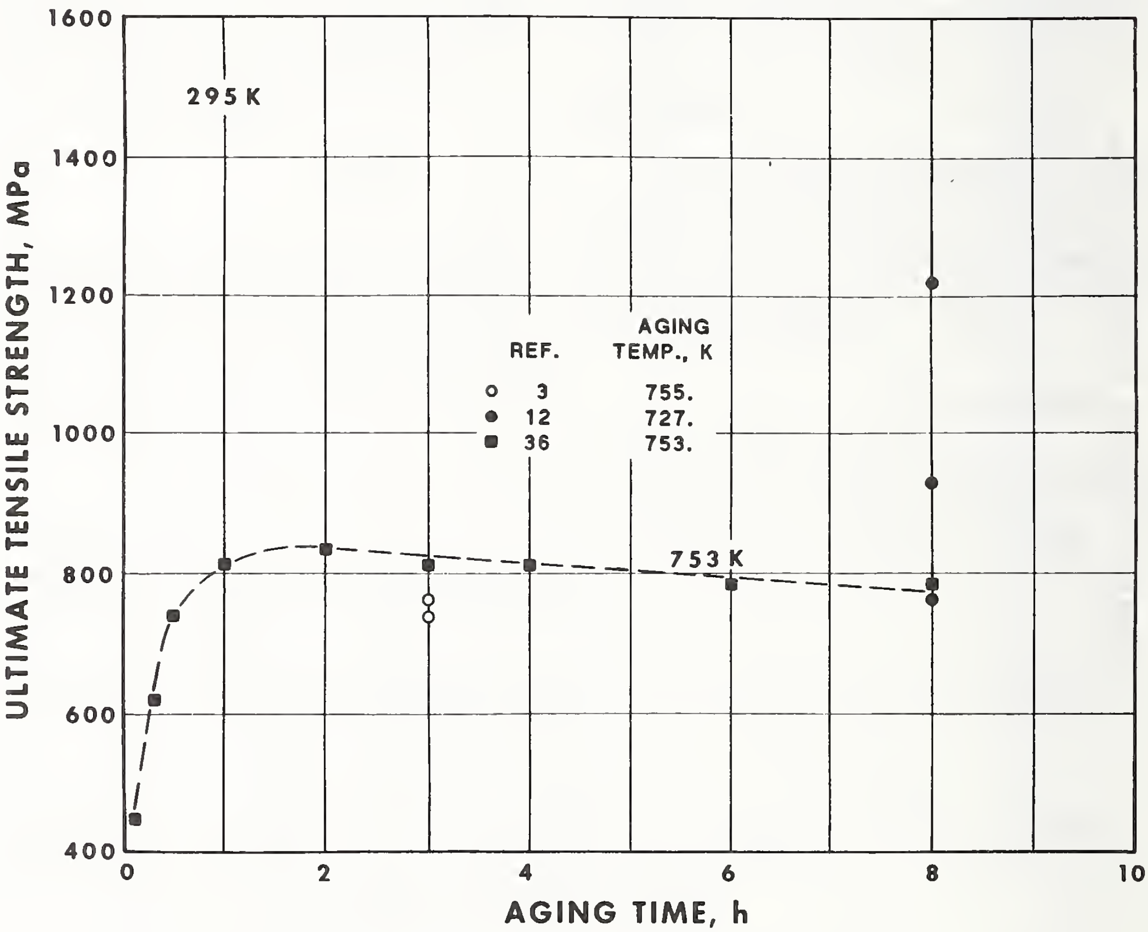

Figure 9.37. Tensile strength measurements for annealed C17500 beryllium copper at 295 K are shown as a function of aging time. All data are presented in Table 8.25. Product was in strip form (Reference 9.3) or not specified (References 9.12 and 9.36).

C17500: Annealed and Aged; Cold-worked; Cold-worked and Aged

Ultimate Tensile Strength vs. Temperature (20–300 K)

DATA SOURCES AND ANALYSIS

Measurements of the tensile strength of annealed and aged, cold-worked, and cold-worked and aged C17500 beryllium copper between 20 and 300 K were obtained from three sources (References 9.6, 9.12, and 9.25). Measurements from Reference 9.38 on cold-worked material at 295 K only are presented for comparison. Products were in sheet and bar form (not specified in References 9.12 and 9.38).

RESULTS

All measurements are reported in Table 9.26, which presents the tensile strength (σ_u), test temperature, percent of cold work (reduction in thickness or area), aging temperature and time, and the reference number. The available characterization of materials and measurements is given in Table 9.57 at the end of the tensile properties section. Figure 9.38 presents the σ_u measurements as a function of test temperature.

The higher set of σ_u values from Reference 9.12 were obtained on notched specimens. The stress concentration factor, K_t, is 4.2, where K_t is defined as $(a/r)^{1/2}$. The notch radius is r and a is one-half the distance between the notches.

Table 9.26. Tensile Strength Dependence of Annealed and Aged, Cold-worked, and Cold-worked and Aged C17500 Beryllium Copper upon Temperature (20–300 K).

Tensile Strength, MPa	Test Temperature, K	Cold Work, %	Aging Temperature, K	Aging Time, h	Reference No.
945	20	33	755	8	6
558	144	33	755	8	6
876	214	33	755	8	6
852	300	33	755	8	6
917	299	0	727	8	12
758	299	0	727	8	12
752	197	0	727	8	12
824	197	0	727	8	12
903	77	0	727	8	12
1296	77	0	727	8	12
1214	20	0	727	8	12
1203	20	0	727	8	12
1224	299	0	727	8	12
1224	299	0	727	8	12
1300	197	0	727	8	12
1296	197	0	727	8	12
1462	77	0	727	8	12
1462	77	0	727	8	12
1544	20	0	727	8	12
648	20	21	0	0	25
662	20	21	0	0	25
558	76	21	0	0	25
572	76	21	0	0	25
758	755	21	0	0	25
462	195	21	0	0	25
414	300	21	0	0	25
421	300	21	0	0	25
505	295	50	0	0	38

Aging Temperature, 0 K = not aged.

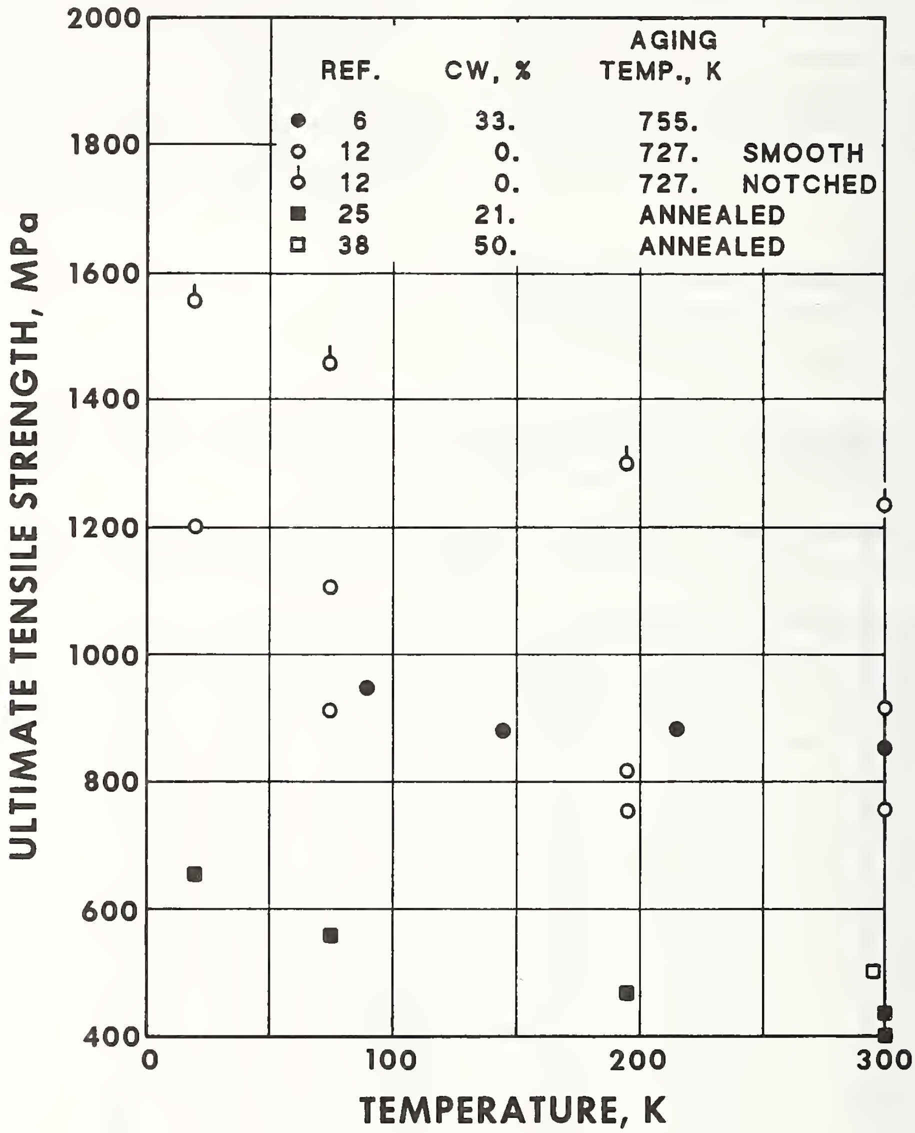

Figure 9.38. Tensile strength measurements of annealed and aged, cold-worked, and cold-worked and aged C17500 beryllium copper are shown as a function of test temperature. For clarity, overlapping data points are omitted from the figure. All data are presented in Table 9.26. Products were in sheet and bar form (not specified in References 9.12 and 9.38).

DATA SOURCES AND ANALYSIS

Measurements of the tensile strength of cold-worked C17500 beryllium copper at 295 K as a function of aging temperature and time were obtained from five sources (References 9.3, 9.6, 9.36, 9.38, and 9.39). Products were in strip and bar form (not specified in References 9.36 and 9.38). Cold work, *CW*, (carried out before aging) ranged from 3 to 65% (reduction in thickness or area). Reported aging temperatures ranged from 723 to 755 K; aging times ranged from 0.13 to 8 h. These parameters were not specified in Reference 9.39. Sufficient data were available to estimate a range of optimum aging times, but not aging temperatures. Since the original data points were not presented in Reference 9.36, data were extracted from the curves at appropriate intervals.

RESULTS

All measurements are reported in Table 9.27, which presents tensile strength (σ_u), *CW* (reduction in thickness or area in percent), aging temperature and time, and the reference number. The available characterization of materials and measurements is given in Table 9.57 at the end of the tensile properties section. Figures 9.39 and 9.40 present the σ_u measurements as a function of aging temperature and time, respectively. Unspecified values of temperature or time are plotted on the *y*-axis.

Not enough data are available in the literature to determine an optimum aging temperature, but in Figure 9.40, optimum aging times appear to range from approximately 1.5 to 2.5 h (for an aging temperature of about 750 K). Reference 9.37 states that it is standard commercial practice to overage at 753 K in order to develop the most favorable combination of strength and electrical conductivity. See also the electromagnetic properties section and Reference 9.36.

DISCUSSION

In Reference 9.36, a comparable set of measurements of yield and tensile strengths on both C17500 and C17510 beryllium copper are reported. The C17500 alloy was found to have slightly higher strengths after aging in both the annealed and cold-worked conditions.

Table 9.27. Tensile Strength Dependence of Cold-worked C17500 Beryllium Copper on Aging Temperature and Time (295 K).

Tensile Strength, MPa	Cold Work, %	Aging Temperature, K	Aging Time, h	Reference No.
852	33	755	2.00	6
8[illegible]2	50	723	0.75	38
692	50	723	1.00	38
736	50	723	1.50	38
741	50	723	2.00	38
755	50	723	2.50	38
755	50	723	3.00	38
615	50	N.S.	N.S.	38
745	50	N.S.	N.S.	38
760	3	755	3.00	3
738	3	755	3.00	3
802	11	755	2.50	3
756	11	755	2.00	3
680	N.S.	753	0.13	36
880	N.S.	753	0.25	36
920	N.S.	753	0.50	36
910	N.S.	753	1.00	36
900	N.S.	753	2.00	36

Table 9.27, continued

Tensile Strength, MPa	Cold Work, %	Aging Temperature, K	Aging Time, h	Reference No.
880	N.S.	753	3.00	36
870	N.S.	753	4.00	36
840	N.S.	753	6.00	36
800	N.S.	753	8.00	36

N.S. = not specified.

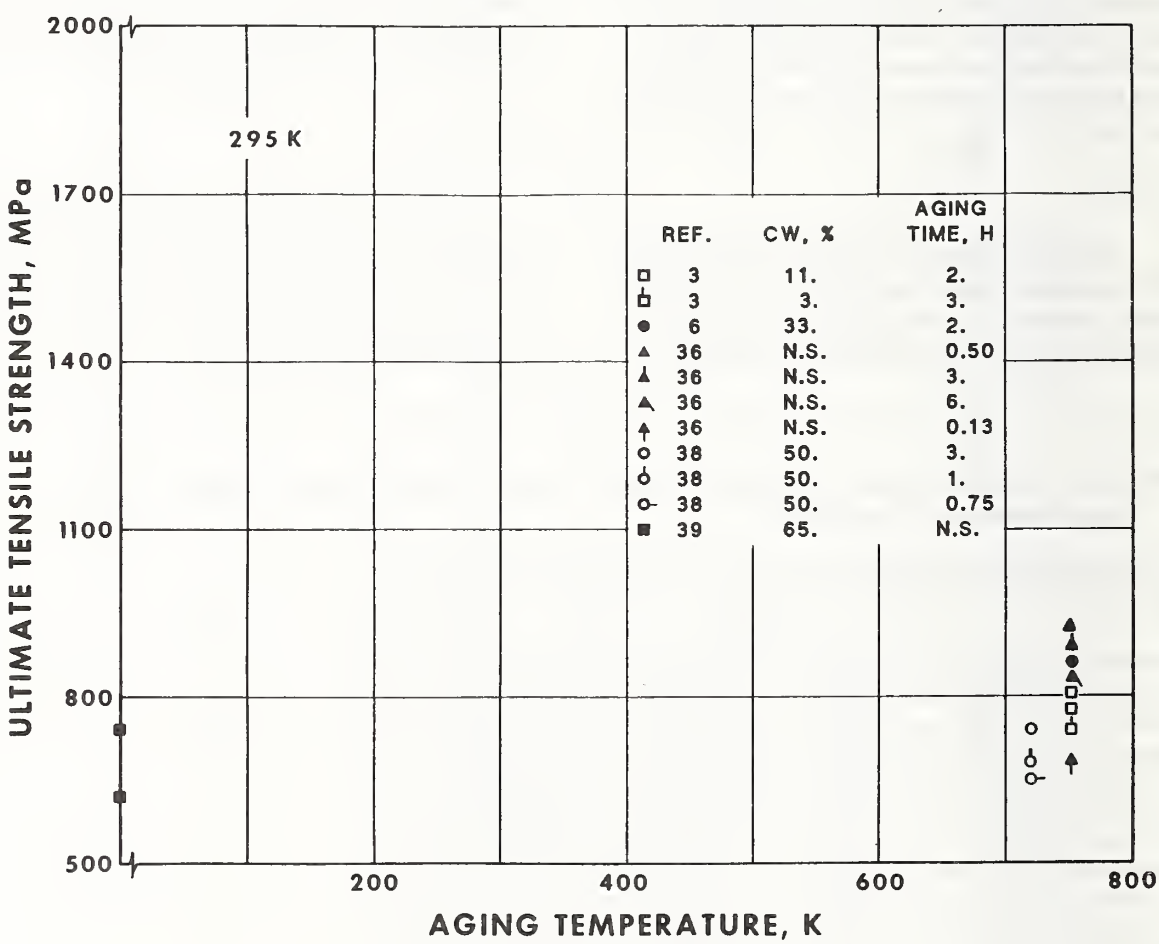

Figure 9.39. Tensile strength measurements on cold-worked C17500 beryllium copper at 295 K are shown as a function of aging temperature. If this parameter was not specified, tensile strength is plotted on the *y*-axis. For clarity, overlapping data points are omitted from the figure. All data are presented in Table 9.27. Products were in strip and bar form (not specified in Reference 9.38).

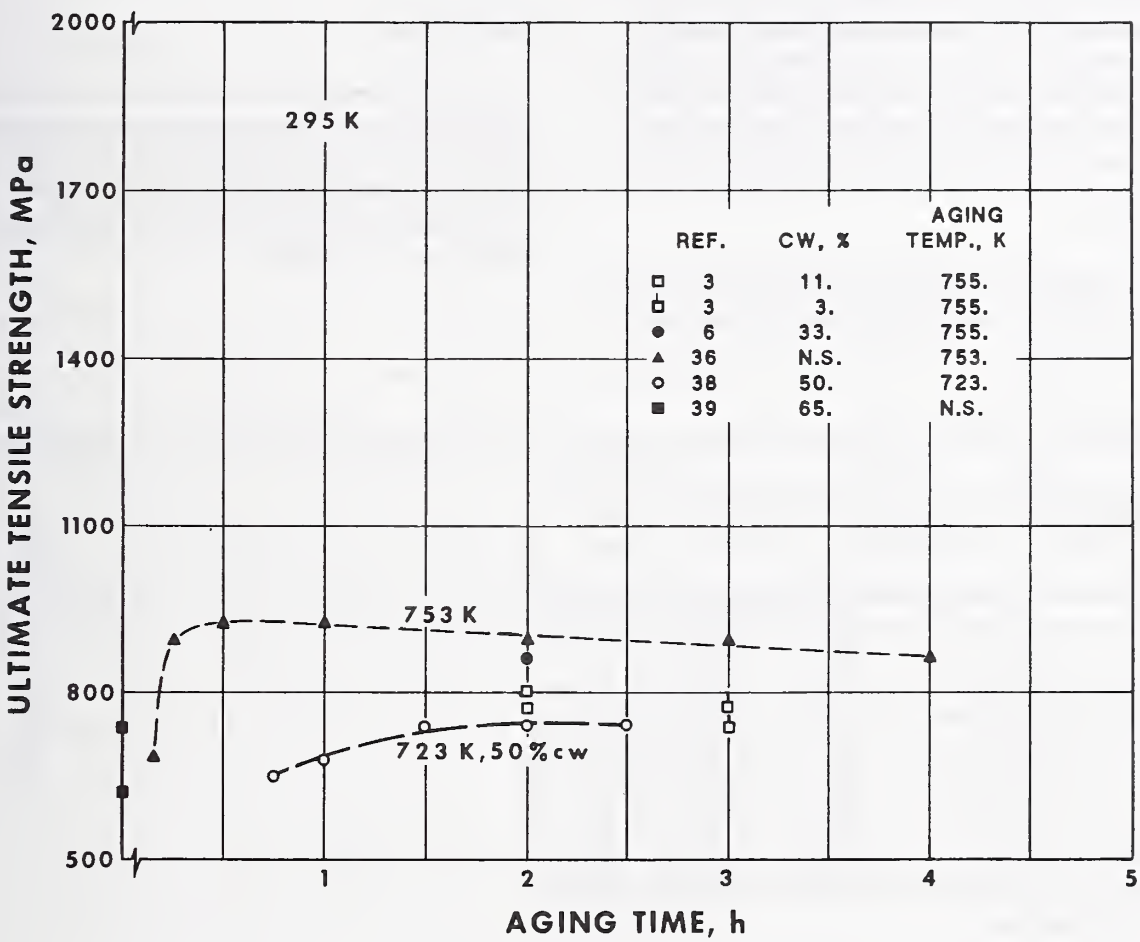

Figure 9.40. Tensile strength measurements on cold-worked C17500 beryllium copper at 295 K are shown as a function of aging time. If this parameter was not specified, tensile strength is plotted on the *y*-axis. For clarity, overlapping data points are omitted from the figure. All data are presented in Table 9.27. Products were in strip and bar form (not specified in Reference 9.38). (N.S. in legend for Reference 9.39 indicates not specified.)

DATA SOURCES AND ANALYSIS

Measurements of the tensile strength of annealed C17510 beryllium copper at 295 K as a function of aging time were obtained from two sources (References 9.36 and 9.40). Product was in strip form (Reference 9.40) or was not specified (Reference 9.36). Aging temperature was 753 K (Reference 9.36) or was not specified. Aging times ranged from 0.13 to 8 h (Reference 9.36) or were not specified. Since the original data points were not presented in Reference 9.36, data were extracted from the curves at appropriate intervals.

RESULTS

All measurements are reported in Table 9.28, which presents tensile strength, aging time, and the reference number. The available characterization of materials and measurements is given in Table 9.57 at the end of the tensile properties section. Figure 9.41 presents the tensile strength measurements as a function of aging time. Unspecified values of time are plotted on the *y*-axis.

DISCUSSION

In Reference 9.36, a comparable set of measurements of yield and tensile strengths on both C17500 and C17510 beryllium copper is reported. The C17500 alloy was found to have slightly higher strengths after aging in both the annealed and cold-worked conditions.

Table 9.28. Tensile Strength Dependence of Annealed C17510 Beryllium Copper on Aging Time (295 K).

Tensile Strength, MPa	Aging Temperature, K	Aging Time, h	Reference No.
834	N.S.	N.S.	40
380	753	0.13	36
834	753	0.25	36
680	753	0.50	36
720	753	1.00	36
780	753	2.00	36
768	753	3.00	36
755	753	4.00	36
740	753	6.00	36
740	753	8.00	36

N.S. = not specified.

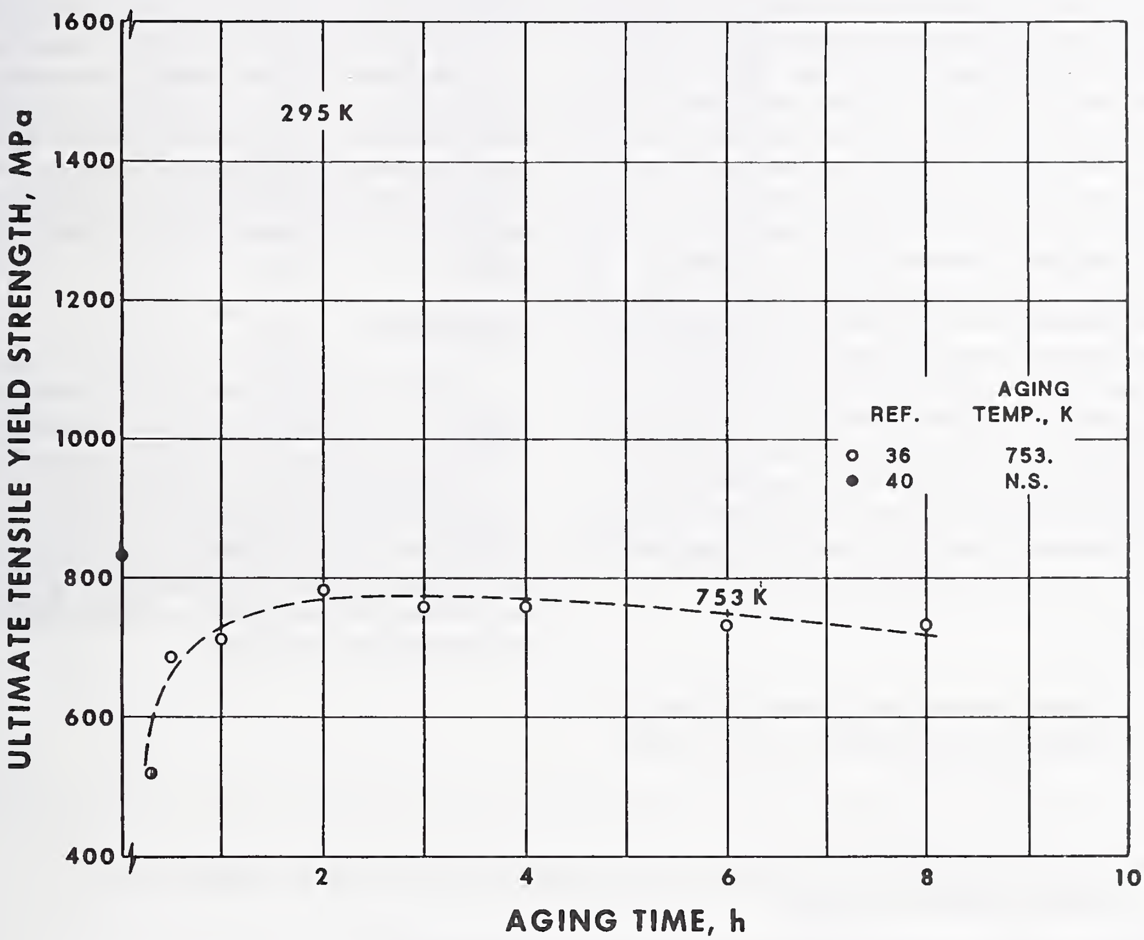

Figure 9.41. Tensile strength measurements on annealed C17510 beryllium copper at 295 K are shown as a function of aging time. If this parameter was not specified, tensile strength is plotted on the *y*-axis. All data are presented in Table 9.28. Product form was not specified. (N.S. in legend for Reference 9.40 indicates not specified.)

DATA SOURCES AND ANALYSIS

Measurements of the tensile strength of cold-worked C17510 beryllium copper at 295 K as a function of aging temperature and time were obtained from six sources (References 9.36, 9.41, and 9.43–9.46). Products were in strip and plate form (not specified in References 9.36 and 9.41). Cold work, *CW*, (carried out before aging) ranged from 37 to 80% (reduction in thickness). Aging temperatures ranged from 573 to 755 K; aging times from 0.13 to 70 h. These parameters were not specified in References 9.43 and 9.50. Before cold rolling, some material was pre-aged at temperatures from 573 to 758 K, usually for 3 h (Reference 9.45). Since the original data points were not presented in Reference 9.36, data were extracted from the curves at appropriate intervals. Data presented here from Reference 9.46 include tensile measurements at 295 K from a commercial supplier, Princeton Plasma Physics Laboratory, and Massachusetts Institute of Technology. Reference 9.44 also reports tensile test data on one of the heats (A) included in the tests summarized in Reference 9.46. Cryogenic test results from Reference 9.44 on this heat are presented in Part B of the tensile properties section.

RESULTS

All measurements are reported in Table 9.29, which presents tensile strength (σ_u), *CW* (reduction in thickness in percent), aging temperature and time, and the reference number. The available characterization of materials and measurements is given in Table 9.57 at the end of the tensile properties section. Figures 9.42 and 9.43 present the σ_u measurements as a function of aging temperature and time, respectively. Unspecified values of temperature or time are plotted on the *y*-axis. Several σ_u measurements at long aging times are not shown in Figure 9.43.

The figures indicate that optimum aging temperatures for high σ_u range from about 573 to 593 K with aging times ranging from 1 to 20 h. However, these conclusions are based on a limited number of measurements, and some material was pre-aged, as described above (Reference 9.45).

DISCUSSION

Further information on the microstructure resulting from the aging processes reported in Reference 9.43 may be found in Reference 9.47.

In Reference 9.36, a comparable set of measurements of yield and tensile strengths on both C17500 and C17510 beryllium copper are reported. The C17500 alloy was found to have slightly higher strengths after aging in both the annealed and cold-worked conditions.

Table 9.29. Tensile Strength Dependence of Cold-worked C17510 Beryllium Copper on Aging Temperature and Time (295 K).

Tensile Strength, MPa	Cold Work, %	Aging Temperature, K	Aging Time, h	Reference No.
931	40	755	3.00	41
1000	37	N.S.	N.S.	43
1034	37	N.S.	N.S.	43
827	37	N.S.	N.S.	43
972	37	N.S.	N.S.	43
783	37	755	2.00	44
777	37	755	2.00	44
1090	60	593	70.00	45
1068	80	573	6.00	45
1045	60	673	1.00	45
1048	60	633	4.00	45

C17510: Cold-worked and Aged

Ultimate Tensile Strength vs. Aging Temperature, Time (295 K)

Table 9.29, continued

Tensile Strength, MPa	Cold Work, %	Aging Temperature, K	Aging Time, h	Reference No.
1070	80	593	5.00	45
1057	60	673	1.00	45
1035	80	593	24.00	45
1049	60	593	16.00	45
1030	60	593	16.00	45
1005	80	633	1.00	45
1046	80	633	2.00	45
1040	60	673	2.00	45
860	N.S.	753	0.13	36
880	N.S.	753	0.25	36
860	N.S.	753	0.50	36
880	N.S.	753	1.00	36
870	N.S.	753	2.00	36
850	N.S.	753	1.00	36
840	N.S.	753	4.00	36
880	N.S.	753	6.00	36
760	N.S.	753	8.00	36
841	37	755	8.00	46A
793	N.S.	N.S.	N.S.	46B
765	N.S.	N.S.	N.S.	46C
793	37	755	2.00	46A
803	N.S.	N.S.	N.S.	46C

N.S. = not specified.

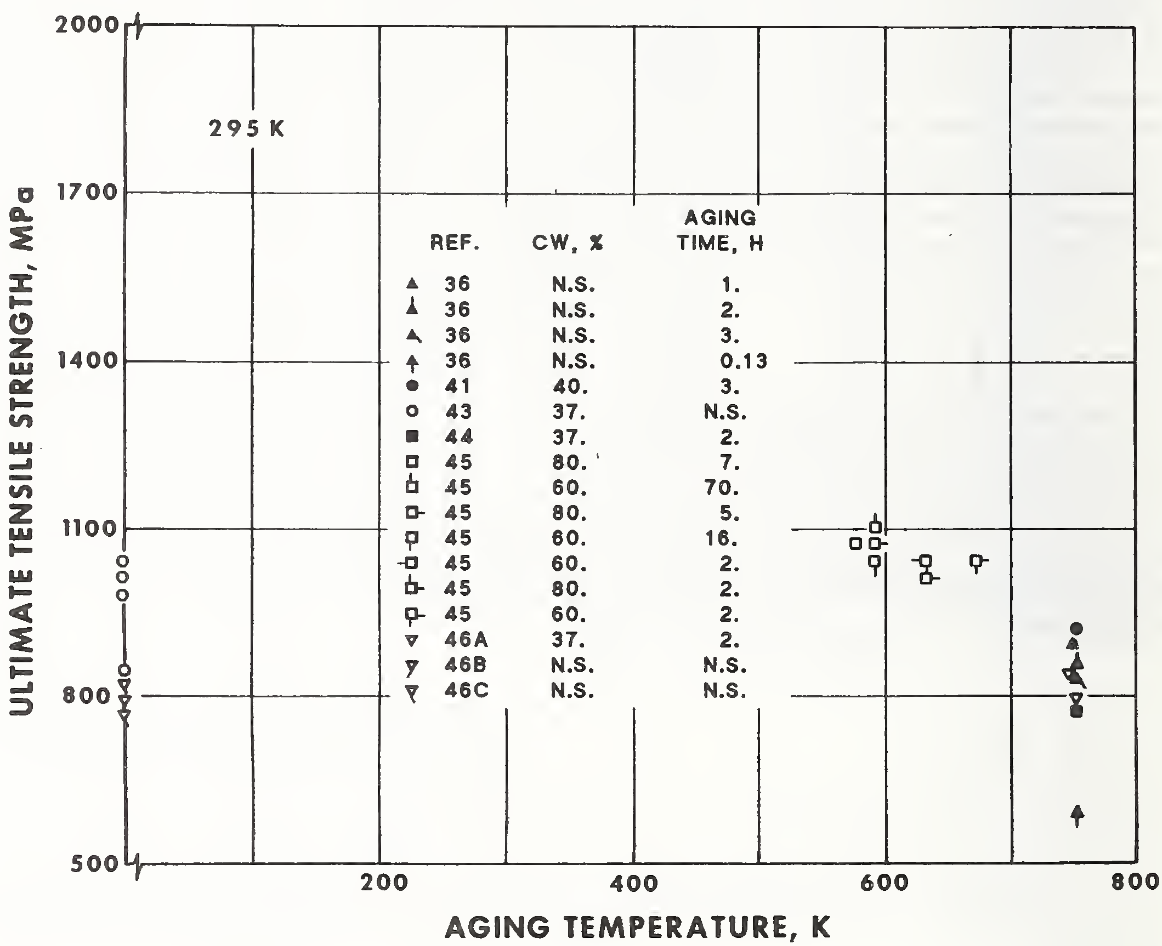

Figure 9.42. Tensile strength measurements on cold-worked C17510 beryllium copper at 295 K are shown as a function of aging temperature. If this parameter was not specified, tensile strength is plotted on the *y*-axis. For clarity, overlapping data points are omitted from the figure. All data are presented in Table 9.29. Products were in strip and plate form (not specified in References 9.36 and 9.41). (N.S. in legend for References 9.43 and 9.46 indicates not specified.)

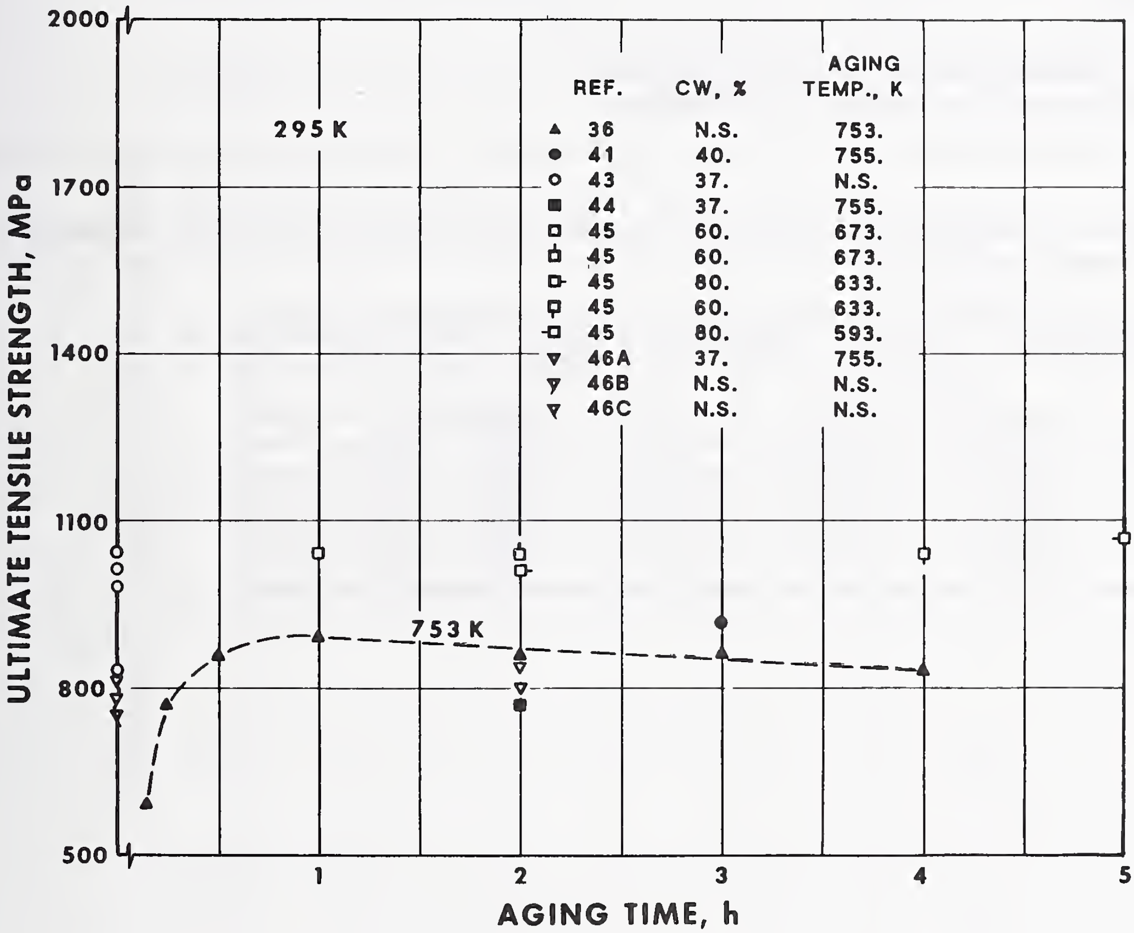

Figure 9.43. Tensile strength measurements on cold-worked C17510 beryllium copper at 295 K are shown as a function of aging time. If this parameter was not specified, tensile strength is plotted on the *y*-axis. Several data points from Reference 9.45 at long aging times do not appear in the figure. For clarity, overlapping data points are omitted from the figure. All data are presented in Table 9.29. Products were in strip and plate form (not specified in References 9.36 and 9.41). (N.S. in legend for References 9.43 and 9.46 indicates not specified.)

DATA SOURCES AND ANALYSIS

Measurements of the tensile strength of cold-worked and aged C17510 beryllium copper from 4 to 295 K were obtained from Reference 9.44. Product form was plate.

RESULTS

All measurements are reported in Table 9.30, which presents tensile strength, test temperature, percent of cold work (reduction in thickness), aging temperature and time, and the reference number. The available characterization of materials and measurements is given in Table 9.57 at the end of the tensile properties section. Figure 9.44 presents the tensile strength measurements as a function of test temperature.

Table 9.30. Tensile Strength Dependence of Cold-worked and Aged C17510 Beryllium Copper upon Temperature (4–295 K).

Tensile Strength, MPa	Test Temperature, K	Cold Work, %	Aging Temperature, K	Aging Time, h	Reference No.
783	295	37	755	2	44
888	76	37	755	2	44
972	4	37	755	2	44
777	295	37	755	2	44
890	76	37	755	2	44
937	4	37	755	2	44

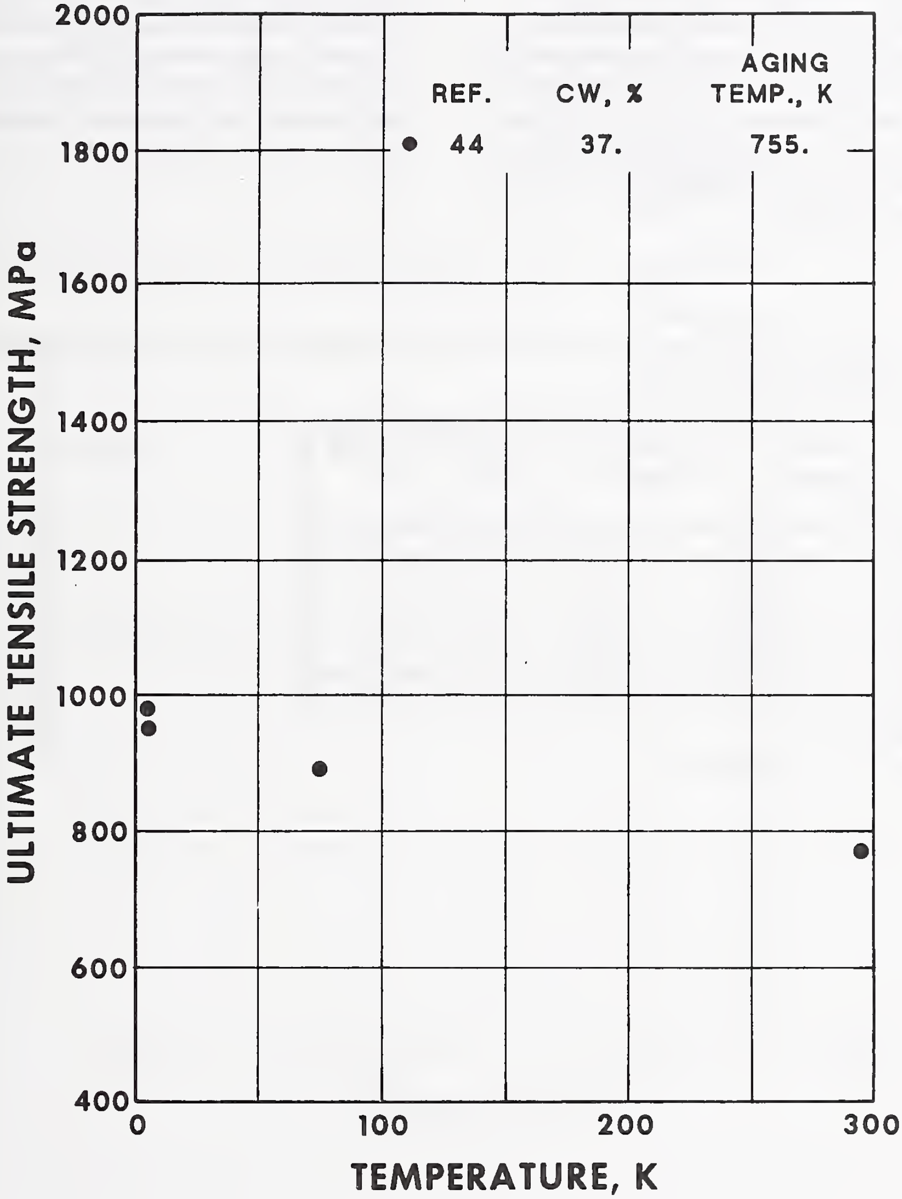

Figure 9.44. Tensile strength measurements of cold-worked and aged C17510 beryllium copper are shown as a function of test temperature. For clarity, overlapping data points are omitted from the figure. All data are presented in Table 9.30. Product was in plate form.

DATA SOURCES AND ANALYSIS

Measurements of the elongation of annealed and aged C17000 beryllium copper between 20 and 290 K were obtained from Reference 9.49. Measurements from References 9.2 and 9.50 on annealed material at 295 K only are presented for comparison. Products were in strip (Reference 9.2) and bar form (Reference 9.50), or not specified (Reference 9.49). Gage lengths were 25 cm (Reference 9.50), 5 cm (Reference 9.2) or not specified (Reference 9.49).

RESULTS

All measurements are reported in Table 9.31, which presents elongation, test temperature, aging temperature and time, and the reference number. The available characterization of materials and measurements is given in Table 9.57 at the end of the tensile properties section. Figure 9.45 presents the elongation measurements as a function of test temperature.

Table 9.31. Elongation Dependence of Annealed, and Annealed and Aged C17000 Beryllium Copper upon Temperature (20–295 K).

Elongation, %	Test Temperature, K	Aging Temperature, K	Aging Time, h	Reference No.
20.6	295	0	0	50
53.2	295	0	0	2
51.8	295	0	0	2
20	290	N.S.	N.S.	49
20	77	N.S.	N.S.	49
40	20	N.S.	N.S.	49

N.S. = not specified.
Aging Temperature, 0 K = not aged.

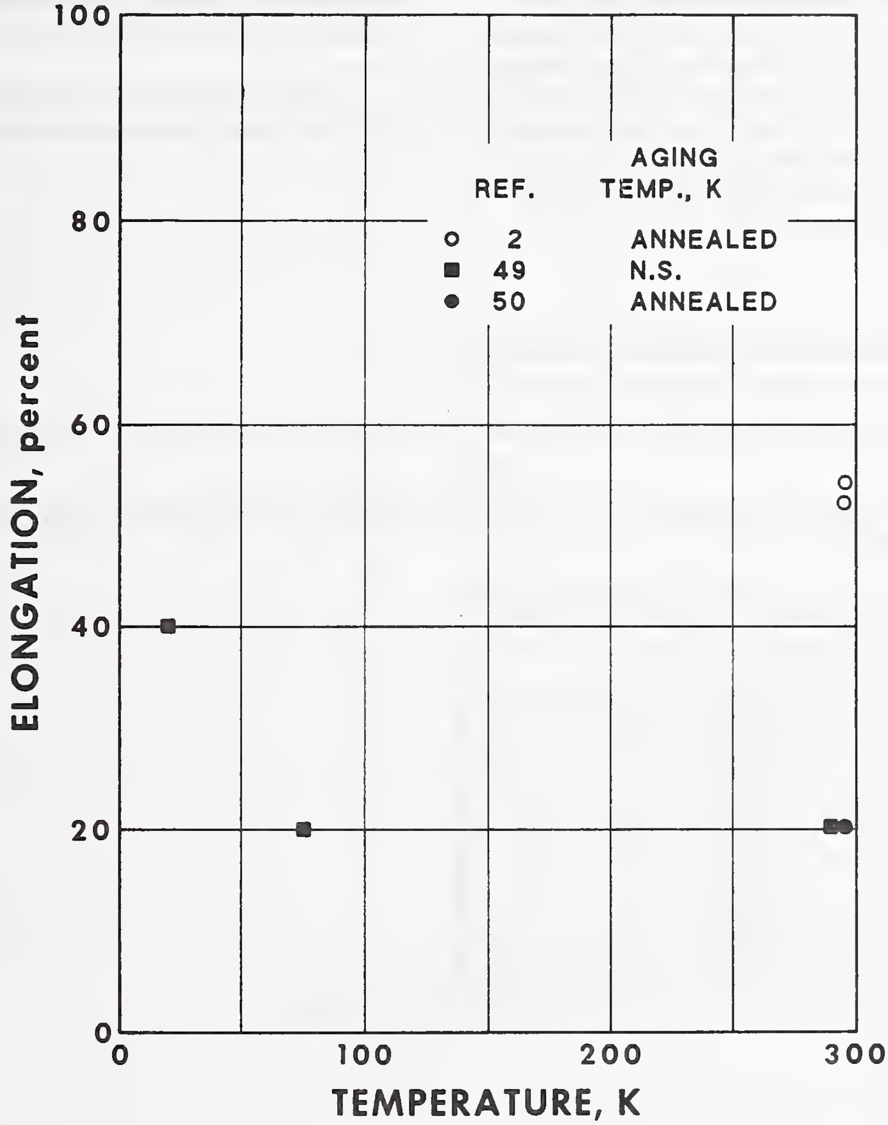

Figure 9.45. Elongation measurements of annealed, and annealed and aged C17000 beryllium copper are shown as a function of test temperature. For clarity, overlapping data points are omitted from the figure. All data are presented in Table 9.31. Products were in strip (Reference 9.2) and bar form (Reference 9.50), or not specified (Reference 9.49).

DATA SOURCES AND ANALYSIS

Measurements of the elongation of annealed C17000 beryllium copper at 295 K as a function of aging temperature and time were obtained from three sources (References 9.2, 9.3, and 9.49). Product was in strip form or was not specified (Reference 9.49). Reported aging temperatures ranged from 588 to 630 K; aging times from 2 to 3 h. Aging parameters were not specified in References 9.3 and 9.49, sometimes for proprietary reasons. Gage lengths were 5 cm (not specified in Reference 9.49).

RESULTS

All measurements are reported in Table 9.32, which presents elongation, aging temperature and time, and the reference number. The available characterization of materials and measurements is given in Table 9.57 at the end of the tensile properties section. Figures 9.46 and 9.47 present the elongation measurements as a function of aging temperature and time, respectively. Unspecified values of temperature and time are plotted on the *y*-axis.

Not enough data are available to determine optimum aging temperature and time.

Table 9.32. Elongation Dependence of Annealed C17000 Beryllium Copper on Aging Temperature and Time (295 K).

Elongation, %	Aging Temperature, K	Aging Time, h	Reference No.
17.8	N.S.	N.S.	3
13.4	602	3	2
10.0	6[illegible]	3	2
12.8	630	2	2
11.5	630	2	2
12.[illegible]	616	3	2
11.1	616	3	2
15.9	588	3	2
12.4	588	3	2
20.0	N.S.	N.S.	49

N.S. = not specified.

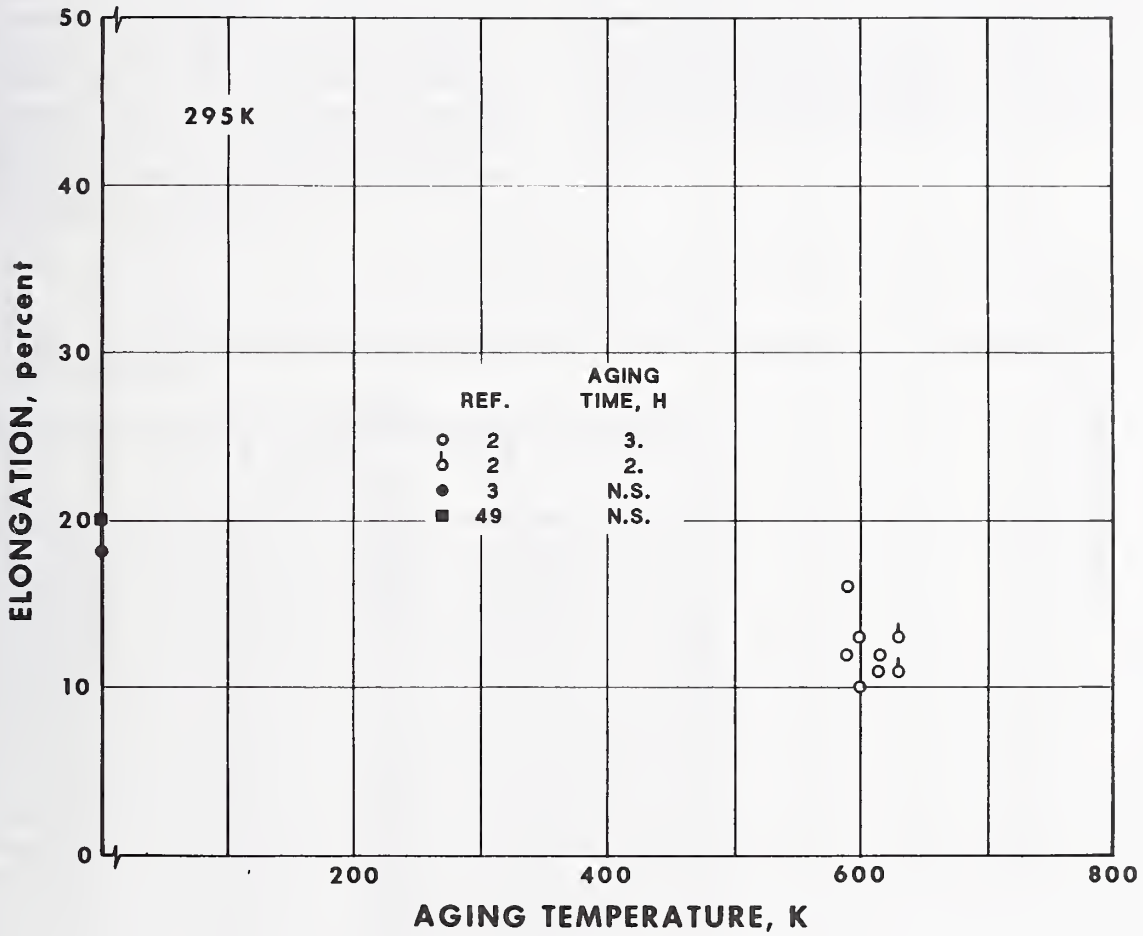

Figure 9.46. Elongation measurements on annealed C17000 beryllium copper at 295 K are shown as a function of aging temperature. If this parameter was not specified, elongation is plotted on the *y*-axis. All data are presented in Table 9.32. Product, where specified, was in strip form. (N.S. in legend for References 9.3 and 9.49 indicates not specified.)

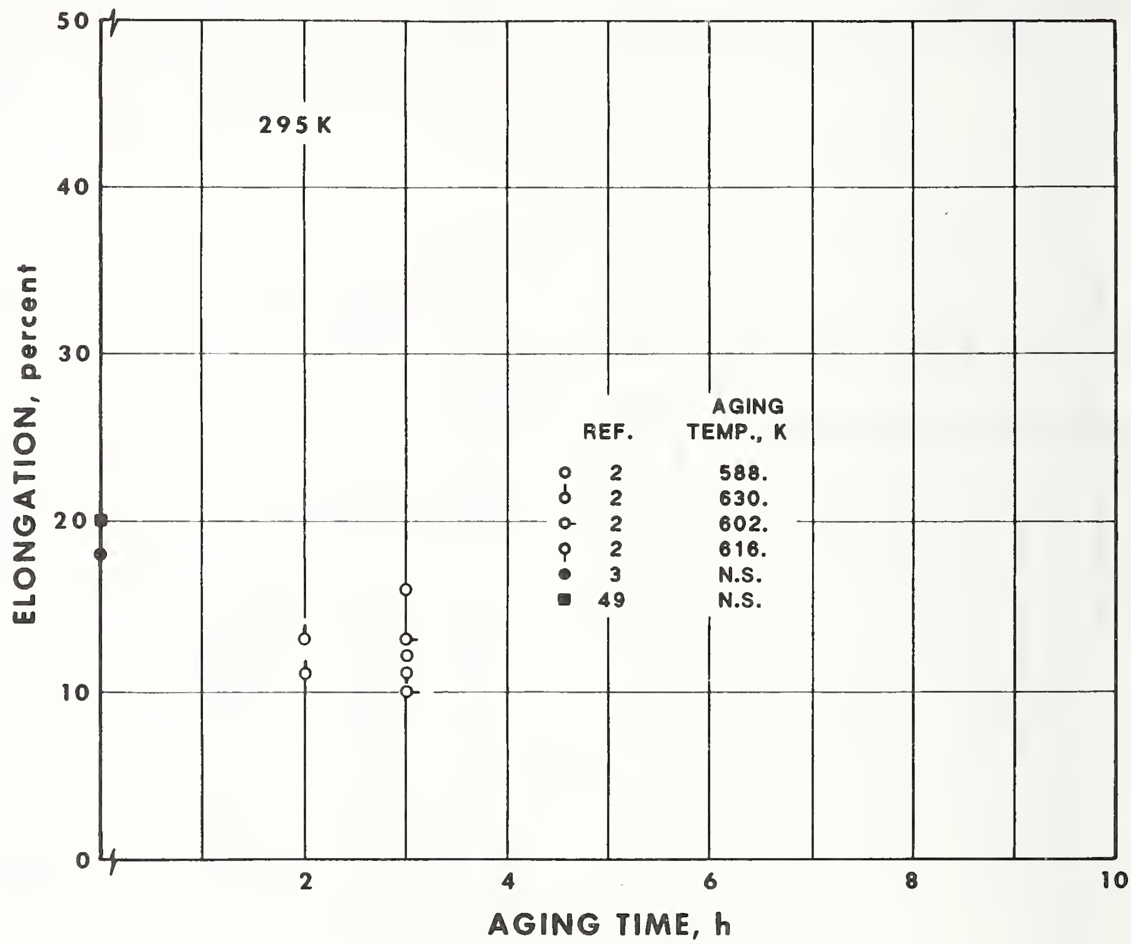

Figure 9.47. Elongation measurements on annealed C17000 beryllium copper at 295 K are shown as a function of aging time. If this parameter was not specified, elongation is plotted on the *y*-axis. All data are presented in Table 9.32. Product, where specified, was in strip form. (N.S. in legend for References 9.3 and 9.49 indicates not specified.)

C17000: Cold-worked and Aged

Tensile Elongation vs. Aging Temperature, Time (295 K)

DATA SOURCES AND ANALYSIS

Measurements of the elongation of cold-worked C17000 beryllium copper at 295 K as a function of aging temperature and time were obtained from three sources (References 9.2, 9.3, and 9.5). Product was in strip form. Cold work, *CW*, (carried out before aging) ranged from 11 to 50% (reduction in thickness). Reported aging temperatures ranged from 588 to 630 K; aging times from 2 to 3 h. For proprietary reasons, aging temperatures and times were not specified in Reference 9.5 (for one elongation measurement) and in Reference 9.3. Gage lengths were 2.5 cm (Reference 9.5) and 5 cm.

RESULTS

All measurements are reported in Table 9.33, which presents elongation, *CW* (reduction in thickness in percent), aging temperature and time, and the reference number. The available characterization of materials and measurements is given in Table 9.57 at the end of the tensile properties section. Figures 9.48 and 9.49 present the elongation measurements as a function of temperature and time, respectively. Unspecified values of temperature and time are plotted on the *y*-axis.

Table 9.33. Elongation Dependence of Cold-worked C17000 Beryllium Copper on Aging Temperature and Time (295 K).

Elongation, %	Cold Work, %	Aging Temperature, K	Aging Time, h	Reference No.
12.6	11	N.S.	N.S.	5
3.7	11	616	2.0	5
13.6	11	N.S.	N.S.	3
21.6	11	N.S.	N.S.	3
11.6	21	N.S.	N.S.	3
10.0	21	N.S.	N.S.	3
4.1	50	N.S.	N.S.	3
4.5	50	N.S.	N.S.	3
11.6	11	602	3.0	2
10.6	21	602	2.0	2
7.0	37	602	2.0	2
10.6	11	602	3.0	2
7.0	21	602	2.0	2
6.3	37	602	2.0	2
11.6	11	616	2.0	2
11.6	21	630	2.0	2
7.0	37	616	2.0	2
11.6	11	602	2.0	2
10.6	21	602	2.0	2
7.0	37	602	2.0	2
11.6	11	616	3.0	2
10.6	21	616	2.0	2
7.3	37	602	2.0	2
10.6	11	602	3.0	2
6.3	21	616	2.0	2
7.3	37	616	2.0	2
11.6	11	616	2.0	2
11.6	21	602	2.0	2
6.4	37	588	2.0	2
11.8	11	588	2.0	2
10.0	21	588	2.0	2
6.0	37	588	2.0	2

N.S. = not specified.

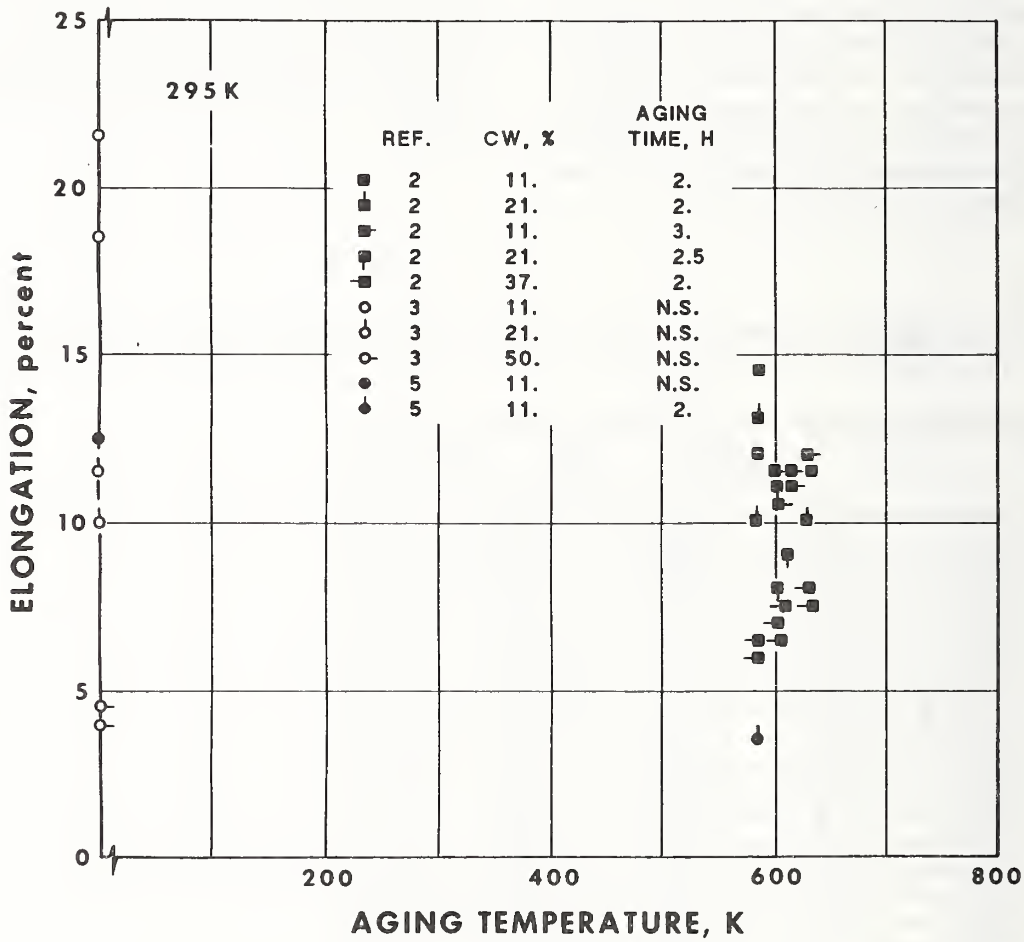

Figure 9.48. Elongation measurements on cold-worked C17000 beryllium copper at 295 K are shown as a function of aging temperature. If this parameter was not specified, elongation is plotted on the *y*-axis. For clarity, overlapping data points are omitted from the figure. All data are presented in Table 9.33. Product was in strip form. (N.S. in legend for Reference 9.3 indicates not specified.)

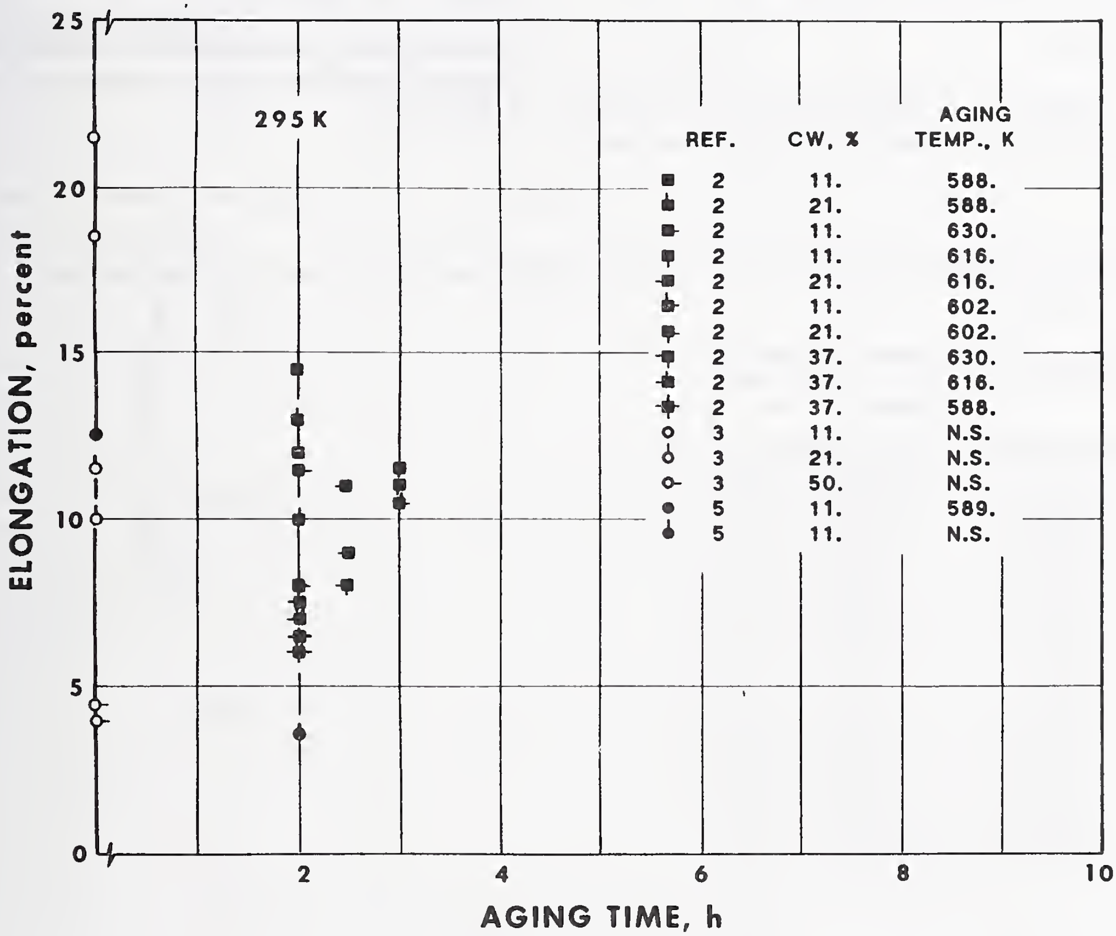

Figure 9.49. Elongation measurements on cold-worked C17000 beryllium copper at 295 K are shown as a function of aging time. If this parameter was not specified, elongation is plotted on the *y*-axis. For clarity, overlapping data points are omitted from the figure. All data are presented in Table 9.33. Product was in strip form. (N.S. in legend for Reference 9.3 indicates not specified.)

C17200: Annealed

Tensile Elongation vs. Temperature (20–300 K)

DATA SOURCES AND ANALYSIS

Measurements of the elongation of annealed C17200 beryllium copper between 20 and 300 K were obtained from three sources (References 9.6, 9.7, and 9.9). Product was in bar form. Gage lengths were 2, 3.2, and 5 cm for References 9.6, 9.7, and 9.9, respectively.

RESULTS

All measurements are reported in Table 9.34, which presents elongation, test temperature, and the reference number. The available characterization of materials and measurements is given in Table 9.57 at the end of the tensile properties section. Figure 9.50 presents the elongation measurements as a function of test temperature.

Reference 9.10 presents measurements from 93 to 293 K on the elongation of a 2.6-wt% beryllium-copper alloy in an annealed condition. These data exhibit an increase in elongation as the temperature decreases that is similar to the trend shown by the data from Reference 9.7 in Figure 9.50.

Table 9.34. Elongation Dependence of Annealed C17200 Beryllium Copper upon Temperature (20–300 K).

Elongation, %	Test Temperature, K	Reference No.
51.8	300	6
55.0	214	6
51.8	144	6
55.0	76	6
62.4	295	7
62.9	295	7
68.9	195	7
69.0	195	7
72.8	76	7
66.7	76	7
68.9	20	7
68.1	76	7
46.5	295	9
46.5	232	9

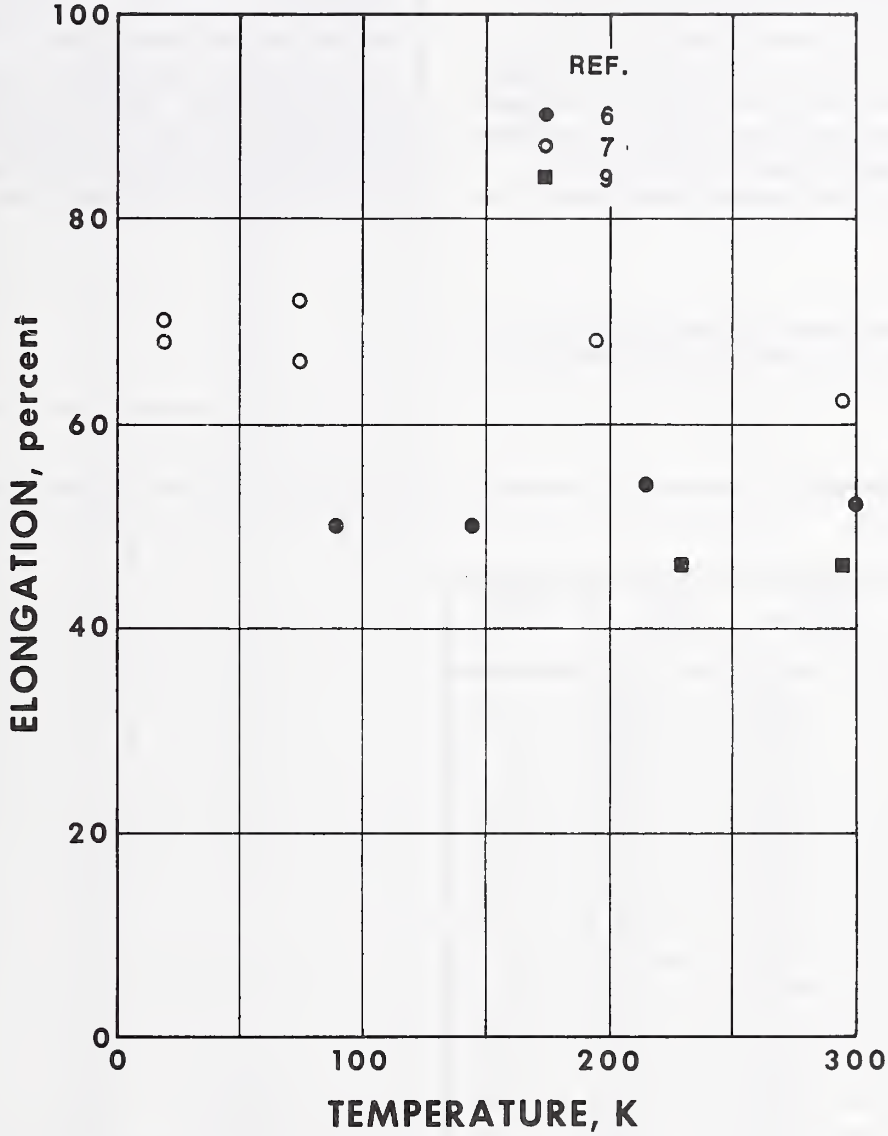

Figure 9.50. Elongation measurements of annealed C17200 beryllium copper are shown as a function of test temperature. For clarity, overlapping data points are omitted from the figure. All data are presented in Table 9.34. Product was in bar form.

DATA SOURCES AND ANALYSIS

Measurements of the elongation of cold-worked C17200 beryllium copper at 295 K as a function of aging temperature and time were obtained from 15 sources (References 9.2, 9.3, 9.6, 9.11–9.15, 9.18–9.21, 9.51, 9.52, and 9.54). Products were in wire, sheet, strip, bar, and plate form. Reported aging temperatures ranged from 293 to 763 K; aging times from 0.067 to 5 h. Gage lengths, where specified, were 2 and 5 cm.

RESULTS

All measurements are reported in Table 9.35, which presents elongation, aging temperature and time, and the reference number. The available characterization of materials and measurements is given in Table 9.57 at the end of the tensile properties section. Figures 9.51 and 9.52 present the elongation measurements as a function of temperature and time, respectively.

As expected, elongation correlates inversely with yield strength. Thus, minima of elongation vs. temperature and time in Figures 9.51 and 9.52 (References 9.14, 9.15 and 9.51) correspond to maxima in yield strength in Figures 9.7 and 9.8.

Table 9.35. Elongation Dependence of Annealed C17200 Beryllium Copper on Aging Temperature and Time (295 K).

Elongation, %	Aging Temperature, K	Aging Time, h	Reference No.
4.5	588	3.000	11
4.5	588	3.000	11
26.5	622	0.067	51
16.0	622	0.170	51
10.0	622	0.250	51
7.0	622	0.330	51
5.5	622	0.420	51
5.0	622	0.500	51
5.5	622	0.580	51
6.0	622	0.670	51
6.5	622	0.750	51
7.0	622	0.830	51
7.8	622	0.920	51
8.8	622	1.000	51
9.7	622	1.100	51
9.0	672	1.500	6
6.2	588	3.000	6
10.0	588	3.000	12
9.0	588	3.000	12
2.5	588	3.000	13
2.5	588	3.000	13
2.5	588	3.000	13
2.5	588	3.000	13
2.5	588	3.000	13
2.0	588	3.000	13
2.0	588	3.000	13
16.7	566	0.330	14
12.7	566	0.670	14
15.0	566	0.500	14

Table 9.35, continued

Elongation, %	Aging Temperature, K	Aging Time, h	Reference No.
10.8	588	0.830	14
10.8	566	1.000	14
5.9	588	1.500	14
8.8	588	2.000	14
5.0	588	3.000	15
50.0	293	1.000	15
50.0	373	1.000	15
32.0	423	1.000	15
22.0	473	1.000	15
43.0	588	1.000	15
10.0	573	1.000	15
7.0	622	1.000	15
10.0	763	1.000	15
43.0	588	0.800	15
5.0	633	5.000	15
7.9	588	3.000	52
7.6	575	3.000	52
10.8	588	3.000	52
7.6	588	3.000	52
7.0	588	3.000	14
3.5	630	0.500	15
7.0	644	0.500	15
7.6	588	2.000	3
7.0	588	2.000	3
4.3	588	3.000	20
43.0	588	2.000	21
5.0	588	2.000	54
8.8	588	3.000	2
5.2	588	3.000	2
8.9	588	3.000	2
5.8	616	3.000	2
4.3	630	3.000	2
5.0	616	3.000	2
8.8	630	2.000	2
7.6	630	2.000	2
7.0	580	2.000	2
5.6	602	3.000	2
3.8	602	3.000	2
5.0	602	3.000	2

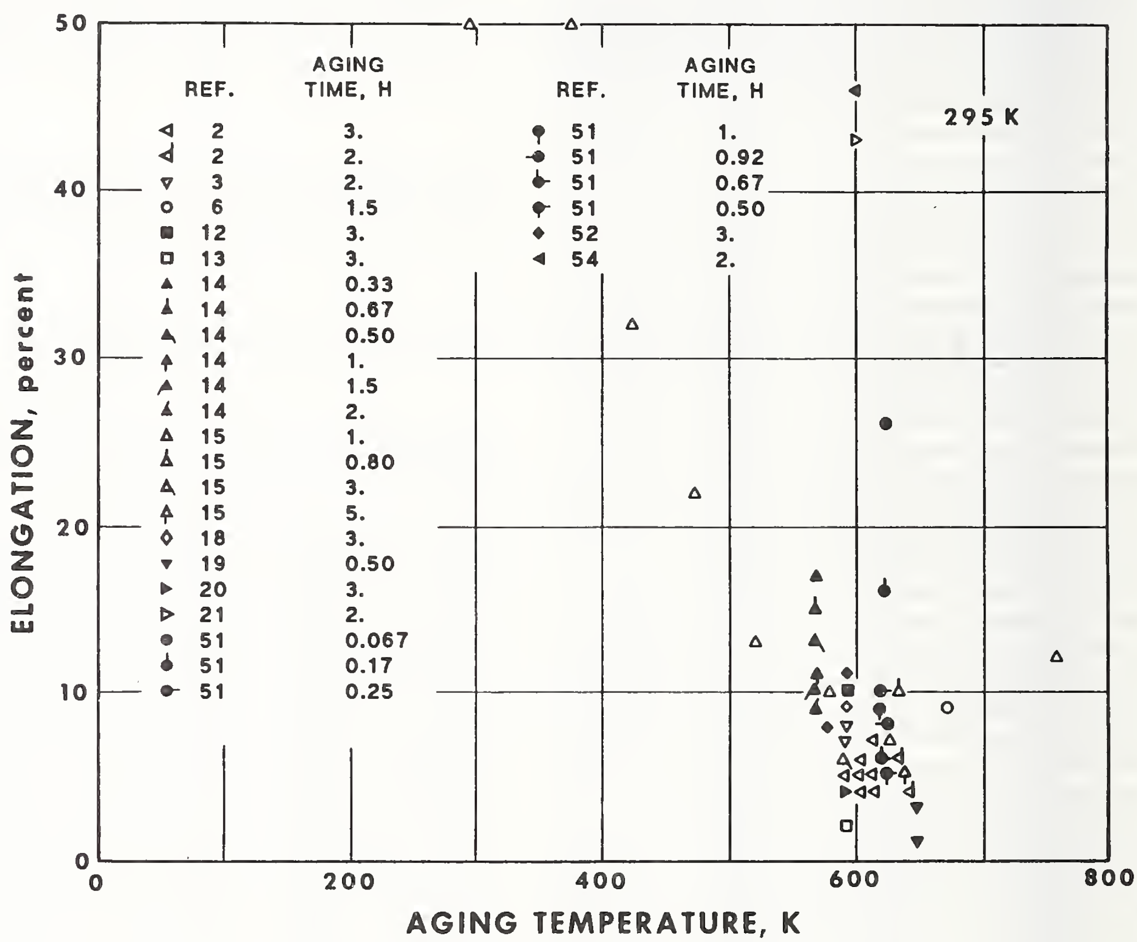

Figure 9.51. Elongation measurements on annealed C17200 beryllium copper at 295 K are shown as a function of aging temperature. For clarity, overlapping data points are omitted from the figure, including all points from Reference 9.11. All data are presented in Table 9.35. Products were in wire, sheet, strip, bar, and plate form.

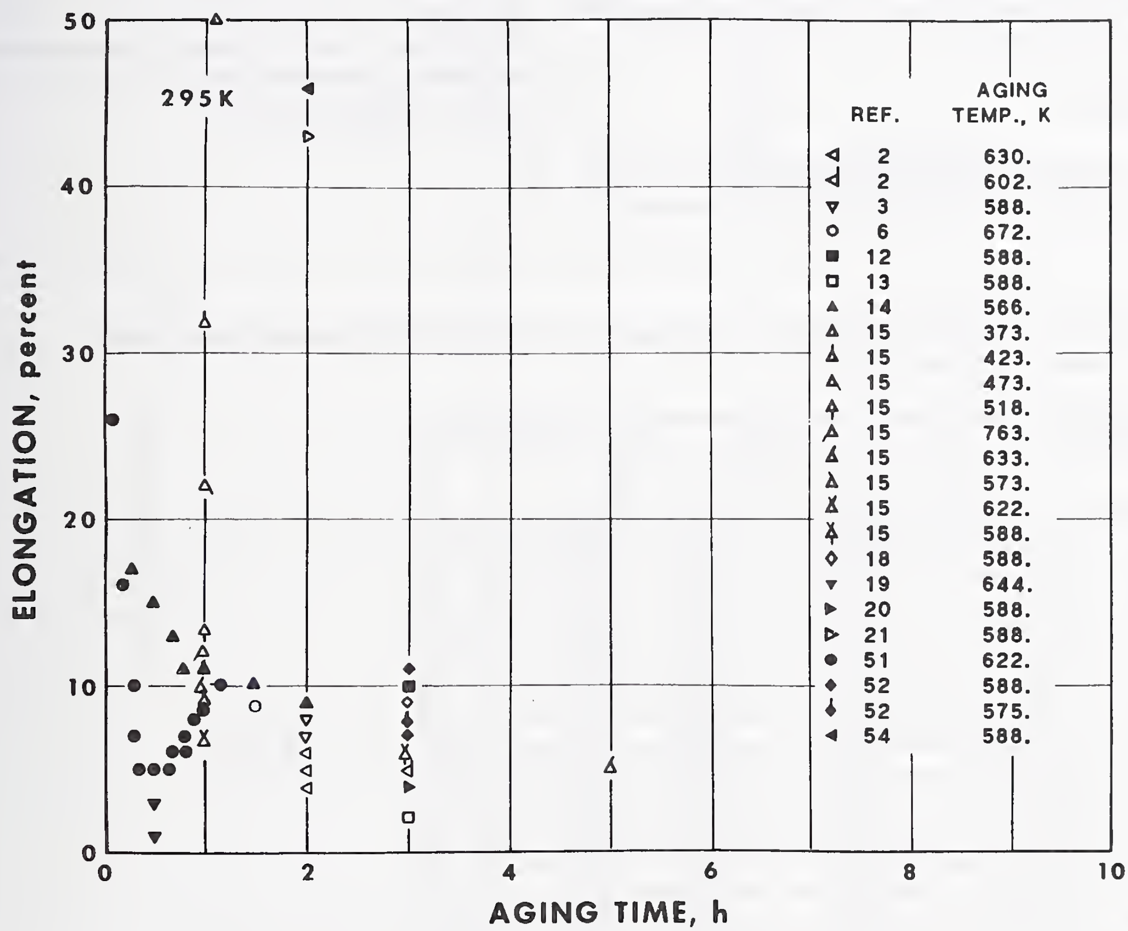

Figure 9.52. Elongation measurements on annealed C17200 beryllium copper at 295 K are shown as a function of aging time. For clarity, overlapping data points are omitted from the figure, including all points from Reference 9.11. All data are presented in Table 9.35. Products were in wire, sheet, strip, bar, and plate form.

DATA SOURCES AND ANALYSIS

Measurements of the elongation of annealed and aged C17200 beryllium copper between 20 and 300 K were obtained from four sources (References 9.6, 9.11, 9.12, and 9.19). Products were in sheet and bar form (not specified in Reference 9.12). Gage lengths were 2 cm (References 9.6 and 9.12), 5 cm (Reference 9.19) or not specified (Reference 9.11).

RESULTS

All measurements are reported in Table 9.36, which presents the elongation, the test temperature, the aging temperature and time, and the reference number. The available characterization of materials and measurements is given in Table 9.57 at the end of the tensile properties section. Figure 9.53 presents the elongation measurements as a function of test temperature.

Reference 9.10 presents measurements from 93 to 293 K on the elongation of a 2.6-wt% beryllium-copper alloy in an aged condition. These data exhibit a slight increase in elongation as the temperature decreases that is similar to the trend shown in Figure 9.53.

Table 9.36. Elongation Dependence of Annealed and Aged C17200 Beryllium Copper upon Temperature (20–300 K).

Elongation, %	Test Temperature, K	Aging Temperature, K	Aging Time, h	Reference No.
8.6	299	588	3.0	11
9.6	299	588	3.0	11
8.6	20	588	3.0	11
12.0	80	588	3.0	11
8.6	20	588	3.0	11
6.2	300	588	3.0	6
8.6	214	588	3.0	6
9.6	88	588	3.0	6
8.6	20	588	3.0	6
15.5	88	672	1.5	6
10.8	197	672	1.5	6
12.0	214	672	1.5	6
8.6	300	672	3.0	6
9.6	299	588	3.0	12
10.0	299	588	3.0	12
9.6	197	588	3.0	12
8.6	197	588	3.0	12
12.0	77	588	3.0	12
16.0	77	588	3.0	12
3.5	300	644	0.5	19
5.0	200	644	0.5	19
1.3	300	644	0.5	19
2.8	200	644	0.5	19

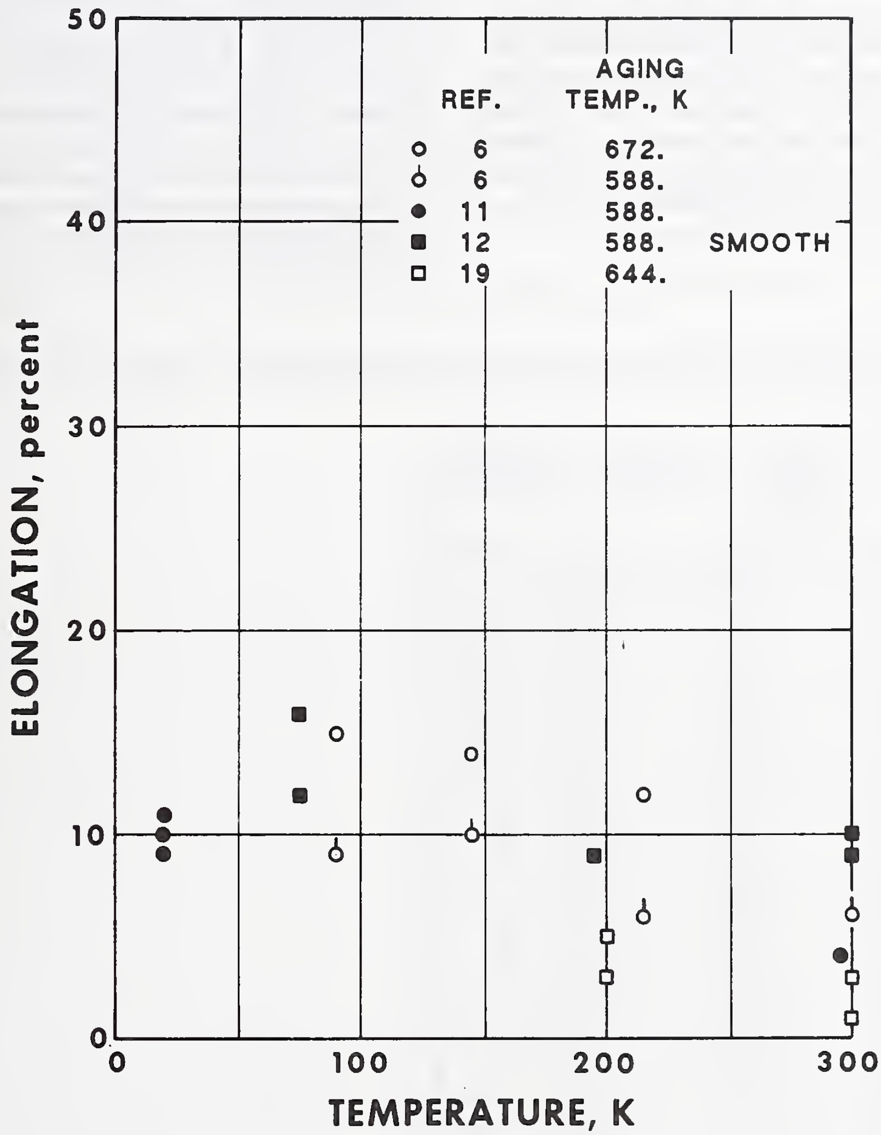

Figure 9.53. Elongation measurements of annealed and aged C17200 beryllium copper are shown as a function of test temperature. For clarity, overlapping data points are omitted from the figure. All data are presented in Table 9.36. Products were in sheet and bar form (not specified in Reference 9.12).

C17200: Cold-worked

Tensile Elongation vs. Temperature (20–300 K)

DATA SOURCES AND ANALYSIS

Measurements of the elongation of cold-worked C17200 beryllium copper between 20 and 300 K were obtained from five sources (References 9.6, 9.7, 9.9, 9.25, and 9.26). Data from Reference 9.27 at 295 K only are presented for comparison because measurements were made for varying amounts of cold work, *CW*. Products were in sheet, strip, and bar form (not specified in Reference 9.26). Gage lengths were 2 cm (References 9.6 and 9.26), 3.2 cm (Reference 9.7) or 5 cm (References 9.9, 9.26, and 9.27).

RESULTS

All measurements are reported in Table 9.37, which presents elongation, test temperature, *CW* (reduction in thickness or area in percent), and the reference number. (The percent of *CW* could not be determined from Reference 9.26: it was 21% if the material was rolled or 37% if it was drawn.) The available characterization of materials and measurements is given in Table 9.57 at the end of the tensile properties section. Figure 9.54 presents the elongation measurements as a function of test temperature.

Table 9.37. Elongation Dependence of Cold-worked C17200 Beryllium Copper upon Temperature (20–300 K).

Elongation, %	Test Temperature, K	Cold Work, %	Reference No.
20.0	88	33	6
22.0	144	33	6
18.0	300	33	6
39.0	20	21	25
12.0	20	21	26
44.0	20	21	25
18.0	20	21	26
46.0	20	21	25
31.0	76	21	26
46.0	76	21	26
18.0	76	21	25
14.0	195	21	26
21.0	195	21	26
19.6	300	21	25
18.0	300	21	26
19.6	295	37	7
18.8	295	37	7
23.7	195	37	7
22.1	195	37	7
31.5	76	37	7
30.5	76	37	7
31.4	20	37	7
31.0	20	37	7
19.6	300	N.S.	25
12.0	300	N.S.	26
12.0	300	N.S.	26
18.0	300	N.S.	26
22.0	77	N.S.	26
18.0	77	N.S.	26
21.0	77	N.S.	26
21.0	77	N.S.	26
26.0	20	N.S.	26

Table 9.37, continued

Elongation, %	Test Temperature, K	Cold Work, %	Reference No.
21.0	20	N.S.	26
20.0	20	N.S.	26
19.0	20	N.S.	26
20.0	20	N.S.	26
19.0	295	60	9
11.5	232	60	9
23.0	295	11	27
14.0	295	21	27
6.0	295	37	27

N.S. = not specified.

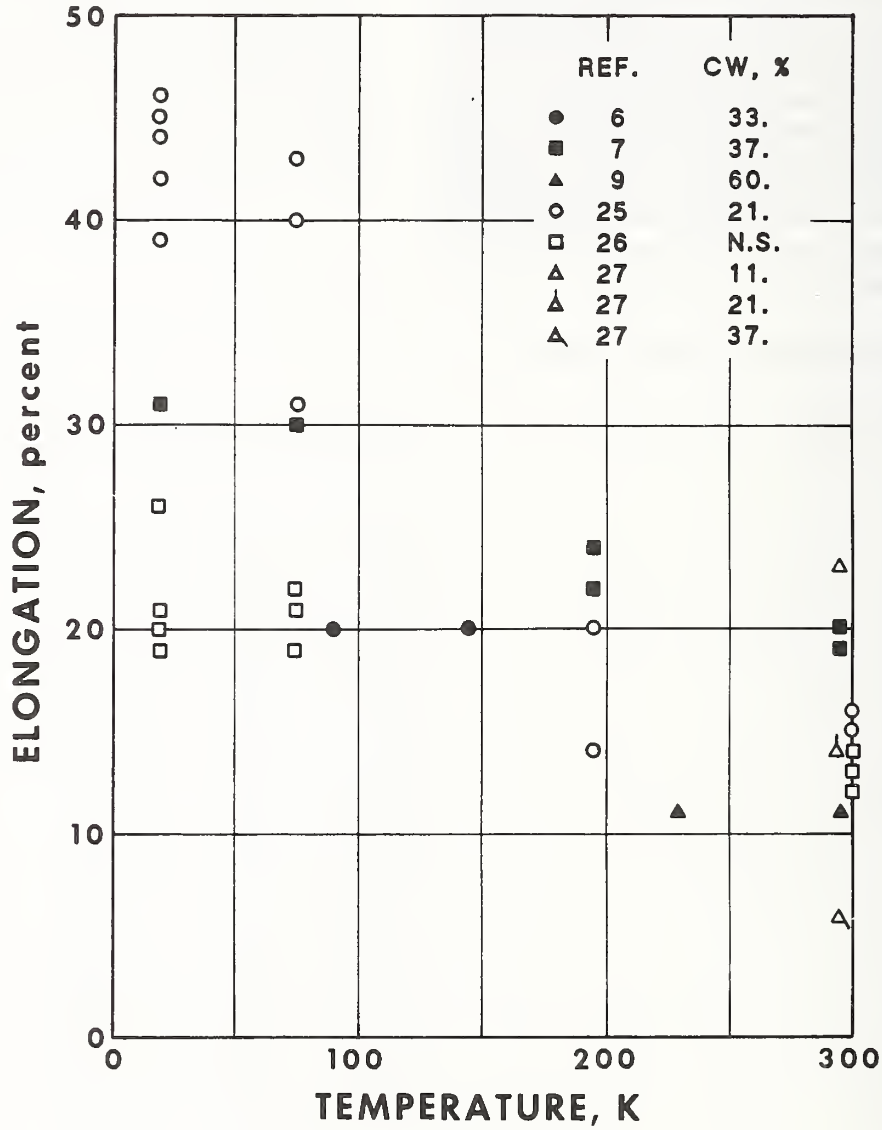

Figure 9.54. Elongation measurements of cold-worked C17200 beryllium copper are shown as a function of test temperature. For clarity, overlapping data points are omitted from the figure. All data are presented in Table 9.37. Products were in sheet, strip, and bar form (not specified in Reference 9.26).

DATA SOURCES AND ANALYSIS

Measurements of the elongation of cold-worked C17200 beryllium copper at 295 K as a function of aging temperature and time were obtained from 18 sources (References 9.2, 9.3, 9.5, 9.6, 9.9, 9.13–9.15, 9.18, 9.19, 9.21, 9.29, 9.31, 9.32, 9.52, 9.55, 9.57, and 9.58). Products were in wire, sheet, strip, bar, and plate form. Cold work, *CW*, ranged from 11 to 97% (reduction in thickness or area). *CW* was carried out before aging, except in the measurements reported in Reference 9.55. Reported aging temperatures ranged from 297 to 748 K; aging times from 0.25 to 5 h. For proprietary reasons, some elongation data were reported in References 9.3 and 9.5 without specifying aging temperatures and times. Gage lengths, where specified, ranged from 2 to 5 cm except for Reference 9.32 (25 cm).

RESULTS

All measurements are reported in Table 9.38, which presents elongation, *CW* (reduction in thickness or area in percent), aging temperature and time, and the reference number. The available characterization of materials and measurements is given in Table 9.57 at the end of the tensile properties section. Figures 9.55 and 9.56 present the elongation measurements as a function of aging temperature and time, respectively. Unspecified values of temperature or time are plotted on the *y*-axis.

As expected, elongation correlates inversely with yield strength. Thus, minima of elongation vs. temperature and time in Figures 9.55 and 9.56 (References 9.14 and 9.15) correspond to maxima of yield strength in Figures 9.11 and 9.12. [Elongation values reported in Reference 9.29 are uniformly low due to the high level of *CW* (97%).]

Table 9.38. Elongation Dependence of Cold-worked C17200 Beryllium Copper on Aging Temperature and Time (295 K).

Elongation, %	Cold Work, %	Aging Temperature, K	Aging Time, h	Reference No.
3.5	50	575	7.00	55
1.0	75	588	7.00	55
1.0	97	575	7.00	55
1.0	33	588	2.00	6
1.2	97	297	2.00	29
1.0	97	525	2.00	29
1.0	97	544	2.00	29
1.0	97	588	2.00	29
1.0	97	588	2.00	29
2.4	97	619	2.00	29
0.5	97	647	2.00	29
1.0	97	297	2.00	29
0.5	97	452	2.00	29
1.0	97	619	2.00	29
0.1	97	647	2.00	29
3.7	33	588	2.00	31
3.0	35	588	2.00	31
2.0	44	588	2.00	31
5.0	37	588	3.00	13
14.0	15	566	0.33	14
8.0	15	566	0.50	14
6.0	15	566	0.67	14
6.0	15	566	0.83	14
6.0	15	566	1.00	14

Table 9.38, continued

Elongation, %	Cold Work, %	Aging Temperature, K	Aging Time, h	Reference No.
1.0	15	566	1.50	14
4.5	15	566	2.00	14
3.0	11	588	3.00	15
2.0	34	588	3.00	15
5.0	21	293	1.00	15
9.0	21	423	3.00	15
4.6	21	573	1.00	15
13.0	21	748	3.00	15
2.0	37	633	0.25	15
2.5	37	633	0.67	15
5.0	37	633	5.00	15
2.0	37	594	3.00	32
1.0	37	588	3.00	32
1.9	34	588	3.00	32
1.0	37	588	3.00	32
5.0	34	594	3.00	32
2.5	37	594	3.00	32
1.9	21	638	2.00	52
1.0	21	575	2.00	52
1.9	34	588	2.00	52
4.6	37	575	2.00	52
6.7	21	588	1.50	57
6.0	37	633	2.00	52
2.8	21	588	2.00	18
2.8	37	644	0.33	15
3.0	34	644	0.33	15
2.0	11	588	2.00	5
1.9	21	588	2.00	5
2.0	37	588	2.00	5
16.1	11	N.S.	N.S.	5
12.8	21	N.S.	N.S.	5
3.0	60	588	2.00	5
5.9	11	588	2.00	3
4.7	11	588	2.00	3
2.3	21	588	2.00	3
2.0	21	588	2.00	3
2.0	37	588	2.00	3
1.9	34	588	2.00	3
12.8	37	N.S.	N.S.	3
11.7	34	N.S.	N.S.	3
6.0	11	588	2.00	21
2.0	34	588	2.00	21
2.0	50	588	2.00	21
6.5	11	630	2.00	2
6.0	21	580	2.00	2
6.5	37	580	2.00	2
3.8	11	594	2.00	2
4.5	21	580	2.00	2
4.0	37	630	2.00	2
5.0	11	630	2.00	2
4.3	21	630	2.00	2

Table 9.38, continued

Elongation, %	Cold Work, %	Aging Temperature, K	Aging Time, h	Reference No.
3.8	37	602	2.00	2
6.3	11	616	2.00	2
5.0	21	616	2.00	2
3.4	37	616	2.00	2
4.0	11	616	2.00	2
3.4	21	616	2.00	2
3.3	37	616	2.00	2
4.6	11	616	2.00	2
3.8	21	616	2.00	2
3.3	37	616	2.00	2
5.0	11	602	3.00	2
4.6	21	602	2.00	2
3.8	37	602	2.00	2
4.6	11	602	3.00	2
3.5	21	602	2.00	2
2.8	37	602	2.00	2
4.8	11	602	3.00	2
3.4	21	602	2.00	2
2.8	37	602	2.00	2
6.8	11	588	2.00	2
4.8	21	588	2.00	2
3.4	37	616	2.00	2
4.8	11	588	2.00	2
3.4	21	682	2.00	2
2.5	37	588	2.00	2
4.9	11	588	2.00	2
3.2	21	588	2.00	2
2.5	37	588	2.00	2

N.S. = not specified.

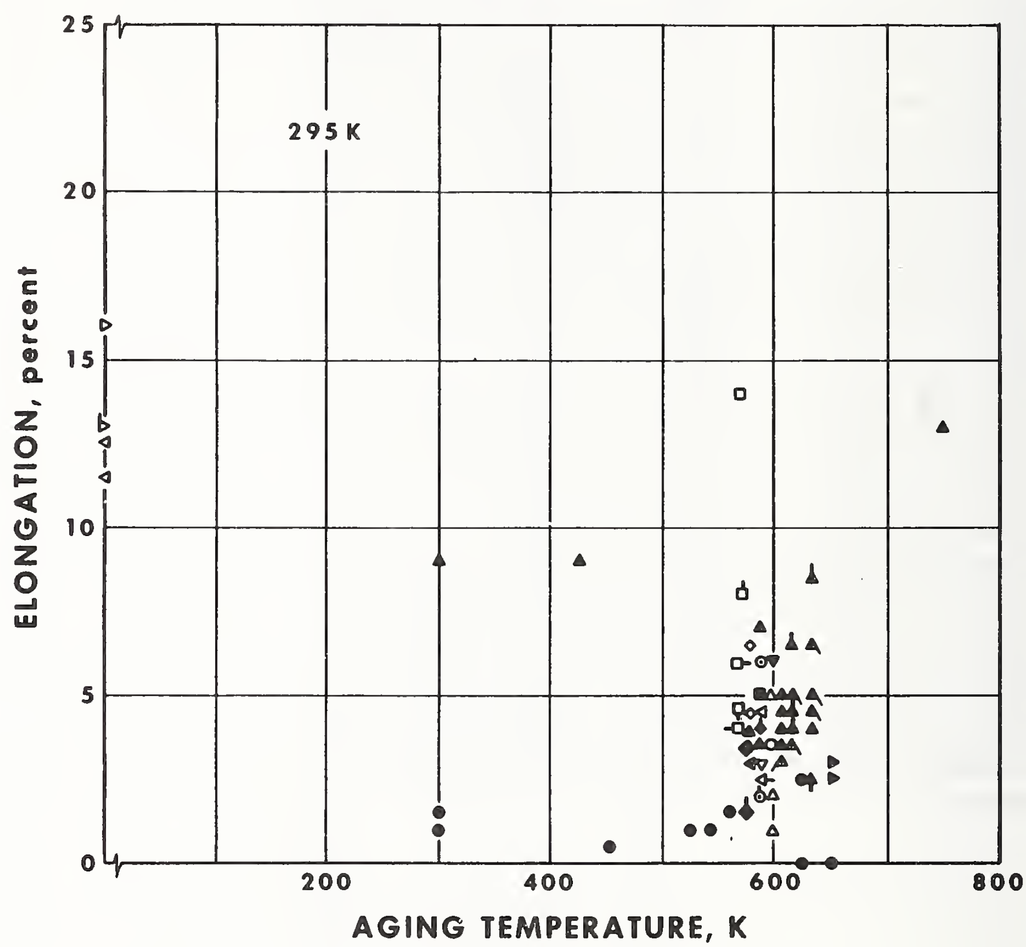

Figure 9.55. Elongation measurements on cold-worked C17200 beryllium copper at 295 K are shown as a function of aging temperature. If this parameter was not specified, elongation is plotted on the *y*-axis. For clarity, overlapping data points are omitted from the figure, including all points from References 9.6 and 9.55. All data are presented in Table 9.38. The legend for this graph is given on the next page. Products were in wire, sheet, strip, bar, and plate form. (N.S. in legend for References 9.3 and 9.5 indicates not specified.) The values from Reference 9.29 for room-temperature (297-K) aging are presented for comparison with values for higher aging temperatures.

REF.	CW, %	AGING TIME, H
2	11.	2.
2	11.	2.5
2	21.	2.
2	11.	3.
2	37.	2.
2	21.	2.5
3	37.	N.S.
3	11.	2.
3	21.	2.
5	11.	N.S.
5	21.	N.S.
9	60.	2.
13	37.	3.
14	15.	0.33
14	15.	0.50
14	15.	1.
14	15.	2.
14	15.	1.5
15	21.	1.
15	34.	0.25
15	34.	5.
15	34.	0.67
18	21.	2.
19	37.	0.33
21	18.	2.
21	50.	2.
29	97.	2.
31	37.	2.
32	37.	3.
52	37.	2.
52	21.	2.
55	50.	7.
55	90.	7.
57	21.	1.5
58	30.	2.

Figure 9.55, continued. Legend for preceding graph.

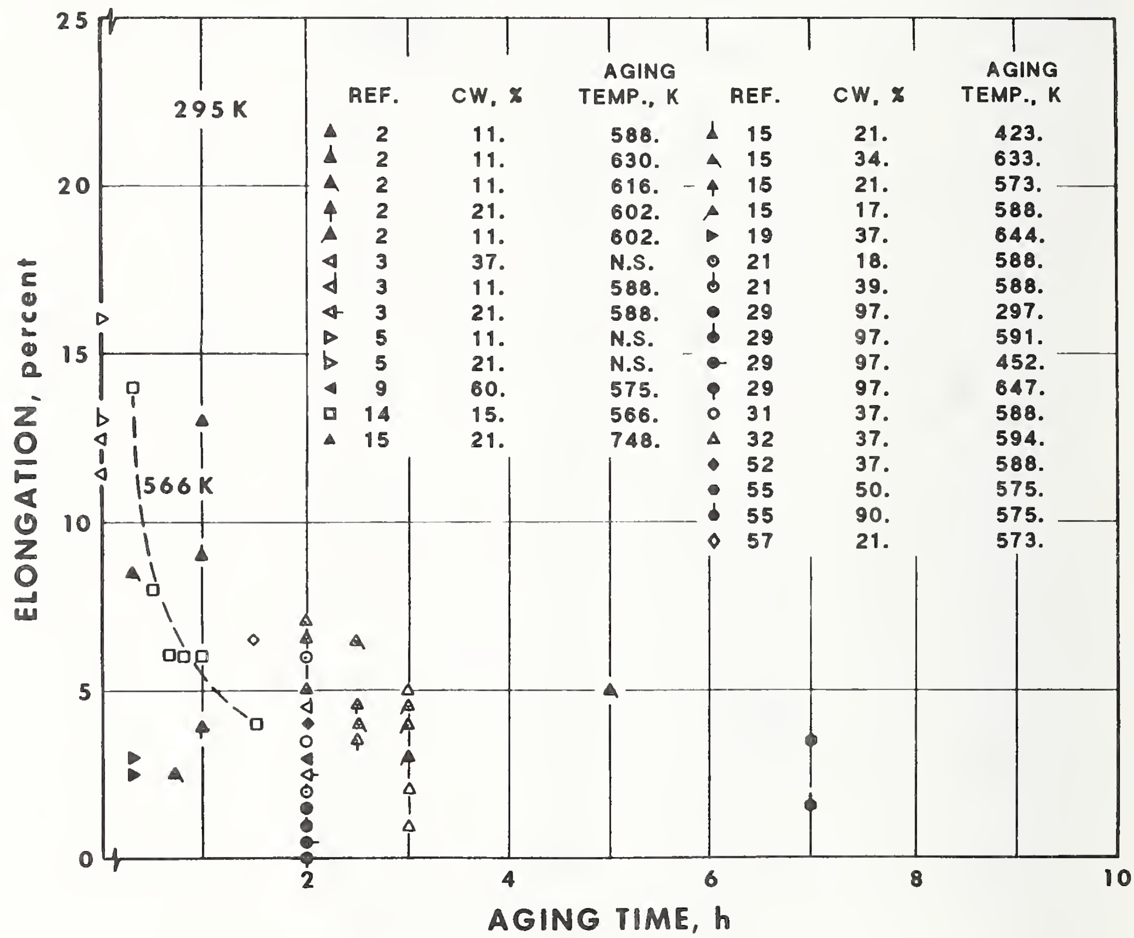

Figure 9.56. Elongation measurements on cold-worked C17200 beryllium copper at 295 K are shown as a function of aging time. If this parameter was not specified, elongation is plotted on the *y*-axis. For clarity, overlapping data points are omitted from the figure, including all points from References 9.6, 9.18, and 9.58. All data are presented in Table 9.38. Products were in wire, sheet, strip, bar, and plate form. (N.S. in legend for References 9.3 and 9.5 indicates not specified.) The values from Reference 9.29 for room-temperature (297-K) aging are presented for comparison with values for higher aging temperatures.

DATA SOURCES AND ANALYSIS

Measurements of the elongation of cold-worked and aged C17200 beryllium copper between 48 and 300 K were obtained from four sources (References 9.6, 9.9, 9.19, and 9.51). Products were in sheet and bar form (not specified in Reference 9.51). Gage lengths were 2 cm (Reference 9.6), 5 cm (References 9.9 and 9.19), or not specified (Reference 9.51).

RESULTS

All measurements are reported in Table 9.39, which presents elongation, test temperature, percent of cold work (reduction in thickness or area), aging temperature and time, and the reference number. The available characterization of materials and measurements is given in Table 9.57 at the end of the tensile properties section. Figure 9.57 presents the elongation measurements as a function of test temperature.

Table 9.39. Elongation Dependence of Cold-worked and Aged C17200 Beryllium Copper upon Temperature (48–300 K).

Elongation, %	Test Temperature, K	Cold Work, %	Aging Temperature, K	Aging Time, h	Reference No.
2.68	48	N.S.	N.S.	N.S.	51
2.[illegible]0	73	N.S.	N.S.	N.S.	51
2.40	98	N.S.	N.S.	N.S.	51
2.25	123	N.S.	N.S.	N.S.	51
2.20	98	N.S.	N.S.	N.S.	51
2.[illegible]0	173	N.S.	N.S.	N.S.	51
2.10	198	N.S.	N.S.	N.S.	51
2.00	223	N.S.	N.S.	N.S.	51
2.60	98	N.S.	N.S.	N.S.	51
2.00	273	N.S.	N.S.	N.S.	51
2.00	293	N.S.	N.S.	N.S.	51
4.00	300	33	588	2.00	6
5.50	88	33	588	2.00	6
4.[illegible]0	144	33	588	2.00	6
4.50	214	33	588	2.00	6
2.60	300	37	644	0.33	19
2.60	200	37	644	0.33	19
3.00	300	37	644	0.33	19
3.20	200	37	644	0.33	19
3.00	295	60	575	2.00	9
2.50	232	60	575	2.00	9

N.S. = not specified.

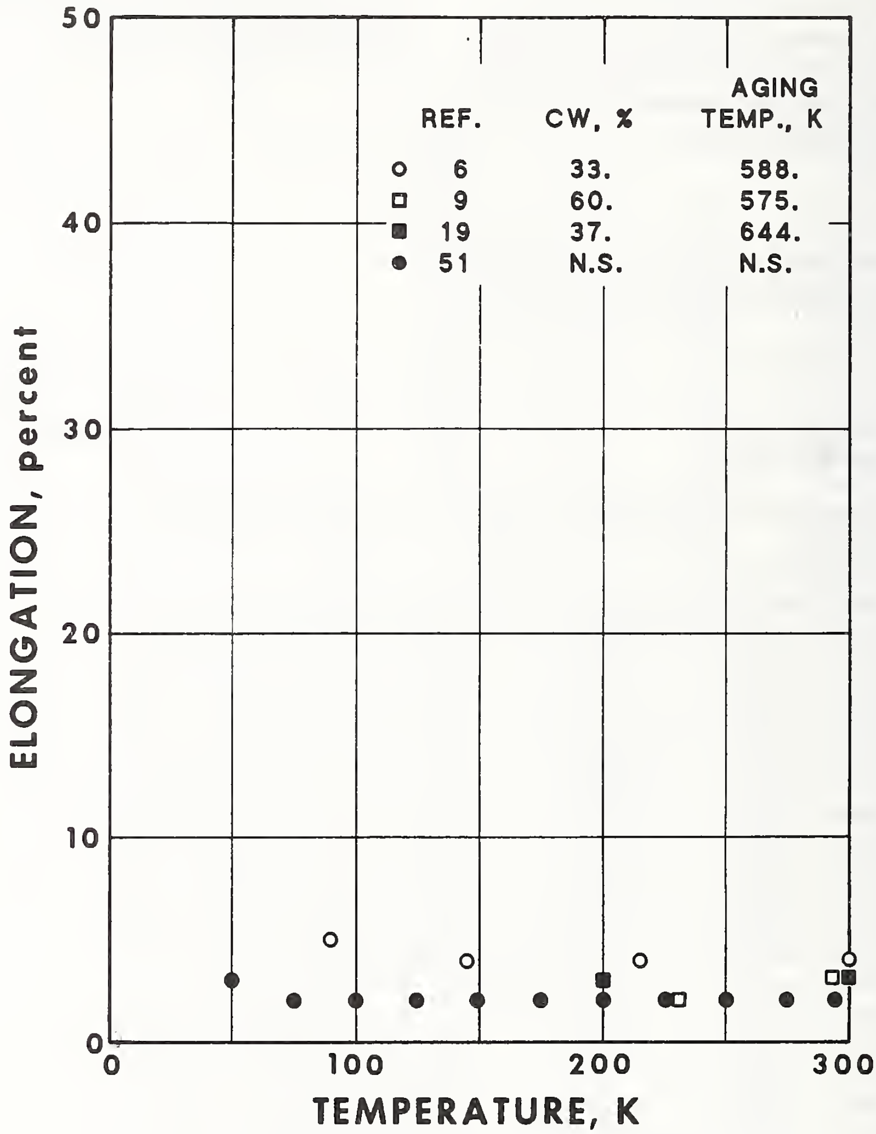

Figure 9.57. Elongation measurements of cold-worked and aged C17200 beryllium copper are shown as a function of test temperature. For clarity, overlapping data points are omitted from the figure. All data are presented in Table 9.39. Products were in sheet and bar form (not specified in Reference 9.51).

C17500: Annealed and Aged

Tensile Elongation vs. Aging Temperature, Time (295 K)

DATA SOURCES AND ANALYSIS

Measurements of the elongation of annealed C17500 beryllium copper at 295 K as a function of aging temperature and time were obtained from three sources (References 9.3, 9.12, and 9.36). Product was in strip form (Reference 9.3) or not specified (References 9.12 and 9.36). Reported aging temperatures ranged from 727 to 755 K; aging times ranged from 0.13 to 8 h. Gage lengths were 2 cm (Reference 9.12) and 5 cm (Reference 9.3). Since the original data points were not presented in Reference 9.36, data were extracted from the curves at appropriate intervals.

RESULTS

All measurements are reported in Table 9.40, which presents the elongation, the aging temperature and time, and the reference number. The available characterization of materials and measurements is given in Table 9.57 at the end of the tensile properties section. Figures 9.58 and 9.59 present the elongation measurements as a function of aging temperature and time, respectively.

Table 9.40. Elongation Dependence of Annealed C17500 Beryllium Copper on Aging Temperature and Time (295 K).

Elongation, %	Aging Temperature, K	Aging Time, h	Reference No.
15.0	727	8.00	12
1[illegible].4	727	8.00	12
17.3	755	3.00	3
18.4	755	3.00	3
25.5	753	0.13	36
20.[illegible]	753	0.25	36
20.0	753	0.50	36
1[illegible].4	753	1.00	36
19.0	753	2.00	36
18.5	753	1.00	36
17.5	753	4.00	36
16.0	753	6.00	36
15.8	753	8.00	36

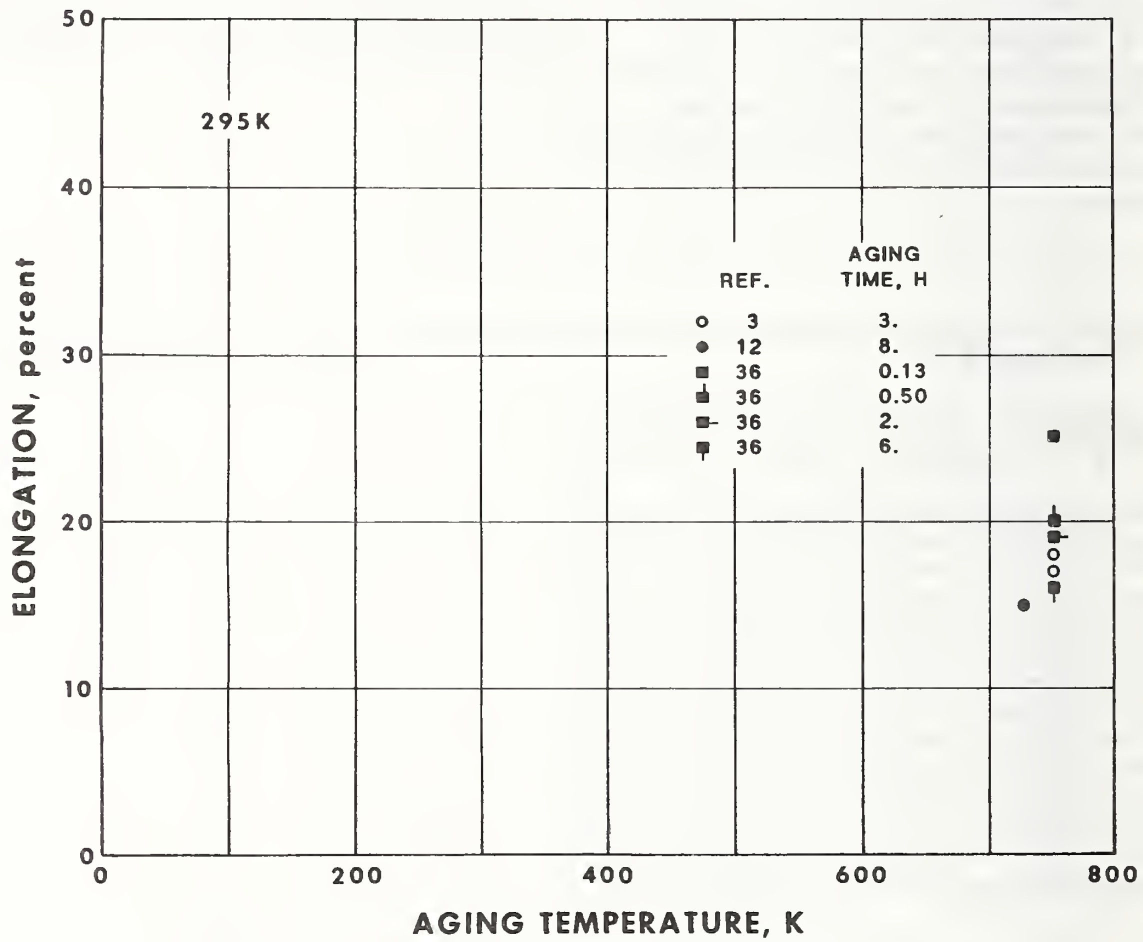

Figure 9.58. Elongation measurements on annealed C17500 beryllium copper at 295 K are shown as a function of aging temperature. For clarity, overlapping data points are omitted from the figure. All data are presented in Table 9.40. Product was in strip form (Reference 9.3) or not specified (References 9.12 and 9.36).

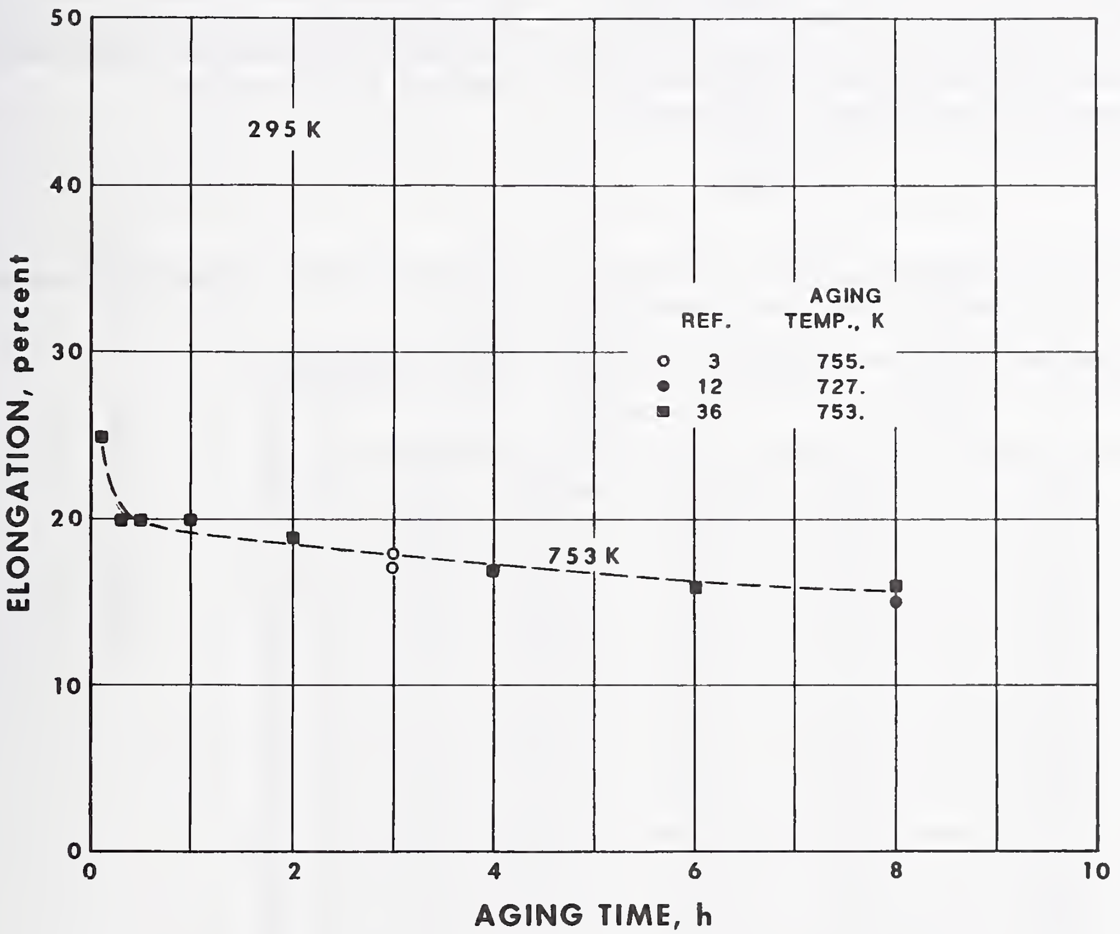

Figure 9.59. Elongation measurements on annealed C17500 beryllium copper at 295 K are shown as a function of aging time. For clarity, overlapping data points are omitted from the figure. All data are presented in Table 9.40. Product was in strip form (Reference 9.3) or not specified (References 9.12 and 9.36).

C17500: Annealed and Aged; Cold-worked; Cold-worked and Aged

Tensile Elongation vs. Temperature (20–300 K)

DATA SOURCES AND ANALYSIS

Measurements of the elongation of annealed and aged, cold-worked, and cold-worked and aged C17500 beryllium copper between 20 and 300 K were obtained from three sources (References 9.6, 9.12, and 9.25). Measurements from Reference 9.38 on cold-worked material at 295 K only are presented for comparison. Products were in sheet and bar form (not specified in References 9.12 and 9.38). Gage lengths were 2 cm (References 9.6 and 9.12) or 5 cm (References 9.25 and 9.38).

RESULTS

All measurements are reported in Table 9.41, which presents elongation, test temperature, percent of cold work (reduction in thickness or area), aging temperature and time, and the reference number. The available characterization of materials and measurements is given in Table 9.57 at the end of the tensile properties section. Figure 9.60 presents the elongation measurements as a function of test temperature.

Table 9.41. Elongation Dependence of Annealed and Aged, Cold-worked, and Cold-worked and Aged C17500 Beryllium Copper upon Temperature (20–300 K).

Elongation, %	Test Temperature, K	Cold Work, %	Aging Temperature, K	Aging Time, h	Reference No.
15.2	28	33	755	8	6
18.0	144	33	755	2	6
49.0	300	33	755	2	6
18.0	299	0	727	8	12
49.0	299	0	727	8	12
18.0	197	0	727	8	12
49.0	197	0	727	8	12
21.0	77	0	727	2	12
21.0	77	0	727	8	12
25.0	20	0	727	8	12
21.0	20	0	727	8	12
18.0	20	21	0	0	25
49.0	20	21	0	2	25
30.0	76	21	0	0	25
32.0	76	21	0	0	25
16.0	195	21	0	0	25
21.0	755	21	0	2	25
10.0	300	21	0	0	25
10.0	300	21	0	0	25
8.0	295	50	0	0	38

Aging Temperature, 0 K = not aged.

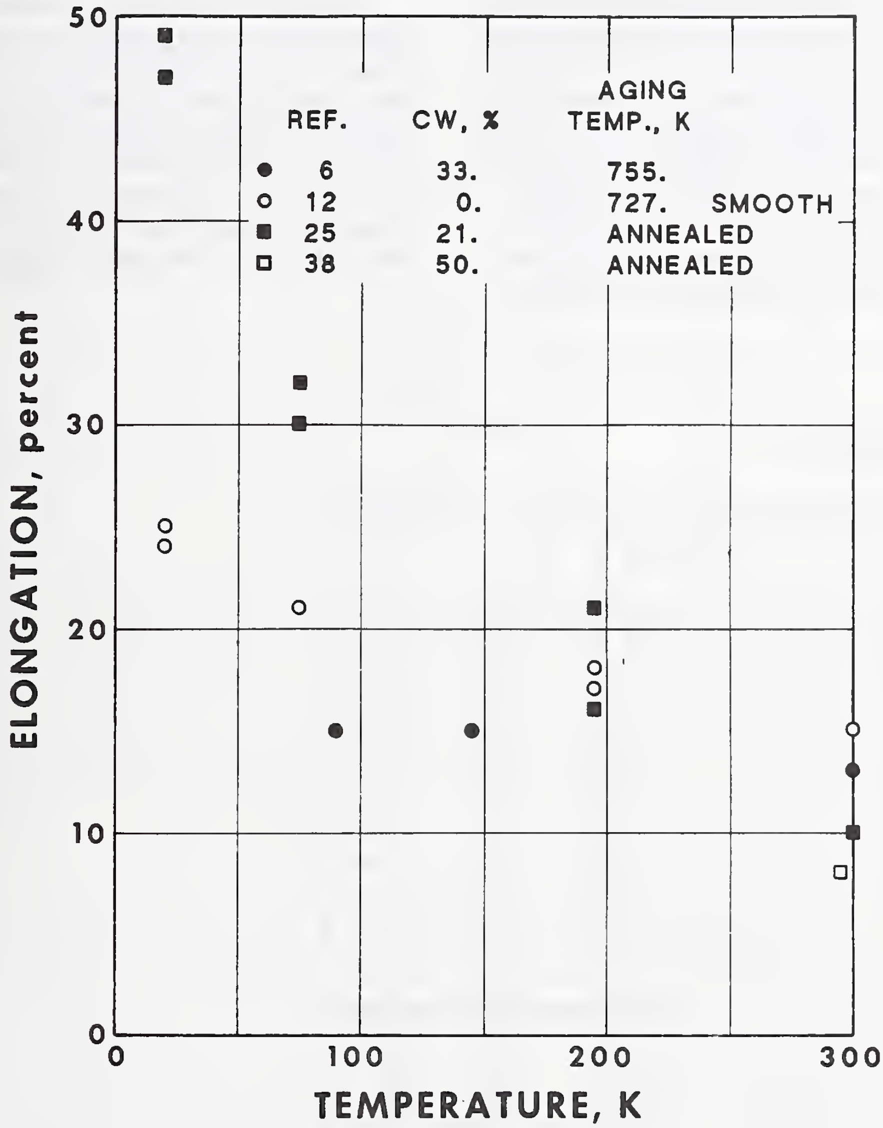

Figure 9.60. Elongation measurements of annealed and aged, cold-worked, and cold-worked and aged C17500 beryllium copper are shown as a function of test temperature. For clarity, overlapping data points are omitted from the figure. All data are presented in Table 9.41. Products were in sheet and bar form (not specified in References 9.12 and 9.38).

DATA SOURCES AND ANALYSIS

Measurements of the elongation of cold-worked C17500 beryllium copper at 295 K as a function of aging temperature and time were obtained from four sources (References 9.3, 9.6, 9.36, and 9.38). Products were in bar (Reference 9.6) and strip form (Reference 9.3) or not specified (Reference 9.36 and 9.38). Cold work, *CW*, (carried out before aging) ranged from 3 to 50% (reduction in thickness or area). Reported aging temperatures ranged from 723 to 755 K; aging times ranged from 0.13 to 8 h. Gage lengths were 2 cm (Reference 9.6) and 5 cm. Since the original data points were not presented in Reference 9.36, data were extracted from the curves at appropriate intervals.

RESULTS

All measurements are reported in Table 9.42, which presents elongation, *CW* (reduction in thickness or area in percent), aging temperature and time, and the reference number. The available characterization of materials and measurements is given in Table 9.57 at the end of the tensile properties section. Figures 9.61 and 9.62 present the elongation measurements as a function of aging temperature and time, respectively.

Table 9.42. Elongation Dependence of Cold-worked C17500 Beryllium Copper on Aging Temperature and Time (295 K).

Elongation, %	Cold Work, %	Aging Temperature, K	Aging Time, h	Reference No.
13.0	33	755	2.00	6
12.[illegible]	50	723	0.75	38
11.8	50	723	1.00	36
15.3	50	723	1.50	38
19.2	50	723	2.00	36
15.3	50	723	2.50	38
11.[illegible]	50	723	3.00	38
15.3	3	755	3.00	3
19.2	3	755	3.00	3
13.3	11	755	2.50	3
14.3	11	755	2.00	3
9.0	N.S.	753	0.13	38
11.0	N.S.	753	0.25	36
12.0	N.S.	753	1.50	36
11.[illegible]	N.S.	753	1.00	36
13.3	N.S.	753	2.50	36
9.8	N.S.	753	3.00	36
9.0	N.S.	753	1.50	38
8.2	N.S.	753	6.00	36
8.0	N.S.	753	8.00	36

N.S. = not specified.

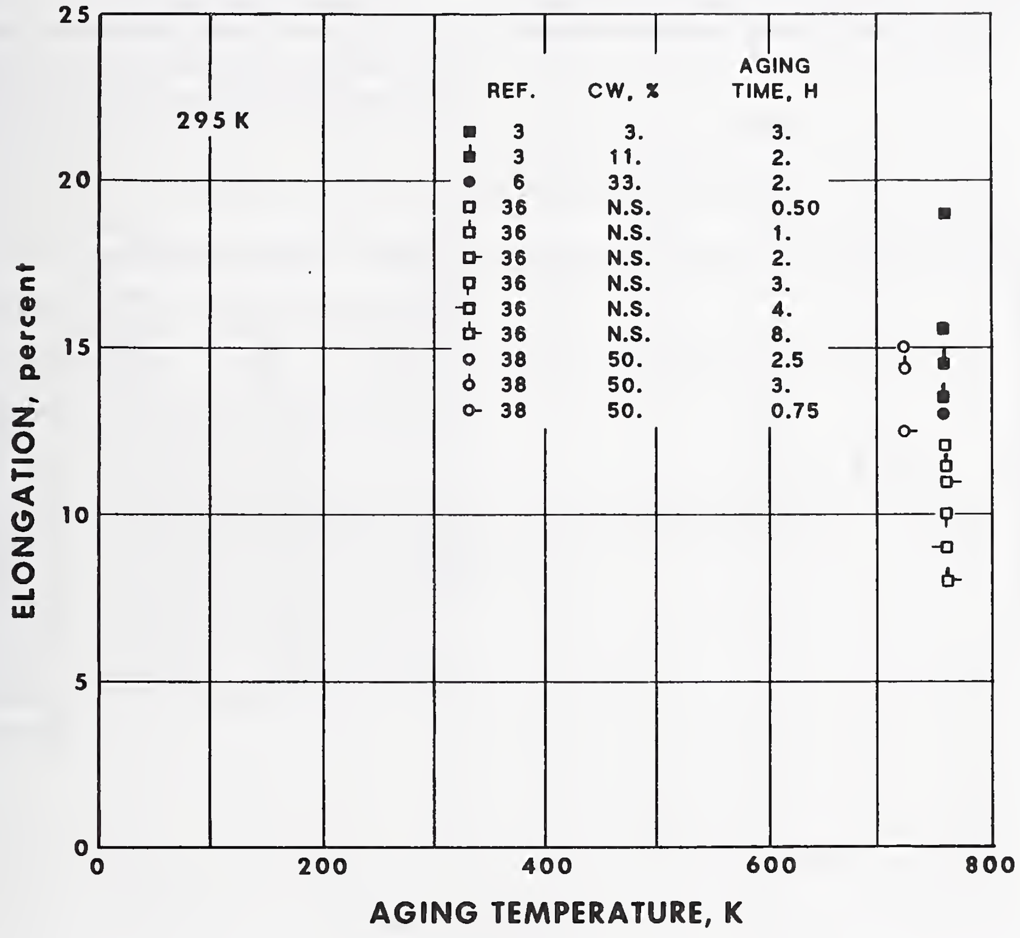

Figure 9.61. Elongation measurements on cold-worked C17500 beryllium copper at 295 K are shown as a function of aging temperature. For clarity, overlapping data points are omitted from the figure. All data are presented in Table 9.42. Products were in bar (Reference 9.6) and strip form (Reference 9.3), or not specified (Reference 9.38).

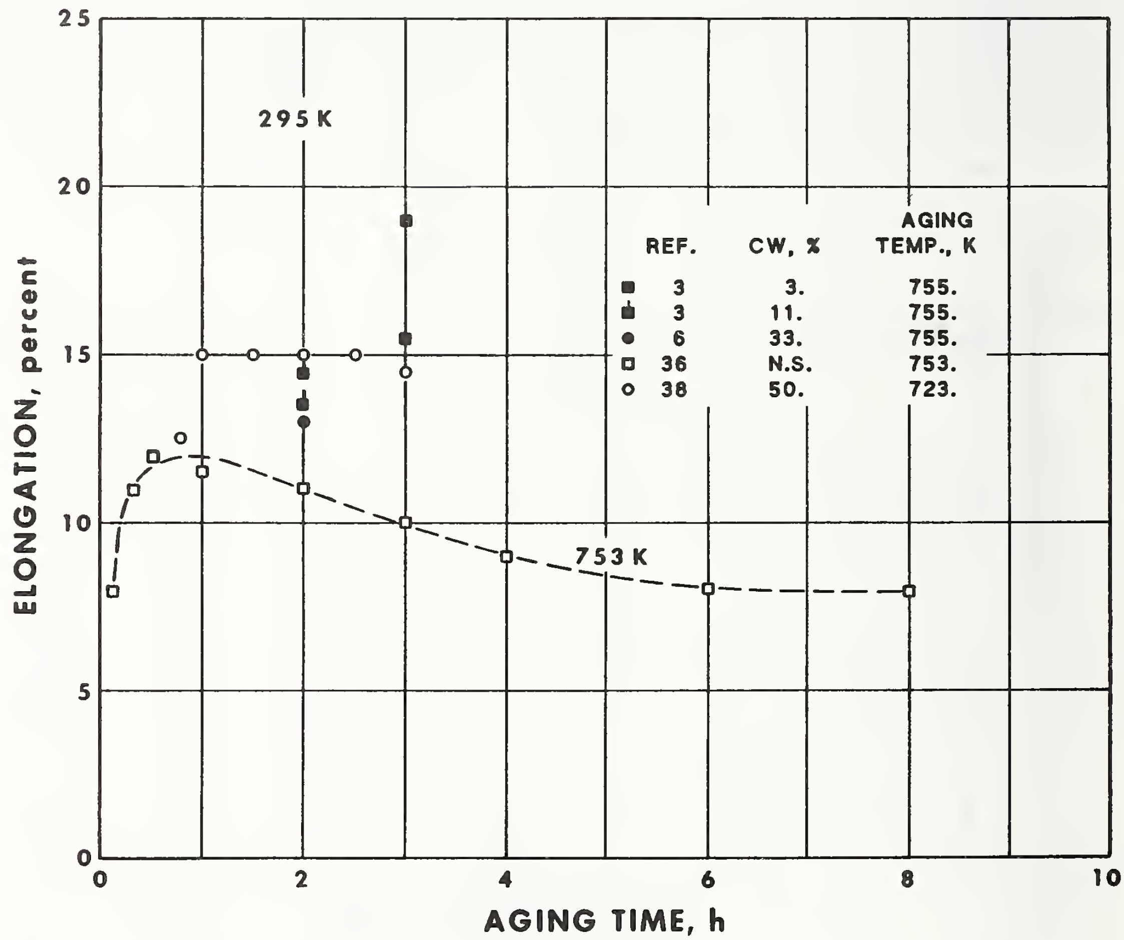

Figure 9.62. Elongation measurements on cold-worked C17500 beryllium copper at 295 K are shown as a function of aging time. All data are presented in Table 9.42. Products were in bar (Reference 9.6) and strip form (Reference 9.3), or not specified (Reference 9.38).

C17510: Annealed and Aged

Tensile Elongation vs. Aging Temperature, Time (295 K)

DATA SOURCES AND ANALYSIS

Measurements of the tensile elongation of annealed C17510 beryllium copper at 295 K as a function of aging time were obtained from two sources (References 9.36 and 9.40). Product was in strip form (Reference 9.40) or was not specified (Reference 9.36). Aging temperature was 753 K (Reference 9.36) or not specified (Reference 9.40). Aging times ranged from 0.13 to 8 h. Since the original data points were not presented in Reference 9.36, data were extracted from the curves at appropriate intervals.

RESULTS

All measurements are reported in Table 9.43, which presents elongation, aging time, and the reference number. The available characterization of materials and measurements is given in Table 9.57 at the end of the tensile properties section. Figure 9.63 presents the elongation measurements as a function of aging time. Unspecified values of time are plotted on the *y*-axis.

Table 9.43. Elongation Dependence of Annealed C17510 Beryllium Copper on Aging Time (295 K).

Elongation, %	Aging Temperature, K	Aging Time, h	Reference No.
15.0	N.S.	N.S.	40
33.5	753.0	0.13	36
22.5	753.0	0.25	36
20.0	753.0	0.50	36
22.5	753.0	1.00	36
19.6	753.0	8.00	36
19.0	753.0	1.00	36
19.6	753.0	4.00	36
17.1	753.0	6.00	36
19.6	753.0	8.00	36

N.S. = not specified.

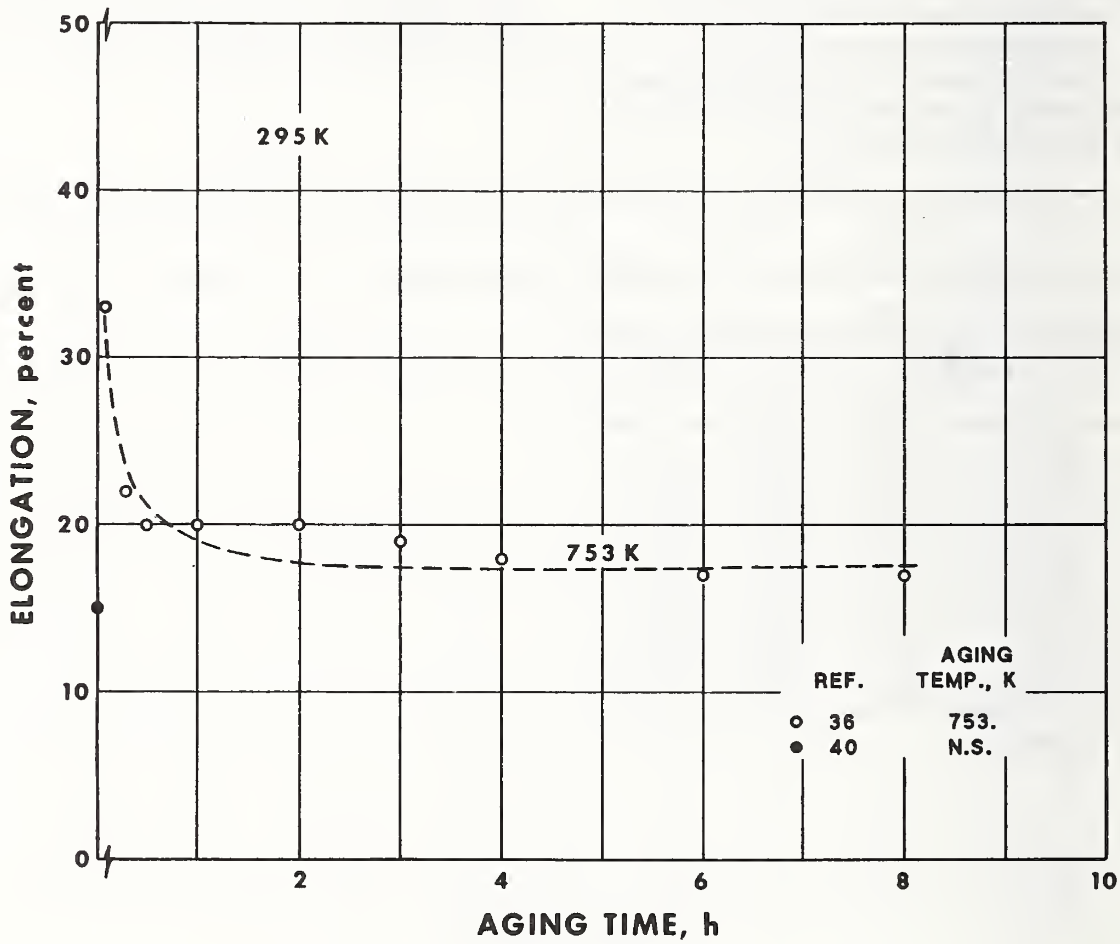

Figure 9.63. Elongation measurements on annealed C17510 beryllium copper at 295 K are shown as a function of aging time. If this parameter was not specified, elongation is plotted on the y-axis. All data are presented in Table 9.43. Product was in strip form (Reference 9.40) or was not specified (Reference 9.36). (N.S. in legend for Reference 9.40 indicates not specified.)

C17510: Cold-worked and Aged

Tensile Elongation vs. Aging Temperature, Time (295 K)

DATA SOURCES AND ANALYSIS

Measurements of the elongation of cold-worked C17510 beryllium copper at 295 K as a function of aging temperature and time were obtained from six sources (References 9.36, 9.40, 9.41, 9.43, 9.44, and 9.46). Products were in strip and plate form (not specified in References 9.36 and 9.41). Cold work, *CW*, (carried out before aging) ranged from 21 to 40% (reduction in thickness). Reported aging temperatures ranged from 727 to 838 K. Aging times ranged from 0.13 to 8 h. Aging parameters were not specified in Reference 9.43. Gage lengths, where specified, were 2 (Reference 9.43), 3.8 (Reference 9.44), and 5 cm (Reference 9.40). Since the original data points were not presented in Reference 9.36, data were extracted from the curves at appropriate intervals. Data presented here from Reference 9.46 include tensile measurements at 295 K from a commercial supplier, Princeton Plasma Physics Laboratory, and Massachusetts Institute of Technology. Reference 9.44 also reports tensile test data on one of the heats (A) included in the tests summarized in Reference 9.46. Cryogenic test results from Reference 9.44 on this heat are presented on pages 9-142 and 9-145 of this section.

RESULTS

All measurements are reported in Table 9.44, which presents elongation, *CW* (reduction in thickness in percent), aging temperature and time, and the reference number. The available characterization of materials and measurements is given in Table 9.57 at the end of the tensile properties section. Figures 9.64 and 9.65 present the elongation measurements as a function of aging temperature and time, respectively. Unspecified values of temperature or time are plotted on the *y*-axis.

Table 9.44. Elongation Dependence of Cold-worked C17510 Beryllium Copper on Aging Temperature and Time (295 K).

Elongation, %	Cold Work, %	Aging Temperature, K	Aging Time, h	Reference No.
15.90	40	755.0	3.00	41
7.00	37	N.S.	N.S.	43
11.00	37	N.S.	N.S.	43
12.00	37	N.S.	N.S.	43
2.00	37	N.S.	N.S.	43
9.76	37	755.0	8.00	44
9.36	37	755.0	2.00	44
12.00	21	727.0	8.00	40
10.10	21	755.0	8.00	40
9.76	21	753.0	8.00	40
9.30	21	811.0	8.00	40
9.30	21	838.0	8.00	40
10.00	N.S.	753.0	0.13	36
14.00	N.S.	753.0	0.25	36
11.00	N.S.	753.0	0.50	36
13.20	N.S.	753.0	1.00	36
10.00	N.S.	753.0	2.00	36
13.20	N.S.	753.0	3.00	36
10.00	N.S.	753.0	4.00	36
9.50	N.S.	753.0	6.00	36
9.50	N.S.	753.0	8.00	36
12.00	37	755.0	2.00	46A
13.00	N.S.	N.S.	N.S.	46B

Table 9.44, continued

Elongation, %	Cold Work, %	Aging Temperature, K	Aging Time, h	Reference No.
10.00	N.S.	N.S.	N.S.	46C
12.50	37	755	2.00	46A
10.50	N.S.	N.S.	N.S.	46C

N.S. = not specified.

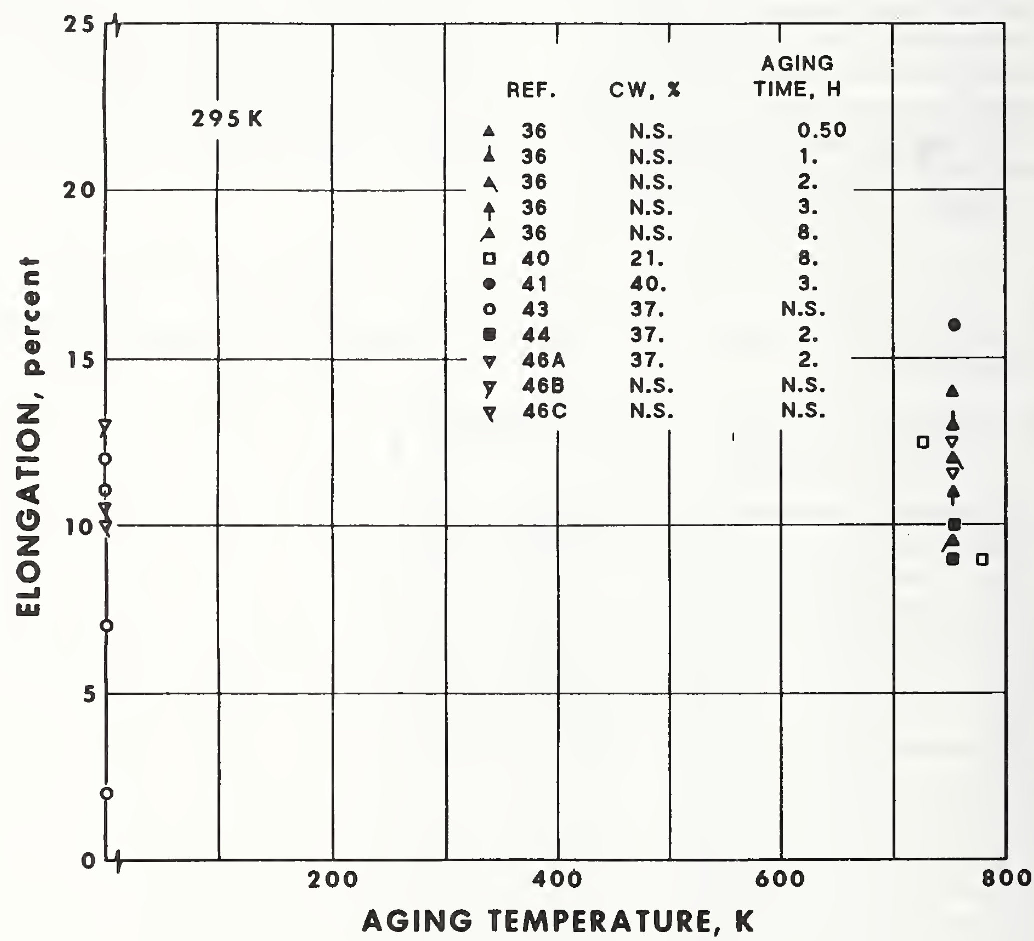

Figure 9.64. Elongation measurements on cold-worked C17510 beryllium copper at 295 K are shown as a function of aging temperature. If this parameter was not specified, elongation is plotted on the y-axis. For clarity, overlapping data points are omitted from the figure. All data are presented in Table 9.44. Products were in strip and plate form (not specified in References 9.36 and 9.41).

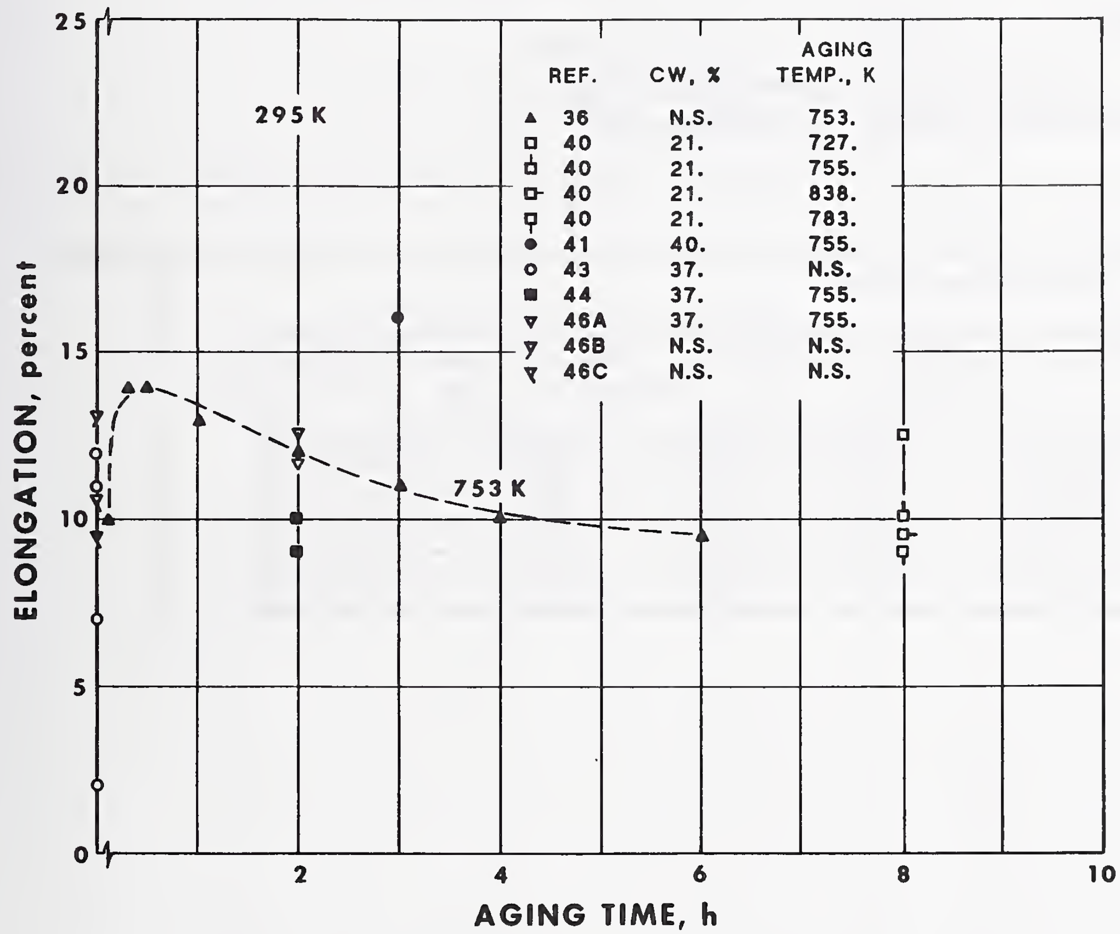

Figure 9.65. Elongation measurements on cold-worked C17510 beryllium copper at 295 K are shown as a function of aging time. If this parameter was not specified, elongation is plotted on the *y*-axis. For clarity, overlapping data points are omitted from the figure. All data are presented in Table 9.44. Products were in strip and plate form (not specified in References 9.36 and 9.41). (N.S. in legend for References 9.43 and 9.46 indicates not specified.)

DATA SOURCES AND ANALYSIS

Measurements of the elongation of cold-worked and aged C17510 beryllium copper from 4 to 295 K were obtained from Reference 9.44. Product was in plate form. Gage lengths were 3.8 cm.

RESULTS

All measurements are reported in Table 9.45, which presents elongation, test temperature, percent of *CW* (reduction in thickness), aging temperature and time, and the reference number. The available characterization of materials and measurements is given in Table 9.57 at the end of the tensile properties section. Figure 9.66 presents the elongation measurements as a function of test temperature.

Table 9.45. Elongation Dependence of Cold-worked and Aged C17510 Beryllium Copper upon Temperature (4–295 K).

Elongation, %	Test Temperature, K	Cold Work, %	Aging Temperature, K	Aging Time, h	Reference No.
9.76	295	37	755	2	44
15.30	76	37	755	2	44
16.90	4	37	755	2	44
9.06	295	37	755	2	44
13.50	76	37	755	2	44
17.60	4	37	755	2	44

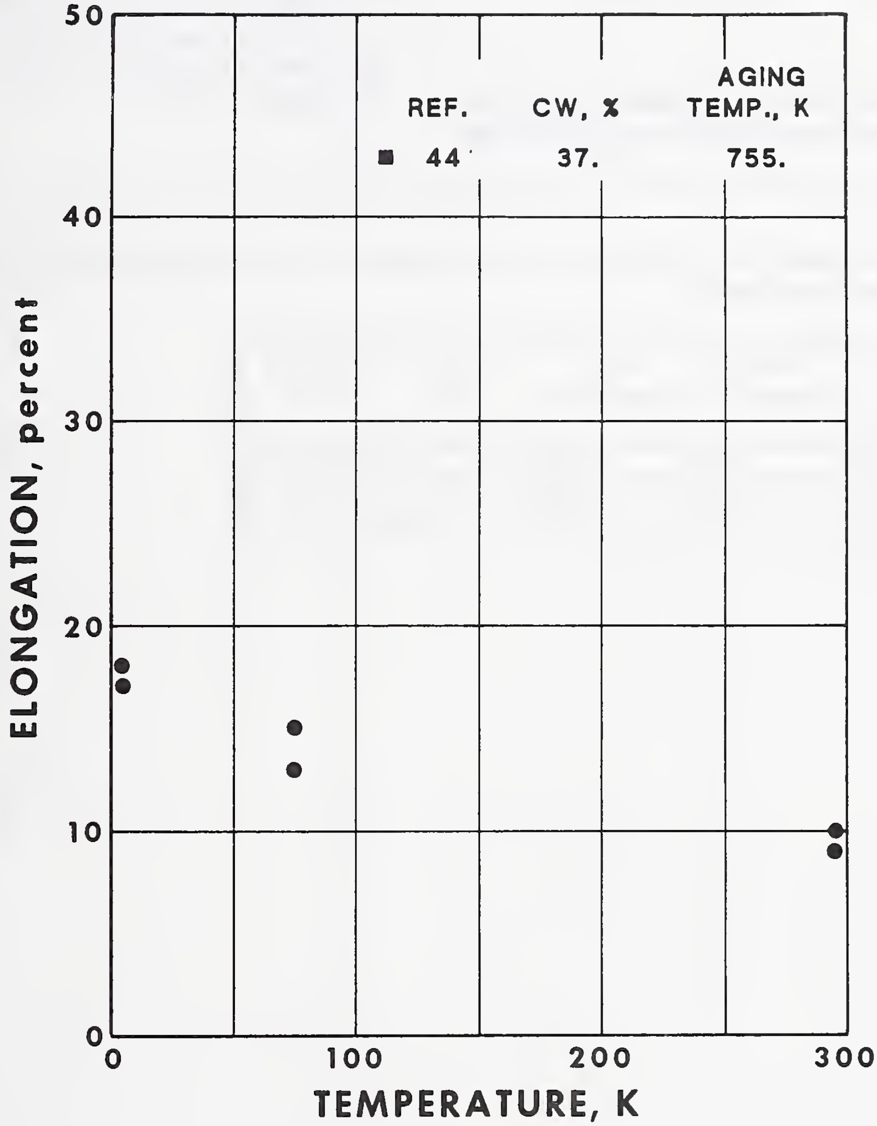

Figure 9.66. Elongation measurements of cold-worked and aged C17510 beryllium copper are shown as a function of test temperature. All data are presented in Table 9.45. Product was in plate form.

DATA SOURCES AND ANALYSIS

Measurements of the reduction of area of annealed and aged C17000 beryllium copper from 20 to 290 K were obtained from Reference 9.49. Product form was not specified.

RESULTS

All measurements are reported in Table 9.46, which presents the reduction of area, test temperature, aging temperature and time, and the reference number. The available characterization of materials and measurements is given in Table 9.57 at the end of the tensile properties section. Figure 9.67 presents the reduction of area measurements as a function of test temperature.

The trend of a small decrease in reduction of area as the temperature is decreased is in agreement with results on C10100–C10400 copper (Reference 9.44).

Table 9.46. Reduction of Area Dependence of Annealed and Aged C17000 Beryllium Copper upon Temperature (20–295 K).

Reduction of Area, %	Test Temperature, K	Aging Temperature, K	Aging Time, h	Reference No.
68	290	N.S.	N.S.	49
64	77	N.S.	N.S.	49
62	20	N.S.	N.S.	49

N.S. = not specified.

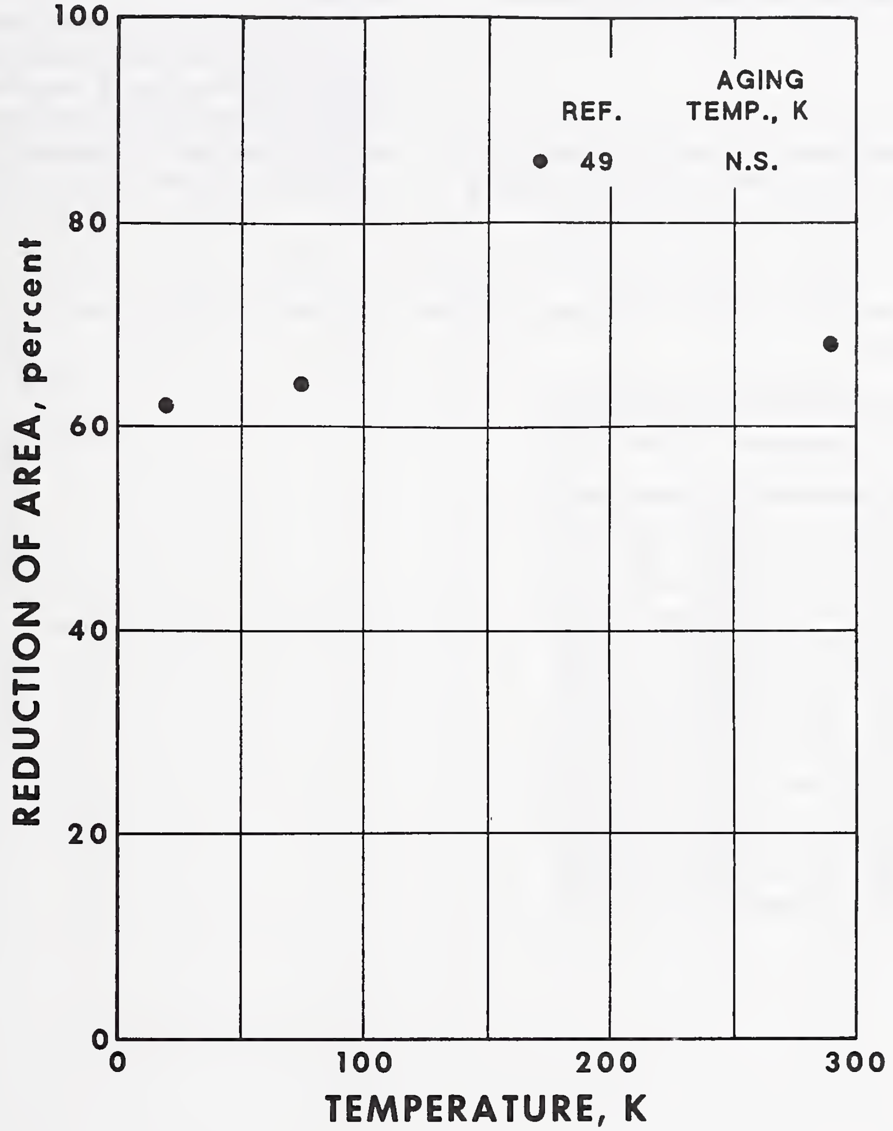

Figure 9.67. Reduction of area measurements of annealed and aged C17000 beryllium copper are shown as a function of test temperature. All data are presented in Table 9.59. Product form was not specified.

C17200: Annealed

Tensile Reduction of Area vs. Temperature (20-300 K)

DATA SOURCES AND ANALYSIS

Measurements of the reduction of area of annealed C17200 beryllium copper between 20 and 300 K were obtained from three sources (References 9.6, 9.7, and 9.9). Product was in bar form.

RESULTS

All measurements are reported in Table 9.47, which presents the reduction of area, test temperature, and the reference number. The available characterization of materials and measurements is given in Table 9.57 at the end of the tensile properties section. Figure 9.68 presents the reduction of area measurements as a function of test temperature.

Reference 9.10 presents measurements from 93 to 293 K on the reduction of area of a 2.6-wt% beryllium-copper alloy in an annealed condition. These data exhibit an increase in reduction of area as the temperature decreases that is similar to the trend shown in Figure 9.68.

Table 9.47. Reduction of Area Dependence of Annealed C17200 Beryllium Copper upon Temperature (20–300 K).

Reduction of Area, %	Test Temperature, K	Reference No.
73.5	300	6
74.5	214	6
79.7	144	6
68.5	76	6
79.7	295	7
79.4	295	7
77.6	195	7
60.5	195	7
75.7	76	7
68.5	76	7
71.0	20	7
68.5	20	7
58.5	295	9
59.0	232	9

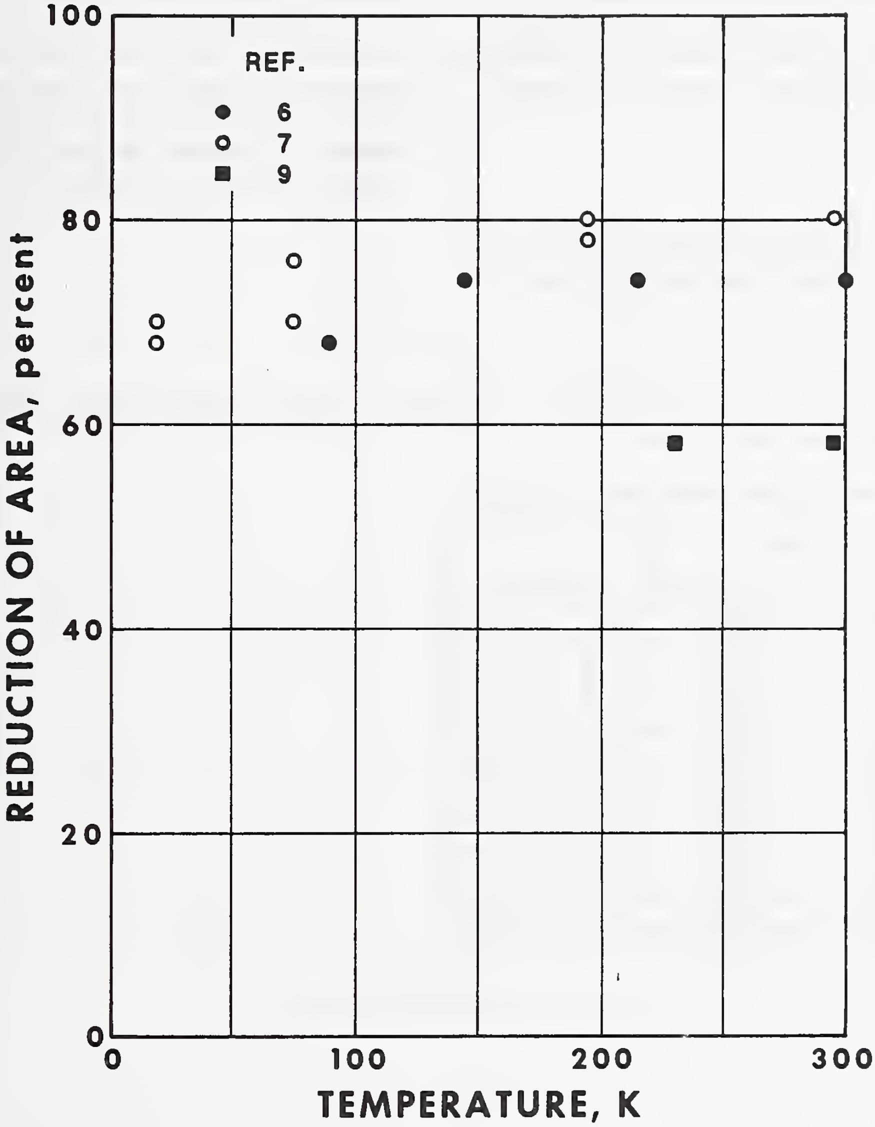

Figure 9.68. Reduction of area measurements of annealed C17200 beryllium copper are shown as a function of test temperature. For clarity, overlapping data points are omitted from the figure. All data are presented in Table 9.47. Product was in bar form.

DATA SOURCES AND ANALYSIS

Measurements of the reduction of area of annealed C17200 beryllium copper at 295 K as a function of aging time and temperature were obtained from four sources (References 9.6, 9.12, 9.13, and 9.20). Products were in bar and plate form, or not specified (Reference 9.12). Reported aging temperatures were 588 and 672 K; aging times were 1.5 and 3 h.

RESULTS

All data are reported in Table 9.48, which presents the reduction of area, aging temperature and time, and the reference number. The available characterization of materials and measurements is given in Table 9.57 at the end of the tensile properties section. Figures 9.69 and 9.70 present the reduction of area measurements as a function of temperature and time, respectively.

Although the range of aging temperatures and times reported is rather narrow, the aging temperature of 588 K and aging time of 3 h correspond to optimum values for maximizing the yield strength of annealed and aged C17200 beryllium copper (see Figures 9.7 and 9.8).

Table 9.48. Reduction of Area Dependence of Annealed C17200 Beryllium Copper on Aging Temperature and Time (295 K).

Reduction of Area, %	Aging Temperature, K	Aging Time, h	Reference No.
11.0	672	1.5	6
7.0	588	3.0	6
12.0	588	3.0	12
12.0	588	3.0	12
6.4	588	3.0	13
7.8	588	3.0	13
9.4	588	3.0	13
6.5	588	3.0	13
9.2	588	3.0	13
7.1	588	3.0	13
8.1	588	3.0	13
5.9	588	3.0	20

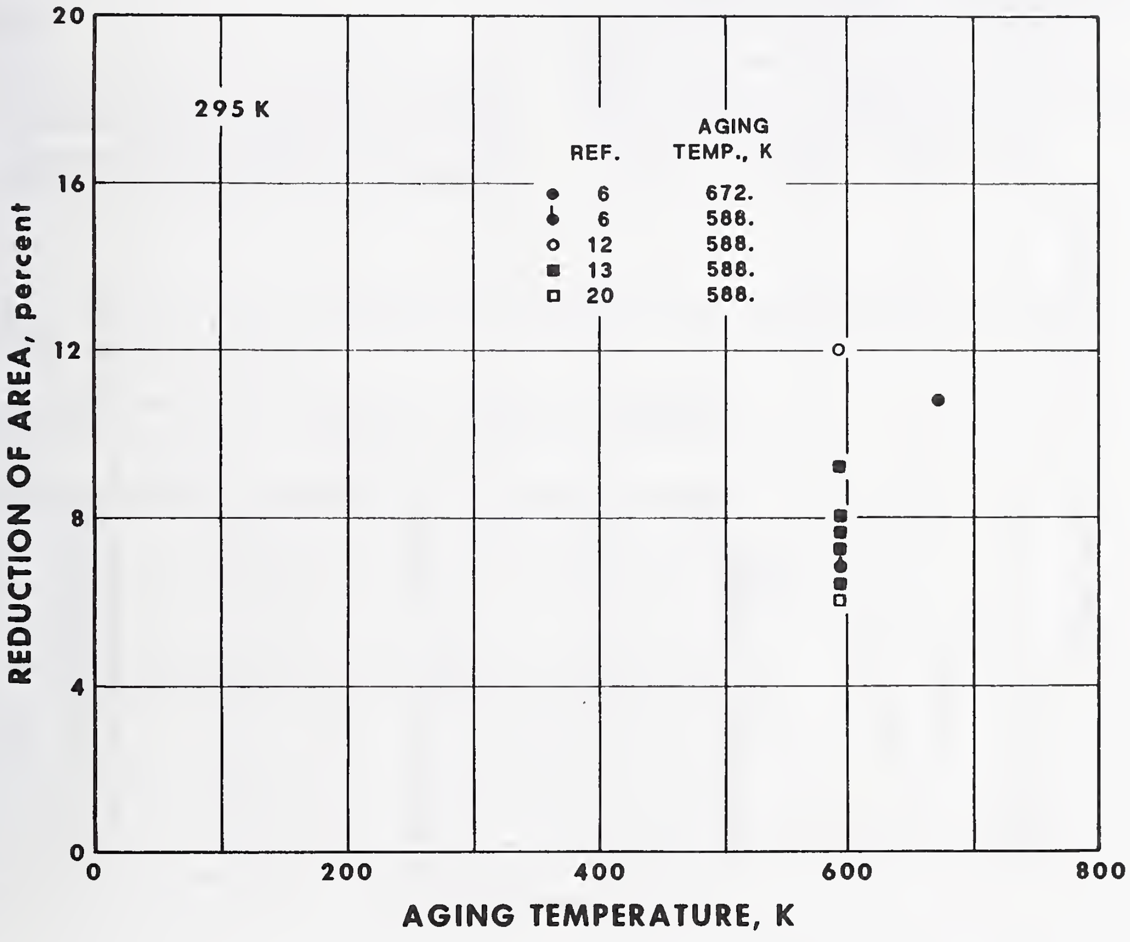

Figure 9.69. Reduction of area measurements for annealed C17200 beryllium copper at 295 K are shown as a function of aging temperature. For clarity, overlapping data points are omitted from the figure. All data are presented in Table 9.48. Products were in bar and plate form, or not specified (Reference 9.12).

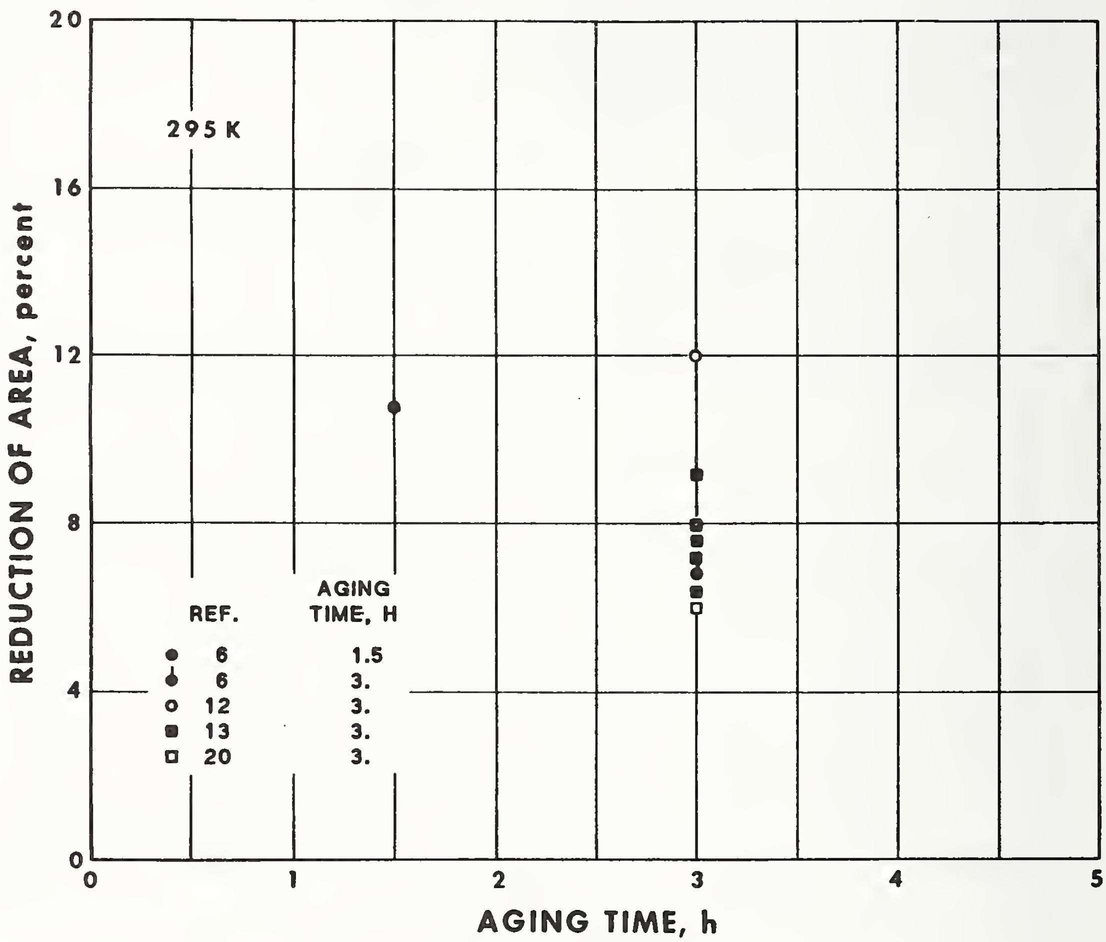

Figure 9.70. Reduction of area measurements for annealed C17200 beryllium copper at 295 K are shown as a function of aging time. For clarity, overlapping data points are omitted from the figure. All data are presented in Table 9.48. Products were in bar and plate form, or not specified (Reference 9.12).

DATA SOURCES AND ANALYSIS

Measurements of the reduction of area of annealed and aged C17200 beryllium copper between 77 and 300 K were obtained from two sources (References 9.6 and 9.12). Product was in bar form (Reference 9.6) or not specified (Reference 9.12).

RESULTS

All measurements are reported in Table 9.49, which presents the reduction of area, test temperature, aging temperature and time, and the reference number. The available characterization of materials and measurements is given in Table 9.57 at the end of the tensile properties section. Figure 9.71 presents the reduction of area measurements as a function of test temperature.

The lower set of values for reduction of area from Reference 9.6 correspond to the higher yield strengths attained with the aging temperature of 588 K.

Reference 9.10 presents measurements from 93 to 293 K on the reduction of area of a 2.6-wt% beryllium-copper alloy in an aged condition. These data exhibit a slight increase in reduction of area as the temperature decreases that is similar to the trend shown in Figure 9.71.

Table 9.49. Reduction of Area Dependence of Annealed and Aged C17200 Beryllium Copper upon Temperature (77–300 K).

Reduction of Area, %	Test Temperature, K	Aging Temperature, K	Aging Time, h	Reference No.
7.0	300	388	3.0	6
19.0	214	588	3.0	6
14.0	388	588	3.0	6
28.0	88	672	1.5	6
25.0	144	672	3.0	6
19.8	214	672	3.0	6
11.0	300	672	1.5	6
12.0	299	588	3.0	12
12.0	299	588	3.0	12
14.5	197	588	3.0	12
11.0	197	588	3.0	12
20.0	77	588	3.0	12
24.5	77	588	3.0	12

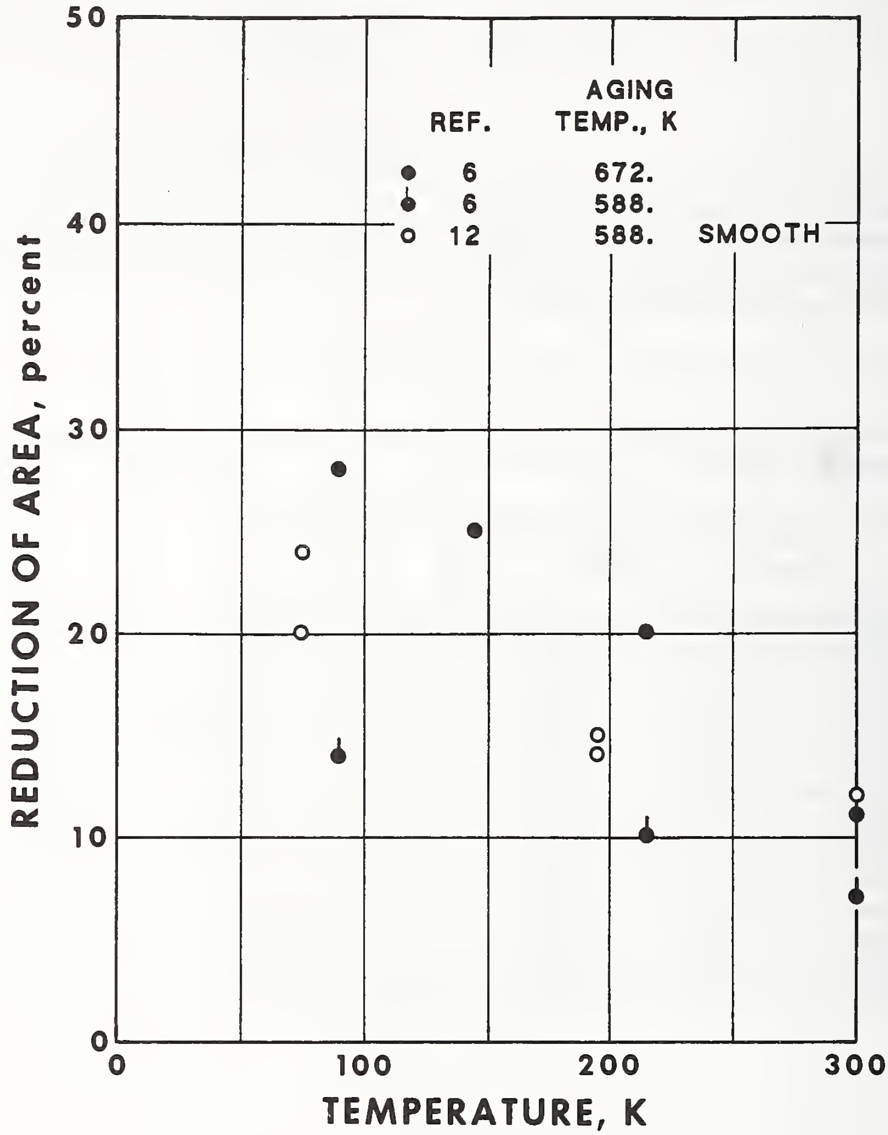

Figure 9.71. Reduction of area measurements of annealed and aged C17200 beryllium copper are shown as a function of test temperature. A duplicate value from Reference 9.12 at 299 K is omitted from the figure. All data are presented in Table 9.49. Product was in bar form (Reference 9.6) or not specified (Reference 9.12).

C17200: Cold-worked

Tensile Reduction of Area vs. Temperature (20–300 K)

DATA SOURCES AND ANALYSIS

Measurements of the reduction of area of cold-worked C17200 beryllium copper between 20 and 300 K were obtained from four sources (References 9.6, 9.7, 9.9, and 9.26). Data from Reference 9.27 at 295 K only are presented for comparison because measurements were made for varying amounts of cold work, *CW*. Products were in strip and bar form (not specified in Reference 9.26).

RESULTS

All measurements are reported in Table 9.50, which presents the reduction of area, test temperature, *CW* (reduction in thickness or area in percent), and the reference number. (The percent of *CW* could not be determined from Reference 9.26: it was 21% if the material was rolled or 37% if it was drawn.) The available characterization of materials and measurements is given in Table 9.57 at the end of the tensile properties section. Figure 9.72 presents the reduction of area measurements as a function of test temperature.

Table 9.50. Reduction of Area Dependence of Cold-worked C17200 Beryllium Copper upon Temperature (20–300 K).

Reduction of Area, %	Test Temperature, K	Cold Work, %	Reference No.
50.0	88	33	6
70.0	144	33	6
57.0	300	33	6
68.0	295	37	7
68.0	295	37	7
56.0	195	37	7
70.0	195	37	7
66.0	76	37	7
65.8	76	37	7
60.0	20	37	7
60.0	20	37	7
70.0	300	N.S.	26
68.0	300	N.S.	26
70.0	20	N.S.	26
70.0	300	N.S.	26
67.0	77	N.S.	26
68.0	77	N.S.	26
57.0	77	N.S.	26
68.0	77	N.S.	26
57.0	20	N.S.	26
55.0	20	N.S.	26
56.0	20	N.S.	26
56.0	20	N.S.	26
60.0	20	N.S.	26
42.5	295	60	6
70.0	232	60	6
56.0	295	0	27
56.0	295	11	27
46.0	295	21	27
24.0	295	37	27

N.S. = not specified.

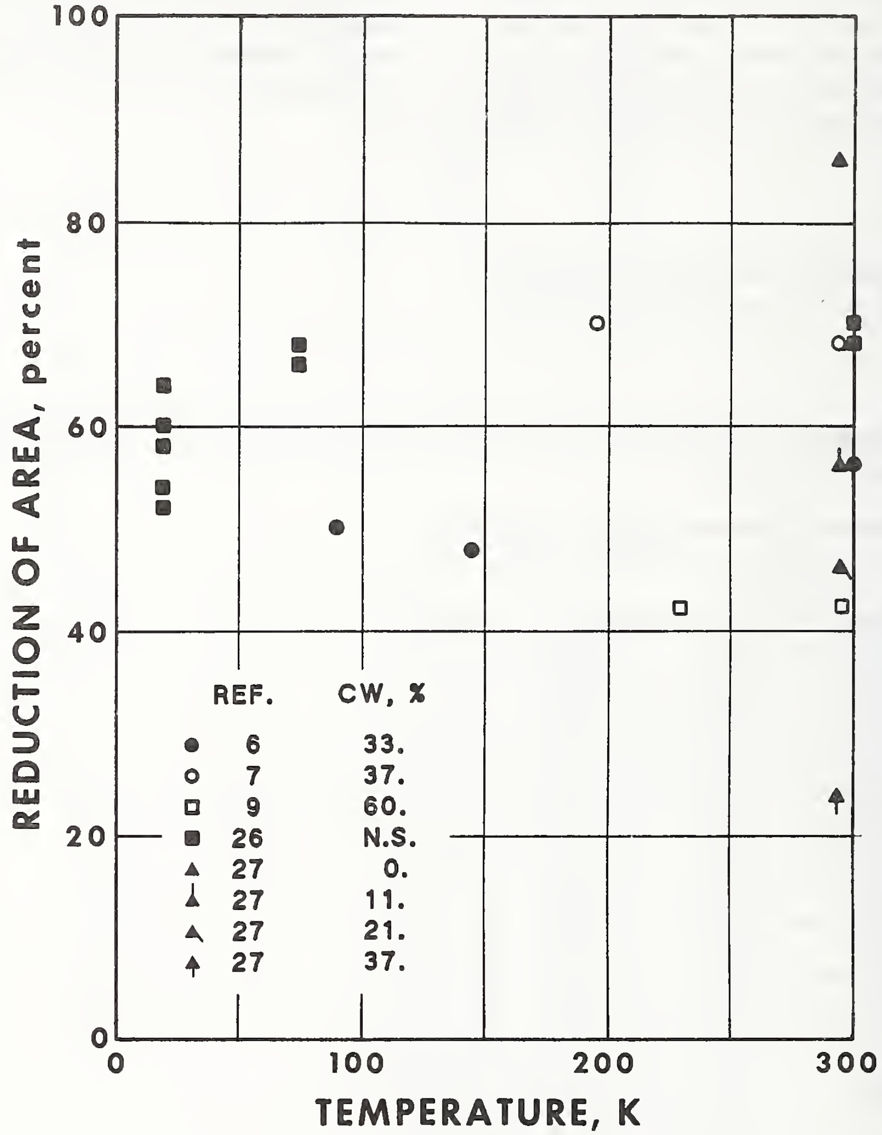

Figure 9.72. Reduction of area measurements of cold-worked C17200 beryllium copper are shown as a function of test temperature. All data are presented in Table 9.50. Products were in strip and bar form (not specified in Reference 9.26).

DATA SOURCES AND ANALYSIS

Measurements of the reduction of area of cold-worked C17200 beryllium copper at 295 K as a function of aging temperature and time were obtained from six sources (References 9.6, 9.9, 9.31, 9.32, 9.57, and 9.58). Products were in wire and bar form. Cold work, *CW*, (carried out before aging) ranged from 21 to 60% (reduction in thickness or area). Reported aging temperatures ranged from 573 to 594 K; aging times from 1.5 to 3 h.

RESULTS

All data are reported in Table 9.51, which presents the reduction of area, aging temperatures and time, *CW* (reduction in thickness or area in percent), and the reference number. The available characterization of materials and measurements is given in Table 9.57 at the end of the tensile properties section. Figures 9.73 and 9.74 present the reduction of area measurements as a function of temperature and time, respectively.

Although the range of aging temperatures and times reported is rather narrow, aging temperatures near 588 K and aging times of 2 to 3 h correspond to optimum values for maximizing the yield strength of cold-worked and aged C17200 beryllium copper (see Figures 9.11 and 9.12). In general, the reduction of area values obtained correlate inversely with the degree of *CW* before aging.

Table 9.51. Reduction of Area Dependence of Cold-worked C17200 Beryllium Copper on Aging Temperature and Time (295 K).

Reduction of Area, %	Cold Work, %	Aging Temperature, K	Aging Time, h	Reference No.
12.0	33	588	2.0	6
16.0	35	588	2.0	31
8.0	33	588	2.0	31
11.0	37	588	3.0	32
16.0	37	594	3.0	32
6.0	37	594	3.0	32
16.0	37	594	3.0	32
18.9	21	573	1.5	57
13.6	30	593	2.0	58
6.0	60	575	2.0	9

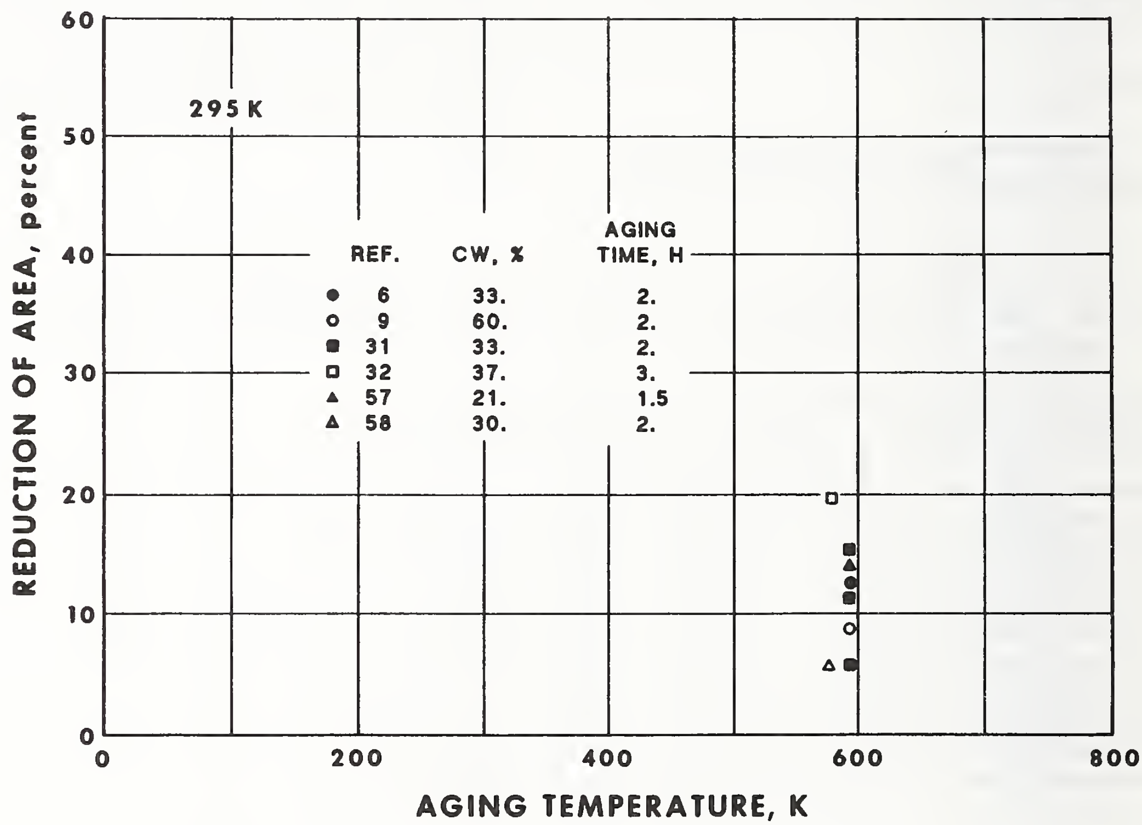

Figure 9.73. Reduction of area measurements for cold-worked C17200 beryllium copper at 295 K are shown as a function of aging temperature. All data are presented in Table 9.51. Products were in wire and bar form.

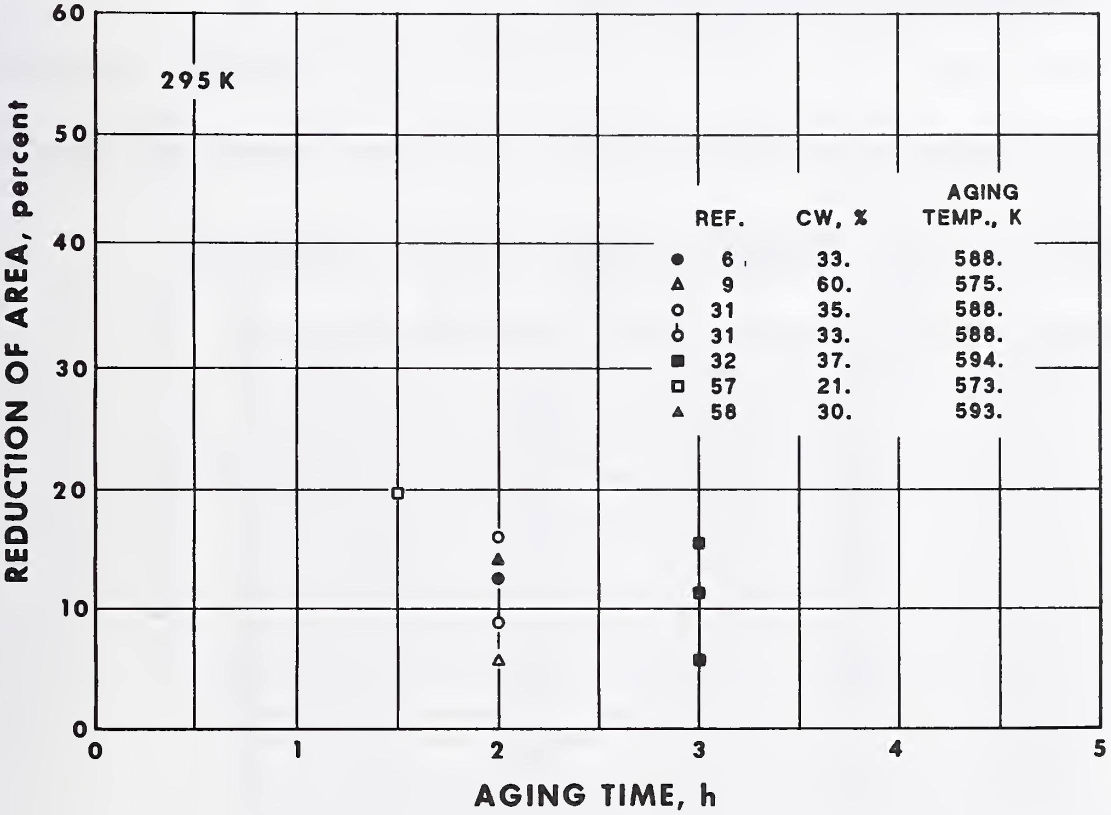

Figure 9.74. Reduction of area measurements on cold-worked C17200 beryllium copper at 295 K are shown as a function of aging time. All data are presented in Table 9.51. Products were in wire and bar form.

DATA SOURCES AND ANALYSIS

Measurements of the reduction of area of cold-worked and aged C17200 beryllium copper between 48 and 300 K were obtained from three sources (References 9.6, 9.9, and 9.51). Product was in bar form (not specified in Reference 9.51).

RESULTS

All measurements are reported in Table 9.52, which presents the reduction of area, test temperature, percent of cold work (reduction in area), aging temperature and time, and the reference number. The available characterization of materials and measurements is given in Table 9.57 at the end of the tensile properties section. Figure 9.75 presents the reduction of area measurements as a function of test temperature.

Table 9.52. Reduction of Area Dependence of Cold-worked and Aged C17200 Beryllium Copper upon Temperature (48–300 K).

Reduction of Area, %	Test Temperature, K	Cold Work, %	Aging Temperature, K	Aging Time, h	Reference No.
5.60	48	N.S.	N.S.	N.S.	51
5.50	73	N.S.	N.S.	N.S.	51
5.10	98	N.S.	N.S.	N.S.	51
4.90	123	N.S.	N.S.	N.S.	51
4.80	98	N.S.	N.S.	N.S.	51
4.60	173	N.S.	N.S.	N.S.	51
4.50	198	N.S.	N.S.	N.S.	51
4.40	223	N.S.	N.S.	N.S.	51
4.35	248	N.S.	N.S.	N.S.	51
4.35	273	N.S.	N.S.	N.S.	51
4.30	293	N.S.	N.S.	N.S.	51
12.00	300	33	588	2	6
10.00	88	33	588	2	6
13.80	144	33	588	2	6
13.00	214	33	588	2	6
6.00	295	60	575	2	9
4.00	232	60	575	2	9

N.S. = not specified.

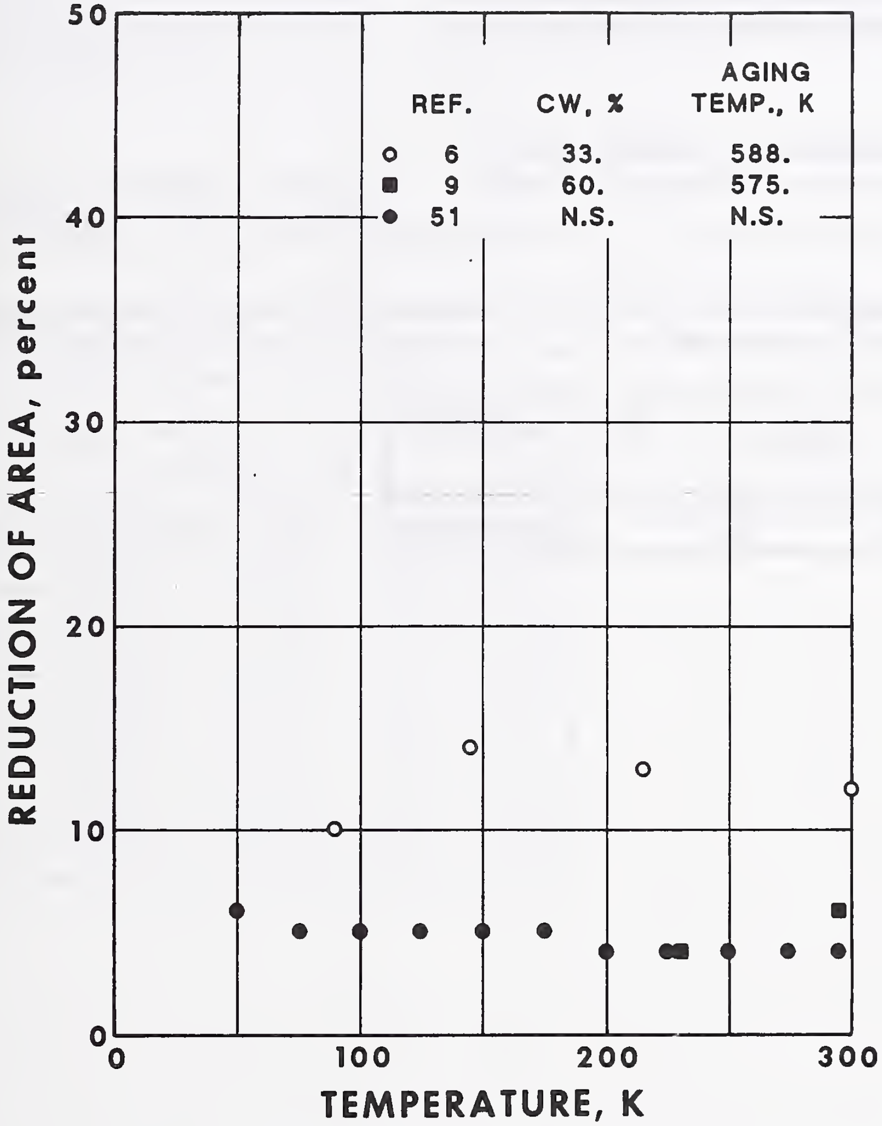

Figure 9.75. Reduction of area measurements of cold-worked and aged C17200 beryllium copper are shown as a function of test temperature. All data are presented in Table 9.52. Product was in bar form (not specified in Reference 9.51).

DATA SOURCES AND ANALYSIS

A limited amount of data on the reduction of area of annealed C17500 beryllium copper at 295 K was obtained from Reference 9.12. Product form was not specified. Measurements were reported on material aged at 727 K for 8 h.

RESULTS

The measurements are reported in Table 9.53, which presents the reduction of area, aging temperature and time, and the reference number. The available characterization of materials and measurements is given in Table 9.57 at the end of the tensile properties section.

Table 9.53. Reduction of Area Dependence of Annealed C17500 Beryllium Copper on Aging Temperature and Time (295 K).

Reduction of Area, %	Aging Temperature, K	Aging Time, h	Reference No.
30.0	727	8	12
37.5	727	8	12

DATA SOURCES AND ANALYSIS

Measurements of the reduction of area of annealed and aged, and cold-worked and aged C17500 beryllium copper between 20 and 300 K were obtained from two sources (References 9.6 and 9.12). Product was in bar form (Reference 9.6) or not specified (Reference 9.12).

RESULTS

All measurements are reported in Table 9.54, which presents the reduction of area, test temperature, percent of cold work (reduction in area), aging temperature and time, and the reference number. The available characterization of materials and measurements is given in Table 9.57 at the end of the tensile properties section. Figure 9.76 presents the reduction of area measurements as a function of test temperature.

Table 9.54. Reduction of Area Dependence of Annealed and Aged, and Cold-worked and Aged C17500 Beryllium Copper upon Temperature (20–300 K).

Reduction of Area, %	Cold Work, %	Aging Temperature, K	Aging Time, h	Reference No.
22.0	33	755	2	6
23.0	33	755	2	6
23.5	33	755	2	6
24.0	33	755	2	6
30.0	0	727	2	12
37.5	0	727	2	12
44.0	0	727	8	12
43.5	0	727	8	12
48.5	0	727	8	12
41.0	0	727	8	12
41.0	0	727	8	12
42.5	0	727	8	12

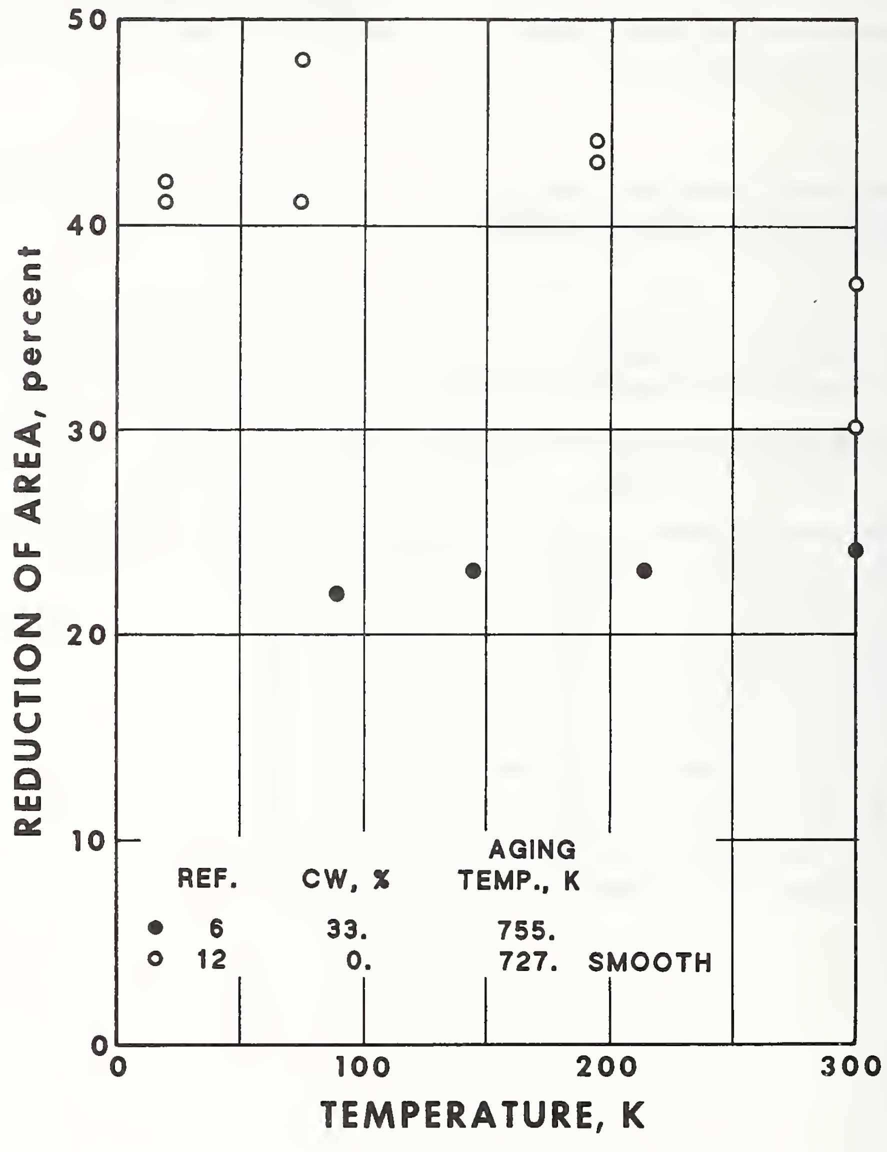

Figure 9.76. Reduction of area measurements of annealed and aged, and cold-worked and aged C17500 beryllium copper are shown as a function of test temperature. All data are presented in Table 9.54. Product was in bar form (Reference 9.6) or not specified (Reference 9.12).

DATA SOURCES AND ANALYSIS

A limited amount of data on the reduction of area of cold-worked C17500 beryllium copper at 295 K was obtained from References 9.6 and 9.39. Product was in bar form. Cold work, *CW*, was 33% (reduction area, Reference 9.6) or 65% (type not specified, Reference 9.39). *CW* was carried out before aging. Aging conditions were 755 K, 2 h (Reference 9.6) or not specified (Reference 9.39).

RESULTS

The measurements are reported in Table 9.55, which presents the reduction of area, percent of *CW* (reduction in area), aging temperature and time, and the reference number. The available characterization of materials and measurements is given in Table 9.57 at the end of the tensile properties section.

Table 9.55. Reduction of Area Dependence of Cold-worked C17500 Beryllium Copper on Aging Temperature and Time (295 K).

Reduction of Area, %	Cold Work, %	Aging Temperature, K	Aging Time, h	Reference No.
24	33	755	2	6
63	65	N.S.	N.S.	39
48	65	N.S.	N.S.	39

N.S. = not specified.

DATA SOURCES AND ANALYSIS

Measurements of the reduction of area of cold-worked and aged C17510 beryllium copper from 4 to 295 K were obtained from Reference 9.44. Product was in plate form.

RESULTS

All measurements are reported in Table 9.56, which presents the reduction of area, test temperature, percent of cold work (reduction in thickness), aging temperature and time, and the reference number. The available characterization of materials and measurements is given in Table 9.57 at the end of the tensile properties section. Figure 9.77 presents the reduction of area measurements as a function of test temperature.

Table 9.56. Reduction of Area Dependence of Cold-worked and Aged C17510 Beryllium Copper upon Temperature (4–295 K).

Reduction of Area, %	Test Temperature, K	Cold Work, %	Aging Temperature, K	Aging Time, h	Reference No.
23.5	295	37	755	2	44
48.8	76	37	755	2	44
35.2	4	37	755	2	44
34.0	295	37	755	2	44
46.8	76	37	755	2	44
45.8	4	37	755	2	44

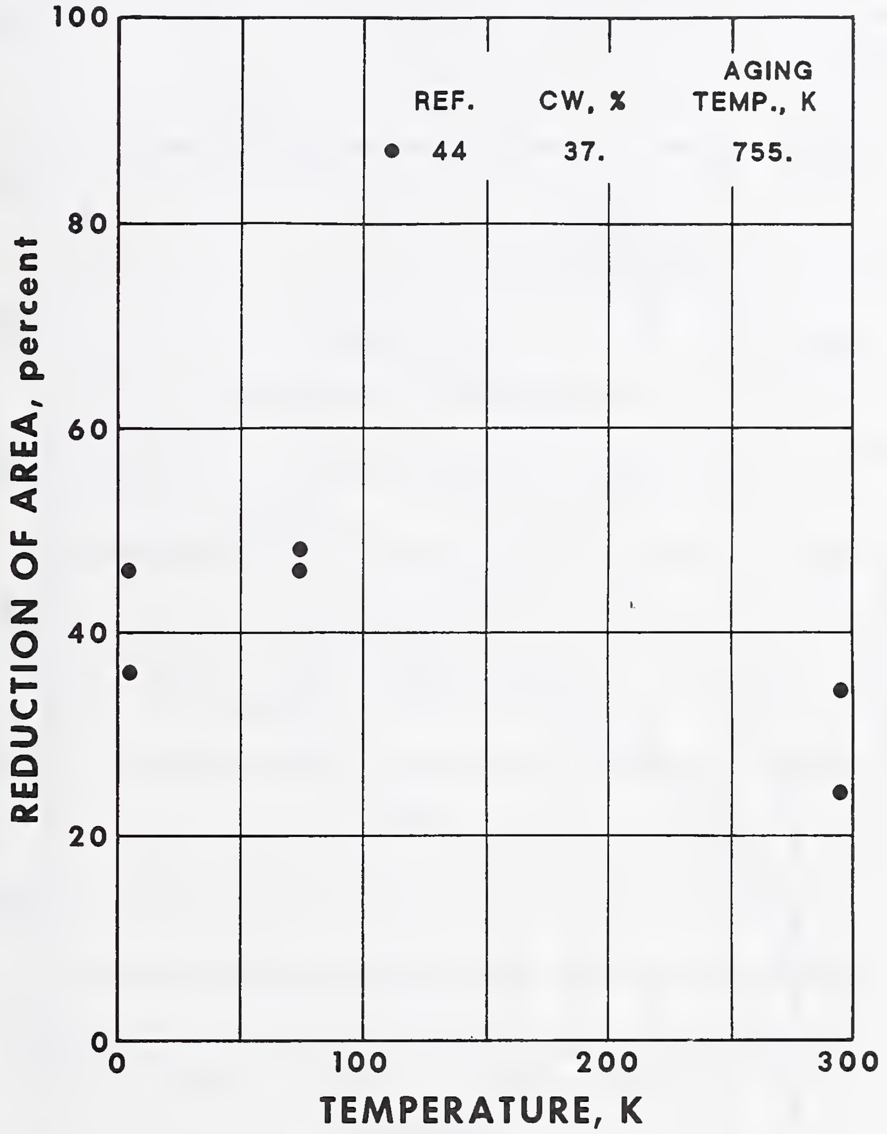

Figure 9.77. Reduction of area measurements of cold-worked and aged C17510 beryllium copper are shown as a function of test temperature. All data are presented in Table 9.56. Product was in plate form.

DATA SOURCE

Stress-strain curves at 20, 76, 195, and 295 K for annealed and 37% cold-rolled C17200 beryllium copper are presented in Figures 9.78 and 9.79. Reference 9.15 is the source of these data. The available characterization of materials and measurements is given in Table 9.57 at the end of the tensile properties section. Measurements were displacement-controlled.

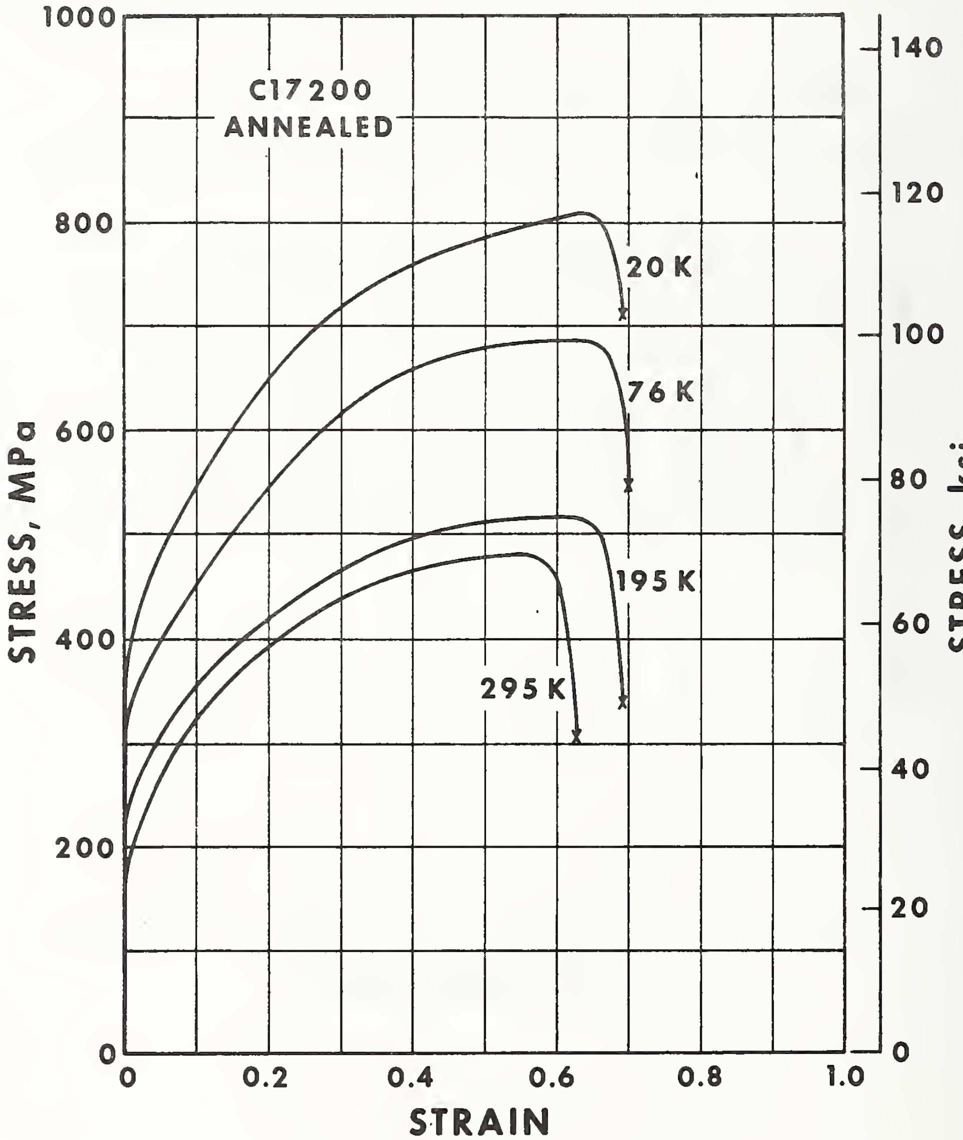

Figure 9.78. Stress-strain curves at four temperatures for annealed C17200 beryllium copper bar are shown. Reference 9.7 is the source of these data.

C17200: Annealed; Cold-worked

Engineering Stress vs. Strain (20, 76, 195, 295 K)

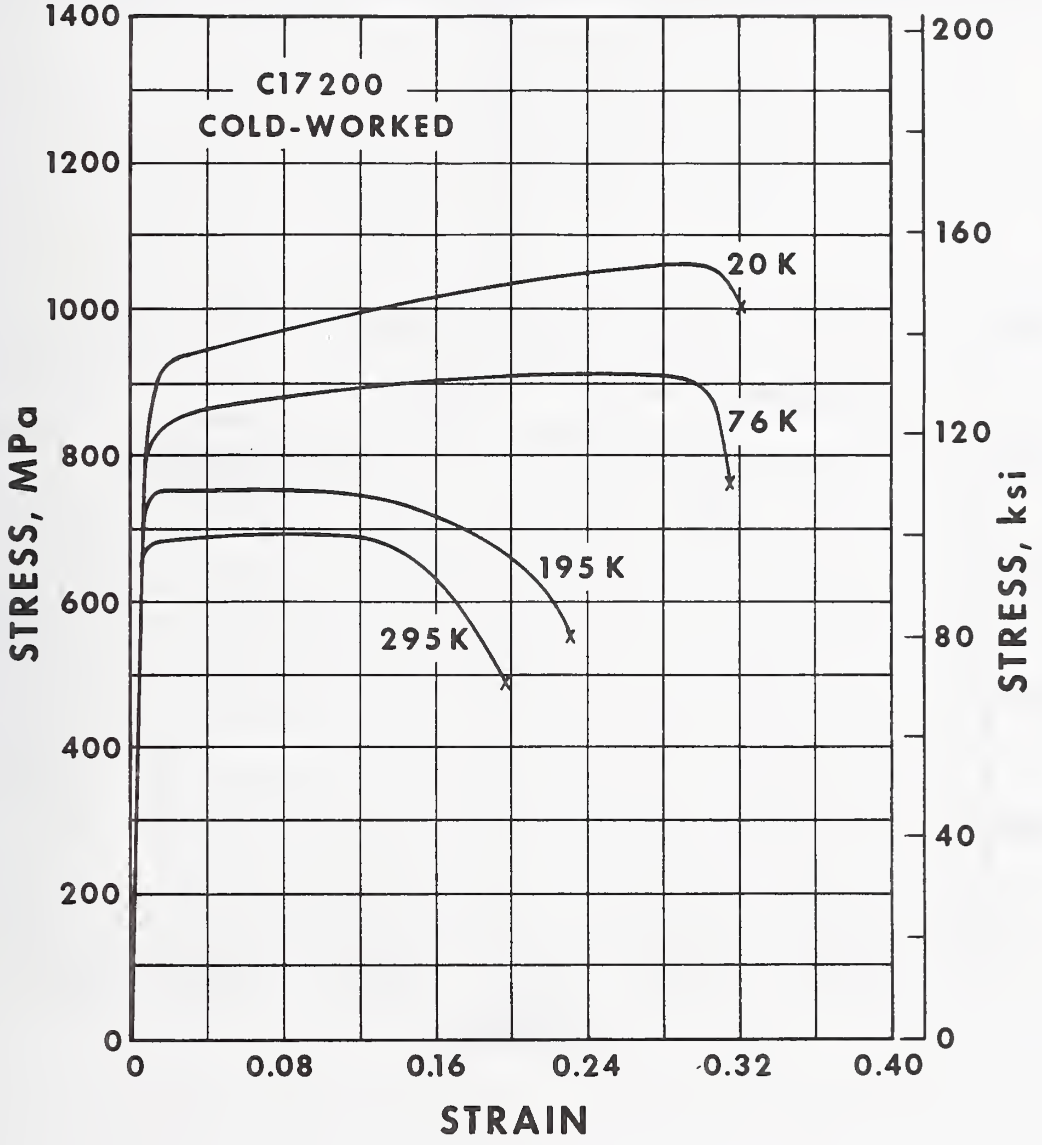

Figure 9.79. Stress-strain curves at four temperatures for 37% cold-worked C17200 beryllium copper bar are shown. Reference 9.7 is the source of these data.

DATA SOURCES AND ANALYSIS

Stress-strain curves at 4, 76, and 295 K for 37% cold-rolled and aged C17510 beryllium copper are presented in Figure 9.80. Reference 9.44 is the source of these data. The available characterization of materials and measurements is given in Table 9.57 at the end of the tensile properties section. Measurements were displacement-controlled.

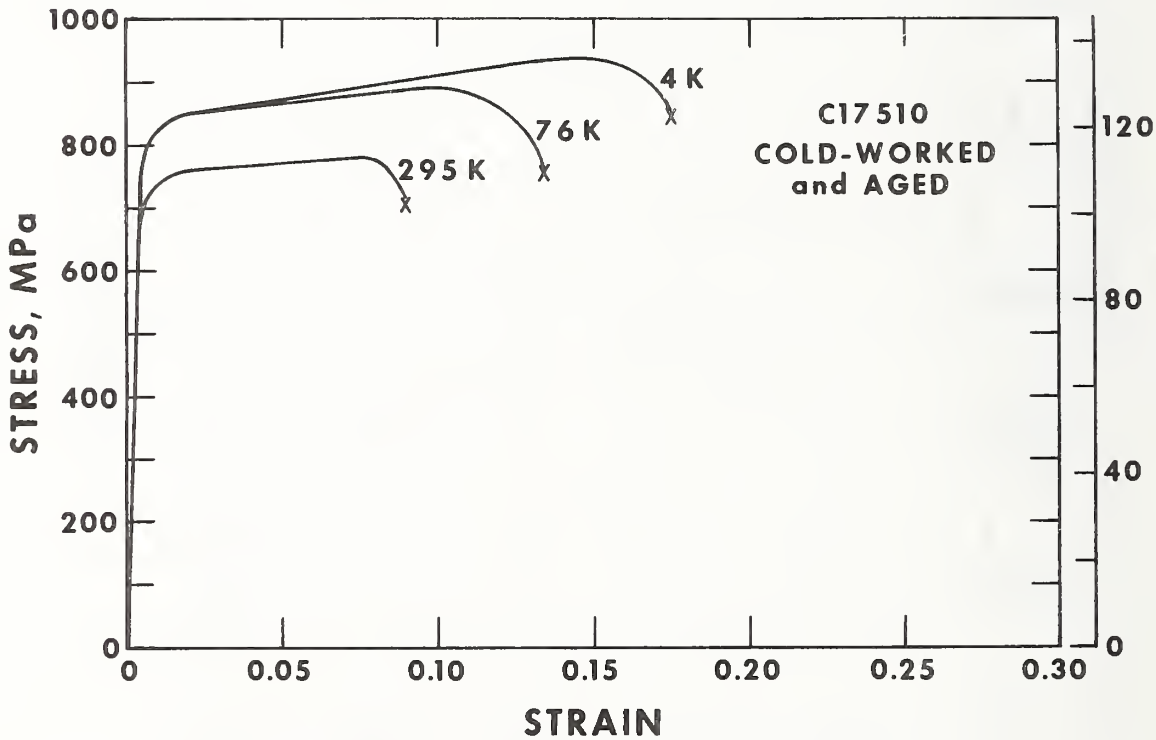

Figure 9.80. Stress-strain curves at three temperatures for cold-worked and aged C17510 beryllium copper plate are shown. Reference 9.44 is the source of these data.

Table 9.57. Characterization of Materials and Measurements.

Reference No.	1A	1B	1C	1D
Specification	C17000	C17000	C17200	C17200
Composition (wt%)				
Cu	> 98.37	> 98.37	> 97.86	> 97.86
Cu + Ag	—	—	—	—
Be	1.57	1.57	2.08	2.08
Ni	—	—	—	—
Co	—	—	—	—
Ni + Co	—	—	—	—
Ni + Fe + Co	—	—	—	—
Al	—	—	—	—
Fe	—	—	—	—
Si	—	—	—	—
Others (Only ≥ 0.001 wt%)	< 0.06 impurities	< 0.06 impurities	< 0.06 impurities	< 0.06 impurities
Material Condition	Annealed, 1073 K, 3 h	Aged (a)	Annealed, 1073 K, 3 h	Aged (a)
Grain Size	300 μm	—	300 μm	—
Hardness	—	—	—	—
Product Form	Strip, 0.32-cm-thick	Strip, 0.32-cm-thick	Strip, 0.32-cm-thick	Strip, 0.32-cm-thick
Specimen Type	Flat	Flat	Flat	Flat
Width or Dia.	0.35 cm	0.35 cm	0.35 cm	0.35 cm
Thickness	0.3 cm	0.3 cm	0.3 cm	0.3 cm
Gage Length	1.0 cm	1.0 cm	1.0 cm	1.0 cm
Strain or Load Rate	0.012 cm/min (crosshead)	0.012 cm/min (crosshead)	0.012 cm/min (crosshead)	0.012 cm/min (crosshead)
No. of Specimens	—	—	—	—
Test Temperature	77, 175, 293 K	77, 175, 293 K	77, 175, 293 K	77, 175, 293 K

(a) Aged: 458 K, 45 h; 408 K, 48 h; 360 K, 20 h.

2A	2B	2C	2D	2E
C17000	C17000	C17000	C17000	C17000
> 97.85 > 97.86 1.59 0.01 0.25 — — 0.05 0.12 0.07 (a)	97.78 97.79 1.70 0.002 0.20 — — 0.05 0.11 0.07 (b)	> 97.85 > 97.86 1.59 0.01 0.25 — — 0.05 0.12 0.07 (a)	97.78 97.79 1.70 0.002 0.20 — — 0.05 0.11 0.07 (b)	> 97.85 > 97.86 1.59 0.01 0.25 — — 0.05 0.12 0.07 (a)
Annealed, 1066 K, 0.12 h	Annealed, 1066 K, 0.12 h	Aged, 588–616 K, 3 h; 630 K, 2 h	Aged, 588–616 K, 3 h; 630 K, 2 h	Cold-rolled, 11%, 21%, 37%, then aged (c)
25 μm	25 μm	25 μm	25 μm	20, 25 μm
R_B 53	R_B 55	R_C 31–36	R_C 34–37	R_C 32–38
Strip, 0.25-cm-thick	Strip, 0.25-cm-thick	Strip, 0.25-cm-thick	Strip, 0.25-cm-thick	Strip, 0.25-cm-thick
Flat — 0.08 cm 5.0 cm	Flat — 0.08 cm 5.0 cm	Flat 1.9 cm 0.08 cm 5.0 cm	Flat 1.9 cm 0.08 cm 5.0 cm	Flat 1.9 cm 0.08 cm 5.0 cm
—	—	—	—	—
—	—	—	—	—
295 K	295 K	295 K	295 K	295 K

(a) Sn: < 0.01; Pb: 0.002; Zn: < 0.03; Cr: 0.005; Mn: 0.005.
(b) Sn: 0.02; Pb: 0.003; Zn: 0.051; Cr: 0.002; Mn: 0.002.
(c) Aged: 588–630 K; 2–3 h.

Table 9.57, continued

Reference No.	2F	2G	2H	2I
Specification	C17000	C17200	C17200	C17200
Composition (wt%)				
Cu	97.78	> 97.49	> 97.36	> 97.20
Cu + Ag	97.79	> 97.50	> 97.38	> 97.22
Be	1.70	1.81	1.96	2.09
Ni	0.002	0.01	0.01	0.02
Co	0.20	0.30	0.26	0.26
Ni + Co	—	—	—	—
Ni + Fe + Co	—	—	—	—
Al	0.05	0.05	0.07	0.05
Fe	0.11	0.15	0.14	0.14
Si	0.07	0.13	0.11	0.17
Others (Only ≥ 0.001 wt%)	(a)	(c)	(d)	(e)
Material Condition	Cold-rolled, 11% 21%, 37%, then aged (b)	Aged, 588–616 K, 3 h; 630 K, 2 h	Aged, 588–616 K, 3 h; 630 K, 2 h	Aged, 588–616 K, 3 h, 630 K, 2 h
Grain Size	20, 25 μm	25 μm	25 μm	20, 25 μm
Hardness	R_C 36–39	R_C 38–40	R_C 41–43	R_C 41–43
Product Form	Strip, 0.25-cm-thick	Strip, 0.25-cm-thick	Strip, 0.25-cm-thick	Strip, 0.25-cm-thick
Specimen Type	Flat	Flat	Flat	Flat
Width or Dia.	1.9 cm	1.9 cm	1.9 cm	1.9 cm
Thickness	0.08 cm	0.08 cm	0.08 cm	0.08 cm
Gage Length	5.0 cm	5.0 cm	5.0 cm	5.0 cm
Strain or Load Rate	—	—	—	—
No. of Specimens	—	—	—	—
Test Temperature	295 K	295 K	295 K	295 K

(a) Sn: 0.02; Pb: 0.003; Zn: 0.051; Cr: 0.002; Mn: 0.002.
(b) Aged: 588–630 K; 2–3 h.
(c) Sn: 0.01; Pb: 0.001; Zn: < 0.03; Cr: 0.003; Mn: 0.003.
(d) Sn: 0.03; Pb: 0.001; Zn: < 0.03; Cr: 0.005, Mn: 0.008.
(e) Sn: 0.01; Pb: 0.001; Zn: < 0.03; Cr: 0.005; Mn: 0.008.

C17000–C17510: Annealed; Annealed and Aged; Cold-worked; Cold-worked and Aged — *Tensile Properties (All)*

2J	2K	2L	3A	3B
C17200	C17200	C17[illegible]00	C17000	C17000
> 97.49 > 97.50 1.81 0.01 0.30 — — 0.05 0.15 0.13 (a)	> 97.36 > 97.38 1.96 0.01 0.26 — — 0.07 0.14 0.11 (c)	> 97.20 > 97.22 2.09 0.02 0.26 — — 0.05 0.14 0.17 (d)	Balance — 1.6–1.79 0.01 0.25 0.26 0.36 0.05 0.10 0.08 (e)	Balance — 1.6–1.79 0.01 0.25 0.26 0.36 0.05 0.10 0.08 (e)
Cold-rolled, 11%, 21%, 37%, then aged (b)	Cold-rolled, 11%, 21%, 37%, then aged (b)	Cold-rolled, 11%, 21%, 37%, then aged (b)	Aged (f)	Cold-rolled, 11%, 21%, 50%, then aged (f)
25 μm	25 μm	20, 25 μm	—	—
R_C 39–42	R_C 40–44	R_C 40–44	—	—
Strip, 0.25-cm-thick	Strip, 0.25-cm-thick	Strip, 0.25-cm-thick	Strip	Strip
Flat 1.9 cm 0.08 cm 5.0 cm	Flat 1.9 cm 0.08 cm 5.0 cm	Flat 1.9 cm 0.08 cm 5.0 cm	Flat (g) (h) 0.025 cm 5.0 cm	Flat (g) (h) 0.025 cm 5.0 cm
—	—	—	—	—
—	—	—	—	—
295 K	295 K	295 K	295 K	295 K

(a) Sn: 0.01; Pb: 0.001; Zn: < 0.03; Cr: 0.003; Mn: 0.003.
(b) Aged: 588–630 K; 2–3 h.
(c) Sn: 0.03; Pb: 0.001; Zn: < 0.03; Cr: 0.005; Mn: 0.008.
(d) Sn: 0.01; Pb: 0.001; Zn: < 0.03; Cr: 0.005; Mn: 0.008.
(e) Sn: 0.015; Zn: < 0.01; Cr: < 0.015; Pb: < 0.05.
(f) Aging conditions considered proprietary.
(g) Longitudinal and transverse orientations.
(h) Ultimate tensile strength and tensile elongation measurements obtained using 1.27-cm-wide specimens, tensile yield strength obtained using 0.64-cm-wide specimens.

Table 9.57, continued

Reference No.	3C	3E	3E	3F
Specification	C17200	C17200	C17200	C17500
Composition (wt%)				
Cu	Balance	Balance	Balance	Balance
Cu + Ag	—	—	—	—
Be	1.8–2.0	1.8–2.0	1.8–2.0	0.40–0.70
Ni	0.01	0.01	0.01	0.01
Co	0.25	0.25	0.25	2.5
Ni + Co	0.26	0.26	0.26	2.51
Ni + Fe + Co	0.36	0.36	0.36	2.56
Al	0.05	0.05	0.05	0.01
Fe	0.10	0.10	0.10	0.05
Si	0.08	0.08	0.08	0.05
Others (Only ≥ 0.001 wt%)	(a)	(a)	(a)	(e)
Material Condition	Aged, 588 K, 2 h	Cold-rolled, 11%, 21%, 37%, then aged, 588 K, 2 h	Cold-rolled, 37% 50%, then aged (d)	Aged, 755 K, 3 h
Grain Size	—	—	—	—
Hardness	—	—	—	—
Product Form	Strip	Strip	Strip	Strip
Specimen Type	Flat (b)	Flat (b)	Flat (b)	Flat (b)
Width or Dia.	(c)	(c)	(c)	1.27 cm
Thickness	0.025 cm	0.025 cm	0.025 cm	0.025 cm
Gage Length	5.0 cm	5.0 cm	5.0 cm	5.0 cm
Strain or Load Rate	—	—	—	—
No. of Specimens	—	—	—	—
Test Temperature	295 K	295 K	295 K	295 K

(a) Sn: 0.015; Zn: < 0.01; Cr: < 0.005; Pb: < 0.005.
(b) Longitudinal and transverse orientations.
(c) Ultimate tensile strength and tensile elongation measurements obtained using 1.27-cm-wide specimens, tensile yield strength obtained using 0.64-cm-wide specimens.
(d) Aging conditions considered proprietary.
(e) Sn: 0.005; Zn: < 0.01; Cr: < 0.005; Pb: < 0.005.

C17000–C17510: Annealed; Annealed and Aged; Cold-worked; Cold-worked and Aged

Tensile Properties (All)

3G	4A	4C	4C	4D
C17500	C17000	C17000	C17000	C17200
Balance — 0.40–0.70 0.01 2.5 2.51 2.56 0.01 0.05 0.05 (a)	Balance — 1.6–1.79 — 0.20–0.60 — — — — — —	Balance — 1.6–1.79 — 0.20–0.60 — — — — — —	Balance — 1.8–2.0 — 0.20–0.60 — — — — — —	Balance — 1.8–2.0 — 0.20–0.60 — — — — — —
Cold-rolled, 3%, then aged, 755 K, 3 h (b)	Aged (d)	Cold-rolled, 37% then aged (d)	Aged (d)	Cold-rolled, 37%, then aged (d)
—	—	—	—	—
—	—	—	—	—
Strip	Strip	Strip	Strip	Strip
Flat (c) 1.27 cm 0.025 cm 5.0 cm	Flat 1.3 cm — 10.0 cm	Flat 1.3 cm — 10.0 cm	Flat 1.3 cm — 10.0 cm	Flat 1.3 cm — 10.0 cm
—	—	—	—	—
—	—	—	—	—
295 K	295 K	295 K	295 K	295 K

(a) Sn: 0.005; Zn: < 0.01; Cr: < 0.005; Pb: < 0.005.
(b) Other specimens cold-rolled, 11%, then aged, 755 K, 2 h.
(c) Longitudinal and transverse orientations.
(d) Aging conditions not specified.

Table 9.57, continued

Reference No.	4E	4F	4G	4H
Specification	C17500	C17500	C17510	C17510
Composition (wt%)				
Cu	Balance	Balance	Balance	Balance
Cu + Ag	—	—	—	—
Be	2.4–2.7	2.4–2.7	0.20–0.60	0.20–0.60
Ni	—	—	1.4–2.20	1.4–2.20
Co	0.40–0.75	0.40–0.75	—	—
Ni + Co	—	—	—	—
Ni + Fe + Co	—	—	—	—
Al	—	—	—	—
Fe	—	—	—	—
Si	—	—	—	—
Others (Only ≥ 0.001 wt%)	—	—	—	—
Material Condition	Aged (a)	Cold-rolled, 37% then aged (a)	Aged (a)	Cold-rolled, 37%, then aged (a)
Grain Size	—	—	—	—
Hardness	—	—	—	—
Product Form	Strip	Strip	Strip	Strip
Specimen Type	Flat	Flat	Flat	Flat
Width or Dia.	1.3 cm	1.3 cm	1.3 cm	1.3 cm
Thickness	—	—	—	—
Gage Length	10.0 cm	10.0 cm	10.0 cm	10.0 cm
Strain or Load Rate	—	—	—	—
No. of Specimens	—	—	—	—
Test Temperature	295 K	295 K	295 K	295 K

(a) Aging conditions not specified.

5A	5B	5C	5D	5E
C17000	C17000	C17200	C17200	C17200
98.1 — 1.68 — 0.23 — — — — — —	98.0 — 1.77 — 0.24 — — — — — —	98.0 — 1.8 — 0.21 — — — — — —	97.98 — 1.81 — 0.21 — — — — — —	97.99 — 1.80 — 0.21 — — — — — —
Cold-rolled, 11%, then aged, 589 K, 2 h	Cold-rolled, 11%, then aged (a)	Cold-rolled, 11% then aged (a)	Cold-rolled, 11% then aged, 589 K, 2 h	Cold-rolled, 21% then aged (a)
—	—	—	—	—
—	—	—	—	—
Strip	Strip	Strip	Strip	Strip
Flat — 0.041 cm 2.5 cm	Flat — 0.041 cm 2.5 cm	Flat — 0.038 cm 2.5 cm	Flat — 0.041 cm 2.54 cm	Flat — 0.038 cm 2.54 cm
—	—	—	—	—
—	—	—	—	—
295 K	295 K	295 K	295 K	295 K

(a) Aging conditions considered proprietary.

Table 9.57, continued

Reference No.	5F	5G	6A	6B
Specification	C17200	C17200	C17200	C17200
Composition (wt%)				
Cu	97.92	97.86	97.56	97.56
Cu + Ag	—	—	—	—
Be	1.84	1.85	1.85	1.85
Ni	—	—	0.02	0.02
Co	0.24	0.29	0.28	0.28
Ni + Co	—	—	—	—
Ni + Fe + Co	—	—	—	—
Al	—	—	0.02	0.02
Fe	—	—	0.12	0.12
Si	—	—	0.14	0.14
Others (Only ≥ 0.001 wt%)	—	—	Sn: 0.01	Sn: 0.01
Material Condition	Cold-rolled, 21%, then aged, 589 K, 2 h	Cold-rolled, 37%, then aged, 589 K, 2 h	Annealed	Aged, 588 K, 3 h; or 672 K, 1.5 h
Grain Size	—	—	25 μm	25 μm
Hardness	—	—	R_B 64	(a)
Product Form	Strip	Strip	Bar, 1.4-cm-dia.	Bar, 1.4-cm-dia.
Specimen Type	Flat	Flat	Round	Round
Width or Dia.	—	—	0.64 cm	0.64 cm
Thickness	0.038 cm	0.038 cm	—	—
Gage Length	2.54 cm	2.54 cm	2.0 cm	2.0 cm
Strain or Load Rate	—	—	—	—
No. of Specimens	—	—	—	—
Test Temperature	295 K	295 K	88–300 K	88–300 K

(a) Aged: 588 K, R_C 39; 672 K, R_C 35.

C17000–C17510: Annealed; Annealed and Aged; Cold-worked; Cold-worked and Aged — *Tensile Properties (All)*

6C	6D	6E	7A	7B
C17200	C17200	C17500	C17200	C17200
97.68	97.68	96.48	97.7	97.7
—	—	—	—	—
1.86	1.86	0.58	1.8	1.8
0.01	0.01	0.03	—	—
0.22	0.22	2.64	0.2	0.2
—	—	—	—	—
—	—	—	—	—
0.02	0.02	0.02	0.1	0.1
0.13	0.13	0.13	0.1	0.1
0.07	0.07	0.11	0.1	0.1
Sn: 0.01	Sn: 0.01	Sn: 0.01	—	—
Cold-drawn, 33%	Cold-drawn, 33%, then aged, 588 K, 2 h	Cold-drawn, 33%, then age, 755 K, 2 h	Annealed	Cold-rolled, 37%
35 μm	35 μm	—	16 μm (a)	13 μm (a)
R_C 21	R_C 42	R_C 22	R_B 55	R_B 95
Bar, 1.4-cm-dia.	Bar, 1.4-cm-dia.	Bar, 1.4-cm-dia.	Bar, 1.4-cm-dia.	Bar, 1.9-cm-dia.
Round 0.64 cm — 2.0 cm	Round 0.64 cm — 2.0 cm	Round 0.64 cm — 2.0 cm	Round 0.45 cm — 3.2 cm	Round 0.45 cm — 3.2 cm
—	—	—	0.02 cm/min (crosshead)	0.02 cm/min (crosshead)
—	—	—	—	—
88–300 K	88–300 K	88–300 K	20–295 K	20–295 K

(a) Grain size converted from ASTM number using ASTM standard E112-85.

Table 9.57, continued

Reference No.	8A	8B	9A	9B
Specification	C17200	C17200	C17200	C17200
Composition (wt%)				
Cu	—	—	97.63	97.63
Cu + Ag	—	—	—	—
Be	1.9	1.9	2.02	2.02
Ni	—	—	0.26	0.26
Co	—	—	—	—
Ni + Co	—	—	—	—
Ni + Fe + Co	—	—	—	—
Al	—	—	—	—
Fe	—	—	0.09	0.09
Si	—	—	—	—
Others (Only ≥ 0.001 wt%)	—	—	—	—
Material Condition	Annealed, 1073 K, 1 h	Cold-rolled, then aged, 588 K, 2 h; or 698 K, 24 h	Annealed	Cold-drawn, 60%
Grain Size	—	—	—	—
Hardness	—	—	Brinell 188	Brinell 225
Product Form	—	—	Bar, 1.6-cm-dia.	Bar, 1.6-cm-dia.
Specimen Type	Flat	Flat	Round	Round
Width or Dia.	0.45 cm	0.45 cm	0.95 cm	0.95 cm
Thickness	0.16 cm	0.16 cm	—	—
Gage Length	2.0 cm	2.0 cm	5.0 cm	5.0 cm
Strain or Load Rate	0.05 cm/min (crosshead)	0.05 cm/min (crosshead)	—	—
No. of Specimens	—	—	—	—
Test Temperature	215, 255, 303 K	215, 255, 303 K	232, 295 K	232, 295 K

C17000–C17510: Annealed; Annealed and Aged; Cold-worked; Cold-worked and Aged | *Tensile Properties (All)*

9C	11	12A	12B	13A
C17200	C17200	C17200	C17500	C17200
97.63	97.6–97.4	98.1	97.4	—
—	—	—	—	—
2.02	1.8–2.05	1.9	0.5	1.8–2.05
0.26	—	—	—	0.2–0.6 (c)
—	—	—	2.0	0.2–0.6 (c)
—	—	—	—	—
—	< 0.6	—	—	—
—	—	—	—	—
0.09	—	—	0.1	—
—	—	—	—	—
—	—	Sn: 0.01	—	—
Cold-drawn, 60%, then aged, 575 K, 2 h	Aged, 588 K, 3 h	Aged, 588 K, 3 h	Aged, 727 K, 8 h	Aged, 588 K, 3 h
—	—	—	—	—
Brinell 375	—	R_C 31–40	R_C 18–27	—
Bar, 1.6-cm-dia.	Sheet, 0.10-cm-thick	—	—	Plate, 1.3-cm-thick
Round 0.95 cm — 5.0 cm	Flat 0.51 cm — 5.7 cm	Round (a) 0.64 cm — 2.70 cm	Round (a) 0.64 cm — 2.7 cm	Round 0.64 cm — 5.87 cm
—	—	0.13 cm/min (b) (crosshead)	0.13 cm/min (b) (crosshead)	—
—	—	12	15	—
232, 295 K	20, 295 K	77–299 K	77–299 K	295 K

(a) Smooth and notched specimens. Notch radius, 0.013 cm. Distance between notches, 0.45 cm.
(b) Prior to 0.2% offset, then at 0.25 cm/min.
(c) Percent nickel or cobalt, or both.

Table 9.57, continued

Reference No.	13B	14B	14B	15A
Specification	C17200	C17200	C17200	C17200
Composition (wt%)				
Cu	—	—	—	97.65
Cu + Ag	—	—	—	—
Be	1.8–2.05	—	—	1.86
Ni	0.2–0.6 (a)	—	—	0.01
Co	0.2–0.6 (a)	—	—	0.19
Ni + Co	—	—	—	0.20
Ni + Fe + Co	—	—	—	0.36
Al	—	—	—	0.02
Fe	—	—	—	0.16
Si	—	—	—	0.07
Others (Only ≥ 0.001 wt%)	—	—	—	Sn: 0.01; Zn: 0.03
Material Condition	Cold-drawn, 37%, then aged, 588 K, 3 h	Aged, 566 K, 0.33–2 h	Cold-rolled, 15%, then aged, 561 K, 0.33–2 h	Aged, 588–633 K, 0.08–5 h
Grain Size	—	—	—	30 μm
Hardness	—	R_{30N} 44–57 (b)	R_{30N} 38.5–54 (b)	—
Product Form	Bar, 2.86-cm-dia.	Strip	Strip	Strip, 0.056-cm-thick
Specimen Type	Round	Flat	Flat	—
Width or Dia.	0.64 cm	—	—	—
Thickness	—	—	—	—
Gage Length	5.87 cm	5.0 cm	5.0 cm	5.0 cm
Strain or Load Rate	—	—	—	—
No. of Specimens	—	—	—	—
Test Temperature	295 K	295 K	295 K	295 K

(a) Percent nickel or cobalt, or both.
(b) To convert hardness to Rockwell C scale see Reference 9.2.

15B	15C	15D	16A	16B
C17200	C17200	C17200	C17200	C17200
97.65 — 1.86 0.01 0.19 0.20 0.36 0.02 0.16 0.07 Sn: 0.01; Zn: 0.03	97.34 — 1.91 0.02 0.29 0.31 0.55 0.06 0.24 0.14 —	97.39 — 1.87 0.02 0.39 0.41 0.63 0.03 0.22 0.08 —	97.54 — 2.16 0.22 — — 0.33 — 0.11 — —	97.46 — 2.20 0.21 — — 0.36 — 0.15 — —
Cold-rolled, 17%, 34%, then aged, 588 K, 3 h	Aged, 293–763 K, 1 h	Cold-rolled, 21%, then aged, 293–763 K, 1 h	Aged, 573 K, 3 h	Cold-drawn, 15%, then aged, 573 K, 3 h
30 μm	30 μm	30 μm	—	75 μm
—	—	—	—	—
Strip, 0.056-cm-thick	Strip, 0.05-cm-thick	Strip, 0.055-cm-thick	Bar, 1.9-cm-dia.	Bar, 1.9-cm-dia.
— — — 5.0 cm	— — — 5.0 cm	— — — 5.0 cm	Round 1.28 cm — 5.0 cm	Round 1.28 cm — 5.0 cm
—	—	—	—	—
—	—	—	—	—
295 K	295 K	295 K	295 K	295 K

Table 9.57, continued

Reference No.	17	18A	18B	19A
Specification	C17200	C17200	C17200	C17200
Composition (wt%)				
Cu	97.75	97.40	97.35	97.59
Cu + Ag	—	97.42	97.37	—
Be	1.93	1.89	1.94	1.89
Ni	—	0.01	0.015	0.01
Co	0.19	0.29	0.27	0.24
Ni + Co	—	0.30	0.285	0.25
Ni + Fe + Co	—	0.45	0.425	0.34
Al	0.02	0.06	0.09	0.06
Fe	0.02	0.15	0.14	0.09
Si	0.08	0.13	0.12	0.11
Others (Only ≥ 0.001 wt%)	Mg: 0.006	(b)	(d)	Sn: 0.01
Material Condition	Aged, 473 K, 0.5–167 h	Aged, 388 K, 3 h	Cold-rolled, 21%, then aged, 588 K, 2 h	Aged, 644 K, 0.5 h
Grain Size	—	—	—	25 μm (f)
Hardness	(a)	(c)	(e)	R_C 42
Product Form	—	—	—	Sheet, 0.16-cm-thick
Specimen Type	—	Flat	Flat	—
Width or Dia.	—	—	—	—
Thickness	—	0.05	0.20 cm	—
Gage Length	—	—	—	5.0 cm
Strain or Load Rate	—	0.005 cm/min (crosshead)	0.005 cm/min (crosshead)	0.002/cm
No. of Specimens	—	—	—	—
Test Temperature	295 K	295 K	295 K	200, 300 K

(a) Micro-Vickers hardness, 130–250.
(b) Mn: 0.005; Cr: 0.006; Sn: 0.010; Pb: 0.002; Zn: 0.30.
(c) Vickers Diamond, 5 kg load, 362.
(d) Mn: 0.004; Cr: 0.001; Sn: 0.02; Pb: 0.002; Zn: 0.03.
(e) Vickers Diamond, 5-kg load, 368.
(f) Grain size converted from grains/cm^3 using ASTM standard E112-85.

C17000–C17510: Annealed; Annealed and Aged; Cold-worked; Cold-worked and Aged

Tensile Properties (All)

19B	19C	19D	20	21A
C17200	C17200	C17200	C17200	C17200
97.49 — 1.95 0.01 0.25 0.26 0.33 0.02 0.13 0.07 Sn: 0.02; Zn: 0.06	97.59 — 1.89 0.02 0.26 0.28 0.37 0.06 0.09 0.09 —	97.69 — 1.84 0.02 0.18 0.20 0.32 0.03 0.12 0.09 Sn: 0.03	97.46 — 2.08 — — 0.40 — — — — —	Balance — 1.81–1.86 0.01–0.03 0.23–0.27 — — 0.01–0.07 0.08–0.10 0.06–0.09 Sn: 0.01
Aged, 644 K, 0.5 h	Cold-rolled, 37%, then aged, 644 K, 0.33 h	Cold-rolled, 37% then aged, 644 K, 0.33 h	Aged, 588 K, 3 h	Aged, 588 K, 2 h
82 µm (a)	75 µm (a)	41 µm (a)	—	—
R_C 42	R_C 42	R_C 42	R_C 37	—
Sheet, 0.16-cm-thick	Sheet, 0.16-cm-thick	Sheet, 0.16-cm-thick	Bar, 0.62-cm-wide	—
— — — 5.0 cm	— — — 5.0 cm	— — — 5.0 cm	Round 0.8 cm — —	Wire 0.14–0.20 cm — —
0.002/min	0.002/min	0.002/min	—	—
—	—	—	—	—
200, 300 K	200, 300 K	200, 300 K	295 K	295 K

(a) Grain size converted from grains/cm^3 using ASTM standard E112-85.

Table 9.57, continued

Reference No.	21B	22	25A	25B
Specification	C17200	C17200	C17200	C17500
Composition (wt%)				
Cu	Balance	97.742	97.7	96.8
Cu + Ag	—	—	—	—
Be	1.81–1.86	1.95	1.9	0.51
Ni	0.01–0.03	—	—	—
Co	0.23–0.27	0.248	0.21	2.6
Ni + Co	—	—	—	—
Ni + Fe + Co	—	—	—	—
Al	0.01–0.07	—	—	—
Fe	0.08–0.10	—	0.07	0.05
Si	0.06–0.09	—	0.08	0.05
Others (Only ≥ 0.001 wt%)	Sn: 0.01	All others, 0.06	—	—
Material Condition	Cold-drawn, 18%, 39%, 50%, then aged (a)	Aged, 473–723 K, times not given	Cold-rolled, 21%	Cold-rolled, 21%
Grain Size	—	—	—	—
Hardness	—	—	R_B 98	R_B 73
Product Form	—	Plate, 0.15-cm-thick	Sheet, 0.32-cm-thick	Sheet, 0.32-cm-thick
Specimen Type	Wire	Flat	Flat	Flat
Width or Dia.	0.14–0.20 cm	1.5 cm	1.3 cm	1.3 cm
Thickness	—	0.15 cm	0.12 cm	0.12 cm
Gage Length	—	7.3 cm	5.0 cm	5.0 cm
Strain or Load Rate	—	—	(b)	(b)
No. of Specimens	—	—	—	—
Test Temperature	295 K	295 K	2–300 K	20–300 K

(a) Aged: 588–644 K; 0.05–24 h.
(b) 0.0005/min to yield strength, then 0.02/min.

26	27A	27B	28	29
C17200	C17200	C17200	C17200	C17200
97.43 — 1.89 — 0.29 0.30 0.45 0.06 0.15 0.13 Cr: 0.006; Mn: 0.005; Zn: 0.03; Pb: 0.002	Balance — 1.9–1.99 0.00–0.02 0.23–0.31 0.23–0.33 0.30–0.45 0.05–0.08 0.07–0.12 0.07–0.13 —	Balance — 1.9–1.99 0.00–0.02 0.23–0.31 0.23–0.33 0.30–0.45 0.05–0.08 0.07–0.12 0.07–0.13 —	97.54–97.55 97.56 1.92 0.03 0.25 0.28 0.33 0.05 0.05 0.1 Zn: 0.025; Mn: 0.009; Cr: 0.003; Pb: 0.004	97.62 97.63 1.87 0.011 0.24 0.251 0.311 0.06 0.06 0.014 (c)
Cold-worked, ½ hard	Annealed	Cold-rolled, 11%, 21%, 37%	Cold-drawn, then aged (b)	Cold-rolled, 96.5%, then aged, 297–647 K, 2 h
—	10–120 μm	10–120 μm	—	—
R_B 100	—	—	—	—
—	Strip	Strip	Bar, 1.91-cm-dia.	Plate, 0.73-cm-thick
Round 0.405 cm — 2.0 cm	Flat (a) — 0.01–0.1 cm 5.0 cm	Flat (a) — 0.01–0.11 cm 5.0 cm	Round 0.762 cm — —	Flat (a) — 0.025 cm 5.0 cm
0.012–1.2 cm/min (crosshead)	—	—	0.06/min	0.05/min
—	—	—	—	—
20, 77, 300 K	295 K	295 K	295 K	295 K

(a) Longitudinal and transverse orientations.
(b) Aging conditions not specified.
(c) Sn: 0.01; Zn: 0.12; Mn: 0.001; Cr: 0.006; Pb: 0.004.

Table 9.57, continued

Reference No.	30	31A	31B	31C
Specification	C17200	C17200	C17200	C17200
Composition (wt%)				
Cu	97.55	97.53	97.49	97.48
Cu + Ag	97.56	—	—	—
Be	1.91	1.83	1.82	1.86
Ni	—	—	—	—
Co	0.21	0.22	0.18	0.22
Ni + Co	—	0.23	0.21	0.23
Ni + Fe + Co	0.34	—	—	—
Al	0.05	—	—	—
Fe	0.07	0.11	0.12	0.13
Si	0.07	0.07	0.15	0.07
Others (Only ≥ 0.001 wt%)	(a)	Sn: 0.01	Sn: 0.02; Pb: 0.002	Sn: 0.01
Material Condition	Cold-rolled, 2.5–37%, then aged, 573 K (b)	Cold-drawn, 44%, then aged, 588 K, 2 h	Cold-drawn, 35%, then aged, 588 K, 2 h	Cold-drawn, 33% then aged, 588 K, 2 h
Grain Size	—	25 μm	25 μm	35 μm
Hardness	—	—	R_B 95	R_B 99
Product Form	Strip, 2. 54 × 10.16 × 0.089 cm	Bar	Bar	Bar
Specimen Type	Flat	Round	Round	Round
Width or Dia.	1.2 cm	0.23 cm	0.56 cm	1.42 cm
Thickness	—	—	—	—
Gage Length	2.0 cm	5.0 cm	5.0 cm	5.0 cm
Strain or Load Rate	0.02/min	—	—	—
No. of Specimens	—	—	—	—
Test Temperature	295 K	295 K	295 K	295 K

(a) Cr: 0.003; Mn: 0.007; Sn: 0.03; Zn: 0.02; Pb: 0.005.
(b) Aging times up to 6 h.

C17000–C17510: Annealed; Annealed and Aged; Cold-worked; Cold-worked and Aged

Tensile Properties (All)

32	33	36A	36B	36C
C17200	C17200	C17500	C17500	C17510
— — 1.93 — 0.24 — — — — — —	— — 1.80–2.05 — — — — — — — —	97.05 — 0.5 — 2.35 — — — — — All others, ~ 0.1	97.05 — 0.5 — 2.35 — — — — — All others, ~ 0.1	97.59 — 0.41 1.90 — — — — — — All others, ~ 0.1
Cold-drawn, 37% then aged, 594 K, 3 h	Cold-drawn, 50% then aged, 588–644 K, 1–8 h	Aged, 753 K, 0.13–8 h	Cold-worked, hard, then aged, 753 K, 0.13–8 h	Aged, 753 K, 0.13–8 h
3–40 μm	—	—	—	—
—	—	Vickers 110–251	Vickers 160–278	Vickers 110–240
Wire, 0.089-cm-dia.	—	—	—	—
Wire 0.089 cm — 25.0 cm	Wire — — —	— — — 5.0 cm	— — — 5.0 cm	— — — 5.0 cm
—	—	—	—	—
—	—	—	—	—
295 K	295 K	295 K	295 K	295 K

Table 9.57, continued

Reference No.	36D	38A	38B	39A
Specification	C17510	C17500	C17500	C17500
Composition (wt%)				
Cu	97.59	96.35	96.35	96.7
Cu + Ag	—	—	—	—
Be	0.41	0.44	0.44	0.5
Ni	1.90	0.13	0.13	(a)
Co	—	2.61	2.61	2.6
Ni + Co	—	2.74	2.74	—
Ni + Fe + Co	—	2.89	2.89	—
Al	—	—	—	—
Fe	—	0.15	0.15	—
Si	—	0.32	0.32	—
Others (Only ≥ 0.001 wt%)	All others, ~ 0.1	—	—	—
Material Condition	Cold-worked, hard then aged, 753 K, 0.13–8 h	Cold-worked, 50%	Cold-worked, 50% then aged, 723 K, 0.75–3 h	Cold-worked, 65%, then aged (b)
Grain Size	—	—	—	—
Hardness	Vickers 160–251	—	—	—
Product Form	—	—	—	Bar, 1.6-cm-dia.
Specimen Type	—	—	—	—
Width or Dia.	—	—	—	(c)
Thickness	—	—	—	—
Gage Length	5.0 cm	5.0 cm	5.0 cm	7.0 cm
Strain or Load Rate	—	—	—	0.2/min
No. of Specimens	—	—	—	—
Test Temperature	295 K	295 K	295 K	295 K

(a) Fe + Ni: 0.25 wt%.
(b) Aging conditions not specified.
(c) Specimen geometry not specified, cross-section = 0.32 cm^2.

C17000–C17510: Annealed; Annealed and Aged; Cold-worked; Cold-worked and Aged — *Tensile Properties (All)*

39B	40A	40B	41A	41B
C17500	C17510	C17510	C17510	C17510
96.7 — 0.54 (a) 2.6 — — — — — —	98.1 — 0.38 1.53 — — — — — — —	98.1 — 0.38 1.53 — — — — — — —	(e) — 0.2–0.6 1.4–2.2 — — — — — — —	(e) — 0.2–0.6 1.4–2.2 — — — — — — —
Cold-worked, 65%, then aged (b)	Aged, 728–755 K (d)	Cold-rolled, 21%, then aged, 727–838 K, 8 h	Cold-worked, 40%, then aged, 755 K, 3 h	Cold-worked, then aged (b)
—	—	—	—	—
—	—	—	—	—
Bar, 1.6-cm-dia.	Strip	Strip	—	—
— (c) — 7.0 cm	Flat — — 5.0 cm	Flat — 0.04 —	— — — —	(f) — — —
0.2/min	—	—	—	—
—	—	—	—	—
295 K	295 K	295 K	293 K	293 K

(a) Fe + Ni: 0.25 wt%.
(b) Aging conditions not specified.
(c) Specimen geometry not specified, cross-section = 0.32 cm^2.
(d) Aging times not specified.
(e) Cu + Be + Ni: 99.5 wt%.
(f) Longitudinal and transverse orientations.

Table 9.57, continued

Reference No.	42	43	44	45
Specification	C17510	C17510	C17510	C17510
Composition (wt%)				
Cu	97.6	97.8	—	97.95
Cu + Ag	—	—	97.6	—
Be	0.4	0.4	0.38	0.38
Ni	2.0	1.8	1.8	1.67
Co	—	—	0.05	—
Ni + Co	—	—	—	—
Ni + Fe + Co	—	—	—	—
Al	—	—	0.01	—
Fe	—	—	0.03	—
Si	—	—	0.02	—
Others (Only ≥ 0.001 wt%)	—	—	(e)	—
Material Condition	Cold-worked, 40%, then aged, 755 K (a)	Cold-rolled, 37%, then aged (b)	Cold-rolled, 37% then aged, 755 K, 2 h	Cold-rolled, 60%, 80%, then aged (f)
Grain Size	—	—	—	—
Hardness	—	(c)	R_F 92	—
Product Form	—	Strip, 0.02-cm-thick	Plate, 2.5-cm-thick	Plate, 1.3-cm-thick
Specimen Type	—	(d)	Round (d)	Flat
Width or Dia.	—	—	0.64 cm	0.64 cm
Thickness	—	—	—	1.3 cm
Gage Length	—	2.0 cm	3.8 cm	2.54 cm
Strain or Load Rate	—	—	0.20 cm/min (crosshead)	—
No. of Specimens	—	—	2 per temperature	—
Test Temperature	295 K	295 K	4, 76, 295 K	295 K

(a) Aging times not specified.
(b) Aging conditions not specified.
(c) Diamond pyramid hardness, 250–305.
(d) Longitudinal and transverse orientations.
(e) Zr: 0.03; Sn: 0.01; Zn: 0.01; Ag: 0.01; Cr: 0.005; Pb: 0.002; Mn: 0.002.
(f) Aged: 573–673 K; 1–70 h.

46A	46B	46C	49	50
C17510	C17510	C17510	C17000	C17000
Balance — 0.38 1.79 0.05 — — 0.01 0.03 0.02 (a)	Balance — 0.40 1.91 0.01 — — 0.01 0.01 0.02 (c)	Balance — 0.41 1.95 0.10 — — 0.01 0.04 0.03 (e)	98.49 — 1.5 — — — — — 0.10 — —	98.37 — 1.62 — — — — — 0.06 — —
Cold-rolled, 37%, then aged, 755 K, 2 h	(d)	(d)	Aged (g)	Annealed
—	—	—	—	—
—	—	R_B 95–99	—	—
Plate, 2.5-cm-thick	Plate, 2.5-cm-thick	Rod	—	Bar, 2.5-cm-dia.
Round (b) 0.64 cm — 3.8 cm	— — — —	Round (f) 0.32 cm — 2.5 cm	Round 0.62 cm — —	Wire — — 25.0 cm
< 21 MPa/s	—	—	—	—
Several	—	3	—	—
295 K	295 K	295 K	20, 77, 290 K	295 K

(a) Zr: 0.03; Sn: 0.01; Zn: 0.01; Ag: 0.01; Cr: 0.005; Pb: 0.002; Mn: 0.002.
(b) Specimen details from PPPL tests. Measurements from a commercial supplier also reported.
(c) Zn: 0.02; Ag: 0.01; Zr: 0.01; Sn: < 0.01; Ti: < 0.01; Cr: 0.004; Pb: 0.003; Mn: 0.001.
(d) Percent cold work and aging conditions not specified.
(e) Ag: 0.09; Sn: 0.02; Zn: 0.02; Cr: 0.007; Mn: 0.004; Pb: 0.003.
(f) Specimen details from MIT tests. Measurements from a commercial supplier also reported.
(g) Aging conditions not specified.

Table 9.57, continued

Reference No.	51A	51B	52A	52B
Specification	C17200	C17200	C17200	C17200
Composition (wt%)				
Cu	Balance	Balance	97.91	97.88
Cu + Ag	—	—	—	—
Be	1.90–2.15	1.90–2.15	1.87	1.88
Ni	—	—	< 0.01	< 0.01
Co	0.25–0.35	0.25–0.35	0.10	0.09
Ni + Co	—	—	< 0.011	< 0.10
Ni + Fe + Co	—	—	0.22	0.22
Al	—	—	—	—
Fe	—	—	0.12	0.13
Si	—	—	0.11	0.11
Others (Only ≥ 0.001 wt%)	—	—	—	—
Material Condition	Aged, 622 K, 0.067–1.1 h	Cold-worked, then aged (a)	Aged, 575 or 588 K, 3 h	Cold-rolled, 21%, then aged, 575 or 588 K, 2 h
Grain Size	—	—	—	—
Hardness	—	—	(b)	(c)
Product Form	—	—	Strip	Strip
Specimen Type	Strip	—	Flat	Flat
Width or Dia.	—	—	—	—
Thickness	—	—	0.082 cm	0.082 cm
Gage Length	—	—	5.0 cm	5.0 cm
Strain or Load Rate	—	—	—	—
No. of Specimens	—	—	—	—
Test Temperature	295 K	48–293 K	295 K	295 K

(a) Type of cold work and aging conditions not specified.
(b) Aged: 575 K, R_C 35.5; 588 K, in purified nitrogen, R_C 31.7; in muffle furnace, R_C 26.
(c) Aged: 575 K, R_C 36; 588 K, R_C 36.7.

52C	53A	53B	54A	54B
C17200	C17200	C17200	C17200	C17200
97.89	> 97.54	> 97.54	97.58	97.58
—	—	—	—	—
1.86	1.91	1.91	1.89	1.89
< 0.01	0.01	0.01	—	—
0.08	0.26	0.26	0.27	0.27
< 0.09	0.27	0.27	—	—
0.20	0.39	0.39	—	—
—	0.04	0.04	0.04	0.04
0.12	0.12	0.12	0.13	0.13
0.11	0.10	0.10	0.09	0.09
—	Sb: 0.005; Zn, Pb, Cr: < 0.005	Sb: 0.005; Zn, Pb, Cr: < 0.005	—	—
Cold-rolled, 37%, then aged, 575 or 588 K, 2 h	Aged, 588 K, 3 h	Cold-rolled, 37%, then aged, 588 K, 2 h	Aged, 561–644 K, 0.5–8 h	Cold-rolled, 3–83%, then aged, 588 K, 2 h
—	—	—	15 μm	—
(a)	R_{30N} 60 (b)	R_{30N} 62 (b)	—	R_{30N} 59–64 (b)
Strip	Strip, 0.05-cm-thick	Strip, 0.05-cm-thick	Strip	Strip
Flat — 0.082 cm 5.0 cm	Flat 1.3 cm — 5.0 cm	Flat 1.3 cm — 5.0 cm	Flat — — —	Flat — 0.02–0.13 cm —
—	0.005/min	0.005/min	—	—
—	—	—	—	—
295 K	295 K	295 K	295 K	295 K

(a) Aged: 575 K, R_C 38.6; 588 K, R_C 37.7.
(b) To convert hardness to Rockwell C scale see Reference 9.2.

Table 9.57, continued

Reference No.	54C	56	56	57
Specification	C17200	C17200	C17200	C17200
Composition (wt%)				
Cu	97.58	—	—	97.42
Cu + Ag	—	—	—	—
Be	1.89	1.91	1.80–2.05	2.12
Ni	—	—	—	0.40
Co	0.27	—	0.20–0.35	—
Ni + Co	—	—	—	—
Ni + Fe + Co	—	—	—	—
Al	0.04	—	—	—
Fe	0.13	—	—	0.09
Si	0.09	—	—	—
Others (Only ≥ 0.001 wt%)	—	—	—	—
Material Condition	Cold-rolled, 11% 21%, 37%, then aged (a)	Aged, 575 K, 7 h, then cold-rolled 50%, 75%, 90%	Cold-drawn, 30%, 67%, then aged, 561–602 K, 1 h	Cold-drawn, 21%, then aged, 573 K, 1.5 h
Grain Size	15 μm	—	—	25 μm
Hardness	—	(b)	—	R_G 98.2
Product Form	Strip	Strip, 0.20-cm-thick	Wire, 0.064-cm-dia.	Bar, 1.3-cm-dia.
Specimen Type	Flat	Flat	Wire	Round
Width or Dia.	—	—	0.064 cm	0.80 cm
Thickness	—	—	—	—
Gage Length	—	5.0 cm	—	3.0 cm
Strain or Load Rate	—	—	—	—
No. of Specimens	—	—	—	—
Test Temperature	295 K	295 K	295 K	295 K

(a) Aged: 561–644 K; 0.5–8 h.
(b) Monotron hardness. Cold-rolled: 50%, 275; 75%, 280; 90%, 285.

58	59
C17200	C17200
— — — — — — — — — — —	— — — — — — — — — — —
Cold-rolled, 30% then aged, 593 K, 2 h	Cold-rolled, 6–50%, then aged, 588 K, 3 h
—	—
—	R_C 36–40
Bar, 1.6-cm-dia.	Strip
— — — —	Flat — 0.13, 0.16 cm —
—	—
—	—
293 K	295 K

REFERENCES

1. Hornbuckle, J., and Martin, J. W., "Plastic Yield in Some Copper-Beryllium Alloys," Metallurgia 75, 195–198 (1967).

2. Gohn, G. R., Herbert, G. J., and Kuhn, J. B., "The Mechanical Properties of Copper-Beryllium Alloy Strip," ASTM Special Technical Publication No. 367, American Society for Testing and Materials, Philadelphia, PA, 109 pp. (1964).

3. Harkness, J. C., and Lorenz, C. S., "Stress Relaxation of Beryllium Copper in Bending," in Proceedings of the Twelfth Annual Connector Symposium, Electronic Connector Study Group, Inc., Fort Washington, PA, 38–52 (1979).

4. Filer, E. W., and McClelland, H. T., "Stress Relaxation of Copper-Beryllium and Nickel-Beryllium Alloys," in Proceedings of the Thirteenth Annual Symposium, Electronic Connector Study Group, Fort Washington, PA, 179–186 (1980).

5. Fox, A., "Stress Relaxation in Bending of Copper Beryllium Alloy Strip," Journal of Testing and Evaluation 8, 119–126 (1980).

6. Richards, J. T., and Brick, R. M., "Mechanical Properties of Beryllium Copper At Subzero Temperatures," Journal of Metals 6, 574–580 (1954).

7. Warren, K. A., and Reed, R. P., "Tensile and Impact Properties of Selected Materials From 20 to 300 °K," National Bureau of Standards, Washington, D.C., Monograph 63, 51 pp. (1963).

8. Bonfield, W., "The Temperature Dependence of Microyielding in Polycrystalline Cu 1.9 Wt pct Be," Transactions of the Metallurgical Society of AIME 242, 2163–2167 (1968).

9. Gillett, H. W., "Impact Resistance and Tensile Properties of Metals at Subatmospheric Temperatures," American Society for Testing Materials, Philadelphia, PA, Project No. 13 (1941).

10. Colbeck, E. W., and MacGillivray, W. E., "The Mechanical Properties of Metals at Low Temperatures, Part II--Non-ferrous Materials," Transactions of the Institute of Chemical Engineers (London) 11, 107–123 (1933).

11. Baughman, R. A., "Interim Progress Report #2 on Gas Atmosphere Effects on Materials," General Electric Company, Flight Propulsion Laboratory Department, Aircraft Gas Turbine Division, Evendale, OH, R58AGT823, unpaged (1958).

12. Belton, J. H., Godby, L. L., and Taft, B. L., "Materials for Use at Liquid Hydrogen Temperature," American Society for Testing Materials, Special Technical Publication 287, 108–121 (1961).

13. Weisman, M. H., Melill, J., and Matsuda, T., "Uni-directional Axial Tension Fatigue Tests of Beryllium Copper and Several Precipitation Hardening Corrosion-Resistant Steels," American Society for Testing Materials, Philadelphia, PA, Special Technical Publication 196, 123–142 (1956).

14. Roach, D. B., Fischer, R. B., and Jackson, J. H., "A Precipitation-Hardenable Copper-Nickel-Silicon-Aluminum Alloy," Transactions of the American Society for Metals 46, 329–347 (1954).

REFERENCES

15. Richards, J. T., and Murakawa, K., "Effect of Cold Rolling and Heat Treatment on the Directional Properties of Beryllium Copper Strip," Proceedings of the American Society for Testing Materials 57, 791–807 (1957).

16. Smith, C. S., and Van Wagner, R. W., "The Tensile Properties of Some Copper Alloys," American Society for Testing Materials 41, 825–848 (1941).

17. Murakami, Y., Yoshida, H., and Yamamoto, S., "On the Aging Characteristics of Copper-2 wt% Beryllium Alloys with or without Additional Elements," Transactions of the Japan Institute of Metals 9, 11–18 (1968).

18. Favor, R. J., Gideon, D. N., Grover, H. J., Hayes, J. E., and McClure, G. M., "Investigation of Fatigue Behavior of Certain Alloys in the Temperature Range Room Temperature to –423 F," Wright-Patterson Air Force Base, OH, WADD Technical Report 61-132, 116 pp. (1961).

19. Bornemann, A., and Gela, T., "Studies in the Behavior of Certain Non-ferrous Metals at Low Temperatures, Final Report Vol. I, Improved Non-ferrous Alloys for Use at Temperatures Down to –100 °F," Pierce Memorial Laboratory for Metallurgy, Stevens Institute of Technology, Contract No. DA-36-039-SC-15393, Signal Corps Project 2005-M08-METALS, 152 pp. (1953).

20. Cummings, H. N., Stulen, F. B., and Schulte, W. C., "Investigation of Materials Fatigue Problems," Wright-Patterson Air Force Base, OH, WADC-TR-56-611 (1957).

21. Richards, J. T., Levan, R. K., and Smith, E. M., "The Influence of Cold Work and Heat Treatment on the Engineering Properties of Beryllium Copper Wire," Proceedings of the American Society for Testing Materials 51, 771–789 (1951).

22. Kayaba, T., Akazawa, M., and Ko, M., "Studies on the Influences of Strain-Hardening on the Plastic Workability of Cu-Be Alloy," Technology Reports, Tohoku University 38, 269–286 (1973).

23. Kuhn, J. B., "How to Heat Treat Beryllium Copper," Metallurgia 68, 155–159 (1963).

24. Richards, J. T., and Smith, E. M., "Problems Associated with Hardness Conversion of Several Copper Alloys," Proceedings of the American Society for Testing Materials 57, 161–169 (1957).

25. McClintock, R. M., Van Gundy, D. A., and Kropschot, R. H., "Low-Temperature Tensile Properties of Copper and Four Bronzes," American Society for Testing Materials Bulletin 240, 47–50 (1959).

26. Eash, D. T., "Cryogenic Tensile Testing of Project Rover Materials," Los Alamos Scientific Laboratory of the University of California, Los Alamos, NM, LA-3161, 66 pp. (1965).

27. Richards, J. T., and Smith, E. M., "The Forming Characteristics of Beryllium Copper Strip," Proceedings of the American Society for Testing Materials 50, 1085–1100 (1950).

28. Benson, D. K., and Hancock, J. R., "The Effect of Strain Rate on the Cyclic Response of Metals," Metallurgical Transactions 5, 1711–1715 (1974).

29. Hart, R. R., Wonsiewicz, B. C., and Chin, G. Y., "High Strength Copper Alloys by Thermomechanical Treatments," Metallurgical Transactions 1, 3163–3172 (1970).

REFERENCES

30. Nordstrom, T. V., Rohde, R. W., and Mottern, D. J., "Explosive Strengthening of a Cu-Be Alloy," Metallurgical Transactions 6A, 1561–1568 (1975).

31. Richards, J. T., "An Evaluation of Several Static and Dynamic Methods for Determining Elastic Moduli," in Symposium on Determination of Elastic Constants, American Society for Testing Materials, Philadelphia, PA, 71–100 (1952).

32. Ogden, H. R., Hodge, W., Williams, D. N., and Wood, R. A., "Effect of Fabrication on Be-Cu Hardness and Grain Size," Wire Journal 2, 52–57 (1969).

33. Richards, J. T., "Beryllium Copper Wire: Property and Design Considerations," Wire and Wire Products 27, 257–307 (1952).

34. Drobnjak, Dj., Jovanović, M., and Djurić, B., "Dynamic Strain Age Hardening of Cu-Be Alloys," Metal Science 11, 196–199 (1977).

35. Jovanić, M., Djurić, B., and Drobnjak, Dj., "Strain Hardening Behaviour of Cu-Be Alloys at Elevated Temperatures," in Deformation of Polycrystals: Mechanisms and Microstructures, Riso National Laboratory, Roskilde, Denmark, 311–314 (1981).

36. Weinlich, W., "CuNiBe--eine Variante der Aushärtbaren CuCoBe--Knetlegierungen," Metallwissenschaft und Technik 34, 135–138 (1980).

37. Mollard, F. R., Wikle, K. G., and Chaudhry, A. R., "Copper-Beryllium for Elevated Temperature Electronic and Electrical Applications," in High Conductivity Copper and Aluminum Alloys, Eds. E. Ling and P. W. Taubenblat, The Metallurgical Society of AIME, New York, 147–168 (1984).

38. Pfeiffer, I., and Hönig, A., "Berylliumleitbronzen," Metallwissenschaft und Technik 22, 1125–1129 (1968).

39. Taplin, D. M. R., and Collins, A. L. W., "The Cyclic Stress Response of Copper Alloys at 100–500 °C," International Copper Research Association, Inc., New York, NY, INCRA Project No. 228(B) (1976).

40. Spiegelberg, W. D., and Guha, A., "Properties of Beryllium Copper Alloy C17510," in Copper and Copper Alloys for Fusion Reactor Applications, Eds. F. W. Wiffen and R. E. Gold, Oak Ridge National Laboratory, TN, CONF-830466, (1984).

41. Stevenson, R. D., and Rosenwasser, S. N., "Characteristics, Properties and Fabrication of CuBeNi Alloy (C17510)," Pacific-Sierra Research Corporation, Del Mar, CA, PSR Report 1545, MIT P.O.FCA-534436, 19 pp. (1985).

42. Nir, N., "Isochronous Creep of Copper-Beryllium-Nickel Alloy (Cu-0.4Be-2.0Ni) Solution Treated and Aged," in Second Israel Materials Engineering Conference, Ben Gurion, University of the Negev, Beer-Sheva, Israel, 122–127 (1984).

REFERENCES

43. Guha, A., "High Performance Mill Hardened Beryllium Copper C17510 Strip for Electrical and Electronic Applications," in Proceedings of the Sixteenth Annual Connectors and Interconnection Technology Symposium, Electronic Connector Study Group, Inc., Fort Washington, PA, 131–140 (1983).

44. Reed, R. P., Walsh, R. P., and Fickett, F. R., "Properties of CDA 104, 155, and 175 Copper Alloys," in Materials Studies for Magnetic Fusion Energy Applications at Low Temperatures--X, National Bureau of Standards, Boulder, CO, NBSIR 87-3067, 83–126 (1987).

45. Rotem, A., and Rosen, A., "Improvement of Strength and Electrical Conductivity of Copper Alloy by Means of Thermo-Mechanical Treatment," Metallurgical Transactions 16A, 2073–2077 (1985).

46. Bushnell, C. W., "A Compendium of Beryllium Copper (Alloy C17510) Data for the CIT Device," Princeton Plasma Physics Laboratory, Princeton, NJ, F-880909-PPL-01 (1988).

47. Guha, A., "Development of a High Strength High Conductivity Cu-Ni-Be Alloy," in High Conductivity Copper and Aluminum Alloys, Eds. E. Ling and P. W. Taubenblat, The Metallurgical Society of AIME, New York, 133–145 (1984).

48. Mihajlović, A., Malcić, S., and Nesić, O., "Precipitation-Hardening of Cast Cu-Be-Ni-Zr Alloy," Journal of the Institute of Metals 99, 19–24 (1971).

49. Kostenets, V. I., "Mechanical Properties of Metals under Static Load at Low Temperatures, Part II--Nonferrous Alloys," Journal of Technical Physics, U.S.S.R. 16, 527–538 (1946).

50. Bassett, W. H., "Beryllium-Copper Alloys," Proceedings of the Institute of Metals Division, American Institute of Mining and Metallurgical Engineers E27, 218–232 (1927).

51. Richards, J. T., "Beryllium Copper," Materials and Methods 31, 76–89 (1950).

52. Gohn, G. R., and Arnold, S. M., "The Fatigue Properties of Beryllium-Copper Strip and Their Relation to Other Physical Properties," Proceedings of the American Society for Testing Materials 46, 741–775 (1946).

53. Wikle, K. G., and Sarle, N. P., "Properties of Hardened Copper-Beryllium Strip After Exposures to Elevated Temperatures," Proceedings of the American Society for Testing Materials 61, 988–1007 (1961).

54. Richards, J. T., and Smith, E. M., "The Properties of Beryllium Copper Strip as Affected by Cold Rolling and Heat Treatment," American Society for Testing Materials, Papers on Metals, STP 196, 143–156 (1956).

55. Smith, J. K., "Copper-Beryllium 'Bronzes'," Transactions of the American Institute of Mining and Metallurgical Engineers 99, 65–77 (1932).

56. Crooks, R. D., and Johnson, W. R., "Mechanical Properties of Beryllium Copper Wire and Springs," Metal Progress 85, 89–91 (1964).

REFERENCES

57. Anderson, A. R., and Smith, C. S., "Fatigue Tests on Some Copper Alloys," Proceedings of the American Society for Testing Materials 41, 849–858 (1941).

58. Smirnov, M. A., Shteynberg, M. M., Kareva, N. T., Teplov, V. A., and Koryagin, Yu. D., "Influence of Plastic Deformation Temperature on the Structure and Properties of Beryllium Bronze," Physics of Metals and Metallography 38, 173–178 (1974).

59. Gohn, G. R., "A Hardness Conversion Table for Copper-Beryllium Alloy Strip," Proceedings of the American Society for Testing Materials 55, 230–239 (1955).

C17200: Cold-worked

Impact Energy (Charpy V-Notch) vs. Temperature (24–296 K)

DATA SOURCE

Charpy V-notch impact energy measurements from 20 to 296 K on 37% cold-drawn C17200 beryllium copper were obtained from Reference 10.1. Product form was not reported. Data at 20 K are included because a large temperature rise in the specimen from absorbed energy is not expected from the relatively brittle material.

RESULTS

The measurements for impact energy, test temperature, and reference number are tabulated in Table 10.1. The available characterization of materials and measurements is given in Table 10.3 at the end of the impact properties section. Figure 10.1 presents the impact data as a function of temperature.

DISCUSSION

The fracture appearance was reported to be moderately granular, and the shear area remained constant in size at the different temperatures. At all temperatures, the specimens were almost completely broken through.

Table 10.1. Impact Energy Dependence on Temperature (20–296 K).

Impact Energy, J	Test Temperature, K	Reference No.
67.2	24	1
79.2	196	1
73.5	24	1
77.7	24	1
79.2	24	1
77.7	24	1
80.0	80	1
81.9	196	1
82.1	80	1
96.9	196	1
87.2	196	1
87.4	196	1
105.7	296	1
104.6	296	1
98.8	296	1
97.8	296	1
97.7	296	1
92.2	296	1

C17200: Cold-worked

Impact Energy (Charpy V-Notch) vs. Temperature (24–296 K)

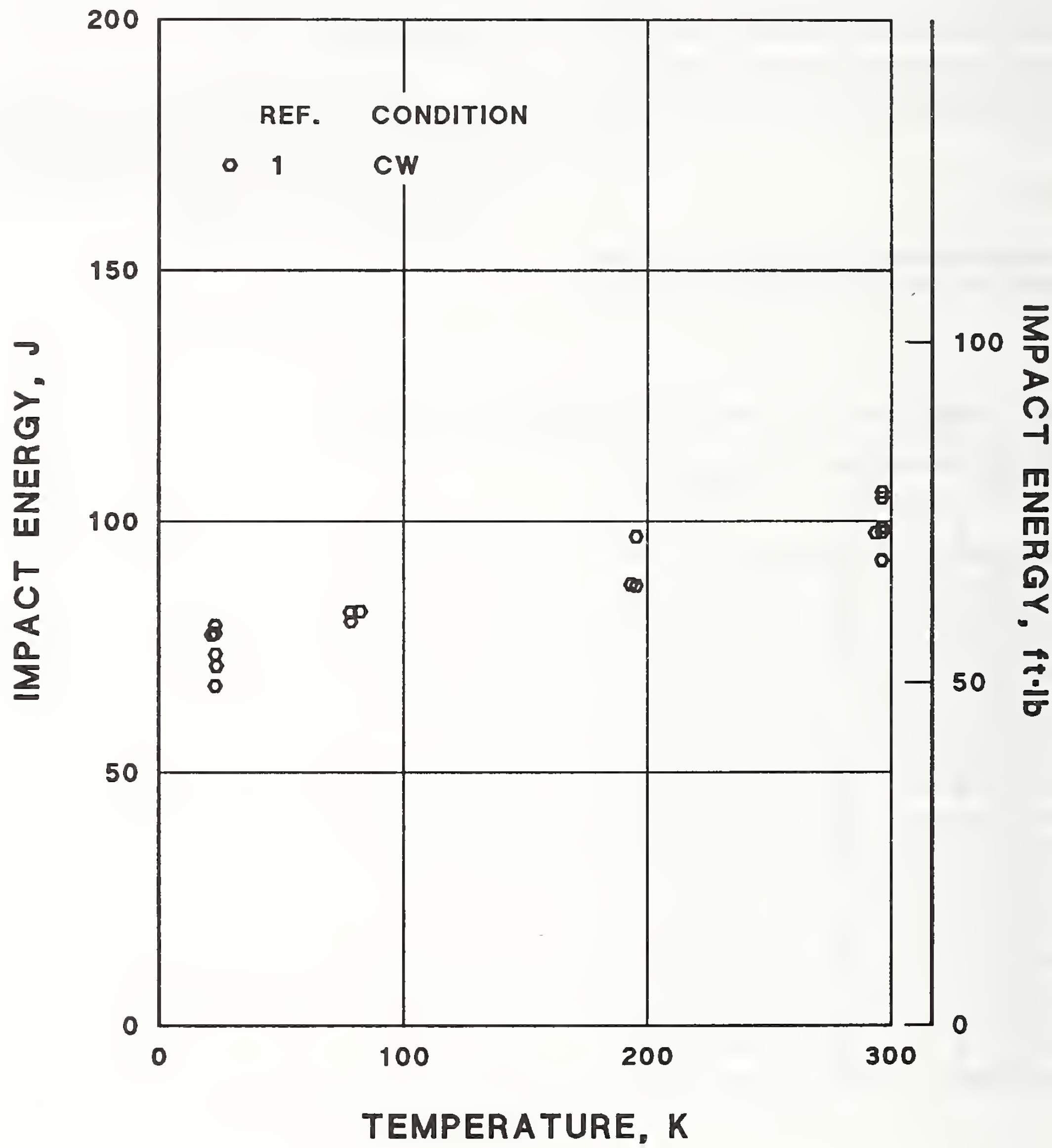

Figure 10.1. The impact energy dependence on test temperature indicates an increase in impact energy with increasing temperature (Reference 10.1). All data are presented in Table 10.1. Product form was not reported.

C17500: Cold-worked and Aged

Impact Energy (Charpy V-Notch) vs. Temperature (24–296 K)

DATA SOURCE

Charpy V-notch impact energy measurements from 20 to 296 K on 37% cold-drawn and aged C17500 beryllium copper were obtained from Reference 10.1. Product form was not reported. Data at 24 K are included because the material is relatively brittle so that a large temperature rise in the specimen from absorbed energy is not expected.

RESULTS

The measurements for impact energy, test temperature, and reference number are tabulated in Table 10.2. The available characterization of materials and measurements is given in Table 10.3 at the end of the impact properties section. Figure 10.2 presents the impact data as a function of temperature.

DISCUSSION

The fracture appearance was reported to be granular, and the shear area remained constant in size at all temperatures. The specimens were completely broken through at all temperatures. In the majority of specimens, the crack did not propagate to the point of impact.

Table 10.2. Impact Energy Dependence on Temperature (24–296 K).

Impact Energy, J	Test Temperature, K	Reference No.
32.9	24	1
34.4	80	1
33.1	80	1
33.5	80	1
33.8	196	1
33.2	196	1
29.8	196	1
32.9	296	1
32.2	296	1
31.2	296	1

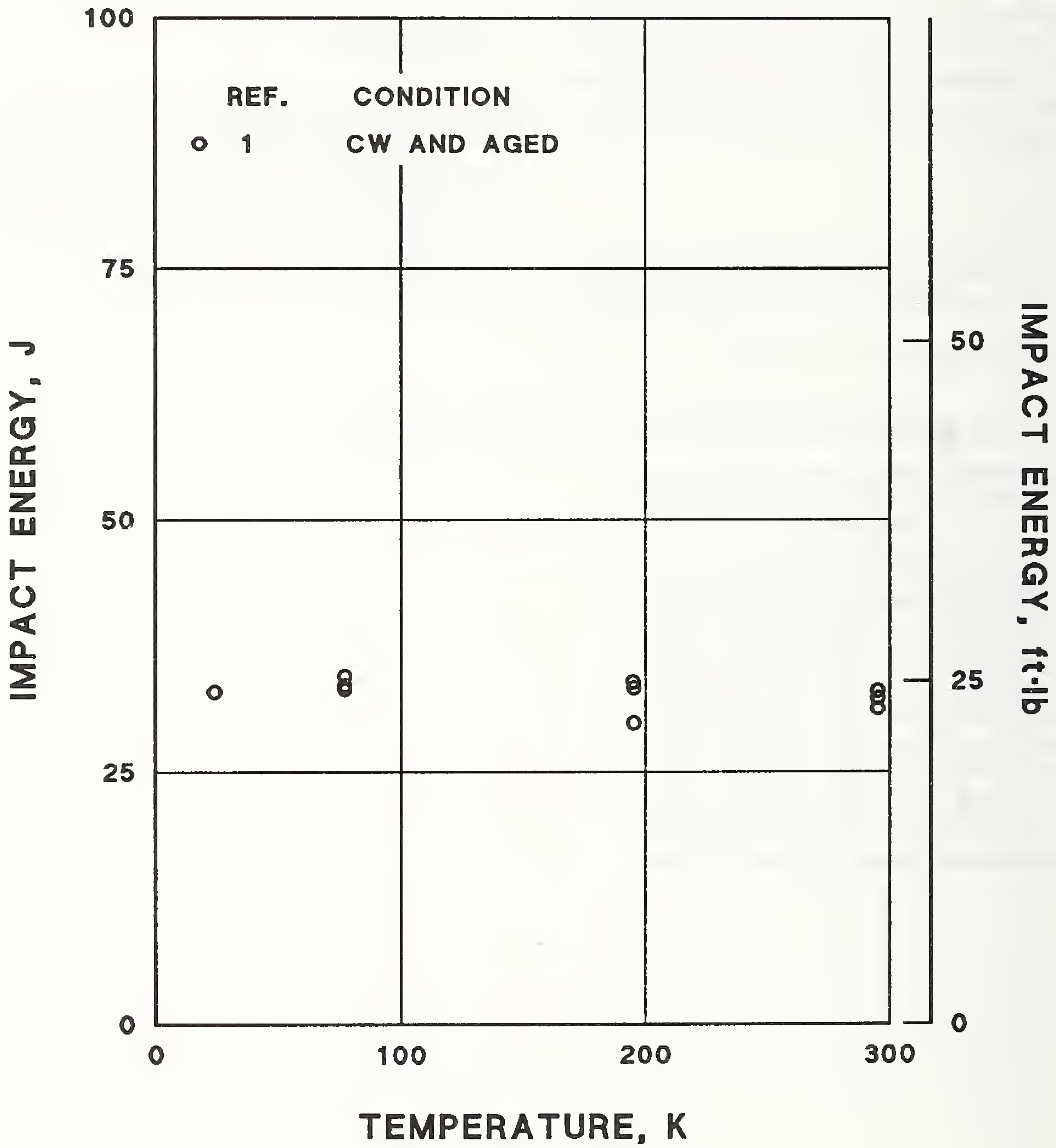

Figure 10.2. The impact energy is independent of test temperature for C17500 material in the cold-worked and aged condition (Reference 10.1). All data are presented in Table 10.2. Product form was not reported.

Table 10.3. Characterization of Materials and Measurements.

Reference No.	1A	1B
Specification	C17200	C17500
Composition (wt%)		
Cu	—	—
Cu + Ag	—	—
Be	2.0	0.5
Ni	—	—
Co	0.2	2.6
Ni + Co	—	—
Ni + Fe + Co	—	—
Al	—	—
Fe	—	—
Si	—	—
Others (Only ≥ 0.001 wt%)	—	—
Material Condition	Cold worked, 1/2-hard	Cold worked, 1/2-hard, aged
Grain Size	—	—
Hardness	R_B 91–93	R_B 97–100
Product Form	—	—
Specimen Type	Charpy V-notch	Charpy V-notch
No. of Specimens	3–6 per temperature	1–3 per temperature
Test Temperature	24–296 K	24–296 K

REFERENCE

1. Mikesell, R. P., and Reed, R. P., "The Results of the Impact Testing of Copper Alloys," U.S. Atomic Energy Commission, Memorandum of Understanding AT(29-1)-1500, 16 pp (1958).

Mikesell, R. P., and Reed, R. P., "The Impact Testing of Various Alloys at Low Temperatures," in Advances in Cryogenic Engineering, Vol. 3, Ed., K. D. Timmerhaus, Plenum Press, NY, 316–324 (1960).

C17000: Annealed and Aged

Stress-controlled Flexural Fatigue Life, Air (295 K)

DATA SOURCES AND ANALYSIS

Measurements at 295 K of the maximum stress (σ_m) versus the number of cycles to failure (N) for annealed and aged C17000 beryllium copper were obtained from Reference 11.1. The fatigue mode was flexural (R-ratio equals –1). Product was in strip form. Aging temperatures were 588 and 616 K; aging time was 3 h. Beryllium content, [Be], was 1.59 and 1.70 wt%.

In the analysis, N is treated as the dependent variable, and the Equation (11-1) used to analyze the data (Reference 11.2) is

$$\log N = N_0 + N_1 \log(\sigma_m - \sigma_0). \qquad (11\text{-}1)$$

The measurements were fitted to this equation by a nonlinear least-squares regression procedure that determines the constants N_0, N_1, and σ_0. If duplicate results (same N for a given σ_m) were obtained, both test results were included in the measurement set used for the regression analysis.

RESULTS

The equation obtained from the measurements was

$$\log N = 9.60 - 2.98 \log(\sigma_m - 189), \qquad (11\text{-}2)$$

where σ_m is in MPa. The standard deviation of the fit (in units of log N) is 0.30. The standard deviations of the three constants are 0.68, 0.28, and 8.

Table 11.1 presents N, σ_m, [Be], the aging temperature, and the reference number. The available characterization of materials and measurements is given in Table 11.14 at the end of the fatigue properties section. Figure 11.1 indicates the fit of the data to Equation (11-2). The scatter band represents two standard deviations about the regression curve. The variance of the data about the line was assumed to be normally distributed and constant throughout the range of the independent variable, σ_m.

DISCUSSION

The constants N_0, N_1, and σ_0 from Equation (11-1) fitted to the data of Reference 11.1 only are shown as a function of cold work in Figure 11.10. For both C17000 and C17200 beryllium coppers, a systematic variation of these constants with cold work was observed.

Table 11.1. Fatigue Life Measurements for Annealed and Aged C17000 Beryllium Copper (295 K).

Cycles, N (10^3)	Maximum Stress, MPa	[Be], wt%	Aging Temperature, K	Reference No.
151	486	1.59	616	1
191	490	1.70	616	1
170	490	1.70	616	1
170	490	1.70	616	1
182	490	1.70	588	1
191	486	1.59	616	1
191	486	1.59	616	1
200	490	1.70	616	1
200	490	1.70	616	1
219	490	1.70	588	1
224	462	1.59	616	1
234	490	1.70	588	1
234	486	1.59	616	1
237	460	1.59	588	1
237	460	1.59	588	1
237	460	1.59	588	1
251	486	1.59	616	1

Table 11.1, continued

Cycles, N (10^3)	Maximum Stress, MPa	[Be], wt%	Aging Temperature, K	Reference No.
263	403	1.59	588	1
269	499	1.70	588	1
331	410	1.70	588	1
372	403	1.59	588	1
372	403	1.70	588	1
372	403	1.70	616	1
398	410	1.70	588	1
427	403	1.70	588	1
437	403	1.59	588	1
457	403	1.59	588	1
468	403	1.70	616	1
479	490	1.70	588	1
479	410	1.70	588	1
513	403	1.59	616	1
562	403	1.59	588	1
562	402	1.70	616	1
603	410	1.70	588	1
617	390	1.59	588	1
617	334	1.59	588	1
661	328	1.59	588	1
661	328	1.59	588	1
708	398	1.59	588	1
832	334	1.70	588	1
851	330	1.70	588	1
1070	334	1.70	588	1
1120	334	1.59	588	1
1170	328	1.59	588	1
1170	328	1.59	588	1
1170	334	1.70	588	1
1200	334	1.59	588	1
1200	334	1.70	588	1
1200	390	1.70	588	1
1260	334	1.70	588	1
1350	334	1.70	588	1
1480	328	1.59	588	1
1480	334	1.70	588	1
1660	314	1.59	588	1
1660	332	1.70	588	1
1660	328	1.59	588	1
1660	290	1.59	588	1
1480	279	1.59	588	1
1780	293	1.70	588	1
1480	290	1.70	588	1
2090	293	1.70	588	1
2090	279	1.59	588	1
2090	315	1.59	588	1
2090	279	1.59	588	1
2090	293	1.70	588	1
2400	293	1.70	588	1
2400	328	1.59	616	1
2450	279	1.59	588	1

C17000: Annealed and Aged

Stress-controlled Flexural Fatigue Life, Air (295 K)

Table 11.1, continued

Cycles, N (10^3)	Maximum Stress, MPa	[Be], wt%	Aging Temperature, K	Reference No.
2820	293	1.70	588	1
2950	290	1.70	616	1
3160	279	1.59	616	1
3980	290	1.59	588	1
4170	293	1.70	616	1
4220	250	1.59	588	1
4270	290	1.70	616	1
4220	290	1.59	616	1
4570	290	1.70	616	1
5010	290	1.59	616	1
5010	290	1.70	616	1
5310	290	1.59	588	1
5370	290	1.70	616	1
5620	290	1.59	616	1
6310	290	1.59	616	1
5310	290	1.59	616	1
7410	293	1.70	616	1
8320	290	1.70	616	1
11000	290	1.59	616	1
13300	290	1.59	616	1
21900	246	1.59	616	1
23400	221	1.59	616	1
26300	228	1.59	616	1
29500	255	1.70	588	1
63100	290	1.70	616	1
64600	290	1.59	616	1
77600	252	1.59	616	1
81300	250	1.70	616	1
81300	290	1.70	616	1
100000	221	1.59	588	1
100000	279	1.59	616	1
100000	221	1.59	616	1
100000	228	1.59	616	1
100000	245	1.59	588	1
100000	279	1.59	616	1
100000	245	1.59	588	1
100000	221	1.70	588	1
100000	221	1.70	588	1
100000	223	1.70	616	1
100000	223	1.70	588	1
100000	228	1.70	616	1
100000	250	1.59	588	1
100000	221	1.59	616	1
100000	250	1.59	616	1
100000	228	1.59	616	1
100000	221	1.59	588	1
100000	228	1.59	616	1
100000	221	1.59	588	1
100000	252	1.70	616	1
100000	221	1.70	616	1
100000	252	1.70	616	1

Table 11.1, continued

Cycles, N (10^3)	Maximum Stress, MPa	[Be], wt%	Aging Temperature, K	Reference No.
100000	221	1.70	616	1
100000	221	1.70	616	1
100000	221	1.70	616	1
100000	221	1.70	616	1

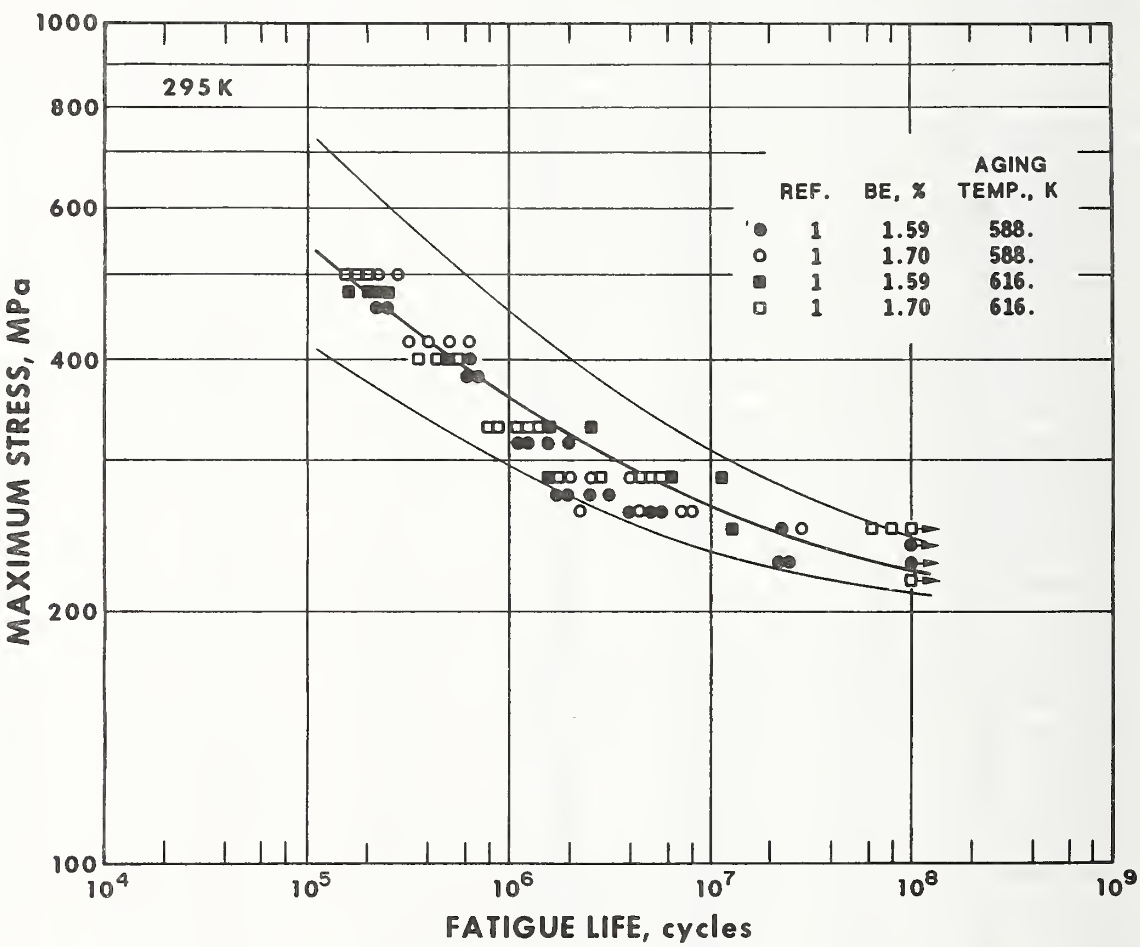

Figure 11.1. Fatigue life curves at 295 K for annealed and aged C17000 beryllium copper are shown. The scatter band represents two standard deviations about a nonlinear regression curve given by Equation (11-2), in which *N* is the dependent variable. For clarity, overlapping data points are omitted from the figure. All data are presented in Table 11.1. Product was in strip form. Arrows denote completion of test before failure.

C17000: Cold-worked 11% and Aged

Stress-controlled Flexural Fatigue Life, Air (295 K)

DATA SOURCES AND ANALYSIS

Measurements at 295 K of the maximum stress (σ_m) versus the number of cycles to failure (N) for cold-worked, C17000 beryllium copper were obtained from Reference 11.1. The fatigue mode was flexural (R-ratio equals −1). Product was in strip form. Cold work, *CW*, was 11% (reduction in thickness). Aging temperatures were 588 and 616 K; aging time was 3 h. Beryllium content, [Be], was 1.59 and 1.70 wt%.

In the analysis, N is treated as the dependent variable, and the equation used to analyze the data (Reference 11.2) is

$$\log N = N_0 + N_1 \log(\sigma_m - \sigma_0). \qquad (11\text{-}1)$$

The measurements were fitted to this equation by a nonlinear least-squares regression procedure that determines the constants N_0, N_1, and σ_0. If duplicate results (same N for a given σ_m) were obtained, both test results were included in the measurement set used for the regression analysis.

RESULTS

The equation obtained from the measurements was

$$\log N = 14.3 - 4.66 \log(\sigma_m - 162), \qquad (11\text{-}3)$$

where σ_m is in MPa. The standard deviation of the fit (in units of log N) is 0.3. The standard deviations of the three constants are 2.0, 0.76, and 29.

Table 11.2 presents N, σ_m, [Be], percent of *CW*, aging temperature, and the reference number. The available characterization of materials and measurements is given in Table 11.14 at the end of the fatigue properties section. Figure 11.2 indicates the fit of the data to Equation (11-3). The scatter band represents two standard deviations about the regression curve. The variance of the data about the line was assumed to be normally distributed and constant throughout the range of the independent variable, σ_m.

DISCUSSION

The constants N_0, N_1, and σ_0 from Equation (11-1) fitted to the data of Reference 11.1 only are shown as a function of *CW* in Figure 11.10. For both C17000 and C17200 beryllium coppers, a systematic variation of these constants with *CW* was observed.

Table 11.2. Fatigue Life Measurements for C17000 Beryllium Copper Cold-worked 11% Before Aging (295 K).

Cycles, N (10^3)	Maximum Stress, MPa	[Be], wt%	Cold Work, %	Aging Temperature, K	Reference No.
126	524	1.59	11	616	1
148	524	1.59	11	616	1
155	524	1.59	11	616	1
174	602	1.70	11	616	1
195	600	1.70	11	616	1
195	524	1.59	11	616	1
195	524	1.59	11	616	1
204	602	1.70	11	616	1
251	600	1.70	11	616	1
263	507	1.59	11	616	1
295	507	1.59	11	616	1
295	507	1.59	11	588	1
302	507	1.70	11	588	1
363	507	1.59	11	588	1

C17000: Cold-worked 11% and Aged

Stress-controlled Flexural Fatigue Life, Air (295 K)

Table 11.2, continued

Cycles, N (10^3)	Maximum Stress, MPa	[Be], wt%	Cold Work, %	Aging Temperature, K	Reference No.
363	507	1.59	11	616	1
407	507	1.70	11	588	1
479	507	1.70	11	588	1
525	507	1.70	11	588	1
562	431	1.59	11	616	1
676	425	1.59	11	616	1
562	431	1.59	11	616	1
692	431	1.59	11	616	1
724	425	1.59	11	616	1
741	425	1.59	11	588	1
741	431	1.59	11	616	1
813	424	1.70	11	616	1
851	424	1.59	11	588	1
851	424	1.70	11	616	1
1230	424	1.70	11	616	1
1320	424	1.70	11	588	1
1500	424	1.70	11	616	1
1780	352	1.59	11	616	1
1860	352	1.59	11	616	1
2000	345	1.59	11	616	1
2400	345	1.59	11	616	1
2400	345	1.59	11	616	1
2400	345	1.70	11	616	1
3090	352	1.59	11	616	1
3310	345	1.59	11	616	1
3310	345	1.59	11	616	1
3390	352	1.59	11	616	1
3690	352	1.59	11	616	1
4070	303	1.70	11	616	1
4680	345	1.59	11	616	1
4680	345	1.59	11	616	1
5130	345	1.70	11	616	1
6030	307	1.59	11	616	1
6310	345	1.70	11	588	1
6830	345	1.70	11	616	1
7410	303	1.70	11	616	1
8130	307	1.59	11	616	1
8320	345	1.70	11	616	1
8510	287	1.59	11	616	1
8510	307	1.59	11	616	1
8510	293	1.59	11	616	1
10700	305	1.59	11	616	1
11200	305	1.59	11	616	1
12000	267	1.59	11	616	1
13500	287	1.59	11	616	1
14800	305	1.59	11	616	1
1[illegible]200	293	1.59	11	588	1
20000	310	1.70	11	616	1
20900	305	1.59	11	588	1
26300	305	1.70	11	588	1
38900	287	1.59	11	588	1

C17000: Cold-worked 11% and Aged

Stress-controlled Flexural Fatigue Life, Air (295 K)

Table 11.2, continued

Cycles, N (10^3)	Maximum Stress, MPa	[Be], wt%	Cold Work, %	Aging Temperature, K	Reference No.
38900	305	1.70	11	588	1
40700	310	1.70	11	616	1
46800	310	1.70	11	616	1
53700	293	1.59	11	616	1
56200	272	1.59	11	616	1
58900	265	1.59	11	616	1
58900	303	1.70	11	588	1
58900	293	1.59	11	616	1
60300	310	1.70	11	616	1
66100	310	1.70	11	616	1
68300	283	1.70	11	588	1
70800	293	1.59	11	616	1
77600	293	1.59	11	616	1
77600	265	1.70	11	616	1
82200	290	1.70	11	616	1
85100	272	1.59	11	616	1
100000	286	1.59	11	588	1
100000	265	1.59	11	588	1
100000	246	1.59	11	588	1
100000	265	1.59	11	588	1
100000	265	1.59	11	588	1
100000	246	1.59	11	588	1
100000	246	1.59	11	588	1
100000	246	1.59	11	616	1
100000	246	1.59	11	588	1
100000	283	1.70	11	588	1
100000	265	1.70	11	588	1
100000	293	1.70	11	588	1
100000	283	1.70	11	588	1
100000	265	1.70	11	588	1
100000	265	1.70	11	588	1
100000	265	1.70	11	588	1
100000	290	1.70	11	588	1
100000	265	1.70	11	588	1
100000	272	1.59	11	616	1
100000	272	1.59	11	616	1
100000	272	1.59	11	616	1
100000	290	1.70	11	616	1
100000	290	1.70	11	616	1
100000	290	1.70	11	616	1

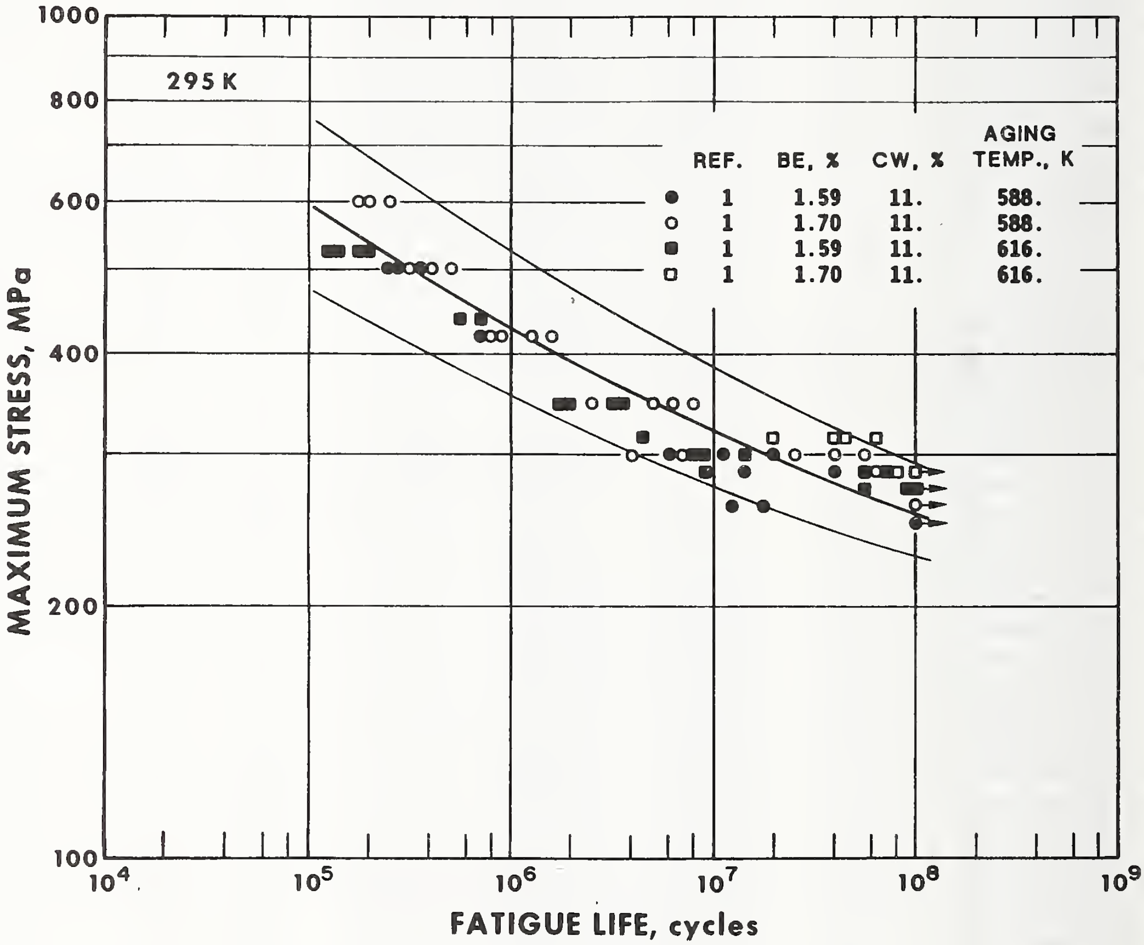

Figure 11.2. Fatigue life curves at 295 K for C17000 beryllium copper cold-worked 11% before aging are shown. The scatter band represents two standard deviations about a nonlinear regression curve given by Equation (11-3), in which *N* is the dependent variable. For clarity, overlapping data points are omitted from the figure. All data are presented in Table 11.2. Product was in strip form. Arrows denote completion of test before failure.

DATA SOURCES AND ANALYSIS

Measurements at 295 K of the maximum stress (σ_m) versus the number of cycles to failure (N) for cold-worked and aged C17000 beryllium copper were obtained from Reference 11.1. The fatigue mode was flexural (R-ratio equals –1). Product was in strip form. Cold work, *CW*, was 21% (reduction in thickness). Aging temperatures were 588 and 616 K; aging time was 3 h. Beryllium content, [Be], was 1.59 and 1.70 wt%.

In the analysis, N is treated as the dependent variable, and the equation used to analyze the data (Reference 11.2) is

$$\log N = N_0 + N_1 \log(\sigma_m - \sigma_0). \qquad (11\text{-}1)$$

The measurements were fitted to this equation by a nonlinear least-squares regression procedure that determines the constants N_0, N_1, and σ_0. If duplicate results (same N for a given σ_m) were obtained, both test results were included in the measurement set used for the regression analysis.

RESULTS

The equation obtained from the measurements was

$$\log N = 14.8 - 4.79 \log(\sigma_m - 160), \qquad (11\text{-}4)$$

where σ_m is in MPa. The standard deviation of the fit (in units of log N) is 0.3. The standard deviations of the three constants are 1.6, 0.59, and 25.

Table 11.3 presents N, σ_m, [Be], percent of *CW*, aging temperature, and the reference number. The available characterization of materials and measurements is given in Table 11.14 at the end of the fatigue properties section. Figure 11.3 indicates the fit of the data to Equation (11-4). The scatter band represents two standard deviations about the regression curve. The variance of the data about the line was assumed to be normally distributed and constant throughout the range of the independent variable, σ_m.

DISCUSSION

The constants N_0, N_1, and σ_0 from Equation (11-1) fitted to the data of Reference 11.1 only are shown as a function of *CW* in Figure 11.10. For both C17000 and C17200 beryllium coppers, a systematic variation of these constants with *CW* was observed.

Table 11.3. Fatigue Life Measurements for C17000 Beryllium Copper Cold-worked 21% Before Aging (295 K).

Cycles, N (10^3)	Maximum Stress, MPa	[Be], wt%	Cold Work, %	Aging Temperature, K	Reference No.
132	598	1.59	21	616	1
132	598	1.59	21	616	1
132	598	1.59	21	616	1
132	602	1.70	21	616	1
145	598	1.59	21	616	1
145	598	1.59	21	616	1
151	602	1.70	21	616	1
166	602	1.70	21	616	1
182	600	1.70	21	588	1
182	602	1.70	21	616	1
191	600	1.70	21	588	1
200	598	1.59	21	616	1
224	600	1.70	21	588	1
224	602	1.70	21	616	1

C17000: Cold-worked 21% and Aged

Stress-controlled Flexural Fatigue Life, Air (295 K)

Table 11.3, continued

Cycles, N (10^3)	Maximum Stress, MPa	[Be], wt%	Cold Work, %	Aging Temperature, K	Reference No.
240	600	1.70	21	588	1
269	508	1.59	21	616	1
282	600	1.70	21	588	1
295	508	1.59	21	616	1
295	508	1.59	21	616	1
316	507	1.59	21	588	1
355	507	1.59	21	588	1
355	507	1.59	21	588	1
355	507	1.59	21	588	1
355	514	1.70	21	616	1
372	507	1.59	21	588	1
372	508	1.59	21	616	1
372	514	1.70	21	616	1
380	515	1.70	21	616	1
380	515	1.70	21	616	1
479	507	1.70	21	588	1
479	507	1.70	21	588	1
589	507	1.70	21	588	1
589	507	1.70	21	588	1
741	508	1.59	21	616	1
759	424	1.70	21	616	1
851	423	1.59	21	588	1
851	423	1.59	21	588	1
912	421	1.59	21	588	1
912	421	1.59	21	616	1
1000	424	1.70	21	616	1
1000	424	1.70	21	616	1
1020	423	1.70	21	588	1
1050	421	1.59	21	616	1
1100	424	1.70	21	616	1
1150	421	1.59	21	616	1
1200	422	1.59	21	588	1
1200	423	1.70	21	588	1
1200	421	1.59	21	616	1
1450	423	1.70	21	588	1
1480	422	1.59	21	588	1
1500	424	1.70	21	616	1
1740	423	1.70	21	588	1
1860	423	1.70	21	588	1
1910	345	1.70	21	588	1
2290	341	1.70	21	616	1
2880	345	1.59	21	588	1
3390	345	1.59	21	588	1
3800	317	1.70	21	616	1
4170	336	1.59	21	616	1
4170	336	1.59	21	616	1
4470	345	1.70	21	588	1
5370	334	1.59	21	616	1
5750	293	1.59	21	616	1
5890	345	1.59	21	588	1
5890	345	1.59	21	588	1

C17000: Cold-worked 21% and Aged

Stress-controlled Flexural Fatigue Life, Air (295 K)

Table 11.3, continued

Cycles, N (10^3)	Maximum Stress, MPa	[Be], wt%	Cold Work, %	Aging Temperature, K	Reference No.
8910	345	1.70	21	588	1
6310	334	1.59	21	616	1
8910	334	1.59	21	616	1
6760	346	1.70	21	588	1
8910	306	1.59	21	616	1
9550	317	1.70	21	616	1
10400	341	1.70	21	616	1
10500	345	1.59	21	616	1
11700	341	1.70	21	616	1
13200	317	1.70	21	616	1
13200	341	1.70	21	616	1
13200	317	1.70	21	616	1
19100	285	1.59	21	616	1
16200	290	1.59	21	616	1
17400	285	1.70	21	588	1
17400	291	1.59	21	616	1
17400	307	1.70	21	616	1
17400	317	1.70	21	616	1
19100	307	1.70	21	616	1
20400	317	1.70	21	616	1
23400	341	1.70	21	588	1
24000	346	1.70	21	588	1
26300	292	1.59	21	616	1
26300	276	1.59	21	616	1
28200	307	1.70	21	616	1
78800	306	1.59	21	588	1
30200	307	1.59	21	588	1
38000	276	1.59	21	616	1
40700	302	1.70	21	616	1
44700	285	1.70	21	588	1
47300	276	1.59	21	616	1
50100	276	1.59	21	616	1
57500	290	1.59	21	616	1
60300	302	1.70	21	616	1
66100	285	1.70	21	616	1
70800	308	1.59	21	588	1
77600	307	1.70	21	588	1
79400	250	1.59	21	588	1
85100	276	1.59	21	616	1
89100	305	1.70	21	588	1
91200	303	1.59	21	588	1
100000	290	1.59	21	588	1
100000	285	1.59	21	588	1
100000	250	1.59	21	588	1
100000	290	1.59	21	588	1
100000	290	1.59	21	588	1
100000	285	1.59	21	588	1
100000	250	1.59	21	588	1
100000	269	1.59	21	588	1
100000	269	1.59	21	588	1
100000	250	1.59	21	588	1

C17000: Cold-worked 21% and Aged

Stress-controlled Flexural Fatigue Life, Air (295 K)

Table 11.3, continued

Cycles, N (10^3)	Maximum Stress, MPa	[Be], wt%	Cold Work, %	Aging Temperature, K	Reference No.
100000	250	1.59	21	588	1
100000	250	1.59	21	588	1
100000	250	1.59	21	588	1
100000	286	1.70	21	588	1
100000	269	1.70	21	588	1
100000	286	1.70	21	588	1
100000	269	1.70	21	588	1
100000	286	1.70	21	588	1
100000	269	1.70	21	616	1
100000	286	1.70	21	588	1
100000	269	1.70	21	588	1
100000	259	1.59	21	616	1
100000	269	1.59	21	616	1
100000	259	1.59	21	616	1
100000	269	1.59	21	616	1
100000	259	1.59	21	616	1
100000	302	1.70	21	616	1
100000	286	1.70	21	616	1
100000	302	1.70	21	616	1
100000	286	1.70	21	616	1
100000	286	1.70	21	616	1
100000	286	1.70	21	616	1

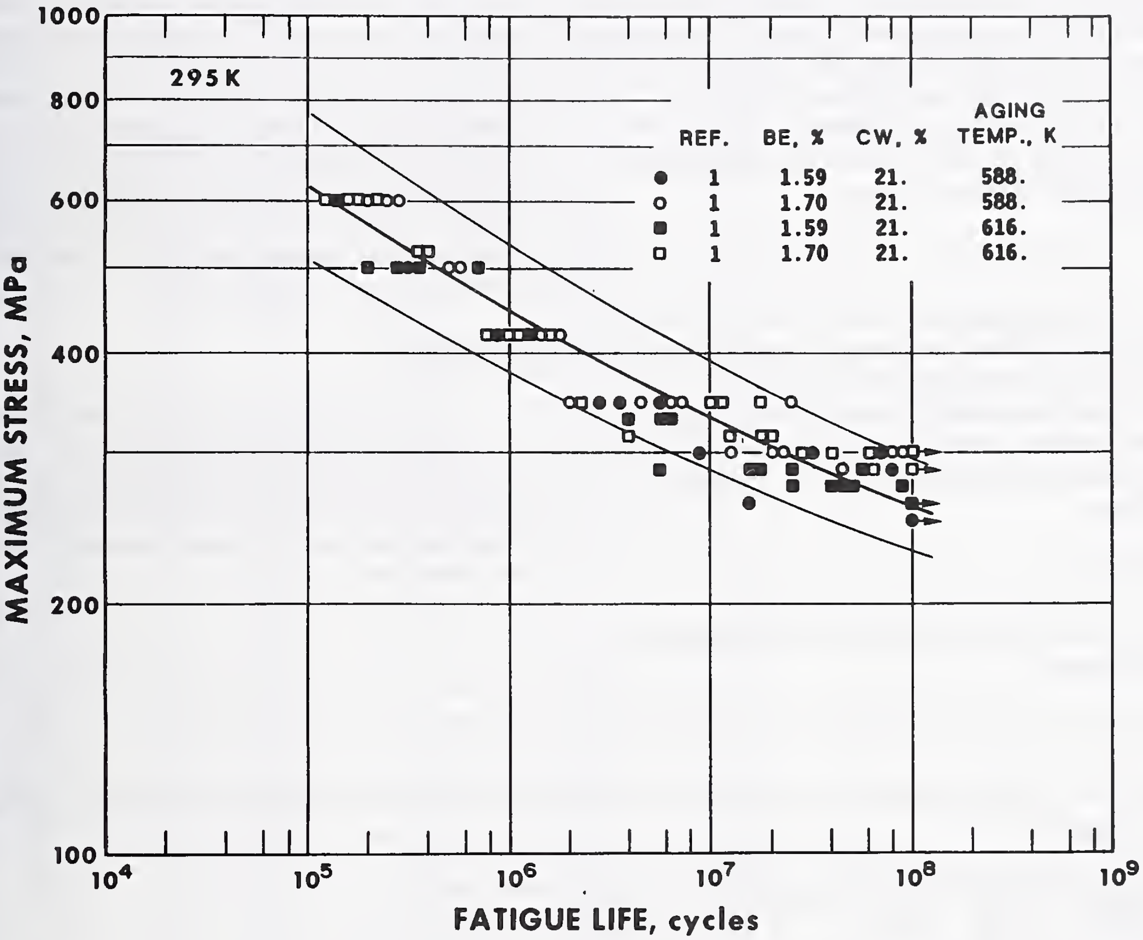

Figure 11.3. Fatigue life curves at 295 K for C17000 beryllium copper cold-worked 21% before aging are shown. The scatter band represents two standard deviations about a nonlinear regression curve given by Equation (11-4), in which N is the dependent variable. For clarity, overlapping data points are omitted from the figure. All data are presented in Table 11.3. Product was in strip form. Arrows denote completion of test before failure.

DATA SOURCES AND ANALYSIS

Measurements at 295 K of the maximum stress (σ_m) versus the number of cycles to failure (N) for cold-worked and aged C17000 beryllium copper were obtained from Reference 11.1. The fatigue mode was flexural (R-ratio equals −1). Product was in strip form. Cold work, *CW*, was 37% (reduction in thickness). Aging temperatures were 588 and 616 K; aging time was 3 h. Beryllium content, [Be], was 1.59 and 1.70 wt%.

In the analysis, N is treated as the dependent variable, and the equation used to analyze the data (Reference 11.2) is

$$\log N = N_0 + N_1 \log(\sigma_m - \sigma_0). \qquad (11\text{-}1)$$

The measurements were fitted to this equation by a nonlinear least-squares regression procedure that determines the constants N_0, N_1, and σ_0. If duplicate results (same N for a given σ_m) were obtained, both test results were included in the measurement set used for the regression analysis.

RESULTS

The equation obtained from the measurements was

$$\log N = 31.5 - 10.3 \log(\sigma_m + 107), \qquad (11\text{-}5)$$

where σ_m is in MPa. The standard deviation of the fit (in units of $\log N$) is 0.3. The standard deviations of the three constants are 11.0, 3.5, and 167.

Table 11.4 presents N, σ_m, [Be], *CW*, aging temperature, and the reference number. The available characterization of materials and measurements is given in Table 11.14 at the end of the fatigue properties section. Figure 11.4 indicates the fit of the data to Equation (11-5). The scatter band represents two standard deviations about the regression curve. The variance of the data about the line was assumed to be normally distributed and constant throughout the range of the independent variable, σ_m.

DISCUSSION

The constants N_0, N_1, and σ_0 from Equation (11-1) fitted to the data of Reference 11.1 only are shown as a function of *CW* in Figure 11.10. For both C17000 and C17200 beryllium coppers, a systematic variation of these constants with *CW* was observed.

Table 11.4. Fatigue Life Measurements for C17000 Beryllium Copper Cold-worked 37% Before Aging (295 K).

Cycles, N (10^3)	Maximum Stress, MPa	[Be], wt%	Cold Work, %	Aging Temperature, K	Reference No.
170	569	1.59	37	616	1
170	593	1.70	37	616	1
178	593	1.59	37	616	1
178	593	1.70	37	616	1
204	597	1.70	37	588	1
204	593	1.70	37	616	1
204	593	1.70	37	616	1
209	593	1.59	37	616	1
214	593	1.70	37	616	1
229	593	1.59	37	616	1
2[illegible]4	569	1.59	37	616	1
245	458	1.59	37	588	1
269	459	1.59	37	588	1
269	459	1.59	37	588	1

C17000: Cold-worked 37% and Aged

Stress-controlled Flexural Fatigue Life, Air (295 K)

Table 11.4, continued

Cycles, N (10^3)	Maximum Stress, MPa	[Be], wt%	Cold Work, %	Aging Temperature, K	Reference No.
288	596	1.70	37	588	1
302	596	1.70	37	588	1
302	501	1.70	37	588	1
331	457	1.59	37	588	1
347	501	1.70	37	588	1
355	596	1.70	37	588	1
355	490	1.59	37	588	1
355	457	1.59	37	588	1
417	501	1.70	37	616	1
422	596	1.70	37	588	1
447	490	1.59	37	616	1
447	490	1.59	37	588	1
501	490	1.59	37	616	1
501	490	1.59	37	588	1
501	501	1.70	37	616	1
501	501	1.70	37	588	1
603	517	1.70	37	588	1
741	517	1.70	37	588	1
813	517	1.70	37	588	1
933	517	1.70	37	588	1
1050	421	1.70	37	616	1
1150	410	1.59	37	588	1
1170	421	1.70	37	616	1
1170	421	1.70	37	588	1
1230	417	1.70	37	616	1
1480	517	1.70	37	588	1
1740	421	1.70	37	588	1
1950	410	1.59	37	588	1
1950	490	1.59	37	588	1
2340	490	1.59	37	616	1
2510	421	1.70	37	588	1
2510	427	1.70	37	588	1
2510	427	1.70	37	588	1
2880	374	1.59	37	588	1
2950	427	1.70	37	588	1
3310	372	1.59	37	588	1
3550	372	1.59	37	588	1
3800	374	1.59	37	588	1
4570	421	1.70	37	588	1
4680	374	1.59	37	588	1
5130	279	1.59	37	588	1
6460	341	1.70	37	588	1
8130	341	1.70	37	588	1
8910	331	1.59	37	588	1
10500	279	1.59	37	588	1
11000	279	1.59	37	588	1
12600	341	1.70	37	588	1
12600	341	1.70	37	616	1
13500	331	1.59	37	616	1
14100	314	1.59	37	616	1
14100	314	1.59	37	616	1

C17000: Cold-worked 37% and Aged

Stress-controlled Flexural Fatigue Life, Air (295 K)

Table 11.4, continued

Cycles, N (10^3)	Maximum Stress, MPa	[Be], wt%	Cold Work, %	Aging Temperature, K	Reference No.
15000	348	1.70	37	588	1
15100	331	1.59	37	588	1
15800	308	1.59	37	616	1
37200	341	1.70	37	616	1
22400	348	1.70	37	588	1
22400	331	1.59	37	616	1
24000	308	1.59	37	588	1
25100	310	1.70	37	588	1
25700	232	1.59	37	588	1
26900	292	1.59	37	616	1
28800	312	1.59	37	588	1
29500	348	1.70	37	588	1
31600	308	1.70	37	588	1
33100	299	1.59	37	616	1
34700	348	1.70	37	588	1
35500	292	1.59	37	616	1
37200	348	1.70	37	588	1
40700	327	1.70	37	588	1
45700	299	1.59	37	588	1
47900	261	1.59	37	616	1
56200	301	1.70	37	588	1
57500	262	1.59	37	616	1
64600	308	1.70	37	588	1
74100	299	1.59	37	588	1
95500	308	1.70	37	588	1
95500	303	1.70	37	616	1
100000	299	1.59	37	588	1
100000	279	1.59	37	588	1
100000	261	1.59	37	588	1
100000	292	1.59	37	588	1
100000	279	1.59	37	588	1
100000	261	1.59	37	588	1
100000	261	1.59	37	588	1
100000	261	1.59	37	588	1
100000	232	1.59	37	588	1
100000	292	1.59	37	588	1
100000	232	1.59	37	588	1
100000	232	1.59	37	588	1
100000	328	1.70	37	588	1
100000	316	1.70	37	588	1
100000	261	1.70	37	588	1
100000	316	1.70	37	588	1
100000	328	1.70	37	588	1
100000	328	1.70	37	588	1
100000	308	1.70	37	588	1
100000	308	1.70	37	588	1
100000	308	1.70	37	588	1
100000	269	1.70	37	616	1
100000	269	1.70	37	588	1
100000	269	1.70	37	588	1
100000	269	1.70	37	588	1

C17000: Cold-worked 37% and Aged

Stress-controlled Flexural Fatigue Life, Air (295 K)

Table 11.4, continued

Cycles, N (10^3)	Maximum Stress, MPa	[Be], wt%	Cold Work, %	Aging Temperature, K	Reference No.
100000	314	1.59	37	616	1
100000	292	1.59	37	616	1
100000	276	1.59	37	616	1
100000	292	1.59	37	616	1
100000	276	1.59	37	616	1
100000	276	1.59	37	616	1
100000	276	1.59	37	616	1
100000	276	1.59	37	616	1
100000	303	1.70	37	616	1
100000	276	1.70	37	616	1
100000	276	1.70	37	616	1
100000	276	1.70	37	616	1
100000	286	1.70	37	616	1
100000	286	1.70	37	616	1

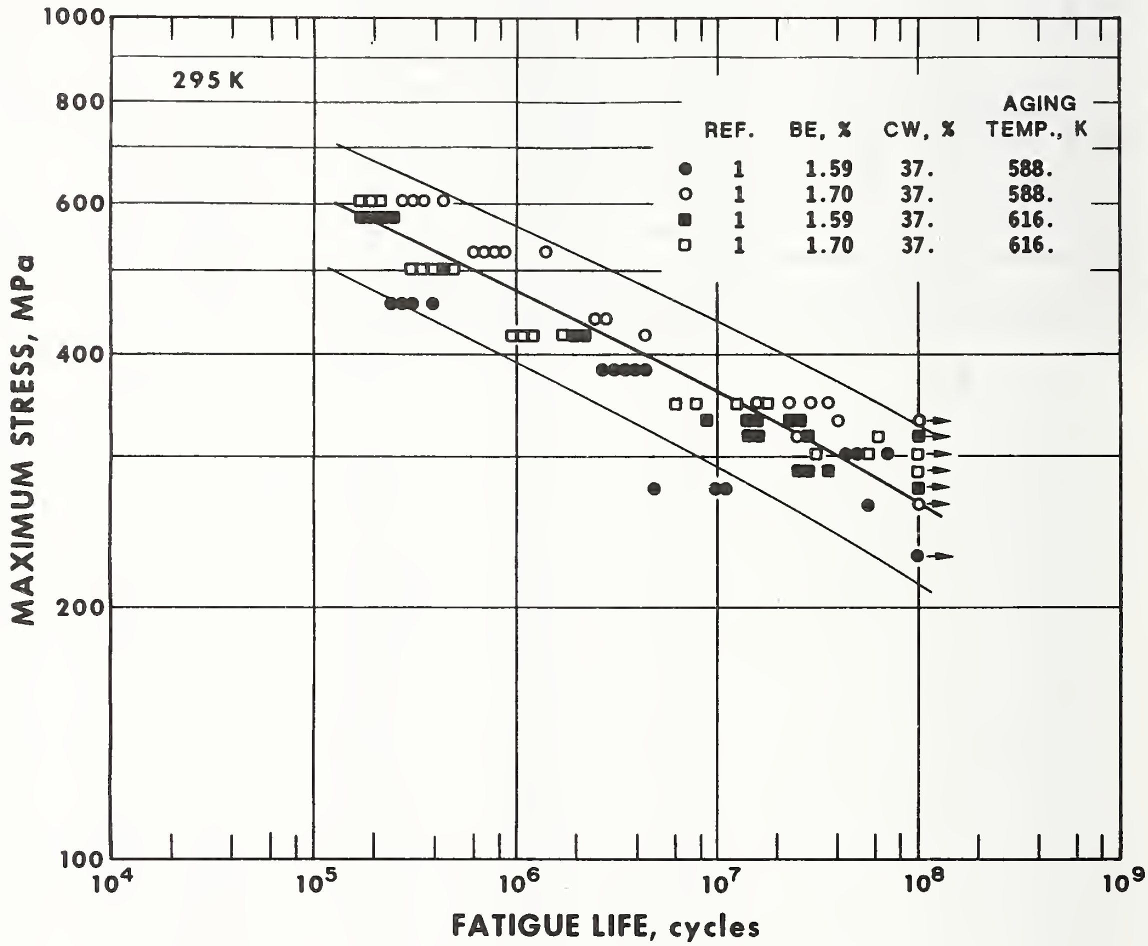

Figure 11.4. Fatigue life curves at 295 K for C17000 beryllium copper cold-worked 37% before aging are shown. The scatter band represents two standard deviations about a nonlinear regression curve given by Equation (11-5), in which *N* is the dependent variable. For clarity, overlapping data points are omitted from the figure. All data are presented in Table 11.4. Product was in strip form. Arrows denote completion of test before failure.

C17200: Annealed; Annealed and Aged; Cold-worked and Aged

Stress-controlled Axial Fatigue Life, Air (295 K)

DATA SOURCES AND ANALYSIS

Measurements at 295 K of the maximum stress (σ_m) versus the number of cycles to failure (N) of C17200 beryllium copper were obtained from References 11.3 and 11.4. The fatigue mode was axial (R-ratio equals 0). The measurements reported in Reference 11.3 were on specimens tested in four different conditions: annealed, annealed and aged (600 K for 0.28 h), cold-worked (60% reduction of area) and aged (600 K for 0.28 h), and cold-worked (60% reduction of area) and overaged (600 K for 24 h). The data reported in Reference 11.4 were obtained on notched and unnotched specimens cold-worked 21% before aging at 588 K for 3 h. Product was in bar form.

Attempts were made to fit the measurements to Equation (11-1) by a nonlinear least-squares regression procedure, but convergent results could not be obtained with this expression.

RESULTS

Table 11.5 presents N, σ_m, CW, aging temperature and time, and the reference number. The available characterization of materials and measurements is given in Table 11.14 at the end of the fatigue properties section. The fatigue life curves are shown in Figure 11.5. The measurements from Reference 11.3 fall in two distinct bands: specimens that were cold-worked before aging have longer fatigue lives at a given stress than specimens that were not cold-worked. The measurements from Reference 11.4 on notched specimens fall considerably below those on unnotched specimens.

Table 11.5. Fatigue Life Measurements for Annealed, Annealed and Aged, and Cold-worked and Aged C17200 Beryllium Copper (295 K).

Cycles, N (10^3)	Maximum Stress, MPa	Cold Work, %	Aging Temperature, K	Aging Time, h	Reference No.
2.82	483	N.S.	588	3.0	4
3.90	690	N.S.	588	3.0	4
9.60	690	N.S.	588	[illegible].0	4
13.40	414	N.S.	588	3.0	4
15.80	690	N.S.	588	[illegible].0	4
15.80	278	60	N.S.	N.S.	3
20.00	576	60	500	0.3	3
23.40	314	60	0	3.0	3
27.10	345	N.S.	588	[illegible].0	4
31.60	452	60	600	24.0	3
37.10	564	60	600	0.3	3
39.80	276	60	0	3.0	3
42.60	237	60	0	0.0	3
44.70	266	60	N.S.	N.S.	3
48.10	552	N.S.	588	[illegible].0	4
50.10	576	60	600	0.[illegible]	3
63.10	240	60	N.S.	N.S.	3
84.30	278	N.S.	588	[illegible].0	4
63.10	400	60	600	24.0	3
112.00	247	60	N.S.	N.S.	3
112.00	206	60	0	0.0	3
117.00	278	N.S.	588	3.0	4
120.00	4[illegible]	60	600	0.3	3
190.00	196	60	N.S.	N.S.	3
251.00	414	N.S.	588	3.0	4
251.00	200	60	N.S.	N.S.	3

C17200: Annealed; Annealed and Aged; Cold-worked and Aged

Stress-controlled Axial Fatigue Life, Air (295 K)

Table 11.5, continued

Cycles, N (10^3)	Maximum Stress, MPa	Cold Work, %	Aging Temperature, K	Aging Time, h	Reference No.
275.00	406	60	500	0.3	3
275.00	492	60	600	0.3	3
282.00	138	N.S.	588	3.0	4
316.00	145	60	0	0.0	3
355.00	358	60	500	24.0	3
398.00	353	60	600	24.0	3
398.00	176	60	N.S.	N.S.	3
602.00	364	60	600	0.3	3
759.00	305	60	600	24.0	3
955.00	163	60	0	0.3	3
1000.00	160	60	N.S.	N.S.	3
1359.00	345	N.S.	588	0.3	4
1698.00	158	60	0	0.3	3
2239.00	317	60	600	0.3	3
3631.00	144	60	0	3.0	3
3981.00	145	60	N.S.	N.S.	3
9550.00	276	60	600	24.0	3
9822.00	163	N.S.	588	0.3	4
14125.00	136	60	0	0.0	3
19953.00	140	60	N.S.	N.S.	3
25704.00	288	60	600	0.3	3

N.S. = not specified.
Aging Temperature, 0 K = not aged.

C17200: Annealed; Annealed and Aged; Cold-worked and Aged

Stress-controlled Axial Fatigue Life, Air (295 K)

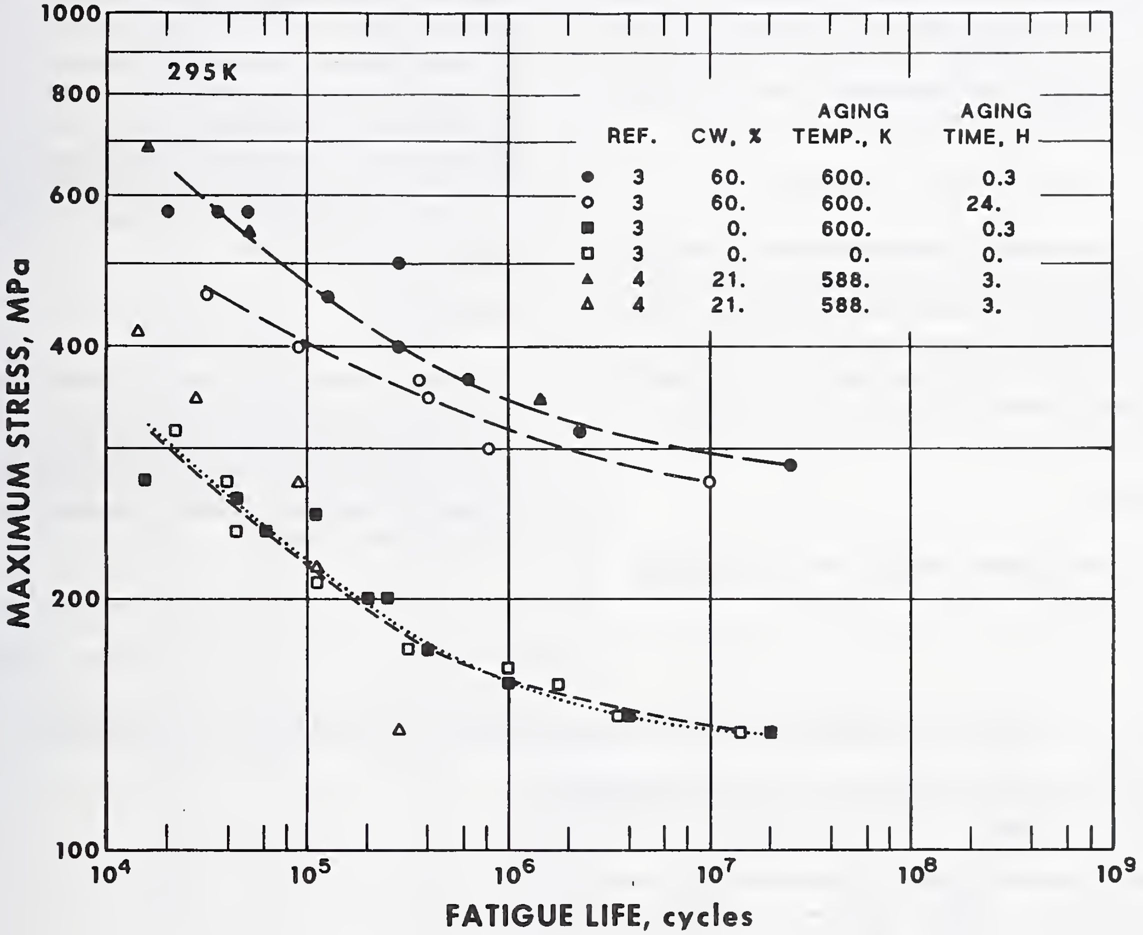

Figure 11.5. Fatigue life curves at 295 K for C17200 beryllium copper for four different material conditions and notched and unnotched specimens are shown. The lower set of measurements from Reference 11.4 were obtained on V-notched specimens. A few points from Reference 4 are off the scale of the graph. All data are presented in Table 11.5. Product was in bar form.

DATA SOURCES AND ANALYSIS

Measurements at 295 K of the maximum stress (σ_m) versus the number of cycles to failure (N) for annealed and aged C17200 beryllium copper were obtained from Reference 11.1. The fatigue mode was flexural (R-ratio equals −1). Product was in strip form. Aging temperatures were 588 and 616 K; aging time was 3 h. Beryllium content, [Be], was 1.81, 1.96, and 2.09 wt%.

In the analysis, N is treated as the dependent variable, and the equation used to analyze the data (Reference 11.2) is

$$\log N = N_0 + N_1 \log(\sigma_m - \sigma_0). \qquad (11\text{-}1)$$

The measurements were fitted to this equation by a nonlinear least-squares regression procedure that determines the constants N_0, N_1, and σ_0. If duplicate results (same N for a given σ_m) were obtained, both test results were included in the measurement set used for the regression analysis.

RESULTS

The equation obtained from the measurements was

$$\log N = 13.0 - 4.20 \log(\sigma_m - 150), \qquad (11\text{-}6)$$

where σ_m is in MPa. The standard deviation of the fit (in units of log N) is 0.4. The standard deviations of the three constants are 1.4, 0.52, and 20.

Table 11.6 presents N, σ_m, [Be], aging temperature, and the reference number. The available characterization of materials and measurements is given in Table 11.14 at the end of the fatigue properties section. Figure 11.6 indicates the fit of the data to Equation (11-6). The scatter band represents two standard deviations about the regression curve. The variance of the data about the line was assumed to be normally distributed and constant throughout the range of the independent variable, σ_m.

DISCUSSION

The constants N_0, N_1, and σ_0 from Equation (11-1) fitted to the data of Reference 11.1 only are shown as a function of cold work in Figure 11.10. For both C17000 and C17200 beryllium coppers, a systematic variation of these constants with cold work was observed.

Table 11.6. Fatigue Life Measurements for Annealed and Aged C17200 Beryllium Copper (295 K).

Cycles, N (10^3)	Maximum Stress, MPa	[Be], wt%	Aging Temperature, K	Reference No.
105	520	2.09	588	1
107	534	1.96	588	1
119	552	1.96	616	1
120	534	1.96	588	1
126	534	1.96	616	1
129	552	1.96	588	1
141	590	2.09	616	1
145	552	1.96	588	1
150	552	1.96	616	1
166	552	1.96	588	1
158	590	2.09	616	1
170	520	2.09	588	1
174	515	1.81	588	1
174	590	2.09	616	1
178	520	2.09	588	1
184	590	2.09	616	1
184	590	2.09	616	1

C17200: Annealed and Aged

Stress-controlled Flexural Fatigue Life, Air (295 K)

Table 11.6, continued

Cycles, N (10^3)	Maximum Stress, MPa	[Be], wt%	Aging Temperature, K	Reference No.
186	515	1.81	616	1
186	499	1.81	588	1
191	499	1.81	588	1
204	499	1.81	616	1
269	448	1.96	588	1
214	499	1.81	588	1
234	499	1.81	588	1
229	457	1.96	588	1
234	520	2.09	588	1
240	514	1.81	588	1
245	457	1.96	588	1
263	514	1.81	588	1
269	458	1.96	588	1
263	448	1.96	616	1
269	520	2.09	588	1
282	448	1.96	588	1
234	514	1.81	588	1
282	444	2.09	588	1
372	426	1.81	588	1
316	457	1.96	588	1
331	431	2.09	588	1
331	417	1.81	616	1
347	448	1.96	588	1
347	448	1.96	616	1
372	457	1.96	588	1
372	417	1.81	616	1
372	417	1.81	588	1
380	499	2.09	588	1
417	445	2.09	616	1
437	445	2.09	616	1
457	499	2.09	616	1
468	431	2.09	588	1
473	417	1.81	588	1
479	445	2.09	588	1
490	424	1.81	588	1
490	424	1.81	588	1
501	445	2.09	616	1
525	431	2.09	588	1
537	365	1.96	616	1
575	424	1.81	588	1
589	417	1.81	616	1
603	424	1.81	588	1
646	327	1.96	588	1
661	365	1.96	588	1
708	365	1.96	588	1
724	293	1.81	588	1
741	327	1.96	588	1
759	327	1.96	588	1
832	365	1.96	616	1
933	534	1.96	616	1
933	328	1.96	616	1

Table 11.6, continued

Cycles, N (10^3)	Maximum Stress, MPa	[Be], wt%	Aging Temperature, K	Reference No.
955	341	1.81	588	1
977	534	1.96	616	1
1200	343	1.81	588	1
1000	293	1.81	616	1
1050	341	1.81	588	1
1080	321	1.96	616	1
1170	328	1.96	588	1
1200	321	1.96	616	1
1200	348	2.09	588	1
1000	348	2.09	616	1
1260	341	1.81	588	1
1080	359	1.96	616	1
1260	359	2.09	588	1
1320	348	2.09	616	1
1820	348	2.09	588	1
1080	341	1.81	616	1
1480	341	1.81	588	1
1000	348	2.09	616	1
1510	341	1.81	616	1
1510	359	2.09	616	1
1850	341	1.81	588	1
1700	359	2.09	616	1
1820	341	1.81	588	1
1880	341	1.81	616	1
2240	359	2.09	588	1
2240	321	2.09	616	1
2290	288	1.96	588	1
2340	359	2.09	616	1
2400	328	1.96	588	1
2570	293	1.81	616	1
2630	321	2.09	588	1
2630	321	2.09	616	1
2630	288	1.81	588	1
2630	286	1.96	588	1
2950	266	1.81	616	1
2950	293	1.81	588	1
2630	287	1.96	588	1
2950	293	1.81	616	1
2950	288	2.09	588	1
2950	286	1.96	616	1
3160	288	1.81	588	1
3160	323	1.96	616	1
3880	288	1.96	588	1
3720	328	1.96	616	1
3800	283	1.81	588	1
1690	252	1.96	616	1
4170	286	1.96	588	1
4570	293	1.81	616	1
4570	286	1.96	616	1
4790	286	1.96	616	1
5010	248	1.96	616	1

Table 11.6, continued

Cycles, N (10^3)	Maximum Stress, MPa	[Be], wt%	Aging Temperature, K	Reference No.
5130	299	1.96	588	1
5190	319	2.09	588	1
5500	319	2.09	588	1
5620	231	1.96	588	1
5750	299	1.81	588	1
5750	293	1.81	588	1
6310	248	1.96	588	1
6760	231	1.81	588	1
6760	248	1.96	588	1
7940	273	1.81	588	1
6310	319	2.09	588	1
9120	293	2.09	588	1
10700	314	2.09	588	1
11500	293	1.81	588	1
14800	252	1.81	588	1
19100	293	2.09	588	1
17400	319	2.09	588	1
19100	252	1.96	588	1
21400	299	2.09	588	1
23700	273	2.09	588	1
25700	252	1.81	588	1
30200	314	2.09	588	1
35500	319	2.09	588	1
35500	293	2.09	588	1
41700	299	1.81	588	1
46800	252	2.09	588	1
67600	299	2.09	588	1
85100	292	2.09	588	1
100000	299	1.81	588	1
100000	231	1.81	588	1
100000	214	1.81	588	1
100000	293	1.81	588	1
100000	231	1.81	588	1
100000	231	1.81	588	1
100000	231	1.81	588	1
100000	231	1.81	588	1
100000	214	1.81	588	1
100000	214	1.81	588	1
100000	214	1.81	588	1
100000	214	1.81	588	1
100000	299	1.96	588	1
100000	293	1.96	588	1
100000	299	1.96	588	1
100000	252	2.09	588	1
100000	273	2.09	588	1
100000	273	2.09	588	1
100000	273	2.09	588	1
100000	273	2.09	588	1
100000	273	2.09	588	1
100000	262	1.81	616	1
100000	224	1.81	616	1

Table 11.6, continued

Cycles, N (10^3)	Maximum Stress, MPa	[Be], wt%	Aging Temperature, K	Reference No.
100000	262	1.81	616	1
100000	262	1.81	616	1
100000	262	1.81	616	1
100000	224	1.81	616	1
100000	224	1.81	616	1
100000	224	1.81	616	1
100000	224	1.81	616	1
100000	248	1.96	616	1
100000	248	1.96	616	1
100000	299	2.09	616	1
100000	279	2.09	616	1
100000	241	2.09	616	1
100000	279	2.09	616	1
100000	279	2.09	616	1
100000	279	2.09	616	1
100000	241	2.09	616	1
100000	241	2.09	616	1
100000	241	2.09	616	1
100000	241	2.09	616	1

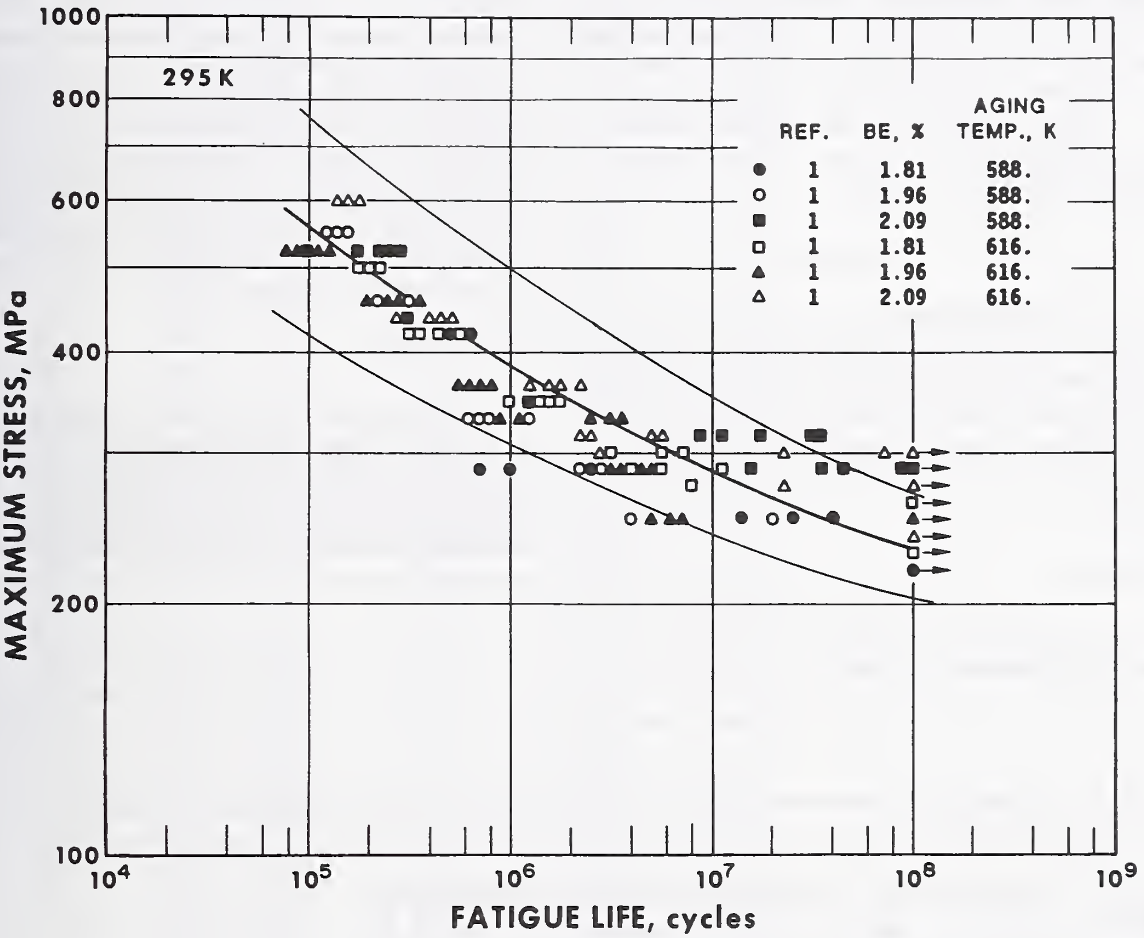

Figure 11.6. Fatigue life curves at 295 K for annealed and aged C17200 beryllium copper are shown. The scatter band represents two standard deviations about a nonlinear regression curve given by Equation (11-6), in which *N* is the dependent variable. For clarity, overlapping data points are omitted from the figure. All data are presented in Table 11.6. Product was in strip form. Arrows denote completion of test before failure.

DATA SOURCES AND ANALYSIS

Measurements at 295 K of the maximum stress (σ_m) versus the number of cycles to failure (N) for cold-worked and aged C17200 beryllium copper were obtained from Reference 11.1. The fatigue mode was flexural (R-ratio equals −1). Product was in strip form. Cold work, *CW*, was 11% (reduction in thickness). Aging temperatures were 588 and 616 K; aging time was 3 h. Beryllium content, [Be], was 1.81, 1.96, and 2.09 wt%.

In the analysis, N is treated as the dependent variable, and the equation used to analyze the data (Reference 11.2) is

$$\log N = N_0 + N_1 \log(\sigma_m - \sigma_0). \qquad (11\text{-}1)$$

The measurements were fitted to this equation by a nonlinear least-squares regression procedure that determines the constants N_0, N_1, and σ_0. If duplicate results (same N for a given σ_m) were obtained, both test results were included in the measurement set used for the regression analysis.

RESULTS

The equation obtained from the measurements of Reference 11.1 was

$$\log N = 12.4 - 3.92 \log(\sigma_m - 190), \qquad (11\text{-}7)$$

where σ_m is in MPa. The standard deviation of the fit (in units of log N) is 0.3. The standard deviations of the three constants are 0.9, 0.34, and 13.

Table 11.7 presents N, σ_m, [Be], *CW*, aging temperature, and the reference number. The available characterization of materials and measurements is given in Table 11.14 at the end of the fatigue properties section. Figure 11.7 indicates the fit of the data to Equation (11-7). The scatter band represents two standard deviations about the regression curve. The variance of the data about the line was assumed to be normally distributed and constant throughout the range of the independent variable, σ_m.

DISCUSSION

The constants N_0, N_1, and σ_0 from Equation (11-1) fitted to the data of Reference 11.1 only are shown as a function of *CW* in Figure 11.10. For both C17000 and C17200 beryllium coppers, a systematic variation of these constants with *CW* was observed.

Table 11.7. Fatigue Life Measurements for C17200 Beryllium Copper Cold-worked 11% Before Aging (295 K).

Cycles, N (10^3)	Maximum Stress, MPa	[Be], wt%	Cold Work, %	Aging Temperature, K	Reference No.
100	645	1.96	11	616	1
107	645	1.96	11	616	1
110	617	1.81	11	588	1
117	645	1.96	11	616	1
120	621	2.09	11	588	1
141	519	1.81	11	616	1
148	602	1.96	11	588	1
155	621	2.09	11	616	1
158	617	1.81	11	588	1
155	602	1.96	11	588	1
166	602	1.96	11	588	1
167	617	1.81	11	616	1
167	617	1.81	11	588	1
167	617	1.81	11	588	1

C17200: Cold-worked 11% and Aged

Stress-controlled Flexural Fatigue Life, Air (295 K)

Table 11.7, continued

Cycles, N (10^3)	Maximum Stress, MPa	[Be], wt%	Cold Work, %	Aging Temperature, K	Reference No.
168	621	2.09	11	616	1
168	621	2.09	11	588	1
178	621	2.09	11	616	1
178	519	1.81	11	588	1
168	602	1.96	11	588	1
195	427	1.81	11	588	1
204	510	1.96	11	588	1
209	519	1.81	11	616	1
209	534	2.09	11	588	1
234	534	2.09	11	616	1
269	510	1.81	11	588	1
269	519	1.81	11	588	1
269	534	2.09	11	588	1
269	510	1.96	11	588	1
269	529	1.96	11	616	1
282	510	1.96	11	588	1
282	534	2.09	11	616	1
299	529	1.96	11	588	1
299	529	1.96	11	616	1
299	529	1.96	11	616	1
309	534	2.09	11	588	1
309	517	1.81	11	616	1
309	510	1.96	11	588	1
309	517	1.81	11	588	1
331	512	1.81	11	588	1
331	529	1.96	11	616	1
331	510	2.09	11	616	1
339	519	2.09	11	616	1
355	534	2.09	11	616	1
369	510	1.81	11	588	1
372	534	2.09	11	616	1
389	510	1.81	11	588	1
398	534	2.09	11	588	1
398	427	1.81	11	588	1
447	438	1.96	11	588	1
468	510	1.96	11	588	1
562	534	1.96	11	588	1
562	427	1.81	11	616	1
575	425	1.81	11	588	1
631	441	2.09	11	616	1
661	425	1.81	11	588	1
661	438	2.09	11	588	1
661	427	1.81	11	616	1
661	441	2.09	11	616	1
675	438	1.96	11	588	1
692	427	1.81	11	616	1
741	438	2.09	11	588	1
741	438	1.96	11	588	1
741	441	2.09	11	616	1
794	438	1.96	11	616	1
813	425	1.81	11	588	1

C17200: Cold-worked 11% and Aged

Stress-controlled Flexural Fatigue Life, Air (295 K)

Table 11.7, continued

Cycles, N (10^3)	Maximum Stress, MPa	[Be], wt%	Cold Work, %	Aging Temperature, K	Reference No.
813	438	1.96	11	616	1
832	438	2.09	11	588	1
813	438	1.96	11	616	1
841	438	1.96	11	616	1
933	414	1.96	11	588	1
955	441	2.09	11	616	1
977	438	2.09	11	616	1
1120	438	2.09	11	588	1
1260	424	1.81	11	616	1
1260	414	1.96	11	616	1
1260	441	2.09	11	616	1
1330	414	1.96	11	588	1
1460	348	1.81	11	616	1
1580	348	1.81	11	616	1
1910	353	1.96	11	616	1
2000	359	2.09	11	616	1
2340	345	1.81	11	616	1
2340	348	1.81	11	616	1
2400	359	1.96	11	616	1
2510	354	2.09	11	616	1
2630	348	1.81	11	616	1
2680	353	1.96	11	616	1
2630	359	2.09	11	616	1
2750	354	2.09	11	616	1
2820	345	1.81	11	616	1
2880	359	2.09	11	588	1
2950	345	1.81	11	588	1
[illegible]	310	1.81	11	616	1
3090	345	1.81	11	588	1
3310	334	1.96	11	616	1
3310	345	1.81	11	616	1
3470	272	1.81	11	616	1
4070	359	2.09	11	588	1
4170	310	2.09	11	616	1
4790	359	2.09	11	588	1
5010	310	1.81	11	616	1
5370	353	1.96	11	616	1
5500	359	2.09	11	588	1
5500	359	2.09	11	616	1
5750	334	2.09	11	616	1
6030	353	1.96	11	616	1
6170	334	2.09	11	616	1
6170	334	2.09	11	616	1
6760	[illegible]	2.09	11	616	1
7080	345	1.81	11	616	1
7080	354	2.09	11	616	1
7590	299	1.96	11	616	1
[illegible]	310	2.09	11	616	1
7760	306	1.81	11	588	1
9120	334	1.96	11	588	1
9330	310	1.81	11	616	1

C17200: Cold-worked 11% and Aged

Stress-controlled Flexural Fatigue Life, Air (295 K)

Table 11.7, continued

Cycles, N (10^3)	Maximum Stress, MPa	[Be], wt%	Cold Work, %	Aging Temperature, K	Reference No.
9550	334	1.96	11	588	1
10000	334	2.09	11	616	1
11500	306	1.81	11	588	1
11700	334	1.96	11	616	1
12900	306	1.81	11	588	1
13200	299	1.96	11	588	1
15500	319	2.09	11	588	1
15800	261	1.81	11	588	1
15800	319	1.96	11	616	1
15800	312	2.09	11	616	1
16600	299	1.96	11	588	1
15800	314	1.96	11	616	1
16600	312	2.09	11	616	1
17000	306	1.81	11	616	1
18200	319	1.96	11	588	1
21400	312	2.09	11	616	1
22400	319	2.09	11	588	1
23400	261	1.81	11	616	1
24000	296	1.96	11	616	1
25100	312	2.09	11	588	1
25700	319	1.96	11	588	1
26300	319	2.09	11	588	1
29500	319	2.09	11	616	1
33900	306	1.81	11	588	1
34700	299	2.09	11	616	1
35500	261	1.96	11	616	1
38000	251	1.81	11	588	1
42200	301	2.09	11	616	1
47900	300	1.96	11	616	1
50100	306	1.96	11	588	1
50100	293	1.96	11	616	1
53700	301	2.09	11	588	1
57500	296	1.81	11	616	1
58900	303	2.09	11	588	1
58100	251	2.09	11	616	1
61700	303	2.09	11	588	1
70800	294	1.96	11	616	1
75000	261	1.96	11	588	1
81300	296	1.81	11	616	1
83200	272	1.81	11	588	1
89100	296	1.81	11	616	1
100000	301	1.81	11	588	1
100000	299	1.81	11	616	1
100000	261	1.81	11	588	1
100000	299	1.81	11	616	1
100000	261	1.81	11	588	1
100000	251	1.81	11	616	1
100000	251	1.81	11	588	1
100000	251	1.81	11	588	1
100000	261	1.96	11	588	1
100000	261	1.96	11	588	1

C17200: Cold-worked 11% and Aged

Stress-controlled Flexural Fatigue Life, Air (295 K)

Table 11.7, continued

Cycles, N (10^3)	Maximum Stress, MPa	[Be], wt%	Cold Work, %	Aging Temperature, K	Reference No.
100000	261	1.96	11	588	1
100000	303	2.09	11	616	1
100000	279	2.09	11	588	1
100000	279	2.09	11	616	1
100000	279	2.09	11	588	1
100000	279	2.09	11	616	1
100000	279	2.09	11	588	1
100000	279	1.81	11	616	1
100000	272	1.81	11	588	1
100000	272	1.81	11	616	1
100000	272	1.81	11	588	1
100000	272	1.81	11	616	1
100000	314	1.96	11	588	1
100000	296	1.96	11	616	1
100000	279	1.96	11	588	1
100000	296	1.96	11	616	1
100000	279	1.96	11	588	1
100000	279	1.96	11	616	1
100000	276	1.96	11	616	1
100000	276	1.96	11	616	1
100000	296	2.09	11	616	1
100000	296	2.09	11	616	1
100000	296	2.09	11	616	1

C17200: Cold-worked 11% and Aged

Stress-controlled Flexural Fatigue Life, Air (295 K)

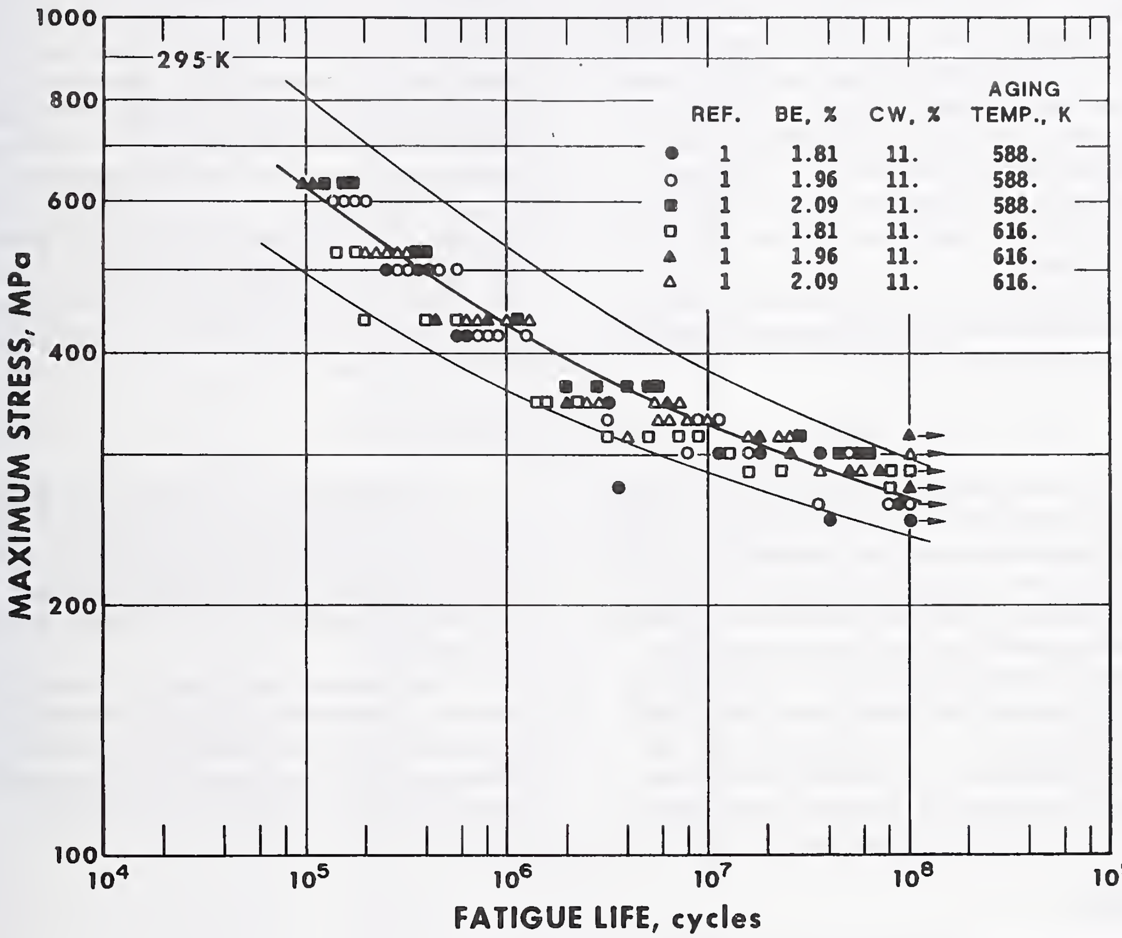

Figure 11.7. Fatigue life curves at 295 K for C17200 beryllium copper cold-worked 11% before aging are shown. The scatter band represents two standard deviations about a nonlinear regression curve given by Equation (11-7), in which N is the dependent variable. For clarity, overlapping data points are omitted from the figure. All data are presented in Table 11.7. Product was in strip form. Arrows denote completion of test before failure.

C17200: Cold-worked 21% and Aged

Stress-controlled Flexural Fatigue Life, Air (295 K)

DATA SOURCES AND ANALYSIS

Measurements at 295 K of the maximum stress (σ_m) versus the number of cycles to failure (N) for cold-worked and aged C17200 beryllium copper were obtained from References 11.1 and 11.5. The fatigue mode was flexural (R-ratio equals −1). Products were in strip and bar form. Cold work, *CW*, was 21% (reduction in thickness). (The degree of *CW* for one set of data from Reference 11.5 was not given, but the authors stated that the material used for all tests was similar). Aging temperatures were 573, 588, and 616 K; aging time was 3 h (Reference 11.1) or 1.5 h (Reference 11.5). Beryllium content, [Be], for the data reported in Reference 11.1 was 1.81, 1.96, and 2.09 wt%.

In the analysis, N is treated as the dependent variable, and the equation used to analyze the data (Reference 11.2) is

$$\log N = N_0 + N_1 \log(\sigma_m - \sigma_0). \qquad (11\text{-}1)$$

The measurements were fitted to this equation by a nonlinear least-squares regression procedure that determines the constants N_0, N_1, and σ_0. If duplicate results (same N for a given σ_m) were obtained, both test results were included in the measurement set used for the regression analysis. Data from Reference 11.5 (bar stock) did not follow the fatigue life trend line of data from Reference 11.1. To determine if the constants in Equation (11-1) varied systematically with *CW*, this equation was fitted to the data of Reference 11.1 only. (See Figure 11.10).

RESULTS

The equation obtained from the measurements of Reference 11.1 was

$$\log N = 16.2 - 5.26 \log(\sigma_m - 146), \qquad (11\text{-}8)$$

where σ_m is in MPa. The standard deviation of the fit (in units of log N) is 0.3. The standard deviations of the three constants are 1.8, 0.62, and 26.

Table 11.8 presents N, σ_m, [Be], *CW*, aging temperature, and the reference number. The available characterization of materials and measurements is given in Table 11.14 at the end of the fatigue properties section. Figure 11.8 indicates the fit of the data to Equation (11-8) and also shows the data of Reference 11.5. The scatter band represents two standard deviations about the regression curve. The variance of the data about the line was assumed to be normally distributed and constant throughout the range of the independent variable, σ_m. The data from Reference 11.5, on bar stock, fall slightly above this scatter band.

DISCUSSION

The constants N_0, N_1, and σ_0 from Equation (11-1) fitted to the data of Reference 11.1 only are shown as a function of *CW* in Figure 11.10. For both C17000 and C17200 beryllium coppers, a systematic variation of these constants with *CW* was observed.

A comparison with Figure 11.5 shows that data from axially fatigued specimens with a similar percent of *CW* and similar aging conditions (Reference 11.4, unnotched specimens) fall just slightly below the scatter band for Equation (11-8).

Table 11.8. Fatigue Life Measurements for C17200 Beryllium Copper Cold-worked 21% Before Aging (295 K).

Cycles, N (10^3)	Maximum Stress, MPa	[Be], wt%	Cold Work, %	Aging Temperature, K	Reference No.
112	590	1.96	21	616	1
135	602	1.81	21	616	1
135	507	1.81	21	616	1
135	602	1.81	21	616	1
151	512	2.09	21	616	1
151	590	1.96	21	616	1
153	507	1.96	21	616	1
162	602	1.81	21	588	1
170	621	1.81	21	616	1
170	621	1.81	21	588	1
170	507	1.81	21	616	1
388	610	1.96	21	588	1
151	621	1.81	21	616	1
209	621	1.81	21	588	1
209	610	1.96	21	616	1
211	610	2.09	21	588	1
211	590	1.96	21	616	1
229	610	2.09	21	616	1
234	621	1.81	21	616	1
240	610	2.09	21	588	1
240	514	2.09	21	616	1
240	417	1.96	21	588	1
269	507	1.81	21	616	1
275	610	1.96	21	616	1
248	512	1.96	21	588	1
289	610	1.96	21	588	1
299	507	1.96	21	616	1
209	610	2.09	21	616	1
209	514	2.09	21	616	1
300	469	2.12	N.S.	588	5
324	507	1.81	21	616	1
331	610	2.09	21	588	1
347	507	1.81	21	616	1
355	590	1.96	21	616	1
355	514	2.09	21	616	1
355	610	2.09	21	616	1
372	500	1.96	21	616	1
380	507	1.81	21	588	1
355	507	1.81	21	616	1
355	590	1.96	21	616	1
437	512	1.81	21	616	1
457	590	1.96	21	588	1
468	552	2.12	N.S.	588	5
468	621	1.96	21	588	1
490	512	1.81	21	616	1
501	427	2.09	21	616	1
525	621	1.96	21	588	1
531	510	2.09	21	588	1
531	510	2.09	21	588	1
550	521	1.96	21	588	1

C17200: Cold-worked 21% and Aged

Stress-controlled Flexural Fatigue Life, Air (295 K)

Table 11.8, continued

Cycles, N (10^3)	Maximum Stress, MPa	[Be], wt%	Cold Work, %	Aging Temperature, K	Reference No.
562	510	1.81	21	588	1
575	512	2.09	21	588	1
575	510	2.09	21	588	1
575	422	2.09	21	616	1
589	521	1.96	21	588	1
603	512	1.81	21	588	1
609	510	2.09	21	588	1
631	427	2.09	21	573	1
676	521	1.96	21	588	1
675	421	1.81	21	616	1
759	421	1.81	21	616	1
813	417	1.81	21	588	1
832	417	1.96	21	573	1
831	506	1.96	21	588	1
933	469	2.12	N.S.	588	5
944	586	2.12	21	573	5
955	421	2.09	21	588	1
955	427	2.09	21	588	1
1000	552	2.12	21	573	5
1000	417	1.96	21	573	1
1000	417	1.96	21	588	1
1020	423	1.81	21	588	1
1120	517	2.12	N.S.	588	5
1120	423	2.09	21	588	1
1150	421	1.81	21	588	1
1150	421	1.81	21	588	1
1290	421	2.09	21	588	1
1380	423	2.09	21	588	1
1410	421	1.81	21	588	1
1585	469	2.12	N.S.	588	1
1620	422	1.81	21	588	1
1680	417	1.96	21	588	1
1660	431	1.96	21	588	1
1800	422	1.81	21	588	1
1800	422	1.81	21	588	1
1380	431	1.96	21	588	1
1860	431	1.96	21	588	1
1910	423	2.09	21	573	1
2138	496	2.12	N.S.	588	5
2291	495	2.12	N.S.	588	5
2399	456	2.12	N.S.	588	5
2570	423	2.09	21	588	1
2818	517	2.12	21	573	5
3020	315	1.96	21	588	1
3550	431	1.96	21	588	1
3890	341	1.81	21	588	1
4070	341	1.81	21	588	1
4467	469	2.12	N.S.	588	5
6610	341	1.81	21	616	1
7240	341	1.81	21	616	1
7940	341	1.81	21	616	1

C17200: Cold-worked 21% and Aged

Stress-controlled Flexural Fatigue Life, Air (295 K)

Table 11.8, continued

Cycles, N (10^3)	Maximum Stress, MPa	[Be], wt%	Cold Work, %	Aging Temperature, K	Reference No.
7943	448	2.12	21	573	5
8320	348	2.09	21	616	1
8910	349	1.81	21	588	1
8910	349	1.96	21	588	1
8910	348	2.09	21	616	1
8912	462	2.12	21	616	5
9120	331	1.96	21	588	1
9330	352	2.09	21	588	1
9770	331	2.09	21	588	1
11200	352	2.09	21	616	1
11500	348	2.09	21	616	1
12000	323	1.81	21	616	1
12600	314	1.96	21	588	1
13183	469	2.12	N.S.	616	5
13200	331	1.96	21	588	1
13964	448	2.12	21	588	5
14100	349	1.96	21	588	1
14500	294	1.96	21	588	1
11500	307	1.81	21	616	1
14800	334	1.81	21	588	1
15000	314	1.96	21	616	1
15300	349	1.96	21	588	1
16200	314	2.09	21	616	1
17783	462	2.12	21	616	5
17800	331	1.81	21	588	1
17800	323	1.81	21	616	1
12600	331	2.09	21	588	1
12800	352	2.09	21	588	1
19500	350	2.09	21	588	1
20400	322	1.81	21	616	1
21400	314	1.96	21	588	1
22400	352	1.81	21	616	1
22900	314	1.96	21	616	1
23400	352	2.09	21	616	1
23714	434	2.12	21	573	5
24000	323	1.81	21	616	1
25700	331	1.81	21	588	1
26900	294	1.96	21	616	1
26900	349	1.96	21	588	1
26900	307	1.81	21	616	1
28200	331	1.81	21	588	1
28200	334	1.96	21	616	1
28200	331	2.09	21	616	1
26900	352	2.09	21	616	1
30200	321	1.81	21	588	1
31600	334	1.96	21	616	1
33900	287	1.81	21	588	1
33900	334	1.96	21	616	1
33900	310	2.09	21	616	1
34700	294	1.96	21	588	1
35500	281	1.96	21	616	1

C17200: Cold-worked 21% and Aged

Stress-controlled Flexural Fatigue Life, Air (295 K)

Table 11.8, continued

Cycles, N (10^3)	Maximum Stress, MPa	[Be], wt%	Cold Work, %	Aging Temperature, K	Reference No.
38900	331	2.09	21	588	1
38904	420	2.12	21	588	5
40700	348	1.96	21	588	1
40700	294	1.96	21	588	1
41700	301	1.96	21	588	1
41700	348	2.09	21	588	1
44668	407	2.12	21	588	5
45700	308	2.09	21	588	1
50100	301	2.09	21	588	1
50100	293	1.96	21	588	1
51300	322	1.96	21	588	1
51300	331	2.09	21	588	1
52481	448	2.12	N.S.	588	5
52500	293	1.96	21	588	1
56200	303	2.09	21	588	1
56200	308	1.81	21	588	1
59566	358	2.12	21	573	5
60300	324	1.96	21	588	1
60300	291	2.09	21	588	1
60300	307	1.81	21	588	1
72400	358	2.09	21	588	1
91200	308	2.09	21	588	1
100000	301	1.81	21	588	1
100000	265	1.81	21	588	1
100000	301	1.81	21	588	1
100000	324	1.81	21	588	1
100000	331	1.81	21	588	1
100000	265	1.81	21	588	1
100000	265	1.81	21	588	1
100000	265	1.81	21	588	1
100000	265	1.81	21	588	1
100000	324	1.96	21	588	1
100000	295	1.96	21	588	1
100000	270	1.96	21	588	1
100000	301	1.96	21	588	1
100000	265	1.96	21	588	1
100000	295	1.96	21	588	1
100000	270	1.96	21	588	1
100000	270	1.96	21	588	1
100000	270	1.96	21	588	1
100000	270	1.96	21	588	1
100000	290	2.09	21	588	1
100000	270	2.09	21	588	1
100000	290	2.09	21	588	1
100000	295	2.09	21	588	1
100000	290	2.09	21	588	1
100000	270	2.09	21	588	1
100000	270	2.09	21	588	1
100000	272	2.09	21	588	1
100000	272	2.09	21	588	1
100000	287	1.81	21	616	1

C17200: Cold-worked 21% and Aged

Stress-controlled Flexural Fatigue Life, Air (295 K)

Table 11.8, continued

Cycles, N (10^3)	Maximum Stress, MPa	[Be], wt%	Cold Work, %	Aging Temperature, K	Reference No.
100000	269	1.81	21	616	1
100000	287	1.81	21	616	1
100000	287	1.81	21	616	1
100000	287	1.81	21	616	1
100000	269	1.81	21	616	1
100000	269	1.81	21	616	1
100000	269	1.81	21	616	1
100000	269	1.81	21	616	1
100000	269	1.96	21	616	1
100000	279	1.96	21	616	1
100000	269	1.96	21	616	1
100000	279	1.96	21	616	1
100000	279	1.96	21	616	1
100000	310	2.09	21	616	1
100000	290	2.09	21	616	1
100000	310	2.09	21	616	1
100000	310	2.09	21	616	1
100000	290	2.09	21	616	1
100000	290	2.09	21	616	1
100000	290	2.09	21	616	1
100000	290	2.09	21	616	1
154882	393	2.12	21	573	5
218776	379	2.12	21	573	5
354813	324	2.12	21	573	5

N.S. = not specified.

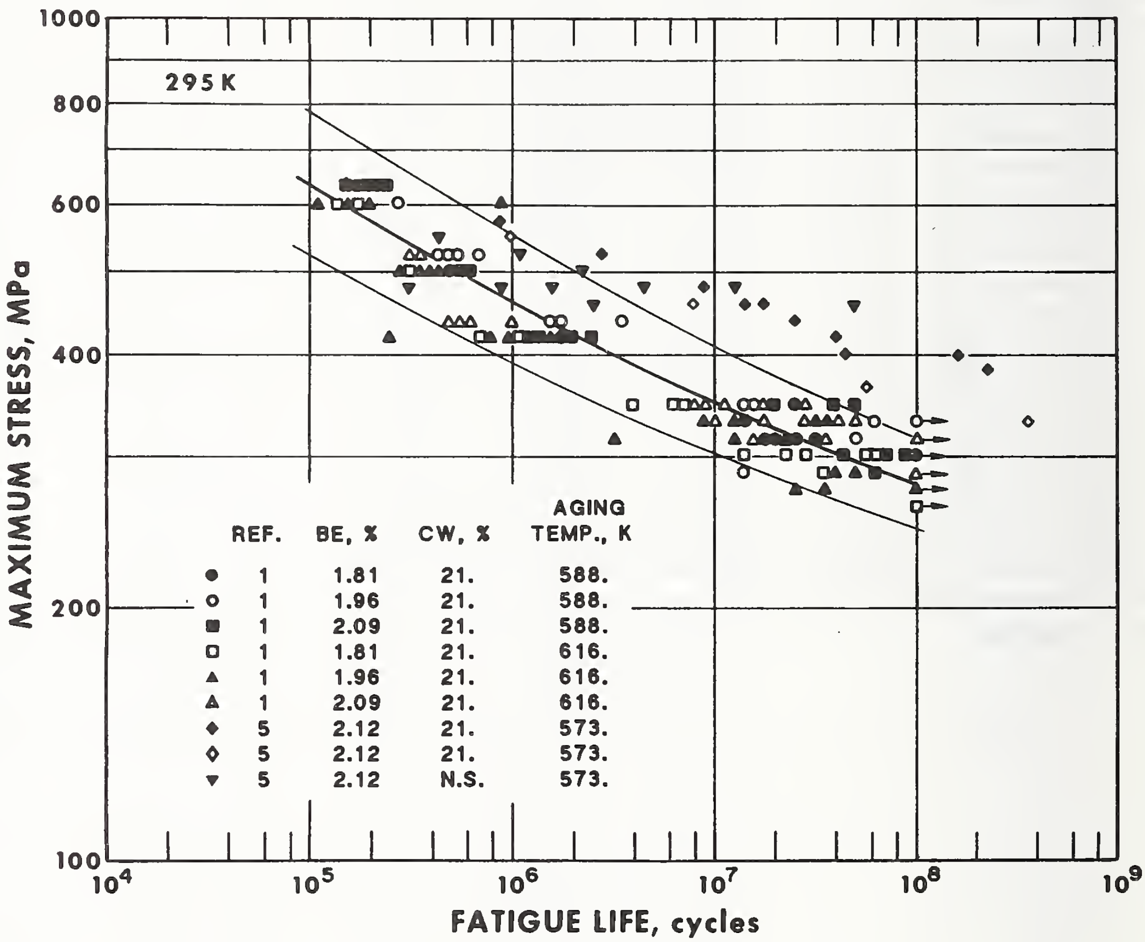

Figure 11.8. Fatigue life curves at 295 K for C17200 beryllium copper cold-worked 21% before aging are shown. The scatter band represents two standard deviations about a nonlinear regression curve given by Equation (11-8), in which N is the dependent variable. For clarity, overlapping data points are omitted from the figure. All data are presented in Table 11.8. Products were in strip (Reference 11.1) and bar form (Reference 11.5). Arrows denote completion of test before failure.

C17200: Cold-worked 37% and Aged

Stress-controlled Flexural Fatigue Life, Air (295 K)

DATA SOURCES AND ANALYSIS

Measurements at 295 K of the maximum stress (σ_m) versus the number of cycles to failure (N) for cold-worked and aged C17200 beryllium copper were obtained from References 11.1 and 11.6. The fatigue mode was flexural (R-ratio equals −1). Product was in strip form. Cold-work, CW, was 37 or 40% (reduction in thickness). Aging temperatures were 588, 616, and 698 K; aging time was 3 h (Reference 11.1) or varied (Reference 11.6). Beryllium content, [Be], for the data reported in Reference 11.1 was 1.81, 1.96, and 2.09 wt%.

In the analysis, N is treated as the dependent variable, and the equation used to analyze the data (Reference 11.2) is

$$\log N = N_0 + N_1 \log(\sigma_m - \sigma_0). \qquad (11\text{-}1)$$

The measurements were fitted to this equation by a nonlinear least-squares regression procedure that determines the constants N_0, N_1, and σ_0. If duplicate results (same N for a given σ_m) were obtained, both test results were included in the measurement set used for the regression analysis. Although the data from Reference 11.6 follows the fatigue life trend line of the data from Reference 11.1 fairly well, for consistency in determining the behavior of the constants of Equation (11-1) with CW, this equation was refitted to the data of Reference 11.1 only. (See Figure 11.10).

RESULTS

The equation obtained from the measurements of Reference 11.1 was

$$\log N = 24.6 - 8.04 \log(\sigma_m + 4.03), \qquad (11\text{-}9)$$

where σ_m is in MPa. The standard deviation of the fit (in units of log N) is 0.4. The standard deviations of the three constants are 7.1, 2.33, and 114.50. Since the uncertainty of the last constant, σ_0, exceeds the value of the constant, σ_0 is not well determined from this data set.

Table 11.9 presents N, σ_m, [Be], CW, aging temperature, and the reference number. The available characterization of materials and measurements is given in Table 11.14 at the end of the fatigue properties section. Figure 11.9 indicates the fit of the data to Equation (11-9) and also shows the data of Reference 11.6. The scatter band represents two standard deviations about the regression curve. The variance of the data about the line was assumed to be normally distributed and constant throughout the range of the independent variable, σ_m. Data from Reference 11.6 are consistent with Equation (11-9) determined from analysis of data from Reference 11.1.

DISCUSSION

The constants N_0, N_1, and σ_0 from Equation (11-1) fitted to the data of Reference 11.1 only are shown as a function of CW in Figure 11.10. For both C17000 and C17200 beryllium coppers, a systematic variation of these constants with CW was observed.

Table 11.9. Fatigue Life Measurements for C17200 Beryllium Copper Cold-worked 37% Before Aging (295 K).

Cycles, N (10^3)	Maximum Stress, MPa	[Be], wt%	Cold Work, %	Aging Temperature, K	Reference No.
63	758	1.90	40	588	6
63	690	1.90	40	588	6
89	548	1.90	40	588	6
108	690	1.90	40	588	6

C17200: Cold-worked 37% and Aged — *Stress-controlled Flexural Fatigue Life, Air (295 K)*

Table 11.9, continued

Cycles, N (10^3)	Maximum Stress, MPa	[Be], wt%	Cold Work, %	Aging Temperature, K	Reference No.
186	627	1.90	40	616	6
150	627	1.90	40	616	6
186	552	1.90	40	616	6
158	545	2.09	37	616	1
158	545	2.09	37	616	1
178	476	1.90	40	616	6
186	627	2.09	37	616	1
186	603	1.81	37	616	1
186	603	1.81	37	616	1
158	545	2.09	37	616	1
191	600	1.96	37	616	1
150	603	1.81	37	616	1
186	603	1.81	37	616	1
195	603	1.81	37	616	1
200	603	1.96	37	616	1
204	603	1.81	37	616	1
209	627	2.09	37	588	1
224	552	1.96	40	588	6
229	545	2.09	37	616	1
229	545	2.09	37	616	1
234	600	1.96	37	616	1
234	603	1.96	37	616	1
240	603	1.96	37	616	1
251	627	2.09	37	588	1
266	508	1.81	37	616	1
269	552	1.96	37	588	1
282	486	2.09	37	616	1
299	552	1.96	37	588	1
299	505	1.96	37	616	1
302	590	1.81	37	588	1
302	590	1.81	37	588	1
331	590	1.81	37	588	1
335	627	2.09	37	588	1
347	590	1.81	37	588	1
355	410	1.90	40	588	6
355	508	1.81	37	616	1
372	486	2.09	37	616	1
380	627	2.09	37	588	1
380	505	1.96	37	616	1
398	508	1.81	37	616	1
407	552	1.96	37	588	1
407	505	1.96	37	616	1
422	486	2.09	37	616	1
437	505	1.96	37	616	1
457	508	1.81	37	616	1
457	508	1.81	37	616	1
468	486	2.09	37	616	1
473	483	1.90	40	588	6
473	505	1.96	37	616	1
501	552	1.96	37	588	1
501	552	1.96	37	588	1

C17200: Cold-worked 37% and Aged

Stress-controlled Flexural Fatigue Life, Air (295 K)

Table 11.9, continued

Cycles, N (10^3)	Maximum Stress, MPa	[Be], wt%	Cold Work, %	Aging Temperature, K	Reference No.
501	515	2.09	37	588	1
525	386	2.09	37	616	1
581	483	1.90	40	588	6
601	501	1.81	37	616	1
603	386	2.09	37	588	1
661	501	1.81	37	588	1
708	501	1.81	37	588	1
724	515	2.09	37	588	1
724	421	1.81	37	588	1
724	421	1.81	37	616	1
832	501	1.81	37	588	1
681	421	1.81	37	588	1
581	501	1.81	37	588	1
912	515	2.09	37	588	1
912	421	1.96	37	588	1
933	474	1.96	37	588	1
933	414	1.96	37	616	1
955	325	2.09	37	616	1
1050	414	1.96	37	588	1
1070	386	2.09	37	616	1
1120	421	1.81	37	588	1
1170	474	1.96	37	588	1
1170	386	2.09	37	588	1
1860	421	1.96	37	588	1
1850	421	1.81	37	588	1
1350	421	1.96	37	616	1
1412	341	1.96	40	588	6
1480	417	1.81	37	588	1
1480	517	2.09	37	588	1
1550	474	1.96	37	588	1
1860	517	2.09	37	588	1
1860	386	2.09	37	616	1
4790	421	1.96	37	588	1
1860	417	1.81	37	588	1
1860	421	1.98	37	588	1
2950	386	1.96	37	616	1
2950	431	2.09	37	588	1
2985	414	1.96	40	588	6
3240	431	2.09	37	588	1
3467	421	1.96	40	588	6
3550	431	2.09	37	588	1
3800	341	1.81	37	616	1
3580	417	1.81	37	588	1
3980	431	2.09	37	588	1
1170	414	1.81	37	588	1
1170	398	1.96	37	616	1
4790	417	1.81	37	588	1
4790	341	1.96	37	616	1
5130	322	2.09	37	616	1
5890	431	2.09	37	588	1
6760	324	2.09	37	616	1

C17200: Cold-worked 37% and Aged

Stress-controlled Flexural Fatigue Life, Air (295 K)

Table 11.9, continued

Cycles, N (10^3)	Maximum Stress, MPa	[Be], wt%	Cold Work, %	Aging Temperature, K	Reference No.
6760	324	2.09	37	616	1
7240	398	1.96	37	588	1
7240	341	1.81	37	616	1
7240	324	1.81	37	588	1
8220	341	1.81	37	616	1
8320	398	1.96	37	588	1
9330	324	2.09	37	616	1
9550	421	2.09	37	588	1
10600	338	1.81	37	616	1
10700	321	1.96	37	588	1
11220	276	1.96	40	616	6
14500	398	1.96	37	588	1
11700	341	1.81	37	616	1
12600	421	2.09	37	588	1
12600	341	1.81	37	616	1
13335	338	1.96	40	588	6
13500	338	1.81	37	616	1
13500	390	1.81	37	588	1
14500	324	1.81	37	616	1
15100	421	2.09	37	588	1
15849	338	1.96	40	616	6
16200	338	1.81	37	588	1
16600	421	2.09	37	616	1
19700	398	1.81	37	588	1
20900	303	2.09	37	616	1
21400	324	1.81	37	588	1
23400	322	1.96	37	616	1
29500	321	1.96	37	588	1
25700	290	1.81	37	616	1
26300	398	1.81	37	588	1
26900	285	1.96	37	616	1
29500	290	2.09	37	588	1
26900	324	1.81	37	616	1
29500	285	1.81	37	588	1
26900	341	1.96	37	616	1
29500	341	1.96	37	588	1
33900	324	1.96	37	616	1
37200	285	1.81	37	588	1
37200	303	2.09	37	616	1
10700	338	1.96	37	588	1
11700	382	2.09	37	616	1
45700	398	1.81	37	588	1
46800	338	1.96	37	616	1
50100	324	1.81	37	588	1
52500	303	2.09	37	616	1
56200	285	1.81	37	588	1
56200	324	1.96	37	616	1
74100	285	1.96	37	588	1
87100	301	1.81	37	588	1
89100	421	2.09	37	588	1
89100	290	2.09	37	616	1

C17200: Cold-worked 37% and Aged

Stress-controlled Flexural Fatigue Life, Air (295 K)

Table 11.9, continued

Cycles, N (10^3)	Maximum Stress, MPa	[Be], wt%	Cold Work, %	Aging Temperature, K	Reference No.
93300	379	1.96	37	616	1
100000	300	1.81	37	588	1
100000	265	1.81	37	588	1
100000	301	1.81	37	588	1
100000	379	1.81	37	588	1
100000	265	1.81	37	588	1
100000	265	1.81	37	588	1
100000	265	1.81	37	588	1
100000	301	1.96	37	588	1
100000	265	1.96	37	588	1
100000	252	1.96	37	588	1
100000	301	1.96	37	588	1
100000	265	1.96	37	616	1
100000	265	1.96	37	588	1
100000	252	1.96	37	588	1
100000	252	1.96	37	588	1
100000	252	1.96	37	588	1
100000	252	1.96	37	588	1
100000	379	2.09	37	588	1
100000	379	2.09	37	588	1
100000	379	2.09	37	588	1
100000	379	2.09	37	616	1
100000	307	1.81	37	616	1
100000	265	1.81	37	616	1
100000	307	1.81	37	616	1
100000	301	1.81	37	616	1
100000	307	1.81	37	616	1
100000	265	1.81	37	616	1
100000	301	1.96	37	616	1
100000	301	1.96	37	616	1
100000	301	1.96	37	616	1
100000	301	1.96	37	616	1
100000	301	1.96	37	616	1
100000	301	1.96	37	616	1
100000	305	2.09	37	616	1
100000	265	2.09	37	616	1
100000	272	2.09	37	616	1
100000	305	2.09	37	616	1
100000	290	2.09	37	616	1
100000	272	2.09	37	616	1
100000	272	2.09	37	616	1
100000	272	2.09	37	616	1
100000	272	2.09	37	616	1

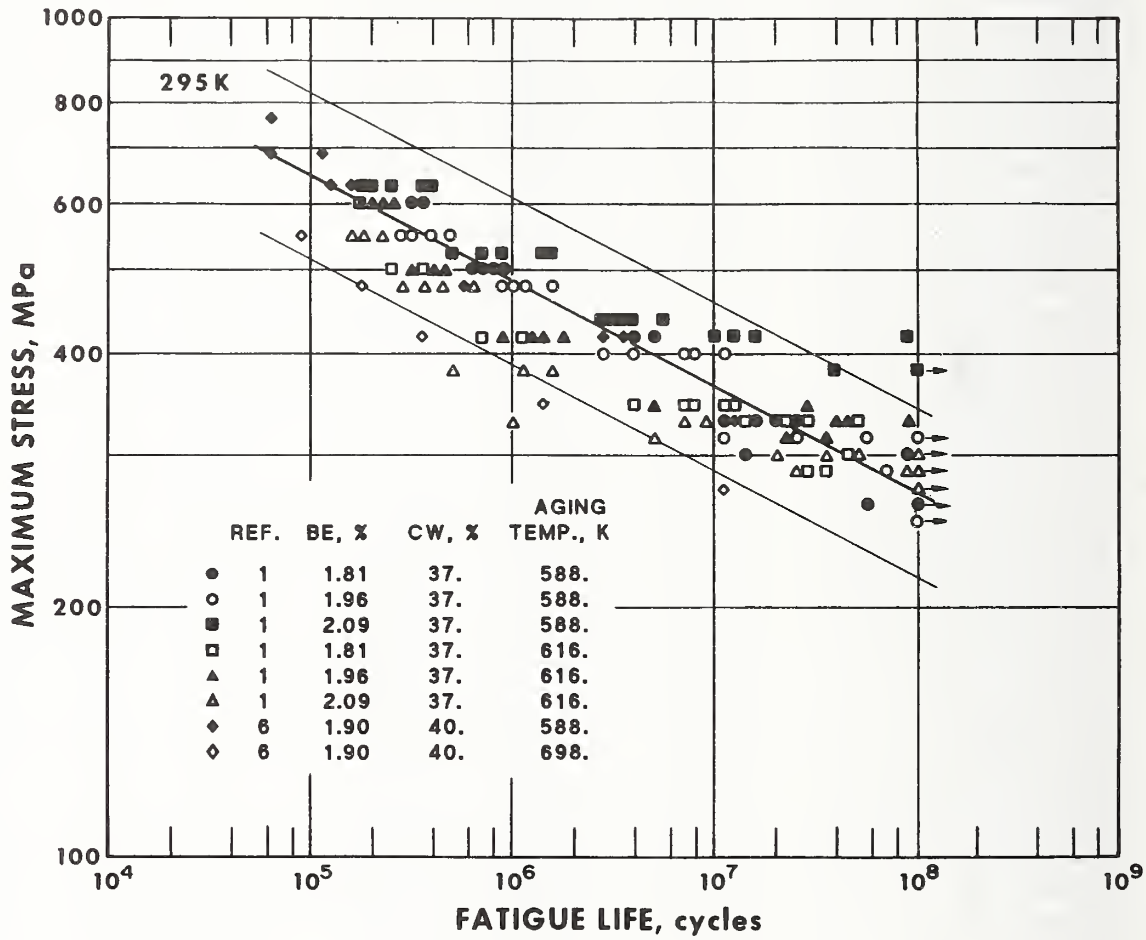

Figure 11.9. Fatigue life curves at 295 K for C17200 beryllium copper cold-worked 37% before aging are shown. The scatter band represents two standard deviations about a nonlinear regression curve given by Equation (11-9), in which *N* is the dependent variable. For clarity, overlapping data points are omitted from the figure. All data are presented in Table 11.9. Product was in strip form. Arrows denote completion of test before failure.

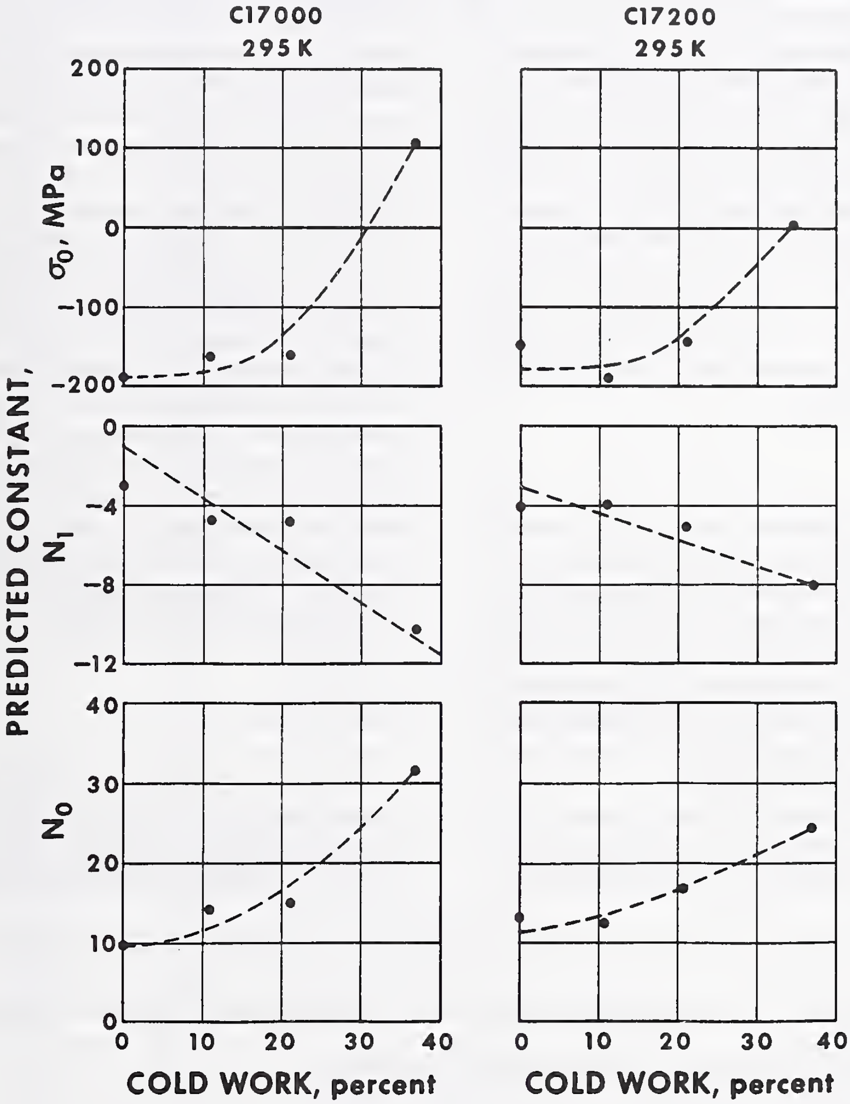

Figure 11.10. The constants N_0, N, and σ_0 from Equation (11-1) fitted to the data of Reference 11.1 only, are shown as a function of cold work.

$$\log N = N_0 + N_1 \log(\sigma_m - \sigma_0) \qquad (11\text{-}1)$$

C17200: Annealed and Aged; Cold-worked and Aged

Stress-controlled Flexural Fatigue Life, Air, Liquid (20–300 K)

DATA SOURCES AND ANALYSIS

Measurements of maximum stress (σ_m) versus the number of cycles to failure (*N*) of C17200 beryllium copper at temperatures ranging from 20 to 300 K were obtained from References 11.7 and 11.8. The fatigue mode was flexural, with an *R*-ratio of –1 (Reference 11.7) or not specified (Reference 11.8). Specimens were tested in the annealed and aged and the cold-worked and aged conditions. Aging temperatures were 588 K (Reference 11.7) and 644 K (Reference 11.8); aging times ranged from 0.33 to 3 h. The amount of cold work, *CW*, was 21 and 31% (reduction in thickness). Product was in sheet form. The effect of grain size, *d*, at 200 and 300 K was reported in Reference 11.8. Tests below room temperature were carried out with the test specimens immersed in the coolant.

RESULTS

Table 11.10 presents values of test temperature, *N*, σ_m, *d*, and the reference number for specimens in the annealed and aged condition. Table 11.11 presents values of test temperature, *N*, σ_m, *CW*, *d*, and the reference number for specimens in the cold-worked and aged condition. The available characterization of materials and measurements is given in Table 11.14 at the end of the fatigue properties section.

Figure 11.11 presents measurements on specimens in the annealed and aged condition, and Figure 11.12 presents measurements on specimens in the cold-worked and aged condition. Both figures show an improvement in fatigue life with decreasing temperature. The data from Reference 11.8 show, in general, a slight improvement with decreasing *d*. Also, if data from Reference 11.8 are compared in Figures 11.11 and 11.12, the specimens in the cold-worked and aged conditions had a longer fatigue life for a given stress level than did specimens in the annealed and aged conditions. This is in agreement with data from Reference 11.3 for axial fatigue shown in Figure 11.5. However, a similar comparison of data from Reference 11.7 in Figures 11.11 and 11.12 leads to a different result: at 294 and 20 K, the fatigue life of the annealed and aged specimens is longer for a given stress level than is the fatigue life of the cold-worked and aged specimens. The aging conditions reported in the two references are somewhat different: Reference 11.7 reports longer aging times at lower temperatures than does Reference 11.8. In both cases, tensile and yield strengths at room temperature are higher in the cold-worked and aged condition than in the annealed and aged condition. Increased tensile strength was found to correlate with longer fatigue life in copper (see Section 4).

DISCUSSION

Data presented in Reference 11.9 on annealed and aged C17200 beryllium copper at $N \approx 10^5$ show an improvement in fatigue strength at 123 K compared with fatigue strength at 412 K.

Table 11.10. Fatigue Life Measurements for Annealed and Aged C17200 Beryllium Copper (20–300 K).

Test Temperature, K	Cycles, N (10^3)	Maximum Stress, MPa	Grain Size, μm	Reference No.
20	132.0	1014	N.S.	7
20	219.0	958	N.S.	7
20	295.0	910	N.S.	7
20	417.0	841	N.S.	7
20	912.0	786	N.S.	7
20	1020.0	724	N.S.	7
77	70.8	903	N.S.	7
77	77.6	848	N.S.	7
77	112.0	765	N.S.	7
77	186.0	696	N.S.	7

C17200: Annealed and Aged; Cold-worked and Aged

Stress-controlled Flexural Fatigue Life, Air, Liquid (20–300 K)

Table 11.10, continued

Test Temperature, K	Cycles, N (10^3)	Maximum Stress, MPa	Grain Size, μm	Reference No.
77	209.0	627	N.S.	8
77	479.0	558	N.S.	8
77	1350.0	440	N.S.	7
194	15.0	938	N.S.	7
194	30.2	848	N.S.	8
194	58.9	786	N.S.	7
194	106.0	717	N.S.	8
194	186.0	593	N.S.	7
194	209.0	648	N.S.	8
194	398.0	524	N.S.	8
194	692.0	448	N.S.	8
200	123.0	483	30	8
200	447.0	414	30	8
200	457.0	379	30	8
200	490.0	345	30	8
200	933.0	310	30	7
200	1350.0	276	30	8
200	3020.0	241	30	7
200	20000.0	228	30	8
200	27500.0	234	30	8
200	141.0	414	100	7
200	234.0	379	100	8
200	447.0	345	100	8
200	741.0	310	100	8
200	1350.0	293	100	8
200	2290.0	262	100	8
200	3020.0	276	100	8
200	6760.0	241	100	8
200	20400.0	276	100	7
200	20400.0	234	100	7
298	12.9	917	N.S.	8
298	43.7	772	N.S.	7
298	47.9	772	N.S.	7
298	132.0	517	N.S.	7
298	473.0	490	N.S.	7
298	1330.0	316	N.S.	8
298	16600.0	283	N.S.	7
194	27.5	517	30	8
300	33.5	448	30	8
194	52.5	414	30	8
300	57.5	448	30	7
300	186.0	379	30	7
300	174.0	345	30	7
300	347.0	276	30	7
300	376.0	310	30	7
194	617.0	255	30	7
300	141.0	276	30	8
300	1060.0	228	30	8
300	1380.0	217	30	8
300	19500.0	207	30	8
300	85.1	345	100	8

Table 11.10, continued

Test Temperature, K	Cycles, N (10^3)	Maximum Stress, MPa	Grain Size, μm	Reference No.
300	186.0	276	100	8
300	427.0	221	100	8
300	525.0	241	100	8
300	741.0	20[illegible]	100	8
300	933.0	193	100	8
300	1550.0	200	100	8
300	1780.0	172	100	8
300	7760.0	179	100	8

N.S. = not specified.

Table 11.11. Fatigue Life Measurements for Cold-worked and Aged C17200 Beryllium Copper (2–300 K).

Test Temperature, K	Cycles, N (10^3)	Maximum Stress, MPa	Cold Work, %	Grain Size, μm	Reference No.
20	39.8	1124	21	N.S.	7
20	42.7	979	21	N.S.	7
20	43.7	814	21	N.S.	8
20	93.3	979	21	N.S.	7
20	93.3	731	21	N.S.	7
20	178.0	655	21	N.S.	8
20	372.0	607	21	N.S.	8
20	1070.0	569	21	N.S.	7
77	23.4	596	21	N.S.	7
77	56.2	862	21	N.S.	7
77	74.1	752	21	N.S.	7
77	100.0	779	21	N.S.	7
77	145.0	703	21	N.S.	7
77	178.0	617	21	N.S.	7
77	912.0	552	21	N.S.	7
77	1000.0	569	21	N.S.	7
194	20.9	821	21	N.S.	7
194	95.5	596	21	N.S.	7
194	266.0	531	21	N.S.	8
194	1350.0	414	21	N.S.	7
200	204.0	783	37	75	8
200	339.0	414	37	75	8
200	1050.0	379	37	75	7
200	2400.0	345	37	75	8
200	8510.0	310	37	75	8
200	8510.0	276	37	75	7
200	15500.0	262	37	75	7
200	33100.0	255	37	75	7
200	41700.0	269	37	75	8
200	50100.0	241	37	75	8
200	841.0	414	37	29	8
200	871.0	448	37	29	8
200	1700.0	396	37	29	8

C17200: Annealed and Aged; Cold-worked and Aged

Stress-controlled Flexural Fatigue Life, Air, Liquid (20–300 K)

Table 11.11, continued

Test Temperature, K	Cycles, N (10^3)	Maximum Stress, MPa	Cold Work, %	Grain Size, μm	Reference No.
294	2950.0	345	37	29	7
200	7080.0	362	37	29	8
294	8710.0	345	37	29	7
200	21900.0	324	37	29	8
294	23400.0	310	37	29	8
200	29500.0	303	37	29	8
294	21.9	676	21	N.S.	7
200	25.1	738	21	N.S.	8
294	27.5	752	21	N.S.	7
200	33.1	627	21	N.S.	8
294	35.5	676	21	N.S.	8
200	41.7	593	21	N.S.	8
294	162.0	517	21	N.S.	7
200	473.0	441	21	N.S.	8
294	1660.0	372	21	N.S.	8
294	1780.0	310	21	N.S.	8
294	10500.0	345	21	N.S.	8
300	56.2	517	37	75	8
300	72.4	414	37	29	8
300	162.0	448	37	75	8
300	162.0	414	37	29	8
300	240.0	379	37	75	8
300	355.0	345	37	29	8
300	531.0	310	37	75	8
300	912.0	276	37	75	7
300	1060.0	255	37	75	8
300	1580.0	241	37	29	8
300	9550.0	207	37	75	8
300	20900.0	221	37	29	8
300	20900.0	207	37	75	8
300	112.0	414	37	41	7
300	263.0	379	37	41	8
300	331.0	414	37	41	8
300	457.0	379	37	41	8
300	603.0	345	37	41	8
300	891.0	207	37	41	8
300	1450.0	262	37	41	8
300	2510.0	248	37	41	8
300	3090.0	234	37	41	8
300	20900.0	214	37	41	8

N.S. = not specified.

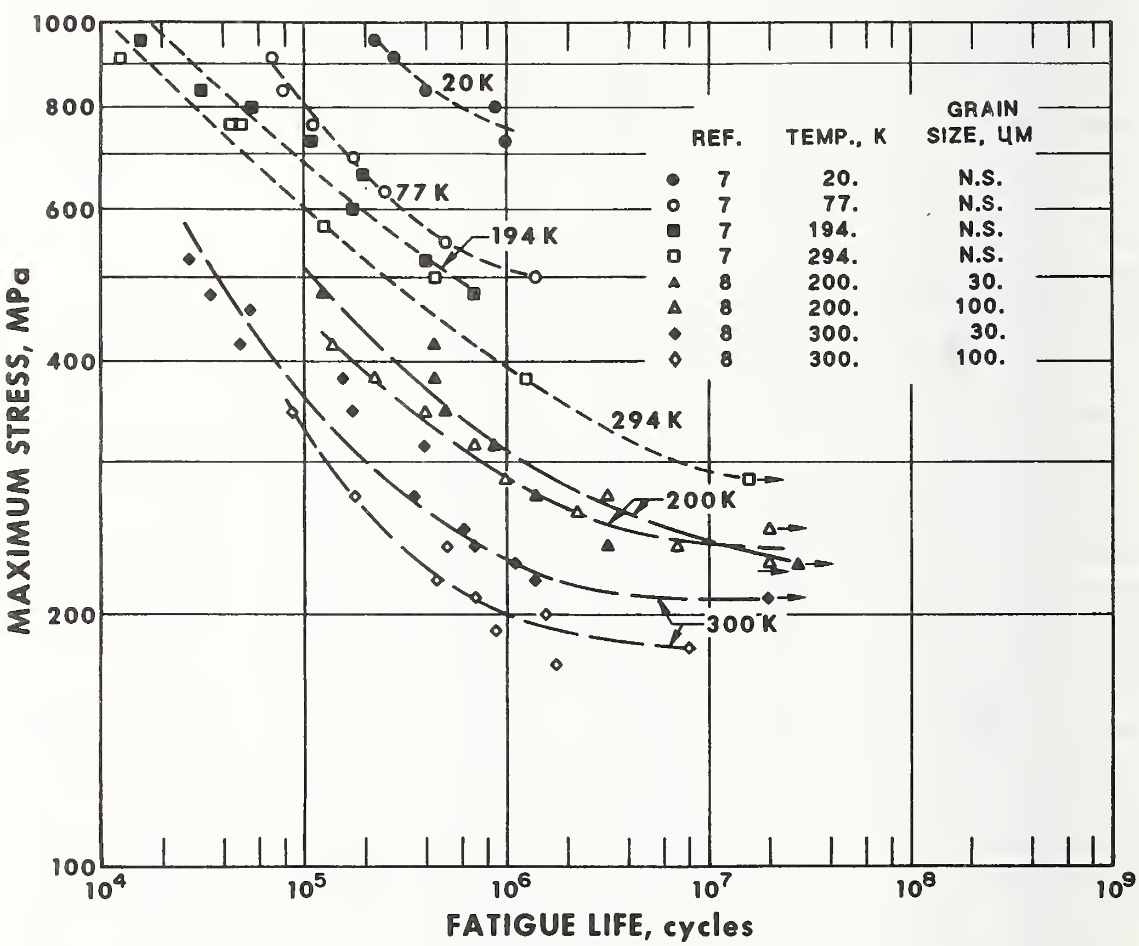

Figure 11.11. Fatigue life curves at 20 to 300 K for C17200 beryllium copper in the annealed and aged condition are shown. One point from Reference 11.7 at 20 K (σ_m = 1020 MPa) does not appear in the figure. All data are presented in Table 11.10. Product was in sheet form. Arrows denote completion of test before failure. (N.S. in legend indicates not specified.)

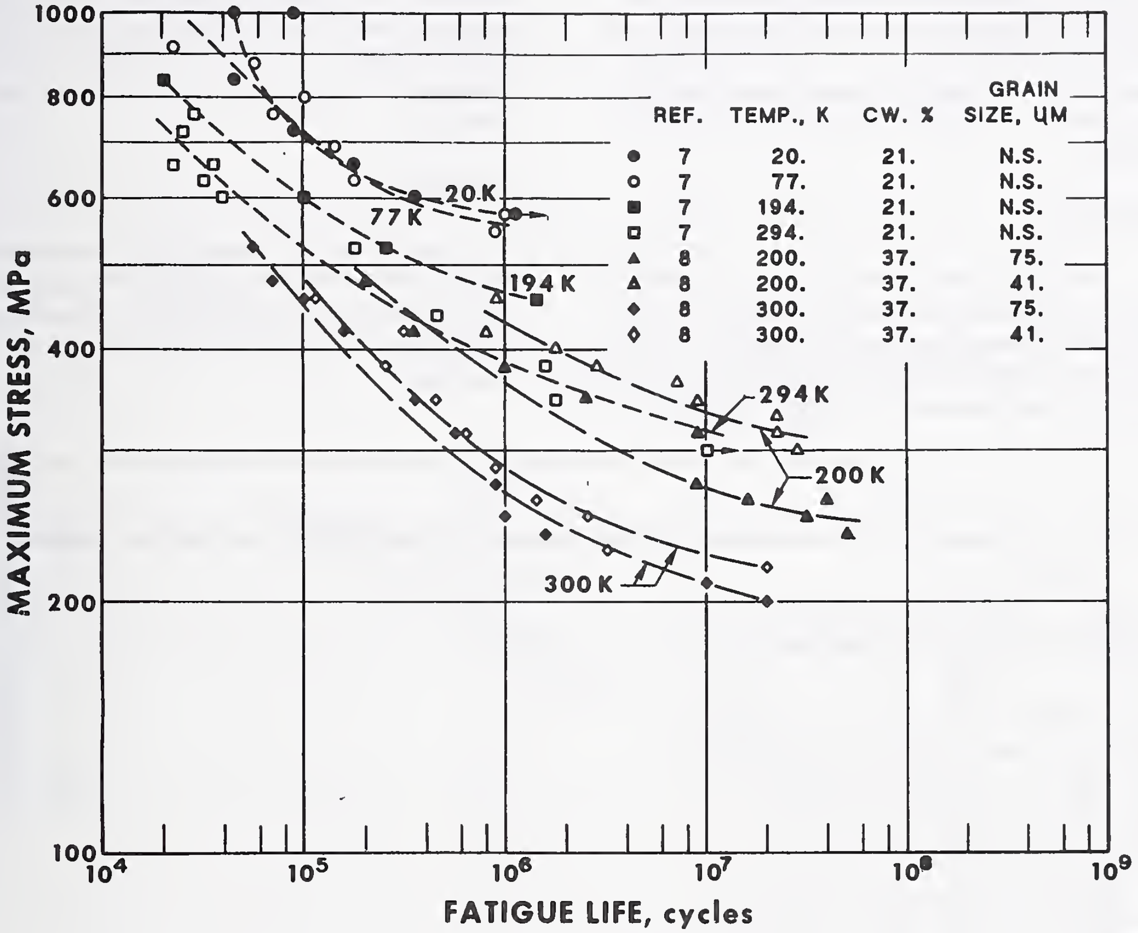

Figure 11.12. Fatigue life curves at 20 to 300 K for C17200 beryllium copper in the cold-worked and aged condition are shown. One point from Reference 11.7 at 194 K (σ_m = 1350 MPa) does not appear in the figure. All data are presented in Table 11.11. Product was in sheet form. Arrows denote completion of test before failure. (N.S. in legend indicates not specified.)

C17500, C17510: Cold-worked and Aged

Stress-controlled Flexural Fatigue Life, Air (295 K)

DATA SOURCES AND ANALYSIS

Measurements at 295 K of the maximum stress (σ_m) versus the number of cycles to failure (N) for cold-worked and aged C17500 and C17510 beryllium copper were obtained from References 11.10, 11.11, and 11.12. The fatigue mode was flexural (R-ratio equals −1). Aging conditions and percent of cold work were not specified. Product was in bar (Reference 11.10) or strip form (References 11.11 and 11.12). In Reference 11.11, data on specimens in both the transverse and longitudinal orientations were reported.

RESULTS

All data are presented in Table 11.12 which gives N, σ_m, and the reference number. The available characterization of materials and measurements is given in Table 11.14 at the end of the fatigue properties section. Figure 11.13 presents the fatigue life curves. The measurements from Reference 11.12 on C17500 and C17510 show that the fatigue life of C17500 was somewhat longer than that of C17510, for a given stress level, although the yield and tensile strengths were identical. Measurements from Reference 11.11 on C17510 indicate that the fatigue life at a given stress level for transverse specimens is considerably longer than that of specimens with a longitudinal orientation. The yield and tensile strengths were higher in the transverse orientation than in the longitudinal orientation.

DISCUSSION

Additional data presented in Reference 11.11 on 37% cold-worked and aged C17200 beryllium copper indicate that its fatigue life characteristics are similar to those of C17510 in the transverse orientation.

Table 11.12. Fatigue Life Measurements for Cold-worked and Aged C17500 and C17510 Beryllium Copper (295 K).

Cycles, N (10^3)	Maximum Stress, MPa	Reference No.
133	414	11
211	414	11
237	345	10
292	379	12
316	345	10
631	345	12
546	483	10
631	379	12
794	486	11
631	381	11
900	345	10
1188	448	11
1334	276	10
1372	448	11
1412	276	10
1412	348	11
2113	276	10
2661	276	12
2818	276	12
3868	417	11
4467	417	11
7000	241	10

Table 11.12, continued

Cycles, N (10^3)	Maximum Stress, MPa	Reference No.
15399	276	11
17783	241	12
23041	310	11
90000	207	10

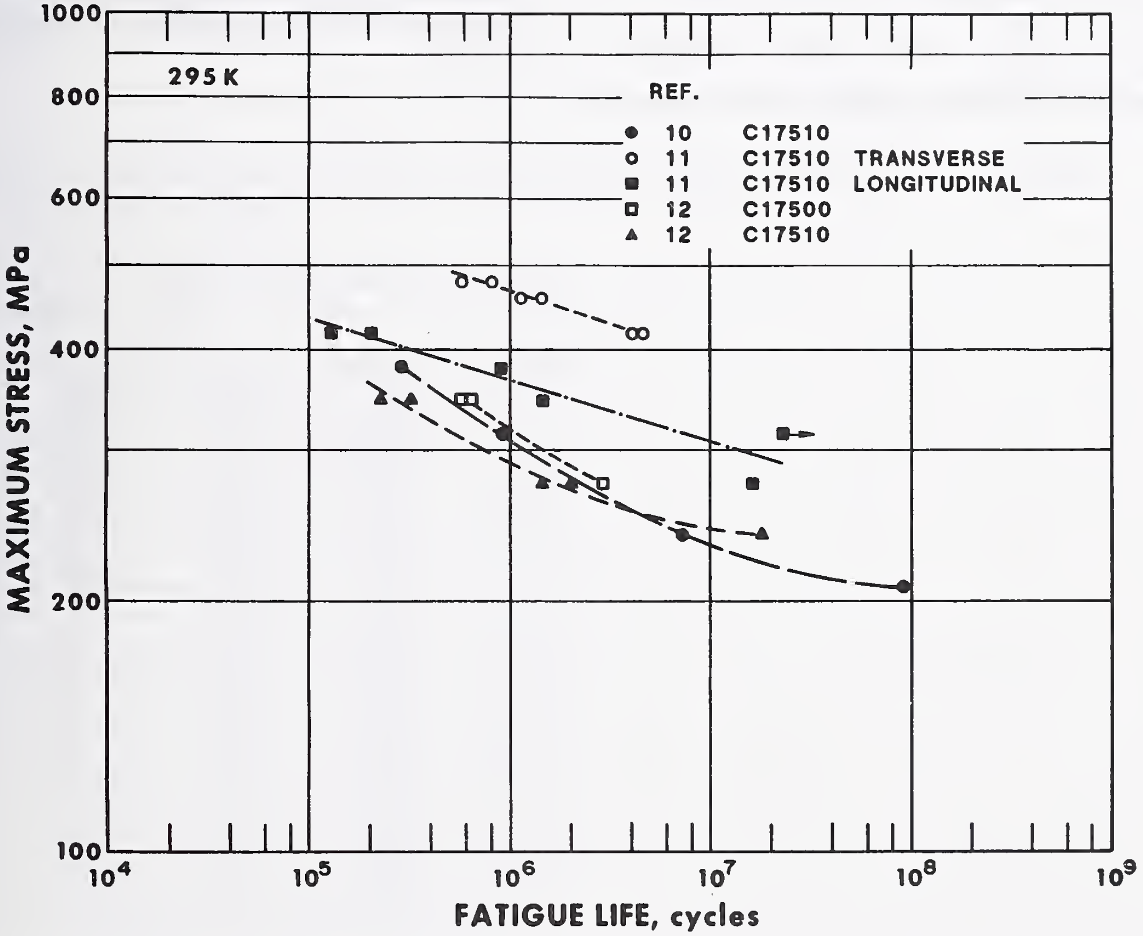

Figure 11.13. Fatigue life curves at 295 K for cold-worked and aged C17500 and C17510 beryllium copper are shown. All data are presented in Table 11.12. Products were in bar (Reference 11.10) and strip form (References 11.11 and 11.12). Arrows denote completion of test before failure.

DATA SOURCES AND ANALYSIS

No measurements of strain-controlled fatigue life on C17200 beryllium copper were located. Such measurements would be expected to follow the Coffin-Manson law (Reference 11.13)

$$\Delta\epsilon_p = k\,N^{-n}, \qquad (11\text{-}10)$$

where $\Delta\epsilon_p$ is the plastic strain range and N is the number of cycles to failure.

Reference 11.14 presents cyclic measurements under fully reversed strain control of cold-worked and aged C17200 beryllium copper. The cyclic strain-hardening parameters K' and n' ($\frac{\Delta\sigma}{2} = K' \left[\frac{\Delta\epsilon_p}{2}\right]^{n'}$ and $\Delta\sigma$ is the stress amplitude) were obtained in these studies. Specimens were subjected to cycles of increasing strain amplitude followed by cycles of decreasing strain amplitude. The available characterization of materials and measurements for these tests is given in Table 11.14 at the end of the fatigue properties section. It is unclear from the reference whether the C17200 beryllium copper was aged after cold working. The degree of cold work was not specified.

DISCUSSION

The cyclic stress-strain coefficient K' and the exponent n' can be related to fatigue life and fatigue crack-growth rate. See Reference 11.14 for discussion of such empirical and theoretical relationships.

C17500, C17510: Cold-worked and Aged

Strain-controlled Axial Fatigue Life, Air (295, 423 K)

DATA SOURCES AND ANALYSIS

Measurements at 295 K of the plastic strain range ($\Delta\epsilon_p$) versus the number of cycles to failure (*N*) for cold-worked and aged C17500 and C17510 beryllium copper were obtained from References 11.15 and 11.16. Plastic strain range values were reported in Reference 11.15; Reference 11.16 reports strain range without specifying whether total strain or plastic strain is meant. The amount of cold work was 40% (Reference 11.16) or 65% (Reference 11.15). Aging conditions were 3 h at 755 K (Reference 11.16) or not specified (Reference 11.15).

Strain-controlled fatigue data are expected to follow the Coffin-Manson law (Reference 11.13),

$$\Delta\epsilon_p = k\,N^n. \qquad (11\text{-}10)$$

RESULTS

Table 11.13 presents test temperature, *N*, $\Delta\epsilon_p$, and the reference number. The available characterization of materials and measurements is given in Table 11.14 at the end of the fatigue properties section. Figure 11.14 presents the fatigue life curve. The data from Reference 11.16 show a decrease in fatigue life for a given $\Delta\epsilon_p$ when the temperature is increased from 295 to 423 K.

Table 11.13. Fatigue Life Measurements of Cold-worked and Aged C17500 and C17510 Beryllium Copper (295 and 423 K).

Test Temperature, K	Cycles, N (10^3)	Plastic Strain Range	Reference No.
295	0.40	0.01800	16
295	2.60	0.01700	16
295	7.00	0.01580	16
295	2.00	0.01410	16
295	7.00	0.01240	16
295	6.00	0.01140	16
295	7.00	0.01100	16
295	0.32	0.00500	16
298	5.72	0.00300	16
295	1.95	0.00200	16
298	5.72	0.00100	16
423	6.00	0.01540	16
423	0.40	0.01630	16
423	6.00	0.01540	16
423	1.00	0.01410	16
423	2.00	0.01540	16
423	7.00	0.01410	16
423	6.00	0.00975	16
423	8.00	0.00900	16

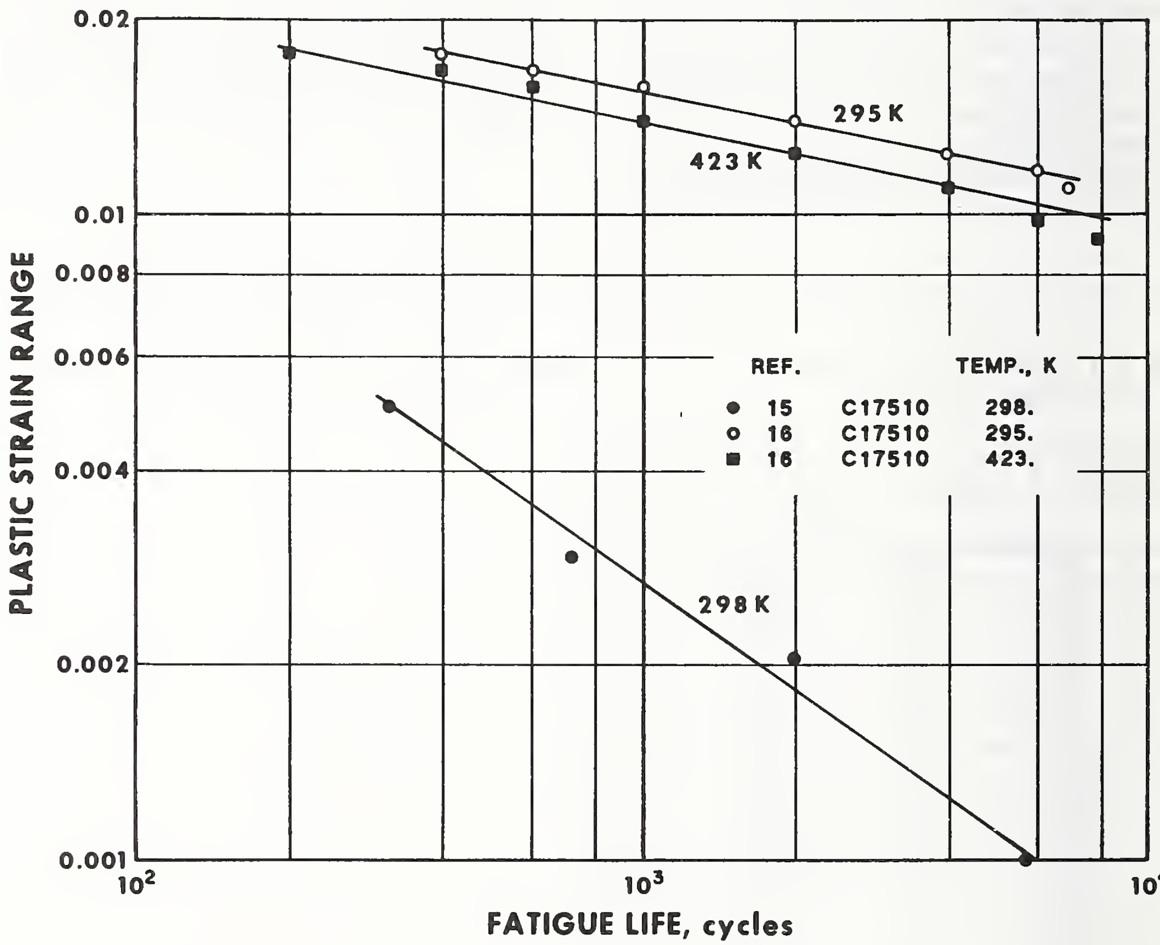

Figure 11.14. Fatigue life curves at 295 and 423 K for cold-worked and aged C17500 and C17510 beryllium copper are shown. All data are presented in Table 11.12. Product was in bar form (Reference 11.15) or not specified (Reference 11.16).

Table 11.14. Characterization of Materials and Measurements.

Reference No.	1A	1B	1C	1D
Specification	C17000	C17000	C17000	C17000
Composition (wt%)				
Cu	> 97.85	97.78	> 97.85	97.78
Cu + Ag	> 97.86	97.79	> 97.86	97.79
Be	1.59	1.70	1.59	1.70
Ni	0.010	0.002	0.010	0.002
Co	0.25	0.20	0.25	0.20
Ni + Co	—	—	—	—
Ni + Fe + Co	—	—	—	—
Al	0.05	0.05	0.05	0.05
Fe	0.12	0.11	0.12	0.11
Si	0.07	0.07	0.07	0.07
Others (Only ≥ 0.001 wt%)	(a)	(b)	(a)	(b)
Material Condition	Aged, 588 K or 616 K, 3 h	Aged, 588 K or 616 K, 3 hr	Cold-rolled, 11%, 21%, 37%, aged (c)	Cold-rolled, 11%, 21%, 37%. aged (c)
Grain Size	25 μm	25 μm	25, 25, 20 μm	25, 20, 20 μm
Hardness	R_c 30.9, 34.4	R_c 34.3, 36.8	R_c 32.2–37.3	R_c 35.7–38.5
Product Form	Strip, 0.25-cm-thick	Strip, 0.25-cm-thick	Strip, 0.25-cm-thick	Strip, 0.25-cm-thick
Specimen Type	Flat	Flat	Flat	Flat
Width or Dia.	—	—	—	—
Thickness	—	—	—	—
Length	—	—	—	—
"R" Ratio	− 1	− 1	− 1	− 1
Test Frequency	—	—	—	—
No. of Measurements	—	—	—	—
Test Temperature	295 K	295 K	295 K	295 K

(a) Sn: < 0.01; Pb: 0.002; Zn: < 0.03; Cr: 0.005; Mn: 0.005.
(b) Sn: 0.02; Pb: 0.003; Zn: 0.051; Cr: 0.002; Mn: 0.002.
(c) Aged: 588 K or 616 K, 3 h.

C17000–C17510: Annealed; Annealed and Aged; Cold-worked and Aged

Fatigue Constants (All)

1E	1F	1G	1H	1I
C17200	C17200	C17200	C17200	C17200
> 97.49 > 97.50 1.81 0.01 0.30 — — 0.05 0.15 0.13 (a)	> 97.36 > 97.38 1.96 0.01 0.26 — — 0.07 0.14 0.11 (b)	> 97.20 > 97.22 2.09 0.02 0.26 — — 0.05 0.14 0.17 (c)	> 97.49 > 97.50 1.81 0.01 0.30 — — 0.05 0.15 0.13 (a)	> 97.36 > 97.38 1.96 0.01 0.26 — — 0.07 0.14 0.11 (b)
Aged, 588 K or 616 K, 3 h	Aged, 588 K or 616 K	Aged, 588 K or 616 K, 3 hr	Cold-rolled, 11%, 21%, 37%, aged (d)	Cold-rolled, 11%, 21%, 37%, aged (d)
25 μm	25 μm	20 μm	25 μm	25 μm
R_c 38, 39.4	R_c 40.8, 41.9	R_c 41.2, 42.3	R_c 39–41.5	R_c 40.1–43
Strip, 0.25-cm-thick	Strip, 0.25-cm-thick	Strip, 0.25-cm-thick	Strip, 0.25-cm-thick	Strip, 0.25-cm-thick
Flat — — —	Flat — — —	Flat — — —	Flat — — —	Flat — — —
– 1 —	– 1 —	– 1 —	– 1 —	– 1 —
—	—	—	—	—
295 K	295 K	295 K	295 K	295 K

(a) Sn: 0.01; Pb: 0.001; Zn: < 0.03; Cr: 0.003; Mn: 0.003.
(b) Sn: 0.03; Pb: 0.001; Zn: < 0.03; Cr: 0.005; Mn: 0.008.
(c) Sn: 0.01; Pb: 0.001; Zn: < 0.03; Cr: 0.005; Mn: 0.008.
(d) Aged: 588 K or 616 K, 3 h.

Table 11.14, continued

Reference No.	1J	3A	3B	3C
Specification	C17200	C17200	C17200	C17200
Composition (wt%)				
Cu	> 97.20	98.2	98.2	98.2
Cu + Ag	> 97.22	—	—	—
Be	2.09	1.8	1.8	1.8
Ni	0.02	—	—	—
Co	0.26	—	—	—
Ni + Co	—	—	—	—
Ni + Fe + Co	—	—	—	—
Al	0.05	—	—	—
Fe	0.14	—	—	—
Si	0.17	—	—	—
Others (Only ≥ 0.001 wt%)	(a)	—	—	—
Material Condition	Cold-rolled, 11% 21%, 37%, aged (b)	Annealed, 1073 K	Annealed, 1073 K, aged (d)	Annealed, 1073 K, cold-drawn, 60%, and aged (e)
Grain Size	20, 25, 20 μm	—	—	—
Hardness	R_c 40.4–44.2	—	—	—
Product Form	Strip, 0.25-cm-thick	Bar, 1.27-cm-dia.	Bar, 1.27-cm-dia.	Bar, 1.27-cm-dia.
Specimen Type	Flat	Round (c)	Round (c)	Round (c)
Width or Dia.	—	—	—	—
Thickness	—	—	—	—
Length	—	—	—	—
"R" Ratio	– 1	0	0	0
Test Frequency	—	158 Hz	158 Hz	158 Hz
No. of Measurements	—	—	—	—
Test Temperature	295 K	295 K	295 K	295 K

(a) Sn: 0.01; Pb: 0.001; Zn: < 0.03; Cr: 0.005; Mn: 0.008.
(b) Aged: 588 K or 616 K, 3 h.
(c) Specimens chemically and electrolytically polished before testing.
(d) Aging conditions not specified.
(e) Aged: 600 K, 0.3 h.

C17000–C17510: Annealed; Annealed and Aged; Cold-worked and Aged

Fatigue Constants (All)

3D	4	5A	5B	6
C17200	C17200	C17200	C17200	C17200
98.2 — 1.8 — — — — — — — —	— — 1.8–2.05 0.20–0.60 (c) 0.20–0.60 (c) — — — — — —	97.54 — 2.12 0.31 — — — — 0.07 — —	97.42 — 2.12 0.40 — — — — 0.09 — —	97.9 — 1.9 — 0.2 — — — — — —
Annealed, 1073 K, cold-drawn, 60%, and over-aged (a)	Cold-worked, 21%, aged, 588 K, 3 h	Aged, 573 K, 1.5 h (f)	Cold-drawn, 21%, aged, 573 K, 1.5 h	Cold-worked, 40%, aged (h)
—	—	—	25 μm	—
—	—	R_G 99.1	R_c 98.2, 102.2	—
Bar, 1.27-cm-dia.	Bar, 2.8-cm-dia.	Bar, 1.3-cm-dia.	Bar, 1.3-cm-dia.	—
Round (b) — — —	Round (d) (e) — —	Round (g) 0.76 cm — 4.6 cm	Round (g) 0.76 cm — 4.6 cm	(i) — — —
0 158 Hz	0 20–25 Hz	— 58 Hz	— 58 Hz	— 30 Hz
—	—	—	—	—
295 K	295 K	295 K	295 K	295 K

(a) Aged: 600 K, 24 h.
(b) Specimens chemically and electrolytically polished before testing.
(c) Nickel or cobalt, or both.
(d) Unnotched specimens sanded lightly before testing.
(e) Unnotched speciments, 0.76-cm-dia.; notched specimens, 1.2-cm-dia.
(f) Extent of previous cold work not specified.
(g) Specimens polished mechanically before testing.
(h) Aged: 588 K, 2 hr; 588 K, 24 h; 698 K, 24 h.
(i) Specimens chemically polished before testing.

Table 11.14, continued

Reference No.	7A	7B	8A	8B
Specification	C17200	C17200	C17200	C17200
Composition (wt%)				
Cu	97.40	97.35	97.59	97.49
Cu + Ag	97.42	97.37	—	—
Be	1.89	1.94	1.89	1.95
Ni	0.01	0.015	0.01	0.01
Co	0.29	0.27	0.24	0.25
Ni + Co	—	—	—	—
Ni + Fe + Co	—	—	—	—
Al	0.06	0.09	0.06	0.02
Fe	0.15	0.14	0.09	0.13
Si	0.13	0.12	0.11	0.07
Others (Only ≥ 0.001 wt%)	(a)	(e)	Sn: 0.01	Sn: 0.02, Zn: 0.06
Material Condition	Aged, 588 K, 3 h	Cold-rolled, 21%, aged, 588 K, 2 h	Aged, 644 K, 0.5 h	Aged, 644 K, 0.5 h
Grain Size	—	—	30 μm	100 μm
Hardness	Vickers Diamond 362 (b)	Vickers Diamond 368 (b)	R_c 42	R_c 42
Product Form	Sheet, 0.053-cm-thick	Sheet, 0.20-cm-thick	Sheet, 0.16-cm-thick	Sheet, 0.16-cm-thick
Specimen Type	Flat (c)	Flat (c)	Flat	Flat
Width or Dia.	—	—	—	—
Thickness	—	—	—	—
Length	—	—	5.7 cm	5.7 cm
"R" Ratio	− 1	− 1	—	—
Test Frequency	(d)	(d)	—	—
No. of Measurements	—	—	—	—
Test Temperature	20–294 K	20–294 K	200, 300 K	200, 300 K

(a) Mn: 0.005; Cr: 0.006; Sn: 0.01; Pb: 0.002; Zn: 0.03.
(b) 5-kg load.
(c) Specimens mechanically polished before testing.
(d) Frequency: 20 K, 58 Hz; all other temperatures, 30 Hz.
(e) Mn: 0.004; Cr: 0.001; Sn: 0.02; Pb: 0.002; Zn: 0.03.

C17000–C17510: Annealed; Annealed and Aged; Cold-worked and Aged

Fatigue Constants (All)

8C	8D	10	10	12A
C17200	C17200	C17510	C17510	C17500
97.59 — 1.89 0.02 0.26 — — 0.06 0.09 0.09 —	97.69 — 1.84 0.02 0.18 — — 0.03 0.12 0.09 Sn: 0.03	— — 0.2–0.6 1.4–2.2 — — — — — — —	— — — — — — — — — — —	— — — — — — — — — — —
Cold-rolled, 37%, aged, 644 K, 0.33 h	Cold-rolled, 37%, aged, 644 K, 0.33 h	Cold-worked and aged (b)	Cold-worked and aged (b)	Cold-worked and aged (b)
75 μm (a)	41 μm (a)	—	—	—
R_c 42	R_c 42	—	—	—
Sheet, 0.16-cm-thick	Sheet, 0.16-cm-thick	Bar	Strip	Strip
Flat — — 5.7 cm	Flat — — 5.7 cm	— — — —	Flat (c) — 0.02 cm —	Flat — 0.05 cm —
— —	— —	– 1 —	– 1 27 Hz	– 1 26 Hz
—	—	—	—	—
200, 300 K	200, 300 K	295 K	295 K	295 K

(a) Grain size converted from grains/cm^3 using ASTM standard E112-85.
(b) Percent cold work and aging conditions not specified.
(c) Longitudinal and transverse orientations.

Table 11.14, continued

Reference No.	12B	14	15	16
Specification	C17510	C17200	C17500	C17510
Composition (wt%)				
Cu	—	—	96.7	(i)
Cu + Ag	—	—	—	—
Be	—	1.92	0.54	0.2–0.6
Ni	—	0.03	(e)	1.4–2.2
Co	—	0.25	2.6	—
Ni + Co	—	—	—	—
Ni + Fe + Co	—	—	—	—
Al	—	0.05	—	—
Fe	—	0.05	—	—
Si	—	0.1	—	—
Others (Only ≥ 0.001 wt%)	—	(b)	—	—
Material Condition	Cold-worked and aged (a)	(c)	Cold-worked, 65%, aged (f)	Cold-worked, 40%, aged, 755 K, 3 h
Grain Size	—	—	10 μm	—
Hardness	—	—	—	—
Product Form	—	Bar, 1.9-cm-dia.	Bar, 1.6-cm-dia.	—
Specimen Type	Flat	Round	(g)	—
Width or Dia.	—	0.76 cm	(h)	—
Thickness	0.05 cm	—	—	—
Length	—	11.5 cm	0.7 cm	—
"R" Ratio	– 1	(d)	—	– 1
Test Frequency	26 Hz	—	0.17 Hz	—
No. of Measurements	—	—	—	—
Test Temperature	295 K	295 K	298 K	295, 423 K

(a) Percent cold work and aging conditions not specified.
(b) Zn: 0.025; Ag: 0.013–0.02; Mn: 0.009; Pb: 0.004; Cr: 0.003.
(c) The degree of cold work and whether or not specimens were aged were unspecified.
(d) Specimens subjected to cyclic tests of variable strain amplitude and variable strain rate.
(e) Fe + Ni: 0.25.
(f) Aging conditions not specified.
(g) Specimens polished before testing.
(h) Specimen geometry not specified, cross section = 0.32 cm^2.
(i) Cu + Be + Ni: 99.5 wt%.

REFERENCES

1. Gohn, G. R., Herbert, G. J., and Kuhn, J. B., "The Mechanical Properties of Copper-Beryllium Alloy Strip," American Society for Testing and Materials Special Technical Publication No. 367, 109 pp (1964).

2. "Metallic Materials and Elements for Aerospace Vehicle Structures," Vol. 1, Department of Defense, Washington, D.C., MIL-HDBK-5E (1987).

3. Lloyd, C. H., and Loretto, M. H., "The Effect of Precipitate Distribution on the Tensile and Fatigue Behaviour of a Copper–1.8% Beryllium Alloy," Metal Science 9, 195–200 (1975).

4. Weisman, M. H., Melill, J., and Matsuda, T., "Uni-directional Axial Tension Fatigue Tests of Beryllium Copper and Several Precipitation Hardening Corrosion-Resistant Steels," in American Society for Testing Materials, Special Technical Publication 196, 123–142 (1956).

5. Anderson, A. R., and Smith, C. S., "Fatigue Tests on Some Copper Alloys," Proceedings of the American Society for Testing Materials 41, 849–858 (1941).

6. Bonfield, W., "Precipitate Substructure and Fatigue of Cu 1.9 Wt% Be," Scripta Metallurgica 6, 77–80 (1972).

7. Favor, R. J., Gideon, D. N., Grover, H. J., Hayes, J. E., and McClure, G. M., "Investigation of Fatigue Behavior of Certain Alloys in the Temperature Range Room Temperature to –423 F," Wright-Patterson Air Force Base, OH, WADD Technical Report 61–132, 116 pp (1961).

8. Bornemann, A., and Gela, T., "Studies in the Behavior of Certain Non-ferrous Metals at Low Temperatures," Vol. I, Pierce Memorial Laboratory for Metallurgy, Stevens Institute of Technology, Hoboken, NJ, Contract No. DA 36–039–SC–15393, Signal Corps Project 2005–M08–METALS, 95–109 (1953).

9. Wolff, R. P., and Dodd, R. A., "Fatigue Properties of Some Age-hardened Alloys," Materials Research and Standards 3, 734–735 (1963).

10. Guha, A., and Spiegelberg, W. D., "Development of a Nickel-containing Beryllium Copper Alloys for Connector Applications," in Annual Connector and Interconnection Technology Symposium, Fort Washington, PA, 133–140 (1979).

11. Guha, A., "High Performance Mill Hardened Beryllium Copper C17510 Strip for Electrical and Electronic Applications," in Sixteenth Annual Connectors and Interconnection Technology Symposium Proceedings, Electronic Connector Study Group Inc., Fort Washington, PA, 131–140 (1983).

12. Guha, A., "Properties of Beryllium Copper Alloy C17510," in Copper and Copper Alloys for Fusion Reactor Applications, Eds. F. W. Wiffen and R. E. Gold, Oak Ridge National Laboratory, TN, CONF–830466, 144–150 (1984).

13. Coffin, L. F., Jr., and Tavernelli, J. F., "The Cyclic Straining and Fatigue of Metals," Transactions of the American Institute of Mining and Metallurgical Engineers 215, 794–807 (1959). Also in a report from General Electric Research Laboratory, Research Information Section, The Knolls, Schenectady, New York, Report No. 58-RL-2100, 32 pp. (1958).

REFERENCES

14. Benson, D. K., and Hancock, J. R., "The Effect of Strain Rate on the Cyclic Stress-Strain Response of Metals," National Technical Information Service, Springfield, VA, AD-762 610, 28 pp. (1973).

15. Taplin, D. M. R., and Collins, A. L. W., "The Cyclic Stress Response of Copper Alloys at 100–500 °C," in International Copper Research Association, Inc., New York, NY, INCRA Project No. 228(B), unpaged (1976).

16. Stevenson, R. D., and Rosenwasser, S. N., "Characteristics, Properties and Fabrication of CuBeNi Alloy (C17510)," Pacific-Sierra Research Corp., Components and Materials Technology Group, Del Mar, CA, PSR Report 1545, 19 pp. (1985).

C17200: Cold-worked and Aged

Creep Strain vs. Elapsed Time (313 K)

DATA SOURCES AND ANALYSIS

A search of the literature for creep data of C17200 at 295 K and lower temperatures was unproductive; therefore, data at 313 K from Reference 12.1 are presented. These data were obtained on wire that was cold-worked 50% and aged. Both commercially fabricated wire with a grain size of 40 μm and laboratory-processed wire with a grain size of 5 μm were tested. The available characterization of materials and measurements is given in Table 12.2 at the end of the creep properties section.

Reference 12.1 does not present instantaneous creep strain as a function of elapsed time, but instead cumulative data are reported for first-stage creep (transient regime) and second-stage creep (steady-state regime).

RESULTS

The deformation in first-stage creep is presented in Table 12.1 in addition to the creep rate during second-stage creep and the total plastic deformation. The second-stage creep rate is plotted against the applied stress in Figure 12.1. For the smaller grain size of 5 μm, there was no measurable second-stage creep rate, at 313 K, but the specimens with an average 40-μm grain size showed an increase in creep rate with applied stress above a threshold of 552–931 MPa.

DISCUSSION

Since the instantaneous creep data were not presented in Reference 12.1, there is no assurance that a steady-state regime was actually attained. As discussed in Section 5 on oxygen-free copper, careful examination of the creep strain plotted as a function of time showed that the creep rate did not attain a constant value, even after elapsed time periods of more than 20 000 h.

Table 12.1. Dependence of Deformation upon Time for the First and Second Stages of Creep (313 K).

			First Stage		Second Stage				
Hardness, VHN	Grain Size, μm	Applied Stress, MPa	Deformation, ϵ, 10^{-6}	Time, min	Deformation, ϵ, 10^{-6}	Time, min	Rate, μs^{-1}	Total Plastic Deformation, 10^{-6}	Total Elapsed Time, min
393	40	0.00	-23	1 440	0	28 800	0	12	30 240
402	40	552	12	5 760	0	24 480	0	–24	30 240
386	40	931	37	2 880	0	15 840	0	175	18 660
39[illegible]	40	1138	200	12 600	25	19 260	0.16	650	31 860
397	40	1138	66	4 320	12	8 640	0.17	224	12 900
398	40	1207	150	4 200	12	8 640	0.17	520	12 780
391	40	1276	267	1 440	63	14 460	0.54	1380	15 900
390	5	552	44	5 760	0	10 080	0	18	15 780
407	5	552	31	12 000	0	18 300	0	18	30 300
371	5	931	129	2 640	0	14 400	0	129	17 040
403	5	931	75	5 760	0	21 660	0	0	27 420
407	5	1138	44	1 140	0	15 900	0	125	17 040
407	5	0.00	56	10 080	0	15 840	0	531	25 900

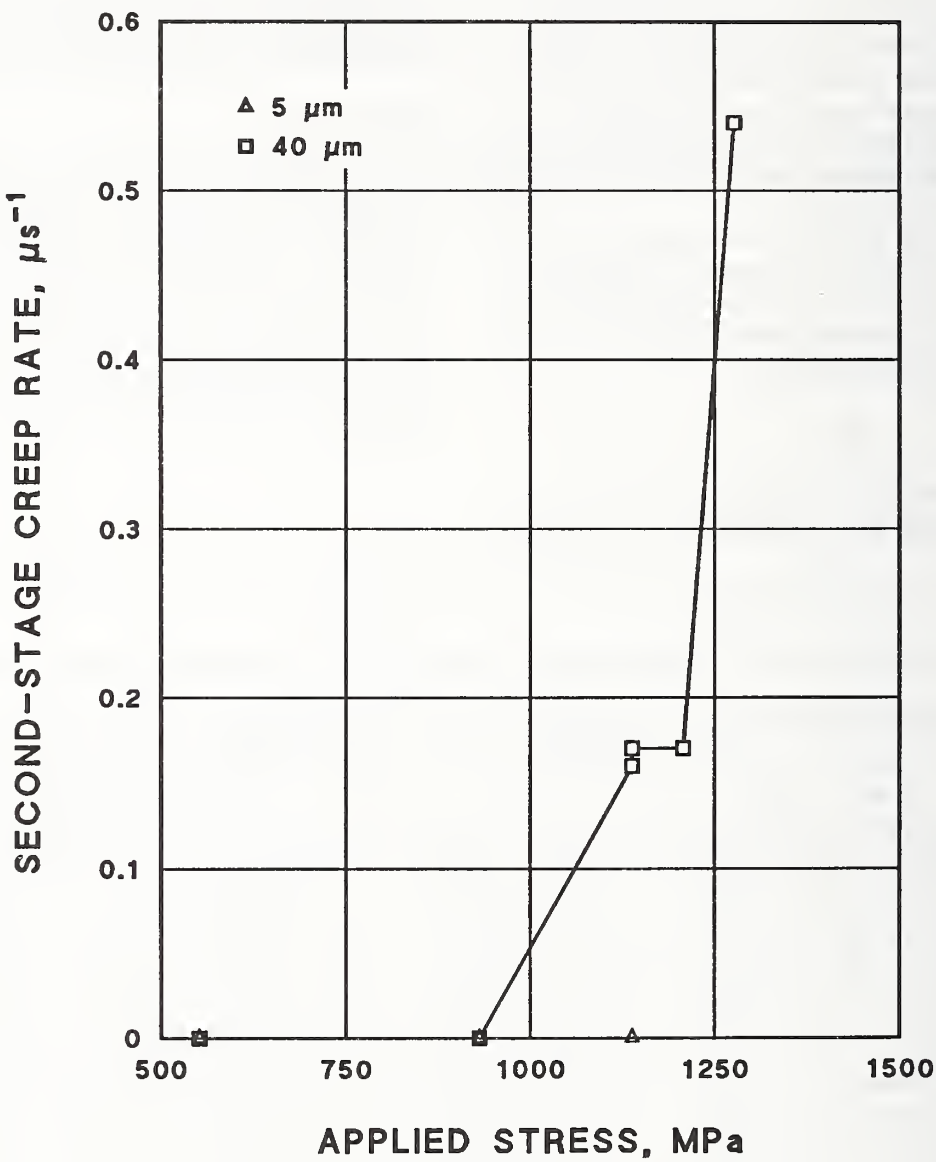

Figure 12.1. The second-stage creep rate versus applied stress for C17200 beryllium copper for two grain sizes (5 and 40 μm). Data from Reference 12.1.

C17510: Cold-worked and Aged

Creep Strain vs. Elapsed Time (295 K)

DATA SOURCES AND ANALYSIS

The only available creep data on C17510 were obtained at 295 K on plate that was cold-worked 37% and aged at 755 K for 2 h (Reference 12.2). The test duration was brief, 18 h. Only one level of applied stress, 646 MPa, was utilized. This is 90% of the tensile yield strength of about 718 MPa. The available information on characterization of materials and measurements is given in Table 12.2 at the end of the creep properties section.

RESULTS

Figure 12.2 shows the creep strain as a function of elapsed time.

DISCUSSION

Test duration was not long enough to determine if a steady-state creep regime had been reached. Also, since only one specimen was tested, the data were not subjected to any further analysis.

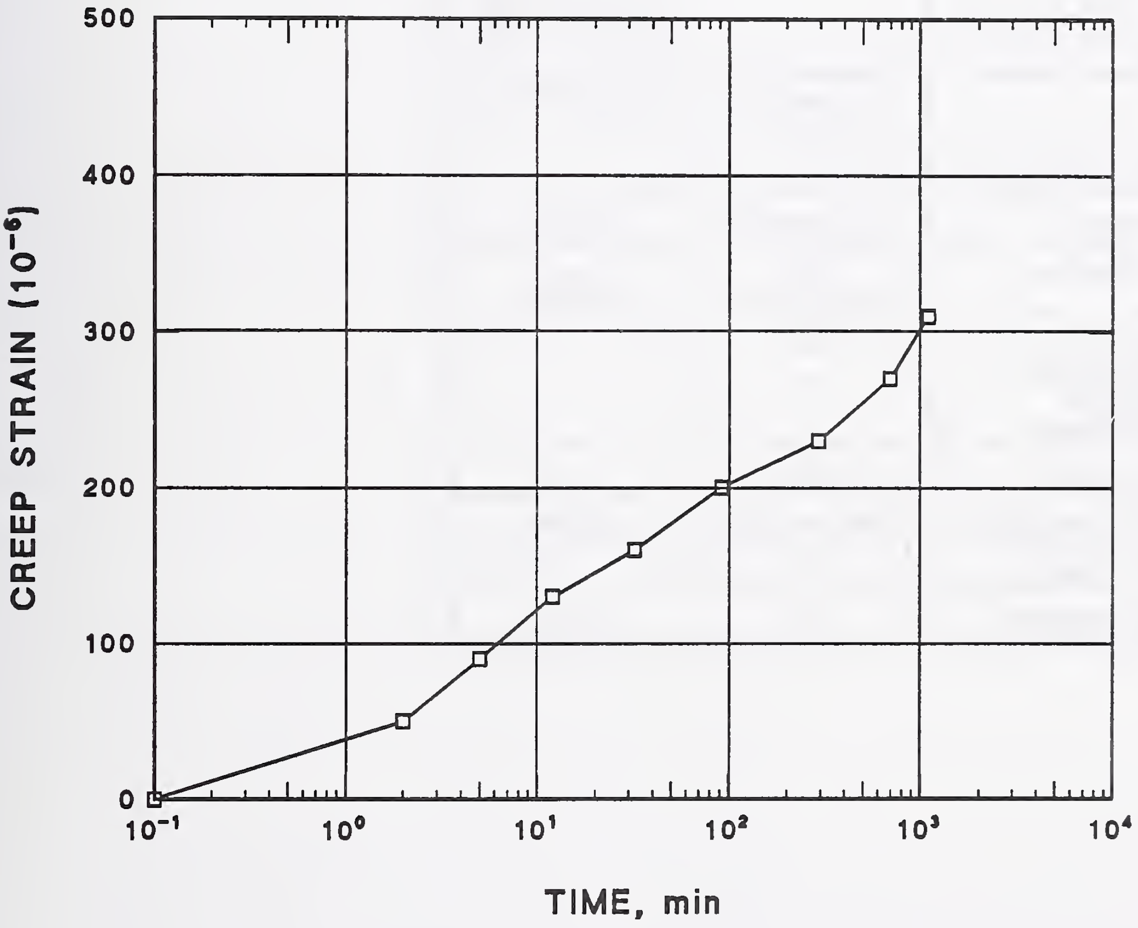

Figure 12.2. The dependence of creep strain of C17500 beryllium copper upon elapsed time. Data from Reference 12.2.

Table 12.2. Characterization of Materials and Measurements.

Reference No.	1	2
Specification	C17200	C17200
Composition (wt%)		
Cu	—	—
Cu + Ag	—	97.6
Be	1.8–2.05	0.38
Ni	—	1.79
Co	0.18–0.30	0.05
Ni + Co	—	—
Ni + Fe + Co	—	—
Al	—	0.01
Fe	—	0.03
Si	—	0.02
Others (Only ≥ 0.001 wt%)	—	Sn, 0.01; Pb, 0.002; Zn, 0.01; Cr, 0.005; Mn, 0.002; Ag, 0.01
Material Condition	Cold-worked, 50%; aged, 588–616 K, 2–5 h	Cold-worked, 50%; aged, 755 K, 2 h
Grain Size (μm)	40 or 5 μm	—
Hardness	371–407 VHN	R_F 92 (b)
Product Form	Wire, 0.089-cm-dia.	Plate, 2.5-cm-thick
Specimen Type	Wire	
Width or Dia.	—	
Thickness	—	
Gage Length	—	
Time Range	211–531 h	18 h
Appl. Stress Range	552–1276 MPa	646 MPa
No. of Specimens	13	1
Test Temperature	313 K	295 K

REFERENCES

1. Wood, R. A., Williams, D. N., Hodge, W., and Ogden, H. R., "Creep Behavior of Copper ~2% Beryllium Wire at Slightly Elevated Temperatures," Transactions of the American Society for Metals 57, 362–364 (1964).

2. Reed, R. P., and Walsh, R. P., National Institute of Standards and Technology, Boulder, CO, private communication (1991).

   Reed, R. P., Walsh, R. P., and Fickett, F. R., "Properties of CDA 104, 155, and 175 Copper Alloys," in Materials Studies for Magnetic Fusion Energy Applications at Low Temperatures--X, Ed., R. P. Reed, National Institute of Standards and Technology, Boulder, CO, NBSIR 87-3067, 83–126 (1987).

C17200: Annealed; Annealed and Aged; Cold-worked; Cold-worked and Aged

Young's Modulus vs. Aging Temperature, Time (295 K)

DATA SOURCES AND ANALYSIS

Only measurements of Young's modulus based upon dynamic methods were considered. These methods determine the adiabatic rather than the isothermal modulus, but the difference between the two moduli of 0.28% at 295 K for beryllium copper (Reference 13.1) is smaller than the errors usually associated with static methods. Dynamic measurements at 295 K of Young's modulus, *E*, of annealed and cold-worked C17200 beryllium copper as a function of aging temperature and time were obtained from References 13.1, 13.2, and 13.3. Measurements from References 13.1 and 13.2 on both annealed and cold-worked material that was not aged were included for comparison. Aging temperatures ranged from 523 to 823 K; aging times from 1 to 3 h. Cold work, *CW*, ranged from 33 to 44% (reduction in thickness or area). Products were in strip (Reference 13.3) and bar form (References 13.1 and 13.2). The results presented here from Reference 13.1 are the averages of several different dynamic methods carried out at different laboratories on the same test material; the variation in results between these measurement methods was less than 2%.

RESULTS

All measurements are reported in Table 13.1, which presents *E*, *CW* (reduction in thickness or area), aging temperature and time, and the reference number. The available characterization of materials and measurements is given in Table 13.5 at the end of the elastic properties section. Figures 13.1 and 13.2 present *E* measurements at 295 K as a function of aging temperature and time, respectively. Measurements on specimens that were not aged are plotted on the *y*-axis. Aging evidently raises the modulus a few percent (References 13.1 and 13.2); the effect of *CW* before aging is small (Reference 13.3).

DISCUSSION

Data are presented in Reference 13.3 on the decrease in *E* as a function of exposure to temperatures up to 750 K for annealed and aged, and cold-worked and aged C17200 beryllium copper. The change is less than 5% when a dynamic method is used to measure the modulus. The dynamic method used is not described in the reference.

Table 13.1. Young's Modulus Measurements of C17200 Beryllium Copper in the Annealed, Annealed and Aged, Cold-worked, and Cold-worked and Aged Conditions (295 K).

Young's Modulus, GPa	Cold Work, %	Aging Temperature, K	Aging Time, h	Reference No.
115	44	0	0	1A
122	44	588	2	1B
118	35	0	0	1F
126	35	588	2	1D
115	33	0	0	1F
130	33	588	2	1[illegible]
130	0	0	0	2A
133	0	523	1	2B
140	0	623	1	2B
140	0	823	1	2B
175	0	588	3	3A
172	37	588	2	3B

Aging Temperature, 0 K = not aged.

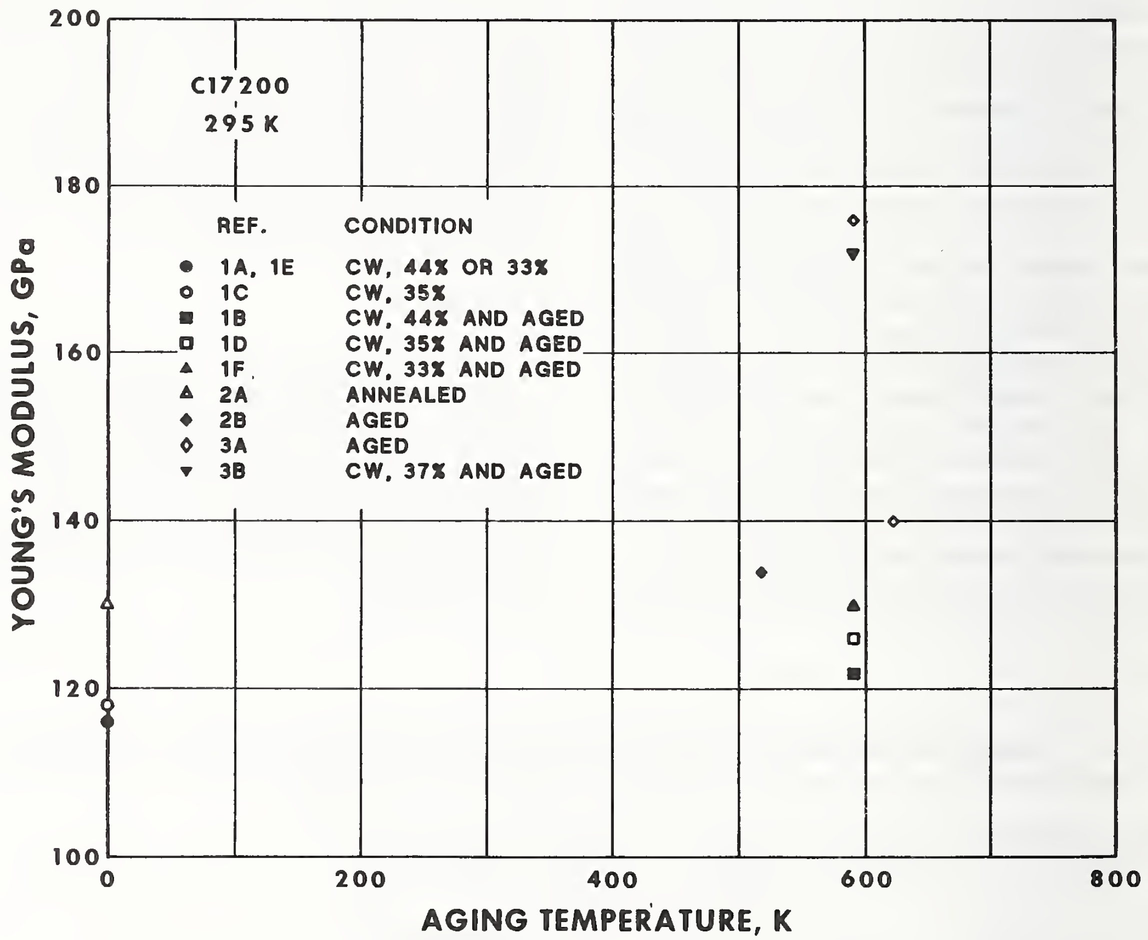

Figure 13.1. Young's modulus measurements at 295 K on C17200 beryllium copper are shown as a function of aging temperature. The material condition is indicated in the graph legend and is further described in Table 13.6. Modulus values for specimens that were not aged are plotted on the *y*-axis. One modulus value from Reference 13.2 at an aging temperature of 823 K does not appear in the graph. All data are presented in Table 13.1. Products were in bar (References 13.1 and 13.2) and strip form (Reference 13.3).

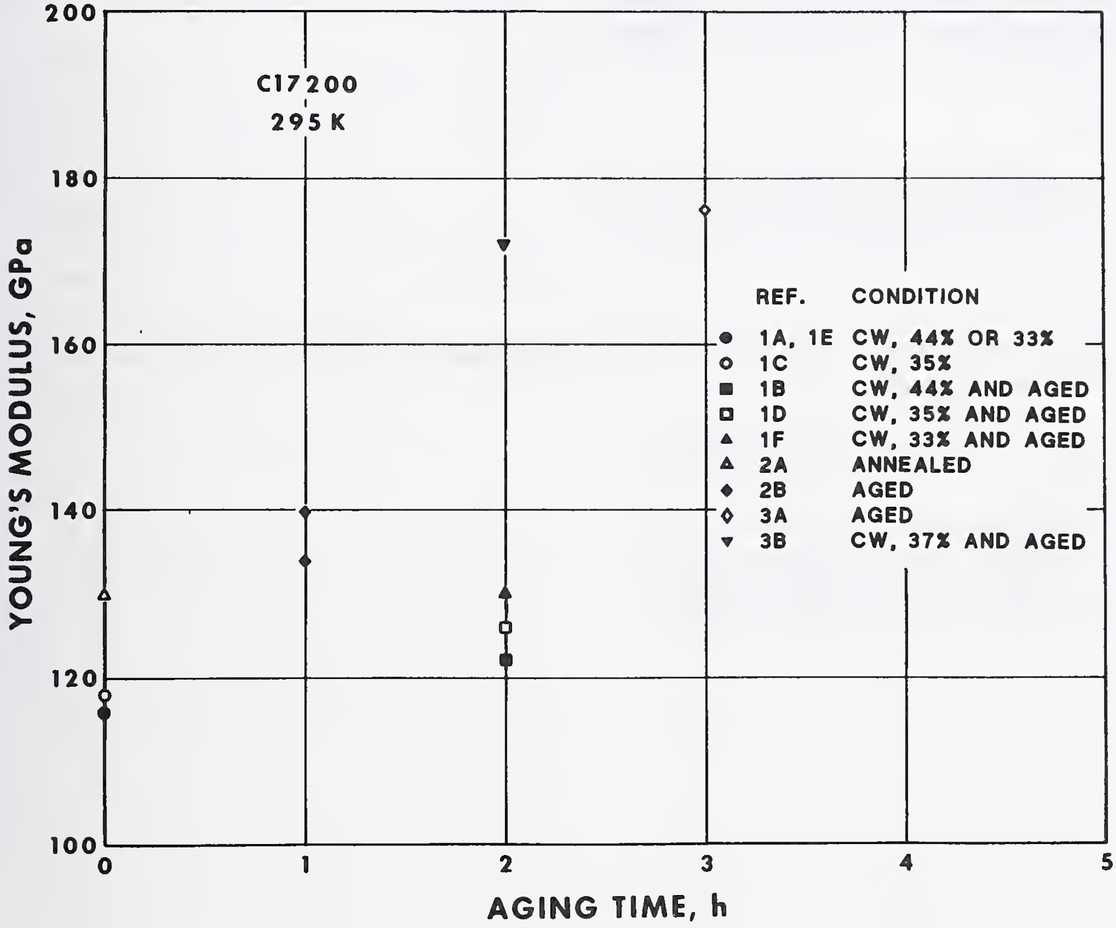

Figure 13.2. Young's modulus measurements at 295 K on C17200 beryllium copper are shown as a function of aging time. The material condition is indicated in the graph legend and is further described in Table 13.6. Modulus values for specimens that were not aged are plotted on the *y*-axis. All data are presented in Table 13.1. Products were in bar (References 13.1 and 13.2) and strip form (Reference 13.3).

DATA SOURCES AND ANALYSIS

Measurements of Young's modulus from 227 to 297 K of cold-worked and aged C17200 beryllium copper were obtained from Reference 13.1. The dynamic method used was that of longitudinal vibration. The amount of cold work, *CW,* was 44% (reduction in area), the aging temperature was 588 K and the aging time was 2 h. Product was in bar form.

RESULTS

All measurements are reported in Table 13.2, which presents test temperature, Young's modulus, *E*, and the reference number. The available characterization of materials and measurements is given in Table 13.5 at the end of the elastic properties section. Figure 13.3 presents the *E* measurements as a function of test temperature. The modulus increases with decreasing temperature, in accord with results on high-purity copper. (See Section 6 in this volume.)

Table 13.2. Dependence of Young's Modulus upon Temperature for Cold-worked and Aged C17200 Beryllium Copper (227–297 K).

Test Temperature, K	Young's Modulus, GPa	Reference No.
227	124	1B
261	122	1B
297	120	1B

C17200: Cold-worked and Aged

Young's Modulus vs. Temperature (227–297 K)

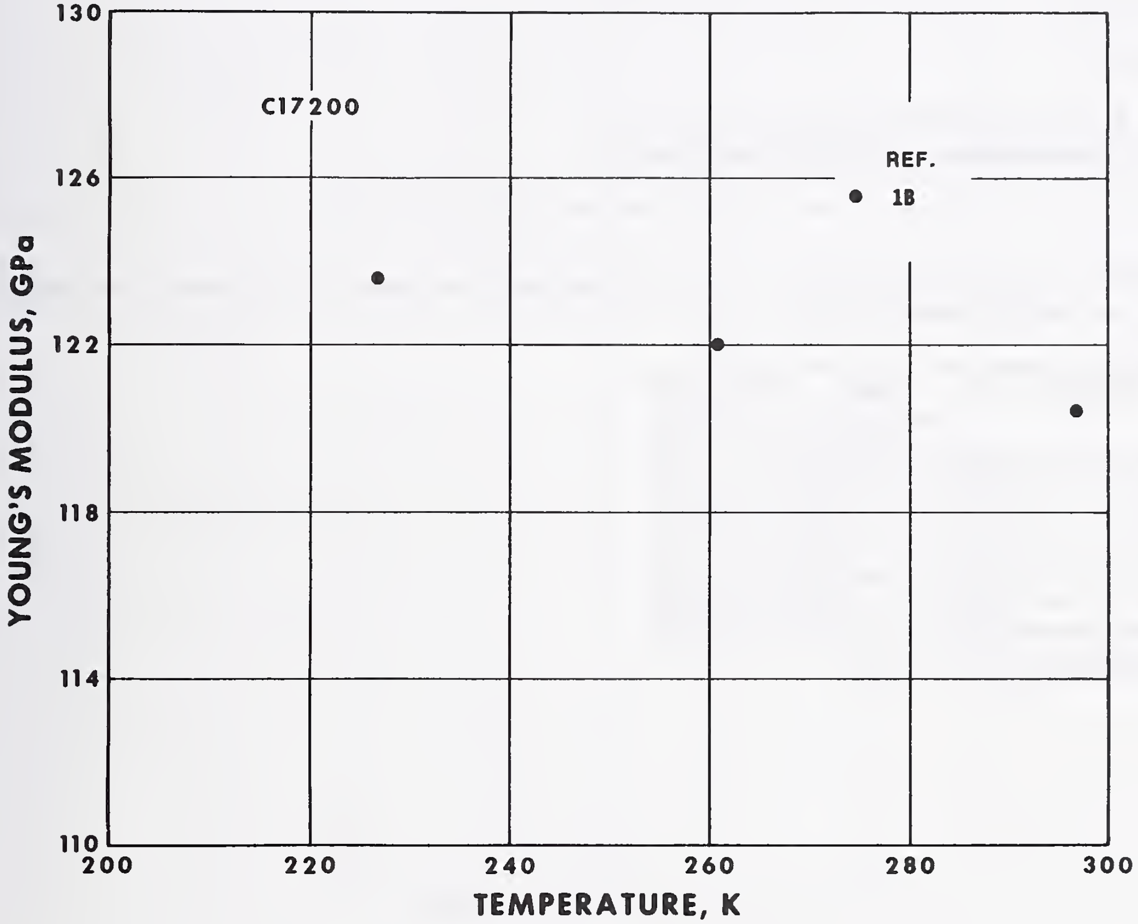

Figure 13.3. Young's modulus measurements of cold-worked and aged C17200 beryllium copper are shown as a function of test temperature. All data are presented in Table 13.2. Product was in bar form.

DATA SOURCES AND ANALYSIS

Measurements of the shear modulus at 295 K of annealed C17200 beryllium copper as a function of aging temperature were obtained from Reference 13.4. A measurement on an annealed specimen was included for comparison. The test method was torsional vibration of a wire. Aging temperature varied from 473 to 723 K; aging time was 0.5 h.

RESULTS

All measurements are reported in Table 13.3, which presents shear modulus (*G*), aging temperature, and the reference number. The available characterization of materials and measurements is given in Table 13.5 at the end of the elastic properties section. Figure 13.4 presents *G* measurements as a function of aging temperature. A measurement on a specimen that was not aged is plotted on the *y*-axis. High aging temperatures (above 673 K) caused a noticeable increase in *G*.

Table 13.3. Shear Modulus Measurements of C17200 Beryllium Copper in the Annealed, and Annealed and Aged Condition (295 K).

Shear Modulus, GPa	Aging Temperature, K	Reference No.
49.6	0	4A
50.8	473	4B
49.8	573	4B
49.7	623	4B
51.8	673	4B
53.4	723	4B

Aging Temperature, 0 K = not aged.

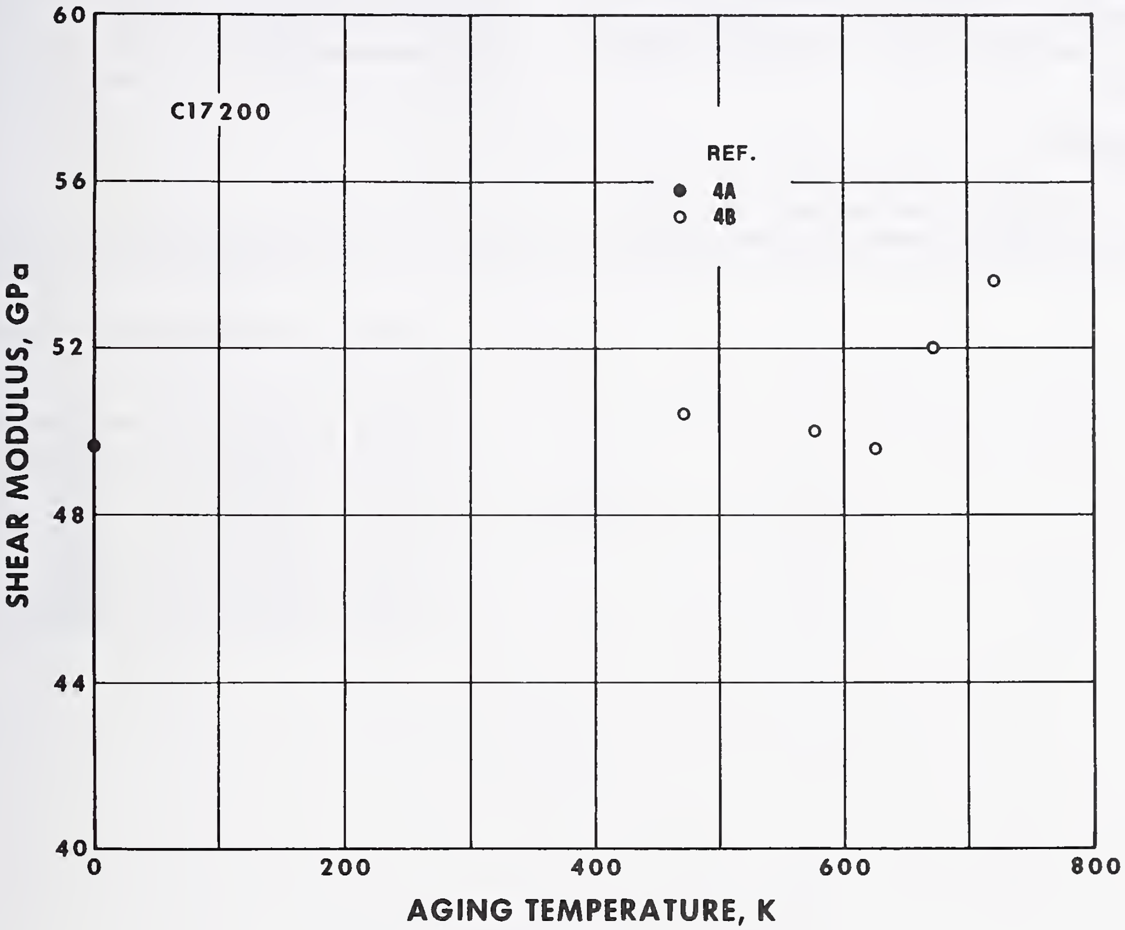

Figure 13.4. Shear modulus measurements at 295 K on annealed C17200 beryllium copper are shown as a function of aging temperature. A modulus value for a specimen that was not aged is plotted on the *y*-axis. All data are presented in Table 13.3. Product was in wire form.

C17200: Cold-worked; Cold-worked and Aged

Shear Modulus (295 K)

DATA SOURCES AND ANALYSIS

Dynamic shear modulus data at 295 K for cold-worked, and cold-worked and aged C17200 beryllium copper were obtained from Reference 13.1. This reference reports results of round-robin tests made at several different laboratories by different dynamic methods on the same test material. The amount of cold work ranged from 33 to 44% (reduction in area). The specimens were aged at 588 K for 2 h. Product was in bar form.

RESULTS

The average shear modulus, G, for cold-worked C17200 beryllium copper was 42.5 GPa; the average for cold-worked and aged material was significantly higher, 47.1 GPa. The variation was less than ± 2.8% for cold-worked specimens, and less than ± 2.5% for cold-worked and aged specimens. The available characterization of materials and measurements is given in Table 13.5 at the end of the elastic properties section. (References 13.1A, 13.1C, and 13.1E refer to the cold-worked material and References 13.1B, 13.1D, and 13.1F refer to the material that was cold-worked and aged.)

DATA SOURCES AND ANALYSIS

Measurements of the shear modulus from 200 to 297 K of cold-worked and aged C17200 beryllium copper were obtained from Reference 13.1. The shear modulus, *G*, was obtained from the deflection rate of a compression spring; these static-method results are presented here because no low-temperature dynamic test data were found. The amount of cold work was 44% (reduction in area), the aging temperature was 588 K and the aging time was 2 h. Product was in bar form.

RESULTS

All measurements are reported in Table 13.4, which presents test temperature, G, and the reference number. The available characterization of materials and measurements is given in Table 13.5 at the end of the elastic properties section. Figure 13.5 presents G as a function of test temperature. The modulus increases slightly with decreasing temperature, in accord with results on high purity copper.

Table 13.4. Shear Modulus Dependence of Cold-worked and Aged C17200 Beryllium Copper upon Temperature (200–297 K).

Test Temperature, K	Shear Modulus, GPa	Reference No.
297	46.7	1B
200	48.0	1B
222	47.4	1B
250	47.2	1B
261	47.0	1B
272	46.9	1B
283	46.8	1B

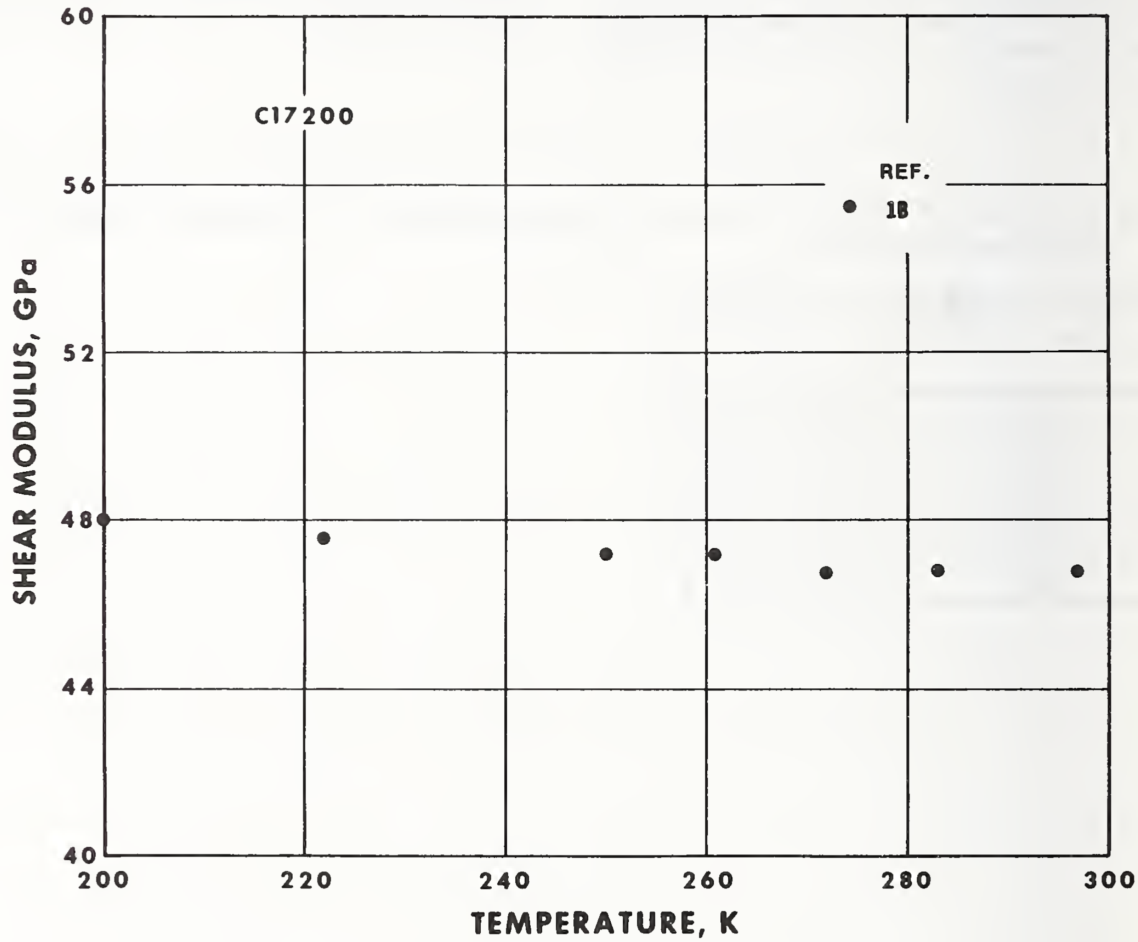

Figure 13.5. Shear modulus measurements of cold-worked and aged C17200 beryllium copper are shown as a function of test temperature. All data are presented in Table 13.4. Product was in bar form.

DATA SOURCES AND ANALYSIS

Direct measurements of Poisson's ratio, ν, on cold-worked and aged C17200 beryllium copper were obtained from Reference 13.1. This source also gives a series of ν values determined from the ratio of the shear modulus to Young's modulus, where both moduli were determined experimentally in the same laboratory. These measurements were carried out in a round-robin in which the material to be tested was supplied to several laboratories. The available material characterization of this material is given in Table 13.5 at the end of the elastic properties section. Coid work, *CW*, varied from 33 to 44% (reduction of area). About half of the specimens were aged at 588 K for 2 h.

RESULTS

Poisson's ratio determined directly from tension was 0.39, and from compression, 0.40. Specimens were cold-worked 33% before aging.

The indirect determinations of ν gave an average value of 0.37 for cold-worked material, and an average value of 0.33 when the material was aged after *CW*. The standard deviations of the two measurements were 0.01 and 0.03, respectively.

DISCUSSION

The expression used in Reference 13.1 to relate ν to Young's modulus and the shear modulus is valid only for isotropic material. Since the specimens were cold-worked, this assumption was probably not correct.

Table 13.5. Characterization of Materials and Measurements.

Reference No.	1A	1B	1C	1D
Specification	C17200	C17200	C17200	C17200
Composition (wt%)				
Cu	97.72	97.72	97.64	97.64
Cu + Ag	—	—	—	—
Be	1.83	1.83	1.82	1.82
Ni	0.01	0.01	0.03	0.03
Co	0.22	0.22	0.18	0.18
Ni + Co	—	—	—	—
Ni + Fe + Co	—	—	—	—
Al	0.03	0.03	0.04	0.04
Fe	0.11	0.11	0.12	0.12
Si	0.07	0.07	0.15	0.15
Others (Only ≥ 0.001 wt%)	Sn: 0.01	Sn: 0.01	Sn: 0.02; Pb: 0.002	Sn: 0.02; Pb: 0.002
Material Condition	Cold-drawn, 44%	Cold-drawn, 44%, then aged, 588 K, 2 h	Cold-drawn, 35%	Cold-drawn, 35%, then aged, 588 K, 2 h
Grain Size	25 μm	25 μm	25 μm	25 μm
Hardness	—	—	R_B 95	R_C 42
Product Form	Bar	Bar	Bar	Bar
Specimen Type	Round (a)	Round (a)	Round (a)	Round (a)
Width or Dia.	0.23 cm	0.23 cm	0.56 cm	0.56 cm
Thickness	—	—	—	—
Gage Length	—	—	—	—
No. of Specimens	—	—	—	—
Test Temperature	293 K	227–297 K	293 K	293 K

(a) Specimen type and diameter refer only to the test material supplied to different investigators.

1E	1F	2A	2B	3A
C17200	C17200	C17200	C17200	C17200
97.68 — 1.86 0.01 0.22 — — 0.02 0.13 0.07 Sn: 0.01	97.68 — 1.86 0.01 0.22 — — 0.02 0.13 0.07 Sn: 0.01	— — 2.0 — — — — — — — —	— — 2.0 — — — — — — — —	> 97.54 — 1.91 0.01 0.26 — — 0.04 0.12 0.10 Sn: 0.005; Zn, Pb, Cr: < 0.005
Cold-drawn, 33%	Cold-drawn, 33%, then aged, 588 K 2 h	Annealed	Aged, 1 h (b)	Aged, 588 K, 3 h
35 μm	35 μm	—	—	20 μm
R_B 99	R_C 42	—	—	R_{30N} 60 (c)
Bar	Bar	—	—	Strip
Round (a) 1.42 cm — —	Round (a) 1.42 cm — —	Cylinder 0.6 cm — 16 cm	Cylinder 0.6 cm — 16 cm	Flat 1.27 cm 0.05 cm 5.0 cm
—	—	—	—	—
293 K	293 K	295 K	295 K	295 K

(a) Specimen type and diameter refer only to the test material supplied to different investigators.
(b) Aging temperatures: 523 K, 623 K, or 823 K.
(c) To convert hardness to Rockwell C scale see Reference 13.5.

Table 13.5, continued

Reference No.	3B	4A	4B
Specification	C17200	C17200	C17200
Composition (wt%)			
Cu	> 97.54	—	—
Cu + Ag	—	—	—
Be	1.91	2.0	2.0
Ni	0.01	—	—
Co	0.26	—	—
Ni + Co	—	—	—
Ni + Fe + Co	—	—	—
Al	0.04	—	—
Fe	0.12	—	—
Si	0.10	—	—
Others (Only ≥ 0.001 wt%)	Sn: 0.005; Zn, Pb, Cr: < 0.005	—	—
Material Condition	Cold-rolled, 37%, then aged, 588 K, 2 h	Annealed	Aged, 473–723 K, 0.5 h
Grain Size	22 μm	—	—
Hardness	R_{30N} 62 (a)	—	—
Product Form	Strip	—	—
Specimen Type	Flat	Wire	Wire
Width or Dia.	1.27 cm	0.025 cm	0.025 cm
Thickness	0.05 cm	—	—
Gage Length	5.0 cm	—	—
No. of Specimens	—	—	—
Test Temperature	295 K	295 K	295 K

(a) To convert hardness to Rockwell C scale see Reference 13.5.

REFERENCES

1. Richards, J. T., "An Evaluation of Several Static and Dynamic Methods for Determining Elastic Moduli," in Symposium on Determination of Elastic Constants, American Society for Testing Materials, Philadelphia, PA, 71–100 (1952).

2. Grachev, S. V., and Grigoryeva, V. N., "Variation in the Elastic Modulus of Alloys with a Metastable Structure," Fizika Metallov I Metallovedenie 32, 155–161 (1971).

3. Wikle, K. G., and Sarle, N. P., "Properties of Hardened Copper-Beryllium Strip after Exposures to Elevated Temperatures," Proceedings of the American Society for Testing Materials 61, 988–1006 (1961).

4. Masing, G., and Haase, C., "Über die Ånderung des Elastizitätsmoduls bei der Vergütung von Beryllium-Kupferlegierungen," Wiss. Veroffentlich. aus den Siemens-Konzern, 142–148 (1929).

5. Gohn, G. R., Herbert, G. J., and Kuhn, J. B., "The Mechanical Properties of Copper-Beryllium Alloy Strip," American Society for Testing and Materials Special Technical Publication No. 367, 109 pp (1964).

6. Guillet, M. L., "Contribution à l'Etude du Module d'Elasticité des Alliages Métalliques," Revue de Métallurgie 36, 497–521 (1939).

C17000–C17510: Annealed; Cold-worked

Specific Heat vs. Temperature (4–345 K)

DATA SOURCES AND ANALYSIS

Reference 14.1 presents data for the specific heat, C_p, of C17510 beryllium copper from 83 to 345 K in the annealed and aged, and cold-worked and aged conditions. No measurements of C_p of other beryllium copper alloys below room temperature were found (see Discussion below). Since C_p is generally insensitive to alloy condition, a polynomial expression was fitted to all the measurements from Reference 14.1.

RESULTS

The best fit to the data was obtained with the equation

$$C_p = 104.5 + 1.883\,T - 0.002987\,T^2 \qquad (14\text{-}1)$$

for three different heat treatments of C17510 only; where $83\ \text{K} \leq T \leq 345\ \text{K}$. The standard deviation of the fit of the data to this equation is 8.4 J/(kg·K). The standard deviations of the three constants are 14.8, 0.156, and 3.64×10^{-4}.

Table 14.1 presents the test temperature, and the measured and calculated values of C_p. The available characterization of materials and methods is given in Table 14.7 at the end of the thermal properties section. Figure 14.1 indicates the fit of the data to Equation (14-1). The scatter bands represent two standard deviations about the curve.

DISCUSSION

As noted above, no measurements were found for C_p of beryllium copper alloys C17000, C17200, and C17500 below room temperature. The C_p of C17000, C17200, C17500, and C17510 beryllium coppers at 295 K is reported by Reference 14.2 to be 418 J/(kg·K) or 0.10 cal/(g·K). The C_p of beryllium at 295 K is 1970 J/(kg·K) (Reference 14.3); that of copper is 384 J/(kg·K) (Reference 14.2). If the additivity principle is valid, the expected specific heat of a 2% binary beryllium copper alloy would be 415 J/(kg·K), approximately in agreement with the value quoted in Reference 14.2. A discussion of the limits of the additivity principle for C_p of alloys can be found in Reference 14.4. Since most of the contribution to C_p of beryllium coppers is from copper, cryogenic values could be estimated by multiplying the specific heats presented in Section 7 of this volume by the ratio 1.1. This ratio is equal to 418/377, the 295-K value for beryllium copper divided by the average value at 295 K found for the C10100–C10200 coppers. Alternatively, measurements of the thermal expansion coefficient of C17200 (see pp 7-23–7-34) could be scaled to give a estimate of the cryogenic C_p. See Reference 14.4 for a more detailed discussion of the limitations of this procedure. The C_p is proportional to the thermal expansion coefficient only for ideal solids that obey a Debye equation of state in which the Grüneisen constant, γ, is temperature independent.

Table 14.1. Dependence of the Specific Heat of C17510 Beryllium Copper upon Temperature (83–345 K).

Test Temperature, K	Specific Heat, Measured, J/(kg·K)	Specific Heat, Predicted, J/(kg·K)	Reference No.
83.2	228.	241.	1A
113.	289.	280.	1A
143.	328.	312.	1A
182.	359.	349.	1A
212.	371.	369.	1A
242.	381.	385.	1A

Table 14.1, continued

Test Temperature, K	Specific Heat, Measured, J/(kg·K)	Specific Heat, Predicted, J/(kg·K)	Reference No.
273.	391.	396.	1A
297.	396.	400.	1A
345.	404.	396.	1A
321.	279.	287.	1B
160.	321.	329.	1B
221.	367.	375.	1B
299.	400.	401.	1B
99.4	261.	262.	1C
125.	297.	293.	1C
150.	328.	319.	1C
250.	383.	389.	1C
325.	406.	401.	1C

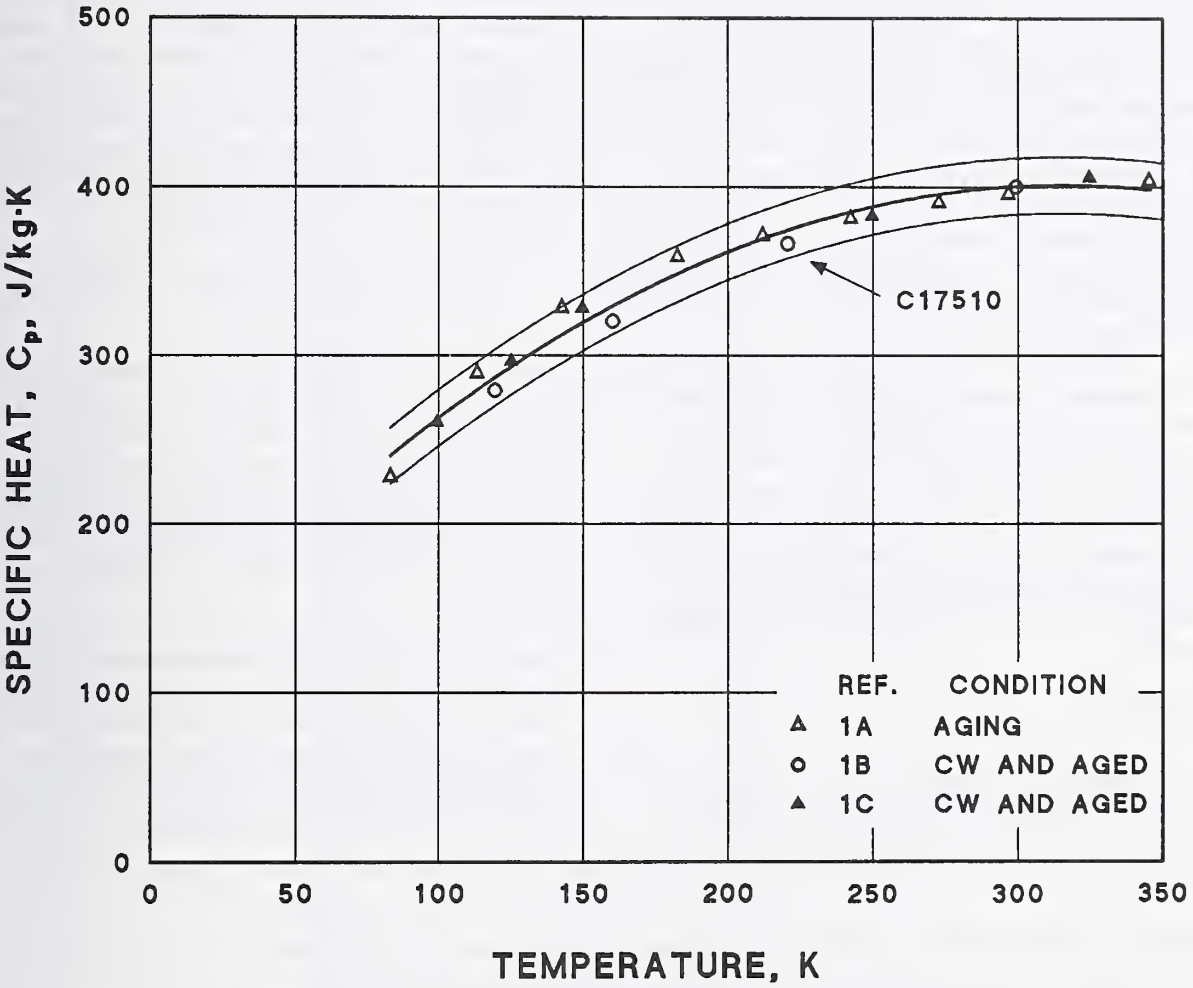

Figure 14.1. Data from three separate heat treatments were used to calculate the regression curve of the specific heat of C17510 beryllium copper upon temperature [Equation (14-1)]. All data are presented in Table 14.1.

DATA SOURCES AND ANALYSIS

Measurements of the thermal conductivity, λ, of C17200 beryllium copper between 2 and 300 K were obtained from References 14.5 and 14.6. Measurements at 295 K only were obtained from References 14.7, 14.8, and 14.9. Measurements of λ for C17510 beryllium copper between 77 and 293 K were obtained from Reference 14.10. Measurements of λ for C17000, C17500, and C17510 beryllium coppers at 295 K only were obtained from References 14.9, 14.11, and 14.12. Material conditions were varied: see Table 14.7 at the end of the thermal properties section and the legend of Figure 14.2 described below. Polynomial regression analysis was carried out on the C17200 beryllium copper data set of 43 measurements, and the C17510 beryllium-copper data set of 37 measurements.

Table 14.2 presents the test temperature, T, the measured values of λ, the values calculated from the regression equation (for C17200 and C17510 only), and the reference number. The notation "N.C." in the table refers to alloys other than C17200 and C17510 which were not used in the regression analyses. The available characterization of materials and methods is given in Table 14.7 at the end of the thermal properties section.

RESULTS

Figure 14.2 presents a plot of the data from all beryllium-copper alloys. The polynomial regression analysis carried out on the C17200 data set indicated that a satisfactory fit could be obtained with a second-order equation

$$\lambda(\mathrm{W/m{\cdot}K}) = 0.93 + 0.492\,T - 0.000594\,T^2 \quad \text{(C17200 only)} \qquad (14\text{-}2)$$

where $2\ \mathrm{K} \leq T \leq 300\ \mathrm{K}$. The standard deviation of the fit of the data to this equation is 8.4 W/(m·K); the standard deviations of the three constants are 2.72, 0.049, and 0.000159. The value of the first constant is not well-determined from the data set.

The polynomial regression analysis carried out on the C17510 data set also gave a satisfactory fit with a second-order equation

$$\lambda(\mathrm{W/m{\cdot}K}) = 64.7 + 0.987\,T - 0.00138\,T^2 \quad \text{(C17510 only)} \qquad (14\text{-}3)$$

where $77\ \mathrm{K} \leq T \leq 293\ \mathrm{K}$. The standard deviation of the fit to this equation is 1.9 W/(m·K); the standard deviations of the three constants are 2.5, 0.032, and 9×10^{-5}. One value, from Reference 14.9D, was eliminated from the analysis because of lack of agreement with the other data. This may be due to the difference in material condition.

Figure 14.2 indicates the fit of the C17200 data to Equation (14-2), and that of the C17510 data to Equation (14-3). The scatter bands represent two standard deviations about the curve. The variance of the data was assumed to be normally distributed and constant throughout the range of the independent variable, T.

Table 14.2. Dependence of Thermal Conductivity upon Temperature (2–300 K).

Test Temperature, K	Thermal Conductivity, Measured, W/(m·K)	Thermal Conductivity, Predicted, W/(m·K)	Material	Reference No.
2.00	0.900	1.91	C17200	5
3.00	1.40	2.40	C17200	5
4.00	1.90	2.89	C17200	5
5.00	2.30	3.37	C17200	5
6.00	2.90	3.86	C17200	5
8.00	3.90	4.83	C17200	5
10.0	4.90	5.79	C17200	5
15.0	7.80	8.18	C17200	5
20.0	10.7	10.5	C17200	5
25.0	13.5	12.9	C17200	5

C17000, C17200, C17500, and C17510: Annealed; Annealed and Aged; Cold-worked; Cold-worked and Aged

Thermal Conductivity vs. Temperature (2–300 K)

Table 14.2, continued

Test Temperature, K	Thermal Conductivity, Measured, W/(m•K)	Thermal Conductivity, Predicted, W/(m•K)	Material	Reference No.
30.0	16.2	15.2	C17200	5
40.0	21.5	19.7	C17200	5
50.0	26.2	24.1	C17200	5
60.0	30.4	28.3	C17200	5
70.0	34.0	32.5	C17200	5
80.0	34.0	36.5	C17200	5
125.	63.5	53.2	C17200	6A
128.	61.0	54.2	C17200	6A
160.	56.5	64.5	C17200	6B
193.	71.0	65.4	C17200	6A
160.	63.5	71.1	C17200	6B
193.	61.0	72.5	C17200	6B
125.	78.5	78.8	C17200	6A
193.	78.5	73.8	C17200	6A
213.	74.0	78.8	C17200	6B
213.	36.4	73.8	C17200	6A
228.	78.5	78.8	C17200	6B
228.	61.0	82.3	C17200	6A
293.	74.0	86.5	C17200	6B
293.	61.0	87.4	C17200	6A
263.	80.0	89.3	C17200	6B
293.	61.0	54.2	C17200	7B
293.	105.	94.2	C17200	7C
293.	74.0	53.2	C17200	7B
293.	106.	94.2	C17200	7D
293.	74.0	54.2	C17200	7B
293.	63.5	94.2	C17200	7C
293.	100.	N.C.	C17200	11A
293.	105.	94.2	C17200	11B
263.	180.	N.C.	C17500	11C
293.	80.0	94.2	C17200	6A
293.	104.	54.2	C17200	6B
293.	63.5	N.C.	C17200	6A
293.	105.	94.2	C17200	6B
293.	180.	N.C.	C17500	9C
293.	180.	N.C.	C17500	9D
293.	230.	N.C.	C17500	12
120.	61.0	95.1	C17200	6B
300.	108.	95.1	C17200	6A
76.0	132.5	131.8	C17510	10
77.2	133.0	132.7	C17510	10
78.46	133.5	135.6	C17510	10
80.93	135.5	135.6	C17510	10
83.41	137.3	137.5	C17510	10
90.95	143.1	143.1	C17510	10
96.0	146.7	146.8	C17510	10
106.3	153.6	154.1	C17510	10
192.7	202.4	203.8	C17510	10
193.5	202.0	204.1	C17510	10

Table 14.2, continued

Test Temperature, K	Thermal Conductivity, Measured, W/(m•K)	Thermal Conductivity, Predicted, W/(m•K)	Material	Reference No.
194.9	207.7	204.8	C17510	10
197.7	207.2	206.0	C17510	10
27[illegible].[illegible]	209.5	214.2	C17510	10
215.4	213.0	213.4	C17510	10
217.4	214.1	214.2	C17510	10
273.9	232.5	231.8	C17510	10
27[illegible].8	231.9	231.[illegible]	C17510	10
276.0	232.5	232.2	C17510	10
278.8	233.5	232.9	C17510	10
281.7	2[illegible]7.7	233.5	C17510	10
284.5	235.4	234.1	C17510	10
290.2	237.4	235.2	C17510	10
293.2	238.0	235.7	C17510	10
299.0	230.0	236.7	C17510	10

N.C. = not calculated (not C17200 or C17510 data set)

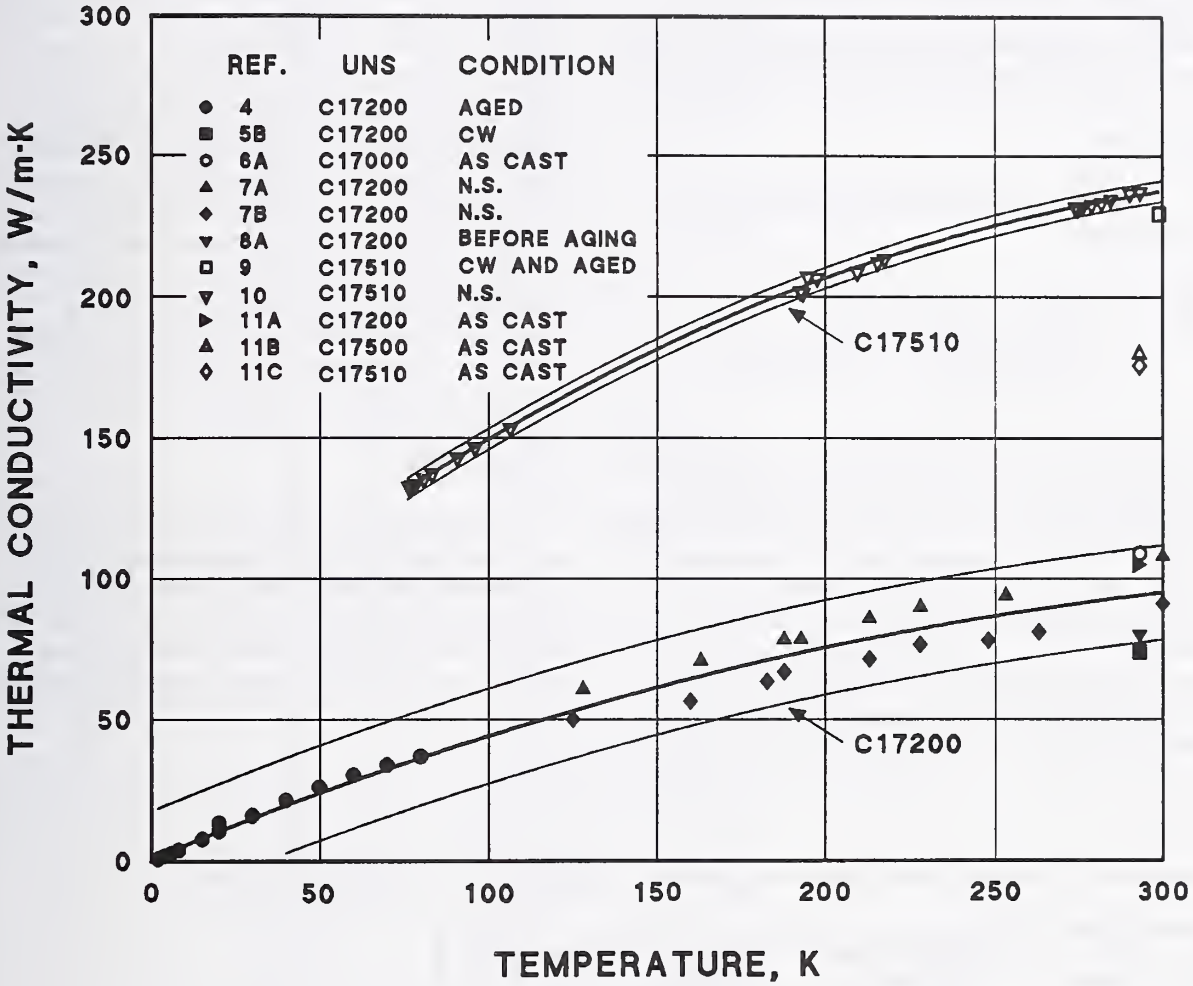

Figure 14.2. The data keyed as C17200 and C17510 in the legend were used to compute the regression of the thermal conductivity of C17200 beryllium copper upon temperature [Equation (14-2)], and the thermal conductivity of C17510 beryllium copper upon temperature [Equation (14-3)]. For clarity, overlapping data points were omitted from the figure. Consequently, some points for different material conditions (References 14.7A, 14.7C, 14.7D, 14.8B, and 14.9A) do not appear in the figure. All data are presented in the table. (N.S. in legend indicates not specified.)

C17200: Annealed; Annealed and Aged
Cold-worked; Cold-worked and Aged

Thermal Expansion Coefficient
vs. Temperature (6–300 K)

DATA SOURCES AND ANALYSIS

Measurements of the coefficient of thermal expansion, α, of C17200 beryllium copper were obtained from four sources (References 14.13–14.16). A variety of material conditions were represented. A total of 97 measurements between 6 and 320 K were used in the regression analysis. A logarithmic transformation of the data was made to avoid a large number of constants.

RESULTS

The best fit to the data was obtained with the equation

$$\log \alpha = -25.30 + 95.96 (\log T) - 164.5 (\log T)^2 + 147.6 (\log T)^3 - 70.83 (\log T)^4 + 17.28 (\log T)^5 - 1.689 (\log T)^6 \qquad (14\text{-}4)$$

where α has units of 10^{-6} K^{-1} and T is temperature for the range 6 K $\leq T \leq$ 300 K. The logarithmic standard deviation of the fit of this equation to the data is 0.04 and the linear standard deviation is 0.14×10^{-6} K^{-1}. The standard deviations of the seven constants of Equation (14-4) are 6.21, 25.88, 43.5, 37.8, 17.93, 4.42, and 0.443. (The size of the residuals at low temperatures where the magnitude of α decreases is much lower than the linear standard deviation of 0.14×10^{-6} K^{-1}. Residuals near 300 K contribute more to the standard deviation.)

Table 14.3 presents T, the measured values of α, the values calculated from the regression equation, and the reference number. The available characterization of materials and measurements is given in Table 14.7 at the end of the thermal properties section. Figure 14.3 indicates the fit of the data to Equation (14-4). Figure 14.4 presents these results in summary form. The scatter bands in both figures represent two standard deviations about the curve given by Equation (14-4). However, because of the narrowness of the bands, the curve had to be omitted in both figures. The variance of the data was assumed to be normally distributed and constant throughout the range of the independent variable, log T.

Because Equation (14-4) is in logarithmic form, a set of calculated values of α for 5 K $\leq T \leq$ 300 K is presented in Table 14.4.

DISCUSSION

The data shown in Figure 14.3 indicate that α is insensitive to material condition. This is in agreement with results on C10100 and C10200 copper (see Section 7 in this volume). However, data on the mean thermal expansion (pages 14-14–14-17) do show some variation with cold work and aging.

Table 14.3. Dependence of Thermal Expansion Coefficient upon Temperature (6–300 K).

Test Temperature, K	Thermal Expansion Coefficient, Measured, 10^{-6}/K	Thermal Expansion Coefficient, Predicted, 10^{-6}/K	Reference No.
6.00	0.00720	0.00767	13B
6.00	0.00850	0.00767	13A
8.00	0.0146	0.0176	13B
8.00	0.0166	0.0176	13A
10.0	0.0269	0.0317	13B
10.0	0.0301	0.0317	13B
10.0	0.0600	0.0317	14
1[illegible].0	0.0461	0.0522	13A
1[illegible].0	0.06[illegible]	0.0522	13B
1[illegible].0	0.0747	0.0818	13A
1[illegible].0	0.0828	0.0818	13B
16.0	0.115	0.123	13B
16.0	0.127	0.123	13A

C17200: Annealed; Annealed and Aged; Cold-worked; Cold-worked and Aged

Thermal Expansion Coefficient vs. Temperature (6–300 K)

Table 14.3, continued

Test Temperature, K	Thermal Expansion Coefficient, Measured, 10^{-6}/K	Thermal Expansion Coefficient, Predicted, 10^{-6}/K	Reference No.
18.0	0.172	0.179	13A
78.0	0.204	0.179	13A
20.0	0.248	0.251	13B
25.0	0.265	0.251	13A
25.0	0.210	0.251	14
25.0	0.528	0.517	13B
25.0	0.550	0.517	13A
30.0	0.948	0.915	13A
30.0	0.961	0.915	13A
30.0	0.760	0.915	14
35.0	1.49	1.44	13B
35.0	1.49	1.44	13A
40.0	2.13	2.07	13B
40.0	2.10	2.07	13A
40.0	2.08	2.07	14
40.0	2.83	2.78	13A
40.0	2.78	2.78	13B
50.0	3.55	9.57	13A
90.0	3.48	3.54	13B
80.0	3.55	3.54	14
90.0	5.02	5.07	13B
80.0	4.92	5.07	13A
90.0	5.38	5.07	14
70.0	6.39	6.50	13A
70.0	6.27	6.50	13A
70.0	6.75	6.50	14
90.0	12.4	7.76	13B
80.0	7.51	7.76	13A
80.0	7.82	7.76	14
80.0	8.69	9.57	13A
90.0	8.61	3.54	13B
80.0	8.68	6.50	14
100.	9.63	9.74	13A
140.	9.57	9.74	13A
100.	9.57	9.74	14
110.	10.5	10.5	14
120.	11.3	11.2	13B
120.	11.8	11.2	13A
120.	11.3	11.2	14
130.	11.8	11.2	14
140.	12.3	12.2	13A
140.	12.3	12.2	13A
140.	12.4	12.2	14
150.	12.8	12.7	14
160.	13.2	13.1	13A
150.	11.8	13.1	13A
160.	6.27	13.1	14
170.	13.6	13.4	14
180.	13.9	13.8	13B
180.	14.0	13.8	13A
180.	13.9	13.8	14

Table 14.3, continued

Test Temperature, K	Thermal Expansion Coefficient, Measured, 10^{-6}/K	Thermal Expansion Coefficient, Predicted, 10^{-6}/K	Reference No.
190.	14.2	14.1	14
200.	14.4	14.4	13B
230.	14.6	14.4	13A
260.	14.4	14.4	14
210.	14.7	14.7	14
220.	14.9	15.0	13B
230.	15.8	15.0	13A
260.	14.9	15.0	14
230.	15.8	15.2	14
240.	16.3	15.8	13B
240.	15.8	15.8	13A
240.	15.3	15.8	14
290.	15.5	15.7	14
260.	15.6	15.8	13B
290.	15.8	15.8	13A
260.	15.6	15.8	14
210.	15.8	15.0	14
273.	15.6	16.2	13B
273.	15.0	15.0	13A
260.	16.3	15.8	13B
290.	15.8	15.8	13A
260.	16.3	15.8	14
290.	16.2	15.8	14
293.	16.1	15.8	13B
293.	16.2	16.2	13B
260.	15.6	15.7	16
300.	16.2	15.8	13B
300.	16.3	16.3	13B
300.	16.2	15.8	15A
300.	16.3	16.3	15A
300.	16.4	16.3	15B
320.	16.4	16.2	13B
320.	16.6	16.2	13A

C17200: Annealed; Annealed and Aged; Cold-worked; Cold-worked and Aged

Thermal Expansion Coefficient vs. Temperature (6–300 K)

Table 14.4. Calculated Values of the Thermal Expansion Coefficient [Equation (14-4)] (6–300 K).

Test Temperature, K	Thermal Expansion Coefficient, 10^{-6}/K
5.00	0.00380
10.0	0.0317
15.0	0.101
20.0	0.251
25.0	0.517
30.0	0.915
95.0	1.44
40.0	2.07
45.0	7.15
60.0	8.84
55.0	9.31
60.0	5.07
65.0	5.80
80.0	8.84
75.0	7.15
80.0	7.76
25.0	8.32
30.0	8.84
95.0	9.31
100.	9.74
115.	10.1
110.	10.5
115.	10.8
100.	11.2
125.	11.4
130.	11.7
135.	12.0
140.	12.2
145.	12.4
150.	12.7
155.	12.9
190.	13.3
185.	13.3
170.	13.4
175.	13.6
190.	13.6
185.	14.0
190.	14.1
195.	14.3
200.	14.7
285.	14.8
200.	14.7
215.	14.9
220.	15.0
225.	15.1
200.	15.2
235.	15.4
240.	15.5
215.	15.6
250.	15.7
235.	15.4
200.	15.5
235.	15.4
200.	16.0
275.	16.1
280.	16.1
285.	16.2
290.	16.2
295.	16.2
300.	16.3

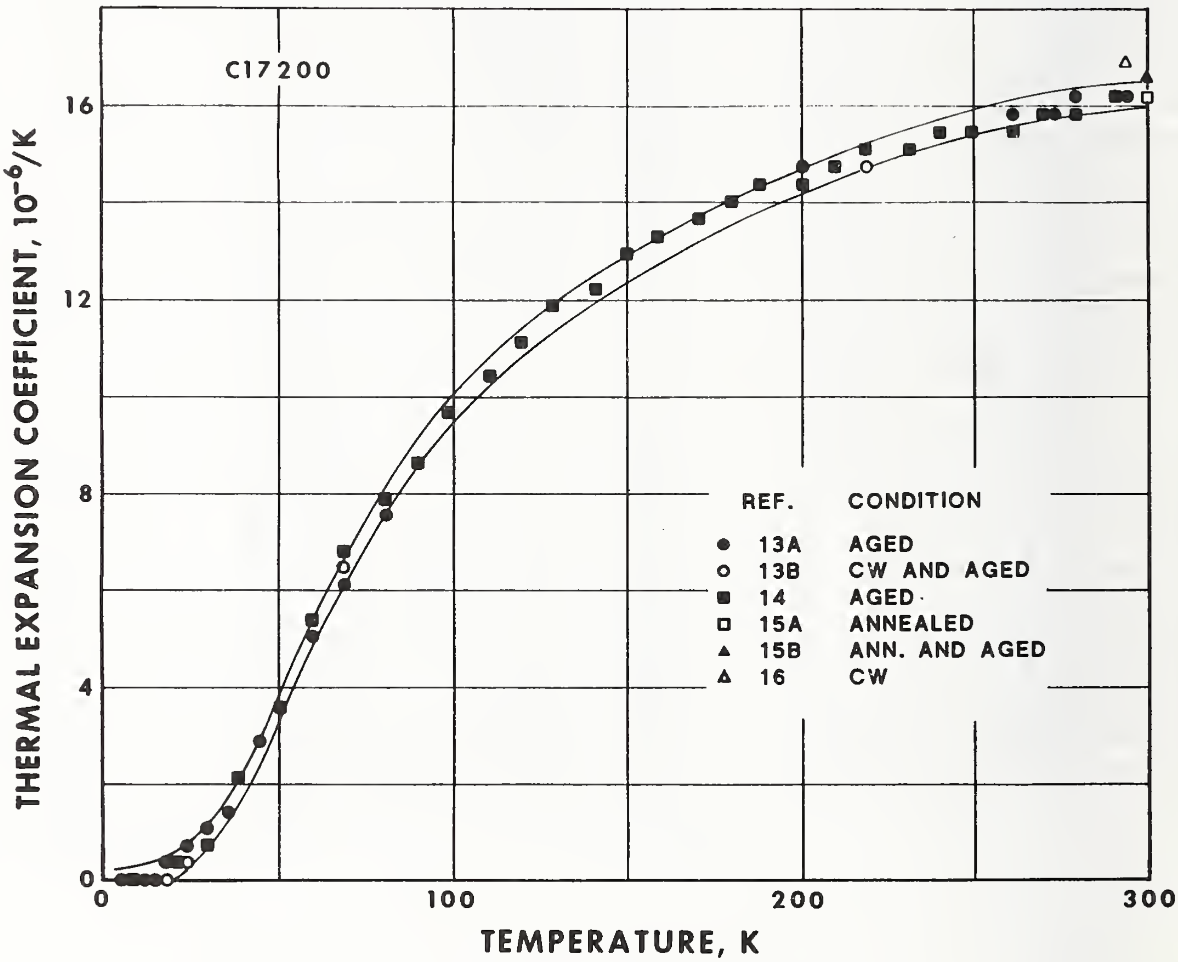

Figure 14.3. The data shown were used to compute the regression of the thermal expansion coefficient, α, upon temperature [Equation (14-4)]. For clarity, overlapping data points are omitted from the figure. Two points at 320 K used in the regression do not appear in the figure. All data are presented in Table 14.3.

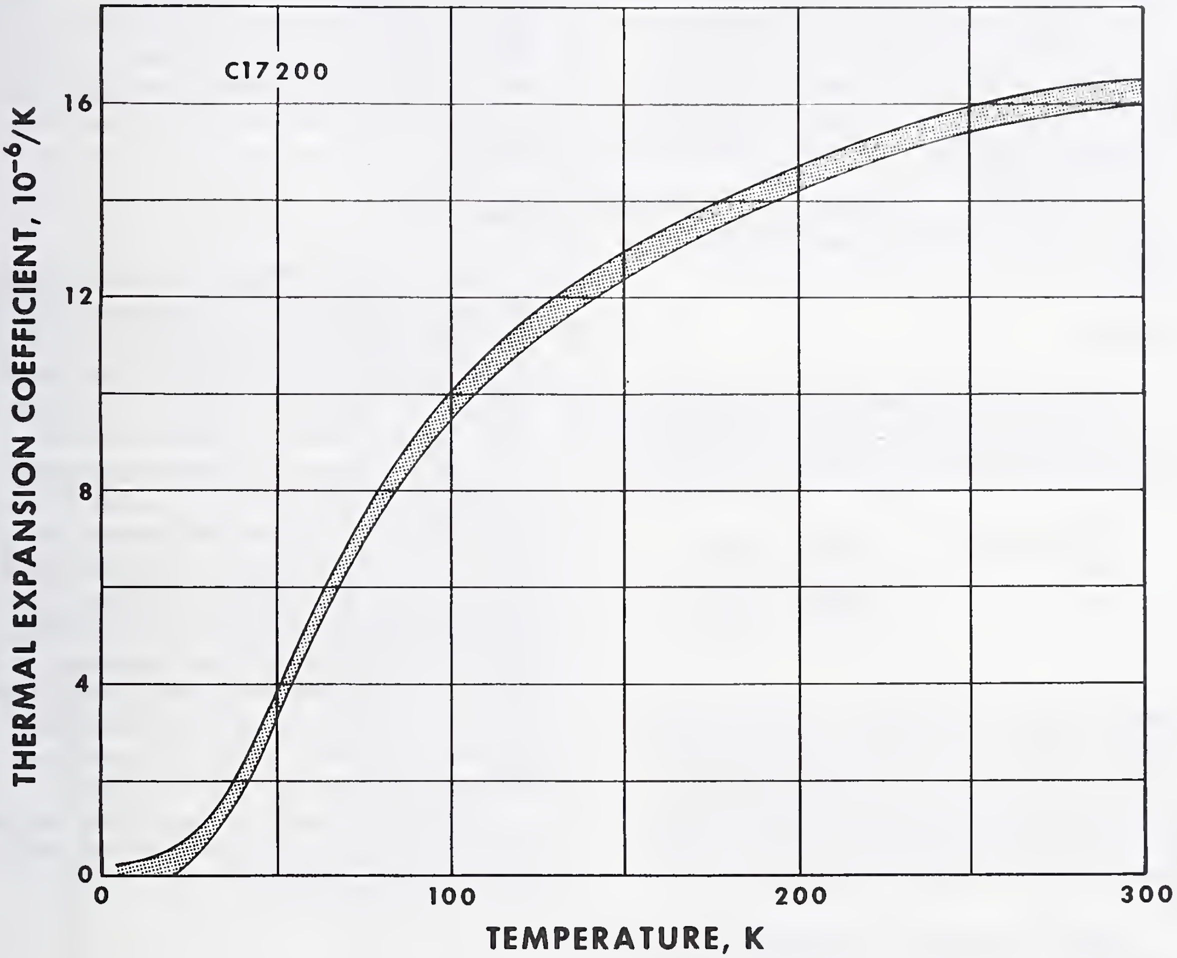

Figure 14.4. Dependence of the thermal expansion coefficient, α, upon temperature, T; 6–300 K. The scatter band represents two standard deviations about a sixth-order logarithmic regression equation based upon 97 measurements on annealed, annealed and aged, cold-worked, and cold-worked and aged C17200 beryllium copper. The regression equation Is

$$\log \alpha = -25.30 + 95.96 (\log T) - 164.5 (\log T)^2 + 147.6 (\log T)^3 - 70.83 (\log T)^4 + 17.28 (\log T)^5 - 1.689 (\log T)^6$$

where α has units of 10^{-6} K^{-1} and $6 K \leq T \leq 300 K$.

DATA SOURCES AND ANALYSIS

Measurements of the mean thermal expansion, $\Delta L/(L \cdot \Delta T)$ (where T is temperature), of C17200 beryllium copper were obtained from six sources (References 14.13, 14.14, and 14.17–14.20). A variety of material conditions were represented. A total of 142 measurements between 6 and 320 K were obtained; after outliers were omitted, 126 data points were used in the regression analysis.

Measurements of $\Delta L/(L \cdot \Delta T)$ of aged C17500 beryllium copper were obtained from Reference 14.19.

RESULTS

The polynomial regression analysis carried out on the data set indicated that a satisfactory fit could be obtained with a second-order equation

$$\frac{1}{L}\frac{\Delta L}{\Delta T}\ (10^{-6} K^{-1}) = +\ 10.66 + 0.04023T - 7.362 \times 10^{-5}T^2 \qquad (14\text{–}5)$$

where $\Delta L/(L \cdot \Delta T) = [L(293\text{ K}) - L(T)]/[L(293\text{ K}) \cdot (293\text{ K} - T)]$ for $6\text{ K} \leq T \leq 300\text{ K}$ except that at $T = 293$ K, this quantity is $(1/L)\ (dL/dT)$. The standard deviation of the fit to this equation is $0.36 \times 10^{-6}\ K^{-1}$; the standard deviations of the three constants are 0.08, 0.00134, and 0.447×10^{-5}.

Table 14.5 presents T, the measured values of $\Delta L/(L \cdot \Delta T)$, the values calculated from the regression equation, and the reference number. The available characterization of materials and measurements is given in Table 14.7 at the end of the thermal properties section. Figure 14.5 indicates the fit of the data to Equation (14-5). The scatter bands represent two standard deviations about the curve in each figure. The variance of the data was assumed to be normally distributed and constant throughout the range of the independent variable, T.

DISCUSSION

Table 14.6 and Figure 14.6 present some of the data of Figure 14.5, and other data that were excluded from the regression analysis, in a different format that shows the effect of changes in the material condition upon $\Delta L/(L \cdot \Delta T)$. Data from Reference 14.13 shows a slight decrease in $\Delta L/(L \cdot \Delta T)$ in cold-worked material after aging. Data from Reference 14.17 shows that $\Delta L/(L \cdot \Delta T)$ is slightly higher for annealed material than for material that is cold-worked. Data from Reference 14.18 on specimens that were aged at 473 K may indicate that aging at a low T results in a significant decrease in thermal expansion, since this curve lies considerably below those of References 14.13 and 14.19 which reported aging temperatures of 603 and 588 K. However, the difference could be due to other factors.

Figure 14.6 also presents a limited number of measurements from Reference 14.19 on C17500 beryllium copper.

Table 14.5. Dependence of Mean Thermal Expansion of C17200 Beryllium Copper upon Temperature (6–320 K).

Test Temperature, K	$\Delta L/(L \cdot \Delta T)$, Measured, 10^{-6}/K	$\Delta L/(L \cdot \Delta T)$, Predicted, 10^{-6}/K	Reference No.
6.00	10.7	10.9	13B
6.00	10.8	10.9	13A
8.00	10.8	11.0	13B
6.00	10.8	11.0	13A
10.0	10.8	11.0	13B
10.0	10.8	11.0	13A
10.0	10.9	11.0	14

C17200 and C17500: Annealed; Annealed and Aged Cold-worked; Cold-worked and Aged

Mean Thermal Expansion vs. Temperature (6–300 K)

Table 14.5, continued

Test Temperature, K	ΔL/(L·ΔT), Measured, 10^{-6}/K	ΔL/(L·ΔT), Predicted, 10^{-6}/K	Reference No.
12.0	11.9	11.1	13B
12.0	11.2	11.1	13A
14.0	11.9	11.8	13B
14.0	11.1	11.2	13A
16.0	13.1	11.8	13B
16.0	11.1	13.1	13A
45.0	11.2	11.8	13B
14.0	11.2	13.1	13A
25.0	11.2	11.1	13B
20.0	11.2	13.1	13A
20.0	13.1	11.8	14
25.0	11.6	11.1	17A
20.0	11.9	11.8	17B
25.0	11.1	11.6	13B
25.0	11.9	11.6	13B
27.4	12.6	13.1	19A
30.0	11.9	11.8	13B
30.0	11.2	13.8	13A
30.0	11.7	11.8	14
30.0	13.4	12.0	13B
35.0	11.9	12.0	13B
40.0	12.0	12.2	13B
40.0	12.4	12.2	13B
40.0	12.1	12.2	14
40.0	12.4	12.2	17B
40.0	12.7	12.2	17A
45.0	12.2	12.0	13B
45.0	12.0	12.3	13A
50.0	12.4	12.0	13B
60.0	12.5	12.2	13B
50.0	12.5	12.5	14
60.0	12.5	12.2	13A
50.0	12.4	12.6	13B
80.0	12.6	12.2	14
50.0	13.1	12.8	17B
60.0	13.4	12.6	17A
70.0	13.1	13.1	13B
16.0	13.2	13.1	13B
70.0	11.2	13.1	14
77.4	14.2	13.1	13A
77.4	12.4	13.1	20
80.0	13.4	13.4	13A
50.0	11.9	11.8	13B
80.0	13.4	13.1	14
80.0	13.1	11.8	17B
80.0	11.1	13.1	17A
48.6	11.2	13.6	20
60.0	13.6	13.1	13B
90.0	13.7	13.7	13A
90.0	13.7	13.7	14
100.	13.9	14.0	13B

Table 14.5, continued

Test Temperature, K	ΔL/(L·ΔT), Measured, 10^{-6}/K	ΔL/(L·ΔT), Predicted, 10^{-6}/K	Reference No.
160.	14.9	14.0	13A
100.	13.9	14.0	14
190.	14.4	14.0	17B
100.	14.6	14.0	17A
110.	14.7	14.2	14
120.	14.3	14.0	13A
120.	14.7	14.4	13A
120.	14.3	14.0	14
120.	14.9	14.4	17B
190.	15.7	14.4	17A
160.	14.9	14.6	14
140.	14.6	14.8	13A
140.	14.7	14.8	13A
140.	14.4	14.8	14
140.	15.2	14.8	17B
140.	15.7	14.8	17B
140.	14.7	14.8	20
150.	14.3	15.0	14
160.	14.9	15.2	13A
160.	16.0	15.2	13A
160.	14.9	15.2	14
160.	15.7	15.2	17A
160.	15.2	15.2	17B
170.	16.0	15.7	14
160.	15.1	15.9	13A
160.	16.0	15.9	13A
160.	15.2	15.9	14
180.	15.7	15.9	17B
160.	15.1	15.9	17B
190.	16.3	16.6	14
160.	15.2	15.7	13A
200.	14.6	15.7	20
200.	15.1	15.7	13A
200.	16.0	15.7	13A
200.	15.1	15.7	14
200.	16.8	15.7	17A
200.	16.3	15.7	17B
210.	16.0	15.9	14
210.	15.6	15.9	13A
220.	16.6	15.9	13A
220.	15.6	15.9	14
220.	16.0	15.9	17B
210.	15.6	15.9	17B
230.	15.7	16.0	14
240.	15.7	15.9	13A
240.	16.6	16.0	13A
240.	15.7	16.0	14
240.	15.7	15.9	17B
240.	16.8	16.0	17A
250.	16.0	16.1	14
255.	15.4	16.1	20

C17200 and C17500: Annealed; Annealed and Aged Cold-worked; Cold-worked and Aged

Mean Thermal Expansion vs. Temperature (6–300 K)

Table 14.5, continued

Test Temperature, K	ΔL/(L·ΔT), Measured, 10^{-6}/K	ΔL/(L·ΔT), Predicted, 10^{-6}/K	Reference No.
260.	15.9	16.1	13B
260.	16.0	16.1	13A
260.	16.0	16.1	14
260.	16.0	16.1	17B
260.	17.3	16.1	17A
270.	16.0	16.1	14
273.	16.0	16.1	17A
273.	16.0	16.1	13A
273.	16.0	16.1	13A
280.	16.0	16.1	13B
260.	15.9	16.1	13A
270.	16.0	16.1	14
290.	16.0	16.1	14
300.	16.1	16.0	13B
300.	16.3	16.0	13A
320.	16.2	15.9	13B
320.	16.5	15.9	13A

Table 14.6. Measurements of the Mean Thermal Expansion of C17200 and C17500 Beryllium Copper (6–300 K).

Test Temperature, K	ΔL/(L·ΔT), Measured, 10^{-6}/K	Reference No.
0.	9.69	18
8.00	10.7	13B
6.00	10.8	13A
8.00	10.6	13B
6.00	11.9	13A
10.0	10.7	13B
10.0	11.9	13A
12.0	10.6	13B
12.0	11.0	13A
14.0	11.0	13B
14.0	14.4	13A
16.0	11.9	13A
16.0	11.9	13A
18.0	11.2	13B
14.0	11.2	13A
25.0	11.2	13B
20.0	11.9	13A
25.0	10.6	17B
25.0	11.9	17B
25.0	10.7	13B
20.0	11.9	13A
25.0	10.6	18
20.0	13.8	13A
27.4	10.6	13B
30.0	13.8	13A
10.0	11.2	13B
35.0	11.9	13A
30.0	11.9	13A
40.0	12.4	13B
40.0	12.1	13B
40.0	12.4	17B
40.0	10.7	17B
45.0	12.4	13A
16.0	12.1	13B
60.0	12.4	13A
60.0	10.6	13B
60.0	11.9	18
60.0	10.6	13B
60.0	12.4	13A
60.0	13.1	17B
60.0	11.9	17B
10.0	13.1	13B
14.0	13.8	13A
16.0	12.3	18
77.4	14.4	13A
77.4	10.7	13B
60.0	11.9	13A
60.0	13.8	13A
80.0	13.9	17B
80.0	14.1	17A

C17200 and C17500: Annealed; Annealed and Aged Cold-worked; Cold-worked and Aged

Mean Thermal Expansion vs. Temperature (6–300 K)

Table 14.6, continued

Test Temperature, K	ΔL/(L·ΔT), Measured, 10^{-6}/K	Reference No.
90.0	13.6	13B
90.0	13.7	13A
100.	13.6	13B
100.	14.9	13A
100.	14.4	17B
100.	14.9	17B
100.	12.9	18
125.	14.3	13A
120.	14.4	13B
120.	14.8	17B
120.	16.0	17A
125.	12.9	18
140.	14.6	13B
180.	14.7	13A
140.	15.6	17B
180.	15.4	17B
1[illegible]0.	12.9	18
160.	14.9	13A
180.	15.6	13B
180.	15.4	17B
180.	15.6	17A
125.	12.9	18
180.	15.1	13B
180.	16.0	13A
180.	15.1	17B
180.	16.0	17B
1[illegible].	15.6	13B
1[illegible].	15.4	13A
200.	15.1	13A
200.	16.0	13A
260.	15.6	17B
200.	16.0	17A
260.	12.9	18
220.	15.5	13A
260.	15.6	13A
220.	16.0	17B
260.	15.6	17A
200.	16.0	13B
240.	15.6	13A
200.	16.0	17B
240.	15.6	17A
260.	9.77	18
260.	15.6	13A
260.	16.0	13B
260.	15.1	17A
260.	14.3	17B
273.	15.0	17B
273.	14.9	17A
273.	15.9	13B
273.	16.0	13A
280.	16.0	13B

Table 14.6, continued

Test Temperature, K	$\Delta L/(L\cdot\Delta T)$, Measured, 10^{-6}/K	Reference No.
280.	16.0	13A
280.	16.9	17B
280.	17.7	17A
300.	16.9	13B
300.	16.3	13A
300.	16.2	13B
320.	16.5	13A

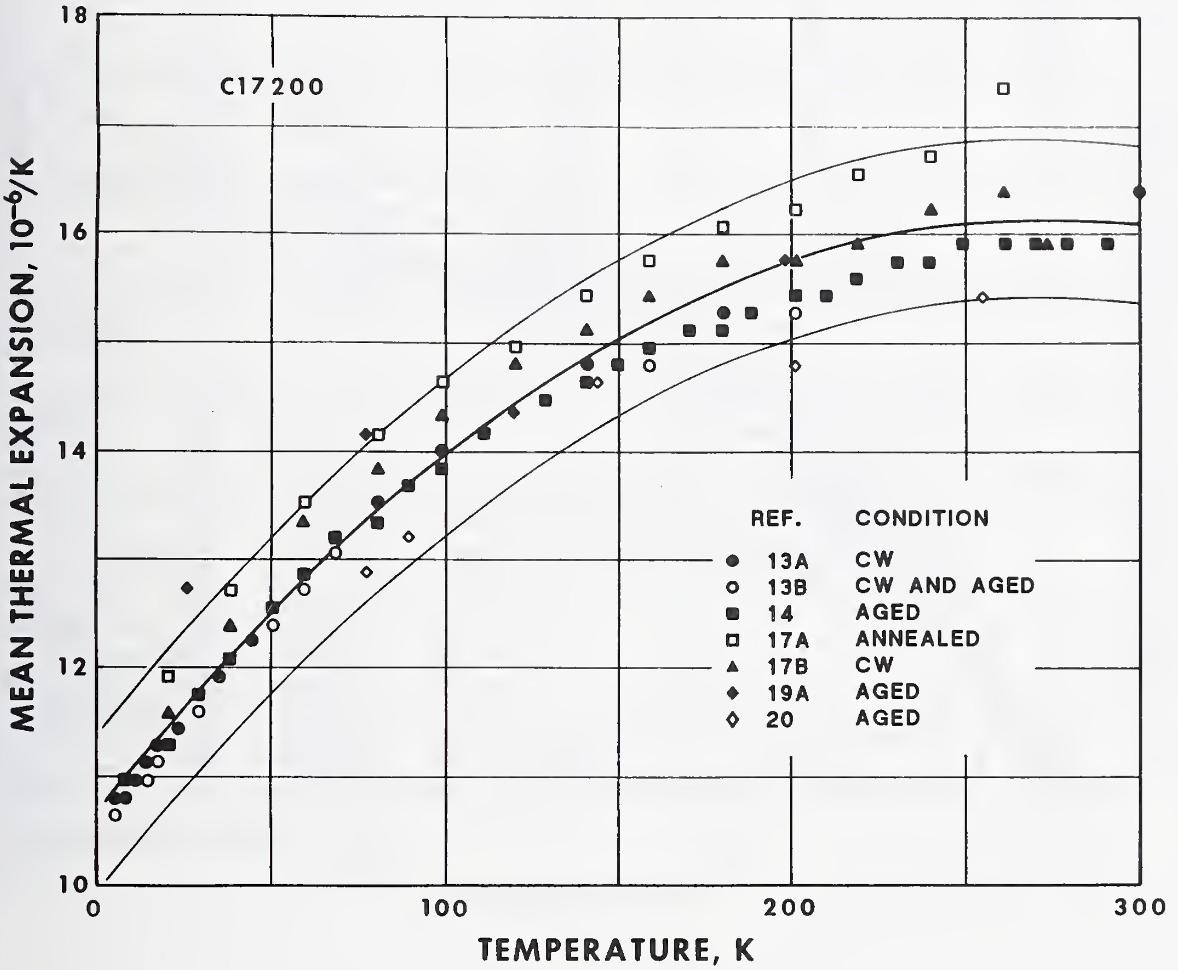

Figure 14.5. The data shown for C17200 beryllium copper were used to compute the regression of the mean thermal expansion upon temperature [Equation (14-5)]. For clarity, overlapping data points are omitted from the figure. Two points from Reference 14.13 at 320 K do not appear in the figure. All data are presented in Table 14.5.

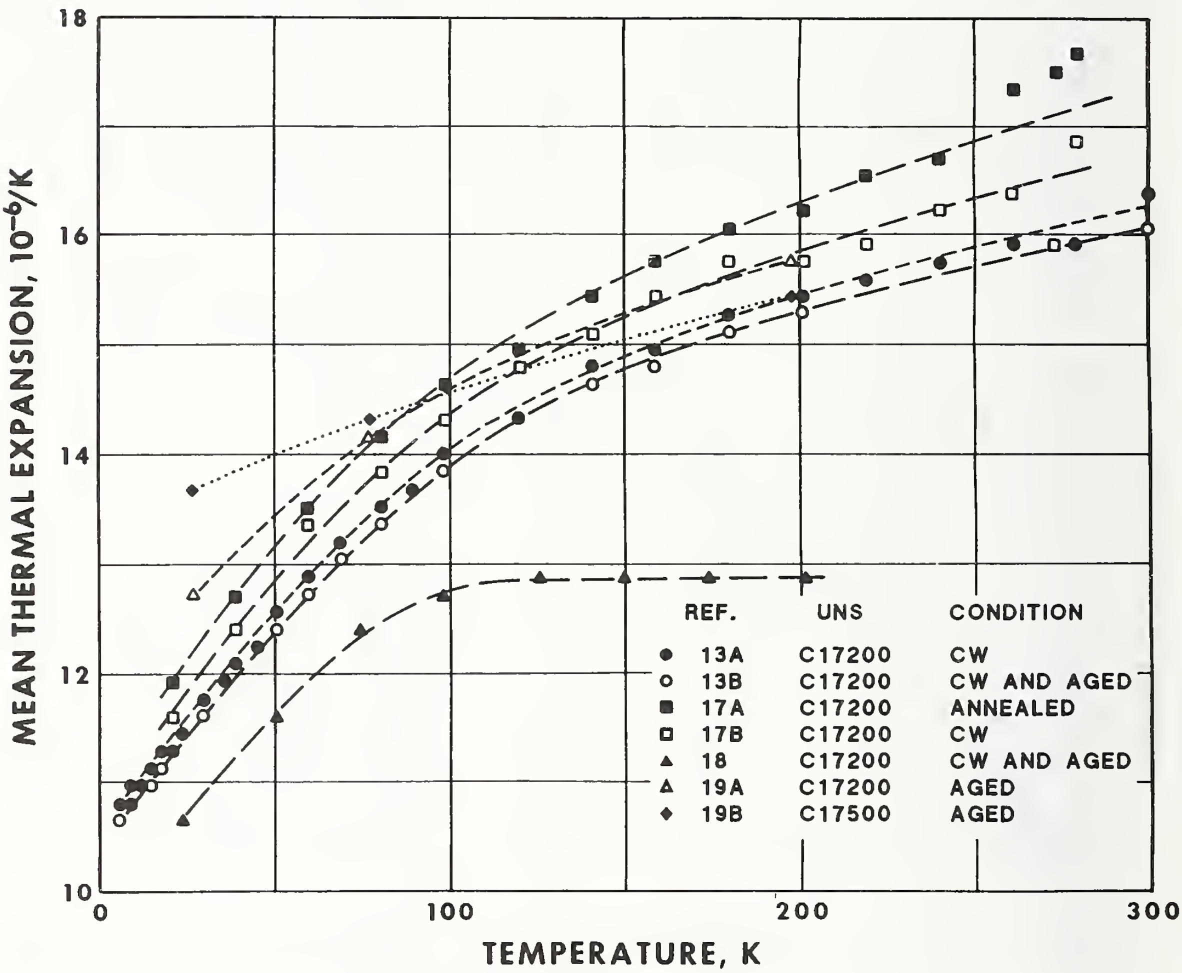

Figure 14.6. The data from Figure 14.5, plus some additional thermal expansion data, are presented to show the effects of aging, aging temperature, and cold work upon mean thermal expansion of C17200 beryllium copper. Some measurements on C17500 beryllium copper are also presented. All data are presented in Table 14.6. The aging temperature reported in Reference 14.18 is considerably below those reported in References 14.13 and 14.19. It is not known if this is the reason for the discrepancy in these results.

Table 14.7. Characterization of Materials and Measurements.

Reference No.	1A	1B	1B	5
Specification	C17510	C17510	C17510	C17200
Composition (wt%)				
Cu	Bal	Bal	Bal	—
Cu + Ag	—	—	—	—
Be	0.39	0.39	0.34	2.0
Ni	1.92	1.92	1.92	—
Co	0.01	0.01	0.02	—
Ni + Co	1.93	1.93	1.94	—
Ni + Fe + Co	1.95	1.95	1.96	—
Al	0.01	0.01	0.01	—
Fe	0.02	0.02	0.02	—
Si	< 0.01	< 0.01	0.02	—
Others (Only ≥ 0.001 wt%)	Cr: 0.007; Pb: < 0.003; Sn: 0.005; Zn: < 0.01	Cr: 0.007; Pb: < 0.003; Sn: 0.005; Zn: < 0.01	Cr: < 0.005; Pb: 0.003; Sn: < 0.005; Zn: < 0.01	—
Material Condition	Aged	Heat-treated	Heat-treated	Aged, 573 K, 2 h
RRR	—	—	—	—
Grain Size	—	—	—	—
Hardness	R_B 88.5	—	R_B 101	Rockwell 41 (a)
Product Form	Plate	Plate	Plate, 3.18-cm-thick	—
Specimen Type	—	—	—	—
Width or Dia.	—	—	—	—
Thickness	—	—	—	—
Gage Length	—	—	—	—
No. of Specimens	—	—	—	—
Test Temperature	83–345 K	120–299 K	99–325 K	2–90 K

(a) Hardness scale not specified.

Table 14.7, continued

Reference No.	6A	6B	7A	7B
Specification	C17200	C17200	C17200	C17200
Composition (wt%)				
Cu	—	—	—	—
Cu + Ag	—	—	—	—
Be	1.80	1.83	—	—
Ni	—	0.01–0.1	—	—
Co	0.1–1.0	—	—	—
Ni + Co	—	—	—	—
Ni + Fe + Co	—	—	—	—
Al	(a)	(d)	—	—
Fe	—	—	—	—
Si	—	—	—	—
Others (Only ≥ 0.001 wt%)	All others < 0.01	—	—	—
Material Condition	Cold-rolled (b)	Cold-rolled (b)	Annealed	Cold-rolled, 21% or 37%
RRR	—	—	—	—
Grain Size	—	—	—	—
Hardness	Knoop 243–332	Knoop 513–541	—	—
Product Form	Strip, 0.005-cm-thick, 5.08-cm-wide	Strip, 0.005-cm-thick, 5.08-cm-wide	Strip	Strip
Specimen Type	Flat (c)	Flat (c)	—	—
Width or Dia.	1.58 cm	1.78 cm	—	—
Thickness	1.08 cm	1.75 cm	—	—
Gage Length	25.4 cm	25.4 cm	—	—
No. of Specimens	—	—	—	—
Test Temperature	128–300 K	125–300 K	293 K	293 K

(a) Al + Fe + Si: 0.01–0.1 wt%.
(b) Percent cold work not specified.
(c) Composite flat specimens were fabricated by stacking together and compressing pieces of strip material, then fastening together with phosphor-bronze screws.
(d) Al + Co + Fe + Si: 0.01–1.0 wt%.

C17000–C17510: Annealed; Annealed and Aged; Cold-worked; Cold-worked and Aged | *Thermal Properties (All)*

7C	7D	8A	8A	9A
C17200	C17200	C17200	C17200	C17000
— — — — — — — — — — —		97.7 — 1.90 (b) — — — — — — —	97.7 — 1.90 (b) — — — — — — —	— — 1.60–1.80 — 0.25–0.35 — — — — — —
Annealed and aged (a)	Cold-worked, 21% or 37%, then aged (a)	Before aging	Aged (a)	As cast
—	—	—	—	—
—	—	—	—	—
—	—	—	—	—
Strip	Strip	—	—	—
— — — —	— — — —	— — — —	— — — —	— — — —
—	—	—	—	—
293 K	293 K	293 K	293 K	293 K

(a) Aging conditions not specified.
(b) Ni + Co + Fe: 0.40 wt%.

Table 14.7, continued

Reference No.	9B	9C	9D	10
Specification	C17200	C17500	C17510	C17510
Composition (wt%)				
Cu	—	—	—	—
Cu + Ag	—	—	—	—
Be	1.80–2.15	0.45–0.65	0.45–0.65	0.39
Ni	—	—	—	1.92
Co	0.25–0.35	2.40–2.60	2.40–2.60	—
Ni + Co	—	—	—	—
Ni + Fe + Co	—	—	—	—
Al	—	—	—	—
Fe	—	—	—	—
Si	—	—	—	—
Others (Only ≥ 0.001 wt%)	—	—	—	—
Material Condition	As cast	As cast	As cast	—
RRR	—	—	—	—
Grain Size	—	—	—	—
Hardness	—	—	—	—
Product Form	—	—	—	—
Specimen Type	—	—	—	Round
Width or Dia.	—	—	—	0.317 cm
Thickness	—	—	—	—
Gage Length	—	—	—	2.54 cm
No. of Specimens	—	—	—	—
Test Temperature	293 K	293 K	293 K	76–293 K

C17000–C17510: Annealed; Annealed and Aged; Cold-worked; Cold-worked and Aged

Thermal Properties (All)

11A	11B	11C	12	13A
C17000	C17200	C17500	C17510	C17200
— — 1.60–1.85 — 0.20–0.65 — — — — — —	— — 2.00–2.25 — 0.35–0.65 — — — — — —	— — 0.55–0.75 — 2.35–2.70 — — — — — —	97.8 — 0.4 1.8 — — — — — — —	97.95 — 1.8 — 0.25 — — — — — —
As cast	As cast	As cast	Cold-rolled, 37%, then aged (a)	Cold-worked, ½ hard
—	—	—	—	—
—	—	—	—	—
—	—	—	—	—
—	—	—	Strip	—
— — — —	— — — —	— — — —	Flat — — —	Cylinder 3.8 cm — 10 cm
—	—	—	—	—
293 K	293 K	293 K	294 K	6–320 K

(a) Aging conditions not specified.

Table 14.7, continued

Reference No.	13B	14	15A	15B
Specification	C17200	C17200	C17200	C17200
Composition (wt%)				
Cu	97.95	98.2	97.78	97.78
Cu + Ag	—	—	—	—
Be	1.8	1.8	2.14	2.14
Ni	—	—	—	—
Co	0.25	—	—	—
Ni + Co	—	—	—	—
Ni + Fe + Co	—	—	—	—
Al	—	—	—	—
Fe	—	—	0.06	0.06
Si	—	—	0.02	0.02
Others (Only ≥ 0.001 wt%)	—	—	—	—
Material Condition	Cold-worked, ½ hard, then aged, 603 K, 4 h	Aged, 600 K, 4 h	Annealed, 1073 K, 0.5 h	Annealed, 1073 K, 0.5 h, aged, 573 K, 2.5 h
RRR	—	—	—	—
Grain Size	—	—	—	—
Hardness	—	—	—	—
Product Form	—	—	—	—
Specimen Type	Cylinder	Cylindrical tube	Round	Round
Width or Dia.	3.8 cm	2.3 cm	0.6 cm	0.6 cm
Thickness	—	—	—	—
Gage Length	10 cm	7.8 cm	30 cm	30 cm
No. of Specimens	—	—	—	—
Test Temperature	6–320 K	10–290 K	293 K	293 K

16	17A	17B	18	19A
C17200	C17200	C17200	C17200	C17200
— — — — — — — — — — —	97.7 — 1.8 — 0.2 — — 0.1 0.1 0.1 —	97.7 — 1.8 — 0.2 — — 0.1 0.1 0.1 —	— — — — — — — — — — —	98.10 — 1.9 — — — — — — — —
Cold-worked (a)	Annealed	Cold-worked, hard	Cold-worked, ½ hard, aged, 473 K, 2 h	Aged, 588 K, 3 h
—	—	—	—	—
—	—	—	—	—
—	R_B 55	R_B 95	—	R_C 22 (b)
—	Bar	Bar	—	—
Wire 0.016 cm — 10 cm	Square bar 0.64 × 0.64 cm — 20 cm	Square bar 0.64 × 0.64 cm — 20 cm	Round 0.64 cm — 7.62 cm	Cylindrical tube (c) 0.82 cm (O.D.) — 13 cm
—	—	—	—	—
293 K	20, 293 K	20, 293 K	0–300 K	27, 77, 197 K

(a) Method not specified.
(b) Average of eight measurements of unnotched tensile specimens.
(c) Inside hole: 0.32 cm in diameter, concentric with outside diameter and 3.2 cm deep from one end.

Table 14.7, continued

Reference No.	19B	20
Specification	C17500	C17200
Composition (wt%)		
Cu	97.40	97.80
Cu + Ag	—	—
Be	0.5	2.0
Ni	—	—
Co	2.0	0.2
Ni + Co	—	—
Ni + Fe + Co	—	—
Al	—	—
Fe	0.1	—
Si	—	—
Others (Only ≥ 0.001 wt%)	—	—
Material Condition	Aged, 727 K, 8 h, AC	Aged (c)
RRR	—	—
Grain Size	—	—
Hardness	R_C 39 (a)	—
Product Form	—	Bar
Specimen Type	Cylindrical tube (b)	Round
Width or Dia.	0.82 cm (O.D.)	0.36 cm
Thickness	—	—
Gage Length	13 cm	5.0 cm
No. of Specimens	—	—
Test Temperature	27, 77, 197 K	77–294 K

(a) Average of six measurements of unnotched tensile specimens.
(b) Inside hole: 0.32 cm in diameter, concentric with outside diameter and 3.2 cm deep from one end.
(c) Aging conditions not specified.

REFERENCES

1. Bushnell, C., Princeton Plasma Physics Laboratory, Princeton, NJ, personal communication (1990).

2. "Standards Handbook, Part 2--Alloy Data, Wrought Copper and Copper Alloy Mill Products," Eighth Edition, Copper Development Association Inc., Greenwich, CN (1985).

3. Touloukian, Y. S., and Buyco, E. H., "Thermophysical Properties of Matter, Vol. 4, Specific Heat, Metallic Elements and Alloys," IFI/Plenum, New York, 16–20 (1970).

4. Corruccini, R. J., "Properties of Materials at Low Temperatures (Part I)," Chemical Engineering Progress 53, 262–267 (1957).

5. Berman, R., Foster, E. L., and Rosenberg, H. M., "The Thermal Conductivity of Some Technical Materials at Low Temperatures," British Journal of Applied Physics 6, 181–182 (1955).

6. Watson, T. W., and Flynn, D. R., "Thermal Conductivity and Electrical Resistivity of Beryllium Copper Foil," Transactions of the Metallurgical Society of AIME 242, 876–880 (1968).

7. Bulow, C. L., "High-Strength Copper-base Alloys," Electro-Technology 71, 113–116 (1963).

8. Weaver, V. P., "Wrought Copper Alloys," in Copper, The Science and Technology of the Metal, Its Alloys and Compounds, Ed. A. Butts, Reinhold Publishing Corporation, New York, 535–572 (1954).

9. Wikle, K. G., "Semicontinuous Casting of Beryllium Copper," Metal Progress 73, 85–89 (1958).

10. Rule, D. L., "Thermal Conductivity of Beryllium-Copper Alloy C17510 from 77 to 300 K," personal communications (1991).

11. Hönig, A., and Koeppen, H., "Über die Vielseitige Verwendung von Kupfer-Beryllium (II)," Metallwissenschaft und Technik 29, 1121–1125 (1975).

12. Guha, A., "High Performance Mill Hardened Beryllium Copper C17510 Strip for Electrical and Electronic Applications," in Proceedings of the Sixteenth Annual Connectors and Interconnection Technology Symposium, Electronic Connector Study Group, Inc., Fort Washington, PA, 131–140 (1983).

13. Holtz, R. L., and Swenson, C. A., "Thermal Expansivity Measurements Below 300 K on a Copper-Beryllium Alloy," Journal of Applied Physics 54, 2844–2846 (1983).

14. Radcliffe, W. J., Gallop, J. C., and Dominique, J., "A Microwave Method for Thermal Expansion Measurement," Journal of Physics E: Scientific Instruments 16, 1200–1202 (1983).

15. Hidnert, P., "Thermal Expansion of Copper-Beryllium Alloys," Journal of Research of the National Bureau of Standards 16, 529–548 (1936).

16. Imai, H., and Bates, W. J., "Measurement of the Linear Thermal Expansion Coefficient of Thin Specimens," Journal of Physics E: Scientific Instruments 14, 883–888 (1981).

REFERENCES

17. Arp, V., Wilson, J. H., Winrich, L., and Sikora, P., "Thermal Expansion of Some Engineering Materials from 20 to 293 °K," Cryogenics 2, 230–235 (1962).

18. Beenakker, J. J. M., and Swenson, C. A., "Total Thermal Contractions of Some Technical Metals to 4.2 °K," Review of Scientific Instruments 26, 1204–1205 (1955).

19. Belton, J. H., Godby, L. L., and Taft, B. L., "Materials for Use at Liquid Hydrogen Temperature," American Society for Testing Materials, Special Technical Publication 287, 108–121 (1961).

20. Williams, L. R., Young, J. D., and Schmidt, E. H., "Thermal Expansion Properties of Aerospace Materials, Technical Support Package for NASA Technical Brief 69-10055," National Technical Information Service, Springfield, VA, PB-184749, 174 pp (1969).

DATA SOURCES AND ANALYSIS

Measurements of the electrical resistivity of annealed C17000 beryllium copper at 295 K as a function of aging time were obtained from Reference 15.1. The aging temperature was 623 K and aging times ranged from 0.001 to 17 h. Product form was not specified.

RESULTS

All measurements are reported in Table 15.1, which presents the electrical resistivity (ρ), the aging temperature and time, and the reference number. The available characterization of materials and measurements is given in Table 15.17 at the end of the electromagnetic properties section. Figure 15.1 presents ρ as a function of aging time.

DISCUSSION

The decrease in ρ with aging time is due to removal of beryllium and other elements from solid solution in copper by precipitation. See also the discussion of electrical resistivity vs. impurity content [Ag] for C10100–C10700 copper (Section 8).

Table 15.1. Electrical Resistivity Dependence of Annealed C17000 Beryllium Copper on Aging Time (295 K).

Electrical Resistivity, nΩm	Aging Temperature, K	Aging Time, h	Reference No.
71.6	0	0	1
69.5	623	0.000833	1
69.3	623	0.001200	1
69.5	623	0.001700	1
68.1	623	0.003330	1
66.6	623	0.006670	1
69.3	623	0.013100	1
69.5	623	0.020000	1
64.5	623	0.033100	1
60.2	623	0.066900	1
57.3	623	0.033100	1
58.0	623	0.083100	1
54.4	623	0.100000	1
47.3	623	0.130000	1
48.8	623	0.170000	1
30.8	623	0.250000	1
27.9	623	0.333000	1
25.1	623	0.670000	1
24.7	623	1.080000	1
22.2	623	3.300000	1
18.6	623	17.000000	1

Aging Temperature, 0 K = not aged.

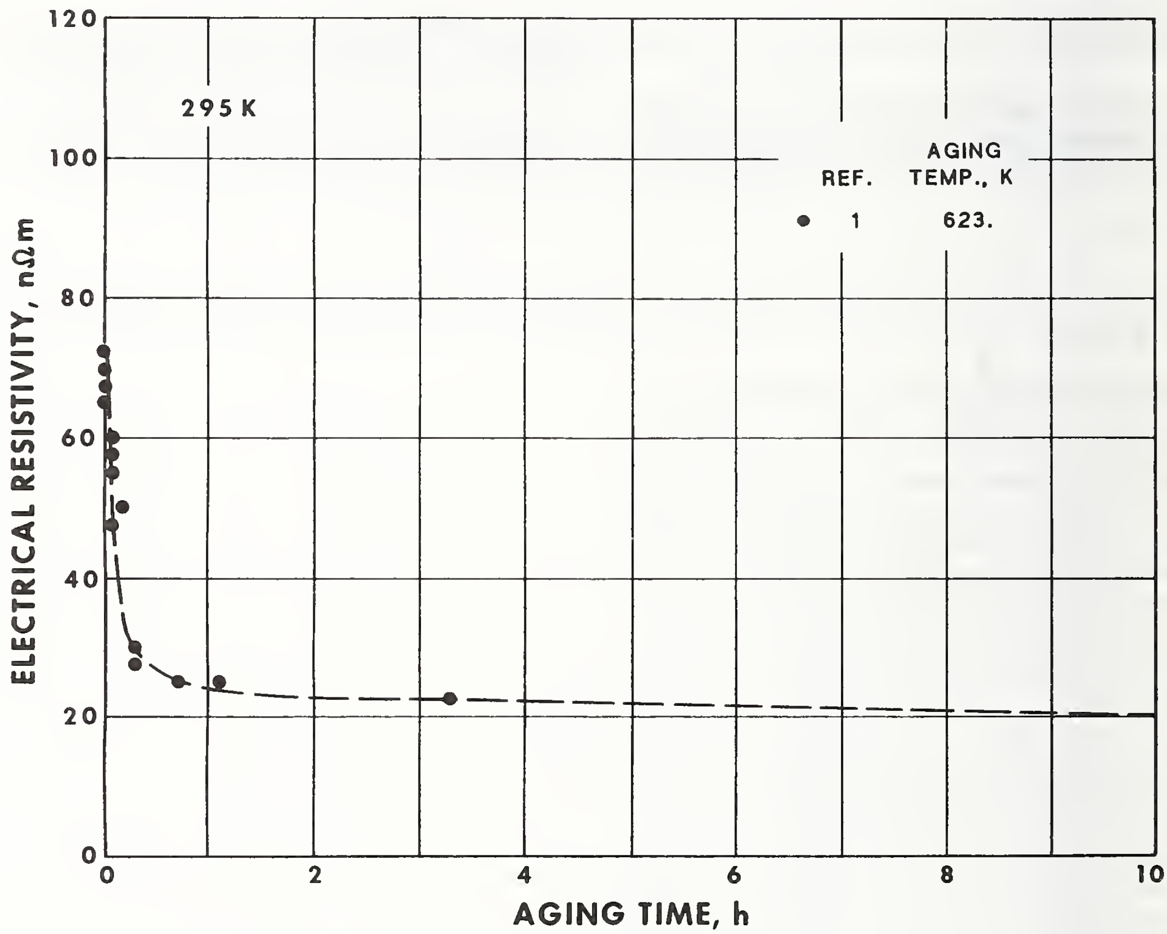

Figure 15.1. Electrical resistivity measurements at 295 K on annealed C17000 beryllium copper are shown as a function of aging time. For clarity, overlapping data points are omitted from the figure. One measurement at an aging time greater than 10 h is also not shown. All data are presented in Table 15.1. Product form was not specified.

C17000: Cold-worked

Electrical Resistivity vs. Cold Work (295 K)

DATA SOURCES AND ANALYSIS

Measurements of the electrical resistivity of C17000 beryllium copper at 295 K as a function of cold work were obtained from References 15.2 and 15.3. Cold work, *CW*, ranged from 0 to 84% (reduction in area). Product was in bar form.

RESULTS

All measurements are reported in Table 15.2, which presents the electrical resistivity (ρ), *CW* (reduction in area), and the reference number. The available characterization of materials and measurements is given in Table 15.17 at the end of the electromagnetic properties section. Figure 15.2 presents ρ as a function of *CW*.

DISCUSSION

The resistivity is essentially unchanged by *CW*. See also Figures 15.8 and 15.12 where similar results are shown.

Table 15.2. Electrical Resistivity Dependence of C17000 Beryllium Copper on Cold Work (295 K).

Electrical Resistivity, nΩm	Cold Work, %	Reference No.
51.60	75	2
42.70	0	2
81.30	0	3
80.96	37	3
80.71	60	3
80.58	84	3

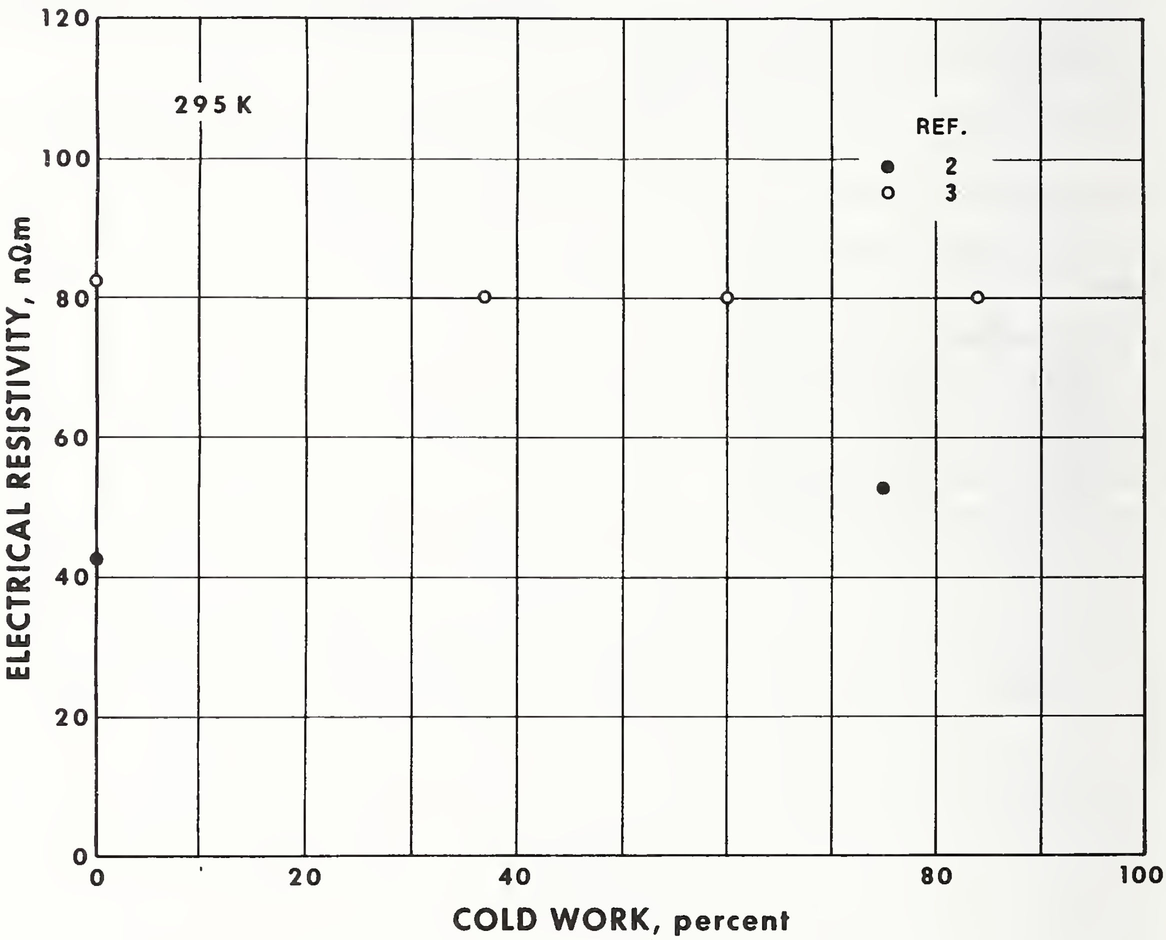

Figure 15.2. Electrical resistivity measurements at 295 K on C17000 beryllium copper are shown as a function of cold work. Product was in bar form.

DATA SOURCES AND ANALYSIS

Measurements of the electrical resistivity of annealed and cold-worked C17200 beryllium copper at 295 K as a function of aging temperature were obtained from three sources (References 15.4, 15.5, and 15.6). Aging temperatures ranged from 373 to 753 K; aging times from 0.5 to 15 h. Cold work, *CW*, ranged from 0 to 50% (reduction in thickness or area). Products were in wire, strip, and bar form.

Measurements of the electrical resistivity, ρ, of annealed C17200 beryllium copper at 295 K as a function of aging time were obtained from four sources (References 15.4, 15.7, 15.8, and 15.9). Aging temperatures ranged up to 573 K; aging times from 0 to 438 h. Products were in wire, strip, and bar form. Measurements at several aging temperatures are reported in Reference 15.8; only data at 573 K are presented here. Reference 15.10 reports similar data in relative form which were not included in this analysis because ρ was not given. Measurements from Reference 15.9 of ρ at aging temperatures were corrected to room-temperature ρ with the temperature coefficient of ρ of 0.009 nΩm/K given in Reference 15.11.

Measurements of ρ of cold-worked C17200 beryllium copper at 295 K as a function of aging time were obtained from seven sources (References 15.4–15.8, 15.12, and 15.13). Aging temperatures ranged from 569 to 644 K; aging times from 0.09 to 100 h. *CW* ranged from 11 to 75% (reduction in thickness or area). Products were in wire, strip, and bar form.

RESULTS

All measurements are reported in Tables 15.3, 15.4, and 15.5 which present ρ, *CW* (reduction in thickness or area), aging temperature and time, and the reference number. The available characterization of materials and measurements is given in Table 15.17 at the end of the electromagnetic properties section. Figure 15.3 presents ρ as a function of aging temperature, and Figures 15.4 and 15.5 present ρ as a function of aging time, for annealed and cold-worked material, respectively. As explained in the figure captions, some of the data are omitted from those figures for clarity.

DISCUSSION

In agreement with Figures 15.2, 15.8, and 15.12, there is little difference in ρ in Figure 15.3 for annealed and 21% cold-worked material (Reference 15.4).

As explained earlier, the decrease in ρ with aging is due to the removal of solute elements from the copper matrix by precipitation. If the aging temperature is below about 500 K, as shown in Figures 15.3 and 15.4 for data from References 15.4 and 15.9, not much precipitation occurs and ρ remains approximately constant.

Data from Reference 15.8 presented in Figure 15.5 and Table 15.5 show that at aging time equal to 0, ρ is somewhat higher for the largest amount of *CW*. However, after aging begins, the curves shown in Figure 15.5 cross over and the effect is reversed because *CW* facilitates precipitation.

Table 15.3. Electrical Resistivity Dependence of Annealed and Cold-worked C17200 Beryllium Copper on Aging Temperature (295 K).

Electrical Resistivity, nΩm	Cold Work, %	Aging Temperature, K	Aging Time, h	Reference No.
81.3	0	588	3.0	4
85.4	17	588	3.0	4
82.1	34	588	1.0	4
101.4	0	298	1.0	4
102.0	0	383	1.0	4
114.2	0	473	1.0	4
108.5	0	513	1.0	4
68.0	0	588	1.0	4
71.9	0	508	1.0	4
70.4	0	633	1.0	4
55.6	0	703	1.0	4
52.6	0	753	1.0	4
104.5	21	293	1.0	4
108.5	21	383	1.0	4
104.5	21	438	1.0	4
108.5	21	588	1.0	4
87.7	21	588	1.0	4
72.5	21	508	1.0	4
81.3	21	588	1.0	4
52.6	21	753	1.0	4
78.7	44	588	2.0	6
68.0	35	588	2.0	6
71.9	33	588	2.0	6
66.2	50	588	0.5	6
87.7	50	588	1.0	6
69.0	50	588	2.0	6
55.6	50	644	1.0	6
52.6	50	644	3.0	6
71.9	50	588	0.5	6
68.0	50	633	1.0	6
63.7	50	633	2.0	6
68.0	50	633	1.0	6
57.8	50	633	1.0	6
68.9	50	633	15.0	6
53.8	50	588	15.0	6
87.0	50	588	0.5	6
82.0	50	588	1.0	6
75.2	50	588	2.0	6
70.4	50	588	4.0	6
66.2	50	588	7.0	6
63.7	50	588	10.0	6
61.7	50	588	15.0	6

Table 15.4. Electrical Resistivity Dependence of Annealed C17200 Beryllium Copper on Aging Time (295 K).

Electrical Resistivity, nΩm	Cold Work, %	Aging Temperature, K	Aging Time, h	Reference No.
104.5	0	633	0.066	8
104.2	0	633	0.270	4
57.0	0	633	0.170	9
88.5	0	633	0.800	4
76.4	0	633	0.640	8
72.5	0	633	1.000	4
76.4	0	633	1.400	7
68.8	0	633	8.900	4
57.8	0	633	6.600	9
76.1	0	0	0.000	4
76.4	0	569	0.083	7
75.0	0	569	0.500	4
57.8	0	569	1.000	7
81.5	0	0	0.000	4
76.4	0	573	1.000	9
68.0	0	573	0.000	4
57.0	0	573	1.000	8
68.8	0	573	18.000	9
57.8	0	573	27.000	8
68.0	0	573	41.000	9
57.0	0	573	61.000	9
53.5	0	573	86.000	4
52.0	0	573	100.000	8
68.8	0	448	0.008	4
57.0	0	448	0.010	9
97.3	0	448	0.017	4
98.3	0	448	0.083	8
99.8	0	448	0.067	9
102.0	0	448	0.170	8
104.3	0	448	6.680	9
104.5	0	496	1.500	8
104.7	0	448	2.640	9
104.5	0	496	4.200	8
104.4	0	448	6.600	9
101.8	0	448	8.006	8
104.2	0	448	10.000	9
103.7	0	496	26.400	8
103.8	0	448	78.700	9
101.8	0	496	100.000	8
103.0	0	448	132.000	9
98.1	0	496	0.006	8
104.4	0	496	0.010	9
101.0	0	496	0.017	8
101.4	0	446	0.086	9
101.6	0	496	0.086	8
101.4	0	496	0.150	9
101.5	0	496	0.886	8
103.9	0	448	0.883	9
100.4	0	496	2.490	9
100.4	0	496	4.180	9

Table 15.4, continued

Electrical Resistivity, nΩm	Cold Work, %	Aging Temperature, K	Aging Time, h	Reference No.
100.0	0	496	5.300	9
99.9	0	496	7.400	9
99.6	0	496	10.000	9
69.9	0	496	13.300	9
98.1	0	496	16.700	9
76.4	0	496	83.300	9
95.2	0	573	0.008	9
95.1	0	573	0.017	9
95.2	0	573	0.030	9
94.7	0	573	0.042	6
94.0	0	573	0.100	9
92.7	0	573	0.170	9
88.7	0	573	0.330	9
83.7	0	573	0.500	9

Aging Temperature, 0 K = not aged.

Table 15.5. Electrical Resistivity Dependence of Cold-worked C17200 Beryllium Copper on Aging Time (295 K).

Electrical Resistivity, nΩm	Cold Work, %	Aging Temperature, K	Aging Time, h	Reference No.
106.4	34	633	0.088	4
108.8	34	633	0.280	4
90.9	34	633	0.380	4
69.9	34	633	0.440	4
88.5	34	633	0.550	4
77.6	34	633	0.670	4
75.2	34	633	0.840	4
69.9	34	633	1.040	4
70.4	34	633	1.430	4
63.7	34	633	1.990	4
61.7	34	633	3.620	4
69.9	34	633	5.940	4
78.4	44	588	2.00	9
69.9	35	588	2.00	9
78.4	33	588	2.00	9
66.2	50	644	0.[illegible]00	9
61.7	50	588	1.000	9
69.9	50	644	2.000	9
55.6	0	644	4.00	9
52.6	50	644	8.000	9
71.9	50	633	0.500	9
69.9	50	633	[illegible].000	6
61.7	50	633	[illegible].000	9
69.9	50	633	4.000	6
57.8	50	633	7.000	6

C17200: Annealed and Aged; Cold-worked and Aged

Electrical Resistivity vs. Aging Temperature, Time (295 K)

Table 15.5, continued

Electrical Resistivity, nΩm	Cold Work, %	Aging Temperature, K	Aging Time, h	Reference No.
55.9	50	633	10.000	6
53.8	50	633	15.000	6
87.0	50	588	0.500	6
82.0	50	588	1.000	6
75.2	50	588	2.000	6
70.4	50	588	1.000	6
66.2	50	588	7.000	6
63.7	50	588	10.000	6
61.7	50	588	15.000	6
79.6	50	569	0.083	7
77.5	50	569	0.250	7
73.4	50	569	0.500	7
82.5	16	0	0.000	8
84.0	36	0	0.000	8
85.8	64	0	0.000	8
86.5	75	0	0.000	8
76.0	16	573	1.000	8
71.0	16	573	1.750	8
69.5	16	573	1.750	8
68.5	16	573	4.000	8
63.0	16	573	8.000	8
58.0	16	573	18.000	8
55.0	16	573	27.000	8
53.5	16	573	41.000	8
51.2	16	573	61.000	8
51.0	16	573	86.000	8
49.5	16	573	100.000	8
75.5	36	573	1.000	8
70.2	36	573	1.750	8
66.5	36	573	4.000	8
61.5	36	573	8.000	8
56.2	36	573	18.000	8
54.0	36	573	27.000	8
51.5	36	573	41.000	8
50.0	36	573	61.000	8
49.0	36	573	86.000	8
47.0	36	573	100.000	8
72.5	64	573	1.000	8
68.5	64	573	1.750	8
62.5	64	573	4.000	8
57.0	64	573	8.000	8
52.8	64	573	18.000	8
51.5	64	573	27.000	8
48.0	64	573	41.000	8
46.5	64	573	61.000	8
45.5	64	573	86.000	8
45.0	64	573	100.000	8
69.9	75	573	1.000	8
64.8	75	573	1.750	8
59.5	75	573	4.000	8
54.5	75	573	8.000	8

Table 15.5, continued

Electrical Resistivity, nΩm	Cold Work, %	Aging Temperature, K	Aging Time, h	Reference No.
43.2	75	573	18.000	8
47.5	75	573	27.000	8
45.7	75	573	41.000	8
44.5	75	573	61.000	8
43.2	75	573	86.000	8
43.0	75	573	100.000	8
78.4	11	573	2.000	12
78.[illegible]	50	644	0.089	13
75.2	50	644	0.160	13
70.0	50	644	0.270	13
64.9	50	644	0.480	13
61.0	50	644	3.000	13
59.0	50	644	2.000	13
56.5	50	644	3.000	13
55.2	50	644	4.600	13
53.2	50	644	7.900	13
84.5	50	622	2.08[illegible]	13
75.2	50	622	0.250	13
69.4	50	622	0.650	13
63.7	50	622	2.000	13
60.6	50	622	4.600	13
58.5	50	622	7.000	13
53.8	50	622	17.000	13
98.0	50	588	0.089	13
86.2	50	588	0.250	13
86.2	50	588	0.480	13
82.0	50	588	1.000	13
78.2	50	588	1.470	13
75.2	50	588	2.000	13
69.4	50	588	4.000	13
66.2	50	588	7.000	13
61.7	50	588	17.000	13

Aging Temperature, 0 K = not aged.

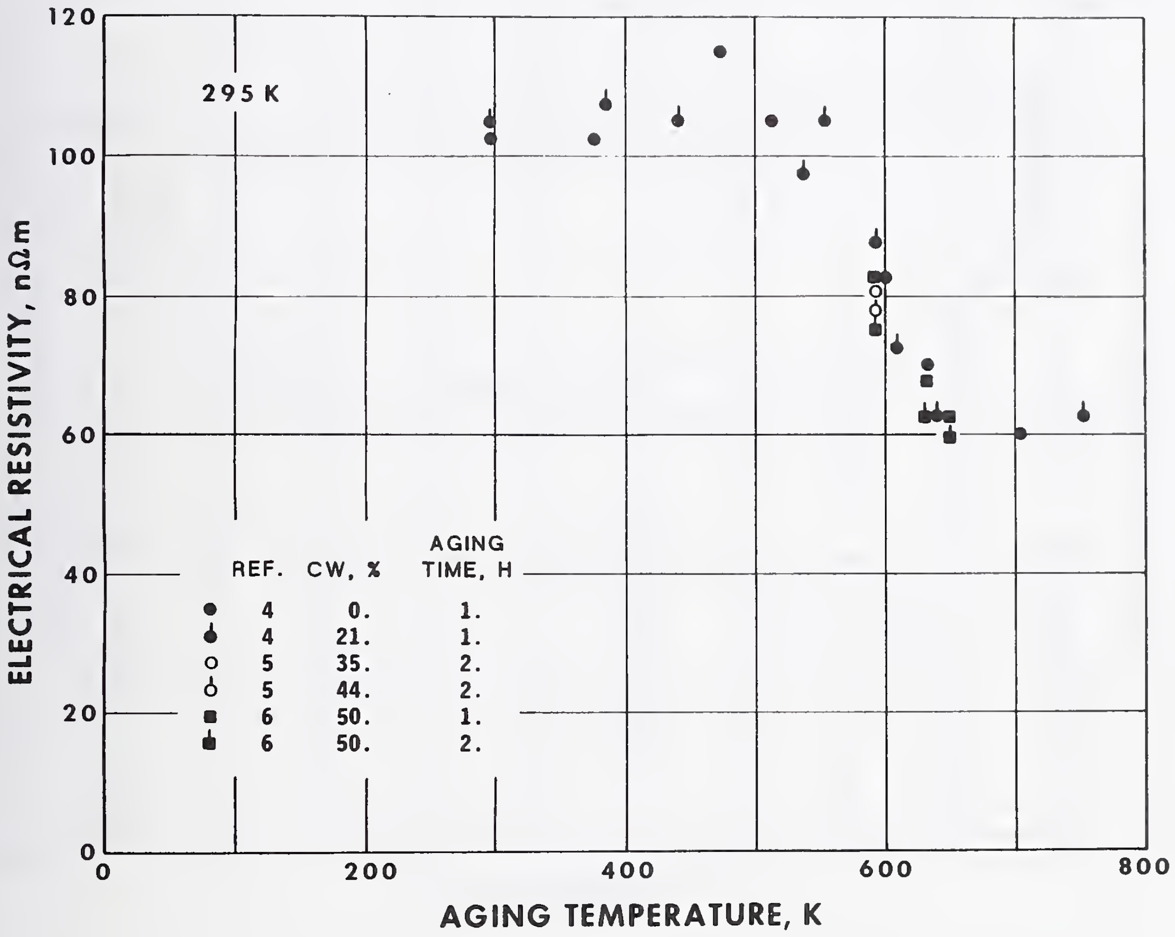

Figure 15.3. Electrical resistivity measurements at 295 K on annealed and cold-worked C17200 beryllium copper are shown as a function of aging temperature. Values from Reference 15.6 at aging times other than 1 or 2 h are omitted from the figure for clarity. All data are presented in Table 15.3. Products were in wire, strip, and bar form.

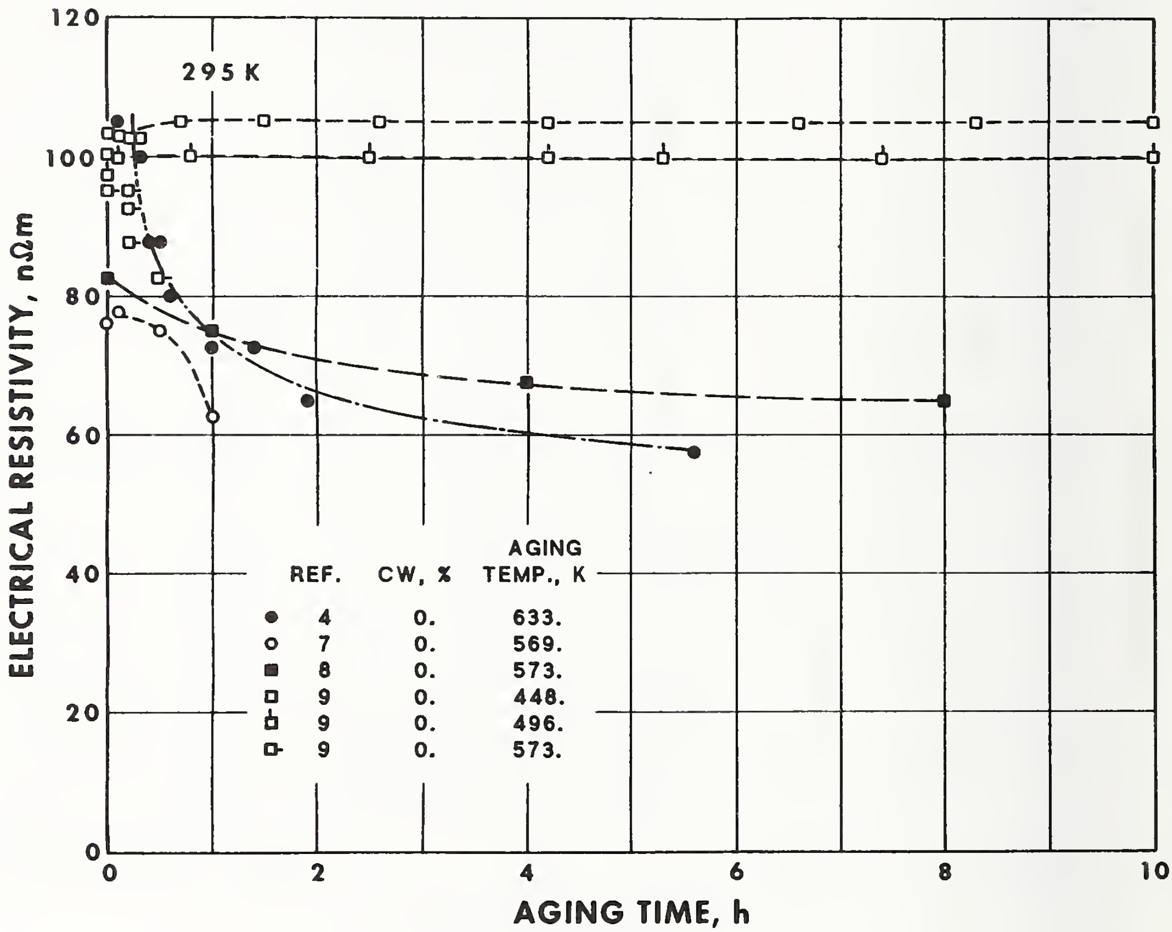

Figure 15.4. Electrical resistivity measurements at 295 K on annealed C17200 beryllium copper are shown as a function of aging time. For clarity, overlapping data points are omitted from the figure. Measurements at aging times greater than 10 h are not shown. All data are presented in Table 15.4. Products were in wire, strip, and bar form.

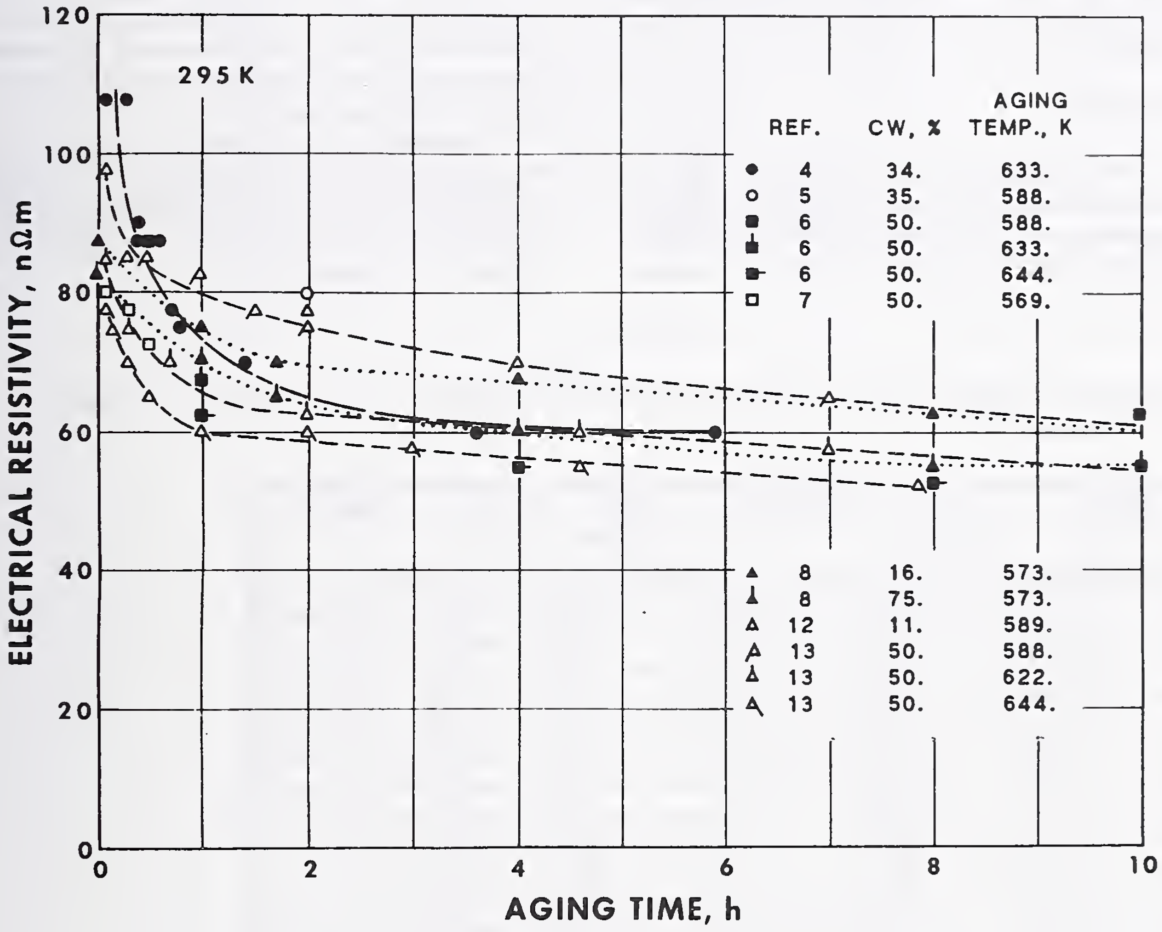

Figure 15.5. Electrical resistivity measurements at 295 K on cold-worked C17200 beryllium copper are shown as a function of aging time. Values from Reference 15.8 for amounts of cold work other than 16 or 75% are omitted from the figure for clarity, as are other overlapping data points. Measurements at aging times greater than 10 h are not shown. All data are presented in Table 15.5. Products were in wire, strip, and bar form.

C17200: Annealed; Annealed and Aged; Cold-worked

Electrical Resistivity vs. Temperature (4–300 K)

DATA SOURCES AND ANALYSIS

Measurements of the electrical resistivity from 4 to 300 K of C17200 beryllium copper were obtained from five sources (References 15.14–15.17). The annealed, annealed and aged, and cold-worked only conditions are represented in this data set. Products were in strip (Reference 15.17) and bar form (Reference 15.15), or not specified.

RESULTS

All measurements are reported in Table 15.6, which presents the electrical resistivity (ρ), test temperature (T), cold work, aging temperature and time, and the reference number. The available characterization of materials and measurements is given in Table 15.17 at the end of the electromagnetic properties section. Figure 15.6 presents ρ as a function of T.

DISCUSSION

Measurements for all material conditions exhibit a decrease In ρ with decreasing T. The small difference in ρ values reported in Reference 15.17 for two specimens is presumably due to differences in composition.

Reference 15.18 presented data at 77 K on the relative values for the change in ρ with aging temperature. Because the absolute values for ρ were not reported the data are not presented in Table 15.6 or Figure 15.6.

Table 15.6. Electrical Resistivity Dependence of C17200 Beryllium Copper on Test Temperature (4–300 K).

Electrical Resistivity, nΩm	Test Temperature, K	Cold Work, %	Aging Temperature, K	Aging Time, h	Reference No.
82.5	295.0	0	573	2.00	15
82.0	77.0	0	573	8.00	14
55.0	4.2	0	573	8.00	14
105.1	273.0	0	0	0.00	16
96.8	192.0	0	0	0.00	15
84.0	75.8	0	0	0.00	16
81.8	19.6	0	0	0.00	15
82.1	4.0	0	0	0.00	16
92.1	273.0	0	N.S.	N.S.	16
84.0	192.0	0	N.S.	N.S.	15
72.4	19.6	0	N.S.	N.S.	15
69.2	19.6	0	N.S.	N.S.	16
81.8	4.0	0	N.S.	N.S.	15
84.0	4.0	0	0	0.00	16
51.8	4.0	0	598	0.90	16
39.7	4.0	0	598	8.90	16
73.5	4.0	0	0	0.00	15
55.0	4.0	0	598	0.90	16
73.5	4.0	0	598	8.90	15
90.8	273.0	0	0	0.00	16
78.5	243.0	0	598	0.90	16
97.0	300.0	0	0	0.00	16
77.0	300.0	0	598	0.90	16
55.0	300.0	0	598	8.90	16
71.0	128.0	N.S.	0	0.00	17
73.0	160.0	N.S.	0	0.00	17
76.0	183.0	N.S.	0	0.00	17
75.0	188.0	N.S.	0	0.00	17

C17200: Annealed; Annealed and Aged; Cold-worked

Electrical Resistivity vs. Temperature (4–300 K)

Table 15.6, continued

Electrical Resistivity, nΩm	Test Temperature, K	Cold Work, %	Aging Temperature, K	Aging Time, h	Reference No.
78.0	215.0	N.S.	0	0.00	17
79.0	230.0	N.S.	0	0.00	17
82.0	248.0	N.S.	0	0.00	17
83.0	260.0	N.S.	0	0.00	17
82.0	133.0	N.S.	0	0.00	17
83.0	160.0	N.S.	0	0.00	17
62.0	188.0	N.S.	0	0.00	17
72.0	191.0	N.S.	0	0.00	17
70.0	215.0	N.S.	0	0.00	17
62.0	238.0	N.S.	0	0.00	17
72.0	250.0	N.S.	0	0.00	17

N.S. = not specified.
Aging Temperature, 0 K = not aged.

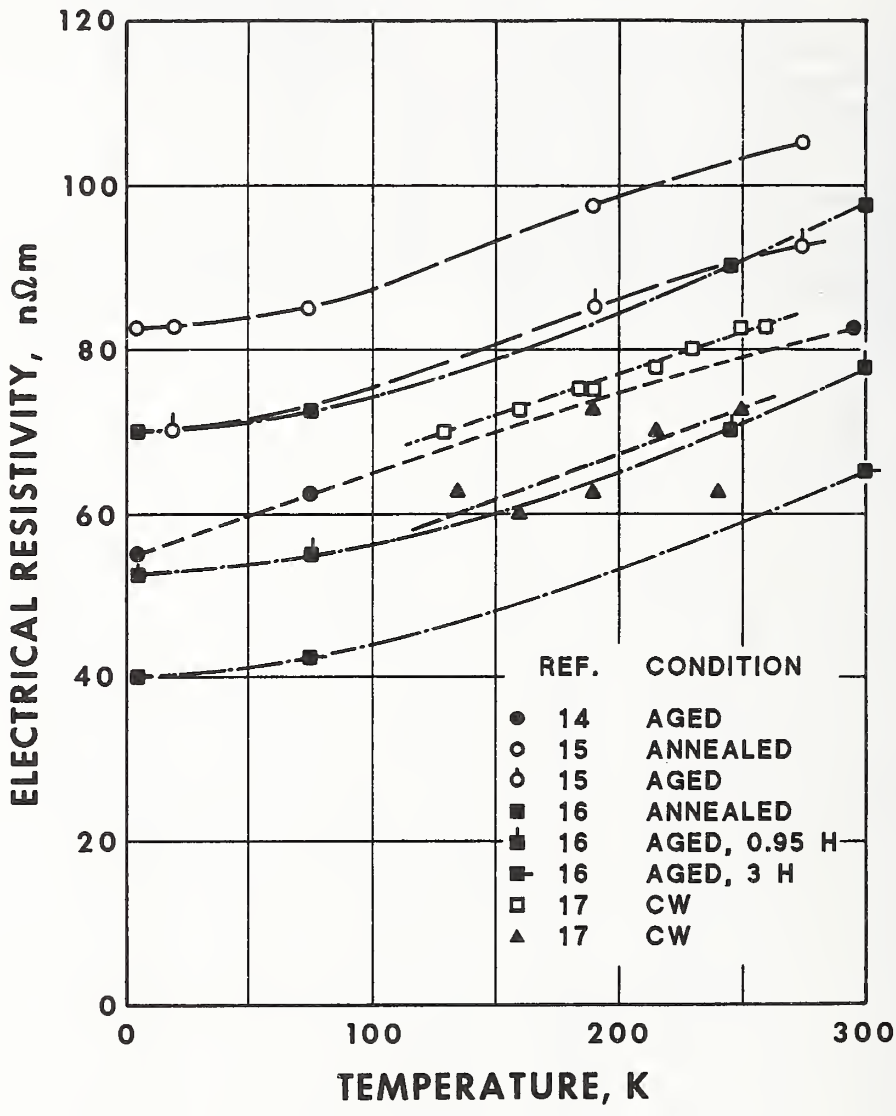

Figure 15.6. Electrical resistivity measurements from 4 to 300 K on C17200 beryllium copper in annealed, annealed and aged, and cold-worked conditions are shown. All data are given in Table 15.6. Products were in strip (Reference 15.17) and bar form (Reference 15.15), or not specified.

C17200: Annealed and Aged

Change in Electrical Resistivity vs. Aging Time (4, 77, 243, 300 K)

DATA SOURCES AND ANALYSIS

Measurements of the change in electrical resistivity at 4, 77, 243 and 300 K of annealed C17200 beryllium copper as a function of aging time were obtained from References 15.16 and 15.19. Aging temperatures were 403 and 598 K; aging times ranged from 0.02 to 167 h. Product form was not specified.

RESULTS

All measurements are reported in Table 15.7, which presents the change in electrical resistivity ($\Delta\rho$), test temperature, aging temperature and time, and the reference number. The available characterization of materials and measurements is given in Table 15.17 at the end of the electromagnetic properties section. Figure 15.7 presents $\Delta\rho$ at several cryogenic temperatures as a function of aging time.

DISCUSSION

The data from Reference 15.19 do not show a decrease in $\Delta\rho$ with aging time because the aging temperature of 403 K is too low to remove beryllium and other elements from solid solution in the copper matrix by precipitation.

Table 15.7. Electrical Resistivity Dependence of Annealed C17200 Beryllium Copper on Aging Time (4, 77, 243, and 300 K).

Change in Electrical Resistivity, nΩm	Test Temperature, K	Cold Work, %	Aging Temperature, K	Aging Time, h	Reference No.
7.3	4	0	4	0.000	16
-18.2	[illegible]	0	598	2.950	16
-30.3	4	0	598	2.950	16
0.0	77	0	0	0.000	16
-18.5	77	0	598	0.950	19
-30.5	77	0	598	[illegible]	16
0.0	243	0	0	0.000	16
-20.3	243	0	598	0.950	16
-31.3	243	0	598	2.950	16
0.0	300	0	4	0.000	16
-20.0	300	0	598	2.950	16
-31.8	300	0	598	2.950	19
7.3	77	0	403	0.022	16
[illegible]	77	0	403	0.111	16
13.1	77	0	403	0.556	19
12.7	77	0	403	1.530	19
13.1	77	0	403	3.140	16
12.9	77	0	403	5.140	19
12.3	77	0	403	167.000	16
7.1	243	0	403	0.022	19
9.2	243	0	403	0.111	16
11.3	243	0	403	0.956	19
12.2	243	0	403	1.530	16
12.9	243	0	403	3.140	19
12.2	243	0	403	5.140	19
11.7	243	0	403	167.000	19

Aging Temperature, 0 K = not aged.

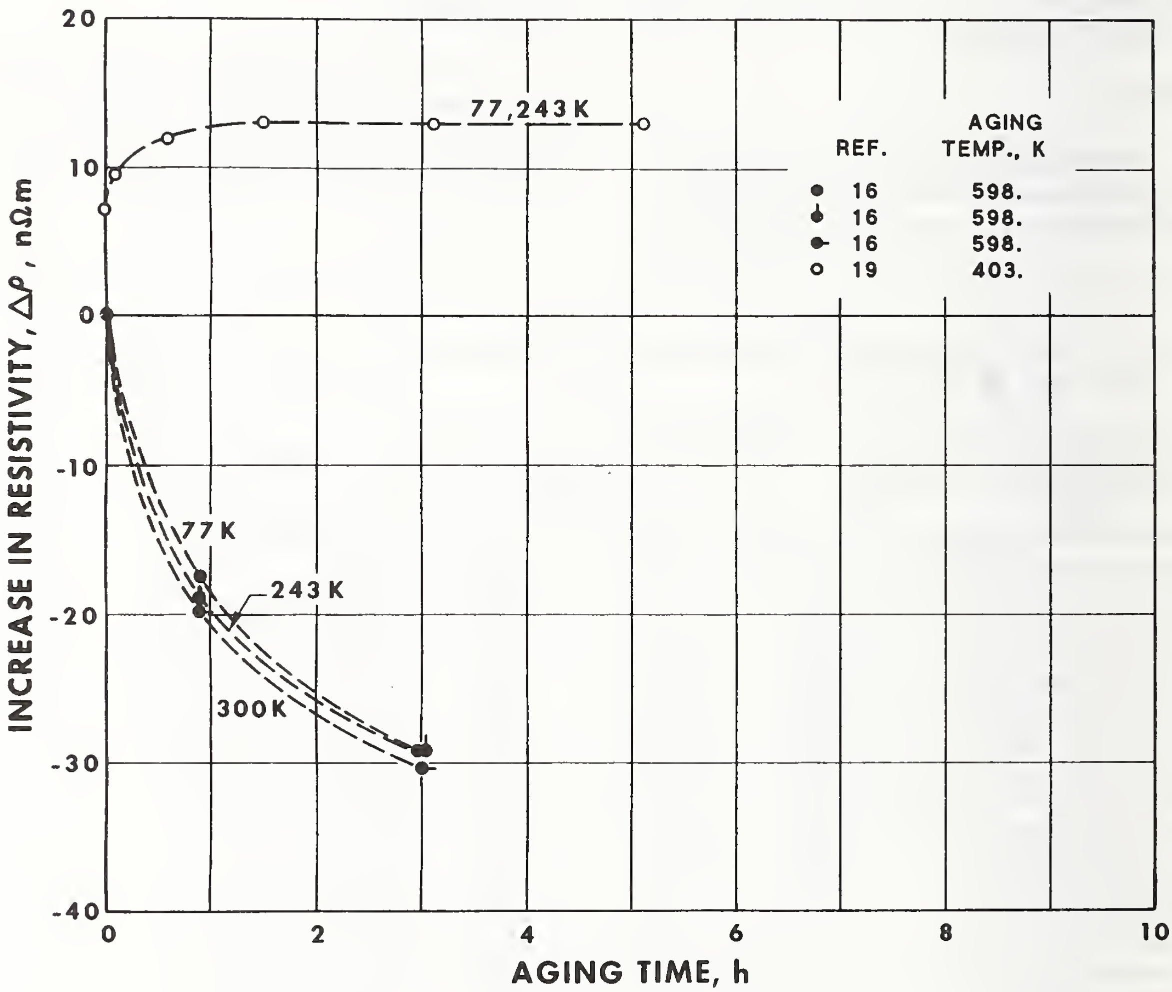

Figure 15.7. Electrical resistivity measurements at cryogenic temperatures on annealed C17200 beryllium copper are shown as a function of aging time. For clarity, overlapping data points are omitted from the figure, and measurements at aging times greater than 10 h are not shown. All data are presented in Table 15.7. Product form was not specified.

C17200: Cold-worked

Electrical Resistivity vs. Cold Work (295 K)

DATA SOURCES AND ANALYSIS

Measurements of the electrical resistivity of C17200 beryllium copper at 295 K as a function of cold work were obtained from five sources (References 15.4, 15.5, 15.7, 15.8, and 15.13). Cold work, *CW*, ranged from 0 to 94% (reduction in thickness or area). Products were in wire, strip, and bar form.

RESULTS

All measurements are reported in Table 15.8, which presents the electrical resistivity (ρ), *CW* (reduction in thickness or area), and the reference number. The available characterization of materials and measurements is presented in Table 15.17 at the end of the electromagnetic properties section. Figure 15.8 presents ρ as a function of *CW*.

DISCUSSION

The resistivity is slightly increased by *CW*. See also Figures 15.2 and 15.12 where similar results are shown.

Table 15.8. Electrical Resistivity Dependence of C17200 Beryllium Copper on Cold Work (295 K).

Electrical Resistivity, nΩm	Cold Work, %	Reference No.
101.4	0	4
108.0	17	4
107.8	34	4
107.8	33	5
102.0	36	8
108.0	44	4
82.8	50	4
98.5	49	8
84.0	36	8
85.8	64	8
86.5	75	8
98.5	0	13
106.0	37	13
108.0	49	13
06.5	70	13
100.0	49	13
107.0	75	13
107.0	49	13
111.0	88	13
114.0	90	13
113.0	92	13
112.0	94	13

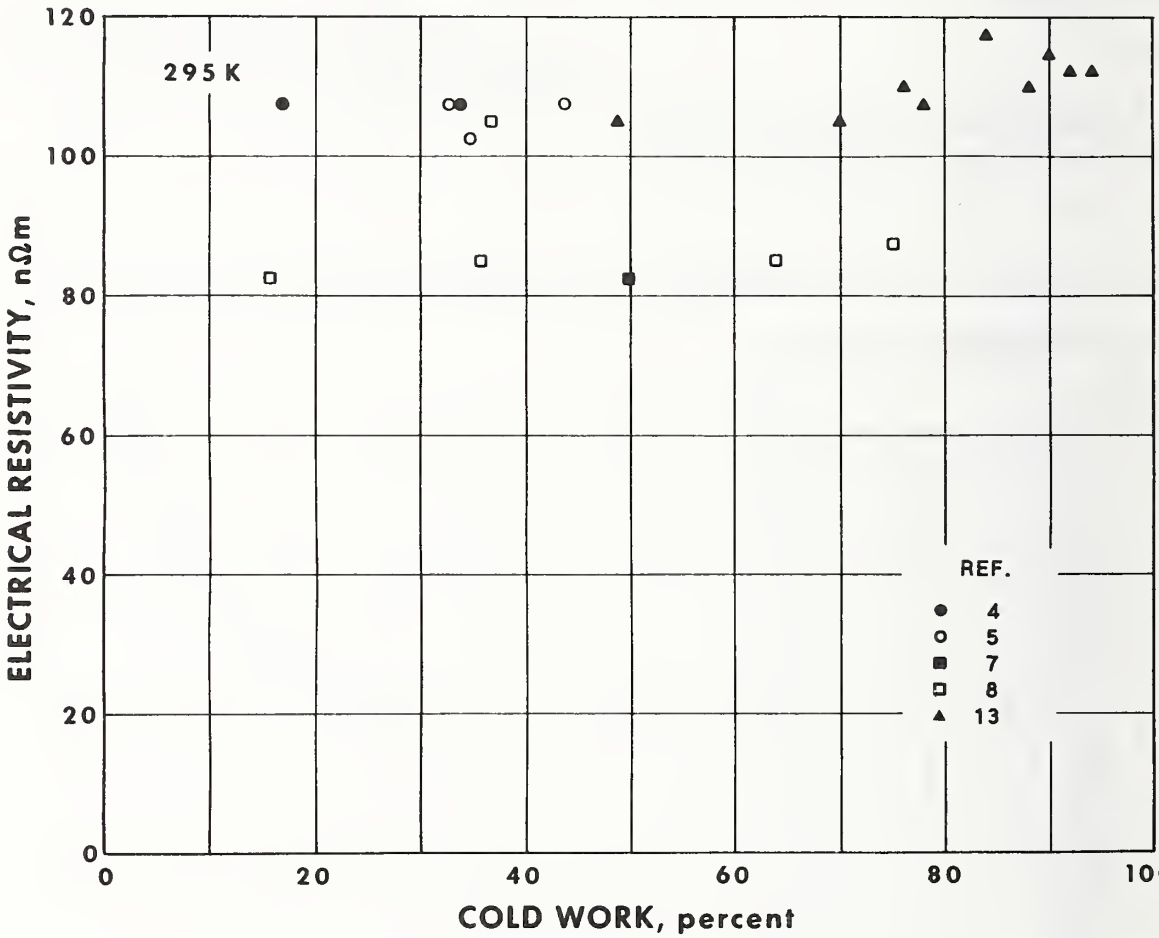

Figure 15.8. Electrical resistivity measurements at 295 K on C17200 beryllium copper are shown as a function of cold work. All data are presented in Table 15.8. Products were in wire, strip, and bar form.

C17200: Annealed; Cold-worked; Cold-worked and Aged

Tensile Yield Strength vs. Electrical Resistivity (295 K)

DATA SOURCES AND ANALYSIS

Measurements of the yield strength of C17200 beryllium copper at 295 K as a function of electrical resistivity were obtained from three sources (References 15.5, 15.12, and 15.13). The annealed, cold-worked, and cold-worked and aged conditions are represented in this data set. The amount of cold work, *CW*, ranged from 0 to 94% (reduction in thickness or area). Products were in wire, strip, and bar form.

RESULTS

All measurements are reported in Table 15.9, which presents the yield strength (σ_y), electrical resistivity (ρ), *CW* (reduction in thickness or area), aging temperature, and the reference number. The available characterization of materials and measurements is presented in Table 15.17 at the end of the electromagnetic properties section. Figure 15.9 presents σ_y as a function of ρ. The shading denotes the two different conditions of cold-worked only and cold-worked and aged.

DISCUSSION

The shaded areas in Figure 15.9 show that for a given level of σ_y, a lower ρ is obtained for material in the cold-worked and aged condition than in the cold-worked only condition.

Table 15.9. Tensile Yield Strength Dependence of C17200 Beryllium Copper on Electrical Resistivity (295 K).

Yield Strength, MPa	Electrical Resistivity, nΩm	Cold Work, %	Aging Temperature, K	Aging Time, h	Reference No.
686	108.0	44	0	0.00	5
1356	78.7	44	588	2.00	5
592	112.0	90	0	0.00	5
1231	98.0	35	588	2.00	5
690	107.8	33	0	0.00	5
1218	78.7	33	588	2.00	5
1169	78.4	94	588	[illegible].00	12
207	98.0	0	0	2.00	13
690	106.0	94	0	0.00	13
760	105.0	76	0	2.00	13
917	106.0	70	0	0.00	13
1076	110.0	76	0	0.00	13
1145	112.0	94	0	0.00	13
1152	111.0	58	0	2.00	13
1200	112.0	90	0	0.00	13
1227	111.0	50	0	2.00	13
1124	112.0	94	0	0.00	13
952	98.0	50	588	0.09	13
1379	86.2	94	588	0.48	13
1434	98.0	50	588	[illegible].00	13
1434	75.2	50	588	[illegible].00	13
1434	98.0	50	588	4.00	13
1400	86.2	94	588	[illegible].00	13
1324	61.7	50	588	17.00	13
1020	84.5	50	622	0.09	13
1324	63.7	50	622	2.00	13
1193	58.5	50	622	7.00	13
1069	53.8	50	622	17.00	13
1214	78.7	50	644	0.09	13

Table 15.9, continued

Yield Strength, MPa	Electrical Resistivity, nΩm	Cold Work, %	Aging Temperature, K	Aging Time, h	Reference No.
1267	75.2	50	644	0.16	13
1276	70.0	50	644	0.27	13
1276	64.9	50	644	0.48	13
1214	61.0	50	644	1.00	13
1034	53.2	50	644	7.90	13

Aging Temperature, 0 K = not aged.

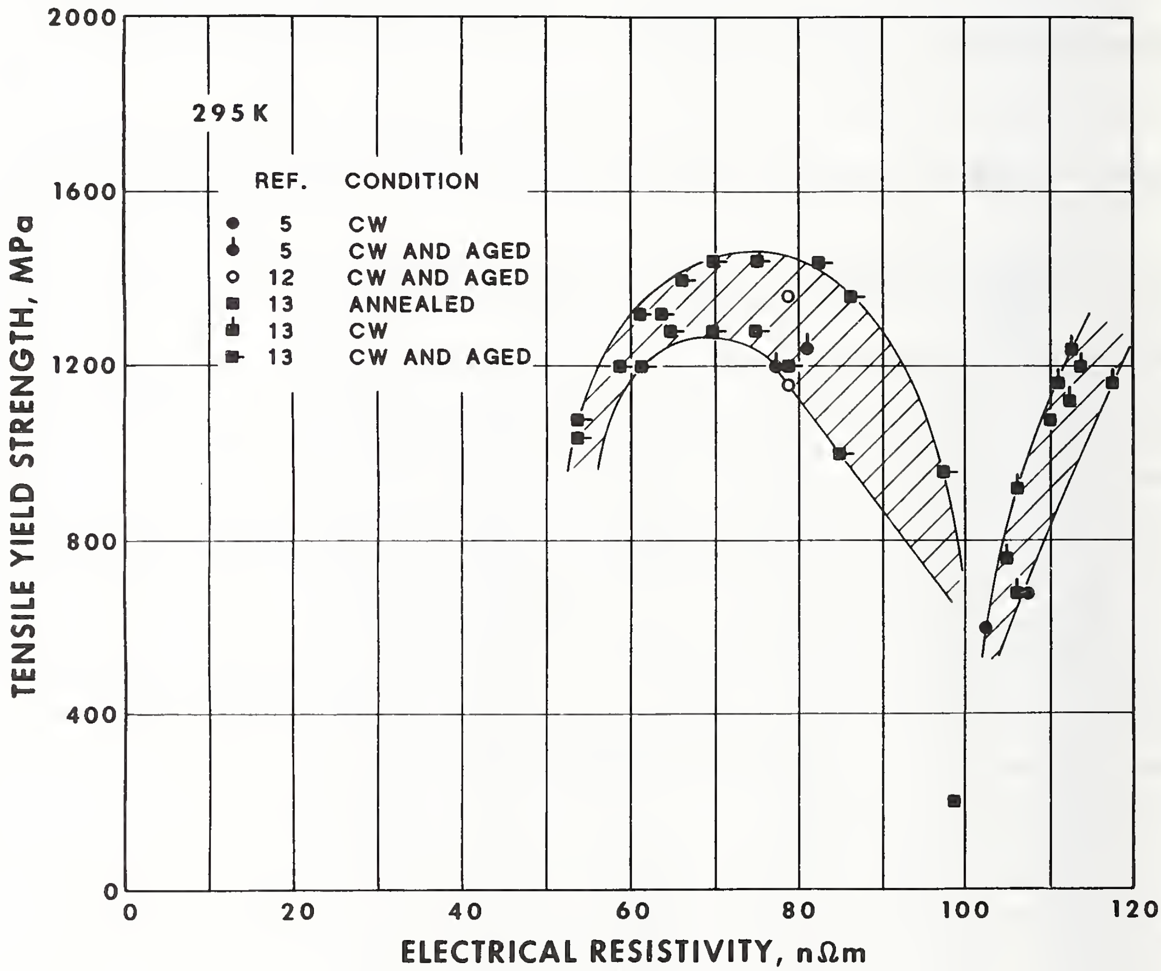

Figure 15.9. Tensile yield strength measurements at 295 K on C17200 beryllium copper are shown as a function of electrical resistivity. The shaded areas denote different material conditions. For clarity, overlapping data points are omitted from the figure. All data are presented in Table 15.9. Products were in wire, strip, and bar form.

DATA SOURCES AND ANALYSIS

Measurements of the electrical resistivity of annealed and cold-worked C17500 beryllium copper at 295 K as a function of aging time were obtained from References 15.20 and 15.21. Aging temperature was 753 K; aging times ranged from 0.15 to 32 h. The percent and type of cold work (Reference 15.21) was not specified (hard condition, product form not specified). Product form also was not specified in Reference 15.20.

RESULTS

All measurements are reported in Table 15.10, which presents the electrical resistivity (ρ), aging temperature and time, and the reference number. The available characterization of materials and measurements is given in Table 15.17 at the end of the electromagnetic properties section. Figure 15.10 presents ρ as a function of aging time.

DISCUSSION

As explained earlier, the decrease in ρ with aging time is due to the removal of impurity elements from the copper matrix by precipitation. The data of Reference 15.22 indicate that ρ remains approximately constant during exposure to 423 K for up to 100 h, with an increase of about 20% that is recovered upon return to room temperature.

Table 15.10. Electrical Resistivity Dependence of Annealed and Cold-worked C17500 Beryllium Copper on Aging Time (295 K).

Electrical Resistivity, nΩm	Cold Work, %	Aging Temperature, K	Aging Time, h	Reference No.
37.3	0	753	0.0[illegible]0	2[illegible]
54.6	0	753	0.150	20
47.2	0	753	0.320	20
45.9	0	753	0.730	20
45.0	0	753	[illegible].000	20
41.3	0	753	2.000	20
40.0	0	753	[illegible].000	20
38.5	0	753	5.750	20
36.8	0	753	15.800	20
36.4	0	753	31.600	20
111.0	N.S.	0	0.000	2[illegible]
63.3	N.S.	753	0.125	2[illegible]
45.[illegible]	N.S.	753	0.250	2[illegible]
42.7	N.S.	753	0.500	2[illegible]
37.3	N.S.	753	[illegible].000	2[illegible]
34.8	N.S.	753	2.000	21
33.9	N.S.	753	[illegible].000	2[illegible]
33.3	N.S.	753	[illegible].000	21
32.7	N.S.	753	6.000	21
32.3	N.S.	753	8.000	21

N.S. = not specified.
Aging Temperature, 0 K = not aged.

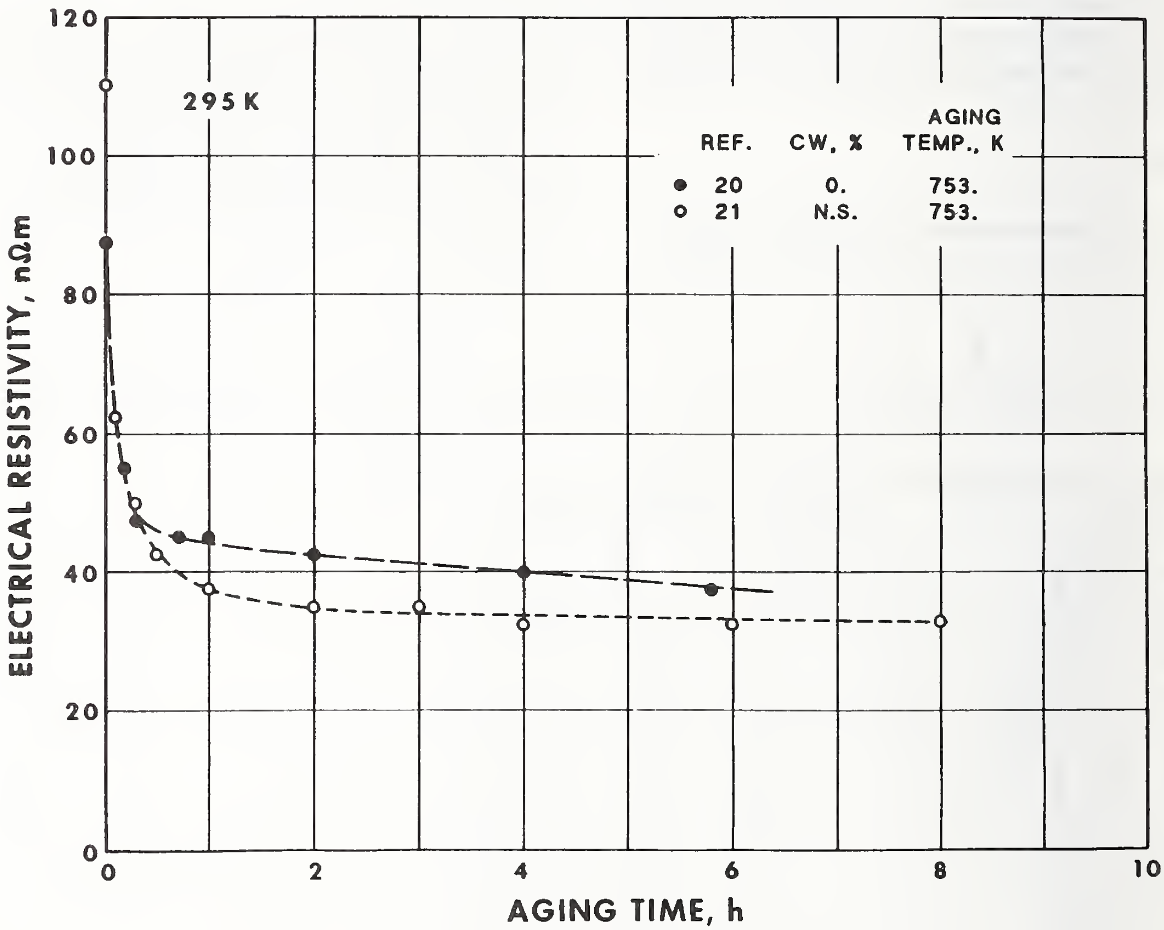

Figure 15.10. Electrical resistivity measurements at 295 K on annealed and cold-worked C17500 beryllium copper are shown as a function of aging time. Two data points from Reference 15.20 at aging times greater than 10 h do not appear on the graph. All data are presented in Table 15.10. Product form was not specified.

DATA SOURCES AND ANALYSIS

Measurements of the electrical resistivity of cold-worked C17510 beryllium copper at 295 K as a function of aging time were obtained from seven sources (References 15.21, and 15.23–15.28). Aging temperatures ranged from 593 to 838 K; aging times from 0.12 to 70 h. The amount of cold work, *CW*, ranged from 21 to 80% (reduction in thickness). In some cases, aging conditions or amount and mode of *CW* was not specified in the reference. Products were in strip and plate form, or not specified (References 15.21, 15.24, and 15.25).

Data presented here from Reference 15.28 include resistivity, ρ, measurements on three heats. Reference 15.26 reports ρ data on one of these heats at 76 and 4 K in addition to 295 K. See Figures 15.13 and 15.14.

RESULTS

All measurements are reported in Table 15.11, which presents ρ, *CW*, aging temperature and time, and the reference number. The available characterization of materials and measurements is given in Table 15.17 at the end of the electromagnetic properties section. Figure 15.11 presents ρ as a function of aging time.

DISCUSSION

As explained earlier, the decrease in ρ with aging time is due to the removal of impurity elements from the copper matrix by precipitation. The data of Reference 15.22 indicate that ρ remains approximately constant during exposure to 423 K for up to 100 h, with an increase of about 20% that is recovered upon return to room temperature.

Reference 15.29 notes that the recent use of higher purity C17510 material and improved thermomechanical processing procedures may result in lower values of ρ.

Table 15.11. Electrical Resistivity Dependence of Cold-worked C17510 Beryllium Copper on Aging Time (295 K).

Electrical Resistivity, nΩm	Cold Work, %	Aging Temperature, K	Aging Time, h	Reference No.
51.30	N.S.	0	0.000	23
48.80	N.S.	753	0.125	21
42.60	N.S.	753	0.250	21
38.20	N.S.	753	0.[illegible]00	21
35.10	N.S.	753	[illegible].000	21
32.80	N.S.	753	8.000	21
31.80	N.S.	753	[illegible].000	21
31.40	N.S.	753	4.000	21
30.80	N.S.	753	6.000	23
30.30	N.S.	753	8.000	21
29.50	21	727	8.000	23
27.20	21	755	8.000	23
27.20	21	753	8.000	23
27.40	21	811	8.000	21
26.90	21	838	8.000	23
38.50	N.S.	N.S.	N.S.	21
41.20	N.S.	N.S.	N.S.	23
27.20	40	755	8.000	21
30.80	N.S.	N.S.	N.S.	24
30.80	N.S.	N.S.	N.S.	24

Table 15.11, continued

Electrical Resistivity, nΩm	Cold Work, %	Aging Temperature, K	Aging Time, h	Reference No.
27.80	N.S.	N.S.	N.S.	24
35.20	N.S.	783	1.000	25
34.50	N.S.	783	2.000	25
33.00	N.S.	783	2.000	25
33.10	N.S.	783	2.000	25
32.80	N.S.	783	1.000	25
32.00	N.S.	783	5.000	25
34.60	N.S.	811	1.000	25
33.40	N.S.	811	2.000	25
32.80	N.S.	811	2.000	25
39.20	N.S.	811	2.000	25
32.00	N.S.	811	1.000	25
31.60	N.S.	811	5.000	25
51.50	N.S.	0	1.000	25
43.70	N.S.	672	4.000	25
42.00	N.S.	672	1.000	25
39.20	N.S.	672	2.000	25
38.80	N.S.	672	3.000	25
39.20	N.S.	672	2.000	25
39.70	N.S.	672	5.000	25
39.20	N.S.	727	2.000	25
37.40	N.S.	727	1.000	25
31.80	N.S.	727	2.000	25
35.70	N.S.	727	3.000	25
31.60	N.S.	727	4.000	25
39.70	N.S.	727	1.000	25
37.40	N.S.	755	2.000	25
36.00	N.S.	755	1.000	25
37.40	N.S.	755	2.000	25
33.30	N.S.	755	1.000	25
33.70	N.S.	755	4.000	25
33.30	N.S.	755	1.000	25
39.20	37	755	2.000	25
33.00	37	0	1.000	27
31.00	60	0	4.000	27
29.00	60	783	1.000	27
31.00	60	693	2.000	27
33.00	60	811	1.000	27
28.00	60	783	2.000	27
31.00	60	811	2.000	27
36.00	60	693	2.000	27
26.70	60	783	3.000	27
29.00	60	693	2.000	27
37.40	60	811	3.000	27
34.10	60	693	4.000	27
28.00	60	693	1.000	27
29.50	60	673	5.000	27
33.00	60	811	1.000	27
36.00	60	593	8.000	27
32.00	60	633	12.000	27
27.20	60	673	16.000	27

Table 15.11, continued

Electrical Resistivity, nΩm	Cold Work, %	Aging Temperature, K	Aging Time, h	Reference No.
30.25	60	593	18.000	27
34.80	60	593	24.000	27
29.50	60	633	36.000	27
34.00	60	593	42.000	27
33.00	60	633	10.000	27
34.65	60	593	70.000	27
33.60	60	573	6.000	27
33.77	60	673	1.000	27
33.00	60	633	7.000	27
33.09	60	593	5.000	27
33.09	60	573	7.000	27
31.93	60	593	24.000	27
31.64	60	633	18.000	27
31.32	60	593	70.000	27
30.25	60	633	2.000	27
31.32	60	593	2.000	27
30.25	60	673	2.000	27
29.70	37	755	2.000	27
28.30	N.S.	N.S.	N.S.	28
30.80	N.S.	N.S.	N.S.	28

N.S. = not specified.
Aging Temperature, 0 K = not aged.

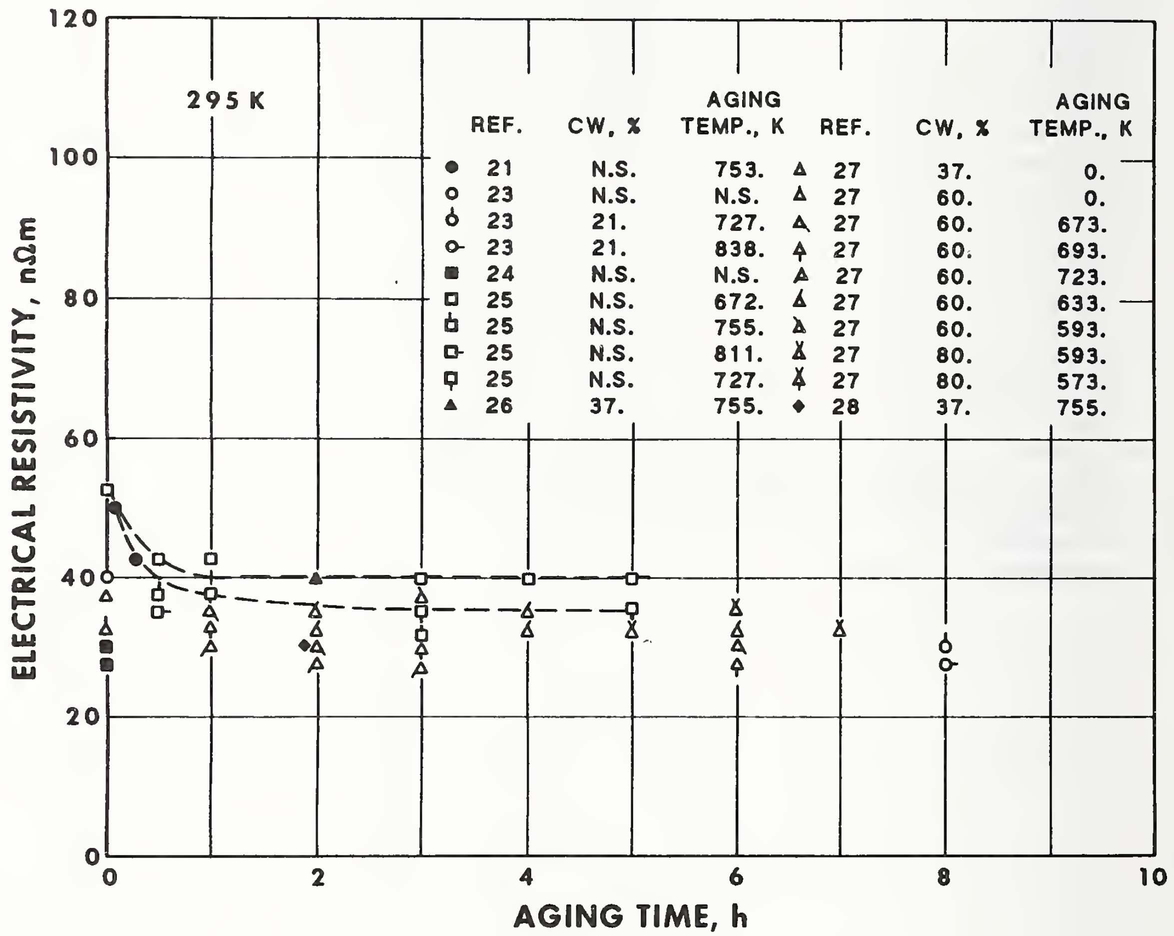

Figure 15.11. Electrical resistivity measurements at 295 K on cold-worked C17510 beryllium copper are shown as a function of aging time. Values from References 15.23, and 15.24, for which aging times were not specified, are plotted on the y-axis. For clarity, overlapping data points are omitted from the figure. A few measurements at aging times greater than 10 h are not shown. All data are presented in Table 15.11. Products were in strip and plate form, or not specified (References 15.21, 15.24, and 15.25).

C17510: Cold-worked; Cold-worked and Aged

Electrical Resistivity vs. Cold Work (295 K)

DATA SOURCES AND ANALYSIS

Measurements of the electrical resistivity of C17510 beryllium copper at 295 K as a function of cold work were obtained from References 15.27 and 15.30. Cold work, *CW*, ranged from 0 to 60% (reduction in thickness). Most of these measurements were made in the not-aged condition; however, Reference 15.30 also reported a series of measurements on material that was aged after varying amounts of *CW*. Also, one measurement from Reference 15.27 was made on material that was pre-aged at 673 K for 3 h and then cold-worked 60%. Products were in strip (Reference 15.30) and plate form (Reference 15.27).

RESULTS

All measurements are reported in Table 15.12, which presents the electrical resistivity (ρ), *CW* (reduction in thickness), aging temperature and time, and the reference number. The available characterization of materials and measurements is presented in Table 15.17 at the end of the electromagnetic properties section. Figure 15.12 presents ρ as a function of *CW*.

DISCUSSION

The resistivity is not changed significantly by *CW*. See also Figures 15.2 and 15.8, where similar results are shown.

Table 15.12. Electrical Resistivity Dependence of C17510 Beryllium Copper on Cold Work (295 K).

Electrical Resistivity, nΩm	Cold Work, %	Aging Temperature, K	Aging Time, h	Reference No.
33	37	0	0	27
38	60	0	0	27
50	0	0	0	30
50	11	0	0	30
50	21	0	0	30
50	37	0	0	30
33	0	755	3	30
34	11	755	N.S.	30
33	21	755	N.S.	30
31	37	755	2	30

N.S. = not specified.
Aging Temperature, 0 K = not aged.

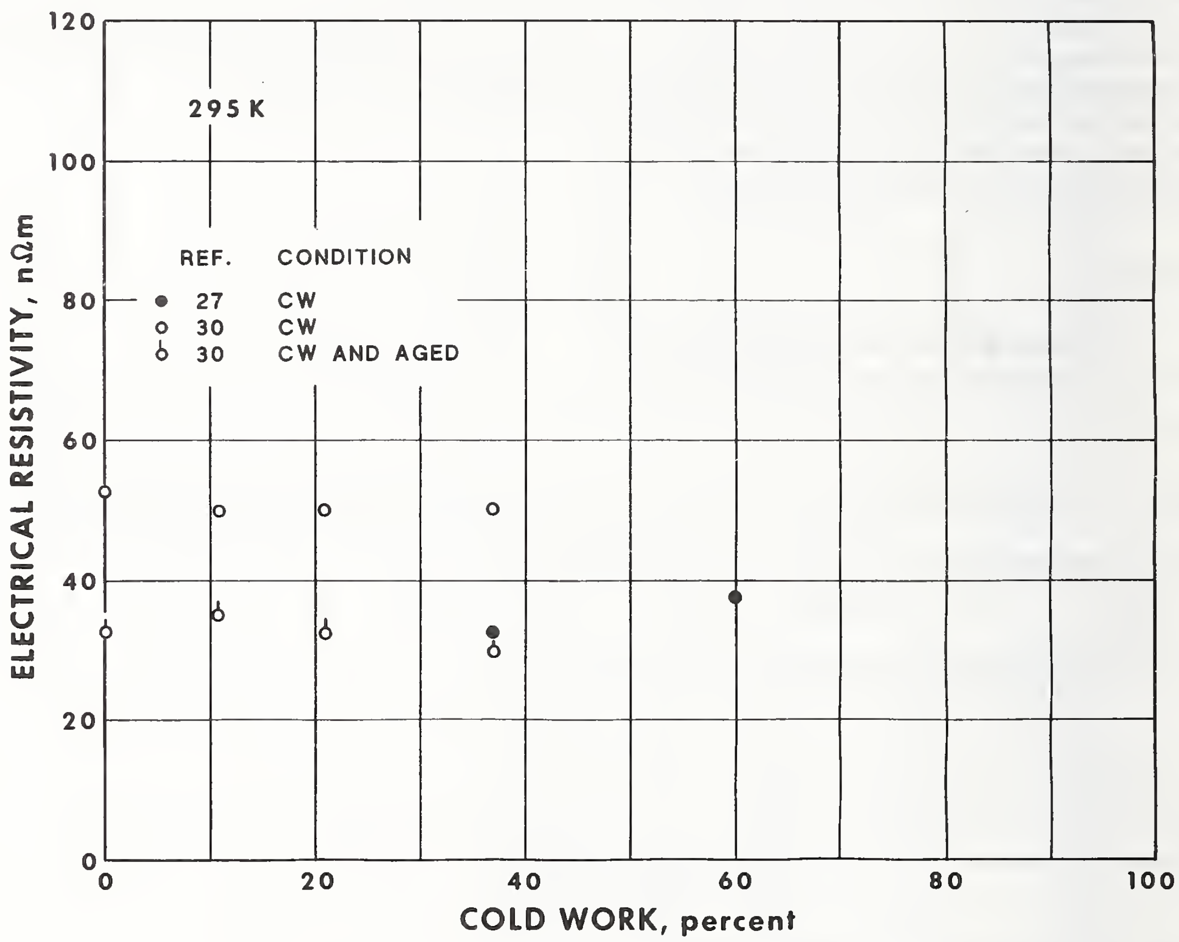

Figure 15.12. Electrical resistivity measurements at 295 K on both aged and not aged C17510 beryllium copper are shown as a function of cold work. All data are presented in Table 15.12. Products were in strip (Reference 15.30) and plate form (Reference 15.27).

DATA SOURCES AND ANALYSIS

Measurements of the electrical resistivity at 4, 76, and 295 K of cold-worked and aged C17510 beryllium copper were obtained from Reference 15.26. Product was in plate form.

RESULTS

All measurements are reported in Table 15.13, which presents the electrical resistivity (ρ), test temperature (T), amount of cold work, aging temperature and time, and the reference number. The available characterization of materials and measurements is given in Table 15.17 at the end of the electromagnetic properties section. Figure 15.13 presents ρ as a function of T.

DISCUSSION

Room temperature results for similar cold work and aging conditions differ from results of Reference 15.30, presented in Table 15.12. The difference may be due to different chemical compositions within the C17510 specifications.

Table 15.13. Electrical Resistivity Dependence of Cold-worked and Aged C17510 Beryllium Copper on Test Temperature (4–295 K).

Electrical Resistivity, nΩm	Test Temperature, K	Cold Work, %	Aging Temperature, K	Aging Time, h	Reference No.
15.0	4	37	755	2	26
18.0	76	37	755	2	26
39.8	295	37	755	2	26

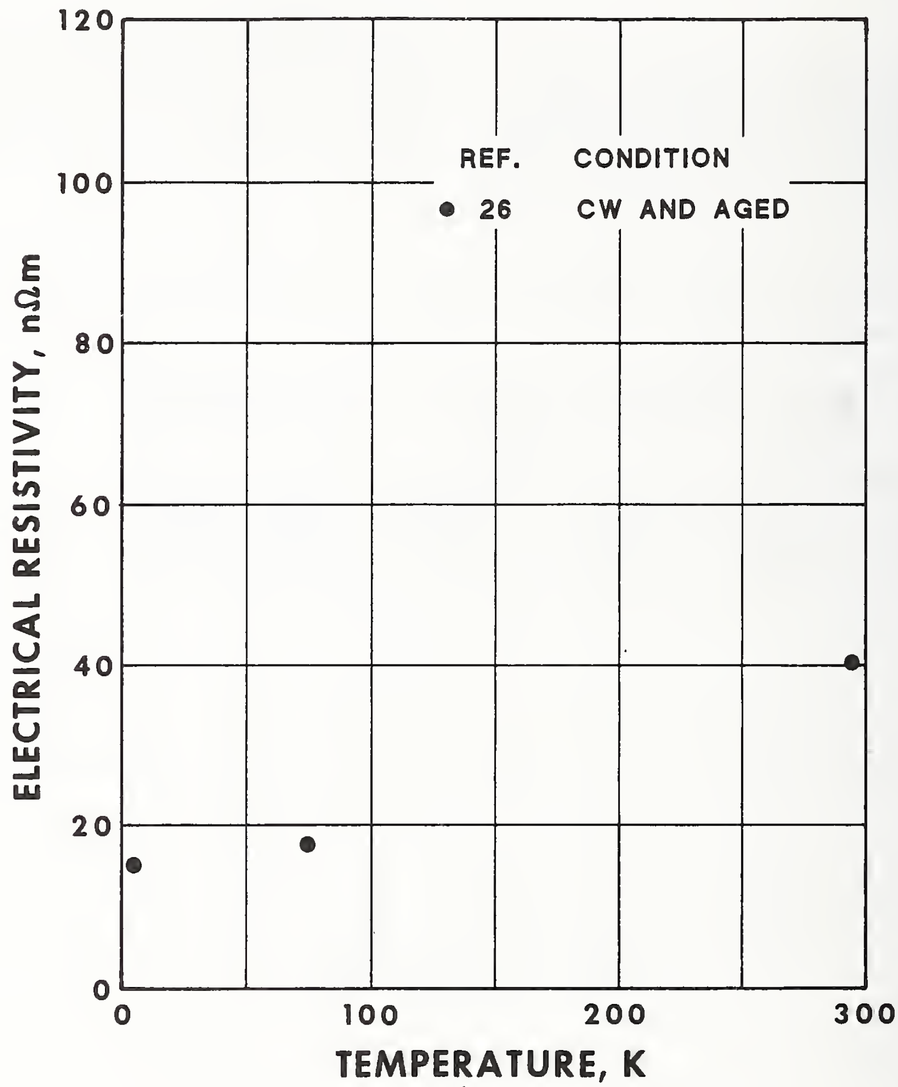

Figure 15.13. Electrical resistivity measurements from 4 to 295 K on cold-worked and aged C17510 beryllium copper are shown. All data are given in Table 15.13. Product was in plate form.

C17510: Cold-worked and Aged

Tensile Yield Strength vs. Electrical Resistivity (295 K)

DATA SOURCES AND ANALYSIS

Measurements of the yield strength at 295 K of cold-worked and aged C17510 beryllium copper as a function of electrical resistivity were obtained from seven sources (References 15.23–15.28, and 15.31). The amount of cold work, *CW*, ranged from 21 to 80% (reduction in thickness). In some cases, the amount or mode of *CW* was not specified. Products were in strip and plate form (not specified in References 15.23 and 15.24).

Data presented here from Reference 15.28 include resistivity, ρ, measurements on three heats. Reference 15.26 reports ρ data on one of these heats at 76 and 4 K in addition to 295 K. See Figures 15.11 and 15.13.

RESULTS

All measurements are reported in Table 15.14, which presents yield strength (σ_y), ρ, *CW* (reduction in thickness), aging temperature and time, and the reference number. The available characterization of materials and measurements is presented in Table 15.17 at the end of the electromagnetic properties section. Figure 15.14 presents σ_y as a function of ρ.

DISCUSSION

Reference 15.22 presents typical values of σ_y and ρ for cold-worked and aged C17500 and C17510 which show that about 30% higher σ_y can be attained with the latter alloy with approximately the same ρ.

Table 15.14. Tensile Yield Strength Dependence of Cold-worked and Aged C17510 Beryllium Copper on Electrical Resistivity (295 K).

Yield Strength, MPa	Electrical Resistivity, nΩm	Cold Work, %	Aging Temperature, K	Aging Time, h	Reference No.
758.0	34.5	N.S.	N.S.	N.S.	31
924.0	32.3	N.S.	N.S.	N.S.	31
896.0	30.8	N.S.	N.S.	N.S.	31
745.0	26.9	21	727	8	23
703.0	27.2	21	755	3	23
641.0	27.8	21	783	8	23
573.0	27.4	21	811	8	23
517.0	26.9	21	838	8	23
814.0	27.2	40	755	3	24
1092.0	35.2	N.S.	N.S.	N.S.	24
096.0	30.8	N.S.	N.S.	N.S.	24
813.0	27.8	N.S.	N.S.	N.S.	24
700.0	38.0	N.S.	N.S.	N.S.	25
725.0	35.2	N.S.	N.S.	N.S.	25
700.0	34.8	N.S.	N.S.	N.S.	25
708.0	34.7	N.S.	N.S.	N.S.	25
720.0	34.8	N.S.	N.S.	N.S.	25
725.0	34.8	N.S.	N.S.	N.S.	25
735.0	34.5	N.S.	N.S.	N.S.	25
695.0	33.6	N.S.	N.S.	N.S.	25
682.0	32.9	N.S.	N.S.	N.S.	25
650.0	32.2	N.S.	N.S.	N.S.	25

Table 15.14, continued

Yield Strength, MPa	Electrical Resistivity, nΩm	Cold Work, %	Aging Temperature, K	Aging Time, h	Reference No.
968.0	32.0	N.S.	N.S.	N.S.	25
650.0	31.7	N.S.	N.S.	N.S.	25
960.0	30.5	N.S.	N.S.	N.S.	25
520.0	27.4	N.S.	N.S.	N.S.	25
500.0	27.0	N.S.	N.S.	N.S.	25
940.0	33.0	N.S.	N.S.	N.S.	25
920.0	31.2	N.S.	N.S.	N.S.	25
885.0	29.8	N.S.	N.S.	N.S.	25
785.0	27.8	N.S.	N.S.	N.S.	25
805.0	26.1	N.S.	N.S.	N.S.	25
716.0	33.8	37	755	2	25
857.0	34.6	37	N.S.	N.S.	27
862.0	34.0	37	N.S.	N.S.	27
865.0	33.8	37	N.S.	N.S.	27
856.0	33.0	37	N.S.	N.S.	27
885.0	34.6	37	N.S.	N.S.	27
920.0	29.9	37	N.S.	N.S.	27
805.0	29.8	37	N.S.	N.S.	27
862.0	27.4	37	N.S.	N.S.	27
942.5	34.6	60	593	70	27
1005.0	33.8	80	573	6	27
960.0	33.8	60	673	1	27
960.0	33.0	80	593	4	27
1022.0	33.8	60	593	5	27
1005.0	33.0	60	573	7	27
940.0	31.9	60	593	24	27
955.0	31.6	60	593	16	27
931.0	31.9	60	593	16	27
960.0	31.3	80	593	2	27
948.0	31.9	60	593	2	27
927.0	30.3	60	673	2	27
765.0	29.7	37	755	2	28A
717.0	28.3	N.S.	N.S.	N.S.	28B
703.0	30.8	N.S.	N.S.	N.S.	28C

N.S. = not specified.

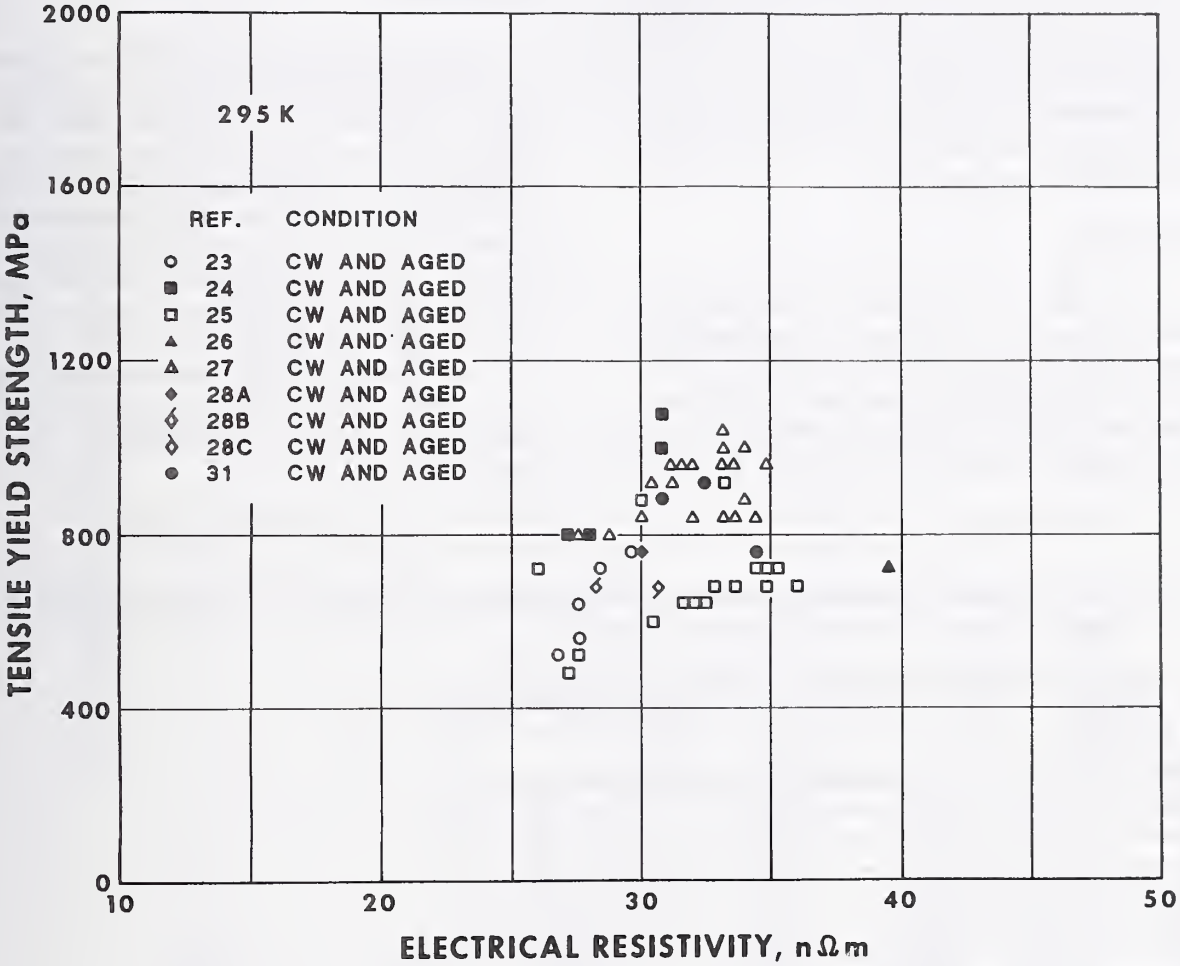

Figure 15.14. Tensile yield strength measurements at 295 K on cold-worked and aged C17510 beryllium copper are shown as a function of electrical resistivity. For clarity, overlapping data points are omitted from the figure. All data are presented in Table 15.14. Products were in strip and plate form (not specified in References 15.23 and 15.24).

DATA SOURCES AND ANALYSIS

Measurements of the magnetic susceptibility at 295 K of annealed and aged C17200 beryllium copper with varying Fe content, [Fe], were obtained from Reference 15.32. The susceptibility, κ, was measured after the annealed and solution-treated material had been initially aged at 588 K for 3 h and then held at various exposure temperatures from 588 to 866 K for 1 h. Some arbitrary values (off-scale) reported in Reference 15.32 are not included in this analysis, but curves based on these values are included in the figure. Product was in a cast-cylinder form.

RESULTS

All measured κ are reported in Table 15.15, which presents κ, [Fe], exposure temperature and time, and the reference number. The available characterization of materials and methods is given in Table 15.17 at the end of the electromagnetic properties section. Figure 15.15 presents κ obtained under the conditions described above. The data show that the alloy is magnetically stable after 1-h exposures at temperatures up to about 755 K. Temperatures of about 811 K were required to precipitate the ferromagnetic iron phase.

DISCUSSION

The specifications for C17200 given by the Copper Development Association Inc., Greenwich, CT, allow Ni + Fe + Co $\leq$ 0.6 wt%. The effects noted here are so small that for many applications, the magnetic permeability is equal to 1 to a good approximation. The susceptibility, in SI units, is defined as $\kappa = M/H$ (dimensionless), where H = applied field and M = magnetization (both in A/m). The relative permeability (μ_r), also dimensionless, is related to κ by $\mu_r = \mu/\mu_o = 1 + \kappa$. Reference 15.33 states that values of μ_r for C17000–C17500 beryllium coppers are normally below 1.020 and are reducible to <1.001 if desired.

Table 15.15. Magnetic Susceptibility Dependence of Annealed and Aged C17200 Beryllium Copper on Exposure Temperature and Fe Content (295 K).

Magnetic Susceptibility, 10^{-6}	[Fe], wt%	Exposure Temperature, K	Exposure Time, h	Reference No.
251	0.30	588	1	32
7504	0.40	588	1	32
327	0.30	644	1	32
4775	0.40	644	1	32
113	0.15	755	1	32
126	0.20	755	1	32
452	0.30	755	1	32
4775	0.40	700	1	32
113	0.10	755	1	32
151	0.15	755	1	32
239	0.20	755	1	32
628	0.30	755	1	32
5529	0.40	755	1	32
239	0.10	811	1	32
377	0.15	811	1	32
892	0.20	811	1	32
4524	0.30	811	1	32
3267	0.10	866	1	32
5906	0.15	866	1	32

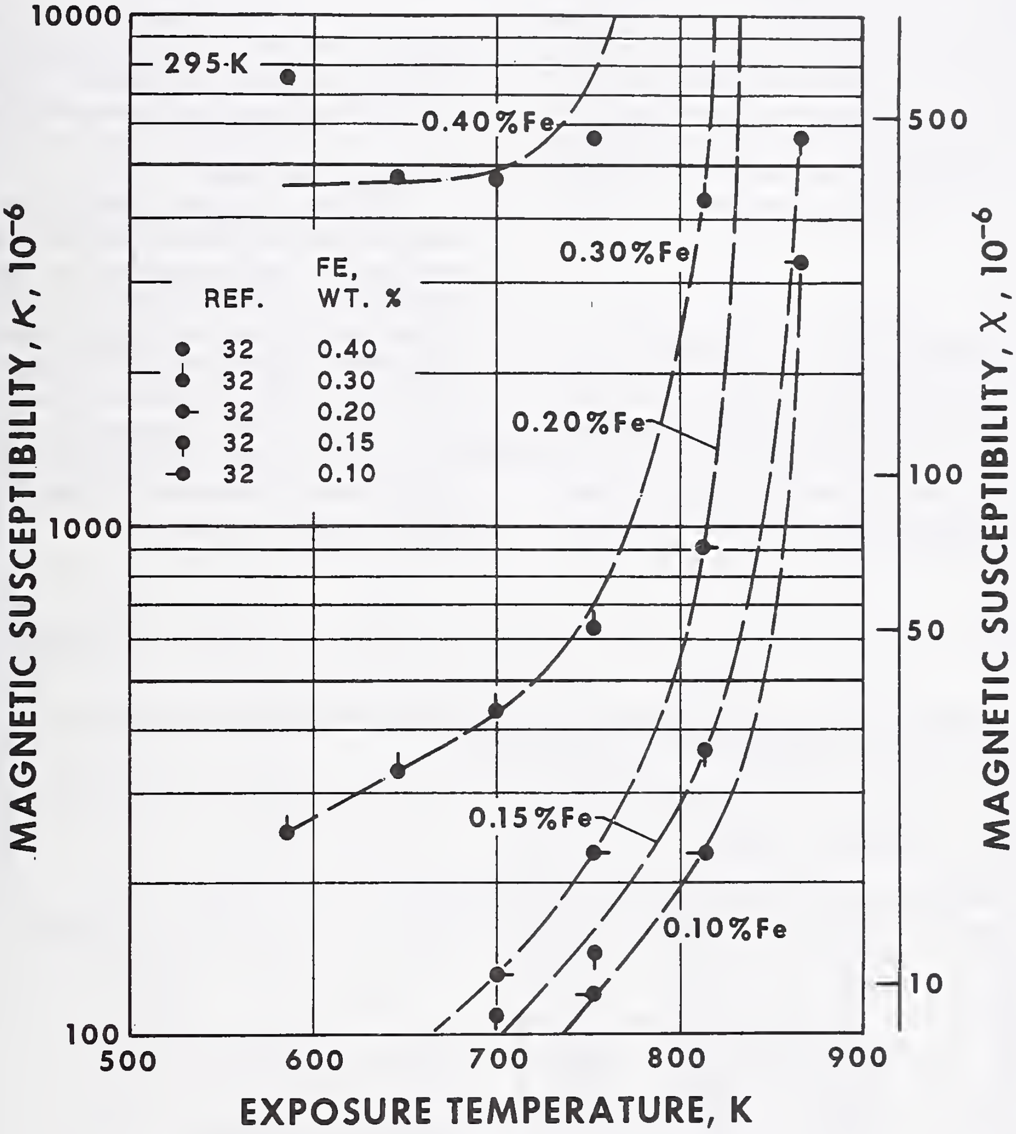

Figure 15.15. Magnetic susceptibility measurements at 295 K from Reference 15.32 on annealed and aged C17200 beryllium copper are shown as a function of exposure temperature and Fe content. The time at the exposure temperature was 1 h. All data are presented in Table 15.15. Product was in a cast-cylinder form.

DATA SOURCES AND ANALYSIS

Measurements of the magnetic susceptibility at 295 K of annealed C17200 beryllium copper with varying Fe content were obtained from Reference 15.32. The susceptibility, κ, was measured after aging at 588 K for 3 h preceded by solution treatments of 1 h at varying temperatures. Some arbitrary values (off-scale) reported in Reference 15.32 are not included in this analysis, but curves based on these values are included in the figure. Product was in a cast-cylinder form.

RESULTS

All measured values of κ are reported in Table 15.16, which presents κ, solution treatment temperature, Fe content, and the reference number. The available characterization of materials and methods is given in Table 15.17 at the end of the electromagnetic properties section. Figure 15.16 presents κ obtained under the conditions described above. The data show that the κ of the alloy can be reduced to about 2×10^{-4} by raising the solution temperature to 1116 K.

DISCUSSION

Iron loses its ferromagnetic characteristics when it is dissolved in copper solid solution. The usual solution-treating temperature is about 1060 K, and the data show that a temperature about 56 K higher is necessary to effect the solution of Fe in the copper matrix.

The effects noted here are so small that for many applications, the magnetic permeability is equal to 1 to a good approximation. The susceptibility, in SI units, is defined as $\kappa = M/H$ (dimensionless), where H = applied field and M = magnetization (both in A/m). The relative permeability (μ_r), also dimensionless, is related to κ by $\mu_r = \mu/\mu_o = 1 + \kappa$. Reference 15.33 states that values for μ_r for C17000–C17500 beryllium copper normally are below 1.020 and are reducible to < 1.001 if desired.

Table 15.16. Magnetic Susceptibility Dependence of Annealed and Aged C17200 Beryllium Copper on Solution-Treating Temperature, Fe Content (295 K).

Magnetic Susceptibility, 10^{-6}	Solution Temperature, K	[Fe], wt%	Reference No.
224.	866.	0.050	32
3343.	866.	0.120	32
9425.	866.	0.215	32
12280	866.	0.305	32
2111.	1061.	0.215	32
3544.	1061.	0.305	32
1257.	1088.	0.305	32
3971.	1088.	0.395	32
126.	1116.	0.215	32
214.	1116.	0.305	32
201.	1116.	0.395	32
201.	1116.	0.490	32

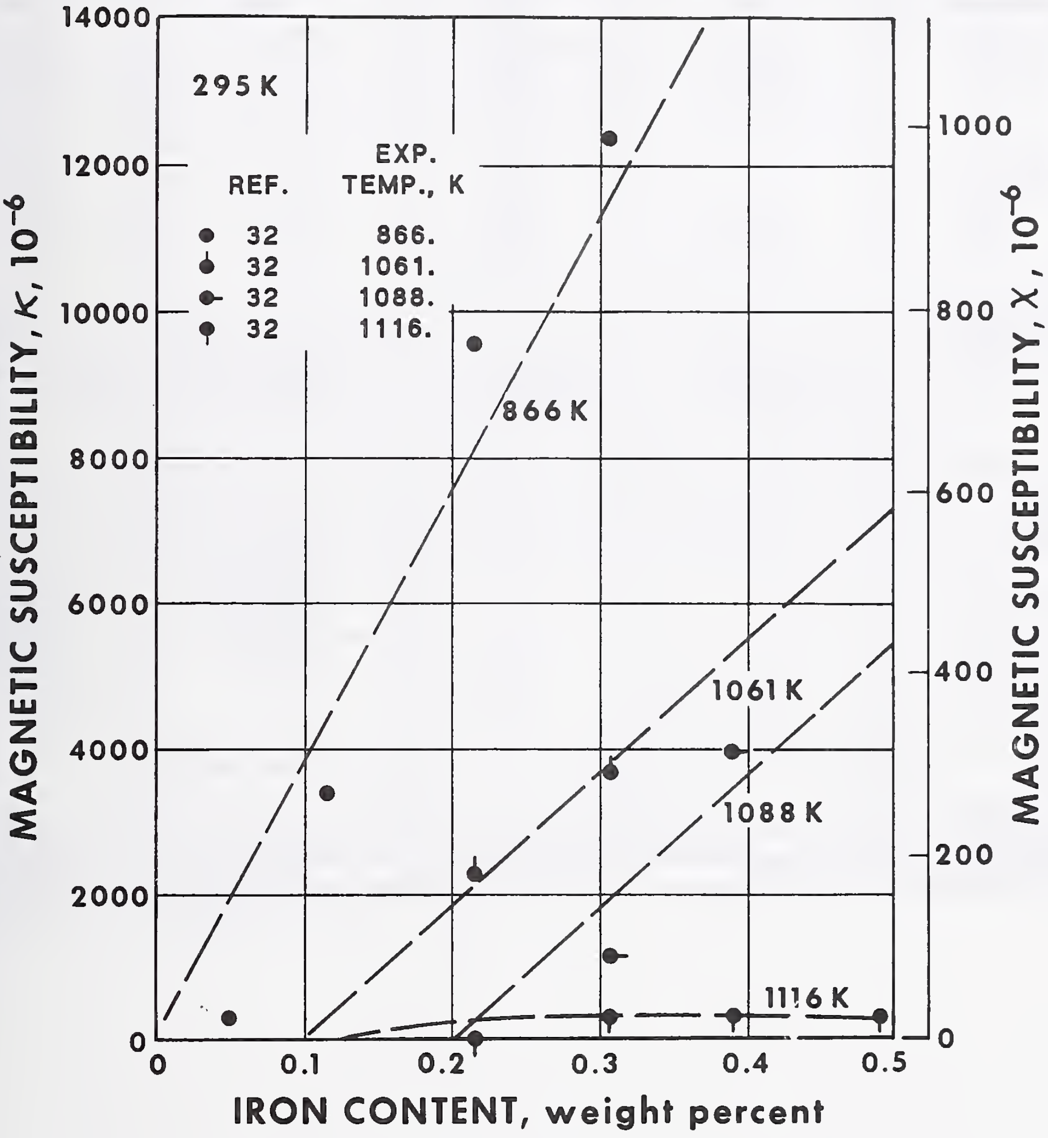

Figure 15.16. Magnetic susceptibility measurements at 295 K on annealed and aged C17200 beryllium copper are shown as a function of iron content and solution temperature. All data are presented in Table 15.16. Product was in a cast-cylinder form.

Table 15.17. Characterization of Materials and Measurements.

Reference No.	1A	1B	2A	2B
Specification	C17000	C17000	C17000	C17000
Composition (wt%)				
Cu	> 98.49	> 98.49	98.37	98.37
Cu + Ag	—	—	—	—
Be	1.50	1.50	1.62	1.62
Ni	—	—	—	—
Co	—	—	—	—
Ni + Co	—	—	—	—
Ni + Fe + Co	—	—	—	—
Al	—	—	—	—
Fe	< 0.01	< 0.01	0.06	0.06
Si	—	—	—	—
Others (Only ≥ 0.001 wt%)	—	—	—	—
Material Condition	Annealed, 1053 K, 0.33 h	Aged, 623 K, 0.0008–17 h	Mill annealed	Cold-drawn, 75%
RRR	—	—	—	—
Grain Size	—	—	—	—
Hardness	—	—	R_B 103	—
Product Form	—	—	Bar, 2.5-cm-dia.	Bar, 2.5-cm-dia.
Specimen Type	—	—	Wire	Wire
Width or Dia.	—	—	—	0.328 cm
Thickness	—	—	—	—
Length	—	—	—	—
No. of Measurements	—	—	—	—
Test Temperature	295 K	295 K	295 K	295 K

C17000–C17510: Annealed; Annealed and Aged
Cold-worked; Cold-worked and Aged

Electromagnetic Properties (All)

3A	3B	4B	4B	4C
C17000	C17000	C17200	C17200	C17200
98.35	98.35	97.65	97.65	97.65
—	—	—	—	—
1.53	1.53	1.86	1.86	1.86
—	—	0.01	0.01	0.01
—	—	0.19	0.19	0.19
—	—	—	—	—
—	—	—	—	—
0.08	0.08	0.02	0.02	0.02
0.04	0.04	0.16	0.16	0.16
—	—	0.07	0.07	0.07
—	—	Sn: 0.01; Zn: 0.03	Sn: 0.01; Zn: 0.03	Sn: 0.01; Zn: 0.03
Annealed	Cold-drawn, 37%, 60%, 84%	Solution treated, 1058 K	Cold-rolled, 17%, 34%	Aged, 588 K, 3 h (b)
—	—	—	—	—
—	—	30 μm	30 μm	30 μm
—	—	—	—	—
Bar, 0.52-cm-dia.	Bar, 0.52-cm-dia.	Strip	Strip	Strip
Round	Round	Flat	Flat	Flat
0.53 cm	(a)	—	—	—
—	—	0.056 cm	0.037, 0.046 cm	0.056 cm
—	—	—	—	—
2	2 per condition	—	—	—
295 K	295 K	295 K	295 K	295 K

(a) Diameter: 37%, 0.041 cm; 60%, 0.33 cm; 84%, 0.21 cm.
(b) Others: Aged, 633 K, 0.088–5.6 h.

Table 15.17, continued

Reference No.	4D	4E	4F	5A
Specification	C17200	C17200	C17200	C17200
Composition (wt%)				
Cu	97.65	97.34	97.39	97.72
Cu + Ag	—	—	—	—
Be	1.86	1.91	1.87	1.83
Ni	0.01	0.02	0.02	0.01
Co	0.19	0.29	0.39	0.22
Ni + Co	—	—	—	—
Ni + Fe + Co	—	—	—	—
Al	0.02	0.06	0.03	0.03
Fe	0.16	0.24	0.22	0.11
Si	0.07	0.14	0.08	0.07
Others (Only ≥ 0.001 wt%)	Sn: 0.01; Zn: 0.03	—	—	Sn: 0.01
Material Condition	Cold-rolled, 17%, 34%, then aged 588 K, 3 h (a)	Aged, 298–753 K, 1 h	Cold-rolled, 21%, then aged, 293–753 K, 1 h	Cold-drawn, 44%
RRR	—	—	—	—
Grain Size	30 μm	30 μm	30 μm	25 μm
Hardness	—	—	—	—
Product Form	Strip	Strip	Strip	Bar
Specimen Type	Flat	Flat	Flat	—
Width or Dia.	—	—	—	—
Thickness	0.037, 0.046 cm	0.051 cm	0.055 cm	—
Length	—	—	—	—
No. of Measurements	—	—	—	—
Test Temperature	295 K	295 K	295 K	295 K

(a) Others: Cold-rolled 34%, then aged, 633 K, 0.088–5.9 h.

5B	5C	5D	5E	5F
C17200	C17200	C17200	C17200	C17200
97.72 — 1.83 0.01 0.22 — — 0.03 0.11 0.07 Sn: 0.01	97.64 — 1.82 0.03 0.18 — — 0.04 0.12 0.15 Sn: 0.02; Pb: 0.002	97.64 — 1.82 0.03 0.18 — — 0.04 0.12 0.15 Sn: 0.02; Pb: 0.002	97.68 — 1.86 0.01 0.22 — — 0.02 0.13 0.07 Sn: 0.01	97.68 — 1.86 0.01 0.22 — — 0.02 0.13 0.07 Sn: 0.01
Cold-drawn, 44%, then aged, 588 K, 2 h	Cold-drawn, 35%	Cold-drawn, 35%, then aged, 588 K, 2 h	Cold-drawn, 33%	Cold-drawn, 33%, then aged, 588 K, 2 h
—	—	—	—	—
25 μm	25 μm	25 μm	35 μm	35 μm
—	R_B 95	R_C 42	R_B 99	R_C 42
Bar	Bar	Bar	Bar	Bar
— — — —	— — — —	— — — —	— — — —	— — — —
—	—	—	—	—
295 K	295 K	295 K	295 K	295 K

Table 15.17, continued

Reference No.	6	7A	7A	7C
Specification	C17200	C17200	C17200	C17200
Composition (wt%)				
Cu	—	97.65	97.65	97.65
Cu + Ag	—	—	—	—
Be	—	2.15	2.15	2.15
Ni	—	—	—	—
Co	—	—	—	—
Ni + Co	—	—	—	—
Ni + Fe + Co	—	—	—	—
Al	—	(a)	(a)	(a)
Fe	—	—	—	—
Si	—	—	—	—
Others (Only ≥ 0.001 wt%)	—	—	—	—
Material Condition	Cold-drawn, 50%, then aged, 588–644 K, 0.5–15 h	Annealed, 1072 K, 1 h	Aged, 569 K, 0.08–1 h	Cold-worked, 50%
RRR	—	—	—	—
Grain Size	—	—	—	—
Hardness	—	—	—	—
Product Form	—	—	—	—
Specimen Type	Wire	Round	Round	Round
Width or Dia.	—	0.48 cm	0.48 cm	0.48 cm
Thickness	—	—	—	—
Length	—	—	—	—
No. of Measurements	—	—	—	—
Test Temperature	295 K	295 K	295 K	295 K

(a) Al + Fe + Si: 0.2 wt%.

C17000–C17510: Annealed; Annealed and Aged
Cold-worked; Cold-worked and Aged

Electromagnetic Properties (All)

7D	8A	8B	8C	8D
C17200	C17200	C17200	C17200	C17200
97.65 — 2.15 — — — — (a) — — —	98.18 — 1.82 — — — — — — — —	98.18 — 1.82 — — — — — — — —	98.18 — 1.82 — — — — — — — —	98.18 — 1.82 — — — — — — — —
Cold-worked, 50%, then aged, 569 K, 0.08–1 h	Annealed	Aged, 573 K, 1–100 h	Cold-drawn, 16–75%	Cold-drawn, 16–75%, then aged, 573 K, 1–100 h
—	—	—	—	—
—	—	—	—	—
—	—	—	—	—
—	—	—	—	—
Round 0.48 cm — —	Wire 0.05 cm — —	Wire 0.05 cm — —	Wire 0.05 cm — —	Wire 0.05 cm — —
—	—	—	—	—
295 K	293 K	293 K	293 K	293 K

(a) Al + Fe + Si: 0.2 wt%.

Table 15.17, continued

Reference No.	9	12	13A	13B
Specification	C17200	C17200	C17200	C17200
Composition (wt%)				
Cu	97.8	—	—	—
Cu + Ag	—	—	—	—
Be	2.2	—	1.81–1.86	1.81–1.86
Ni	—	—	0.01–0.03	0.01–0.03
Co	—	—	0.23–0.27	0.23–0.27
Ni + Co	—	—	—	—
Ni + Fe + Co	—	—	—	—
Al	—	—	0.01–0.03	0.01–0.07
Fe	—	—	0.08–0.10	0.08–0.10
Si	—	—	0.06–0.09	0.06–0.09
Others (Only ≥ 0.001 wt%)	—	—	Sn: 0.01	Sn: 0.01
Material Condition	Aged, 448, 496, or 573 K (a)	Cold-rolled, 11%, then aged, 589 K, 2 h	Annealed	Cold-drawn, 37–94%
RRR	—	—	—	—
Grain Size	9	—	—	—
Hardness	—	—	—	—
Product Form	—	Strip	—	—
Specimen Type	Bar	Flat	Wire	Wire
Width or Dia.	0.32-cm dia.	—	—	—
Thickness	—	0.04 cm	—	—
Length	6.3 cm	—	—	—
No. of Measurements	—	—	—	—
Test Temperature	293 K	293 K	295 K	295 K

(a) Aging times: 488 K, 0.0059–132 h; 496 K, 0.0059–83.3 h; 573 K, 0.008–0.5 h.

*C17000–C17510: Annealed; Annealed and Aged
Cold-worked; Cold-worked and Aged* | *Electromagnetic Properties (All)*

13C	14	15A	15A	16A
C17200	C17200	C17200	C17200	C17200
— — 1.81–1.86 0.01–0.03 0.23–0.27 — — 0.01–0.07 0.08–0.10 0.06–0.09 Sn: 0.01	98.00 — 2.0 — — — — — — — —	~ 97.00 — 1.84 < 0.1 0.22 — — < 0.1 0.12 0.11 Sn, Ag, Zn, Pb, Cr, Mn: < 0.1	~ 97.00 — 1.84 < 0.1 0.22 — — < 0.1 0.12 0.11 Sn, Ag, Zn, Pb, Cr, Mn: < 0.1	97.7 — 2.0 — 0.3 — — — — — —
Cold-drawn, 50%, then aged, 588, 622, or 644 K (a)	Aged, 573 K, 2 h	Annealed	Aged (c)	Annealed
—	1.5	1.28	1.33	1.38
—	—	16 μm	35 μm	—
—	Rockwell 41 (b)	R_B 65	R_C 31	—
—	—	Bar	Bar	—
Wire — — —	— — — —	Round 0.635 cm — 15.2 cm	Round 0.635 cm — 15.2 cm	Flat 0.6 cm 0.01 cm 10 cm
—	—	1 per temperature	1 per temperature	—
295 K	4.2, 77, 295 K	4–273 K	4–273 K	4–300 K

(a) Aging times 0.089–17 h.
(b) Hardness scale not specified.
(c) Aging condition not specified.

Table 15.17, continued

Reference No.	16B	17A	17B	19
Specification	C17200	C17200	C17200	C17200
Composition (wt%)				
Cu	97.7	—	—	97.87
Cu + Ag	—	—	—	—
Be	2.0	1.80	1.83	2.08
Ni	—	—	—	—
Co	0.3	0.1–1.0	0.01–0.1	0.009
Ni + Co	—	—	—	—
Ni + Fe + Co	—	—	—	—
Al	—	(b)	(f)	0.008
Fe	—	—	—	0.018
Si	—	—	—	0.013
Others (Only ≥ 0.001 wt%)	—	All others < 0.01	All others < 0.01	—
Material Condition	Aged, 598 K, 0.95 h or 2.95 h	Cold-rolled (c)	Cold-rolled (c)	Aged, 403 K, 0.02–167 h
RRR	(a)	—	—	—
Grain Size	—	—	—	—
Hardness	—	Knoop 243–332	Knoop 513–541	—
Product Form	—	Strip (d)	Strip (d)	—
Specimen Type	Flat	Flat (e)	Flat (e)	—
Width or Dia.	0.6 cm	1.58 cm	1.78 cm	—
Thickness	0.01 cm	1.08 cm	1.75 cm	—
Length	10 cm	25.4 cm	25.4 cm	—
No. of Measurements	—	—	—	—
Test Temperature	4–300 K	133–250 K	128–260 K	77, 243 K

(a) Aged: 0.95 h, RRR = 1.49; 2.95 h, RRR = 1.64.
(b) Al + Fe + Si: 0.01–0.1 wt%.
(c) Percent cold work not specified.
(d) 0.005-cm-thick and 5.08-cm-wide.
(e) Composite flat specimens fabricated by stacking and compressing pieces of strip material, then fastening together with phosphor-bronze screws.
(f) Al + Co + Fe + Si: 0.01–1.0 wt%.

C17000–C17510: Annealed; Annealed and Aged
Cold-worked; Cold-worked and Aged

Electromagnetic Properties (All)

20	21A	21B	21C	21D
C17500	C17500	C17500	C17510	C17510
96.96 — 0.49 0.06 2.28 — — — 0.09 0.12 —	97.05 — 0.5 — 2.35 — — — — — All others ~ 0.1	97.05 — 0.5 — 2.35 — — — — — All others ~ 0.1	97.59 — 0.41 1.90 — — — — — — All others ~ 0.1	97.59 — 0.41 1.90 — — — — — — All others ~ 0.1
Aged, 753 K, 0.01–31.6 h	Cold-worked, hard	Cold-worked, hard, then aged, 753 K, 0.125–8 h	Cold-worked, hard	Cold-worked, hard, then aged, 753 K, 0.125–8 h
—	—	—	—	—
—	—	—	—	—
Vickers 75–280	Vickers 170	Vickers 220–280	Vickers 160	Vickers 212–255
—	—	—	—	—
— — — —	— — — —	— — — —	— — — —	— — — —
—	—	—	—	—
295 K	295 K	295 K	295 K	295 K

Table 15.17, continued

Reference No.	23A	23B	23C	24A
Specification	C17510	C17510	C17510	C17510
Composition (wt%)				
Cu	—	—	98.02	(b)
Cu + Ag	—	—	—	—
Be	—	—	0.38	0.2–0.6
Ni	—	—	1.60	1.4–2.2
Co	—	—	—	—
Ni + Co	—	—	—	—
Ni + Fe + Co	—	—	—	—
Al	—	—	—	—
Fe	—	—	—	—
Si	—	—	—	—
Others (Only ≥ 0.001 wt%)	—	—	—	—
Material Condition	Aged (a)	Cold-worked, ¼ hard, then aged (a)	Cold-rolled, 21%, then aged, 727–838 K, 8 h	Cold-worked, 40%, then aged, 755 K, 3 h
RRR	—	—	—	—
Grain Size	—	—	—	—
Hardness	—	—	—	—
Product Form	—	—	Strip	—
Specimen Type	—	—	Flat	—
Width or Dia.	—	—	—	—
Thickness	—	—	0.04 cm	—
Length	—	—	—	—
No. of Measurements	—	—	—	—
Test Temperature	295 K	295 K	295 K	293 K

(a) Aging conditions not specified.
(b) Cu + Be + Ni: 99.5 wt%.

24B	25A	25B	25C	25D
C17510	C17510	C17510	C17510	C17510
(a) — 0.2–0.6 1.4–2.2 — — — — — — —	97.7 — 0.40 1.90 — — — — — — —	97.7 — 0.40 1.90 — — — — — — —	97.7 — 0.40 1.90 — — — — — — —	97.7 — 0.40 1.90 — — — — — — —
Cold-worked, then aged (b)	Cold-rolled (c)	Cold-rolled, then aged, 672–811 K, 0.5–5 h (c)	Cold-rolled, then aged (b)	Cold-worked, then aged (d)
—	—	—	—	—
—	—	—	—	—
—	—	—	—	—
—	Sheet, 0.02-cm-thick	—	—	—
— — — —	Flat — — —	— — — —	— — — —	— — — —
—	—	—	—	—
293 K	295 K	295 K	295 K	295 K

(a) Cu + Be + Ni: 99.5 wt%.
(b) Percent cold work and aging conditions not specified.
(c) Percent cold work not specified.
(d) Aging conditions considered proprietary.

Table 15.17, continued

Reference No.	26	27A	27B	27C
Specification	C17510	C17510	C17510	C17510
Composition (wt%)				
Cu	—	97.95	97.95	97.95
Cu + Ag	97.6	—	—	—
Be	0.38	0.38	0.38	0.38
Ni	1.8	1.67	1.67	1.67
Co	—	—	—	—
Ni + Co	—	—	—	—
Ni + Fe + Co	—	—	—	—
Al	—	—	—	—
Fe	—	—	—	—
Si	—	—	—	—
Others (Only ≥ 0.001 wt%)	—	—	—	—
Material Condition	Cold-rolled, 37%, then aged, 755 K, 2 h	Cold-rolled, 37%, 60%	Cold-rolled, 37%, then aged (b)	Cold-rolled, 60%, 80%, then aged, 593–723 K (c)
RRR	2.65	—	—	—
Grain Size	—	—	—	—
Hardness	R_F 92	(a)	—	(d)
Product Form	Plate, 2.5-cm-thick	Plate, 1.27-cm-thick	Plate, 1.27-cm-thick	Plate, 1.27-cm-thick
Specimen Type	—	Flat	Flat	Flat
Width or Dia.	—	0.64 cm	0.64 cm	0.64 cm
Thickness	—	—	—	—
Length	14.0 cm	—	—	—
No. of Measurements	—	—	—	—
Test Temperature	4, 76, 295 K	295 K	295 K	295 K

(a) 37%, R_C 27.5; 60%, R_C 29.5.
(b) Aging conditions not specified.
(c) Aging times: 593 K, 3–70 h; 633 K, 2–36 h; 673 K, 1–16 h; 693 K, 1–6 h; 723 K, 1–3 h.
(d) 593 K, R_C 33.5–34; 633 K, R_C 31.5–33; 673 K, R_C 21.5–31.5; 693 K, R_C 24–29.5; 723 K, R_C 19.5–24.5.

C17000–C17510: Annealed; Annealed and Aged
Cold-worked; Cold-worked and Aged

Electromagnetic Properties (All)

28A	28B	28C	30A	30B
C17510	C17510	C17510	C17510	C17510
Balance	Balance	Balance	—	—
—	—	—	—	—
0.38	0.40	0.41	0.2–0.6	0.2–0.6
1.79	1.91	1.95	1.4–2.2	1.4–2.2
0.05	0.01	0.10	—	—
—	—	—	—	—
—	—	—	—	—
0.01	0.01	0.01	—	—
0.03	0.01	0.04	—	—
0.02	0.02	0.03	—	—
(a)	(b)	(d)	—	—
Cold-rolled, 37%, then aged, 755 K, 2 h	(c)	(c)	Annealed	Aged, 755 K, 3 h
—	—	—	—	—
—	—	—	—	—
—	—	R_B 95–99	DPH 80	DPH 229
Plate, 2.5-cm-thick	Plate, 2.5-cm-thick	Bar	Strip	Strip
—	—	—	Flat	Flat
—	—	—	—	—
—	—	—	—	—
—	—	—	—	—
—	—	—	—	—
295 K	295 K	295 K	295 K	295 K

(a) Zr: 0.03; Sn: 0.01; Zn: 0.01; Ag: 0.01; Cr: 0.005; Pb: 0.002; Mn: 0.002.
(b) Zn: 0.02; Ag: 0.01; Zr: 0.01; Sn: < 0.01; Ti: < 0.01; Cr: 0.004; Pb: 0.003; Mn: 0.001.
(c) Percent cold work and aging conditions not specified.
(d) Ag: 0.09; Sn: 0.02; Zn: 0.02; Cr: 0.007; Mn: 0.004; Pb: 0.003.

Table 15.17, continued

Reference No.	30C	30D	31	32
Specification	C17510	C17510	C17510	C17200
Composition (wt%)				
Cu	—	—	97.8	—
Cu + Ag	—	—	—	—
Be	0.2–0.6	0.2–0.6	0.4	2.0
Ni	1.4–2.2	1.4–2.2	1.8	—
Co	—	—	—	—
Ni + Co	—	—	—	—
Ni + Fe + Co	—	—	—	—
Al	—	—	—	—
Fe	—	—	—	0.05–0.5
Si	—	—	—	—
Others (Only ≥ 0.001 wt%)	—	—	—	—
Material Condition	Cold-rolled, 11%, 21%, 37%	Cold-rolled, 11%, 21%, 37%, then aged, 755 K (b)	Cold-worked, aged (e)	Aged, 588 K, 3 h; others, 644–866 K, 1 h
RRR	—	—	—	—
Grain Size	—	(c)	—	—
Hardness	(a)	(d)	—	—
Product Form	Strip	Strip	Strip	—
Specimen Type	Flat	Flat	Flat	Round
Width or Dia.	—	—	—	0.31 cm
Thickness	—	—	—	—
Length	—	—	—	5.0 cm
No. of Measurements	—	—	—	—
Test Temperature	295 K	295 K	295, 299, 316 K	295 K

(a) DPH: 11%, 110; 21%, 115; 37%, 120.
(b) Aging time: 37%, 2 h; others not given.
(c) Grain size: 11%, 20 μm; others not given.
(d) DPH: 37%, 265; others not given.
(e) Percent cold work and aging conditions not specified.

REFERENCES

1. Yoshida, H., and Murakami, Y., "The Effects of Neutron Irradiation on Aging Characteristics of Copper--1.5 and 2.0 wt% Beryllium Alloys," Journal of the Japan Institute of Metals 33, 775–781 (1969).

2. Bassett, W. H, "Beryllium-Copper Alloys," Proceedings of the Institute of Metals Division, American Institute of Mining and Metallurgical Engineers E27, 218–232 (1927).

3. Crampton, D. K., Burghoff, H. L, and Stacy, J. T., "Effect of Cold-Work upon Electrical Conductivity of Copper Alloys," Transactions of the American Institute of Mining and Metallurgical Engineers 143, 228–245 (1941).

4. Richards, J. T., and Murakawa, K., "Effect of Cold Rolling and Heat Treatment on the Directional Properties of Beryllium Copper Strip," Proceedings of the American Society for Testing Materials 57, 791–807 (1957).

5. Richards, J. T., "An Evaluation of Several Static and Dynamic Methods for Determining Elastic Moduli," in Symposium on Determination of Elastic Constants, American Society for Testing Materials, Philadelphia, PA, 71–100 (1952).

6. Richards, J. T., "Beryllium Copper Wire: Property and Design Considerations," Wire and Wire Products 27, 257–262, 304–307 (1952).

7. Billington, D. S., and Siegel, S., "Effect of Nuclear Radiation on Metal," Metal Progress 58, 847–852 (1950).

8. Gruhl, W., and Wassermann, G., "Über den Verlauf der Ausscheidung bei Kupfer-Beryllium-Legierungen," Metall 5, 93–98 (1951).

9. Murray, G. T., and Taylor, W. E., "Effect of Neutron Irradiation on a Supersaturated Solid Solution of Beryllium in Copper," Acta Metallurgica 2, 52–62 (1954).

10. Murakami, Y., Yoshida, H., and Yamamoto, S., "On the Aging Characteristics of Copper–2 wt% Beryllium Alloys with or without Additional Elements," Transactions of the Japan Institute of Metals 9, 11–18 (1968).

11. Richards, J. T., "Beryllium Copper," Materials & Methods 31, 75–89 (1950).

12. Fox, A., "Stress Relaxation in Bending of Copper Beryllium Alloy Strip," Journal of Testing and Evaluation 8, 119–126 (1980).

13. Richards, J. T., Levan, R. K., and Smith, E. M., "The Influence of Cold Work and Heat Treatment on the Engineering Properties of Beryllium Copper Wire," Proceedings of the American Society for Testing Materials 51, 771–789 (1951).

14. Berman, R., Foster, E. L., and Rosenberg, H. M., "The Thermal Conductivity of Some Technical Materials at Low Temperatures," British Journal of Applied Physics 6, 181–182 (1955).

15. Clark, A. F., Childs, G. E., and Wallace, G. H., "Electrical Resistivity of Some Engineering Alloys at Low Temperatures," Cryogenics 10, 295–305 (1970).

REFERENCES

16. Feid, S., Gröger, and Stangler, F., "Temperaturabhängigkeit der Hallkonstante der Kupferberylliumlegierung CuBe2 zwischen 6 und 300 K," Zeitschrift für Metallkunde 74, 246–249 (1983).

17. Watson, T. W., and Flynn, D. R., "Thermal Conductivity and Electrical Resistivity of Beryllium Copper Foil," Transactions of the Metallurgical Society of AIME 242, 876–880 (1968).

18. Yoshida, H., Yamamoto, S., Murakami, Y., and Kodaka, H., "The Effects of Neutron Irradiation on Ageing and Precipitation Phenomena in Copper-Beryllium Alloys with or without Additional Elements," Transactions of the Japan Institute of Metals 12, 229–237 (1971).

19. Vigier, G., Pelletier, J. M., and Merlin, J., "Temperature Dependence of the Electrical Resistivity of Alloys with Guinier-Preston Zones," Journal of Physics F: Metal Physics 13, 1677–1687 (1983).

20. Pfeiffer, I., and Hönig, A., "Berylliumleitbronzen," Metall 22, 1125–1129 (1968).

21. Weinlich, W., "CuNiBe--eine Variante der aushärtbaren CuCoBe-Knetlegierungen," Metall 34, 135–138 (1980).

22. Mollard, F. R., Wikle, K. G., and Chaudhry, A. R., "Copper-Beryllium for Elevated Temperature Electronic and Electrical Applications," in High Conductivity Copper and Aluminum Alloys, Eds. E. Ling and P. W. Taubenblat, The Metallurgical Society of AIME, New York, 147–168 (1984).

23. Spiegelberg, W. D., and Guha, A., "Properties of Beryllium Copper Alloy C17510," in Copper and Copper Alloys for Fusion Reactor Applications, Eds. F. W. Wiffen and R. E. Gold, Oak Ridge National Laboratory, Oak Ridge, TN, CONF-830466, 143–150 (1984).

24. Stevenson, R. D., and Rosenwasser, S. N., "Characteristics, Properties and Fabrication of CuBeNi Alloy (C17510)," Pacific-Sierra Research Corp., Del Mar, CA, PSR Report 1545, MIT P.O. FCA-534436, 19 pp (1985).

25. Guha, A., "Development of a High Strength High Conductivity Cu-Ni-Be Alloy," in High Conductivity Copper and Aluminum Alloys, Eds. E. Ling and P. W. Taubenblat, The Metallurgical Society of AIME, New York, 133–145 (1984).

26. Reed, R. P., Walsh, R. P., and Fickett, F. R., "Properties of CDA 104, 155, and 175 Copper Alloys, in Materials Studies for Magnetic Fusion Energy Applications at Low Temperatures--X, Ed. R. P. Reed, National Bureau of Standards, Boulder, CO, NBSIR 87-3067, 83–126 (1987).

27. Rotem, A., and Rosen, A., "Improvement of Strength and Electrical Conductivity of Copper Alloy by Means of Thermo-Mechanical Treatment," Metallurgical Transactions 16A, 2073–2077 (1985).

28. Bushnell, C. W., "A Compendium of Beryllium Copper (Alloy C17510) Data for the CIT Device," Princeton Plasma Physics Laboratory, Princeton, NJ, F-880909-PPL-01 (1988).

29. Pawel, R. E., and Williams, R. K., "Survey of Physical Property Data for Several Alloys," Oak Ridge National Laboratory, Oak Ridge, TN, ORNL/TM-9616, 37 pp (1985).

REFERENCES

30. Guha, A., and Spiegelberg, W. D., "Development of a Nickel-containing Beryllium Copper Alloy for Connector Applications," in Annual Connector and Interconnection Technology Symposium, 133–140 (1979).

31. Guha, A., "High Performance Mill Hardened Beryllium Copper C17510 Strip for Electrical and Electronic Applications," in Sixteenth Annual Connectors and Interconnection Technology Symposium Proceedings, Electronic Connector Study Group Inc., 131–140 (1983).

32. Bernstein, H., "Reduction of Magnetic Susceptibility in Beryllium-Copper," Transactions of the Metallurgical Society of AIME 212, 225–226 (1958).

33. Hönig, A., and Koeppen, H., "Über die vielseitige Verwendung von Kupfer-Beryllium," Metall 28, 1059–1062 (1974).

DATA SOURCES AND ANALYSIS

A set of 304 measurements of 0.2%-offset tensile yield strength (σ_y) at temperatures between 4 and 297 K was selected for analysis because degree of cold work, Sn and P content, and grain size were reported (References 16.1–16.11). In a few cases, because the data appeared very useful, reasonable assumptions were made for one of these parameters. For Reference 16.2, P content, [P], was taken as the arithmetic average of the C51000 specification limits. The grain size, *d*, was not specified in References 16.6, 16.9, and 16.10, and values based in part on the heat treatment of the material were assigned (80, 50, and 50 μm, respectively). Degree of *CW* (percent reduction of thickness or area), ranged from 0 to 85%; Sn content, [Sn], ranged from 0 to 10.10 wt%; [P] ranged from 0 to 0.40 wt%; and *d*, from 0.5 to 250 μm. Four measurements from Reference 16.6 at higher cold-work percentages (91, 94.8, 95.7, and 97.3%) were dropped from the data set because they differed by more than two standard deviations from an equation that fitted the rest of the data well.

Products were in sheet (Reference 16.6), wire (Reference 16.9), strip (References 16.1–16.3), and bar form (References 16.4, 16.5, 16.7, 16.10, and 16.11). Product form was not reported in Reference 16.8. Data on wire from Reference 16.9 were included because there are very few measurements at 4 K. Other data on wire at 295 K were not included because an adequate amount of data on other product forms was available at this temperature and tensile measurements on wire may not be comparable to measurements on other product forms. The type of *CW* was cold rolling in all cases except for the bar and wire stock which were drawn. The cold rolling reported in Reference 16.1 was carried out in the laboratory and may have differed somewhat from standard commercial practice. The available information on the characterization of materials and measurements is given in Table 16.5 at the end of the C50100–C52400 tensile properties section.

Because an extensive data set was available, it seemed appropriate to develop a predictive equation for σ_y as a function of temperature (*T*), *CW*, [Sn], [P], *d*, and any other relevant parameters. The alloying element, Fe, although present in commercial material, was judged not to affect σ_y significantly. Reference 16.6 reported that the tensile properties were not affected by the variation in Fe content, [Fe], from 0.02 to 0.12 wt% in two different lots of C51000. Measurements of ultimate tensile strength and strain to failure in high [Sn], low [P] bronzes were in agreement, within the measurement error, for [Fe] of either 0.05 wt% or 0.94 wt% (Reference 16.12). Reference 16.13 states that [Fe] of up to 0.28 wt% causes only a slight Increase of tensile strength and amounts above 0.28% actually cause a decrease because the Fe enters into a secondary phase. Further data on the dependence of tensile properties of phosphor bronzes on [Fe] are not available at present, and [Fe] was generally not reported in References 16.1–16.11.

The data set was not ideal for developing a predictive equation relating σ_y to *T*, [Sn], and *CW*, because only a few measurements from 4 to 295 K on cold-worked material have been reported (see Table 16.1). However, an excellent set of 132 measurements at 295 K is available from Reference 16.1 in which [Sn], *CW*, *d*, and [P] were varied systematically. Therefore, regression analysis of σ_y upon [Sn], *CW*, *d*, and [P] was first carried out on this data set to establish the best functional forms. In particular, this data set was used to develop the best expressions for the interactive effect of *CW* and [Sn]. It is clear from the results presented in Reference 16.1 that such an interactive effect exists: in Figure 16.1, where σ_y is plotted as a function of *CW*, the slope of the curves increases with increasing [Sn]. The data set from Reference 16.1 was also used to test the effect of *d* upon σ_y. Although a $d^{-1/2}$ term fitted the data only slightly better than a d^{-1} term, $d^{-1/2}$ was chosen because it is the traditional Hall-Petch expression.

Analysis of data from 77 to 295 K, as presented in Reference 16.7, led to an examination of interactive terms for [Sn] and temperature, *T*, although the equation that was found to fit the data best was not of the same form as that presented in Reference 16.7. In particular, no evidence was found to justify $[Sn]^{1/2}d^{-1/2}$ and $[Sn]^{1/2}T^{1/3}d^{-1/2}$ terms, but addition of a $[Sn]^{1/2}$ term to [Sn] and $[Sn]^2$ terms, and the use of a negative $[Sn]^{1/2}T^{1/3}$ term for the temperature dependence represented the data well. Figure 16.2, which presents σ_y as a function of *T* for various

[Sn] values, also shows a change in slope with increasing [Sn]. Data on cold-worked material from References 16.10 and 16.11 are included in this graph to indicate that they follow the $T^{1/3}$ temperature dependence to a first approximation. Figure 16.3, which shows σ_y vs. $[Sn]^{1/2}$ for temperatures between 4 and 300 K, illustrates both the dependence on $[Sn]^{1/2}$ and the nonlinear temperature dependence. These data,taken from Reference 16.14, were not used in the analysis because σ_y is not measured with the 0.2% offset method.

When the form of the equation had been established from the data sets with extensive parametric variation, data from References 16.10 and 16.11 were added (8 measurements between 4 and 295 K on drawn bar product) to determine the final coefficients. Table 1.17 in the introductory section gives cold-work equivalents for cold-rolled and drawn tempers. Therefore, for cold-drawn bar product (References 16.4, 16.5, 16.10, and 16.11) percentages for cold rolling were substituted in the *CW* terms in the equation in place of the percentage of reduction of area. This did not improve the fit of the equation to the data, so the percentage reduction of area by drawing was used for *CW* in the analysis for measurements on bar stock. This is discussed further below.

RESULTS

The final equation expressing the dependence of σ_y in MPa upon the parameters reviewed above is

$$\begin{aligned}\sigma_y = & -5.972 + 28.61\,[Sn] - 1.584\,[Sn]^2 \\ & + 84.14\,[Sn]^{1/2} + 12.02\,CW - 0.1024\,(CW)^2 \\ & + 277.9\,d^{-1/2} + 88.08\,[P] + 0.06416\,CW[Sn] \\ & - 0.02421\,CW[Sn]^2 - 13.01\,T^{1/3}[Sn]^{1/2}\end{aligned} \qquad (16\text{-}1)$$

(S.D. = 34.523 MPa),

where 4 K $\leq T \leq$ 297 K. The standard deviations of the coefficients are: constant term, 8.486; [Sn], 5.53; $[Sn]^2$, 0.409; $[Sn]^{1/2}$, 12.01; *CW*, 0.32; CW^2, 0.0043; $d^{-1/2}$, 12.28; [P], 21.01; *CW*[Sn], 0.0898; $CW[Sn]^2$, 0.00903; and $T^{1/3}[Sn]^{1/2}$, 1.19. The set of σ_y measurements and parameters are presented in Table 16.1, which also gives the σ_y value predicted from the analysis described.

Figure 16.4 indicates the fit of the data to Equation (16-1). The scatter band represents two standard deviations about the straight line, which indicates agreement between the measured and predicted values of σ_y. The variance of the data was assumed to be normally distributed and constant throughout the range of the predicted values. Table 16.1 presents the σ_y values calculated from Equation (16-1) as well as the measured σ_y and the parameters [Sn], *CW*, *d*, [P], and *T*. The available characterization of materials and measurements is given in Table 16.5 at the end of the tensile properties section.

DISCUSSION

The few available measurements of σ_y on cold-worked material below 295 K often fall outside the scatter band. This is true also of several measurements on 60% cold-worked sheet not included in the analysis (Reference 16.21). Equation (16-1) represents the best determination of the dependence of σ_y on [Sn], *CW*, *d*, [P], and *T* that could be obtained from the available database, but probably represents cold-worked material only within ± 4 standard deviations.

In agreement with these results for phosphor bronzes, analysis of the dependence of σ_y upon *CW* for C10100–C10700 coppers (pages 2-13–2-19 and 2-22–2-28) also showed that a better fit of the data was obtained when the cold-work term in the equation represents the reduction of thickness for cold-rolled product and reduction of area for drawn product. The alternative, to use the temper equivalents presented in Table 1.5, resulted in a worse fit of the data. Thus, the higher, drawn product value is used in the cold-work term of Equation (16-1). Reference 16.15 reported that as the diameter of their phosphor-bronze specimens from drawn bar decreased, i.e., as specimens were obtained that sampled less of the exterior of the bar, the measured σ_y increased. This apparent anomaly has not been investigated further. The same anomaly may have affected the measurements reported in References 16.4, 16.5, 16.10, and 16.11, i.e., a higher value of σ_y was measured than would be expected from the nominal value of *CW*, since these specimens also were obtained from the interior of the bar stock. If so, the use of higher values for *CW* would improve the agreement of the drawn

C50100–C52400: Annealed; Cold-worked

Tensile Yield Strength vs. [Sn], Cold Work, Grain Size, [P] (4–297 K)

product measurements with the cold-rolled product measurements. It was not feasible, given the limited amount of data available, to develop separate equations for the two types of product.

Reference 16.6 presents additional data (not used in this analysis) on material subjected to other forms of thermomechanical processing. C51000 phosphor bronze was cold rolled to 97.3% and subsequently annealed for 2 h at various temperatures in an attempt to recover ductility without losing strength. Results and mechanisms are discussed in the reference.

Table 16.1. Tensile Yield Strength Dependence on [Sn], *CW*, *d*, and [P] (4–297 K).

Yield Strength, Measured, MPa	Yield Strength, Predicted, MPa	[Sn], wt%	Cold Work, %	Grain Size, μm	[P], wt%	Test Temperature, K	Reference No.
82.3	54.8	0.42	0.0	35.0	0.04	295.0	1
327.0	264.0	0.42	20.6	35.0	0.07	295.0	1
387.0	372.0	0.42	37.6	35.0	0.07	295.0	1
415.0	440.0	0.42	50.2	35.0	0.07	295.0	1
439.0	423.0	0.42	60.6	35.0	0.04	295.0	1
457.0	445.0	0.42	68.7	35.0	0.07	295.0	1
98.5	79.5	0.42	0.0	15.0	0.04	295.0	1
322.0	264.0	0.42	20.6	15.0	0.07	295.0	1
393.0	399.0	0.42	37.4	15.0	0.04	295.0	1
488.0	448.0	0.42	60.6	15.0	0.07	295.0	1
452.0	441.0	0.42	68.6	15.0	0.04	295.0	1
426.0	438.0	0.42	50.2	15.0	0.07	295.0	1
70.6	69.8	0.96	0.0	35.0	0.06	295.0	1
347.0	264.0	0.95	20.6	35.0	0.06	295.0	1
406.0	399.0	0.96	37.6	35.0	0.06	295.0	1
448.0	445.0	0.95	50.2	35.0	0.06	295.0	1
465.0	458.0	0.95	60.5	35.0	0.06	295.0	1
486.0	453.0	0.95	68.6	35.0	0.06	295.0	1
83.7	94.6	0.95	0.0	15.0	0.06	295.0	1
351.0	309.0	0.96	20.9	15.0	0.06	295.0	1
426.0	423.0	0.95	37.4	15.0	0.06	295.0	1
458.0	469.0	0.95	50.2	15.0	0.06	295.0	1
484.0	448.0	0.95	60.6	15.0	0.06	295.0	1
502.0	448.0	0.95	68.7	15.0	0.06	295.0	1
90.5	96.3	2.07	0.0	35.0	0.04	295.0	1
373.0	309.0	2.07	20.9	35.0	0.07	295.0	1
446.0	448.0	2.07	37.4	35.0	0.07	295.0	1
488.0	523.0	2.07	50.1	35.0	0.07	295.0	1
513.0	523.0	2.07	60.4	35.0	0.07	295.0	1
558.0	523.0	2.07	68.6	35.0	0.07	295.0	1
103.0	121.0	2.07	0.0	15.0	0.07	295.0	1
383.0	309.0	2.07	20.6	15.0	0.07	295.0	1
472.0	474.0	2.07	37.6	15.0	0.07	295.0	1
531.0	523.0	2.07	50.1	15.0	0.07	295.0	1
561.0	548.0	2.07	60.6	15.0	0.07	295.0	1
562.0	548.0	2.07	68.6	15.0	0.07	295.0	1
105.0	114.0	2.96	0.0	35.0	0.07	295.0	1
379.0	356.0	2.96	20.9	35.0	0.07	295.0	1
479.0	481.0	2.96	37.0	35.0	0.07	295.0	1
535.0	544.0	2.96	50.1	35.0	0.07	295.0	1
579.0	568.0	2.96	60.3	35.0	0.07	295.0	1

Table 16.1, continued

Yield Strength, Measured, MPa	Yield Strength, Predicted, MPa	[Sn], wt%	Cold Work, %	Grain Size, µm	[P], wt%	Test Temperature, K	Reference No.
696.0	573.0	2.96	68.2	15.0	0.07	295.0	1
170.0	139.0	2.96	0.0	15.0	0.07	295.0	1
411.0	376.0	2.96	20.4	15.0	0.07	295.0	1
507.0	509.0	2.96	37.5	15.0	0.07	295.0	1
567.0	568.0	2.96	49.9	15.0	0.07	295.0	1
603.0	589.0	2.96	60.5	15.0	0.07	295.0	1
620.0	597.0	2.96	68.5	35.0	0.07	295.0	1
117.0	132.0	4.00	0.0	35.0	0.07	295.0	1
390.0	384.0	4.00	20.9	35.0	0.07	295.0	1
603.0	520.0	4.00	37.5	35.0	0.07	295.0	1
577.0	528.0	4.00	50.2	35.0	0.07	295.0	1
645.0	616.0	4.00	60.5	35.0	0.07	295.0	1
646.0	627.0	4.00	68.6	35.0	0.07	295.0	1
202.0	156.0	4.00	0.0	15.0	0.07	295.0	1
457.0	407.0	4.00	20.4	15.0	0.07	295.0	1
583.0	546.0	4.00	37.1	15.0	0.07	295.0	1
620.0	610.0	4.00	50.0	15.0	0.07	295.0	1
683.0	687.0	4.00	60.5	15.0	0.07	295.0	1
696.0	699.0	4.00	68.5	15.0	0.07	295.0	1
152.0	148.0	5.20	0.0	35.0	0.07	295.0	1
431.0	408.0	5.20	20.7	35.0	0.07	295.0	1
583.0	589.0	5.20	36.9	35.0	0.07	295.0	1
696.0	627.0	5.20	50.2	35.0	0.07	295.0	1
671.0	662.0	5.20	60.4	35.0	0.07	295.0	1
696.0	674.0	5.20	68.3	35.0	0.07	295.0	1
220.0	173.0	5.20	0.0	15.0	0.07	295.0	1
451.0	718.0	5.20	20.9	15.0	0.07	295.0	1
571.0	586.0	5.20	36.9	15.0	0.07	295.0	1
696.0	652.0	5.20	50.0	15.0	0.07	295.0	1
683.0	687.0	5.20	60.3	15.0	0.07	295.0	1
706.0	699.0	5.20	68.2	15.0	0.07	295.0	1
169.0	191.0	8.12	0.0	35.0	0.05	295.0	1
405.0	445.0	8.12	20.9	15.0	0.05	295.0	1
683.0	605.0	8.12	37.1	35.0	0.05	295.0	1
663.0	699.0	8.12	50.2	35.0	0.05	295.0	1
727.0	737.0	8.12	60.3	35.0	0.05	295.0	1
757.0	757.0	8.12	68.5	35.0	0.05	295.0	1
235.0	191.0	8.12	0.0	15.0	0.05	295.0	1
514.0	474.0	8.12	20.9	15.0	0.05	295.0	1
645.0	634.0	8.12	37.5	15.0	0.05	295.0	1
696.0	718.0	8.12	50.2	35.0	0.05	295.0	1
738.0	763.0	8.12	60.5	15.0	0.05	295.0	1
786.0	748.0	8.12	68.2	35.0	0.05	295.0	1
177.0	156.0	10.10	0.0	35.0	0.07	295.0	1
447.0	455.0	10.10	20.9	35.0	0.07	295.0	1
587.0	620.0	10.10	37.2	35.0	0.07	295.0	1
681.0	718.0	10.10	50.2	15.0	0.07	295.0	1
741.0	768.0	10.10	60.5	35.0	0.07	295.0	1
779.0	783.0	10.10	68.6	35.0	0.04	295.0	1
243.0	189.0	10.10	0.0	15.0	0.04	295.0	1
489.0	473.0	10.10	20.3	15.0	0.04	295.0	1

C50100–C52400: Annealed; Cold-worked

Tensile Yield Strength vs. [Sn], Cold Work, Grain Size, [P] (4–297 K)

Table 16.1, continued

Yield Strength, Measured, MPa	Yield Strength, Predicted, MPa	[Sn], wt%	Cold Work, %	Grain Size, µm	[P], wt%	Test Temperature, K	Reference No.
647.0	686.0	10.10	37.1	15.0	0.04	295.0	1
706.0	733.0	10.10	49.6	15.0	0.04	295.0	1
756.0	783.0	10.10	60.2	10.0	0.04	295.0	1
796.0	807.0	10.10	68.2	15.0	0.04	295.0	1
134.0	139.0	2.81	0.0	35.0	0.39	295.0	1
418.0	379.0	2.81	20.6	35.0	0.39	295.0	1
538.0	507.0	2.81	37.5	35.0	0.35	295.0	1
569.0	565.0	2.81	50.0	35.0	0.39	295.0	1
638.0	686.0	2.81	60.3	35.0	0.39	295.0	1
672.0	593.0	2.81	68.2	35.0	0.39	295.0	1
153.0	185.0	3.97	0.0	15.0	0.40	295.0	1
458.0	434.0	3.97	20.6	15.0	0.40	295.0	1
572.0	587.0	3.97	37.5	10.0	0.40	295.0	1
652.0	638.0	3.97	49.8	15.0	0.40	295.0	1
638.0	686.0	3.97	60.3	10.0	0.40	295.0	1
727.0	676.0	3.97	68.5	75.0	0.40	295.0	1
122.0	145.0	3.97	0.0	75.0	0.40	295.0	1
443.0	396.0	3.97	20.6	75.0	0.40	295.0	1
525.0	686.0	3.97	37.5	75.0	0.40	295.0	1
589.0	638.0	3.97	50.0	15.0	0.40	295.0	1
598.0	686.0	3.97	60.7	75.0	0.40	295.0	1
589.0	638.0	3.97	58.0	75.0	0.40	295.0	1
166.0	185.0	0.05	0.0	35.0	0.40	295.0	1
466.0	436.0	5.00	20.6	35.0	0.40	295.0	1
598.0	686.0	0.05	37.5	35.0	0.40	295.0	1
671.0	652.0	5.00	60.2	35.0	0.40	295.0	1
711.0	686.0	5.00	60.7	35.0	0.40	295.0	1
756.0	697.0	5.00	68.5	35.0	0.40	295.0	1
63.7	45.4	0.05	0.0	35.0	0.05	295.0	1
266.0	251.0	5.00	20.6	35.0	5.00	295.0	1
338.0	352.0	0.05	37.1	35.0	0.05	295.0	1
335.0	387.0	5.00	50.0	35.0	5.00	295.0	1
352.0	352.0	0.05	60.3	35.0	0.05	295.0	1
371.0	387.0	5.00	50.0	35.0	5.00	295.0	1
70.2	70.2	0.05	0.0	10.0	0.05	295.0	1
273.0	274.0	5.00	20.6	15.0	5.00	295.0	1
331.0	377.0	0.05	37.5	10.0	0.05	295.0	1
355.0	415.0	5.00	50.1	15.0	5.00	295.0	1
374.0	783.0	0.00	60.8	10.0	0.05	295.0	1
355.0	413.0	5.00	58.8	15.0	5.00	295.0	1
214.0	197.0	0.05	0.0	10.0	0.19	295.0	2
372.0	396.0	5.00	11.0	75.0	0.19	295.0	2
166.0	459.0	0.05	21.0	10.0	0.19	295.0	2
569.0	593.0	5.00	37.0	75.0	0.19	295.0	2
641.0	672.0	5.00	50.0	10.0	0.19	295.0	2
589.0	708.0	5.00	50.0	15.0	0.19	295.0	2
152.0	459.0	5.00	0.0	35.0	0.19	295.0	2
310.0	396.0	5.00	11.0	35.0	0.19	295.0	2
400.0	418.0	5.00	21.0	35.0	0.19	295.0	2
503.0	557.0	5.00	37.0	35.0	0.19	295.0	2
579.0	631.0	5.00	50.0	35.0	0.19	295.0	2

Table 16.1, continued

Yield Strength, Measured, MPa	Yield Strength, Predicted, MPa	[Sn], wt%	Cold Work, %	Grain Size, μm	[P], wt%	Test Temperature, K	Reference No.
641.0	667.0	5.00	61.0	35.0	0.19	295.0	2
138.0	148.0	8.07	0.0	50.0	0.19	295.0	2
290.0	297.0	5.00	11.0	50.0	0.19	295.0	2
386.0	415.0	5.00	21.0	50.0	0.19	295.0	2
476.0	619.0	8.07	37.0	50.0	0.19	295.0	2
545.0	624.0	8.07	50.0	50.0	0.19	295.0	2
614.0	659.0	8.07	61.0	50.0	0.19	295.0	2
124.0	141.0	8.07	0.0	75.0	0.19	295.0	2
276.0	290.0	5.00	11.0	10.0	0.19	295.0	2
372.0	403.0	5.00	21.0	75.0	0.19	295.0	2
462.0	542.0	5.00	37.0	10.0	0.19	295.0	2
531.0	646.0	5.00	50.0	75.0	0.19	295.0	2
669.0	652.0	5.00	61.0	75.0	0.19	295.0	2
510.0	545.0	4.91	37.1	35.0	0.07	295.0	3
669.0	619.0	4.91	60.5	40.0	0.07	295.0	3
572.0	635.0	4.91	30.1	8.0	0.07	295.0	3
717.0	693.0	4.91	60.5	10.0	0.07	295.0	3
427.0	415.0	4.91	22.2	40.0	0.07	295.0	3
614.0	184.0	4.91	23.8	10.0	0.07	295.0	3
572.0	542.0	4.91	35.5	25.0	0.07	295.0	3
607.0	659.0	4.91	39.6	10.0	0.07	295.0	3
689.0	559.0	4.91	35.7	35.0	0.07	295.0	3
614.0	619.0	4.91	32.9	35.0	0.07	295.0	3
552.0	564.0	4.91	[illegible]	35.0	0.07	295.0	3
669.0	619.0	4.91	50.3	35.0	0.07	295.0	3
717.0	542.0	4.91	56.2	8.0	0.07	295.0	3
669.0	693.0	4.91	60.5	25.0	0.07	295.0	3
689.0	646.0	4.91	57.9	35.0	0.07	295.0	3
669.0	648.0	4.91	60.5	45.0	0.07	295.0	3
641.0	646.0	4.91	60.5	[illegible]	0.07	295.0	3
667.0	637.0	4.91	45.5	10.0	0.07	295.0	3
124.0	659.0	4.91	65.4	25.0	0.07	295.0	3
669.0	658.0	4.91	65.6	40.0	0.07	295.0	3
196.0	172.0	4.32	0.0	25.0	0.07	295.0	4
343.0	344.0	4.32	15.2	10.0	0.38	295.0	4
425.0	485.0	4.32	30.1	35.0	0.38	295.0	4
614.0	619.0	4.32	50.1	50.0	0.07	295.0	4
641.0	521.0	3.72	36.0	75.0	0.07	295.0	4
177.0	173.0	3.67	0.0	40.0	0.07	295.0	4
765.0	635.0	4.91	36.0	25.0	0.07	295.0	4
196.0	184.0	8.19	0.0	20.0	0.07	295.0	4
138.0	156.0	8.19	0.0	75.0	0.07	295.0	4
339.0	364.0	8.19	15.2	100.0	0.07	295.0	4
445.0	521.0	8.19	30.1	35.0	0.07	295.0	4
642.0	619.0	8.19	50.1	100.0	0.07	295.0	4
196.0	156.0	9.76	0.0	16.0	0.12	295.0	4
146.0	184.0	9.76	0.0	58.0	0.12	295.0	4
347.0	377.0	9.76	15.2	75.0	0.12	295.0	4
485.0	543.0	9.76	30.1	90.0	0.12	295.0	4
752.0	698.0	9.76	50.1	95.0	0.12	295.0	4
434.0	476.0	4.28	27.0	25.0	0.29	295.0	5

C50100–C52400: Annealed; Cold-worked

Tensile Yield Strength vs. [Sn], Cold Work, Grain Size, [P] (4–297 K)

Table 16.1, continued

Yield Strength, Measured, MPa	Yield Strength, Predicted, MPa	[Sn], wt%	Cold Work, %	Grain Size, μm	[P], wt%	Test Temperature, K	Reference No.
479.0	528.0	8.09	30.0	110.0	0.11	295.0	6
603.0	594.0	9.98	36.0	120.0	0.12	295.0	5
606.0	667.0	5.19	60.5	50.0	0.22	295.0	6
683.0	672.0	5.19	70.0	50.0	0.22	295.0	6
755.0	667.0	5.19	79.0	50.0	0.22	295.0	6
26.3	82.6	0.00	0.0	50.0	0.00	79.6	7
25.5	48.0	0.00	0.0	50.0	0.00	153.0	7
24.4	38.7	0.00	0.0	50.0	0.00	223.0	7
22.8	90.6	0.00	0.0	50.0	0.00	297.0	7
52.8	41.8	0.00	0.0	50.0	0.00	79.6	7
43.7	41.8	0.00	0.0	50.0	0.00	155.0	7
97.9	41.8	0.00	0.0	50.0	0.00	175.0	7
40.2	41.8	0.00	0.0	50.0	0.00	192.0	7
97.9	44.7	0.00	0.0	50.0	0.00	223.0	7
36.6	44.1	0.00	0.0	50.0	0.00	224.0	7
33.6	42.3	0.00	0.0	50.0	0.00	263.0	7
31.7	40.5	0.00	0.0	50.0	0.00	295.0	7
86.5	77.6	0.74	0.0	50.0	0.00	81.3	7
74.9	99.6	0.74	0.0	50.0	0.00	155.0	7
66.4	63.4	0.74	0.0	50.0	0.00	175.0	7
60.8	61.3	0.74	0.0	50.0	0.00	153.0	7
66.4	58.2	0.74	0.0	50.0	0.00	224.0	7
68.8	87.1	0.74	0.0	50.0	0.00	297.0	7
53.3	54.4	0.74	0.0	50.0	0.00	263.0	7
60.8	51.5	0.74	0.0	50.0	0.00	297.0	7
127.0	111.0	1.63	0.0	50.0	0.00	81.3	7
105.0	94.2	1.63	0.0	50.0	0.00	155.0	7
69.8	62.6	1.63	0.0	50.0	0.00	171.0	7
95.1	87.1	1.63	0.0	50.0	0.00	195.0	7
31.7	82.6	1.63	0.0	50.0	0.00	224.0	7
84.4	99.6	1.63	0.0	50.0	0.00	295.0	7
79.1	76.8	1.63	0.0	50.0	0.00	297.0	7
74.9	72.8	1.63	0.0	50.0	0.00	295.0	7
143.0	134.0	2.35	0.0	50.0	0.00	82.2	7
121.0	116.0	2.35	0.0	50.0	0.00	195.0	7
143.0	111.0	2.35	0.0	50.0	0.00	156.0	7
114.0	111.0	2.35	0.0	50.0	0.00	171.0	7
143.0	106.0	2.35	0.0	50.0	0.00	177.0	7
105.0	107.0	2.35	0.0	50.0	0.00	155.0	7
127.0	106.0	2.35	0.0	50.0	0.00	194.0	7
99.6	99.6	2.35	0.0	50.0	0.00	226.0	7
97.9	38.7	2.35	0.0	50.0	0.00	236.0	7
69.8	93.1	2.35	0.0	50.0	0.00	264.0	7
85.5	92.6	2.35	0.0	50.0	0.00	224.0	7
83.2	44.0	2.35	0.0	50.0	0.00	297.0	7
211.0	196.0	0.74	0.0	50.0	0.00	81.3	7
165.0	165.0	0.74	0.0	50.0	0.00	155.0	7
160.0	159.0	4.78	0.0	50.0	0.00	176.0	7
153.0	153.0	4.78	0.0	50.0	0.00	195.0	7
138.0	143.0	4.78	0.0	50.0	0.00	234.0	7
129.0	136.0	4.78	0.0	50.0	0.00	263.0	7

Table 16.1, continued

Yield Strength, Measured, MPa	Yield Strength, Predicted, MPa	[Sn], wt%	Cold Work, %	Grain Size, µm	[P], wt%	Test Temperature, K	Reference No.
121.0	129.0	8.78	0.0	50.0	0.00	296.0	7
238.0	211.0	5.67	0.0	50.0	0.00	81.9	7
187.0	173.0	5.67	0.0	50.0	0.00	156.0	7
128.0	178.0	5.67	0.0	50.0	0.00	175.0	7
169.0	155.0	5.67	0.0	50.0	0.00	194.0	7
157.0	157.0	5.67	0.0	50.0	0.00	225.0	7
153.0	154.0	5.67	0.0	50.0	0.00	234.0	7
333.0	147.0	5.67	0.0	50.0	0.00	264.0	7
132.0	139.0	5.67	0.0	50.0	0.00	234.0	7
238.0	246.0	8.78	0.0	50.0	0.00	80.3	7
224.0	249.0	8.78	0.0	50.0	0.00	156.0	7
211.0	159.0	8.78	0.0	50.0	0.00	175.0	7
239.0	189.0	8.78	0.0	50.0	0.00	194.0	7
186.0	178.0	8.78	0.0	50.0	0.00	223.0	7
130.0	175.0	8.78	0.0	50.0	0.00	234.0	7
167.0	159.0	8.78	0.0	50.0	0.00	264.0	7
155.0	155.0	8.78	0.0	50.0	0.00	295.0	7
167.0	159.0	2.35	0.0	20.0	0.00	77.8	7
130.0	137.0	2.35	0.0	20.0	0.00	194.0	8
128.0	133.0	2.35	0.0	20.0	0.00	172.0	7
123.0	137.0	2.35	0.0	20.0	0.00	172.0	7
120.0	425.0	2.35	0.0	20.0	0.00	193.0	7
112.0	129.0	2.35	0.0	20.0	0.00	220.0	7
128.0	116.0	2.35	0.0	20.0	0.00	262.0	7
98.1	111.0	2.35	0.0	20.0	0.00	295.0	7
126.0	178.0	2.35	0.0	250.0	0.00	77.5	7
89.9	88.3	2.35	0.0	250.0	0.00	172.0	7
87.0	84.3	2.35	0.0	250.0	0.00	192.0	7
70.7	71.6	2.35	0.0	250.0	0.00	263.0	7
65.8	66.5	2.35	0.0	250.0	0.00	296.0	7
303.0	249.0	7.80	0.0	20.0	0.00	90.9	7
214.0	203.0	7.80	0.0	20.0	0.00	193.0	7
158.0	171.0	7.80	0.0	20.0	0.00	295.0	7
333.0	285.0	7.80	0.0	8.9	0.00	81.9	7
239.0	238.0	7.80	0.0	8.9	0.00	196.0	7
195.0	207.0	7.80	0.0	8.9	0.00	295.0	7
449.0	405.0	7.80	0.0	1.7	0.00	93.1	8
352.0	358.0	7.80	0.0	1.7	0.00	156.0	7
303.0	328.0	7.80	0.0	1.7	0.00	292.0	7
505.0	502.0	7.80	0.0	0.9	0.00	92.6	7
138.0	155.0	7.80	0.0	0.8	0.00	196.0	7
333.0	425.0	7.80	0.0	0.9	0.00	264.0	7
608.0	584.0	7.80	0.0	0.5	0.00	93.1	7
505.0	502.0	7.80	0.0	0.9	0.00	197.0	8
441.0	504.0	7.80	0.0	0.5	0.00	295.0	7
74.1	96.5	0.00	0.0	50.0	0.00	4.2	7
110.0	178.0	1.35	0.0	50.0	0.00	4.2	7
128.0	174.0	0.00	0.0	50.0	0.00	4.2	8
150.0	203.0	2.70	0.0	50.0	0.00	4.2	9
207.0	152.0	6.40	0.0	50.0	0.00	4.2	9
241.0	344.0	8.30	0.0	50.0	0.00	4.2	9

Table 16.1, continued

Yield Strength, Measured, MPa	Yield Strength, Predicted, MPa	[Sn], wt%	Cold Work, %	Grain Size, μm	[P], wt%	Test Temperature, K	Reference No.
496.0	632.0	4.85	85.0	101.0	0.18	295.0	10
543.0	657.0	4.85	85.0	101.0	0.18	195.0	10
615.0	701.0	4.85	85.0	101.0	0.18	76.0	10
723.0	745.0	4.85	85.0	101.0	0.18	20.0	10
692.0	777.0	4.85	85.0	101.0	0.18	4.0	10
772.0	758.0	8.10	85.0	50.0	0.18	295.0	1[illegible]
958.0	848.0	8.20	75.0	50.0	0.06	76.0	11
1060.0	905.0	8.20	75.0	50.0	0.06	20.0	11

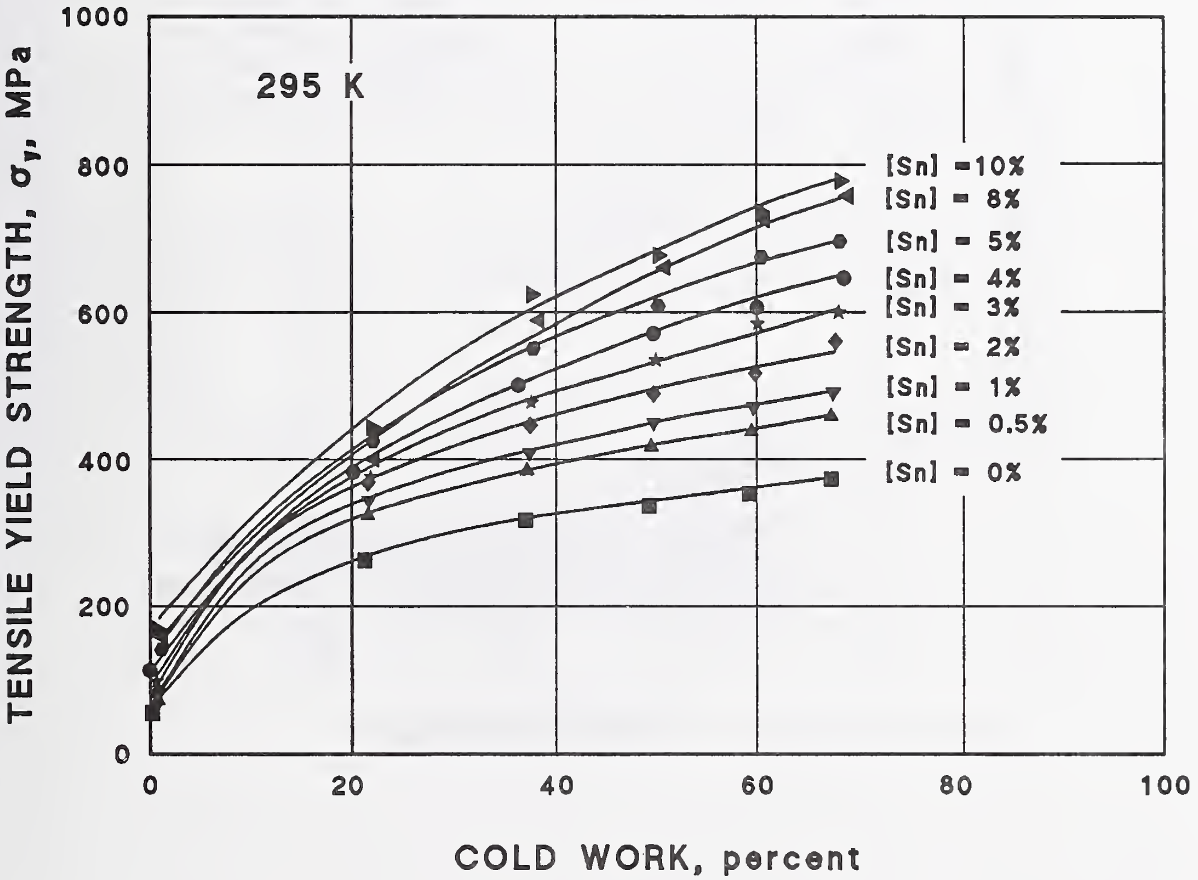

Figure 16.1. Tensile yield strength measurements from Reference 16.1 are plotted as a function of cold work for increasing values of Sn content, [Sn] (in wt%).

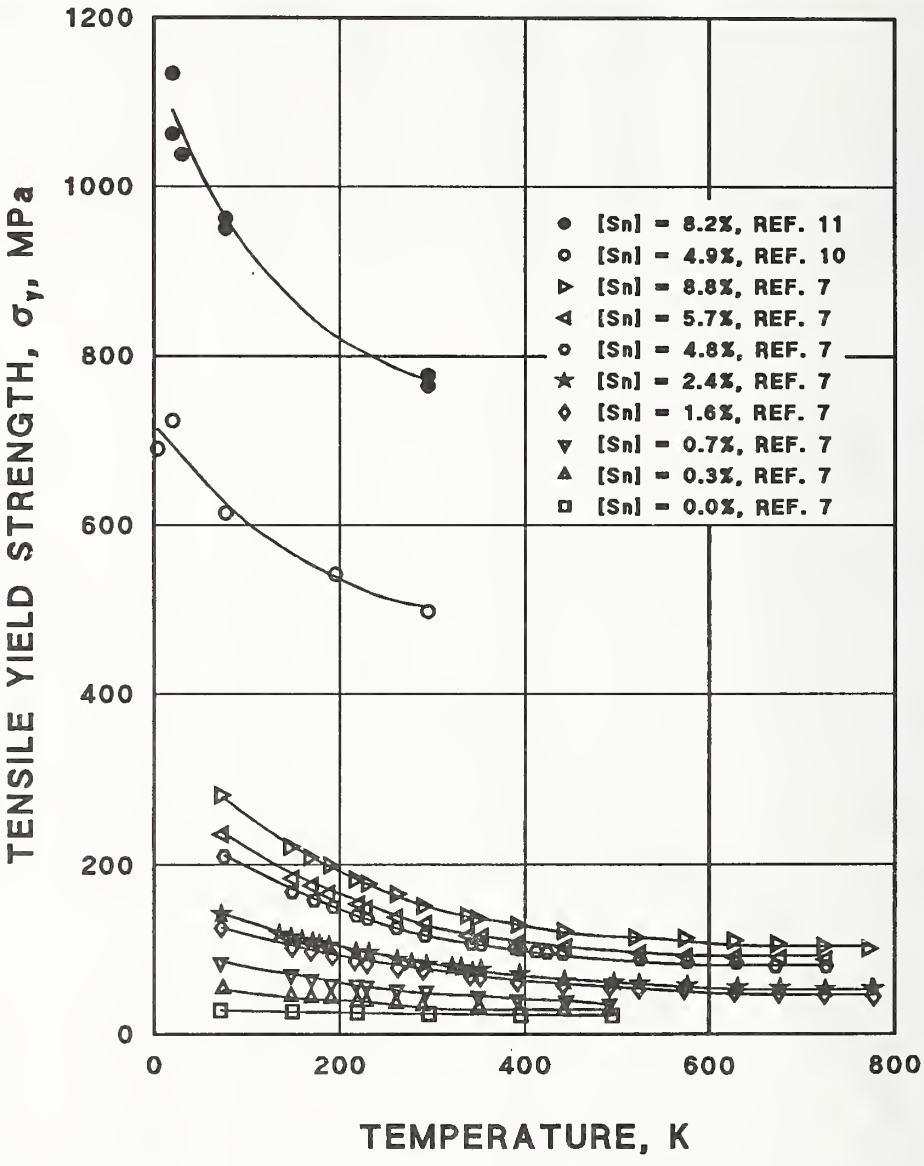

Figure 16.2. Tensile yield strength measurements as a function of temperature for increasing values of Sn content, [Sn] (in wt%). The material from Reference 16.7 was annealed, whereas the materials from References 16.10 and 16.11 were cold worked.

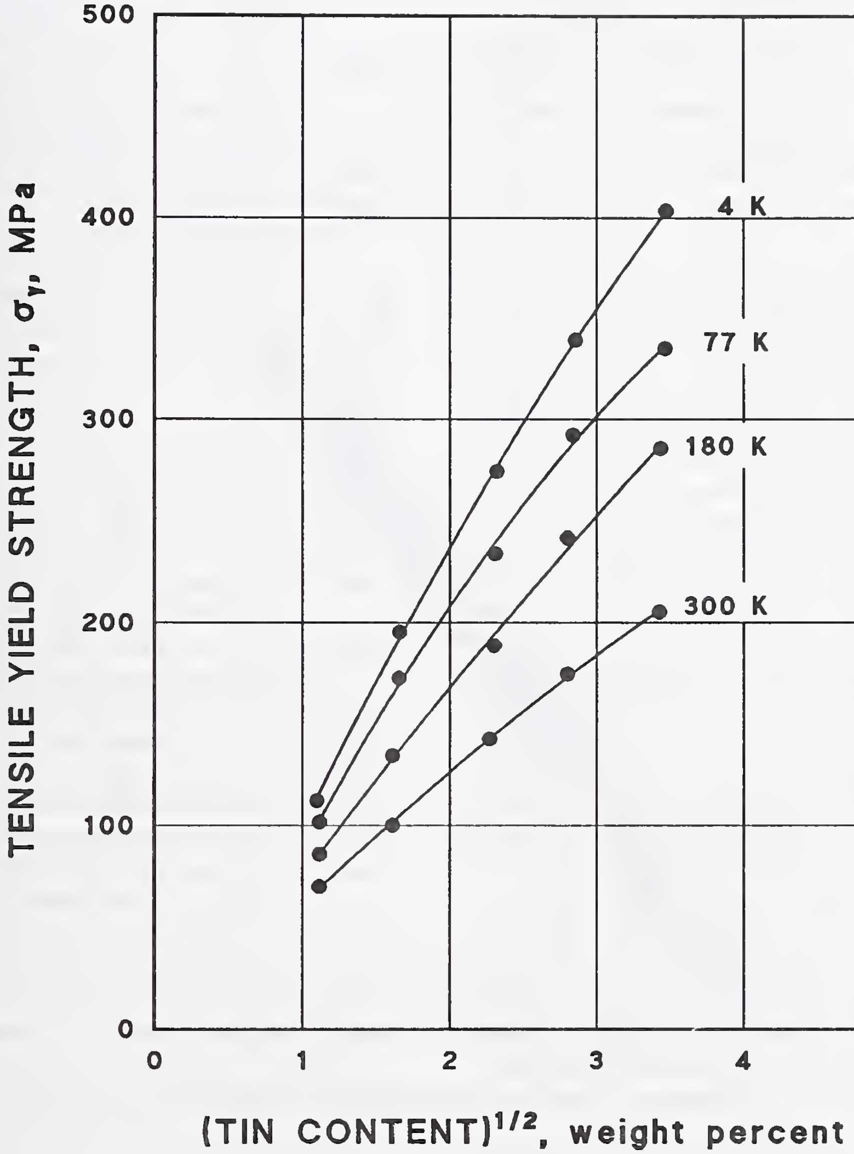

Figure 16.3. Tensile yield strength measurements from Reference 16.14 are plotted as a function of Sn content for decreasing values of the test temperature.

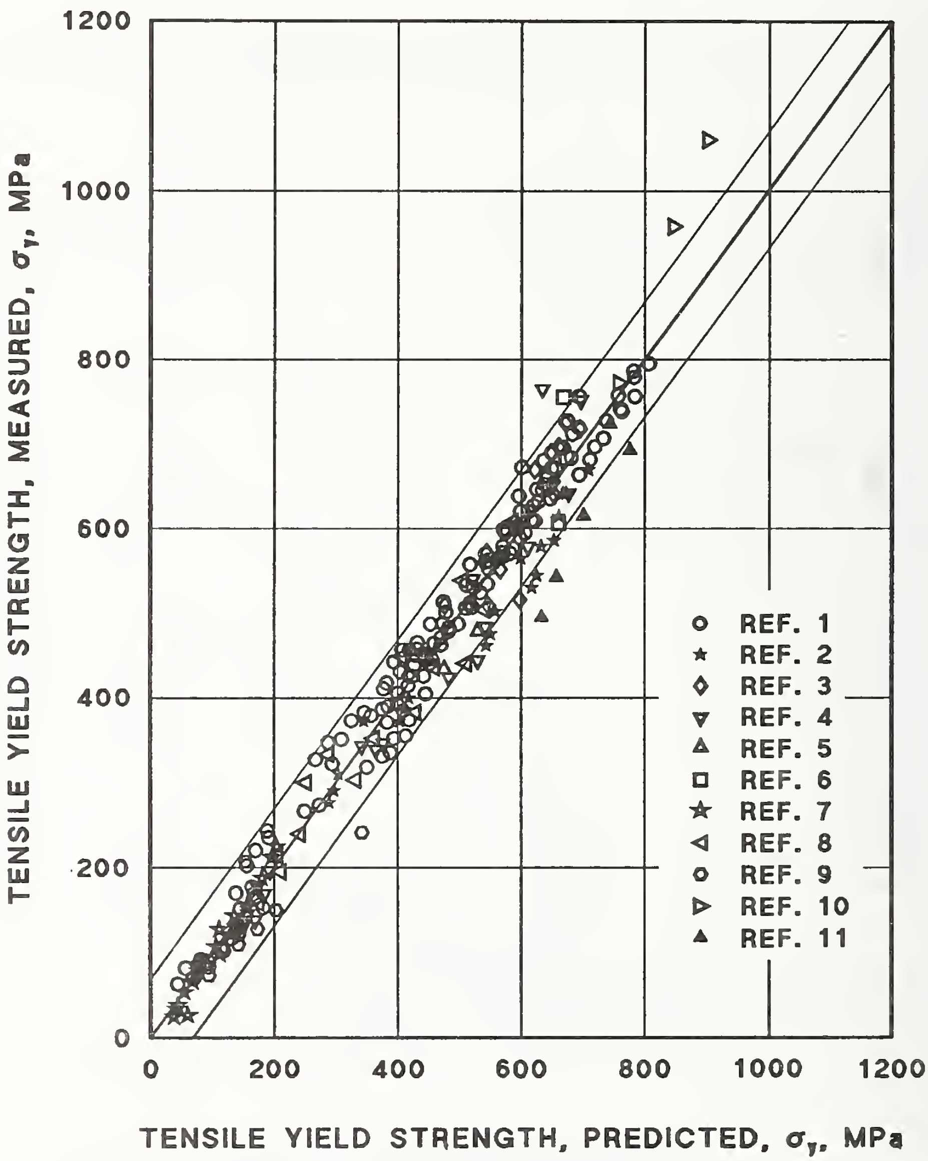

Figure 16.4. The data shown were used to compute the regression of tensile yield strength upon [Sn], *CW*, *d*, [P], and *T* [Equation (16-1)]. For clarity, data points were removed where overlapping occurred to such an extent that symbols could not be discerned. All data are presented in Table 16.1. Products were in sheet, wire, strip, and bar form.

DATA SOURCES AND ANALYSIS

A set of 208 ultimate tensile strength measurements at temperatures between 4 and 297 K was selected for analysis because degree of cold work, Sn and P content, and grain size were reported (References 16.1, 16.3–16.6, 16.10, 16.11, 16.16, and 16.17). In a few cases, because the data appeared very useful, reasonable assumptions were made for one of these parameters. The grain size, *d*, was not specified in References 16.6, 16.10, and 16.17 and values based in part on the heat treatment of the material were assigned (80, 50, and 40 μm, respectively). Degree of cold work, *CW* (percent reduction of thickness or area) ranged from 0 to 85%; Sn content, [Sn], ranged from 0 to 10.10 wt%; P content, [P], ranged from 0 to 0.40 wt%; and *d*, from 0.5 to 250 μm.

Products were in sheet (Reference 16.6), strip (References 16.1 and 16.3), and bar form (References 16.4, 16.5, 16.10, 16.11, and 16.17). Product form was not reported in Reference 16.16. Data on wire at 295 K were not included because a great deal of data was available at this temperature and tensile measurements on wire may not be comparable to measurements on other product forms. The type of cold work was cold rolling in all cases except for the bar stock which was drawn. The cold rolling reported in Reference 16.1 was carried out in the laboratory and may have differed somewhat from standard commercial practice. The available information on the characterization of materials and measurements is given in Table 16.5 at the end of the C50100–C52400 tensile properties section.

Because an extensive data set was available, it seemed appropriate to develop a predictive equation for ultimate tensile strength, σ_u, as a function of potentially relevant parameters, such as temperature (*T*), *CW*, [Sn], *d*, [P]. The alloying element, Fe, although present in commercial material, was judged not to affect σ_u significantly. Reference 16.6 reported that the tensile properties were not affected by the variation in Fe content, [Fe], from 0.02 to 0.12 wt% in two different lots of C51000. Measurements of σ_u and strain to failure in high-[Sn], low-[P] bronzes were in agreement, within the measurement error, for [Fe] of either 0.05 wt% or 0.94 wt% (Reference 16.12). Reference 16.13 states that [Fe] of up to 0.28% causes only a slight increase in σ_u and amounts above 0.28 wt% actually cause a decrease because the Fe enters into a secondary phase. Further data on the dependence of tensile properties of phosphor bronzes on [Fe] are not available at present, and [Fe] was generally not reported in the references used in this analysis.

The data set was not ideal for developing a predictive equation relating σ_u to *T*, [Sn], and *CW*, because only a few measurements from 4 to 295 K on cold-worked material have been reported (see Table 16.2). However, an excellent set of 132 measurements at 295 K is available from Reference 16.1 in which [Sn], *CW*, *d*, and [P] were varied systematically. Therefore, regression analysis of σ_u upon [Sn], *CW*, *d*, and [P] was initially carried out on this data set to establish the best functional forms. In particular, this data set was used to develop the best expressions for the interactive effect of *CW* and [Sn]. It is clear from the results presented in Reference 16.1 that such an interactive effect exists. The data set from Reference 16.1 was also used to test the effect of d and [P] upon σ_u. These parameters were found not to affect σ_u significantly, in contrast to their effect on σ_y [Equation (16-1)]. A trial and error procedure was used to find the best terms to express the temperature dependence, after additional data from Reference 16.16 were added to the data set.

When the form of the equation had been established from the data sets with extensive parameter variation, data from References 16.10, 16.11, and 16.17 were added (8 measurements between 4 and 295 K on drawn bar product and 3 measurements on annealed material) to determine the final coefficients. Table 1.17 in the introductory section gives *CW* equivalents for cold-rolled and drawn tempers. Therefore, for cold-worked bar product (References 16.4, 16.5, 16.10, and 16.11), equivalent temper percentages for cold rolling were substituted in the cold-work terms in the equation in place of the percentage of reduction of area. In contrast to Equation (16-1) for σ_y, a better fit of the equation to the measurements was obtained with this procedure. This is discussed further below.

RESULTS

The final equation expressing the dependence of σ_u in MPa upon the parameters discussed above is

$$\sigma_u = +813.9 + 149.2[\mathrm{Sn}]^{1/2} + 3.005\,CW + 0.3748\,CW[\mathrm{Sn}] - 0.01653\,CW[\mathrm{Sn}]^2 - 2.120\,T - 451.8\,T^{-0.4}[\mathrm{Sn}]^{1/2} \quad (16\text{-}2)$$

(S.D. = 69.8 MPa),

where 4 K ≤ T ≤ 297 K. The standard deviations of the coefficients are: constant term, 46.1; $[\mathrm{Sn}]^{1/2}$, 13.4; CW, 0.456; $CW[\mathrm{Sn}]$, 0.1511; $CW[\mathrm{Sn}]^2$, 0.01253; T, 0.145; and $T^{-0.4}[\mathrm{Sn}]^{1/2}$, 86.4. The set of σ_u measurements and parameters are presented in Table 16.2, which also gives the σ_u value predicted from the analysis described. Figure 16.5 indicates the fit of the data to Equation (16-2). The scatter band represents two standard deviations about the straight line, which corresponds to agreement between the measured and predicted values of σ_u. The variance of the data was assumed to be normally distributed and constant throughout the range of the predicted values. Table 16.2 presents the σ_u values calculated from Equation (16-2) as well as the measured σ_u, and the parameters [Sn], *CW*, and *T*. The available characterization of materials and measurements is given in Table 16.5 at the end of the tensile properties section.

DISCUSSION

It would be advantageous to have more measurements of σ_u on phosphor bronzes of varying *CW* and [Sn] for temperatures below 295 K. Equation (16-2) represents the best determination of the dependence of σ_u on [Sn], *CW*, and *T* that could be obtained from the available database. Several measurements on 60% cold-worked sheet (Reference 16.21) not included in this analysis fell within the scatter band.

In contrast with these results for phosphor bronzes, analysis of the dependence of σ_u upon *CW* for C10100–C10700 coppers (pages 2-35–2-41 and 2-44–2-50) showed that a good fit of the data was obtained when the cold-work term in the equation represents the reduction of thickness for cold-rolled product and reduction of area for drawn product. As explained above, the fit of the σ_u data to the equation was improved if the equivalent *CW* for cold rolled tempers (Table 1.17) was used in the equations in place of the percent reduction of area for drawn product, whereas the opposite was true for σ_y. The difference may be due to the larger effect of a given percent increase in *CW* for σ_u [Equation (16-2)] as compared with σ_y [Equation (16-1)]. Not enough data are available on drawn product to determine why the use of temper equivalents of *CW* gives a better fit of the data to predictive equations for σ_u than for σ_y. Reference 16.15 indicates that smaller specimen sizes increase the measured σ_u and σ_y for this commercial product form, and that tensile data for design purposes should be obtained on full-sized specimens.

Reference 16.6 presents tensile data (not used in this analysis) on material subjected to other forms of thermomechanical processing. C51000 phosphor bronze was cold rolled to 97.3% and subsequently annealed for 2 h at various temperatures in an attempt to recover ductility without losing strength. Results and mechanisms are discussed in the reference. Reference 16.18 reports tensile and other mechanical property data on C52100 spring wire that was cold drawn and straightened.

Table 16.2. Ultimate Tensile Strength Dependence on [Sn] and *CW* (4–297 K).

Tensile Strength, Measured, MPa	Tensile Strength, Predicted, MPa	[Sn], wt%	Cold Work, %	Test Temperature, K	Reference No.
267.0	250.0	0.42	0.0	295.0	1
333.0	318.0	0.42	20.7	295.0	1
391.0	372.0	0.42	37.5	295.0	1

Table 16.2, continued

Tensile Strength, Measured, MPa	Tensile Strength, Predicted, MPa	[Sn], wt%	Cold Work, %	Test Temperature, K	Reference No.
420.0	413.0	0.42	50.2	295.0	1
443.0	447.0	0.42	60.5	295.0	1
465.0	474.0	0.42	68.9	295.0	1
271.0	250.0	0.42	0.0	295.0	1
335.0	318.0	0.42	20.8	295.0	1
402.0	372.0	0.42	37.6	295.0	1
428.0	413.0	0.42	50.3	295.0	1
442.0	447.0	0.42	60.6	295.0	1
456.0	413.0	0.42	68.6	295.0	1
277.0	284.0	0.95	0.0	295.0	1
355.0	355.0	0.95	20.7	295.0	1
414.0	413.0	0.95	37.6	295.0	1
456.0	456.0	0.95	50.2	295.0	1
472.0	492.0	0.95	60.9	295.0	1
495.0	520.0	0.95	68.9	295.0	1
281.0	284.0	0.95	0.0	295.0	1
399.0	354.0	0.95	20.3	295.0	1
428.0	412.0	0.95	37.3	295.0	1
465.0	455.0	0.95	49.9	295.0	1
488.0	492.0	0.95	60.9	295.0	1
511.0	520.0	0.95	58.2	295.0	1
286.0	333.0	2.07	0.0	295.0	1
387.0	412.0	2.07	21.1	295.0	1
454.0	474.0	2.07	37.4	295.0	1
493.0	522.0	2.07	50.1	295.0	1
521.0	561.0	2.07	60.3	295.0	1
565.0	591.0	2.07	68.9	295.0	1
309.0	333.0	2.07	0.0	295.0	1
399.0	410.0	2.07	20.8	295.0	1
475.0	475.0	2.07	37.5	295.0	1
535.0	522.0	2.07	50.1	295.0	1
570.0	562.0	2.07	60.7	295.0	1
577.0	593.0	2.07	68.8	295.0	1
321.0	362.0	2.96	0.0	295.0	1
404.0	448.0	2.96	21.2	295.0	1
491.0	512.0	2.96	37.2	295.0	1
546.0	564.0	2.96	50.1	295.0	1
589.0	606.0	2.96	60.3	295.0	1
607.0	638.0	2.96	68.3	295.0	1
349.0	362.0	2.96	0.0	295.0	1
425.0	445.0	2.96	20.7	295.0	1
517.0	515.0	2.96	37.8	295.0	1
568.0	564.0	2.96	50.1	295.0	1
608.0	606.0	2.96	60.4	295.0	1
627.0	639.0	2.96	68.6	295.0	1
324.0	391.0	4.00	0.0	295.0	1
414.0	481.0	4.00	20.9	295.0	1
518.0	552.0	4.00	37.4	295.0	1
588.0	607.0	4.00	50.1	295.0	1
625.0	651.0	4.00	60.4	295.0	1
662.0	685.0	4.00	68.4	295.0	1
373.0	391.0	4.00	0.0	295.0	1

Table 16.2, continued

Tensile Strength, Measured, MPa	Tensile Strength, Predicted, MPa	[Sn], wt%	Cold Work, %	Test Temperature, K	Reference No.
464.0	480.0	4.00	20.7	295.0	1
564.0	553.0	4.00	37.4	295.0	1
627.0	606.0	4.00	49.6	295.0	1
650.0	651.0	4.00	60.5	295.0	1
558.0	686.0	4.00	68.5	295.0	1
340.0	420.0	5.20	0.0	295.0	1
452.0	618.0	5.20	20.6	295.0	1
570.0	584.0	5.20	38.3	295.0	1
625.0	648.0	5.20	49.9	295.0	1
694.0	696.0	5.20	60.4	295.0	1
719.0	733.0	5.20	68.4	295.0	1
389.0	420.0	5.20	0.0	295.0	1
467.0	515.0	5.20	20.2	295.0	1
583.0	595.0	5.20	38.3	295.0	1
650.0	649.0	5.20	60.4	295.0	1
633.0	696.0	5.20	60.4	295.0	1
733.0	732.0	5.20	68.4	295.0	1
665.0	828.0	8.12	0.0	295.0	1
639.0	823.0	8.12	20.6	295.0	1
638.0	595.0	8.12	37.1	295.0	1
700.0	731.0	8.12	50.2	295.0	1
768.0	782.0	8.12	60.5	295.0	1
791.0	823.0	8.12	68.5	295.0	1
423.0	480.0	8.12	0.0	295.0	1
558.0	686.0	8.12	21.0	295.0	1
668.0	667.0	8.12	37.1	295.0	1
700.0	731.0	8.12	60.4	295.0	1
768.0	783.0	8.12	60.6	295.0	1
818.0	823.0	8.12	68.5	295.0	1
432.0	514.0	10.10	0.0	295.0	1
583.0	622.0	10.10	20.6	295.0	1
668.0	705.0	10.10	37.4	295.0	1
737.0	771.0	10.10	49.8	295.0	1
795.0	420.0	10.10	60.4	295.0	1
833.0	667.0	10.10	68.5	295.0	1
467.0	514.0	10.10	0.0	295.0	1
579.0	618.0	10.10	20.2	295.0	1
695.0	705.0	10.10	37.1	295.0	1
755.0	770.0	10.10	49.6	295.0	1
805.0	420.0	10.10	60.4	295.0	1
847.0	866.0	10.10	68.3	295.0	1
340.0	357.0	2.81	0.0	295.0	1
442.0	441.0	2.81	20.6	295.0	1
547.0	507.0	2.81	37.4	295.0	1
608.0	557.0	2.81	50.0	295.0	1
648.0	638.0	2.81	60.2	295.0	1
687.0	630.0	2.81	68.4	295.0	1
356.0	390.0	3.97	0.0	295.0	1
479.0	478.0	3.97	20.5	295.0	1
586.0	550.0	3.97	37.3	295.0	1
664.0	604.0	3.97	49.8	295.0	1
712.0	650.0	3.97	60.4	295.0	1

Table 16.2, continued

Tensile Strength, Measured, MPa	Tensile Strength, Predicted, MPa	[Sn], wt%	Cold Work, %	Test Temperature, K	Reference No.
703.0	688.0	3.97	68.4	295.0	1
327.0	390.0	3.97	0.0	295.0	1
454.0	479.0	3.97	20.7	295.0	1
547.0	553.0	3.97	37.6	295.0	1
617.0	605.0	3.97	69.0	295.0	4
662.0	651.0	3.97	60.8	295.0	4
703.0	685.0	3.97	68.5	295.0	1
374.0	417.0	5.04	0.0	295.0	1
500.0	511.0	5.04	20.9	295.0	4
616.0	581.0	5.04	37.6	295.0	1
687.0	643.0	5.04	45.5	295.0	1
734.0	691.0	5.04	60.8	295.0	4
776.0	727.0	5.04	69.0	295.0	1
212.0	183.0	0.00	0.0	295.0	1
271.0	247.0	0.00	20.7	295.0	1
379.0	298.0	0.00	37.1	295.0	1
342.0	338.0	0.00	50.3	295.0	1
357.0	371.0	0.00	60.8	295.0	1
374.0	397.0	0.00	69.8	295.0	1
231.0	183.0	0.00	0.0	295.0	1
286.0	247.0	0.00	20.9	295.0	4
337.0	301.0	0.00	38.4	295.0	1
357.0	396.0	0.00	56.2	295.0	1
378.0	371.0	0.00	60.8	295.0	1
342.0	396.0	0.00	69.0	295.0	1
538.0	581.0	4.91	38.4	295.0	3
679.0	686.0	4.91	60.5	295.0	3
696.0	581.0	4.91	37.1	295.0	3
731.0	688.0	4.91	69.0	295.0	3
448.0	514.0	4.91	22.2	295.0	3
524.0	521.0	4.91	23.8	295.0	3
646.0	674.0	4.91	35.5	295.0	3
621.0	592.0	4.91	39.6	295.0	3
646.0	674.0	4.91	38.4	295.0	3
524.0	592.0	4.91	32.9	295.0	3
580.0	691.0	4.91	·0.0	295.0	3
689.0	640.0	4.91	50.3	295.0	3
724.0	651.0	4.91	56.2	295.0	3
703.0	684.0	4.91	60.0	295.0	3
696.0	674.0	4.91	57.9	295.0	3
703.0	688.0	4.91	69.0	295.0	3
662.0	686.0	4.91	60.8	295.0	3
676.0	643.0	4.91	45.5	295.0	3
772.0	103.0	4.91	60.8	295.0	3
745.0	709.0	4.91	69.0	295.0	3
378.0	399.0	4.32	0.0	295.0	4
391.0	437.0	4.32	8.0	295.0	4
481.0	472.0	4.32	45.5	295.0	1
666.0	531.0	4.32	30.0	295.0	4
553.0	469.0	3.72	20.1	295.0	4
376.0	382.0	3.67	0.0	295.0	4
796.0	603.0	9.31	20.1	295.0	4

C50100–C52400: Annealed; Cold-worked

Ultimate Tensile Strength vs. [Sn], Cold Work (4–297 K)

Table 16.2, continued

Tensile Strength, Measured, MPa	Tensile Strength, Predicted, MPa	[Sn], wt%	Cold Work, %	Test Temperature, K	Reference No.
408.0	479.0	8.10	0.0	295.0	4
383.0	479.0	5.19	0.0	295.0	4
455.0	828.0	5.19	8.0	295.0	4
558.0	562.0	8.10	16.5	295.0	4
869.0	630.0	8.70	30.0	295.0	4
469.0	508.0	9.78	0.0	295.0	4
426.0	508.0	9.78	0.0	295.0	4
528.0	552.0	9.78	8.0	295.0	4
889.0	593.0	9.76	16.5	295.0	4
879.0	662.0	9.76	30.0	295.0	4
455.0	462.0	8.28	14.6	295.0	5
341.0	344.0	4.28	0.0	295.0	5
571.0	852.0	4.05	16.5	295.0	5
392.0	479.0	4.05	0.0	295.0	5
687.0	615.0	9.96	20.0	295.0	5
440.0	512.0	9.96	0.0	295.0	5
889.0	1048.0	5.19	60.5	295.0	5
742.0	739.0	5.19	70.0	295.0	6
793.0	861.0	5.19	70.0	295.0	5
865.0	638.0	5.19	90.3	295.0	5
889.0	852.0	5.19	94.7	295.0	6
913.0	684.0	5.19	38.8	295.0	5
972.0	861.0	5.19	97.3	295.0	5
1170.0	1050.0	8.20	50.1	20.0	16
089.0	1070.0	8.20	50.1	76.0	16
574.0	732.0	4.20	90.3	295.0	16
687.0	684.0	4.85	60.5	295.0	11
590.0	861.0	4.85	60.5	195.0	11
725.0	1040.0	4.85	60.5	76.0	11
303.0	1050.0	4.85	60.5	20.0	11
303.0	850.0	4.85	60.5	4.0	11
1100.0	828.0	8.78	0.0	78.7	16
889.0	728.0	8.78	0.0	155.0	16
787.0	617.0	8.78	0.0	223.0	16
865.0	488.0	8.78	0.0	297.0	16
987.0	861.0	5.67	0.0	20.0	16
781.0	674.0	5.67	0.0	154.0	16
574.0	588.0	5.67	0.0	224.0	16
540.0	427.0	5.67	0.0	297.0	16
471.0	769.0	8.78	0.0	77.9	16
676.0	657.0	8.78	0.0	154.0	16
574.0	537.0	8.78	0.0	224.0	16
492.0	408.0	4.78	0.0	297.0	16
722.0	479.0	2.35	0.0	77.9	16
542.0	602.0	2.35	0.0	154.0	16
598.0	859.0	2.35	0.0	175.0	16
471.0	479.0	2.35	0.0	222.0	16
426.0	344.0	2.35	0.0	297.0	16
435.0	383.0	2.35	0.0	273.0	16
510.0	743.0	3.90	0.0	85.0	17
386.0	567.0	3.90	0.0	195.0	17
331.0	379.0	3.90	0.0	300.0	17

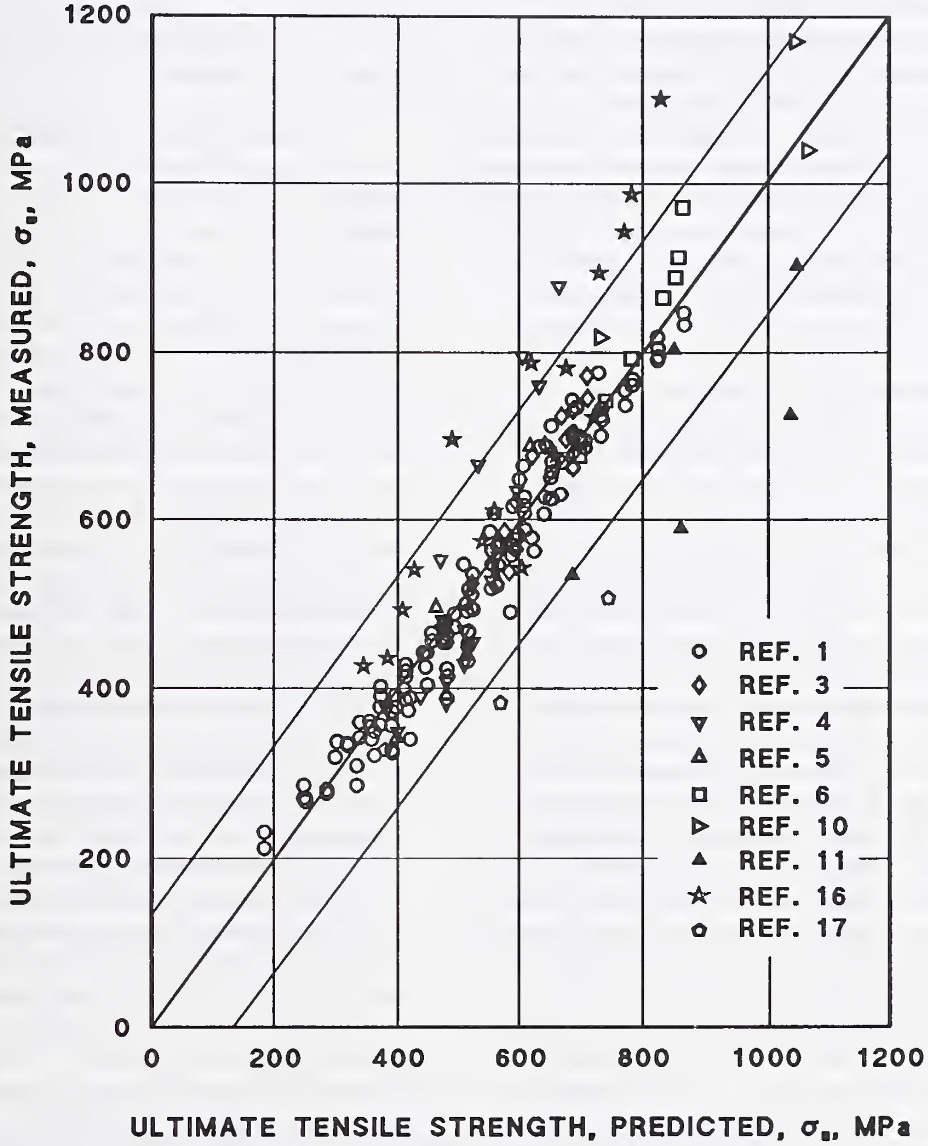

Figure 16.5. The data shown were used to compute the regression of ultimate tensile strength upon [Sn], *CW*, and *T* [Equation (16-2)]. All data are presented in Table 16.2. Products were in sheet, wire, strip, and bar form.

DATA SOURCES AND ANALYSIS

A set of 212 values of tensile strain to failure (as determined by elongation measurements) were selected from measurements at temperatures between 4 and 297 K. These data were chosen for analysis because degree of cold work, Sn and P content, and grain size were reported (References 16.1, 16.3–16.6, 16.10, 16.11, 16.16, and 16.19). In a few cases, because the data appeared very useful, reasonable assumptions were made for one of these parameters. The grain size was not specified in References 16.6 and 16.10 and values based in part on the heat treatment of the material were assigned (80 and 50 μm, respectively). Degree of cold work, *CW* (percent reduction of thickness or area), ranged from 0 to 85%; Sn content, [Sn], ranged from 0 to 10.10 wt%; P content, [P], ranged from 0 to 0.40 wt%; and grain size, *d*, from 0.5 to 250 μm.

Products were in sheet (Reference 16.6), strip (References 16.1 and 16.3), and bar form (References 16.4, 16.5, 16.10, 16.11, and 16.19). Product form was not reported in Reference 16.16. Data on wire at 295 K were not included because a great deal of data was available at this temperature and tensile measurements on wire may not be comparable to measurements on other product forms. The type of cold work was cold rolling in all cases except for the bar stock which was drawn. The cold rolling reported in Reference 16.1 was carried out in the laboratory and may have differed somewhat from standard commercial practice. The available information on the available characterization of materials and measurements is given in Table 16.5 at the end of the C50100–C52400 tensile properties section.

Because an extensive data set was available, it seemed appropriate to develop a predictive equation for strain to failure, ϵ_f, as a function of potentially relevant parameters, such as temperature (*T*), *CW*, [Sn], *d*, and [P]. The alloying element, Fe, although present in commercial material, was judged not to affect ϵ_f significantly. Reference 16.6 reported that the tensile properties were not affected by the variation in Fe content, [Fe], from 0.02 to 0.12 wt% in two different lots of C51000. Measurements of ultimate tensile strength and ϵ_f in high [Sn], low [P] bronzes were in agreement, within the measurement error, for [Fe] of either 0.05 wt% or 0.94 wt% (Reference 16.12). Reference 16.13 states that [Fe] of up to 0.28 wt% causes only a slight increase of tensile strength and amounts above 0.28% actually cause a decrease because the Fe enters into a secondary phase. Further data on the dependence of tensile properties of phosphor bronzes on [Fe] are not available at present, and [Fe] was generally not reported in the references used in this analysis.

The data set was not ideal for developing a predictive equation relating ϵ_f to *T*, [Sn], *CW*, and possibly other parameters, because only a few measurements from 4 to 295 K on cold-worked material have been reported (see Table 16.3). However, an excellent data set of 132 measurements at 295 K is available from Reference 16.1 in which [Sn], *CW*, *d*, and [P] were varied systematically. Therefore, regression analysis of ϵ_f upon [Sn], *CW*, *d*, and [P] was initially carried out on this data set to establish the best functional forms. In particular, this data set was used to develop the best expressions for the interactive effect of *CW* and [Sn]. It is clear from the results presented in Reference 16.1 that such an interactive effect exists. The data set from Reference 16.1 was also used to test the effect of *d* and [P] upon ϵ_f. The [P] was found not to affect ϵ_f significantly, in contrast to its effect on σ_y [Equation (16-1)]. An interactive effect between *d* and *CW* was found. A trial and error procedure was used to find the best terms to express the temperature dependence, after additional data from Reference 16.16 were added to the data set.

When the form of the equation had been established from the data sets with extensive parameter variation, data from References 16.10 and 16.11 were added (8 measurements between 4 and 295 K on drawn bar product) to determine the final coefficients. Table 1.17 in the introductory section gives *CW* equivalents for cold-rolled and drawn tempers. Therefore, for cold-worked bar product (References 16.4, 16.5, 16.10, and 16.11), equivalent temper percentages for cold rolling were substituted in the *CW* terms in the equation in place of the percentage of reduction of area. This did not Improve the fit of the equation to the data, so the percent reduction of area by drawing was used for *CW* in the analysis for measurements on bar stock. This is discussed further below.

C50100–C52400: Annealed; Cold-worked

Strain to Failure vs. [Sn], Cold Work, Grain Size (4–297 K)

RESULTS

The final equation expressing the dependence of ϵ_f upon the parameters discussed above is

$$\begin{aligned}\epsilon_f = {} & +0.477 + 0.0677[\mathrm{Sn}] - 0.00303[\mathrm{Sn}]^2 \\ & - 0.0123\,CW + 0.000152(CW)^2 - 0.474d^{-1/2} \\ & - 0.00136\,CW[\mathrm{Sn}] + 0.0000796\,CW[\mathrm{Sn}]^2 \\ & + 0.00637(CW)d^{-1/2} - 0.0000132\,CW(T)\end{aligned} \qquad (16\text{-}3)$$

(S.D. = 0.066),

where $4\ \mathrm{K} \le T \le 297\ \mathrm{K}$. The standard deviations of the coefficients are: constant term, 0.033; [Sn], 0.0096; $[\mathrm{Sn}]^2$, 0.00089; *CW*, 0.0011; $(CW)^2$, 0.000008; $d^{-1/2}$, 0.110; *CW*[Sn], 0.00021; $CW[\mathrm{Sn}]^2$, 0.0000202; $(CW)d^{-1/2}$, 0.00282; and *CW*(*T*), 0.0000016. The set of ϵ_f measurements and parameters are presented in Table 16.3, which also gives the ϵ_f value predicted from the analysis described. Figure 16.6 indicates the fit of the data to Equation (16-3). The scatter band represents two standard deviations about the straight line, which corresponds to agreement between the measured and predicted values of ϵ_f. The variance of the data was assumed to be normally distributed and constant throughout the range of the predicted values. Table 16.3 presents the ϵ_f values calculated from Equation (16-3) as well as the measured ϵ_f and the parameters [Sn], *CW*, *d*, and *T*. The available characterization of materials and measurements is given in Table 16.5 at the end of the tensile properties section.

DISCUSSION

It would be advantageous to have more measurements of ϵ_f on phosphor bronzes of varying *CW* and [Sn] for temperatures below 295 K. Equation (16-3) represents the best determination of the dependence of ϵ_f on [Sn], *CW*, *d*, and *T* that could be obtained from the available database. The effect of decreasing *d* in Equation (16-3) is to lower the ductility. As expected, the $d^{-1/2}$ term has a negative sign in Equation (16-3) for ϵ_f and a positive sign in Equation (16-1) for yield strength, because an increase in strength generally results in a decrease in ductility. An attempt to correlate ϵ_f directly with σ_y was not successful.

In agreement with the results for yield strength, a better fit of the data was obtained when the cold-work term in the equation represents the reduction of thickness for cold-rolled product and reduction of area for drawn product. The alternative, to use the temper equivalents presented in Table 1.5, resulted in a worse fit of the data. It was not feasible, given the limited amount of data available, to develop separate equations for the two types of product.

Reference 16.6 presents tensile data (not used in this analysis) on material subjected to other forms of thermomechanical processing. C51000 phosphor bronze was cold rolled to 97.3% and subsequently annealed for 2 h at various temperatures in an attempt to recover ductility without losing strength. Results and mechanisms are discussed in the reference. Reference 16.18 reports tensile and other mechanical property data on C52100 spring wire that was cold drawn and straightened.

Table 16.3. Strain to Failure Dependence on [Sn], *CW*, and *d* (4–297 K).

Strain to Failure, Measured	Strain to Failure, Predicted	[Sn], wt%	Cold Work, %	Grain Size, µm	Test Temperature, K	Reference No.
0.4980	0.4250	0.42	0.0	35.0	295.0	1
0.1040	0.1650	0.42	20.7	35.0	295.0	1
0.0379	0.0502	0.42	37.4	35.0	295.0	1
0.0344	0.0198	0.42	60.5	35.0	295.0	1
0.0256	0.0306	0.42	60.3	35.0	295.0	1
0.0218	0.0620	0.42	68.5	35.0	295.0	1
0.4560	0.3830	0.42	0.0	15.0	295.0	1
0.1670	0.1350	0.42	20.7	15.0	295.0	1

Table 16.3, continued

Strain to Failure, Measured	Strain to Failure, Predicted	[Sn], wt%	Cold Work, %	Grain Size, μm	Test Temperature, K	Reference No.
0.0604	0.0308	0.42	37.6	15.0	295.0	1
0.0401	0.0059	0.42	15.6	15.0	295.0	1
0.0367	0.0218	0.42	60.1	15.0	295.0	1
0.0353	0.0554	0.42	67.9	15.0	295.0	1
0.4670	0.4590	0.95	0.0	35.0	295.0	1
0.1240	0.1860	0.95	20.5	35.0	295.0	1
0.0494	0.0604	0.95	37.2	35.0	295.0	1
0.0354	0.0209	0.95	49.7	35.0	295.0	1
0.0311	0.0218	0.95	60.2	35.0	295.0	1
0.0283	0.0482	0.95	68.3	35.0	295.0	1
0.4730	0.4160	0.95	0.0	15.0	295.0	1
0.1280	0.1570	0.95	20.5	15.0	295.0	1
0.0910	0.0401	0.95	37.6	15.0	295.0	1
0.0324	0.0068	0.95	49.7	15.0	295.0	1
0.0277	0.0180	0.95	60.1	15.0	295.0	1
0.0264	0.0452	0.95	68.3	15.0	295.0	1
0.4630	0.5240	2.07	0.0	35.0	295.0	1
0.1410	0.2230	2.07	20.8	35.0	295.0	1
0.0412	0.0796	2.07	37.2	35.0	295.0	1
0.0232	0.0209	2.07	49.7	35.0	295.0	1
0.0150	0.0143	2.07	59.9	35.0	295.0	1
0.0125	0.0289	2.07	68.3	35.0	295.0	1
0.4910	0.4820	2.07	0.0	15.0	295.0	1
0.1410	0.1950	2.07	20.6	15.0	295.0	1
0.0480	0.0604	2.07	37.6	15.0	295.0	1
0.0277	0.0068	2.07	60.8	15.0	295.0	1
0.0150	0.0021	2.07	60.1	15.0	295.0	1
0.0176	0.0289	2.07	68.3	15.0	295.0	1
0.4850	0.5710	2.96	0.0	35.0	295.0	1
0.1410	0.2500	2.96	21.1	35.0	295.0	1
0.0599	0.0959	2.96	37.6	35.0	295.0	1
0.0400	0.0209	2.96	15.9	35.0	295.0	1
0.0325	0.0100	2.96	60.2	35.0	295.0	1
0.0283	0.0184	2.96	68.3	35.0	295.0	1
0.4630	0.5290	2.96	0.0	15.0	295.0	1
0.1690	0.2230	2.96	20.6	15.0	295.0	1
0.0587	0.0108	2.96	37.6	15.0	295.0	1
0.0491	0.0132	2.96	50.2	15.0	295.0	1
0.0386	0.0021	2.96	59.9	15.0	295.0	1
0.0353	0.0156	2.96	68.3	15.0	295.0	1
0.5030	0.0209	4.00	0.0	35.0	295.0	1
0.2040	0.2230	4.00	20.6	35.0	295.0	1
0.0773	0.1140	4.00	37.6	35.0	295.0	1
0.0354	0.0348	4.00	15.9	35.0	295.0	1
0.0306	0.0082	4.00	59.9	35.0	295.0	1
0.0245	0.0099	4.00	68.3	35.0	295.0	1
0.4800	0.5770	4.00	0.0	15.0	295.0	1
0.1410	0.2560	4.00	20.6	15.0	295.0	1
0.0766	0.0883	4.00	37.6	15.0	295.0	1
0.0482	0.0210	4.00	49.9	15.0	295.0	1
0.0302	0.0002	4.00	60.2	15.0	295.0	1

C50100–C52400: Annealed; Cold-worked

Strain to Failure vs. [Sn], Cold Work, Grain Size (4–297 K)

Table 16.3, continued

Strain to Failure, Measured	Strain to Failure, Predicted	[Sn], wt%	Cold Work, %	Grain Size, μm	Test Temperature, K	Reference No.
0.0277	0.0065	4.00	68.8	15.0	295.0	1
0.5680	0.6670	5.20	0.0	35.0	295.0	1
0.2090	0.3190	5.20	20.9	35.0	295.0	1
0.0795	0.1360	5.20	35.8	35.0	295.0	1
0.0476	0.0448	5.20	50.0	35.0	295.0	1
0.0292	0.0103	5.20	60.6	35.0	295.0	1
0.0271	0.0065	5.20	68.2	35.0	295.0	1
0.4850	0.6250	5.20	0.0	15.0	295.0	1
0.2090	0.2840	5.20	20.9	15.0	295.0	1
0.0656	0.1360	5.20	35.0	15.0	295.0	1
0.0487	0.0302	5.20	60.8	15.0	295.0	1
0.0293	0.0025	5.20	60.6	15.0	295.0	1
0.0227	0.0032	5.20	68.8	15.0	295.0	1
0.7280	0.7470	8.12	0.0	35.0	295.0	1
0.4120	0.3190	8.12	20.8	35.0	295.0	1
0.1680	0.1790	8.12	37.3	35.0	295.0	1
0.0824	0.0798	8.12	60.8	35.0	295.0	1
0.0525	0.0374	8.12	60.6	35.0	295.0	1
0.0505	0.0274	8.12	68.8	35.0	295.0	1
0.6340	0.7050	8.12	0.0	15.0	295.0	1
0.2670	0.3460	8.12	20.9	15.0	295.0	1
0.1490	0.1570	8.12	37.3	15.0	295.0	1
0.0709	0.0672	8.12	60.8	15.0	295.0	1
0.0545	0.0300	8.12	60.6	15.0	295.0	1
0.0442	0.0241	8.12	58.6	15.0	295.0	1
0.6820	0.7720	10.10	0.0	35.0	295.0	1
0.3480	0.4090	10.10	20.6	35.0	295.0	1
0.1590	0.2120	10.10	37.2	35.0	295.0	1
0.1000	0.1160	10.10	50.1	35.0	295.0	1
0.0708	0.0745	10.10	60.6	35.0	295.0	1
0.0563	0.0652	10.10	68.5	35.0	295.0	1
0.6200	0.1360	10.10	0.0	15.0	295.0	1
0.3160	0.3190	10.10	20.9	15.0	295.0	1
0.1490	0.1360	10.10	35.0	15.0	295.0	1
0.1070	0.1020	10.10	60.8	15.0	295.0	1
0.0656	0.0658	10.10	60.6	15.0	295.0	1
0.0558	0.0621	10.10	68.8	15.0	295.0	1
0.4980	0.5640	2.81	0.0	35.0	295.0	1
0.1760	0.2460	2.81	20.9	35.0	295.0	1
0.0773	0.0905	2.81	35.0	35.0	295.0	1
0.0429	0.0263	2.81	50.0	35.0	295.0	1
0.0305	0.0106	2.81	60.6	35.0	295.0	1
0.0240	0.0263	2.81	68.8	35.0	295.0	1
0.5570	0.6186	3.97	0.0	35.0	295.0	1
0.2120	0.2820	3.97	20.9	35.0	295.0	1
0.0656	0.1360	3.97	37.5	35.0	295.0	1
0.0478	0.0339	3.97	50.1	35.0	295.0	1
0.0374	0.0078	3.97	60.6	35.0	295.0	1
0.0296	0.0106	3.97	68.6	35.0	295.0	1
0.6240	0.6440	3.97	0.0	75.0	295.0	1
0.2700	0.3020	3.97	20.8	75.0	295.0	1

Table 16.3, continued

Strain to Failure, Measured	Strain to Failure, Predicted	[Sn], wt%	Cold Work, %	Grain Size, µm	Test Temperature, K	Reference No.
0.0900	0.1010	3.97	37.8	75.0	295.0	1
0.0571	0.0433	3.97	15.6	15.0	295.0	1
0.0450	0.0130	3.97	60.3	35.0	295.0	1
0.0419	0.0120	3.97	68.1	15.0	295.0	1
0.6490	0.6620	5.04	0.0	35.0	295.0	1
0.2880	0.3110	5.04	20.8	35.0	295.0	1
0.1140	0.1290	5.04	37.3	35.0	295.0	4
0.0605	0.0441	5.04	15.6	35.0	295.0	1
0.0546	0.0102	5.04	60.3	35.0	295.0	1
0.0359	0.0065	5.04	68.1	35.0	295.0	1
0.3770	0.3970	0.00	0.0	35.0	295.0	1
0.1240	0.1480	0.00	20.8	35.0	295.0	1
0.0531	0.0418	0.00	37.8	35.0	295.0	1
0.0334	0.0197	0.00	60.5	35.0	295.0	1
0.0392	0.0193	0.00	61.2	35.0	295.0	1
0.0359	0.0769	0.00	50.3	35.0	295.0	1
0.4480	0.3550	0.00	0.0	35.0	295.0	1
0.1890	0.1180	0.00	20.8	15.0	295.0	1
0.0676	0.0224	0.00	37.4	35.0	295.0	1
0.0527	0.0059	0.00	50.2	15.0	295.0	1
0.0477	0.0293	0.00	60.3	35.0	295.0	1
0.0397	0.0681	0.00	68.1	15.0	295.0	1
0.0800	0.1280	4.91	37.8	35.0	295.0	1
0.0250	0.0103	4.91	60.5	40.0	295.0	3
0.1300	0.0842	4.91	37.8	8.0	295.0	1
0.0150	-0.0036	4.91	60.5	15.0	295.0	3
0.1540	0.2940	4.91	22.2	9.0	295.0	1
0.1120	0.2220	4.91	20.8	10.0	295.0	3
0.0800	0.1350	4.91	35.0	25.0	295.0	3
0.0359	0.0876	4.91	35.6	15.0	295.0	3
0.0700	0.1180	4.91	35.7	15.0	295.0	3
0.0660	0.1610	4.91	32.9	35.0	295.0	3
0.0800	0.1040	4.91	0.0	35.0	295.0	1
0.0250	0.0407	4.91	50.3	35.0	295.0	3
0.0070	-0.0027	4.91	56.2	8.0	295.0	3
0.0050	0.0073	4.91	50.8	20.0	295.0	3
0.0090	0.0144	4.91	57.9	35.0	295.0	3
0.0100	0.0104	4.91	65.0	15.0	295.0	3
0.0230	0.0103	4.91	60.3	35.0	295.0	3
0.0110	0.0062	4.91	15.0	15.0	295.0	3
0.0050	0.0138	4.91	65.4	25.0	295.0	3
0.0060	0.0062	4.91	65.6	9.0	295.0	3
0.7380	0.6108	4.32	0.0	25.0	295.0	4
0.5490	0.3900	4.32	15.0	70.0	295.0	1
0.3250	0.2010	4.32	37.8	60.3	295.0	4
0.1710	0.0435	4.32	60.1	65.0	295.0	1
0.0660	0.1010	3.72	35.0	35.0	295.0	1
0.5200	0.5270	3.97	9.0	9.0	295.0	1
0.0960	0.1970	9.31	36.0	20.0	295.0	4
0.8360	0.7210	8.10	0.0	20.0	295.0	4
0.8640	0.7710	8.10	0.0	70.0	295.0	4

Table 16.3, continued

Strain to Failure, Measured	Strain to Failure, Predicted	[Sn], wt%	Cold Work, %	Grain Size, μm	Test Temperature, K	Reference No.
0.5650	0.4900	8.10	15.2	110.0	295.0	4
0.3520	0.2740	5.19	30.1	90.0	295.0	4
0.1470	0.0920	5.19	80.0	110.0	295.0	4
0.7570	0.7310	8.78	0.0	16.0	295.0	4
0.8240	0.7920	4.78	0.0	88.0	295.0	4
0.5360	0.5530	8.78	16.0	75.0	295.0	4
0.3040	0.2990	9.76	30.1	80.0	295.0	4
0.1880	0.1190	9.76	90.0	90.0	295.0	4
0.2760	0.2070	4.28	27.0	25.0	295.0	6
0.7300	0.6970	4.28	0.0	70.0	295.0	5
0.3260	0.2770	4.05	30.0	110.0	295.0	6
0.8300	0.7700	8.09	0.0	75.0	295.0	5
0.2660	0.2400	9.96	80.0	110.0	295.0	6
0.7550	0.8010	9.96	0.0	90.0	295.0	5
0.0150	0.0155	5.19	60.5	80.0	295.0	6
0.0500	0.0658	5.19	70.0	90.0	295.0	5
0.0350	0.0297	5.19	79.0	60.5	295.0	6
0.0200	0.0927	5.19	90.8	90.0	295.0	5
0.0090	0.1230	5.19	94.7	80.0	295.0	6
0.0100	0.1330	5.19	96.8	90.0	295.0	5
0.0060	0.1460	5.19	97.3	80.0	295.0	6
0.2520	0.3060	4.20	70.0	50.0	20.0	10
0.3020	0.2510	4.20	75.0	80.0	76.0	10
0.1880	0.0341	4.20	75.0	90.0	295.0	10
0.1800	0.0592	4.85	80.0	101.0	295.0	11
0.2000	0.1710	4.85	90.0	100.0	195.0	10
0.3400	0.3050	4.85	80.0	110.0	76.0	11
0.3900	0.3660	4.85	80.0	101.0	20.0	10
0.3400	0.3650	4.85	80.0	101.0	4.0	11
0.8190	0.7700	8.78	0.0	90.0	72.2	16
0.7940	0.7710	4.78	0.0	80.0	149.0	16
0.8300	0.7710	9.76	0.0	80.0	295.0	16
0.4910	0.7710	4.78	0.0	80.0	292.0	16
0.8700	0.6970	5.67	0.0	90.0	73.0	16
0.8150	0.6970	5.67	0.0	80.0	149.0	16
0.6060	0.6970	5.67	0.0	90.0	220.0	16
0.5960	0.6970	5.67	0.0	80.0	294.0	16
0.9060	0.6650	8.78	0.0	90.0	72.2	16
0.6640	0.6650	4.78	0.0	80.0	152.0	16
0.6060	0.6650	8.78	0.0	90.0	220.0	16
0.4910	0.6650	4.78	0.0	80.0	296.0	16
0.7160	0.5530	2.35	0.0	80.0	72.9	16
0.5120	0.5530	2.35	0.0	80.0	152.0	16
0.4920	0.5530	2.35	0.0	90.0	220.0	16
0.4530	0.5530	2.35	0.0	80.0	294.0	16
0.7250	0.7210	5.82	0.0	100.0	273.0	19
0.7350	0.7210	5.82	0.0	100.0	296.0	19
0.9000	0.7210	5.82	0.0	100.0	20.0	16
0.5890	0.5750	5.82	0.0	6.0	273.0	19
0.6990	0.5750	5.82	0.0	6.0	206.0	19
0.8320	0.5750	5.82	0.0	6.0	86.0	19

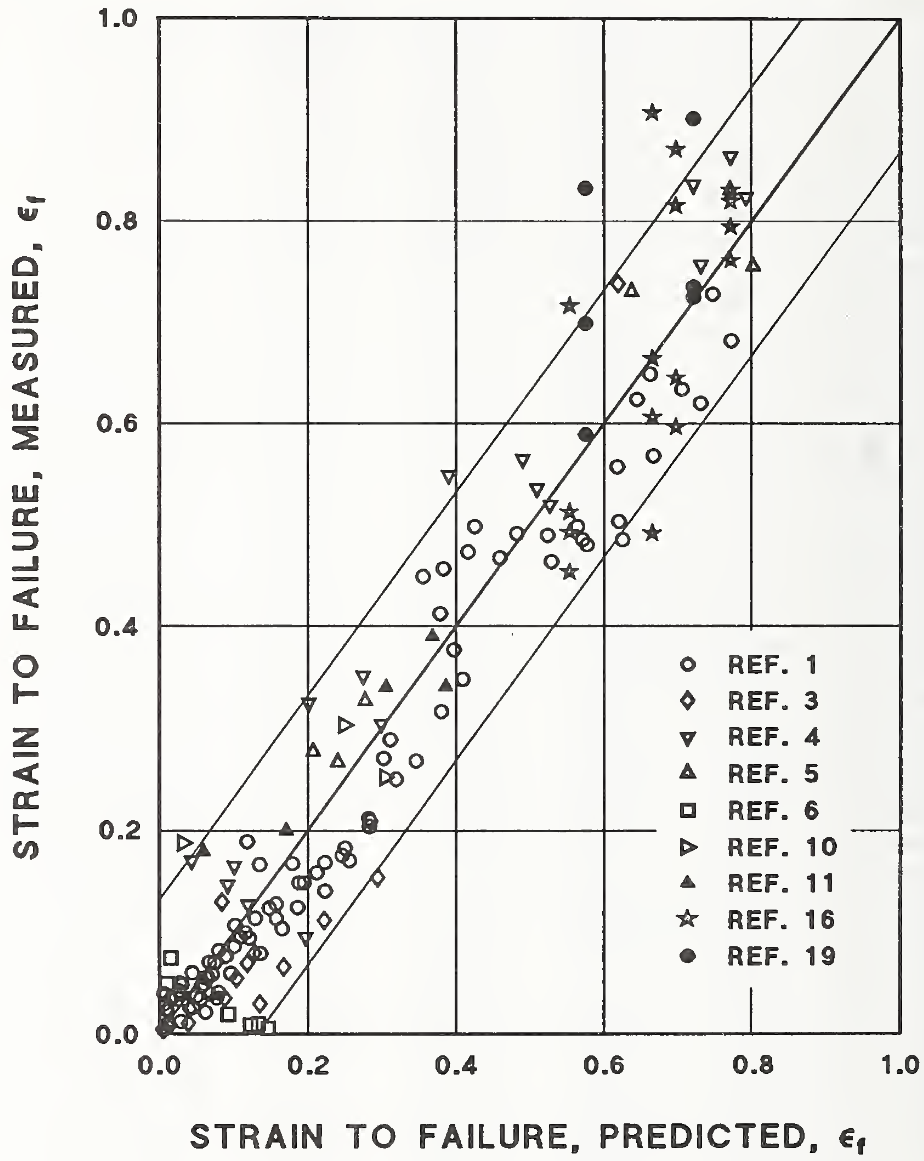

Figure 16.6. The data shown were used to compute the regression of strain to failure upon [Sn], *CW*, *d*, and *T* [Equation (16-3)]. For clarity, data points were removed where overlapping occurred to such an extent that symbols could not be discerned. All data are presented in Table 16.3. Products were in sheet, wire, strip, and bar form.

DATA SOURCES AND ANALYSIS

Relatively few cryogenic reduction of area measurements for phosphor bronzes are available, compared with measurements of other tensile properties. However, results of one systematic investigation of the effects of Sn content, [Sn], and temperature (4–300 K) on annealed material have been reported (Reference 16.14). For analysis, these data were combined with data from Reference 16.4 and 16.5 in which [Sn], P content, [P], cold work (*CW*), and grain size (*d*) were varied. Only five measurements on cold-worked material between 4 and 295 K were available for this analysis (Reference 16.11). The temperature dependence of this set of measurements is shown in Figure 16.7. A total of 67 measurements were used to develop a predictive equation for reduction of area (R.A.). In this set of data, degree of *CW* (percent reduction of thickness or area) ranged from 0 to 85%; [Sn] from 1.5 to 12.20 wt%; [P] from 0 to 0.38 wt%; and *d* from 15 to 150 μm. (An anomalous measurement with a grain size of 9 μm from Reference 16.4 was dropped from the data set.) Product was in bar form (References 16.4, 16.5, 16.11, and 16.14). All cold work was done by drawing (bar stock). The available characterization of materials and measurements are given in Table 16.5 at the end of the tensile properties section.

The analysis of the data set showed that *d* and [P] did not affect R.A. This data set was not ideal for developing a predictive equation relating R.A. to temperature (*T*), [Sn], and *CW*, because only a few measurements from 4 to 295 K on cold-worked material are available.

RESULTS

The equation expressing the dependence of R.A. upon the parameters discussed above is

$$\begin{aligned}\text{R.A.} = &+91.0 - 4.84\,[\text{Sn}] + 0.139\,[\text{Sn}]^2 \\ &- 1.80\,CW + 1.21\,[\text{Sn}]^{1/2}T^{1/3} - 21.5\,[\text{P}] \\ &+ 0.558\,CW[\text{Sn}] - 0.0439\,CW[\text{Sn}]^2 \end{aligned} \tag{16-4}$$

$$(\text{S.D.} = 3.8\%),$$

where $4\ \text{K} \leq T \leq 300\ \text{K}$. The standard deviations of the coefficients are: constant term, 2.1; [Sn], 0.76; $[\text{Sn}]^2$, 0.051; *CW*, 0.40; $[\text{Sn}]^{1/2}T^{1/3}$, 0.11; [P], 5.8; *CW*[Sn], 0.126; and $CW[\text{Sn}]^2$, 0.0090. This set of measurements and parameters are presented in Table 16.4, which also gives the R.A. values predicted from the analysis described. Figure 16.8 indicates the fit of the data to Equation (16-4). The scatter band represents two standard deviations about the straight line, which corresponds to agreement between the measured and predicted values of R.A. The variance of the data was assumed to be normally distributed and constant throughout the range of the predicted values. Table 16.4 presents the R.A. values calculated from Equation (16-4) as well as the measured R.A. and the parameters [Sn], *CW*, *d*, and *T*. The available characterization of materials and measurements is given in Table 16.5 at the end of the tensile properties section.

DISCUSSION

It would be advantageous to have more measurements of R.A. on phosphor bronzes of varying *CW* and [Sn] for temperatures below 295 K. Equation (16-4) represents the best determination of the dependence of R.A. on [Sn], *CW*, and *T* that could be obtained from the available database.

Table 16.4. Reduction of Area Dependence on [Sn], *CW*, and [P] (4–295 K).

Reduction of Area, Measured, %	Reduction of Area, Predicted, %	[Sn], wt%	Cold Work, %	[P], wt%	Test Temperature, K	Reference No.
68.4	81.9	3.72	21.0	0.08	295.0	4
83.9	76.6	3.67	85.0	0.18	295.0	4
92.8	81.3	4.32	0.0	0.38	295.0	4
83.9	73.0	4.32	15.2	0.18	295.0	4
78.7	79.7	4.32	30.1	0.08	295.0	4
71.3	71.0	4.32	50.1	0.18	295.0	4
81.2	82.2	8.09	0.0	0.08	295.0	4
83.9	82.2	2.80	0.0	0.18	295.0	4
84.0	79.8	8.10	15.2	0.08	295.0	4
77.3	77.4	8.10	85.0	0.18	295.0	4
81.2	81.3	8.10	50.1	0.08	295.0	4
81.5	79.7	2.88	0.0	0.18	295.0	4
78.4	79.7	9.76	0.0	0.12	295.0	4
72.0	71.6	2.88	15.2	0.18	295.0	4
84.8	63.6	9.76	30.0	0.12	295.0	4
56.4	90.9	8.10	50.1	0.18	295.0	4
78.7	77.5	4.28	27.0	0.09	295.0	5
82.1	90.9	4.28	0.0	0.09	295.0	5
78.7	79.8	8.09	30.0	0.12	295.0	5
81.5	71.6	2.09	0.0	0.18	295.0	5
84.9	58.1	9.96	30.0	0.12	295.0	5
73.2	76.6	9.96	0.0	0.18	295.0	5
78.7	74.0	8.89	85.0	0.08	295.0	11
73.2	74.9	4.85	85.0	0.18	150.0	14
84.0	81.4	8.89	30.0	0.12	78.7	14
82.1	63.6	4.85	85.0	0.18	20.0	14
83.9	68.6	4.85	85.0	0.18	4.0	14
86.0	86.5	1.50	0.0	0.00	4.0	14
78.7	90.4	1.50	0.0	0.00	4.0	14
93.3	92.0	1.50	0.0	0.00	150.0	14
93.9	93.1	1.50	0.0	0.00	225.0	14
95.0	90.9	1.50	0.0	0.00	300.0	14
82.3	81.3	8.89	0.0	0.00	4.0	14
89.1	87.2	2.80	0.0	0.00	77.0	14
78.7	89.3	8.89	0.0	0.00	150.0	14
91.5	90.9	2.80	0.0	0.10	225.0	14
92.8	92.0	2.80	0.0	0.00	300.0	14
79.5	74.8	2.80	0.0	0.10	4.0	14
84.0	87.2	2.80	0.0	0.00	77.0	14
89.1	90.9	2.80	0.0	0.00	225.0	14
89.7	92.1	8.89	0.0	0.00	300.0	14
83.9	74.0	5.20	0.0	0.00	77.0	14
78.7	81.4	5.20	0.0	0.00	4.0	14
83.9	74.0	5.20	0.0	0.10	150.0	14
89.7	86.4	5.20	0.0	0.00	225.0	14
83.9	88.1	5.20	0.0	0.10	300.0	14
92.8	74.0	5.20	0.0	0.00	4.0	14
83.9	88.1	5.20	0.0	0.10	4.0	14
86.1	86.4	5.20	0.0	0.00	225.0	14
87.1	88.1	5.20	0.0	0.00	300.0	14
66.8	66.5	8.10	0.0	0.00	4.0	14

C50100–C52400: Annealed; Cold-worked

Reduction of Area vs. [Sn], Cold Work (4–300 K)

Table 16.4, continued

Reduction of Area, Measured, %	Reduction of Area, Predicted, %	[Sn], wt%	Cold Work, %	[P], wt%	Test Temperature, K	Reference No.
74.6	75.6	8.10	0.0	0.00	77.0	14
81.1	79.3	8.10	0.0	0.00	150.0	14
85.4	81.9	8.10	0.0	0.00	225.0	14
69.9	84.0	8.10	0.0	0.00	300.0	14
57.8	66.5	8.10	0.0	0.00	77.0	14
69.9	75.6	8.10	0.0	0.00	77.0	14
85.4	81.9	8.10	0.0	0.00	300.0	14
66.3	66.5	12.20	0.0	0.00	4.0	14
73.8	70.7	12.20	0.0	0.00	77.0	14
76.7	75.2	12.20	0.0	0.00	150.0	14
73.8	75.6	12.20	0.0	0.00	225.0	14
79.3	81.0	12.20	0.0	0.00	300.0	14
54.5	59.5	12.20	0.0	0.00	4.0	14
71.2	70.7	12.20	0.0	0.00	77.0	14
76.5	75.2	12.20	0.0	0.00	150.0	14
81.5	81.0	12.20	0.0	0.00	300.0	14

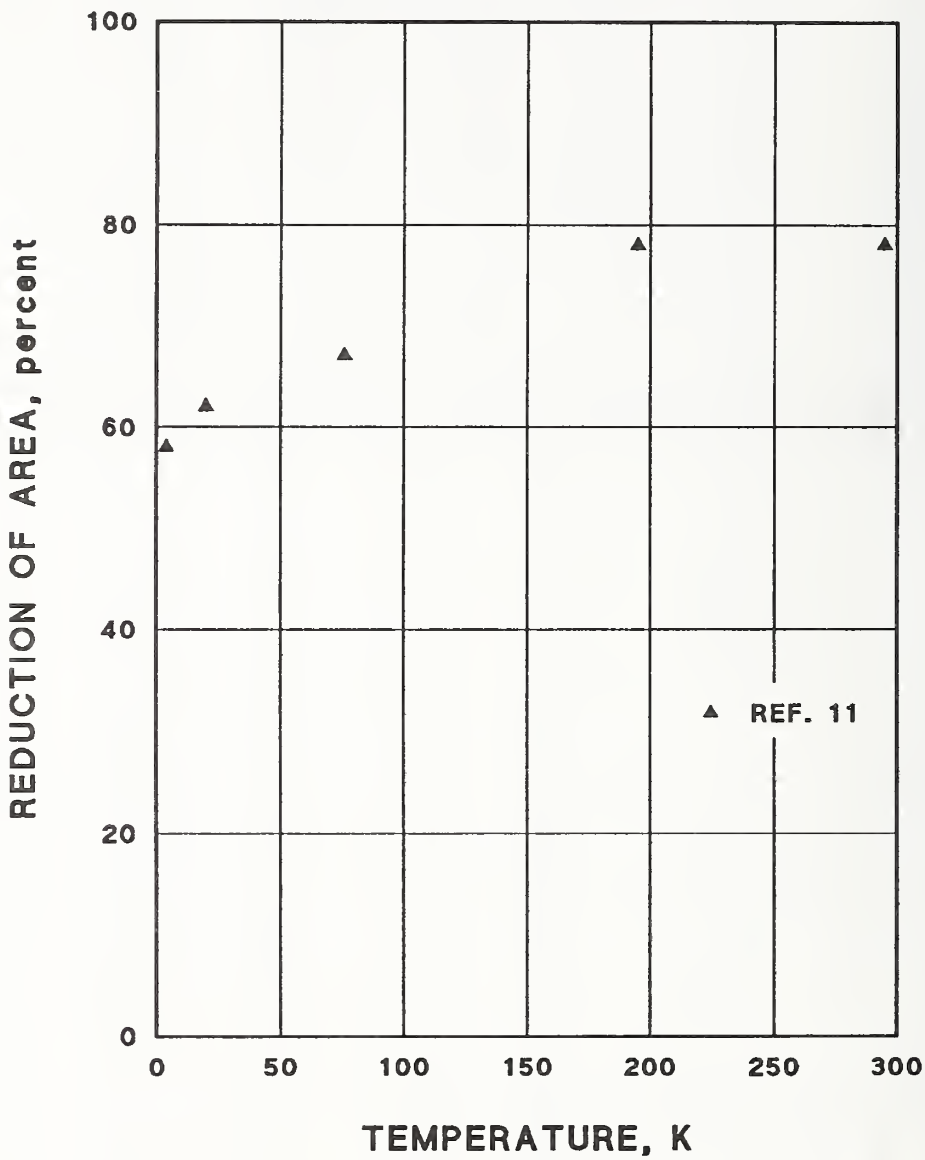

Figure 16.7. These data from Reference 16.11 indicate a decrease in reduction of area as the temperature is reduced below 295 K. Product, in bar form, was cold-worked to 85%.

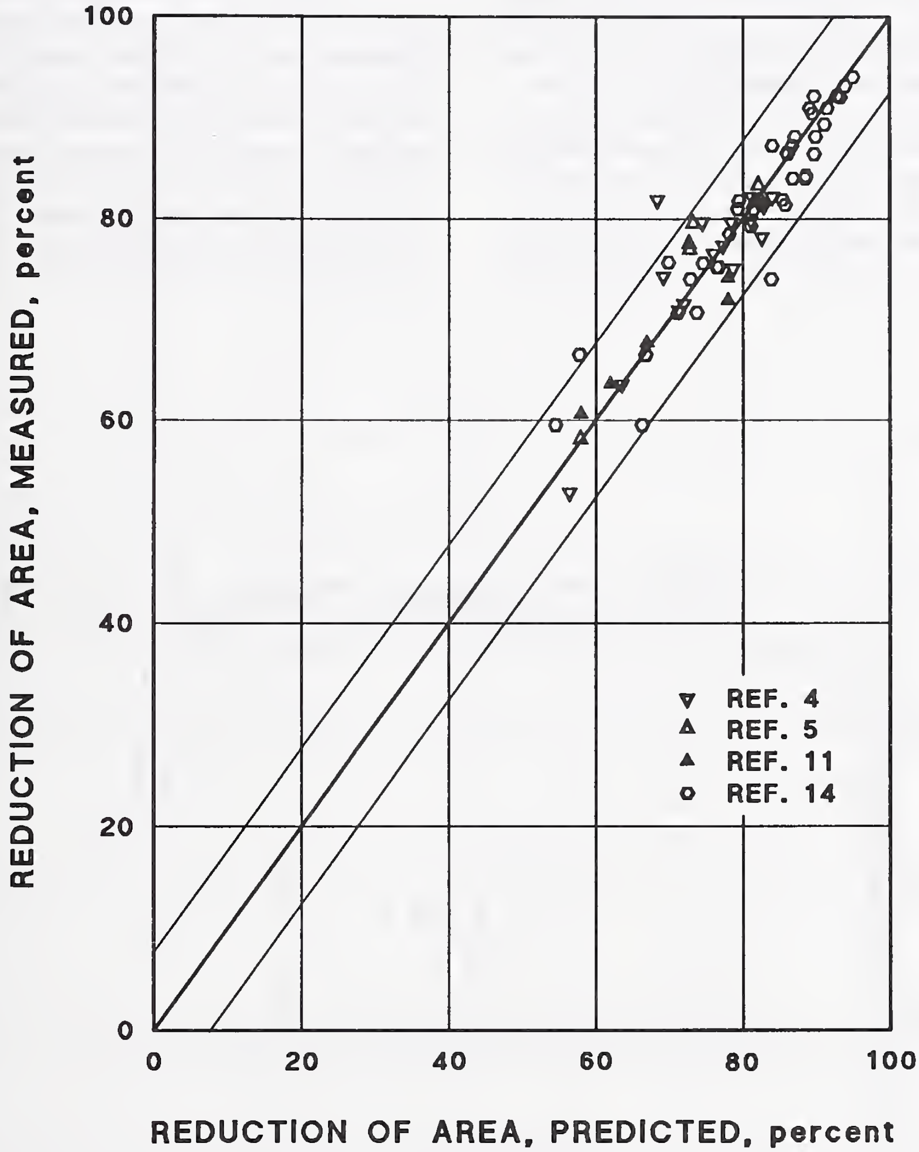

Figure 16.8. The data shown were used to compute the regression of reduction of area upon [Sn], *CW*, *d*, and *T* [Equation (16-4)]. All data are presented in Table 16.4. The product was in bar form.

DATA SOURCE AND ANALYSIS

Engineering stress-strain curves at 4, 20, 76, 195, and 295 K for spring-hard bar (84% reduction of area) containing 4.85 wt% Sn are presented in Figure 16.9. Reference 16.11 is the source of these data. In Figure 16.10, stress-strain data from Reference 16.9 are presented. These data are for annealed wire tested at 4.2 K. The Sn content, [Sn], is indicated on the figure. True stress-strain data at 4 and 77 K from Reference 16.14 on annealed bar are given In Figures 16.11 and 16.12. The [Sn] varies from 0 to 12.2 wt%, and is indicated on the figure. The available characterization of materials and measurements are given in Table 16.5 at the end of the tensile properties section.

DISCUSSION

No 295-K true stress-strain data were presented in Reference 16.14. True stress-strain measurements for a similar range of [Sn] at 295 K are presented in Reference 16.20. For comparable [Sn], these 295-K curves lie below the 77-K curves in Figure 16.12, as would be expected. However, the 295-K data from Reference 16.20 are not presented here, because of the difficulty in comparing stress-strain curves that have been obtained on different material.

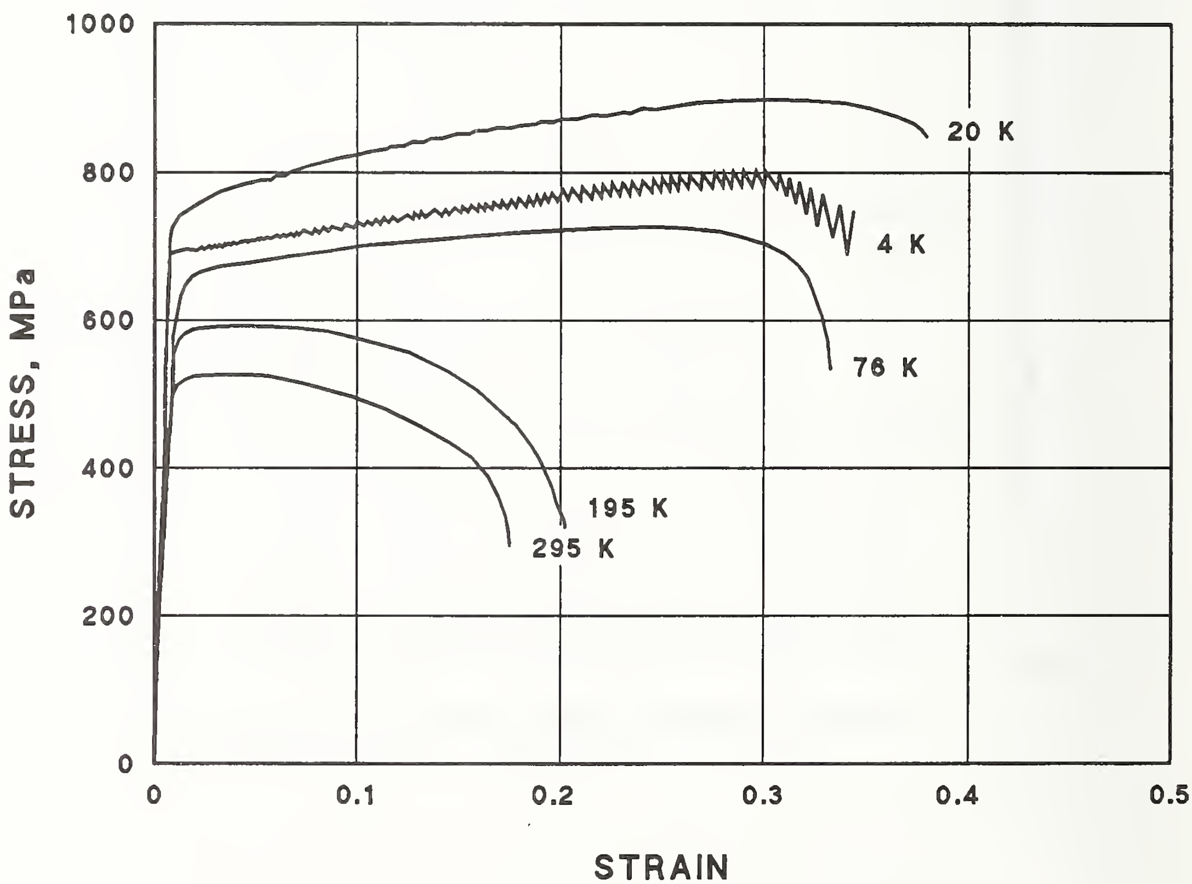

Figure 16.9. Stress-strain curves at five temperatures for spring-drawn bar containing 4.85 wt% Sn. Reference 16.11 is the source of these data.

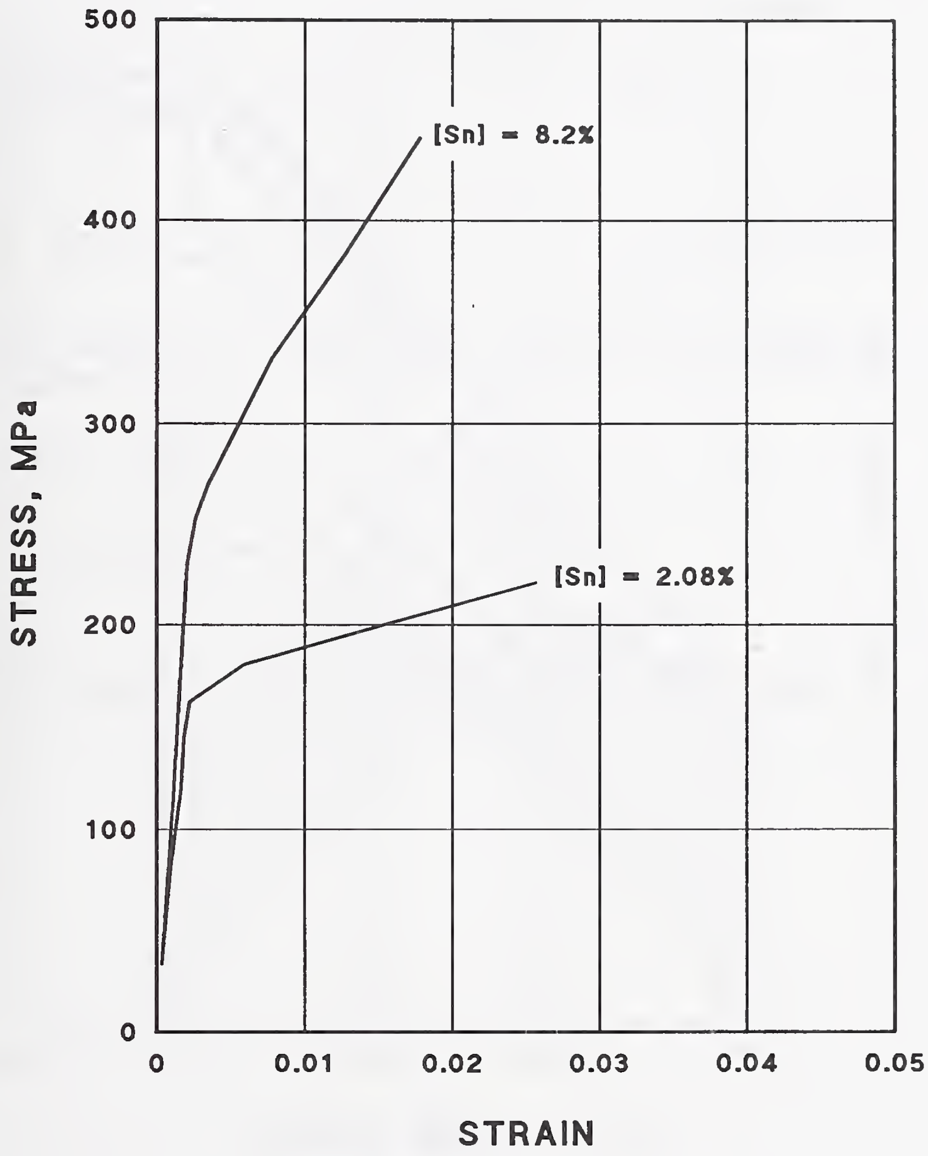

Figure 16.10. Stress-strain curves at 4.2 K for annealed wire at two Sn contents (in wt%). Reference 16.9 is the source of these data.

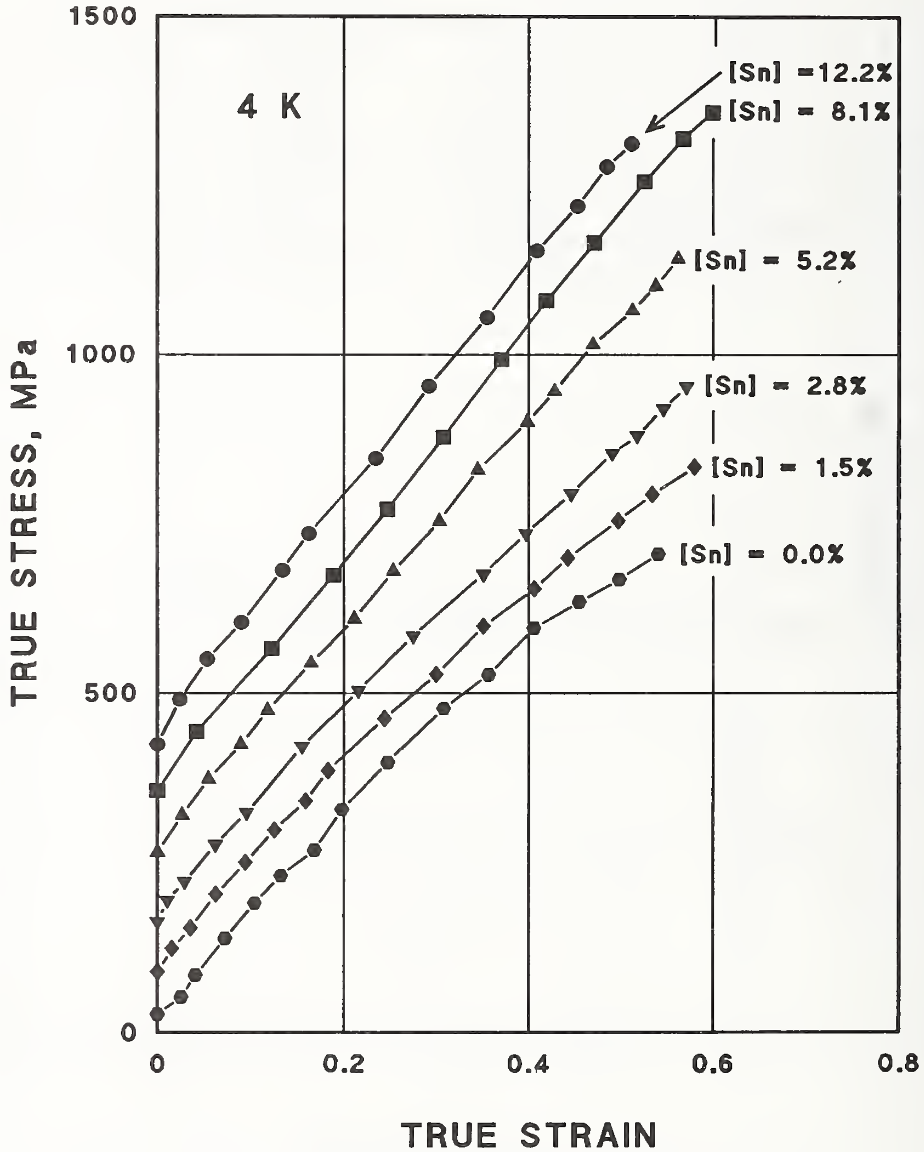

Figure 16.11. True stress-strain curves at 4 K from Reference 16.14 are plotted for increasing values of Sn content, [Sn] (in wt%). The product was in the form of annealed bar.

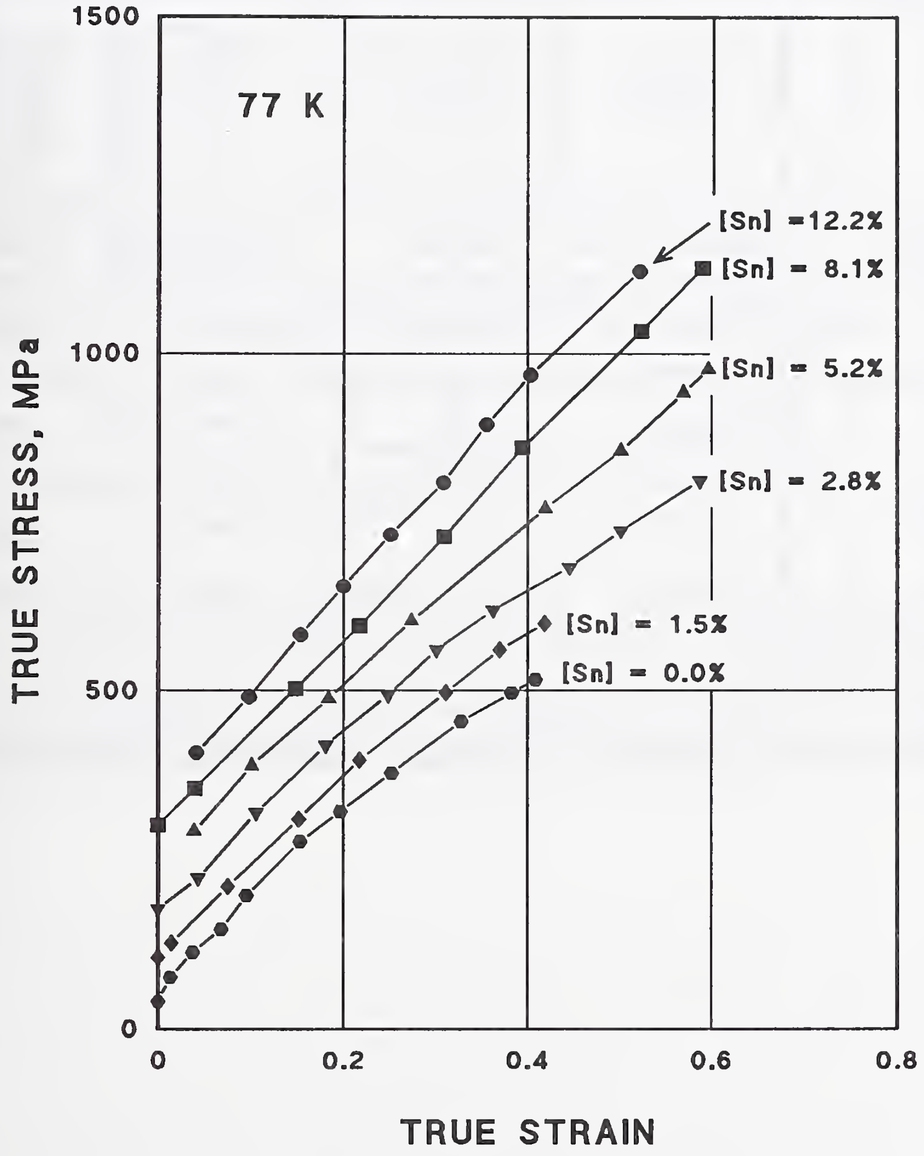

Figure 16.12. True stress-strain curves at 77 K from Reference 16.14 are plotted for increasing values of Sn content, [Sn] (in wt%). The product was in the form of annealed bar.

Table 16.5. Characterization of Materials and Measurements.

Reference No.	1	2	3	4
Specification	—	C51000	C51000	—
Composition (wt%)				
Cu	—	—	94.96	88.5–95.3
Sn	0.5–10	5	4.91	3.72–9.31
P	0.05 or 0.4	~0.19	0.07	0.08–0.38
Pb	—	—	—	0–0.003
Fe	—	—	—	0.025–1.36
Zn	—	—	0.01	0–0.12
Others	—	—	—	Mn: 0.21–0.78
Material Condition	Cold-rolled, 0–68%	Cold-rolled, 0–61%	Cold-rolled, 22.2–65.6%	Cold-drawn 0–50.1%
Grain Size	15 or 35 μm	10–75 μm	8–45 μm	25–90 μm
Hardness	R_B 0.0–106.5	—	—	R_B 34–101
Product Form	Strip, 0.635-cm-thick	Strip, 0.1016–0.1626-cm-thick	Strip, 0.076-cm-thick	Bar, 1.27-cm-dia.
Specimen Type	Flat	—	Rectangular	Round
Width or Dia.	—	—	—	0.795 cm
Thickness	—	—	—	—
Gage Length	5.08 cm	—	5.08 cm	5.08 cm
Strain (Load) Rate	—	—	—	—
No. of Specimens	—	—	5	—
Test Temperature	295 K	295 K	295 K	295 K

C50100–C52400: Annealed; Cold Worked *Tensile Properties (All)*

5	6	7	8	[illegible]	10
—	C51000	—	—	—	C52100
89.76–95.35 4.28–9.96 0.11–0.29 0.003–0.01 0.01–0.02 0–0.10 —	94.03–95.88 4.75–5.64 0.19–0.26 trace–0.01 0.02–0.12 0.02–0.08 —	— 0–8.78 0 — — — —	— 7.8 0 — — — —	— 1.4–8.2 0 — — — —	90.3 8.2 0.06 — — — —
Cold-drawn, 27–36%	Cold-rolled, 60.5–97.3%	—	—	Annealed	Cold-drawn, 75%
25–120 μm	—	20–250 μm	0.5–24 μm	50 μm	50 μm
—	—	—	—	—	R_B 100
Bar, 1.91-cm-dia.	Sheet, 0.025-cm-thick	Bar	—	Wire, 0.025-cm-dia.	Bar, 1.91-cm-dia.
Round 1.28 cm — 5.08 cm	— — — 5.08 cm	Round 0.35 cm — 6.0 cm	— — — —	— — — 5.08 cm	Round 0.635 cm — 2.54 cm
—	—	0.0096/min	—	—	4.98×10^{-4}/min
—	—	—	—	—	—
295 K	295 K	77–297 K	77–297 K	4.2 K	20–300 K

Table 16.5, continued

Reference No.	11	14	16	14	19
Specification	C51000	—	—	C51100	—
Composition (wt%)					
Cu	remainder	—	—	remainder	—
Sn	4.85	0.0–12.2	2.35–8.78	3.9	5.82
P	0.18	—	—	0.3	0.0
Pb	0.02	—	—	—	—
Fe	0.02	—	—	<0.01	—
Zn	0.05	—	—	—	—
Others	—	—	—	—	—
Material Condition	Cold-drawn, 84%	Annealed	—	Annealed	Annealed
Grain Size	101 μm	10–200 μm	50 μm	—	100 and 6 μm
Hardness	R_B 94	—	—	—	—
Product Form	Bar, 1.91-cm-dia.	Bar, 0.953-cm-dia.	—	Bar, 1.91-cm-dia.	Bar, 0.794-cm-dia.
Specimen Type	Round	Round	—	—	Round
Width or Diam.	0.635 cm	0.318 cm	—	—	0.453 cm
Thickness	—	—	—	—	—
Gage Length	3.81 cm	1.75–1.81 cm	—	—	2.45 cm
Strain (Load) Rate	—	0.09/min	0.0096/min	—	0.0096/min
No. of Specimens	—	—	—	—	—
Test Temperature	4–295 K	4–300 K	77–300 K	85–300 K	86–273 K

REFERENCES

1. Gohn, G. P., Guerard, J. P., and Freynik, H. S., "The Mechanical Properties of Wrought Phosphor Bronze Alloys," American Society for Testing Materials, Philadelphia, PA, Special Technical Publication No. 183, 114 pp. (1956).

2. Buell, M. A., "For Cold-worked Copper Alloys Grain Size Is Important," Product Engineering 33, 46–49 (1962).

3. Hart, R. R., "Mechanical Properties of Phosphor Bronze Strip and Their Variations within Temper as Defined by ASTM Practice," Journal of Materials 5, 536–549 (1970).

4. Anderson, A. R., Swan, E. F., and Palmer, E. W., "Fatigue Tests on Some Additional Copper Alloys," Proceedings of the American Society for Testing Materials 46, 678–692 (1946).

5. Smith, C. S., and Van Wagner, R. W., "The Tensile Properties of Some Copper Alloys," Proceedings of the American Society for Testing Materials 41, 825–848 (1941).

REFERENCES

6. Hart, R. R., Wonsiewicz, B. C., and Chin, G. Y., "High Strength Copper Alloys by Thermomechanical Treatments," Metallurgical Transactions 1, 3163–3172 (1970).

7. Vöhringer, O., and Macherauch, E., "The Yield Point of α-Copper–Tin Alloys," Physica Status Solidi 19, 793–803 (1967).

8. Köster, W. and Speidel, M., "Einfluß der Korngröße auf die Streckgrenze von Kupferlegierungen," Physica Status Solidi 3, K401–K405 (1963).

9. Cogan, S. F., and Rose, R. M., "Properties of CuSn Bronze at 4.2 K," Cryogenics 20, 313–315 (1980).

10. McClintock, R. M., Van Gundy, D. A., and Kropschot, R. H., "Low-Temperature Tensile Properties of Copper and Four Bronzes," American Society for Testing and Materials Bulletin 240, 47–50 (1959).

11. Reed, R. P., and Mikesell, R. P., "Low-Temperature (295 to 4 K) Mechanical Properties of Selected Copper Alloys," Journal of Materials 2, 370–392 (1967).

12. Hanson, D., and Pell-Walpole, W. T., "The Effect of Minor Constituents and of Solid Impurites on the Properties of Chill-Cast Bronzes," Chapter XI in Chill-Cast Tin Bronzes, Edward Arnold and Company, London, England, 268–294 (1951).

13. Winterton, K., "Tin Bronzes: Effects of Impurities in the Chill-Cast Condition," Metal Industry 71, 479–482 and 507–509 (1947).

14. Troiano, A. R., and Kochera, J. W., "Temperature-Sensitive Ductility in Face-centered Cubic Copper Alloys," Air Force Materials Laboratory, Wright-Patterson AFB, OH, AFML-TR-67-82, 90 pp. (1967).

15. Gohn, G. R., and Bader, W. G., "The Tensile Properties of Hard-drawn, Alloy A, Phosphor-Bronze Rod," Proceedings of the American Society for Testing Materials 60, 843–848 (1960).

16. Vöhringer, O., "Verformungsverhalten von vielkristallinen α-Kupferlegierungen," Metall 30, 1150–1160 (1976).

17. McAdam, D. J., Jr., Geil, G. W., and Mebs, R. W., "The Effect of Combined Stresses on the Mechanical Properties of Steels between Room Temperature and −188 °C," Proceedings of the American Society for Testing and Materials 45, 448–481 (1945).

18. Nishihata, M., and Kumakaura, Y., "Mechanical Properties of Phosphor-Bronze Wire Spring," Review of the Electrical Communication Laboratory 15, 201–212 (1967).

19. Russell, B., and Jaffrey, D., "The Strain Hardening Characteristics of a Copper–3.2-at.%-Tin Solid Solution," Acta Metallurgica 13, 1–10 (1965).

20. French, R. S., and Hibbard, W. R., Jr., "Effect of Solute Elements on the Tensile Deformation of Copper," Journal of Metals 188, 53–58 (1950).

C51000: Annealed; Cold-worked

Impact Energy (Charpy V-Notch) vs. Temperature (20–300 K)

DATA SOURCES

Charpy V-notch Impact energy measurements from 20 to 300 K were obtained on cold-worked and annealed C51000 phosphor bronze from References 17.1 and 17.2. The product was In bar form (Reference 17.1) or not specified (Reference 17.2). The available characterization of materials and measurements is given in Table 17.3 at the end of the impact properties section.

RESULTS

Figure 17.1 presents the impact data as a function of temperature. All reported measurements are given In Table 17.1.

DISCUSSION

The Impact energy measurements at 295 K on spring-hardened C51000 from References 17.1 and 17.2 differ by a factor of two. Although the tensile yield strength for the material reported in Reference 17.1 Is about 80% of that reported in Reference 17.2, other inaccuracies inherent in the test may explain the discrepancy. Hardness was not reported In Reference 17.2.

The temperature dependence of the impact strength of the annealed material, though available only from 200–300 K, appears to show the same trend, an Increase at low temperatures, as shown by annealed copper (Section 3).

Table 17.1. Impact Energy Dependence on Temperature (20–300 K).

Impact Energy, J	Test Temperature, K	Reference No.
144	295	1
111	195	1
73	76	1
69	20	1
226	300	2
262	200	2
62	300	2
60	200	2

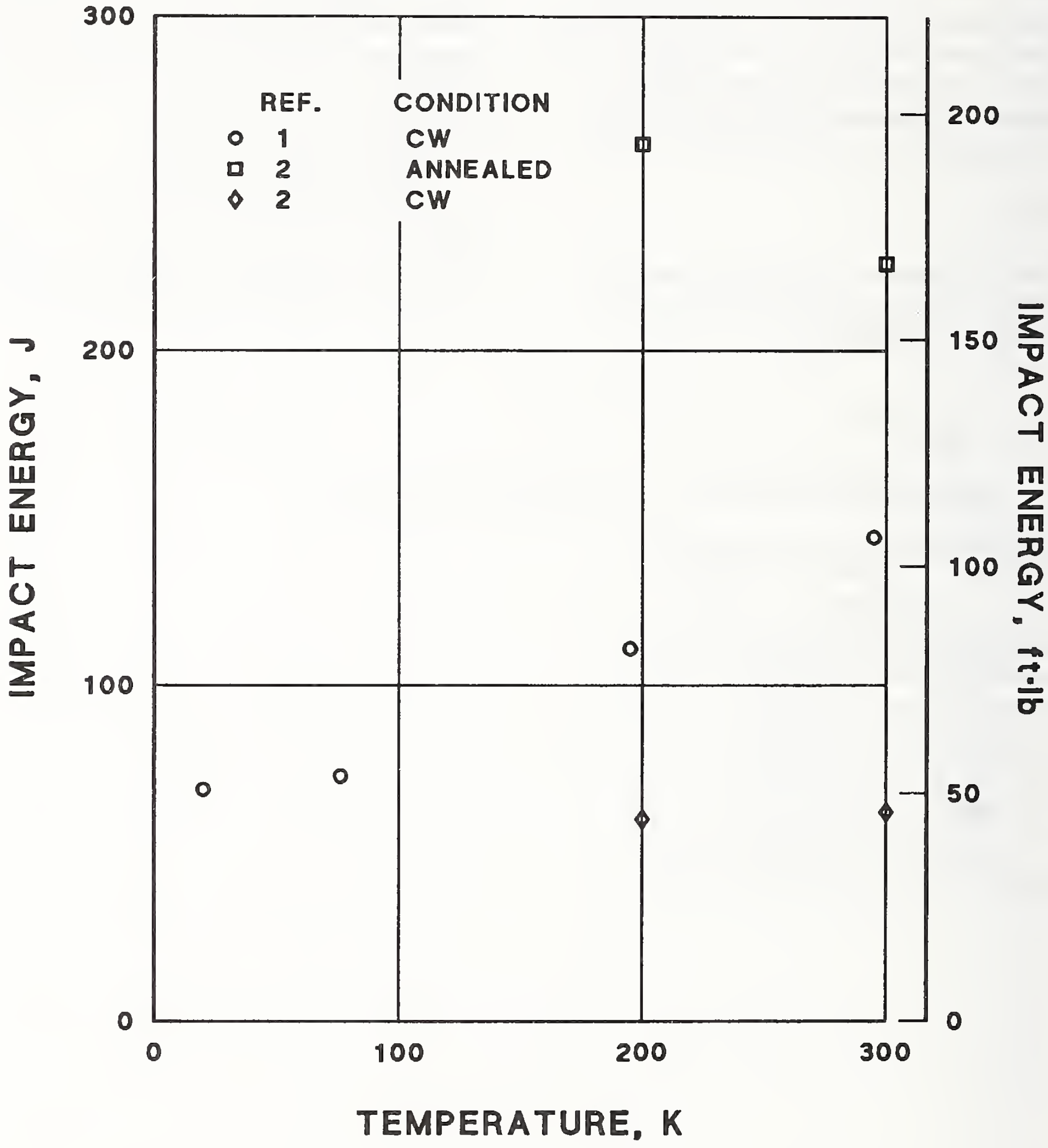

Figure. 17.1. The impact energy dependence on test temperature indicates a decrease in impact energy with increasing temperature for annealed material (Reference 17.2). The temperature dependence for cold-worked material (References 17.1 and 17.2) is unclear. All data are presented in Table 17.1. Product was in bar form for Reference 17.1, and not reported for Reference 17.2.

C52400: Annealed; Cold-worked

Impact Energy (Charpy V-Notch) vs. Temperature (24–296 K)

DATA SOURCE

Charpy V-notch Impact energy measurements from 24 to 296 K on 37% cold-worked C52400 phosphor bronze were obtained from Reference 17.3. The product was in plate form. The available characterization of materials and measurements Is given in Table 17.3 at the end of the impact properties section. Data at 24 K are included because the material is relatively brittle so that a large temperature rise in the specimen from absorbed energy is not expected.

RESULTS

Figure 17.2 presents the impact data as a function of temperature. The measurements are tabulated in Table 17.2.

DISCUSSION

The fracture appearance was reported to be granular at all temperatures, but the area of the shear region decreased as the temperature decreased. The specimens were completely broken through at all temperatures.

Table 17.2. Impact Energy Dependence on Temperature (24–296 K).

Impact Energy, J	Test Temperature, K	Reference No.
28.9	24	3
26.4	80	3
25.7	24	3
26.5	80	3
25.3	80	3
23.1	24	3
21.7	80	3
39.8	196	3
38.8	196	3
37.0	196	3
70.4	296	3
69.0	296	3
56.5	296	3

C52400: Annealed;
Cold-worked

Impact Energy (Charpy V-Notch)
vs. Temperature (24–296 K)

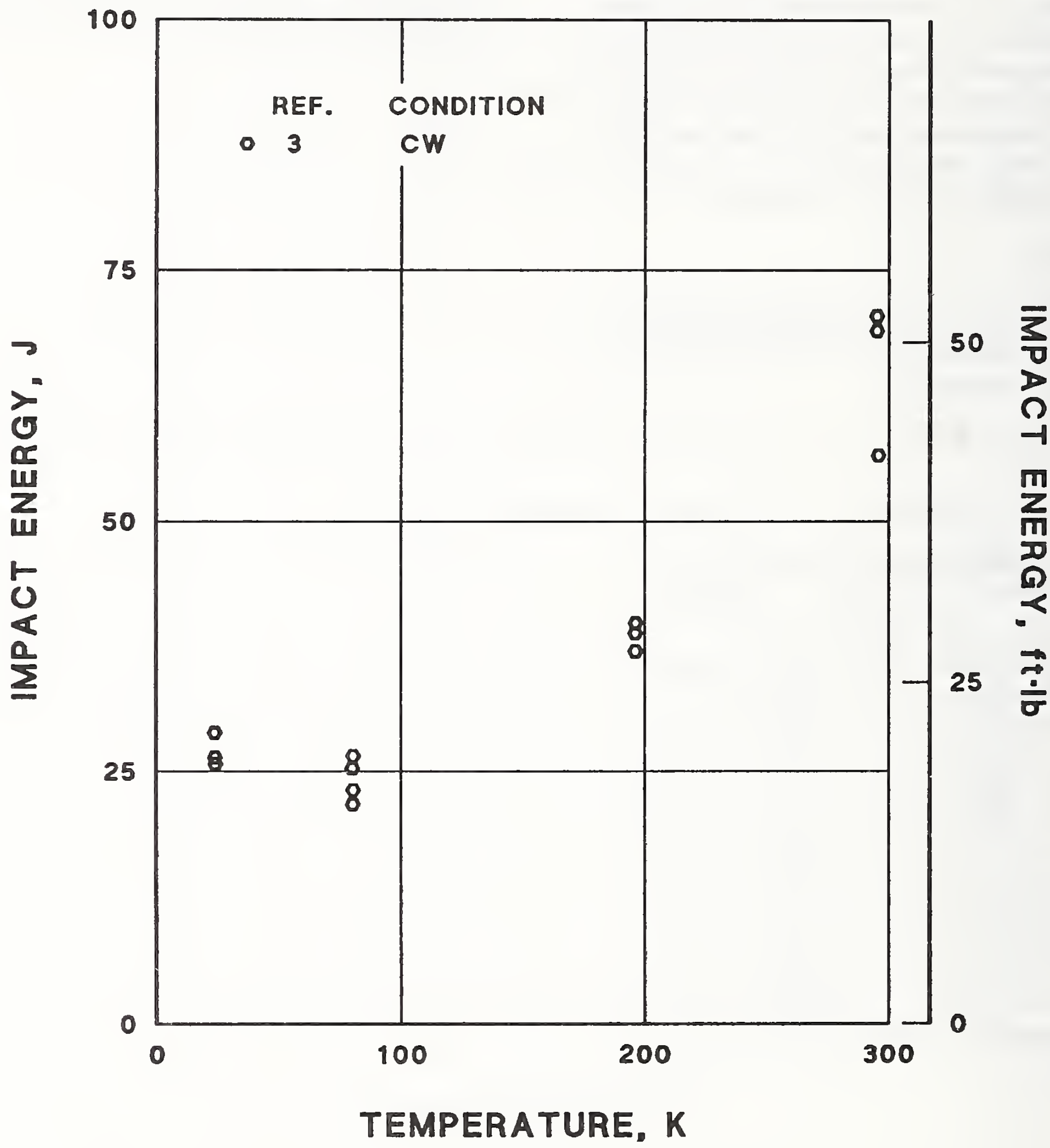

Figure 17.2. The impact energy dependence on test temperature indicates an increase in impact energy with increasing temperature (Reference 17.3). All data are presented in Table 17.2. Product was in plate form.

Table 17.3. Characterization of Materials and Measurements.

Reference No.	1	2A	2B	3
Specification	C51000	C51000	C51000	C52400
Composition (wt%)				
Cu	—	—	—	—
Sn	4.85	5	5	10
P	0.18	—	—	—
Pb	0.02	—	—	—
Fe	0.02	—	—	—
Zn	0.05	—	—	—
Others (Only ≥ 0.001 wt%)	—	—	—	—
Material Condition	Cold-drawn, 85%	Annealed	Cold-worked, 60.5%	Cold-worked, 37%
Grain Size	101 μm	—	—	—
Hardness	R_B 94	—	—	R_B 97–98
Product Form	Bar, 1.91-mm-dia.	—	—	Plate
Specimen Type	Charpy V-notch	Charpy V-notch	Charpy V-notch	Charpy V-notch
No. of Specimens	—	—	—	3–4 per temperature
Test Temperature	20–295 K	200–300 K	200–300 K	24–296 K

REFERENCES

1. Reed, R. P., and Mikesell, R. P., "Low-Temperature (295 to 4 K) Mechanical Properties of Selected Copper Alloys," Journal of Materials 2, 370–392 (1967).

2. Gela, T., Lepkowski, W. J., and Gade, H. M., "How 7 Nonferrous Metals Perform at Low Temperatures," Materials and Methods 44, 116–120 (1956).

3. Mikesell, R. P., and Reed, R. P., "The Results of the Impact Testing of Copper Alloys," U.S. Atomic Energy Commission, Memorandum of Understanding AT(29-1)-1500, 16 pp. (1958).

   Mikesell, R. P., and Reed, R. P., "The Impact Testing of Various Alloys at Low Temperatures," in Advances in Cryogenic Engineering, Vol. 3, Ed., K. D. Timmerhaus, Plenum Press, NY, 316–324 (1960).

C50100–C52400: Annealed; Cold-worked

Reversed Bending Fatigue Life (295 K)

DATA SOURCES AND ANALYSIS

No cryogenic fatigue life measurements on phosphor bronzes were found in the literature. At room temperature, an extensive set of reversed bending measurements on 1-mm strip are available (Reference 18.1). Grain size, Sn content ([Sn]), phosphorus content ([P]), and cold work were varied in these measurements, which are summarized in Figures 18.1, 18.2, and 18.3. The figures present the maximum bending stress at 10^8 cycles. To compare the more limited data of other authors with these measurements, results from Reference 18.1 for [Sn] = 5 and 8 wt% are plotted in Figure 18.4 together with data from References 18.2 to 18.4 for similar [Sn]. (The authors of Reference 18.2 extrapolate bending stress at 10^8 cycles from tests up to 5×10^7 cycles.) Only approximate agreement among the results from different investigators should be expected, since parameters that affect fatigue life, such as grain size, specimen thickness, and [P] varied somewhat. The effects of grain size and specimen thickness are depicted in Figures 18.5 and 18.6, based on data from Reference 18.4. (Figure 18.3 also presents limited data on the effect of grain size.) The available characterization information on specimens and measurements is presented in Table 18.1 at the end of the fatigue properties section.

RESULTS

Figures 18.1 and 18.2 show that fatigue life improves as [Sn] increases, but that this improvement is most marked for [Sn] up to about 3 wt%; there is little improvement as [Sn] is increased further. The improvement in fatigue life with increased cold work also appears to saturate; there is little improvement for cold work above 30 to 40%.

Figure 18.4 shows considerable scatter in the results from References 18.2–18.4 compared to those from Reference 18.1. Thus, fatigue strength endurance data should be used with caution.

Figure 18.5 on the effect of grain size on fatigue life data for C51000 material shows that fine-grained specimens (8, 10 μm) have better fatigue properties than coarse-grained specimens (35, 40 μm). Grain size variability can result in additional scatter in fatigue-life data, as shown in Figure 18.5.

The results from a study of reversed bending fatigue life for C51000 material as a function of specimen thickness are shown in Figure 18.6a and b. Very thin specimens, 0.13-mm thick, have a higher fatigue endurance than specimens that are 0.76-mm thick.

DISCUSSION

Reference 18.1 presents a number of fatigue life curves; the results are summarized here in Figures 18.1–18.3. Most of this fatigue-life data indicate that an asymptotic value of stress has been reached by 10^8 cycles. This is known as the endurance limit. However, the curves presented in Reference 18.4 do not always display this behavior, as the examples given in Figures 18.5 and 18.6 show. See also the fatigue life data presented in the following section on torsional fatigue.

Fatigue testing in bending machines is described in References 18.2 and 18.4. Usually these machines are of the constant displacement or constant-strain type. The load-deflection characteristics used to calculate the bending stress in the specimens are obtained with a separate test fixture. Thus, although the data are presented in the same format as stress-controlled measurements, the data are not strictly stress-controlled.

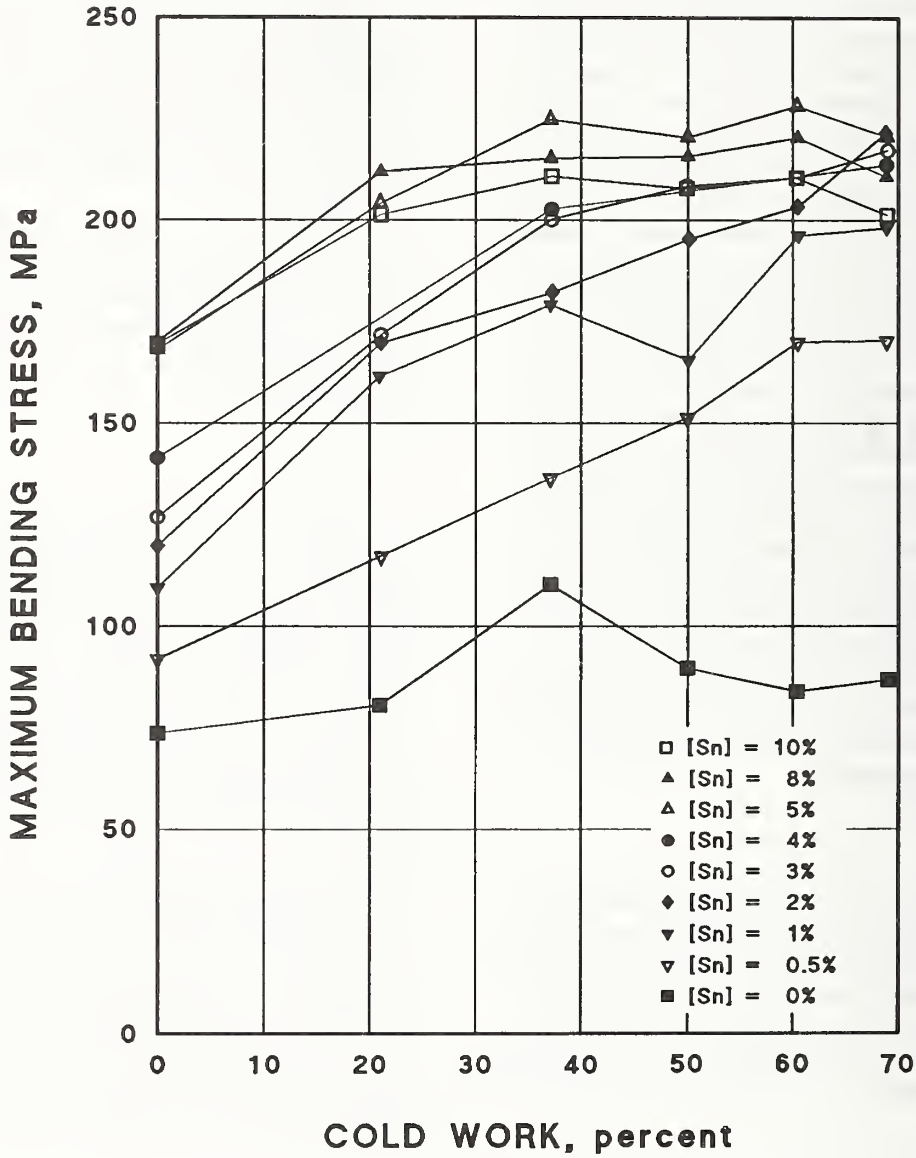

Figure 18.1. The maximum bending stress at 10^8 cycles versus cold work for varying amounts of tin contents in weight percent. Data are from Reference 18.1 on strip containing ~0.05 wt% phosphorus and a nominal grain size of 35 μm.

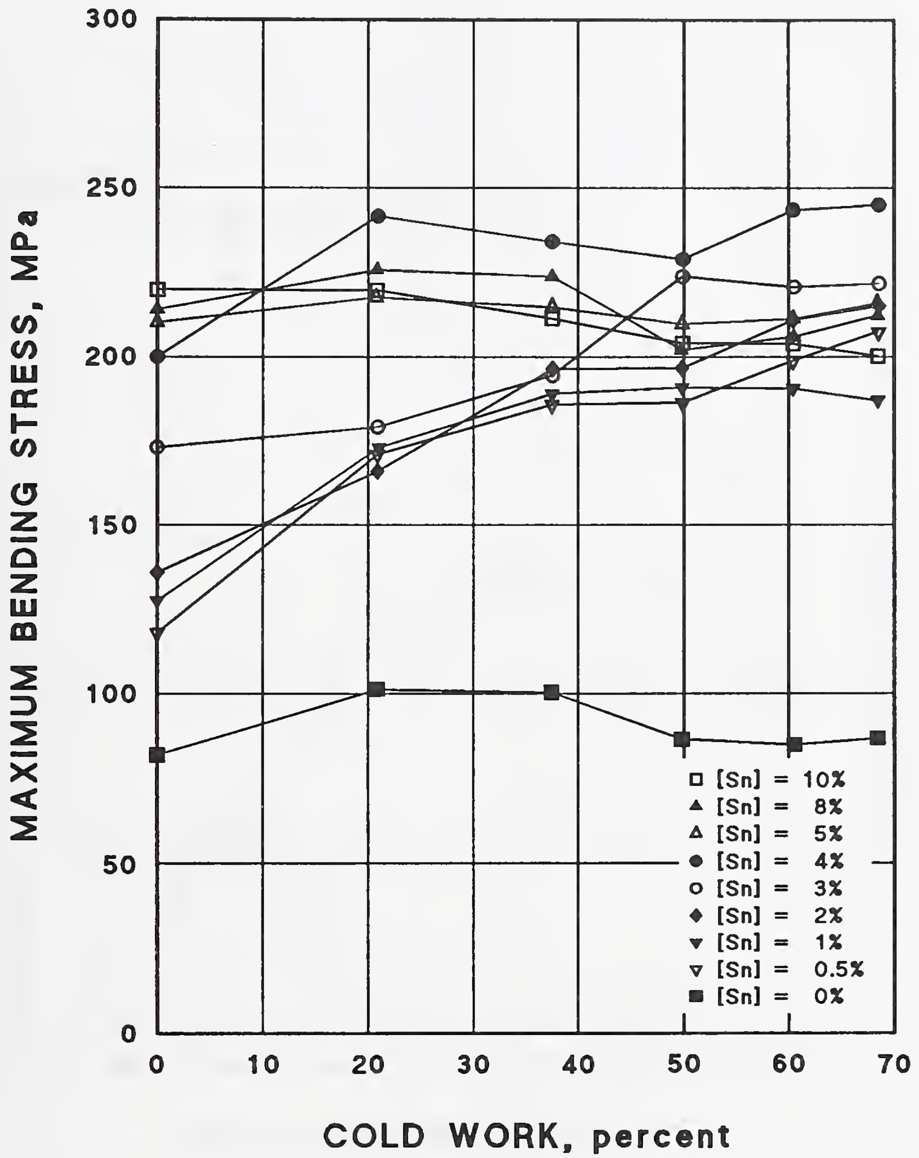

Figure 18.2. The maximum bending stress at 10^8 cycles versus cold work for varying amounts of tin contents in weight percent. Data are from Reference 18.1 on strip containing ~0.05 wt% phosphorus and a nominal grain size of 15 μm.

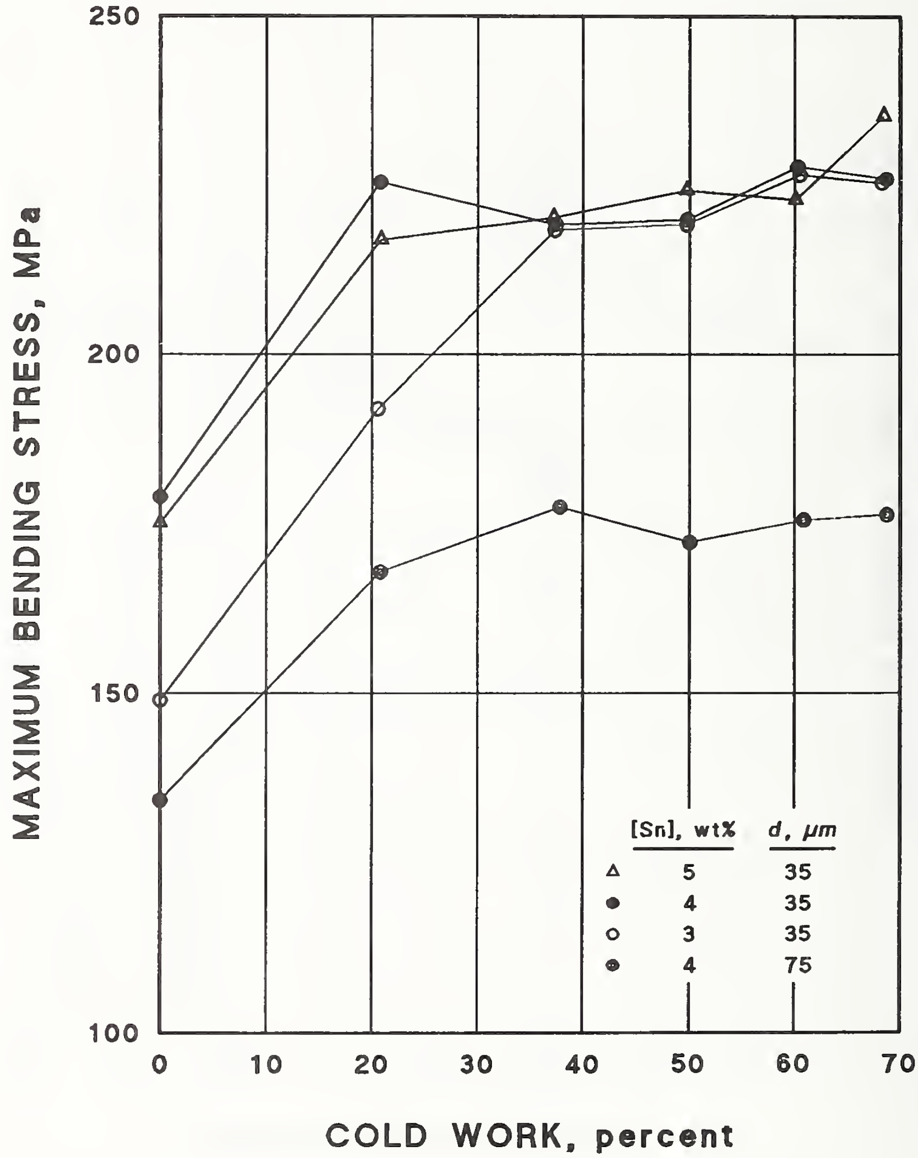

Figure 18.3. The maximum bending stress at 10^8 cycles versus cold work for three tin contents. The nominal grain size, *d*, was 35 μm for the three tin contents, and 75 μm for one (4 wt%) tin content. The data from Reference 18.1 are on strip containing ~0.40 wt% phosphorus.

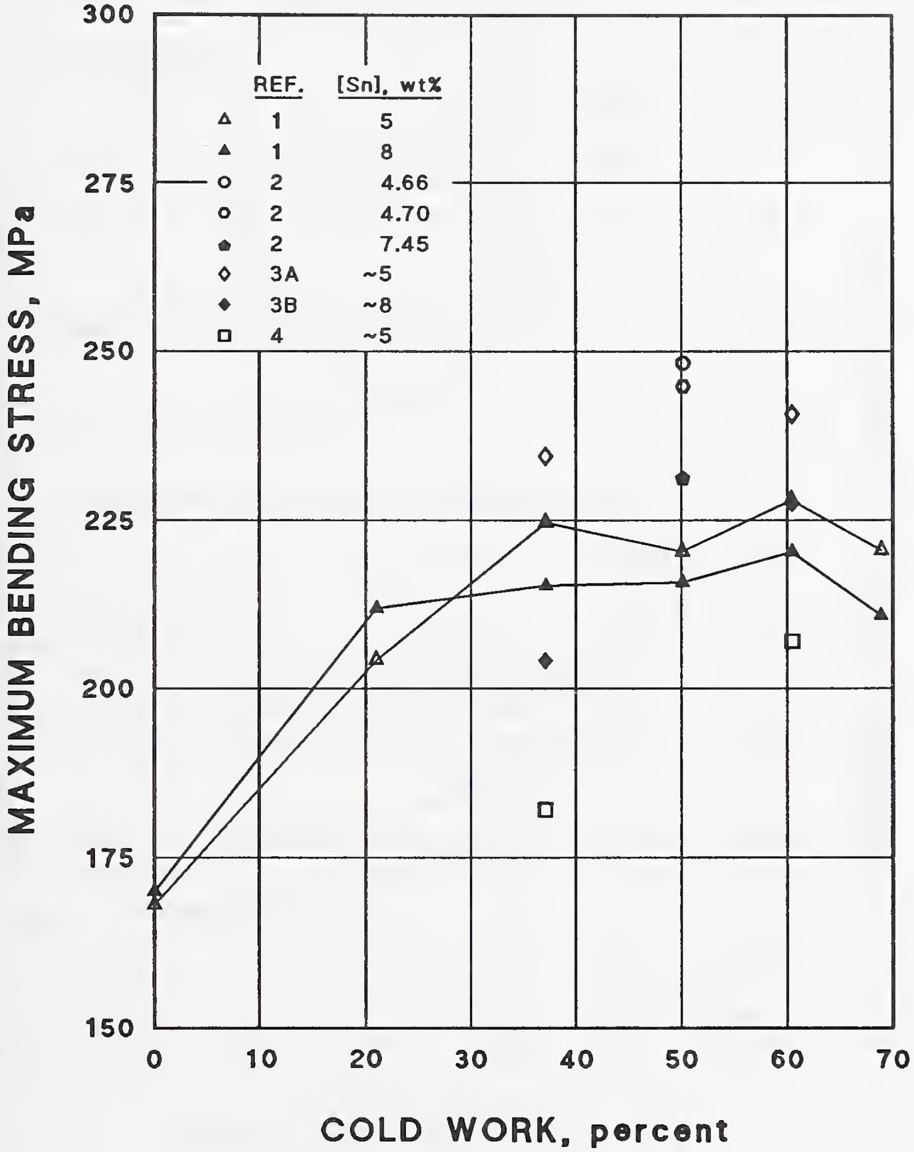

Figure 18.4. The maximum bending stress at 10^8 cycles versus cold work is shown for two approximate tin contents (~5 and ~8 wt%). The product was in strip form for References 18.1 and 18.4, and an unspecified form of cold-rolled product for References 18.2 and 18.3.

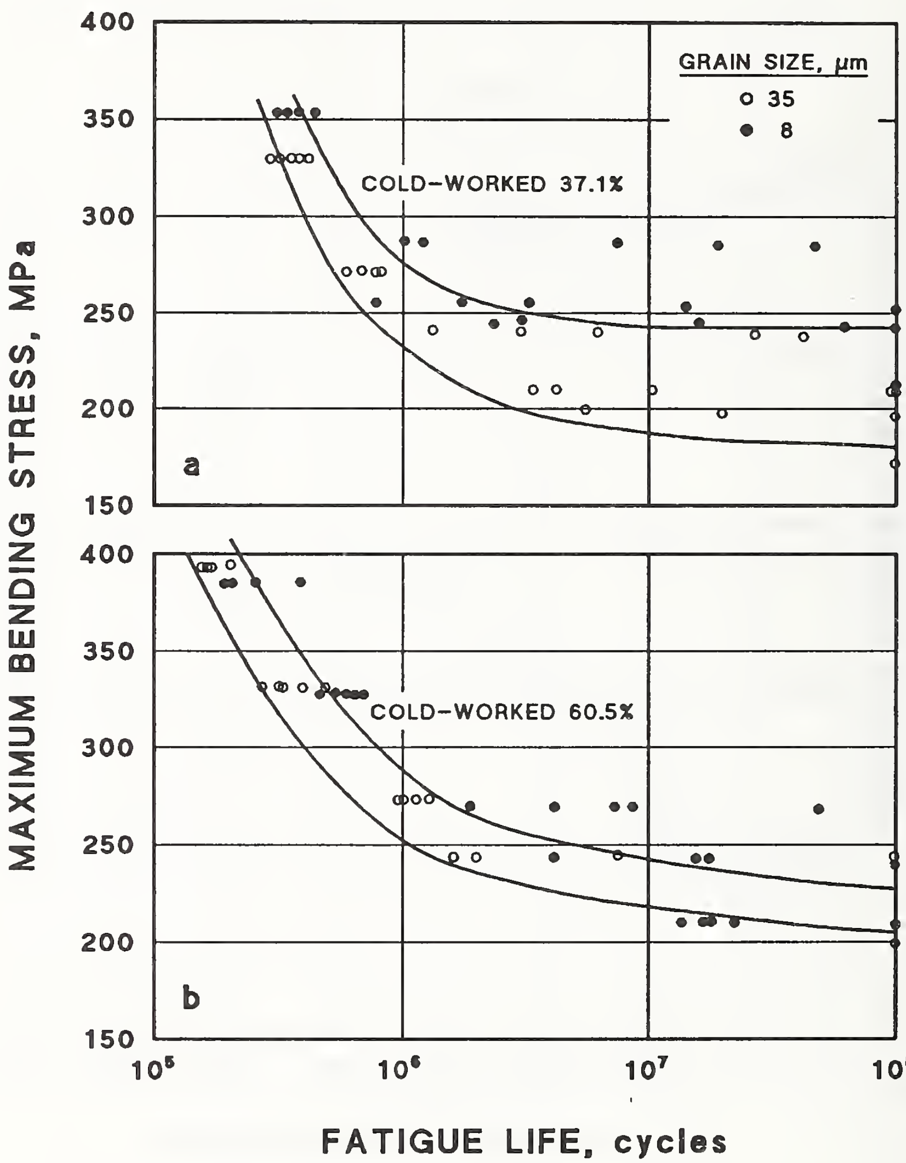

Figure 18.5. The dependence of fatigue life on the maximum bending stress is shown for two amounts of cold work and two grain sizes. The shaded area indicates the variation for the 35-μm material. Data are from Reference 18.4 on C51000 product of strip form.

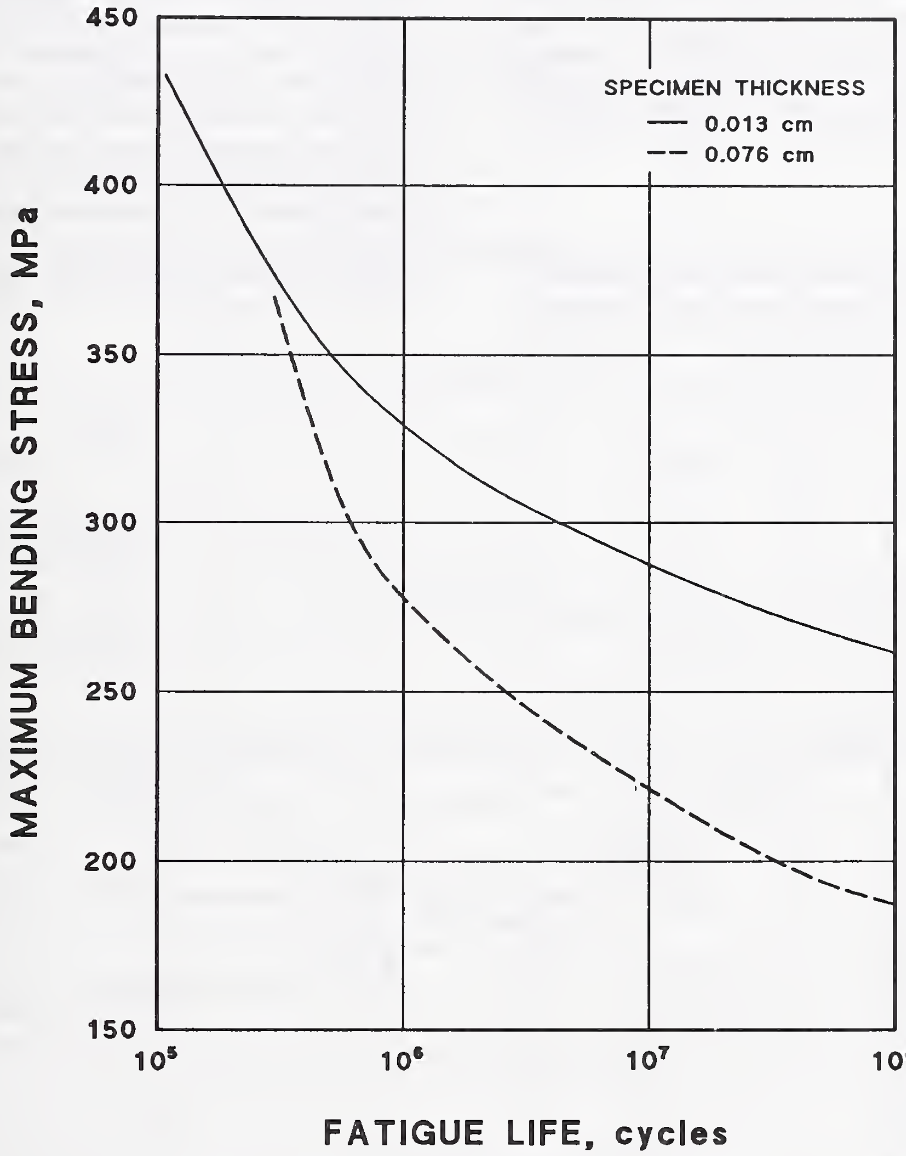

Figure 18.6. The median curves showing the dependence of the fatigue life on the maximum bending stress are plotted for two thicknesses of strip material. The data from Reference 18.4 were obtained on C51000 material that had been cold-worked 37.1% and had a nominal grain size of 35 µm.

DATA SOURCES AND ANALYSIS

Fatigue-life curves from rotating-beam measurements of C5100, C52100, and C52400 phosphor bronzes were obtained from Reference 18.5. The bar specimens were either annealed or cold-drawn 37, 60, or 75%. The available characterization of materials and measurements is given in Table 18.1 at the end of the fatigue properties section.

RESULTS

Figure 18.7 presents results on annealed specimens. The results show that fatigue life improves with decreasing grain size and increasing Sn content, [Sn]. Figure 18.8 a, b, and c presents the results for cold-worked specimens. At stresses above about 250 MPa, Figure 18.8 shows an improvement in fatigue life with increasing [Sn]; however, the improvement is less marked below this stress level and some crossing-over of the curves is observed. With increasing cold work, fatigue life is longer for stresses in the range of about 300–400 MPa. At lower stress levels, the amount of cold work does not appear to have much effect on fatigue life. For the annealed material, an asymptotic endurance life appears to be reached at about 10^8 to 10^9 cycles; but it is less clear whether such a limit exists for cold-worked material.

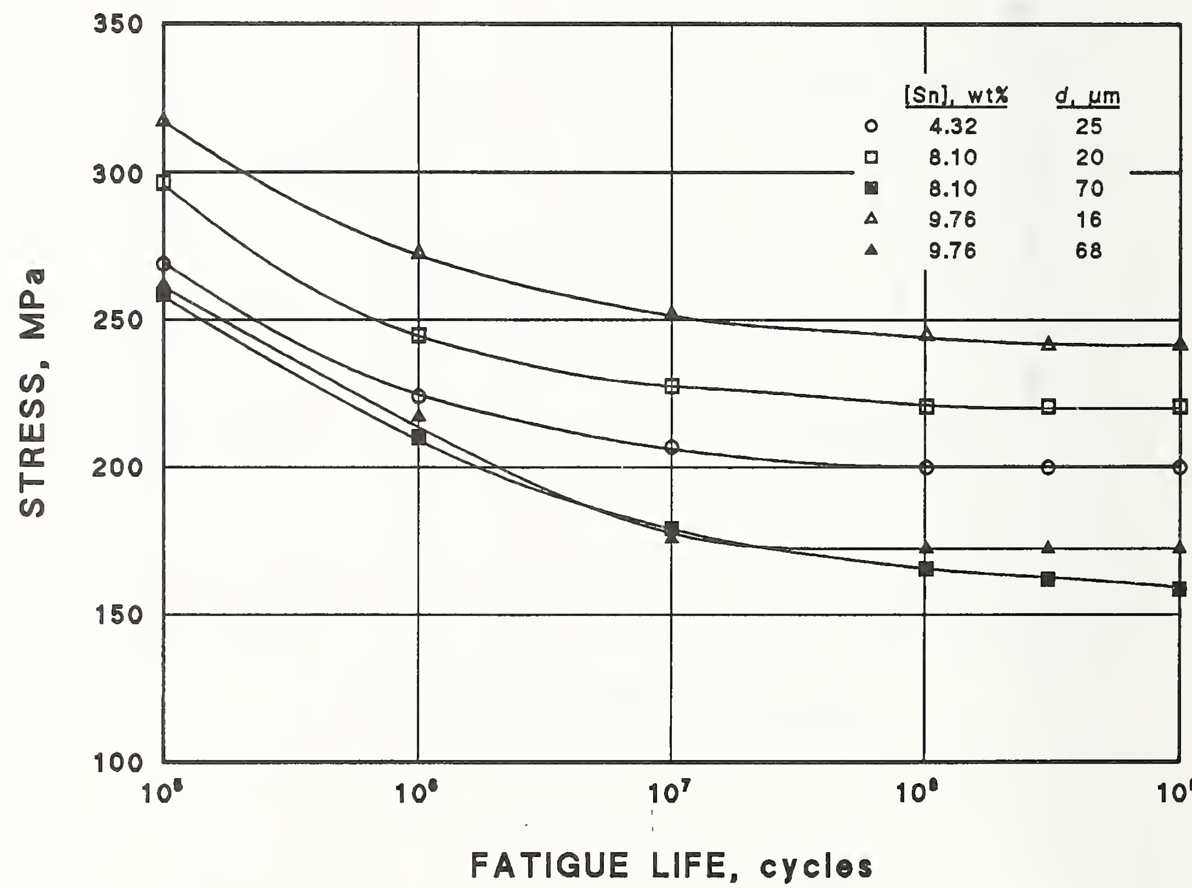

Figure 18.7. Stress-controlled fatigue-life curves showing the effect of tin content, [Sn], and grain size, *d*. Data are from Reference 18.5 on product in the form of annealed bar.

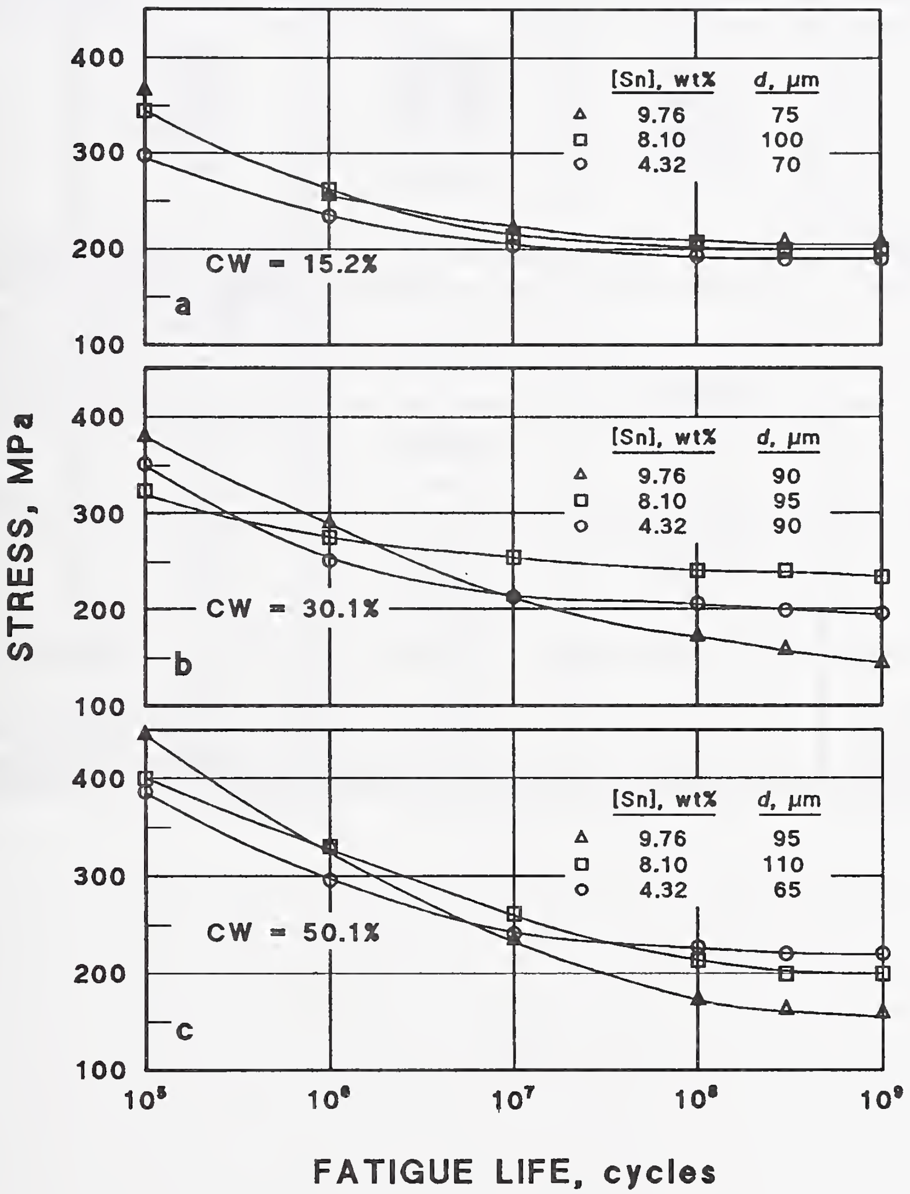

Figure 18.8. Stress-controlled fatigue-life curves showing the effect of cold work (*CW*), tin content ([Sn]), and grain size (*d*). Data are from Reference 18.5 on product in bar form.

Table 18.1. Characterization of Materials and Measurements.

Reference No.	1	2	3A	3B
Specification	1	—	C51000	C52100
Composition (wt%)				
Cu	—	91.98–95.16	—	—
Sn	0–10.11	4.66–7.45	—	—
P	0–0.07	0.032–0.106	—	—
Pb	0–0.009	—	—	—
Fe	0–0.009	—	—	—
Zn	—	0–0.53	—	—
Others (Only ≥ 0.001 wt%)	—	—	—	—
Material Condition	Cold-rolled, 0–68%	Cold-rolled, 50.15%	Cold-rolled, 37.1 and 60.5%	Cold-rolled 37.1 and 60.5%
Grain Size	15 or 35 μm	—	—	—
Hardness	R_B 2.0–106.5	R_B 91–95	—	—
Product Form	Strip 0.635-cm-thick	Strip	—	—
Specimen Type	Flat	Flat	—	—
Width or Dia.	0.102 cm	0.48–1.19 cm	—	—
Thickness	—	—	—	—
Gage Length	—	13.4 cm	—	—
"R" Ratio	—	—	—	—
Test Frequency	—	48 kHz	—	
Test Temperature	295 K	295 K	295 K	295 K

4	5
C51000	—
— 5 — — — — —	89.86–95.27 4.32–9.76 0.08–0.38 0.00–0.003 0.025–0.06 0.0–0.20 —
Cold-rolled, 37.1 and 60.5%	Annealed, 823, 898, or 923 K; or cold-drawn, 15.2–50.1%
35 and 40 μm	16–110 μm
R_A 54.8 and 58.5	R_B 34–103
Strip 0.076-cm-thick	Bar 1.27-cm-dia.
Flat 0.076 cm 0.476 cm 4.56 cm	Round 0.76 cm — —
— —	— 210 kHz
295 K	295 K

REFERENCES

1. Gohn, G. P., Guerard, J. P., and Freynik, H. S., "The Mechanical Properties of Wrought Phosphor Bronze Alloys," American Society for Testing Materials, Philadelphia, PA, Special Technical Publication No. 183, 114 pp. (1956).

2. Price, W. B., and Bailey, R. W., "Fatigue Properties of Five Cold-rolled Copper Alloys," AIME Transactions 124, 271–286 (1937).

3. Mendenhall, J. H., Ed., "Other Engineering Properties, Fatigue, Creep, and Relaxation," Chapter 7 in Understanding Copper Alloys, Olin Corporation, East Alton, IL, 98–109 (1977).

4. Fox, A., "Reversed Bending Fatigue Characteristics of Copper Alloy 510 Strip," Journal of Materials 5, 273–293 (1970).

5. Anderson, A. R., Swan, E. F., and Palmer, E. W., "Fatigue Tests on Some Additional Copper Alloys," Proceedings of the American Society for Testing Materials 46, 678–692 (1946).

C51000, C52100: Annealed; Cold-worked

Creep Strain and Rate vs. Elapsed Time (398, 422 K)

DATA SOURCES

A search of the literature for creep data of phosphor bronzes at 295 K and lower temperatures was unproductive. To provide some guidance, references are given for data within 200 K of room temperature; however, since mechanisms for cryogenic creep are likely to be different from mechanisms at higher temperatures, these data must be interpreted with caution.

Reference 19.1 provides data on hard C51000 phosphor bronze at 398 K. These data are based on applied stresses at 50% of the 0.2% offset yield strength. At 2000 h, total creep was 0.103% and creep rate was 2.12×10^{-5} %/h. On the basis of the information provided, the percent of total creep of C51000 (hard) in 2000 h is about three times higher than that of C17500 (hard), but the creep rate of the C51000 at 2000 h is about twice that of C17500.

References 19.2 and 19.3 present data on creep rate at 1000 h as a function of applied stress for C51000 in both hard-drawn and annealed conditions. The lowest temperature for which data are furnished is 422 K.

Reference 19.4 present data at 295 K for creep of C52100 phosphor-bronze springs used in a switch. The data are not in standard format, and the test period was less than 200 days. Information on the residual deflection of a cantilever strip after the load is removed is supplied, but the load is not specified.

REFERENCES

1. Mendenhall, J. H., Ed., "Other Engineering Properties--Fatigue, Creep and Relaxation," in Understanding Copper Alloys, John Wiley and Sons, New York, NY, 94–106 (1980).

2. Burghoff, H. L., Blank, A. I., and Maddigan, S. E., "The Creep Characteristics of Some Copper Alloys at Elevated Temperatures," Proceedings of the American Society for Testing Materials 42, 668–691 (1942).

3. Burghoff, H. L., and Blank, A. I., "The Creep Characteristics of Copper and Some Copper Alloys at 300, 400, and 500 °F," Proceedings of the American Society for Testing and Materials 47, 725–754 (1947).

4. Shimizu, Y., Nishihata, M., Muta, T., and Matumoto, E., "Mechanical Properties and Weldablities of Small Sized Crossbar Switch Springs," Review of the Electrical Communication Laboratories 20, 71–92 (1972).

DATA SOURCES AND ANALYSIS

Young's modulus (*E*) measurements at 295 K on annealed Cu-Sn alloys were obtained from References 20.1–20.4. All measurements were made with dynamic, rather than static methods. These methods determine the adiabatic, rather than the isothermal, modulus, but the difference of a few percent between the two types of moduli is usually smaller than the errors associated with static methods of measurement (Reference 20.5). The available characterization of materials and measurements is given in Table 20.7 at the end of the elastic properties section. A polynomial regression analysis of the data was carried out to determine the dependence of the modulus upon Sn content, [Sn].

RESULTS

The data were fitted with the equation

$$E(\text{GPa}) = 128.2 - 2.005[\text{Sn}] \quad (\text{S.D.} = 5.7\ \text{GPa}), \qquad (20\text{-}1)$$

where [Sn] is less than 10 wt%. The standard deviations of the coefficients are 2.1 and 0.375. Table 20.1 gives the measured Young's modulus values and the values calculated from Equation (20-1). Figure 20.1 shows the fit of the data to Equation (20-1).

DISCUSSION

Figure 20.1 and Equation (20-1) indicate a decrease of about 6% in the Young's modulus as [Sn] is varied from 5 wt% to 9 wt%, but the specifications for phosphor bronze C51000 and C52400 indicate no change (Reference 20.6).

The Young's modulus for [Sn] = 0 at 295 K [Equation (20-1)] is in agreement with the calculated Young's modulus of 126 GPa for high-purity, annealed copper [Equation (6-2)].

Table 20.1. The Dependence of Young's Modulus on [Sn] (295 K)

[Sn], wt%	Young's Modulus, Measured, GPa	Young's Modulus, Predicted, GPa	Reference No.
0.65	129.2	126.94	1
3.22	128.5	121.78	4
4.21	117.19	119.80	1
8.28	108.76	111.68	4
10.48	100.23	107.22	1
0	124.84	128.24	2
3.31	127.84	121.60	2
4.75	121.83	118.71	2
5.99	119.80	116.22	2
9.98	118.68	108.23	2
0	123.2	128.24	3
[illegible]	102.6	118.21	3
10	105.4	108.19	3
0.28	128.5	127.68	4
0.54	128.3	127.16	1
1.10	127.5	126.03	4
2.18	125.6	123.87	1
[illegible].28	121.7	119.70	4
8.26	115.3	111.66	4

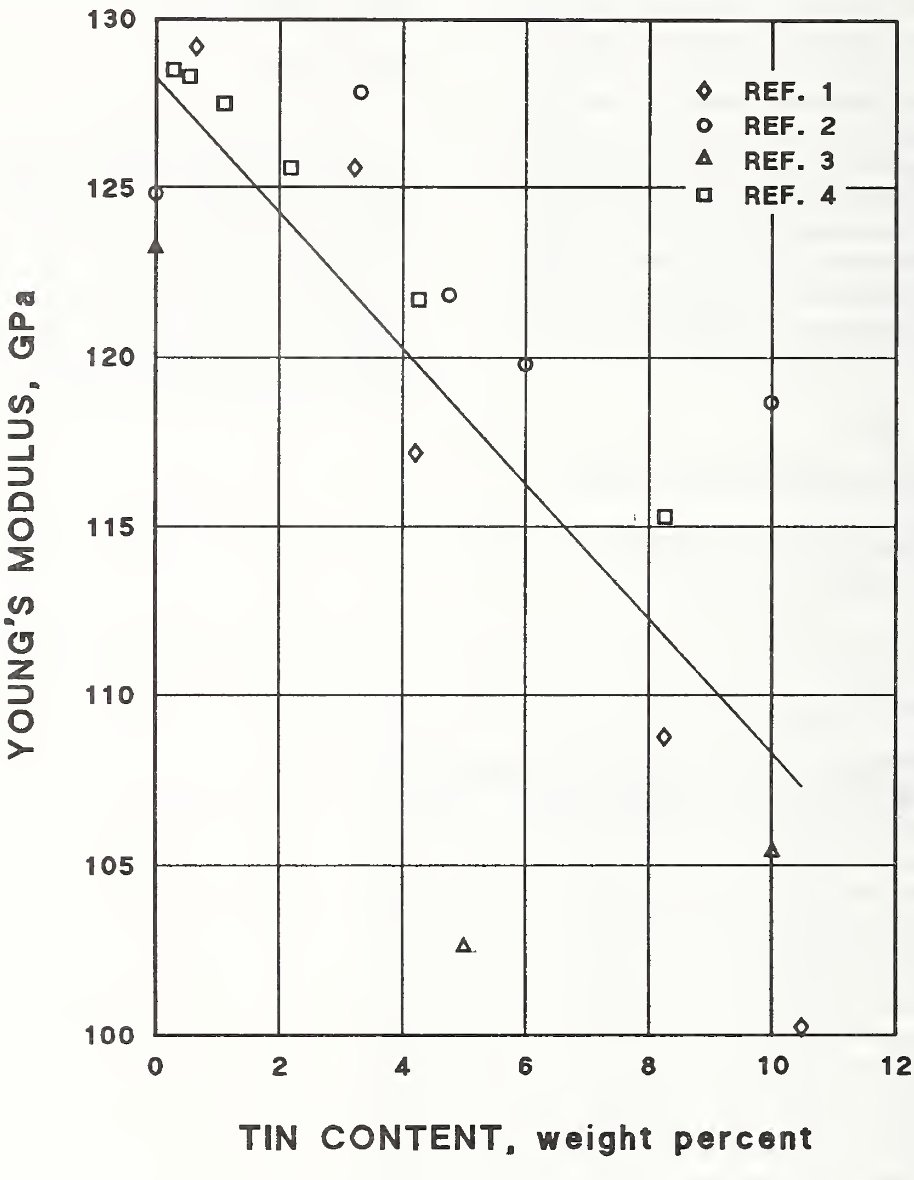

Figure 20.1. Young's modulus versus tin content at 295 K on annealed material (References 20.1–20.4). The product was in cylinder form (References 20.2 and 20.4) or not specified (References 20.1 and 20.3).

C50500, C52100: Cold-worked

Young's Modulus vs. Temperature (4–295 K)

DATA SOURCES

Young's modulus measurements below 295 K on two cold-worked phosphor bronzes were obtained from References 20.7 and 20.8. The measurements were made with static methods; dynamic measurements have not been conducted for phosphor-bronze alloys at cryogenic temperatures. The available characterization of materials and measurements is given in Table 20.7 at the end of the elastic properties section.

RESULTS

Table 20.2 and Figure 20.2 present the measurements. (One data point at 76 K from Reference 20.7 that does not agree with the trend of the other measurements was eliminated from the figure.) According to Equation (20-1), the Young's modulus of the C50500 material should be higher (at least at 295 K) than the Young's modulus of the C52100 material. Perhaps the higher degree of cold-working of the C50500 material lowered the modulus below that of the C52100 material. The influence of cold-working on elastic constants is complex (Reference 20.5).

Table 20.2. The Dependence of Young's Modulus on Temperature (4–295 K).

Alloy Designation	Test Temperature, K	Young's Modulus, GPa	[Sn], wt%	Reference No.
C52100	20	126.9	8.2	7
	20	113.8	8.2	7
	76	124.8	8.2	7
	76	122.0	8.2	7
	76	115.1	8.2	7
	76	113.0	8.2	7
	295	110.3	8.2	7
	295	109.6	8.2	7
C50500	4	113.1	4.85	7
	20	113.8	4.85	7
	76	115.1	4.85	7
	195	113.8	4.85	7
	295	107.6	4.85	8

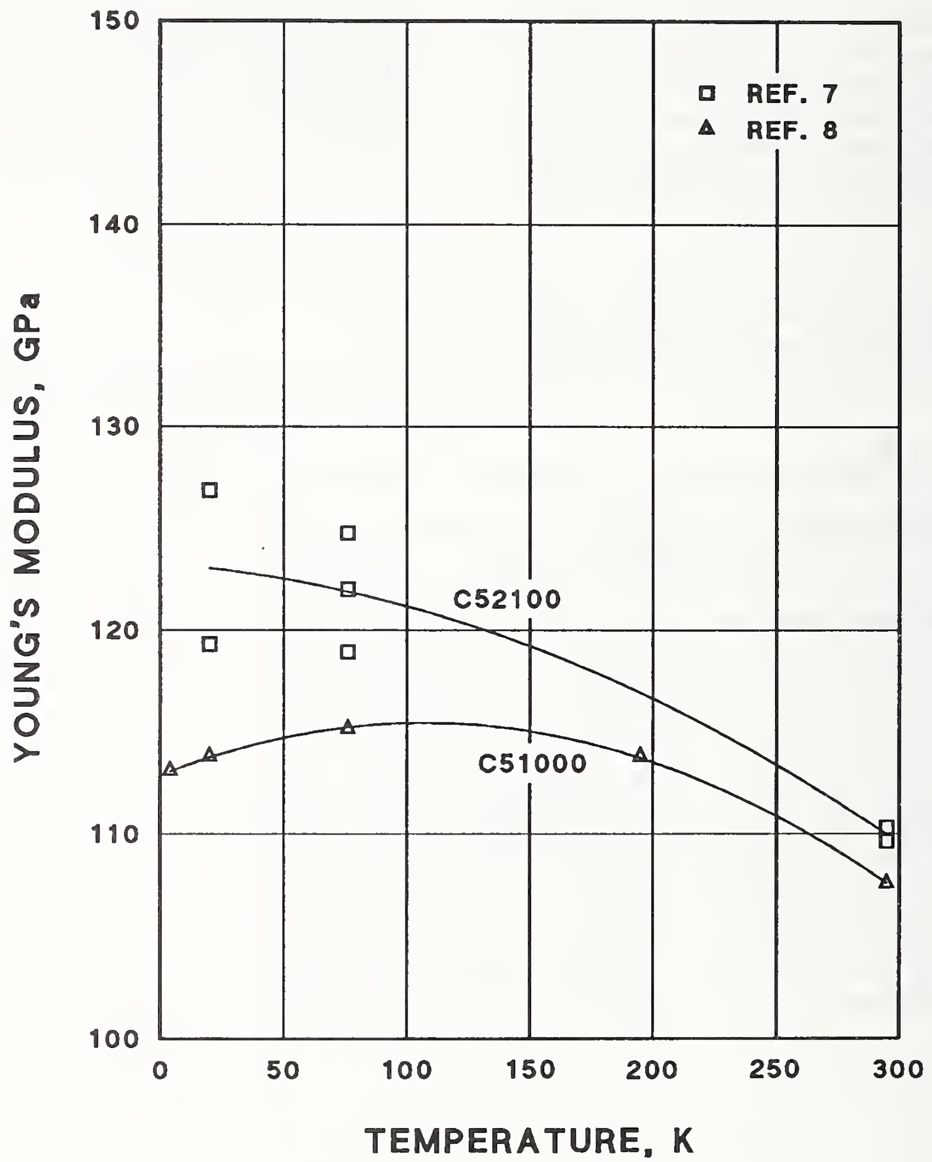

Figure 20.2. Young's modulus versus temperature for cold-worked material. The amount of cold-work was 37% and tin content was 8.2 wt% for measurements taken from Reference 20.7, and cold-work was 85% and tin content was 4.85 wt% for measurements taken from Reference 20.8. Product was in bar form.

C50100–C52400: Annealed

Shear Modulus vs. [Sn] (295 K)

DATA SOURCES AND ANALYSIS

Shear modulus (*G*) measurements at 295 K on annealed Cu-Sn alloys were obtained from References 20.3 and 20.4. All measurements were made with dynamic, rather than static methods. These methods determine the adiabatic, rather than the isothermal, modulus, but the difference of a few percent between the two types of moduli is usually smaller than the errors associated with static methods of measurement (Reference 20.5). The available characterization of materials and measurements Is given In Table 20.7 at the end of the elastic properties section. A polynomial regression analysis of the data was carried out to determine the dependence of the modulus upon Sn content, [Sn].

RESULTS

The data were fitted with the equation

$$G(\text{GPa}) = 47.34 - 0.8950\,[\text{Sn}], \quad (\text{S.D.} = 2.78\ \text{GPa}), \qquad (20\text{-}2)$$

where [Sn] is less than 10 wt%. The standard deviations of the coefficients are 1.32 and 0.2692. Table 20.3 gives the measured shear modulus values and the values calculated from Equation (20-2). Figure 20.3 shows the fit of the data to Equation (20-2).

DISCUSSION

Although Figure 20.3 and Equation (20-2) indicate a decrease of about 10% in the shear modulus as [Sn] is varied from 5 wt% to 9 wt%, the specifications for phosphor bronze C51000 and C52400 indicate no change (Reference 20.6).

The shear modulus for [Sn] = 0 at 295 K [Equation (20-2)] is in agreement with the calculated shear modulus of 47.2 GPa for high-purity, annealed copper [Equation (6-4)].

Table 20.3. The Dependence of the Shear Modulus on [Sn] (295 K).

[Sn], wt%	Shear Modulus, Measured, GPa	Shear Modulus, Predicted, GPa	Reference No.
0	44.9	47.3	4
5	37.2	42.9	3
10	37.7	38.4	3
0.28	47.9	47.1	4
0.54	47.8	46.9	4
1.10	47.9	46.4	4
2.18	46.8	45.4	4
4.26	45.3	43.5	4
8.26	42.7	40.0	4

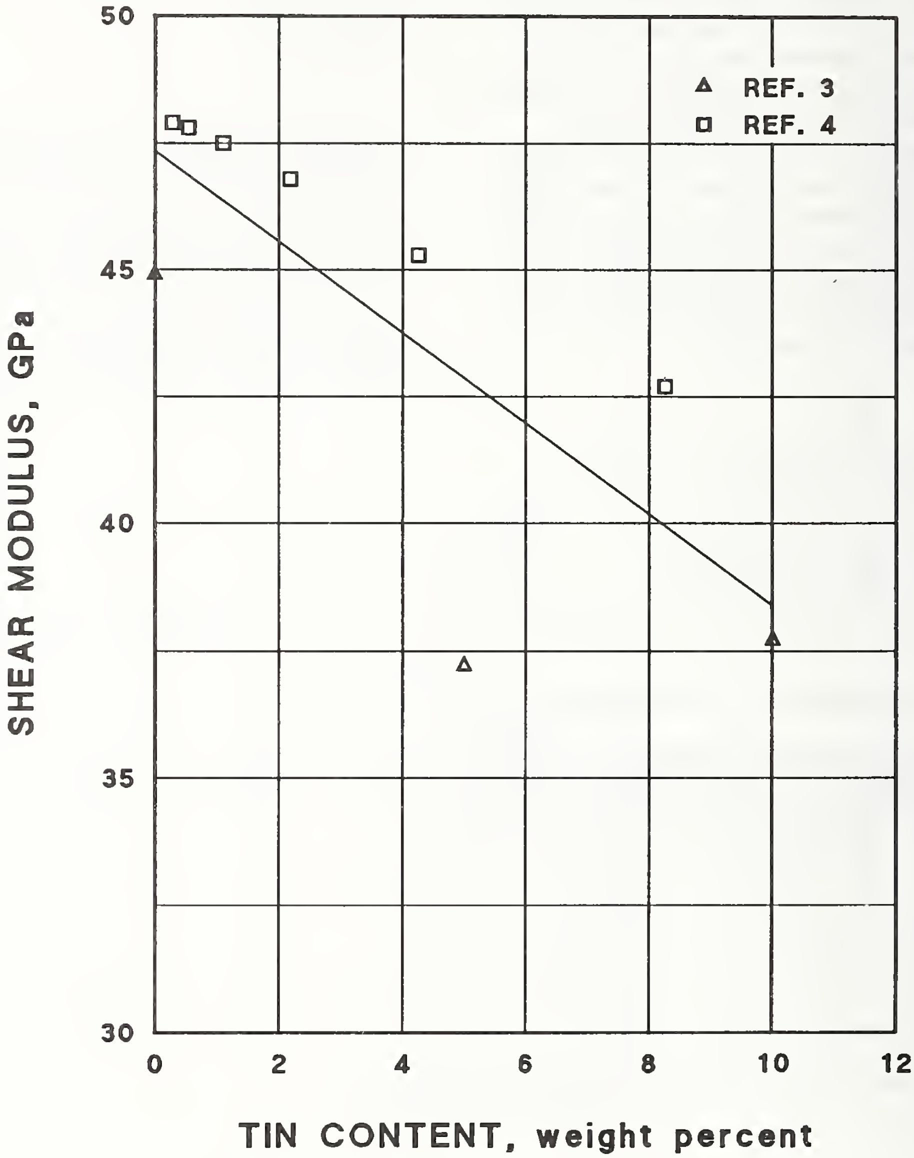

Figure 20.3. Shear modulus versus tin content at 295 K for annealed material. The product was in cylinder form (Reference 20.4) or not specified (Reference 20.3).

C50100–C52100: Annealed

Shear Modulus vs. [Sn] (77 K)

DATA SOURCES AND ANALYSIS

Shear modulus (*G*) measurements at 77 K on annealed Cu-Sn alloys were obtained from Reference 20.9. The measurements were made with dynamic, rather than static methods. These methods determine the adiabatic, rather than the isothermal, modulus, but the difference of a few percent between the two types of moduli is usually smaller than the errors usually associated with static methods of measurement (Reference 20.5). The available characterization of materials and measurements is given in Table 20.7 at the end of the elastic property section. A polynomial regression analysis of the data was carried out to determine the dependence of the modulus upon Sn content, [Sn].

RESULTS

The data were fitted with the equation

$$G(\text{GPa}) = 55.32 - 1.025\,[\text{Sn}] \quad (\text{S.D.} = 0.86\ \text{GPa}), \qquad (20\text{-}3)$$

where [Sn] is less than 8 wt%. The standard deviations of the coefficients are 0.80 and 0.164. Table 20.4 gives the measured shear modulus values and the values calculated from Equation (20-3). Figure 20.4 shows the fit of the data to Equation (20-3).

DISCUSSION

The shear modulus for [Sn] = 0 at 77 K [Equation (20-3)] differs from the calculated shear modulus of 51 GPa for high-purity, annealed copper [Equation (6-4)]. Data for the latter equation were obtained from several references. The reason for the discrepancy with the measurements from Reference 20.9 is not known.

Table 20.4. The Dependence of the Shear Modulus on [Sn] (77 K).

[Sn], wt%	Shear Modulus, Measured, GPa	Shear Modulus, Predicted, GPa	Reference No.
0	55.0	55.3	9
4.0	51.9	51.2	9
7.4	47.4	47.7	9

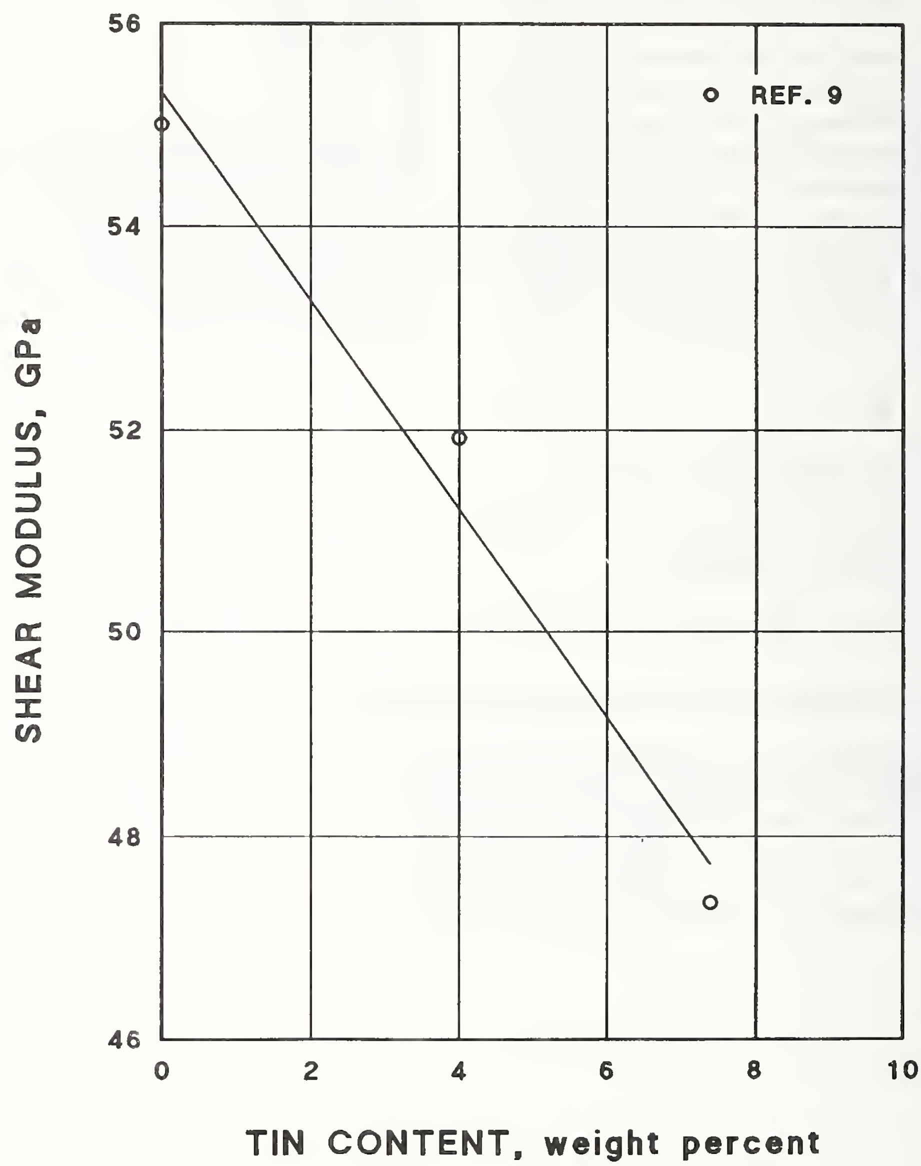

Figure 20.4. Shear modulus versus tin content at 77 K on annealed material (Reference 20.9). The product was in wire form.

C51100: Cold-worked

*Shear Modulus vs.
Temperature (200–289 K)*

DATA SOURCE

Measurements of the shear modulus on a C51100 phosphor bronze at 200 and 300 K were obtained from Reference 20.10. The material was cold-worked to an unreported extent. The product was in wire form. A static, torsional test method was used. The available characterization of materials and measurements is given in Table 20.7 at the end of the elastic properties section.

RESULTS

Table 20.5 and Figure 20.5 present the measurements.

DISCUSSION

The slight decrease in shear modulus as the temperature decreases is not in agreement with the temperature dependence reported in two references for Young's modulus of phosphor bronzes (Figure 20.2). The apparent decrease in modulus with lower temperature might represent data scatter rather than a true temperature effect.

Table 20.5. The Dependence of the Shear Modulus on Temperature (200–289 K).

Test Temperature, K	Shear Modulus, GPa	Reference No.
200	45.4	10
289	45.9	10

C51100: Cold-worked

Shear Modulus vs. Temperature (200–289 K)

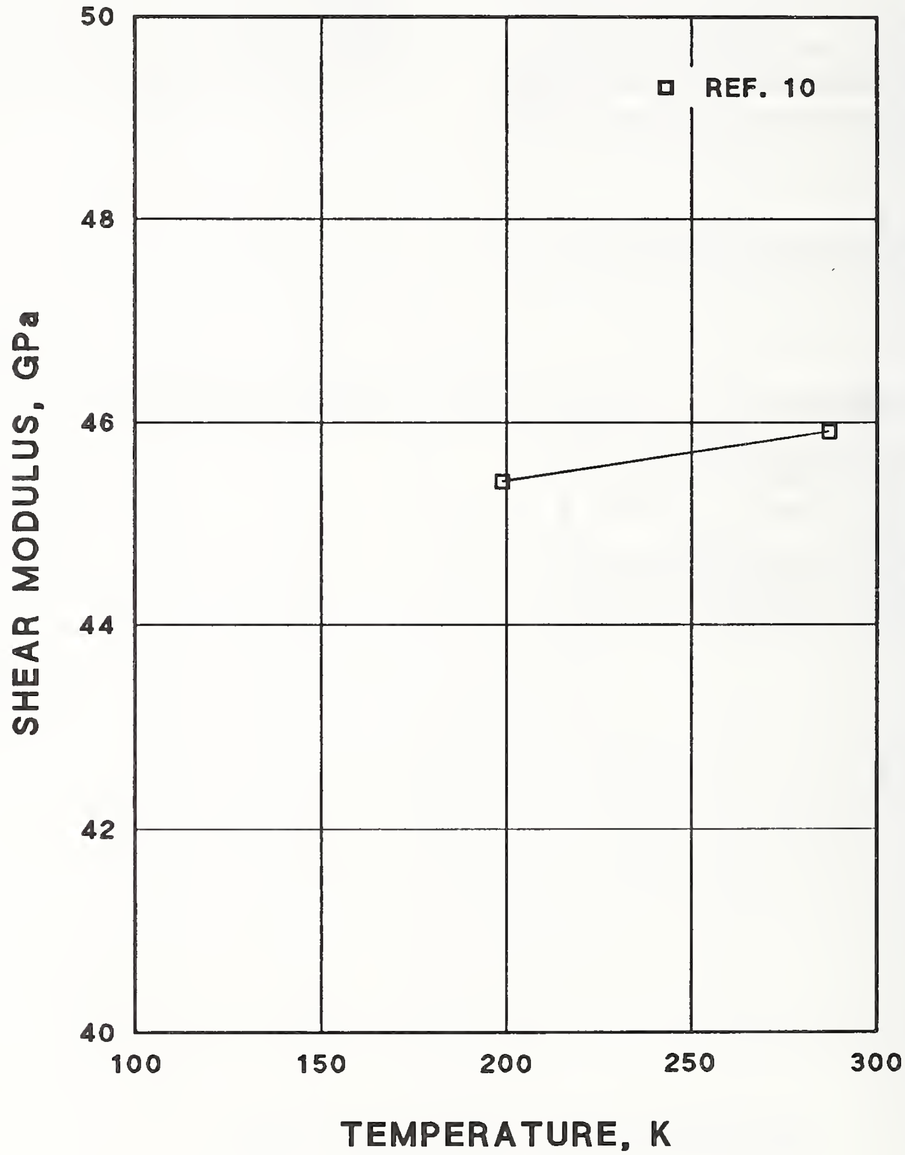

Figure 20.5. Shear modulus versus temperature for cold-worked material (Reference 20.10). The amount of cold drawing was not specified, tin content was 3.57 wt%, and product was in wire form.

DATA SOURCES AND ANALYSIS

Poisson's ratio (ν) measurements at 295 K on annealed Cu-Sn alloys were obtained from References 20.3 and 20.4. All measurements were made with dynamic, rather than static methods. These methods determine the adiabatic, rather than the isothermal, modulus, but this difference of a few percent at most is smaller than the errors usually associated with static methods of measurement (Reference 20.5). The available characterization of materials and measurements is given in Table 20.7 at the end of the elastic properties section. A polynomial regression analysis of the data was carried out to determine the dependence of ν upon Sn content, [Sn].

RESULTS

The data were fitted with the equation

$$\nu = 0.3447 + 0.003459\,[Sn] \quad (S.D. = 0.0184), \qquad (20\text{-}4)$$

where [Sn] is less than 10 wt%. The standard deviations of the coefficients are 0.0088 and 0.001786. Table 20.6 gives the measured Poisson's ratio values and the values calculated from Equation (20-4). Figure 20.6 shows the fit of the data to Equation (20-4).

DISCUSSION

A second-order polynomial gave a better fit than Equation (20-4), but this was an artifact of the small data set available; a linear fit is an adequate description of the dependence on [Sn] when data from each reference are considered separately.

Table 20.6. The Dependence of Poisson's Ration on Tin Content (295 K).

[Sn], wt%	Poisson's Ratio, Measured	Poisson's Ratio, Predicted	Reference No.
0	0.37	0.345	3
5	0.38	0.362	3
10	0.40	0.379	3
0.28	0.340	0.346	4
0.54	0.343	0.347	4
1.10	0.343	0.349	4
2.18	0.343	0.352	4
4.26	0.344	0.359	4
8.26	0.349	0.373	4

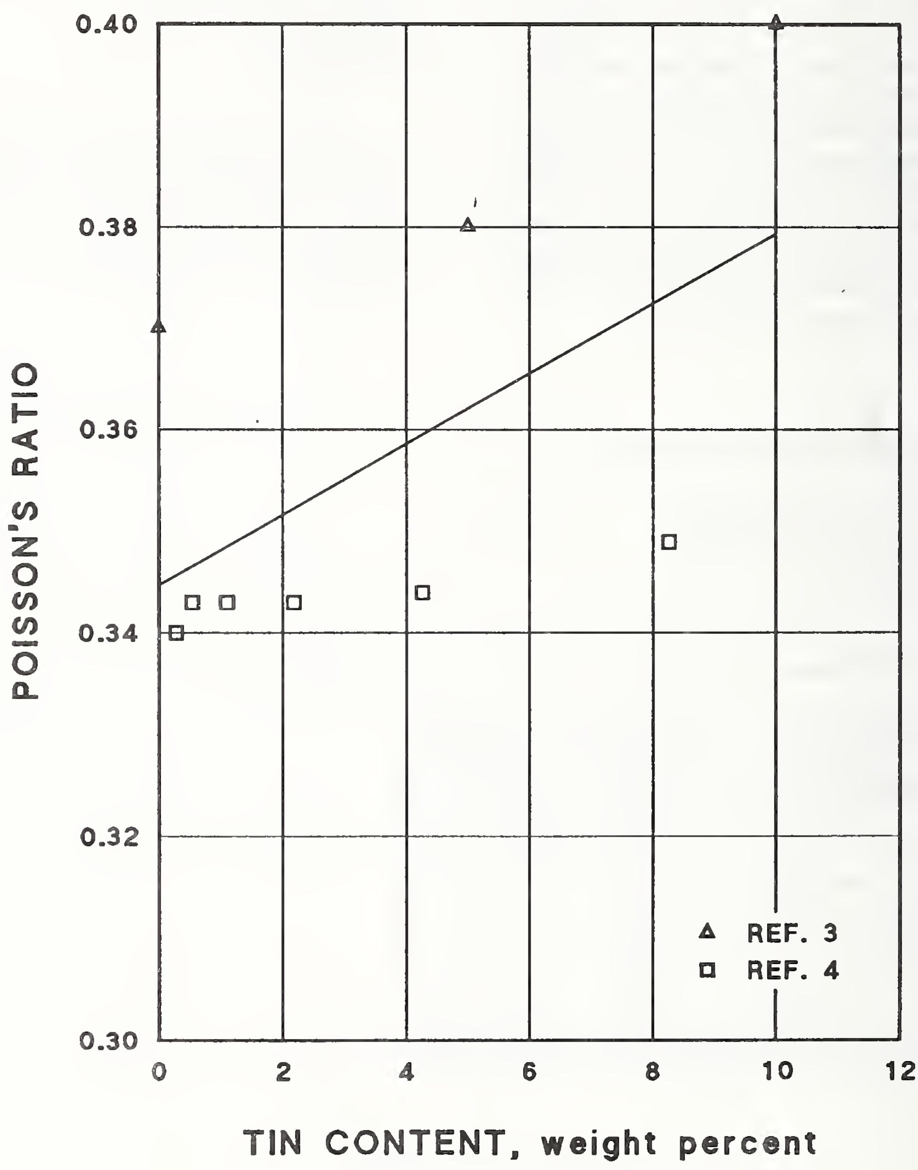

Figure 20.6. Poisson's ratio versus tin content at 295 K on annealed material. The product was in cylinder form (Reference 20.4) or was not specified (Reference 20.3).

C50100–C52400: Annealed; Cold-worked — *Elastic Properties (All)*

Table 20.7. Characterization of Materials and Measurements.

Reference No.	1	2	3	4
Specification	—	—	—	4
Composition (wt%)				
Cu	—	—	—	—
Sn	0.65–10.48	0–9.98	0–10	0.28–8.26
P	—	—	—	—
Pb	—	—	—	—
Fe	—	—	—	—
Zn	—	—	—	—
Others (Only ≥ 0.001 wt%)	—	—	—	—
Material Condition	Annealed	Annealed, 100 h	—	Annealed, 923 K, 1.5 h
Grain Size	1	—	3	—
Hardness	—	—	—	—
Product Form	—	—	—	Rod, 3-cm-dia.
Specimen Type	—	Cylinder	—	Cylinder
Width or Dia.	—	0.8–1.2 cm	—	1.2 cm
Thickness	—	—	—	—
Gage Length	—	14.0 cm	—	10–12 cm
No. of Specimens	5	5	3	—
Test Temperature	295 K	295 K	295 K	295 K

Table 20.7, continued

Reference No.	7	8	9	10
Specification	C52100	C51000	—	C51100
Composition (wt%)				
Cu	90.3	—	—	95.98
Sn	8.2	4.85	0–7.4	3.67
P	0.06	0.18	—	—
Pb	—	0.02	—	—
Fe	—	0.02	—	—
Zn	—	0.05	—	—
Others (Only ≥ 0.001 wt%)	—	—	—	—
Material Condition	Cold-rolled, 37%	Cold-rolled, 85%	Annealed	Cold-drawn
Grain Size	—	101 μm	—	—
Hardness	R_B 100	R_B 94	[illegible]	—
Product Form	Bar, 19.1-cm-dia.	Bar, 19.1-cm-dia.	Wire, 0.07610-cm-dia.	Wire, 0.23-cm-dia.
Specimen Type	Round	Round	Wire	Wire
Width or Dia.	0.635 cm	0.635 cm	0.0761 cm	0.23 cm
Thickness	—	—	—	—
Gage Length	2.54 cm	3.81 cm	2.54 cm	~25.4 cm
No. of Specimens	÷	5	3	2
Test Temperature	20–295 K	4–295 K	77 K	200–289 K

REFERENCES

1. Köster, W., and Rauscher, W., "Beziehungen zwischen dem Elastizitätsmodul von Zweistofflegierungen und ihrem Aufbau," Zeitschrift für Metallkunde 39, 111–120 (1948).

2. Cabarat, R., Guillet, L., and LeRoux, R., "The Elastic Properties of Metallic Alloys," Journal of the Institute of Metals 75, 391–402 (1948–1949).

3. Subrahmanyam, B., and Krishnamurty, B., "Elastic Studies in Polycrystalline Brasses and Bronzes," Indian Journal of Pure and Applied Physics 2, 369–370 (1964).

4. Hopkin, L. M., Pursey, H. and Markham, M. F., "Precise Measurements of the Elastic Constants of Copper and Silver Base Alloys," Zeitschrift für Metallkunde 61, 535–540 (1970).

5. Ledbetter, H. M., and Naimon, E. R., "Elastic Properties of Metals and Alloys. II. Copper," Journal of Physical and Chemical Reference Data 3, 897–935 (1974).

6. Standards Handbook, Part 2, Copper Development Association, Greenwich, CT (1985).

REFERENCES

7. McClintock, R. M., Van Gundy, D. A., and Kropschot, R. H., "Low-Temperature Tensile Properties of Copper and Four Bronzes," American Society for Testing and Materials Bulletin 240, 47–50 (1959).

8. Reed, R. P., and Mikesell, R. P., "Low-Temperature (295 to 4 K) Mechanical Properties of Selected Copper Alloys," Journal of Materials 2, 370–392 (1967).

9. Fleischer, R. L., "Substitutional Solution Hardening," Acta Metallurgica 11, 203–209 (1963).

10. Zimmerli, F. P., Wood, W. P., and Wilson, G. D., "The Effect of Temperature upon the Torsional Modulus of Spring Materials," Proceedings of the American Society for Testing and Materials 30, 350–361 (1930).

DATA SOURCES AND ANALYSIS

There are only a few measurements of the specific heat of Cu-Sn alloys or C50100–C52400 phosphor bronzes below 300 K. Reference 21.1 presents data on Cu-8Sn (extruded) and Cu-11Sn (cast) between 4 and 18 K (Table 21.1). References 21.2 and 21.3 both present values of the electronic specific heat coefficient, γ, and the Debye temperature, θ_D, for a range of Sn contents, [Sn], up to 11%. The quantities γ and θ_D were derived from measurements over the temperature interval from 1.5 to 4 K. Since the theory of specific heat of alloys such as the Cu-Sn series is well-established, the measurements of References 21.2 and 21.3 (below 4 K) allow predictions of the specific heat, C_p, of Cu-Sn alloys between 2 and 300 K. These predictions can be compared with the measurements on two Cu-Sn alloys between 4 and 18 K from Reference 21.1. The measurements, obtained by adiabatic calorimetry, have an expected accuracy of 1%. The available characterization of these measurements and specimens is given in Table 21.8 at the end of the thermal properties section.

The procedure by which predicted specific heats can be obtained from the limited data of References 21.2 and 21.3 follows. First, the specific heat contributions from the electrons, C_e, and the lattice vibrations, C_l, are considered to be additive:

$$C_p = C_e + C_l. \qquad (21\text{-}1)$$

Second, C_e is represented over the entire temperature interval by

$$C_e = \frac{\gamma}{M} T, \qquad (21\text{-}2)$$

where M is the molar mass number and T is the temperature. In practice, this term will be a significant part of the total C_p only at low temperatures, for instance, for $T < 4$ K. Third, at low temperatures the lattice specific heat is well-represented in the Debye approximation by

$$C_l\ (\text{J/kg}\bullet\text{K}) = \frac{1.94 \times 10^6}{M} (T/\theta_D)^3. \qquad (21\text{-}3)$$

This expression can be used when $T \lesssim \theta_D/10$ (Reference 21.4).

Therefore, in the temperature range from 1.5 to 4 K, the expression

$$C_p\ (\text{J/kg}\bullet\text{K}) = \frac{\gamma}{M} T + \frac{1.94 \times 10^6}{M} (T/\theta_D)^3. \qquad (21\text{-}4)$$

is valid, and measurements of C_p will yield values for γ and for θ_D.

To predict C_l at higher temperatures, the value found for θ_D can be substituted into the more general Debye integral expression for C_l (Reference 21.5). This expression is

$$C_l\ (\text{J/kg}\bullet\text{K}) = \frac{7.48 \times 10^4}{M \bullet x_m^3} \int_0^{x_m} \frac{e^x x^4}{(e^x - 1)^2}\, dx,$$

$$x_m = \theta_D/T \qquad \text{or,}$$

$$C_l\ (\text{J/kg}\bullet\text{K}) = \frac{1}{M} D(\theta_D/T). \qquad (21\text{-}5)$$

Values of the integral in this expression are tabulated (Reference 21.6). For $T < \theta_D/10$, Equation (21-5) reduces to Equation (21-3). (C_l in these equations actually refers to the specific heat at constant volume, C_v, which is nearly equivalent to C_p, especially at low temperatures.)

RESULTS

Figures 21.1 and 21.2 show γ and θ_D as a function of [Sn] from the measurements of References 21.2 and 21.3 between 1.5 and 4 K. The equations derived from simple polynomials fitted to the curve of Figure 21.1 and the straight line of Figure 21.2 are

$$\gamma\ ([\text{Sn}]) = +0.698 + 0.00911[\text{Sn}] - 0.00128[\text{Sn}]^2 + 6.54 \times 10^{-5}[\text{Sn}]^3, \qquad (21\text{-}6)$$

and

$$\theta_D\ ([\text{Sn}]) = 344 - 3.11\,[\text{Sn}], \qquad (21\text{-}7)$$

where [Sn] is expressed in wt%. The standard deviation of the fit of the data to Equation (21-6) is 0.00398 and the standard deviation of the fit of the data to Equation (21-7) is 0.876. The units of γ are J/(kmol•K^2); the units of θ_D are K.

When γ and θ_D have been obtained for a particular value of [Sn] from Equations (21-6) and (21-7), the following expression, obtained from Equations (21-1), (21-2), and (21-5), can be used to predict values of C_v for 2 K $\leq T \leq$ 300 K:

$$C_v \text{ (J/kg}\cdot\text{K)} = \frac{1}{M}[\gamma([\text{Sn}])T + D(\theta_D/T)]. \quad (21\text{-}8)$$

Values for $D(\theta_D/T)$ can be obtained from Figure 21.3 or Table 21.2, adapted from Reference 21.6. The molar mass number, M, is given by

$$M \text{ (g/mol)} = 1.187[\text{Sn}] + 0.6354(100 - [\text{Sn}]). \quad (21\text{-}9)$$

See the discussion section below for information on converting C_v to C_p.

DISCUSSION

The only measurements above 4 K that the predictive equation can be compared with are those from Reference 21.1 from 4 to 17 K. At 17 K, Equation (21-8) predicts C_p values of 4.903 J/(kg•K) and 5.034 J/(kg•K) for [Sn] = 8 and 11 wt%, respectively. Allowing for the uncertainty in γ and θ_D given by plus or minus one standard deviation from the fit of Equations (21-6) and (21-7) to the experimental data, the expected uncertainty in the C_p value for 8 wt% [Sn] is ± 0.038 J/(kg•K). For 11 wt% [Sn], the corresponding uncertainty is ± 0.046 J/(kg•K). This calculation assumes that the contributions to the total uncertainty from the standard deviations of Equations (21-6) and (21-7) are additive. The predicted values differ by more than the expected uncertainty from the measurements of C_p at ~17 K from Reference 21.1: these are 6.073 J/(kg•K) for [Sn] = 8 wt% and 6.389 J/(kg•K) for [Sn] = 11 wt%. However, the Cu-Sn alloys used in the work reported in References 21.2 and 21.3 were evidently of a higher degree of purity than the commercial alloys used for the measurements of Reference 21.1. It is also possible that the discrepancy results from a systematic error in the measurements in Reference 21.1; the authors did not compare their results with the earlier work of References 21.2 and 21.3.

The authors of Reference 21.1 also used their measurements to estimate values for γ and θ_D, for [Sn] = 8 and 11 wt%. Perhaps because these measurements were obtained between 4 and 18 K on commercial alloys, the values of γ and θ_D were not consistent with those obtained in References 21.2 and 21.3; consequently, they were not used to establish Equations (21-6) and (21-7). Measurements in a lower temperature range, about 2 to 4 K, as reported in References 21.2 and 21.3, should establish γ and θ_D as a function of [Sn] more accurately.

The specific heat values for Cu-Sn alloys that can be obtained from Equations (21-6), (21-7), and (21-8) must be regarded as approximations of the true values. Using plus or minus one standard deviation as obtained from the fits of Equations (21-6) and (21-7) to the data to estimate the uncertainty in the predicted C_v for [Sn] = 5 wt% gives the following values at 4, 77, and 295 K: 0.09614 (+0.00067, −0.00066) J/(kg•K); 175.3 (± 0.6) J/(kg•K); and 356.71 (+0.14 −0.12) J/(kg•K), respectively. In addition to this uncertainty, the use of the Debye approximation adds a much larger possible error. Even for a pure element, such as copper, the Debye approximation for C_l is of limited validity. The analysis generally used to compare the agreement with theory is based on a plot of θ_D vs. T, in which θ_D is computed separately from each experimental C_p value ($C_p \approx C_v$ at low temperatures; see below). For copper, θ_D varies by about ± 15 K between 2 and 80 K, with a corresponding inaccuracy in the predicted C_p value (Reference 21.7). It must be assumed that at least the same degree of uncertainty pertains to θ_D values obtained for Cu-Sn alloys from Equation (21-7) when these values are used to predict C_p at higher temperatures.

At temperatures near 295 K, there is a difference of a few percent between C_p and C_v. Equation (21-8) predicts C_v, whereas the experimental quantity is C_p. The difference may be calculated from thermodynamic expressions that involve the isothermal compressibility and the isobaric coefficient of volumetric expansion, or an estimate may be obtained from the Grüneisen constant. The relevant formulas are discussed in Reference 21.8. However, since the thermodynamic quantities to use in these formulas may not be well-known for Cu-Sn alloys, and the procedure presented here for estimating C_v is very approximate, this correction is of only academic interest in the present context.

C50100–C52400: Annealed; Cold-worked

Specific Heat vs. [Sn], Temperature (2–300 K)

Table 21.1. Specific Heat Dependence on Temperature (4.0–17.5 K).

Test Temperature, K	Specific Heat, J/(kg·K)	Reference No.
4.0	0.109	1A
4.1	0.120	1A
4.2	0.121	1A
4.5	0.134	1A
4.6	0.140	1A
4.7	0.148	1A
4.9	0.162	1A
5.0	0.168	1A
5.1	0.181	1A
5.3	0.193	1A
5.4	0.202	1A
5.5	0.235	1A
5.8	0.244	1A
6.0	0.262	1A
6.2	0.289	1A
6.4	0.338	1A
6.6	0.338	1A
6.9	0.384	1A
7.1	0.414	1A
7.4	0.466	1A
7.7	0.511	1A
7.9	0.550	1A
8.2	0.610	1A
8.6	0.686	1A
9.0	0.774	1A
9.3	0.859	1A
9.5	0.921	1A
9.8	1.008	1A
10.1	1.103	1A
10.5	1.225	1A
10.9	1.363	1A
11.3	1.528	1A
11.9	1.761	1A
12.3	1.983	1A
12.7	2.161	1A
13.1	2.353	1A
13.5	2.651	1A
14.0	2.933	1A
14.8	3.529	1A
15.4	3.546	1A
16.0	4.484	1A
16.7	5.156	1A
17.5	6.073	1A

Test Temperature, K	Specific Heat, J/(kg·K)	Reference No.
4.4	0.133	1B
4.6	0.155	1B
4.8	0.168	1B
5.1	0.191	1B
5.2	0.203	1B
5.1	0.222	1B
5.6	[illegible]	1B
5.1	0.251	1B
5.9	[illegible]	1B
6.2	0.312	1B
6.3	0.336	1B
6.5	0.348	1B
6.7	0.378	1B
6.8	0.401	1B
6.9	0.424	1B
7.0	0.433	1B
[illegible]	0.453	1B
7.[illegible]	0.433	1B
4.6	0.500	1B
7.6	0.534	1B
4.8	0.588	1B
8.[illegible]	0.654	1B
5.2	0.5[illegible]	1B
5.1	0.726	1B
4.6	0.757	1B
8.8	0.312	1B
8.9	0.856	1B
[illegible]	0.312	1B
9.9	0.5[illegible]	1B
9.8	1.078	1B
5.2	1.123	1B
10.5	1.227	1B
10.2	[illegible]	1B
10.5	1.395	1B
10.9	1.553	1B
1[illegible].5	1.761	1B
11.8	2.044	1B
1[illegible].9	2.407	1B
1[illegible].2	2.799	1B
10.5	3.289	1B
14.7	3.888	1B
1[illegible].5	4.634	1B
16.4	5.419	1B
17.3	6.389	1B

Table 21.2. Numerical Values for the Debye Function (Reference 21.6).

θ_D/T, K	Debye Function, $D(\theta_D/T)$, J/(kmol·K)
0.0	24915.720
0.1	24894.800
6.2	24852.960
0.3	24811.120
6.0	24727.440
0.9	24601.920
6.6	24476.400
0.1	24309.040
6.8	24141.680
0.9	23932.480
1.5	23723.280
1.5	23472.240
1.2	23221.200
1.3	22928.320
[illegible].3	22635.440
1.5	22342.560
1.6	22007.840
1.7	21673.120
[illegible].9	21296.560
1.9	20961.840
2.4	20585.280
2.1	20208.720
2.2	19832.160
[illegible].3	19413.760
2.4	18995.360
2.5	18618.800
2.6	18200.400
2.7	17782.000
6.8	17363.600
2.5	16945.200
3.5	16526.800
9.4	16108.400
1.2	15690.000
3.5	15187.920
9.4	14895.040
3.5	14434.800
3.6	14058.240
3.7	13681.680
9.6	13305.120
3.5	12928.560
6.0	12535.260
6.1	12175.440
4.2	11798.880
4.3	11464.160
4.4	11087.600
4.5	10752.880
4.6	10460.000
4.7	10125.280
4.8	9790.560
4.9	9497.680
5.0	9192.248
5.1	8911.920

θ_D/T, K	Debye Function, $D(\theta_D/T)$, J/(kmol·K)
5.2	8619.040
[illegible].3	8326.160
[illegible].1	8075.120
[illegible].9	7824.080
5.6	7573.040
[illegible].1	7322.000
5.8	7070.960
9.4	6819.920
6.0	6619.088
8.1	6401.520
6.2	6192.320
8.3	5983.120
6.0	5815.760
6.9	5606.560
6.6	5439.200
6.7	5271.840
6.8	5062.640
6.6	4937.120
7.0	4757.208
[illegible].1	4602.400
1.2	4455.960
1.3	4313.704
7.0	4175.632
7.[illegible]	4041.744
6.8	3912.040
[illegible].1	3790.704
7.8	3673.552
7.9	3556.400
6.0	3443.432
9.4	3338.832
6.2	3238.416
8.3	3138.000
6.0	3041.768
6.9	2945.536
6.6	2857.672
8.1	2769.808
6.8	2686.128
8.9	2606.632
0.9	2527.136
9.1	2460.192
9.2	2384.880
8.3	2309.568
9.4	2246.808
9.5	2179.864
5.6	2121.288
9.4	2058.528
0.9	1999.952
0.9	1945.560
10.0	1891.168
10.1	1836.776
10.2	1786.568
10.3	1736.360

θ_D/T, K	Debye Function, $D(\theta_D/T)$, J/(kmol·K)
10.4	1690.336
14.5	1648.496
10.6	1602.472
12.7	1560.632
14.8	1518.792
14.5	1476.952
11.0	1443.480
11.[illegible]	1401.640
14.[illegible]	1355.616
11.[illegible]	1334.696
11.4	1297.040
14.5	1263.568
14.8	1234.280
14.7	1200.808
14.5	1171.520
11.9	1142.232
12.0	1117.128
12.1	1297.840
12.2	1062.736
12.1	1037.632
12.0	1012.528
12.5	991.608
1[illegible].6	966.504
12.7	945.584
12.8	924.664
14.5	903.744
13.0	882.824
13.1	861.904
13.2	845.168
13.3	824.248
13.9	807.512
13.5	786.592
13.6	769.856
12.7	753.120
13.5	736.384
13.9	719.648
14.0	707.096
14.1	690.360
14.2	677.808
14.5	665.256
14.8	648.520
14.5	635.968
14.5	623.416
14.7	610.864
14.8	598.312
14.5	585.760
15.0	573.208
15.[illegible]	564.840
15.2	552.288
15.3	543.920
15.4	531.368
15.5	523.000

Table 21.2, continued

θ_D/T, K	Debye Function, $D(\theta_D/T)$, J/(kmol·K)
15.6	510.448
15.7	502.080
15.8	493.712
15.9	485.344
16.0	472.792
17.0	395.388
18.0	333.046

θ_D/T, K	Debye Function, $D(\theta_D/T)$, J/(kmol·K)
15.6	283.257
20.0	243.090
21.0	210.037
22.0	182.422
23.0	159.829
24.0	140.582

θ_D/T, K	Debye Function, $D(\theta_D/T)$, J/(kmol·K)
25.0	124.683
26.0	110.458
21.0	98.742
28.0	88.366
29.0	79.496
30.0	71.965

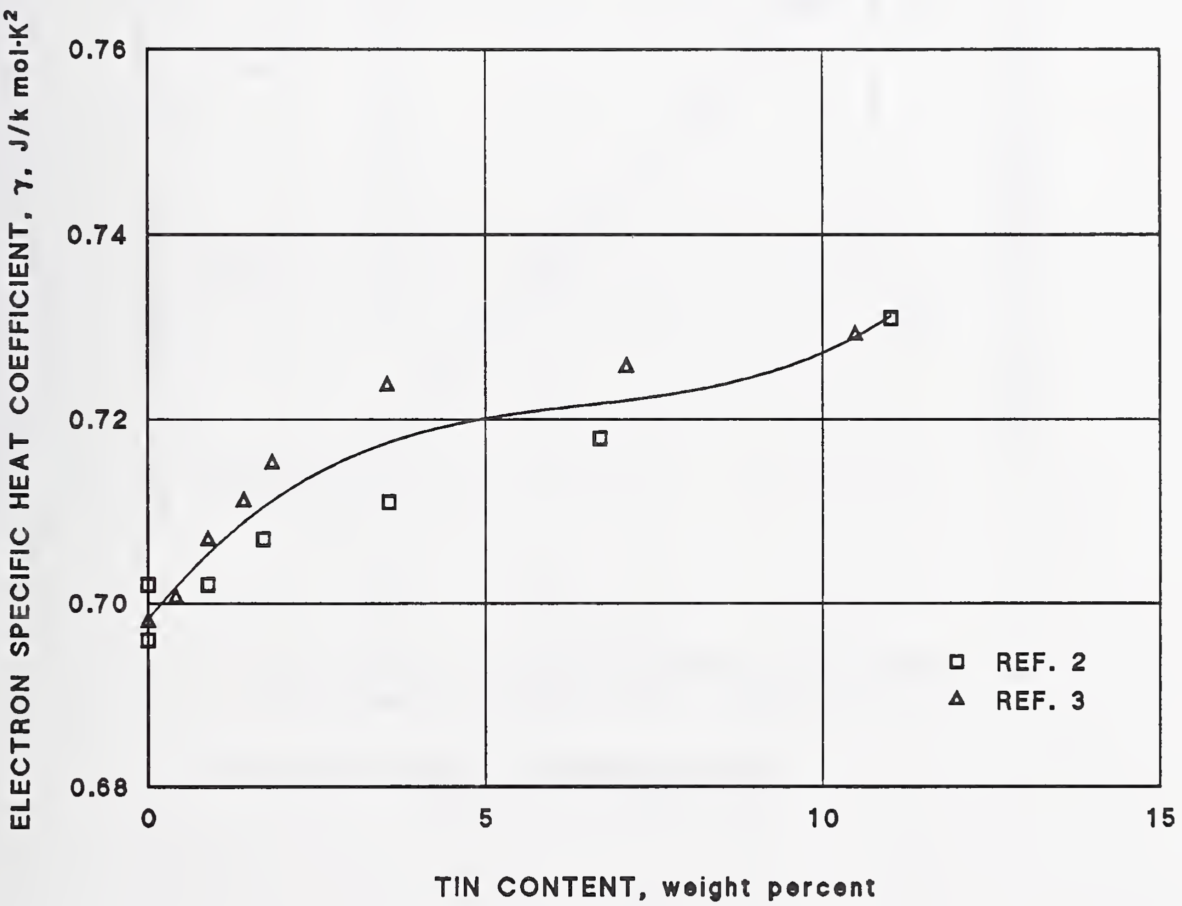

Figure 21.1. The electron specific heat coefficient (γ) is shown as a function of tin content. The data from References 21.2 and 21.3 are fitted to a third-order polynomial [Equation (21-6)].

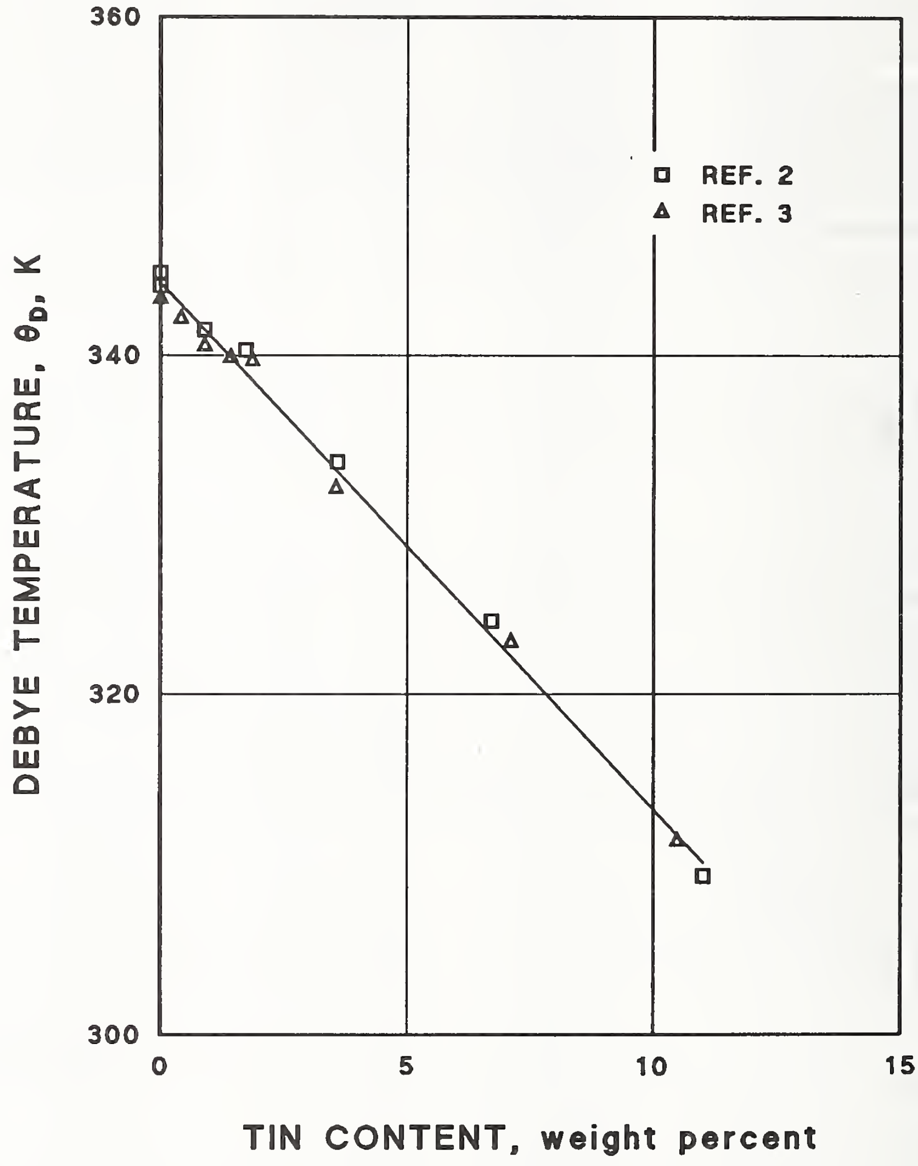

Figure 21.2. The Debye temperature (θ_D) is shown as a function of tin content. The data from References 21.2 and 21.3 follow a linear trend [Equation (21-7)].

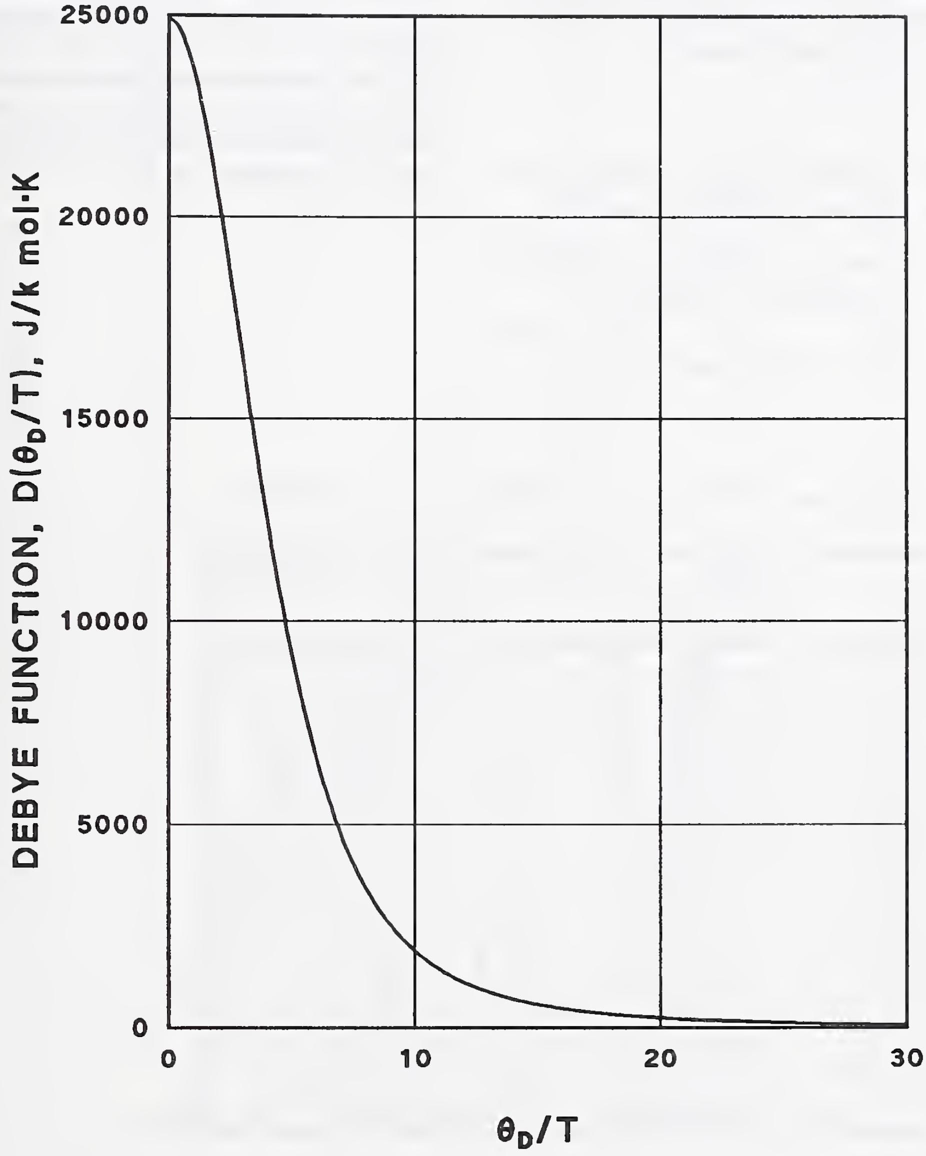

Figure 21.3. This curve, adapted from Reference 21.6, provides values for the Debye function for a known quantity of θ_D/T.

DATA SOURCES AND ANALYSIS

Thermal conductivity (λ) measurements at 295 K on annealed C50715–C52000 phosphor bronzes were obtained from References 21.9–21.12. The available characterization of materials and measurements is given in Table 21.8 at the end of the thermal properties section.

RESULTS

Regression analysis indicated that the best fit to the data was obtained with the equation

$$\lambda\ (W/m{\cdot}K) = +549.2 + 109.9[Sn] - 2.447[Sn]^2 - 425.6[Sn]^{1/2} - 99.72[P] \qquad (21\text{-}10)$$

$$(S.D. = 6.9\ W/m{\cdot}K),$$

where [Sn] is Sn content, and [P] is the phosphorus content, both in wt%. The standard deviations of the coefficients are 44.3, 22.1, 0.773, 60.6, and 13.34. The measurements and thermal conductivity values predicted from Equation (21-10) are given in Table 21.3. The straight line in Figure 21.4 indicates the fit of the data to Equation (21-10); the scatter band represents two standard deviations above and below the line. The variance of the data was assumed to be normally distributed and constant throughout the range of predicted values.

Table 21.3. Dependence of Thermal Conductivity on [Sn] and [P] (295 K).

Thermal Conductivity, Measured, W/(m•K)	Thermal Conductivity, Predicted, W/(m•K)	[Sn], wt%	[P], wt%	Reference No.
167	157	2	0	9
100	[illegible]	4	0	9
75.3	77.8	6	0	9
62.8	67.8	8	0	9
117	115	3.11	0.02	10
66.9	78.3	3.09	0.09	10
66.9	68.9	7.31	0.02	10
46.0	32.5	7.41	0.09	10
83.7	91.4	3.11	0.02	10
75.3	74.2	5.27	0.09	10
62.8	68.9	6.65	0.02	10
165	160	1.92	0.01	11
50.6	51.7	10.4	0.03	11
227	232	0.99	0.002	12
81.6	80.5	4.92	0.06	12
64.4	66.1	7.48	0.04	12
62.8	62.6	4.18	0.33	12

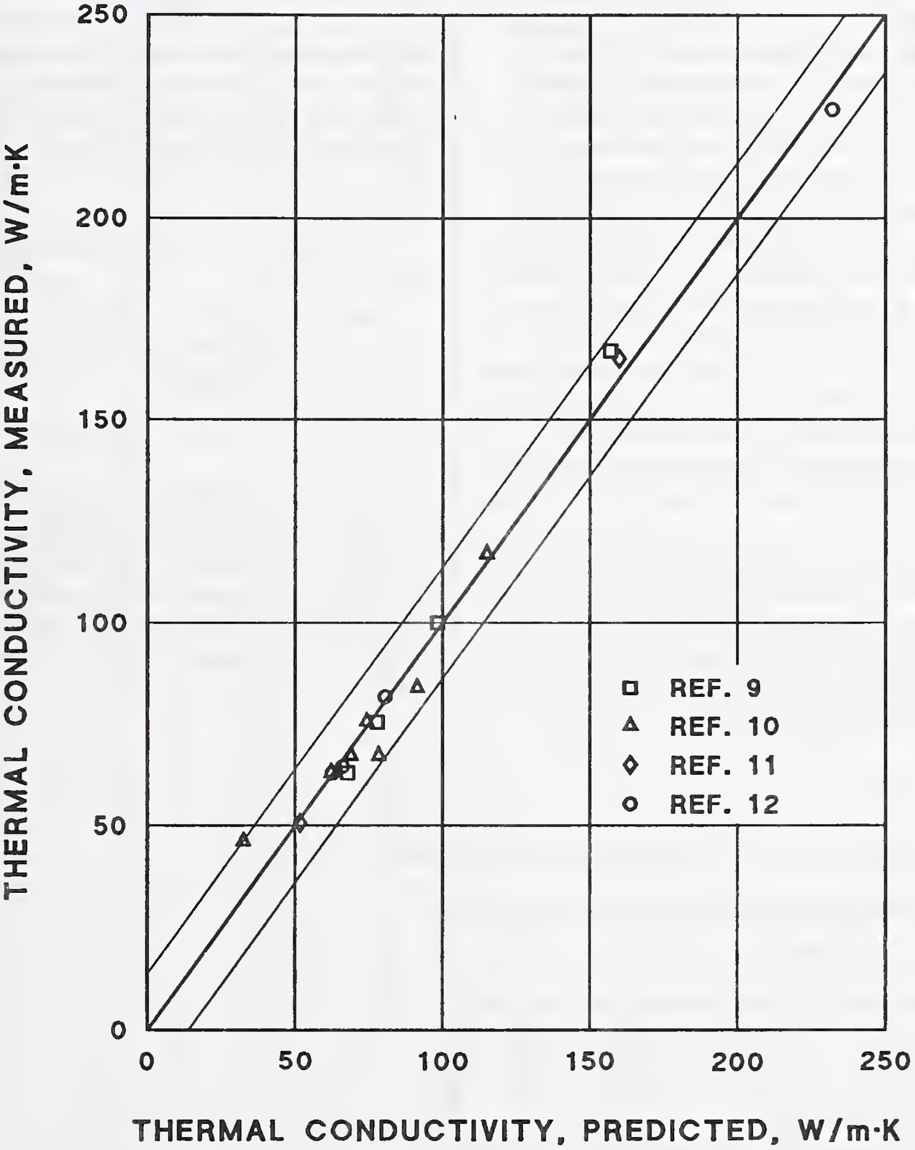

Figure 21.4. The data shown were used to compute the regression of thermal conductivity at 295 K upon Sn and P contents [Equation (21-10)].

DATA SOURCES AND ANALYSIS

Thermal conductivity (λ) measurements between 1 and 473 K were obtained from References 21.10, and 21.13–21.15. The Sn content, [Sn], varied from 0.94 to 7.3 wt%, corresponding to C50100–C52100. The available characterization of materials and measurements is given in Table 21.8 at the end of the thermal properties section. These data are presented in Table 21.4 and Figure 21.5. The data from Reference 21.13 were obtained by adding a Lorentz term for the electronic thermal conductivity to the data the authors presented on the lattice thermal conductivity, since residual resistivity data were provided. Reference 21.4 explains this procedure. However, the procedure is only valid up to about 30 K, so data from 10–30 K only were used from Reference 21.13. As Figure 21.5 shows, the slope of these values does not agree well with that of the other measurements. Consequently, the data from Reference 21.13 were not used in the subsequent analysis.

Because the functional form of the data is a simple polynomial on a log-log plot, logarithmic terms for λ and T (temperature) were used in the multivariate regression analysis of λ on [Sn] and T. A total of 69 measurements were used in the analysis. Values from Reference 21.10 with P content above 0.09 wt% were eliminated, since phosphorus was not present in the other alloys. Also, thermal conductivity values from the annealed, rather than the cold-worked specimens of Reference 21.14 were chosen to not overweight the analysis with data points from one reference. As Figure 21.5 shows, there is not much difference between the thermal conductivity of annealed and 75% cold-worked alloys with the same [Sn], although the effect of cold work may be larger as [Sn] decreases below ~1 wt%.

RESULTS

The best fit to the data was obtained with the equation

$$\log \lambda = +0.4145 + 1.563 \log T - 0.2285 (\log T)^2 - 0.3234\,[\mathrm{Sn}] + 0.02500\,[\mathrm{Sn}]^2 \qquad (21\text{-}11)$$

$$(\mathrm{S.D.} = 0.0796),$$

where λ is in W/(m•K), [Sn] is in wt%, and $4\ \mathrm{K} \leq T \leq 300\ \mathrm{K}$. The standard deviations of the coefficients of this equation are 0.0566, 0.054, 0.0195, 0.0292, and 0.00396. Figure 21.6 indicates the fit of selected data to the curves produced from Equation (21-11) for three values of [Sn].

Table 21.4. Dependence of Thermal Conductivity on [Sn] (1.4–473.2 K).

Test Temperature, K	Thermal Conductivity, W/(m•K)	[Sn], wt%	Reference No.
293	117	3.11	10
473	146	3.71	10
293	62.8	3.71	10
473	83.7	3.71	10
293	83.7	5.27	10
473	108	5.27	10
293	75.3	6.65	10
473	100	6.65	10
293	66.9	7.31	10
473	92.0	7.31	10
8.84	19.9	1.21	13
19.8	66.0	1.21	13
23.5	77.9	1.21	13
11.2	15.0	2.25	13
14.3	21.1	2.25	13
17.3	29.7	2.25	13

Table 21.4, continued

Test Temperature, K	Thermal Conductivity, W/(m•K)	[Sn], wt%	Reference No.
20.6	84.4	2.25	13
24.7	52.2	2.25	13
26.9	53.9	2.25	13
23.6	59.1	2.25	13
10.6	9.48	3.38	13
43.7	13.5	3.38	13
16.8	17.9	3.38	13
17.3	20.8	3.38	13
24.6	88.5	3.38	13
23.6	33.7	3.38	13
28.0	39.9	3.38	13
5.58	28.8	0.937	14B
9.35	32.8	0.937	14B
10.0	34.3	0.937	14B
12.5	43.4	0.937	14B
17.3	88.4	0.937	14B
19.2	66.3	0.937	14A
23.6	74.4	0.937	14B
24.6	84.4	0.937	14A
28.0	88.4	0.937	14B
29.6	96.5	0.937	14B
30.4	59.1	0.937	14B
33.4	66.3	0.937	14A
37.7	112.5	0.937	14B
41.3	122.5	0.937	14B
51.0	134.6	0.937	14B
5.74	15.3	0.937	14B
5.58	16.0	0.937	14B
9.50	25.4	0.937	14B
10.8	29.8	0.937	14B
16.8	43.6	0.937	14A
19.0	54.2	0.937	14B
21.4	69.1	0.937	14A
23.1	54.2	0.937	14B
28.8	69.1	0.937	14A
25.6	71.3	0.937	14B
24.6	76.1	0.937	14B
31.2	88.4	0.937	14B
33.6	88.5	0.937	14A
36.5	94.6	0.937	14B
40.0	101.2	0.937	14B
43.7	107.7	0.937	14B
46.7	112.5	0.937	14A
51.8	118.4	0.937	14B
1.66	1.46	1.85	14C
1.83	1.62	1.85	14B
2.07	1.89	1.85	14B
2.16	1.98	1.85	14B
2.38	2.23	1.85	14C
2.64	2.52	1.85	14C
2.84	2.77	1.85	14C

Table 21.4, continued

Test Temperature, K	Thermal Conductivity, W/(m•K)	[Sn], wt%	Reference No.
3.00	2.96	1.85	14C
3.46	3.86	1.85	14C
3.60	3.72	1.85	14C
3.75	1.49	1.85	14C
1.95	1.35	1.85	14D
2.24	2.31	1.85	14E
2.60	2.71	1.85	14D
2.74	2.89	1.85	14D
2.91	3.07	1.85	14D
3.03	3.86	1.85	14E
3.19	3.07	1.85	14D
3.86	3.55	1.85	14E
3.69	3.87	1.85	14D
3.86	1.49	1.85	14D
9.16	14.7	1.85	14D
10.0	11.9	1.85	14D
12.8	14.7	1.85	14D
10.0	17.3	1.85	14E
14.7	24.0	1.85	14D
21.3	26.1	1.85	14D
20.9	30.9	1.85	14D
30.3	36.0	1.85	14D
32.8	38.9	1.85	14D
34.5	40.9	1.85	14E
40.7	51.4	1.85	14D
10.6	48.9	1.85	14E
1.46	0.589	5.46	14E
1.61	0.665	5.46	14E
1.84	0.775	5.46	14E
2.74	0.940	5.46	14E
2.27	1.35	5.46	14D
2.45	1.49	5.46	14E
2.61	1.35	5.46	14D
2.72	1.26	5.46	14E
2.88	1.35	5.46	14D
3.11	1.49	5.46	14E
3.69	1.84	5.46	14D
3.80	1.91	5.46	14E
5.91	3.23	5.46	14D
6.90	3.86	5.46	14E
9.24	5.52	5.46	14D
10.8	6.38	5.46	14E
12.4	7.66	5.46	14D
16.8	8.46	5.46	14E
20.9	11.2	5.46	14E
22.7	13.6	5.46	14E
20.9	14.7	5.46	14D
31.3	16.8	5.46	14E
33.9	17.8	5.46	14E
43.1	20.7	5.46	14E
46.6	21.8	5.46	14E

Table 21.4, continued

Test Temperature, K	Thermal Conductivity, W/(m•K)	[Sn], wt%	Reference No.
52.9	23.2	5.46	14F
56.9	24.3	5.46	14F
1.60	0.592	5.46	14F
1.79	0.662	5.46	14F
1.60	0.726	5.46	14F
2.22	0.830	5.46	14F
2.42	0.922	5.46	14F
2.58	0.984	5.46	14F
2.71	4.04	5.46	14F
3.13	1.21	5.46	14F
3.43	1.32	5.46	14F
3.80	1.51	5.46	14F
5.99	3.09	5.46	14F
8.32	1.21	5.46	14F
5.99	4.84	5.46	14F
10.9	5.60	5.46	14F
11.9	6.11	5.46	14F
12.6	5.60	5.46	14F
15.6	4.04	5.46	14F
12.6	5.60	5.46	14F
21.7	10.1	5.46	14F
25.1	12.5	5.46	14F
27.4	13.5	5.46	14F
31.6	11.0	5.46	14F
38.1	10.1	5.46	14F
12.6	19.2	5.46	14F
46.3	20.3	5.46	14F
51.6	21.7	5.46	14F
56.6	23.4	5.46	14F
3.80	1.14	5.46	15
4.50	4.04	5.46	15
6.52	2.47	5.46	15
1.60	4.04	5.46	15
12.1	5.60	5.46	15
15.7	4.04	5.46	15
23.3	11.0	5.46	15
29.0	11.6	6.46	15
49.0	16.3	6.46	15
88.0	25.1	6.46	15

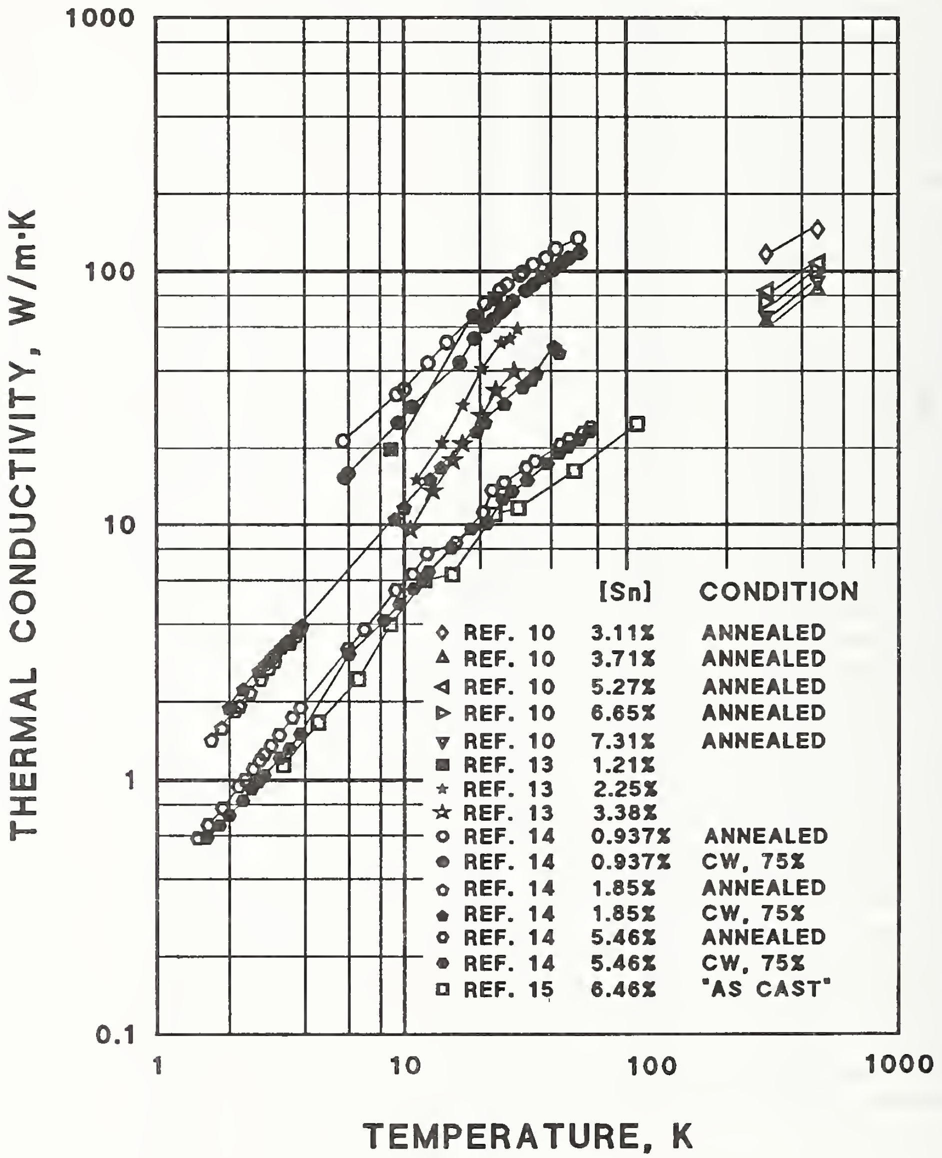

Figure 21.5. Data on the thermal conductivity of phosphor bronzes from four references are shown as a function of temperature. Tin contents are in weight percent.

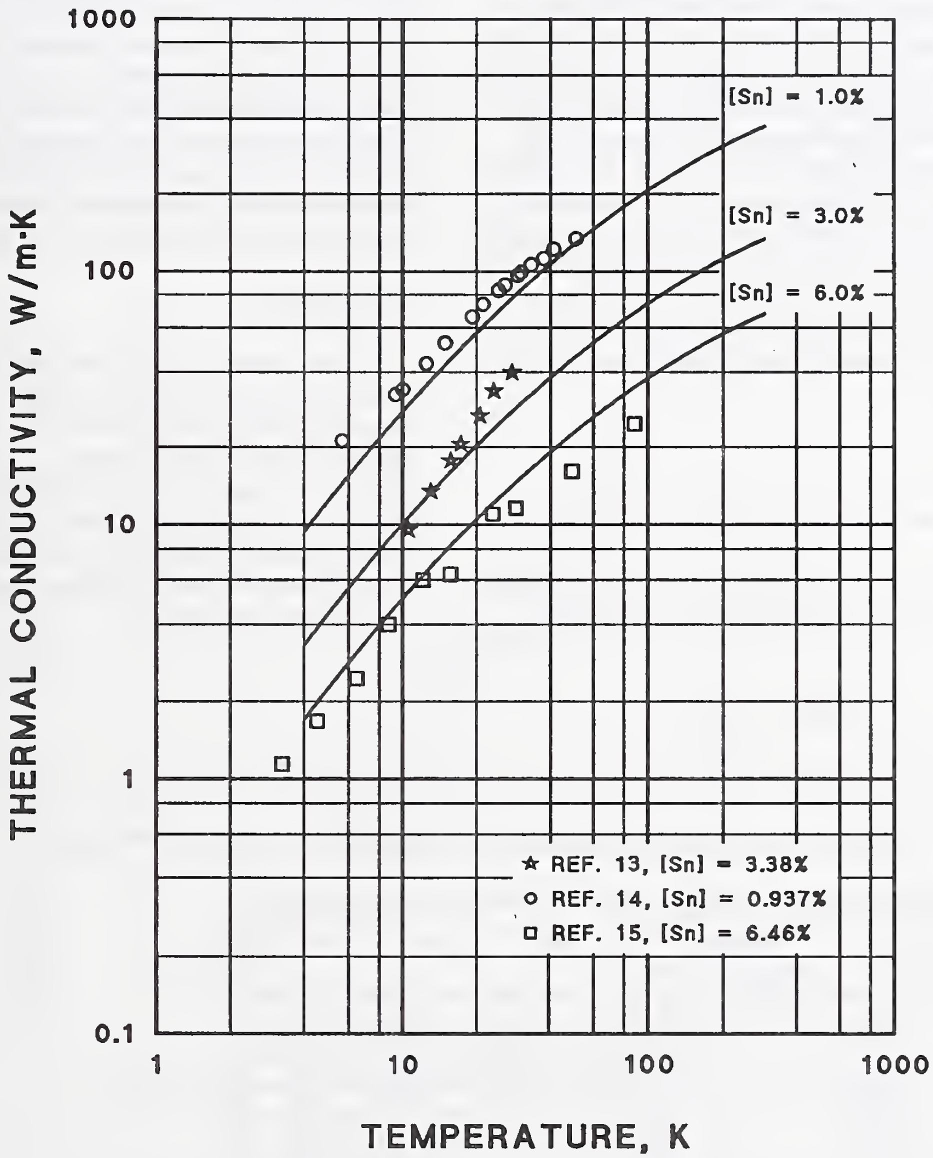

Figure 21.6. Predictive curves are shown for thermal conductivity vs. temperature for three Sn contents, 1, 3, and 6 wt%, based on Equation (21-11). Data from References 21.10, 21.14 (annealed data only) and 21.15 were used to derive the equation. Values for Sn contents approximately equal to 1, 3, and 6 wt% from References 21.14, 21.13, and 21.15, respectively, show the fit of the data to the equation.

DATA SOURCES AND ANALYSIS

Data on the thermal expansion coefficient, α, at 295 K were obtained from References 21.16–21.18 on a total of nine alloys. Composition, including phosphorus content, [P], as well as tin content, [Sn], was reported in these references. The data are presented in Table 21.5. The available characterization of materials and measurements is given in Table 21.8 at the end of the thermal properties section. A linear regression analysis was carried out to obtain the dependence of α upon [Sn] and [P]. The data from Reference 21.19 on a binary Cu-Sn alloy were not included in the analysis owing to lack of agreement with the equation that fitted the rest of the data well.

RESULTS

The regression analysis gave the following equation:

$$\alpha\,(10^{-6}) = 16.24 + 0.1072\,[Sn] + 0.5726\,[P] \qquad (21\text{-}12)$$

(S.D. = 0.12).

The standard deviations of the three coefficients in Equation (21-12) are 0.09, 0.0134, and 0.1384. Figure 21.7 indicates the fit of the data to Equation (21-12). The scatter band represents two standard deviations about the straight line that indicates agreement between the measured and predicted values of α. The variance of the data was assumed to be normally distributed and constant throughout the range of the predicted values. Equation (21-12) indicates that the small amounts of phosphorus usually found in C50100–C52400 can influence α significantly.

DISCUSSION

The reason for the poor fit of the measurements on a binary alloy from Reference 21.19 to Equation (21-12) is unknown. The equation should be used with caution for Cu-Sn alloys with [P] = 0. A measurement from Reference 21.16 with [P] = 0 does agree well with other data. The data from Reference 21.19 pertain to annealed material; other measurements are on cold-worked and cast alloys.

Table 21.5. Dependence of the Thermal Expansion Coefficient on [Sn] and [P] (295 K).

Thermal Expansion Coefficient, Measured, 10^{-6}/K	Thermal Expansion Coefficient, Predicted, 10^{-6}/K	[Sn], wt%	[P], wt%	Reference No.
16.95	16.90	4.25	0.37	16A
16.78	16.59	4.88	0.12	16A
16.99	17.12	7.67	0.11	16A
17.28	17.32	10.14	0.20	16A
16.69	16.59	2.20	0.20	16A
16.61	16.59	2.20	0.20	16B
17.03	17.14	4.70	0.70	16B
17.01	17.14	4.70	0.70	16B
16.99	16.86	4.85	0.18	17
17.95	17.78	10.47	0.74	18A
17.03	17.04	6.46	0.20	18B

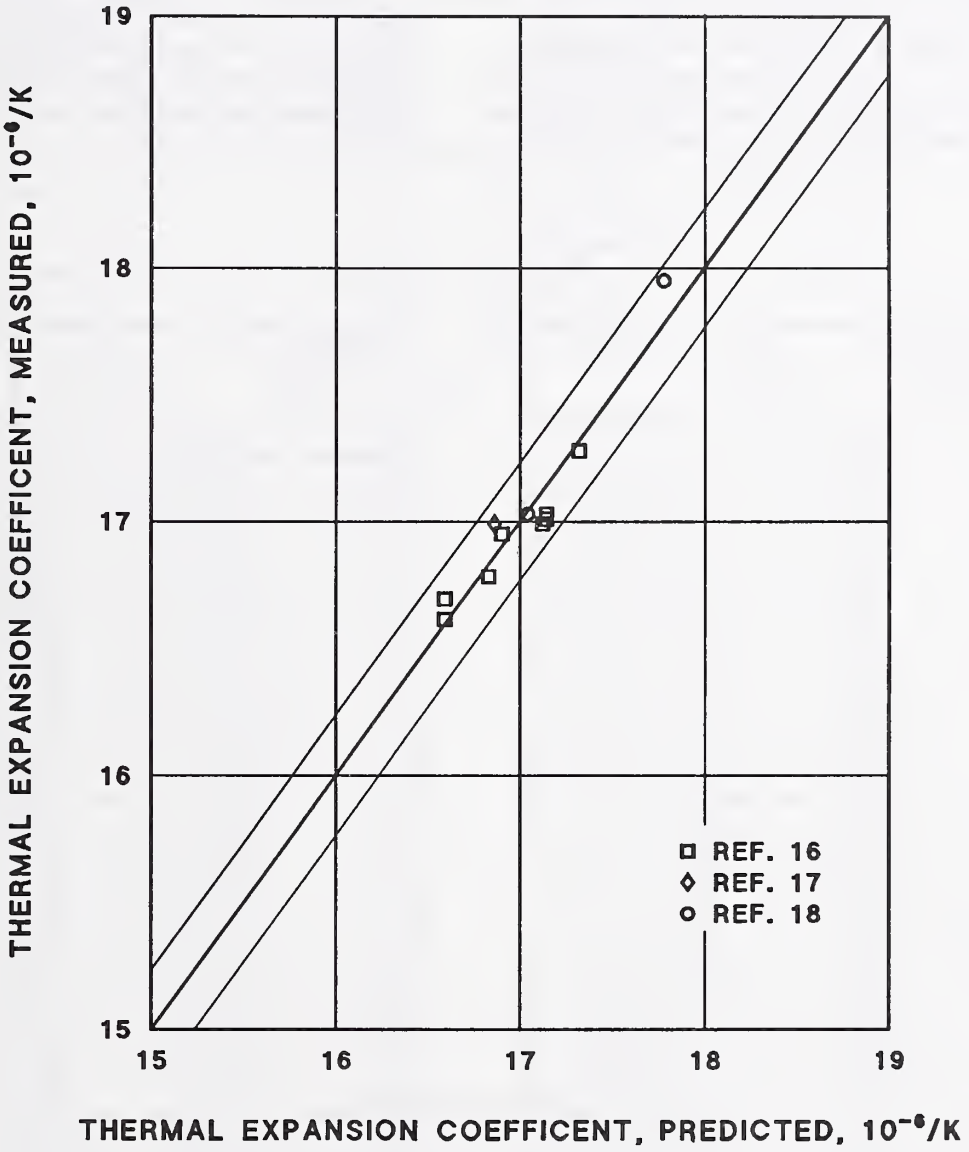

Figure 21.7. The data shown were used to compute the regression of the thermal expansion coefficient at room temperature upon [Sn] and [P] [Equation (21-12)].

C51000: Cold-worked

Thermal Expansion Coefficient vs. Temperature (10–300 K)

DATA SOURCE

Data on the thermal expansion coefficient (α) below 300 K were obtained on three alloys, cold-worked C51000, C51900, and C52400. Reference 21.17 reports α for cold-worked C51000 from 293 to 20 K, and provides an extrapolated value at 10 K. Reference 21.18 reports α for alloys C51900 and C52400 from approximately 300 to 77 K. These data are presented in Table 21.6 and Figure 21.8. The available characterization of materials and measurements is given in Table 21.8 at the end of the thermal properties section.

DISCUSSION

Data on two Sn contents, [Sn], from Reference 21.18 are included in Figure 21.7. It is not understood why the data for [Sn] = 10.47% do not plot as a smooth curve. However, the data from Reference 21.18 show that as the [Sn] Increases, α also increases.

Table 21.6. Dependence of the Thermal Expansion Coefficient on Temperature (10–300 K).

Thermal Expansion Coefficient, 10^{-6}/K	Test Temperature, K	Reference No.
0.06	10	17
0.46	20	17
1.35	30	17
2.67	40	17
4.22	50	17
5.81	80	17
7.29	70	17
8.59	80	17
9.71	30	17
10.66	100	17
12.15	103	17
13.20	80	17
14.09	50	17
14.76	180	17
16.99	50	17
15.78	20	17
16.17	240	17
16.51	280	17
16.71	273	17
16.81	280	17
16.99	293	17
12.40	77	18A
12.70	50	18A
13.20	80	18A
13.70	103	18A
14.10	100	18A
14.50	123	18A
14.70	80	18A
14.80	103	18A
15.00	100	18A
15.20	163	18A
15.50	173	18A
16.00	183	18A
16.70	193	18A
17.20	203	18B
17.65	213	18B
17.60	203	18B
17.65	213	18B
17.80	203	18B
17.75	260	18B
17.80	230	18A
17.65	213	18B
17.90	230	18B
17.65	213	18B
10.03	90	18B
16.45	100	18B
11.69	110	18B
12.37	120	18B
12.96	130	18B
13.46	140	18B
13.88	90	18B
14.23	160	18B
14.53	110	18B
17.65	140	18B
15.05	190	18B
15.28	200	18B
15.05	230	18B
15.71	220	18B
15.91	230	18B
16.45	240	18B
16.28	230	18B
16.45	260	18B
15.91	270	18B
16.76	280	18B
16.90	290	18B
17.03	300	18B

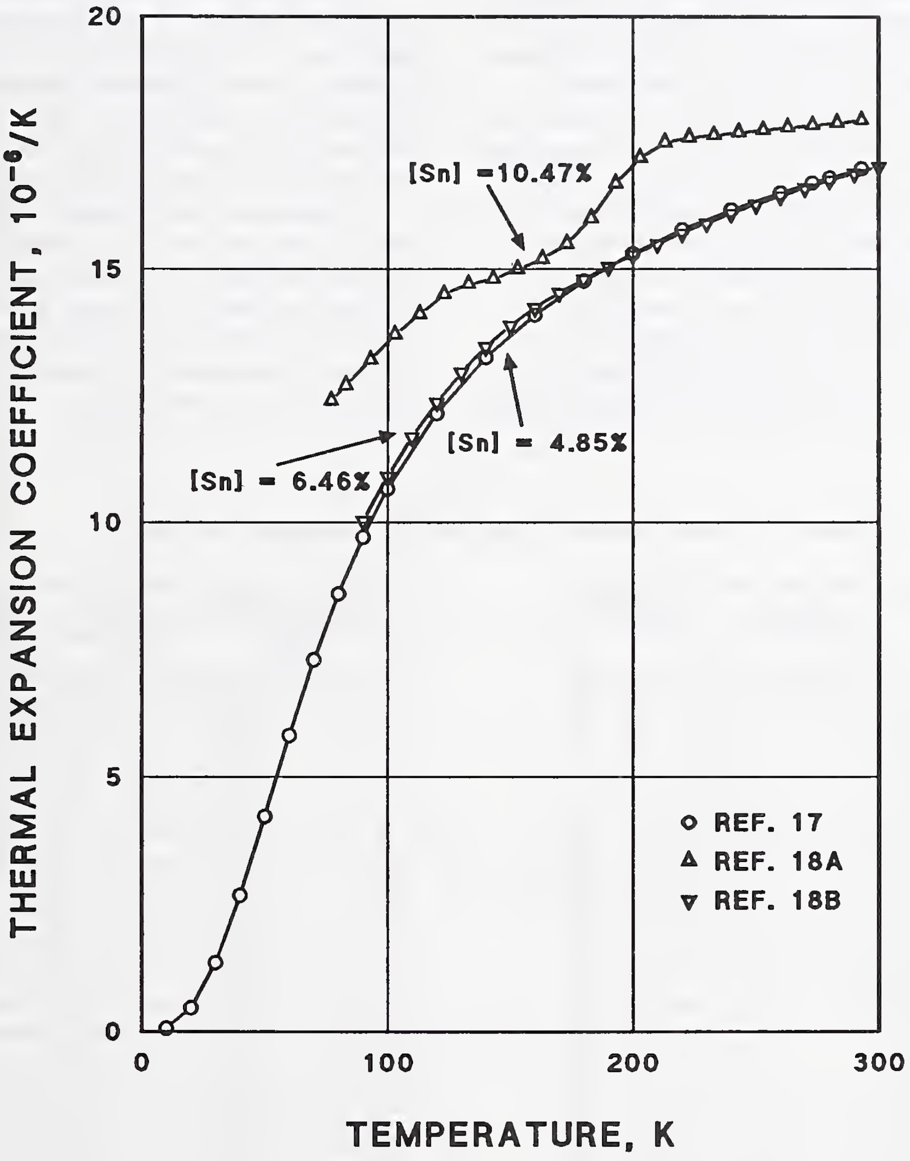

Figure 21.8. Data on the thermal expansion coefficient of phosphor bronzes from two references are shown as a function of temperature. Tin contents are given in weight percent.

DATA SOURCES

Mean thermal expansion data below 300 K were obtained on cold-worked C51000 from Reference 21.17 and on cast C52400 from Reference 21.1. The available characterization of materials and measurements is given in Table 21.8 at the end of the thermal properties section. The mean thermal expansion, $\Delta L/(L \cdot \Delta T)$, is defined as $[L(293\ \mathrm{K}) - L(T)]/[L(293\ \mathrm{K})(293\ \mathrm{K} - T)]$ except at 293 K, where it equals $(1/L)(dL/dT)$. These data are presented in Table 21.7 and Figure 21.9. A few data points above 260 K are eliminated from the figure; data on $\Delta L/(L \cdot \Delta T)$ become less accurate near room temperature as ΔL becomes smaller. Reference 21.17 gives a value for $(1/L)(dL/dT)$ at 293 K; this is presented in the figure. Reference 21.1 does not provide such a value, and the scatter of the mean thermal expansion data reported in this paper makes it difficult to estimate $(1/L)(dL/dT)$ at 293 K.

DISCUSSION

Because the scatter of the data near 295 K is large for both alloys, and since no other cryogenic data on alloys of different [Sn] and [P] are available, it was considered impractical to develop a predictive equation for mean thermal expansion as a function of [Sn], [P], and temperature. The influence of cold work also is unknown.

The reason that the data for both alloys appear to coincide near room temperature (above ~ 240 K) is unclear. As explained above, errors in the data are likely to be larger in this temperature region. However, Equation (21-12) predicts that the thermal expansion for the two alloys would be different at room temperature.

Table 21.7. Dependence of Mean Thermal Expansion on Temperature (5–300 K).

Mean Thermal Expansion, 10^{-6}/K	Test Temperature, K	Reference No.
11.26	0	17
11.66	10	17
12.09	20	17
12.51	30	17
12.92	40	17
13.33	50	17
13.69	60	17
13.99	80	17
14.27	60	17
14.53	50	17
14.77	100	17
15.14	120	17
15.49	140	17
15.71	160	17
16.58	180	17
16.13	200	17
16.30	220	17
16.42	240	17
16.36	260	17

Mean Thermal Expansion, 10^{-6}/K	Test Temperature, K	Reference No.
16.50	273	17
16.15	280	17
16.99	293	17
12.80	4	1
13.52	20	1
14.19	40	1
14.81	60	1
15.31	80	1
15.65	100	1
16.34	120	1
16.21	140	1
16.32	160	1
16.37	180	1
16.34	200	1
16.58	220	1
16.32	240	1
16.36	260	1
16.50	273	1
16.92	280	1

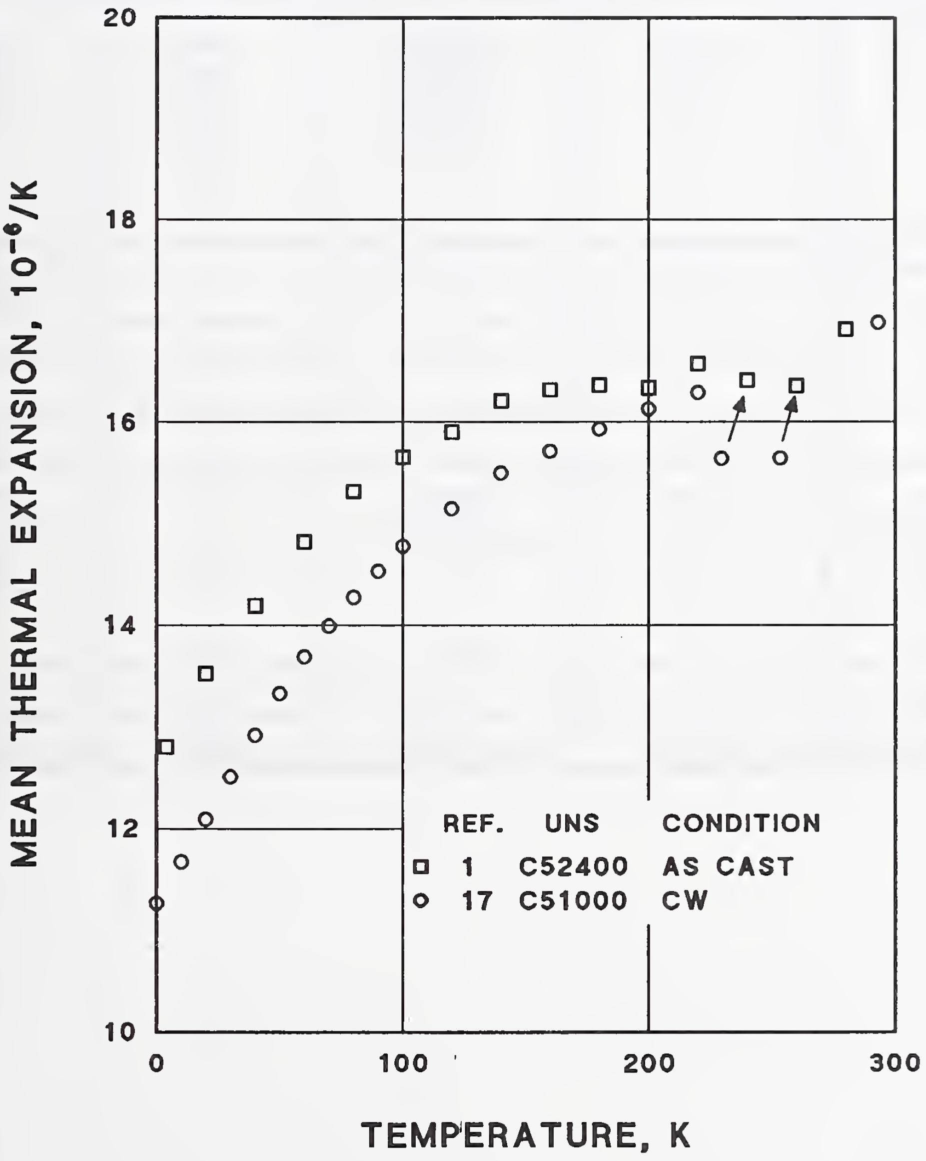

Figure 21.9. Data on the mean thermal expansion of phosphor bronzes from two references are shown as a function of temperature.

Table 21.8. Characterization of Materials and Measurements.

Reference No.	1A	1B	9	10
Specification	—	—	—	—
Composition (wt%)				
Cu	—	—	—	92.2–96.84
Sn	8	11	2–8	3.11–7.41
P	—	—	—	0.02–0.39
Pb	—	—	—	—
Fe	—	—	—	—
Zn	—	—	—	—
Others (Only ≥ 0.001 wt%)	—	—	—	—
Material Condition	As extruded	As cast	—	Annealed, 898 K, 2.5 h
RRR	—	—	—	—
Grain Size	—	—	—	—
Hardness	—	—	—	R_B66–82
Product Form	Extrusion	Casting	—	Strip, 1.91-cm-thick
Specimen Type	—	—	—	Cylinder
Width or Dia.	—	—	—	1.6 cm
Thickness	—	—	—	—
Gage Length	—	—	—	—
No. of Specimens	—	—	—	—
Test Temperature	4.0–17.5 K	4.4–17.3 K	293 K	293, 473 K

11A	11B	12	13	14A
C50715	C52400	—	—	—
98.09	89.52	92.55–99.00	—	—
1.92	10.40	0.99–7.48	1.21–3.38	0.937
0.01	0.03	0.002–0.33	—	—
—	0.01	0.00–0.04	—	—
0.01	0.05	0.01–0.05	—	—
—	—	—	—	—
—	—	—	—	—
—	—	Annealed, 923 K, 0.5 h	—	Annealed, 1123 K, 48 h
—	—	—	—	—
—	—	—	—	—
—	—	—	—	—
—	—	Bar, 2.22-cm-dia.	—	Bar, 0.318-cm-dia.
—	—	—	—	Cylinder
—	—	—	—	0.318 cm
—	—	—	—	—
—	—	—	—	4.86 cm
—	—	—	—	—
293 K	293 K	293 K	5–30 K	5.678–50.979 K

Table 21.8, continued

Reference No.	14B	14C	14D	14E
Specification	—	—	—	—
Composition (wt%)				
Cu	—	—	—	—
Sn	0.937	1.85	1.85	5.46
P	—	—	—	—
Pb	—	—	—	—
Fe	—	—	—	—
Zn	—	—	—	—
Others (Only ≥ 0.001 wt%)	—	—	—	—
Material Condition	Cold-drawn, 75%	Annealed, 1073 K, 24 h	Cold-drawn, 75%	Annealed, 1123 K, 48 h
RRR	—	—	—	—
Grain Size	—	—	—	—
Hardness	—	—	—	—
Product Form	Bar, 0.318-cm-dia.	Bar, 0.318-cm-dia.	Bar, 0.318-cm-dia.	Bar, 0.318-cm-dia.
Specimen Type	Cylinder	Cylinder	Cylinder	Cylinder
Width or Dia.	0.318 cm	0.318 cm	0.318 cm	0.318 cm
Thickness	—	—	—	—
Gage Length	4.99 cm	4.99 cm	5.01 cm	4.71 cm
No. of Specimens	—	—	—	—
Test Temperature	5.739–51.750 K	1.659–3.751 K	1.954–42.616 K	1.438–56.897 K

14F	15	16A	16A	17
—	C51900	—	—	C51000
— 5.46 — — — — —	93.3 6.46 0.20 — — — —	89.69–95.40 4.25–10.14 0.0–0.37 — — — —	94.6–97.6 2.2–4.7 0.2–0.7 — — — —	95.93 4.85 0.18 — — — —
Cold-drawn, 75%	As received	Cold-drawn, 60%	—	Cold-drawn, 85%
—	—	—	—	—
—	—	—	—	100 μm
—	—	—	—	R_B91
Bar, 0.318-cm-dia.	—	Bar, 0.635-cm-dia.	—	—
Cylinder 0.318 cm — 4.77 cm	Cylinder 0.3 cm — —	— — — 30 cm	— — — —	Bar 0.64 cm 0.64 cm 20.32 cm
—	—	—	—	—
1.596–56.578 K	3–88 K	293 K	293 K	20–293 K

Table 21.8, continued

Reference No.	18A	18B
Specification	C52400	C51900
Composition (wt%)		
Cu	88.44	93.3
Sn	10.47	6.46
P	0.74	0.20
Pb	—	—
Fe	—	—
Zn	—	—
Others	—	—
(Only ≥ 0.001 wt%)	—	—
Material Condition	As cast	—
RRR	—	—
Grain Size	—	—
Hardness	R_B67	—
Product Form	Bar, 1.5-cm-dia.	Wire, 0.3-cm-dia.
Specimen Type	—	—
Width or Dia.	—	—
Thickness	—	—
Gage Length	—	—
No. of Specimens	—	—
Test Temperature	77–293 K	90–300 K

REFERENCES

1. Jelinek, F. J., and Collings, E. W., "Low Temperature Thermal Expansion and Specific Heat Properties of Structural Materials," in Semi-Annual Technical Reports on Materials Research in Support of Superconducting Machinery--II, Eds. A. F. Clark, R. P. Reed, and E. C. van Reuth, National Technical Information Service, Springfield, VA, ADA 004586 (1974).

2. Clune, L. C., and Green, B. A., Jr., "Low-Temperature Specific Heats of α-CuSn and α-CuZn Alloys," Physical Review 144, 525–528 (1966).

3. Bevk, J., and Massalski, T. B., "Low-Temperature Specific Heats in α-Phase CuSn Alloys," Physical Review B 5, 4678–4683 (1972).

4. Rosenberg, H. M., "Low Temperature Solid State Physics--Some Selected Topics," Oxford University Press, London, England (1963).

5. Ziman, J. M., "Electrons and Phonons--The Theory of Transport Phenomena in Solids," Oxford University Press, London, England (1960).

REFERENCES

6. Roberts, J. K., "Heat and Thermodynamics, 4th Edition," Interscience Publishers, Inc., New York, NY (1954).

7. de Launay, J., "The Theory of Specific Heats and Lattice Vibrations," in Solid State Physics, Vol. 2, Eds. F. Seitz and D. Turnbull, Academic Press, Inc., New York, NY (1956).

8. Touloukian, Y. S., and Buyco, E. H., "Thermophysical Properties of Matter, Vol. 4, Specific Heat, Metallic Elements and Alloys," IFI/Plenum, New York, NY (1970).

9. Zschötge, S., "Vorwärmtemperaturen beim Schmeizschweißen von Nichteisenmetallen," Schweißen und Schneiden 20, 634–643 (1968).

10. Cook, M., and Tallis, W. G., "The Physical Properties and Annealing Characteristics of Standard Phosphor-Bronze Alloys," The Journal of the Institute of Metals 67, 49–65 (1941).

11. Donaldson, J. W., "Thermal and Electrical Conductivities: Details for Non-ferrous Metals and Alloys," The Metal Industry 58, 342–376 (1941).

12. Smith, C. S., "Thermal Conductivity of Copper Alloys: II. Copper-Tin Alloys and III. Copper-Phosphorus Alloys," Transactions of the American Institute of Mining and Metallurgical Engineering 93, 176–184 (1931).

13. Garber, M., Scott, B. W., and Blatt, F. J., "Thermal Conductivity of Dilute Copper Alloys," Physical Review 130, 2188–2192 (1963).

14. Nanjundiah, S., "Phonon Scattering by Point Defect Impurities in Copper Alloys at Very Low Temperatures," Ph.D. Dissertation from the University of Connecticut (1980).

15. Zavaritskii, N. V., and Zel'dovich, A. G., "Thermal Conductivity of Technical Materials at Low Temperatures," Soviet Physics--Technical Physics 1, 1970–1974 (1956).

16. Hidnert, P., "Thermal Expansion of Copper and Some of Its Important Industrial Alloys," Scientific Papers of the Bureau of Standards 17, 91–159 (1922).

17. Clark, A. F., "Low Temperature Thermal Expansion of Some Metallic Alloys," Cryogenics 8, 282–289 (1968).

18. Gudkov, S. I., "Tin, Aluminum, and Silicon Bronzes, Part 3," in Mechanical Properties of Industrial Nonferrous Metals at Low Temperatures, Publishing House, Moscow, USSR (1971), translation from Joint Publications Research Service, Washington, DC, JPRS-55861, 307–333 (1972).

19. De, M., "Thermal Expansion of Some Cu- and Ag-base Alloys at High Temperatures," Indian Journal of Physics 43, 367–376 (1969).

DATA SOURCES AND ANALYSIS

Measurements at 295 K of the resistivity, ρ, of annealed C51000–C52400 phosphor bronzes and Cu-Sn alloys were obtained from References 22.1–22.7. The form of the product was wire (References 22.2–22.6) or bar (References 22.1 and 22.7). The available characterization information on specimens and measurements is presented in Table 22.10 at the end of the electromagnetic properties section. Regression analysis was carried out on the data to determine the dependence of ρ on Sn content, [Sn], P content, [P], and Fe content, [Fe].

RESULTS

A satisfactory fit to the data was obtained with the expression

$$\rho(\mathrm{n\Omega{\cdot}m}) = + 16.52 + 16.24\,[\mathrm{Sn}] - 0.2906\,[\mathrm{Sn}]^2 + 176.4\,[\mathrm{P}] - 101.8\,[\mathrm{Fe}] \qquad (22\text{-}1)$$

$$(\mathrm{S.D.} = 3.09\ \mathrm{n\Omega{\cdot}m}),$$

where the standard deviations of the coefficients are 0.81, 0.60, 0.0706, 10.3, and 55.9, and $[\mathrm{Sn}] \leq 10.4$ wt%. The element contents are in wt%. Table 22.1 presents the measured values of ρ and the values calculated from Equation (22-1). The straight line in Figure 22.1 indicates the fit of the data to Equation (22-1); the scatter band represents two standard deviations above and below the line. The variance of the data was assumed to be normally distributed and constant throughout the range of predicted values.

DISCUSSION

The coefficient of the [Fe] term is not well-determined, as indicated by the standard deviation of 55.9, which equals about 50% of the coefficient. Iron content was reported for only 6 out of the total of 32 measurements used in the analysis.

As Table 22.10 shows, an additional element, O_2, was present in small amounts in the material reported on in Reference 22.5. From Figure 8.1, the expected change in resistivity of about 0.05 nΩ•m is well below the standard deviation of 3 nΩ•m. Figure 8.1 also shows that the expected change in ρ, for [P] and $[\mathrm{Sn}] < 0.01$ wt%, is in agreement with Equation (22-1).

Table 22.1 Electrical Resistivity of Annealed Material (295 K).

Electrical Resistivity, Measured, nΩ•m	Electrical Resistivity, Predicted, nΩ•m	[Sn], wt%	[P], wt%	[Fe], wt%	Reference No.
31.88	31.65	0.99	0.002	0.01	1
47.27	47.38	4.92	0.01	0.01	1
93.69	94.88	4.92	0.0•	0.05	1
126.67	126.76	7.48	0.01	0.02	1
155.37	154.19	10.4	0.03	0.05	3
136.63	136.51	6.19	0.33	0.01	1
17.16	16.52	0.0	0.0	0.0	2A
33.28	32.31	0.99	0.0	0.0	2A
95.72	89.39	4.92	0.0	0.0	2A
127.93	121.86	7.49	0.0	0.0	2A
17.69	16.52	0.0	0.0	0.0	3
20.46	19.60	0.19	0.0	0.0	3
31.73	31.37	0.93	0.0	0.0	3
51.03	47.84	2.00	0.0	0.0	3
59.49	59.28	2.77	0.0	0.0	3
101.20	96.53	5.46	0.0	0.0	3
16.87	16.52	0.0	0.0	0.0	4A
16.89	16.53	0.0007	0.0	0.0	4A
16.88	16.54	0.0015	0.0	0.0	4A

Table 22.1, continued

Electrical Resistivity, Measured, nΩ·m	Electrical Resistivity, Predicted, nΩ·m	[Sn], wt%	[P], wt%	[Fe], wt%	Reference No.
16.94	16.60	0.005	0.0	0.0	4A
17.00	18.67	0.010	0.0	0.0	7A
17.65	17.33	0.0[illegible]5	0.0	0.0	4A
17.0[illegible]	16.78	0.016	0.0	0.0	6
17.10	17.43	0.056	0.0	0.0	6
17.[illegible]	17.82	0.080	0.0	0.0	5
17.45	18.67	0.133	0.0	0.0	6
31.3	32.47	1.00	0.0	0.0	6
44.0	48.29	2.03	0.0	0.0	6
56.5	62.05	2.96	0.0	0.0	6
70.0	75.16	3.88	0.0	0.0	6
53.7	54.42	2.03	0.0	0.0	7A
127.7	135.59	8.68	0.0	0.0	7A

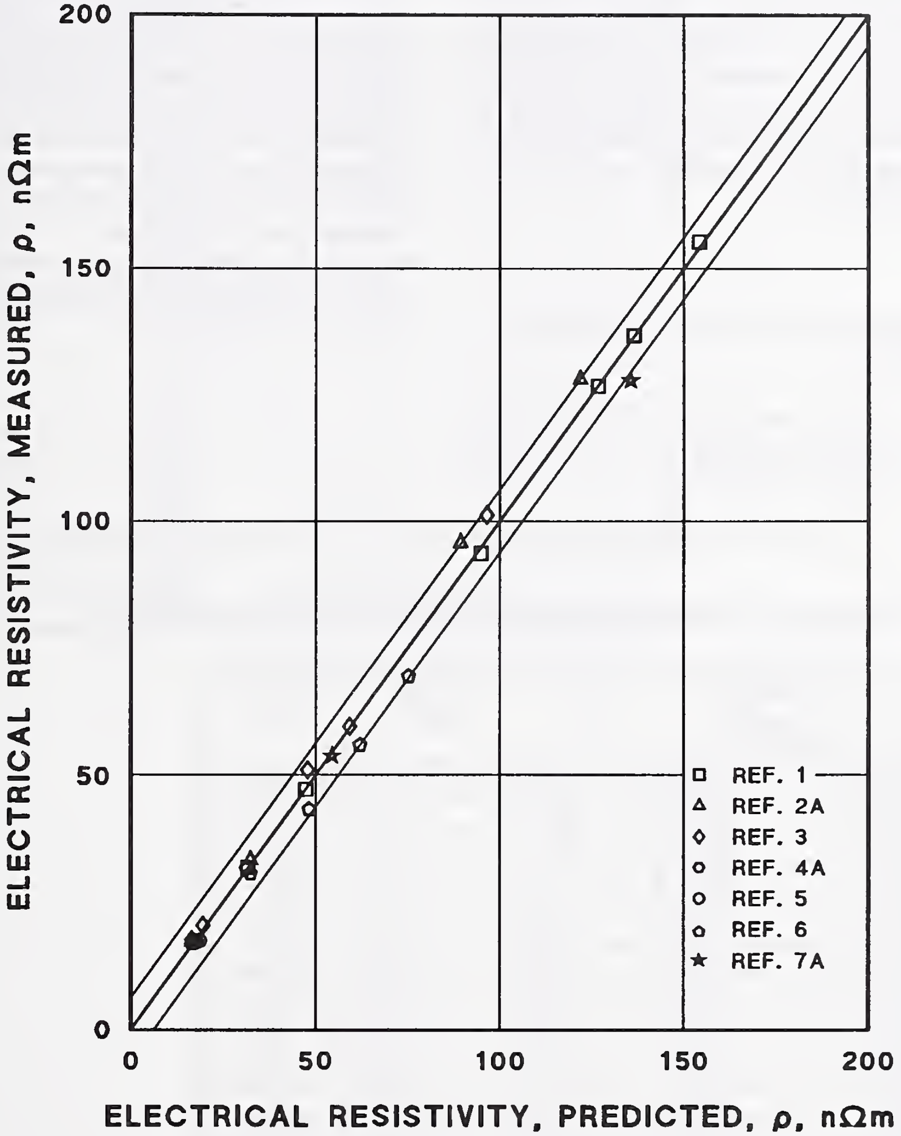

Figure 22.1. The data shown were used to compute the regression of electrical resistivity at 295 K for annealed material upon Sn, P, and Fe content [Equation (22-1)].

DATA SOURCES AND ANALYSIS

Measurements at 295 K of the electrical resistivity (ρ) with both cold work (*CW*) and Sn content ([Sn]) were obtained from References 22.2, 22.4, 22.7, and 22.8. The form of the product was wire (References 22.2, 22.4, and 22.8) or bar (Reference 22.7). The available characterization of specimens and measurements is presented in Table 22.10 at the end of the electromagnetic properties section. Since the effect of *CW* is larger for higher [Sn], the multivariate analysis included cross terms.

RESULTS

A satisfactory fit to the data was obtained with the equation

$$\rho(\mathrm{n\Omega\cdot m}) = +\ 16.72 + 16.91\,[\mathrm{Sn}] - 0.3719\,[\mathrm{Sn}]^2 + 0.01272\,[\mathrm{Sn}](CW) \quad (22\text{-}2)$$
$$(\mathrm{S.D.} = 3.03\ \mathrm{n\Omega\cdot m}),$$

where the standard deviations of the coefficients are 1.12, 0.48, 0.0424, and 0.00233, $[\mathrm{Sn}] \leq 10.4$ wt%, and $CW \leq 90\%$. Table 22.2 presents the measured values of ρ and the values calculated from Equation (22-2). The straight line in Figure 22.2 indicates the fit of the data to Equation (22-2); the scatter band represents two standard deviations above and below the line. The variance of the data was assumed to be normally distributed and constant throughout the range of predicted values. For $CW = 0$, coefficients of Equation (22-2) are in satisfactory agreement with Equation (22-1). Figure 22.3 shows curves for three levels of *CW*, where $5 \leq [\mathrm{Sn}] \leq 11$ wt%, predicted from Equation (22-2). Also shown are data for corresponding amounts of *CW*.

Table 22.2. Dependence of Electrical Resistivity on [Sn] and Cold Work (295 K).

Electrical Resistivity, Measured, nΩ•m	Electrical Resistivity, Predicted, nΩ•m	[Sn], wt%	Cold Work, %	Reference No.
32.27	34.04	0.99	75.	2B
48.55	49.82	1.93	75.	2B
98.55	95.62	4.92	75.	2B
135.95	129.67	7.49	75.	2B
17.22	16.72	0.0	75.	4B
17.22	16.73	0.0007	75.	4B
17.24	16.75	0.0015	75.	4B
17.29	16.81	0.005	75.	4B
17.40	16.90	0.010	75.	4B
17.32	17.61	0.050	75.	4B
54.14	56.77	2.44	32.	7B
54.25	57.60	2.44	59.	7B
54.92	58.38	2.44	84.	7B
132.68	139.03	8.68	32.	7B
136.94	142.01	8.68	59.	7B
138.05	143.66	8.68	74.	7B
96.14	92.59	5.0	10.	8
96.36	93.31	5.0	20.	8
98.08	95.19	5.0	50.	8
99.96	95.83	5.0	60.	8
101.99	97.11	5.0	80.	8
102.21	97.72	5.0	90.	8
104.91	105.52	6.0	10.	8

Table 22.2, continued

Electrical Resistivity, Measured, nΩ•m	Electrical Resistivity, Predicted, nΩ•m	[Sn], wt%	Cold Work, %	Reference No.
106.08	106.38	9.0	20.	8
108.26	108.61	6.0	80.	8
108.20	106.38	6.0	60.	8
108.66	110.93	9.0	80.	8
109.21	111.64	9.0	60.	8
124.05	123.50	7.5	10.	8
125.49	124.62	7.5	20.	8
127.92	127.51	7.5	80.	8
128.74	106.38	7.5	60.	8
130.34	130.31	7.5	80.	8
131.35	131.22	7.5	60.	8
137.09	139.90	9.0	10.	8
139.33	141.14	9.0	20.	8
141.80	144.58	9.0	80.	8
143.23	145.67	9.0	60.	8
144.51	144.58	9.0	80.	8
145.88	106.38	9.0	60.	8
155.91	154.51	10.5	10.	8
159.88	156.01	10.5	20.	8
163.12	160.06	10.5	50.	8
162.96	161.23	10.5	60.	8
167.61	164.01	10.5	80.	8
167.97	165.22	10.5	90.	8

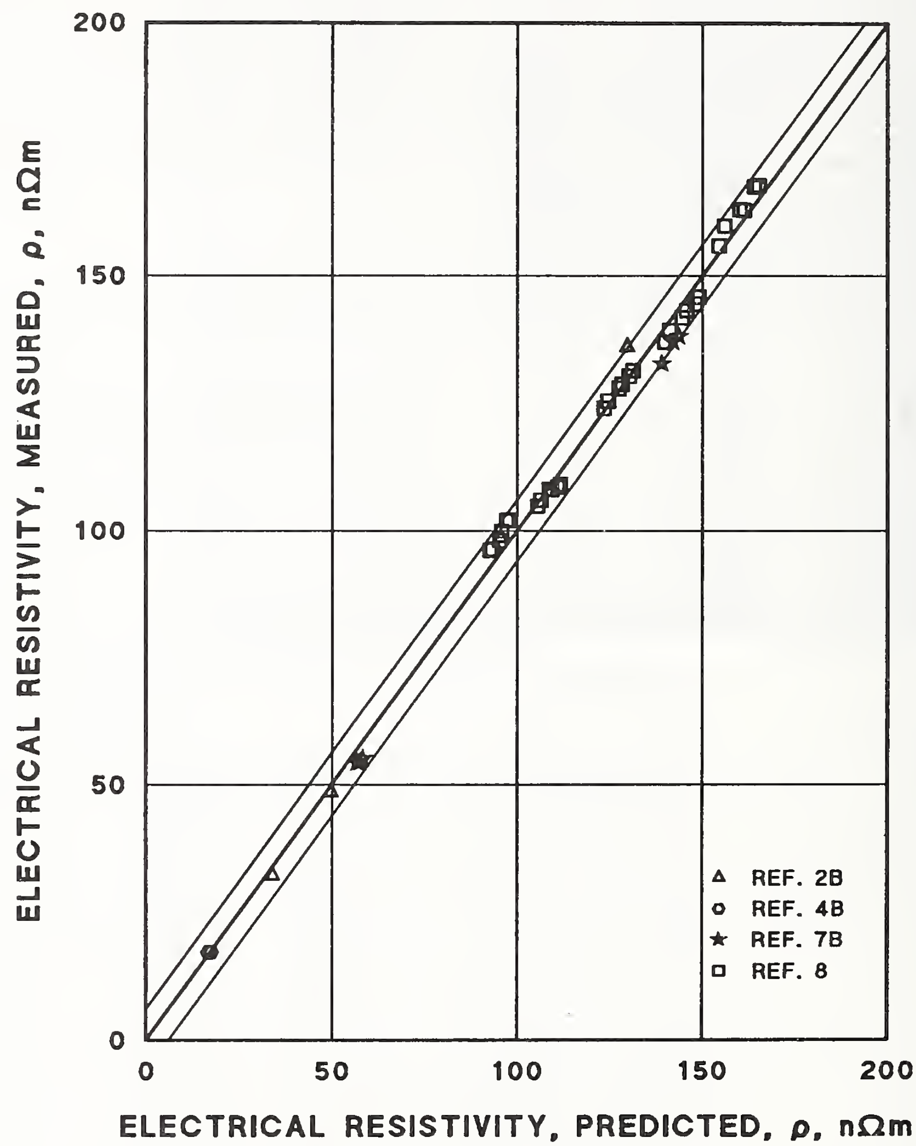

Figure 22.2. The data shown were used to compute the regression of electrical resistivity at 295 K upon cold work and Sn content [Equation (22-2)].

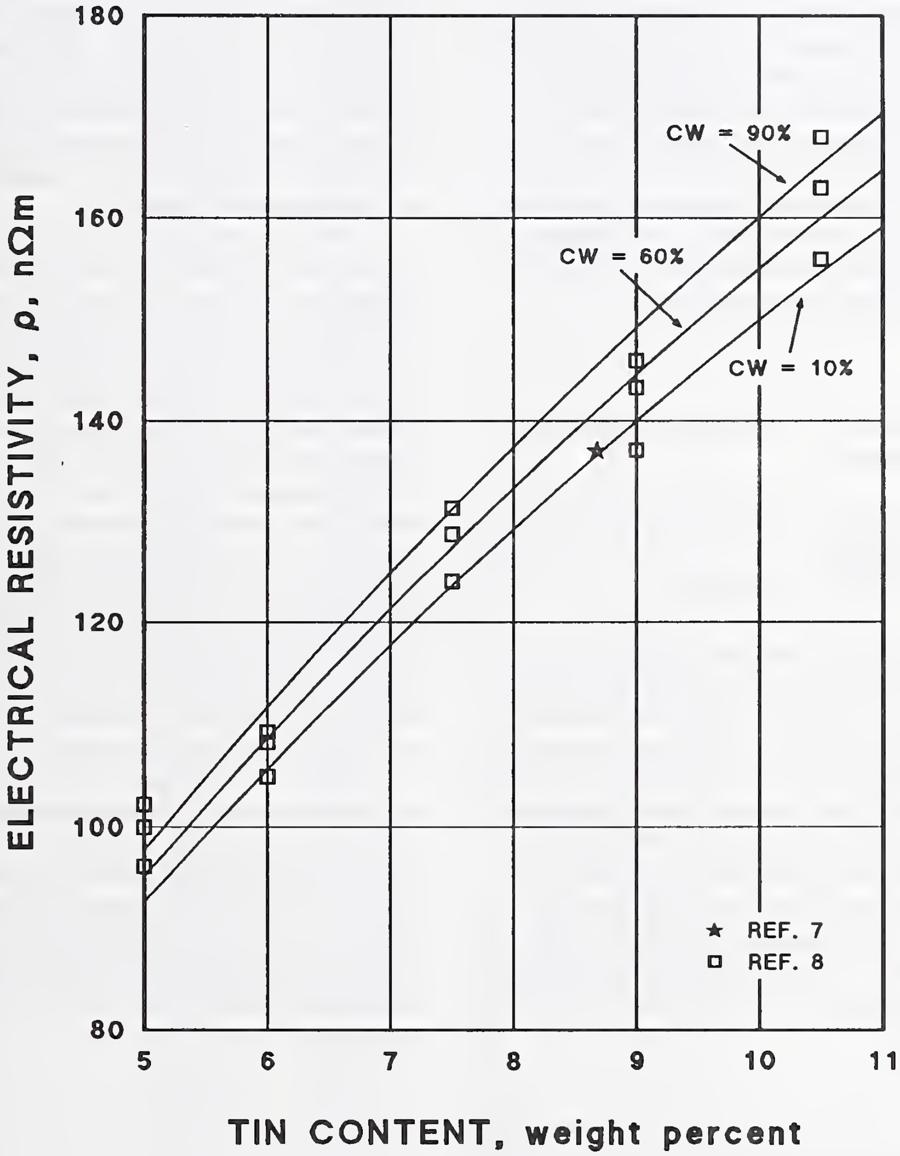

Figure 22.3. The dependence of electrical resistivity upon tin content is illustrated by three curves predicted from Equation (22-2), and data from Reference 22.8 for three levels of cold work.

DATA SOURCES AND ANALYSIS

Measurements of the resistivity (ρ) of annealed Cu-Sn alloys between 4 and 295 K were obtained from References 22.2, 22.3, 22.9, and 22.10. The form of the product was wire. The available characterization of specimens and measurements is presented in Table 22.10 at the end of the electromagnetic properties section. Multi-variate regression analysis was used to obtain an expression for the dependence of the resistivity upon Sn content, [Sn], and temperature, T. The dependence of resistivity upon phosphorus content can be estimated from Equation (22-1); no cryogenic data on annealed phosphorus-containing alloys were available.

RESULTS

A satisfactory fit to the data was obtained with the expression

$$\rho(\mathrm{n\Omega \cdot m}) = -4.513 + 17.96\,[\mathrm{Sn}] - 0.4930\,[\mathrm{Sn}]^2 + 0.07202\,T \quad (22\text{-}3)$$
$$(\mathrm{S.D.} = 2.564\ \mathrm{n\Omega \cdot m}),$$

where the standard deviations of the coefficients are 0.638, 0.34, 0.0334, and 0.00287, $[\mathrm{Sn}] \le 10.4$ wt%, and $4\ \mathrm{K} \le T \le 295\ \mathrm{K}$. Table 22.3 presents the measured values of ρ and the values calculated from Equation (22-3). The straight line in Figure 22.4 indicates the fit of the data to Equation (22-3); the scatter band represents two standard deviations above and below the line. The variance of the data was assumed to be normally distributed and constant throughout the range of predicted values. Figure 22.5 presents families of curves for several [Sn] values calculated from Equation (22-3).

DISCUSSION

The data from Reference 22.10 (at 4 K only) are not in agreement with measurements from other references (Figures 22.4 and 22.5). The wire used in these measurements was processed differently; annealed Cu wire was plated with Sn, which was allowed to dissolve in the wire in an Ar environment below 300 °C. The wire was then homogenized at 800 °C for 140 h. Perhaps the final product was less homogeneous that those used in the other reported measurements (References 22.2, 22.3, and 22.9), which were produced by more conventional methods. However, the diffusion method of alloying may be closer to production methods of Cu-Sn stabilizing material in superconducting cable.

Very dilute Cu-Sn alloys exhibit a minimum in the electrical resistivity at temperatures of about 15 K or less. The effect is most pronounced for $[\mathrm{Sn}] \approx 0.01$ wt% and declines sharply at higher [Sn]. This resistivity minimum is observed only in very pure dilute Cu-Sn alloys, since contamination of as little as 0.002 wt% of Fe can obscure the effect. Experiments have indicated that the phenomenon is due to some type of preferential distribution of the Sn atoms in the interstices of misfit along the grain boundaries (Reference 22.11). Additional discussion of this phenomenon is presented in Reference 22.12. Because this phenomenon is observable only in dilute, high-purity alloys, it is not demonstrable with the present set of measurements and thus is not reflected in Equation (22-3).

At 295 K, Equations (22-3) and (22-1) are very similar, and coefficients generally agree within one or two standard deviations. Exact agreement of the coefficients to like terms, such as $[\mathrm{Sn}]^2$, should not be expected because the 295-K data sets used in the two equations were not identical. Obviously, the negative values for ρ predicted at low temperatures for [Sn] = 0 are not correct.

C50100–C52400: Annealed

Electrical Resistivity vs. [Sn]
Temperature (4–295 K)

Table 22.3. Dependence of Electrical Resistivity on [Sn] and Temperature (4–295 K).

Electrical Resistivity, Measured, nΩ•m	Electrical Resistivity, Predicted, nΩ•m	[Sn], wt%	Test Temperature, K	Reference No.
0.45	-3.52	0.0	14.3	2A
0.26	-3.08	0.0	20.4	2A
1.40	-0.08	0.0	63.5	2A
2.30	1.90	0.0	77.3	2A
3.10	1.90	0.0	90.2	2A
17.16	16.52	0.0	295.0	2A
10.50	19.36	0.99	14.3	2A
14.97	14.25	0.99	20.4	2A
16.41	17.28	0.99	63.5	2A
17.56	18.30	0.93	77.3	2A
18.50	19.16	0.99	90.2	2A
20.08	20.70	0.99	111.6	2A
24.09	24.84	0.99	169.5	2A
31.25	32.82	0.99	273.2	2A
33.28	34.04	0.99	295.0	2A
29.94	20.76	1.93	20.4	2A
31.74	32.82	0.99	63.5	2A
32.54	-3.68	1.93	77.3	2A
33.38	34.76	0.99	90.2	2A
39.48	40.51	1.93	169.5	2A
46.78	47.92	0.99	273.2	2A
75.06	73.46	4.92	20.4	2A
77.03	76.49	4.92	63.5	2A
78.90	77.52	4.92	77.3	2A
78.90	78.46	4.92	90.2	2A
80.96	80.01	4.92	111.6	2A
85.35	84.11	4.92	169.5	2A
93.71	91.67	4.92	273.2	2A
95.73	93.38	4.92	295.0	2A
105.26	103.83	7.49	20.4	2A
107.59	106.91	7.49	63.5	2A
108.72	107.94	7.49	77.3	2A
109.64	108.83	7.49	90.2	2A
111.75	110.42	7.49	111.6	2A
116.76	114.56	7.49	169.5	2A
125.73	122.07	7.49	273.2	2A
127.93	123.82	7.49	295.0	2A
129.75	130.44	10.4	20.4	2A
132.63	133.47	10.4	63.5	2A
133.91	134.56	10.4	77.3	2A
134.88	135.43	10.4	90.2	2A
142.48	141.18	10.4	169.5	2A
152.36	148.57	10.4	273.2	2A
17.7	16.73	0.0	295.	3
20.5	20.13	0.19	295.	3
31.7	33.01	0.93	295.	3
51.0	50.68	2.00	295.	3
59.5	62.69	2.77	295.	3
101.2	100.08	5.46	295.	3
0.133	-4.23	0.0	4.0	3
2.95	-0.83	0.19	4.0	3

Table 22.3, continued

Electrical Resistivity, Measured, nΩ•m	Electrical Resistivity, Predicted, nΩ•m	[Sn], wt%	Test Temperature, K	Reference No.
13.9	12.05	0.93	4.0	9
30.4	29.72	2.00	4.0	3
40.5	41.73	2.77	4.0	9
79.1	79.12	5.46	4.0	3
42.75	45.06	1.65	295.55	9
41.06	43.45	1.65	273.15	9
38.91	41.29	1.65	243.15	9
37.24	39.47	1.65	217.95	9
35.48	37.61	1.65	192.15	9
33.94	36.05	1.65	170.45	9
32.58	34.74	1.65	152.25	9
31.10	33.18	1.65	130.65	9
29.72	31.81	1.65	111.55	9
28.07	30.32	1.65	90.85	9
0.13	-4.21	0.0	4.2	10
0.32	0.25	0.25	4.[illegible]	10
1.60	3.77	0.45	4.[illegible]	10
14.	16.62	1.20	4.[illegible]	10
37.	32.90	2.20	4.2	10
32.	39.91	2.65	4.2	10
120.	130.74	10.60	4.2	10

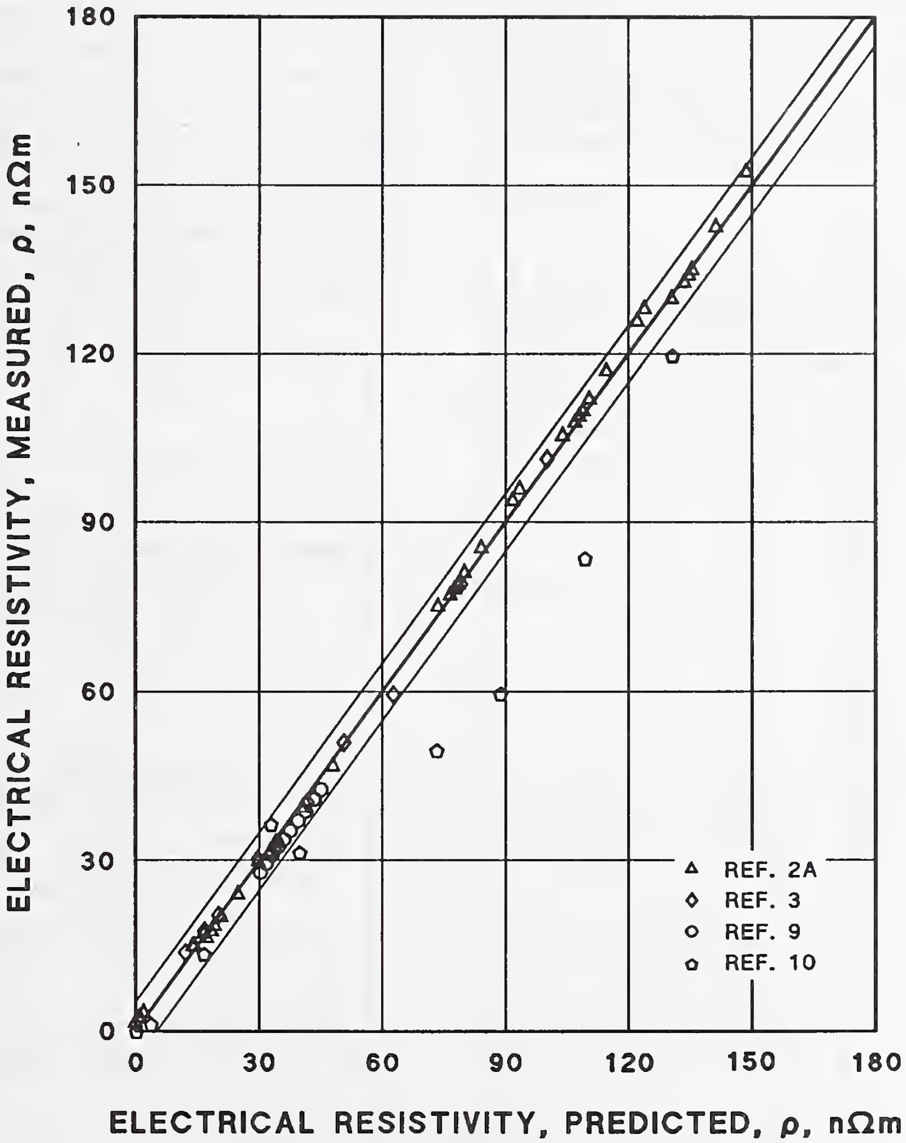

Figure 22.4. The data shown were used to compute the regression of electrical resistivity of annealed material upon Sn content and temperature [Equation (22-3)].

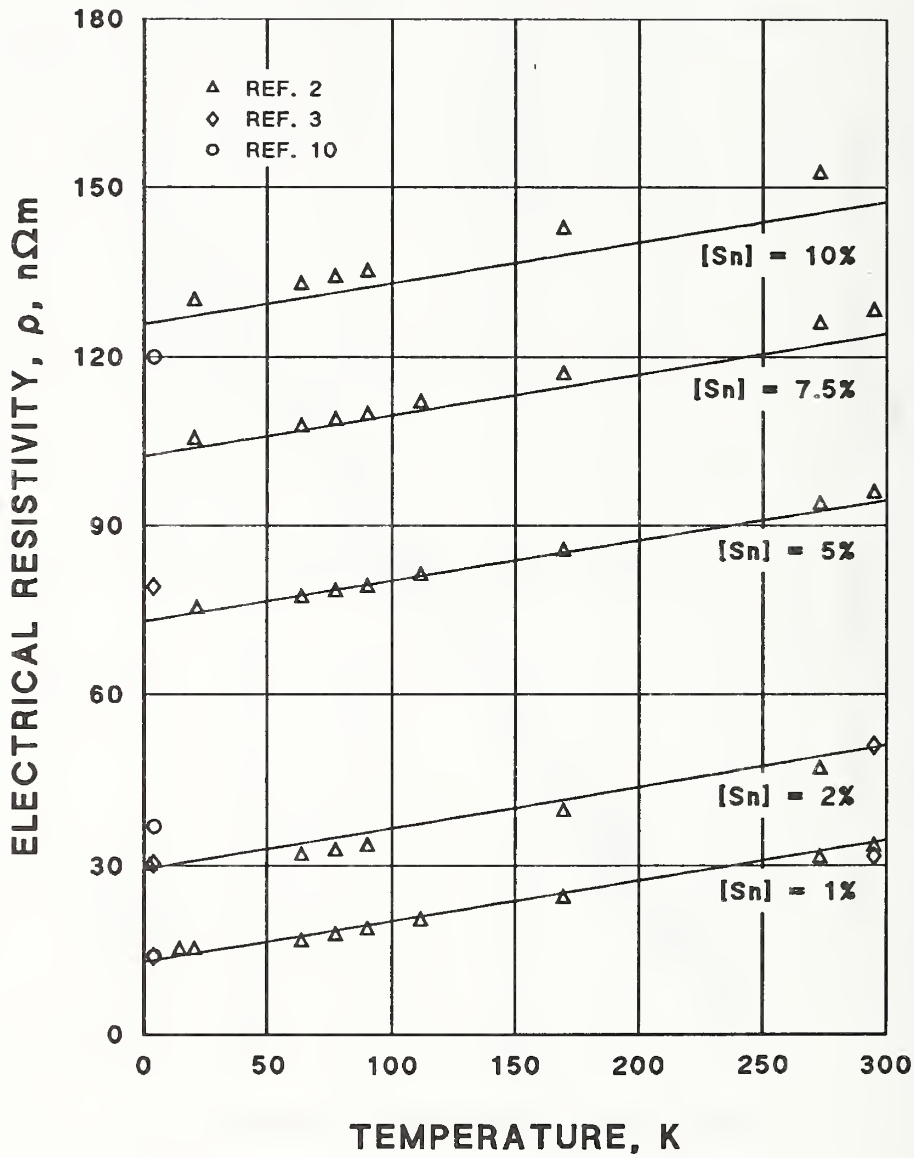

Figure 22.5. The curves for constant Sn content, [Sn], were calculated from Equation (22-3).

DATA SOURCES AND ANALYSIS

Measurements of the resistivity (ρ) of 75% cold-drawn Cu-Sn alloys between 14 and 295 K were obtained from Reference 22.2. The resistivity of an 85% cold-drawn C51000 phosphor bronze was obtained from Reference 22.13. The form of the product was wire (Reference 22.2) or bar or plate (Reference 22.13). The available characterization of materials and measurements is given in Table 22.10 at the end of the electromagnetic properties section. Multivariate regression analysis was used to obtain an expression for the dependence of the resistivity upon Sn content, [Sn], cold work, *CW*, and temperature, *T*. Since the effect of cold work is larger as [Sn] increases, cross-terms were used in this analysis.

RESULTS

A satisfactory fit to the data was obtained with

$$\rho(\mathrm{n\Omega{\cdot}m}) = -92.50 + 17.72\,[\mathrm{Sn}] - 0.3198\,[\mathrm{Sn}]^2 + 0.07430\,T + 1.146\,CW + 0.001793\,[\mathrm{Sn}]\cdot T, \quad (\mathrm{S.D.} = 2.20\ \mathrm{n\Omega{\cdot}m}), \tag{22-4}$$

where the standard deviations of the coefficients are 8.52, 0.38, 0.0337, 0.00564, 0.114, and 0.001063, $[\mathrm{Sn}] \le 10.4$ wt%, and $4\ \mathrm{K} \le T \le 295\ \mathrm{K}$. Table 22.4 presents the measured values of ρ and the values calculated from Equation (22-4). The straight line in Figure 22.6 indicates the fit of the data to Equation (22-4); the scatter band represents two standard deviations above and below the line. The variance of the data was assumed to be normally distributed and constant throughout the range of predicted values.

DISCUSSION

For T = 295 K and CW = 75%, the first five terms of Equation (22-4) are in agreement with the first three terms of Equation (22-2). However, the analysis of the dependence of ρ upon *CW*, [Sn], and *T* is based mostly upon results from one reference for a limited range of *CW* (75-85%); thus, Equation (22-4) should be used with caution.

Table 22.4. Dependence of Electrical Resistivity on [Sn], Cold Work, and Temperature (4–295 K).

Electrical Resistivity, Measured, nΩ•m	Electrical Resistivity, Predicted, nΩ•m	[Sn], wt%	Test Temperature, K	Cold Work, %	Reference No.
0.16	-5.01	0.0	20.4	75.	2B
1.25	-1.85	0.0	63.5	75.	2B
2.01	-0.76	0.0	77.3	75.	2B
3.01	0.10	0.0	90.2	75.	2B
8.38	6.03	0.0	169.5	75.	2B
15.99	13.68	0.0	273.2	75.	2B
10.03	12.25	0.99	20.4	75.	2B
13.72	15.50	0.99	63.5	75.	2B
14.85	16.56	0.99	77.3	75.	2B
16.47	17.55	0.99	90.2	75.	2B
23.15	23.60	0.99	169.5	75.	2B
30.53	31.47	0.99	273.2	75.	2B
32.27	33.31	0.99	295.0	75.	2B
22.60	28.05	1.93	20.4	75.	2B
27.83	31.42	1.93	63.5	75.	2B
29.72	32.50	1.93	77.3	75.	2B
31.21	33.48	1.93	90.2	75.	2B
33.34	35.16	1.93	111.6	75.	2B

Table 22.4, continued

Electrical Resistivity, Measured, nΩ·m	Electrical Resistivity, Predicted, nΩ·m	[Sn], wt%	Test Temperature, K	Cold Work, %	Reference No.
38.57	39.68	1.93	169.5	75.	28
46.40	47.61	1.93	273.2	75.	28
48.55	49.58	1.93	295.0	75.	28
74.06	74.52	4.92	20.4	75.	28
77.37	78.20	4.92	63.5	75.	28
78.81	79.35	4.92	77.3	75.	28
80.42	80.29	4.92	90.2	75.	28
82.51	82.20	4.92	111.6	75.	28
87.99	86.91	4.92	169.5	75.	28
96.20	95.50	4.92	273.2	75.	28
98.55	97.61	4.92	295.0	75.	28
113.5	109.9	7.49	20.4	75.	28
115.7	113.6	7.49	63.5	75.	28
116.7	115.0	7.49	77.3	75.	28
117.9	116.1	7.49	90.2	75.	28
120.3	118.0	7.49	111.6	75.	28
125.1	123.1	7.49	169.5	75.	28
133.8	132.1	7.49	273.2	75.	28
136.0	134.3	7.49	295.0	75.	28
144.9	145.1	10.4	20.4	75.	28
147.2	149.0	10.4	63.5	75.	28
148.7	150.4	10.4	77.3	75.	28
149.9	151.5	10.4	90.2	75.	28
157.5	158.9	10.4	169.5	75.	28
167.0	168.5	10.4	273.2	75.	28
104.8	106.0	4.85	273.0	85.	13
98.3	99.31	4.85	192.4	85.	13
88.8	89.63	4.85	75.75	85.	13
85.8	84.98	4.85	19.65	85.	13
85.9	83.68	4.85	4.0	85.	13

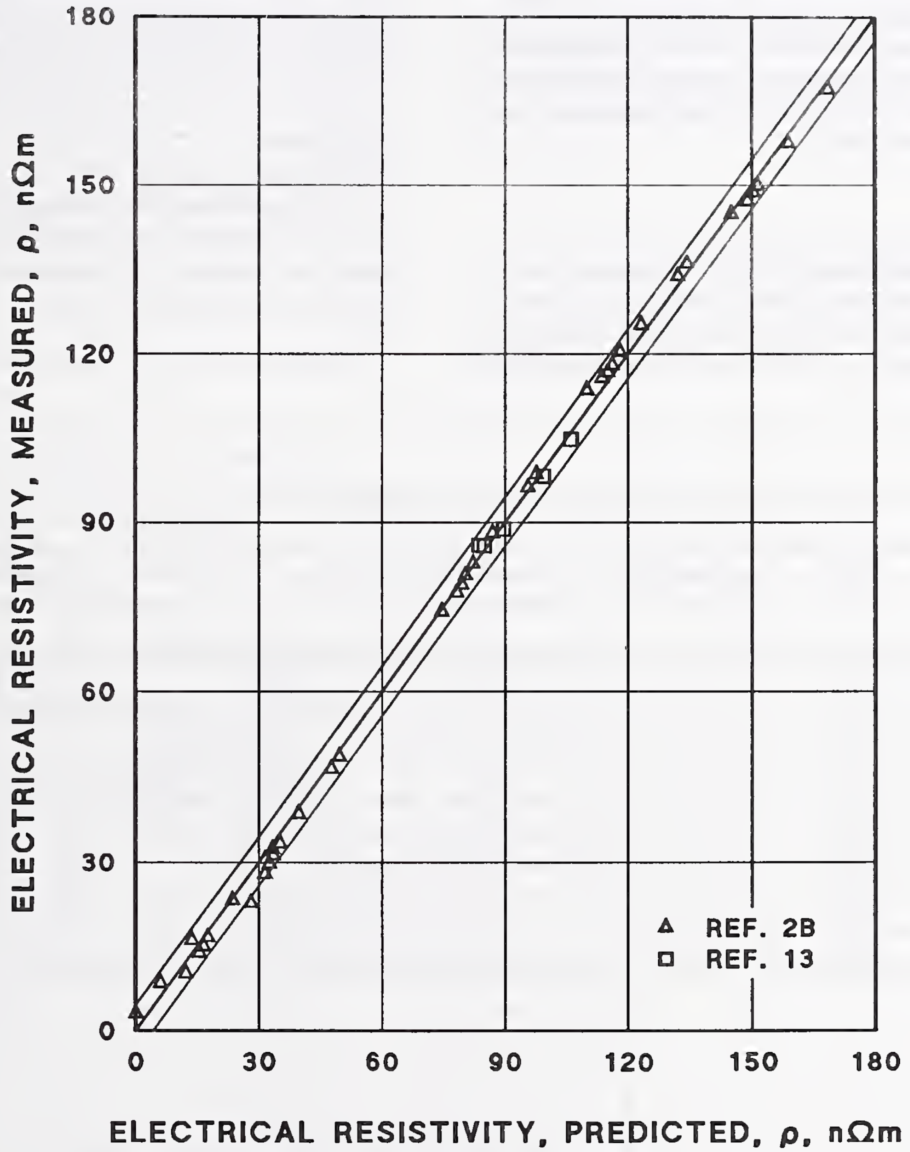

Figure 22.6. The data shown were used to compute the regression of electrical resistivity upon Sn content, cold work, and temperature [Equation (22-4)].

DATA SOURCES

Measurements at both 295 and 4 K of the magnetoresistance of Cu-Sn alloys at 9 T were obtained from Reference 22.3; similar measurements at 4 K on a C51000 phosphor bronze at 14 T were obtained from Reference 22.14. The form of the product was wire. The available characterization of materials and measurements is given in Table 22.10 at the end of the electromagnetic properties section.

RESULTS

The application of a 9-T field resulted in a resistance change of <1% at both 295 and 4 K, except for the 0.19 wt% Sn alloy tested, which gave an increase of 4.6% at 4 K (Reference 22.3). However, the authors suspected that there were small regions of precipitated elemental tin in this alloy, because magnetic susceptibility results on the alloy were also anomalous, compared to other alloys in the series. The application of a 14-T field to several specimens of a C51000 phosphor bronze at 4 K resulted in a resistance change of less than 0.01%, as shown in Table 22.5 below.

DISCUSSION

The higher residual resistivity, ρ_0, of specimens reported on in Reference 22.14, probably reflects the presence of impurities, or differences in annealing procedures or the amount of cold work.

Table 22.5. Magnetoresistance (Resistivity Change) between 0 and 9 or 14 T (4 K).

Specimen No.	[Sn], wt%	Magnetic Flux Density, T	Residual Resistivity, nΩm	$\Delta\rho/\rho_0$	Test Temperature, K	Reference No.
1	0.19	9	2.95	0.046	4	3
2	0.93	9	13.9	<0.01	4, 295	3
3	2.00	9	30.4	<0.01	4, 295	3
4	2.77	9	40.5	<0.01	4, 295	3
5	5.46	9	79.1	<0.01	4, 295	3
1	0.95	14	126	(5 ± 1) ×	4	14
2, Run 1	0.95	14	126	(6 ± 2) × 10	4	14
2, Run 2	0.95	14	136	(7 ± 2) × 10	4	14
3	0.95	14	135	(4 ± 2) × 10	4	14

DATA SOURCES AND ANALYSIS

Measurements of the magnetic susceptibility at 295 K on annealed Cu-Sn alloys were obtained from References 22.3, 22.15, and 22.16. The susceptibility, in SI units, is defined as $\kappa = M/H$ (dimensionless) where H is the applied field and M is the magnetization (both in A/m). The mass susceptibility (κ_ρ) has SI units of m^3/kg. The available characterization of materials and measurements is given in Table 22.10 at the end of the electromagnetic properties section. A polynomial regression analysis of κ_ρ as a function of Sn content, [Sn], was carried out on the data.

RESULTS

A satisfactory fit to the data was obtained with the equation

$$\kappa_\rho = -10.59 - 0.5368\,[Sn] + 0.01386\,[Sn]^2 \qquad (22\text{-}5)$$

$$(S.D. = 0.15\ m^3/kg),$$

where the standard deviations of the coefficients are 0.08, 0.0440, and 0.00452, and $[Sn] \leq 9.2$ wt%. Table 22.6 gives the measured κ_ρ and the values calculated from Equation (22-5). The straight line in Figure 22.7 indicates the fit of the data to Equation (22-5); the scatter band represents two standard deviations above and below the line. The variance of the data was assumed to be normally distributed and constant throughout the range of predicted values.

DISCUSSION

The data from the three references are in reasonable agreement with each other. Methods of correcting data for ferromagnetic iron impurities are discussed in Reference 22.16 and citations therein.

Table 22.6. Dependence of Magnetic Susceptibility on [Sn] (295 K)

Magnetic Susceptibility, Measured, 10^{-10} m^3/kg	Magnetic Susceptibility, Predicted, 10^{-10} m^3/kg	[Sn], wt%	Reference No.
−10.25	−10.59	0.0	3
−12.69	−10.69	0.19	3
−14.45	−11.07	0.93	3
−11.75	−10.69	2.00	3
−12.07	−11.97	2.77	3
−13.11	−13.11	5.46	3
−10.56	−10.59	0.0	15
−12.69	−12.78	4.65	15
−14.45	−14.46	9.60	15
−11.55	−11.53	4.65	16
−12.25	−12.32	9.60	15
−12.73	−12.82	0.19	16
−14.41	−14.36	9.21	16

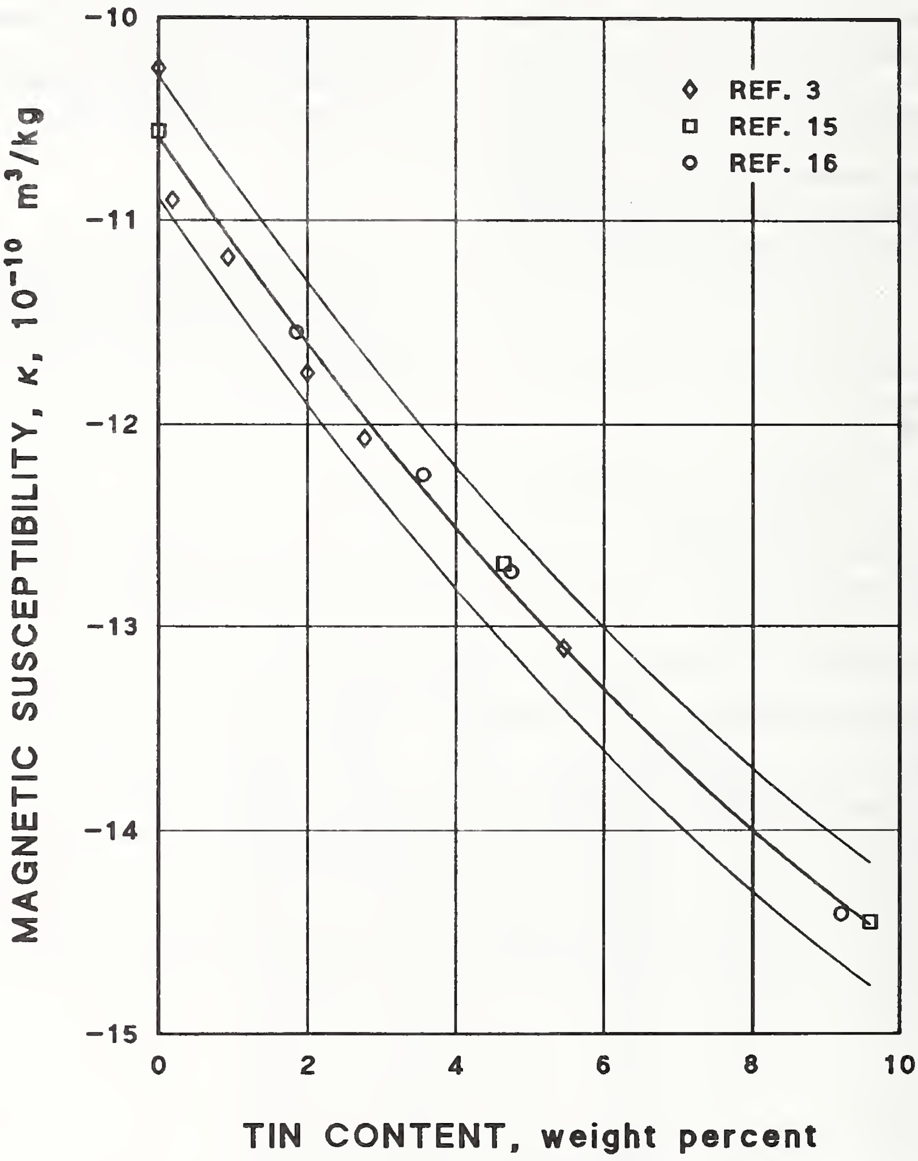

Figure 22.7. The data shown were used to compute the regression of magnetic susceptibility upon Sn content. The curve is fit to Equation (22-5) for the range of Sn contents shown.

DATA SOURCE

Measurements of the mass magnetic susceptibility (κ_ρ) at 295 K as a function of Fe content, [Fe], were obtained from Reference 22.17. The measurements were made on cast C51000 phosphor bronze that had been either cold-rolled or cold-rolled and subsequently annealed . The available characterization of materials and measurements is given in Table 22.10 at the end of the electromagnetic properties section.

RESULTS

Table 22.7 and Figure 22.8 present the increase in absolute magnitude of susceptibility as [Fe] is increased from about 0 to 0.3 wt%.

DISCUSSION

For most phosphor bronze alloys, specifications require [Fe] $\leq$ 0.010 wt%, and in practice, [Fe] is often much lower. However, these measurements show that κ_ρ could vary considerably within phosphor bronze specifications. The results agree approximately with those of Section 8 for the change of κ with addition of Fe to high-purity copper.

Table 22.7. Dependence of Magnetic Susceptibility on [Fe] and Material Condition (295 K).

Material Condition	[Fe], wt%	Magnetic Susceptibility, 10^{-10} m^3/kg
Annealed	0.01	0.0
Annealed	0.15	–16
Annealed	0.15	–26
Annealed	0.20	–31
Annealed	0.25	–36
Annealed	0.30	–43
Cold-rolled 50%	0.01	0.0
Cold-rolled 50%	0.10	–11
Cold-rolled 50%	0.15	–21
Cold-rolled 50%	0.20	–31
Cold-rolled 50%	0.25	–39
Cold-rolled 50%	0.30	–45

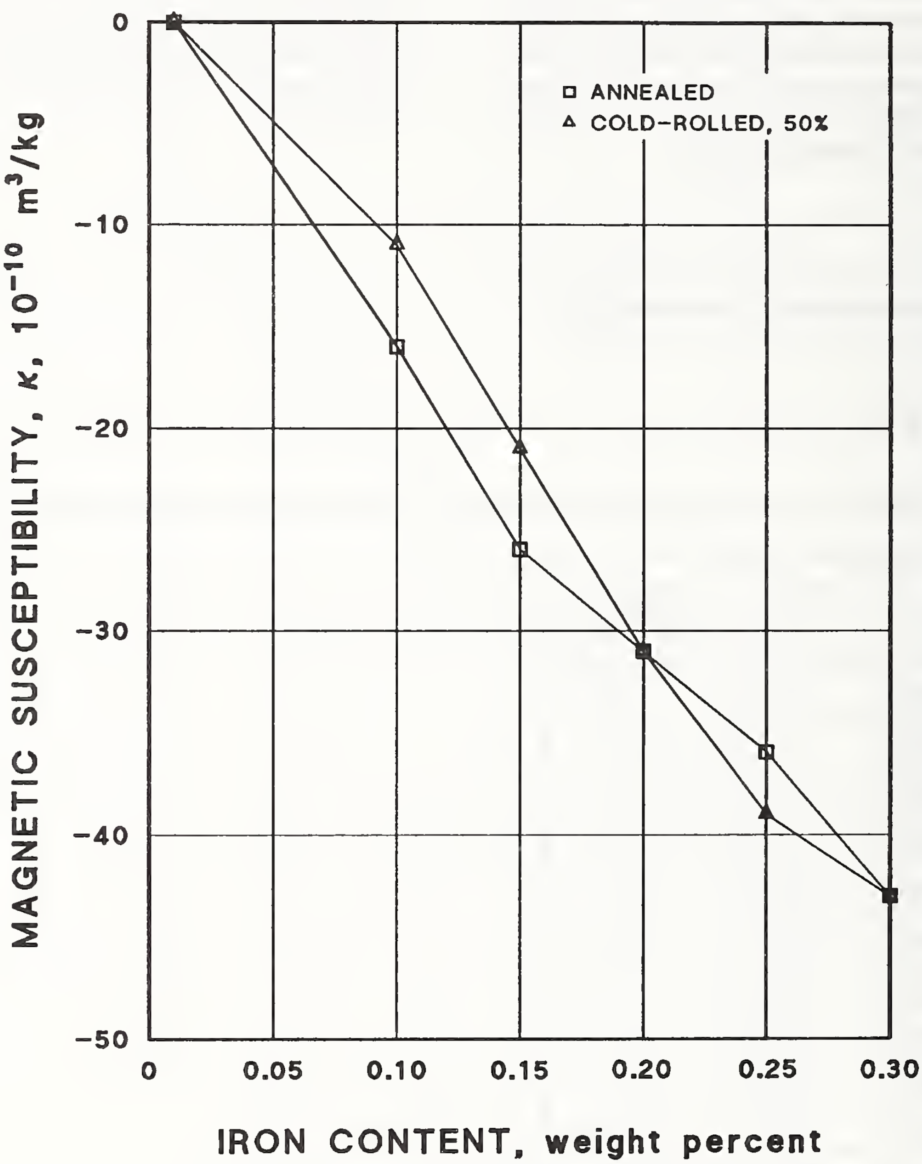

Figure 22.8. Data from Reference 22.17 show the change in magnetic susceptibility with Fe content. The cast product was rolled and then annealed.

C51000: Annealed; Cold-worked

Magnetic Susceptibility vs. Cold Work (295 K)

DATA SOURCE

Mass magnetic susceptibility (κ_ρ) measurements at 295 K on a C51000 phosphor bronze in both the annealed and cold-worked conditions were obtained from Reference 22.18. The cold-worked material was drawn to 16%. The Sn content obtained from chemical analysis was slightly above the C51000 specification, although the specimens were described as commercial, 5 wt% Sn. No attempt was made by the authors of Reference 22.18 to vary the Fe content, since the intention was to test typical alloys as they were being processed in the mill. However, Fe content was low, 0.003 wt%. The form of the product was not specified. The available characterization of materials and measurements is given in Table 22.10 at the end of the electromagnetic properties section.

RESULTS

Table 22.8 shows that the absolute value of the susceptibility of cold-worked C51000 decreases after it is annealed.

DISCUSSION

The magnetic susceptibility depends on both the amount of Fe present and its chemical form and distribution. Since the thermal and mechanical history of the specimen and the presence of other impurities affect Fe chemistry and distribution, these factors can alter κ_ρ significantly. Therefore, these values may not apply to all C51000 phosphor bronzes.

Table 22.8. Magnetic Susceptibility of Annealed and Cold-worked C51000 (295 K).

Magnetic Susceptibility, 10^{-10} m^3/kg	Material Condition	Reference No.
–15.	Annealed	18
–20.	Cold-drawn 16%	18

DATA SOURCE

Measurements of the mass magnetic susceptibility (κ_ρ) at 4 K as a function of Sn content, [Sn], were obtained from Reference 22.3 on annealed Cu-Sn alloys. The available characterization of materials and measurements is given in Table 22.10 at the end of the electromagnetic properties section.

RESULTS

Table 22.9 and Figure 22.9 present the increase in absolute magnitude of susceptibility with [Sn].

Table 22.9. Dependence of the Magnetic Susceptibility on [Sn] (4 K).

[Sn], wt%	Magnetic Susceptibility, 10^{-10} m^3/kg	Reference No.
0.0	−8.55	3
0.93	−10.15	3
2.00	−10.30	3
2.77	−11.50	3
5.46	−11.02	3

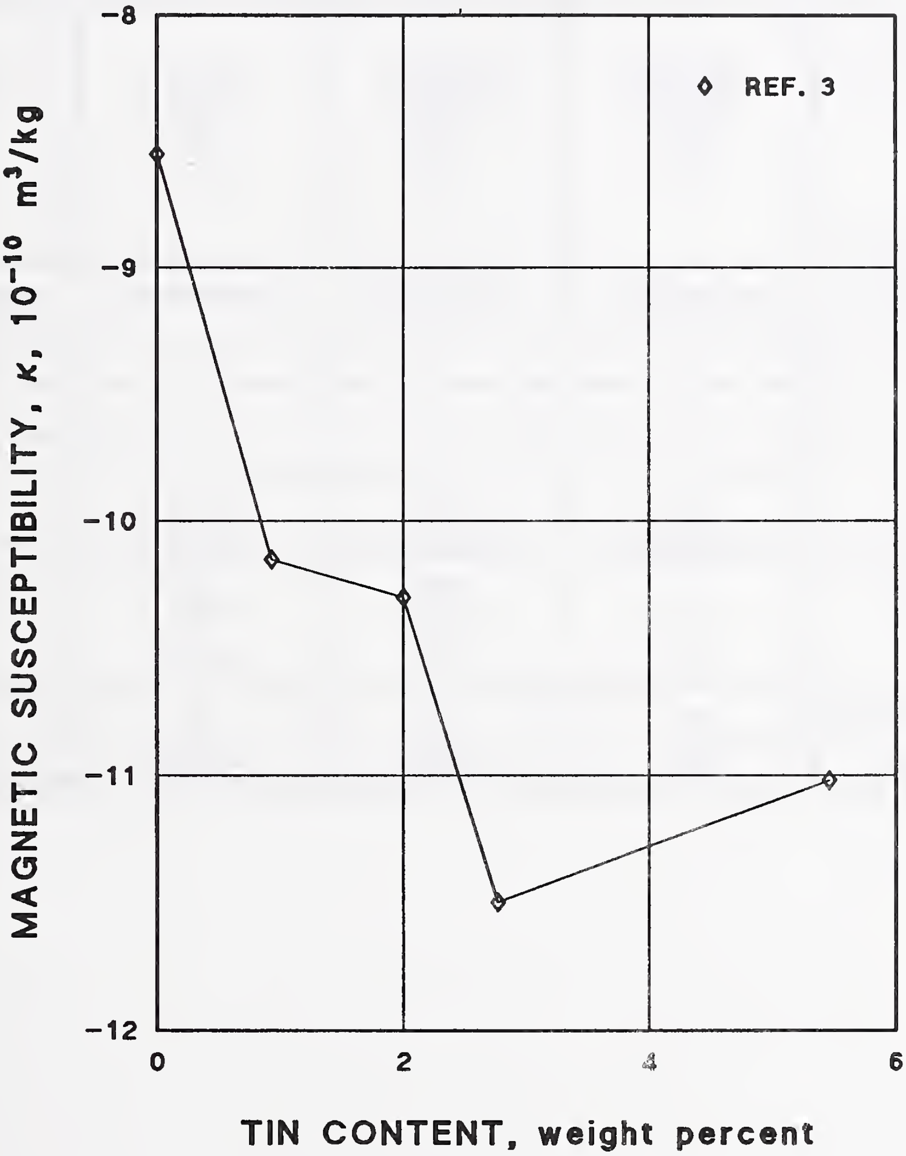

Figure 22.9. Data from Reference 22.3 show the change in magnetic susceptibility with Sn content. Data are on annealed material.

Tables 22.10. Charaterization and Materials and Measurements.

Reference No.	—	2A	2B	3
Specification	—	—	—	—
Composition (wt%)				
Cu	89.52–99.00	—	—	—
Sn	0.99–10.40	0.00–10.4	0.00–10.4	0.00–5.46
P	0.002–0.33	≤0.06	≤0.06	—
Pb	0.00–0.04	≤0.05	≤0.05	—
Fe	0.01–0.05	≤0.01	≤0.01	—
Zn	—	—	—	—
Others (Only ≥ 0.001 wt%)	—	—	—	—
Material Condition	Annealed, 923 K, 0.5 h, AC	Annealed, 973 K, 1 h, WQ	Cold-drawn, 75%	Annealed, 873 K, FC
RRR	—	—	—	1.28–133
Grain Size	—	—	—	—
Hardness	—	—	—	—
Product Form	Bar, 2.22-cm-dia.	Wire, 0.10-cm-dia.	Wire, 0.10-cm-dia.	Wire, 0.11-cm-dia.
Specimen Type	—	Wire	Wire	Wire
Width or Dia.	—	0.10 cm	0.10 cm	0.11 cm
Thickness	—	—	—	—
Gage Length	—	7.62 cm	7.62 cm	20 cm
No. of Measurements	6	6	6	6
Test Temperature	293 K	4.2–295 K	4.2–295 K	4, 295 K

4A	4B	5	6	7A
—	—	—	—	—
— 0.000–0.050 — — — — —	— 0.000–0.050 — — — — —	99.85–99.95 0.016–0.133 — 0.018–0.021 — — O: 0.028–0.040	— 1.00–3.88 — — — — —	97.40 and 91.15 2.44 and 8.68 — — — — —
Annealed, 873 K, 1 h, quenched	Cold-drawn, 75%	Annealed, 648 K	Annealed, 973 K	Annealed, 798 K, 1 h, AC
—	—	—	—	—
—	—	—	—	—
—	—	—	—	—
Wire, 0.206-cm-dia.	Wire, 0.206-cm-dia.	Wire, 0.102-cm-dia.	Wire, 0.25-cm-dia.	Bar, 0.518-cm-dia.
Wire 0.206 cm — —	Wire 0.206 cm — —	Wire 0.102 cm — —	Wire 0.25 cm — 100 cm	Cylinder 0.518 cm — —
6	6	4	4	2
295 K	295 K	293 K	289 K	295 K

Table 22.10, continued

Reference No.	7B	8	9	10
Specification	—	—	—	—
Composition (wt%)				
Cu	97.40 and 91.15	—	—	—
Sn	2.44 and 8.68	5–10.5	1.65	0.0–10.6
P	—	—	—	—
Pb	—	—	—	—
Fe	—	—	—	—
Zn	—	—	—	—
Others (Only ≥ 0.001 wt%)	—	—	—	—
Material Condition	Cold-drawn, 32–84%	Cold-worked, 9–90%	Annealed, 1023 K	Homogenized, 1073 K, 140 h (a)
RRR	—	—	—	—
Grain Size	—	—	—	—
Hardness	—	—	—	—
Product Form	Wire, 0.21–0.43-cm-dia.	—	—	Wire 0.025-cm-dia.
Specimen Type	Wire	—	—	Wire
Width or Dia.	—	—	—	0.025 cm
Thickness	—	—	—	—
Gage Length	—	—	—	4.5 cm
No. of Measurements	5	30	10	10
Test Temperature	295 K	295 K	91–295 K	4.2 K

(a) Copper wire plated with tin, then homogenized to allow the tin to completely diffuse in the copper.

13	14	15	16	17
C51000	C51000	—	—	C51000
~94 4.85 0.18 <0.1 <0.1 <0.1 —	95 5 — — — — —	90.40–100.00 0.00–9.60 — — — — —	— 1.85–9.21 — — — — —	94.6 4.6 0.36 — 0.01–0.30 — —
Cold-drawn, 85%	Annealed	Annealed, 1173 or 1073 K, 10 h	Annealed, 823 K, 504 h, WQ (a)	Annealed, 773 K, 24 h; or cold-rolled, 50%
—	—	—	—	—
100 μm	—	—	—	—
R_B 91	—	—	—	—
Bar	Wire, 1.27- and 2.03-cm-dia.	Bar, 0.6-cm-dia.	—	Strip, 0.508-cm-thick
Cylinder 0.635 cm — 10.0 cm	Wire 1.27 and 2.03 cm — —	Cylinder 0.6 cm — 10 cm	— — — —	Disk 1.27 cm 0.508 cm —
5	—	—	—	12
4.0–273 K	4.2 K	295 K	295 K	295 K

(a) Quenched in ice water.

Table 22.10, continued

Reference No.	18
Specification	C51000
Composition (wt%)	
Cu	93.83
Sn	5.94
P	0.23
Pb	<0.01
Fe	0.003
Zn	<0.01
Others (Only ≥ 0.001 wt%)	—
Material Condition	Annealed, 867 K, 2 h; or cold-rolled, 16%
RRR	—
Grain Size	2
Hardness	R_B 31 or 73
Product Form	Bar, 1.43-cm-dia.
Specimen Type	Cylinder
Width or Dia.	—
Thickness	—
Gage Length	—
No. of Measurements	2
Test Temperature	295 K

REFERENCES

1. Smith, C. S., "Thermal Conductivity of Copper Alloys. II. Copper-Tin Alloys. III. Copper-Phosphorus Alloys," Transactions of the A.I.M.E. 93, 176–184 (1931).

2. Fairbank, H. A., "The Electrical Resistivity of Copper-Zinc and Copper-Tin Alloys at Low Temperatures," Physical Review 66, 274–281 (1944).

3. Fickett, F. R., "Electric and Magnetic Properties of CuSn and CuNi Alloys at 4 K, "Cryogenics 22, 135–137 (1982).

4. Smart, J. S., Jr., and Smith, A. A., Jr., "Effect of Certain Fifth-period Elements on Some Properties of High-purity Copper," Transactions of the A.I.M.E. 152, 103–121 (1943).

5. Pilling, N. B., Bayonne, N. J., and Halliwell, G. P., "The Effect of Lead and Tin with Oxygen on the Conductivity and Ductility of Copper," Transactions of the A.I.M.E. 73, 679–699 (1926).

REFERENCES

6. Norbury, A. L., "Note on the Effects of Certain Elements on the Electrical Resistivity of Copper," Journal of the Institute of Metals 33, 91–94 (1925).

7. Crampton, D. K., Burghoff, H. L., and Stacy, J. T., "Effect of Cold-work upon Electrical Conductivity of Copper Alloys," Transactions of the A.I.M.E. 143, 228–245 (1941).

8. Haase, C., and Pawiek, F., "Zur Kenntnis der Kupfer-Zinnlegierungen," Zeitschrift für Metallkunde 28, 73–80 (1936).

9. Linde, J. O., Elektrische Eigenschaften verdünnter Mischkristallegierungen. III. Widerstand von Kupfer- und Goldlegierungen Gesetzmäßigkeiten der Widerstandserhöhungen," Annalen der Physik 15, 219–251 (1932).

10. Cogan, S. F., and Rose, R. M., "Properties of CuSn Bronze at 4.2 K," Cryogenics 20, 313–315 (1980).

11. Pearson, W. B., Rimek, D. M., and Templeton, I. M., "The Resistance Minimum in Dilute Alloys of Tin in Copper," Philosophical Magazine 4, 612–621 (1959).

12. Knook, B., and Van den Berg, G. J., "The Influence of Unpaired Spins in Transition Elements on the Resistivity of Cu, Ag, and Au," in Proceedings of the Eighth International Conference on Low Temperature Physics, Ed., R. O. Davies, Butterworths, Washington, 239–240 (1963).

13. Clark, A. F., Childs, G. E., and Wallace, G. H., "Electrical Resistivity of Some Engineering Alloys at Low Temperatures," Cryogenics 10, 295–305 (1970).

14. Feldman, R., Talley, L., Rojeski, M., Vold, T., and Woollam, J. A., "Upper Limit for Magnetoresistance in Silicon Bronze and Phosphor Bronze Wire," Cryogenics 17, 31–32 (1977).

15. Endo, H., "On the Relation between the Equilibrium Diagram and the Magnetic Susceptibility in Binary Alloys," Science Reports of the Research Institute of Tohoku University--Physics, Chemistry, and Metallurgy 14, 479–513 (1925).

16. Henry, W. G., and Rogers, J. L., "The Magnetic Susceptibilities of Some Diamagnetic Alloys," Canadian Journal of Physics 38, 908–925 (1960).

17. Butts, A., and Reiber, P. L., "Investigation of the Effect of Impurities on the Ferro-Magnetism of Non-ferrous Alloys," Frankford Arsenal, Philadelphia, PA, Report No. R-652, 102 pp. (1945).

18. Parker, F. G., Winter, R. M., and LaPorta, J. A., "Magnetic Properties of Copper Alloys," Proceedings of the American Society for Testing and Materials 59, 230–261 (1959).

BL-114A
(5-90)

U.S. DEPARTMENT OF COMMERCE
NATIONAL INSTITUTE OF STANDARDS AND TECHNOLOGY

BIBLIOGRAPHIC DATA SHEET

1. PUBLICATION OR REPORT NUMBER
NIST/MN-177

2. PERFORMING ORGANIZATION REPORT NUMBER
B92-0080

3. PUBLICATION DATE
February 1992

4. TITLE AND SUBTITLE
Properties of Copper and Copper Alloys at Cryogenic Temperatures

5. AUTHOR(S)
N.J. Simon, E.S. Drexler, R.P. Reed

6. PERFORMING ORGANIZATION (IF JOINT OR OTHER THAN NIST, SEE INSTRUCTIONS)
U.S. DEPARTMENT OF COMMERCE
NATIONAL INSTITUTE OF STANDARDS AND TECHNOLOGY
BOULDER, COLORADO 80303-3328

7. CONTRACT/GRANT NUMBER
Project No. 434

8. TYPE OF REPORT AND PERIOD COVERED
Final

9. SPONSORING ORGANIZATION NAME AND COMPLETE ADDRESS (STREET, CITY, STATE, ZIP)
International Copper Association, Ltd.
708 Third Avenue
New York, NY 10017

10. SUPPLEMENTARY NOTES

11. ABSTRACT (A 200-WORD OR LESS FACTUAL SUMMARY OF MOST SIGNIFICANT INFORMATION. IF DOCUMENT INCLUDES A SIGNIFICANT BIBLIOGRAPHY OR LITERATURE SURVEY, MENTION IT HERE.)

The mechanical and physical properties at cryogenic temperatures for selected coppers and copper alloys have been compiled, reviewed, and analyzed. Tables, figures, and regression equations are included. The materials are: the oxygen-free coppers (C10100-C10700), beryllium coppers (C17000-C17510), and the phosphor bronzes (C50500-C52400). The temperature range for the property data is from 4 to 295 K. Mechanical properties include tensile, toughness, fatigue, and creep; physical properties include elastic constants, specific heat, thermal conductivity and expansion, and electrical resistivity. In many cases, these properties are a strong function of metallurgical variables, such as cold work and grain size. Regression analyses have been performed in cases where there are sufficient data to ensure reasonable statistical portrayal of the effect of these variables on specific properties.

The original program of data review was sponsored by the Office of Fusion Energy of the U.S. Department of Energy. Its purpose was to assemble and to evaluate property data useful to magnet designers for fusion plasma confinement. Both normal-metal, high-field magnets (using cold-worked C10700 and C17510 alloys) and NbTi and Nb_3Sn superconducting magnets (using C10400 and copper-tin or phosphor bronze alloys) are currently in design or development stages. The review has been re-edited and expanded for those more generally interested in the low-temperature properties of copper and selected copper alloys, under the sponsorship of the International Copper Association, Ltd.

12. KEY WORDS (6 TO 12 ENTRIES; ALPHABETICAL ORDER; CAPITALIZE ONLY PROPER NAMES; AND SEPARATE KEY WORDS BY SEMICOLONS)
beryllium copper alloys; copper; copper alloys; copper-tin alloys; cryogenic; electromagnetic properties; fatigue; mechanical properties; phosphor bronze alloys; tensile properties; thermal properties

13. AVAILABILITY

X	UNLIMITED
	FOR OFFICIAL DISTRIBUTION. DO NOT RELEASE TO NATIONAL TECHNICAL INFORMATION SERVICE (NTIS).
X	ORDER FROM SUPERINTENDENT OF DOCUMENTS, U.S. GOVERNMENT PRINTING OFFICE, WASHINGTON, DC 20402.
X	ORDER FROM NATIONAL TECHNICAL INFORMATION SERVICE (NTIS), SPRINGFIELD, VA 22161.

14. NUMBER OF PRINTED PAGES
850

15. PRICE

ELECTRONIC FORM

NIST Technical Publications

Periodical

Journal of Research of the National Institute of Standards and Technology—Reports NIST research and development in those disciplines of the physical and engineering sciences in which the Institute is active. These include physics, chemistry, engineering, mathematics, and computer sciences. Papers cover a broad range of subjects, with major emphasis on measurement methodology and the basic technology underlying standardization. Also included from time to time are survey articles on topics closely related to the Institute's technical and scientific programs. Issued six times a year.

Nonperiodicals

Monographs—Major contributions to the technical literature on various subjects related to the Institute's scientific and technical activities.

Handbooks—Recommended codes of engineering and industrial practice (including safety codes) developed in cooperation with interested industries, professional organizations, and regulatory bodies.

Special Publications—Include proceedings of conferences sponsored by NIST, NIST annual reports, and other special publications appropriate to this grouping such as wall charts, pocket cards, and bibliographies.

Applied Mathematics Series—Mathematical tables, manuals, and studies of special interest to physicists, engineers, chemists, biologists, mathematicians, computer programmers, and others engaged in scientific and technical work.

National Standard Reference Data Series—Provides quantitative data on the physical and chemical properties of materials, compiled from the world's literature and critically evaluated. Developed under a worldwide program coordinated by NIST under the authority of the National Standard Data Act (Public Law 90-396). NOTE: The Journal of Physical and Chemical Reference Data (JPCRD) is published bi-monthly for NIST by the American Chemical Society (ACS) and the American Institute of Physics (AIP). Subscriptions, reprints, and supplements are available from ACS, 1155 Sixteenth St., NW., Washington, DC 20056.

Building Science Series—Disseminates technical information developed at the Institute on building materials, components, systems, and whole structures. The series presents research results, test methods, and performance criteria related to the structural and environmental functions and the durability and safety characteristics of building elements and systems.

Technical Notes—Studies or reports which are complete in themselves but restrictive in their treatment of a subject. Analogous to monographs but not so comprehensive in scope or definitive in treatment of the subject area. Often serve as a vehicle for final reports of work performed at NIST under the sponsorship of other government agencies.

Voluntary Product Standards—Developed under procedures published by the Department of Commerce in Part 10, Title 15, of the Code of Federal Regulations. The standards establish nationally recognized requirements for products, and provide all concerned interests with a basis for common understanding of the characteristics of the products. NIST administers this program as a supplement to the activities of the private sector standardizing organizations.

Consumer Information Series—Practical information, based on NIST research and experience, covering areas of interest to the consumer. Easily understandable language and illustrations provide useful background knowledge for shopping in today's technological marketplace.

Order the ***above*** *NIST publications from: Superintendent of Documents, Government Printing Office, Washington, DC 20402.*

Order the ***following*** *NIST publications—FIPS and NISTIRs—from the National Technical Information Service, Springfield, VA 22161.*

Federal Information Processing Standards Publications (FIPS PUB)—Publications in this series collectively constitute the Federal Information Processing Standards Register. The Register serves as the official source of information in the Federal Government regarding standards issued by NIST pursuant to the Federal Property and Administrative Services Act of 1949 as amended, Public Law 89-306 (79 Stat. 1127), and as implemented by Executive Order 11717 (38 FR 12315, dated May 11, 1973) and Part 6 of Title 15 CFR (Code of Federal Regulations).

NIST Interagency Reports (NISTIR)—A special series of interim or final reports on work performed by NIST for outside sponsors (both government and non-government). In general, initial distribution is handled by the sponsor; public distribution is by the National Technical Information Service, Springfield, VA 22161, in paper copy or microfiche form.

U.S. Department of Commerce
National Institute of Standards and Technology
Gaithersburg, MD 20899

Official Business
Penalty for Private Use $300